

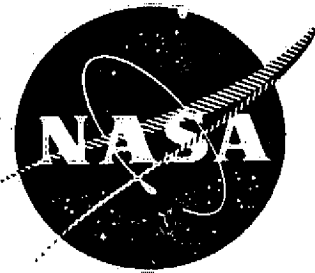
General Disclaimer

One or more of the Following Statements may affect this Document

- This document has been reproduced from the best copy furnished by the organizational source. It is being released in the interest of making available as much information as possible.
- This document may contain data, which exceeds the sheet parameters. It was furnished in this condition by the organizational source and is the best copy available.
- This document may contain tone-on-tone or color graphs, charts and/or pictures, which have been reproduced in black and white.
- This document is paginated as submitted by the original source.
- Portions of this document are not fully legible due to the historical nature of some of the material. However, it is the best reproduction available from the original submission.

NASA

CR-159575 Vol. II



ACOUSTIC AND AERODYNAMIC PERFORMANCE INVESTIGATION OF INVERTED VELOCITY PROFILE COANNULAR PLUG NOZZLES

Comprehensive Data Report

VOLUME II

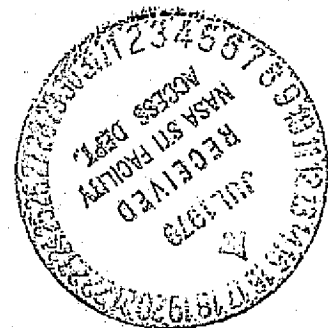
P. R. Knott
J. T. Blozy
P. S. Staid

GENERAL ELECTRIC COMPANY

(NASA-CR-159575-Vol-2) ACOUSTIC AND
AERODYNAMIC PERFORMANCE INVESTIGATION OF
INVERTED VELOCITY PROFILE COANNULAR PLUG NOZZLES, COMPREHENSIVE DATA REPORT, VOLUME 2
Final Report (General Electric Co.) 523 p
N79-26885
HC A22/MF A01
Unclas
G3/71 27855

NATIONAL AERONAUTICS AND SPACE ADMINISTRATION
LEWIS RESEARCH CENTER
21000 BROOKPARK ROAD
CLEVELAND, OHIO 44135

NASA CONTRACT: NAS3-19777



1. Report No. CR-159575		2. Government Accession No.		3. Recipient's Catalog No.	
4. Title and Subtitle ACOUSTIC AND AERODYNAMIC PERFORMANCE INVESTIGATION OF INVERTED VELOCITY PROFILE CO-ANNULAR PLUG NOZZLES -- COMPREHENSIVE DATA REPORT -- VOLUME II				5. Report Date May 1979	
				6. Performing Organization Code	
7. Author(s) P. R. Knott, J. T. Blozy, and P. S. Staid				8. Performing Organization Report No. R79AEG166	
9. Performing Organization Name and Address General Electric Company Aircraft Engine Group Cincinnati, Ohio 45215				10. Work Unit No.	
				11. Contract or Grant No. NAS3-19777	
12. Sponsoring Agency Name and Address National Aeronautics and Space Administration Washington, D.C. 20546				13. Type of Report and Period Covered Contractor Report	
				14. Sponsoring Agency Code	
15. Supplementary Notes Final report. Project Manager, Orlando A. Gutierrez, V/STOL and Noise Division, NASA Lewis Research Center, Cleveland, Ohio 44135.					
16. Abstract This Comprehensive Data Report, comprising three volumes, includes the basic test description and test results which are analyzed and documented in the comparison Final Reports, NASA CR-3149 and CR-2990. Volume I contains a description of the acoustic configurations, test facilities, data reduction techniques, test conditions, and detailed test results from the hot, static acoustic tests at the General Electric Anechoic Chamber. Volume II presents acoustic data comparisons in graphical form. Volume III contains the detailed aerodynamic test results plus the "concept screening and model design report."					
17. Key Words (Suggested by Author(s)) Supersonic jet noise; Noise suppression; Co-annular plug nozzles; Inverted velocity profile; Variable-cycle engine; Acoustic tests; Aerodynamic performance tests				18. Distribution Statement Unclassified - unlimited STAR Category 71	
19. Security Classif. (of this report) Unclassified		20. Security Classif. (of this page) Unclassified		21. No. of Pages 523	
				22. Price*	

* For sale by the National Technical Information Service, Springfield, Virginia 22161 75¢

TABLE OF CONTENTS

<u>Section</u>		<u>Page</u>
	<u>VOLUME I</u>	
1.0	INTRODUCTION	1
2.0	DEFINITION OF ACOUSTIC CONFIGURATIONS	2
3.0	ACOUSTIC TEST FACILITY AND DATA REDUCTION TECHNIQUES	6
	3.1 The Acoustic Arena	6
	3.2 Acoustic Data Systems	21
	3.3 Aero Data Systems	28
	3.4 Analysis of Variance - Overall Precision of the Acoustic Measurements	33
	3.5 Certification	39
4.0	ACOUSTIC TEST POINT DEFINITION	42
5.0	ACOUSTIC DATA SCALING AND NORMALIZATION	58
6.0	DETAILED TABLES OF ACOUSTIC TEST RESULTS	60
	6.1 Coannular Configuration 1	64
	6.2 Coannular Configuration 2	161
	6.3 Coannular Configuration 3	221
	6.4 Coannular Configuration 4	331
	6.5 Coannular Configuration 5	389
	6.6 Coannular Configuration 6	449
	6.7 Coannular Configuration 7	517
	6.8 Conical Nozzle	691
	<u>VOLUME II</u>	
7.0	ACOUSTIC DATA COMPARATIVE PLOTS	715
	7.1 Introduction	715
	7.2 Comparisons of Anechoic Chamber and Outdoor Test Site (JENOTS) Data	716
	7.3 Comparison of Data for IVP Nozzles with Low Amounts of Inner Flow	786
	7.3.1 Zero Inner Flow Study	786
	7.3.2 Low Inner Flow Study	808

TABLE OF CONTENTS (Concluded)

<u>Section</u>	<u>Page</u>
7.4 Comparisons of Data for IVP Nozzles with High Amounts of Inner Flow	879
7.4.1 Effect of Outer Radius Ratio	879
7.4.2 Effect of Inner Radius Ratio	942
7.4.3 Effect of Plug Geometry	1048
7.4.4 Effect of Velocity Ratio	1112
7.4.5 Effect of Inner Pressure Ratio at Constant Velocity Ratio	1155
7.4.6 Effect of Velocity Ratio at Constant Inner Pressure Ratio	1177
7.4.7 Velocity Dependence Study	1213
7.4.8 Temperature Dependence Study	1224
<u>VOLUME III</u>	
8.0 INTRODUCTION TO AERODYNAMIC PERFORMANCE DATA	1237
9.0 AERODYNAMIC FACILITY DESCRIPTION	1238
10.0 AERODYNAMIC DATA REDUCTION PROCEDURES	1242
11.0 AERODYNAMIC MODEL DESCRIPTION	1251
12.0 AERODYNAMIC TEST MATRIX	1263
13.0 AERODYNAMIC DATA TABULATION	1299
14.0 STATIC PRESSURE PLOTS	1346
15.0 CONCEPT SCREENING AND MODEL DESIGN REPORT	1459

7.0 ACOUSTIC DATA COMPARATIVE PLOTS

7.1 INTRODUCTION

In the following sections data plots are presented which examine the noise characteristics of the coannular nozzle. The effect of changes in both the nozzle flow parameters (i.e., velocity, temperature, pressure ratio) and the coannular nozzle geometry are presented. All data are normalized except for PWL spectra and the first 10 points, which are comparisons with JENOTS data.

Unless otherwise specified, the following plots are presented for each study.

For full size (513 in.²) at the 2400-ft sideline:

1. PNL directivity, normalized

For model size (29,399 in.²) at the 40-ft arc:

1. OASPL directivity, normalized
2. 1/3-octave band PWL spectra, unnormalized
3. 1/3-octave band SPL spectra at angles of 50°, 90°, 130°, and 140° to the inlet, normalized

The following normalization factors have been used in the plots:

1. PNL - $10 \text{ LOG}(FT/F_{REF})$

where:

PNL perceived noise level
FT total ideal thrust
F_{REF} reference ideal thrust (F_{REF} = 5130 lbf)

2. OASPL - A

where:

$A = 10 \text{ LOG}(AT/R^2) + 10 \text{ LOG}(FT/(AT \cdot F_{REF}))$
OASPL overall sound pressure level
AT total area
R distance
FT total ideal thrust
F_{REF} reference thrust/reference area (F_{REF} = 10 lbf/in.²)

3. SPL - $10 \text{ LOG}(A/R^2) - 10 \text{ LOG}(FT/(A \cdot F_{REF}))$

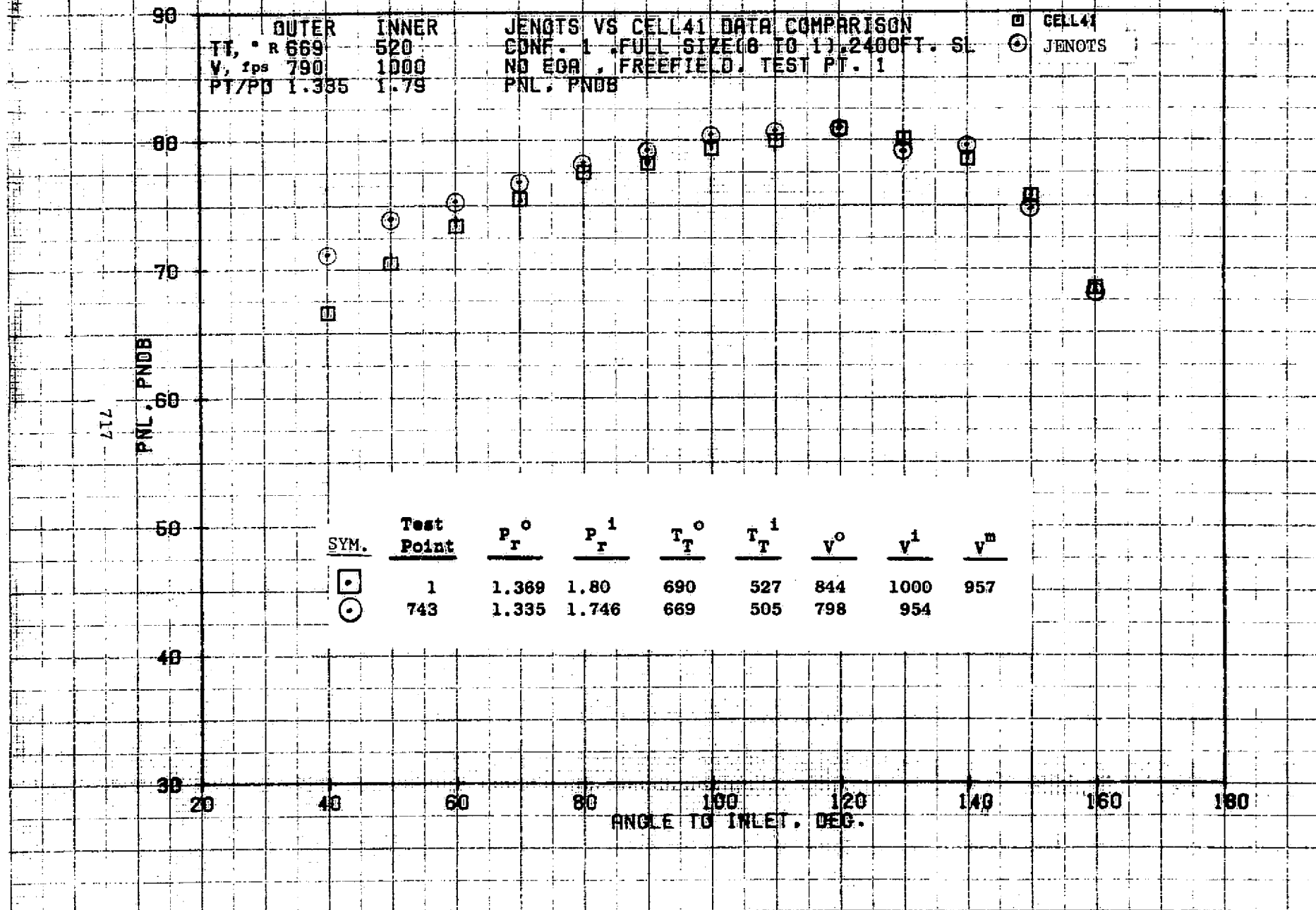
where:

SPL sound pressure level
A total area
R distance
FT total ideal thrust
F_{REF} reference thrust/reference area (F_{REF} = 10 lbf/in.²)

Only a presentation of the data is made in this report. Data analysis is addressed in the main final report. On each plot the measured flow conditions are shown for all data points in the comparison.

7.2 COMPARISON OF ANECHOIC CHAMBER AND OUTDOOR TEST SITE (JENOTS) DATA

The purpose of this data analysis group is to compare data measured previously in the General Electric outdoor acoustic test site (JENOTS) with the acoustic measurements in the General Electric Anechoic Jet Noise Facility (Cell 41). Ten test points were chosen for this comparison. For these points the full-size comparison was made at 1812 in.² and both full-size and model-size data were not normalized since the test model was exactly the same in size and geometry. The JENOTS data was previously reported in NASA CR-135239.

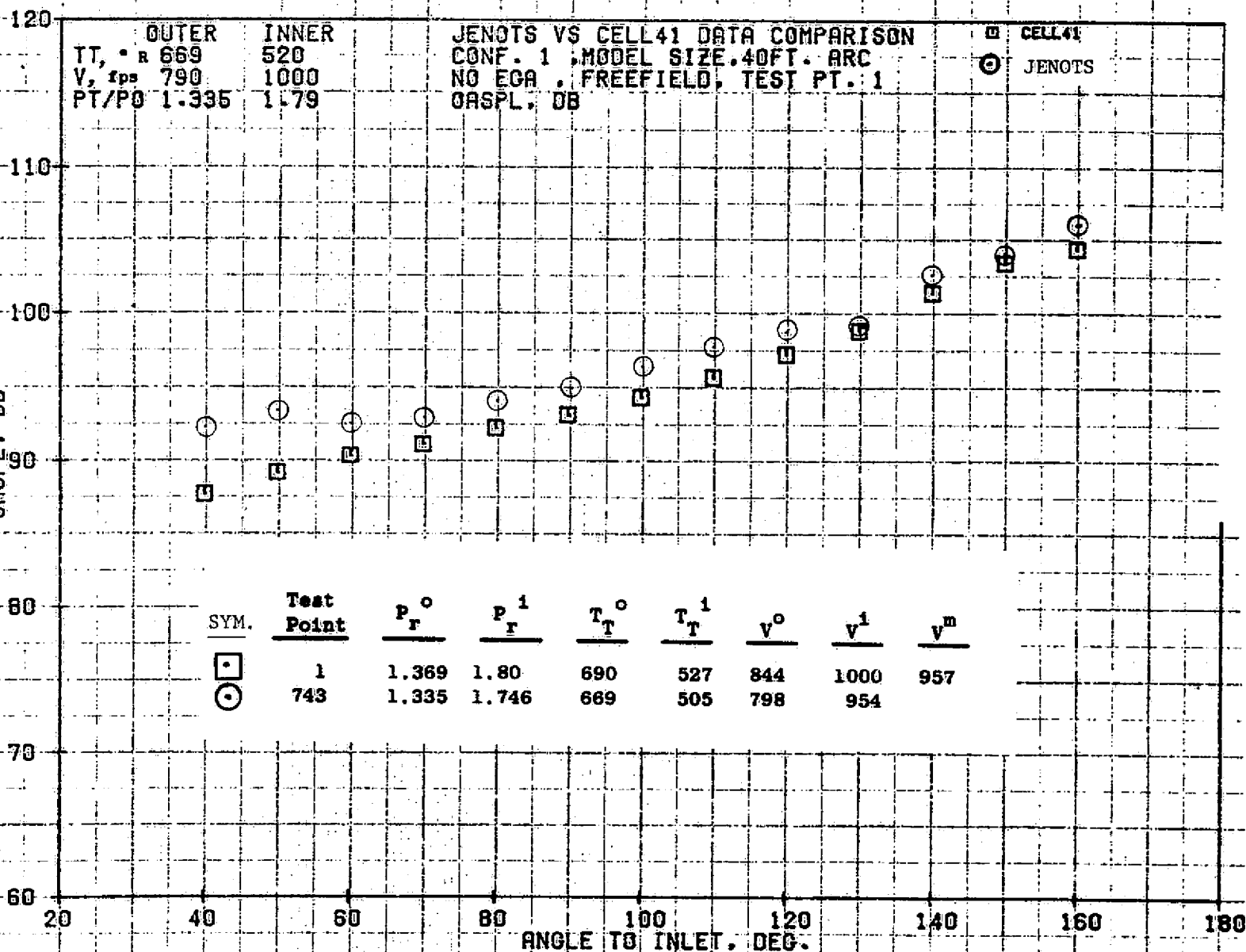


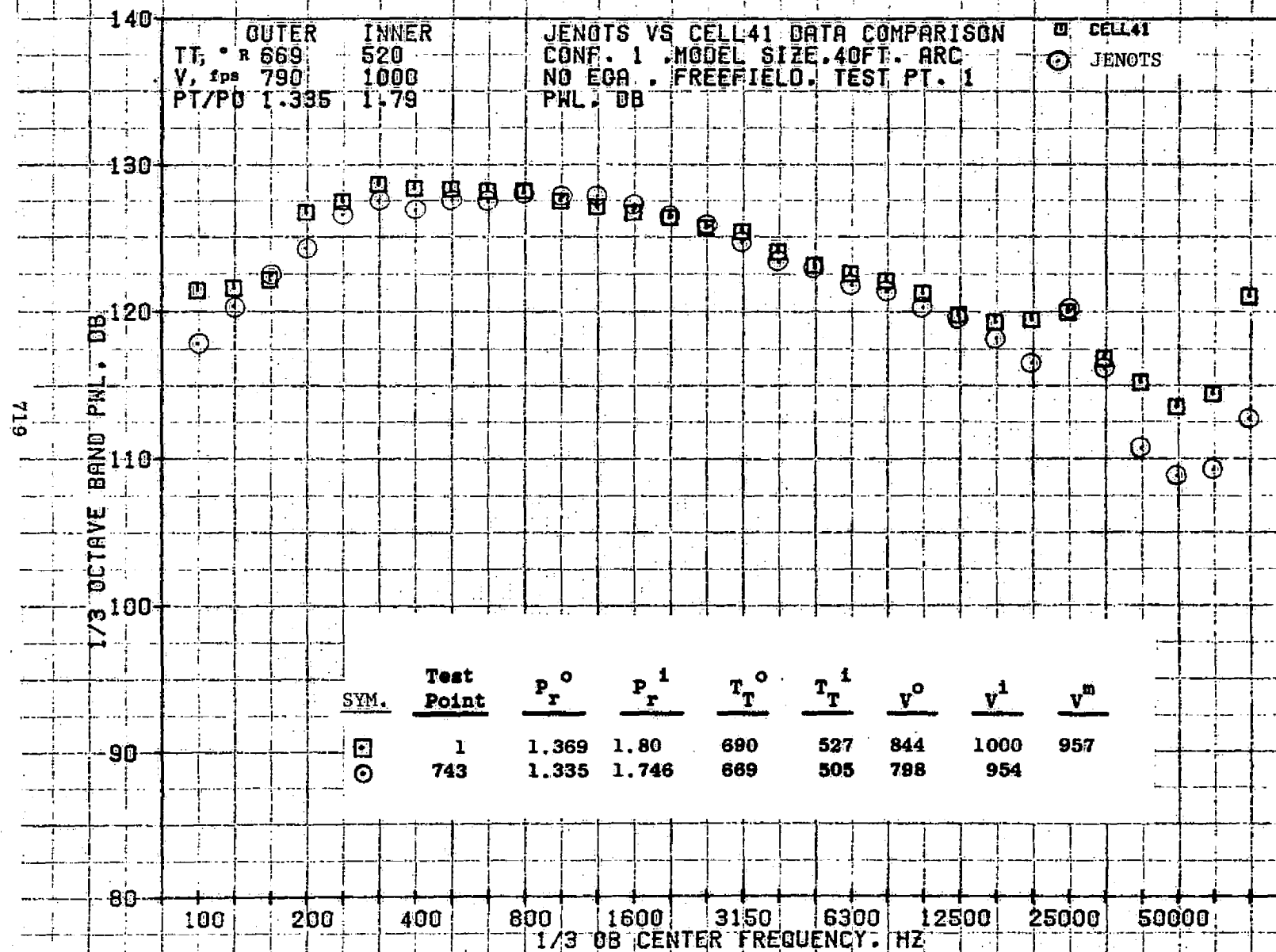
09/28/76
 1X583-001

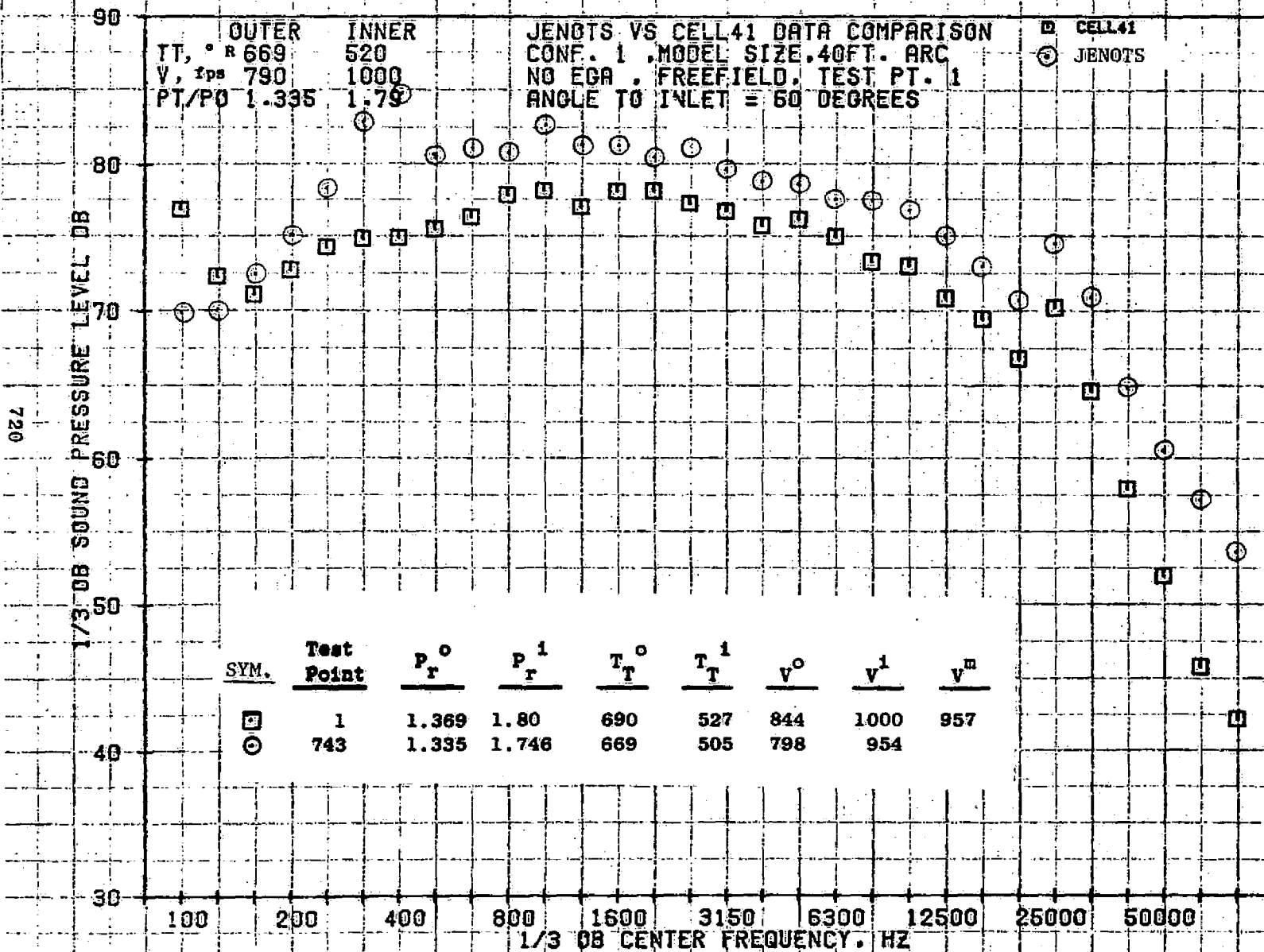
73KOLLSTEDT

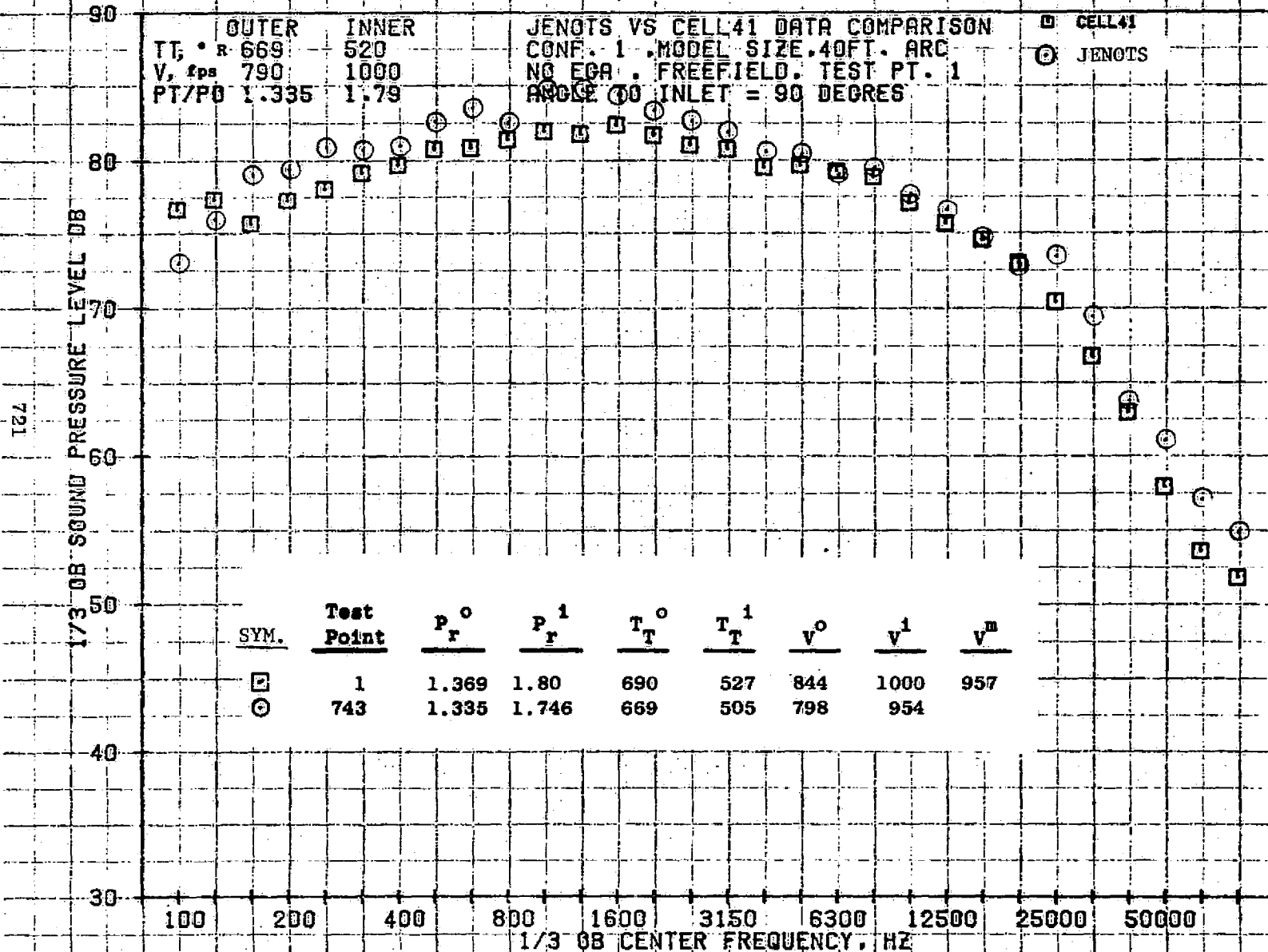
718

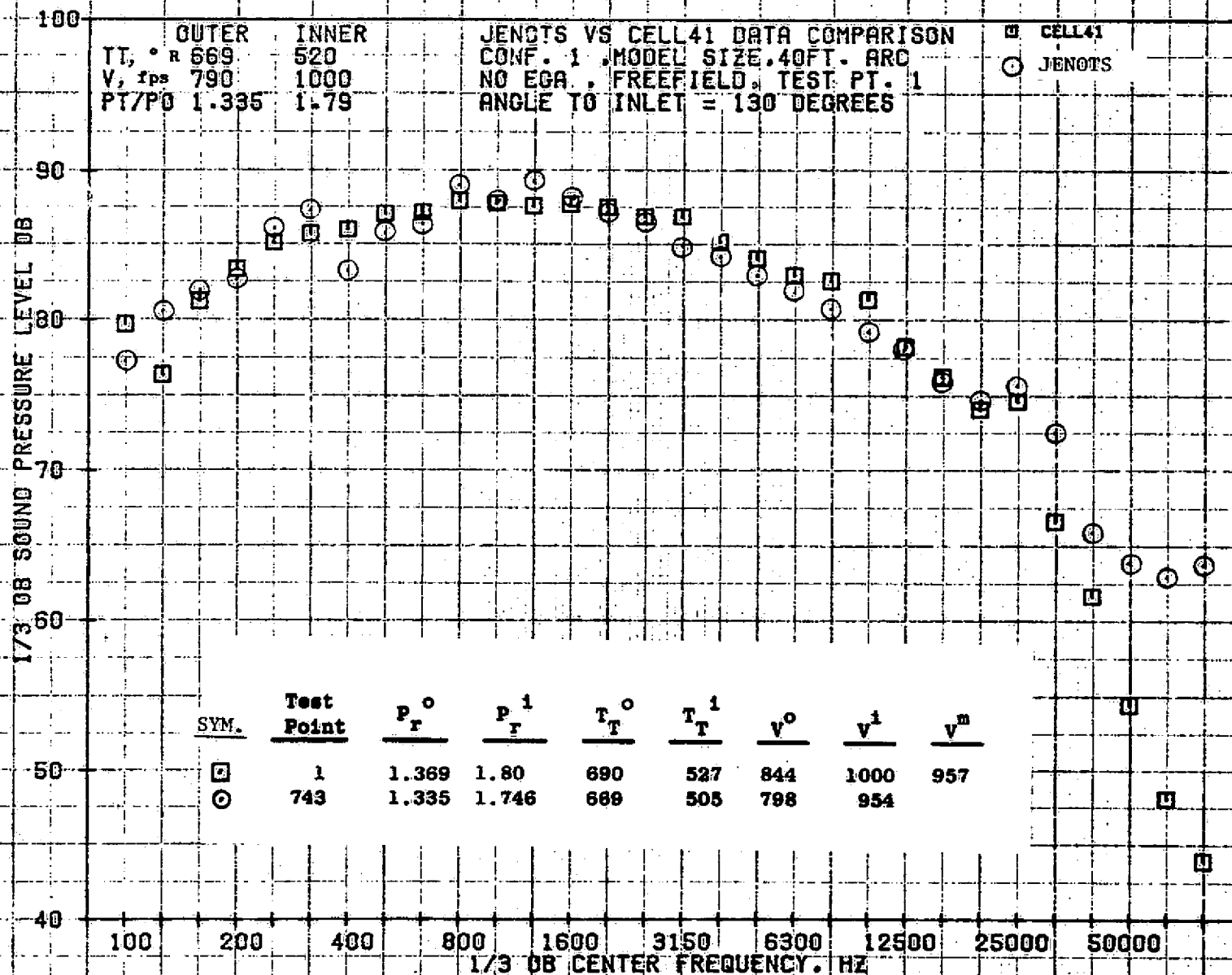
OASPL, DB

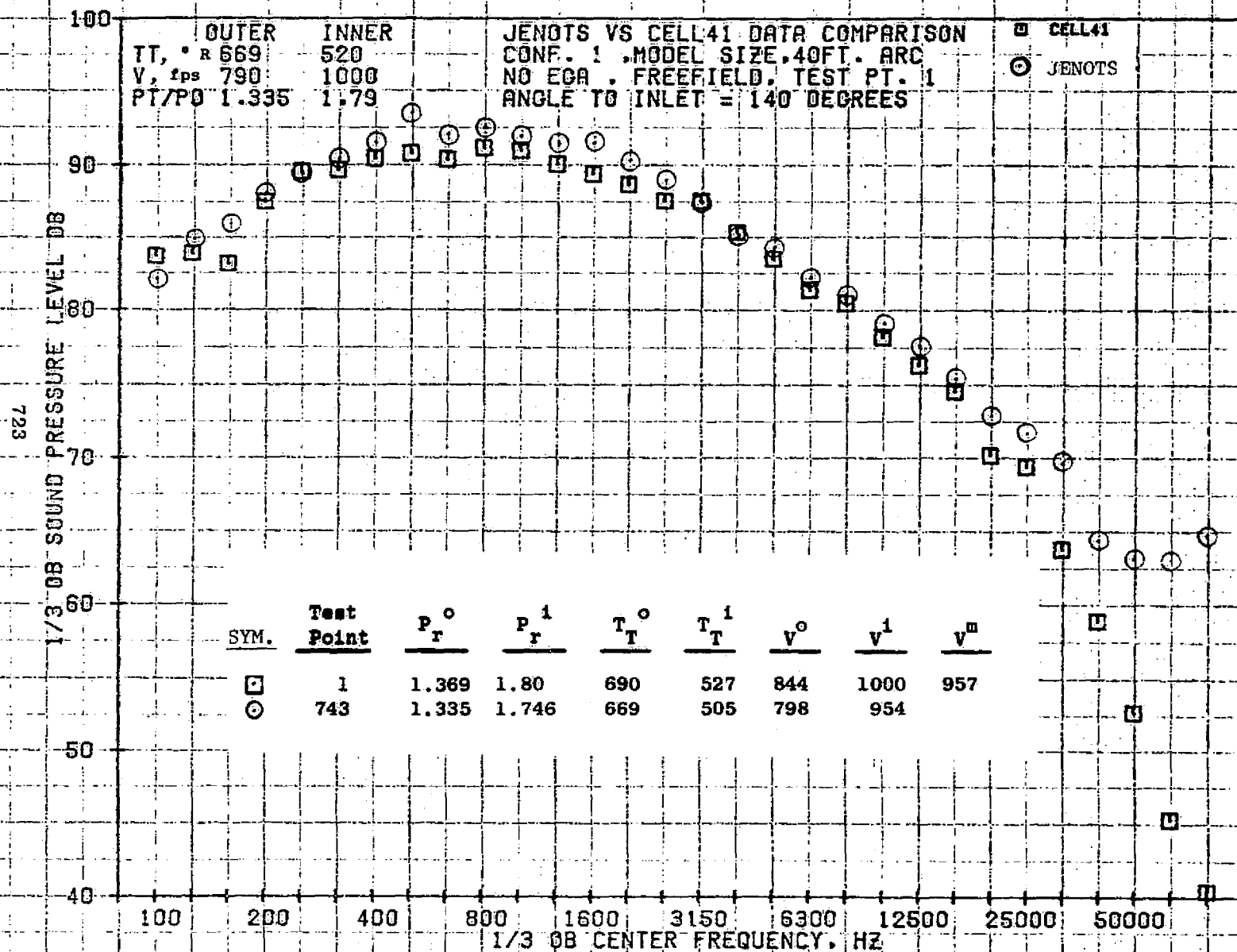


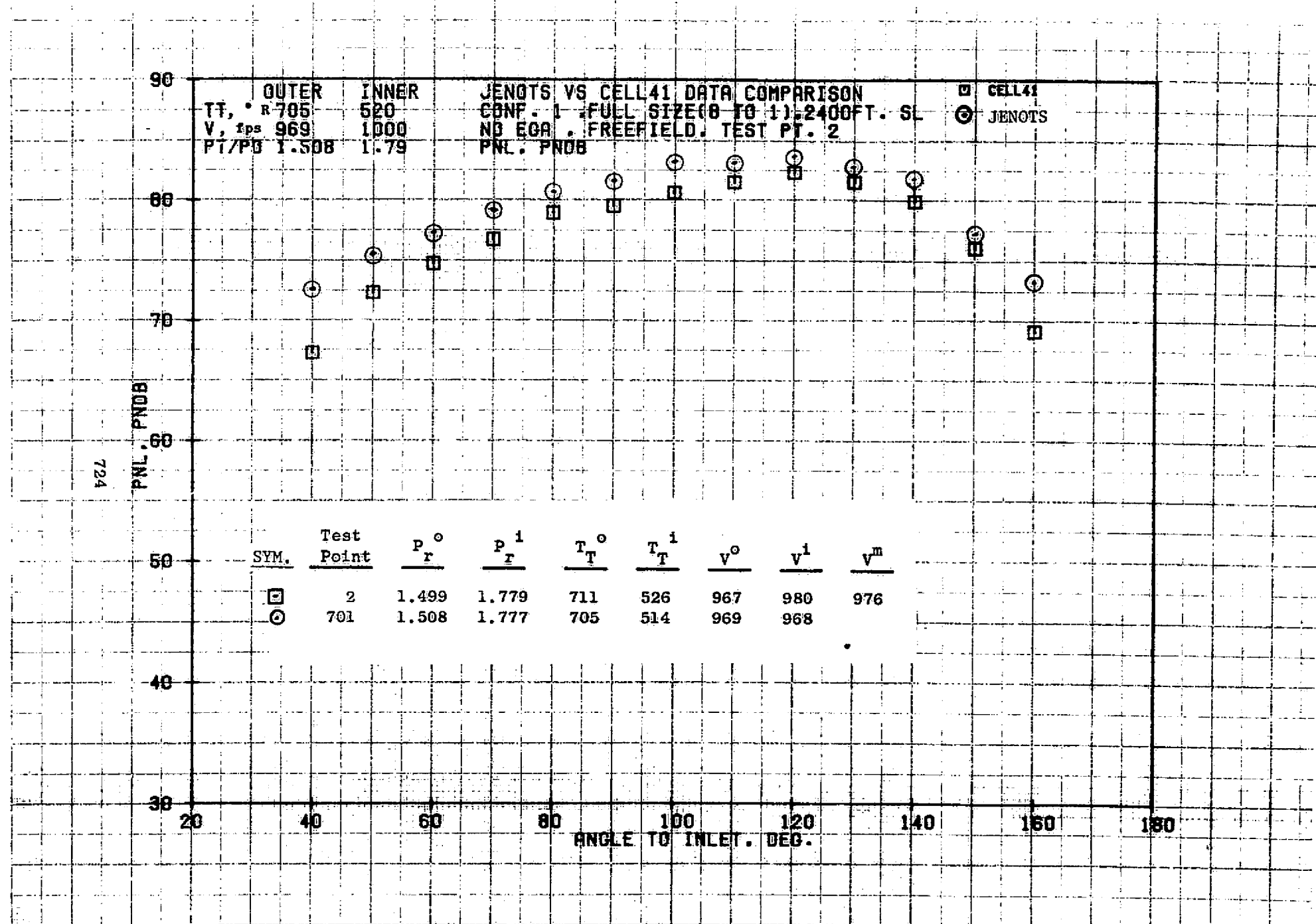






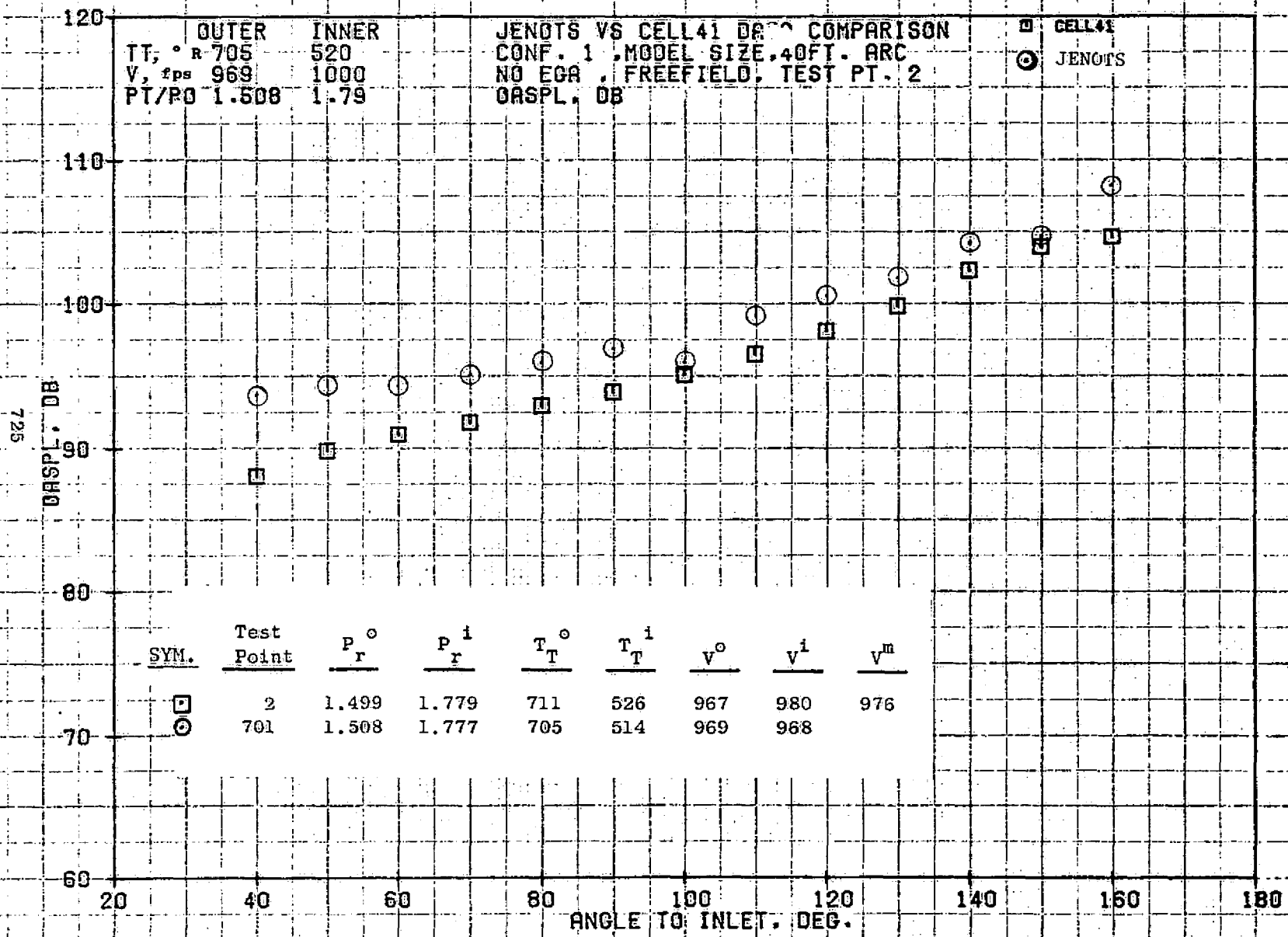


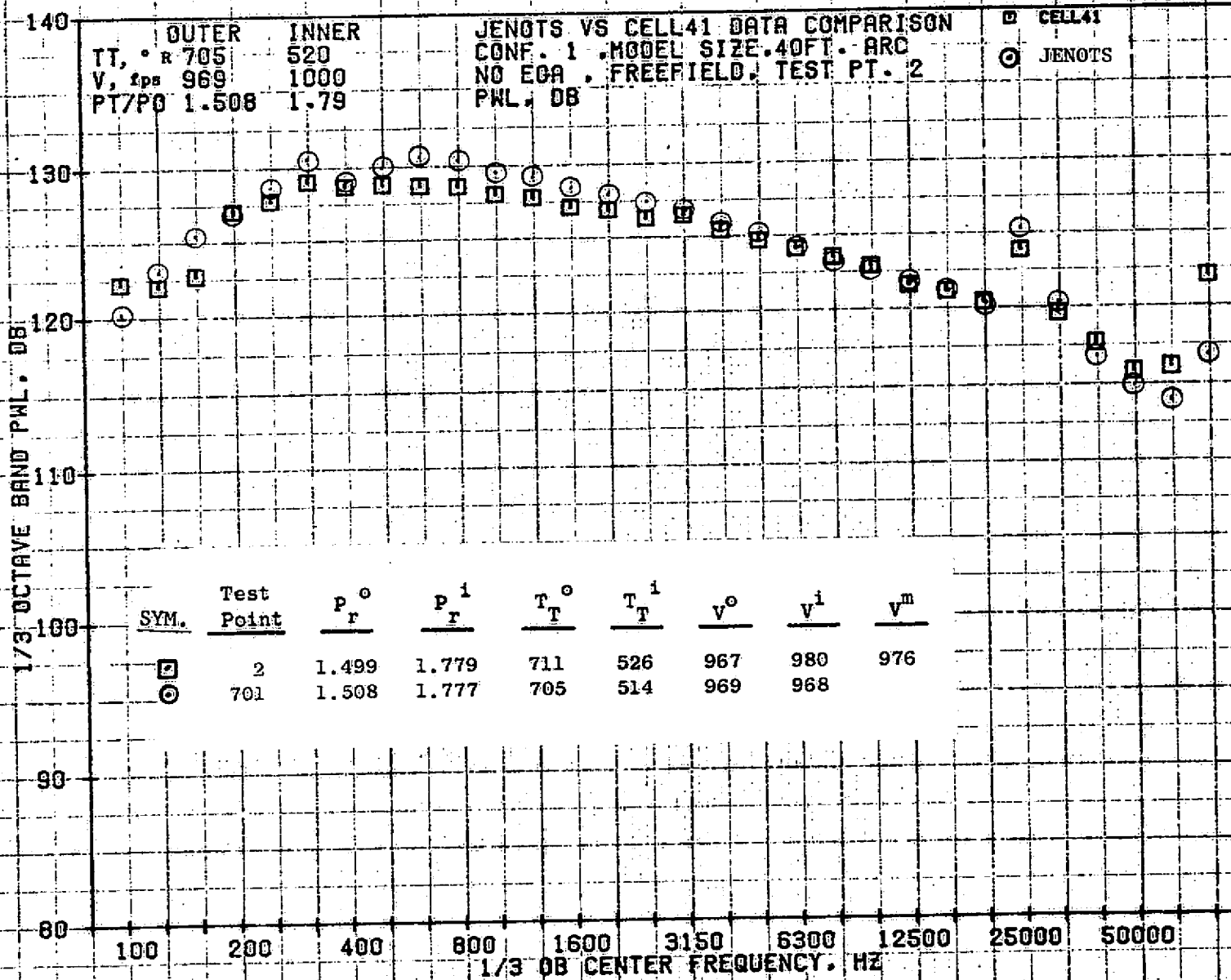


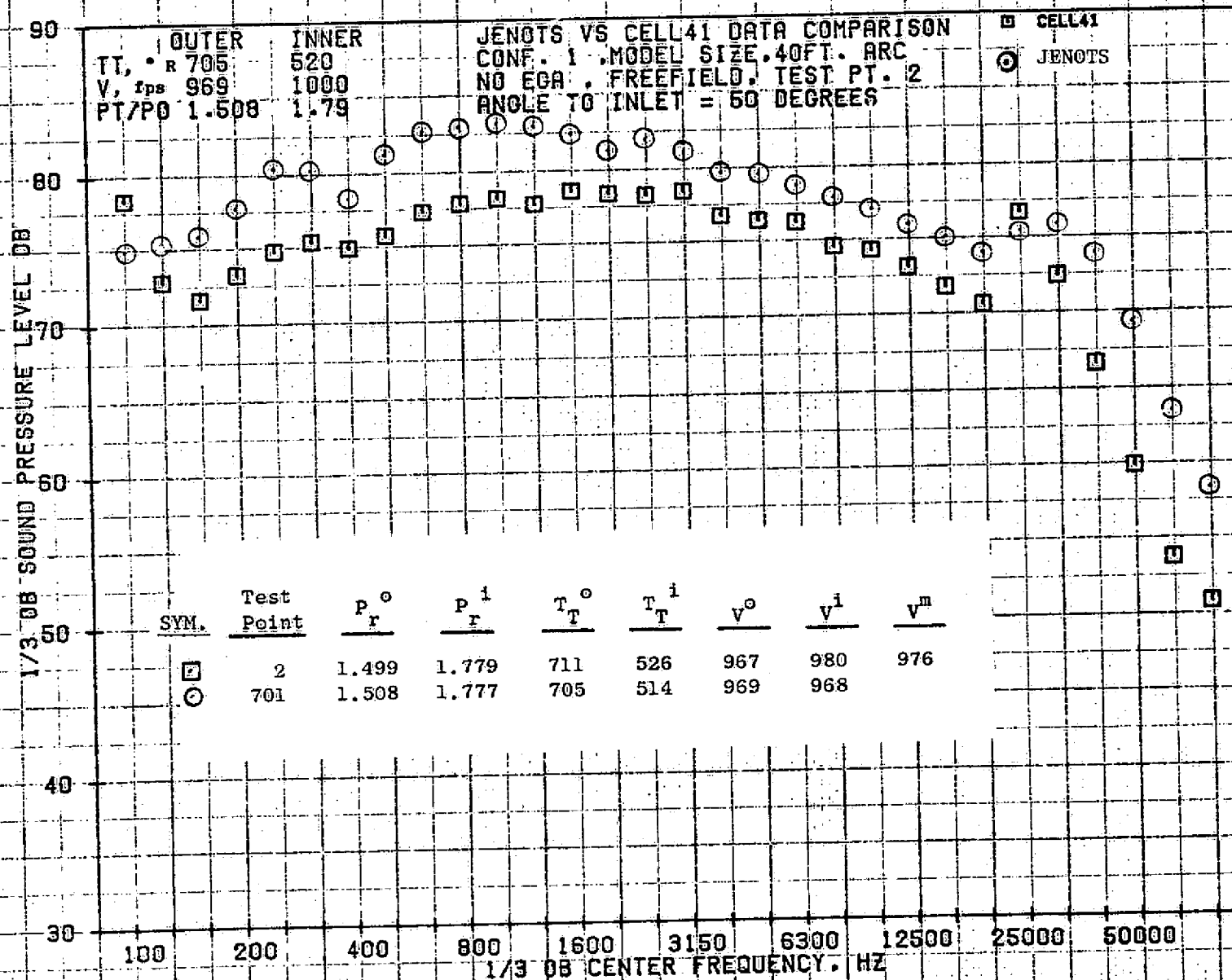


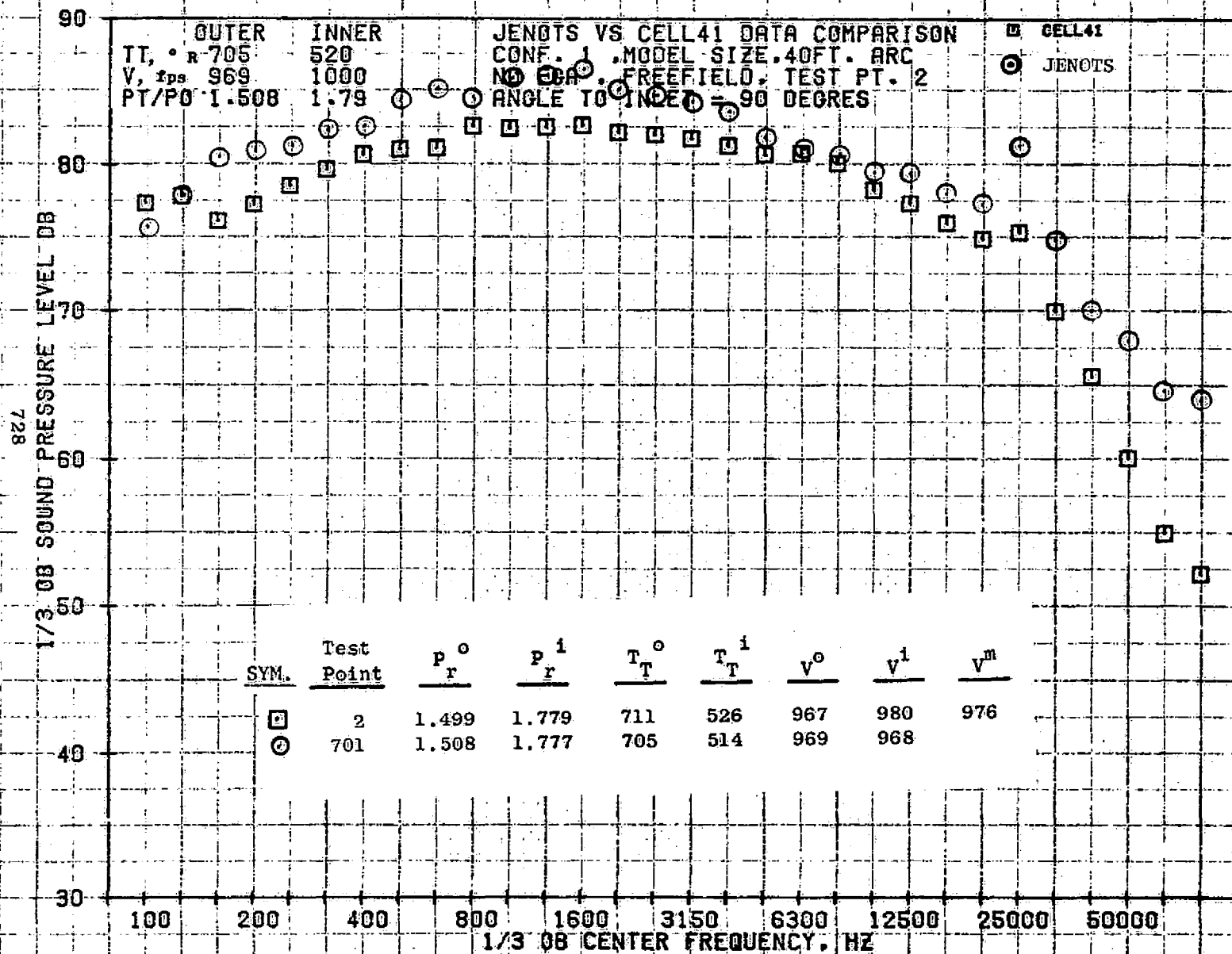
09/28/76
1X583-001

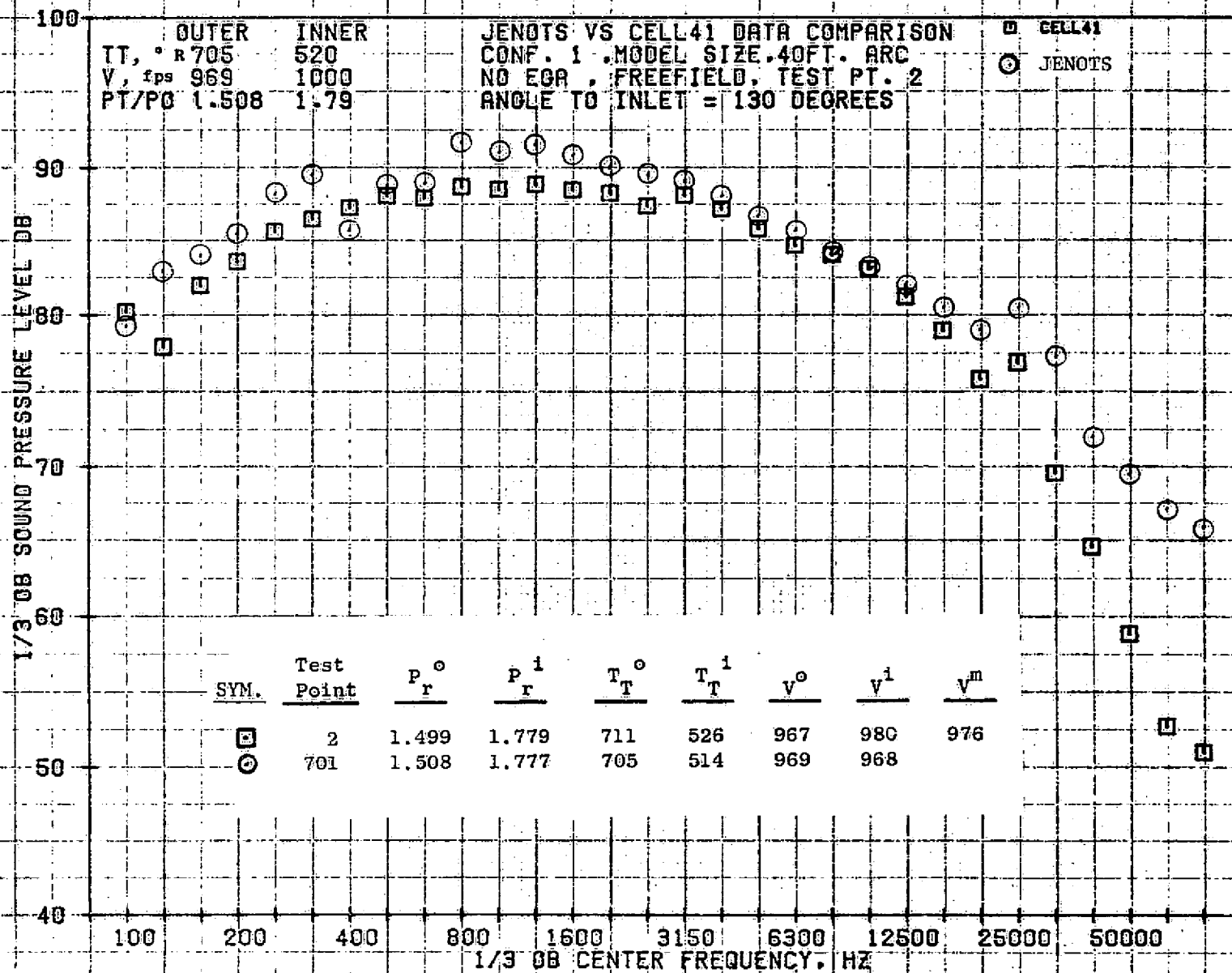
73KOLLSTEDT

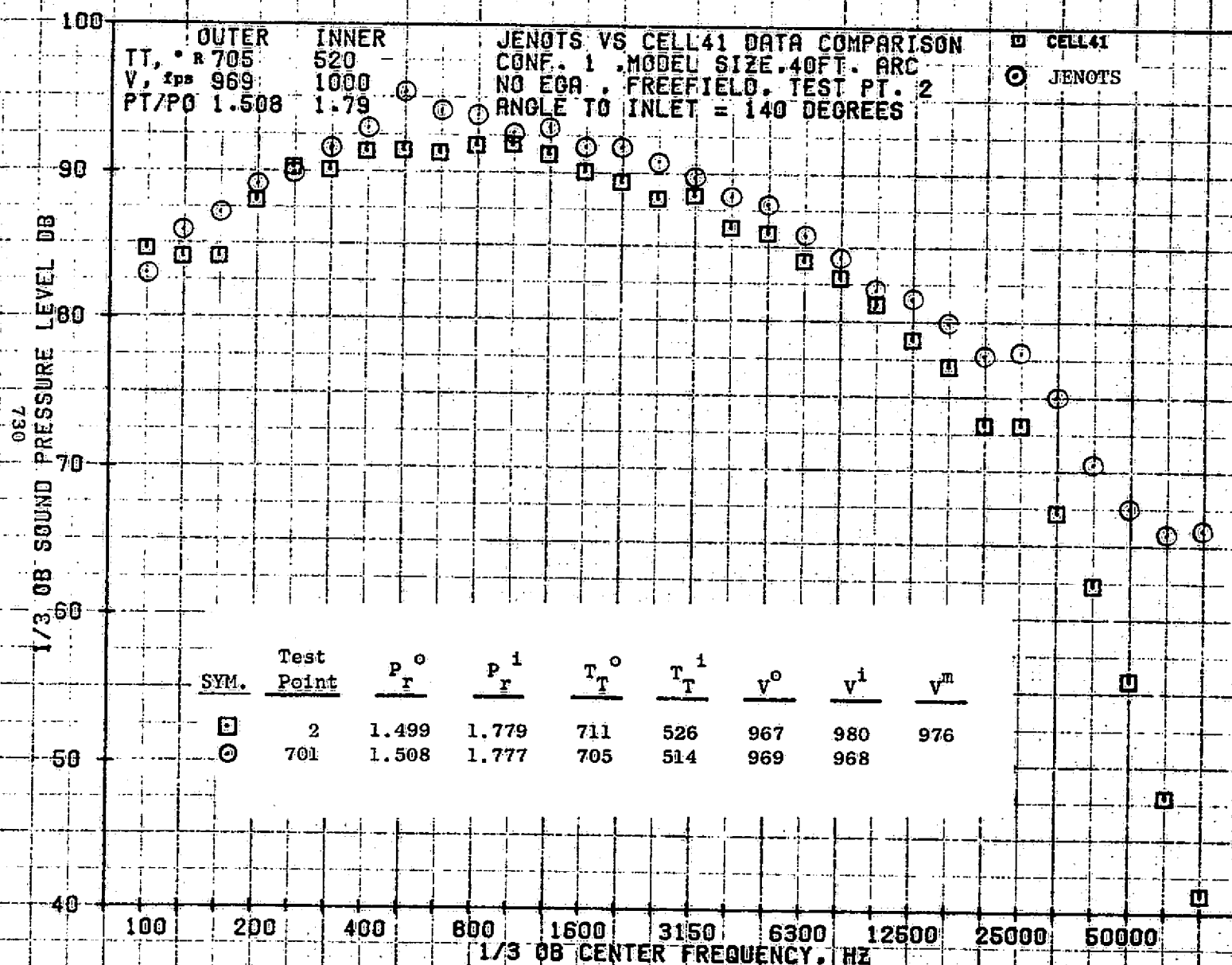


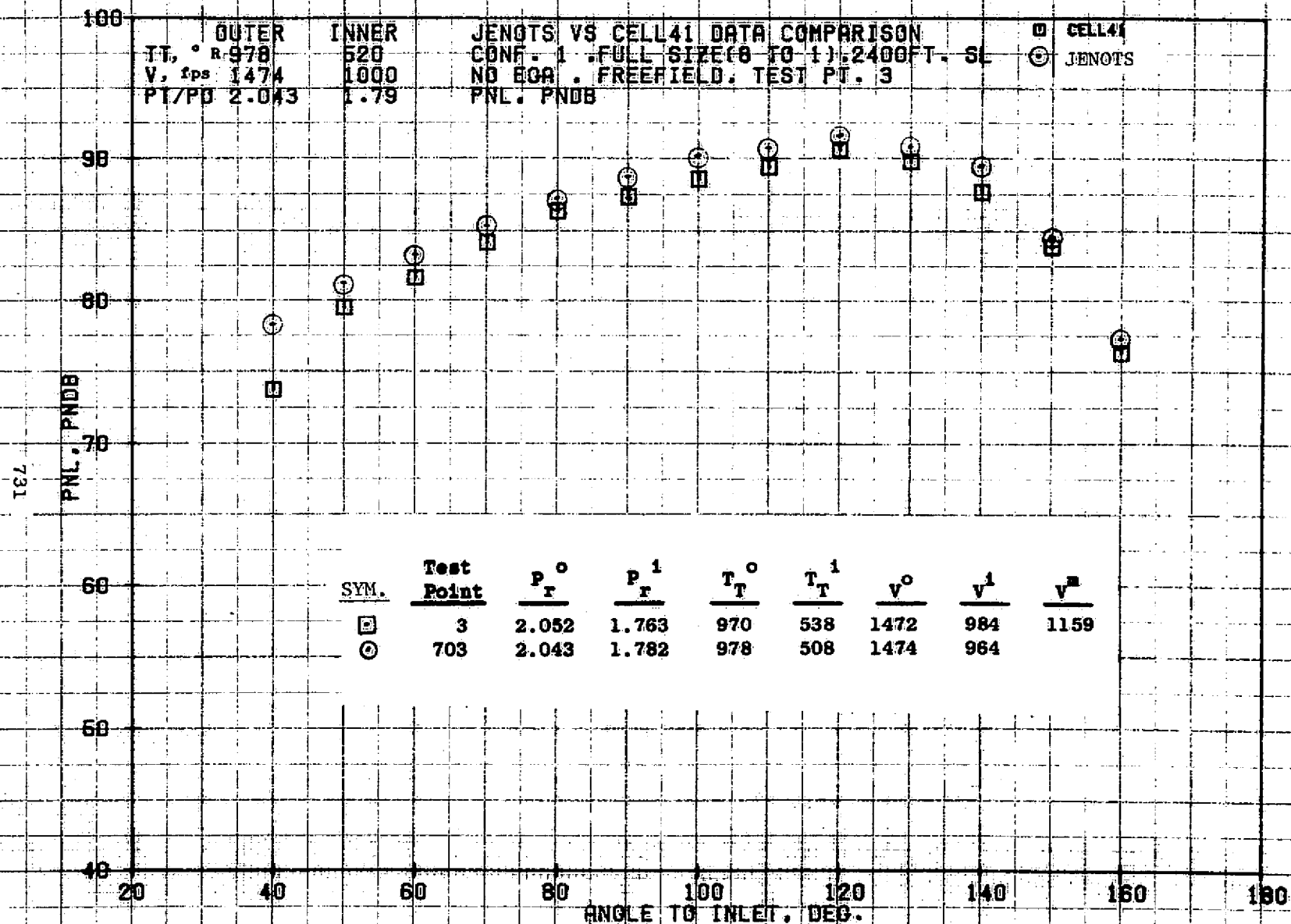












09/28/76
 1X583-001

73KOLLSTEDT

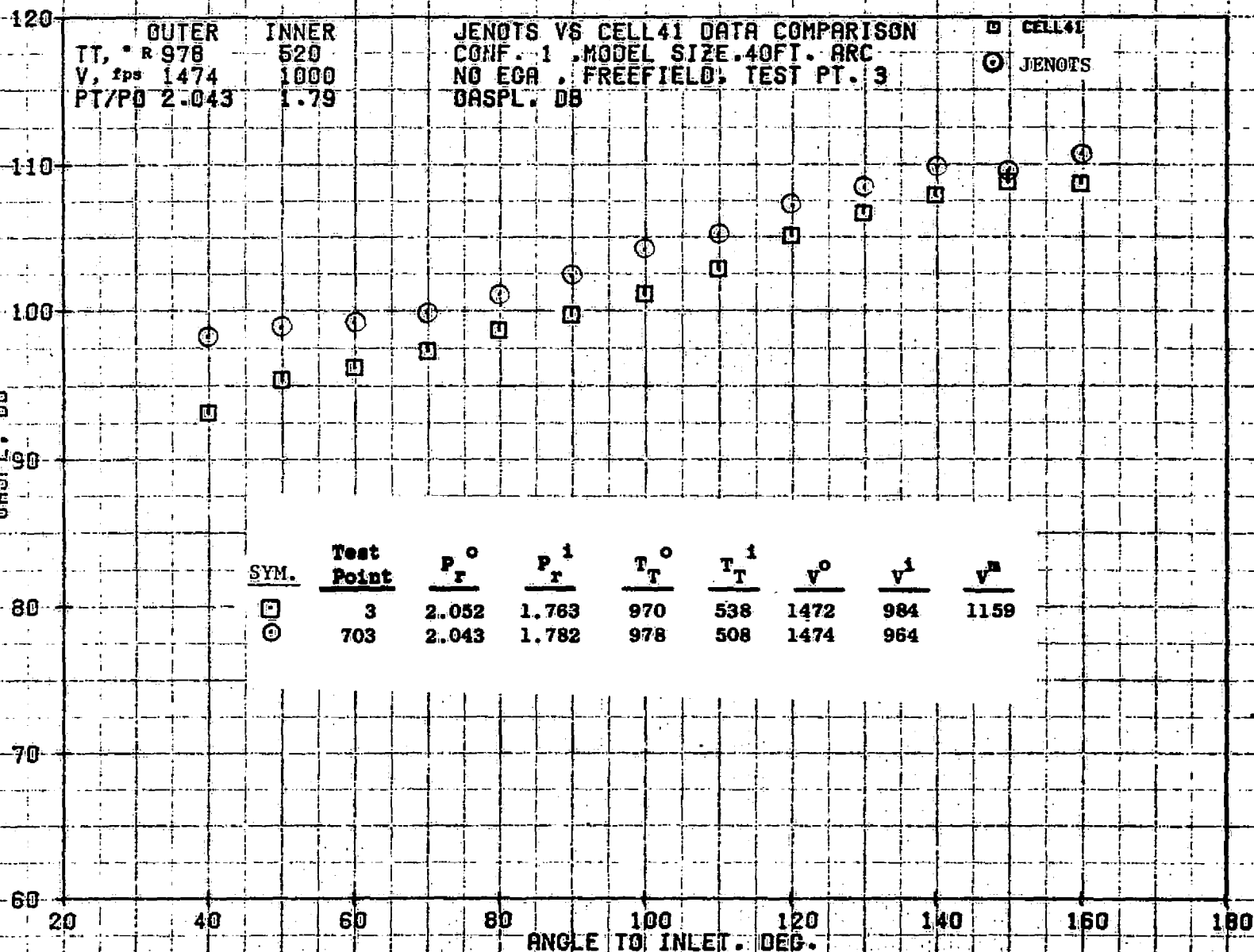
OUTER
TT, ° R 978
V, fps 1474
PT/PO 2.043

INNER
520
1000
1.79

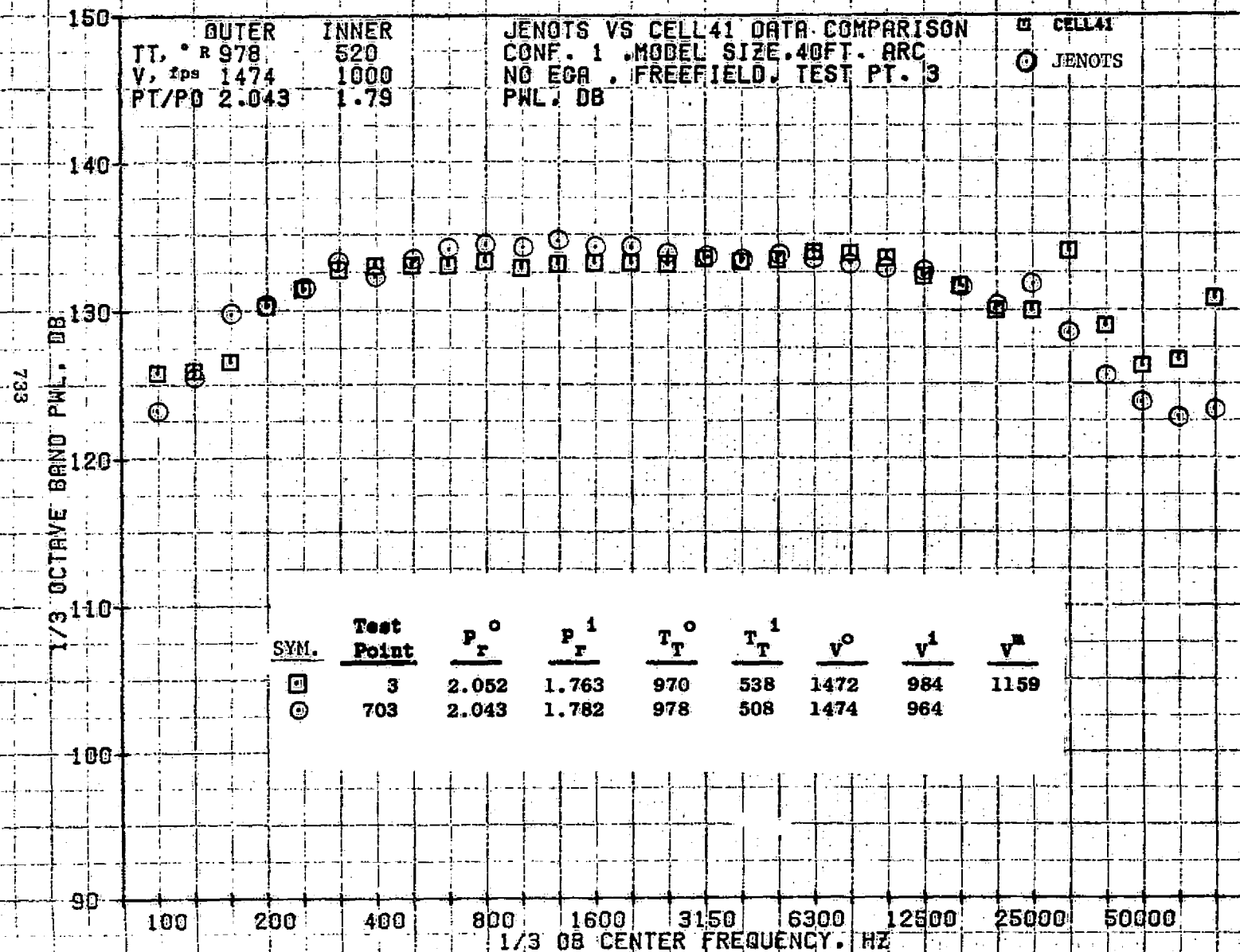
JENOTS VS CELL41 DATA COMPARISON
CONF. 1 MODEL SIZE.40FT. ARC
NO EGA. FREEFIELD; TEST PT. 3
OASPL. DB

□ CELL41
○ JENOTS

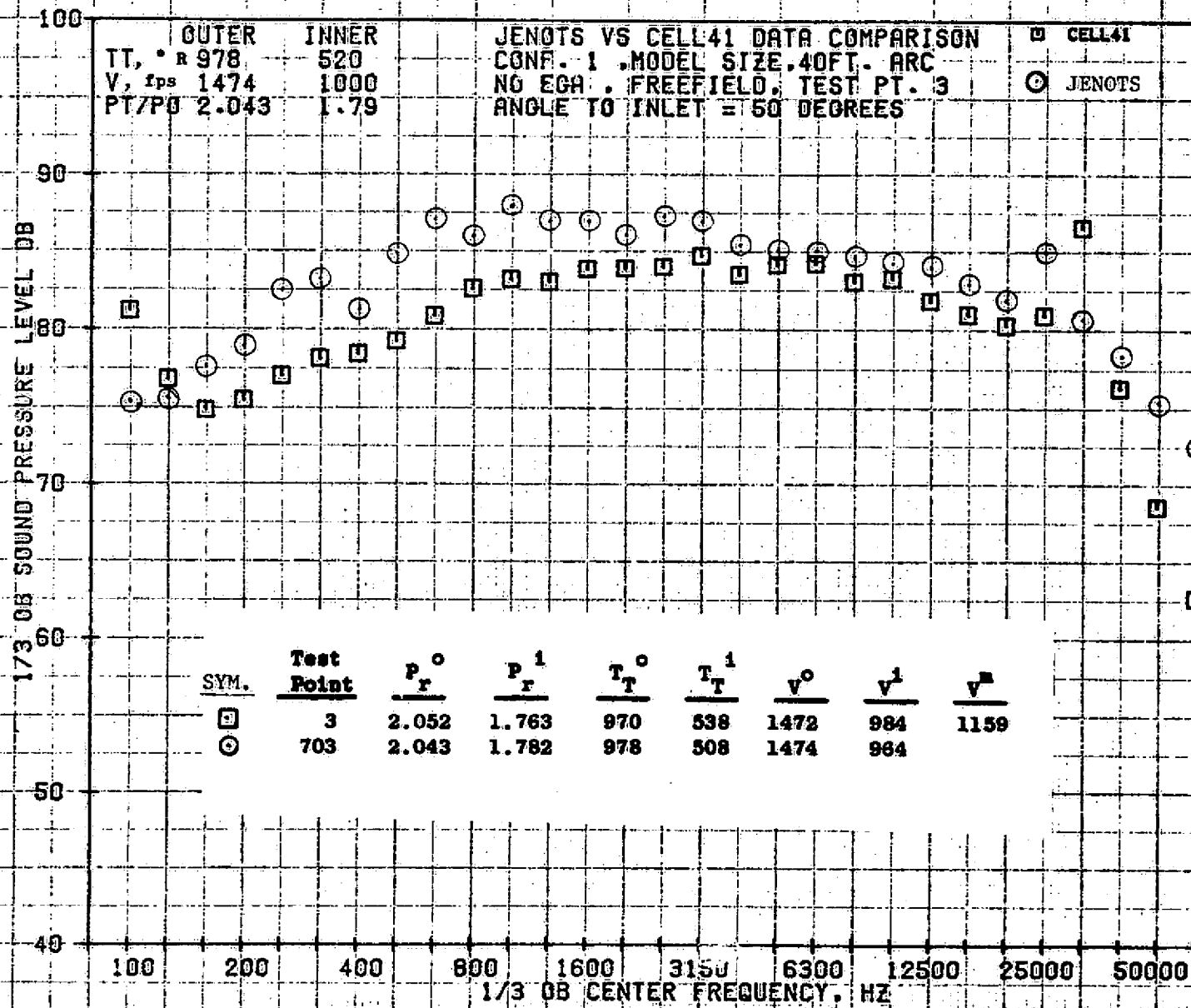
OASPL. DB
732

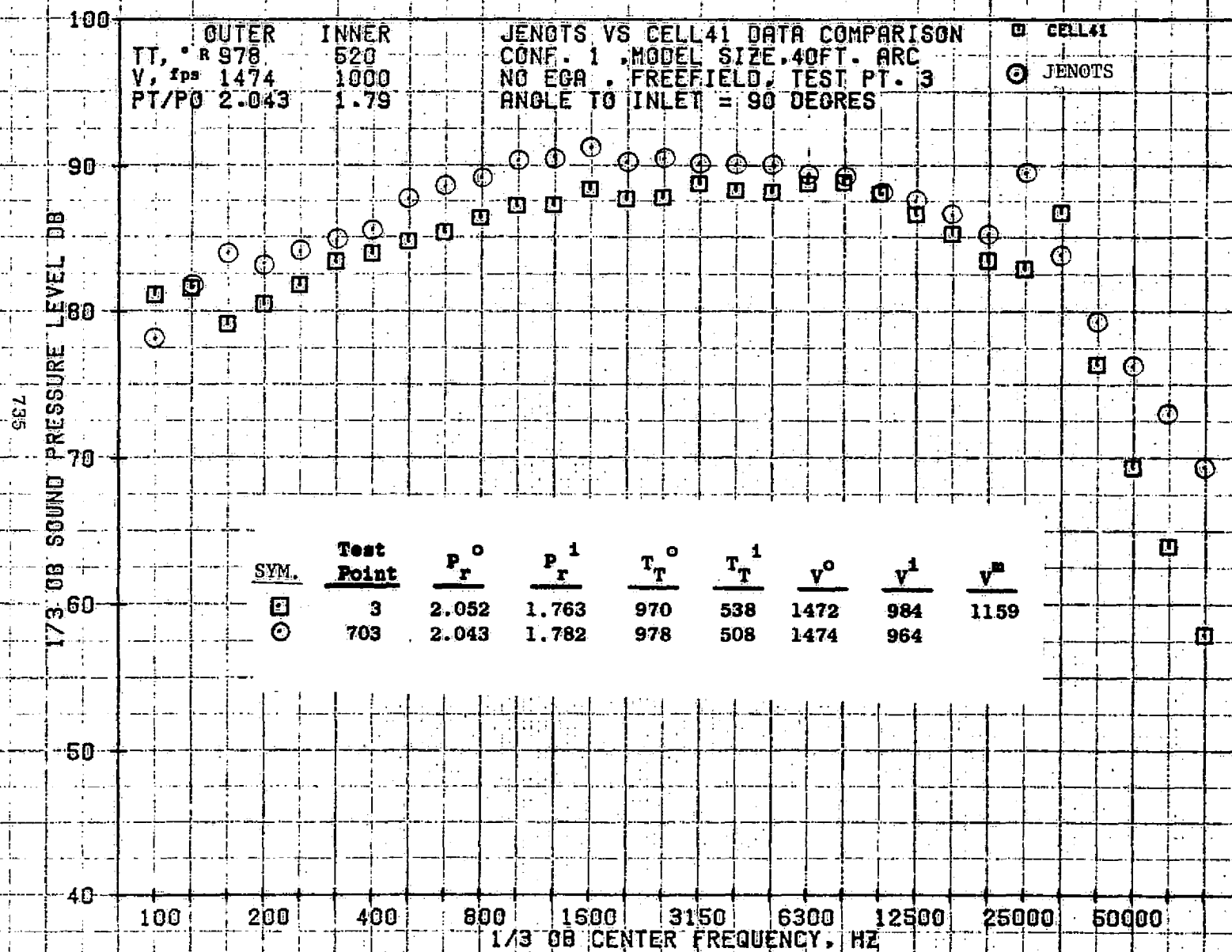


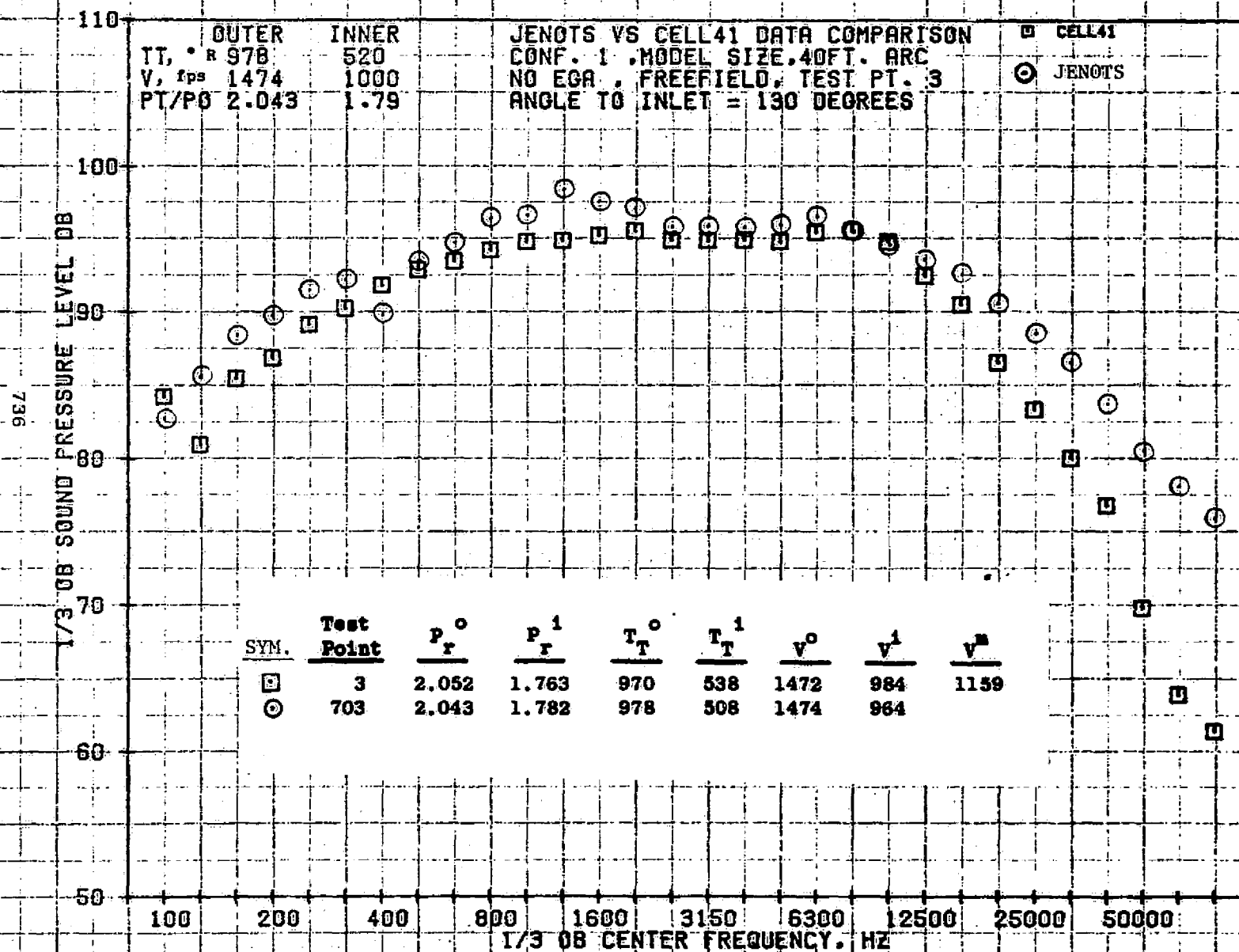
SYM.	Test Point	P_r^o	P_r^i	T_T^o	T_T^i	V^o	V^i	V^m
□	3	2.052	1.763	970	538	1472	984	1159
○	703	2.043	1.782	978	508	1474	964	

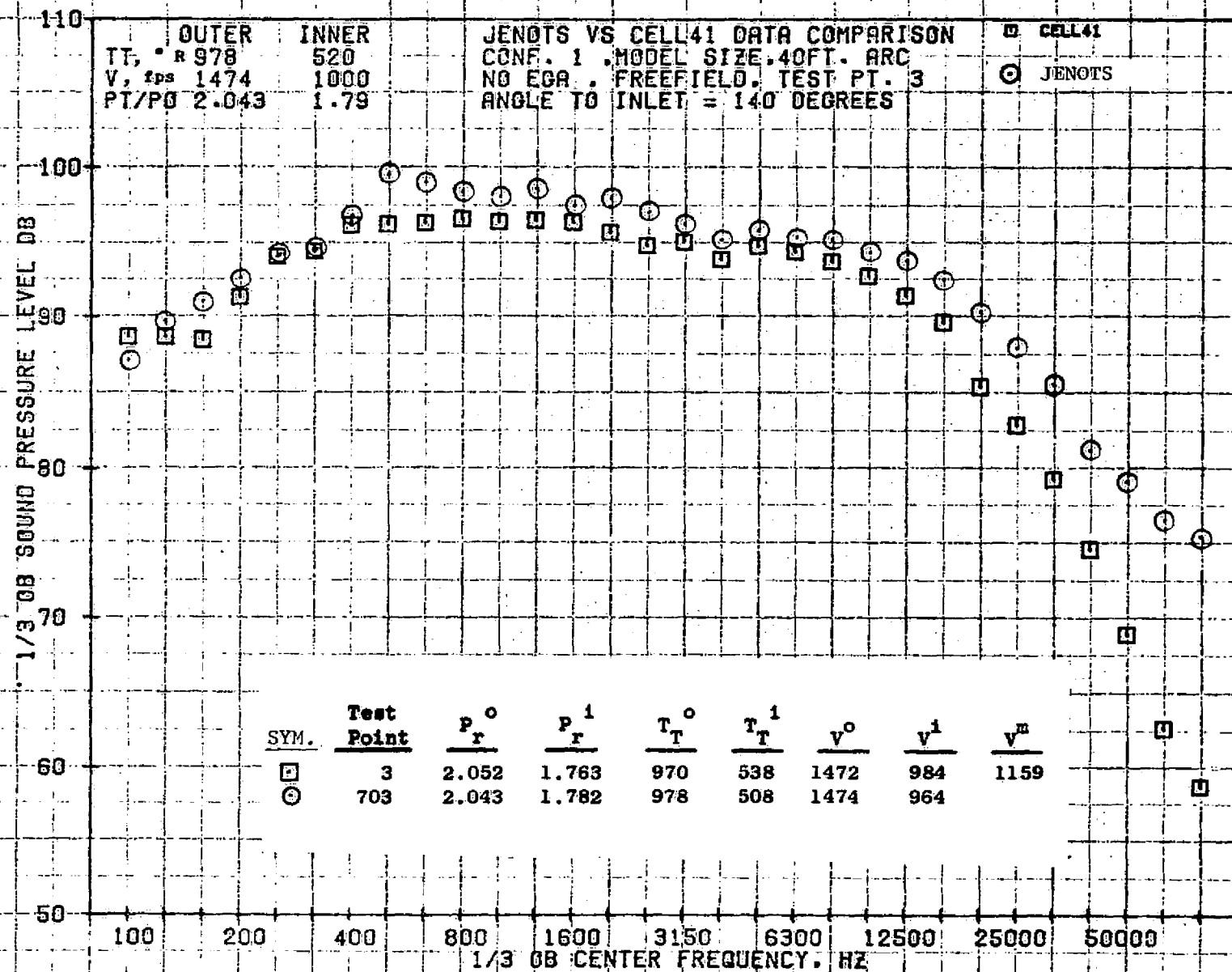


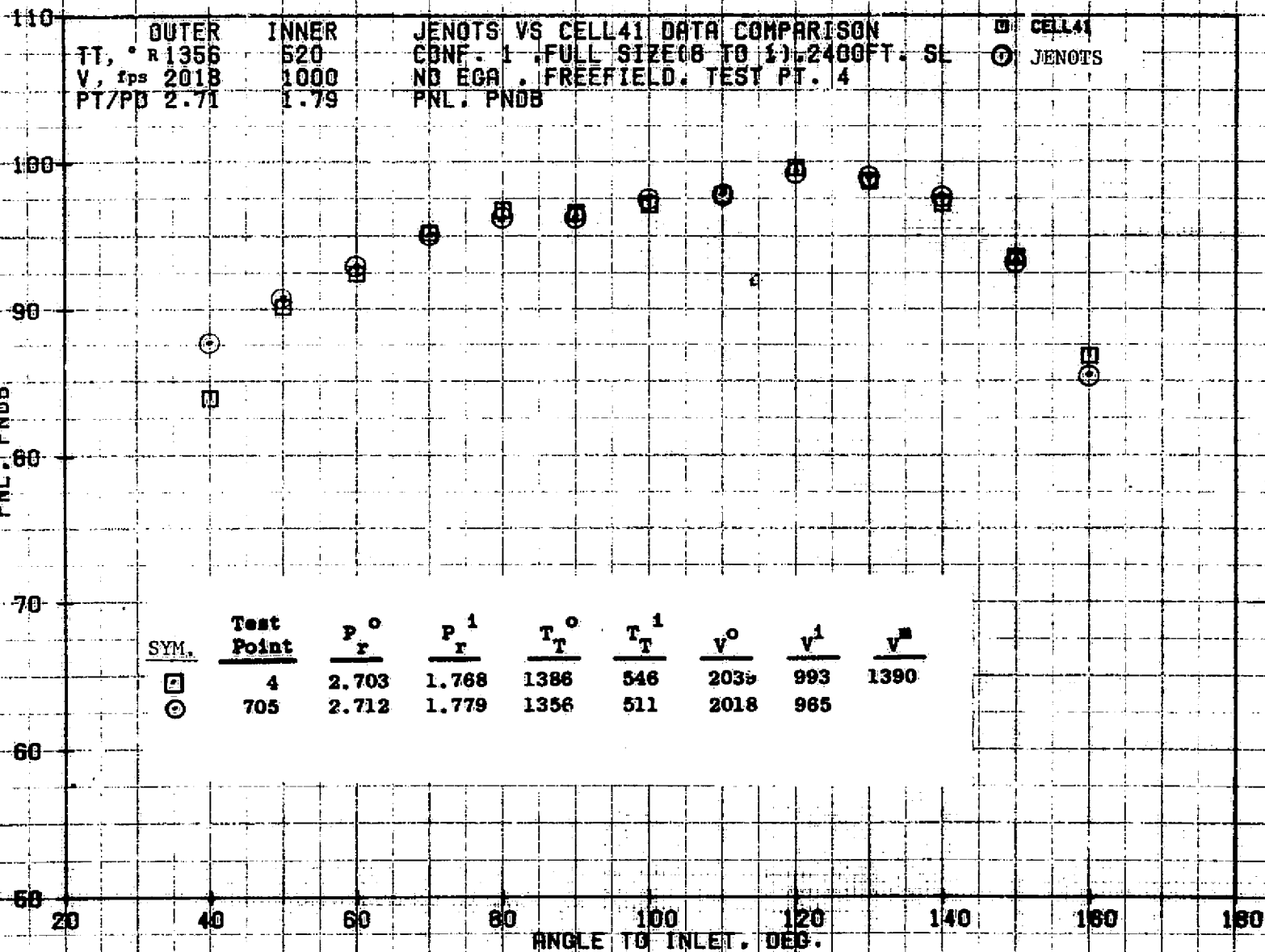
734





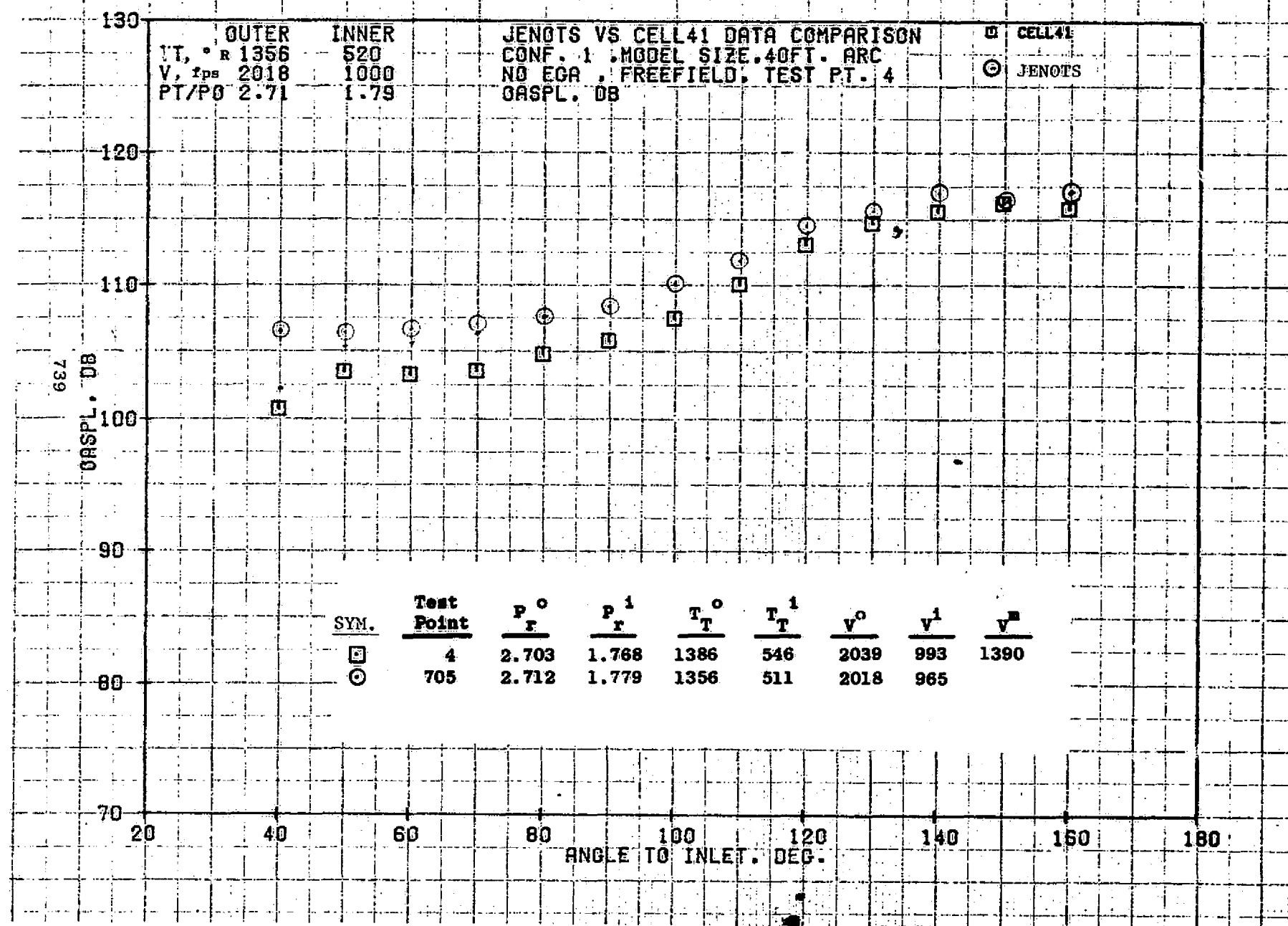


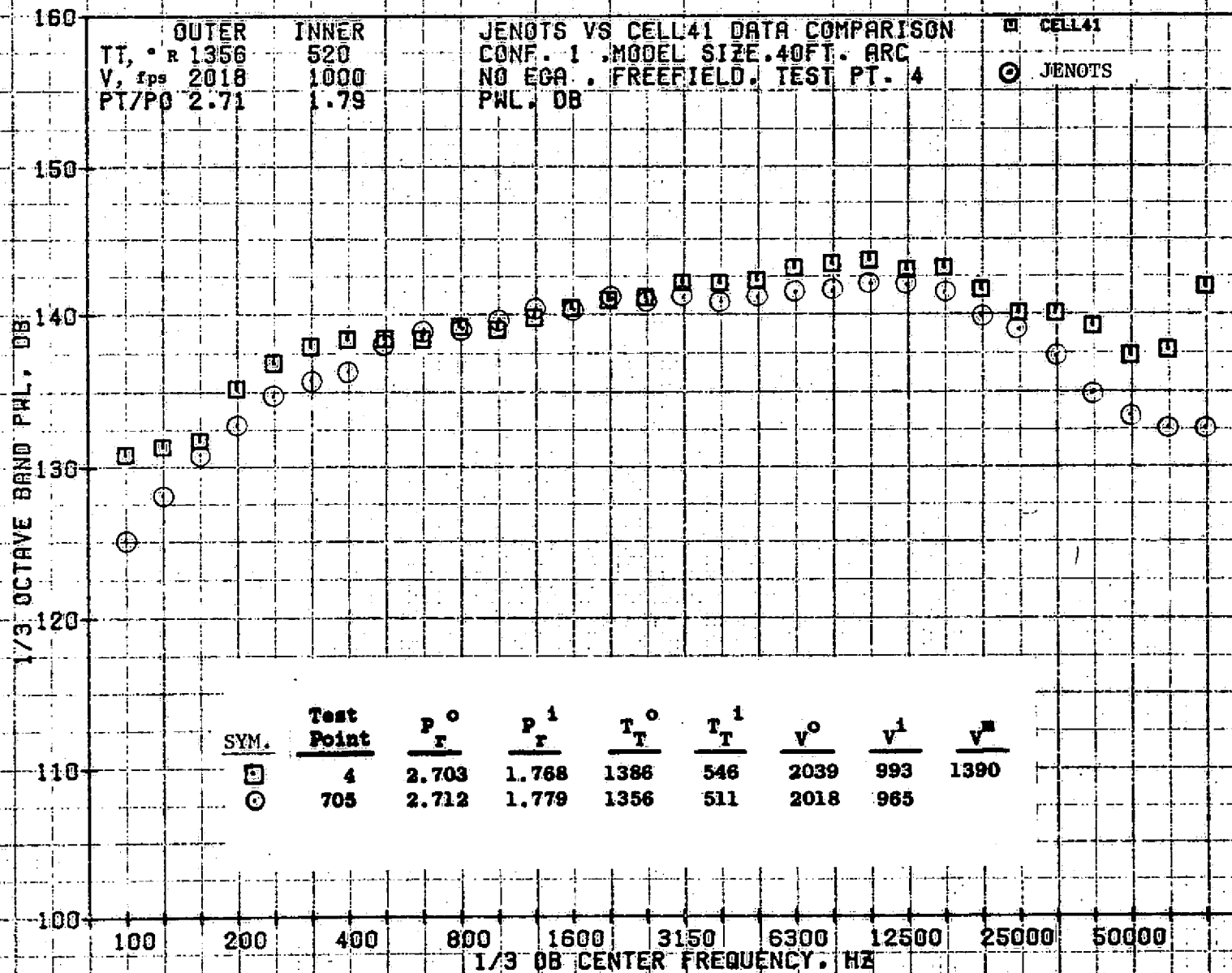


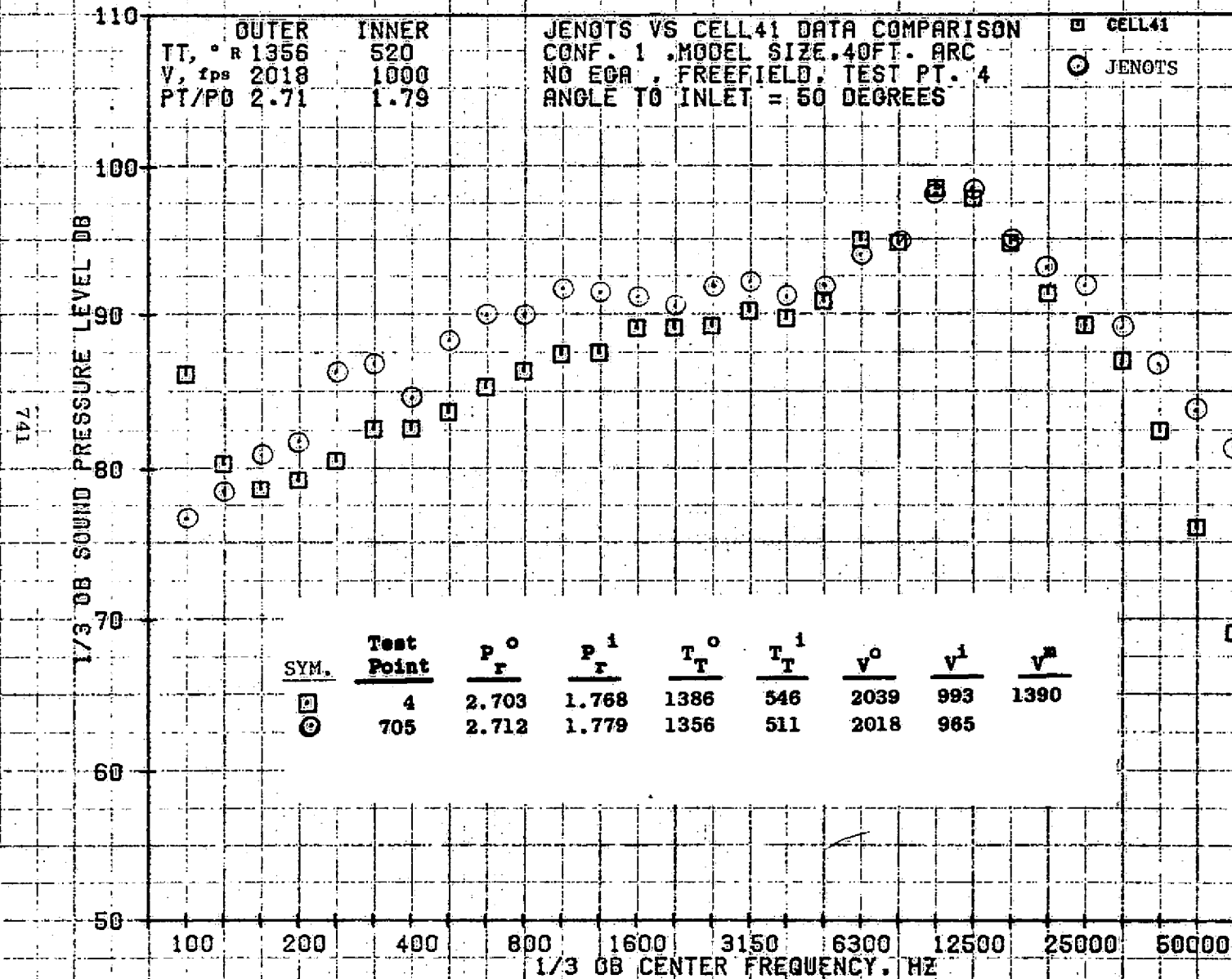


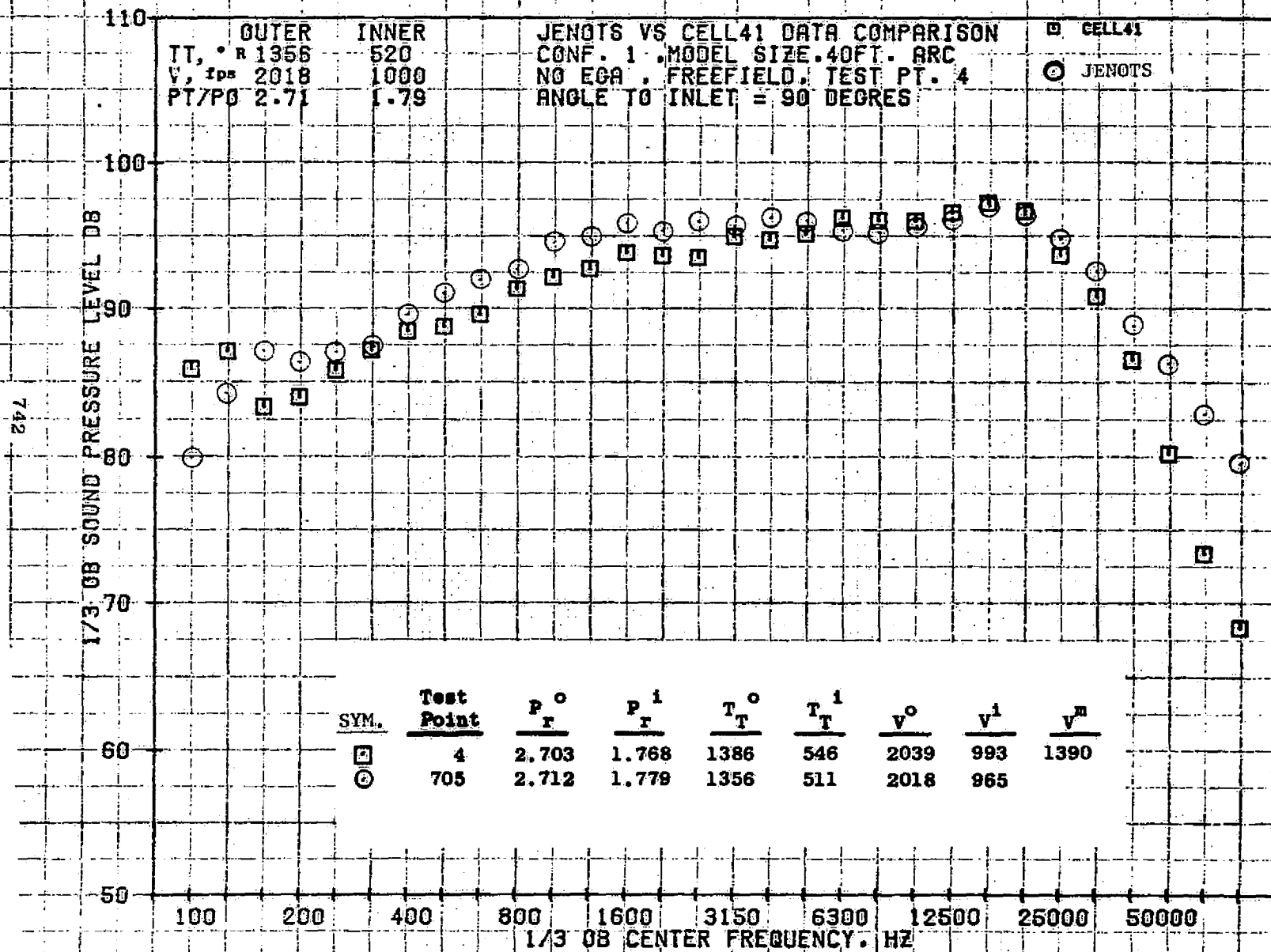
09/28/76
 LX583-001

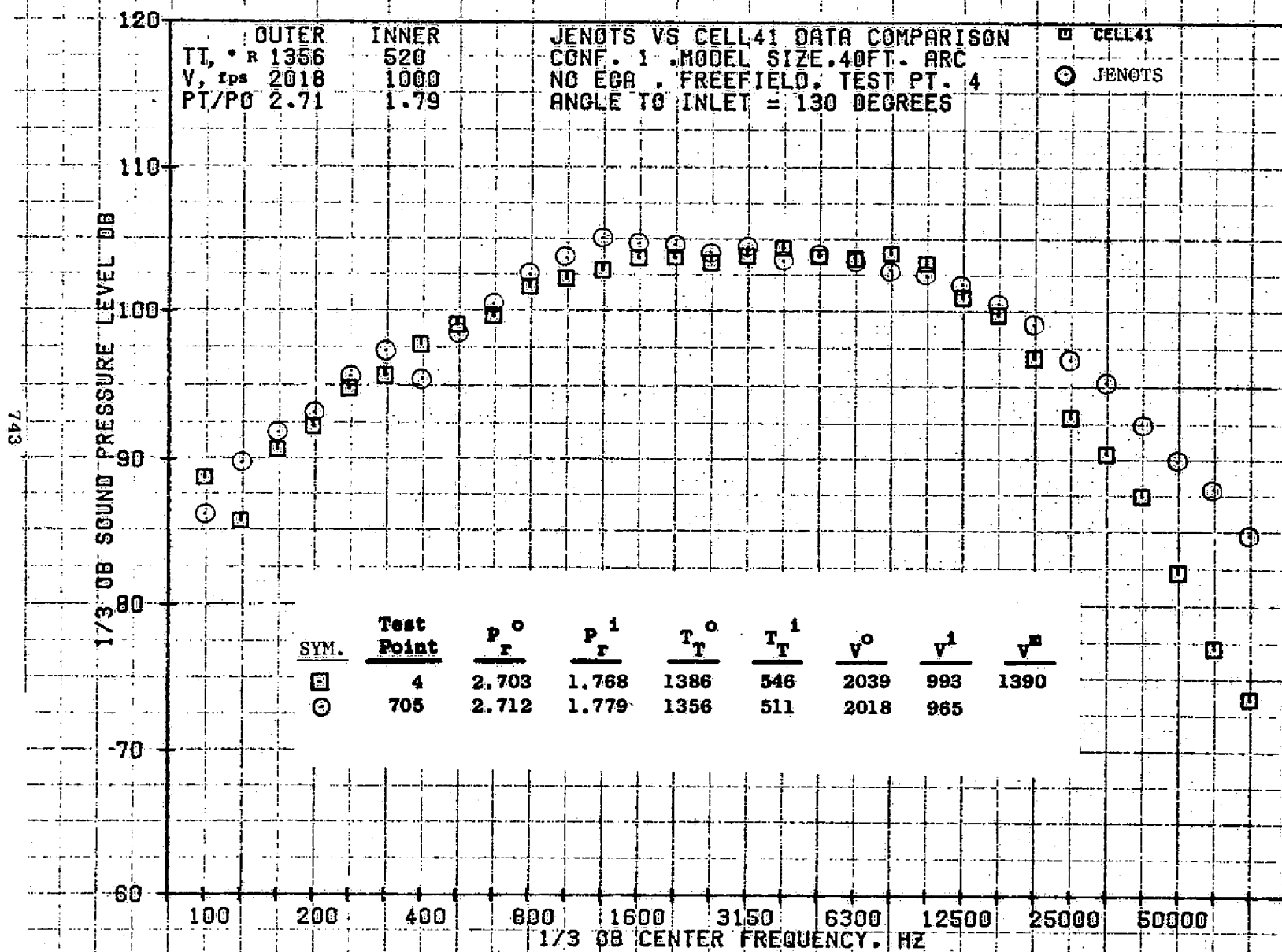
73KOLLSTEDT

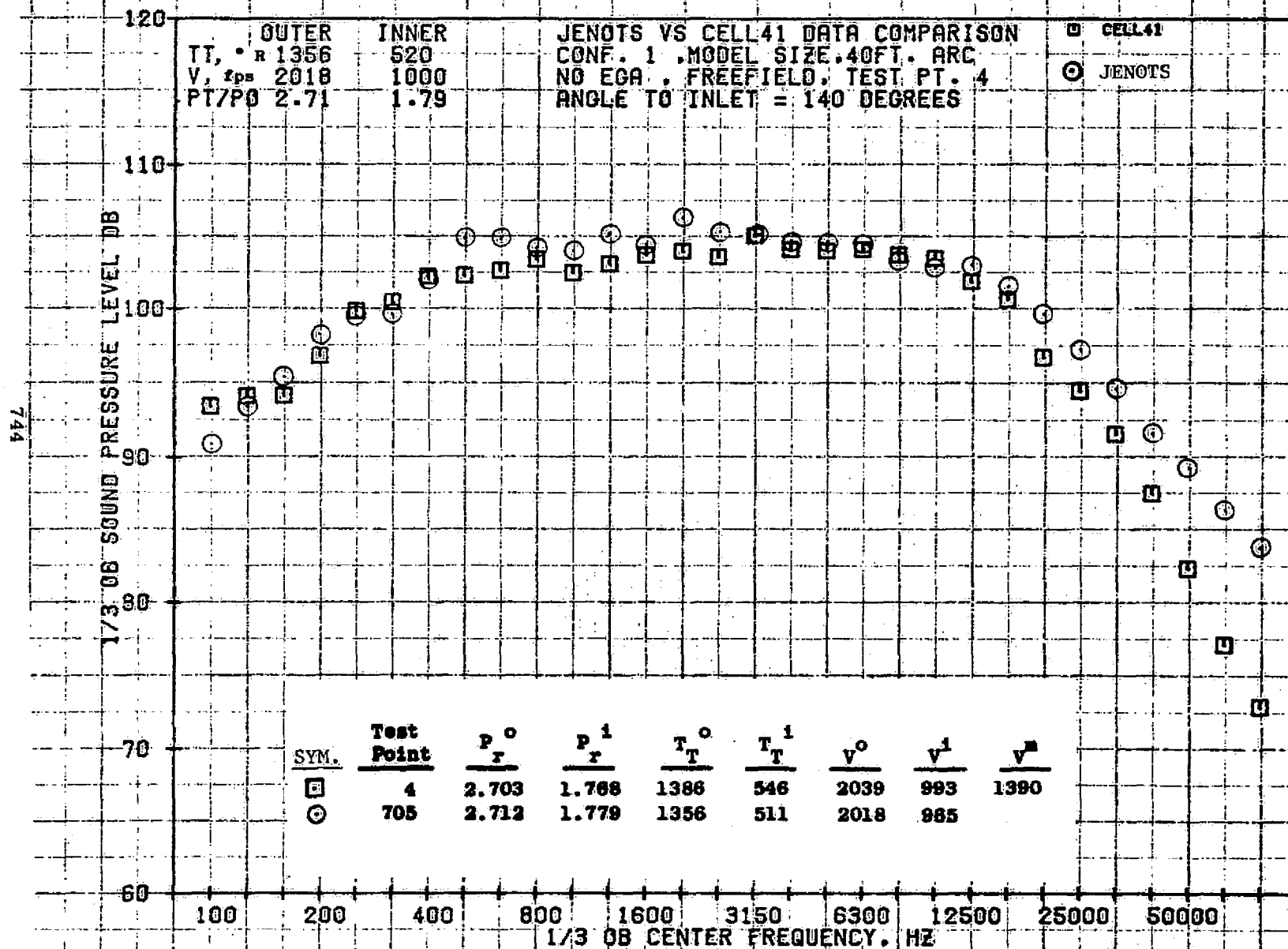


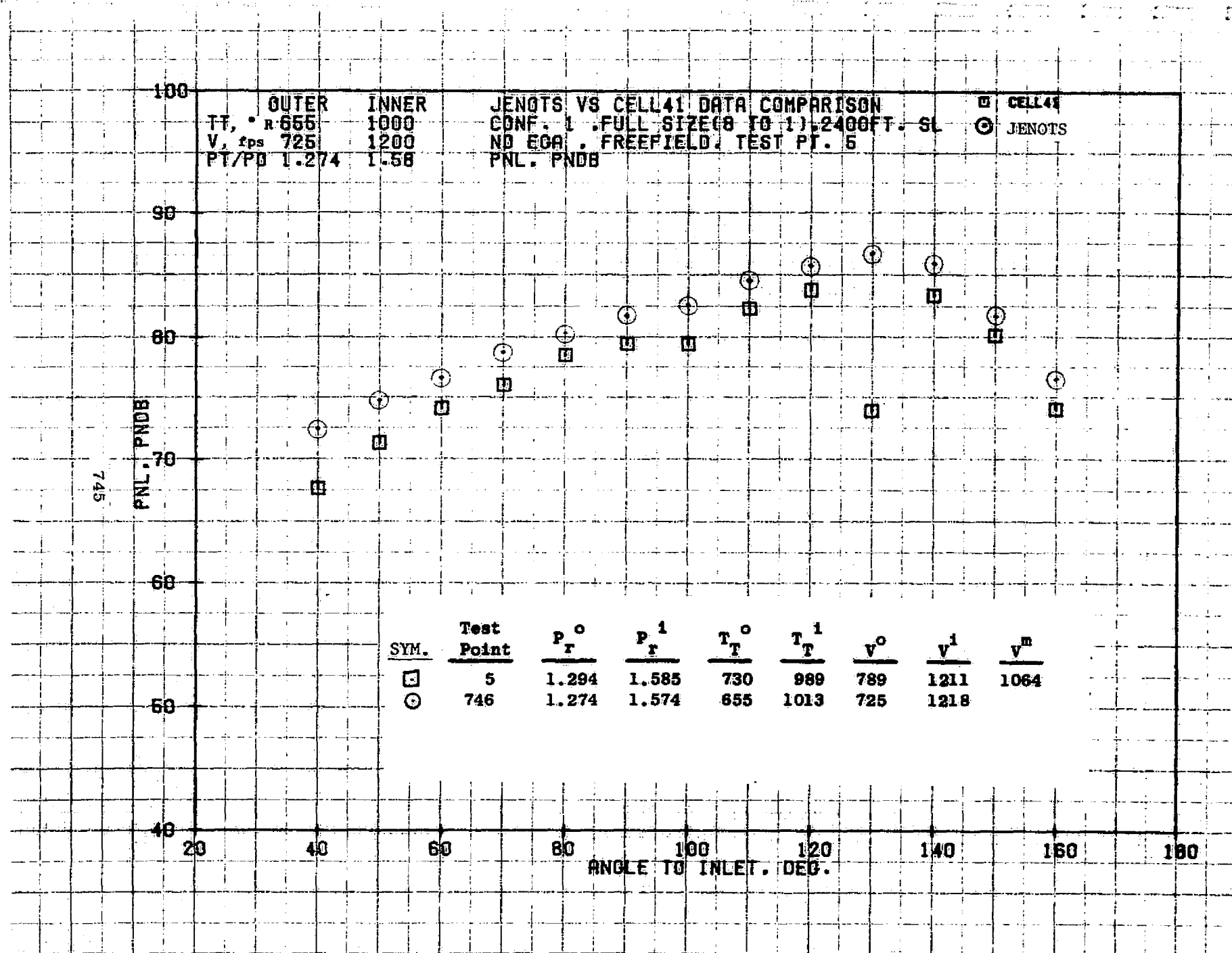








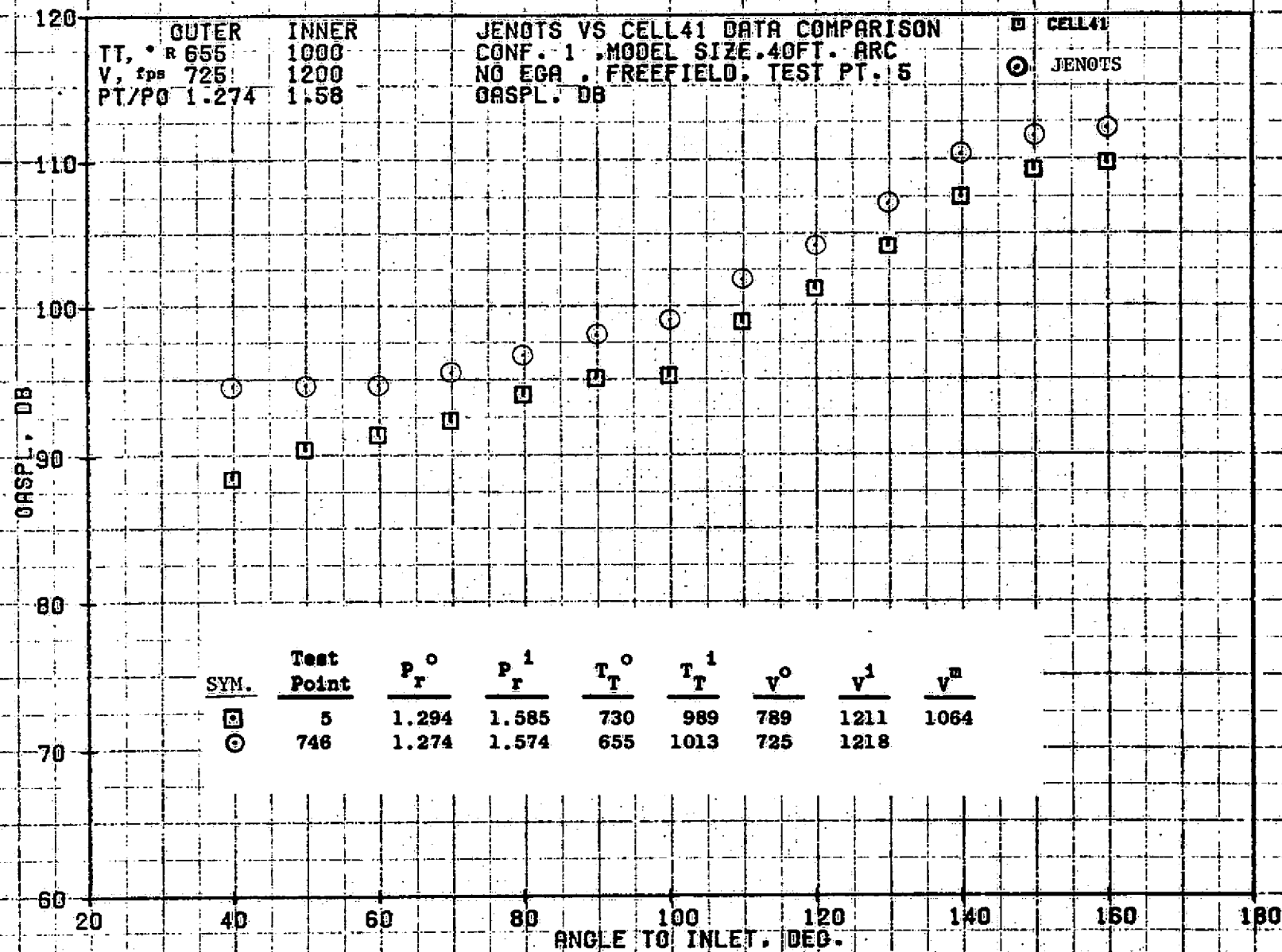




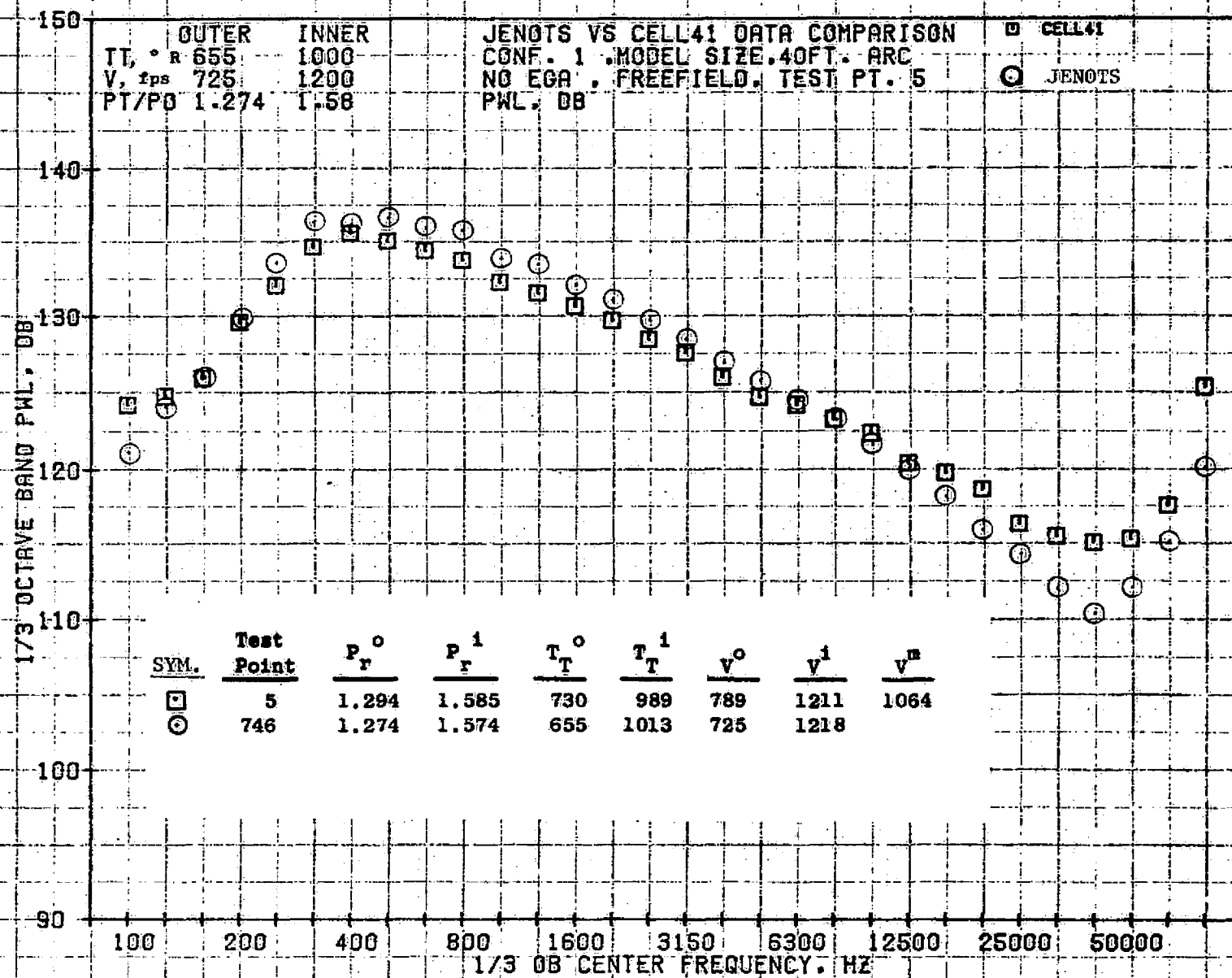
09/28/76
 1X583-001

73KOLLSTEDT

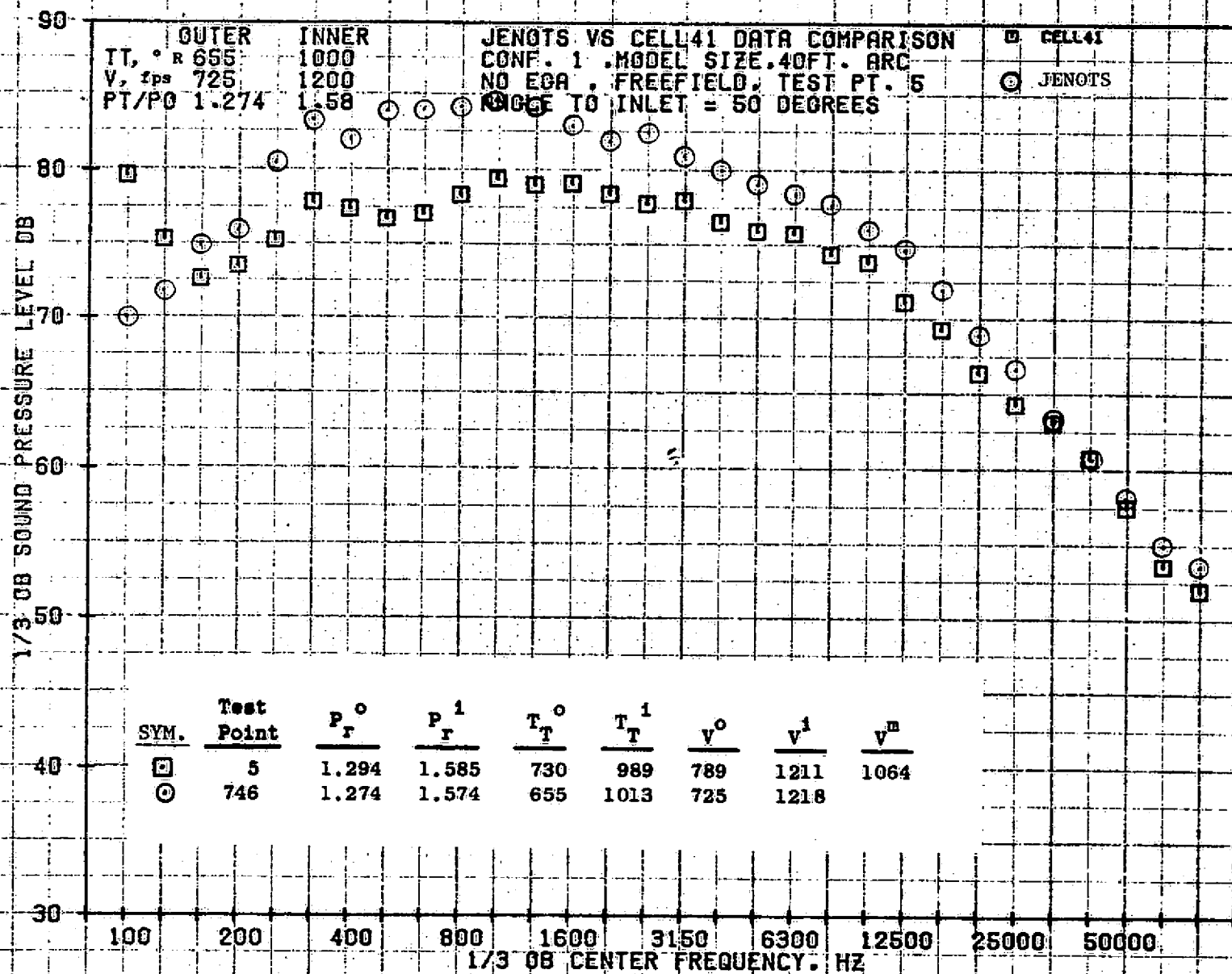
746



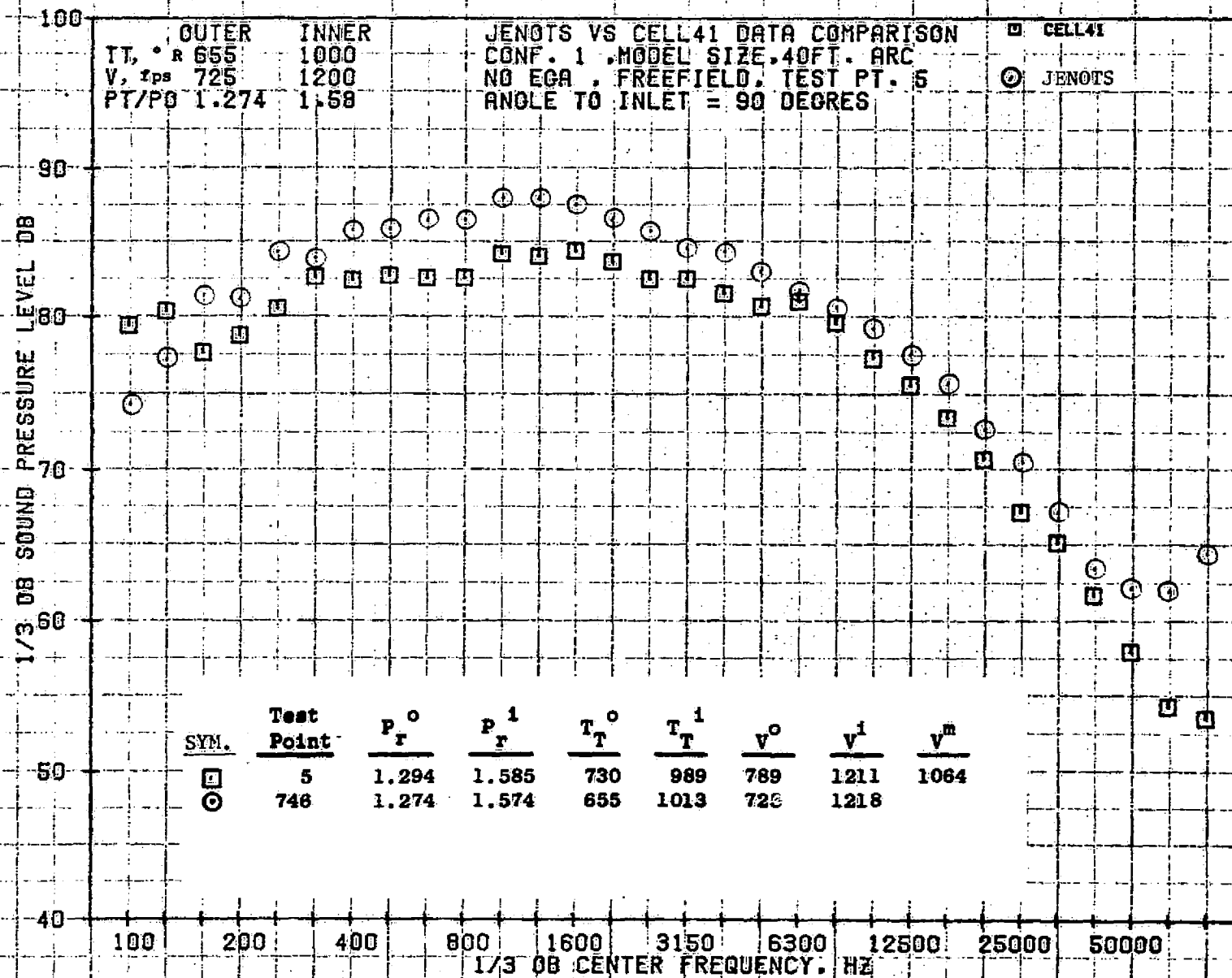
747

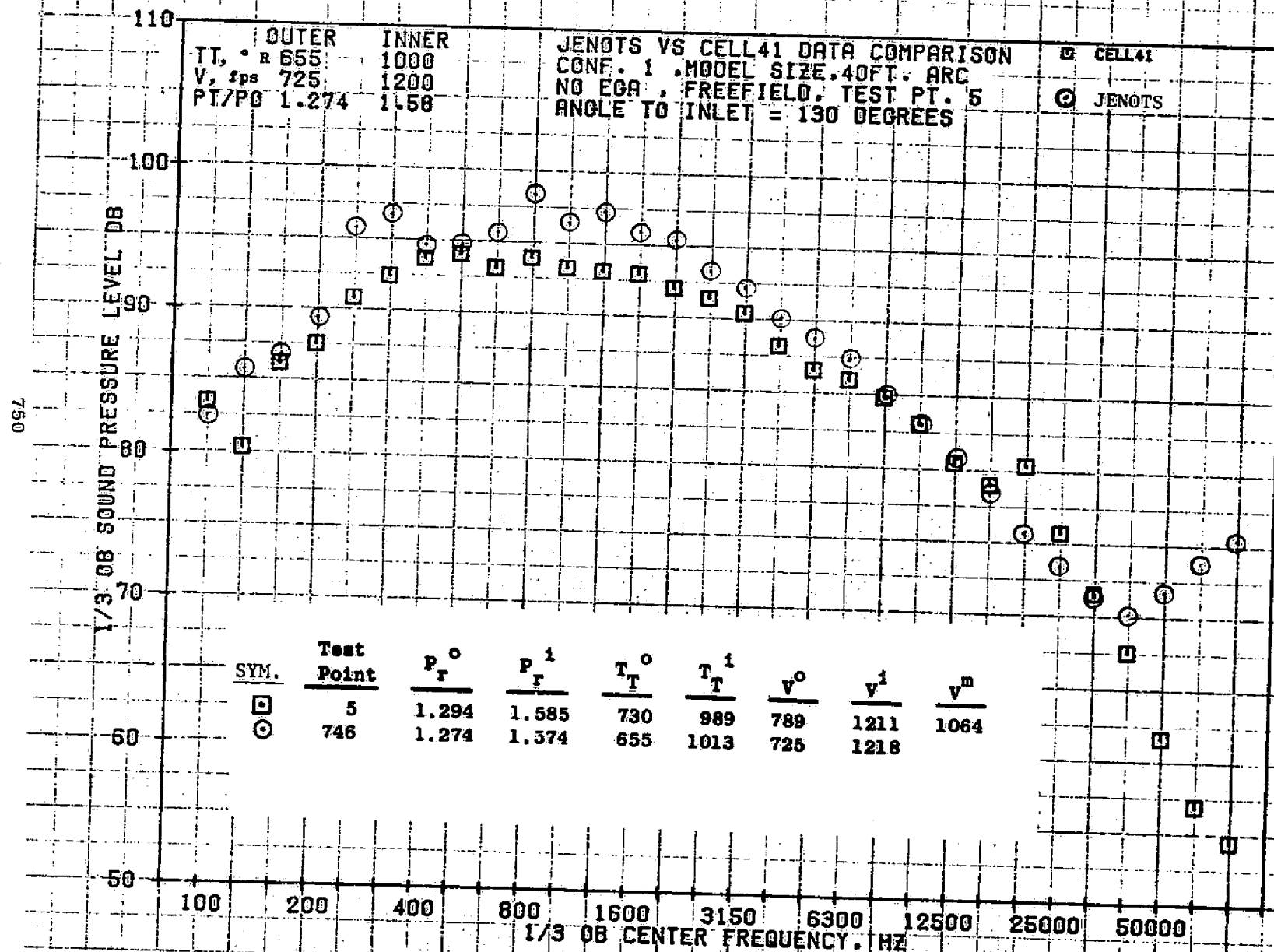


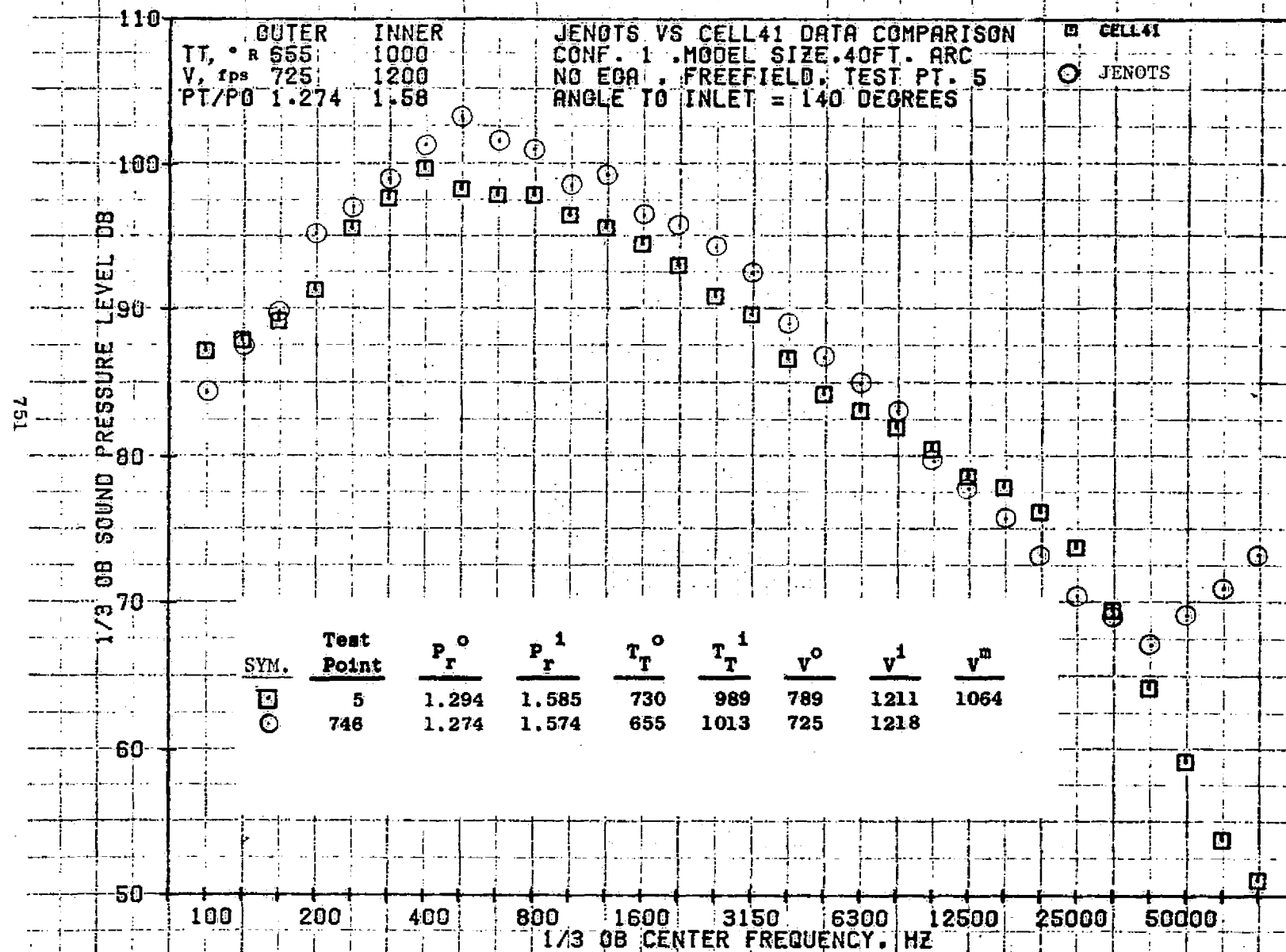
748

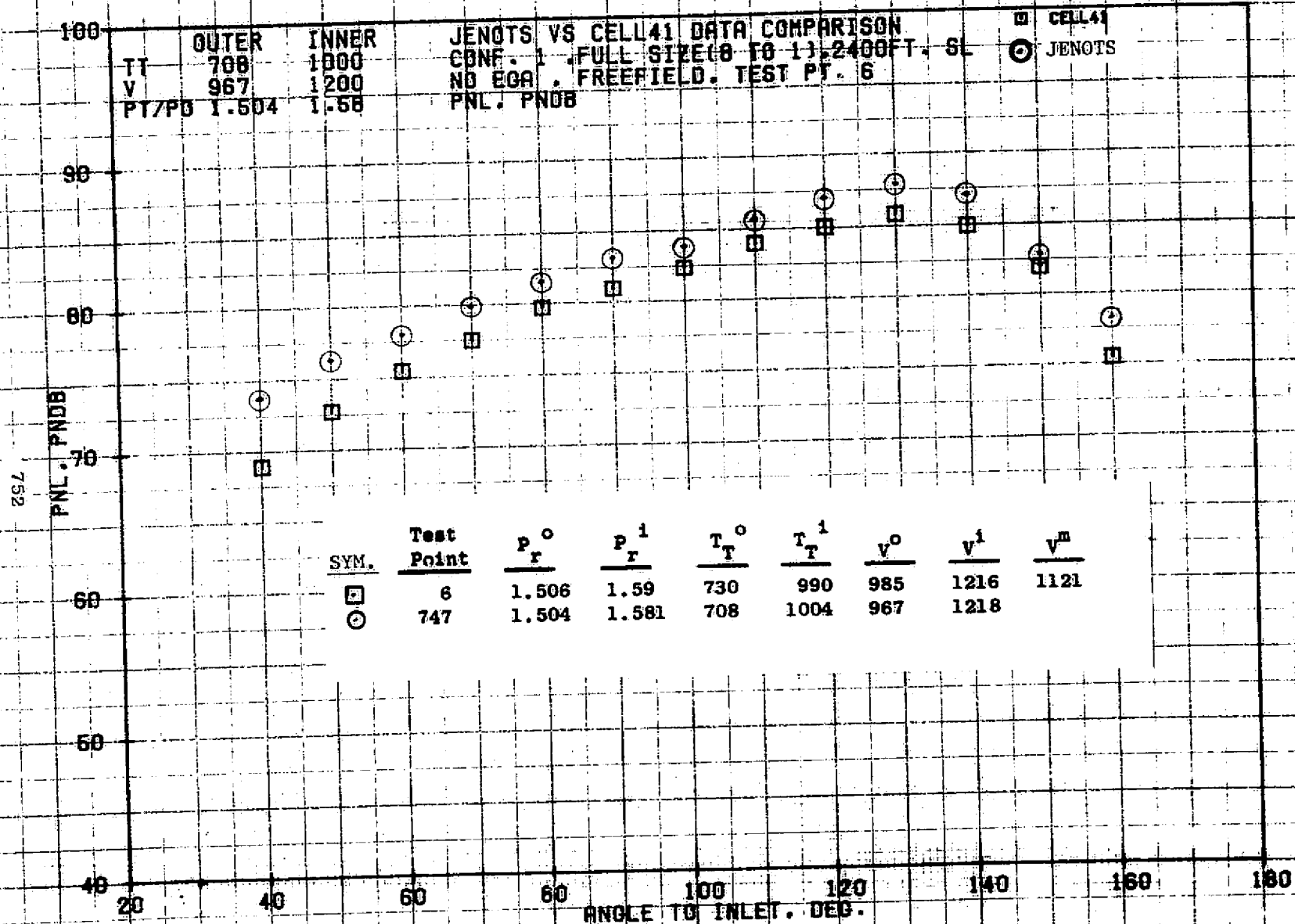


749



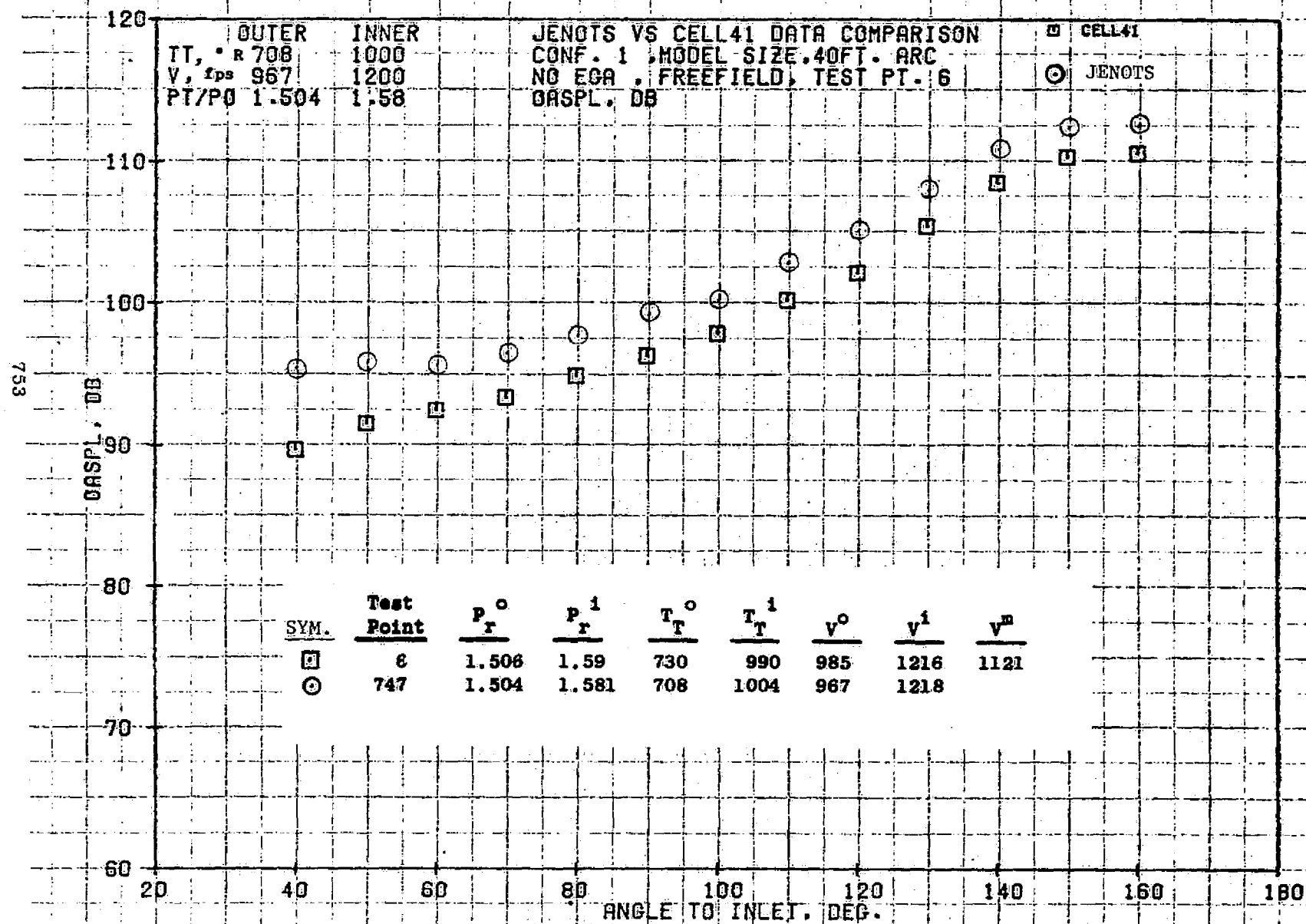


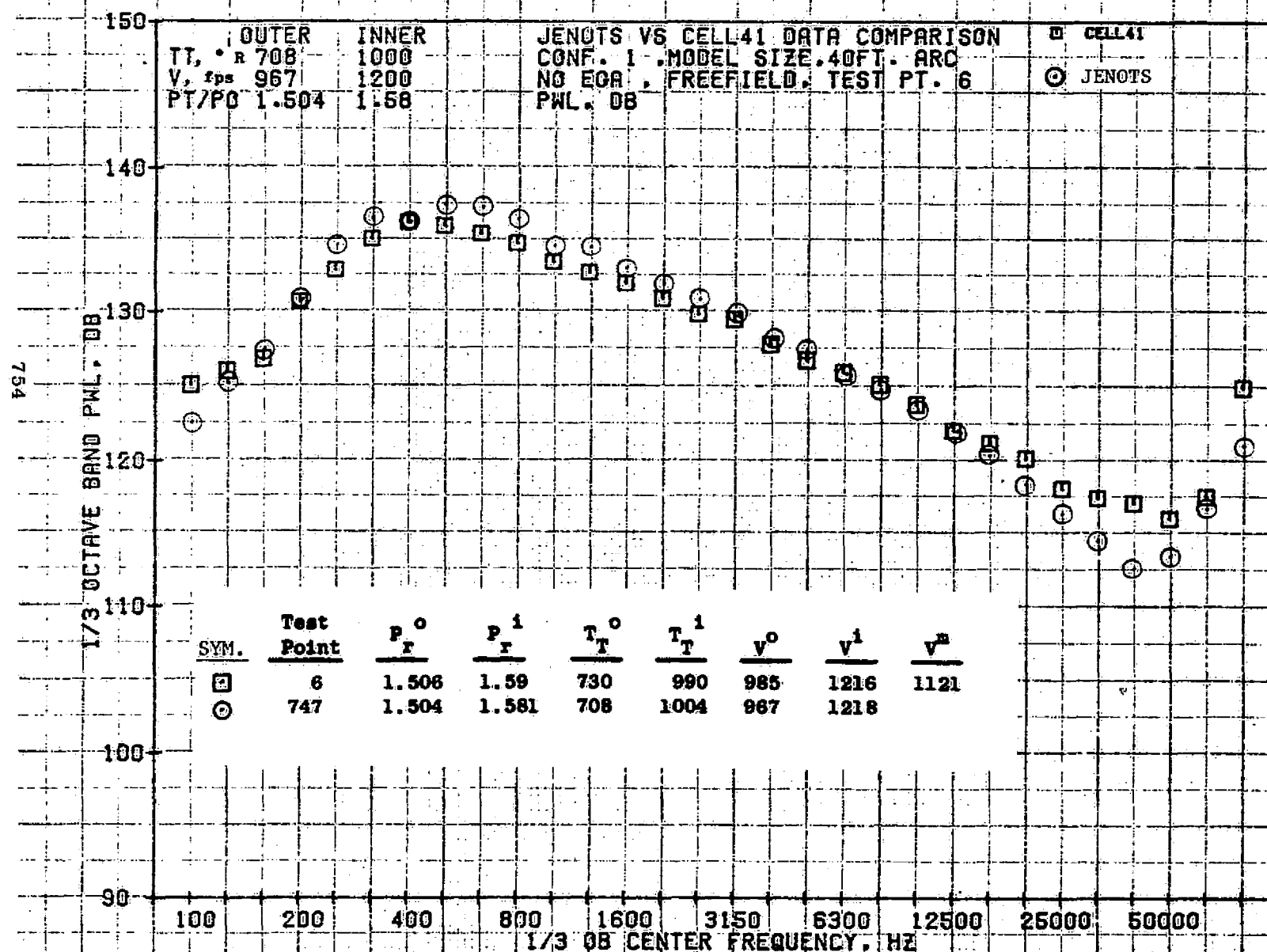


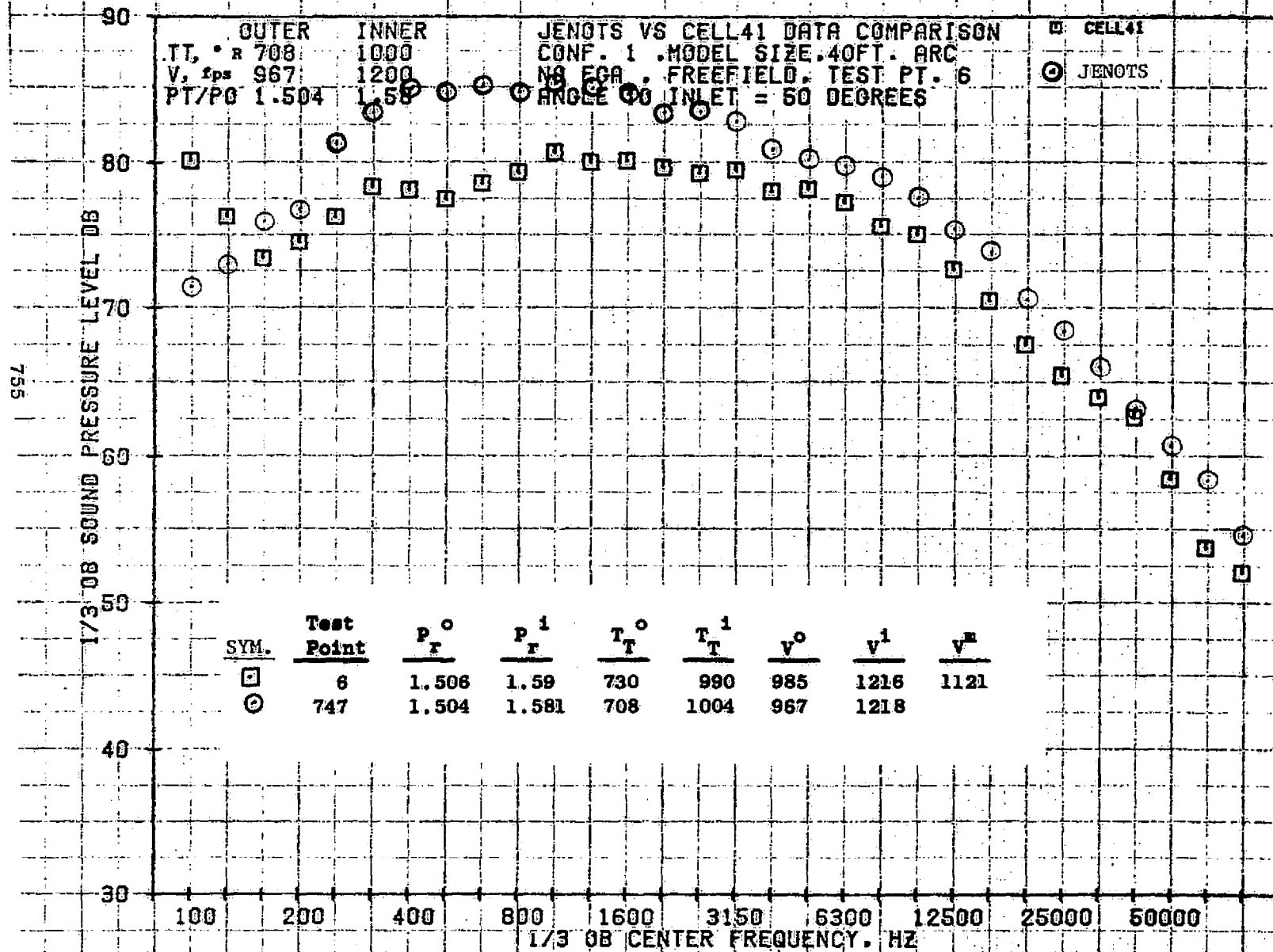


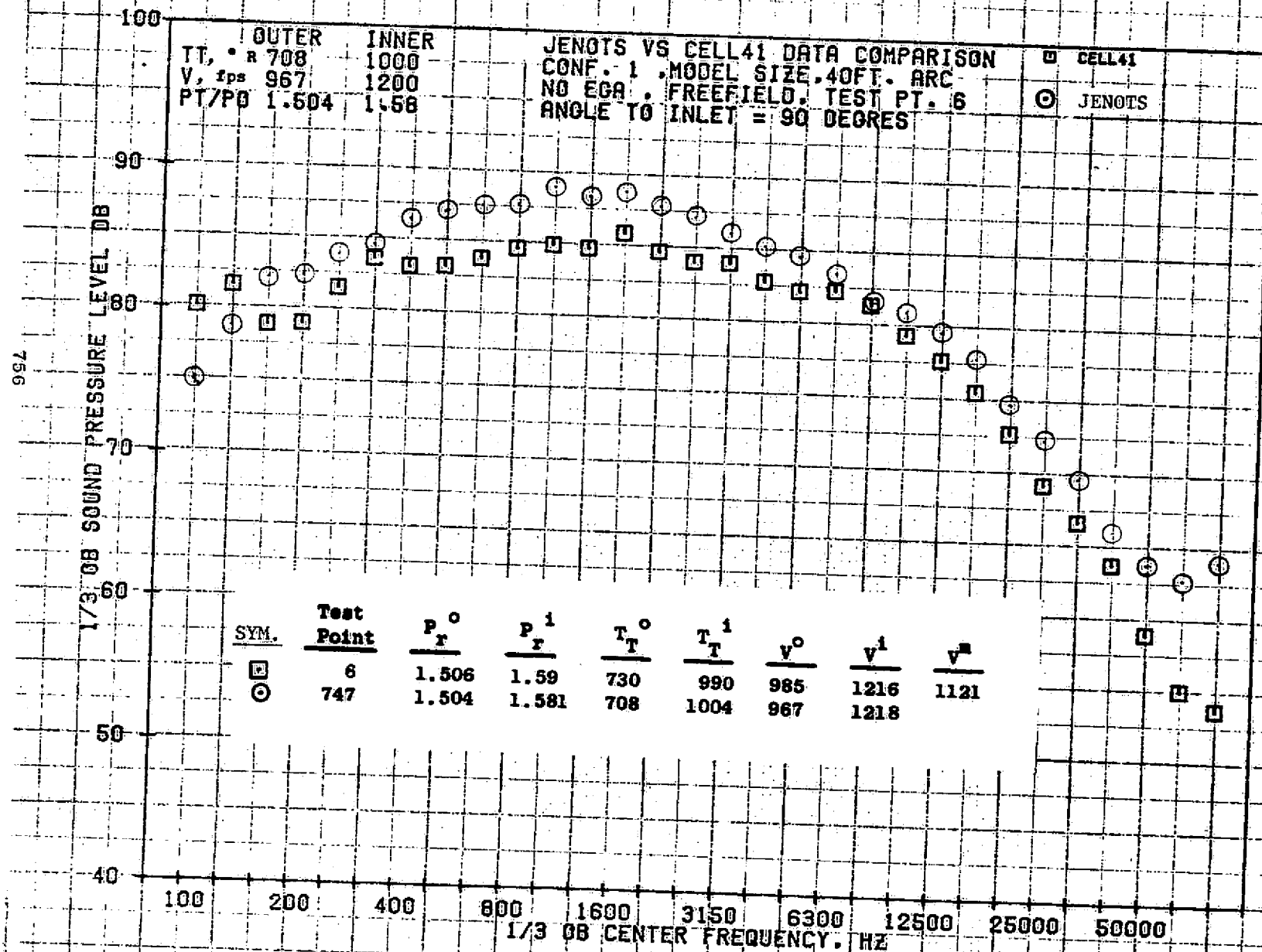
09/28/76
1X583-001

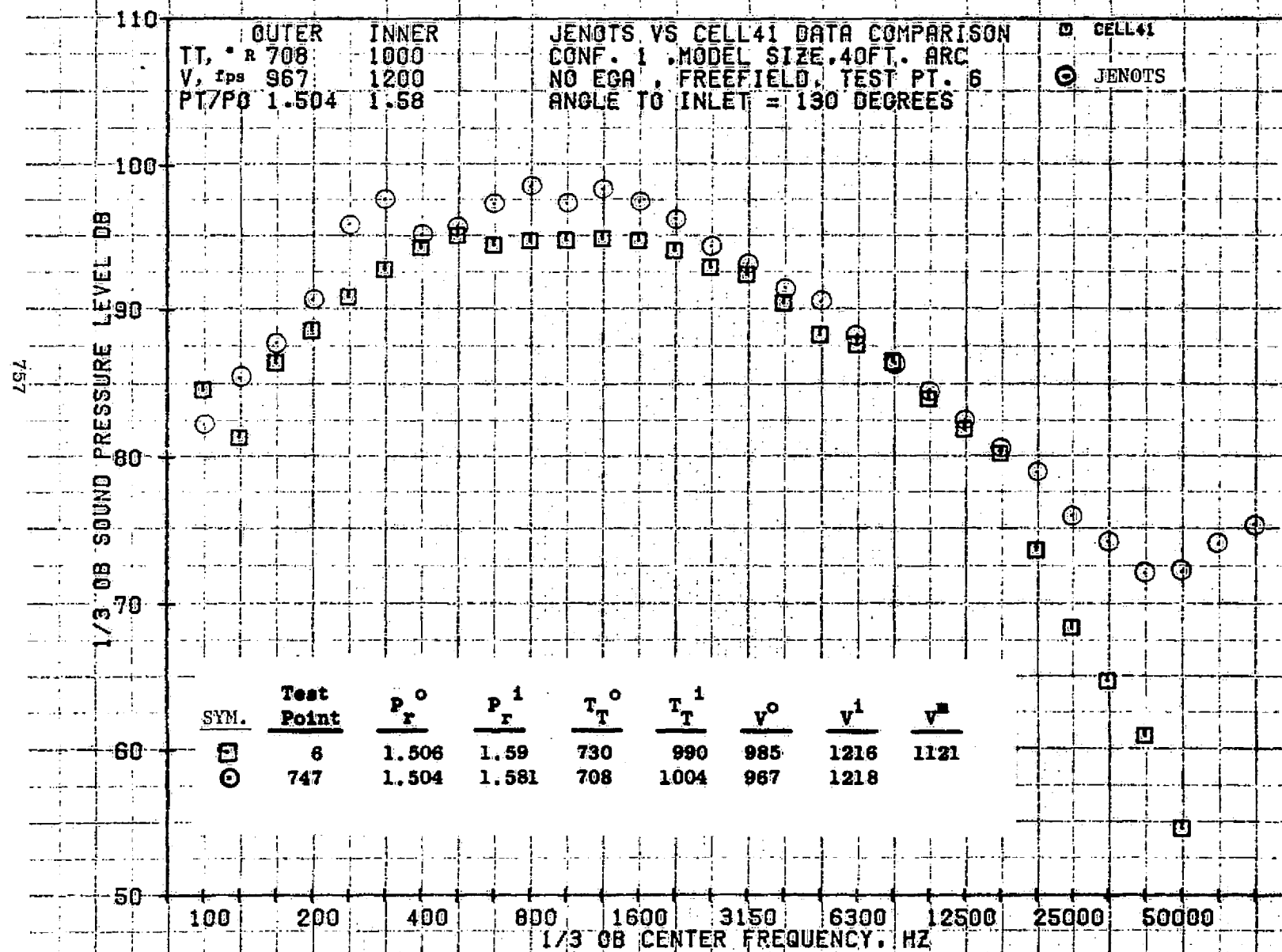
73KOLLSTEDT

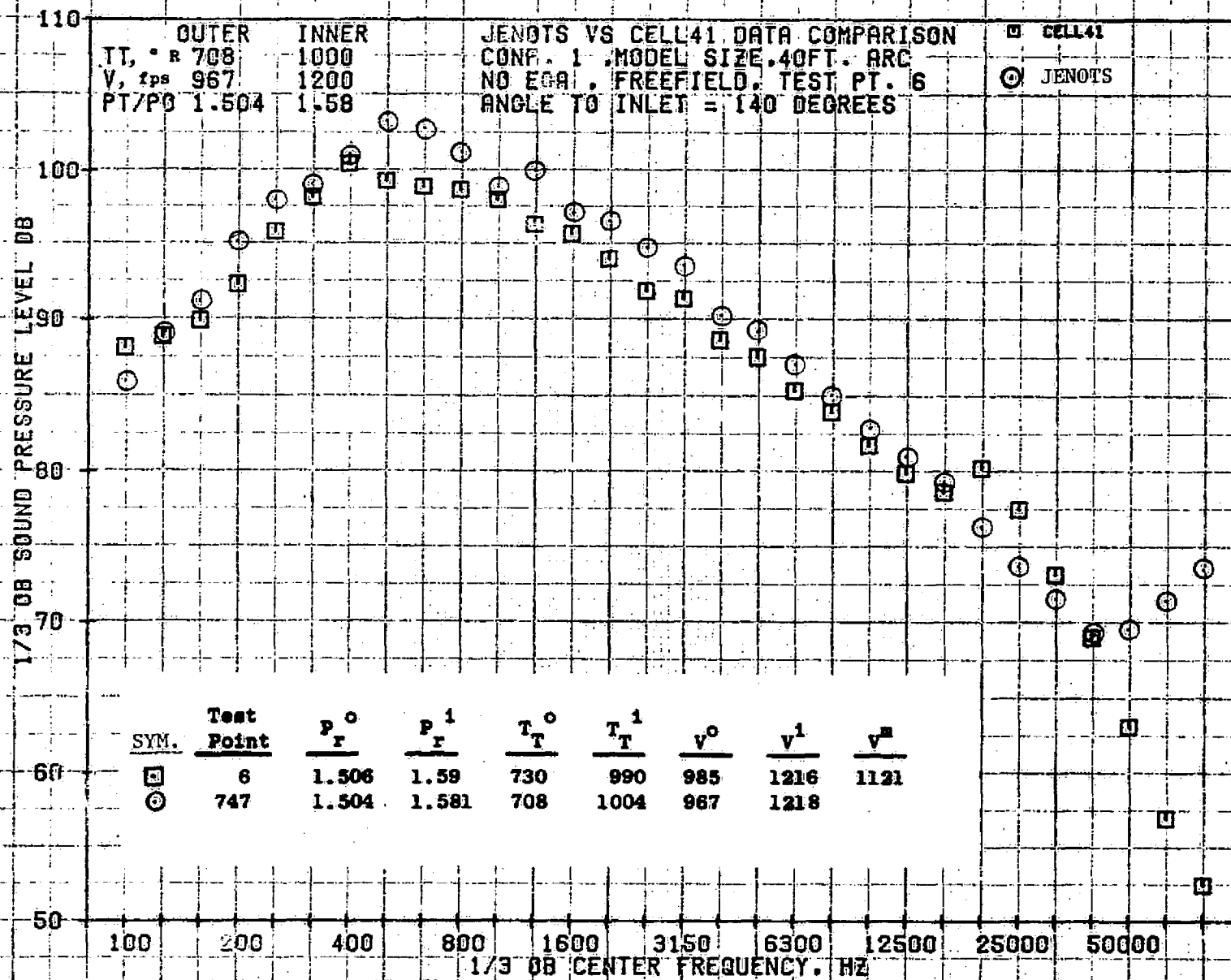


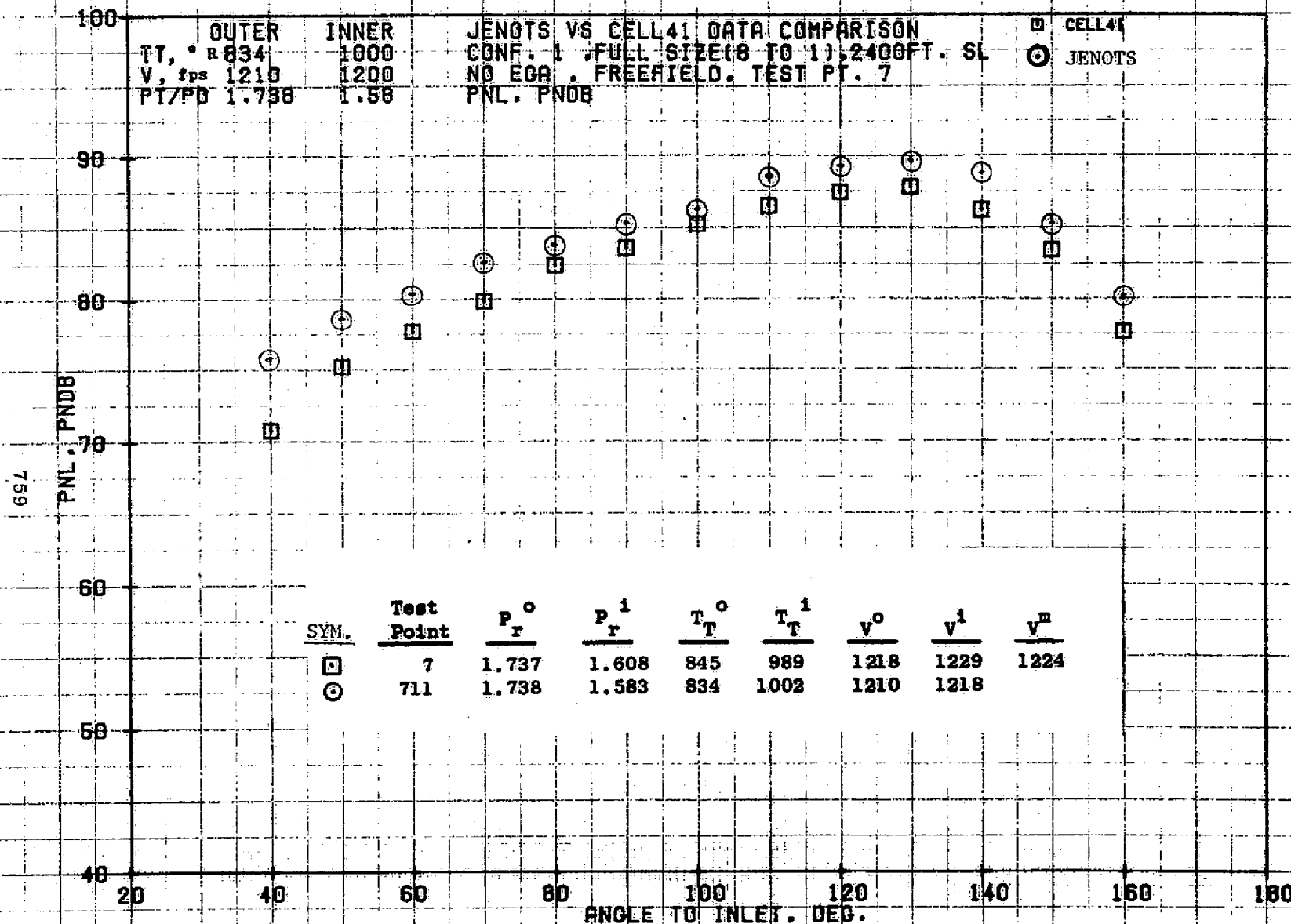






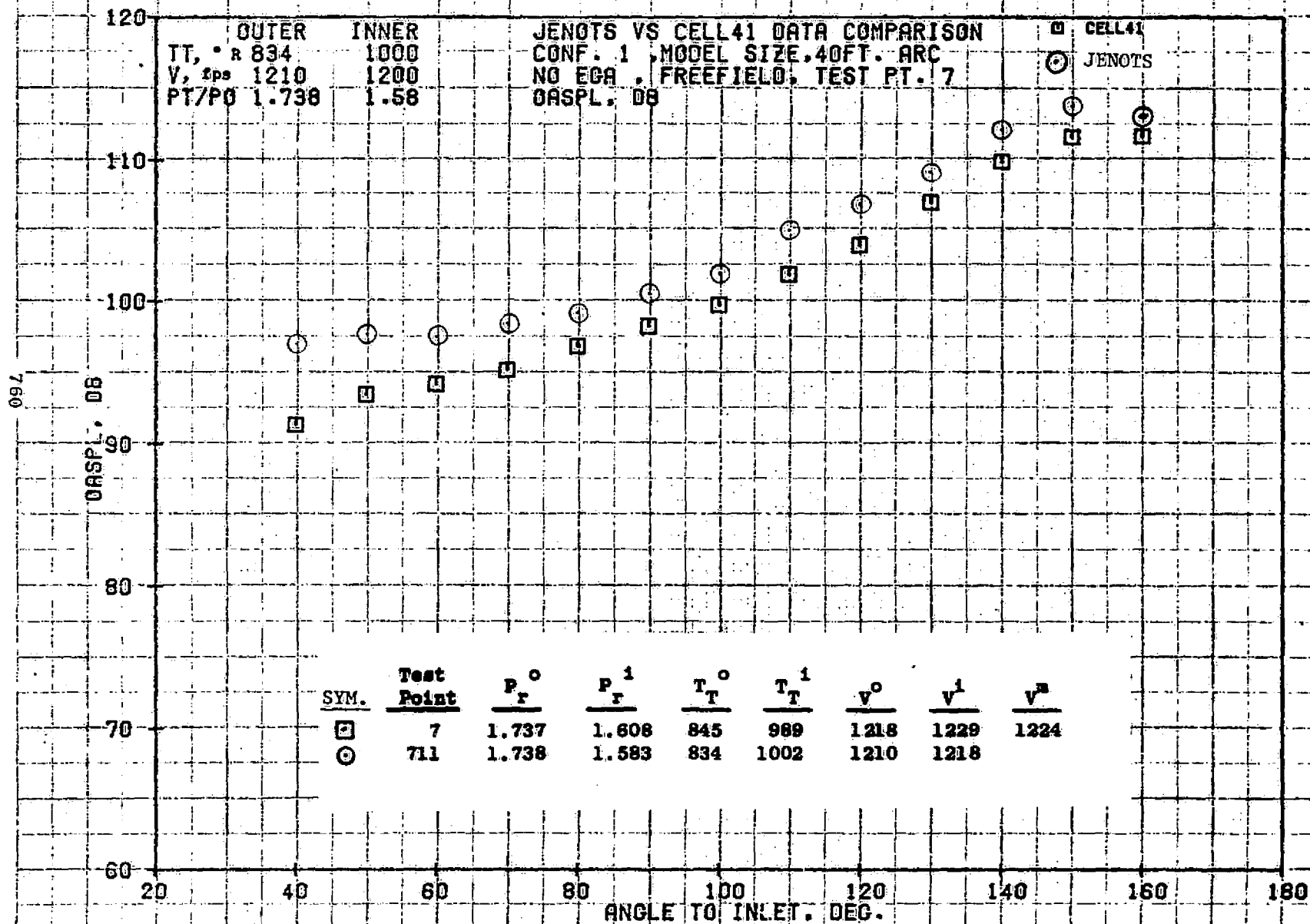


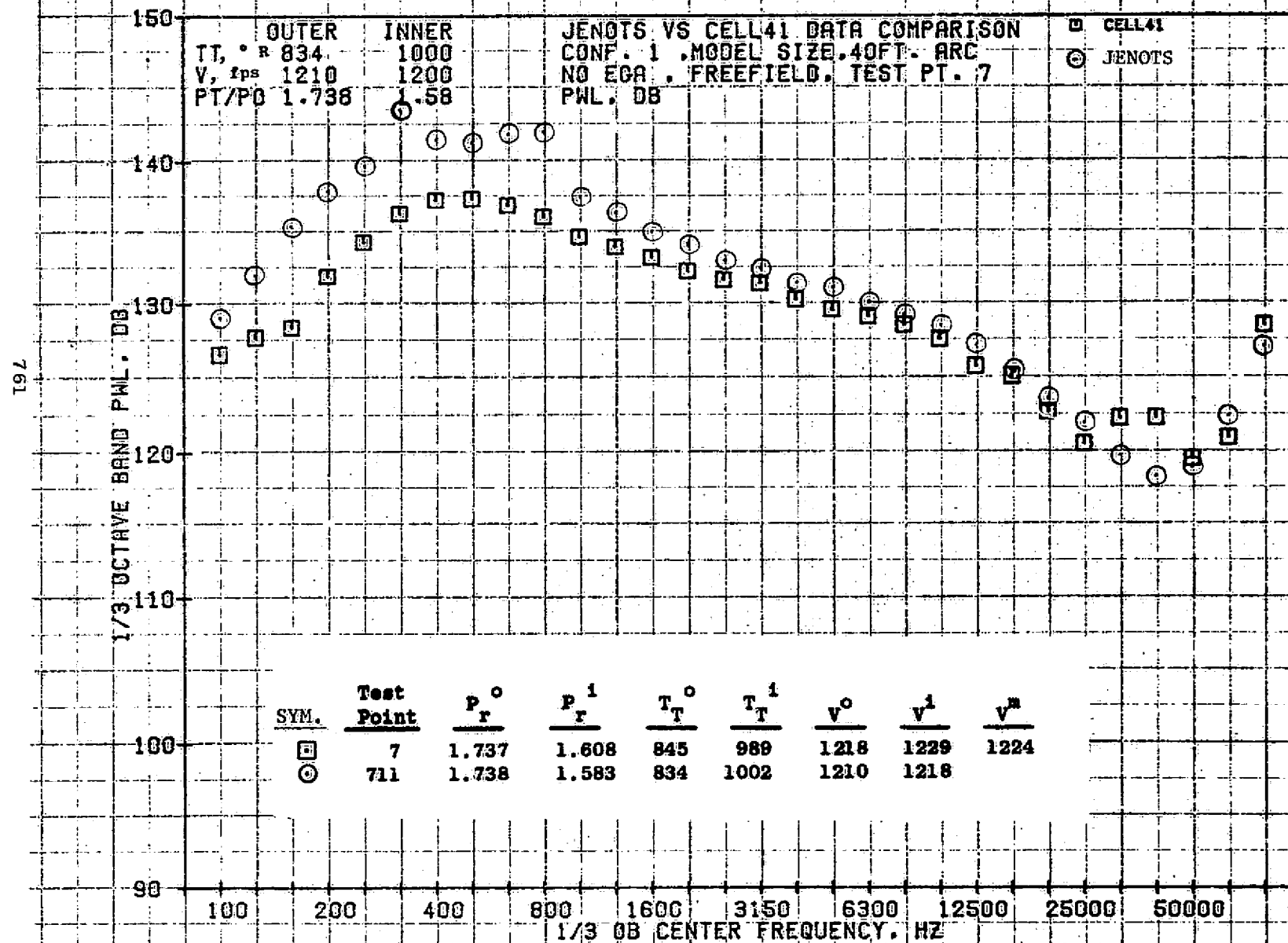


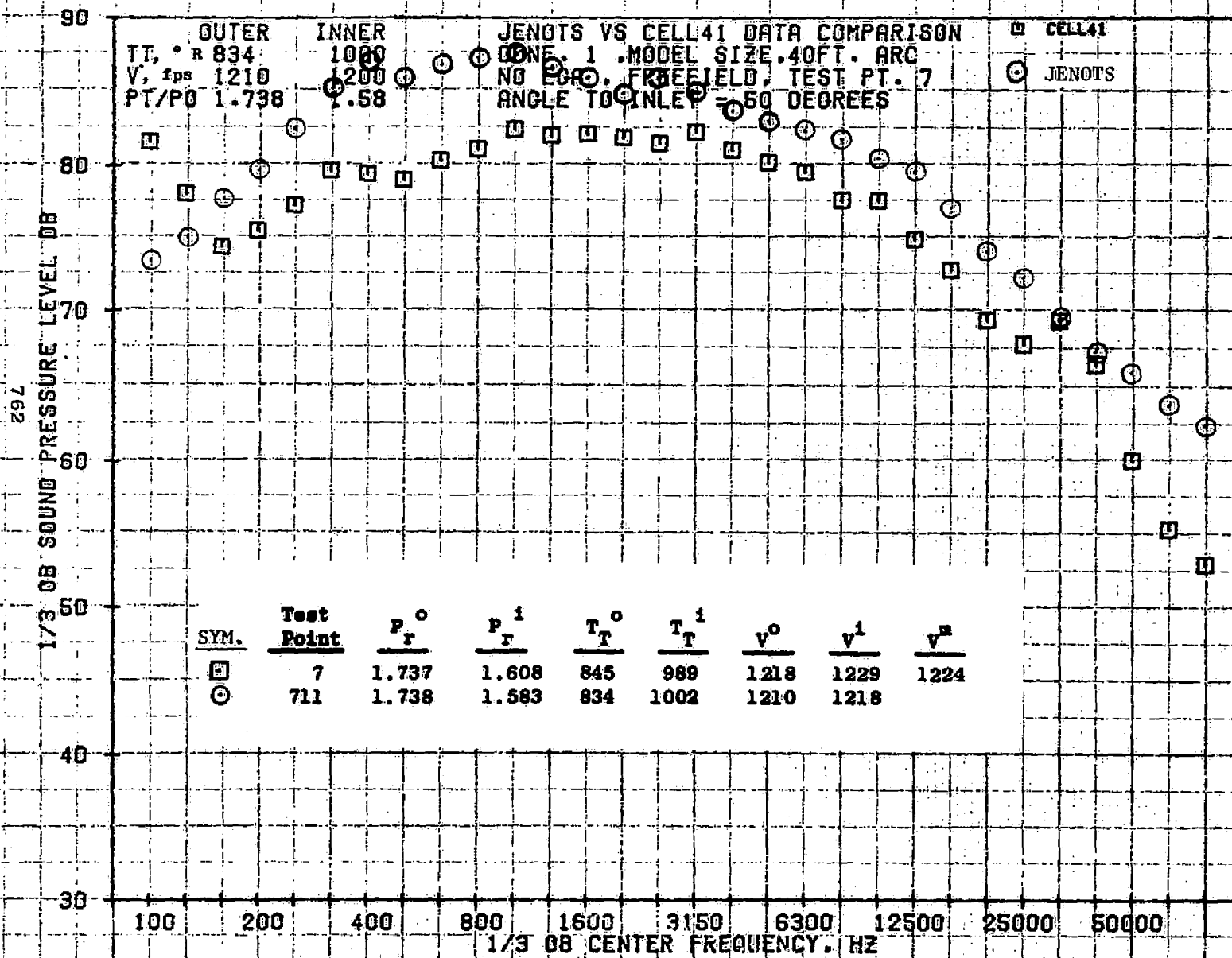


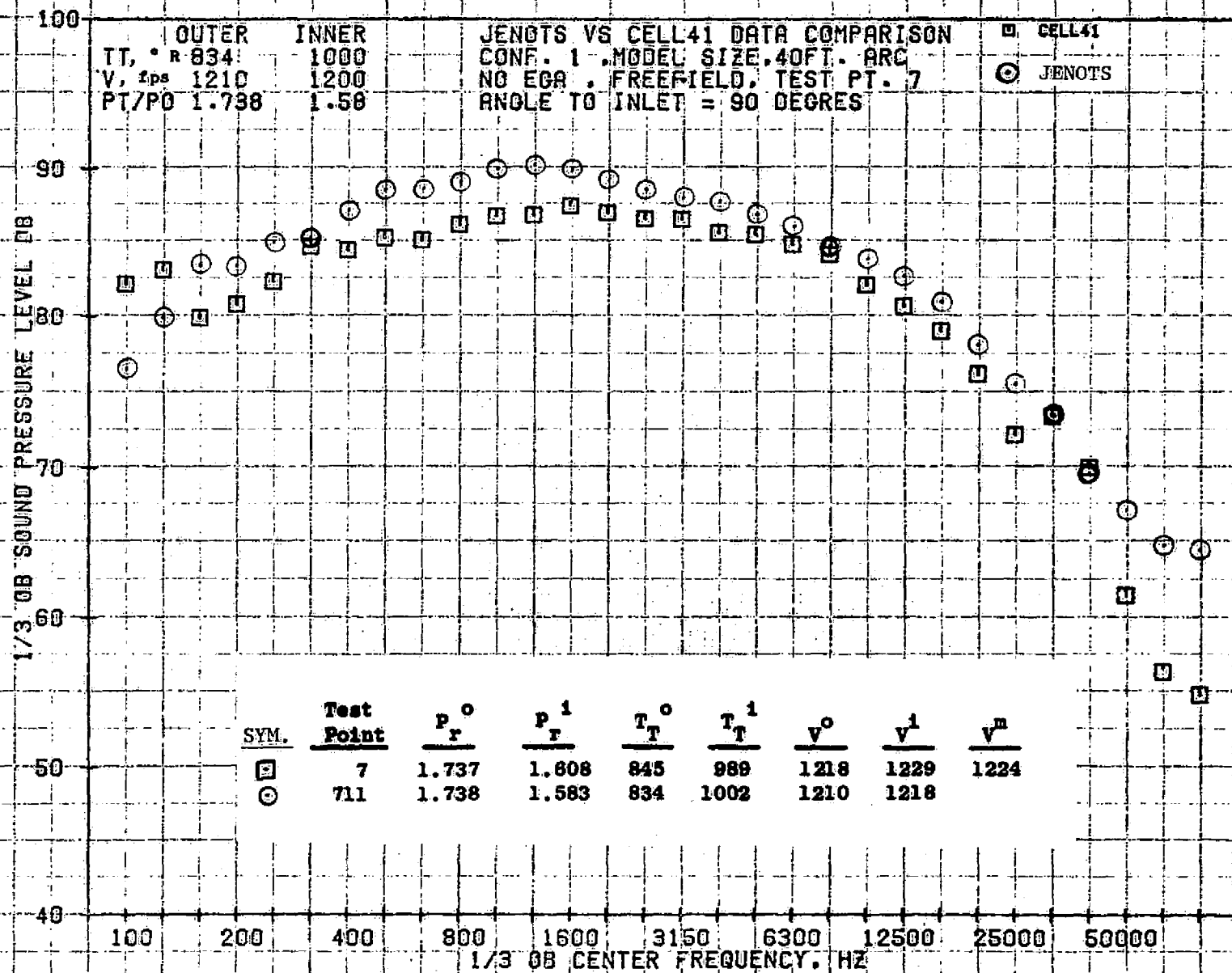
09/28/76
1X583-001

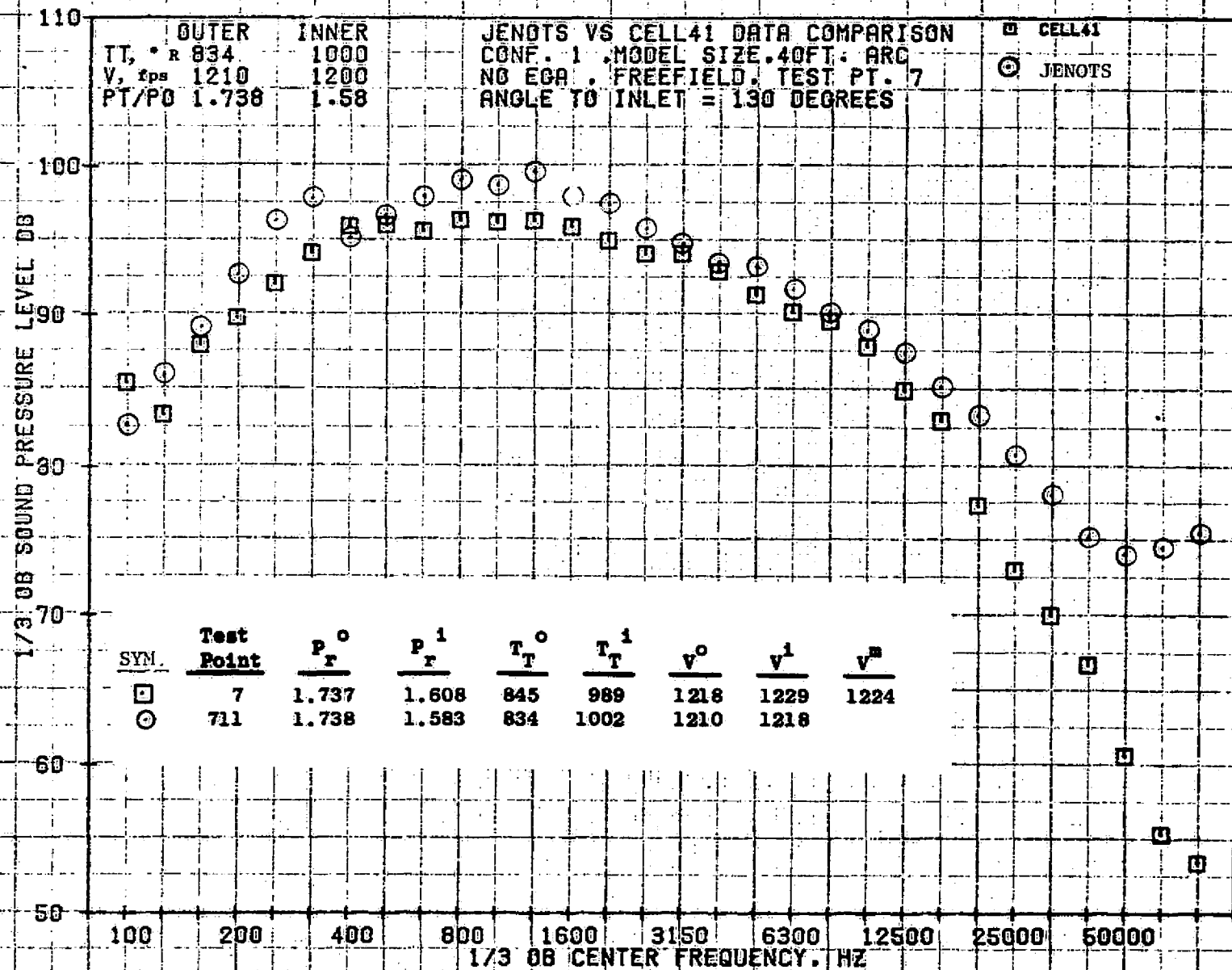
73KOLLSTEDT

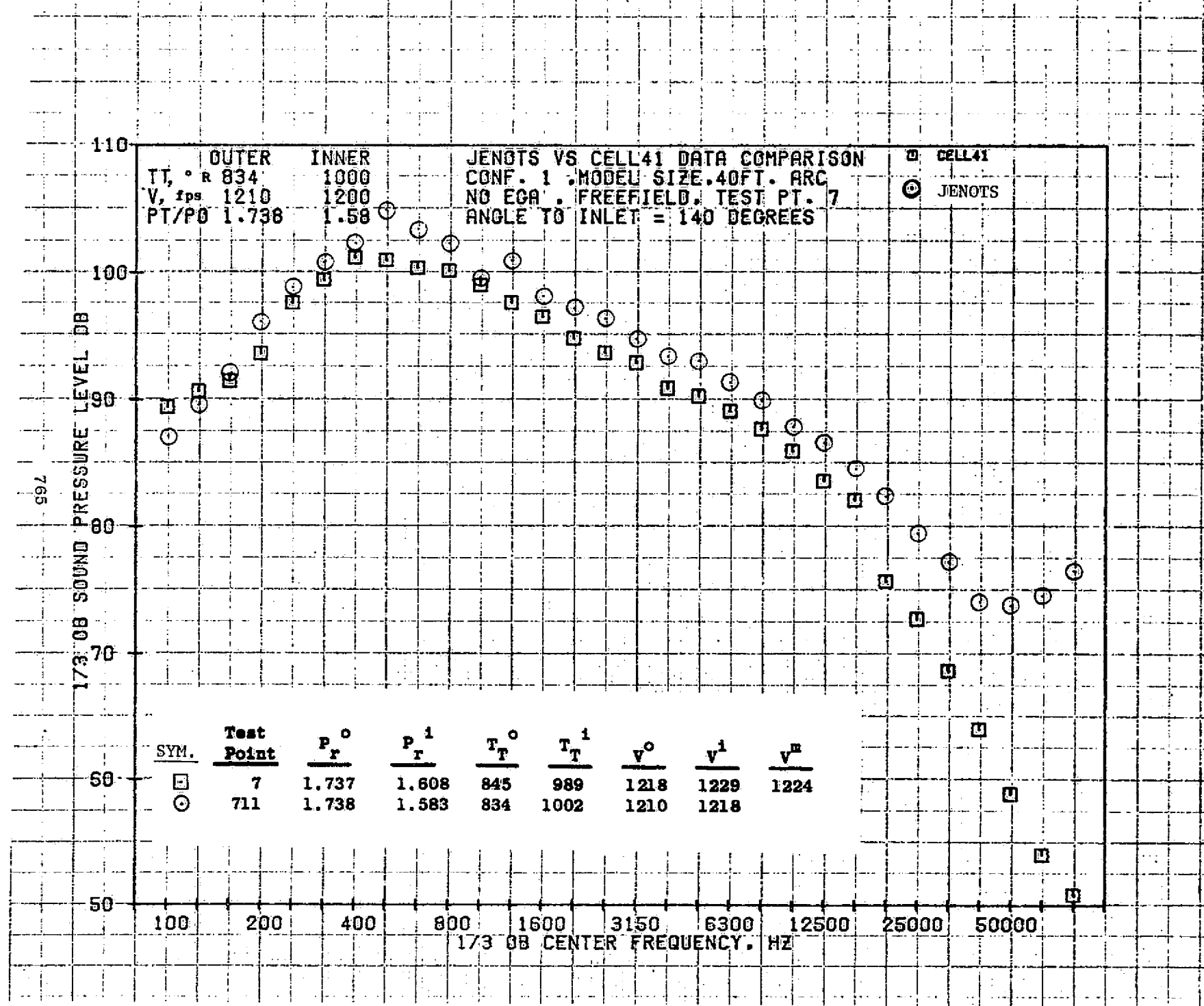


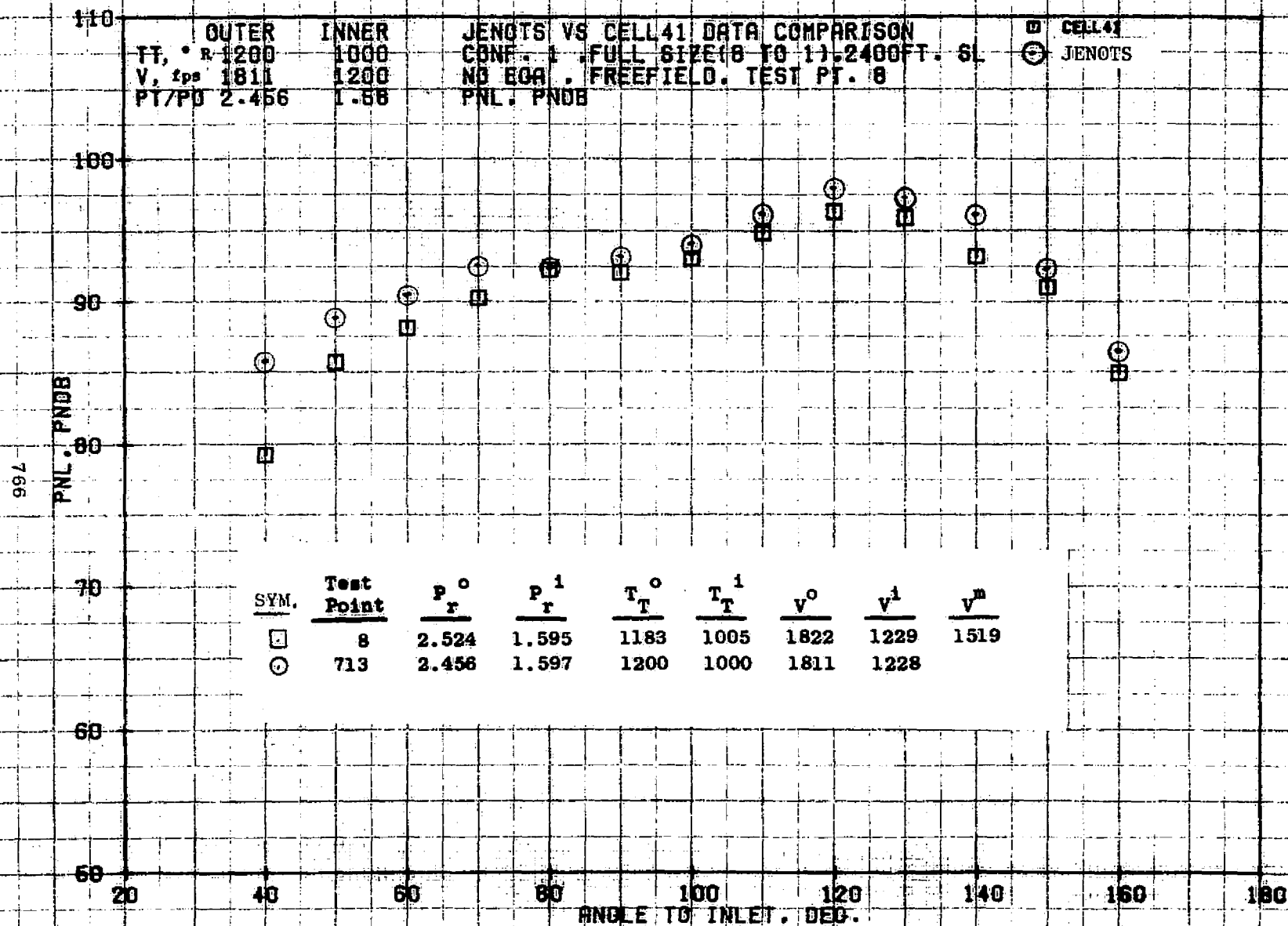






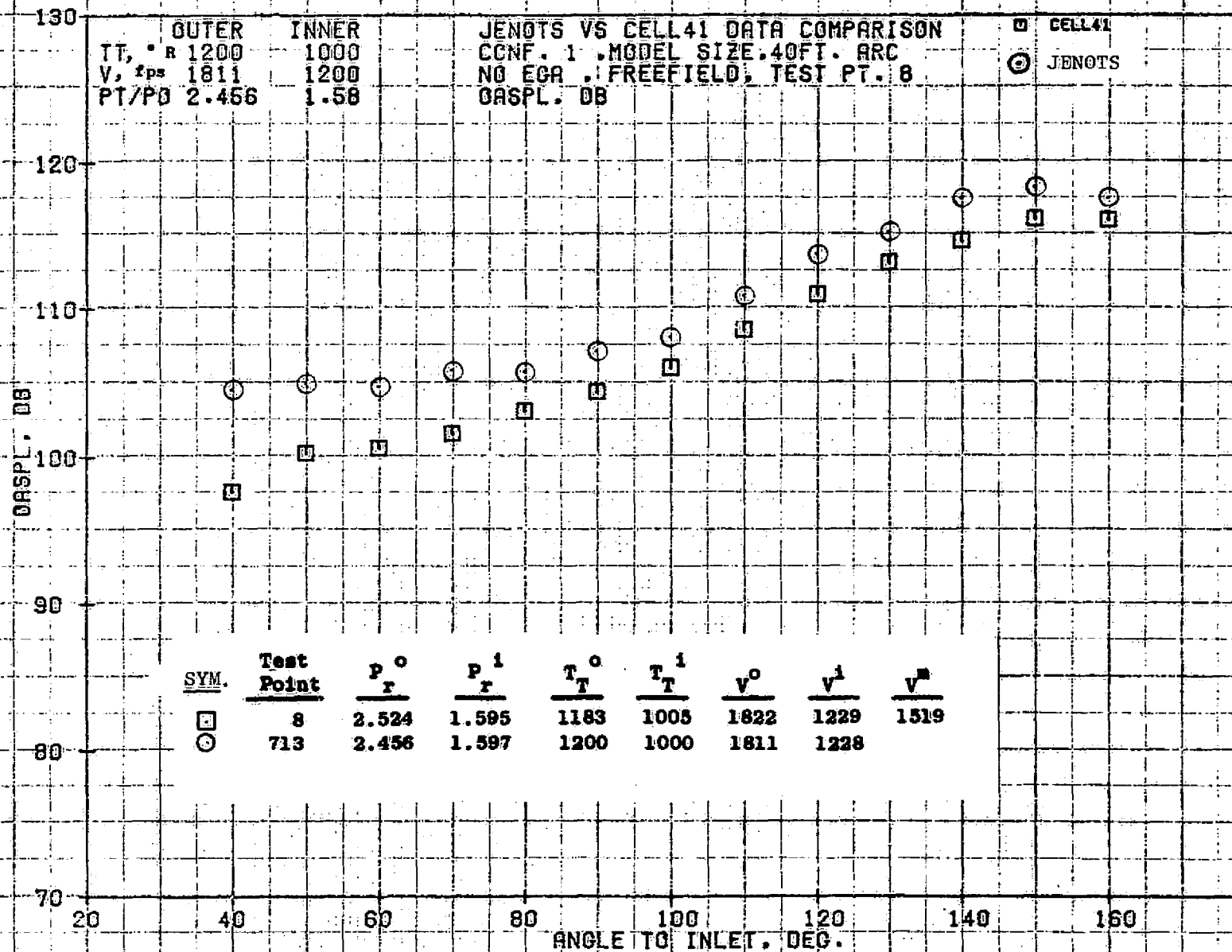




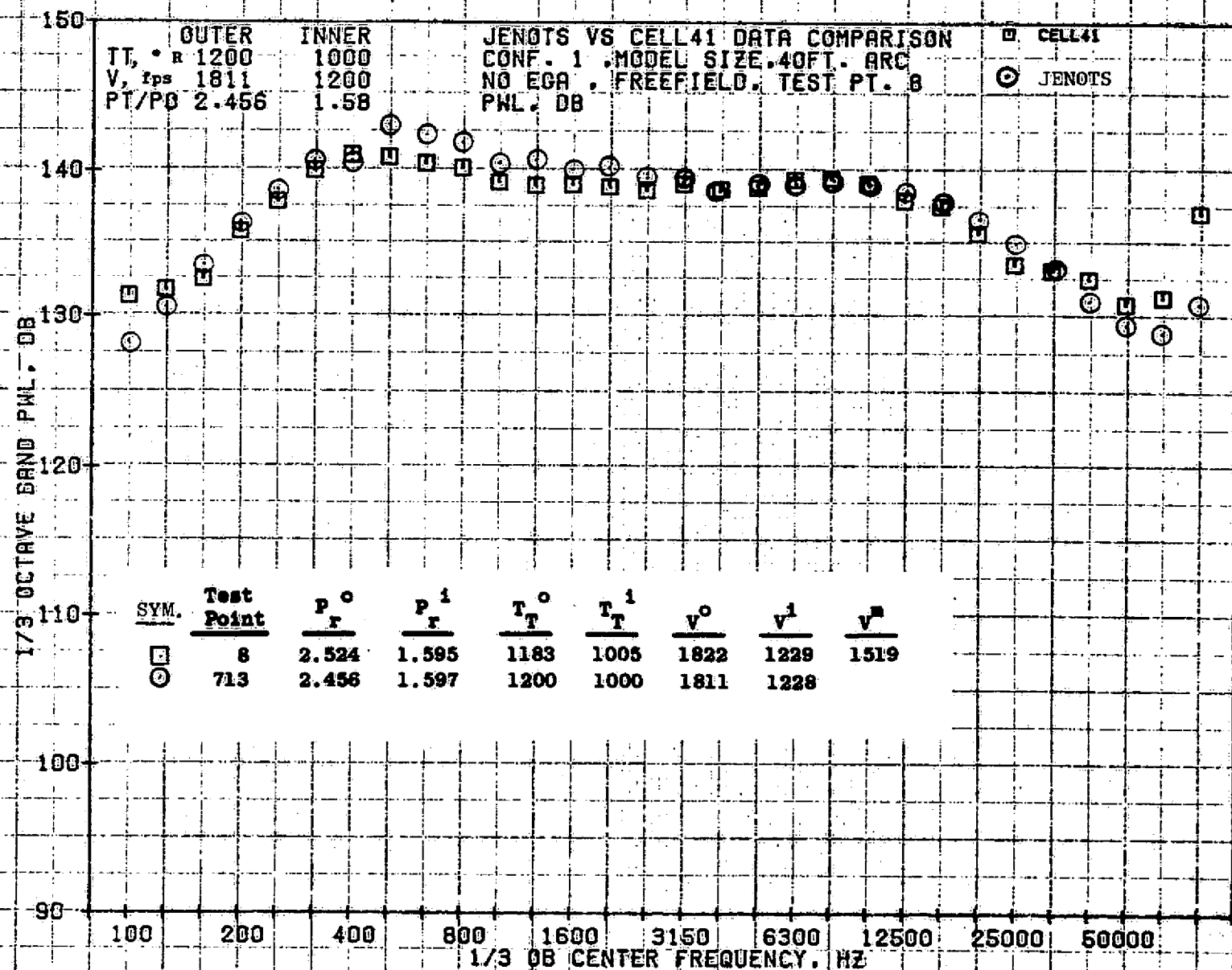


09/28/76
 1X583-001

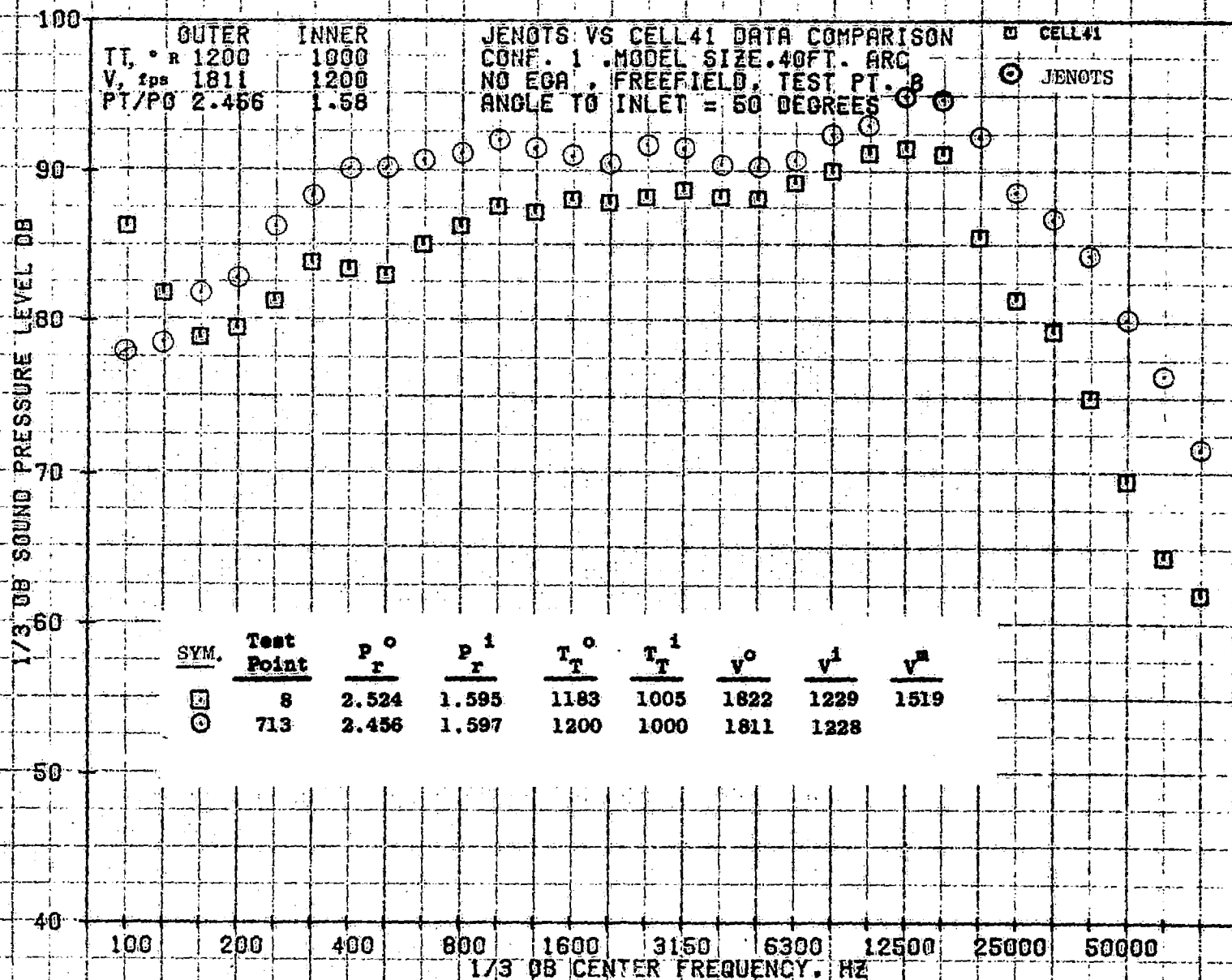
73KOLLSTEDT

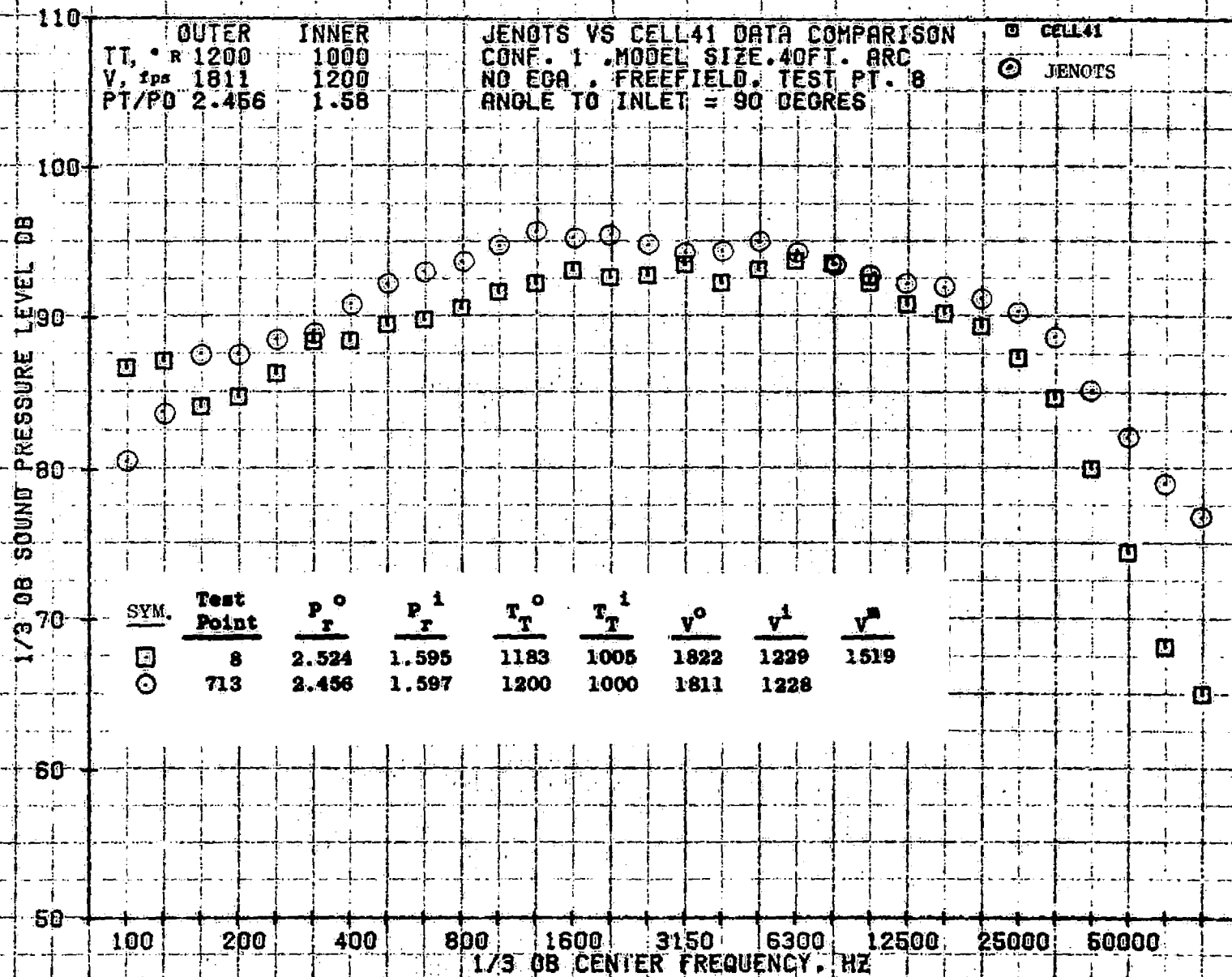


768

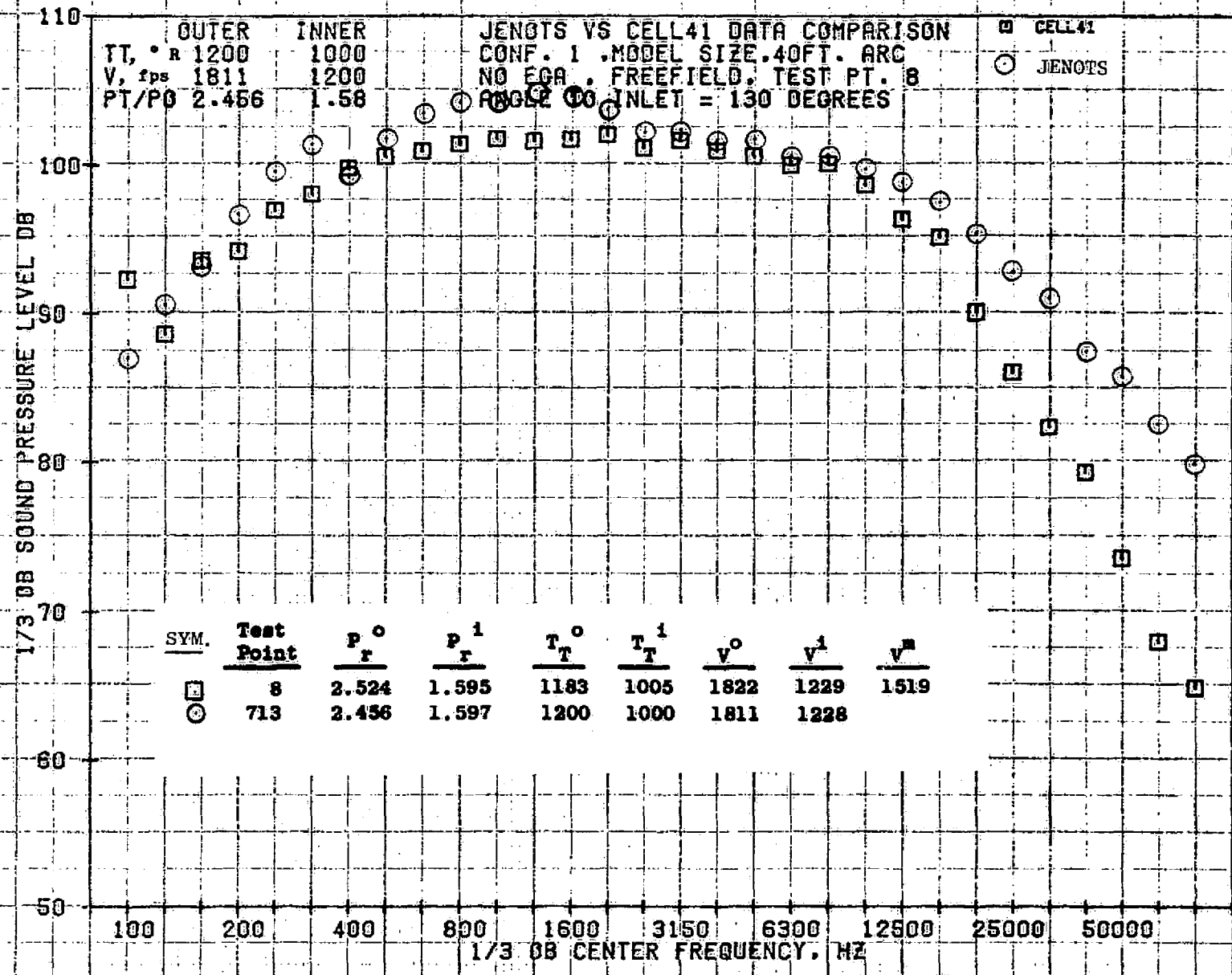


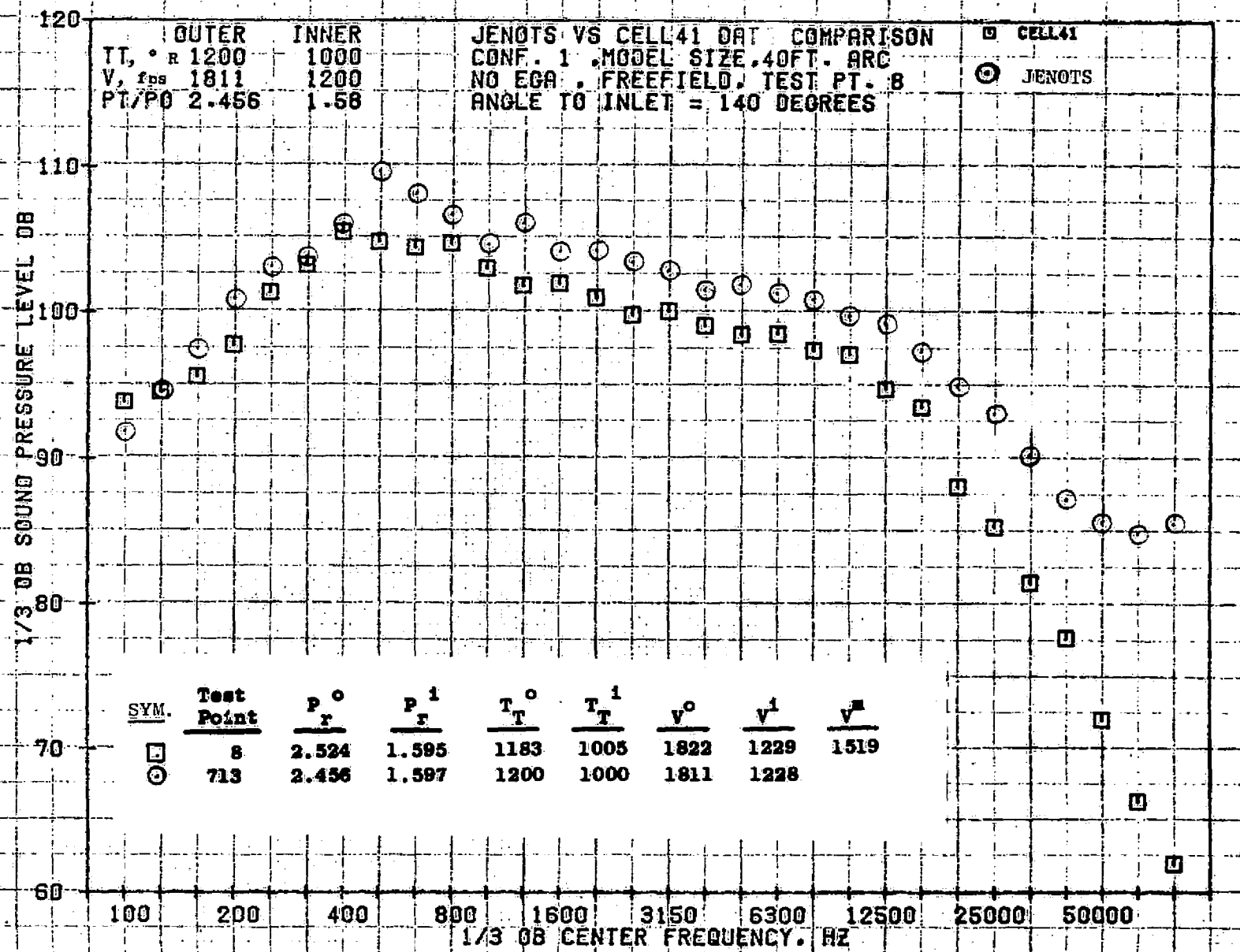
669

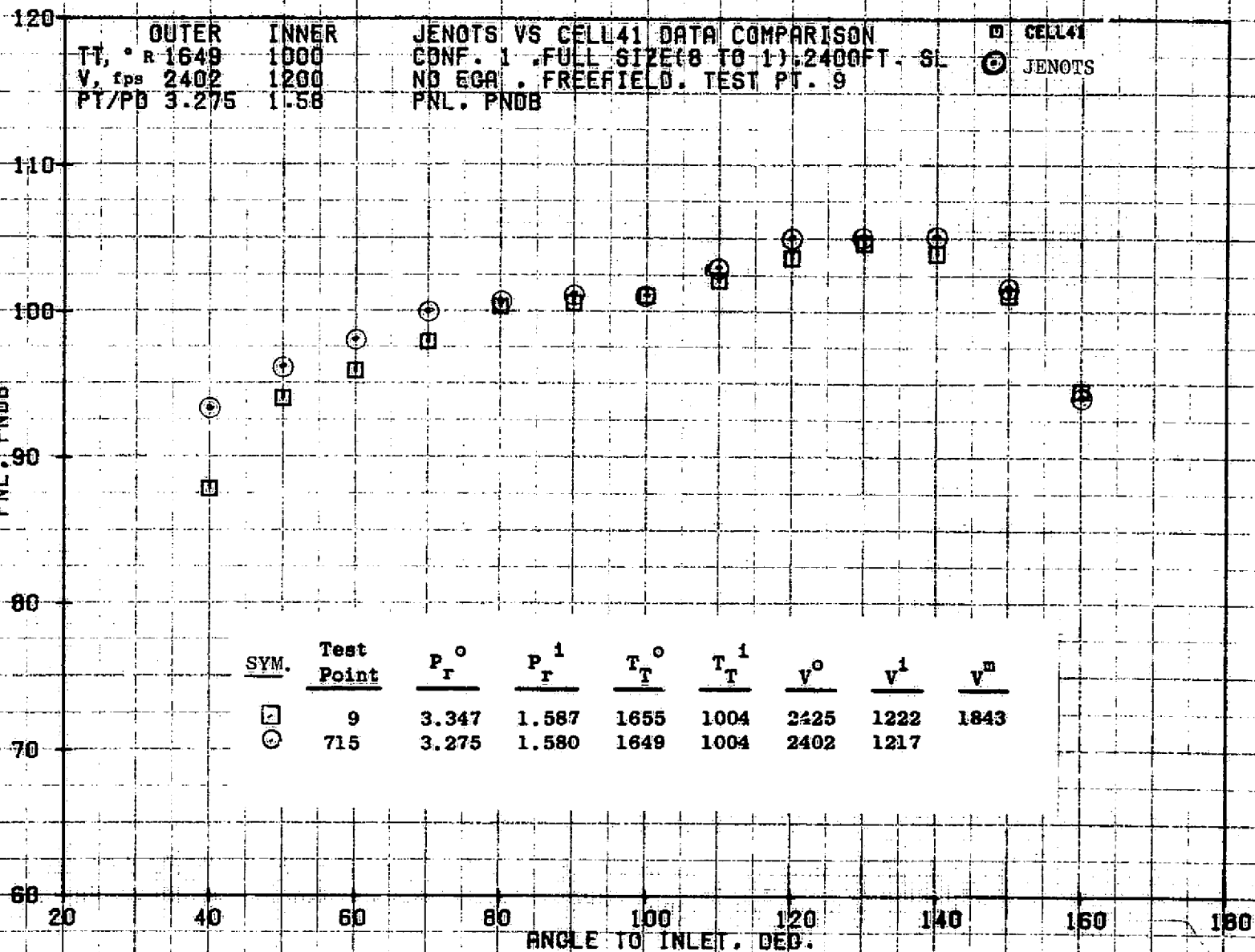




777

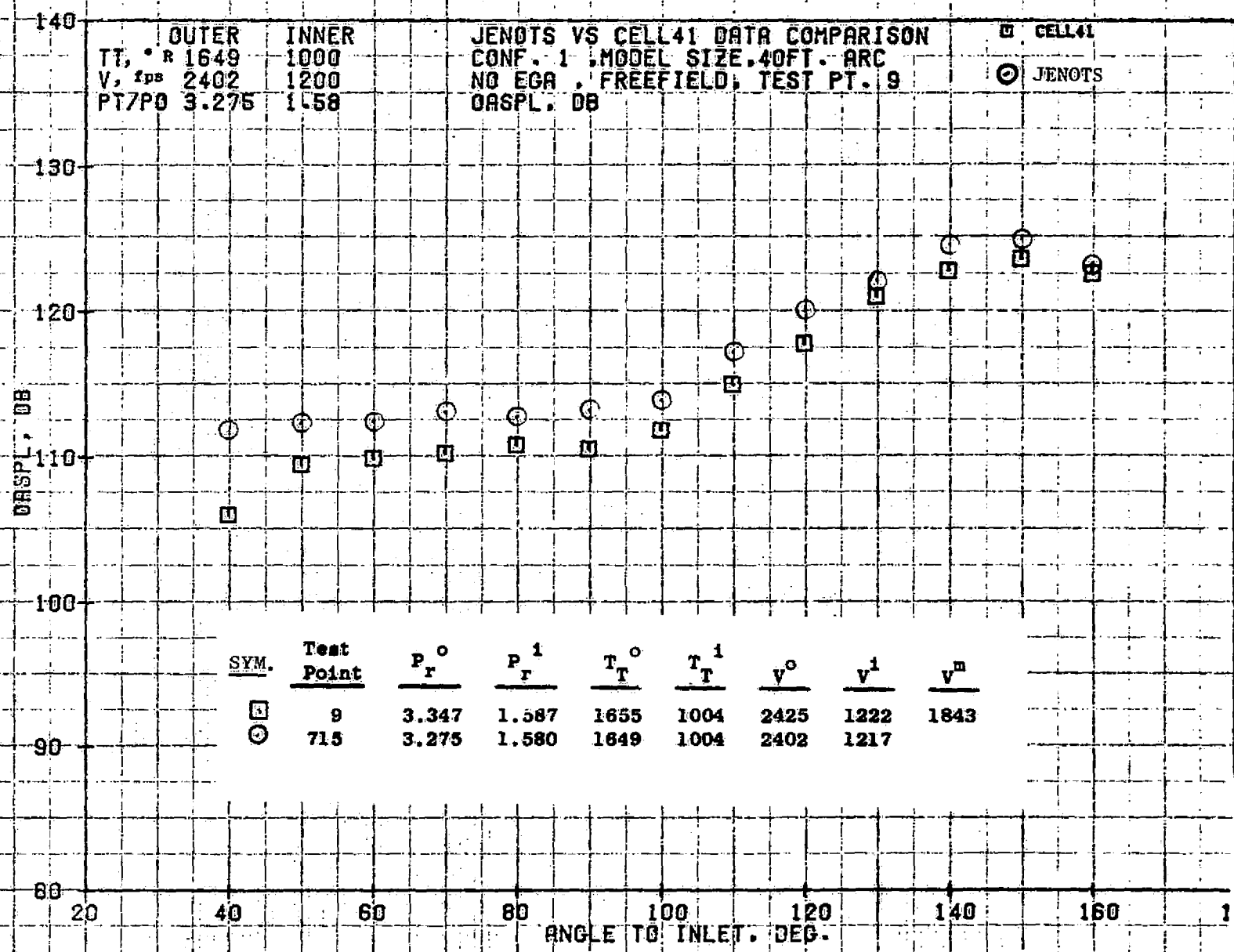


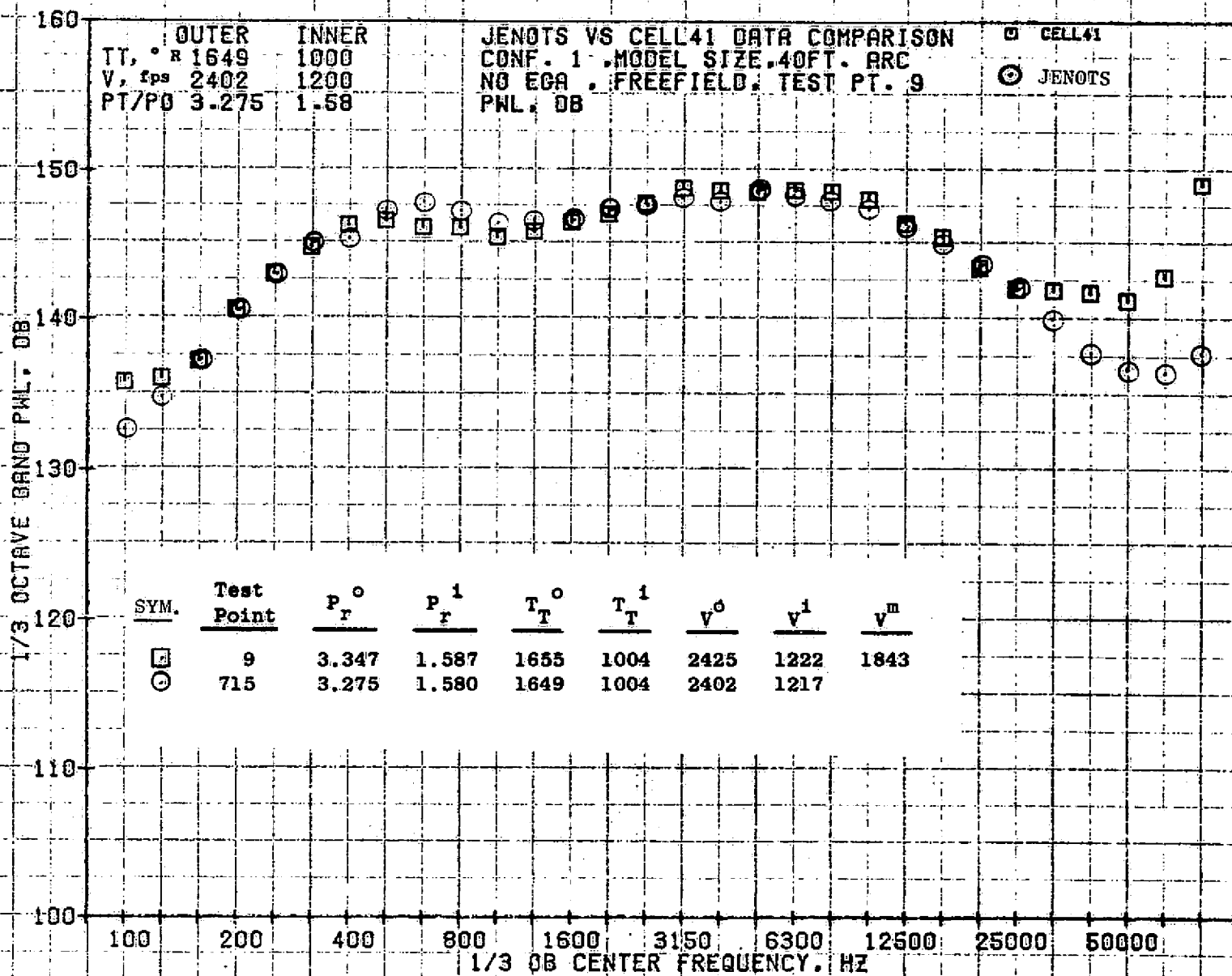


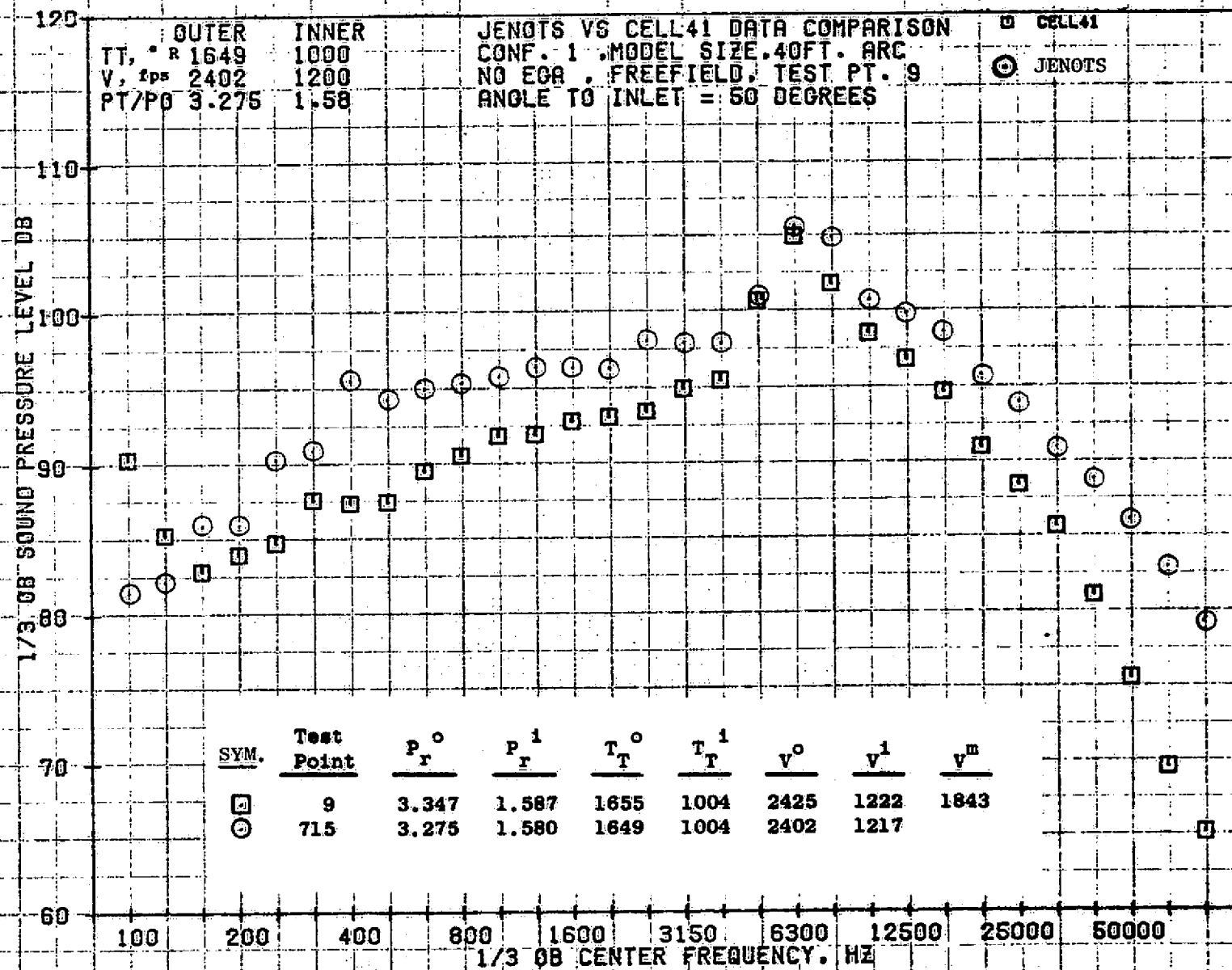


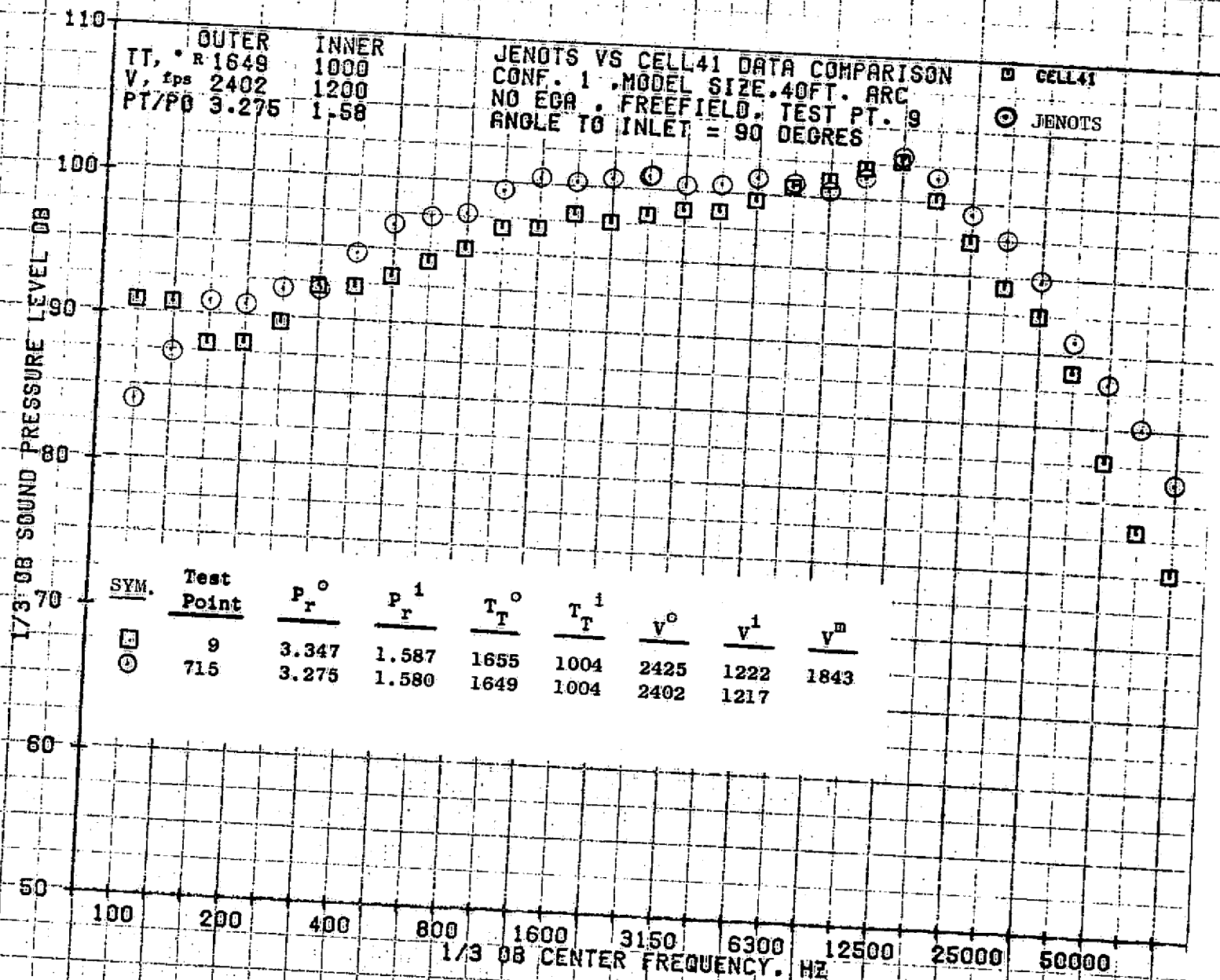
09/28/76
1X583-001

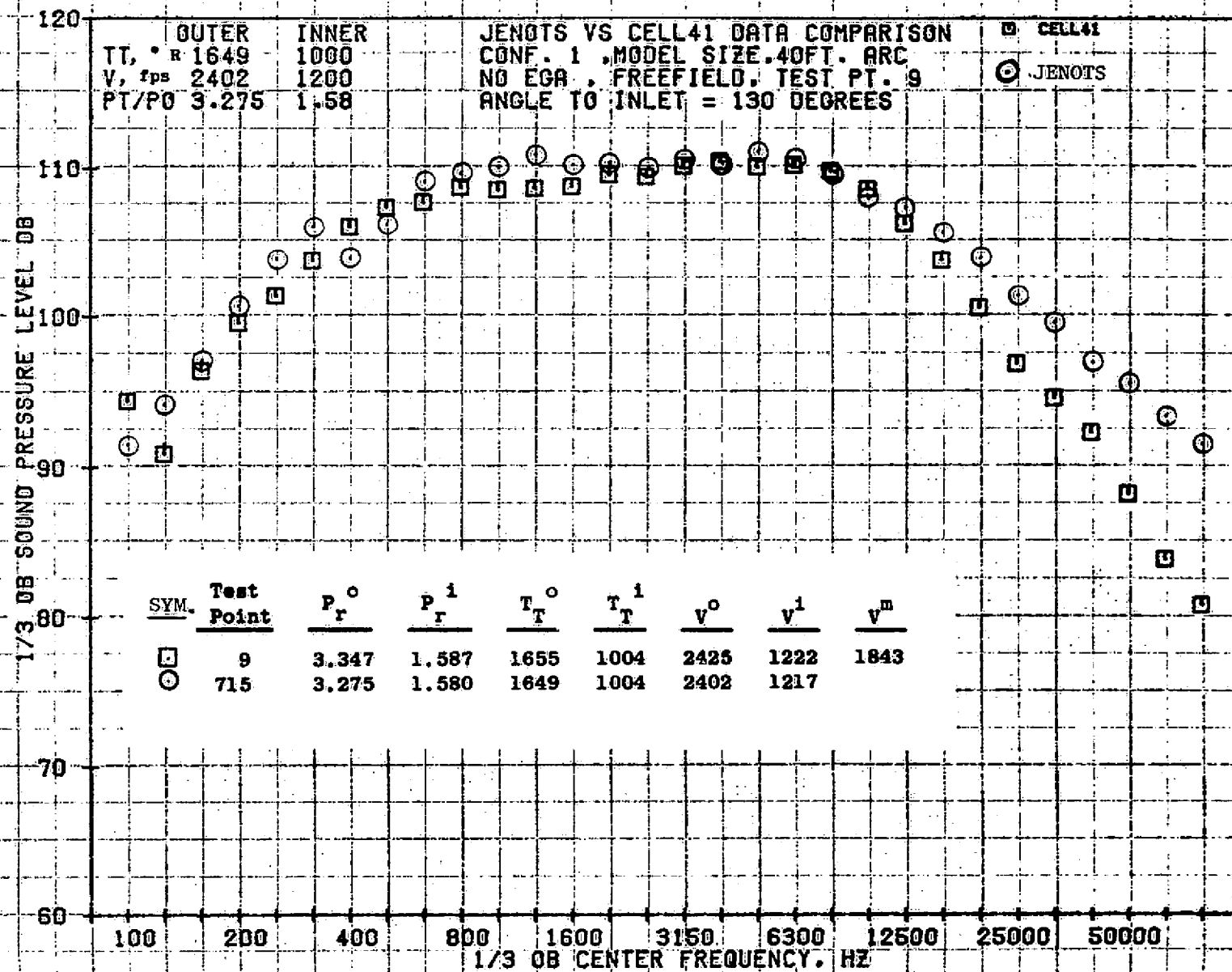
73KOLLSTEOT



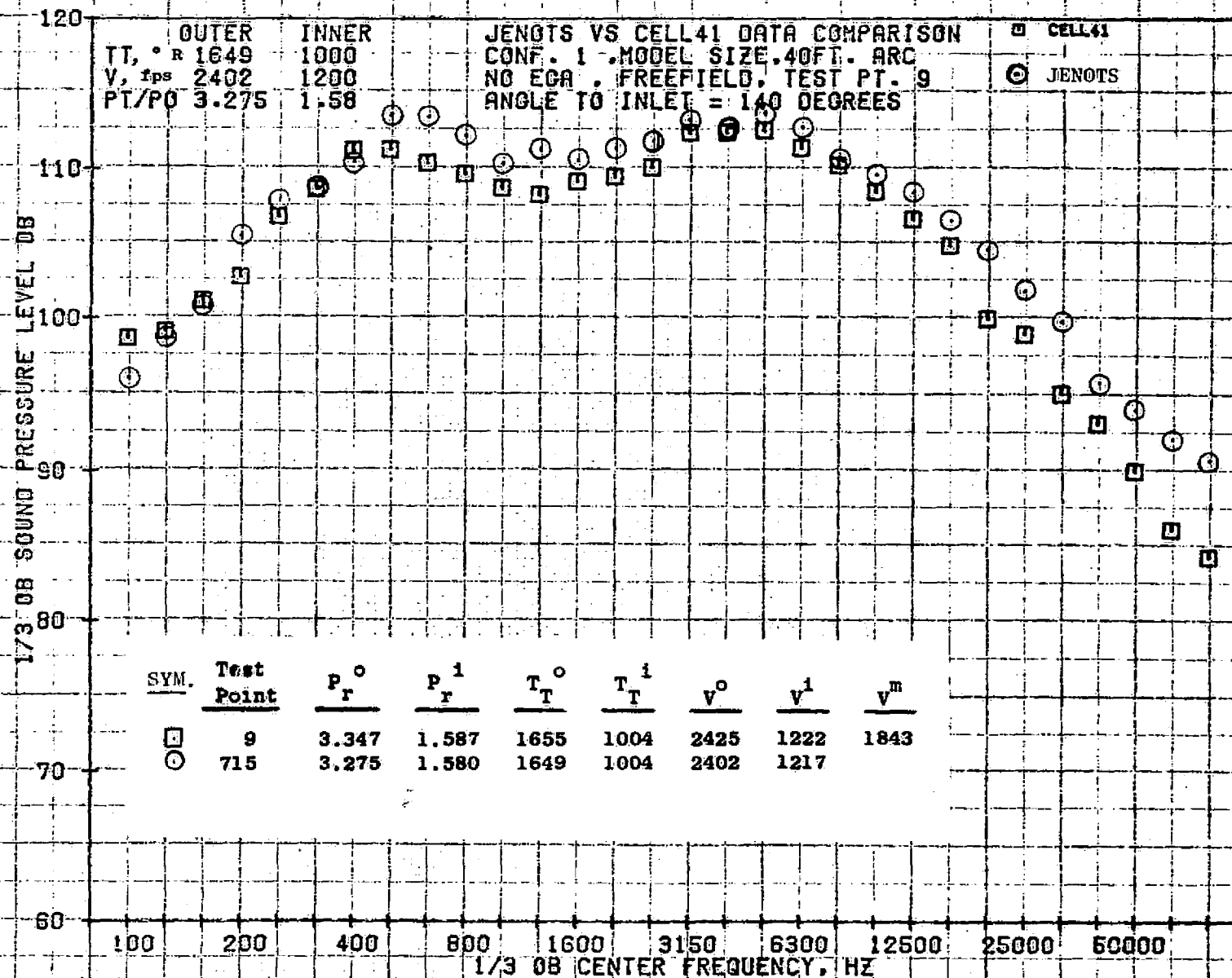


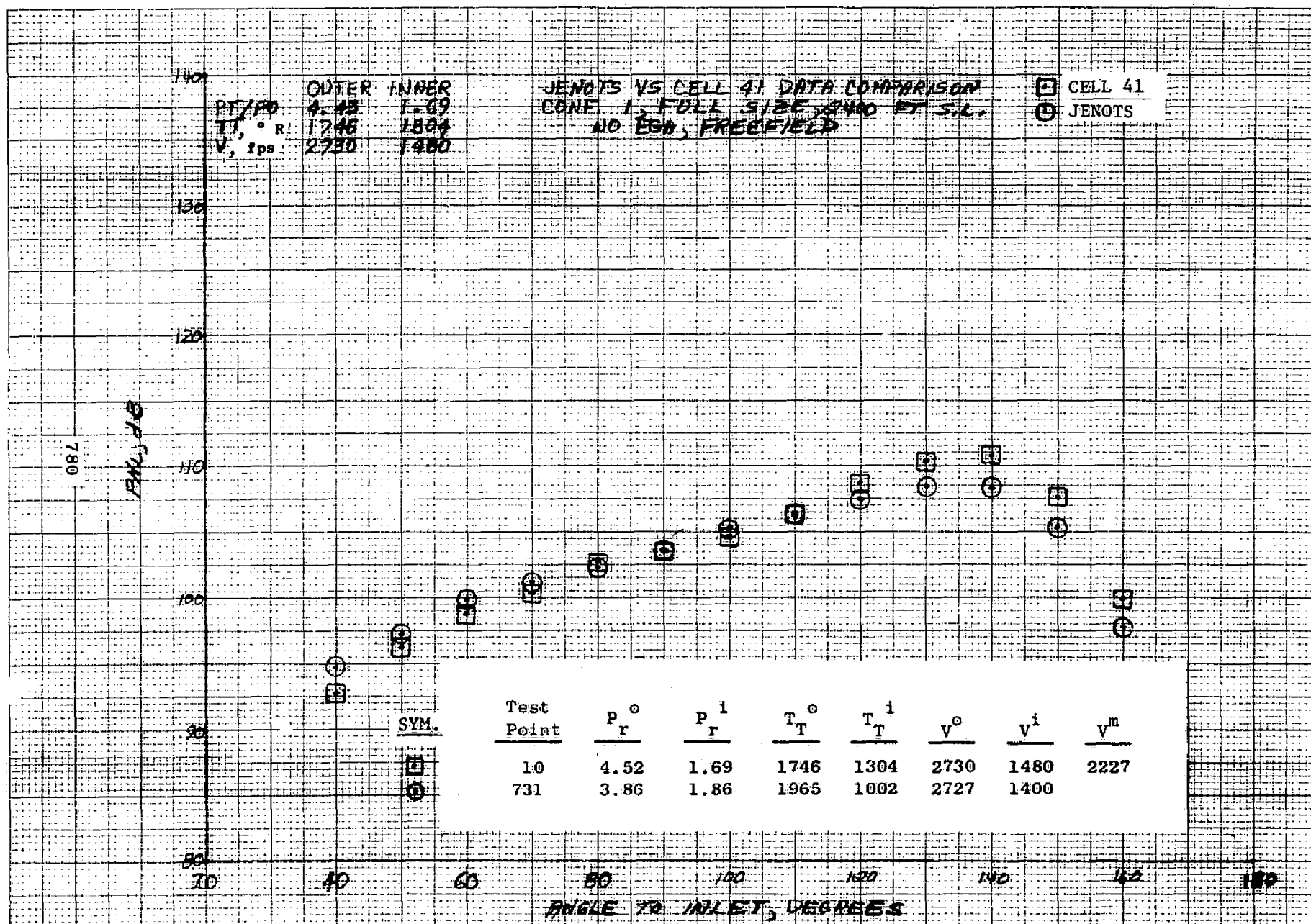


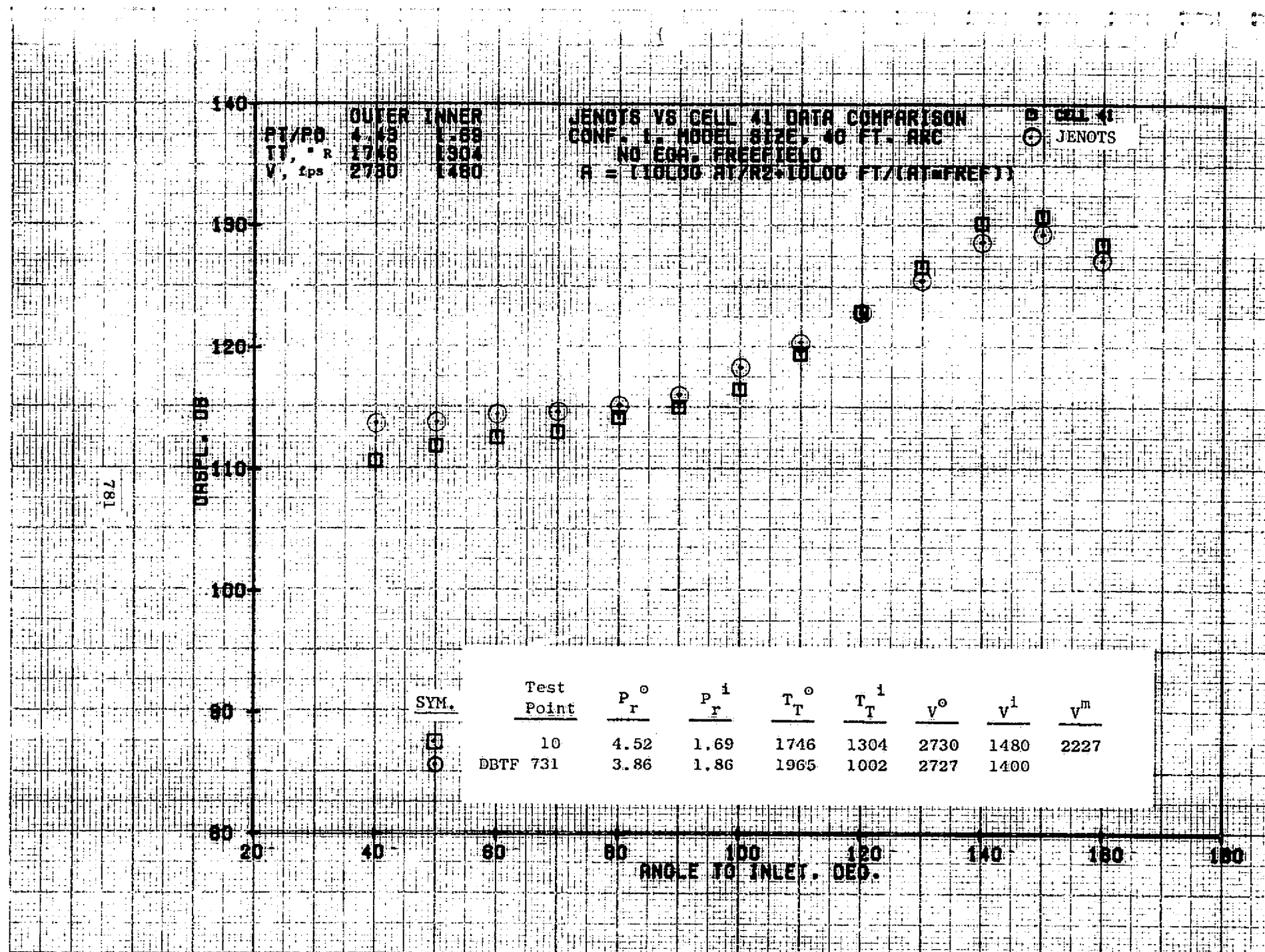




779

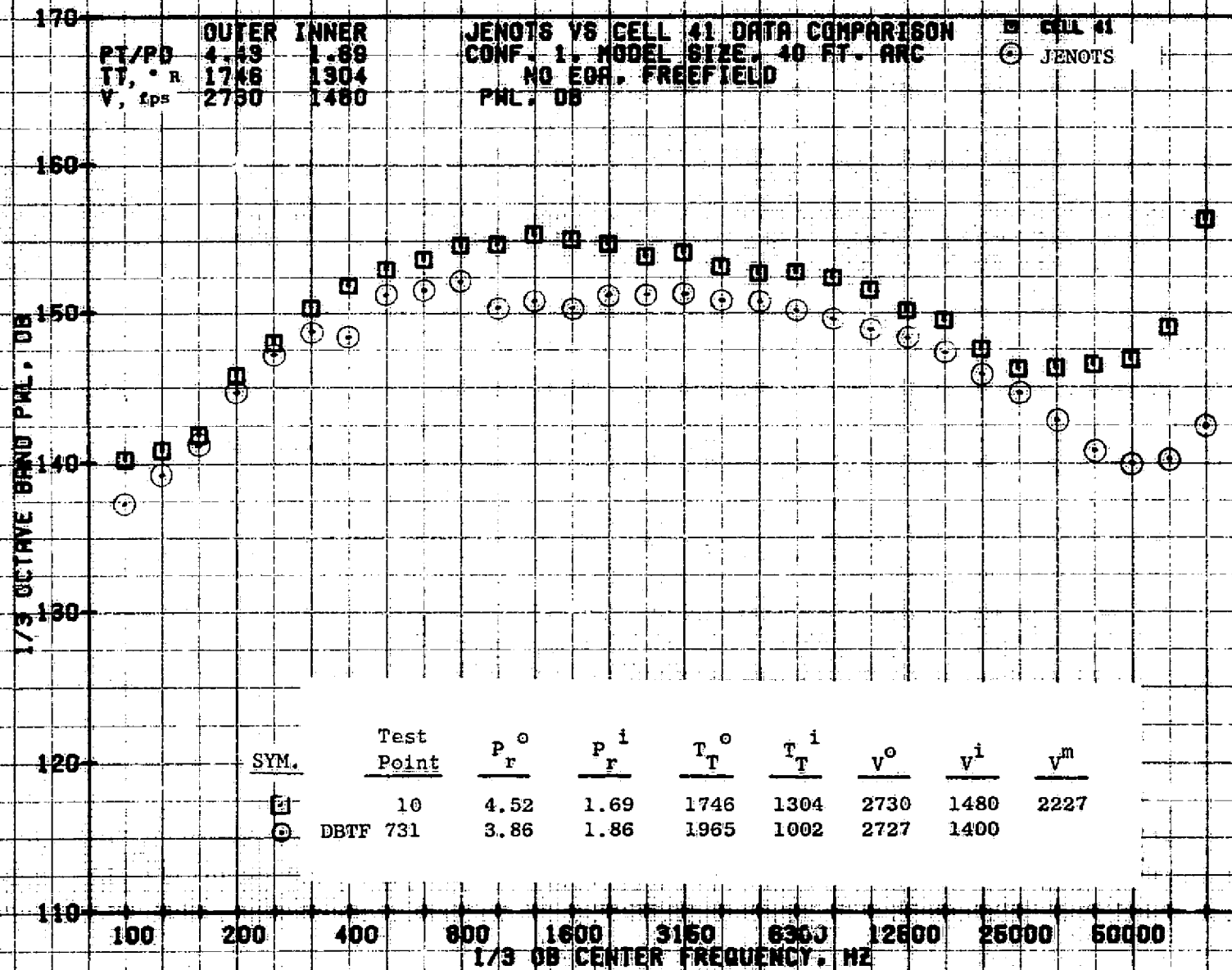






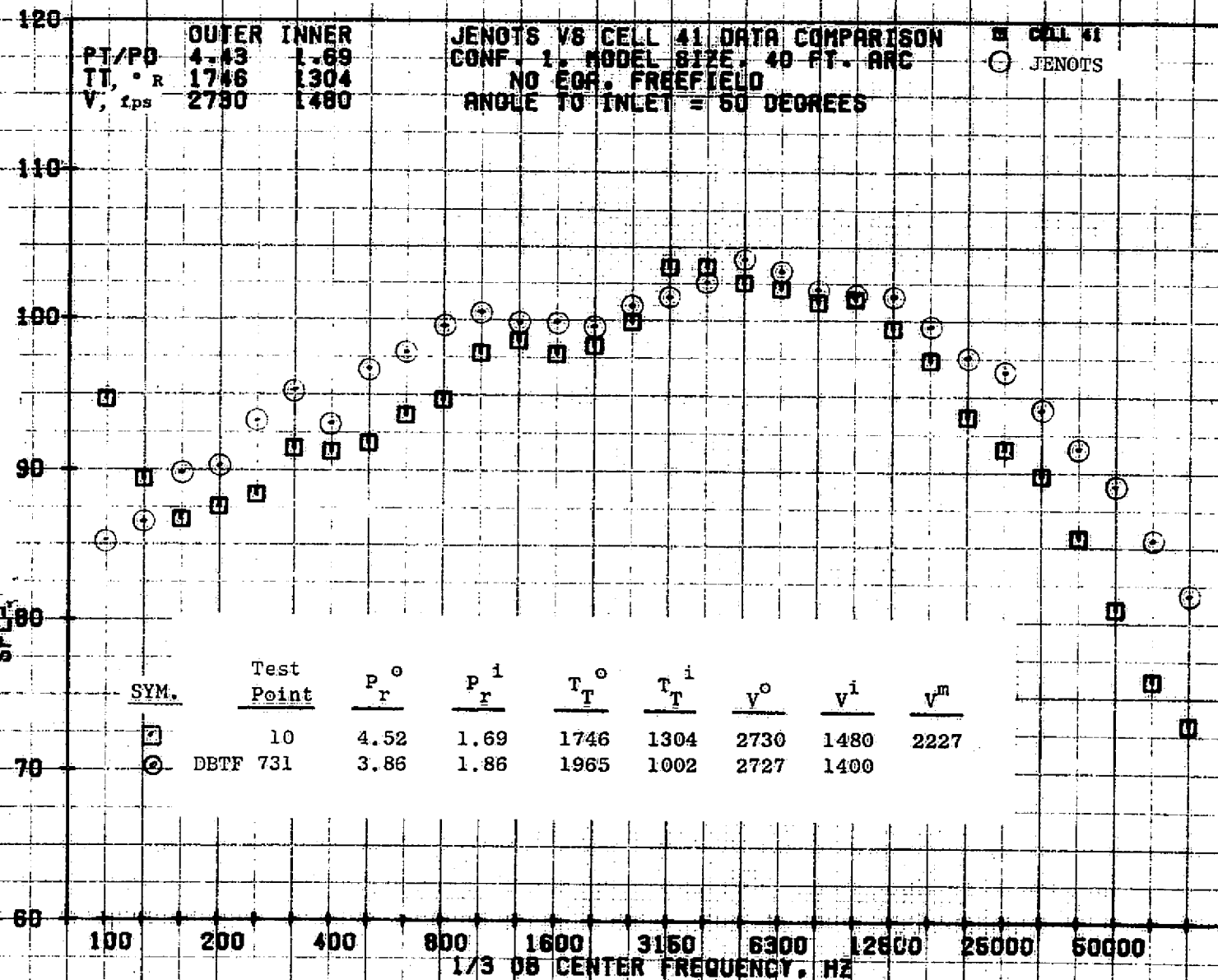
11/09/76
 1A343-001

79 APRCH 2...



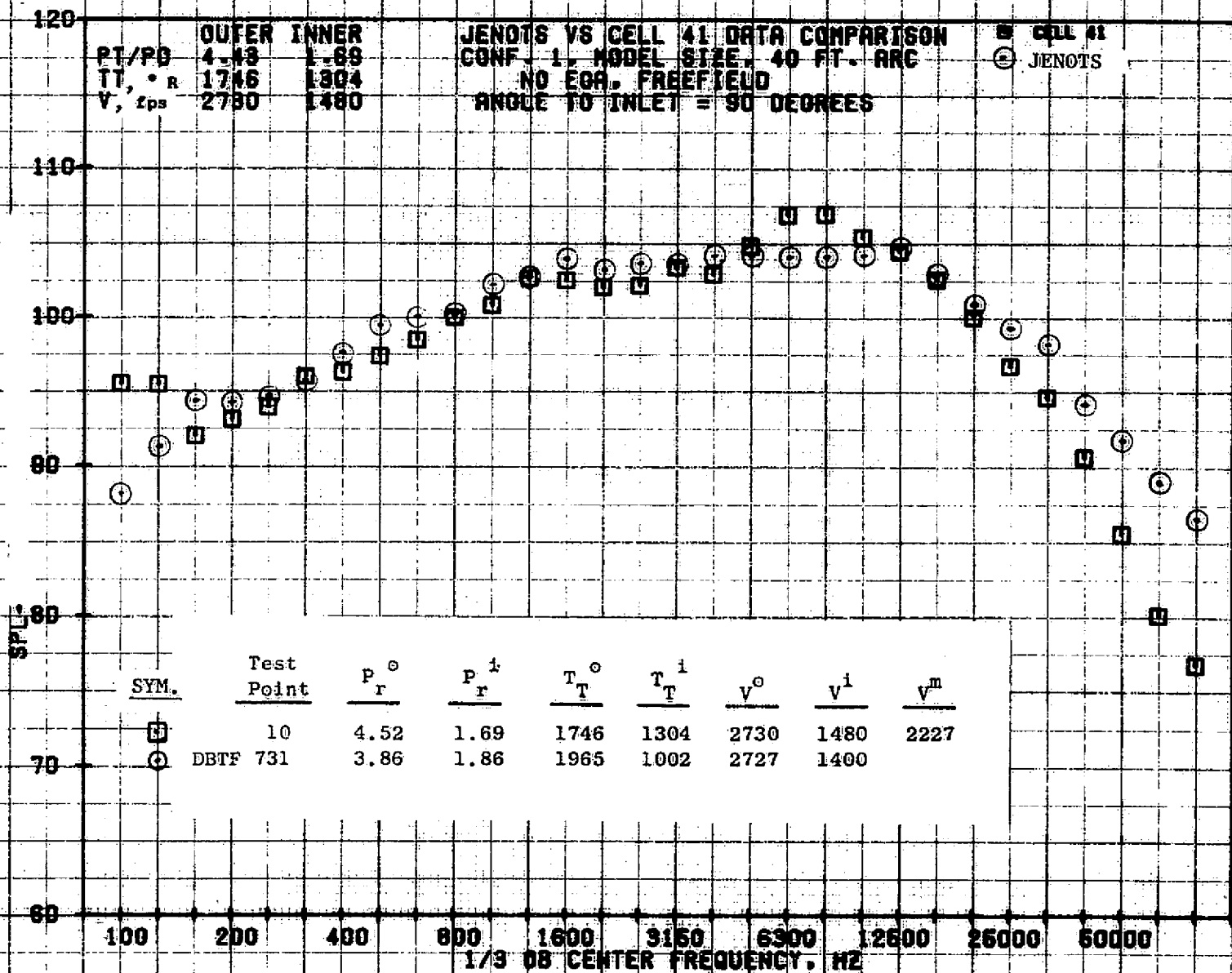
11/01/76
 18391-001

79 BURCH A.



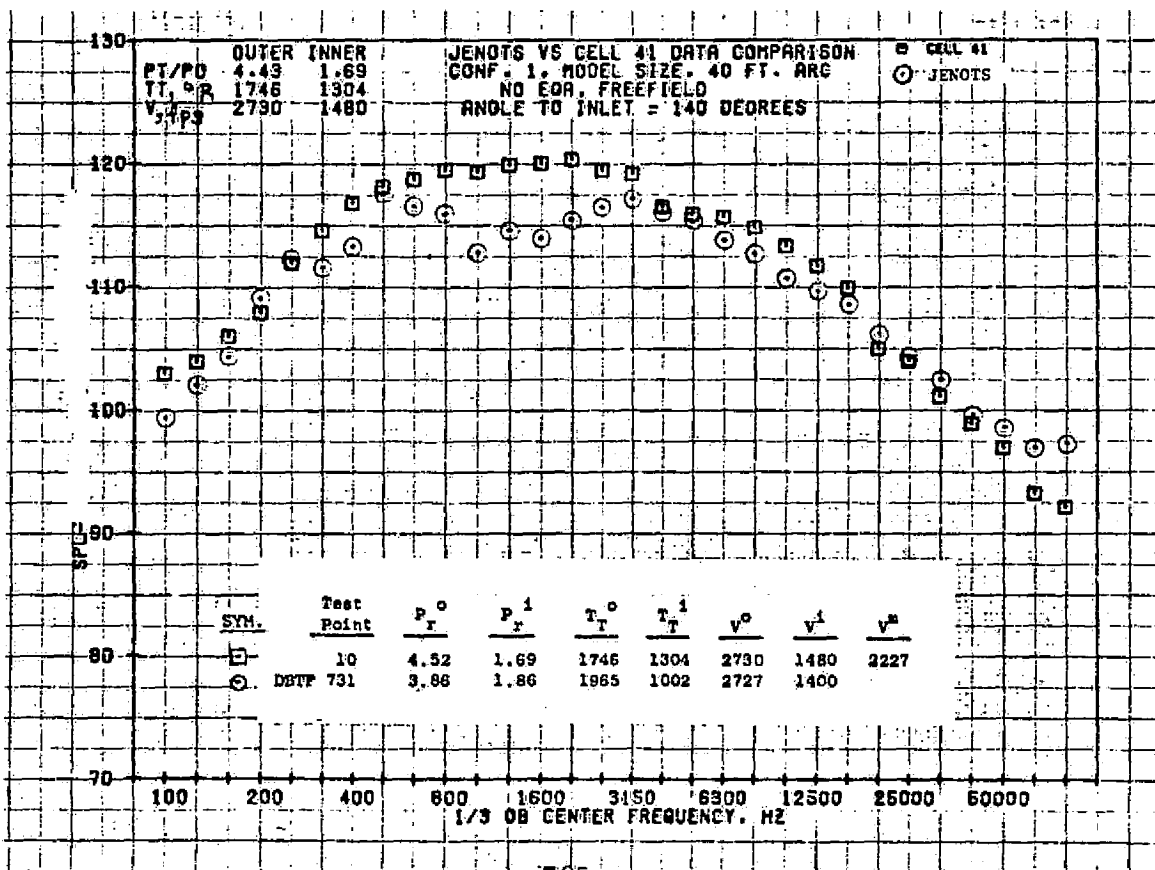
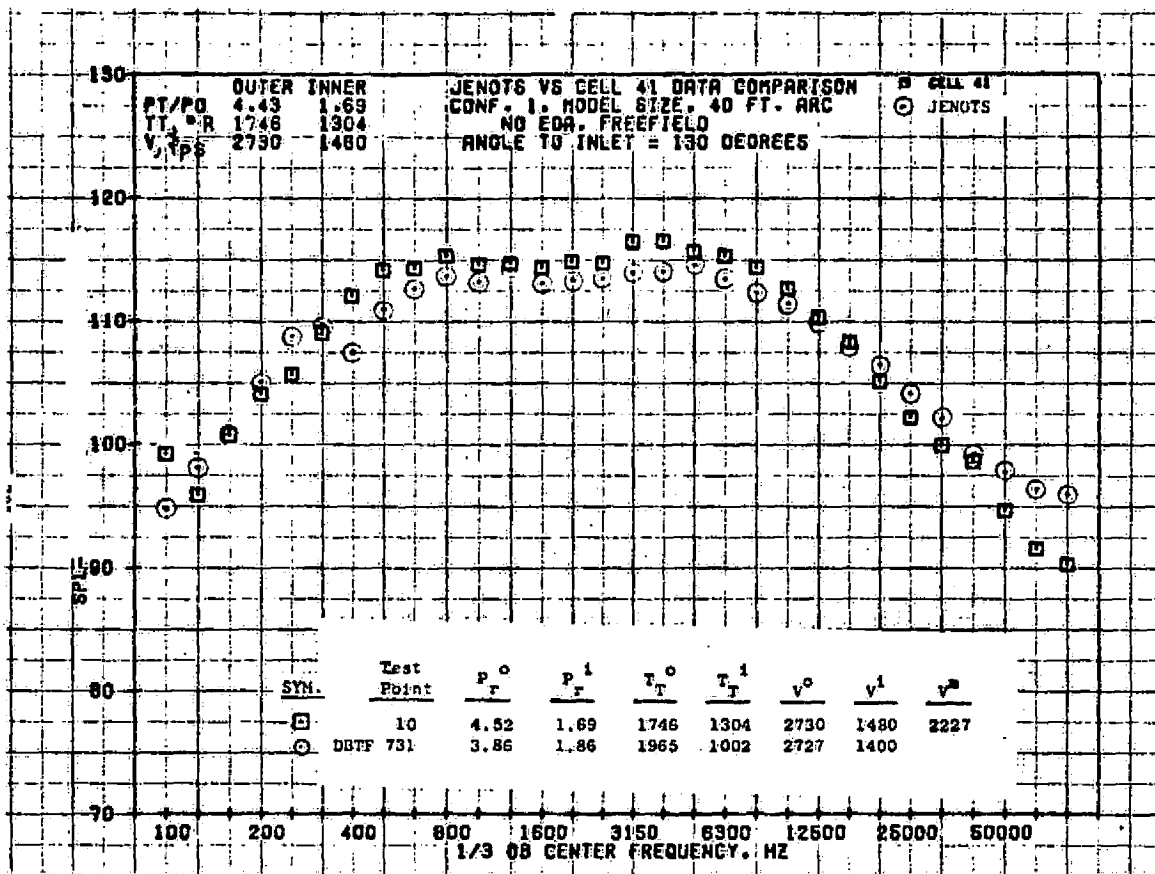
11/01/76
1B391-001

79 BURCH A.



11/01/76
 18391-001

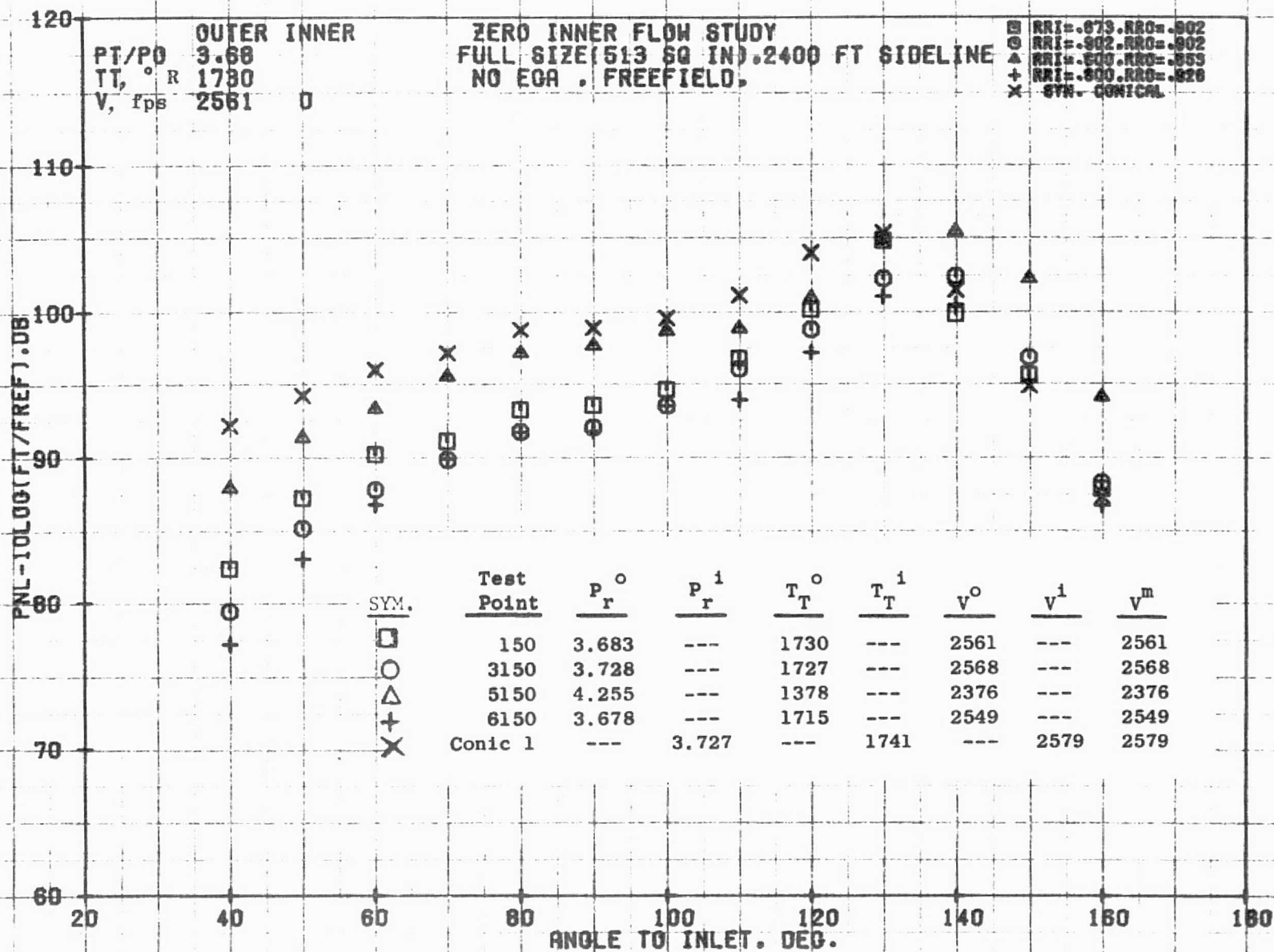
79 BURCH A.



7.3 COMPARISON OF DATA FOR IVP NOZZLES WITH LOW AMOUNTS OF INNER FLOW

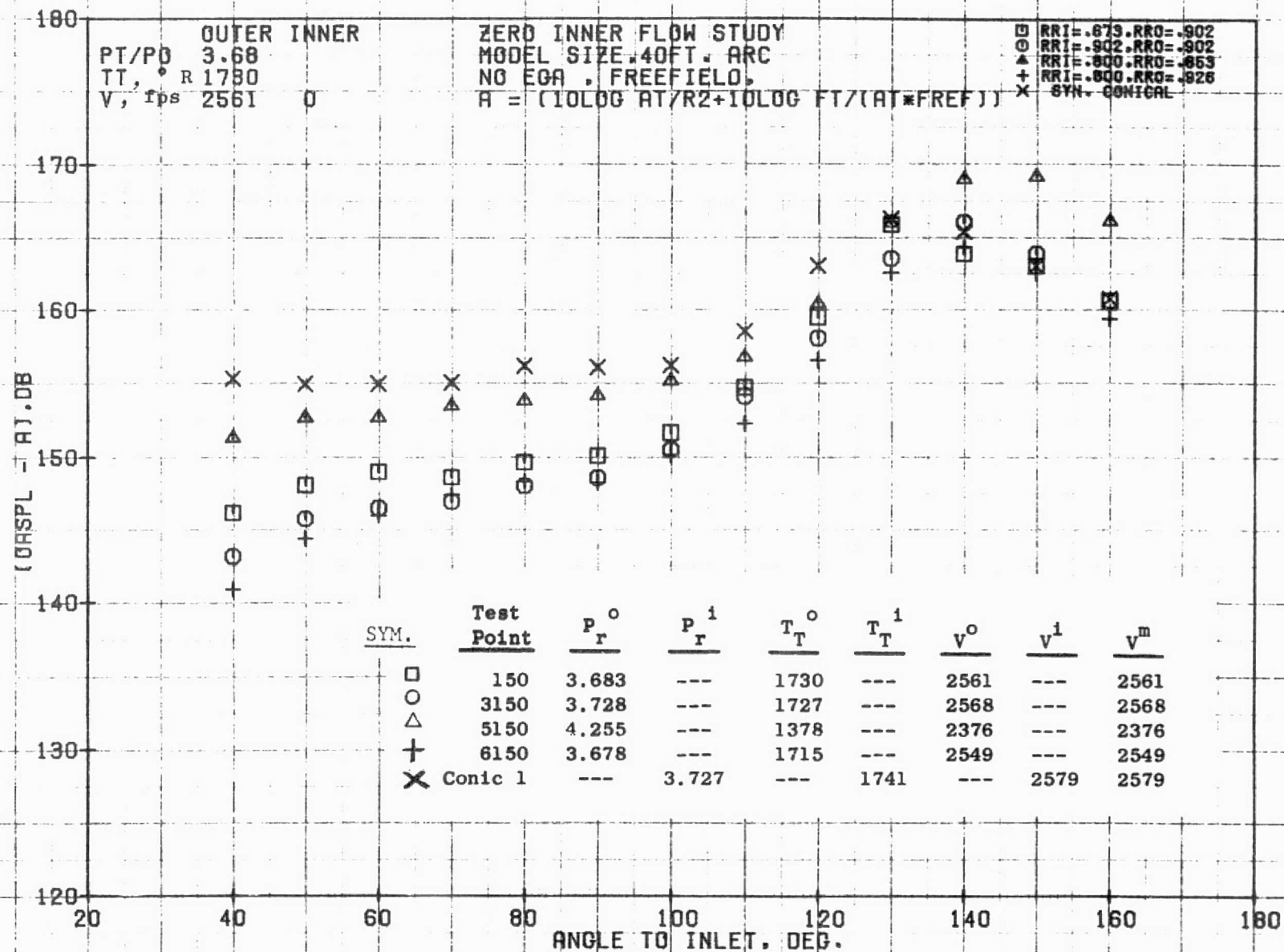
7.3.1 Zero Inner Flow Study

For configurations 1, 3, 5, and 6, acoustic measurements were made with no inner flow. For configurations 1 and 3 the outer radius ratio was 0.902 while for configurations 5 and 6, it was 0.853 and 0.926, respectively. The effect of the outer radius ratio on noise levels with zero inner flow is demonstrated in the following plots.



10/25/76
1X898-001

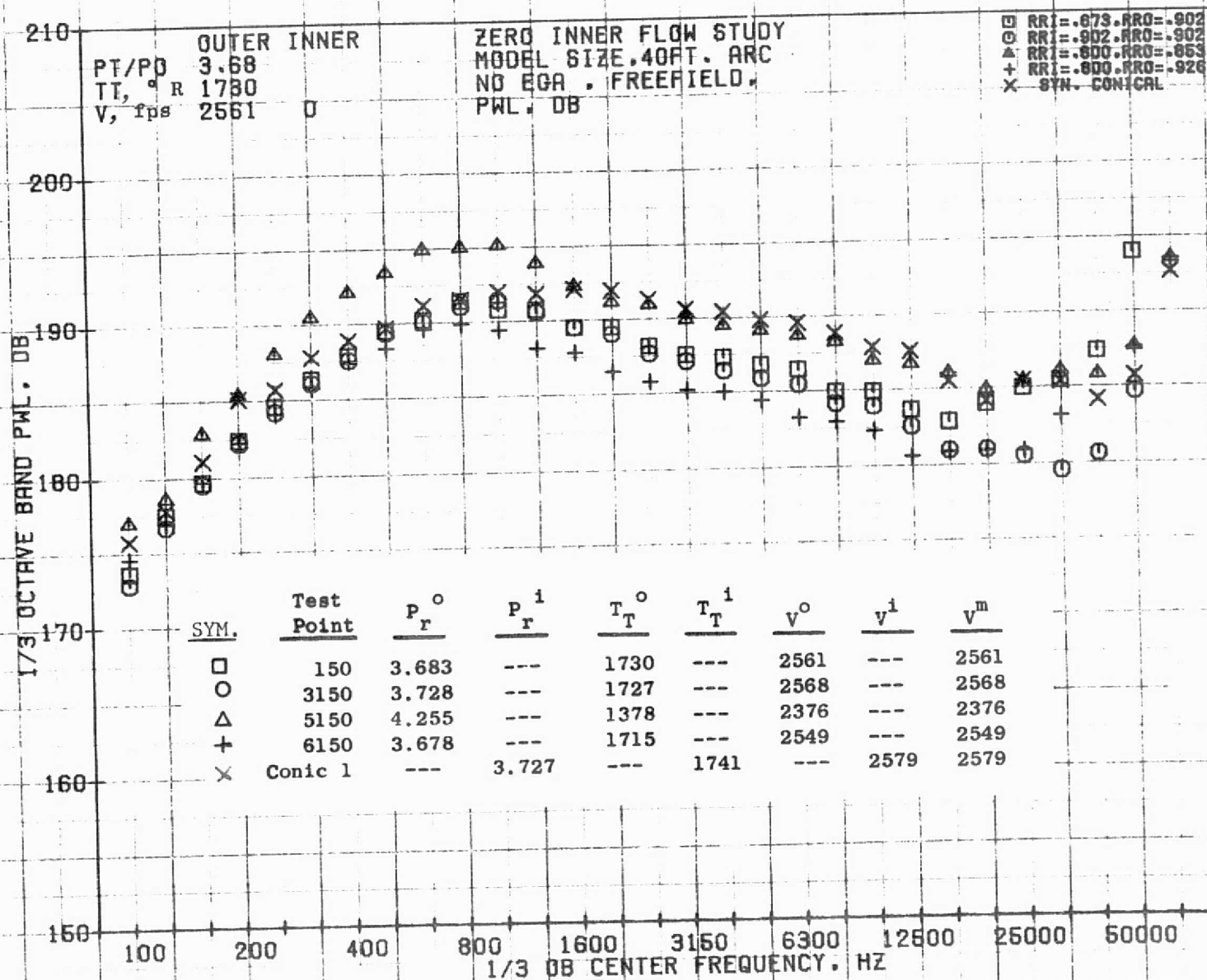
73KOLLSTEDT



10/12/76
1X409-001

73KOLLSTEDT

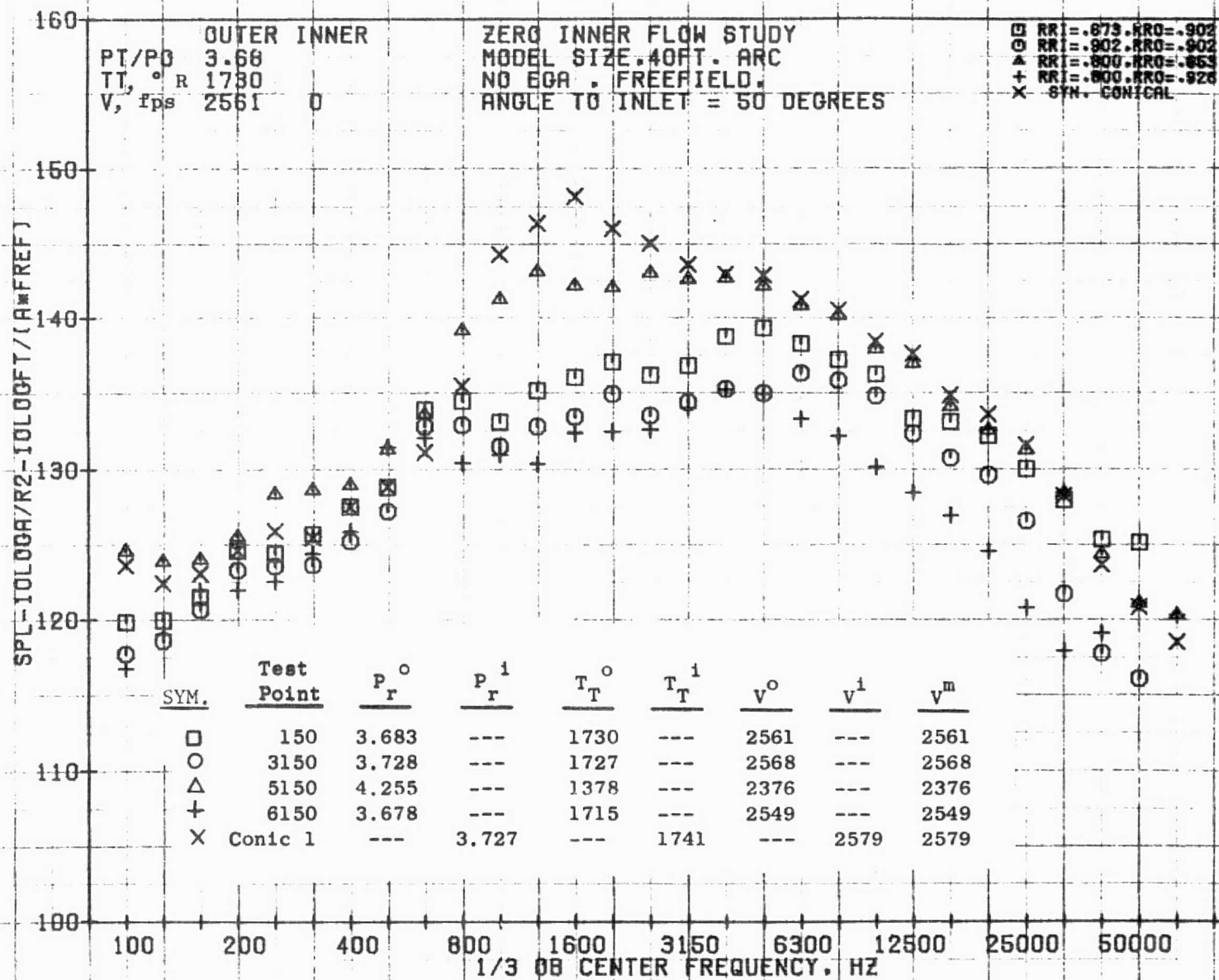
789



10/12/76
1X409-001

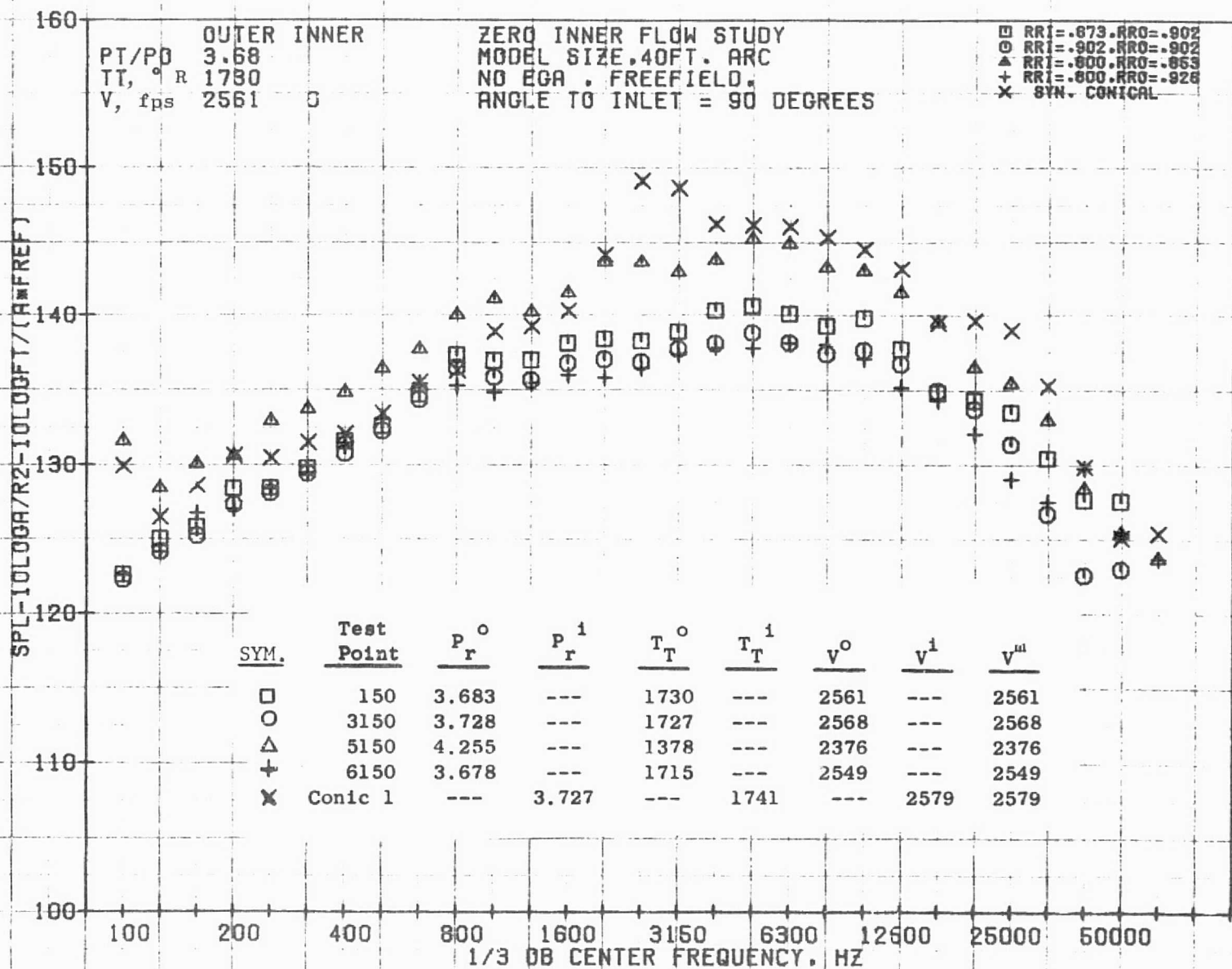
73KOLLSTEDT

790


 10/12/76
 1X409-001

73KOLLSTEDT

791

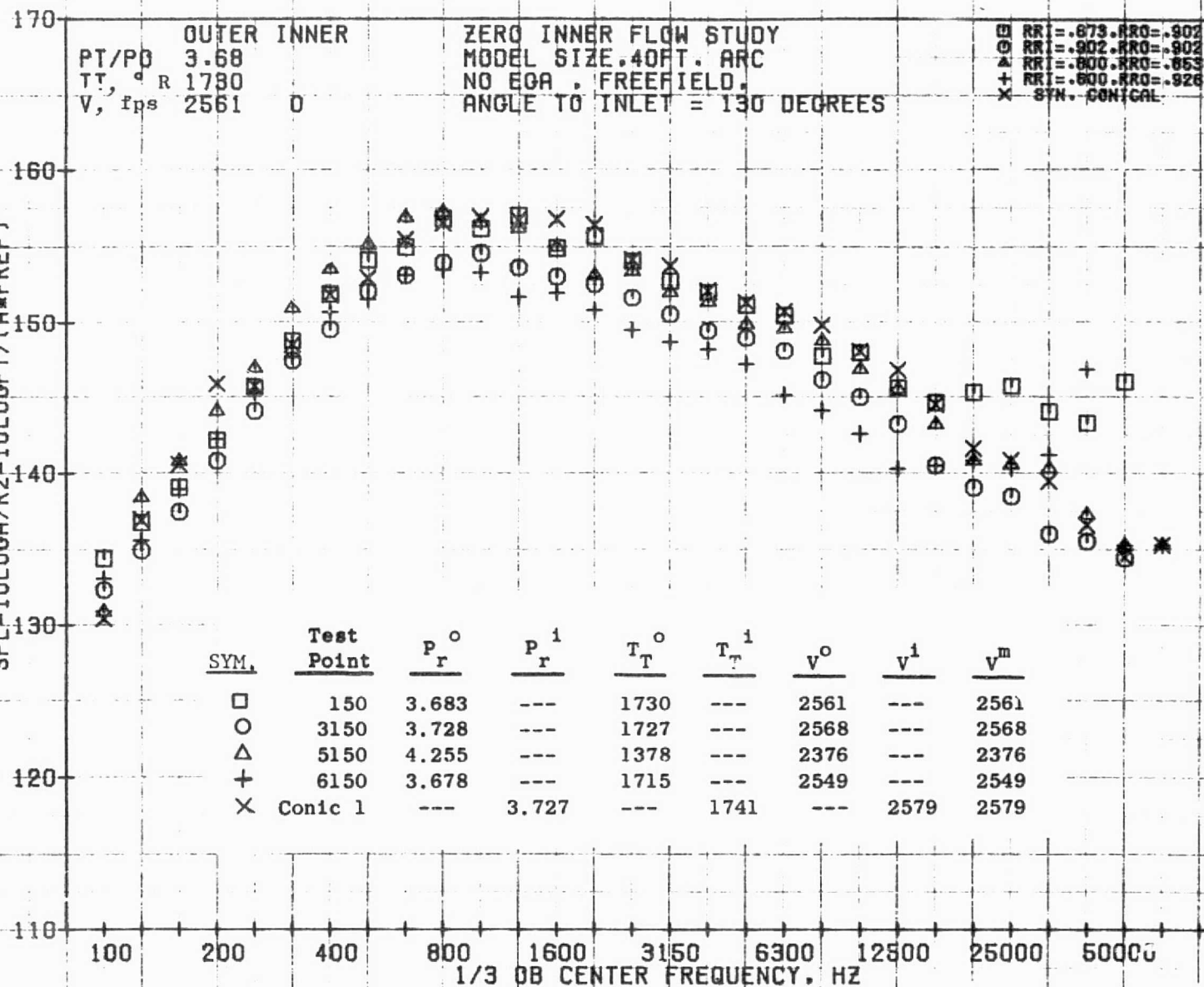


10/12/76
1X409-001

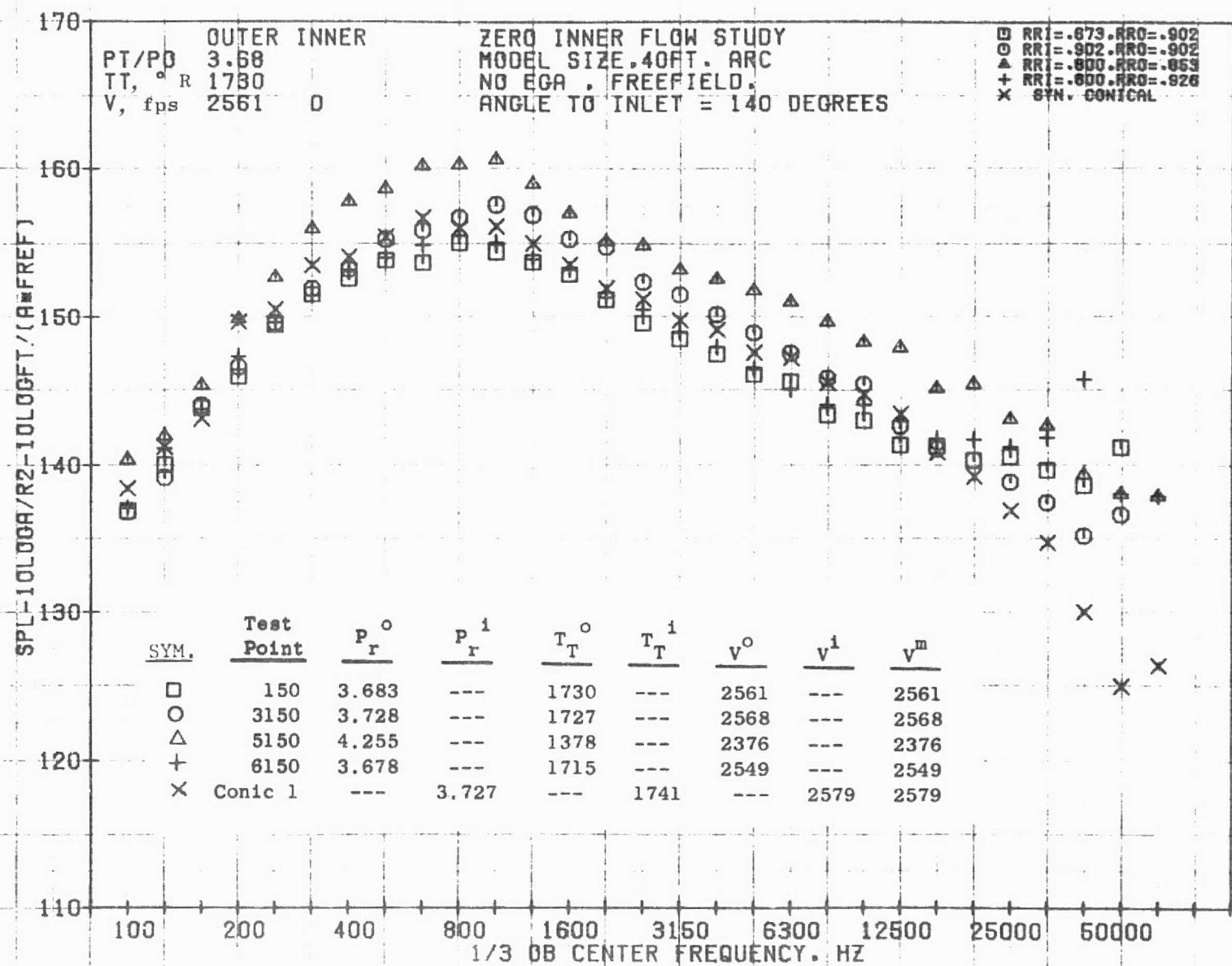
73KOLLSTEST

792

SPL-10LOGH/R2-10LOGT/(H*FREF)

10/12/76
1X409-001

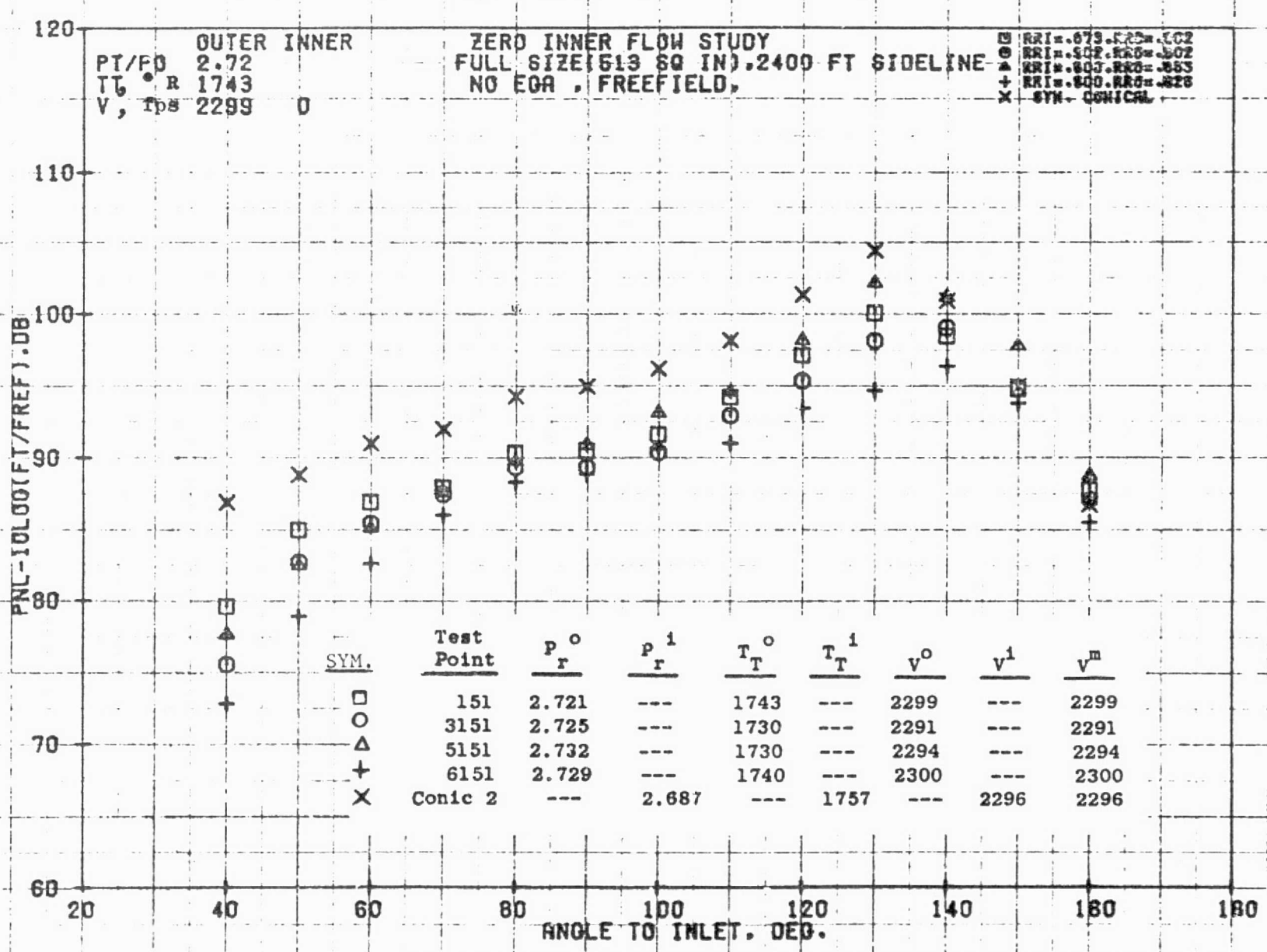
73KOLLSTEDT



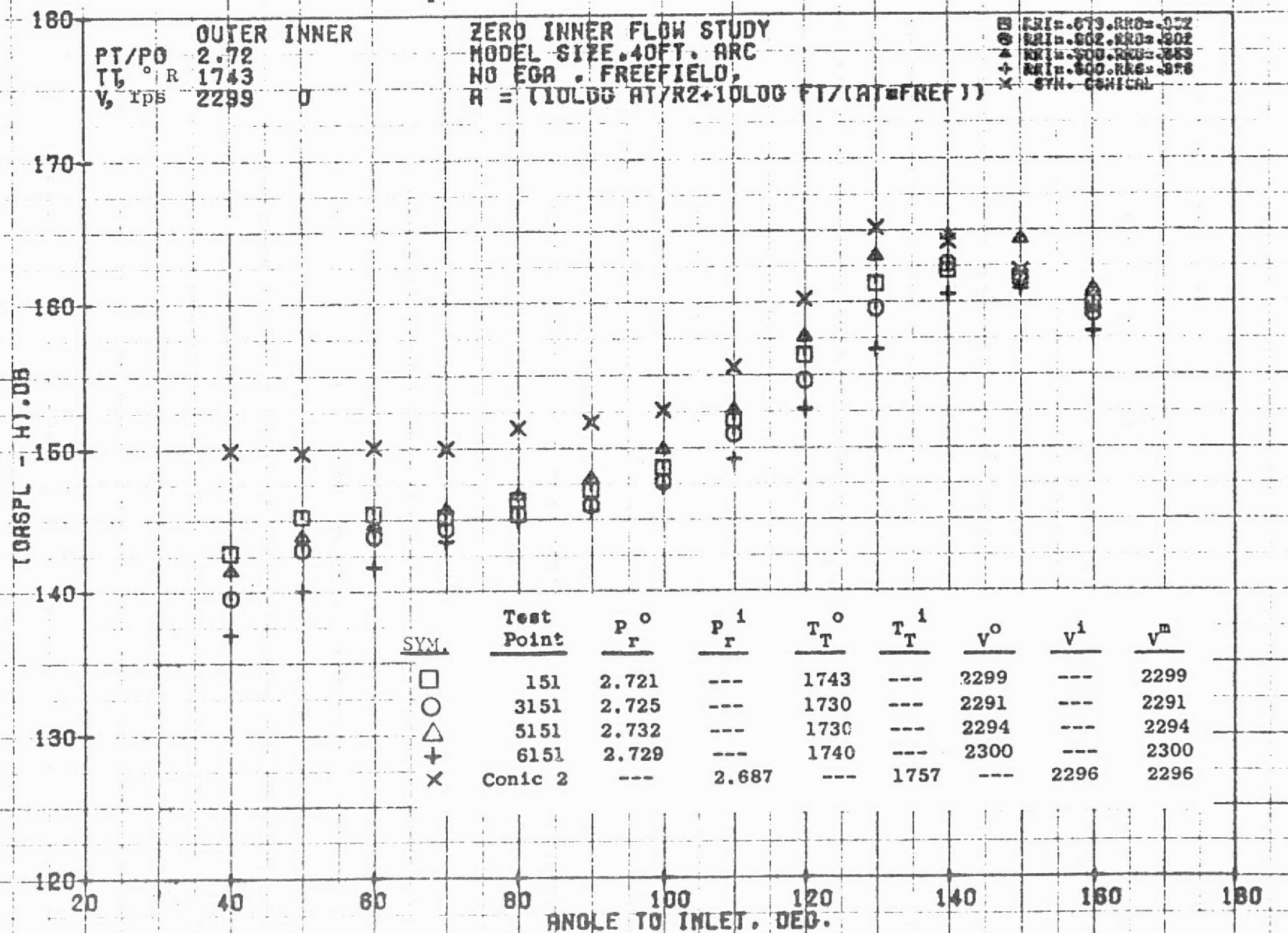
10/12/76
1X409-001

73KOLLSTEDT

761



795



796

1/3 OCTAVE BAND PNL, DB

210

200

190

180

170

160

150

OUTER INNER
 P_i/P_0 2.72
 T_i , °R 1743
 V , fps 2299 0

ZERO INNER FLOW STUDY
 MODEL SIZE .40 FT. ARC
 NO EGA, FREEFIELD.
 PNL, DB

RR1=.878, RR0=.802
 RK1=.802, RK0=.902
 RM1=.800, RM0=.863
 RK1=.800, RK0=.828
 X+46B STM. CONICAL

SYM.	Test Point	P_r^0	P_r^1	T_T^0	T_T^1	V^0	V^1	V^m
□	151	2.721	---	1743	---	2299	---	2299
○	3151	2.725	---	1730	---	2291	---	2291
△	5151	2.732	---	1730	---	2294	---	2294
+	6151	2.729	---	1740	---	2300	---	2300
X	Conic 2	---	2.687	---	1757	---	2296	2296

1/3 DB CENTER FREQUENCY, HZ

100

200

400

800

1600

3150

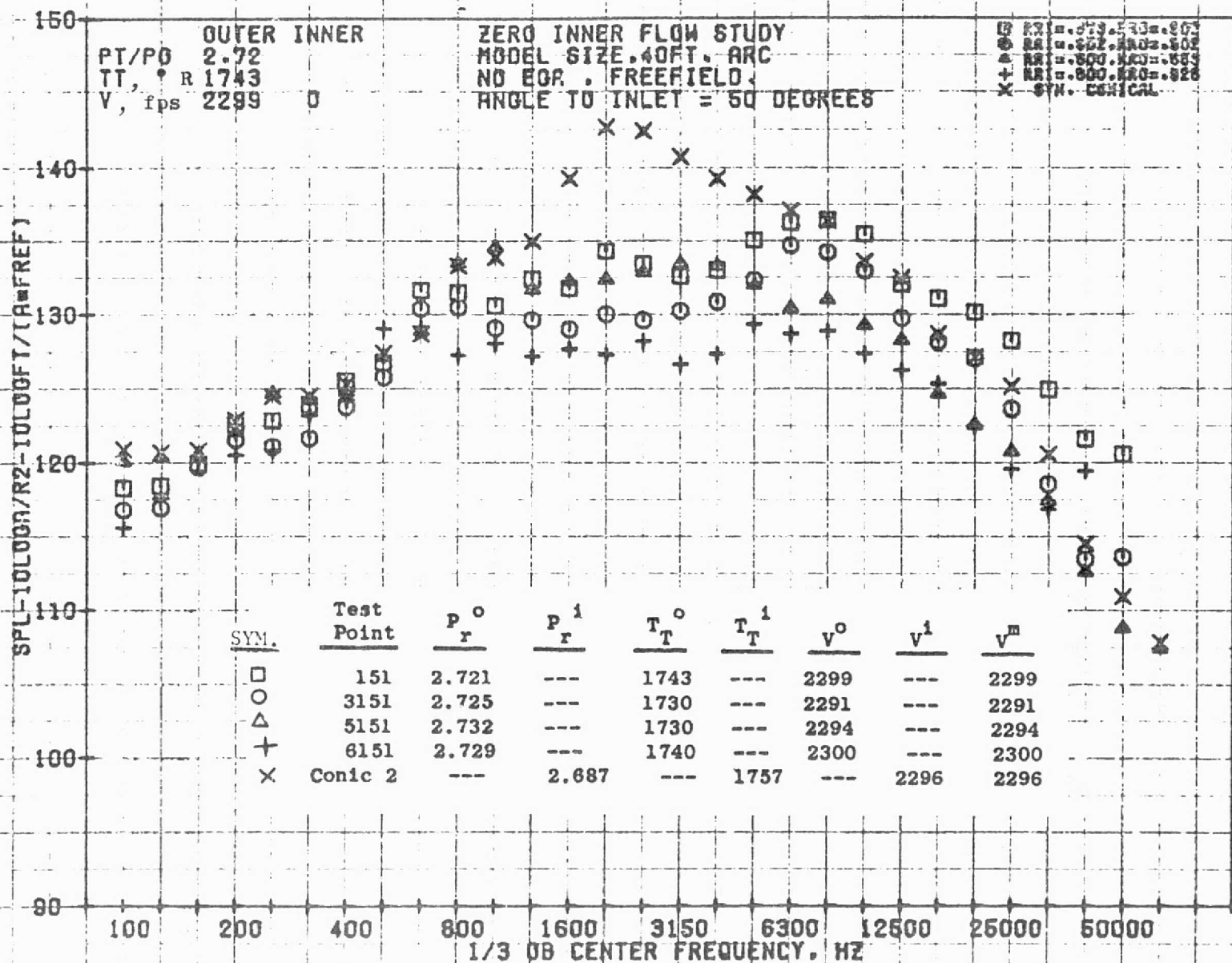
6300

12500

25000

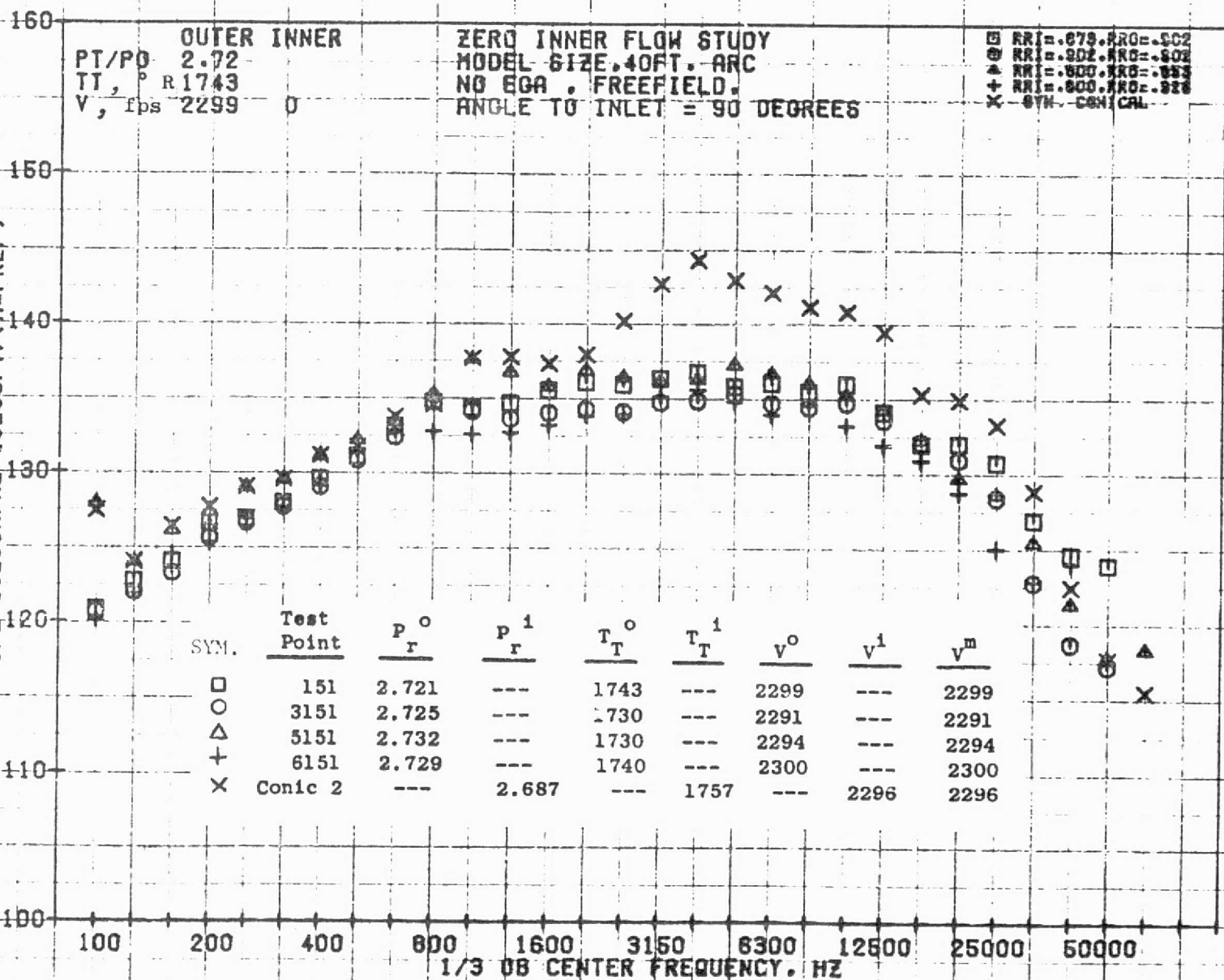
50000

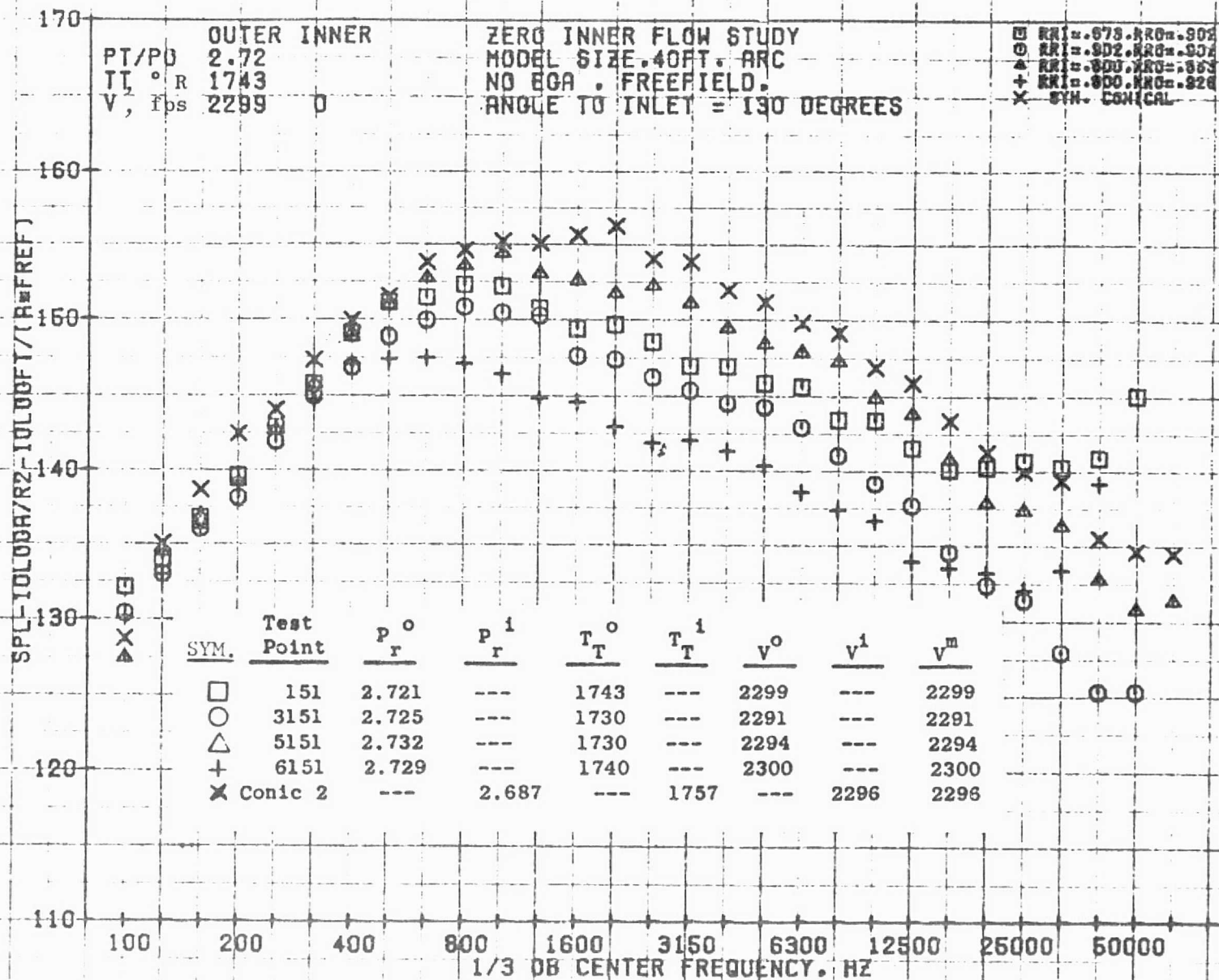
797



782

SPL-10LOGA/R2-10LOGT/(A=REF)





OUTER INNER
 PT/PO 2.72
 TT, °R 1743
 V, fps 2299 0

ZERO INNER FLOW STUDY
 MODEL SIZE, 40FT. ARC
 NO EGA, FREEFIELD
 ANGLE TO INLET = 140 DEGREES

□ RR1=.673,RR2=.638
 ○ RR1=.902,RR2=.902
 △ RR1=.300,RR2=.853
 + RR1=.800,RR2=.928
 X SYN. CONICAL

008

SPL-10LOGA/R2-10LOGFT/(A*REF)

SYM.

Test Point

P_r^0

P_r^1

T_T^0

T_T^1

V^0

V^1

V^m

□
 ○
 △
 +
 X

151
 3151
 5151
 6151
 Conic 2

2.721
 2.725
 2.732
 2.729

 2.687

1743
 1730
 1730
 1740

 1757

2299
 2291
 2294
 2300

 2296

2299
 2291
 2294
 2300
 2296

110

100

200

400

800

1600

3150

6300

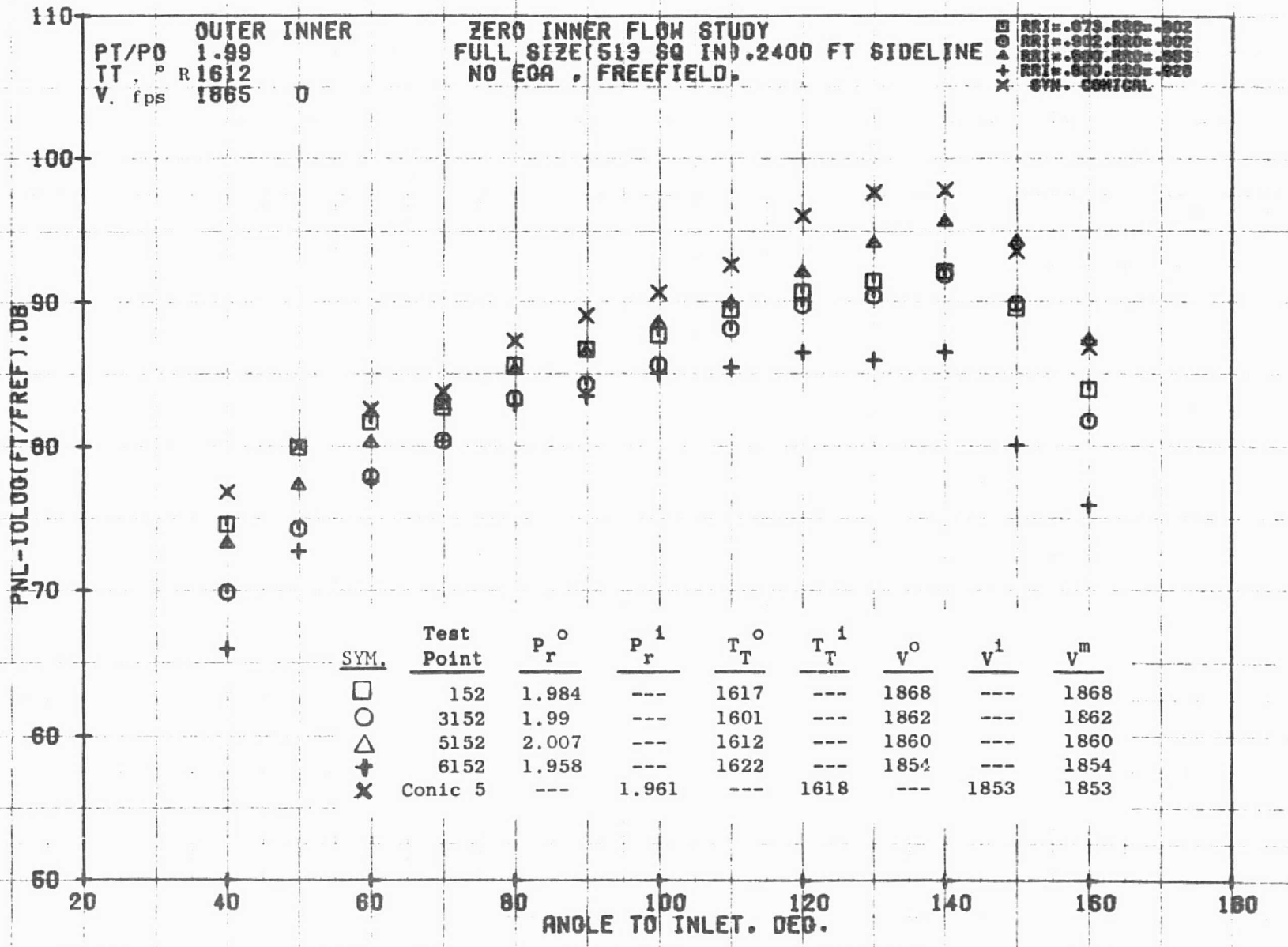
12500

25000

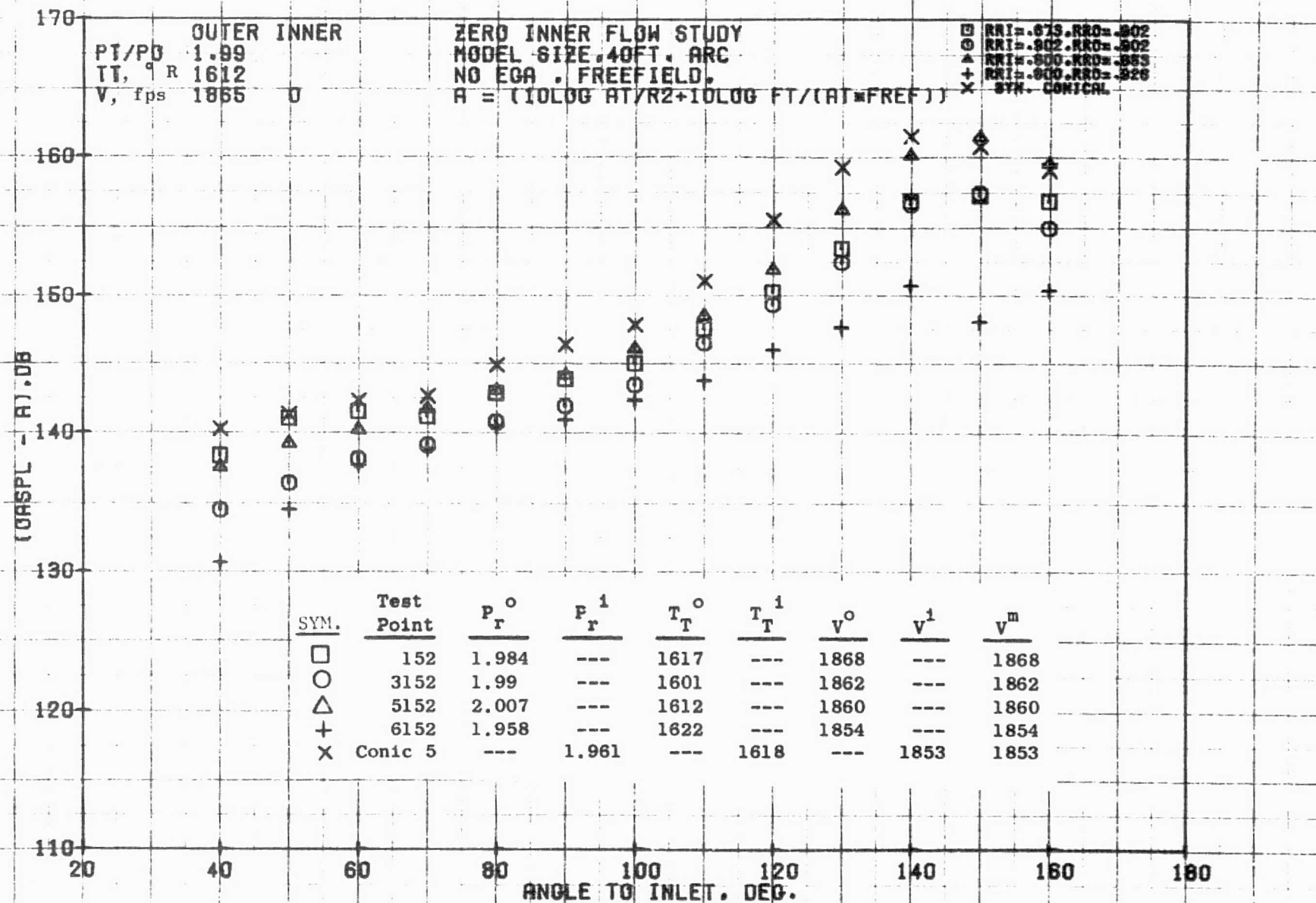
50000

1/3 OB CENTER FREQUENCY, HZ

108



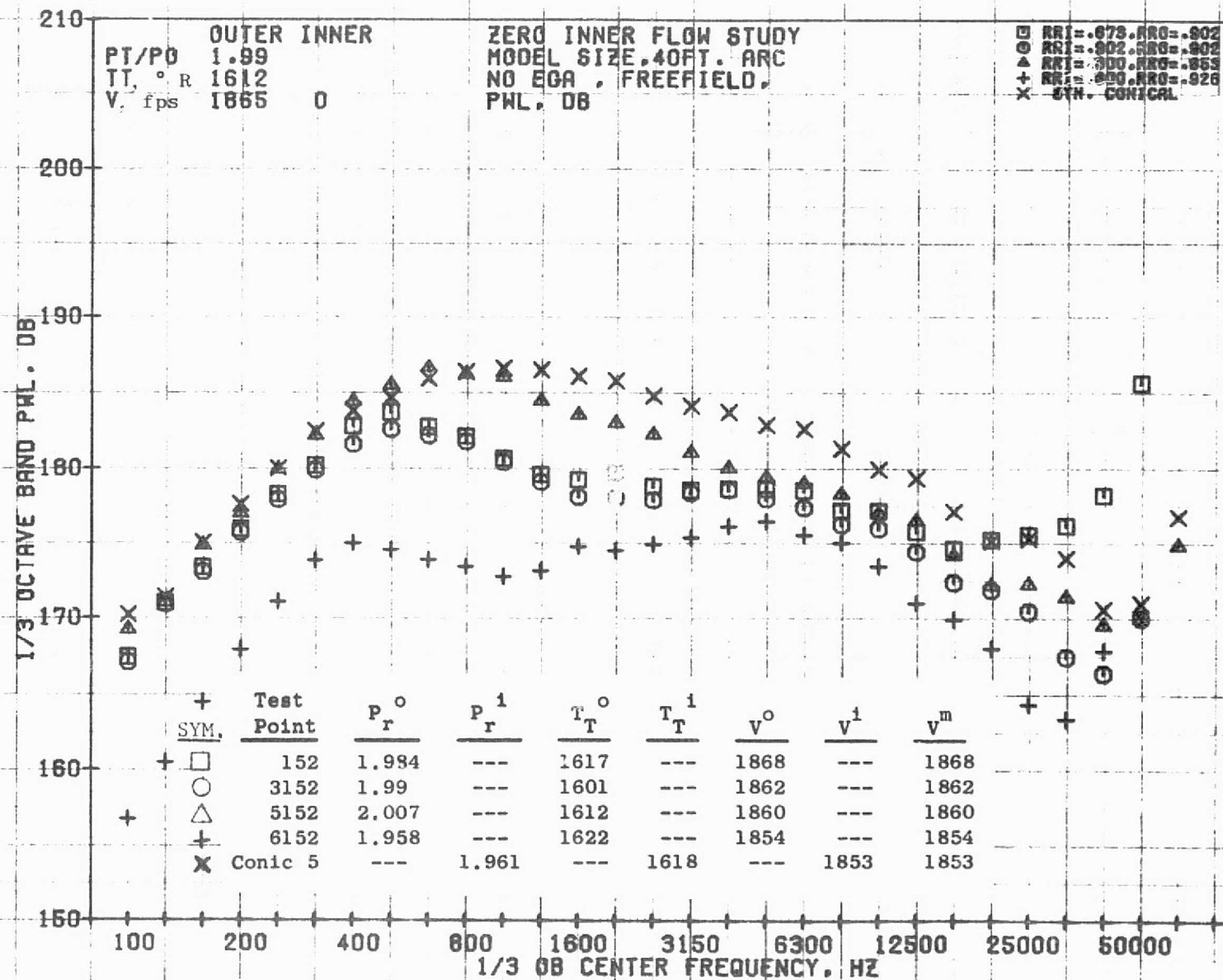
802



10/25/76
1X945-001

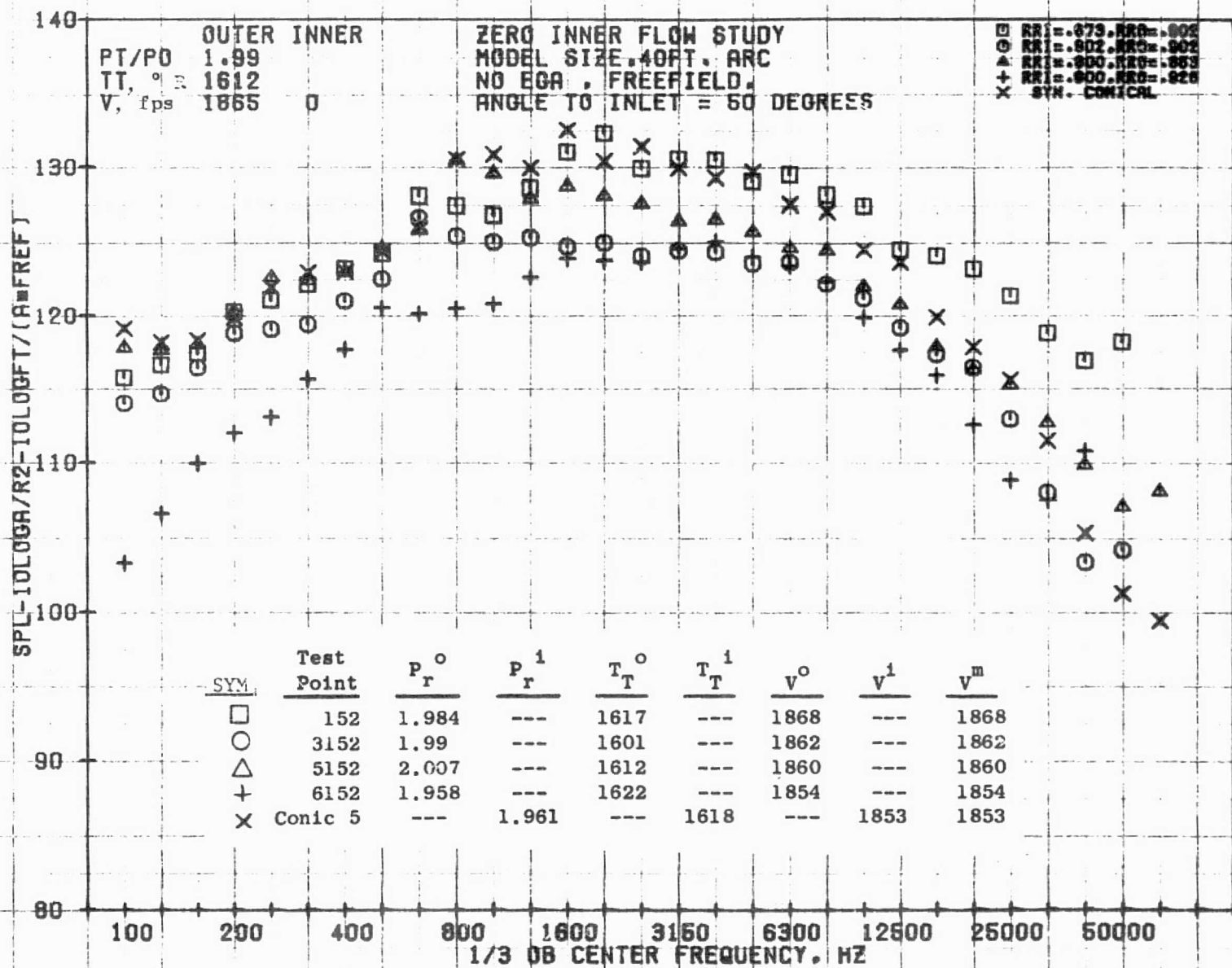
73KOLLSTEDT

803



10/25/76
1X945-001

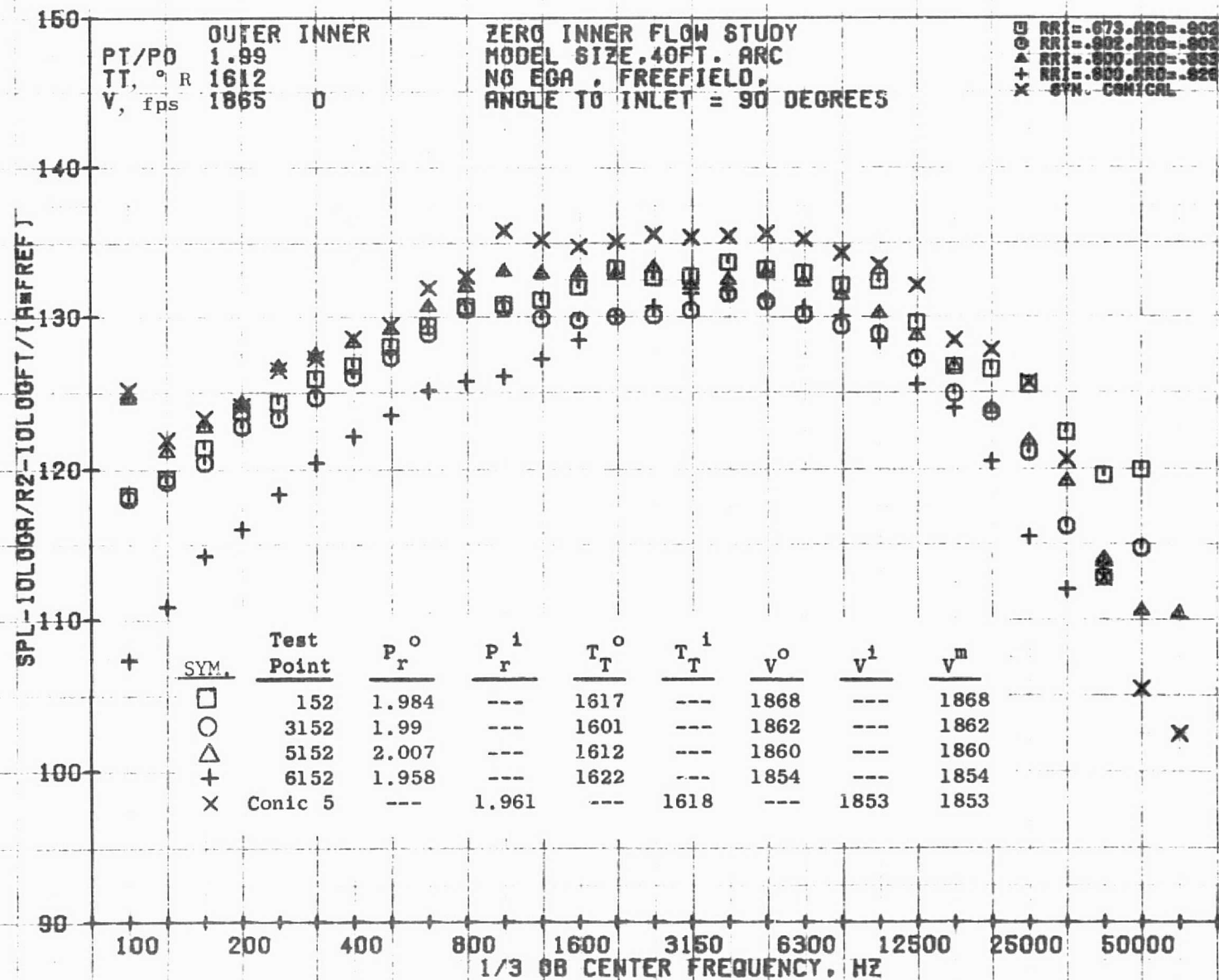
73KOLLSTEDT



10/25/76
1X945-001

73KOLLSTEOT

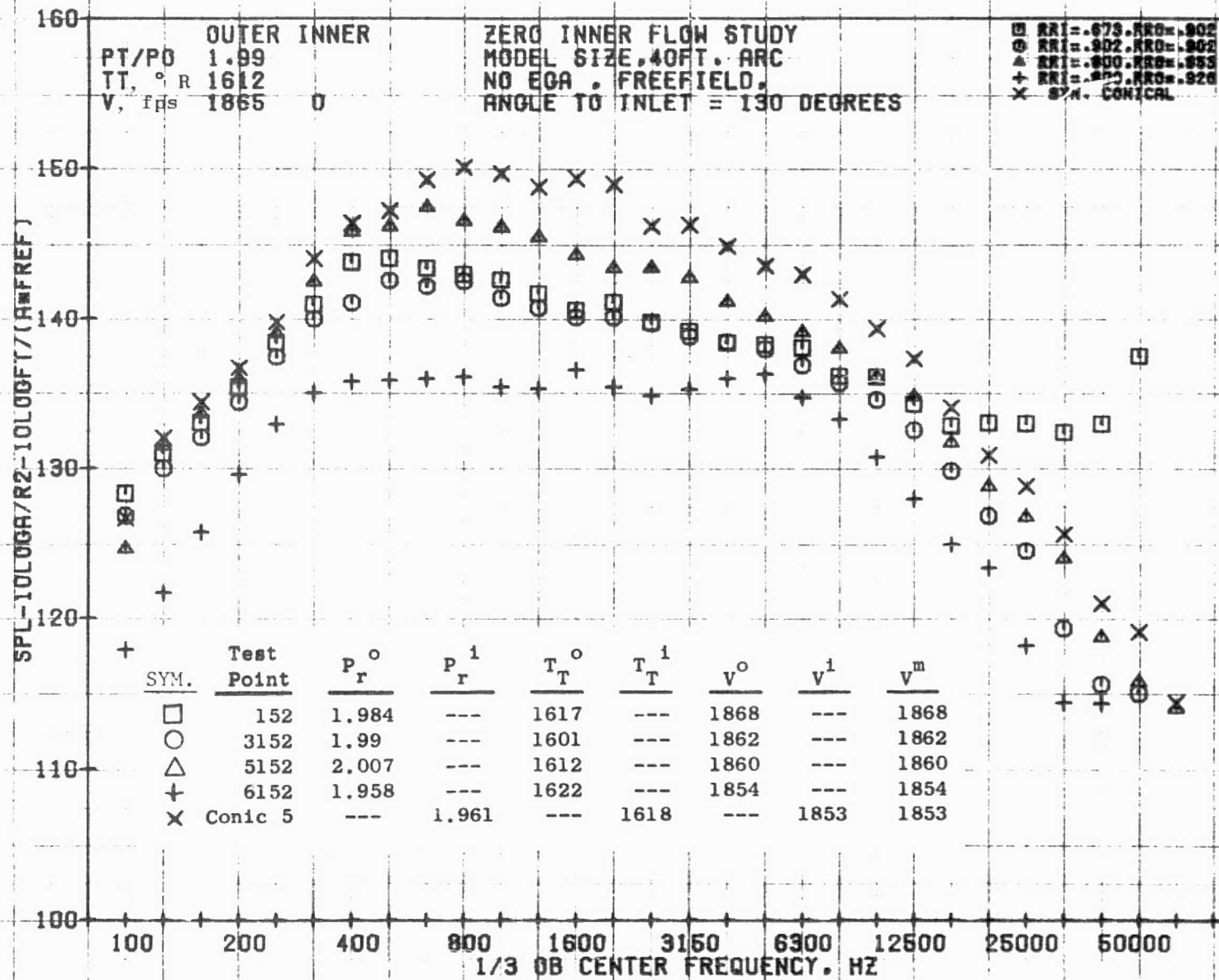
805



10/25/76
1X945-001

73KOLLSTEDT

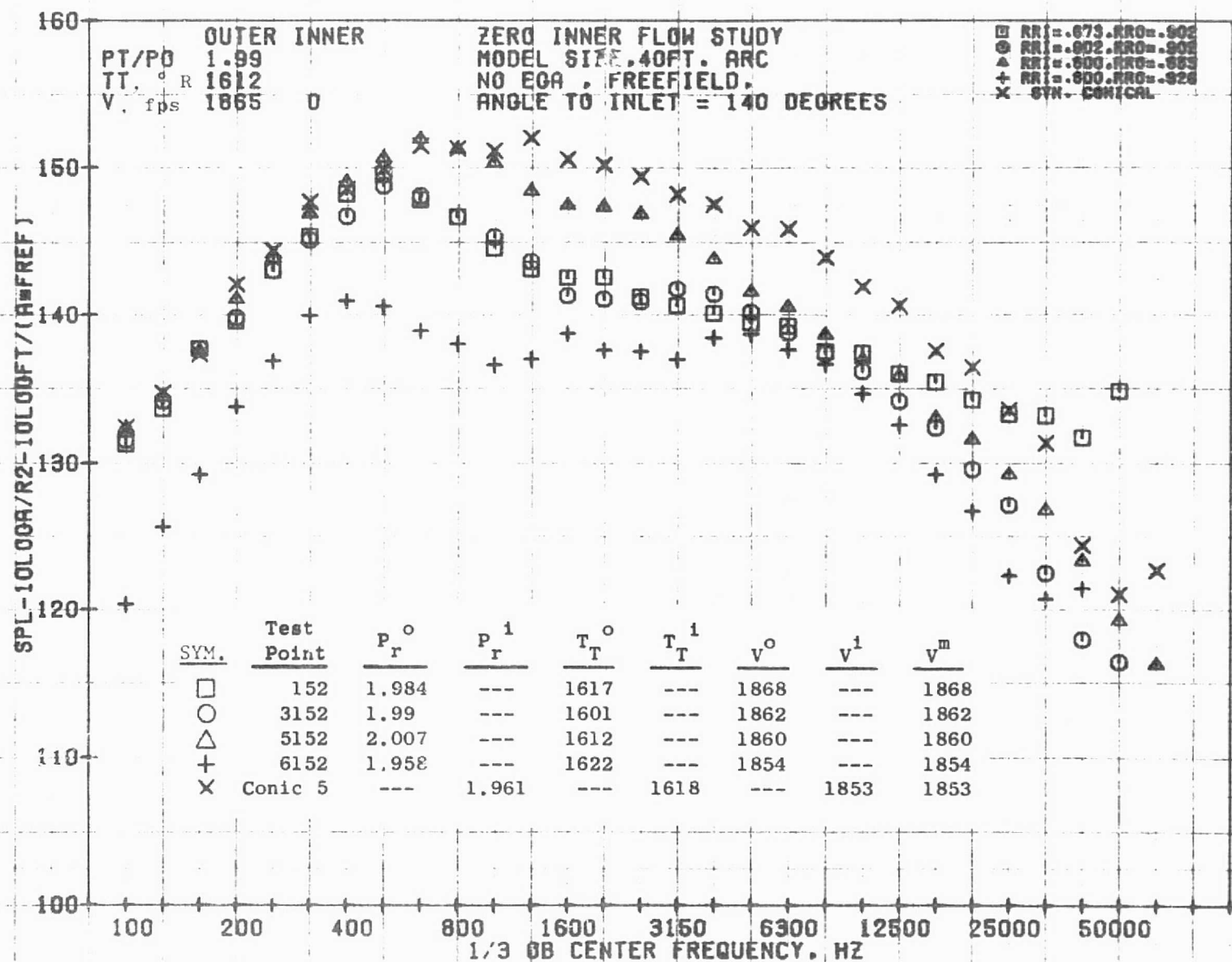
908



10/25/76
1X945-001

73KOLLSTEDT

807



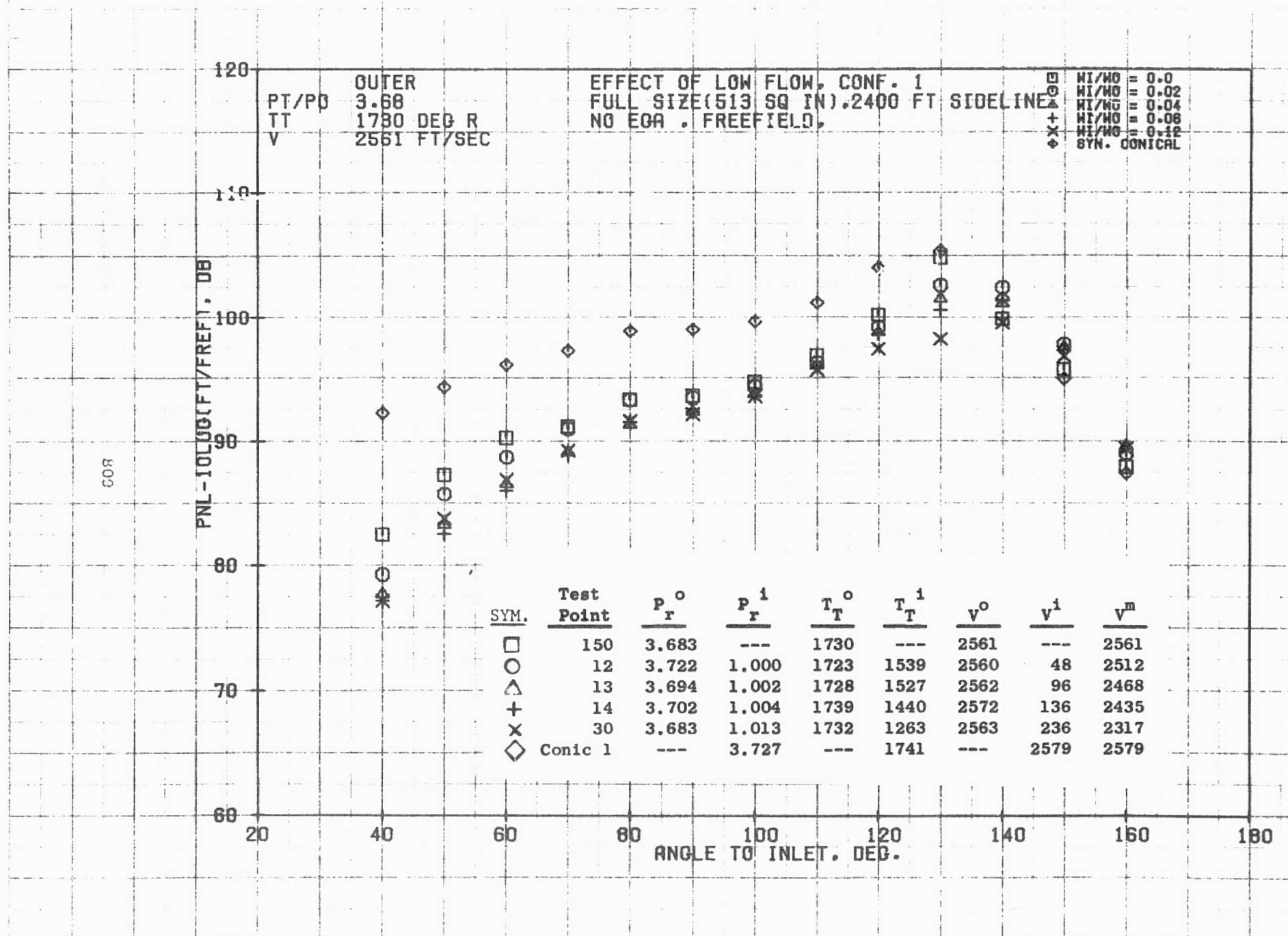
10/25/76
1X945-001

73KOLLSTEOT

7.3.2 Low Inner Flow Study

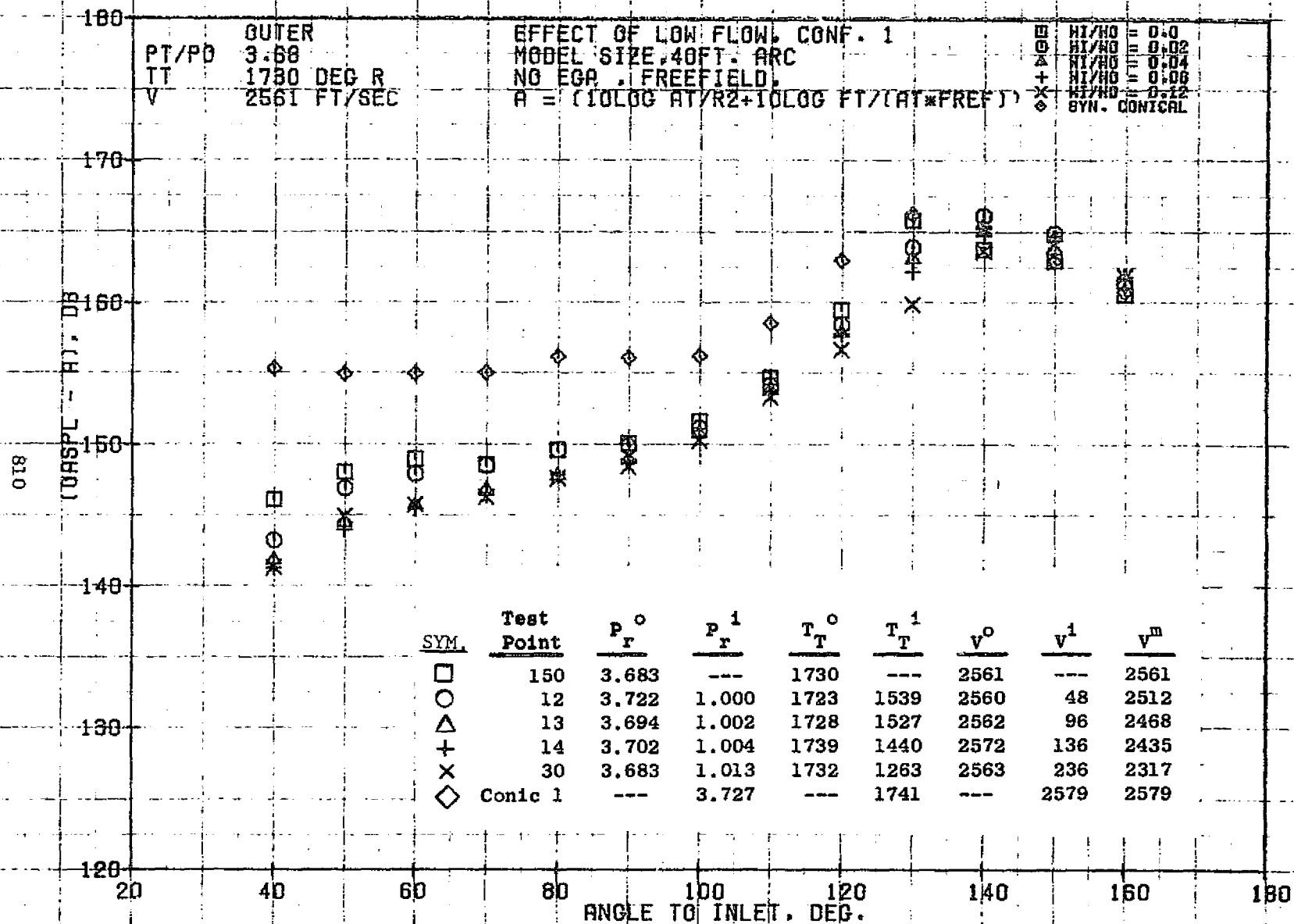
The effect of low inner flows was investigated for configurations 1 and 3. Configurations 1 and 3 both have a 0.902 outer radius ratio, but configuration 1 has a 0.673 inner radius ratio compared to a 0.902 inner radius ratio for configuration 3. Low flow testing was initially performed on configuration 1 at weight flow ratios (W^i/W^o) of 0.02, 0.04, and 0.06. It was found that there was no significant noise suppression relative to the zero inner flow case so higher inner flow rates were tested. Noise suppression was seen at higher flow rates so that for configuration 3 the tests were performed primarily at weight flow ratios of 0.06, 0.09, and 0.12.

The following graphs are based on a variation of W^i/W^o (sometimes expressed as W_8/W_{28}) whereas the Tables 6 and 7 in Volume I used W^i/W_T and W^o/W_T parameters.



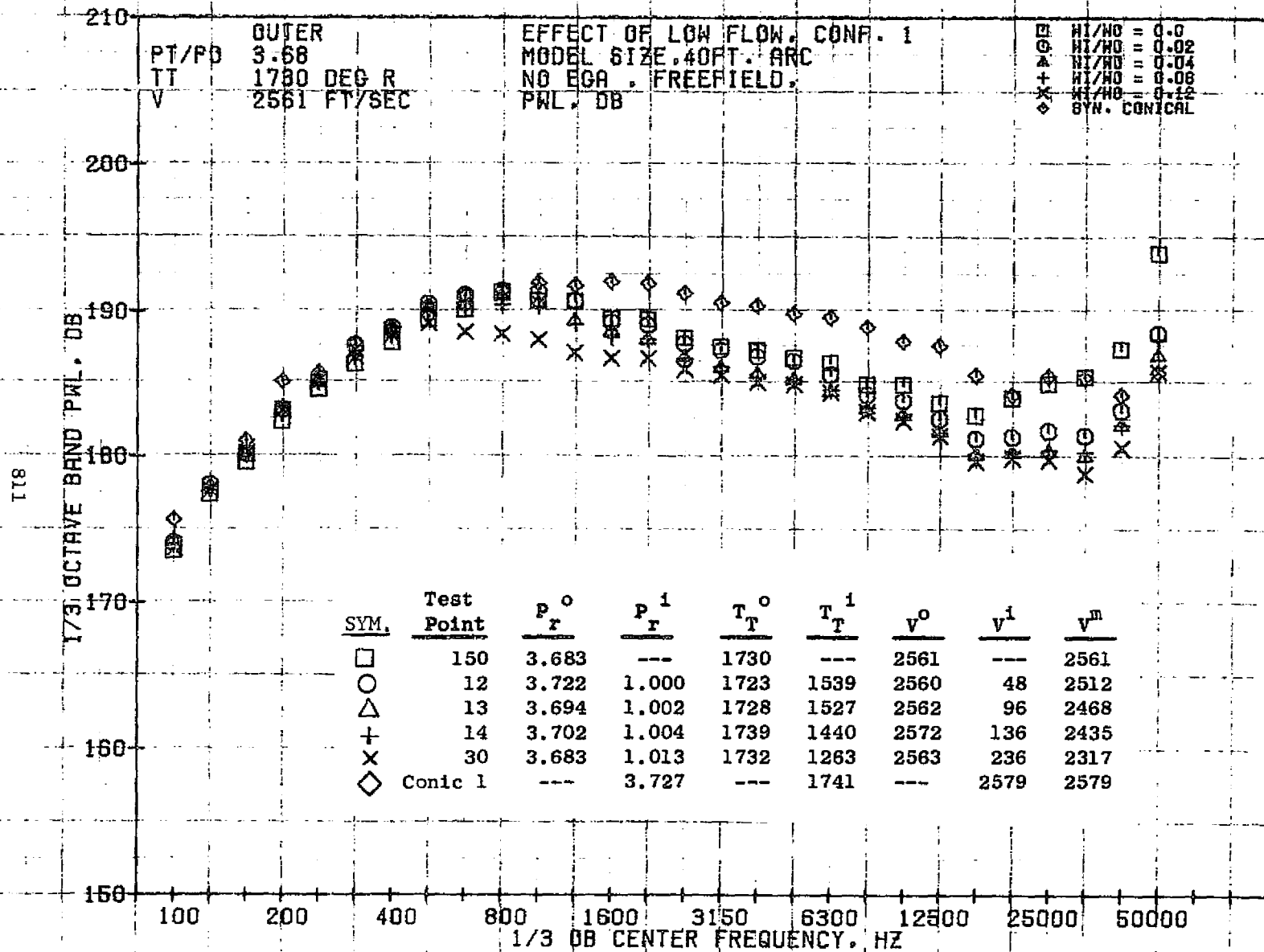
10/25/76
1X285-001

73KOLLSTEDT



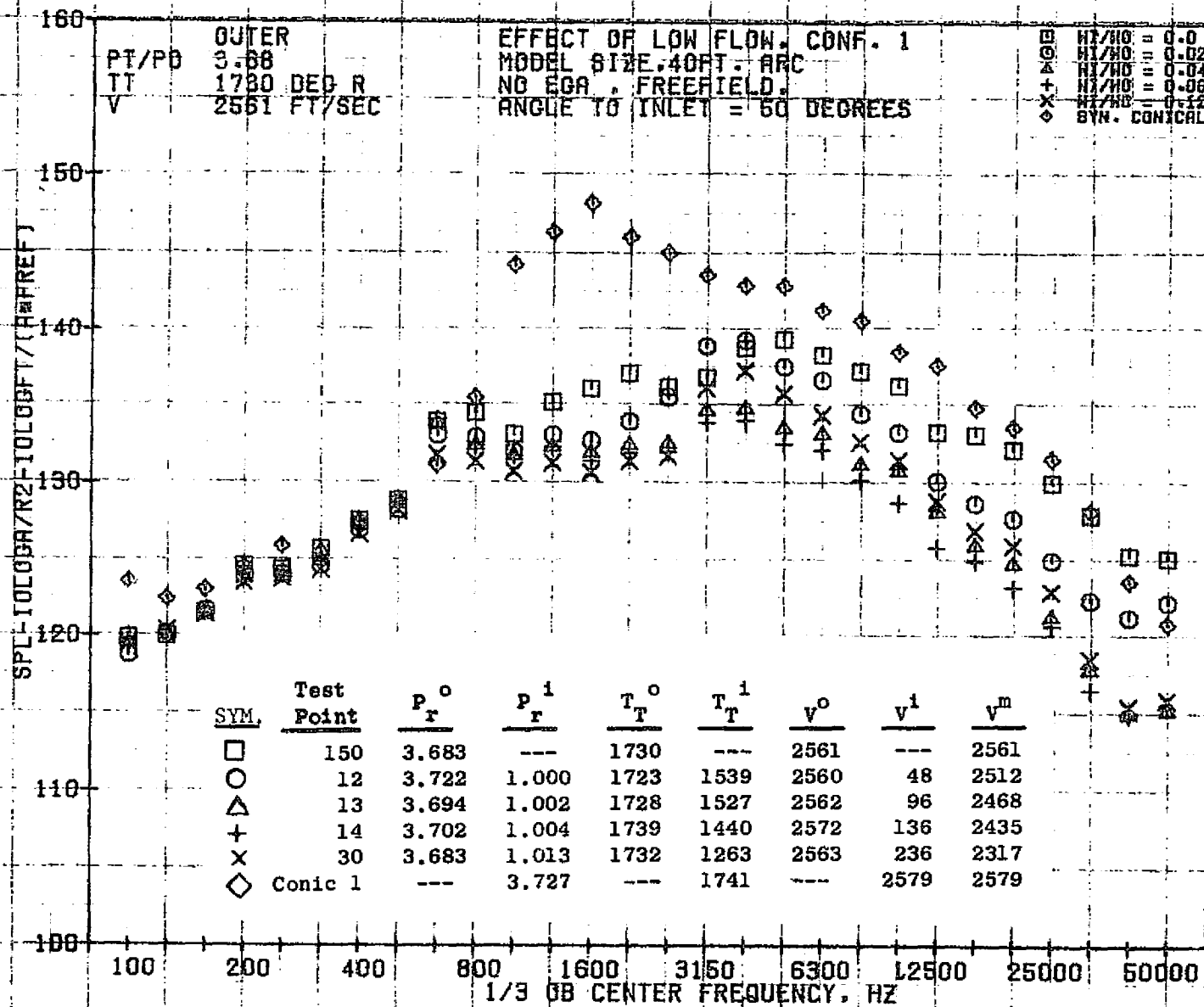
10/06/76
1X583-001

73KOLLSTEDT



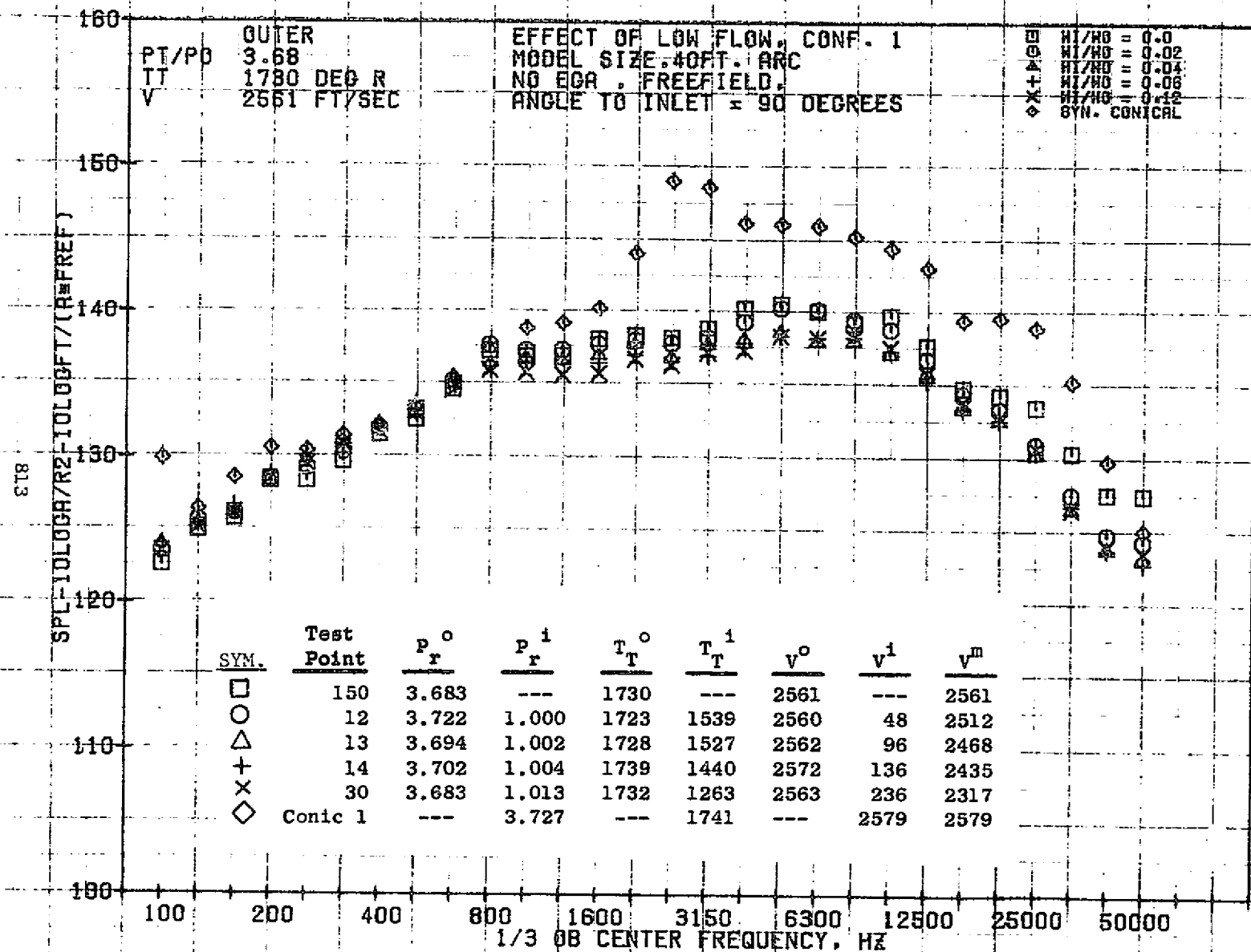
10/05/76
1X583-001

73KOLLSTEDT



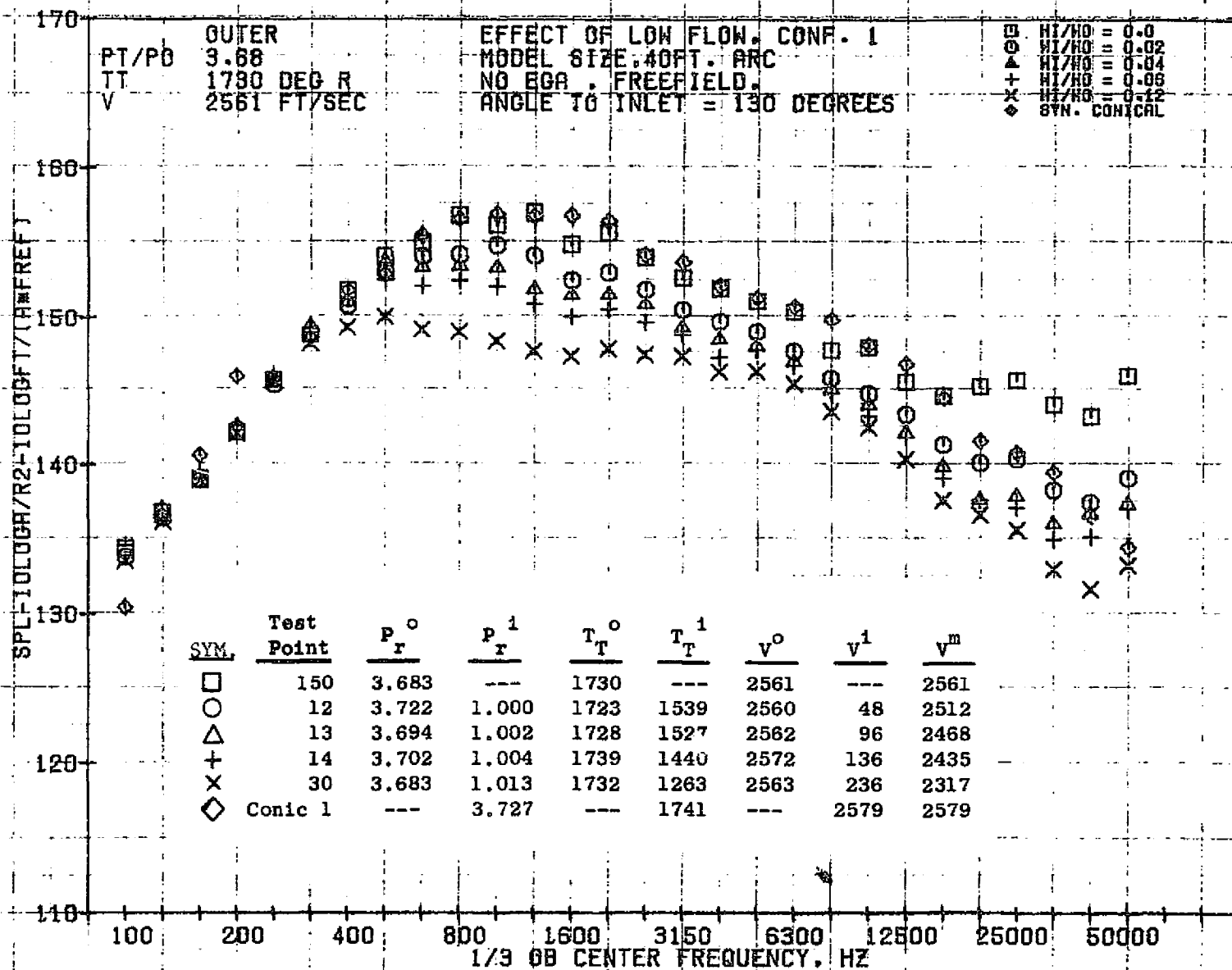
10/06/76
 1X583-001

73KOLLSTEDT



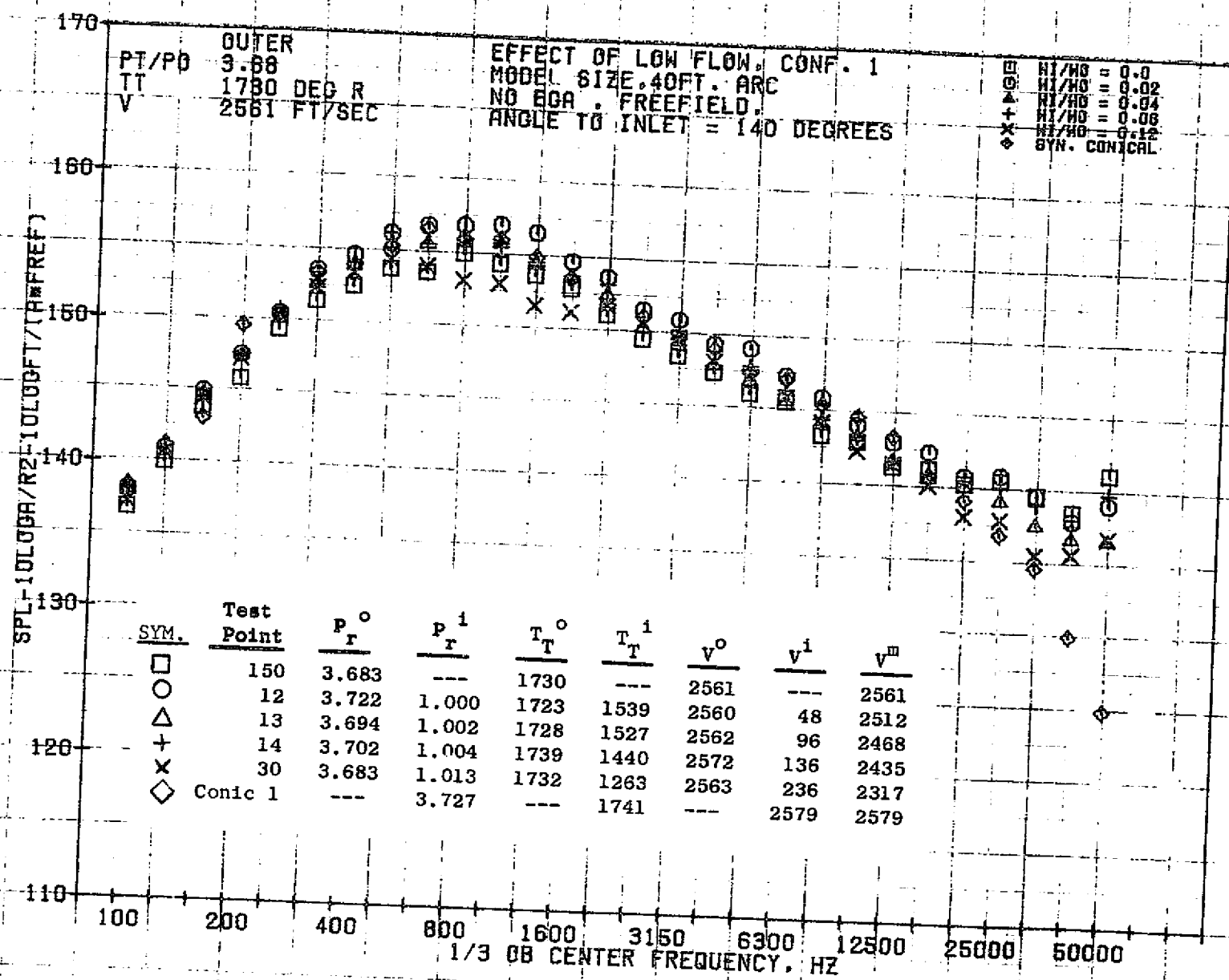
10/05/76
1X583-001

73KOLLSTEDT



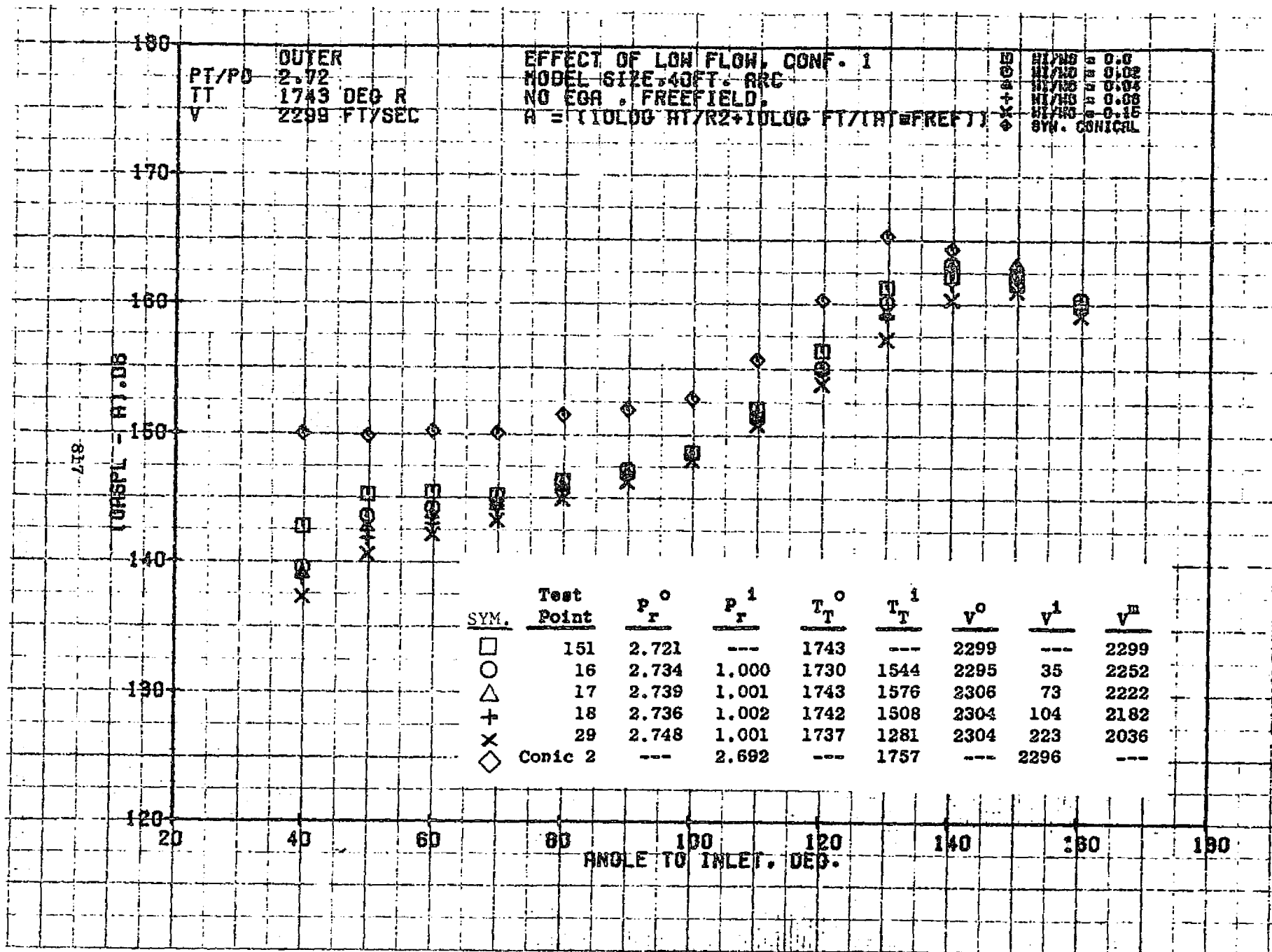
10/05/76
1X583-001

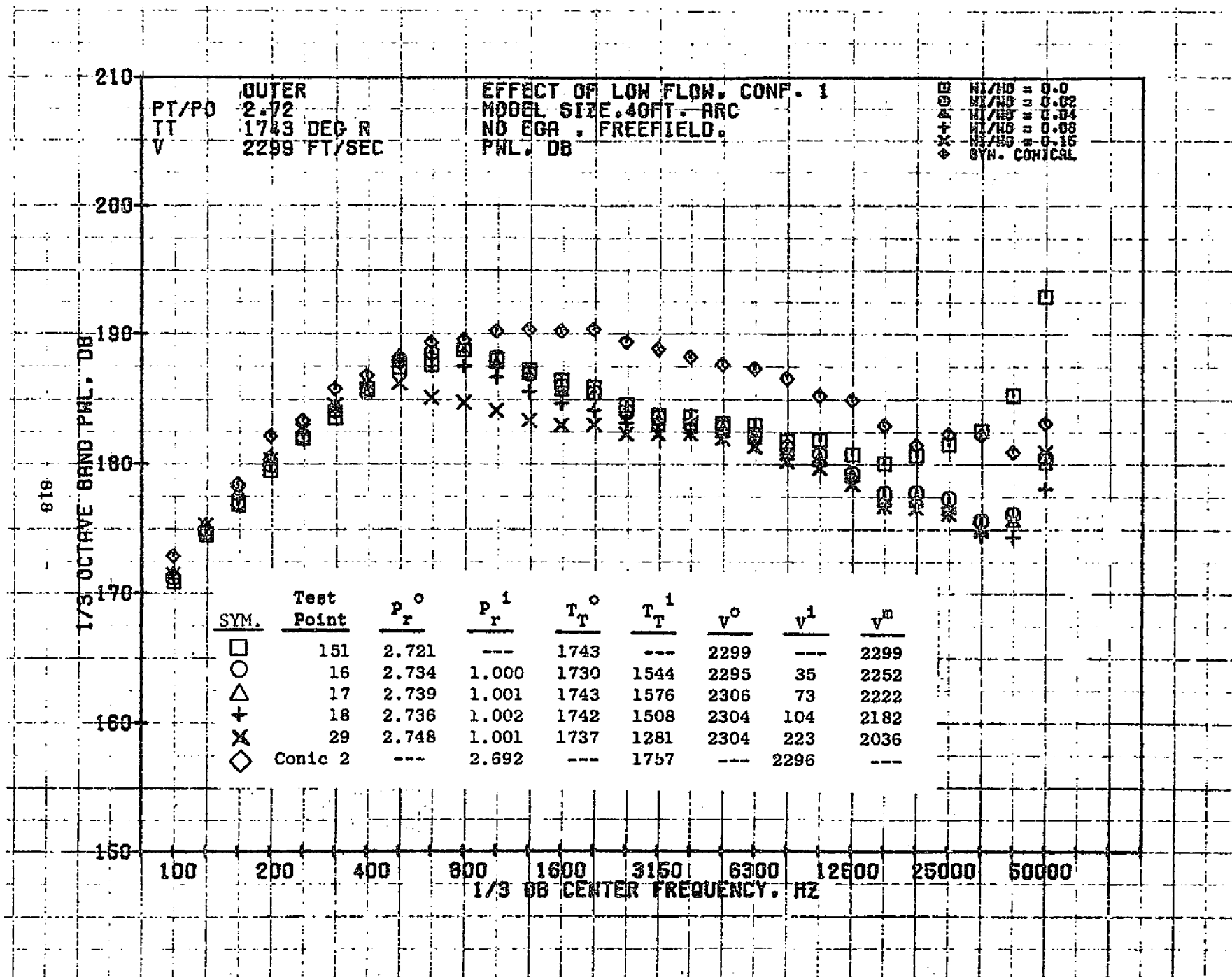
73KOLLSTEDT

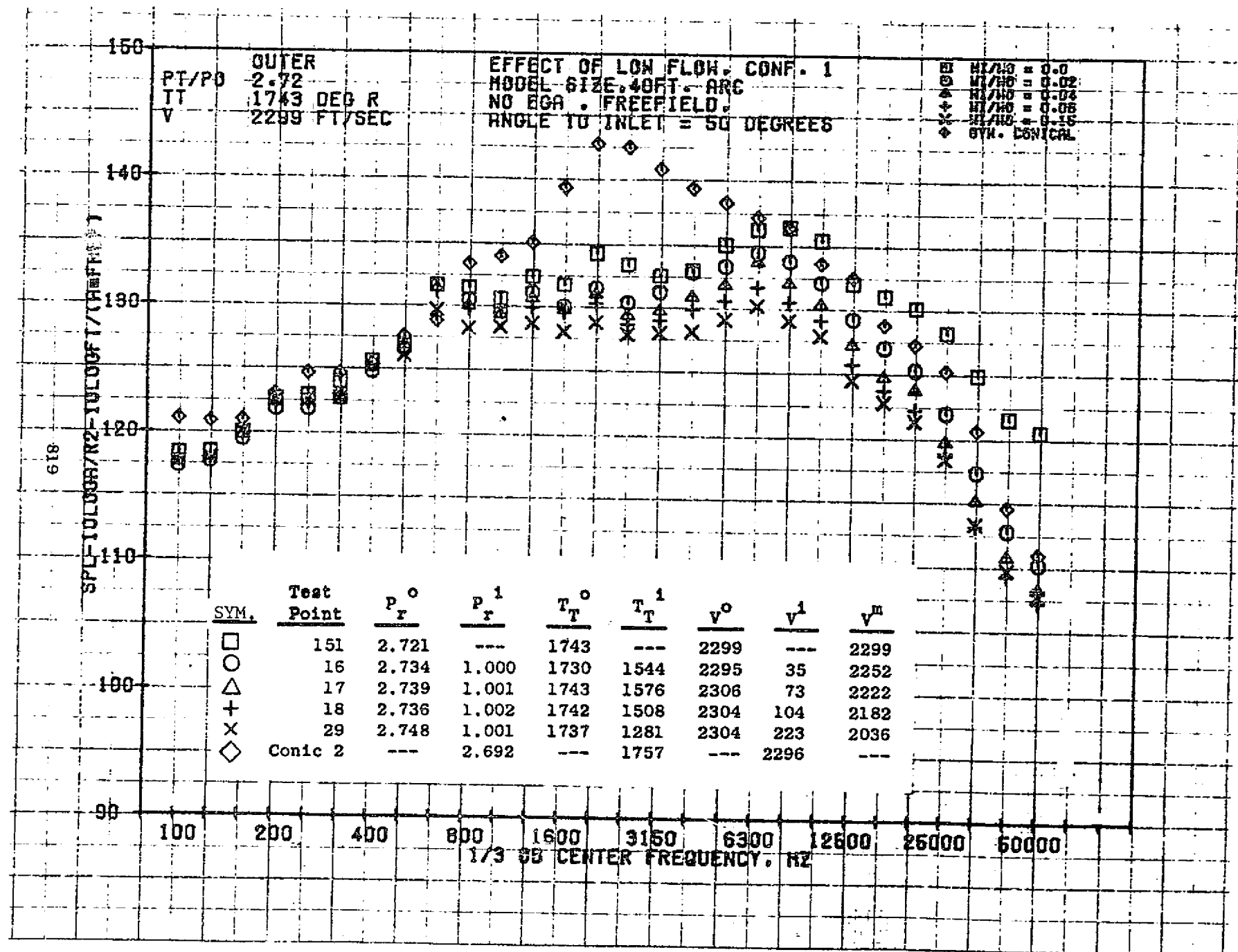


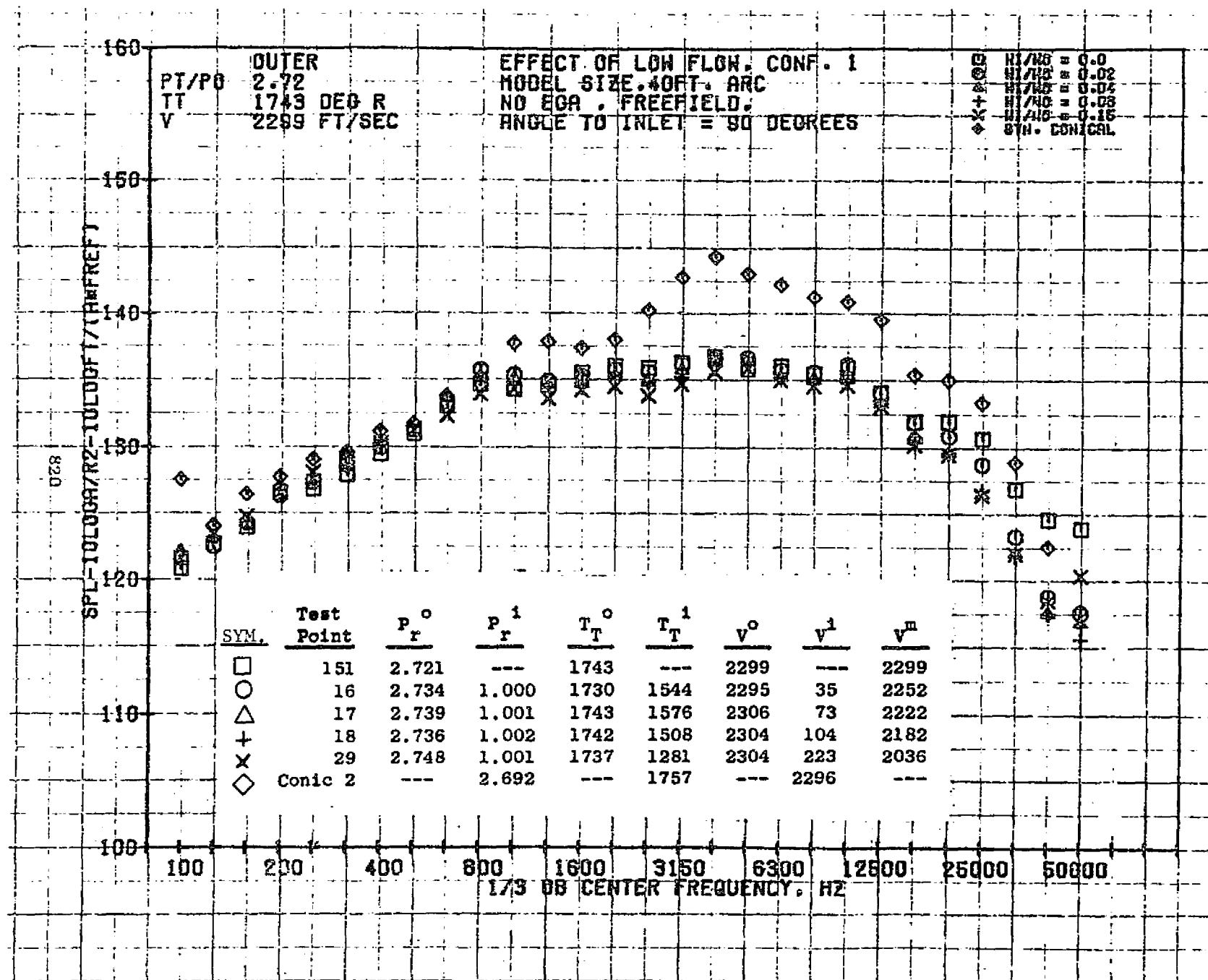
10/05/76
 1X583-001

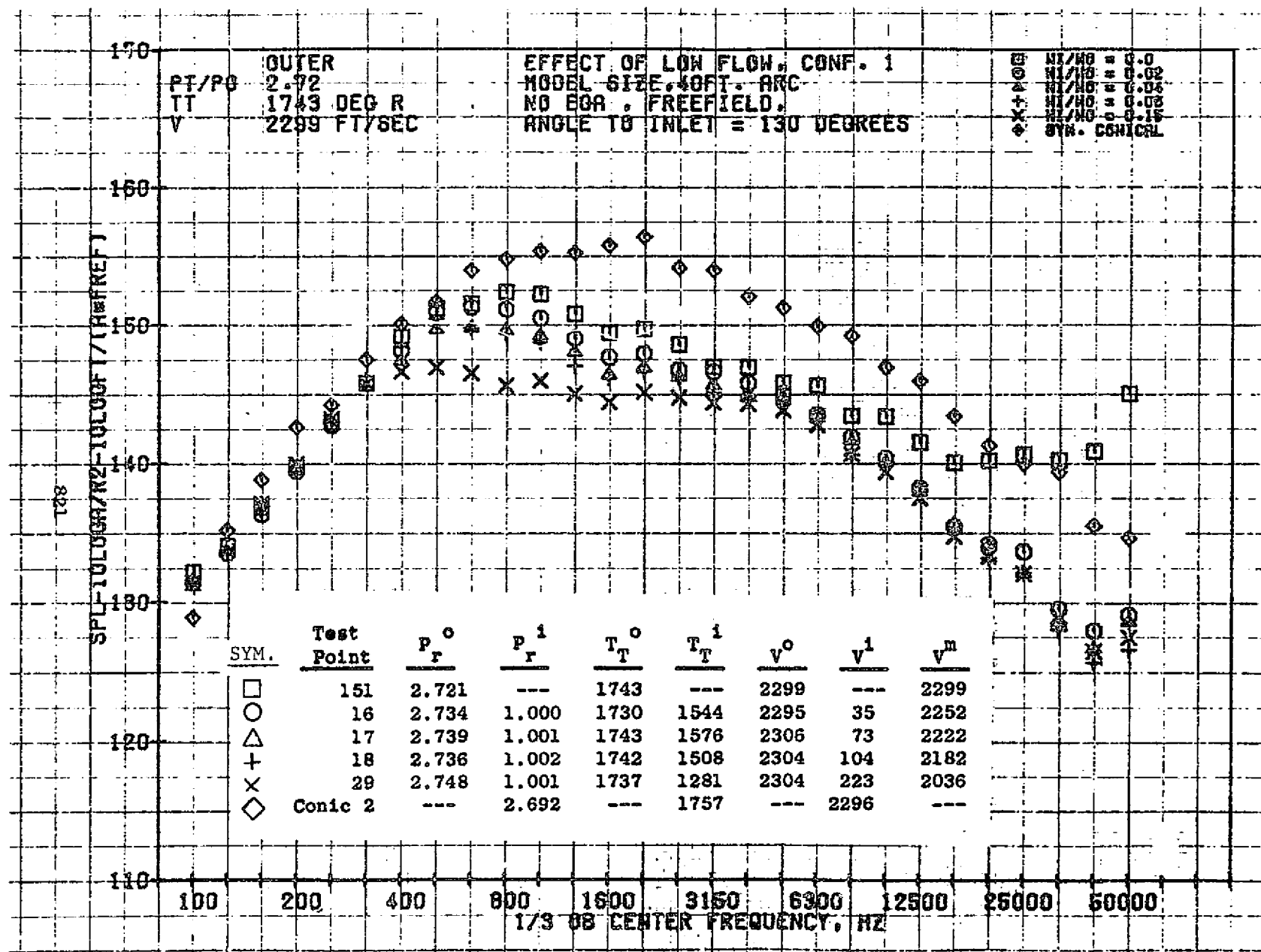
73KOLLSTFDT

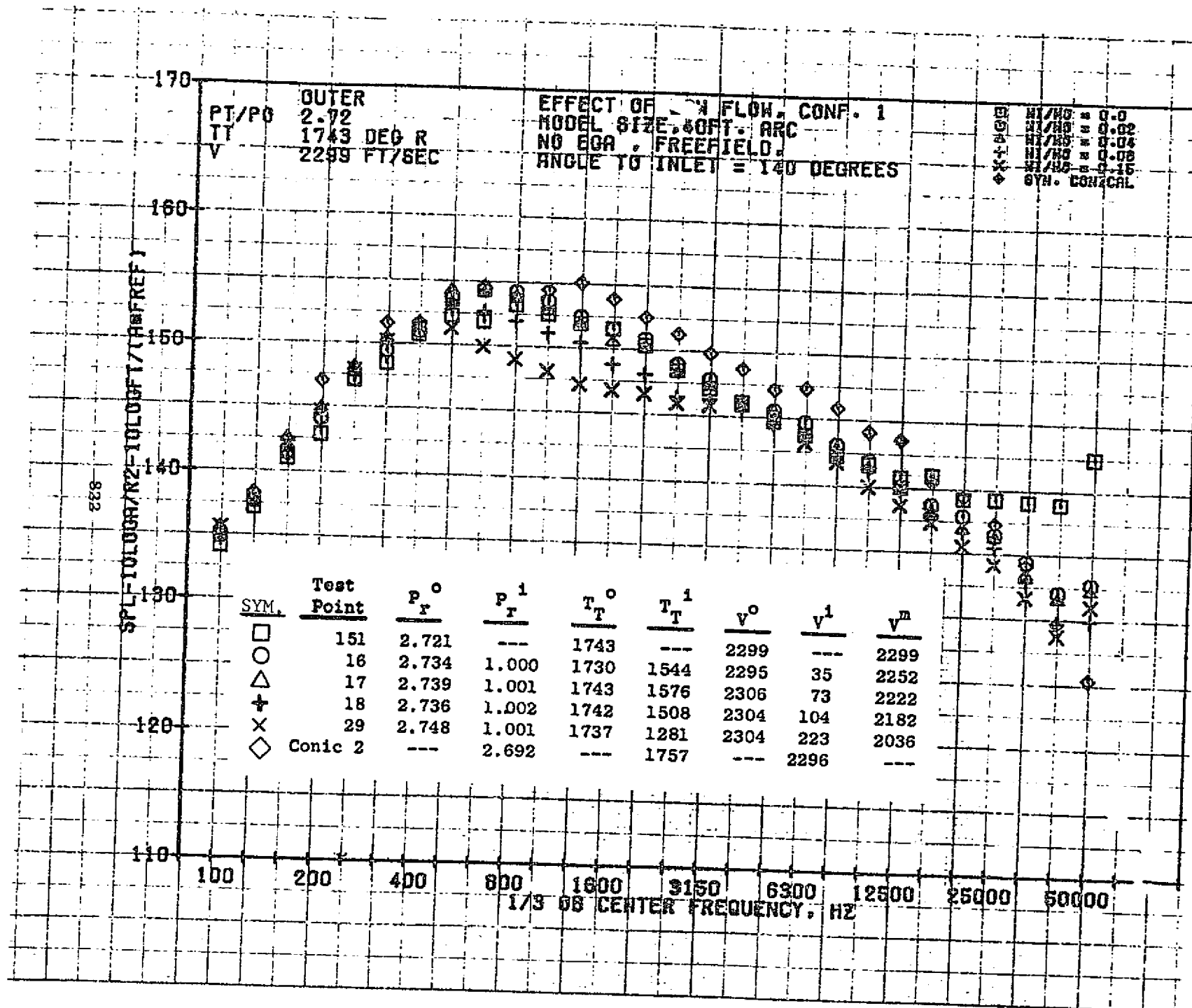


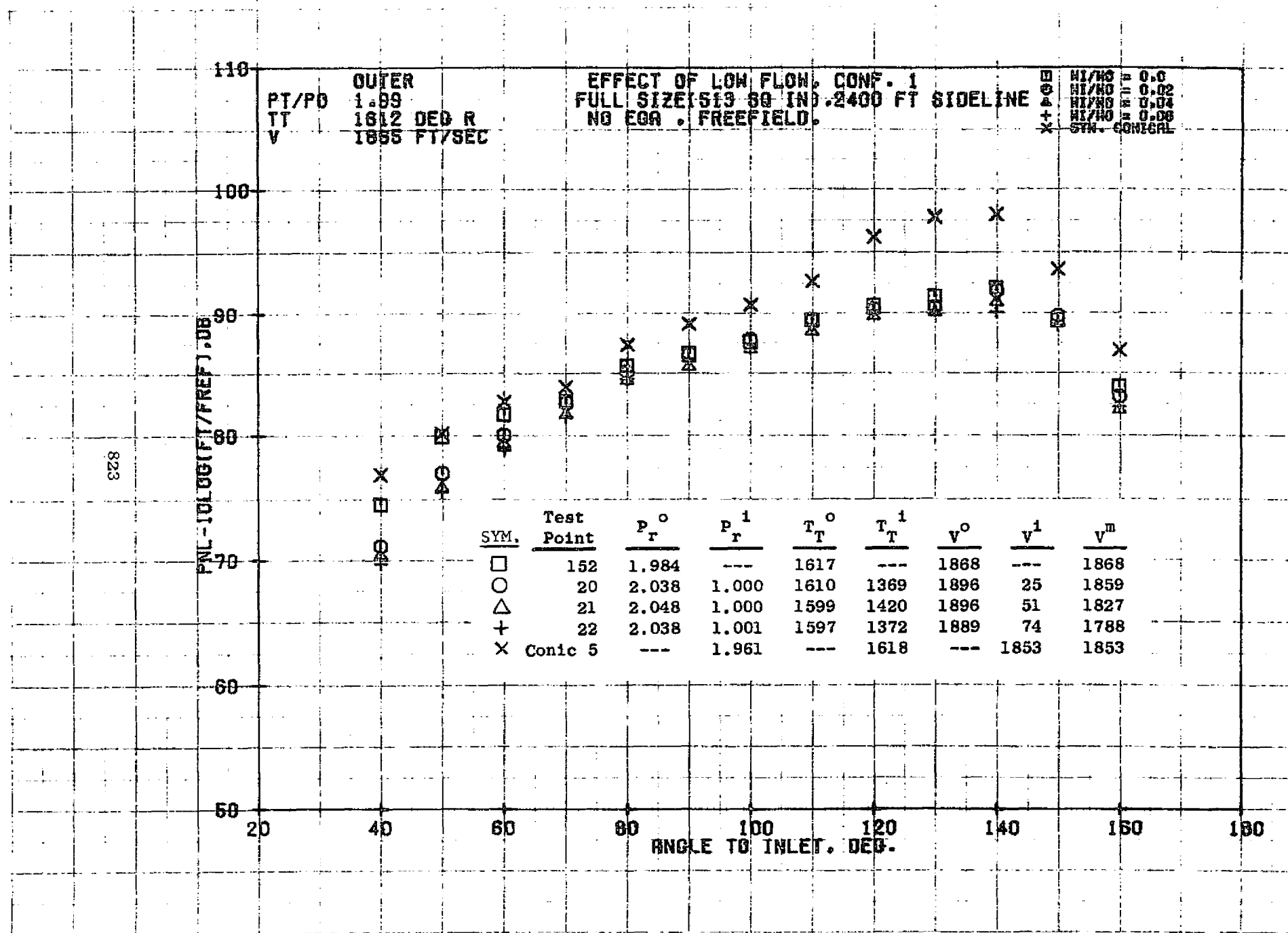






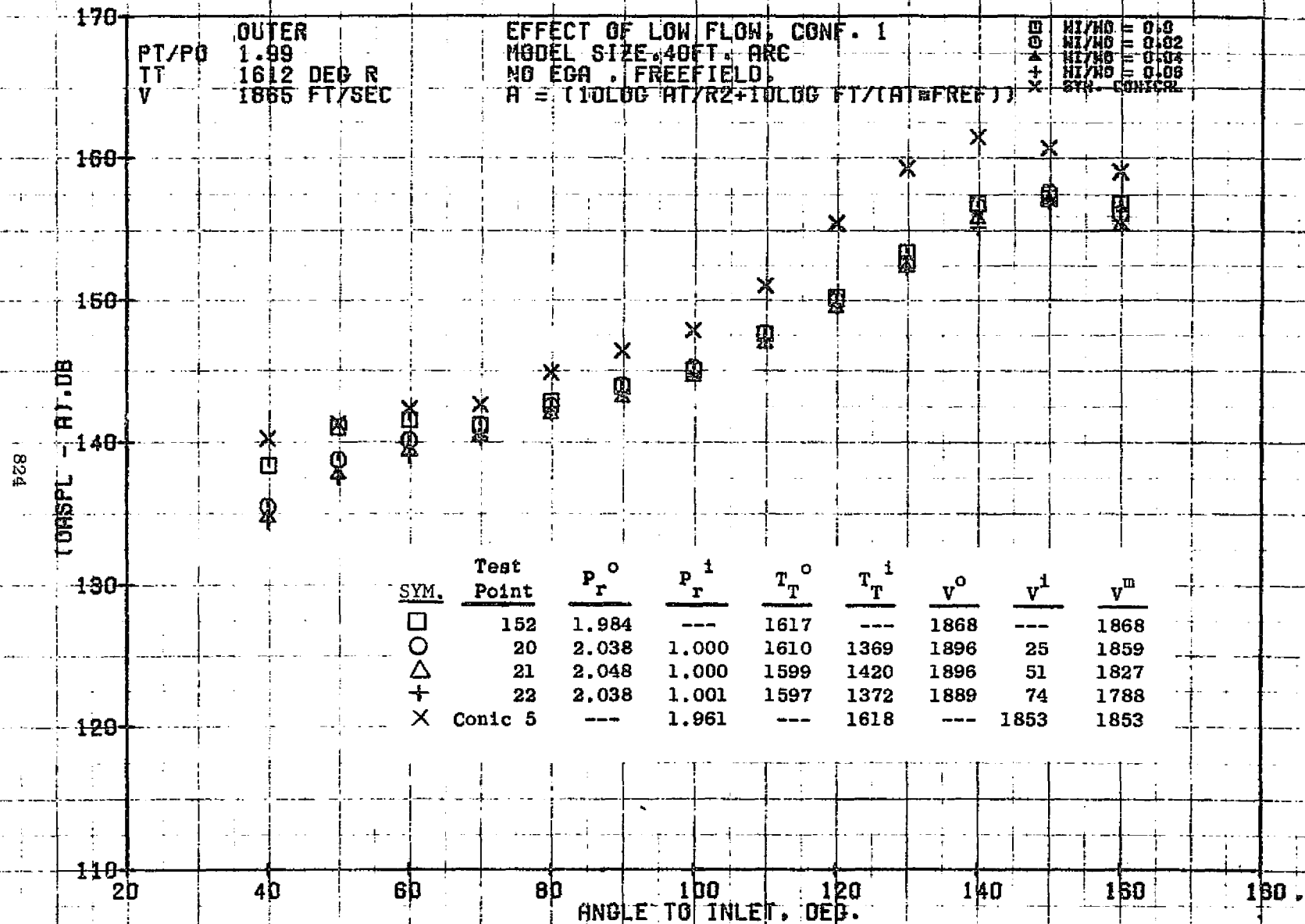






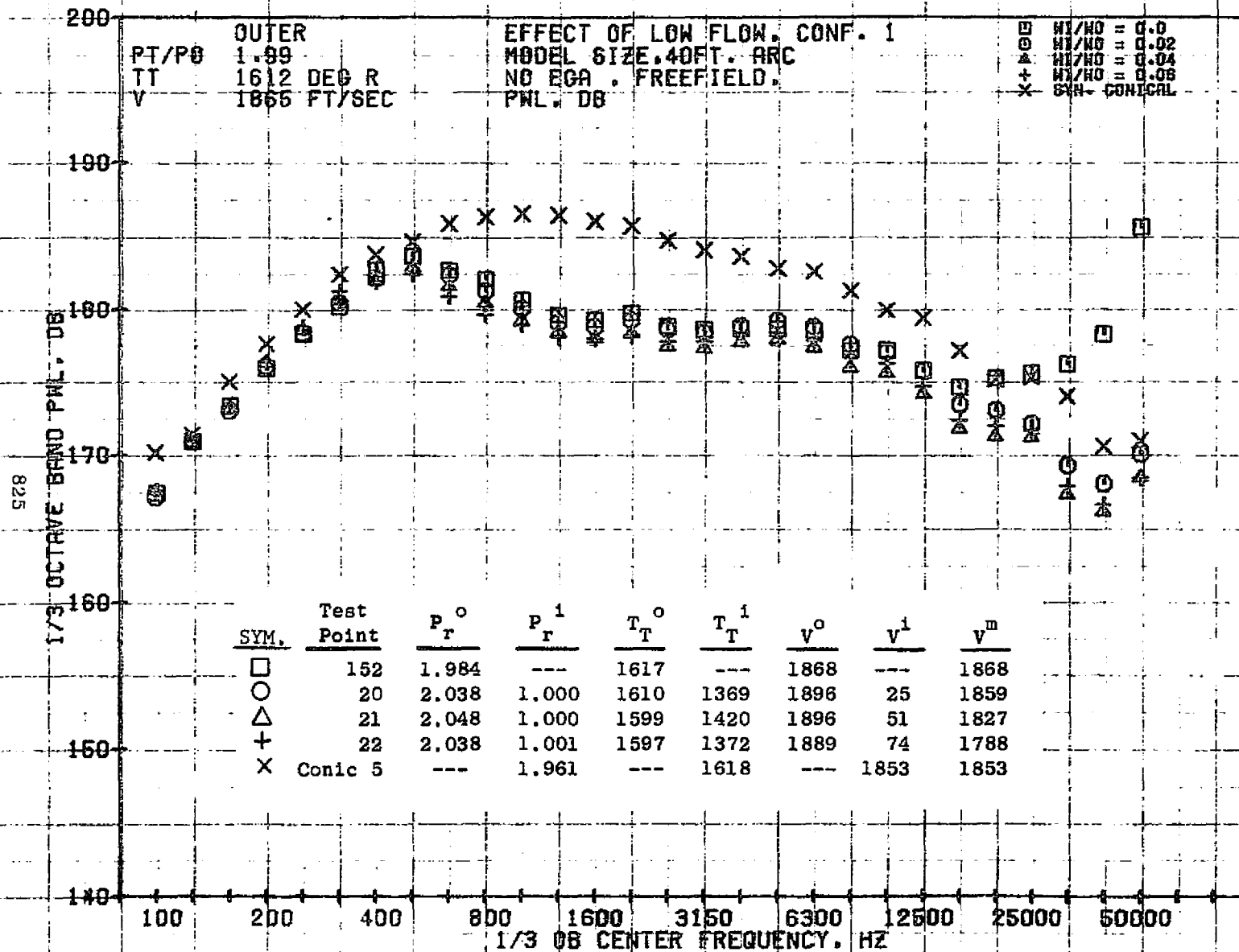
10/25/76
1X556-001

73KOLLSTEOT



10/06/76
1X334-001

73KOLLSTEDT



10/06/76
1X334-001

73KOLLSTEDT

826

SPL-10LOGA/R2-10LOGF1/(A*REF)

140

130

120

110

100

90

80

PT/PO
TT
VOUTER
1.89
1612 DEG R
1865 FT/SECEFFECT OF LOW FLOW, CONF. 1
MODEL SIZE, 40FT. ARC
NO EGA, FREEFIELD,
ANGLE TO INLET = 50 DEGREES

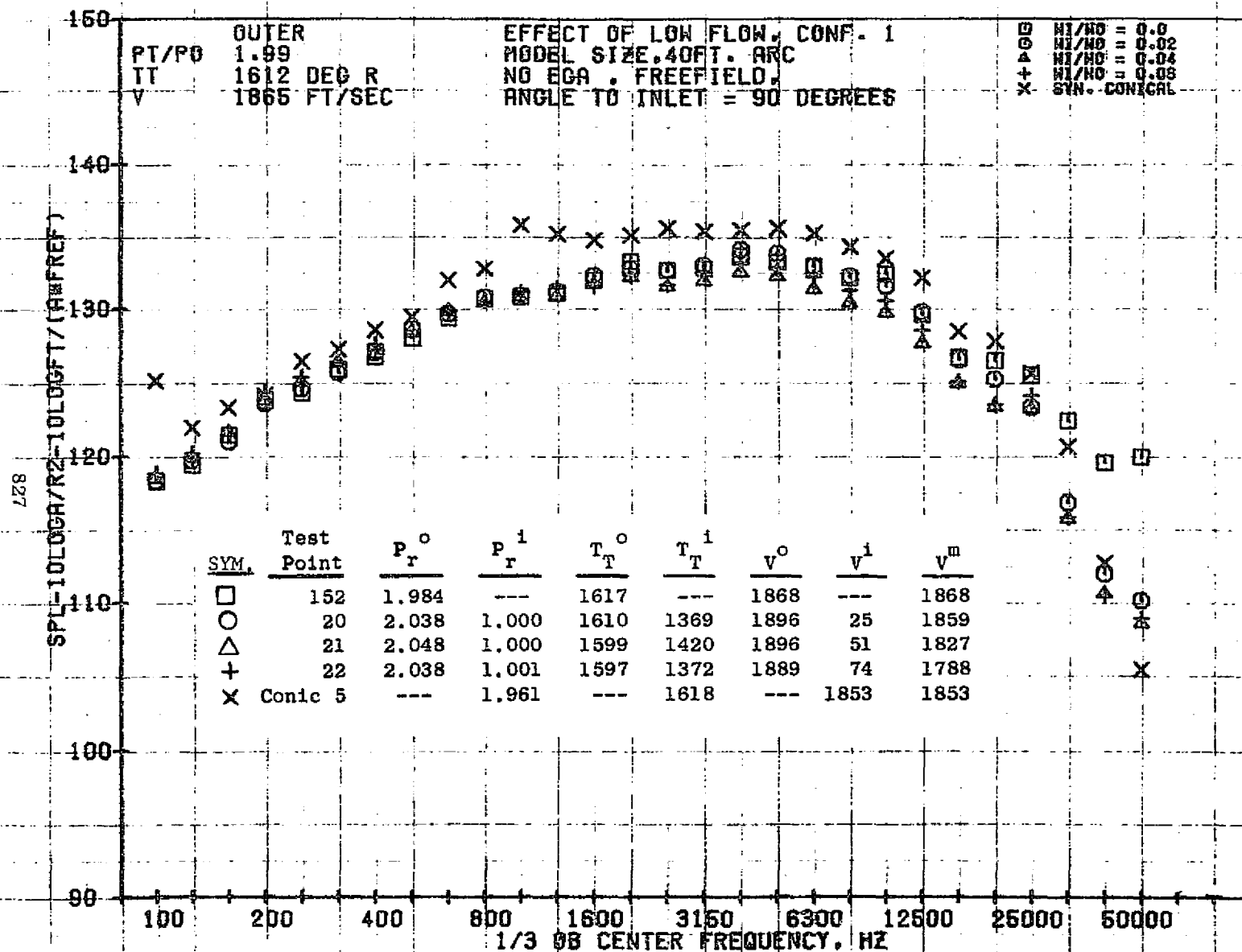
\square M1/M0 = 0.0
 \circ M1/M0 = 0.02
 \triangle M1/M0 = 0.04
 $+$ M1/M0 = 0.06
 \times SYM. CONICAL

SYM	Test Point	P_r^o	P_r^i	T_T^o	T_T^i	V^o	V^i	V^m
\square	152	1.984	---	1617	---	1868	---	1868
\circ	20	2.038	1.000	1610	1369	1896	25	1859
\triangle	21	2.048	1.000	1599	1420	1896	51	1827
$+$	22	2.038	1.001	1597	1372	1889	74	1788
\times	Conic 5	---	1.961	---	1618	---	1853	1853

1/3 OB CENTER FREQUENCY, HZ

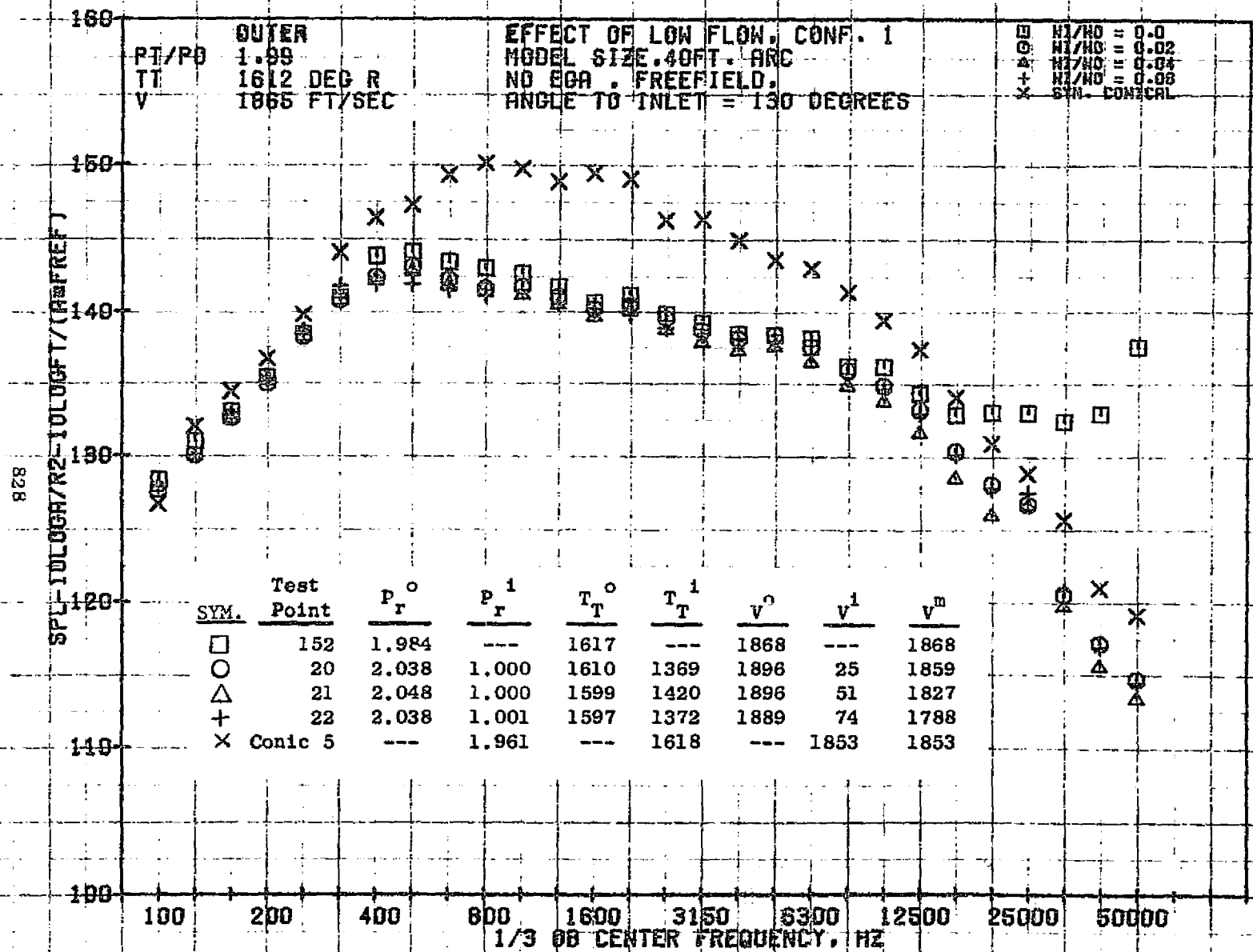
10/06/76
1X334-001

73KOLLSTEDT



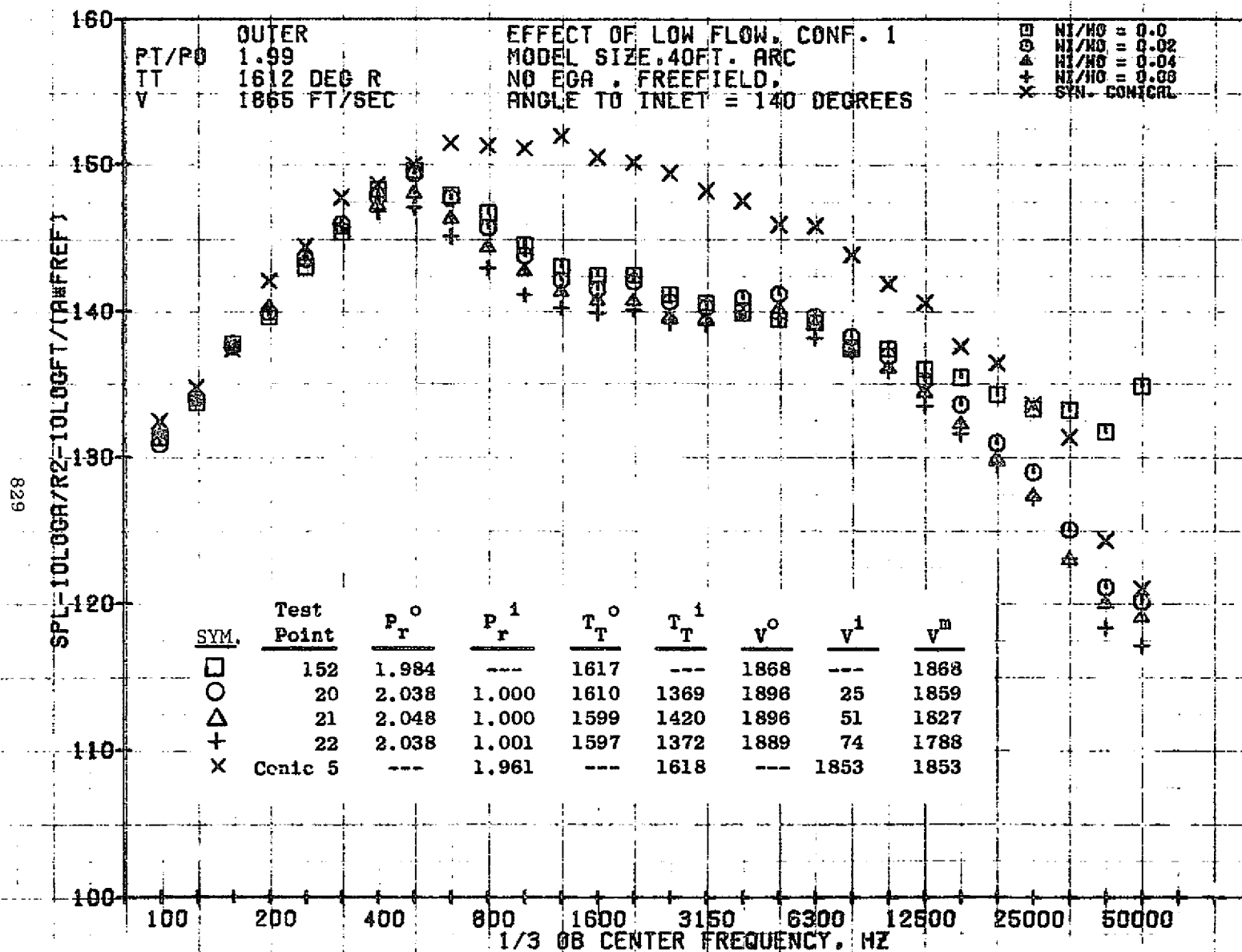
10/06/76
1X334-001

73KOLLSTEDT



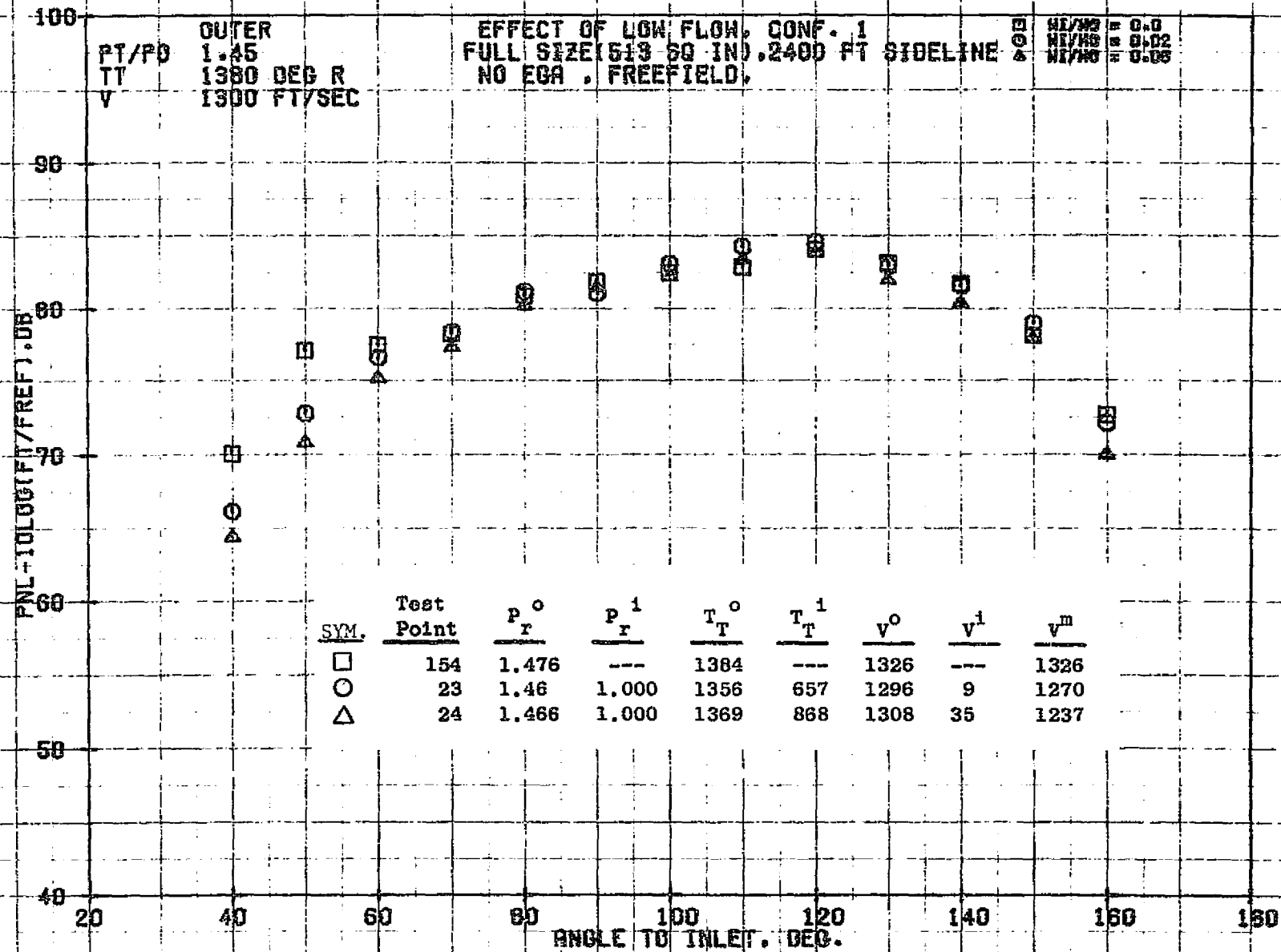
10/06/76
1X334-001

73KOLLSTEDT



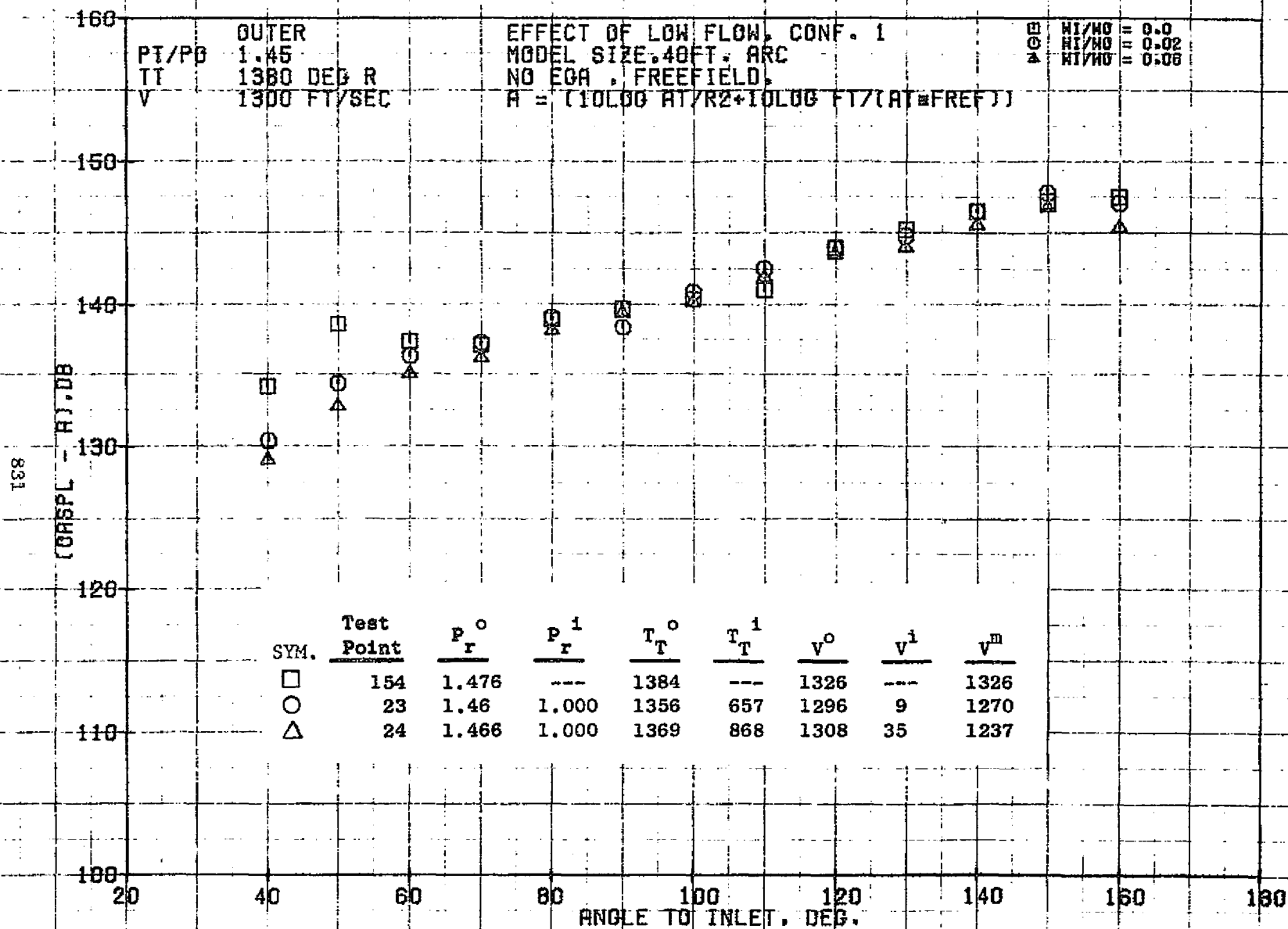
10/06/76
1X334-001

73KOLLSTEDT



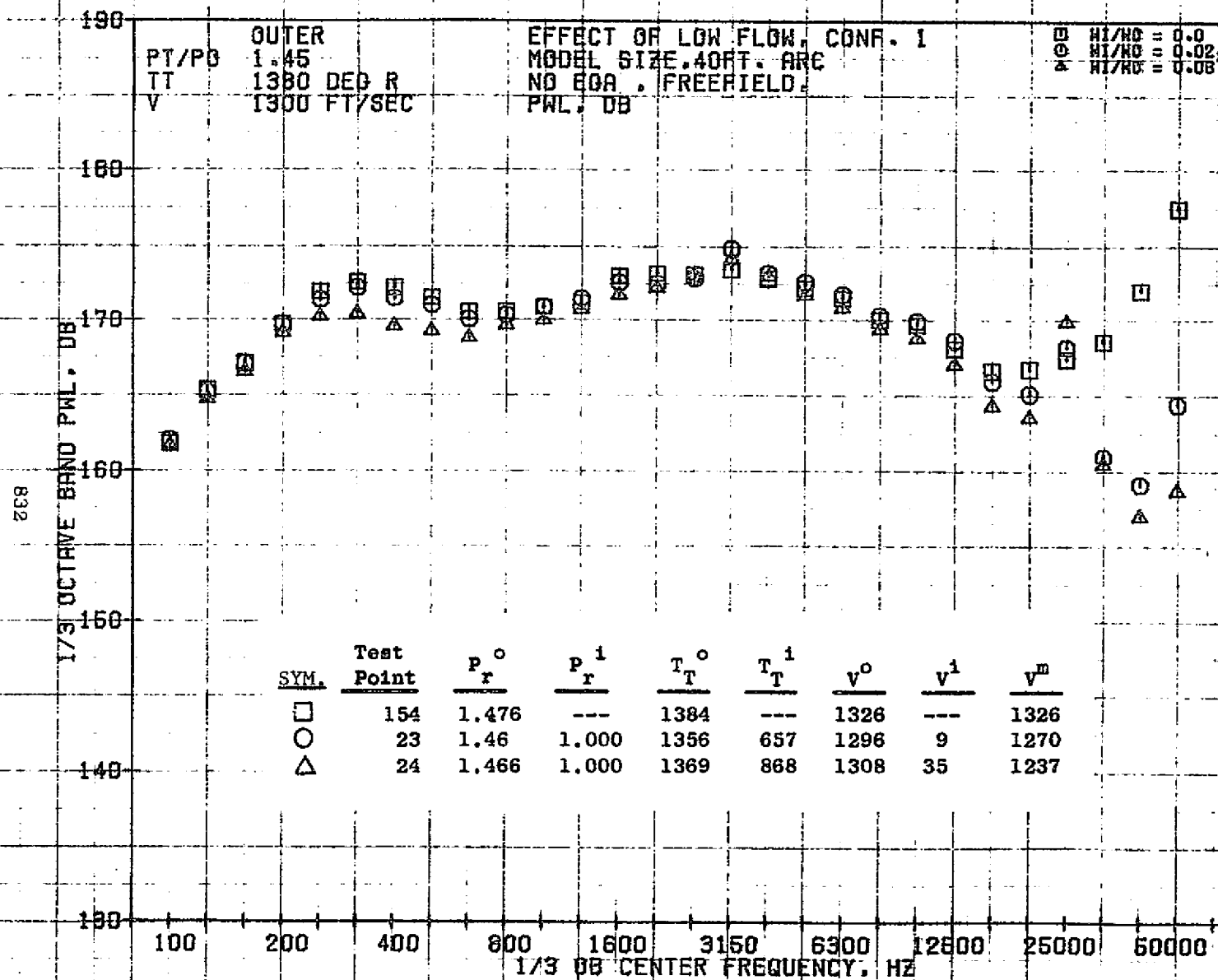
10/25/76
1X556-001

73KOLLSTEDT



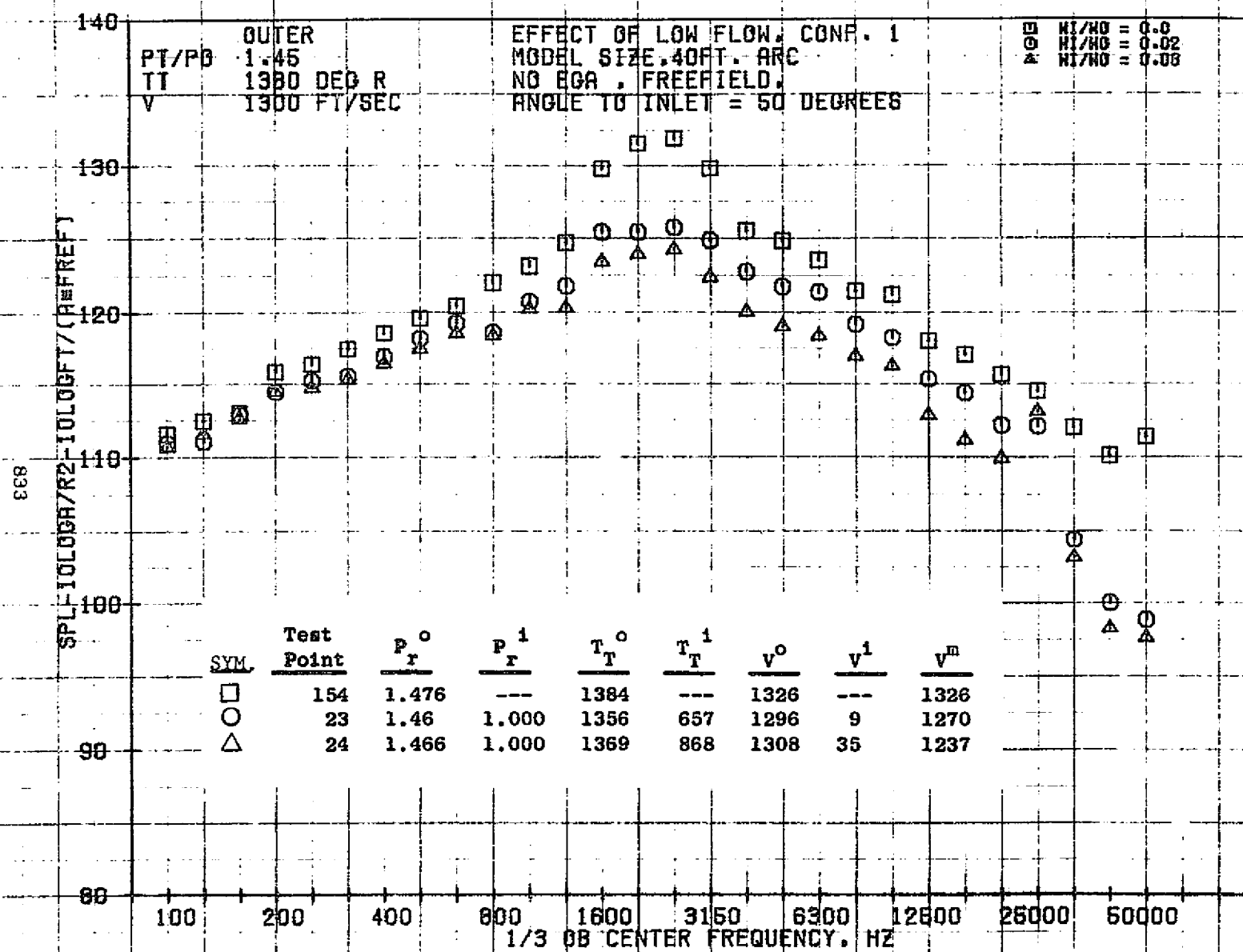
10/08/76
1X746-001

73KOLLSTEDT



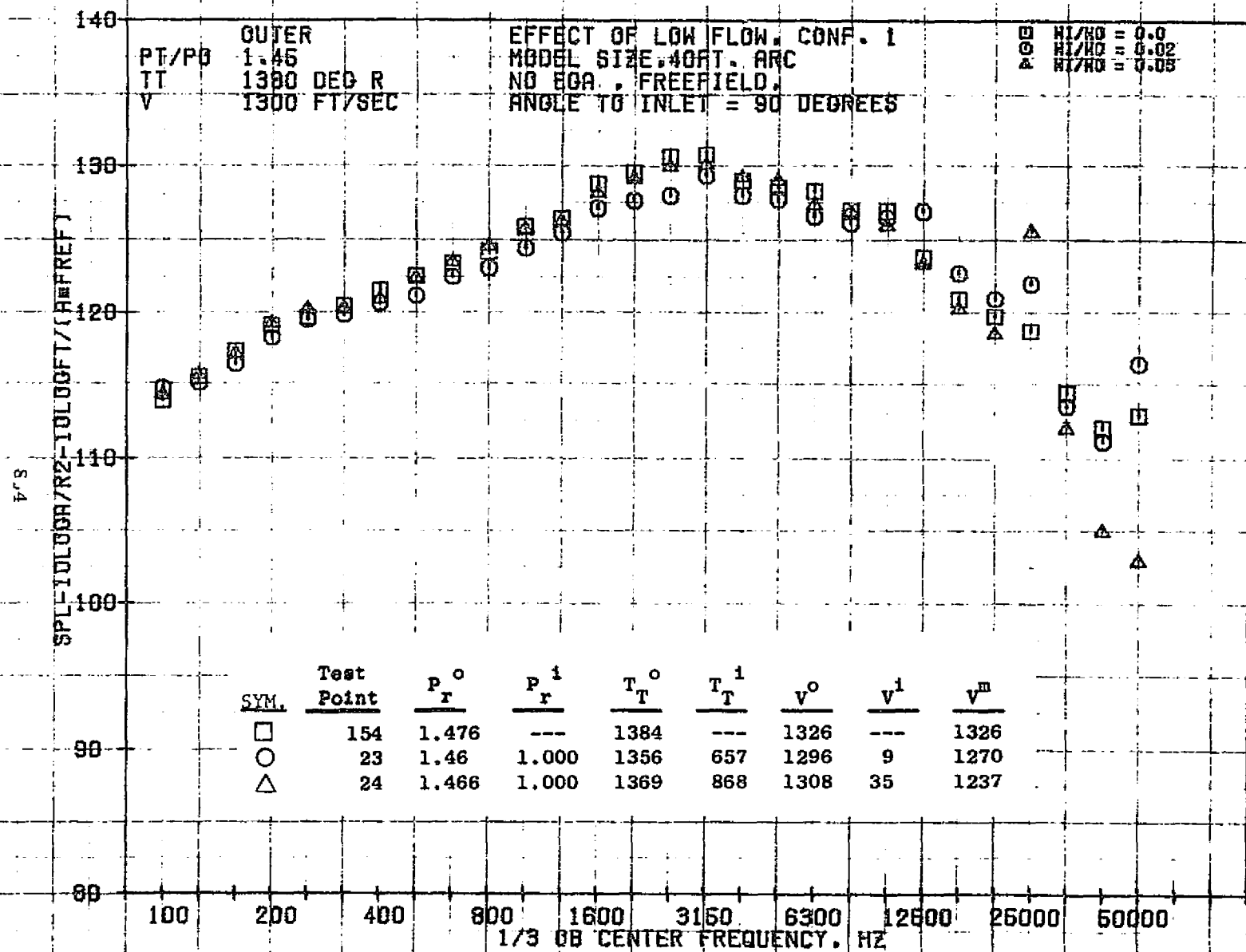
10/08/76
1X746-001

73KOLLSTEDT



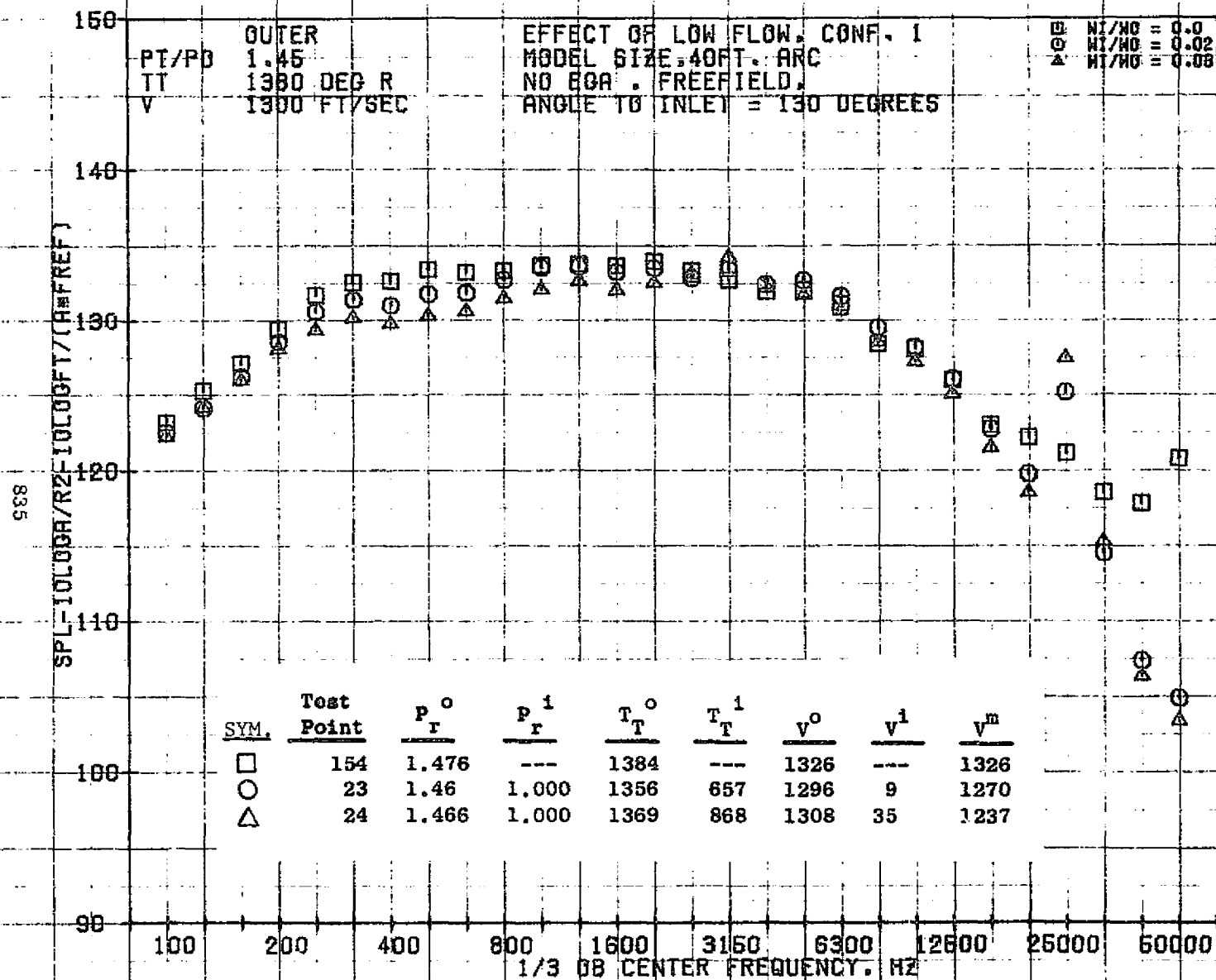
10/08/76
1X746-001

73KOLLSTEDT



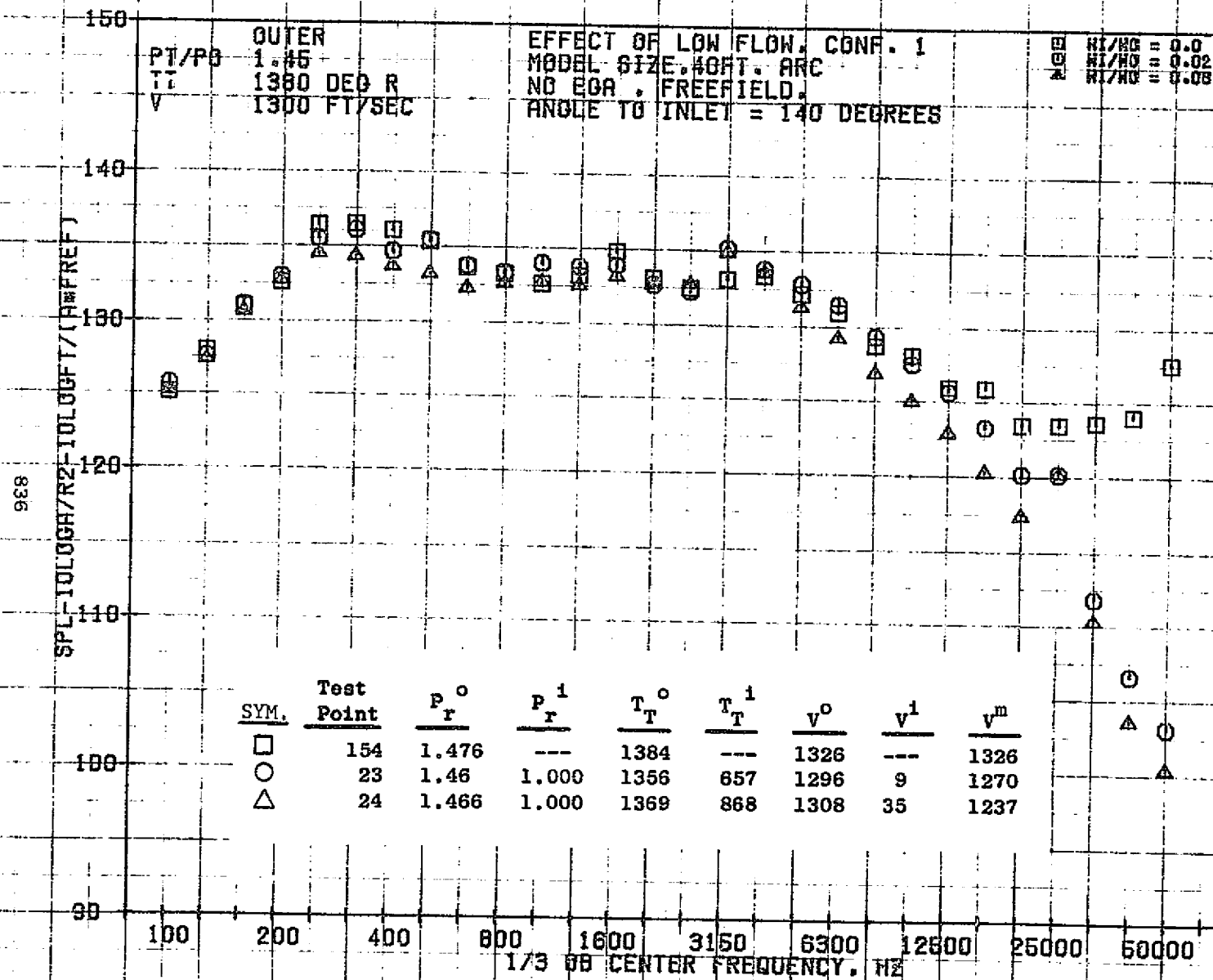
10/08/76
1X746-001

73KOLLSTEDT



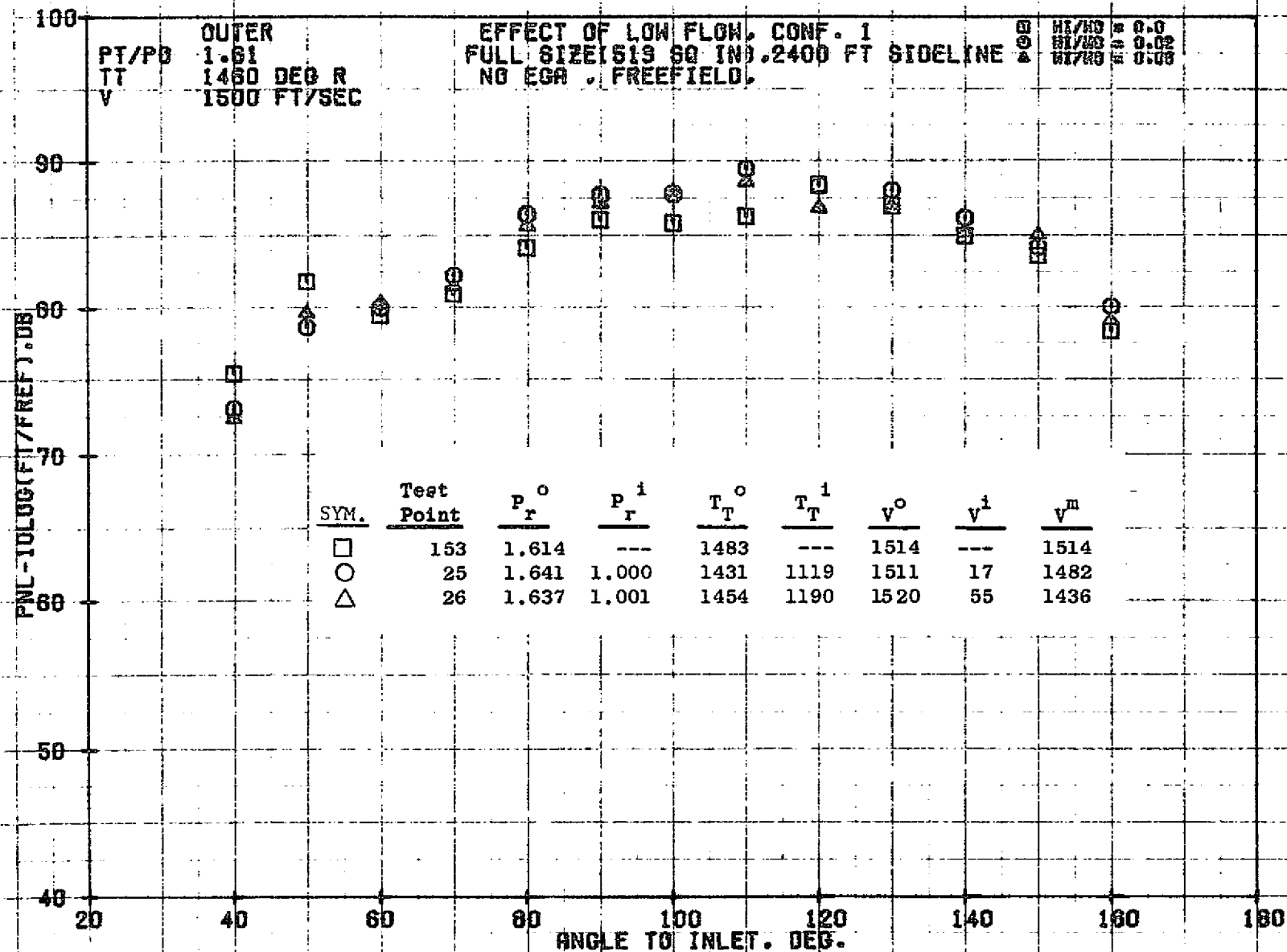
10/08/76
 1X746-001

73KOLLSTEDT



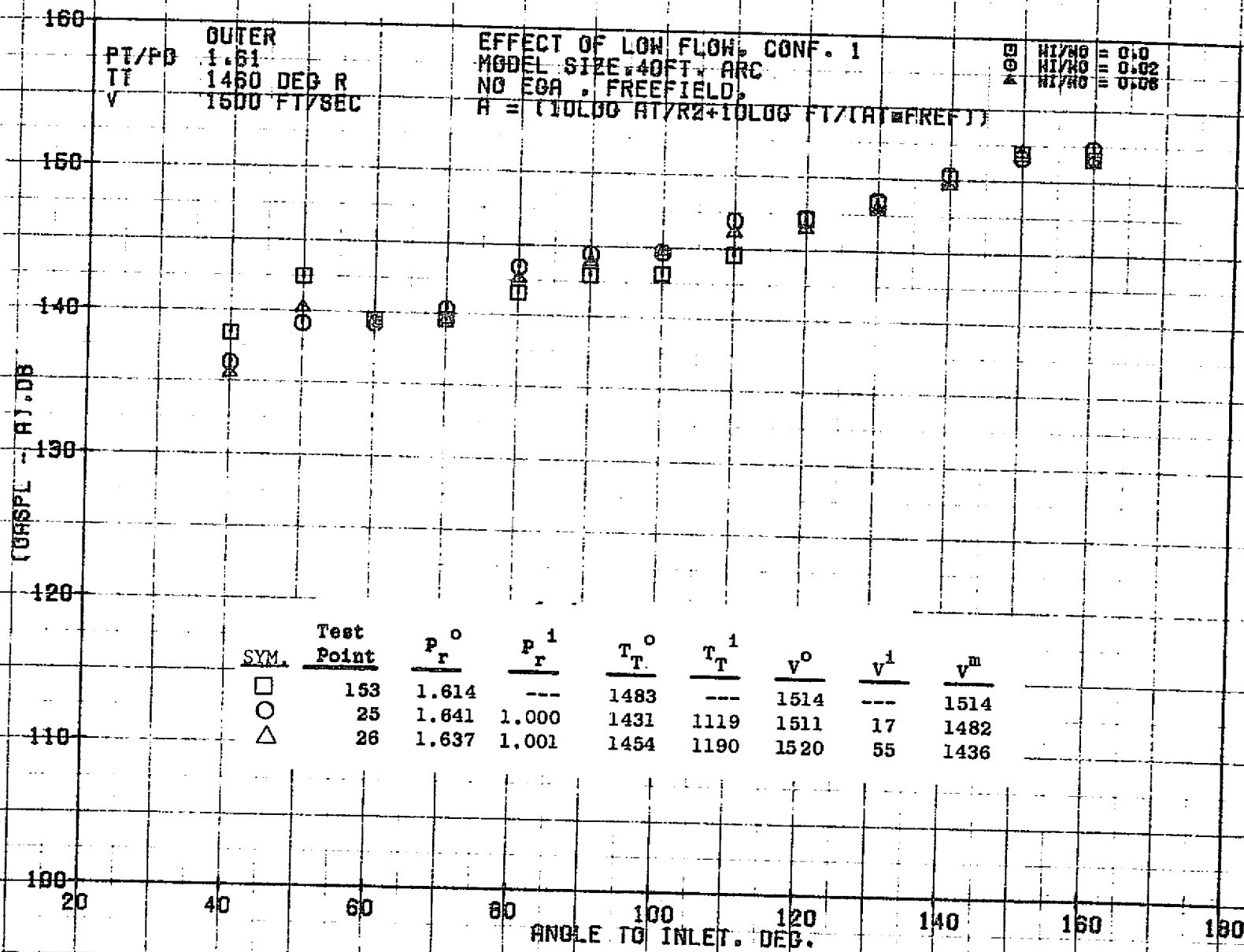
10/08/76
1X746-001

73KOLLSTEDT



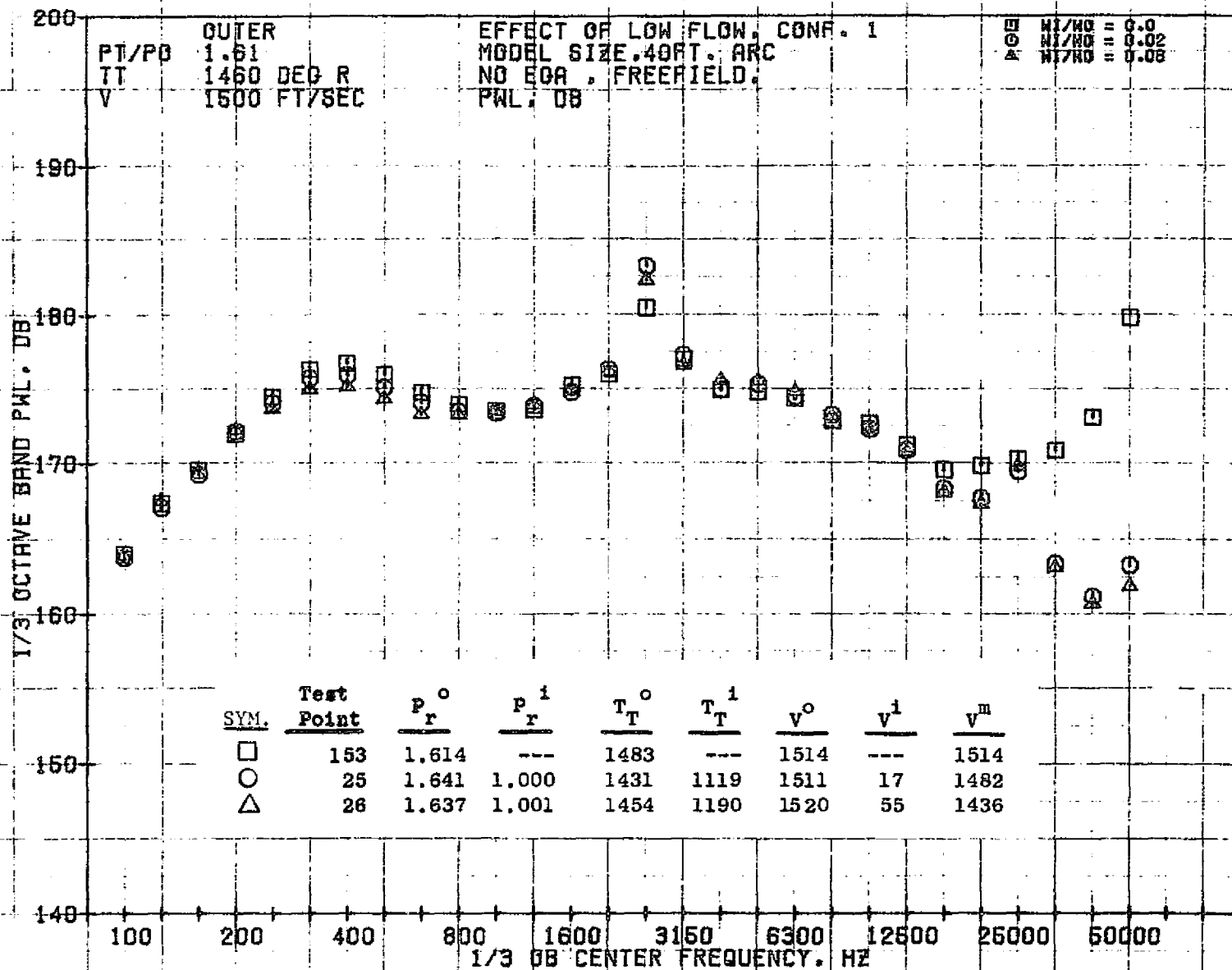
10/25/76
1X556-001

73KOLLSTEDT



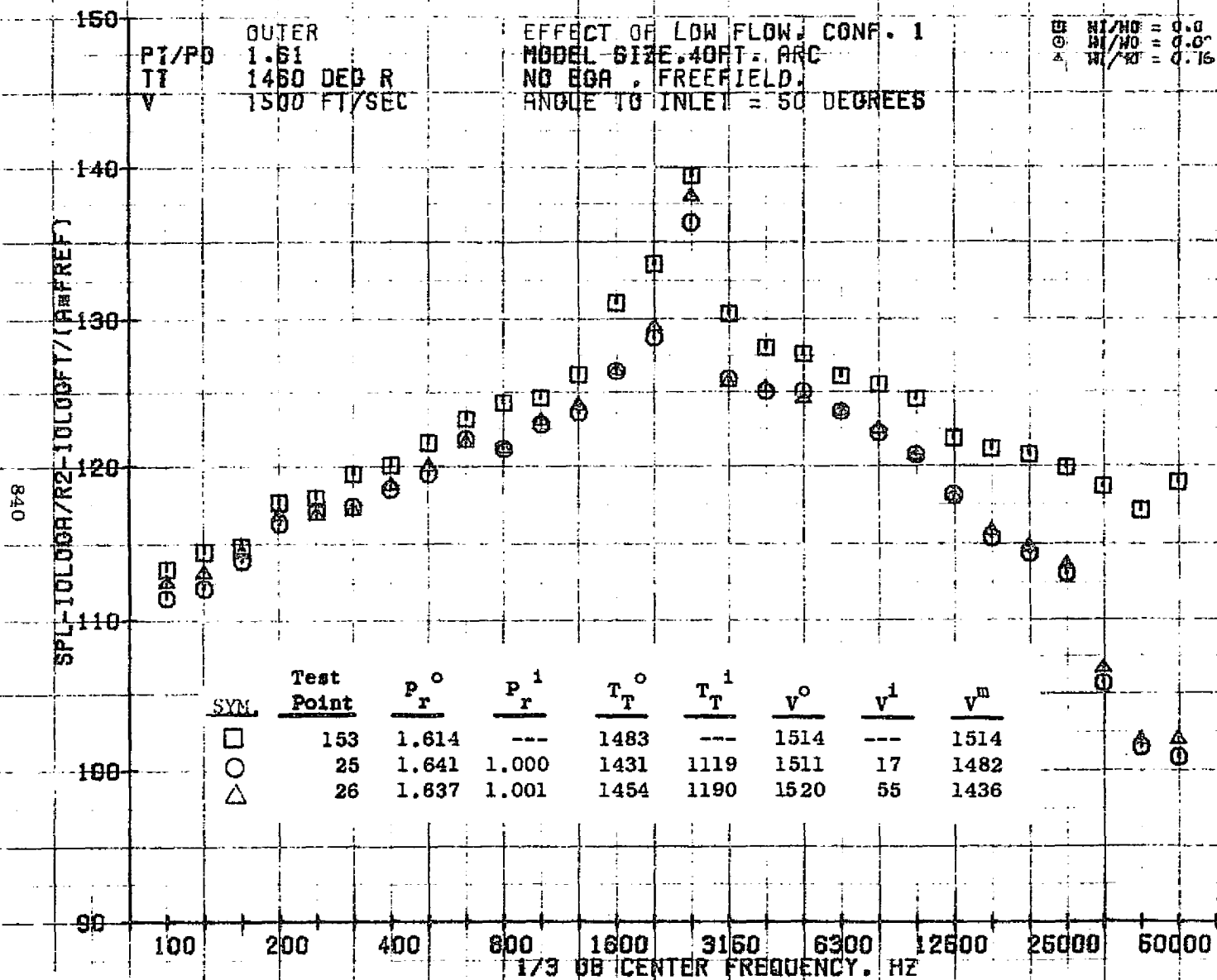
10/08/76
1X746-001

73KOLLSTEDT

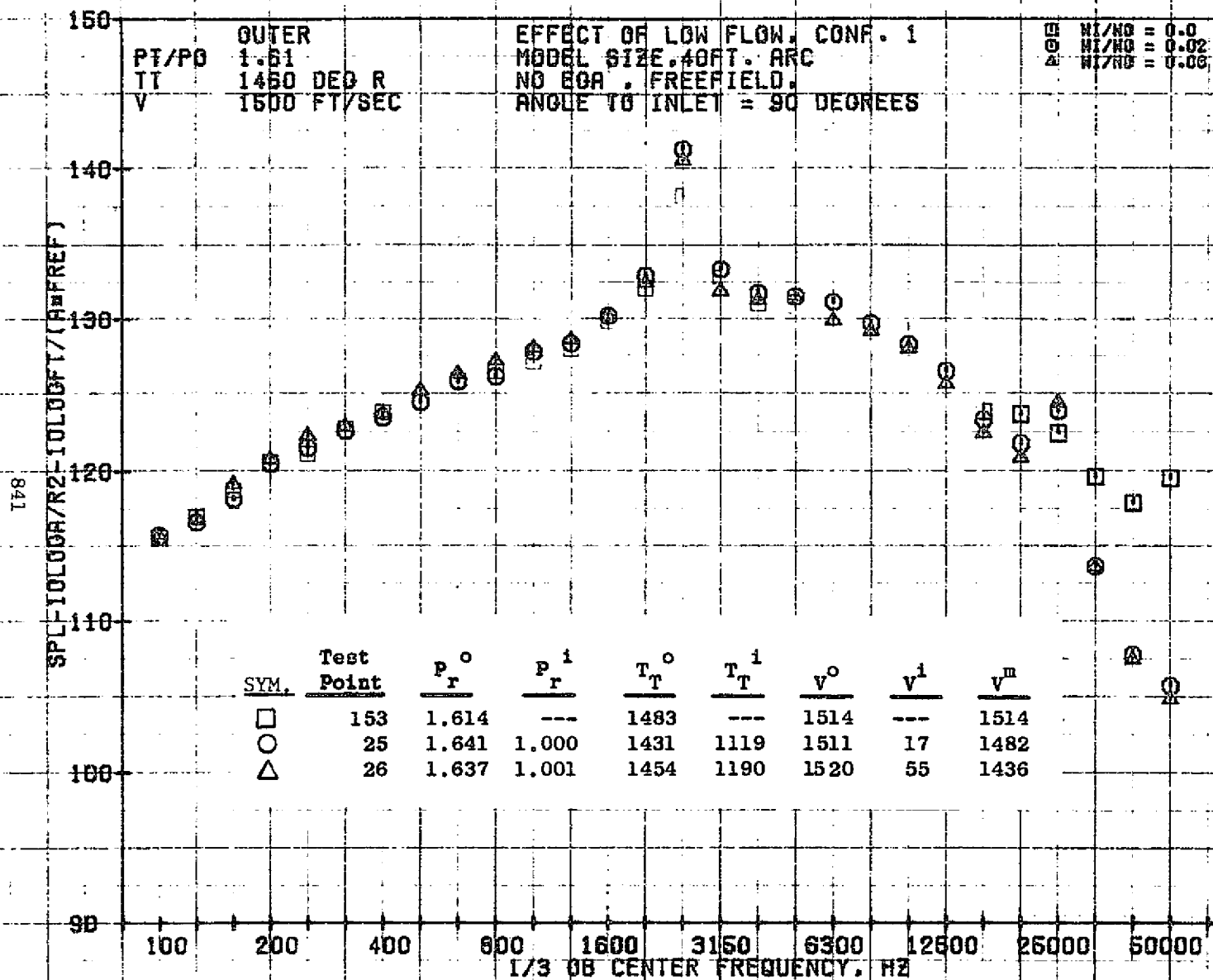


10/08/76
1X746-001

73KOLLSTEDT

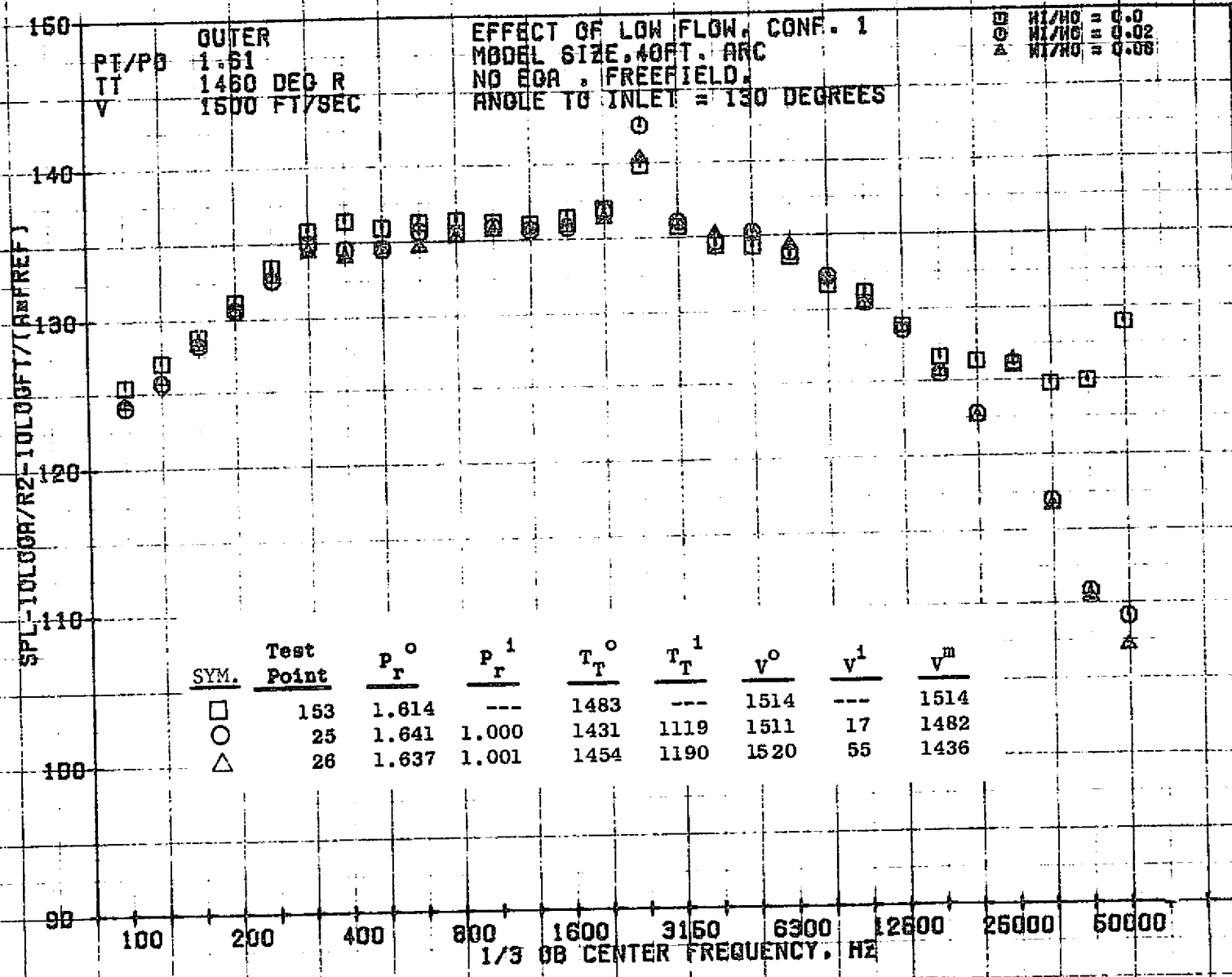


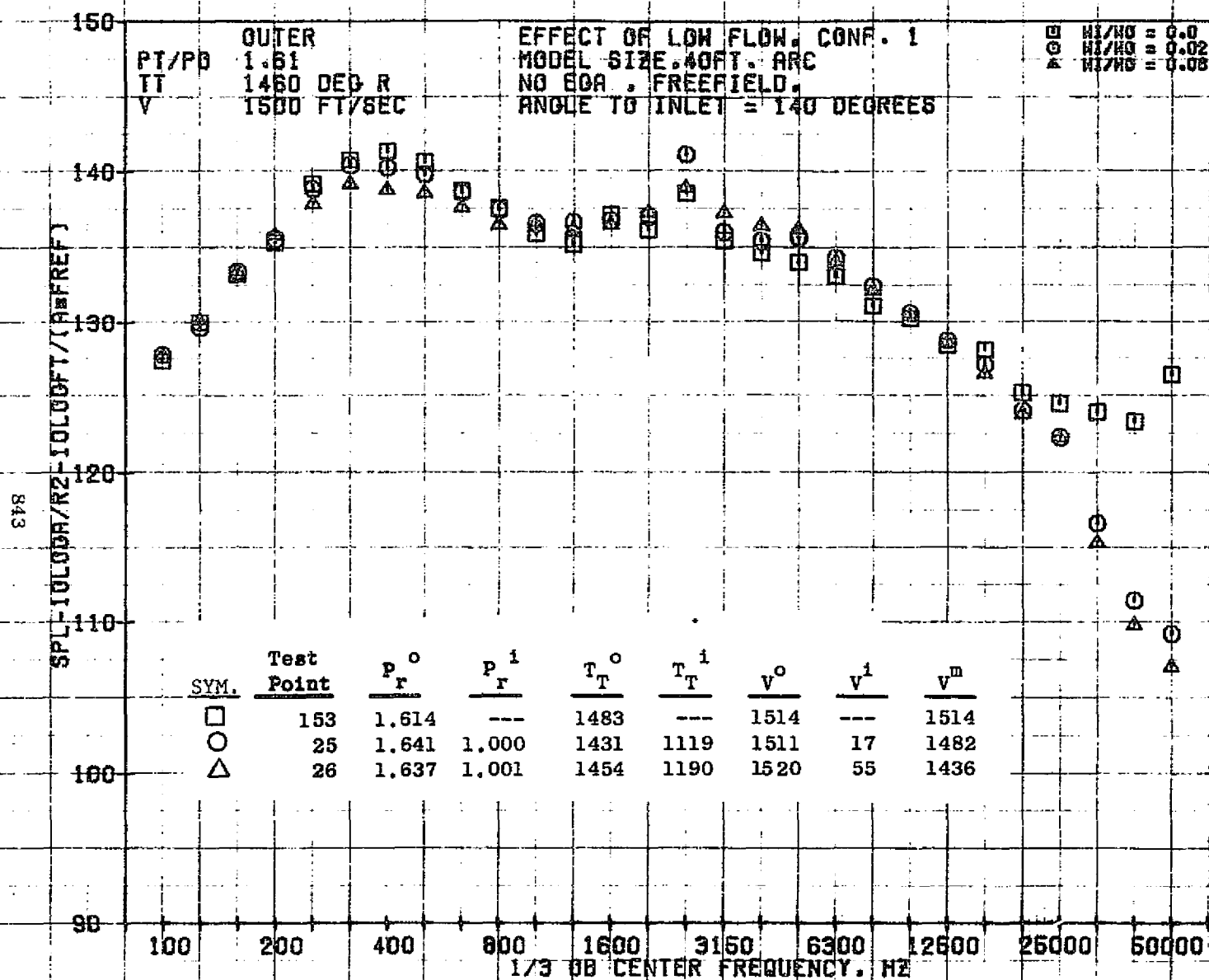
LISTED



10/08/76
1X746-001

73KOLLSTEDT





10/08/76
1X746-001

73KOLLSTEDT

PT/PO
TT
V

OUTER
3.69
1780 DEG R
2561 FT/SEC

EFFECT OF LOW FLOW, CONF. 3
FULL SIZE (513 SQ IN) 2400 FT SIDELINE
NO EOR, FREEFIELD.

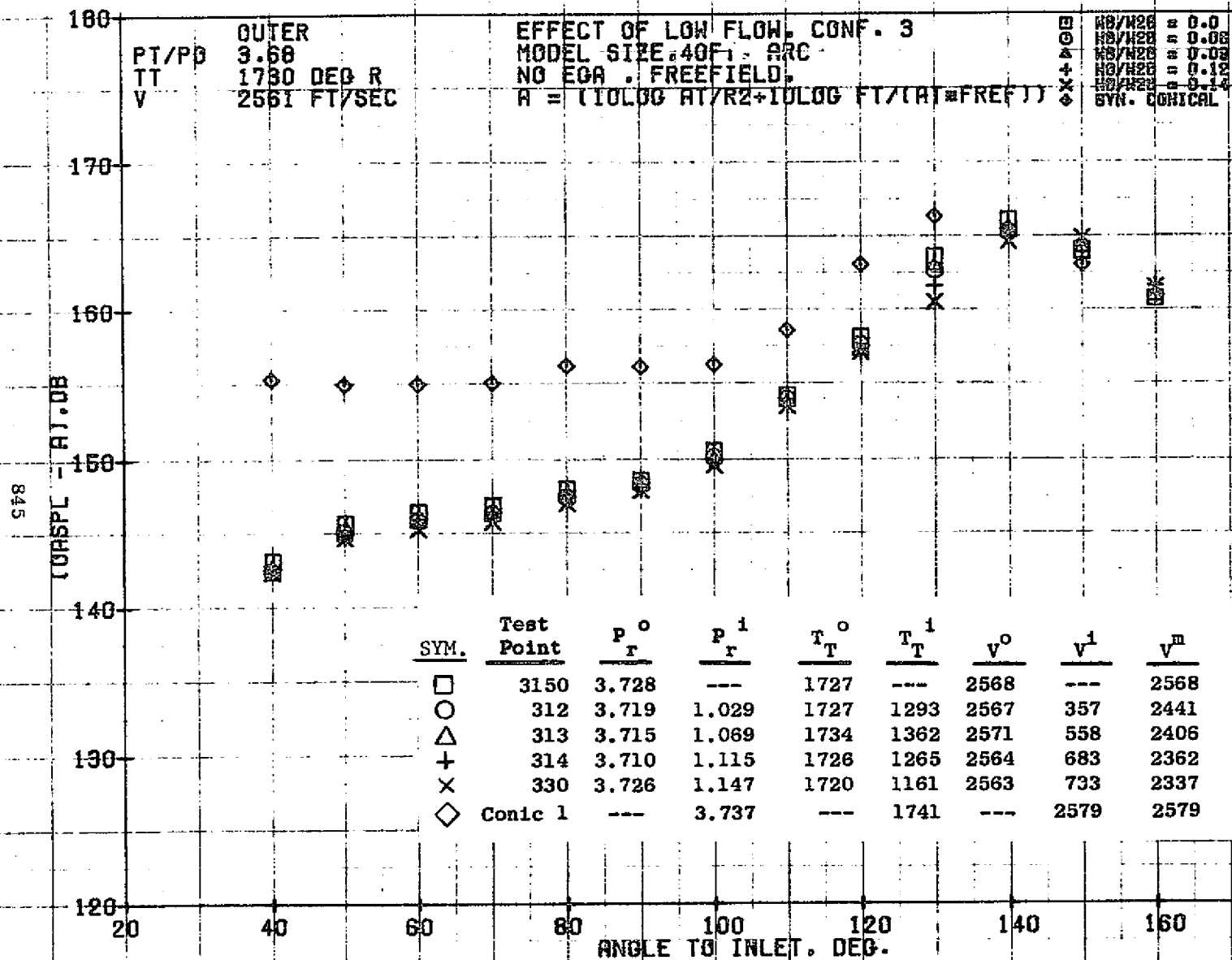
HS/H28 = 0.0
HS/H28 = 0.08
HS/H28 = 0.09
HS/H28 = 0.12
HS/H28 = 0.14
SYM. CONIC

PAL-10 LOG (FT/FREF). DB

844

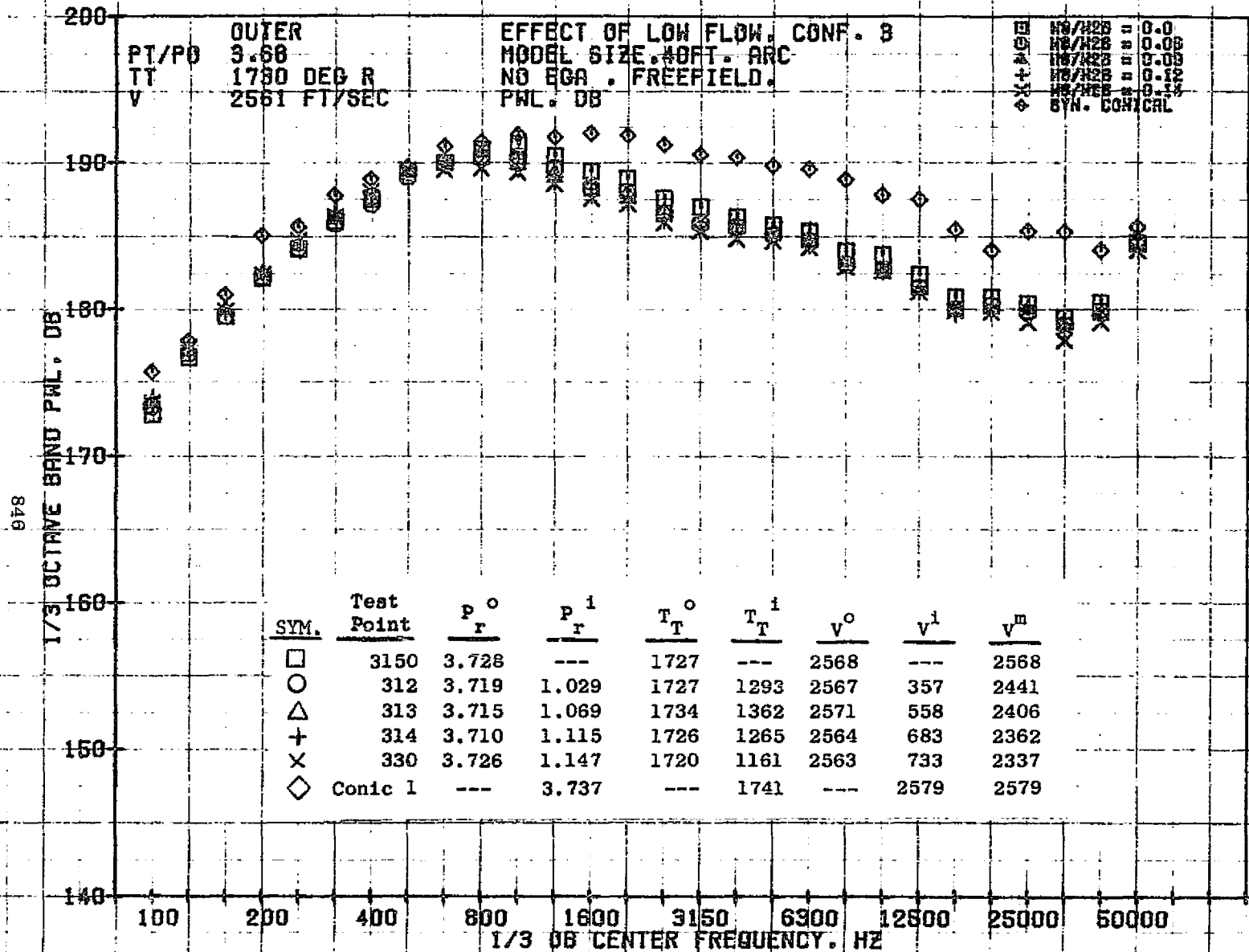
SYM.	Test Point	P_r^o	P_r^i	T_T^o	T_T^i	V^o	V^i	V^m
□	3150	3.728	---	1727	---	2568	---	2568
○	312	3.719	1.029	1727	1293	2567	357	2441
△	313	3.715	1.069	1734	1362	2571	558	2406
+	314	3.710	1.115	1726	1265	2564	683	2362
x	330	3.726	1.147	1720	1161	2563	733	2337
◇	Conic 1	---	3.737	---	1741	---	2579	2579

ANGLE TO INLET, DEG.



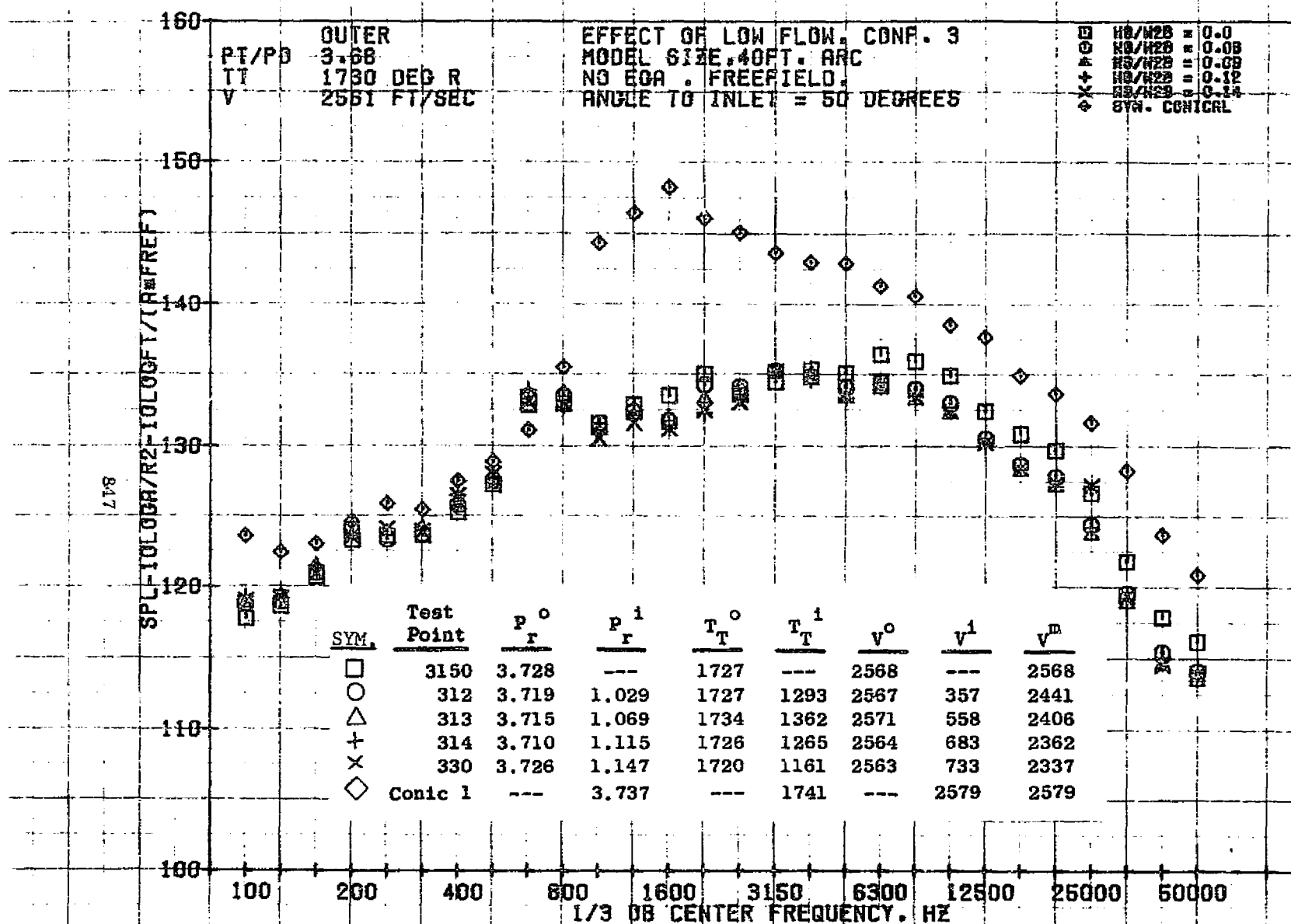
10/11/76
1X207-001

73KOLLSTEDT



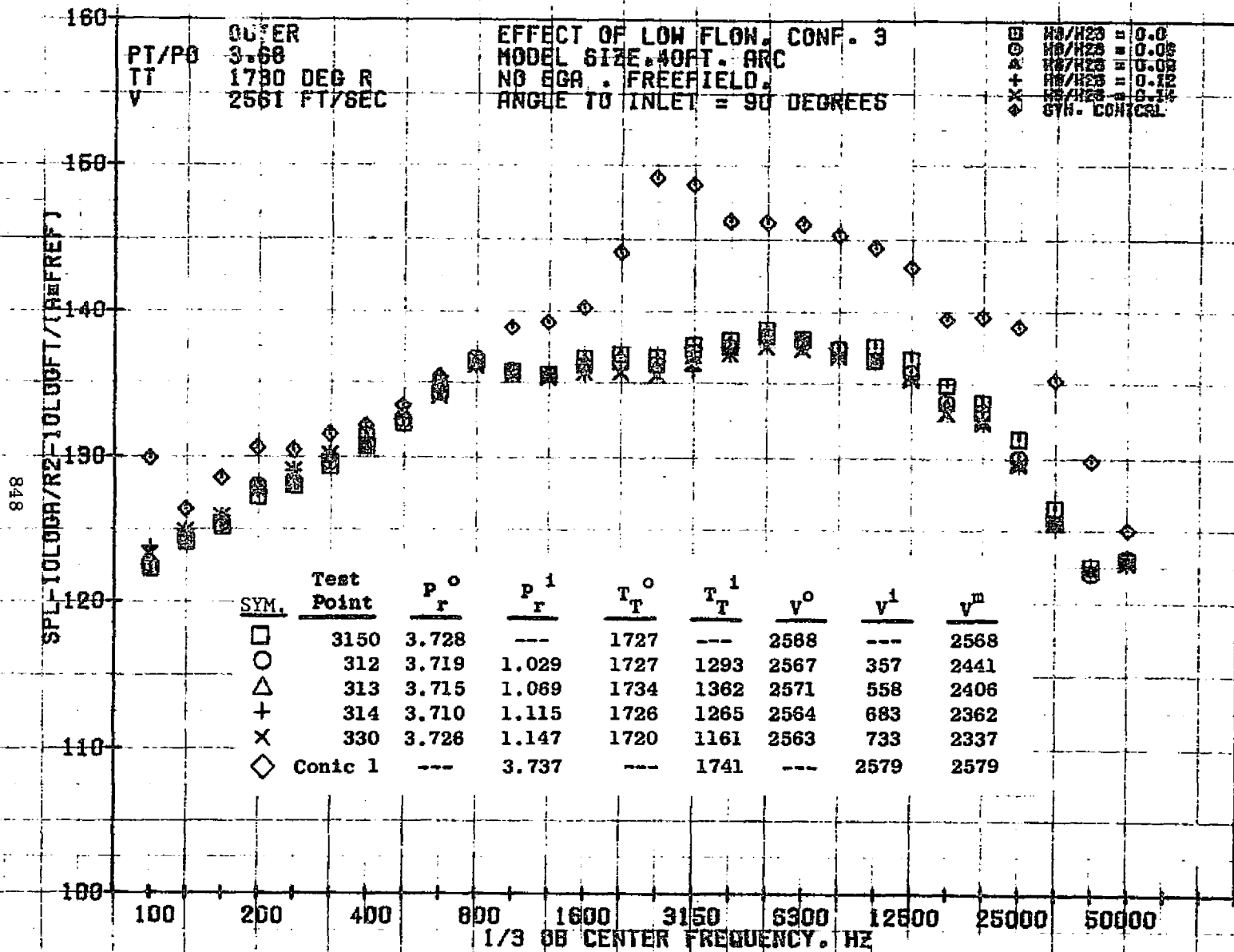
10/11/76
1X207-001

73KOLLSTEDT



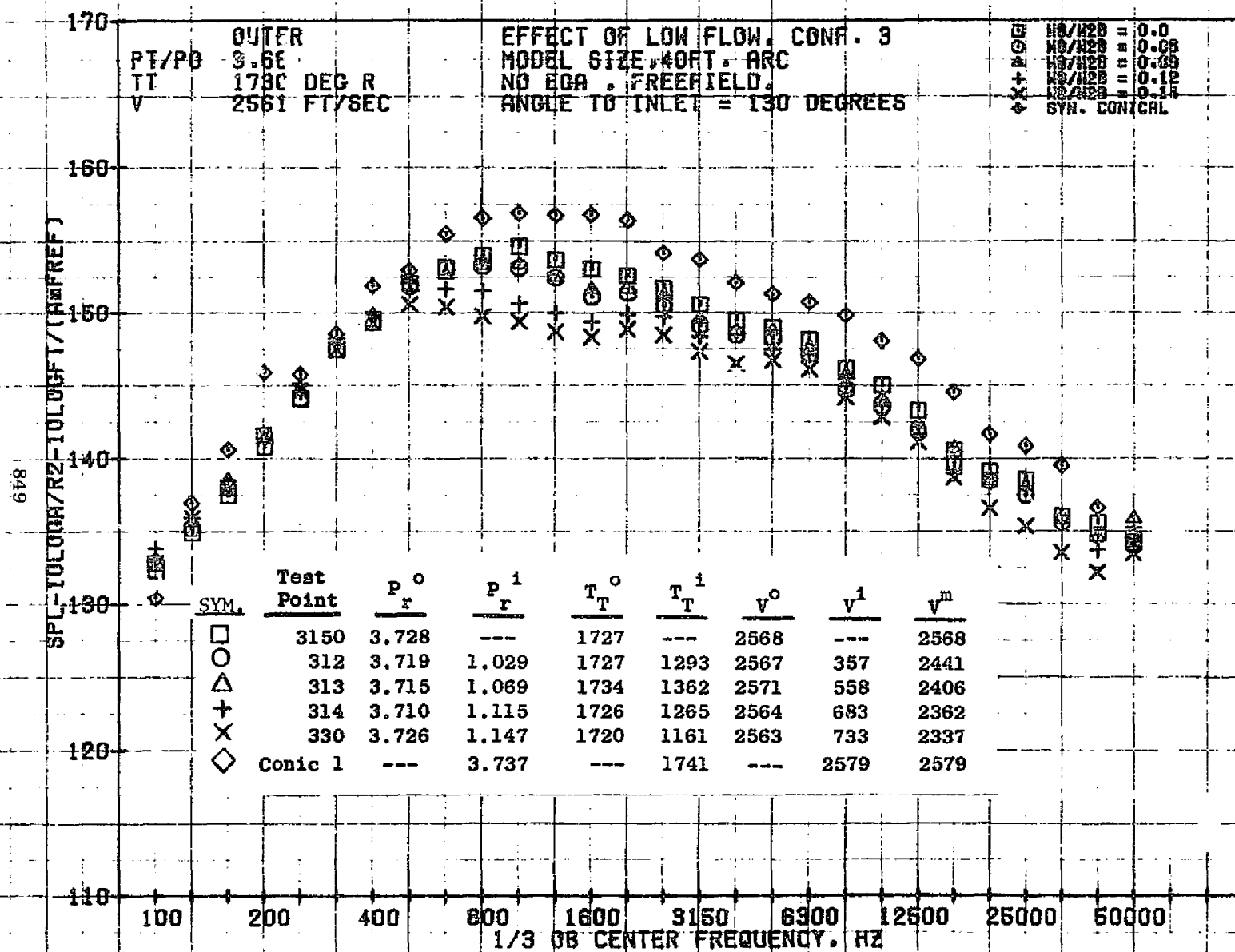
10/11/76
1X207-001

73KOLLSTEDT



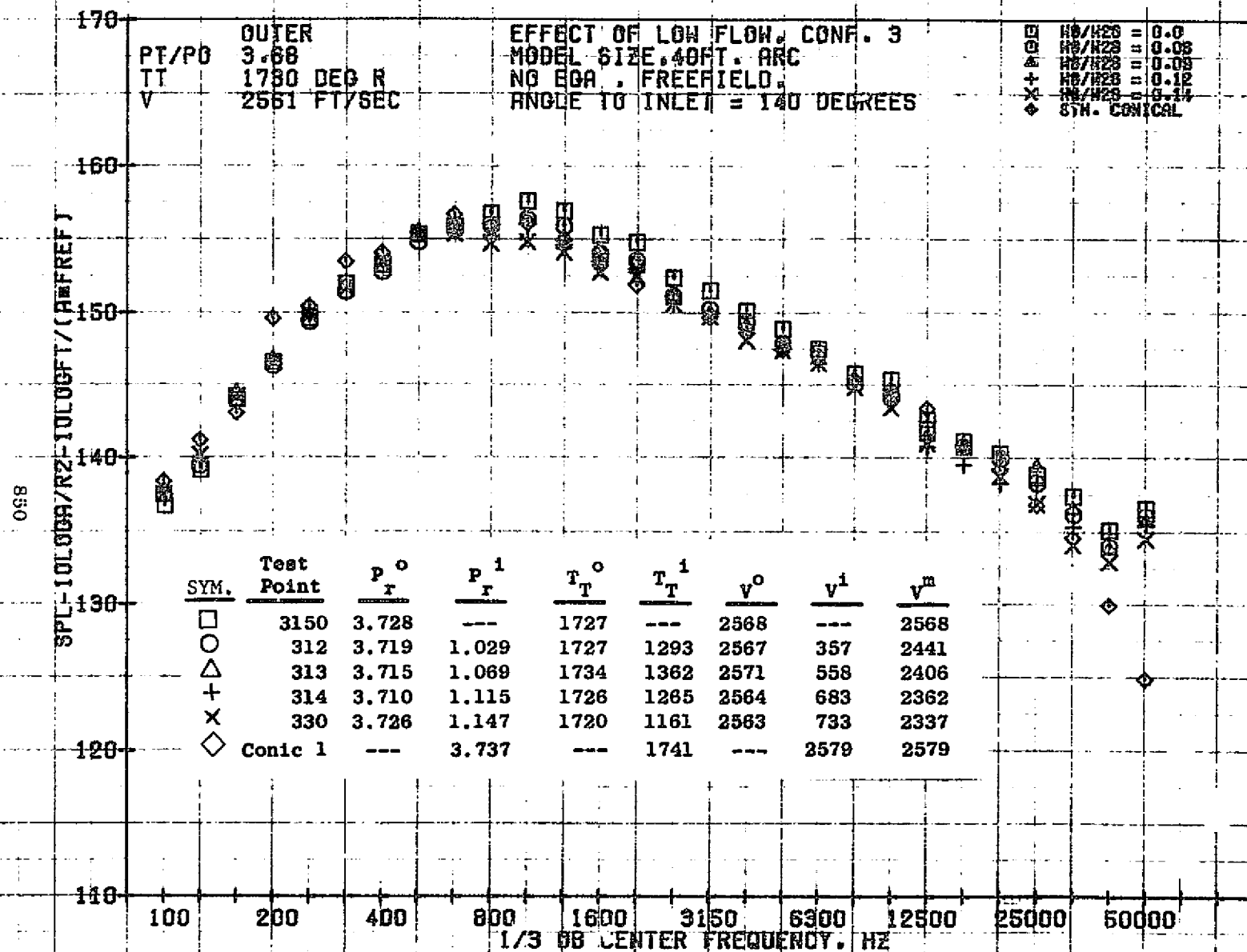
10/11/76
1X207-001

73KOLLSTEDT



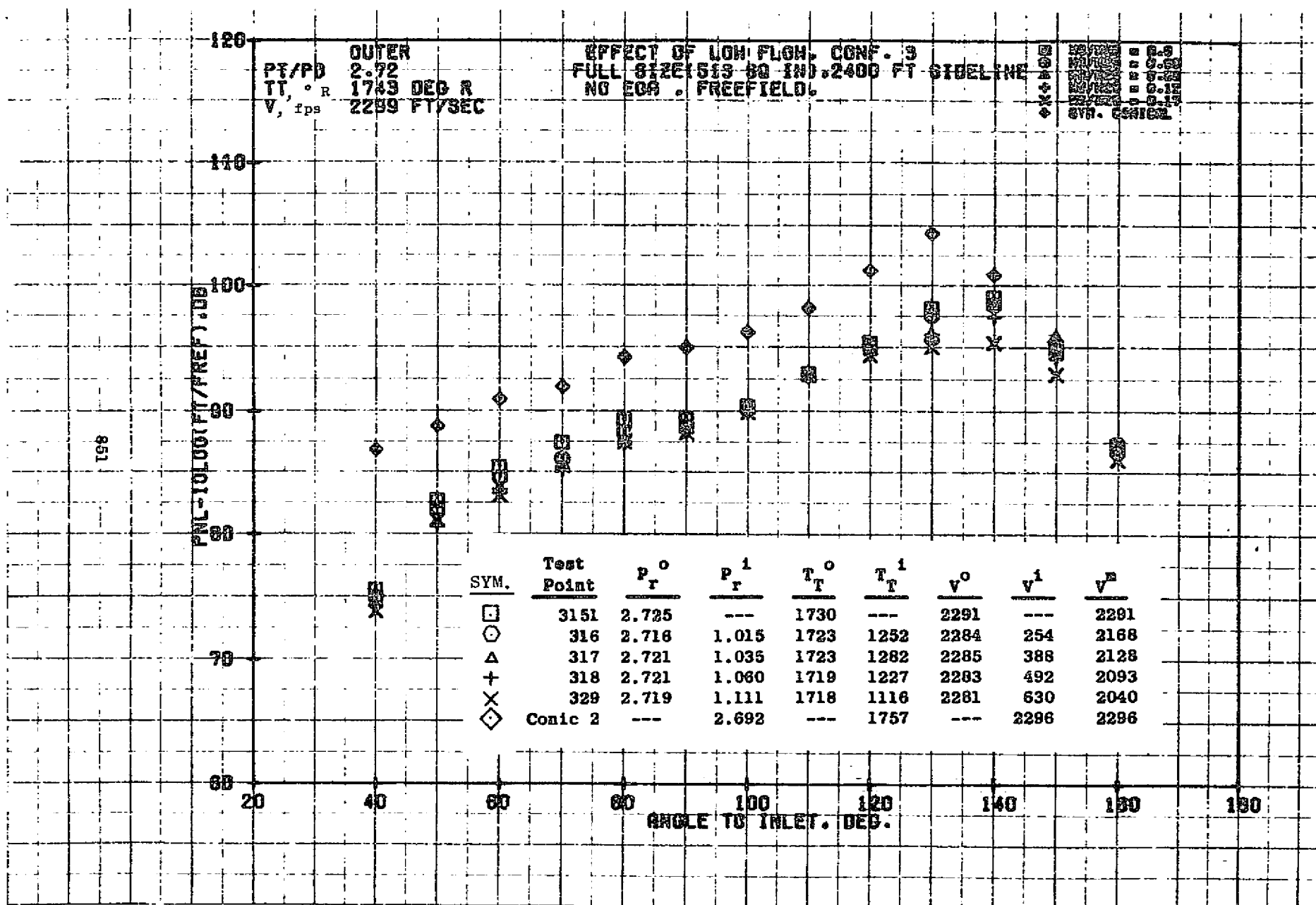
10/11/76
1X207-001

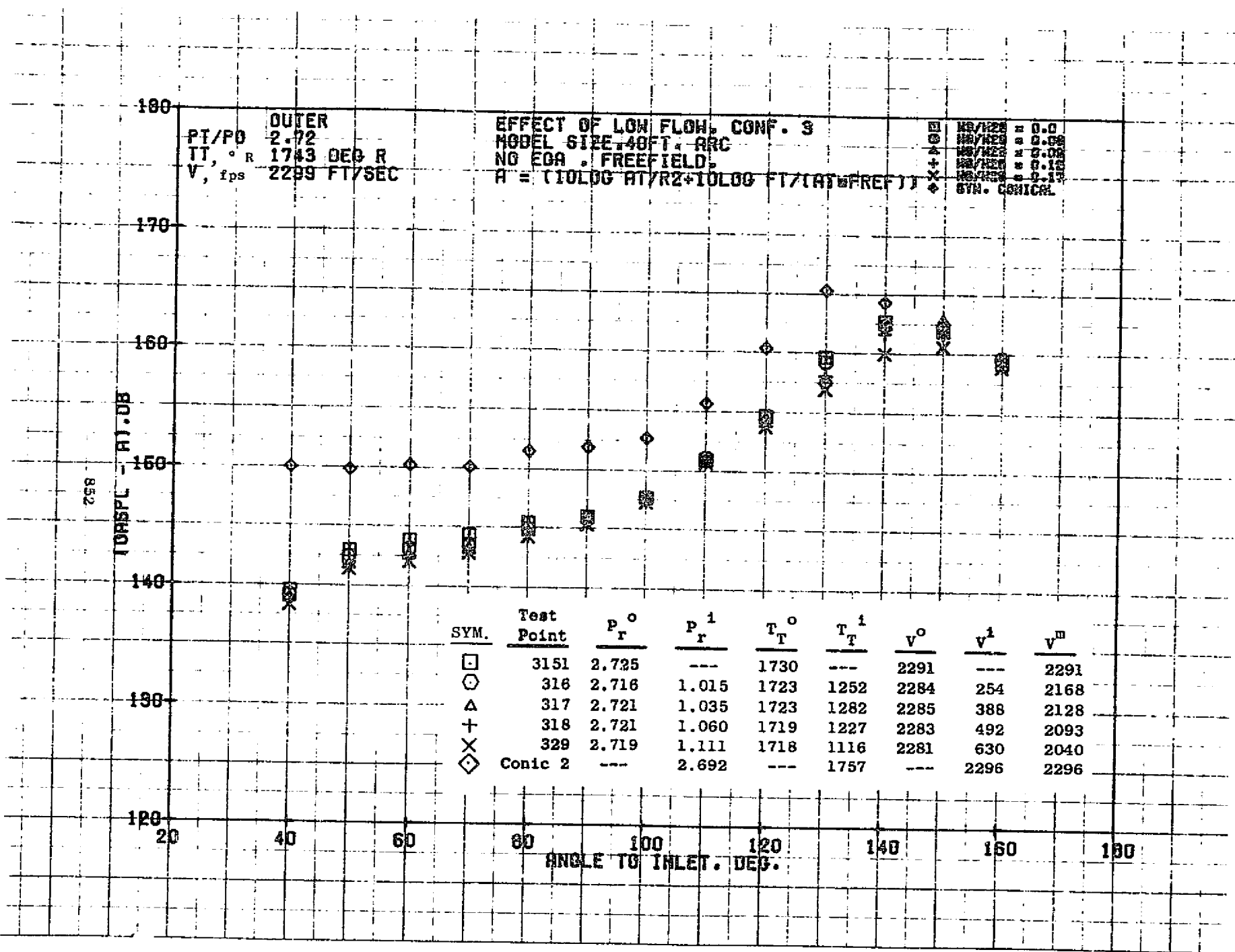
73KOLLSTEDT

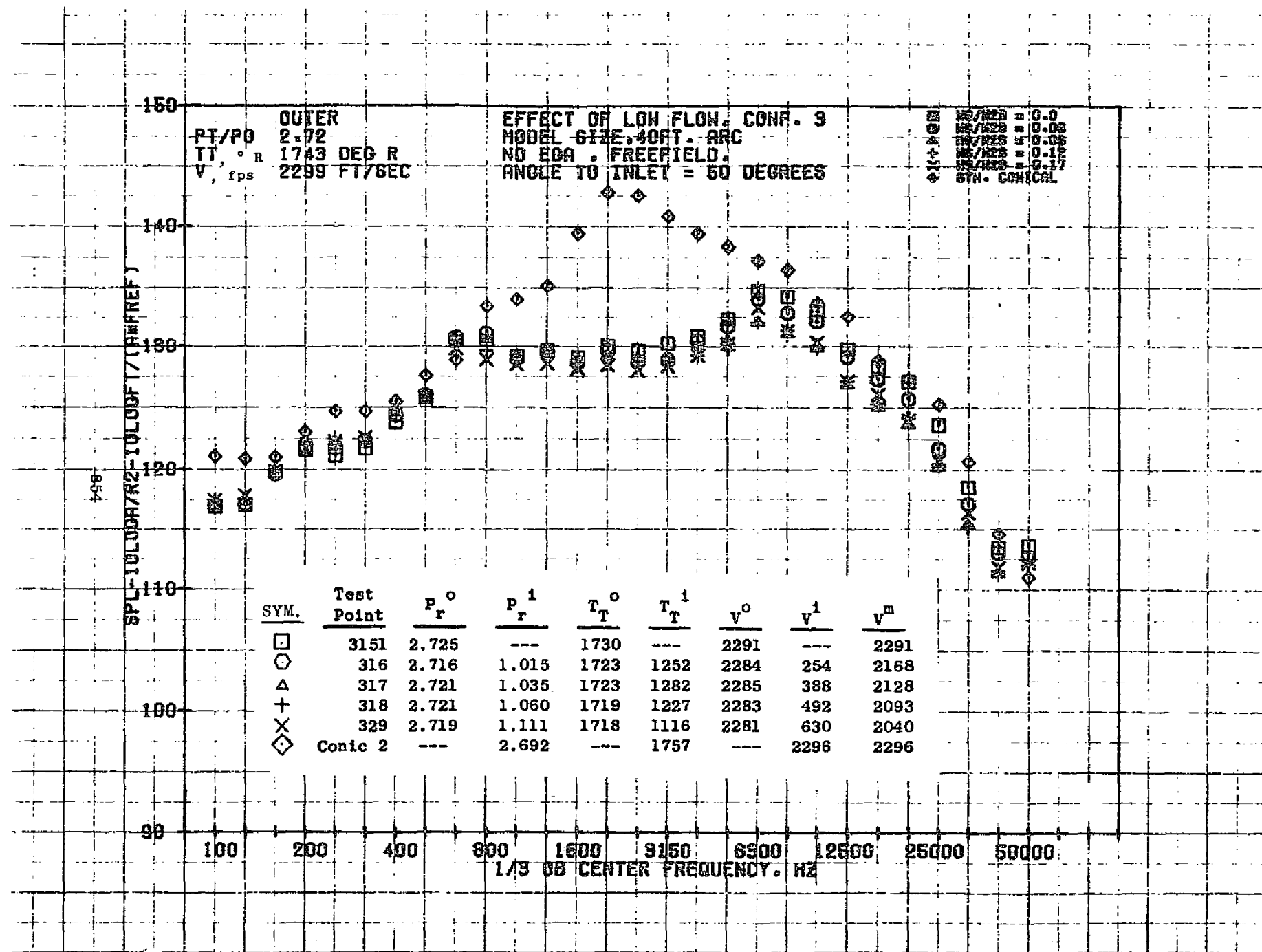


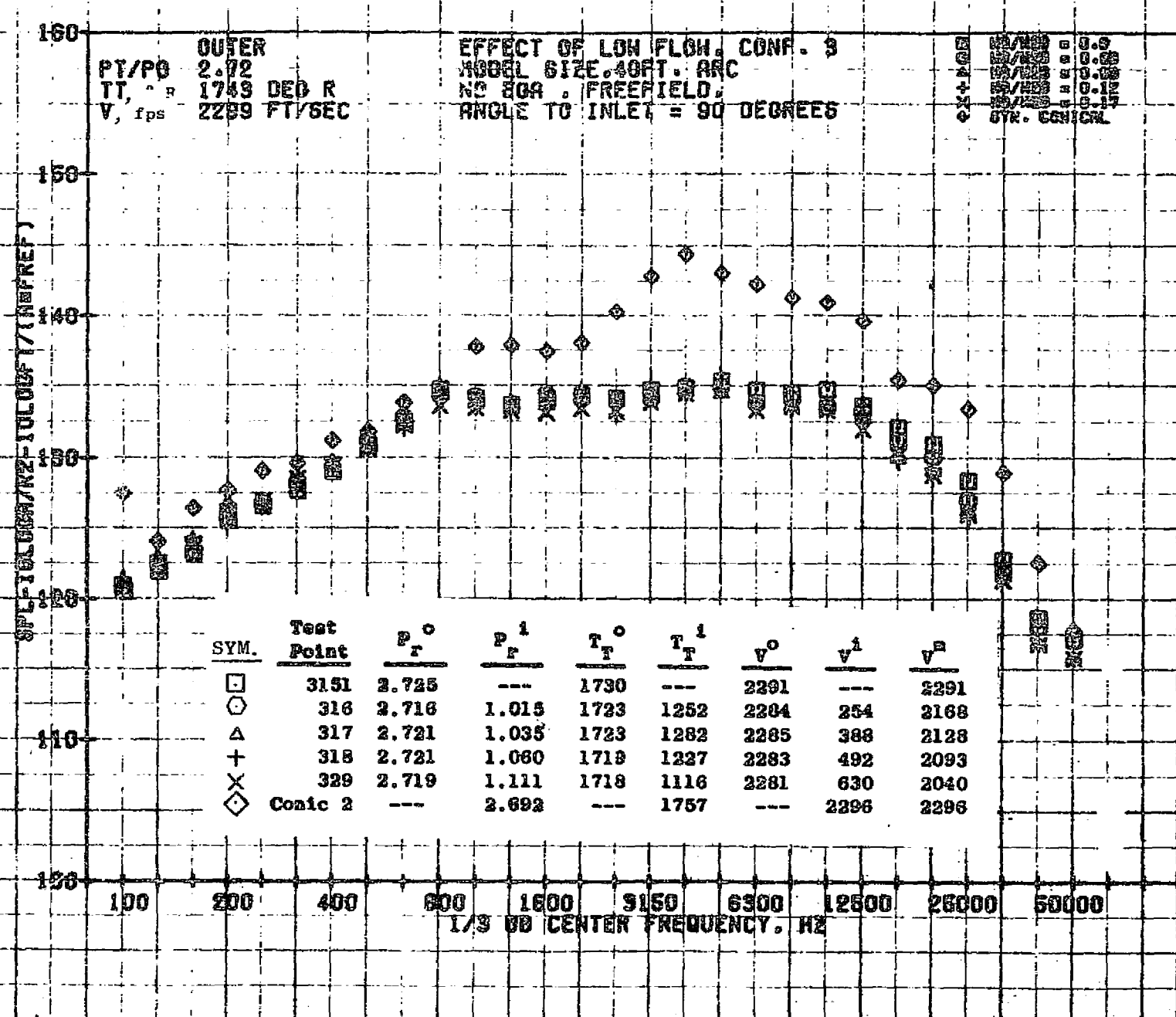
10/11/76
1X207-001

73KOLLSTEDT







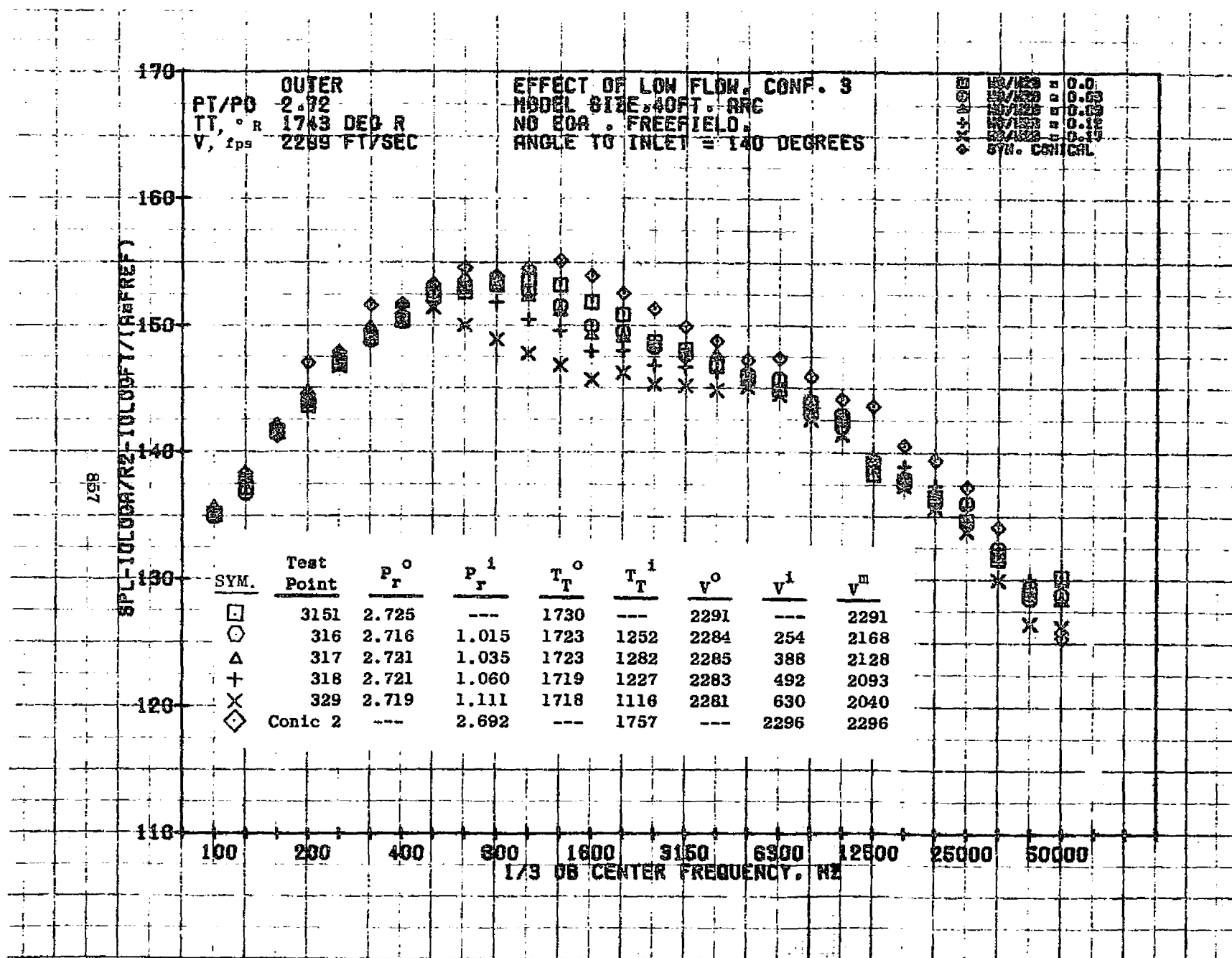


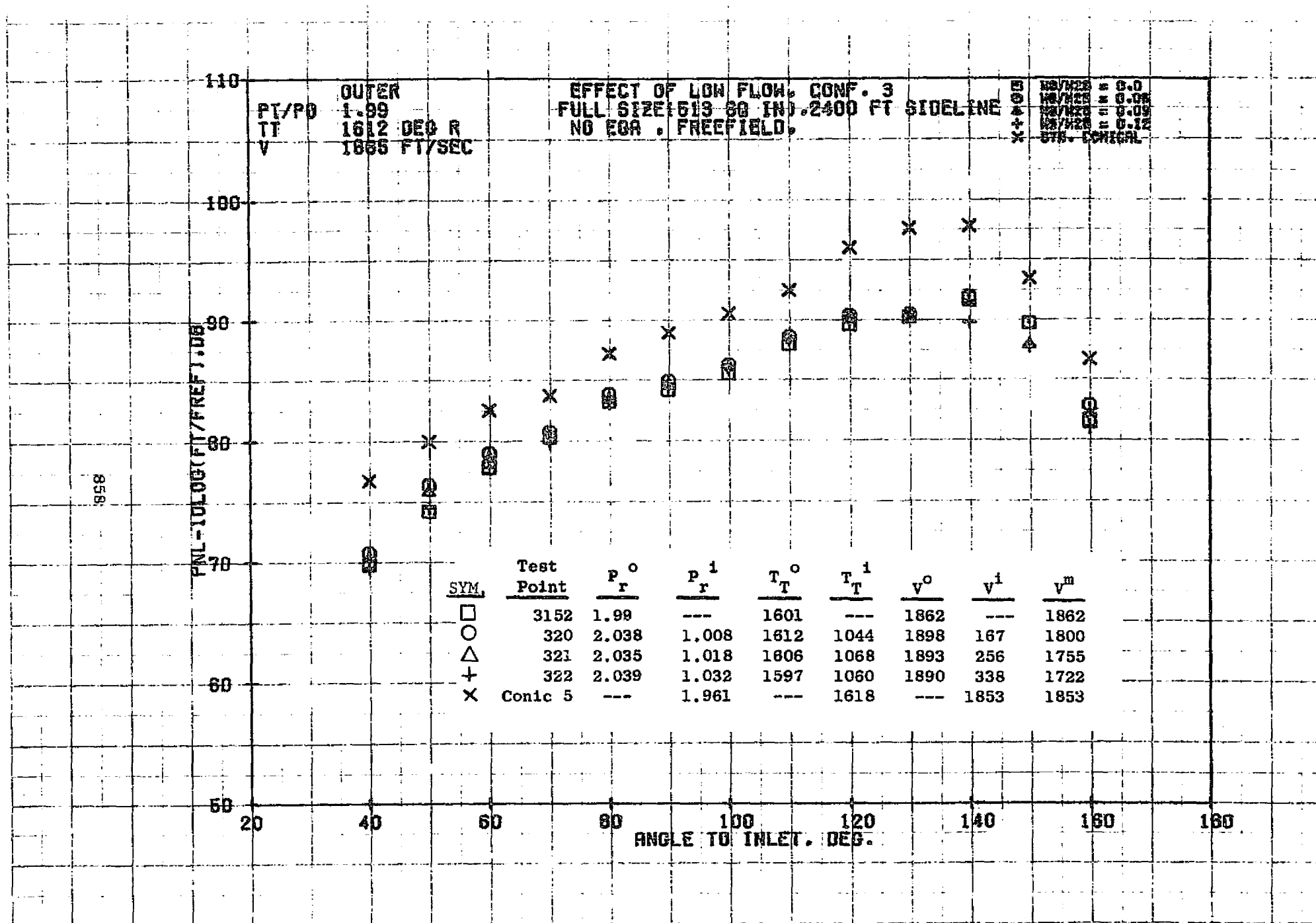
OUTER
 PT/PO 2.72
 TT, " R 1743 DEG R
 V, fps 2299 FT/SEC

EFFECT OF LOW FLOW, CONF. 9
 MODEL SIZE 40FT. ARC
 NO BGA, FREEFIELD
 ANGLE TO INLET = 90 DEGREES

W/W 0.9
 W/W 0.08
 W/W 0.08
 W/W 0.12
 W/W 0.17
 SYN. CONICAL

SYM.	Test Point	P _T ⁰	P _T ¹	T _T ⁰	T _T ¹	V ⁰	V ¹	V ²
□	3151	2.725	---	1730	---	2291	---	2291
○	316	2.716	1.015	1723	1252	2204	254	2168
△	317	2.721	1.035	1723	1282	2285	388	2128
+	318	2.721	1.060	1719	1227	2283	492	2093
x	329	2.719	1.111	1719	1116	2281	630	2040
◇	Conic 2	---	2.692	---	1757	---	2296	2296





10/25/76
1X558-001

73KOLLSTEDT

658

CIRCUPL - RT. DB

170

160

150

140

130

120

110

20

OUTER

PT/PD

1.99

TT

1612 DEG R

V

1865 FT/SEC

EFFECT OF LOW FLOW. CONF. 3

MODEL SIZE .40 FT. ARC

NO EOA, FREEFIELD.

 $A = (10 \log RT/R2 + 10 \log FT/(AT \cdot FREF))$

MOA

+

X

H8/H28 = 0.0

H8/H28 = 0.06

H8/H28 = 0.08

H8/H28 = 0.12

CONICAL

SYM.	Test Point	P_r^0	P_r^1	T_T^0	T_T^1	V^0	V^1	V^m
□	3152	1.99	---	1601	---	1862	---	1862
○	320	2.038	1.008	1612	1044	1898	167	1800
△	321	2.035	1.018	1606	1068	1893	256	1755
+	322	2.039	1.032	1597	1060	1890	338	1722
X	Conic 5	---	1.961	---	1618	---	1853	1853

ANGLE TO INLET. DEG.

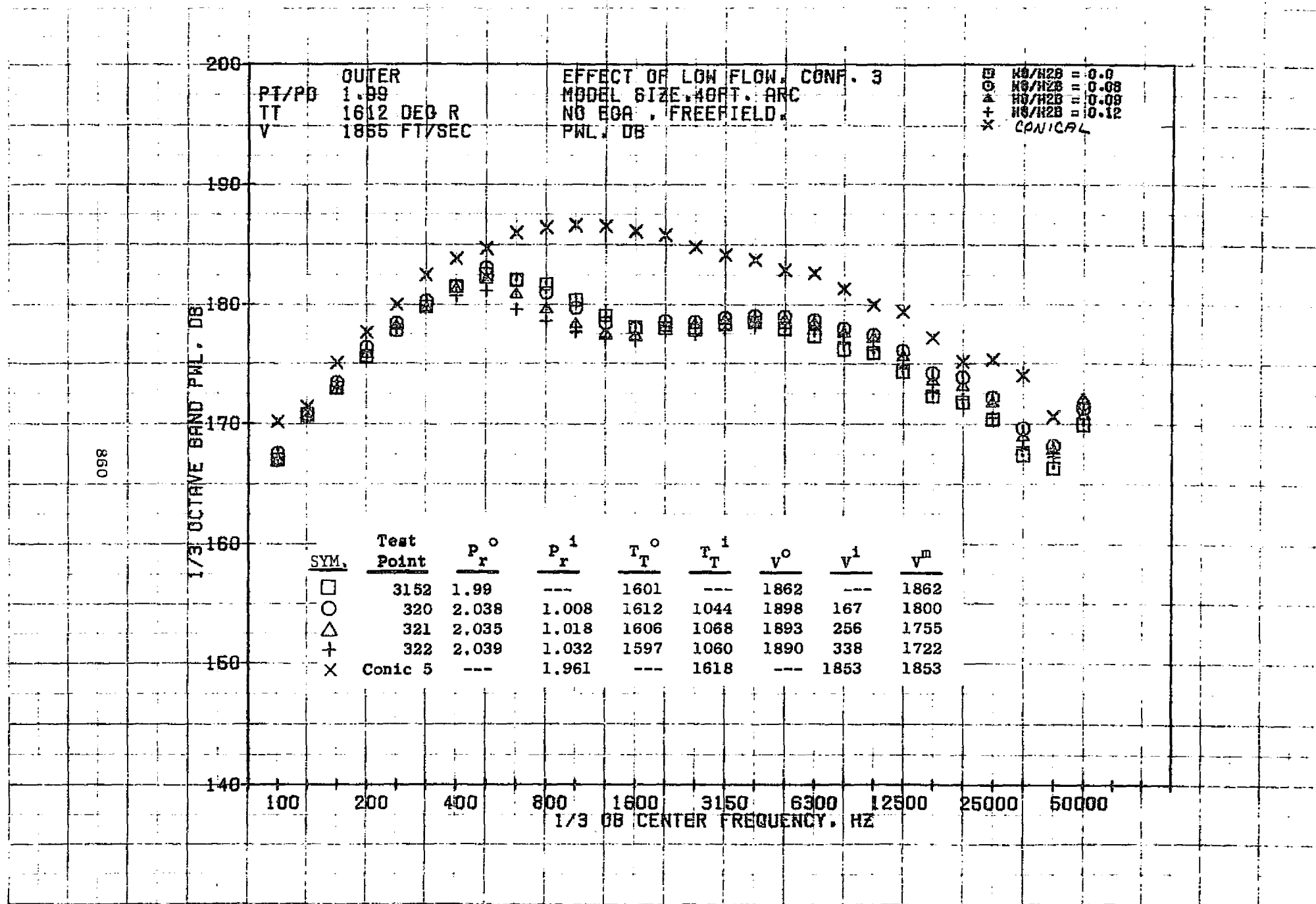
140

160

180

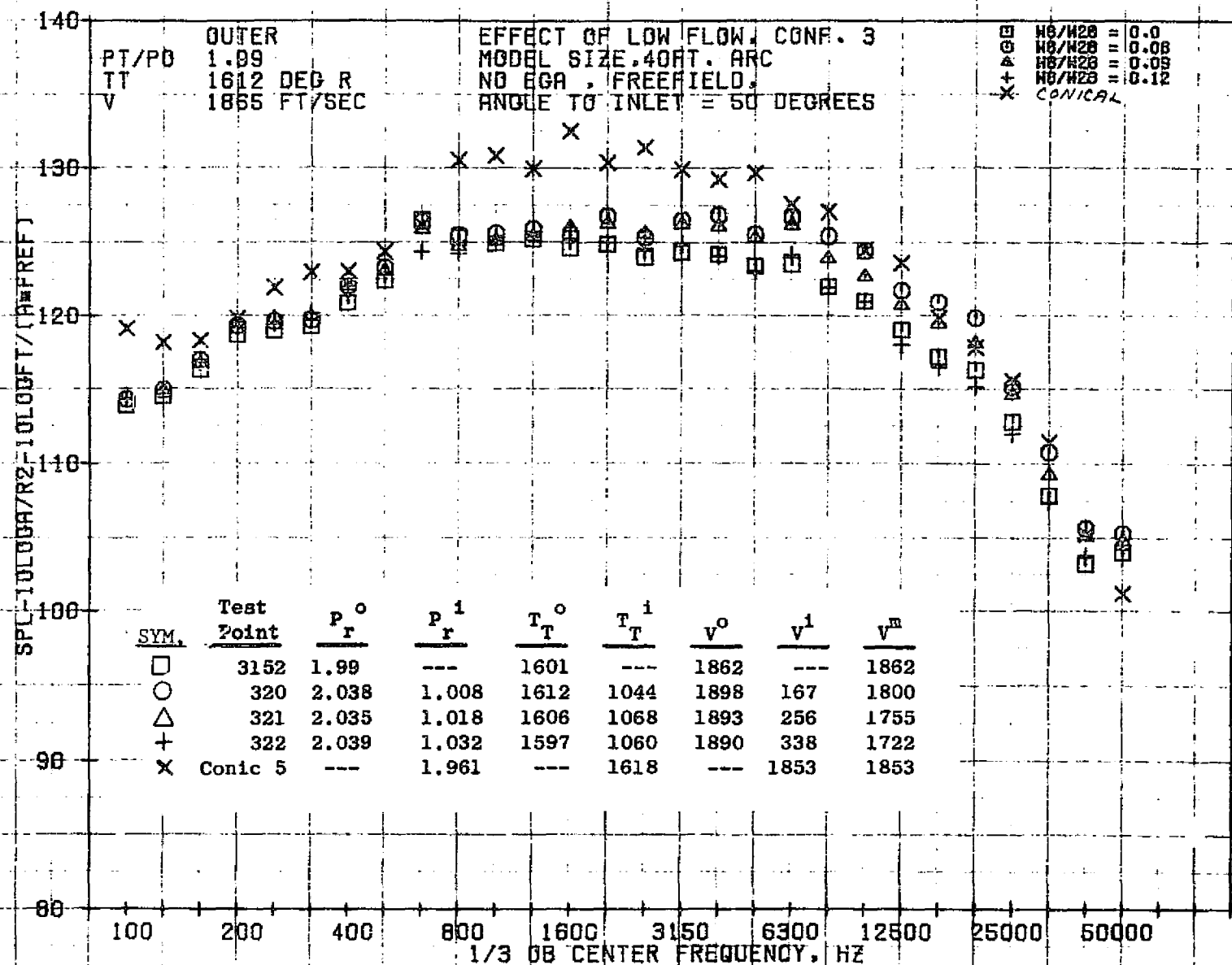
10/12/76
1X525-001

73KOLLSTEOT



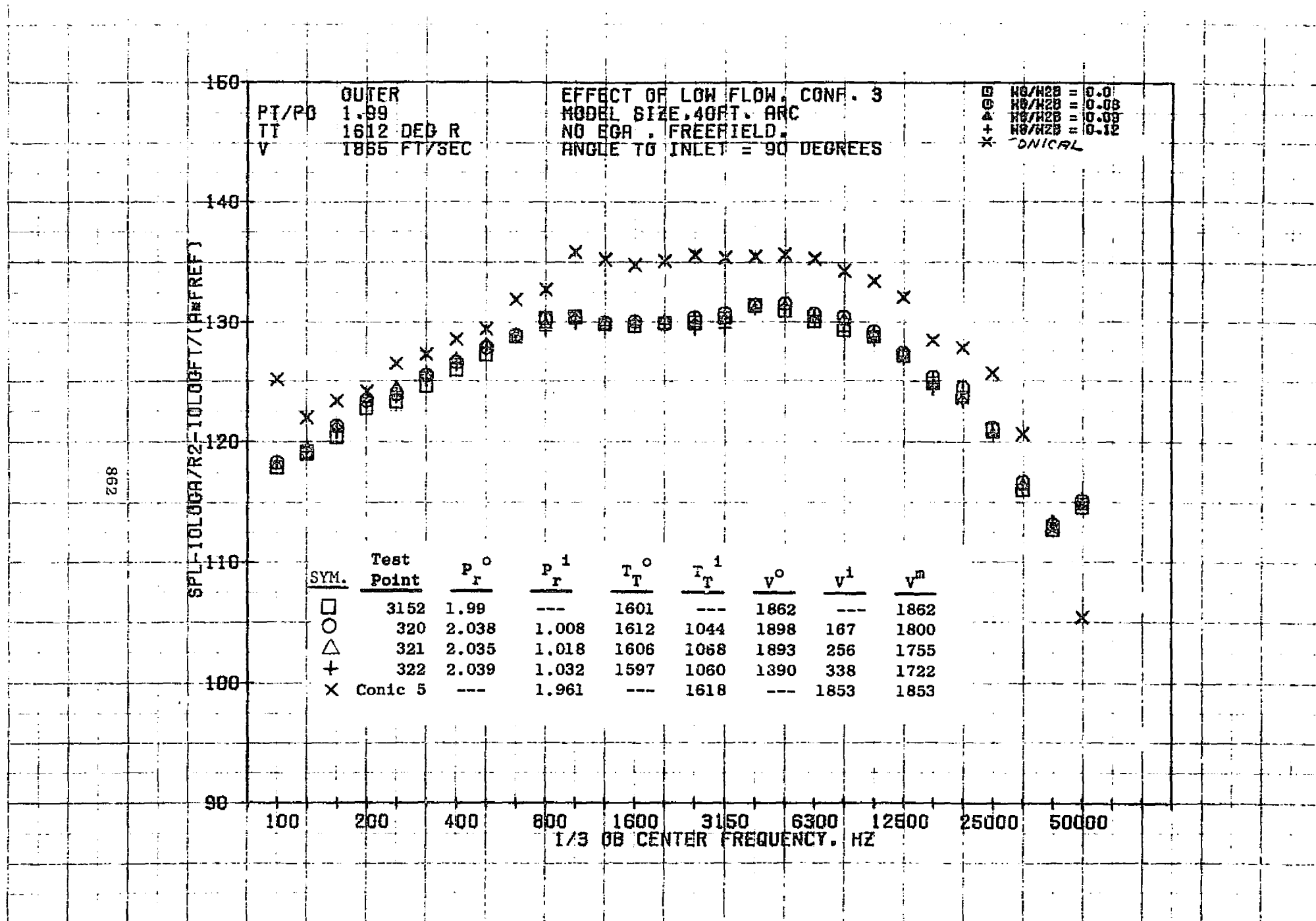
10/12/76
1X525-001

73KOLLSTEDT



10/12/76
1X525-001

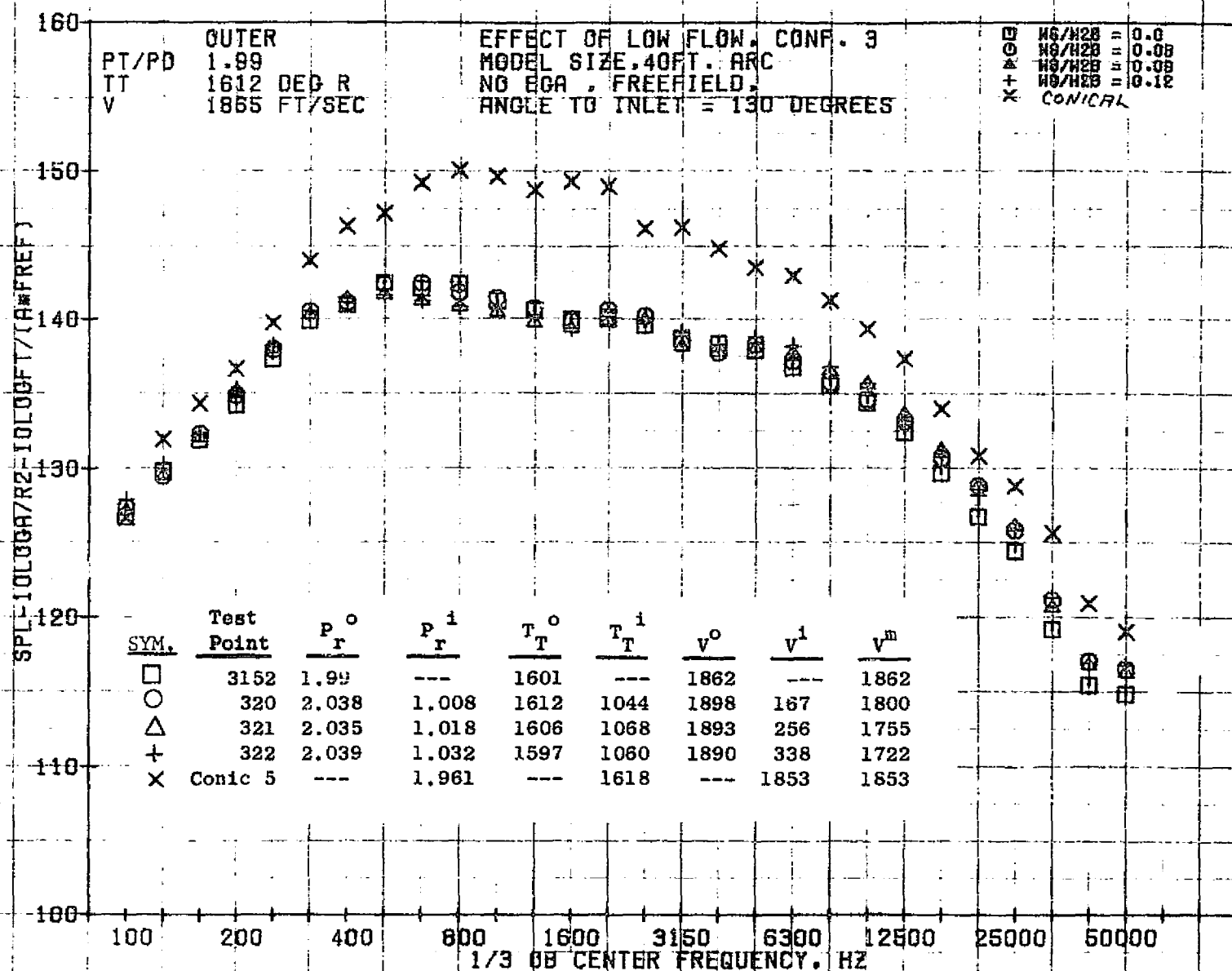
73KOLLSTEDT

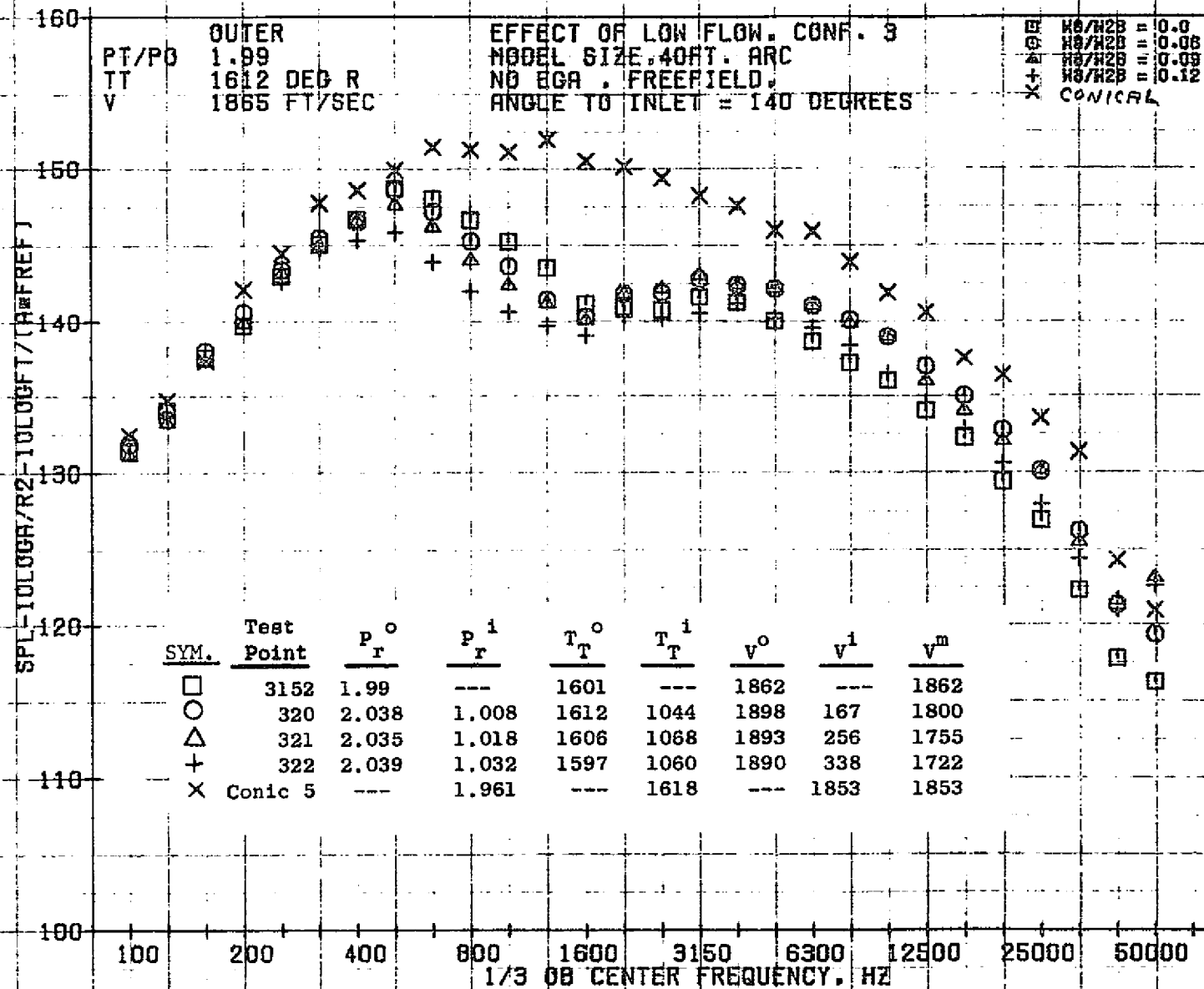


10/12/76
1X525-001

73KOLLSTEDT

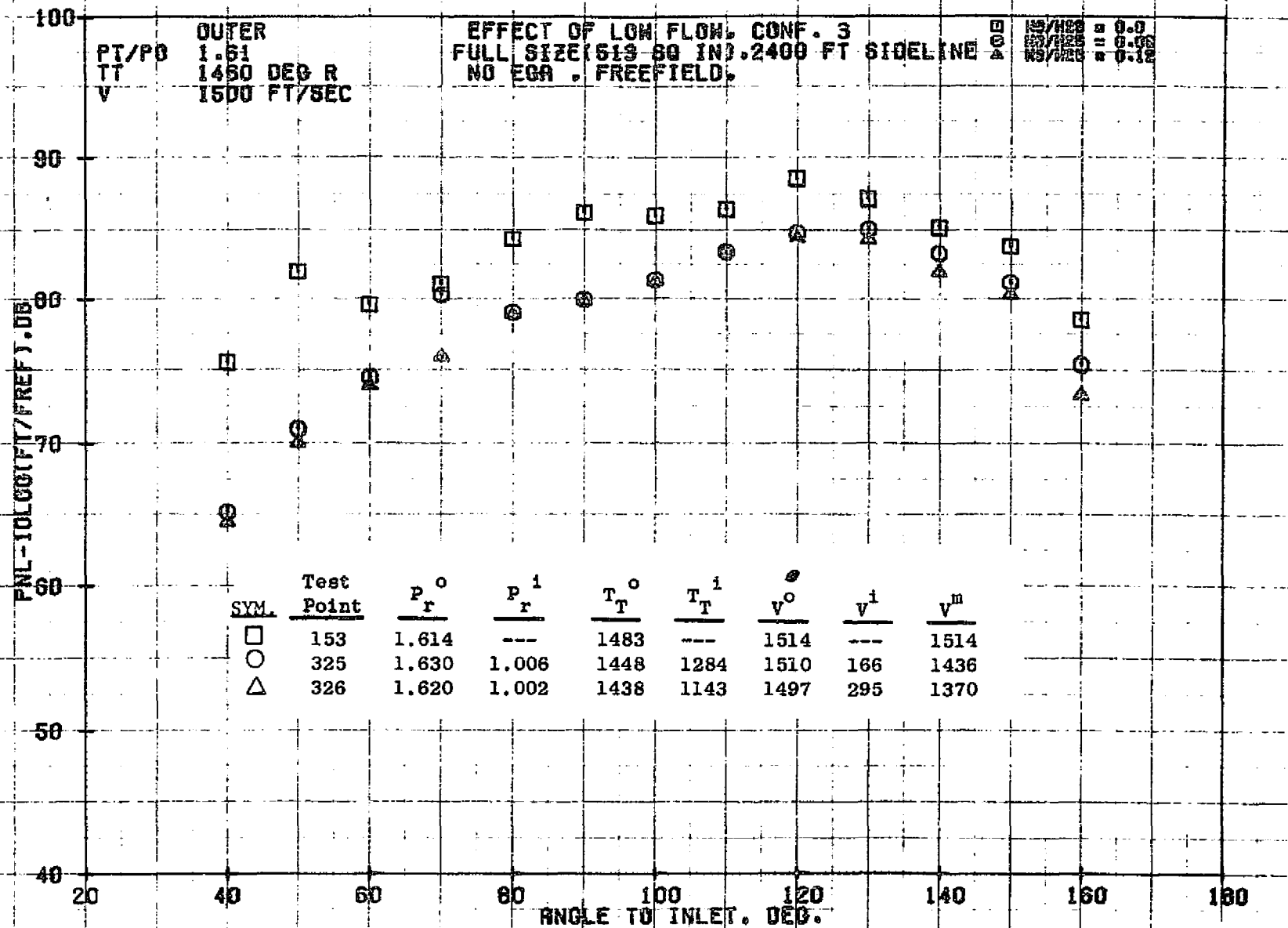
898





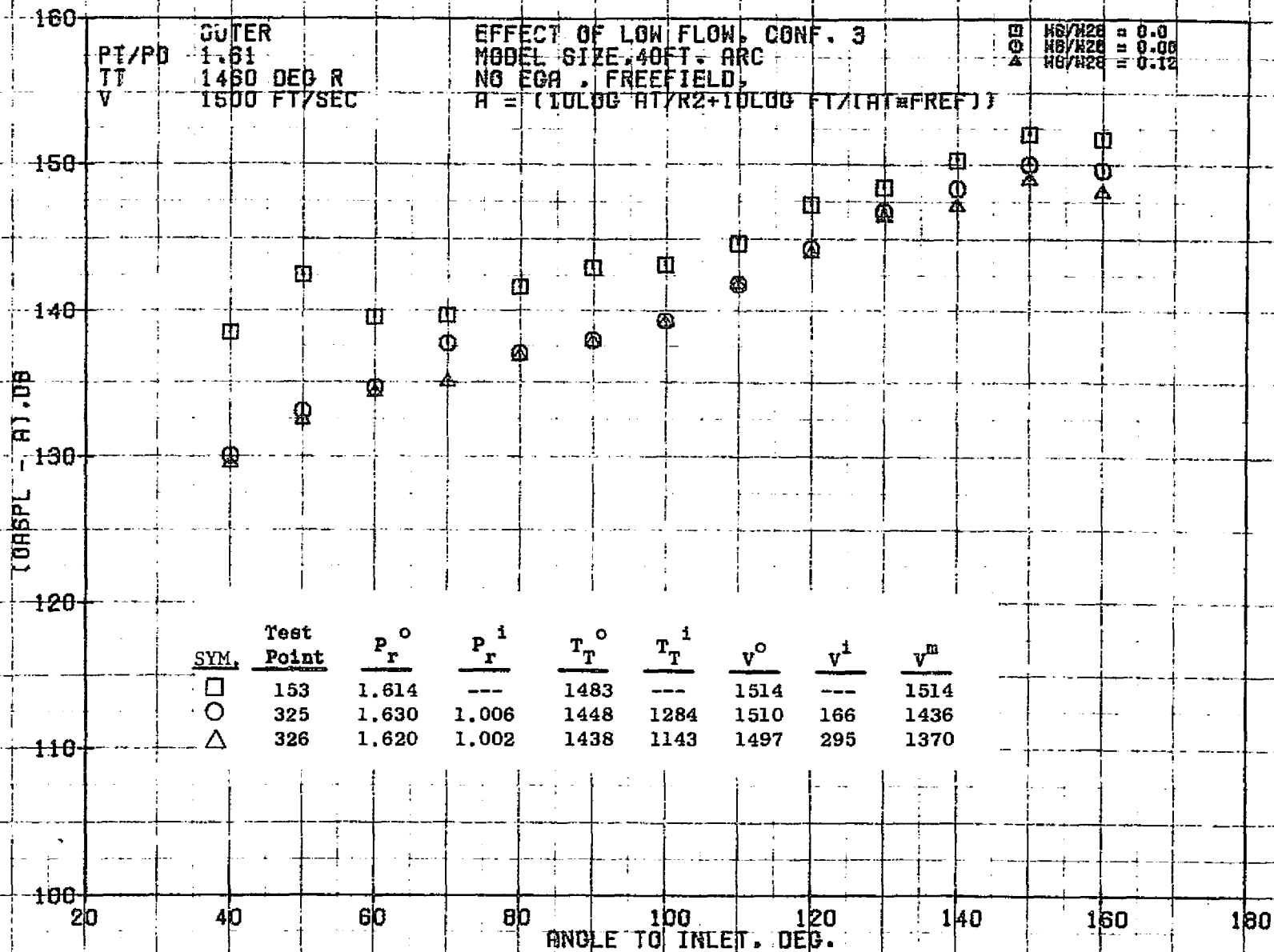
10/12/76
1X525-001

73KOLLSTEOT

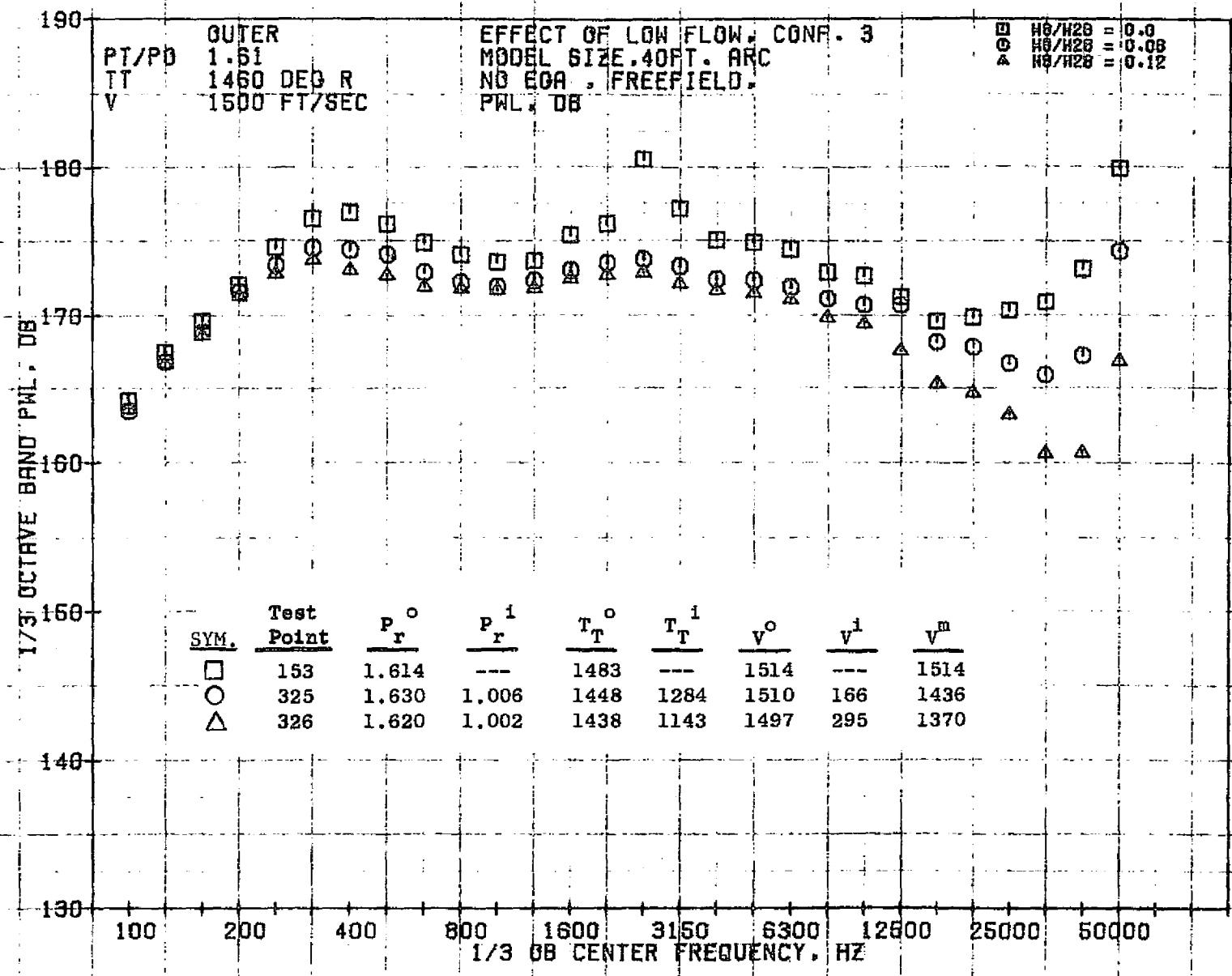


10/25/76
1X558-001

73KOLLSTEDT

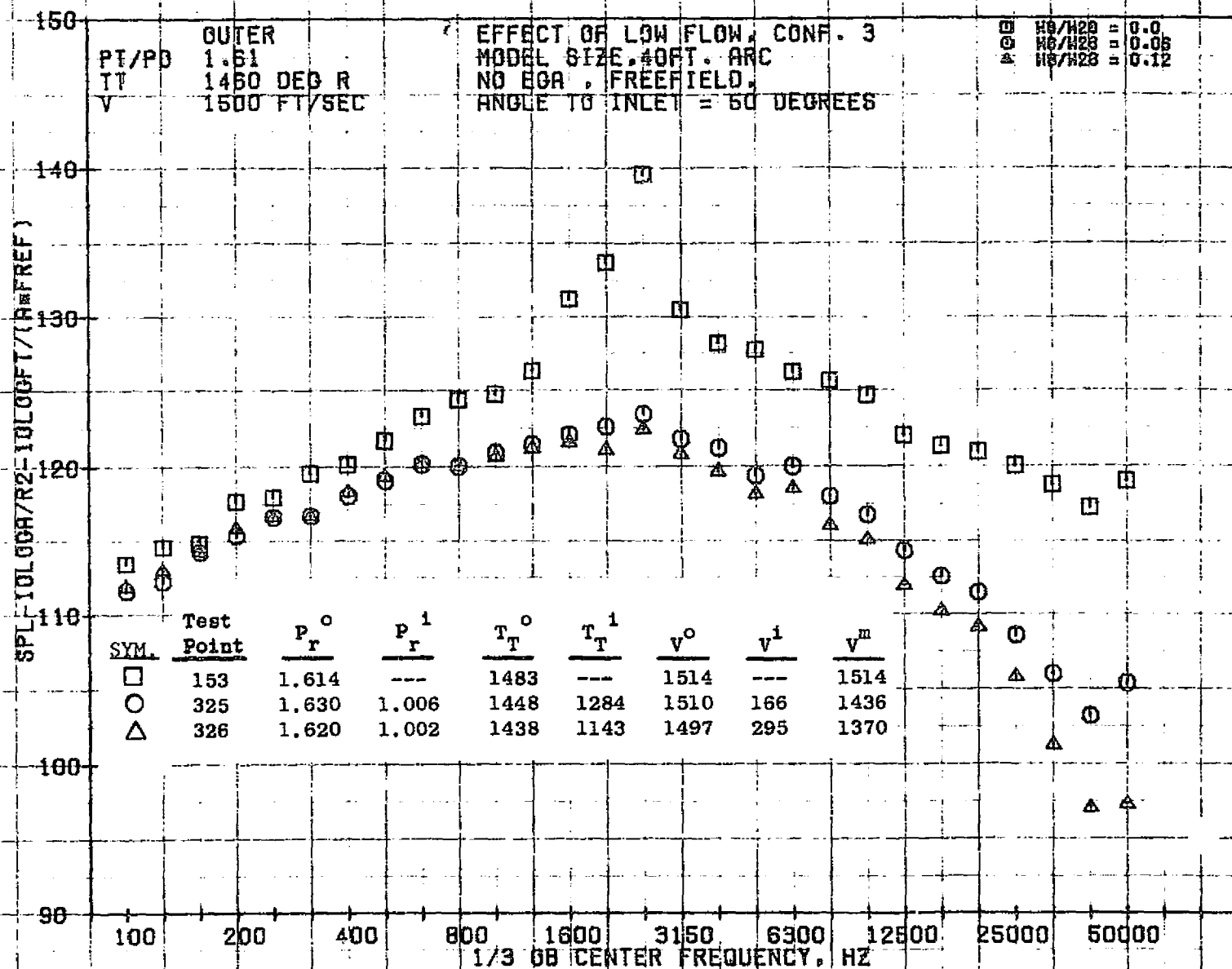


867



10/12/76
1X525-001

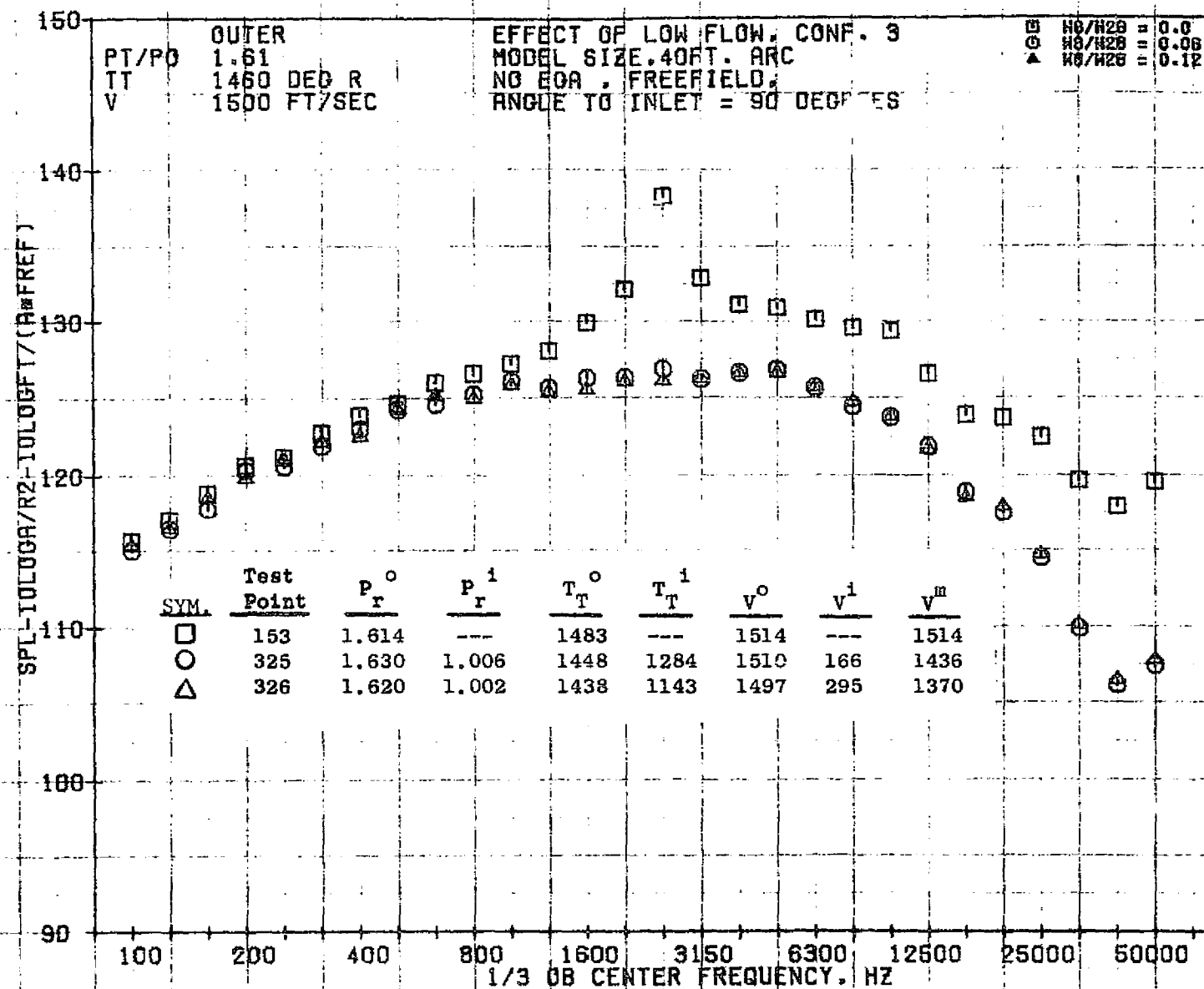
73KOLLSTEDT



10/12/76
1X525-001

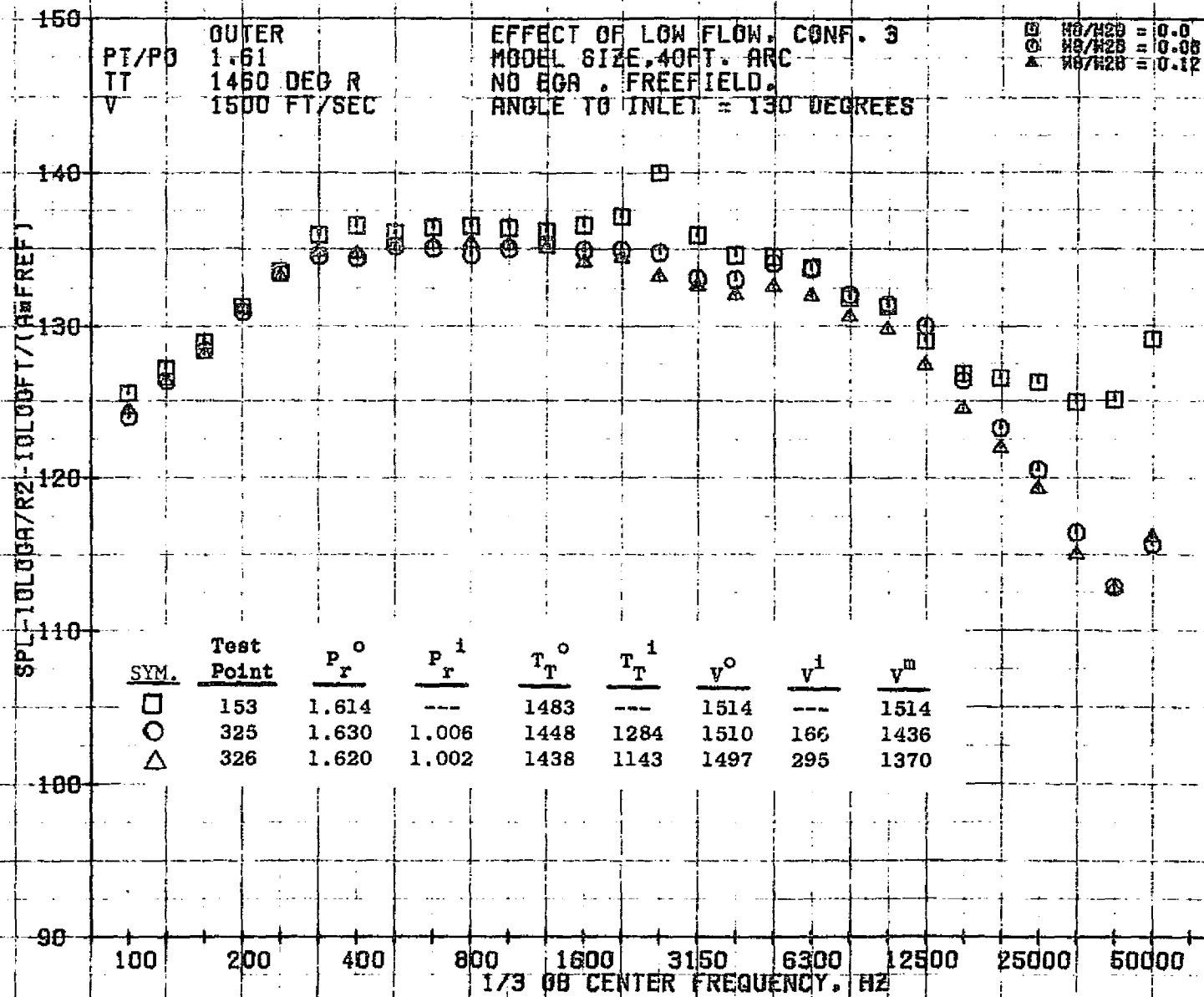
73KOLLSTEDT

698



10/12/76
1X525-001

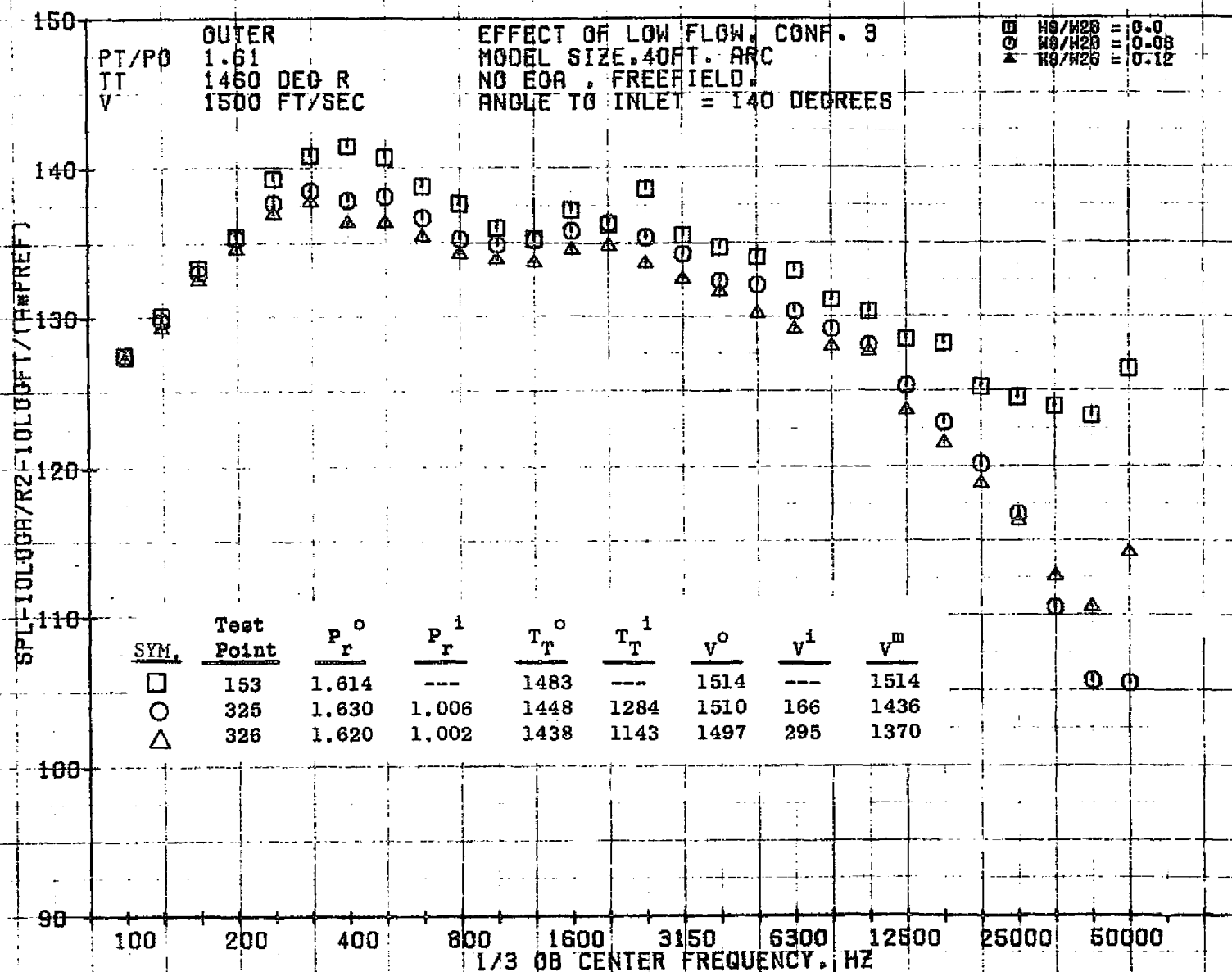
73KOLLSTEDT



10/12/76
1X525-001

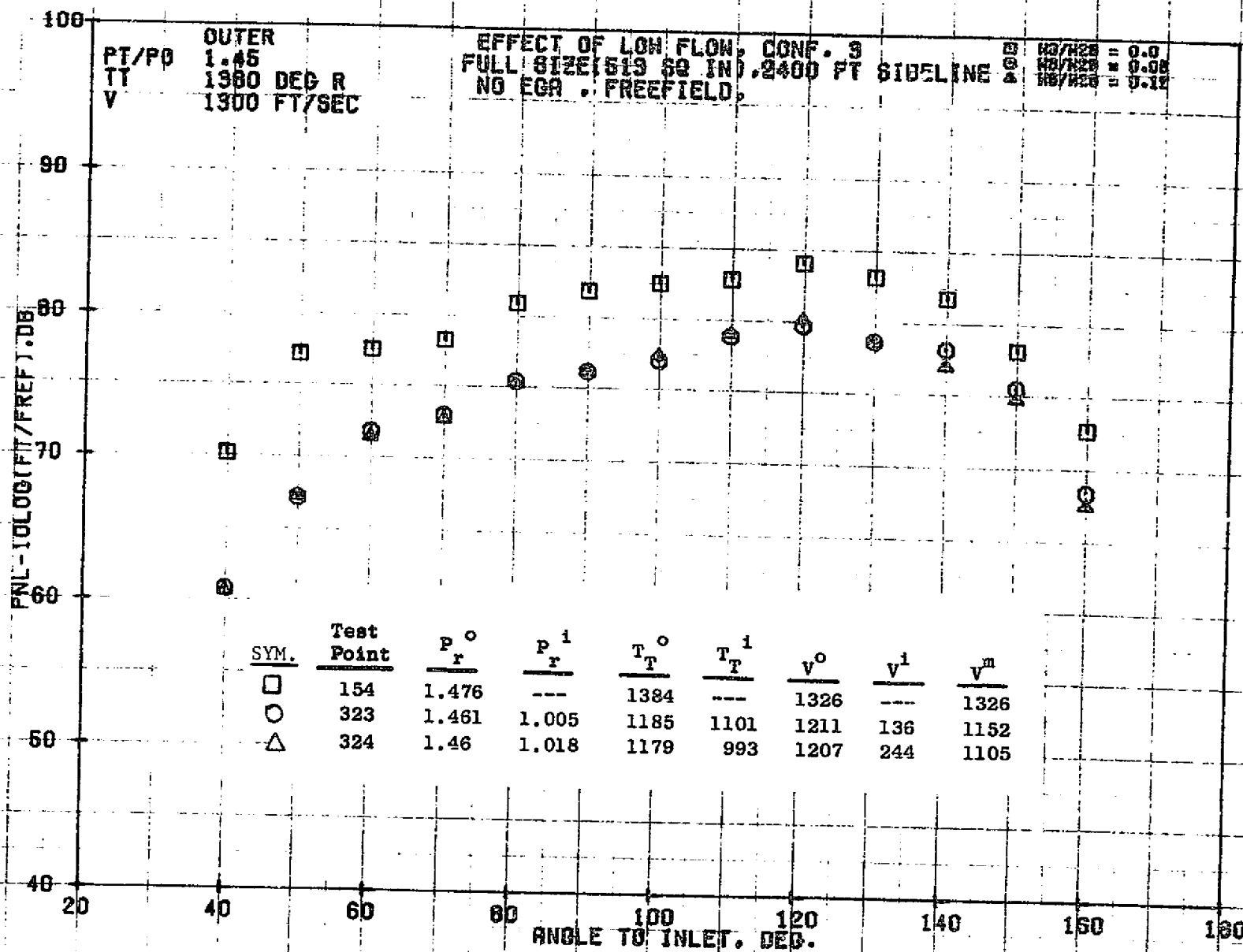
73KOLLSTEDT

871



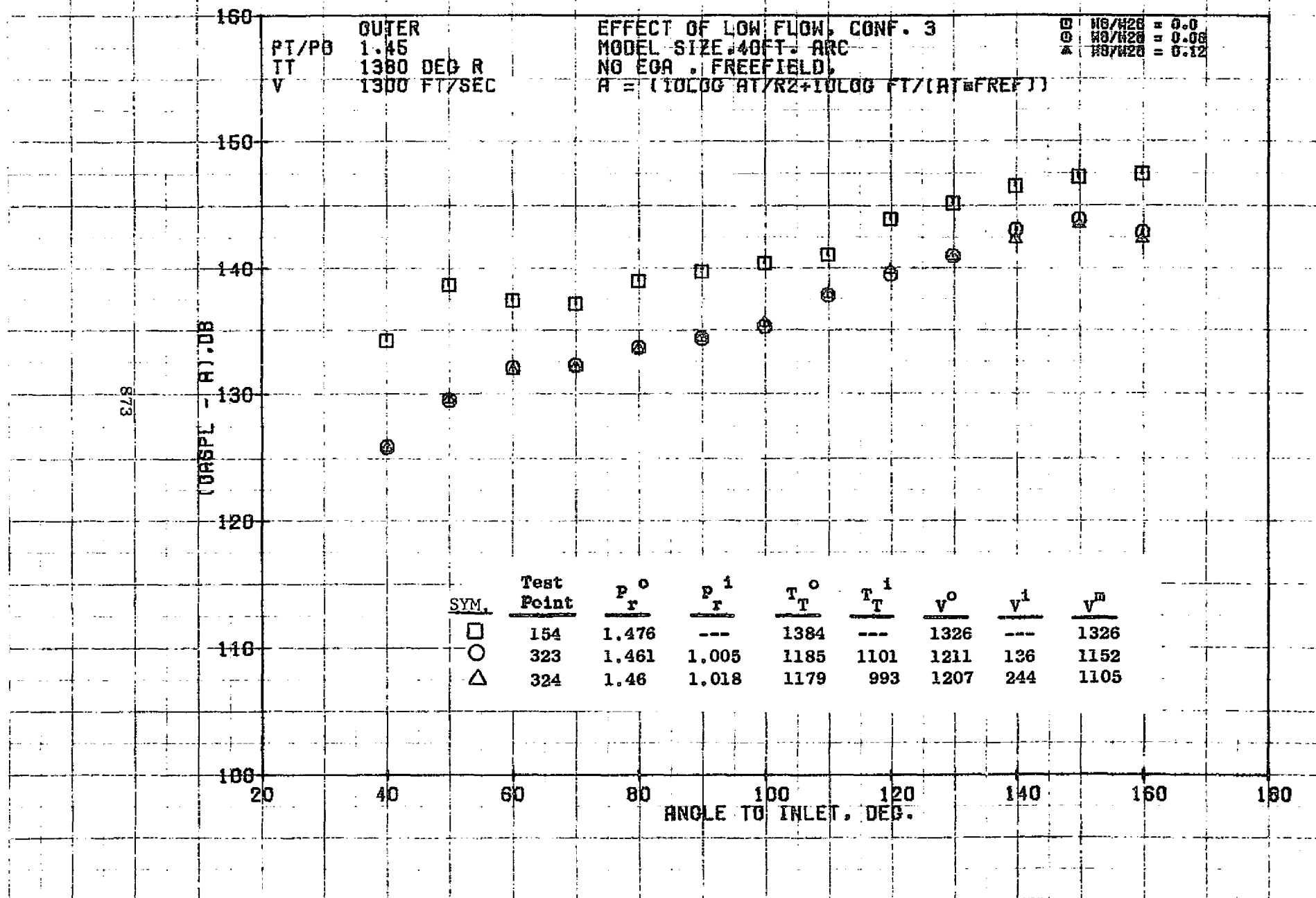
10/12/76
1X525-001

73KOLLSTEOT



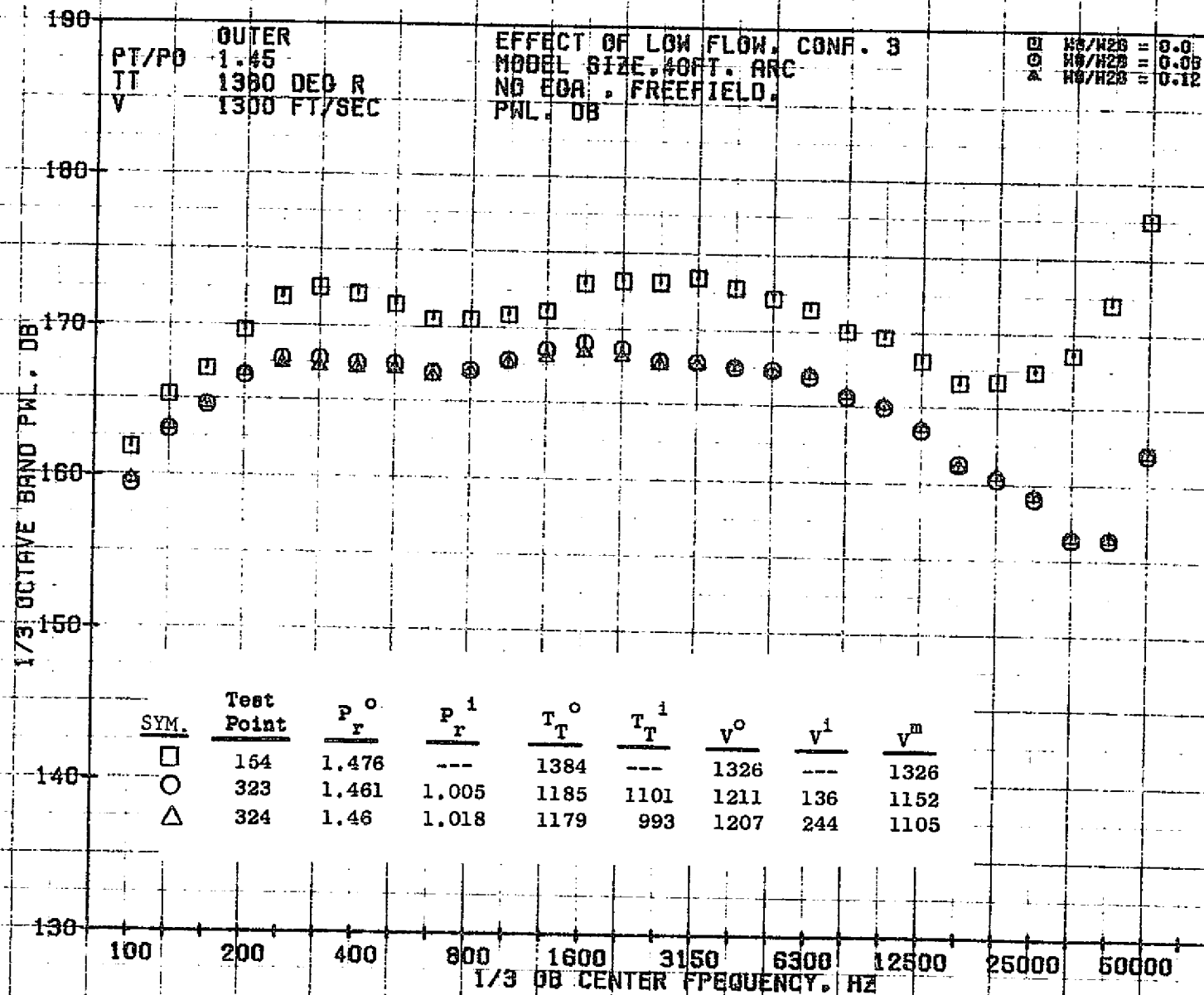
10/25/76
1X556-001

73KOLLSTEDT



10/12/76
1X525-001

73KOLLSTEDT



10/12/76
1X525-001

73KOLLSTEDT

875

SPL-10LOG(R/R2-10LOG(F1/(R-RREF))

OUTER
PT/PO 1.45
TT 1380 DEG R
V 1300 FT/SEC

EFFECT OF LOW FLOW, CONF. 3
MODEL SIZE, 40FT. ARC
NO SGA, FREEFIELD
ANGLE TO INLET = 50 DEGREES

□ H₅/H₂₈ = 0.0
○ H₅/H₂₈ = 0.06
△ H₅/H₂₈ = 0.12

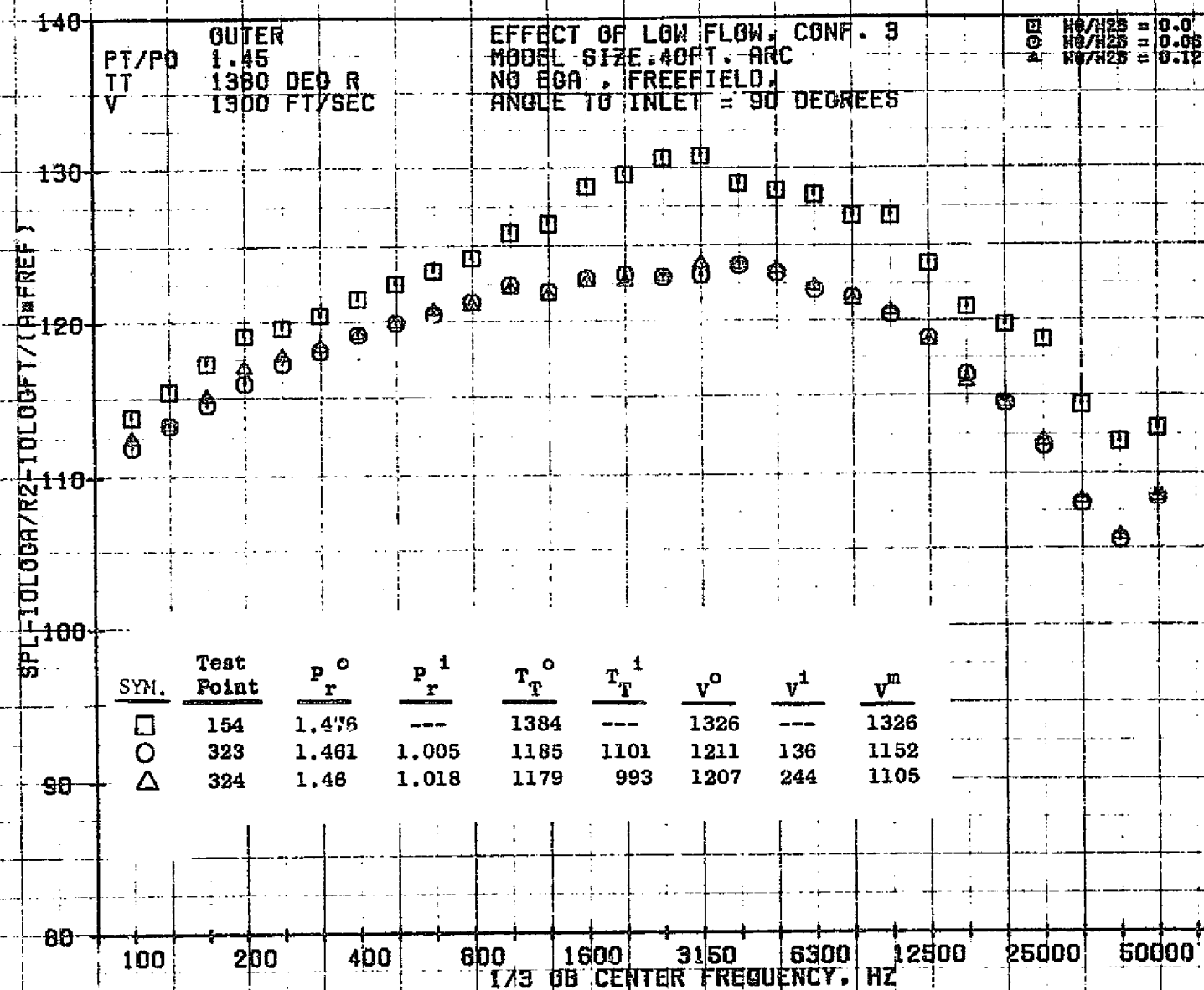
SYM	Test Point	P_r^0	P_r^1	T_T^0	T_T^1	V^0	V^1	V^m
□	154	1.476	---	1384	---	1326	---	1326
○	323	1.461	1.005	1185	1101	1211	136	1152
△	324	1.46	1.018	1179	993	1207	244	1105

100 200 400 800 1600 3150 6300 12500 25000 50000
1/3 OB CENTER FREQUENCY, HZ

10/12/76
1X525-001

73KOLLSTEDT

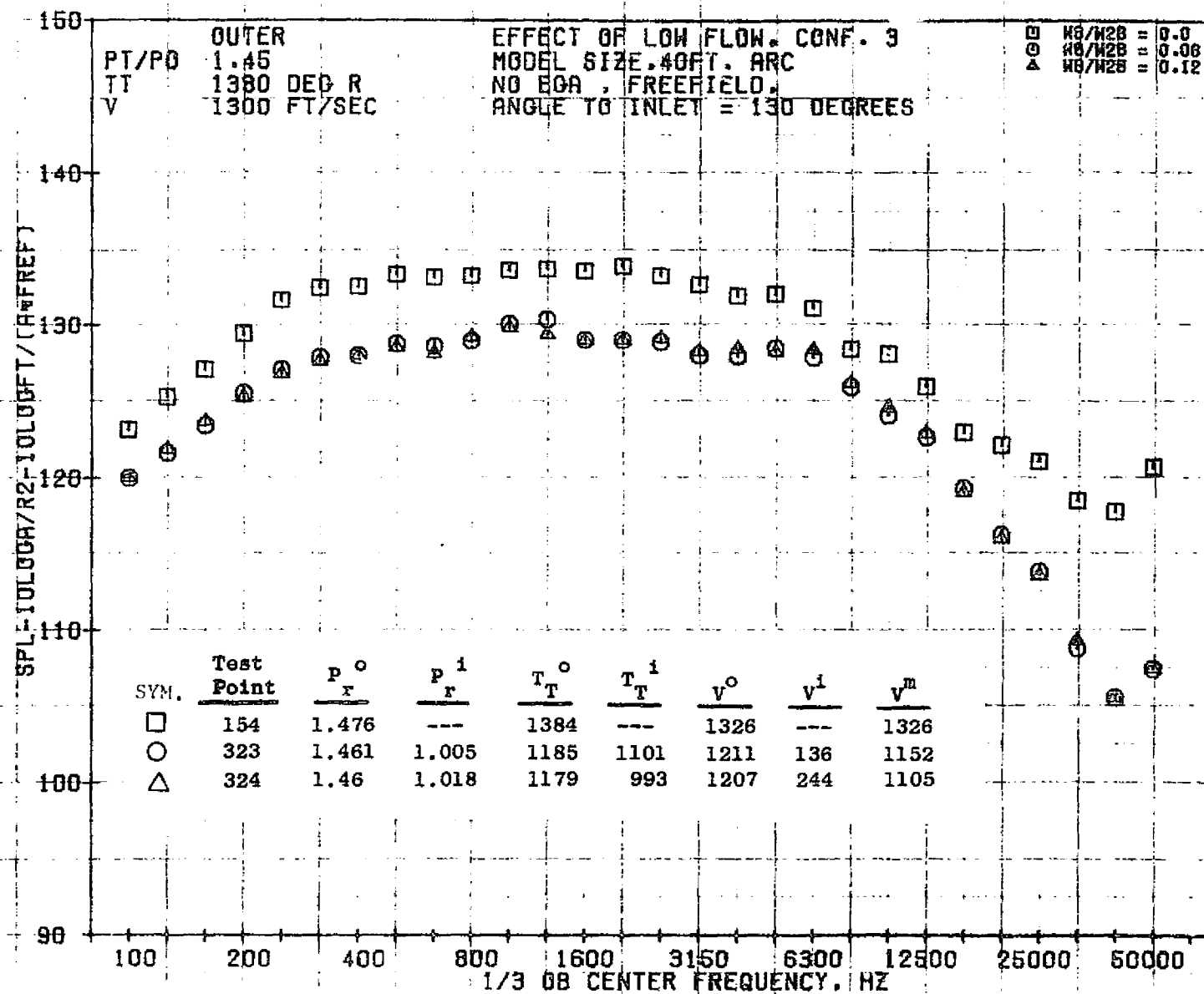
876



10/12/76
1X525-001

73KOLLSTEDT

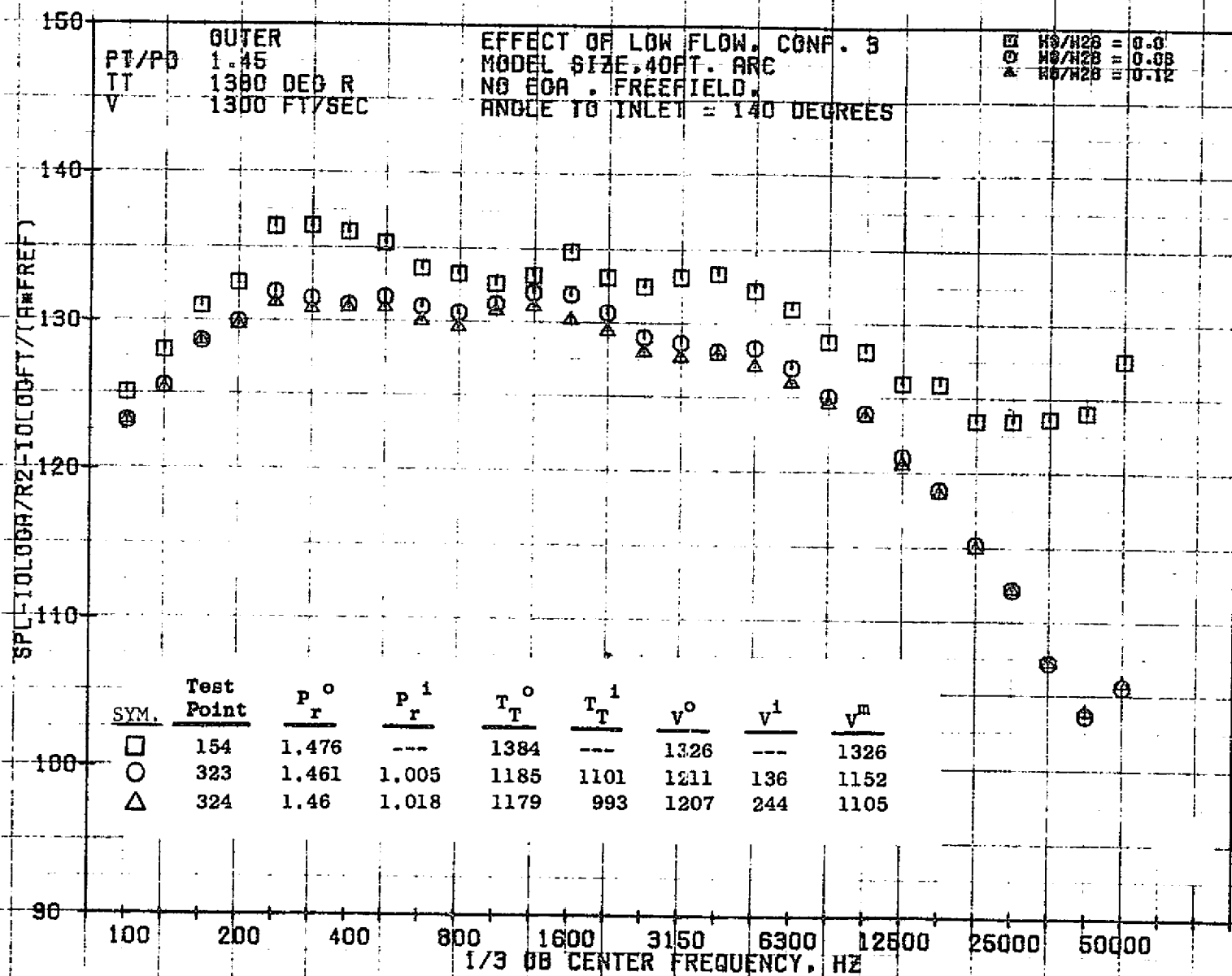
877



10/12/76
1X525-001

73KOLL STEOT

878



10/12/76
1X525-001

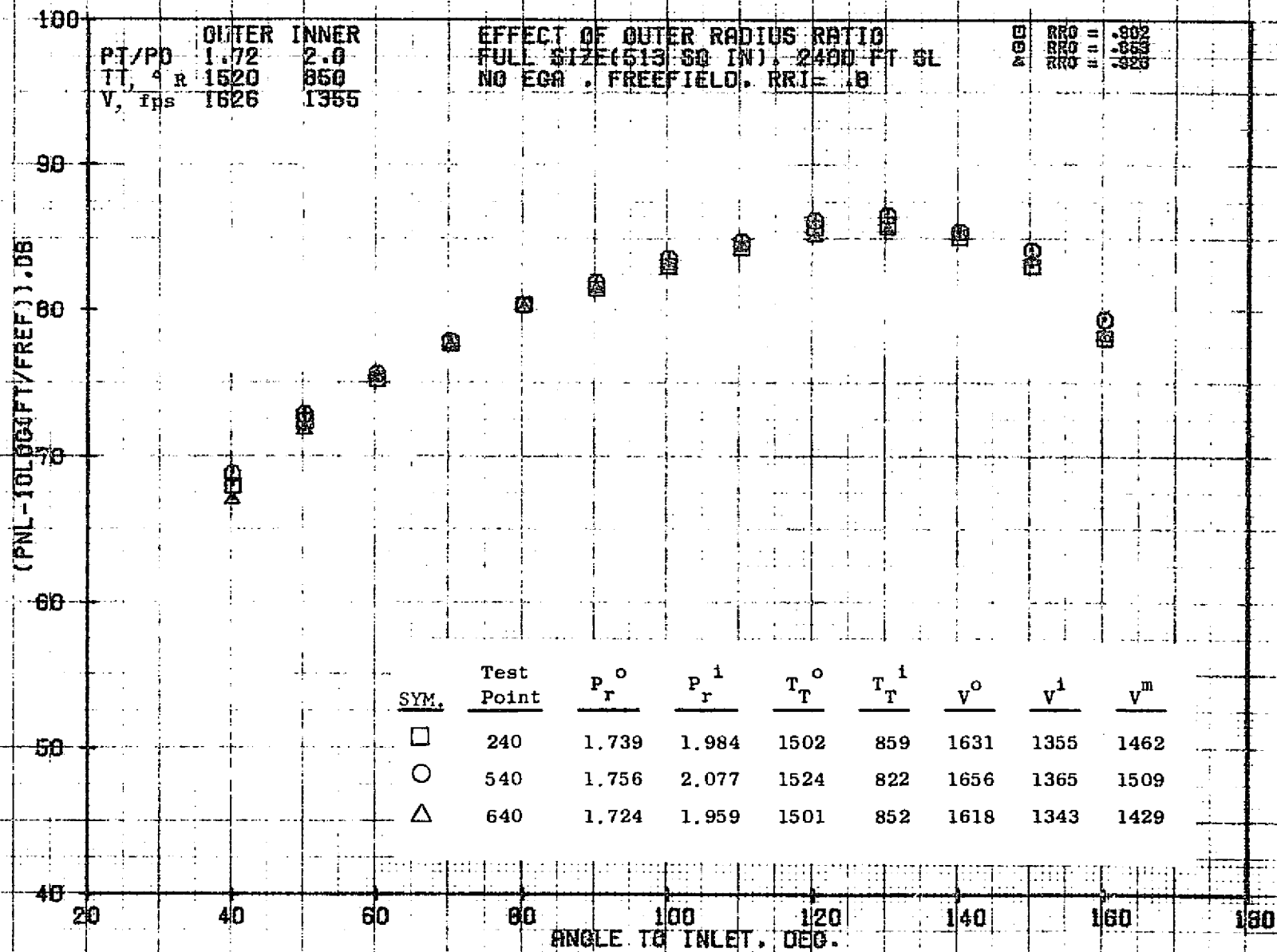
73KOLLSTEDT

7.4 COMPARISONS OF DATA FOR IVP NOZZLES WITH HIGH AMOUNTS OF INNER FLOW

The purpose of this test series was to examine the noise suppression characteristics of coannular nozzle configurations with high inner flows. Data presentations are described in the following sections.

7.4.1 Effect of Outer Radius Ratio

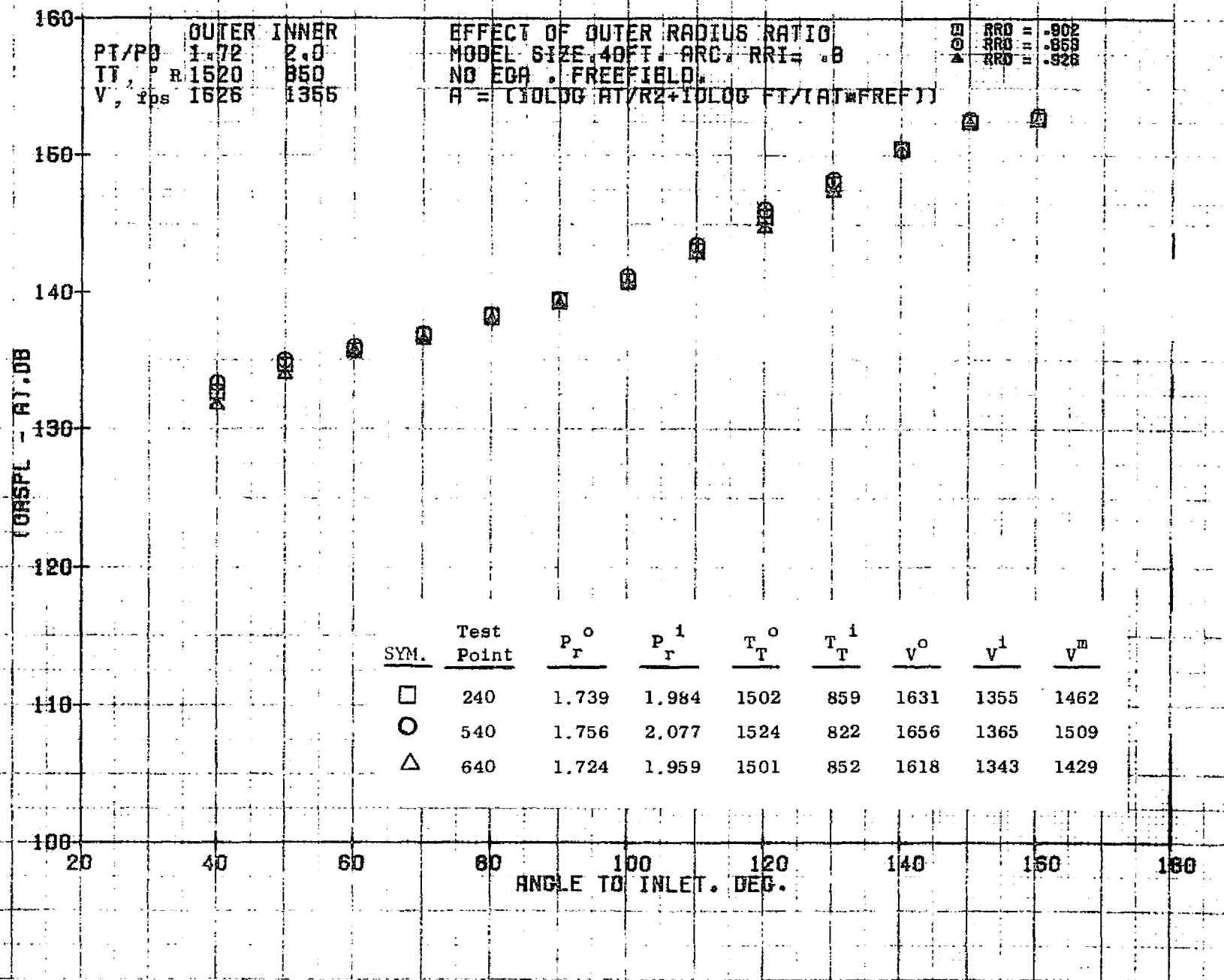
In this section, the test results from Configurations 2, 5, and 6 are compared. All three configurations have the same inner radius ratio (0.8) and plug geometry, but the outer radius ratio varies from 0.853 to 0.926.



10/27/76
1X008-001

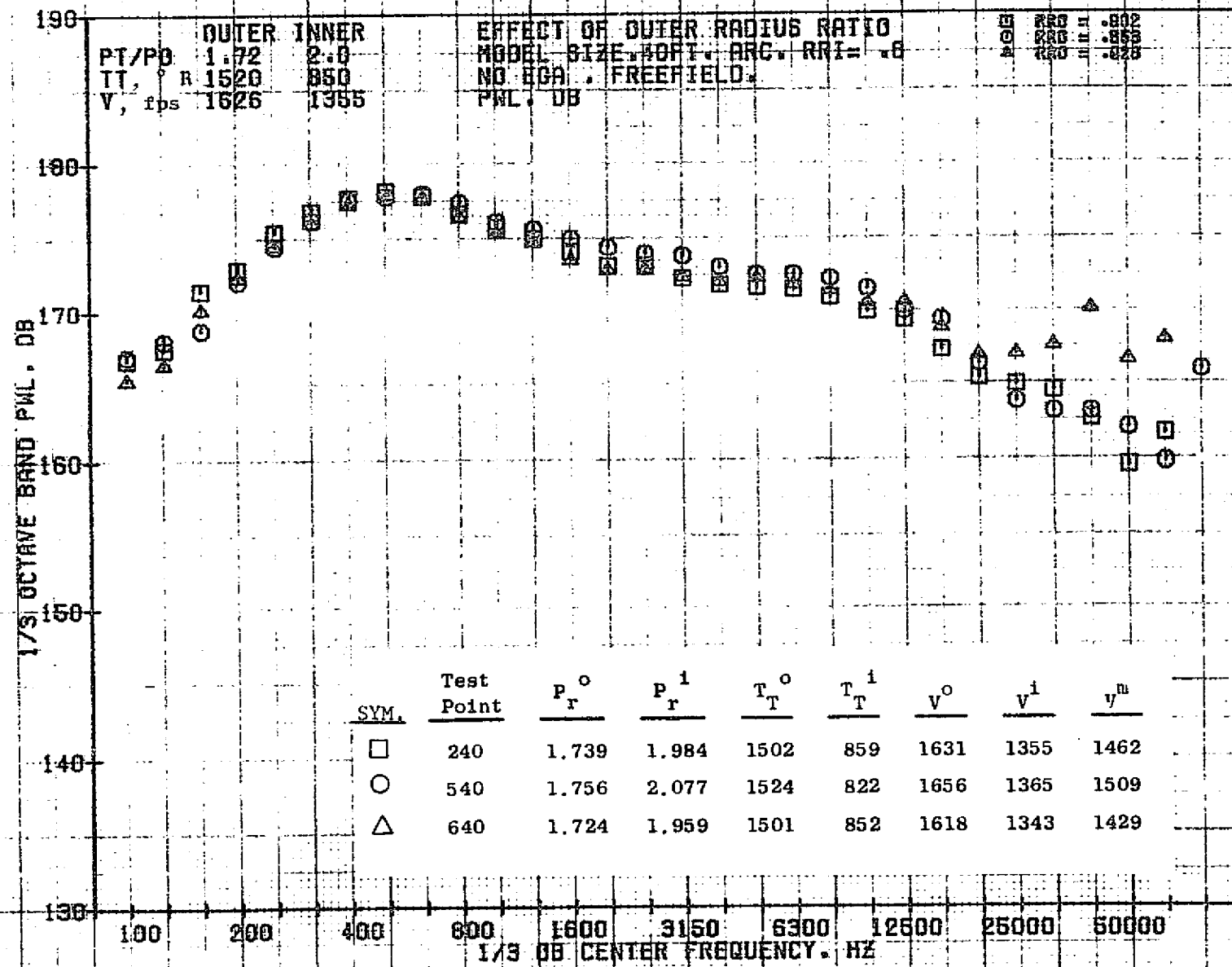
73KOLLSTEDT

188



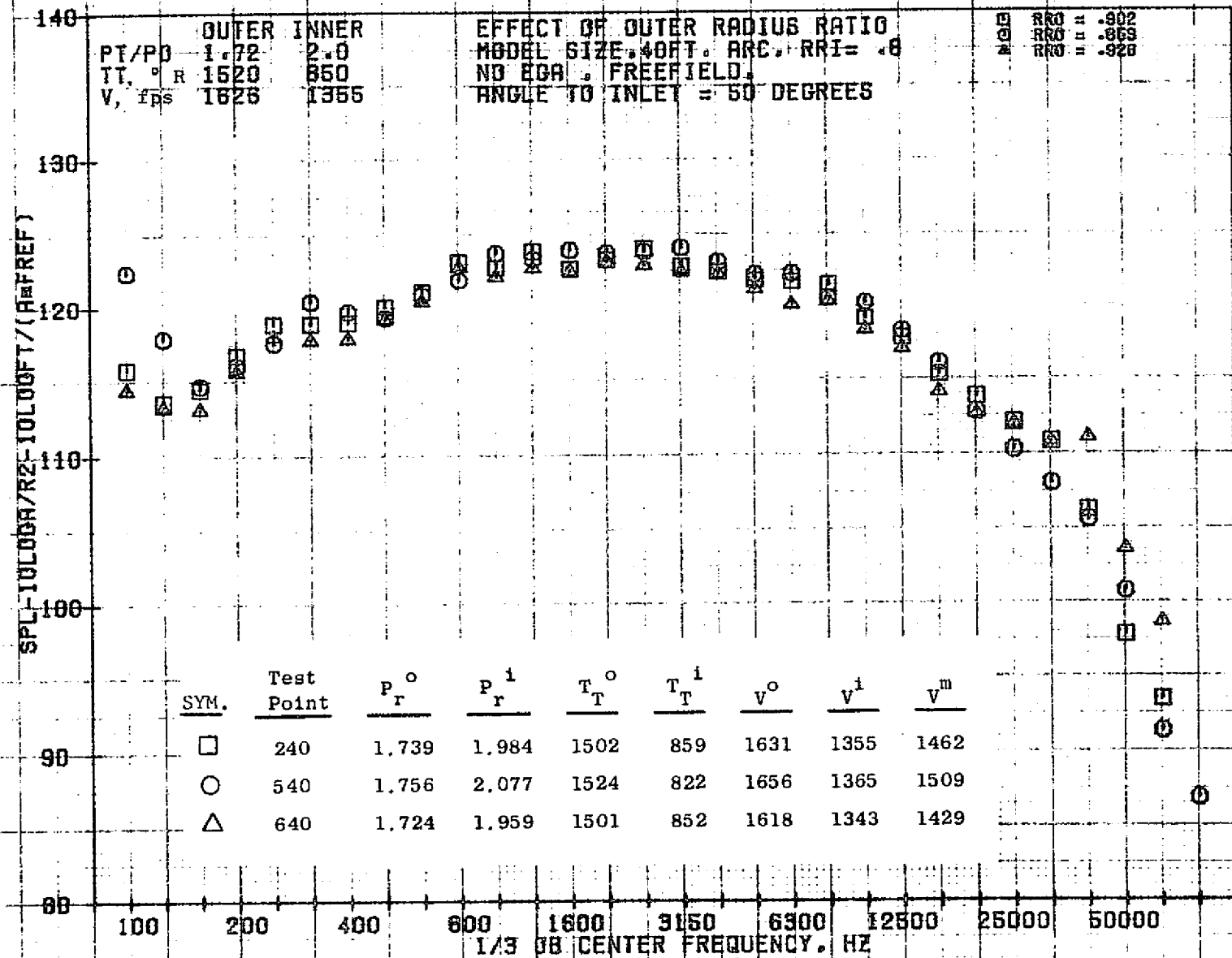
10/27/76
 1X824-001

73KOLLSTEDT



10/27/76
 1X824-001

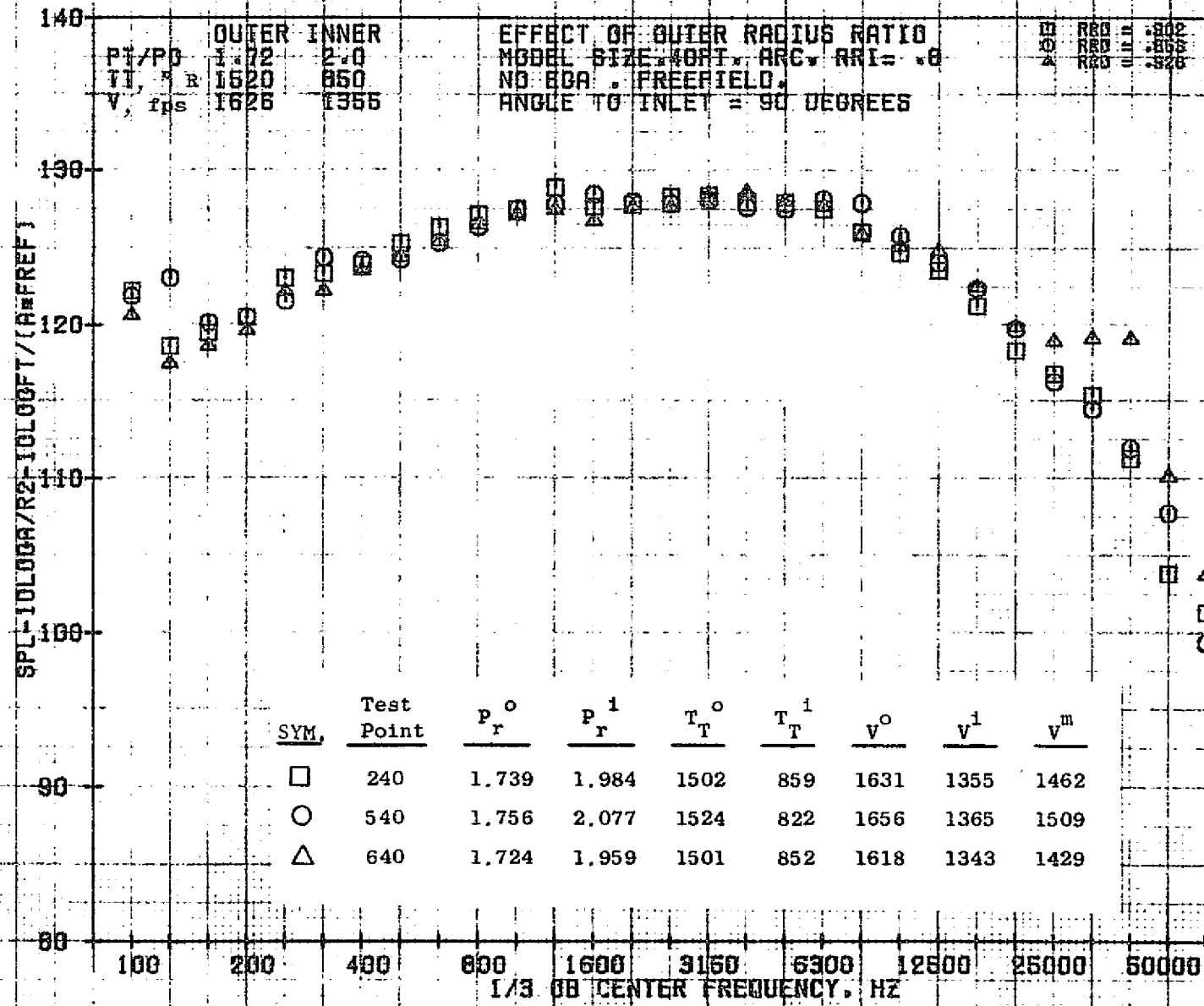
73KOLLSTEDT



10/27/76
 1X824-001

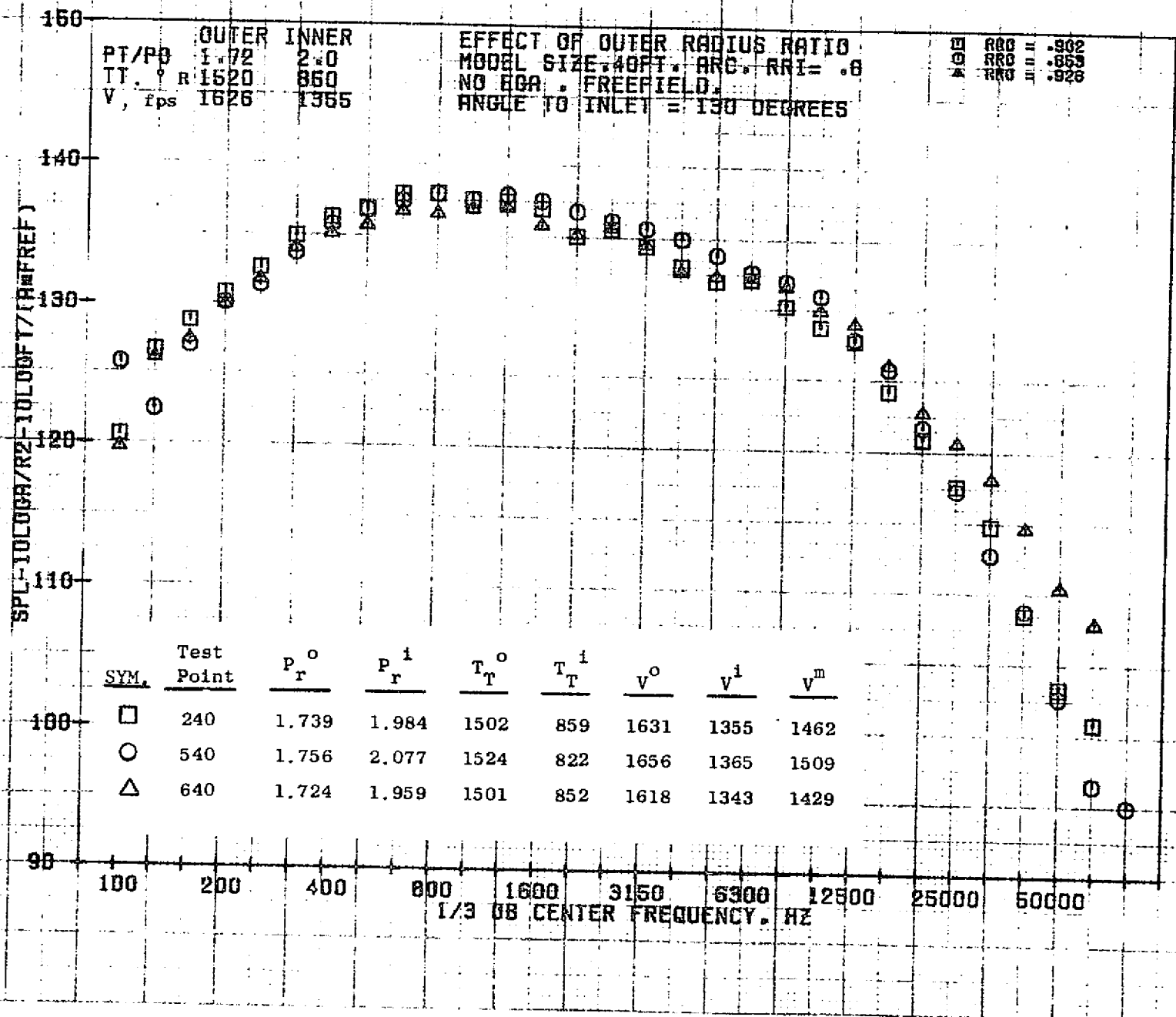
73KOLLSTEDT

884



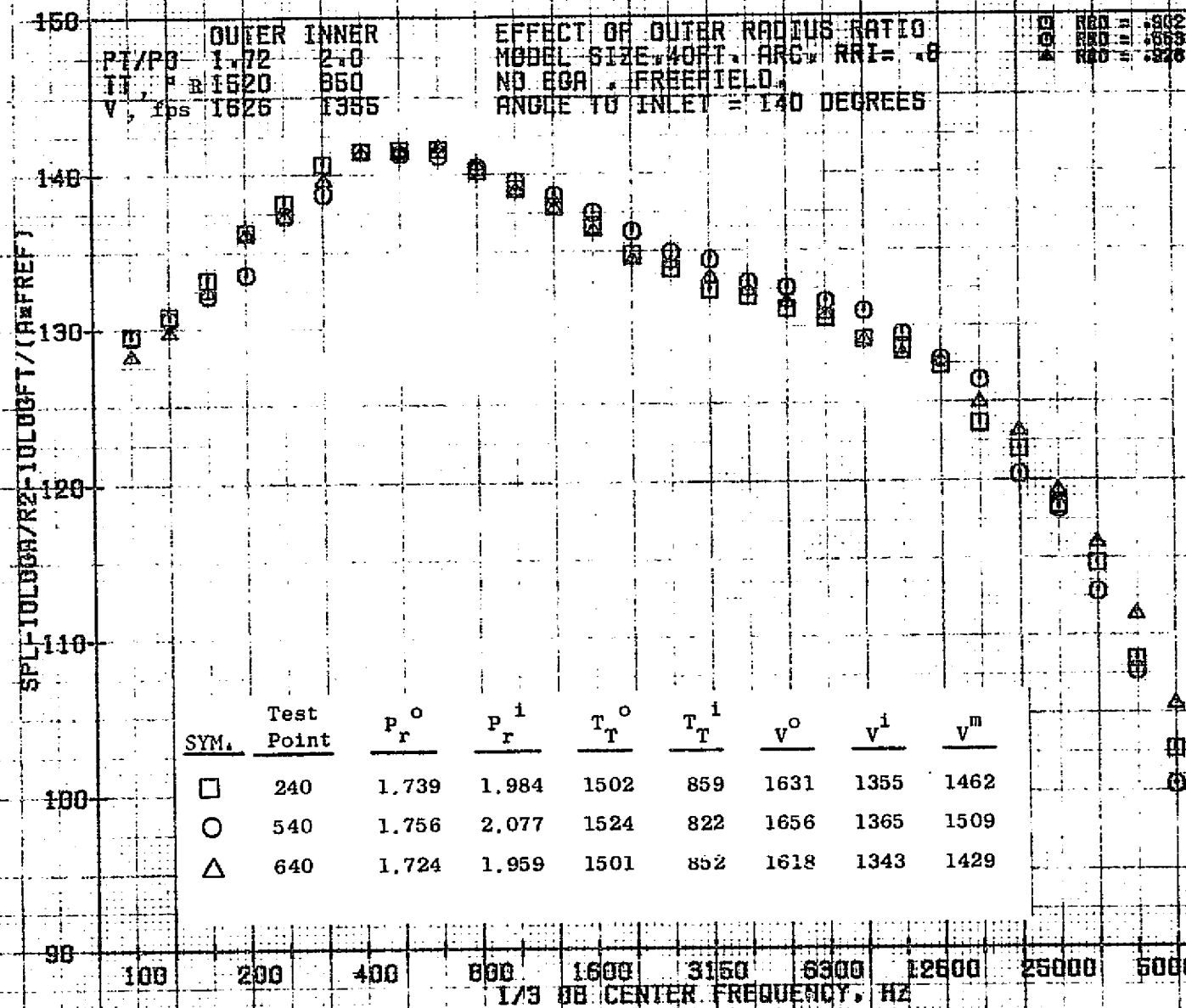
10/27/76
 1X824-001

73K011ST0T



10/27/76
1X824-001

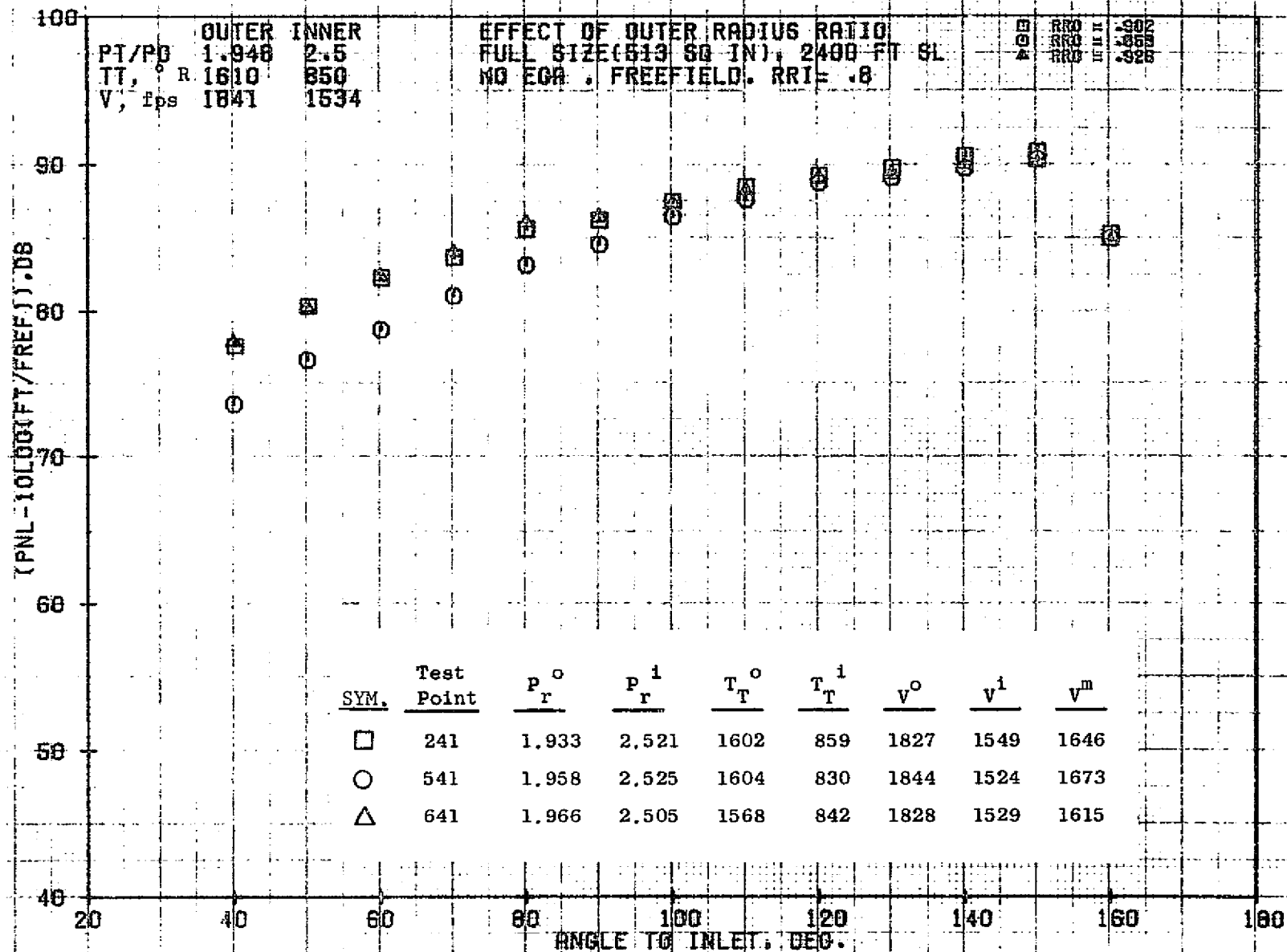
73K011 STFDT



10/27/76
 1X824-001

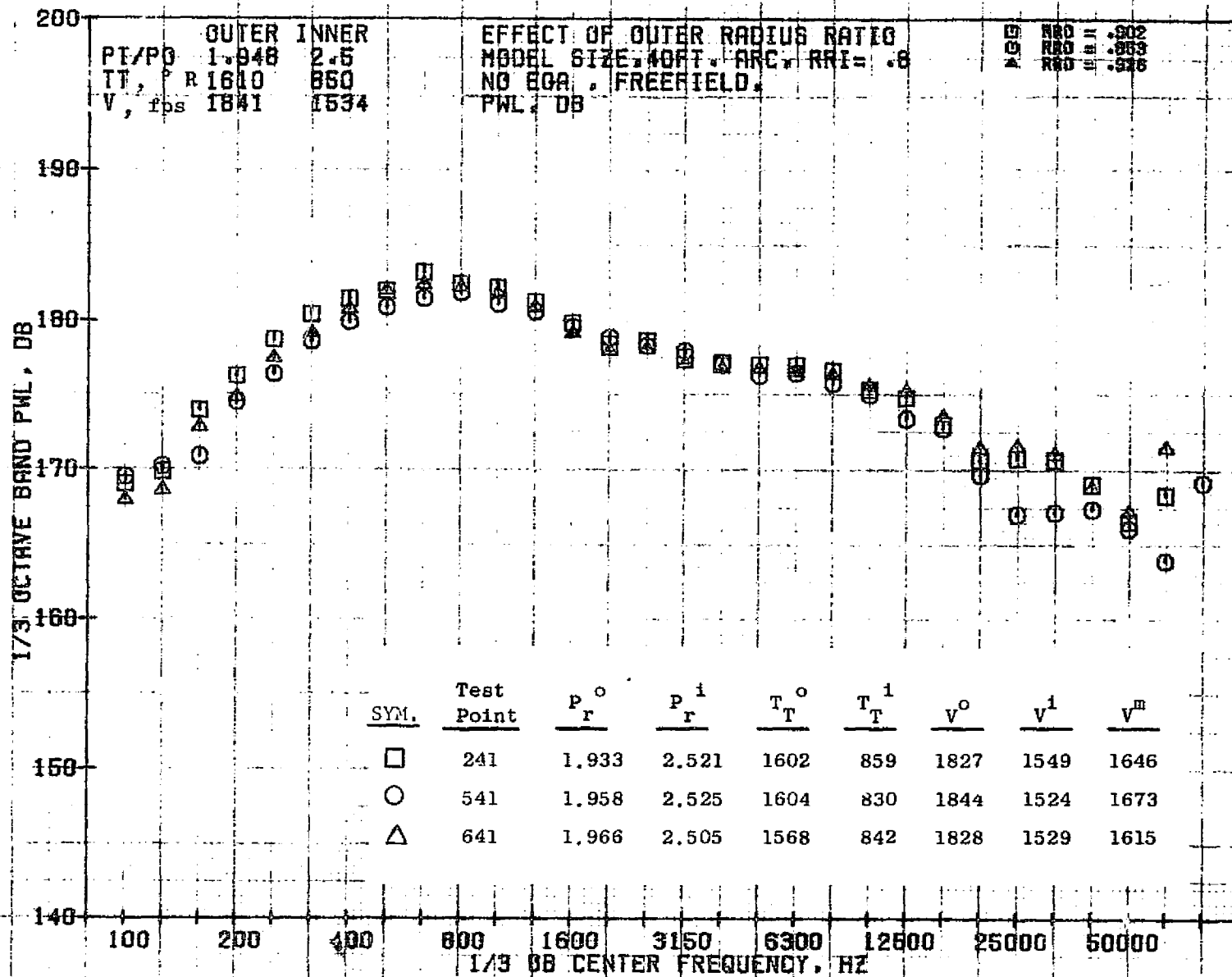
73KOLLSTEDT

887



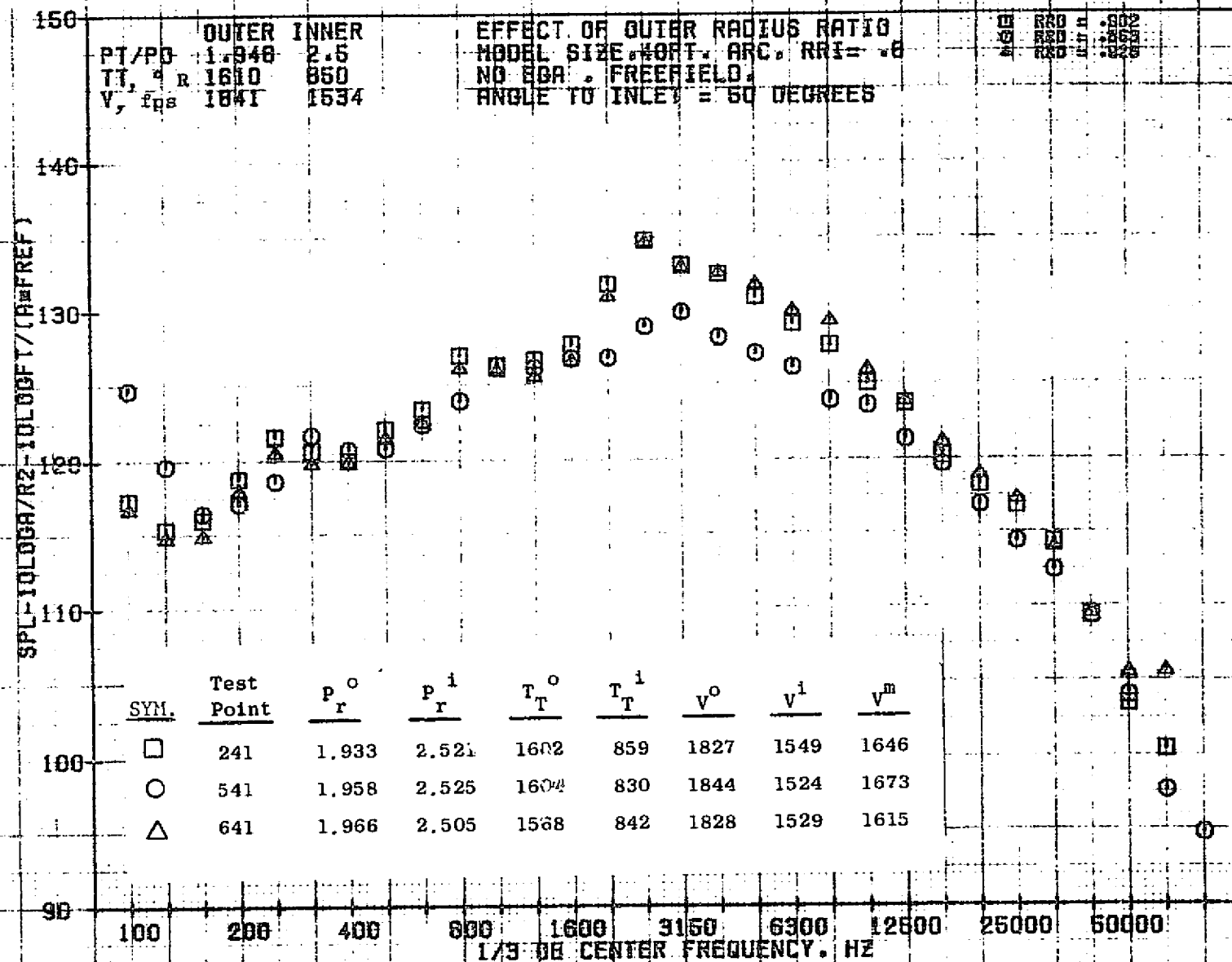
10/27/76
1X008-001

73K011 STFOT



10/27/76
 1X824-001

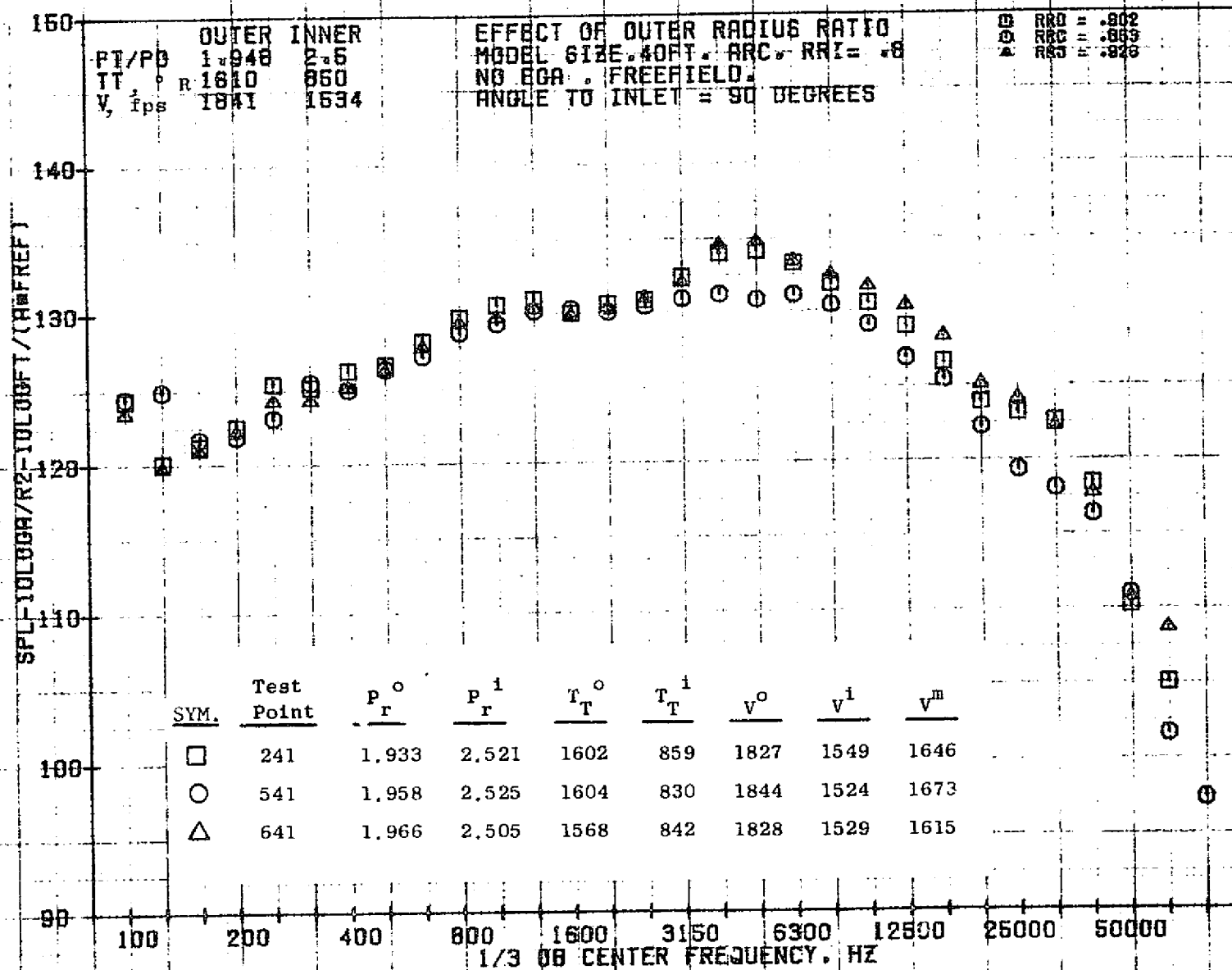
73KOLLSTEDT



10/27/76
1X824-001

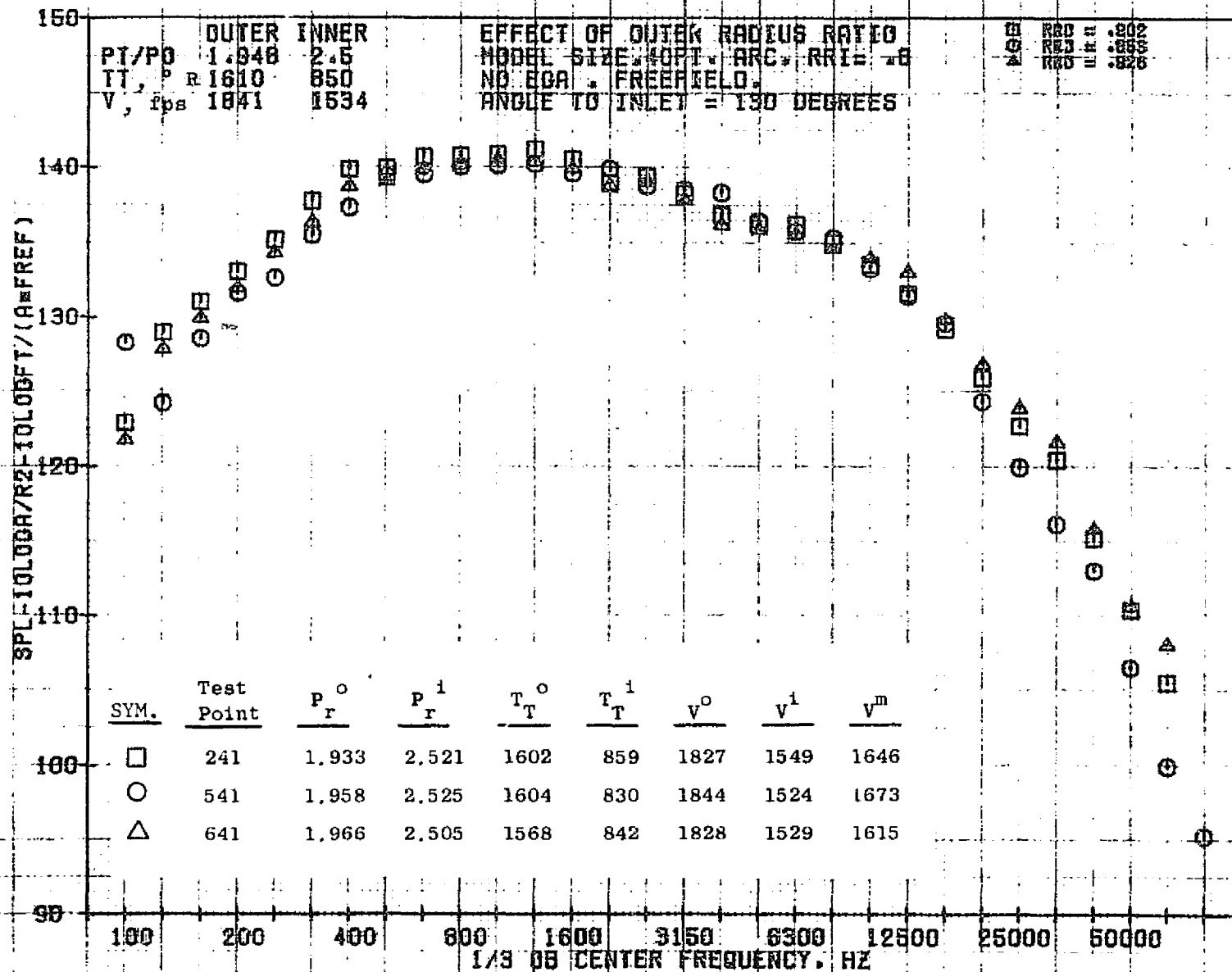
73KOLLSTEDT

168



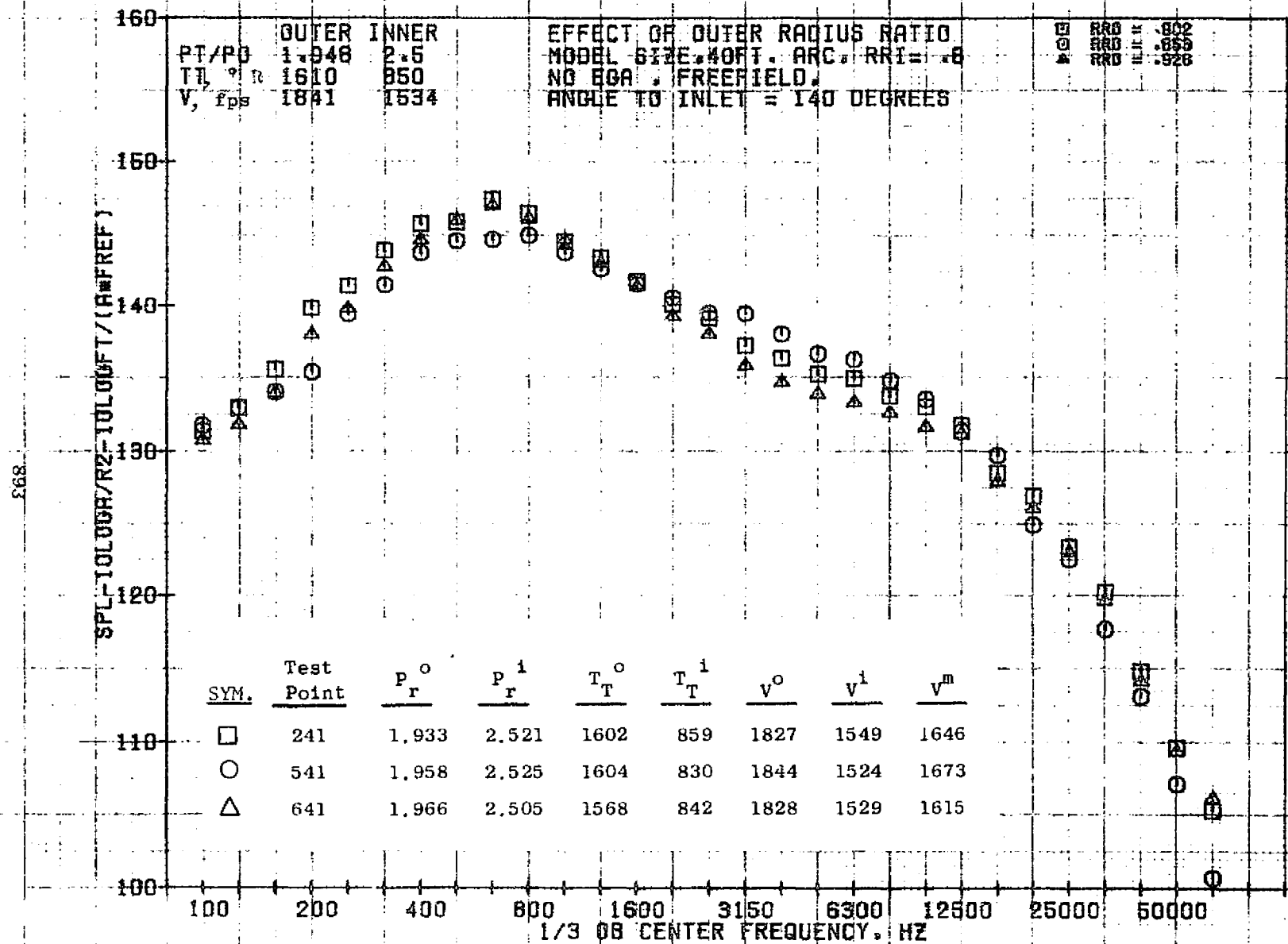
10/27/76
1X824-001

73KOLLSTEDT



10/27/76
 1X824-001

73KOLLSTEDT



10/27/76
 1X824-001

73KOLI STENT

PS8

(PNL - 10 LOG (FT / FREF)), DB

110

100

70

60

50

20

40

60

80

100

120

140

160

180

ANGLE TO INLET, DEG.

PT/P0
T, ° R
V, fps

OUTER
2.14
1668
1991

INNER
3.9
850
1659

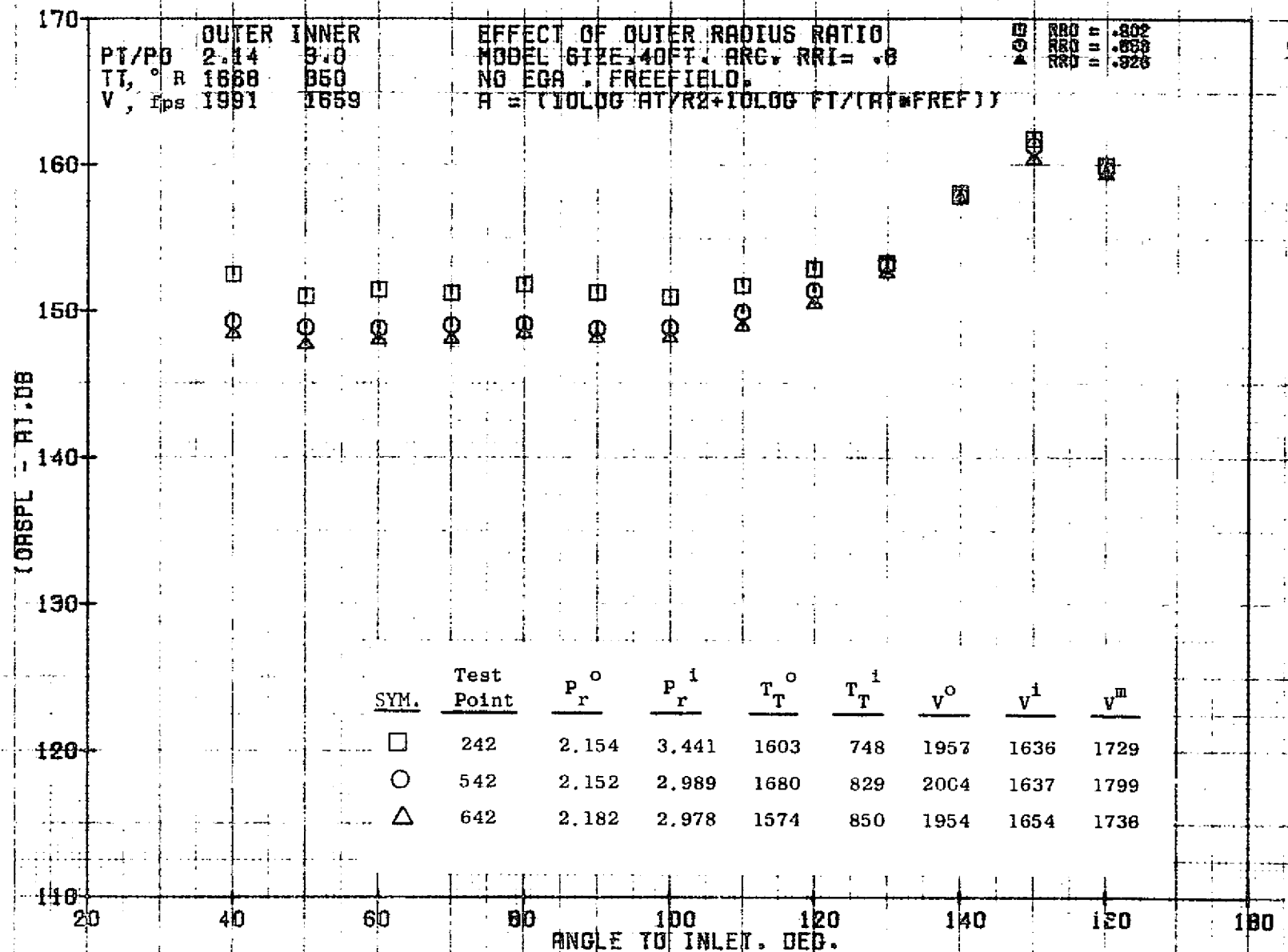
EFFECT OF OUTER RADIUS RATIO
FULL SIZE (513 SQ IN), 2400 FT SL
NO EGA, FREEFIELD, RRI = .8

OUTER
RRI
RRI
RRI

SYM.	Test Point	P_r^o	P_r^1	T_T^o	T_T^1	V^o	V^1	V^m
□	242	2.154	3.441	1603	748	1957	1636	1729
○	542	2.152	2.989	1680	829	2004	1637	1799
△	642	2.182	2.978	1574	850	1954	1654	1738

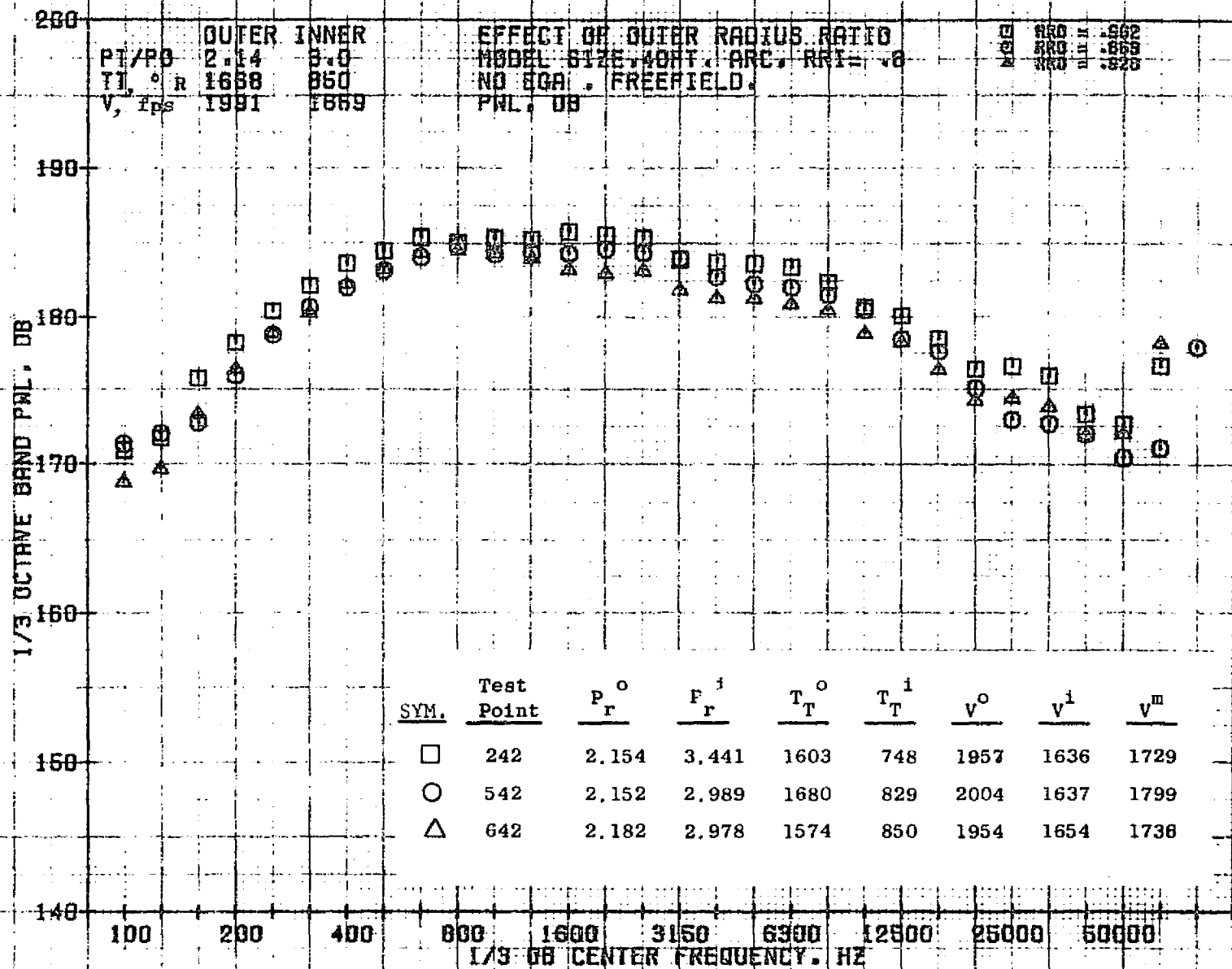
10/27/76
1X008-001

73K01 LSTEDT



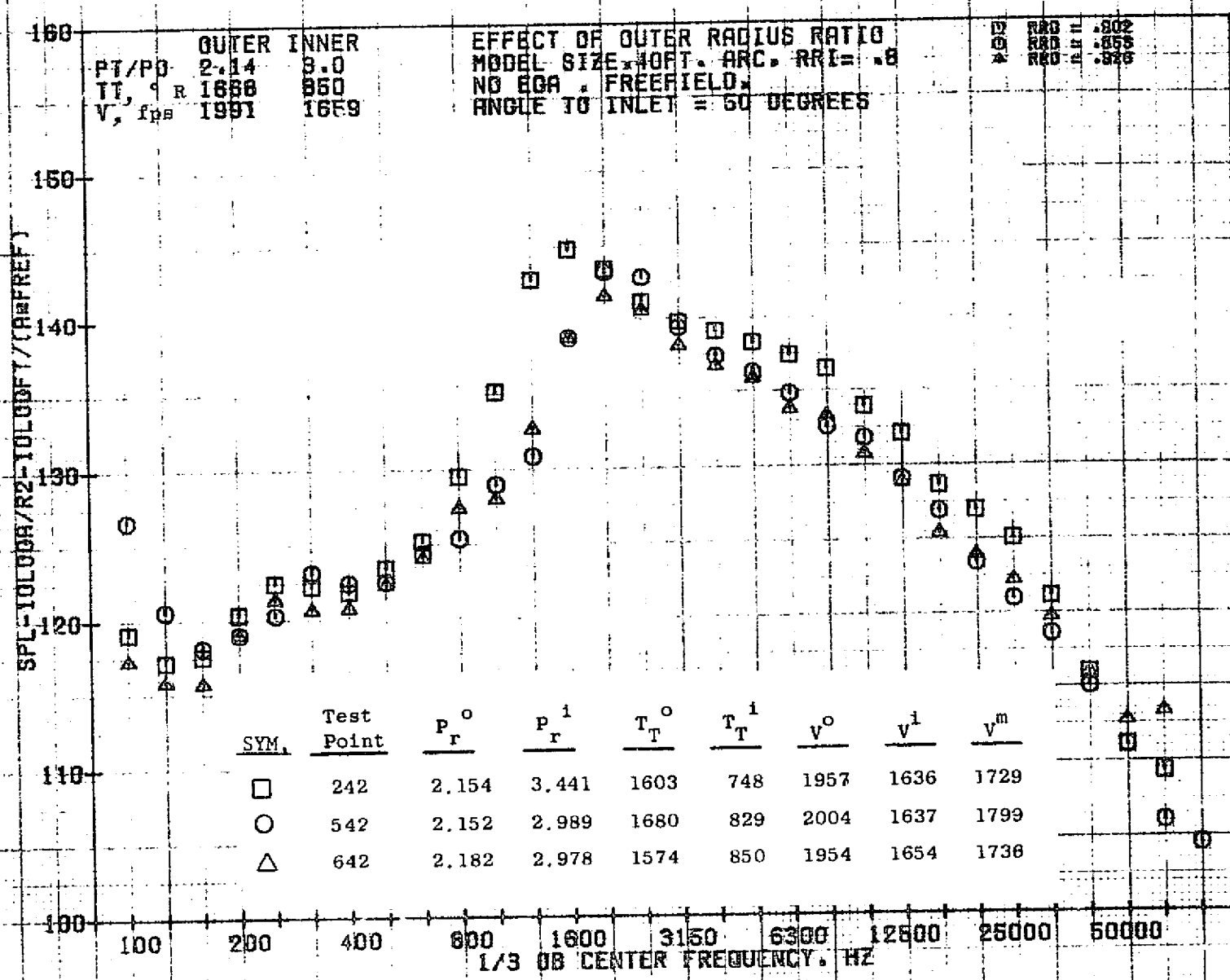
10/27/76
 1X824-001

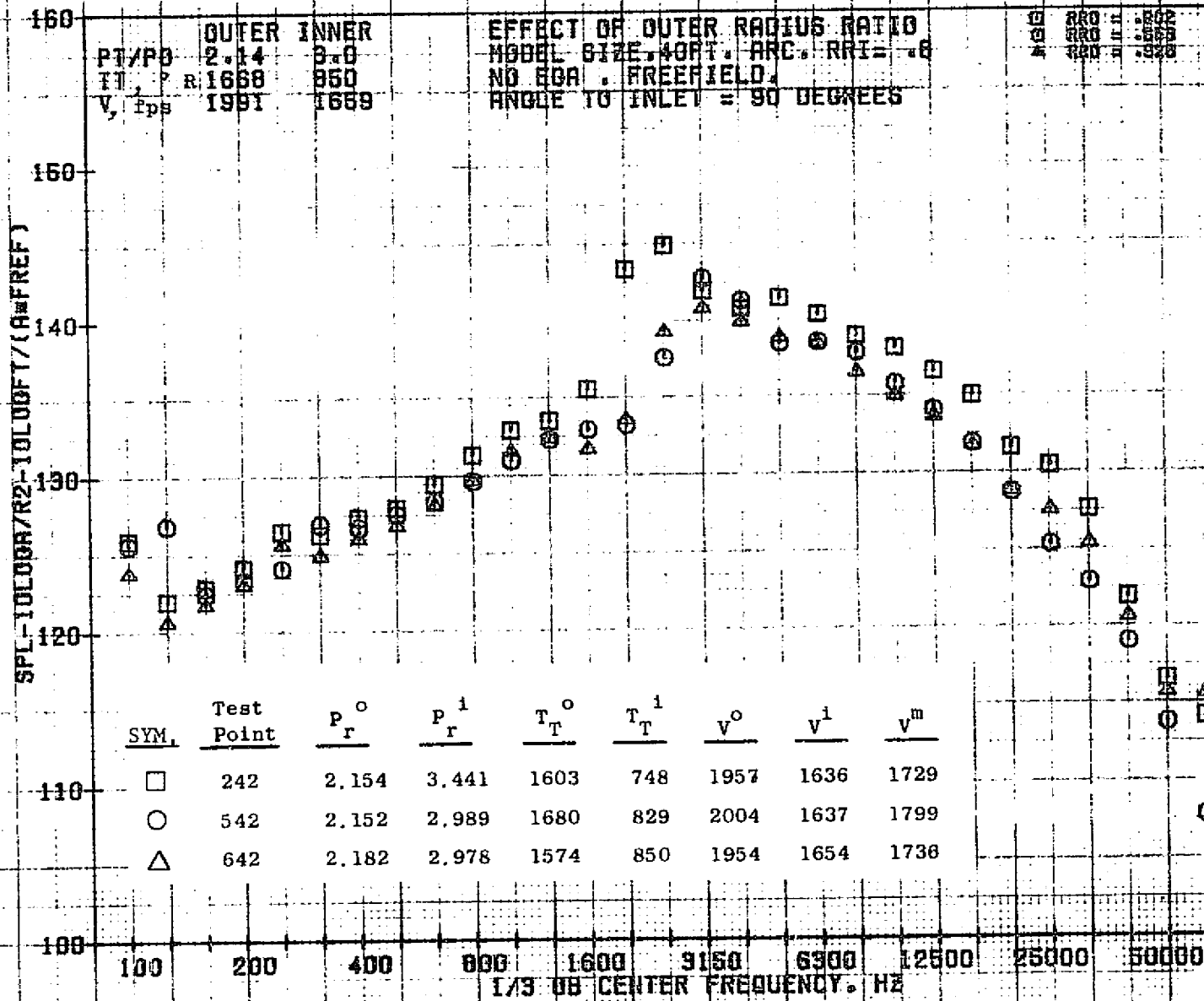
73KOLI STEDT



10/27/76
 1X824-001

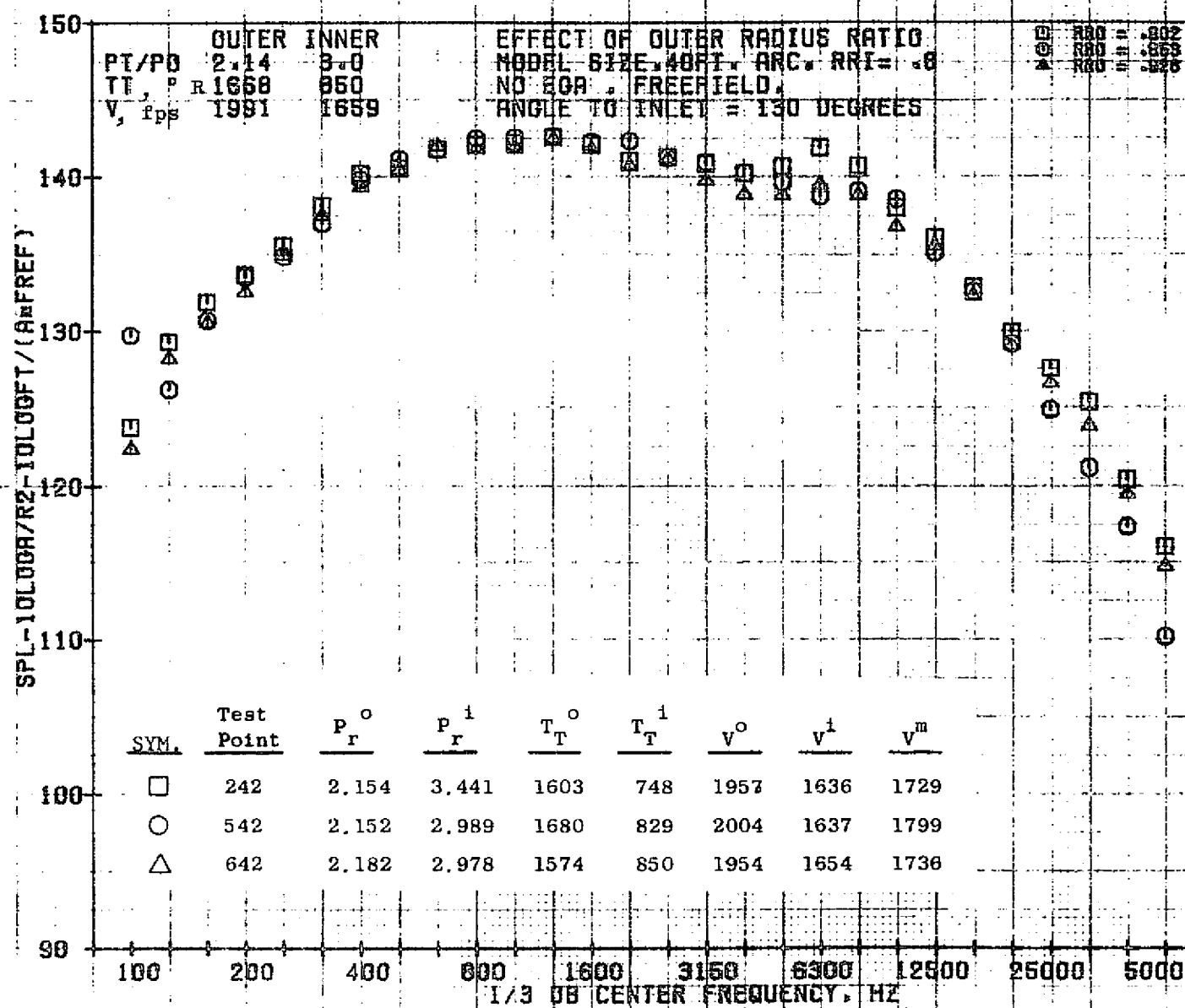
73KOLLSTEDT





10/27/76
 1X824-001

73KOLLSTEDT



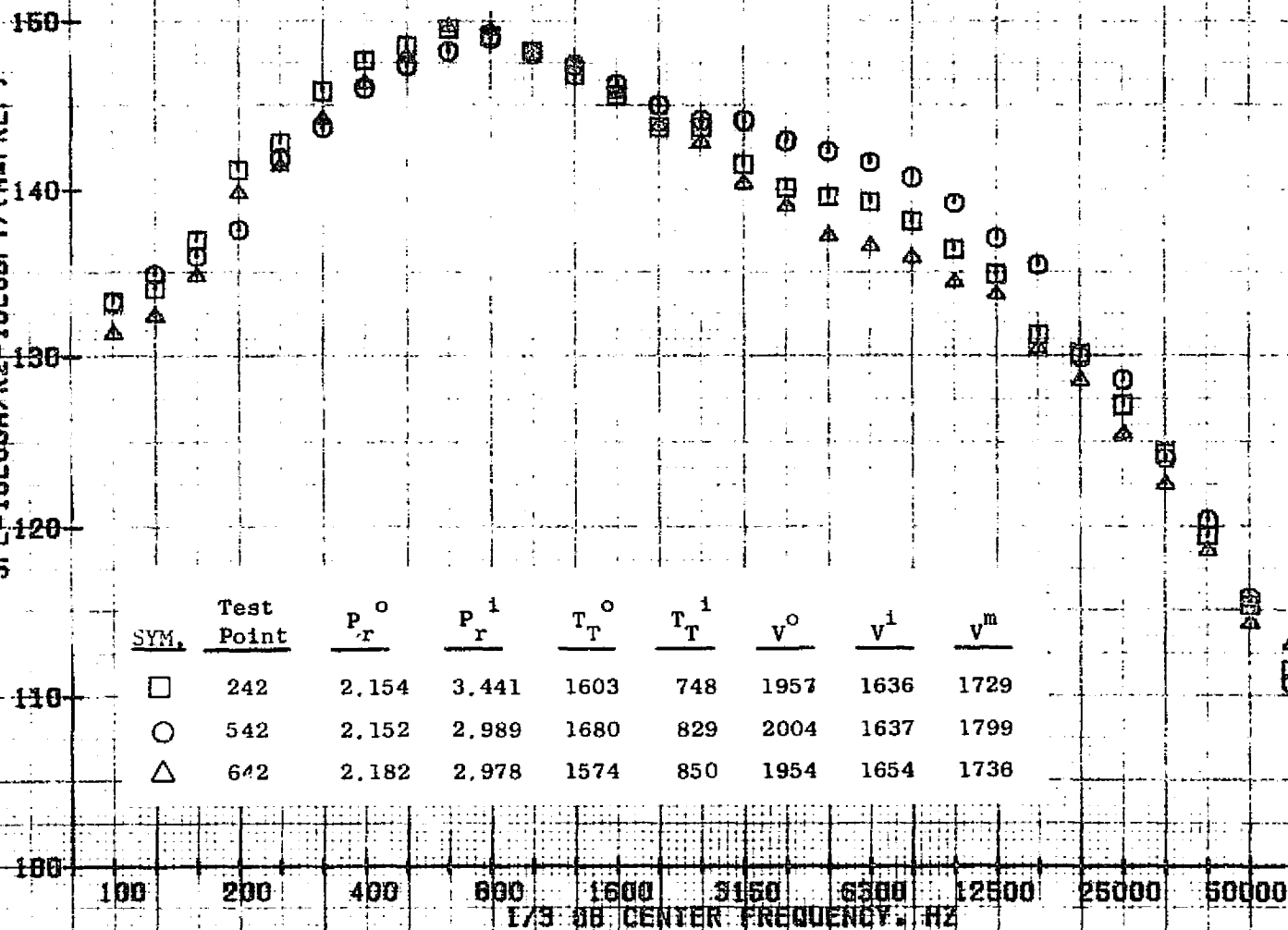
006

SPL-10LOG(PA/R²-10LOG(PY/(A=REF))

PT/PO 2.14 3.0
 TT, ° R 1688 850
 V, fms 1981 1659

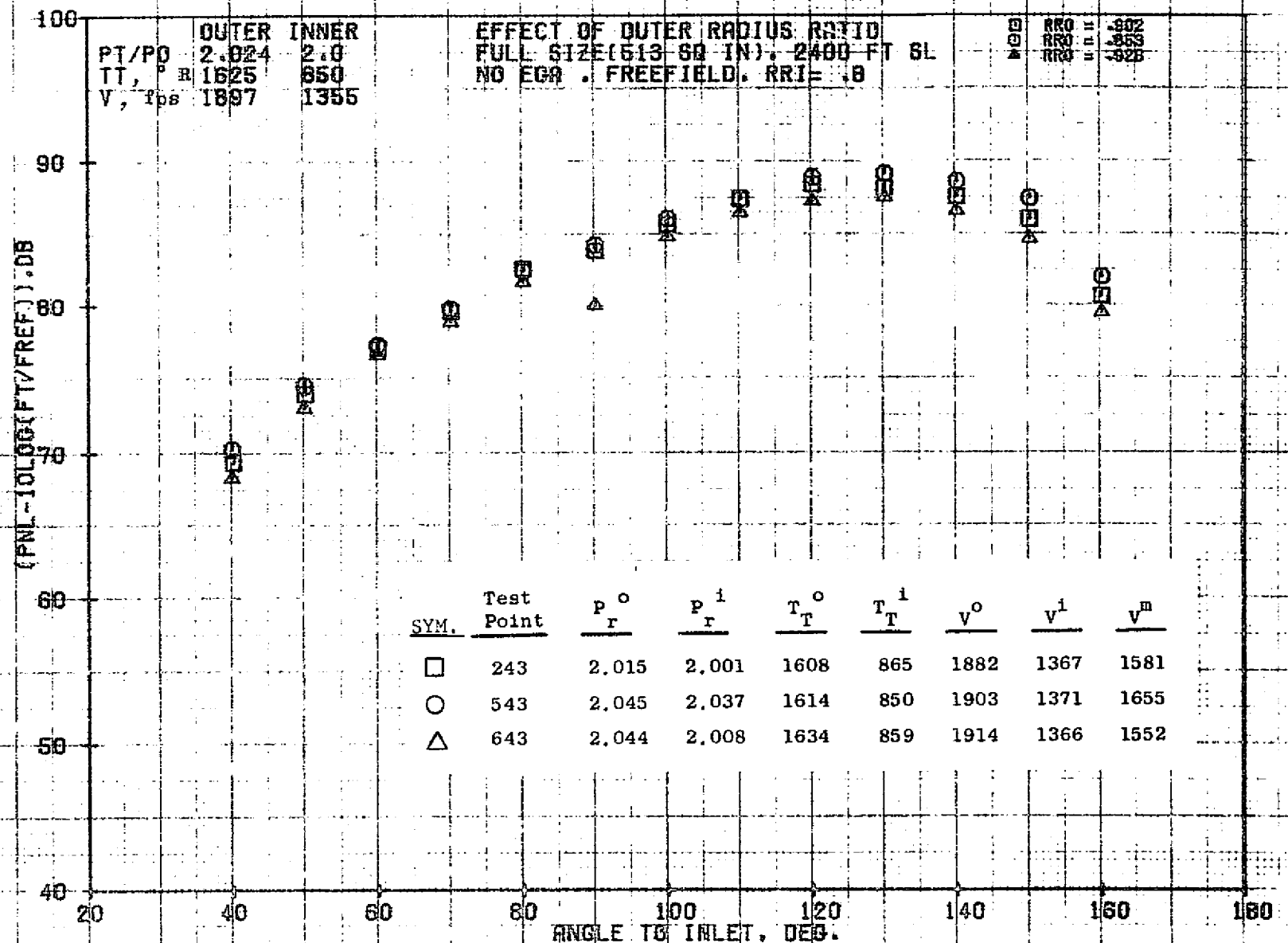
EFFECT OF OUTER RADIUS RATIO
 MODEL SIZE 40FT. ARC. RRI = .8
 NO BGA. FREEFIELD.
 ANGLE TO INLET = 140 DEGREES

□ RRI = .802
 ○ RRI = .858
 △ RRI = .928



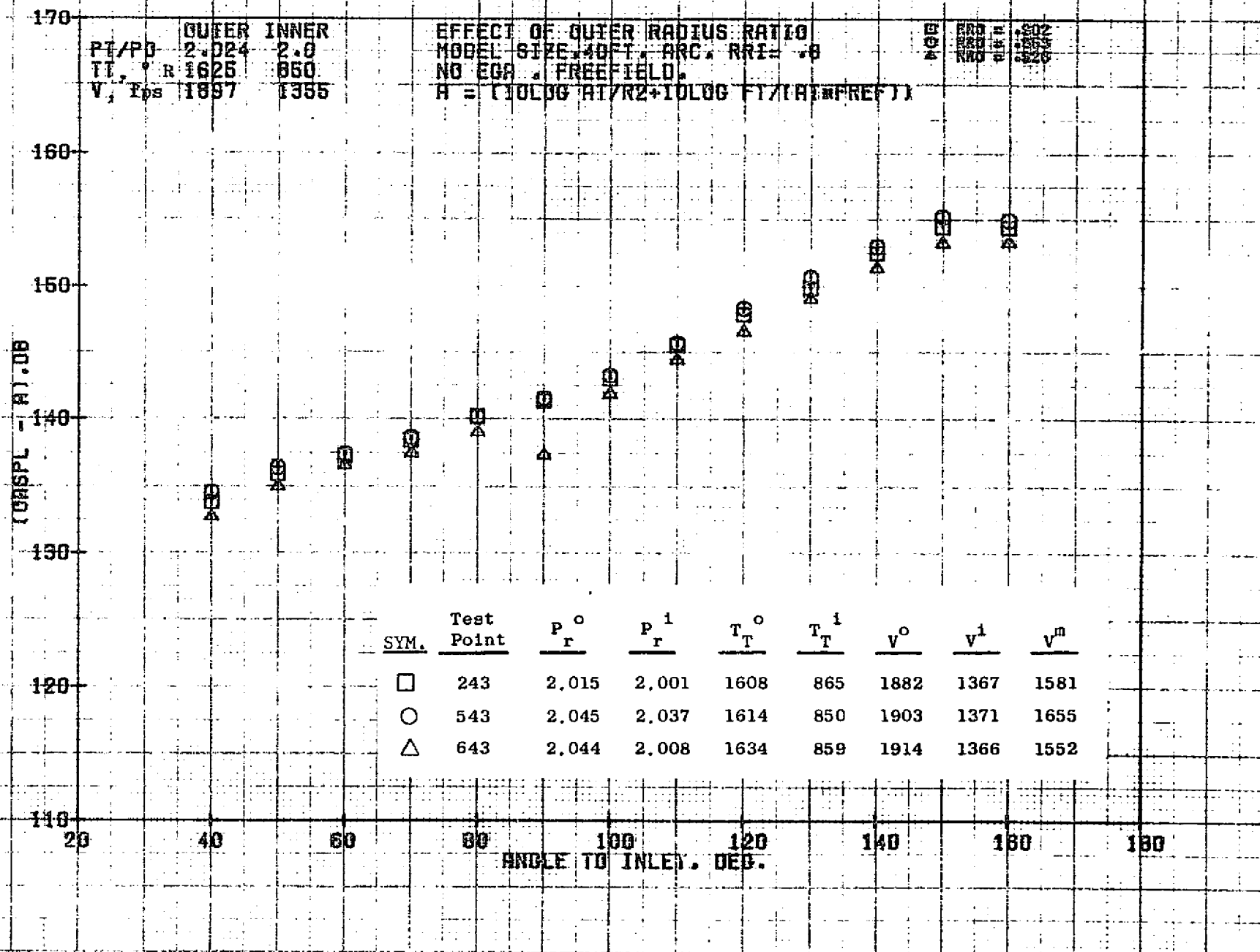
10/27/76
 1X824-001

73KOLLSTEDT



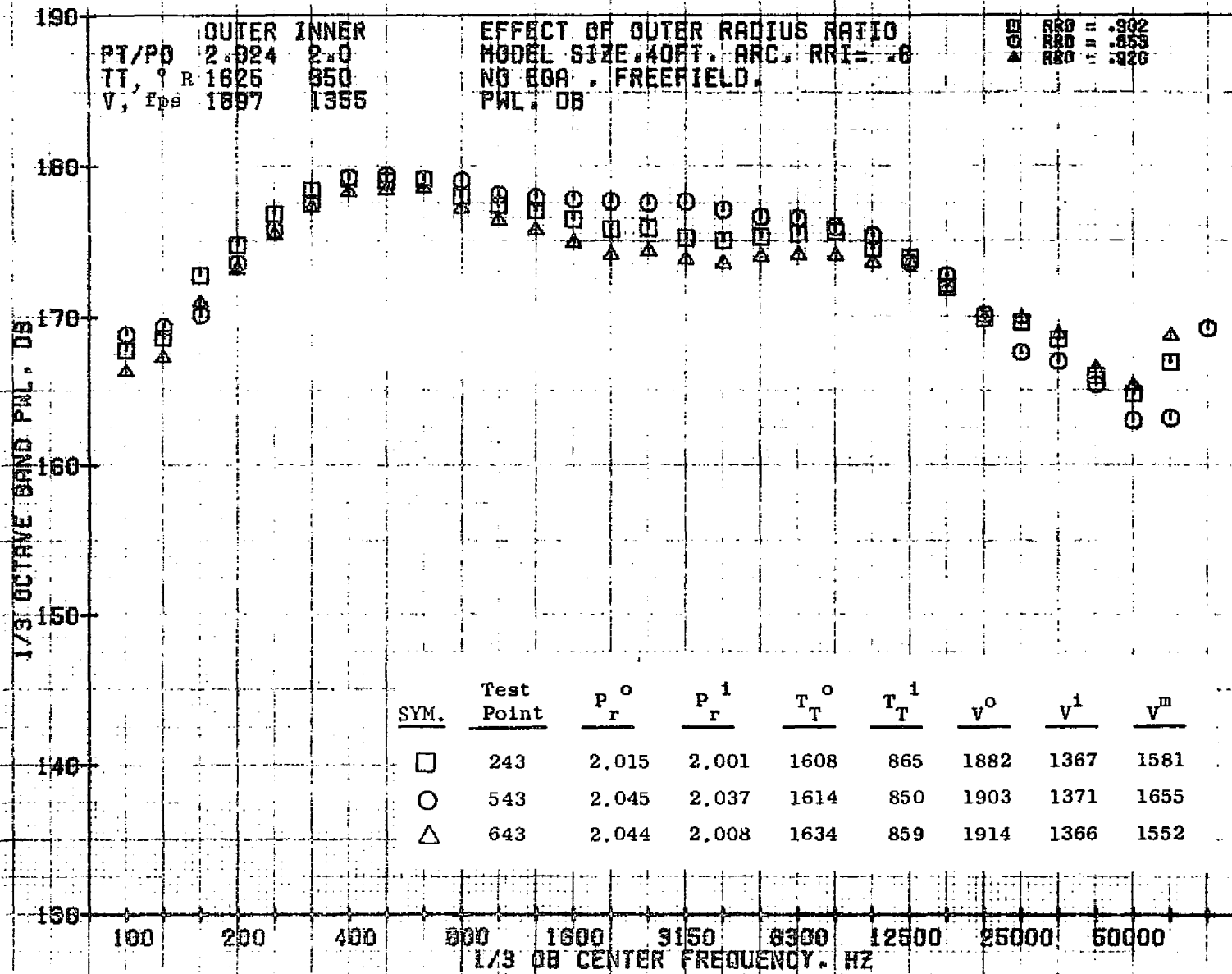
10/27/76
1X008-001

73KOLLSTEDT



10/27/76
1X824-001

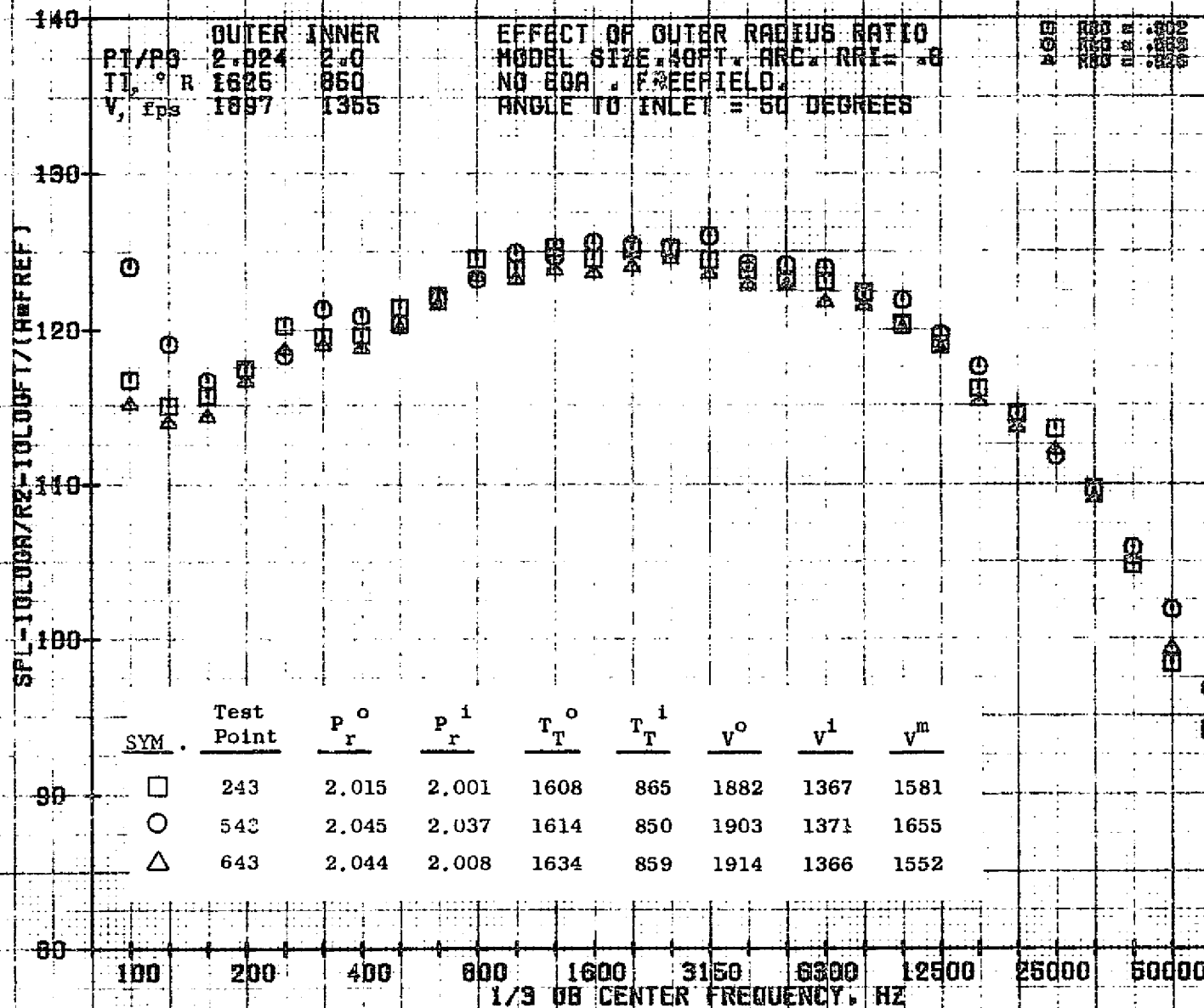
73KOLLSTEDT



10/27/76
1X824-001

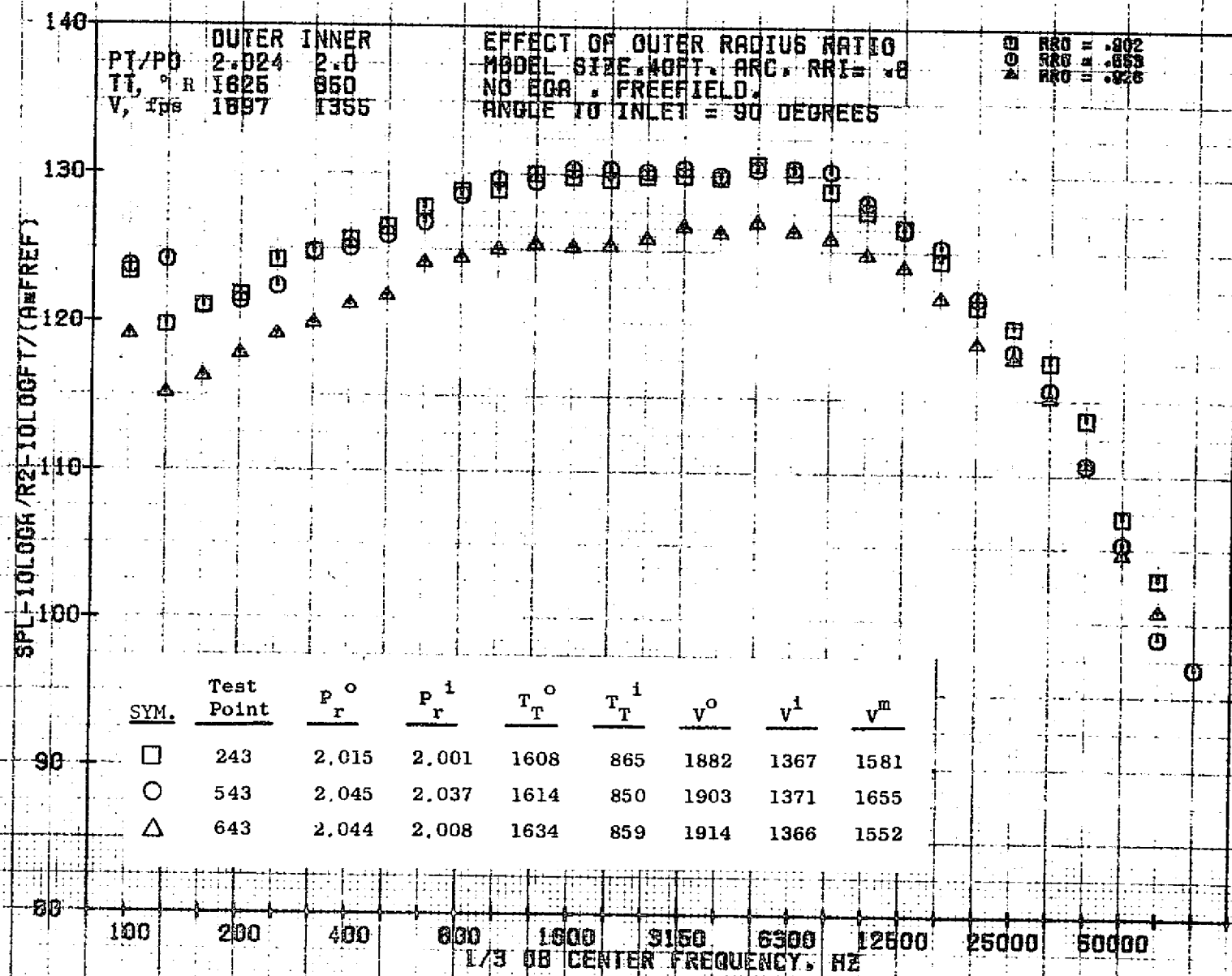
73KOLLSTEDT

904



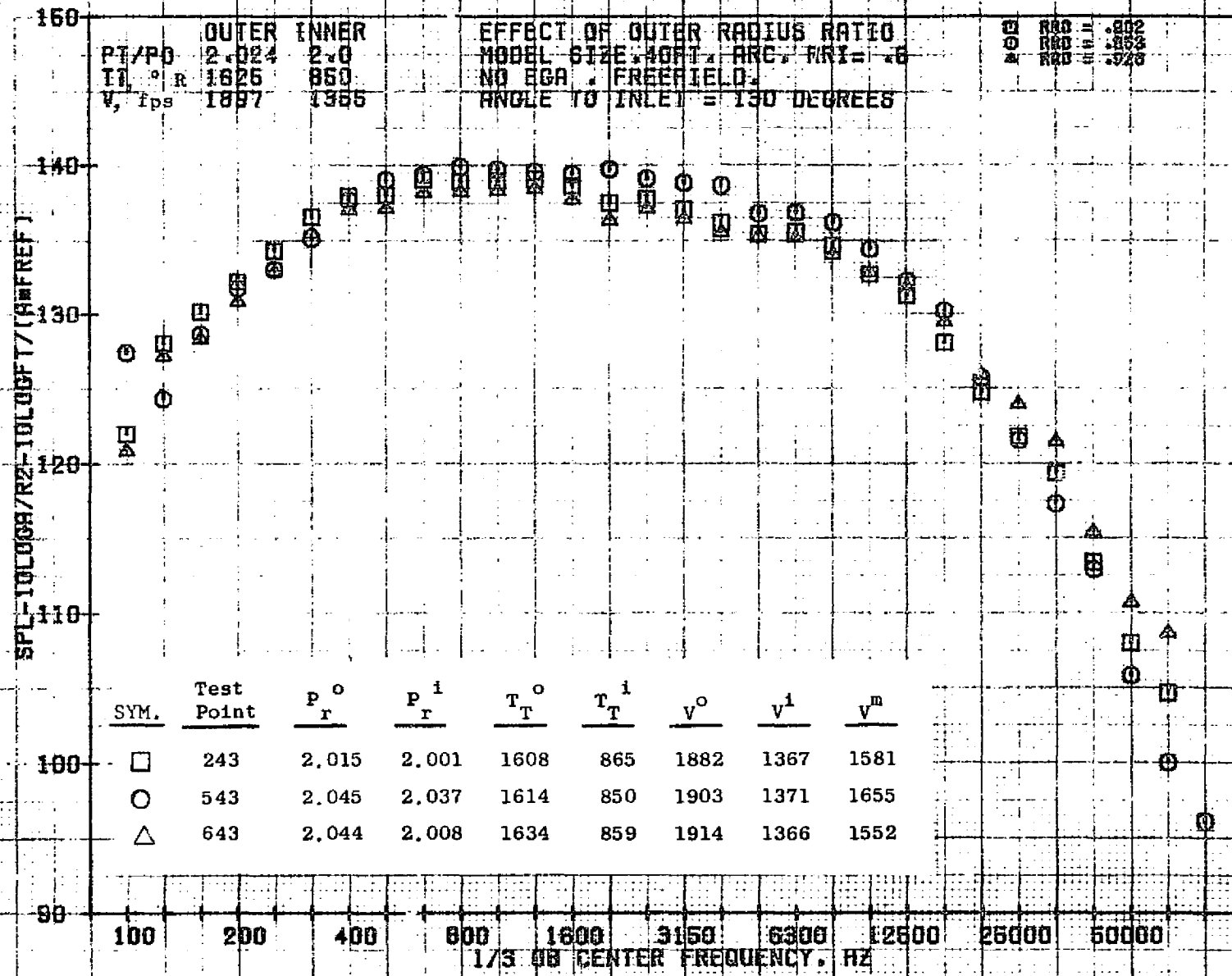
10/27/76
 1X824-001

73KOLLSTEDT



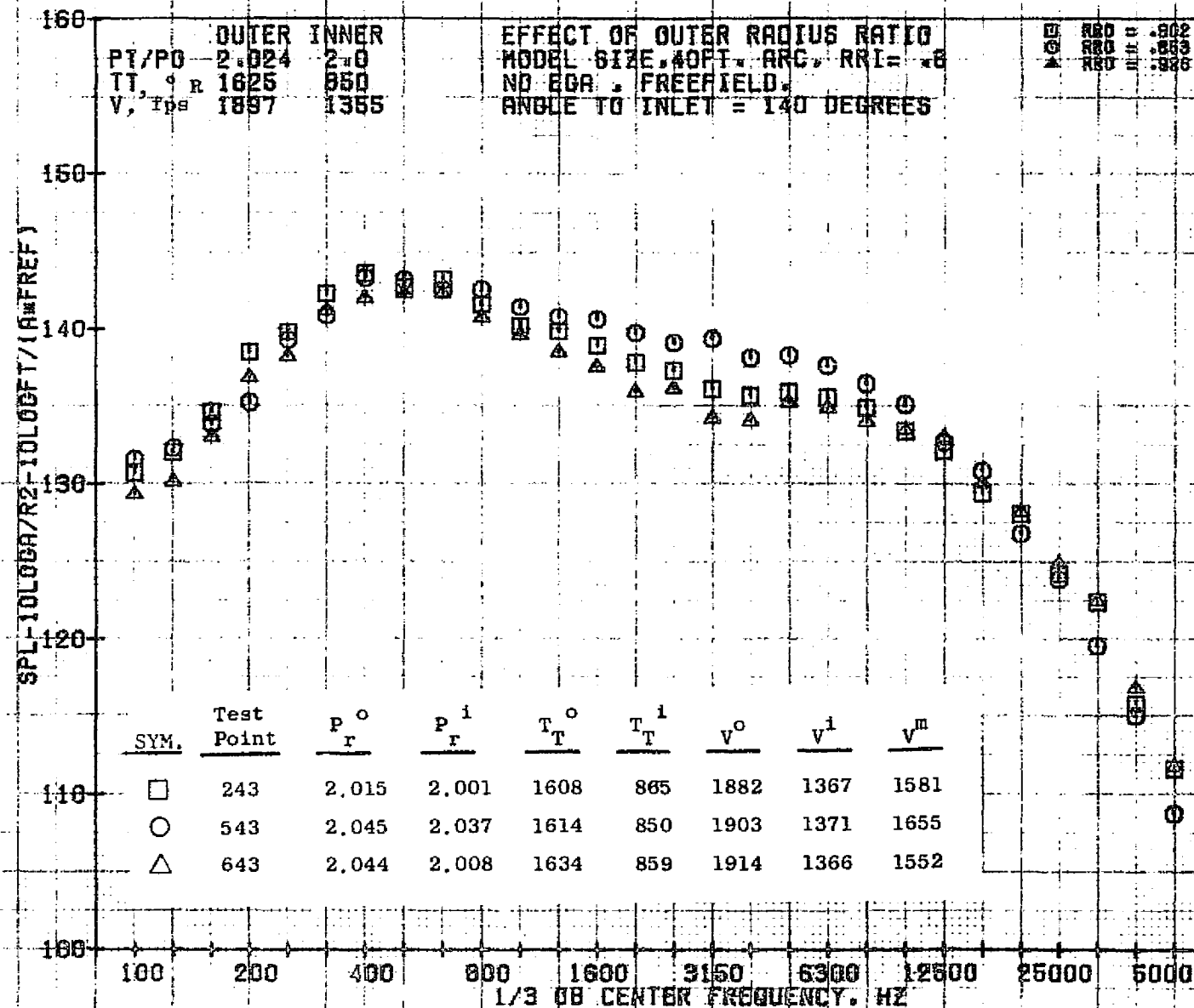
10/27/76
 1X824-001

73KOLLSTEOT



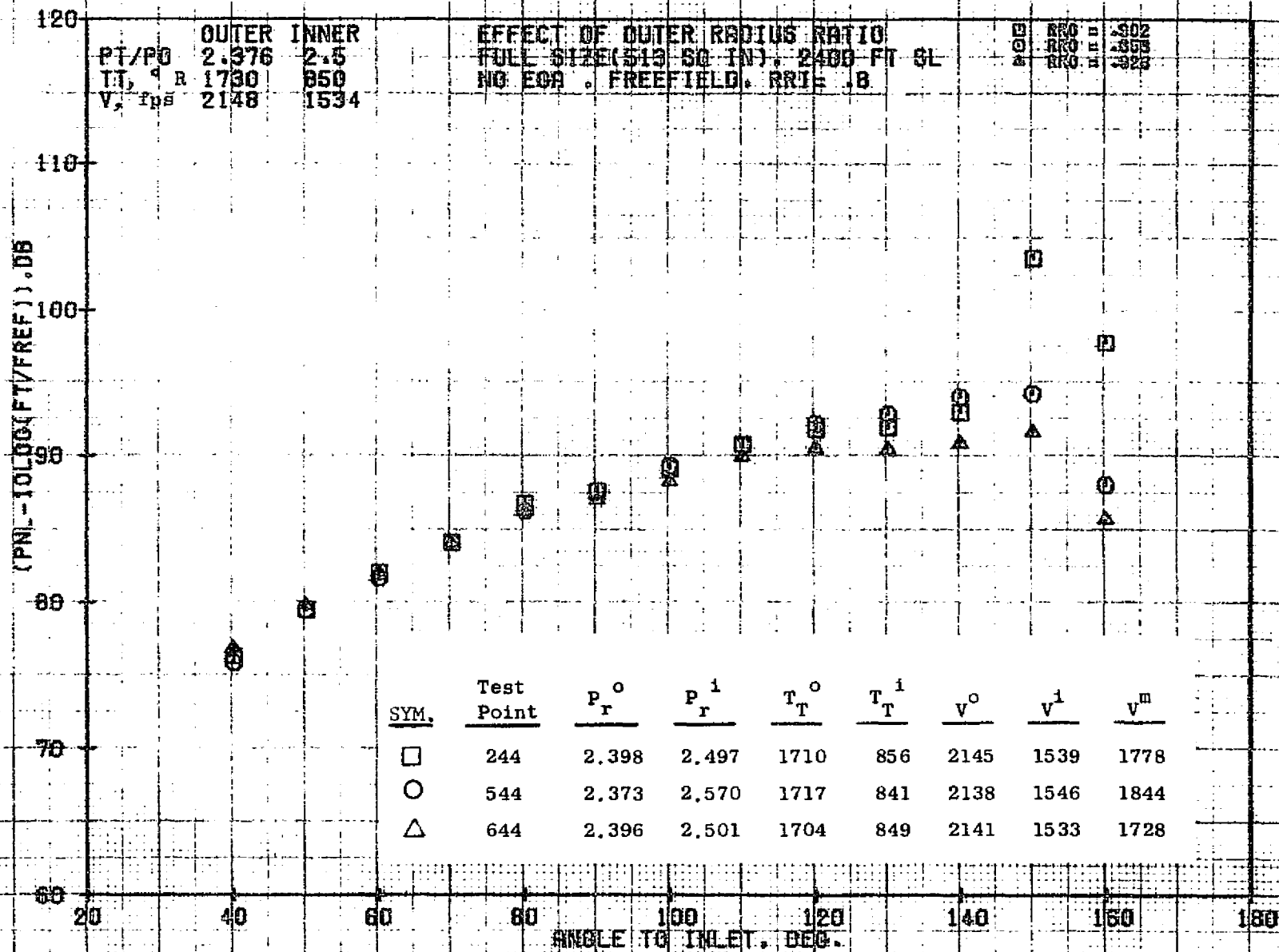
10/27/76
 1X824-001

73KOLLSTEDT



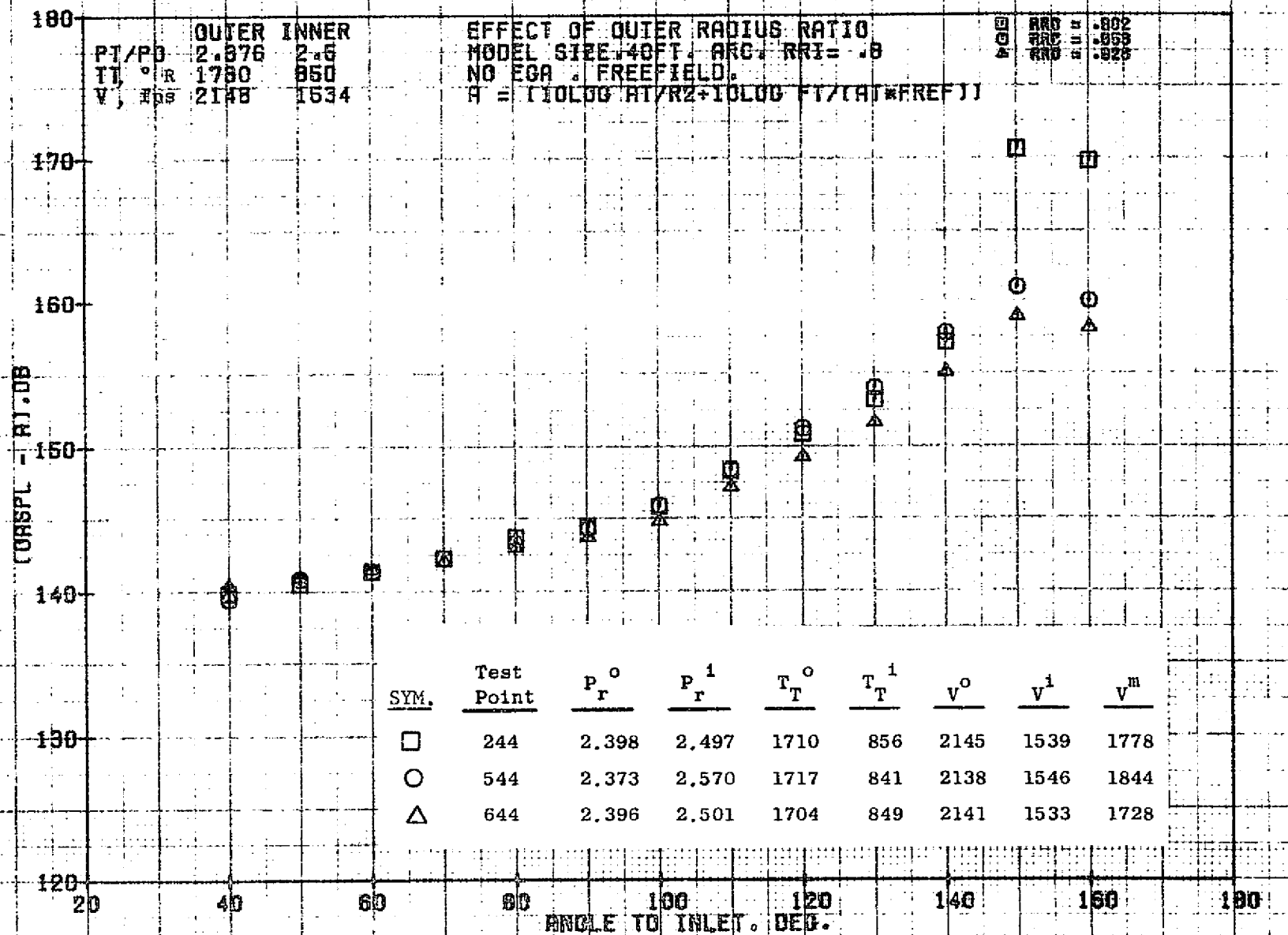
10/27/76
1X824-C01

73KOLLSTEDT



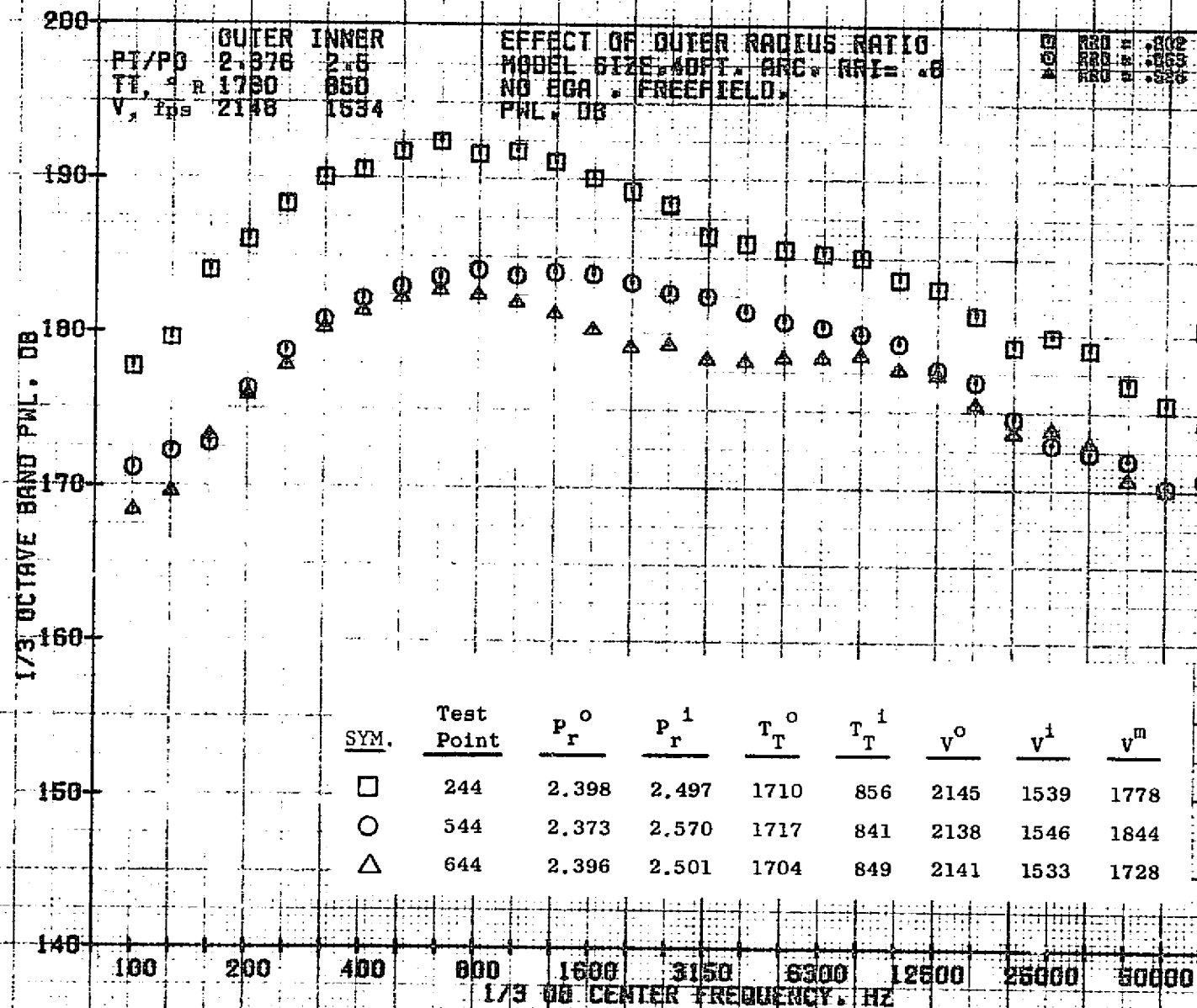
10/27/76
 1X008-001

73KOLLSTEDT



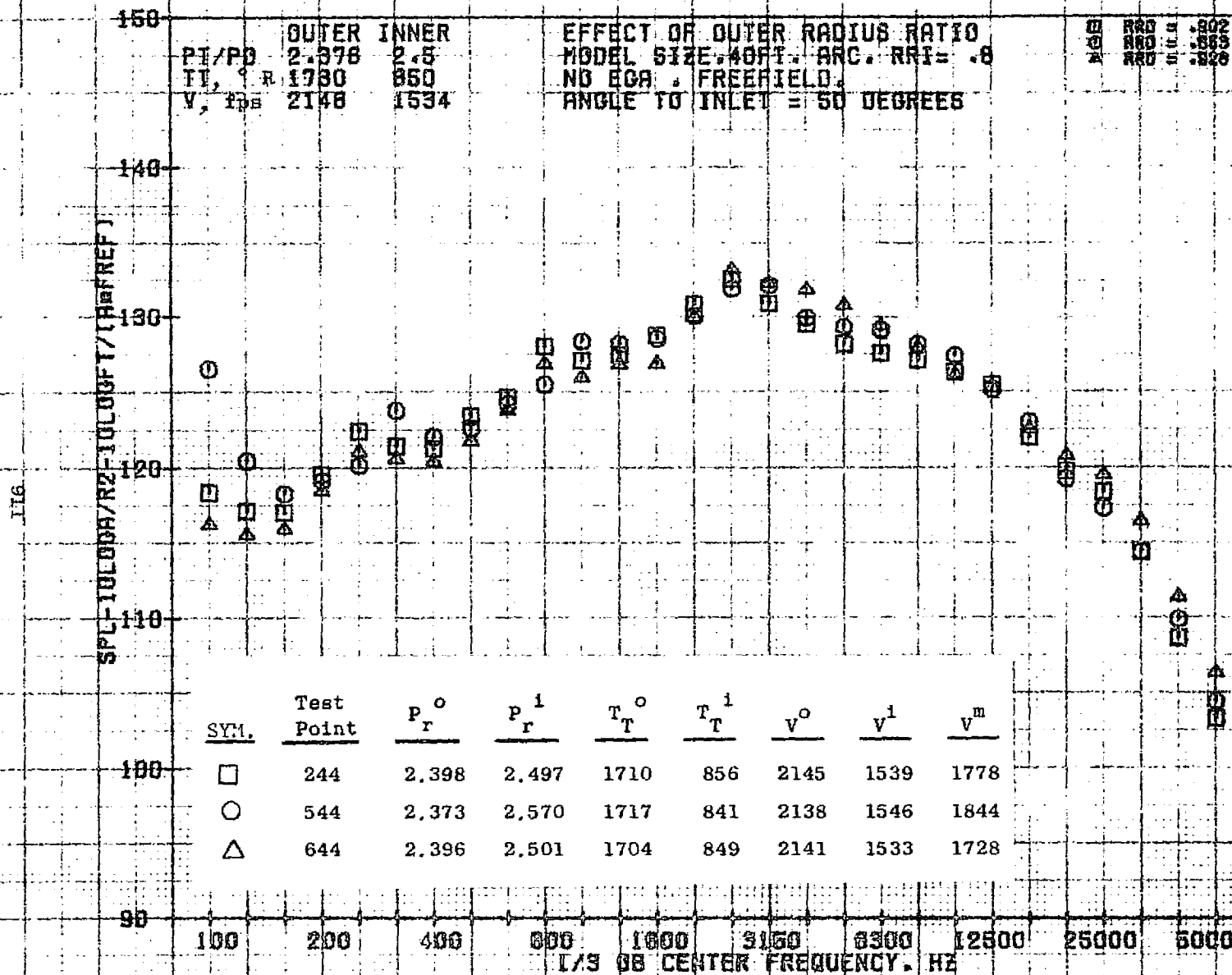
10/27/76
1X824-001

73KOLLSTEDT



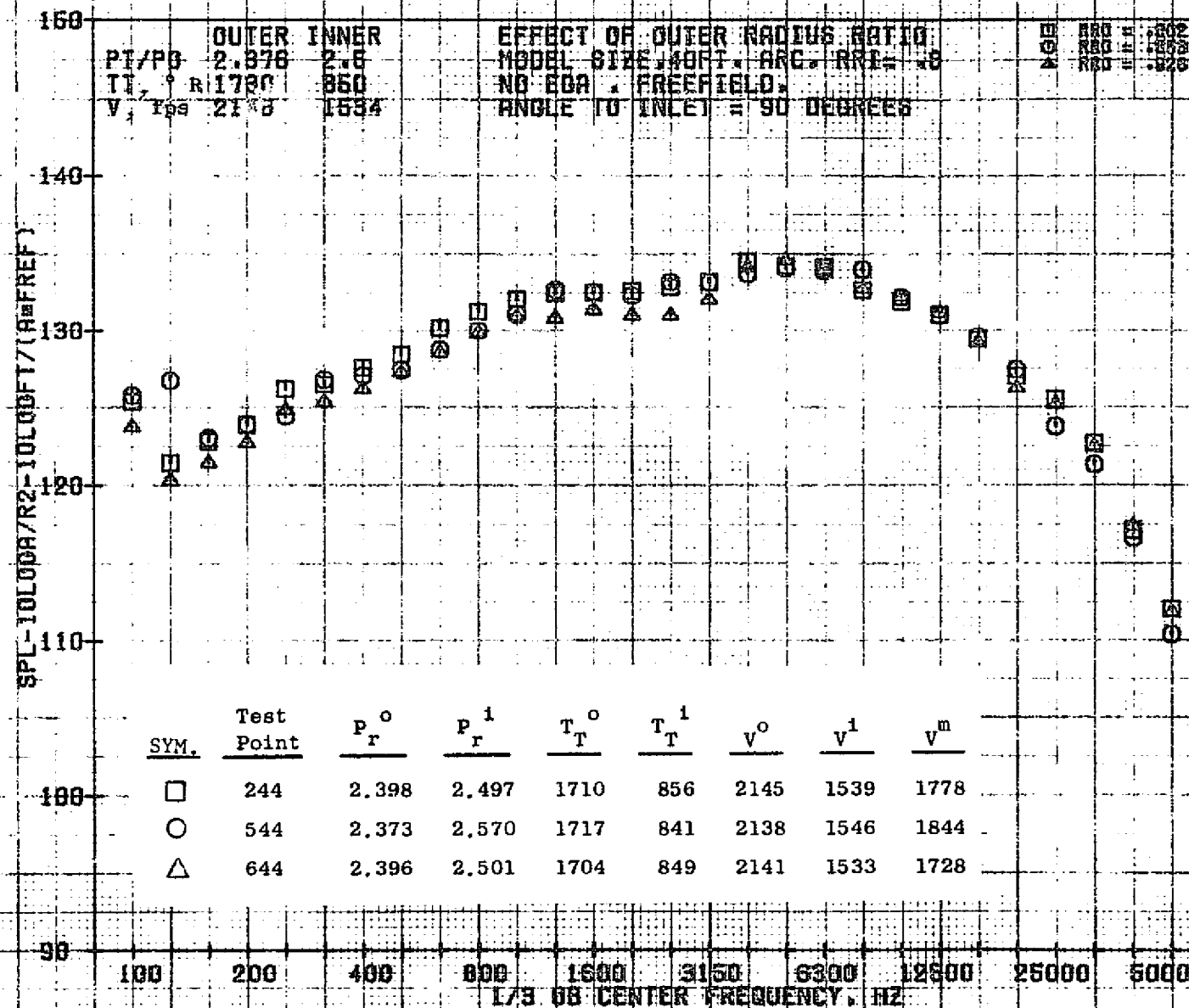
10/27/76
 1X824-001

73KOLLSTEDT



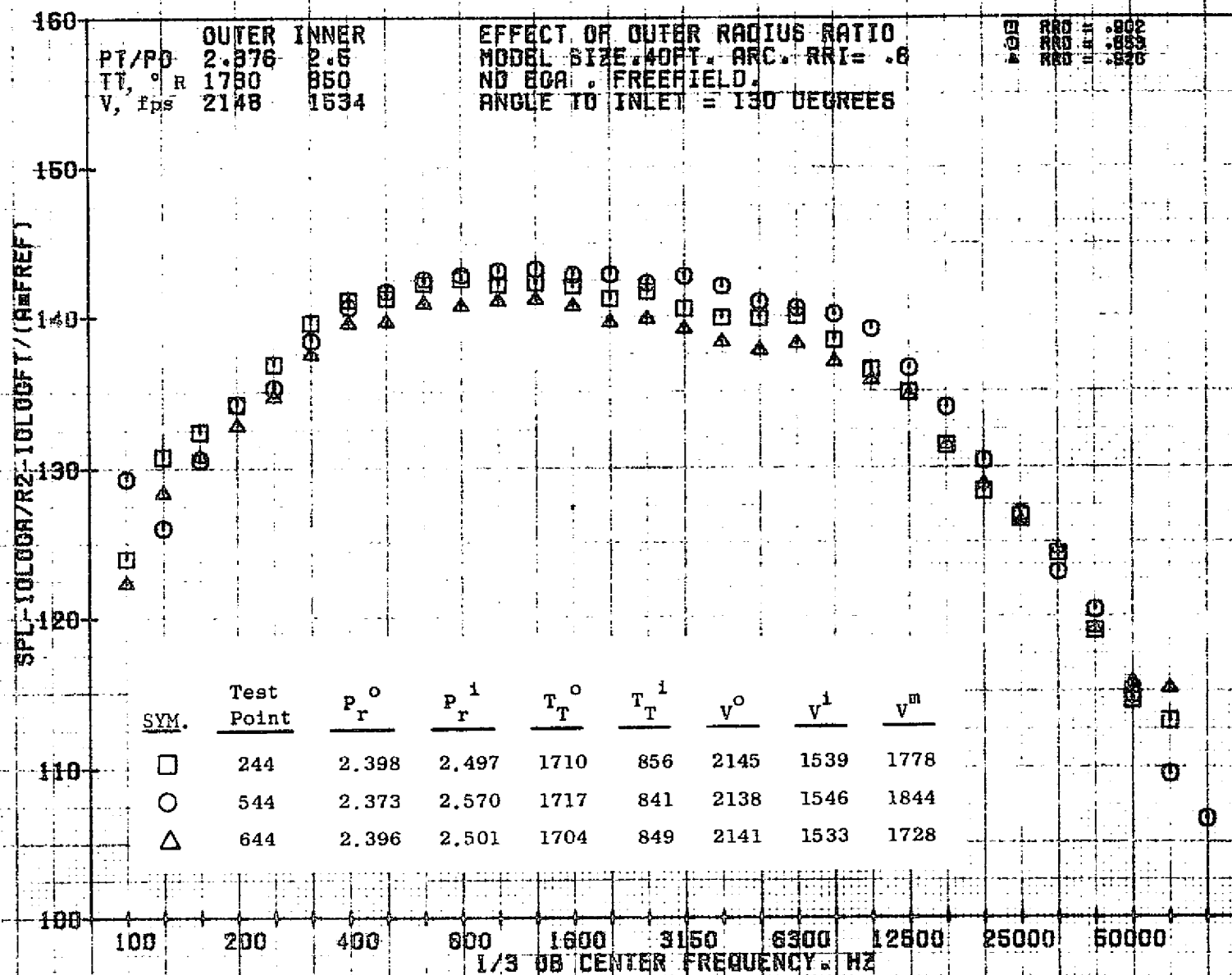
10/27/76
1X824-001

73KOLLSTEDT



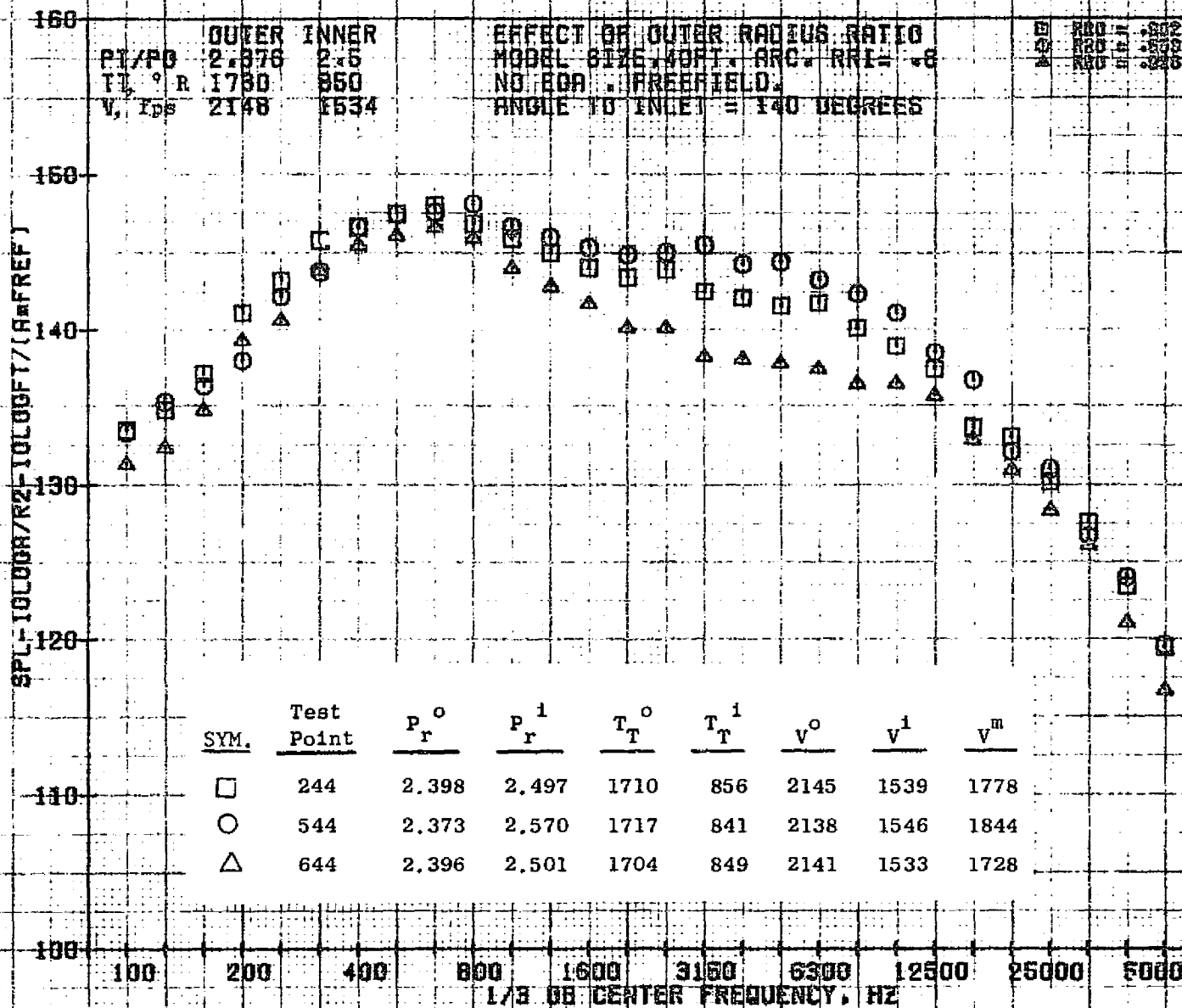
10/27/76
 1X824-001

73KOLLSTEOT



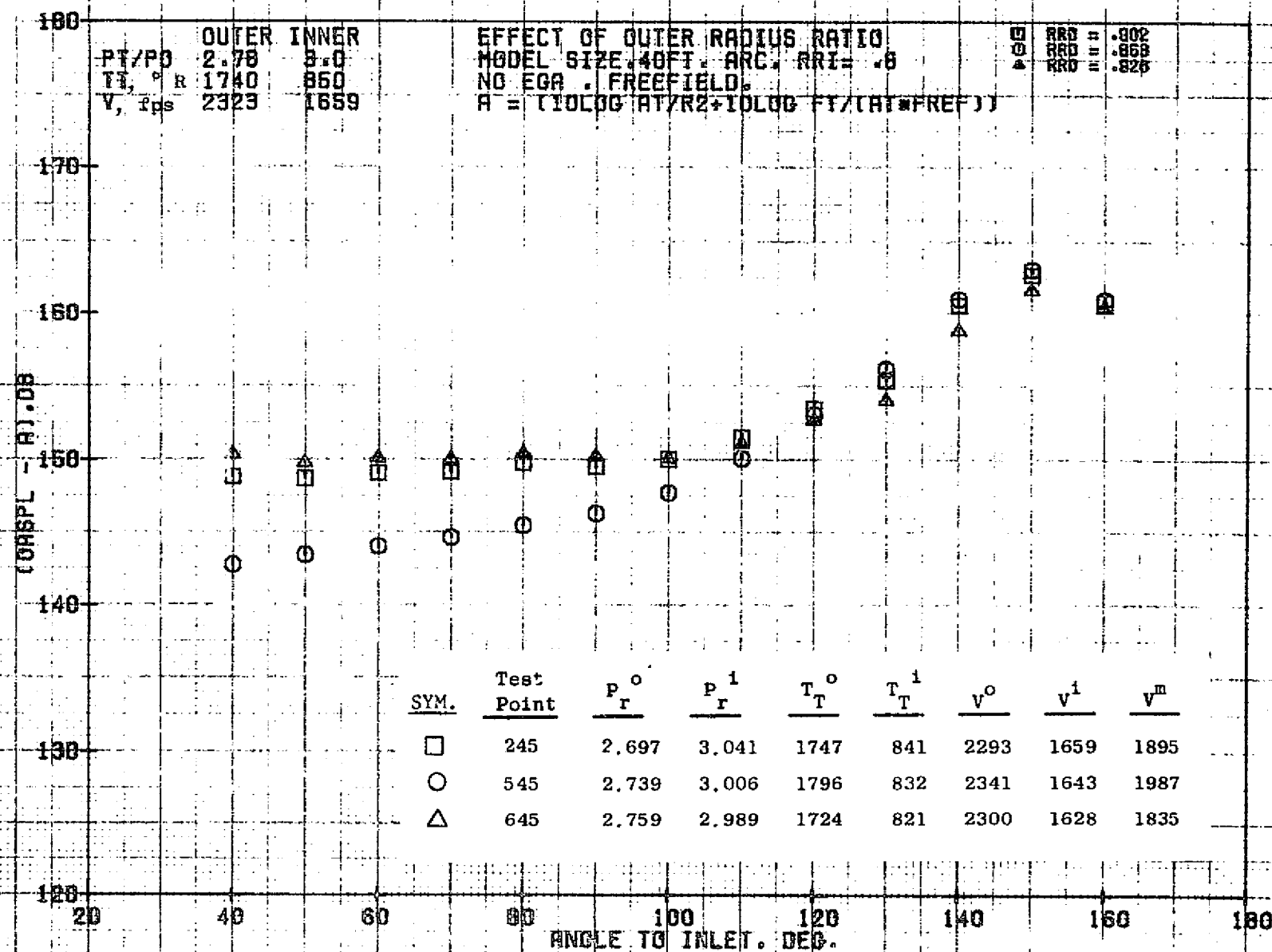
10/27/76
 1X824-001

73KOLLSTEDT



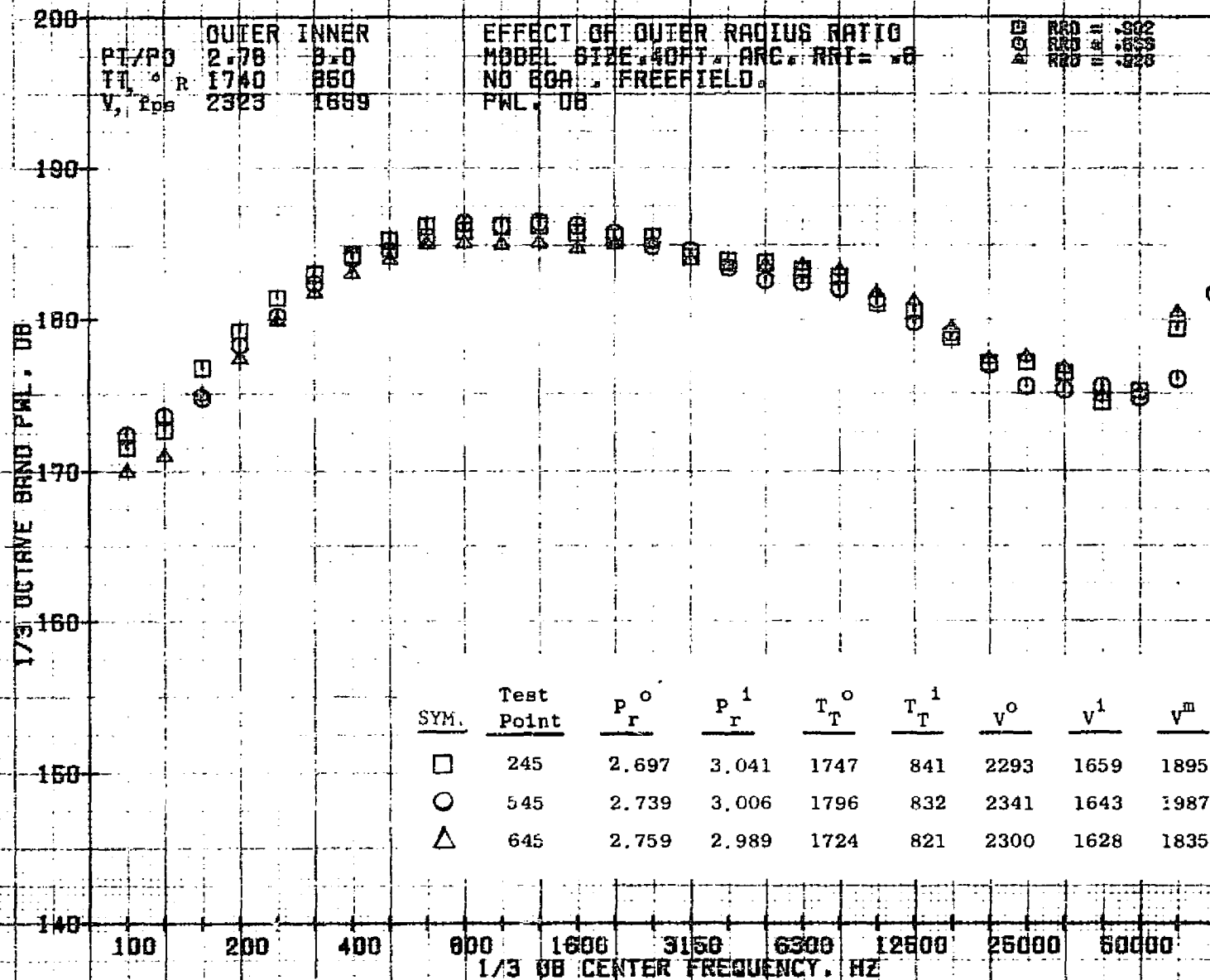
10/27/76
 1X824-001

73KOLLSTEDT



10/27/76
 1X824-001

73KOLLSTERT



10/27/76
1X824-001

73K3LLSTEDT

160
 150+
 140-
 130-
 120-
 110-
 100-

PT/PD 2.78 3.0
 TT, ° R 1740 850
 V, fps 2323 1659

EFFECT OF OUTER RADIUS RATIO.
 MODEL SIZE, 40 FT. ARC. RRI = .8
 NO ECA. FREEFIELD.
 ANGLE TO INLET = 50 DEGREES

□ RRO = .902
 ○ RRO = .853
 △ RRO = .826

SPL - YOLODA/R2-YOLODA/T/(R-REF)

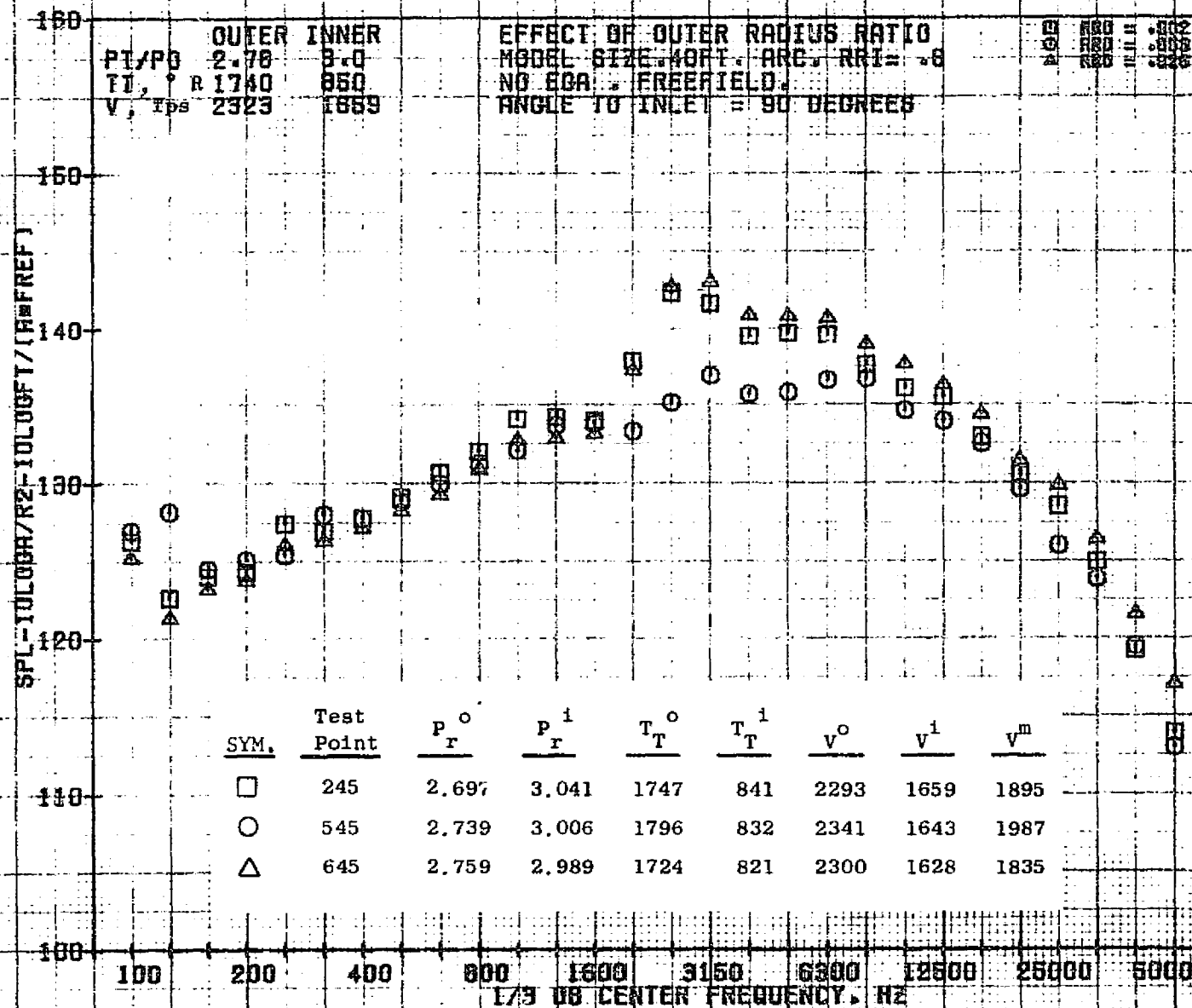
916

SYM.	Test Point	P _r ^o	P _r ⁱ	T _T ^o	T _T ⁱ	V ^o	V ⁱ	V ^m
□	245	2.697	3.041	1747	841	2293	1659	1895
○	545	2.739	3.006	1796	832	2341	1643	1987
△	645	2.759	2.989	1724	821	2300	1628	1835

1/3 DB CENTER FREQUENCY. HZ

10/27/76
18854-001

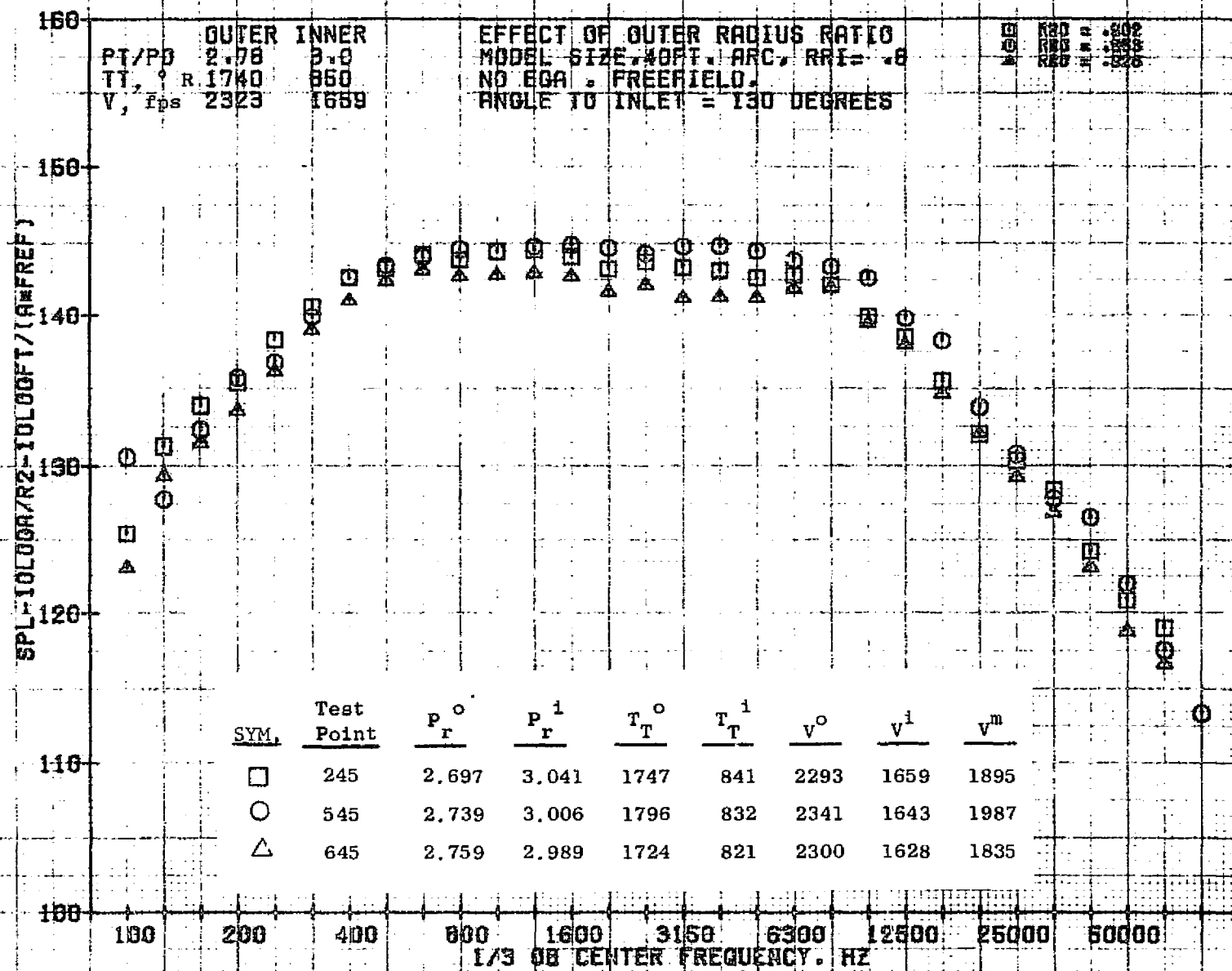
73K011 SIFT



10/27/76
1X824-001

73KOLLSTEOT

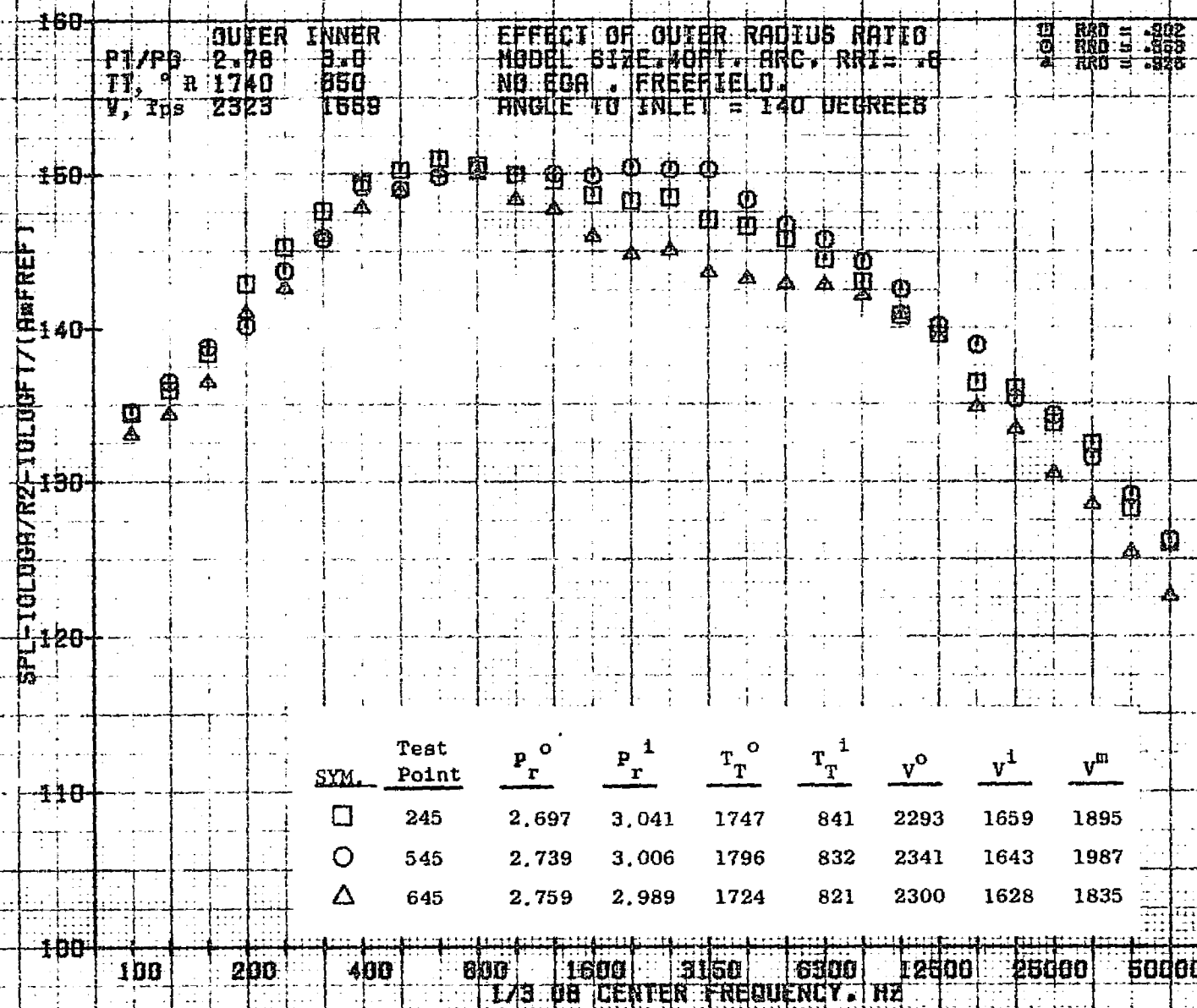
616



10/27/76
1X824-001

73KOLLSTEDT

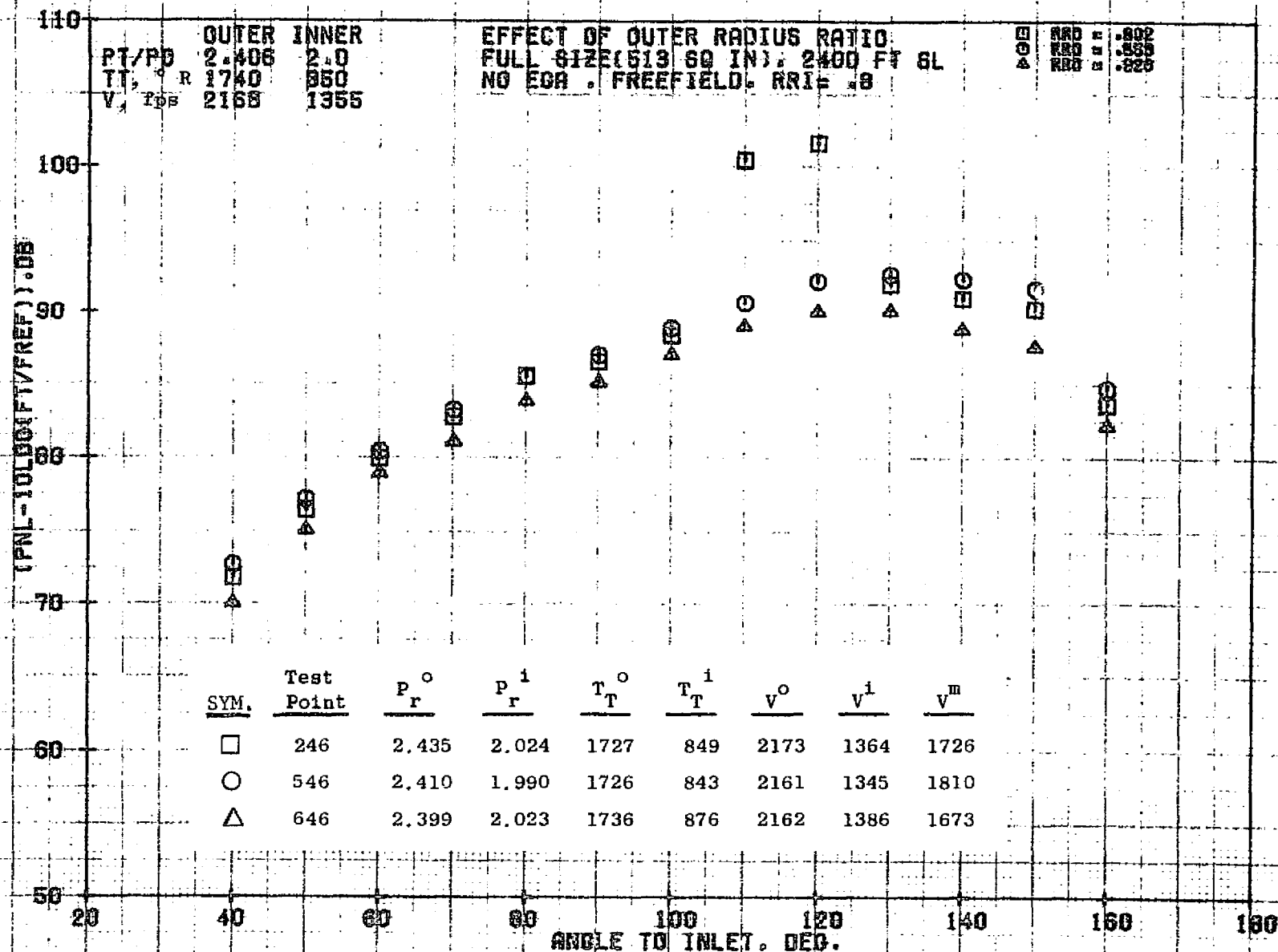
926



10/27/76
1X824-001

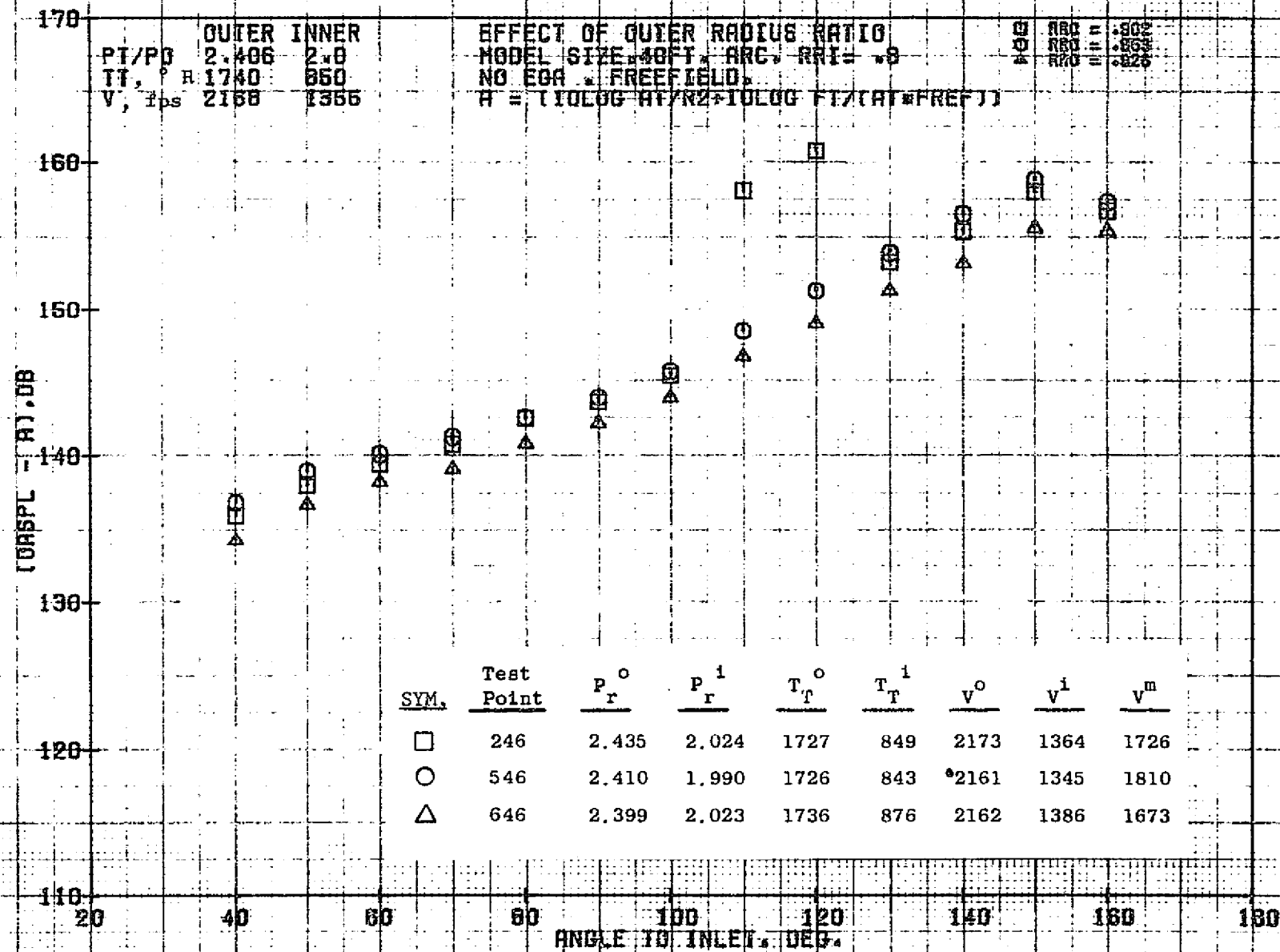
73KOLLSTEDT

921



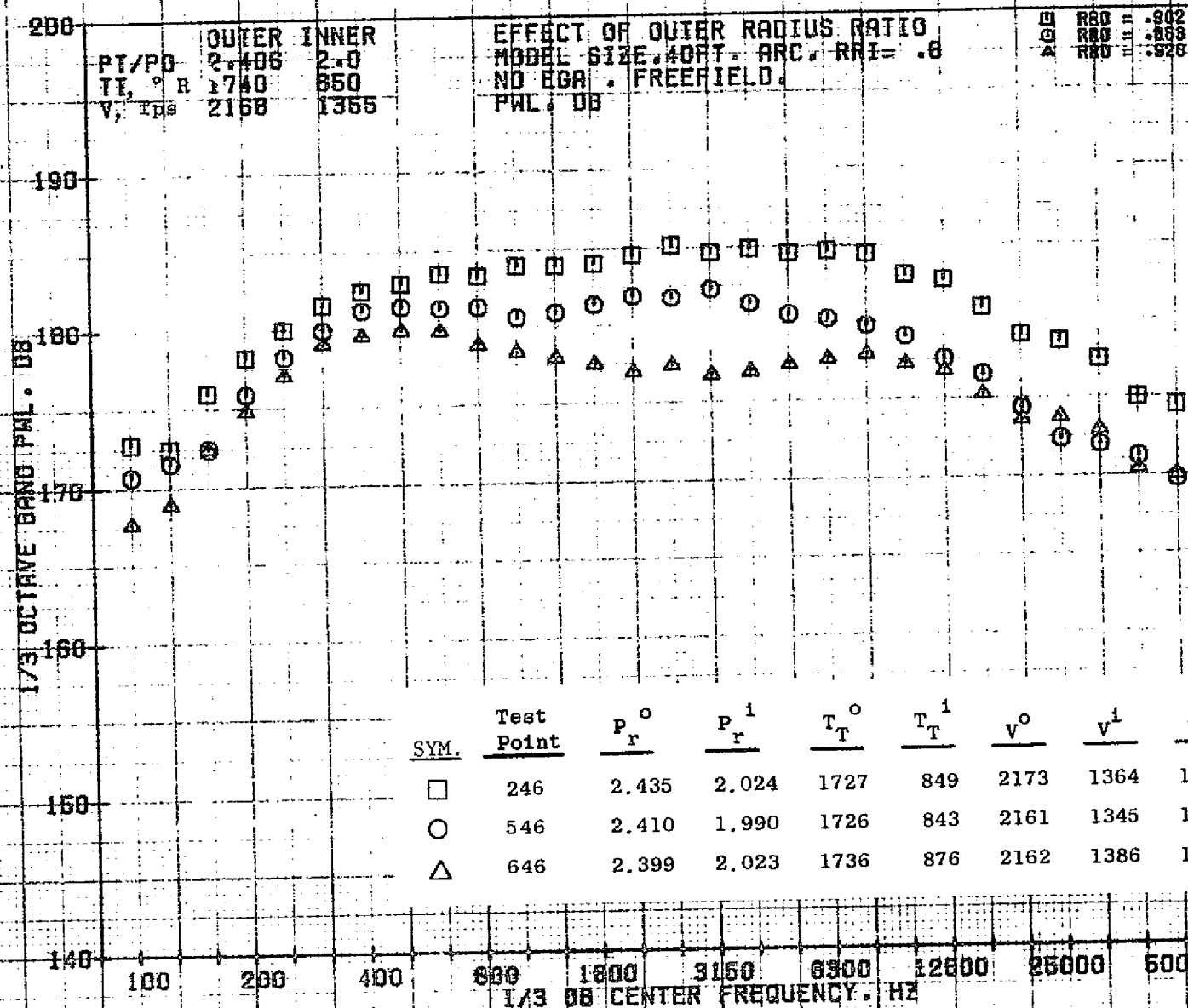
10/29/76
18124-001

79 BURCH A.



10/27/76
1X824-001

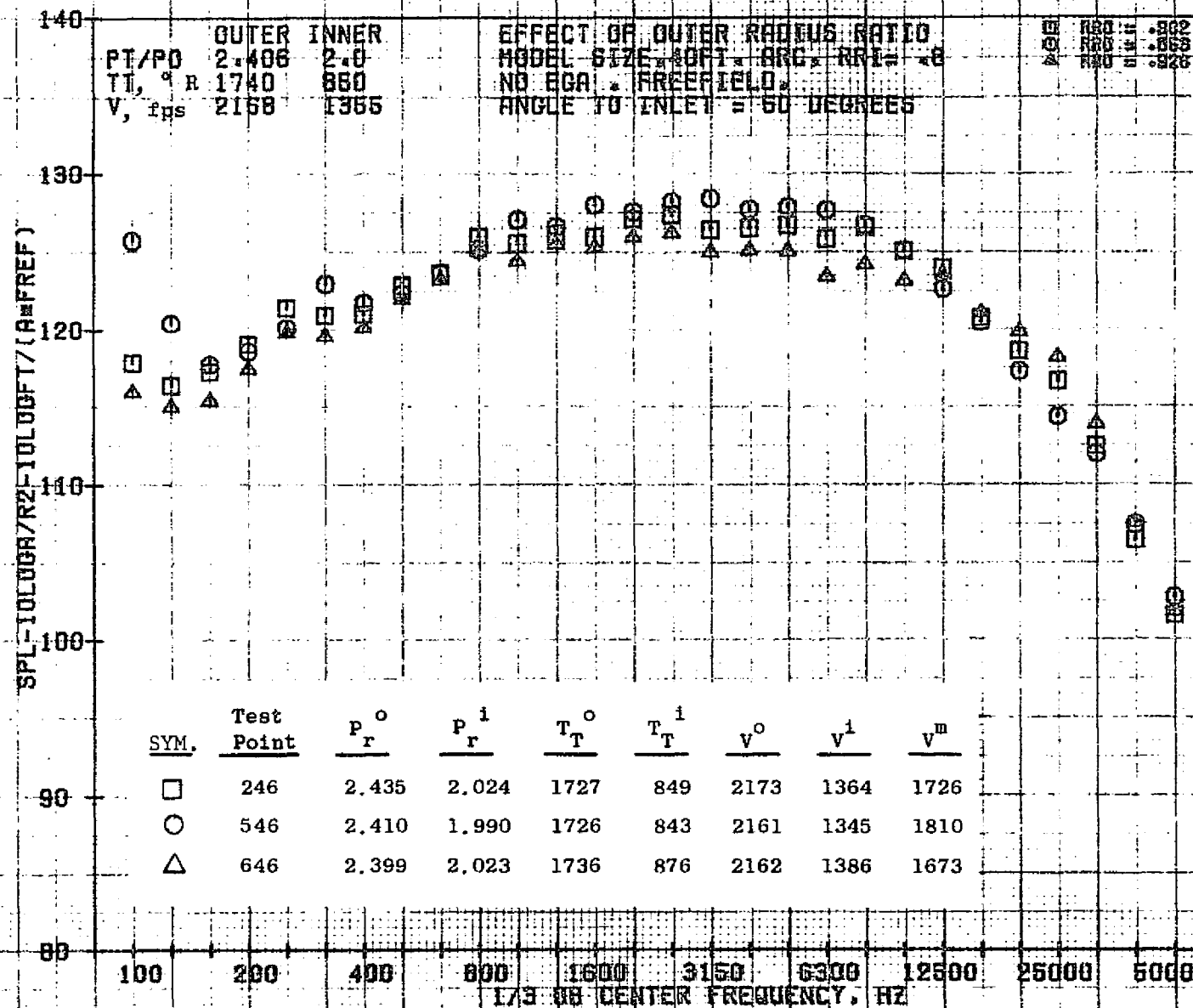
73KOLLSTEDT



10/27/76
 1X824-001

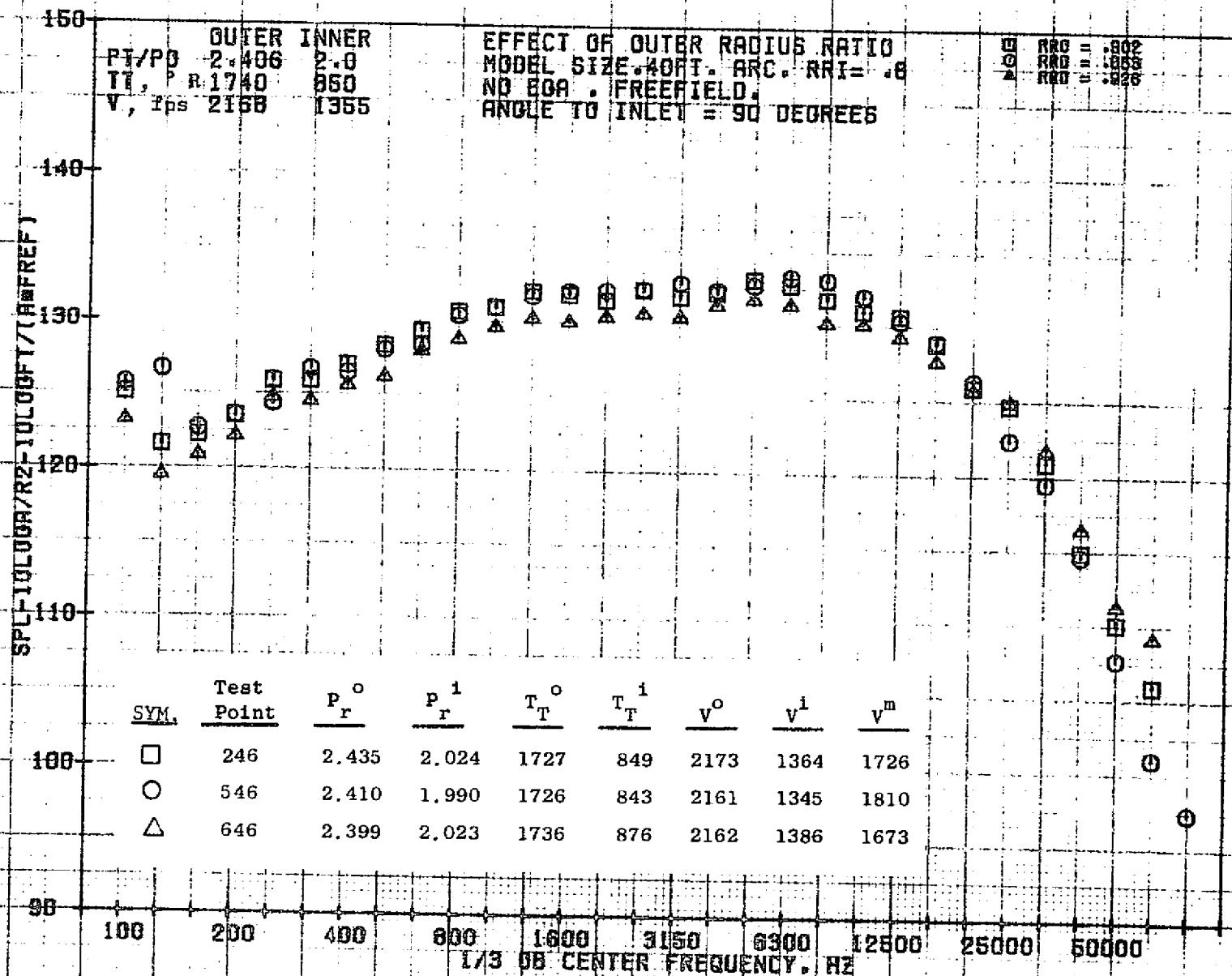
73KOLLSTEDT

924



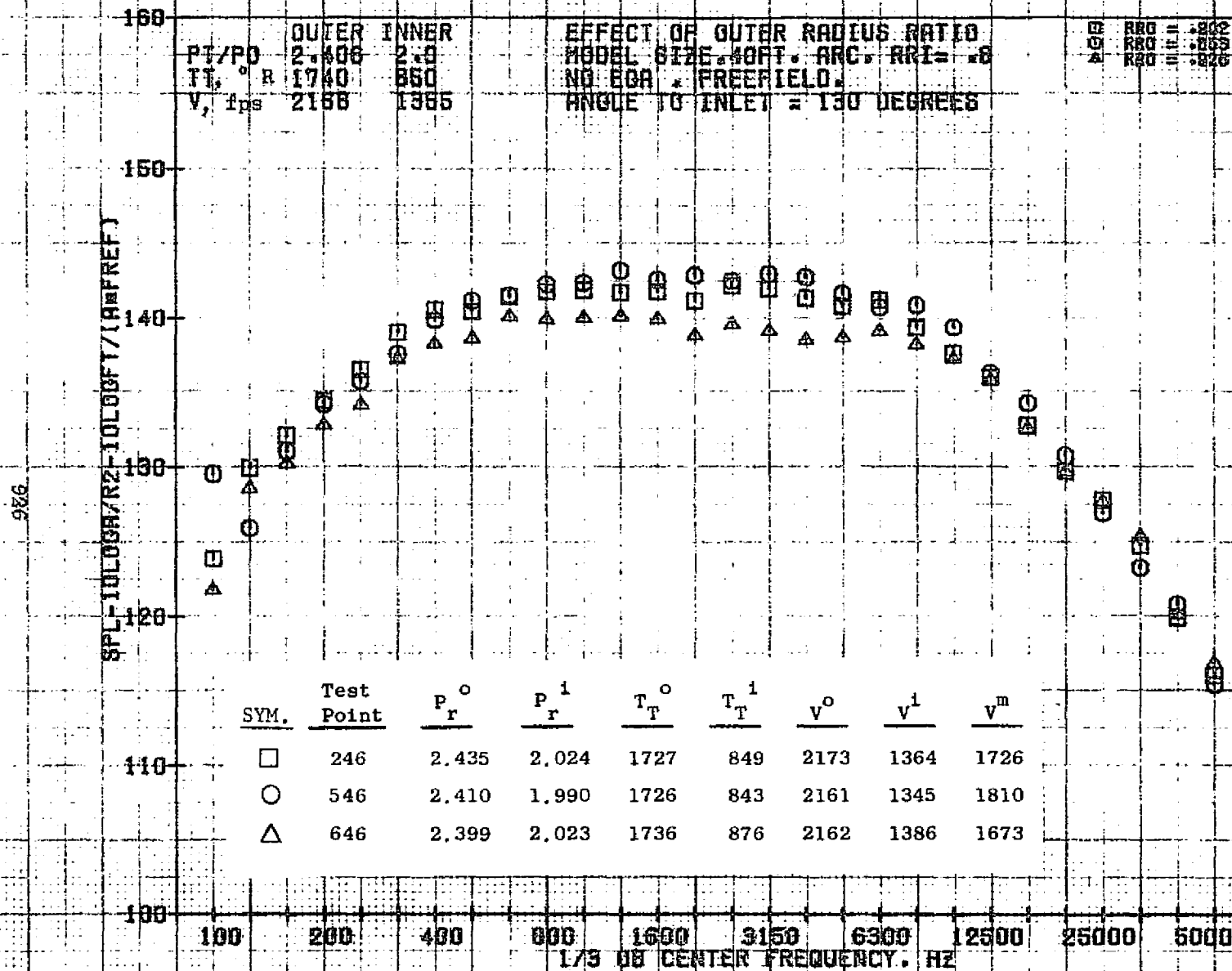
10/27/76
1X824-001

73KOLLSTEDT



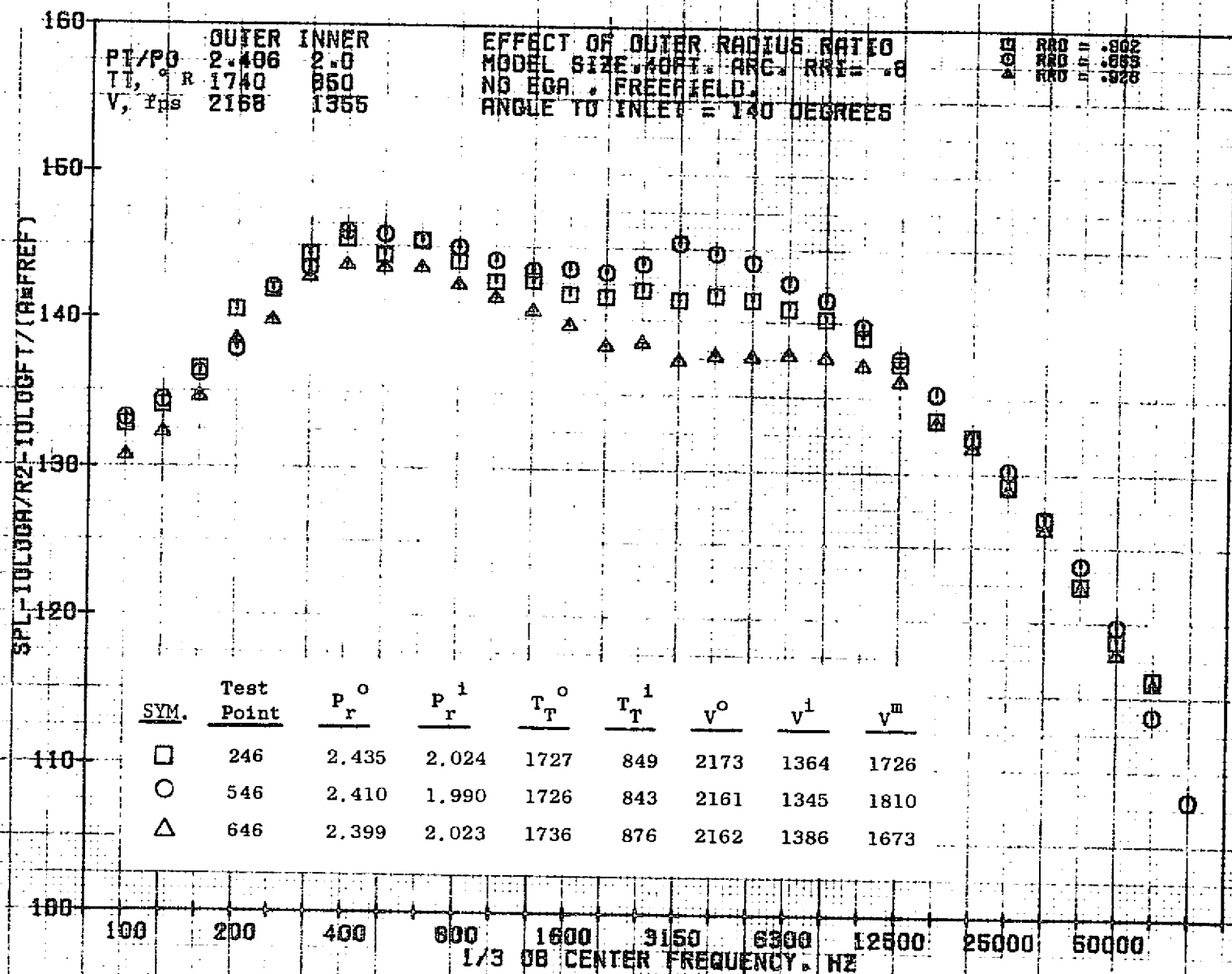
10/27/76
 1X824-001

73KOLLSTEDT



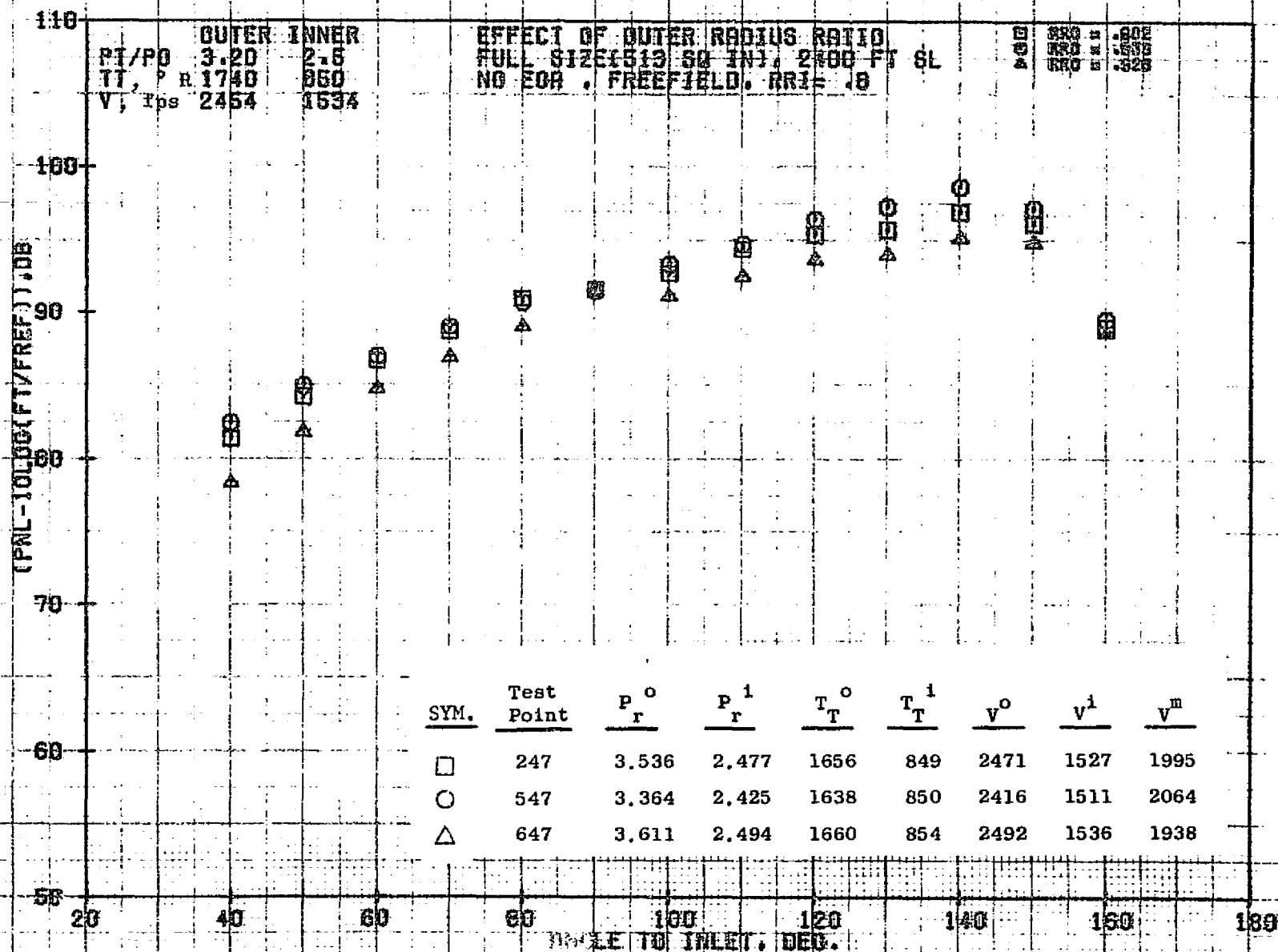
10/27/76
 1X824-001

73KOLLSTEDT



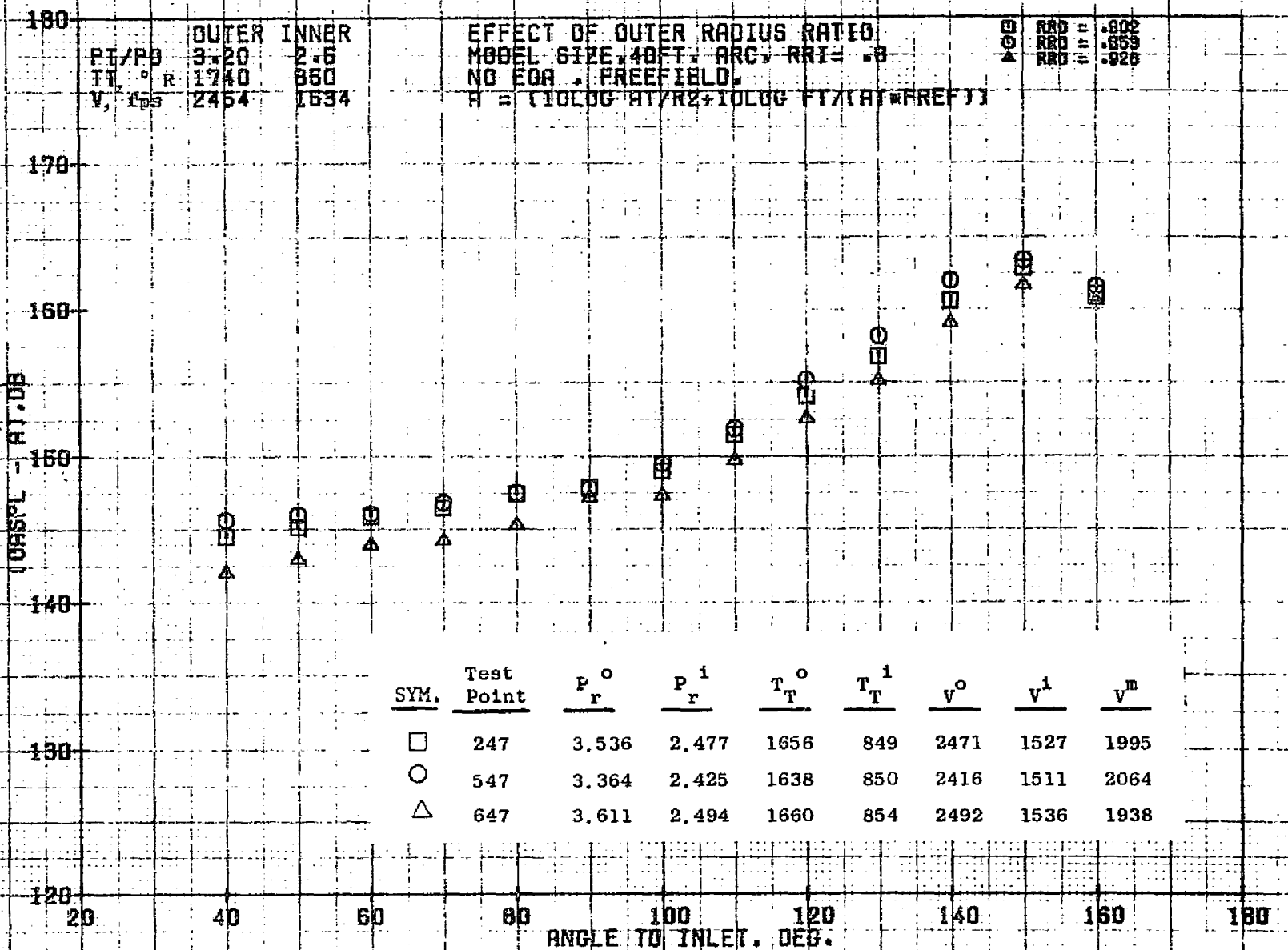
10/27/76
1X824-001

73KOLLSTEDT



10/29/76
18124-001

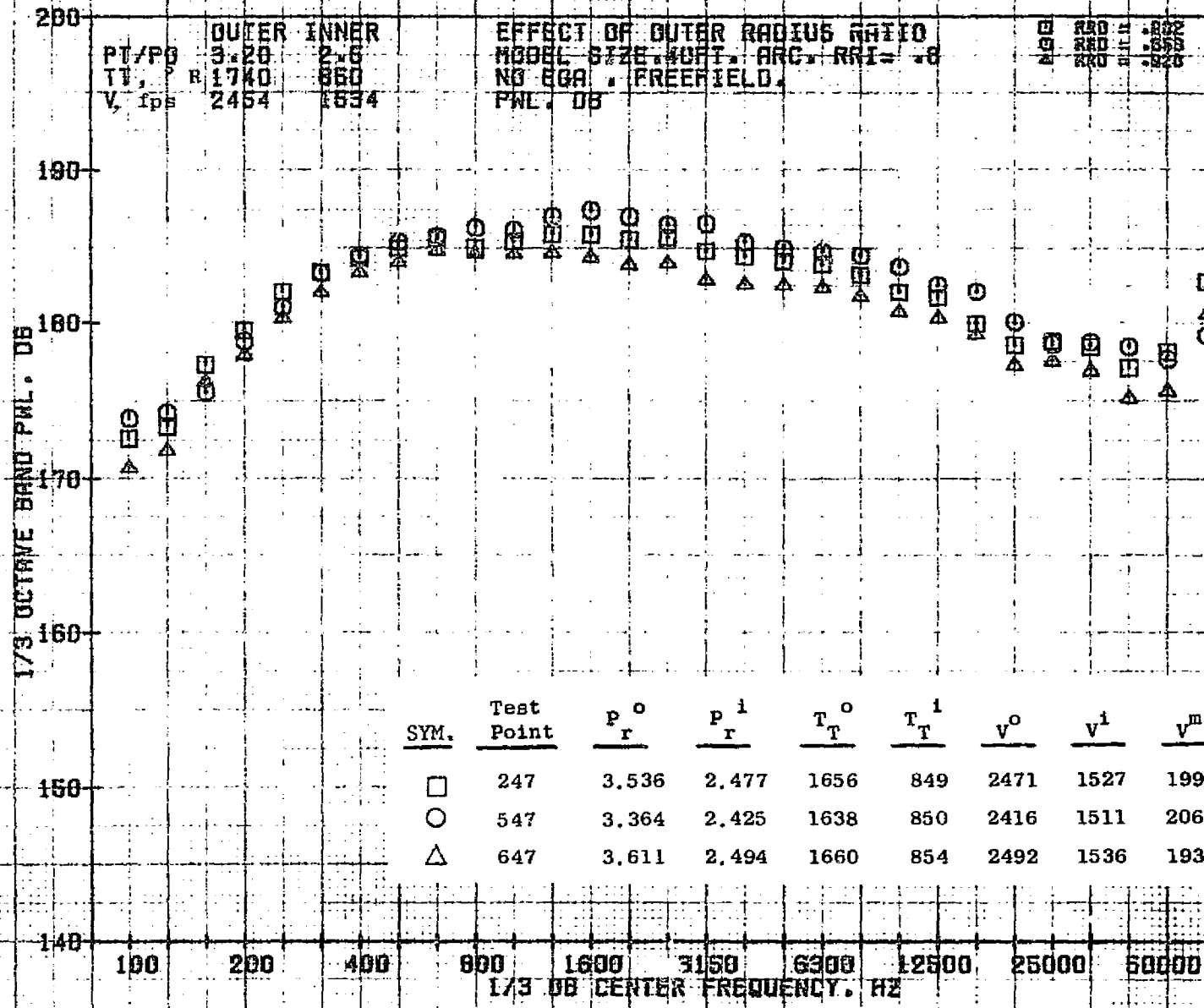
79 BURCH A.



10/27/76
 1X824-001

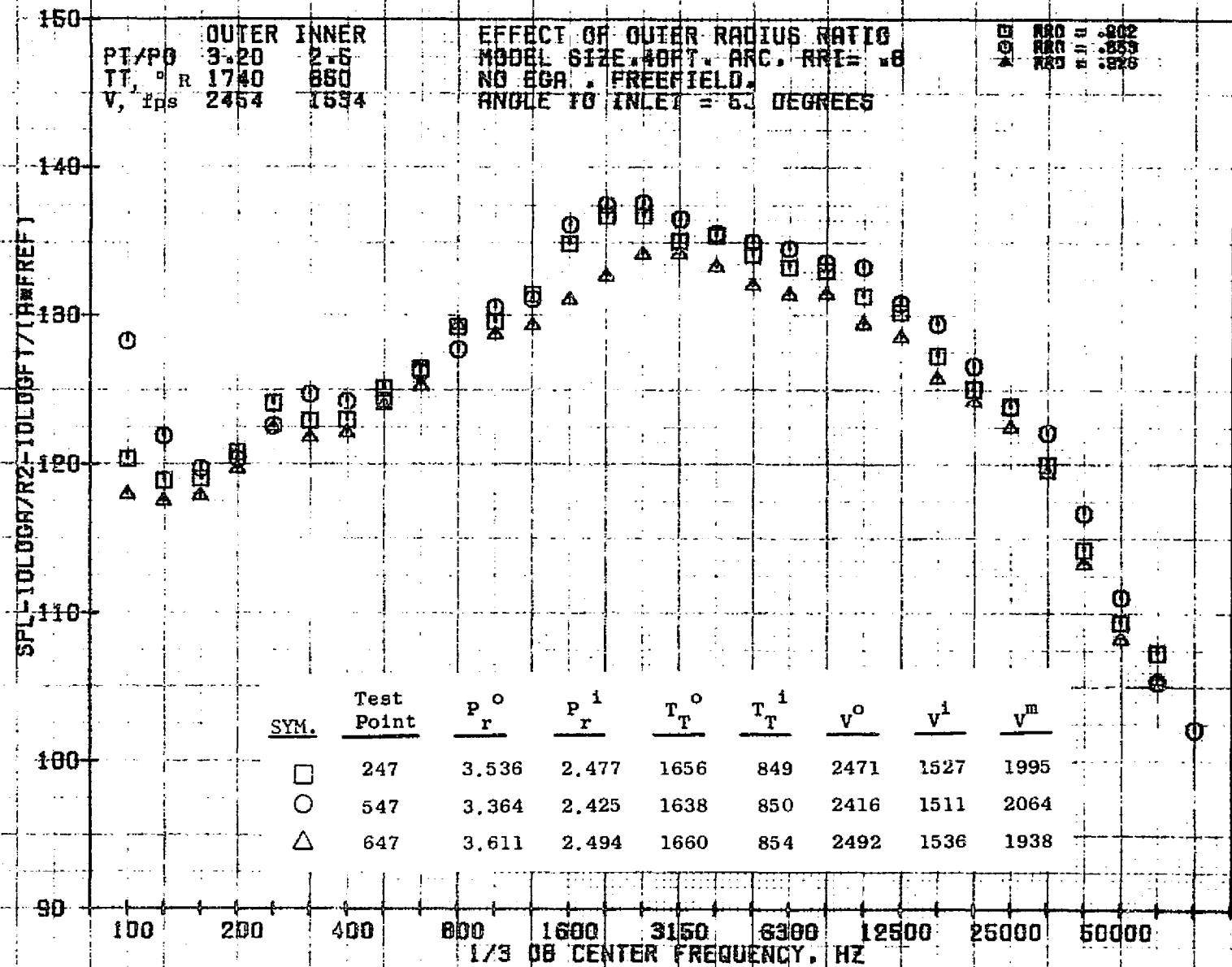
73KOLLSTEDT

QEG



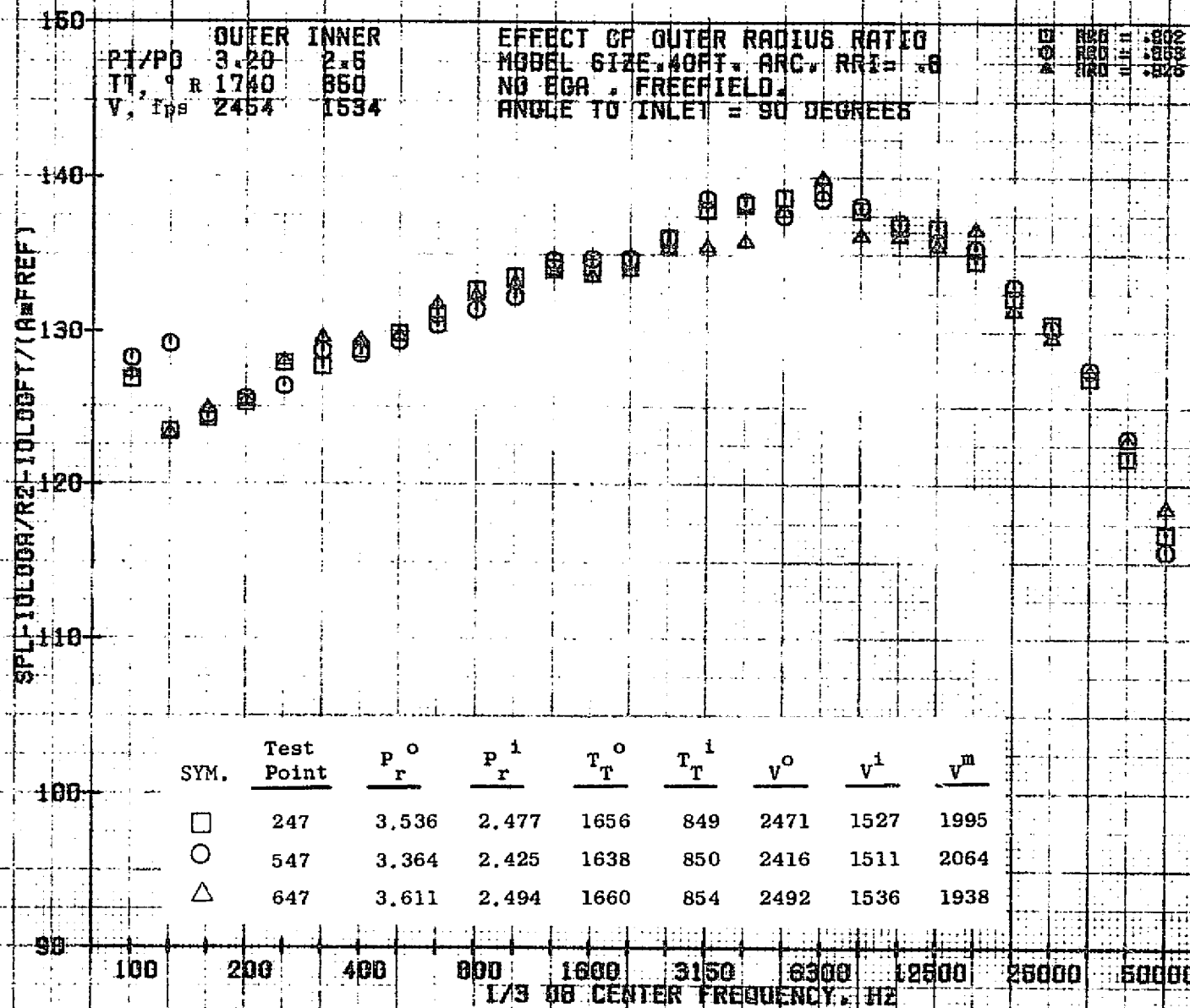
10/27/76
1X824-001

73KOLLSTEDT



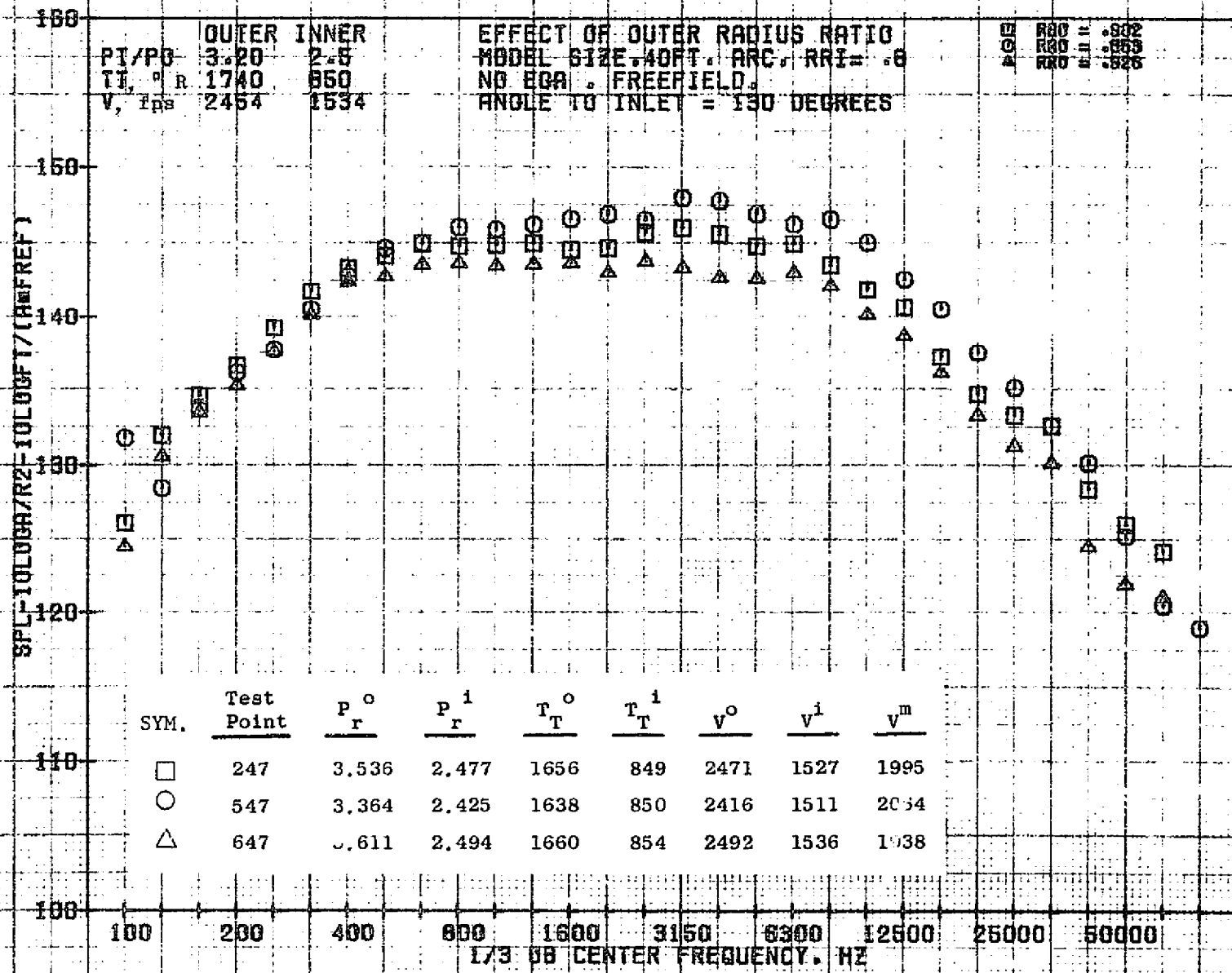
10/27/76
1X824-001

73KOLLSTEDT



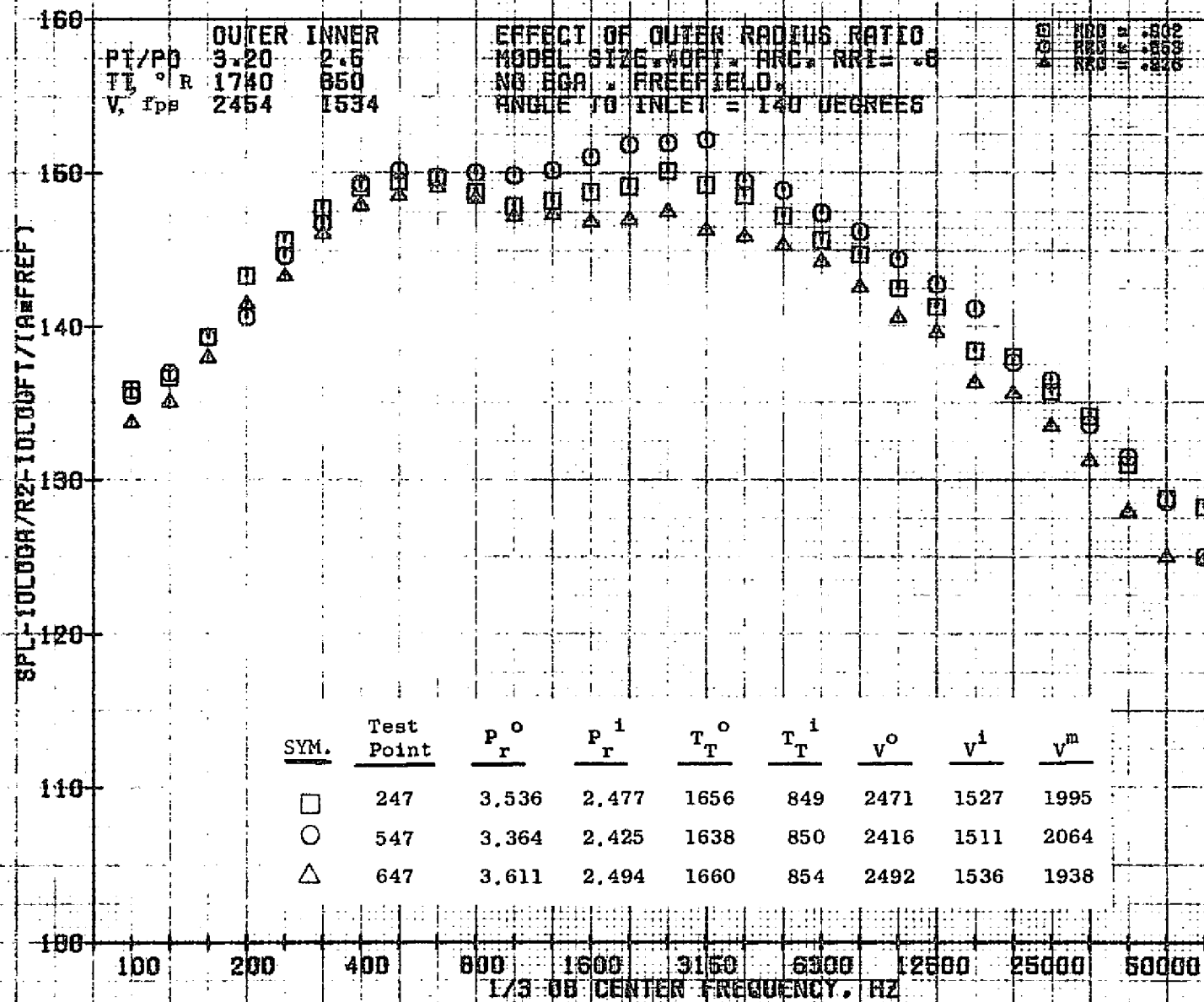
10/27/76
 1X824-001

73KOLLSTEDT



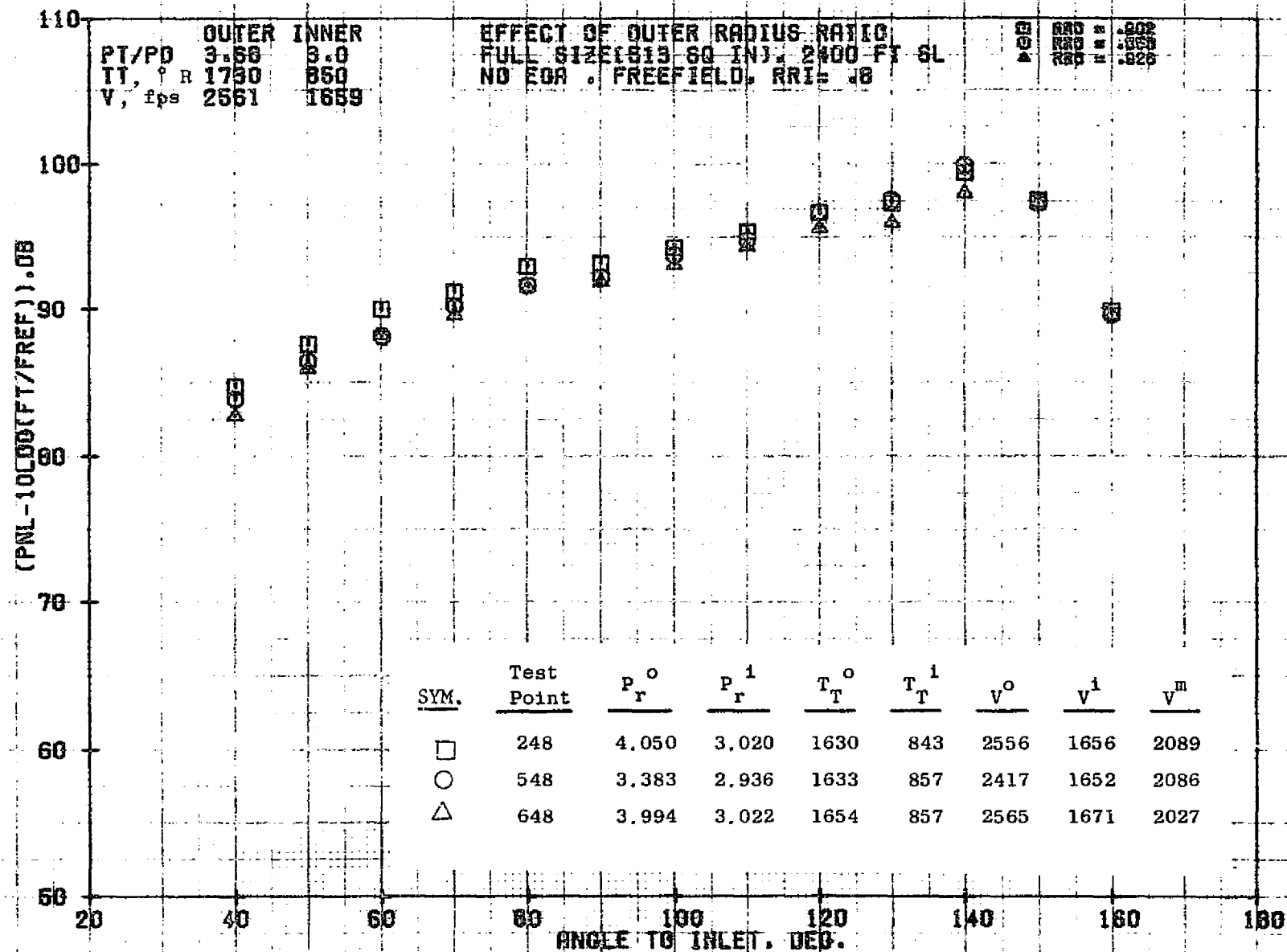
10/27/76
 1X824-001

73KOLI STEDT



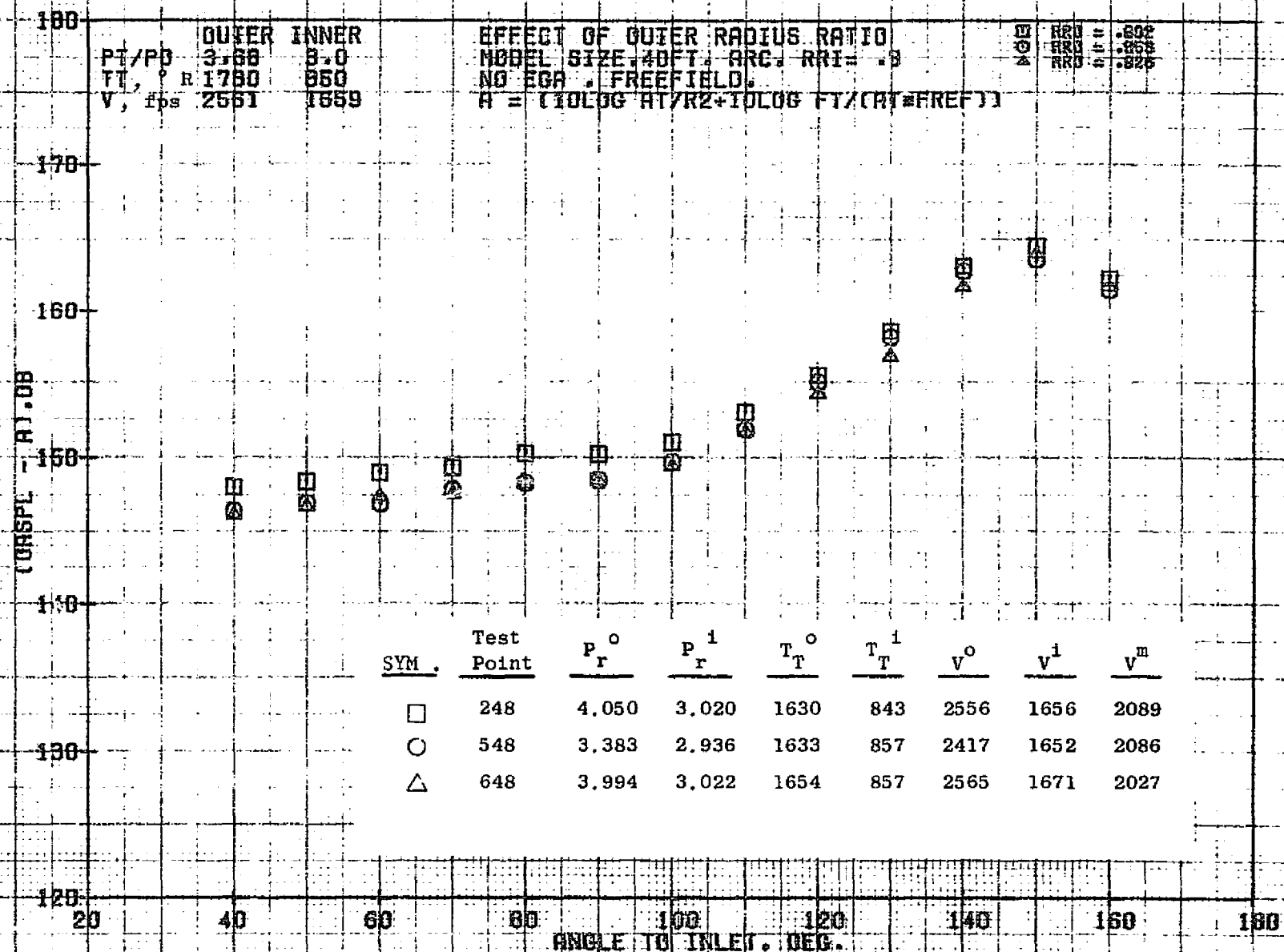
10/27/76
 1X824-001

73KOLLSTEDT



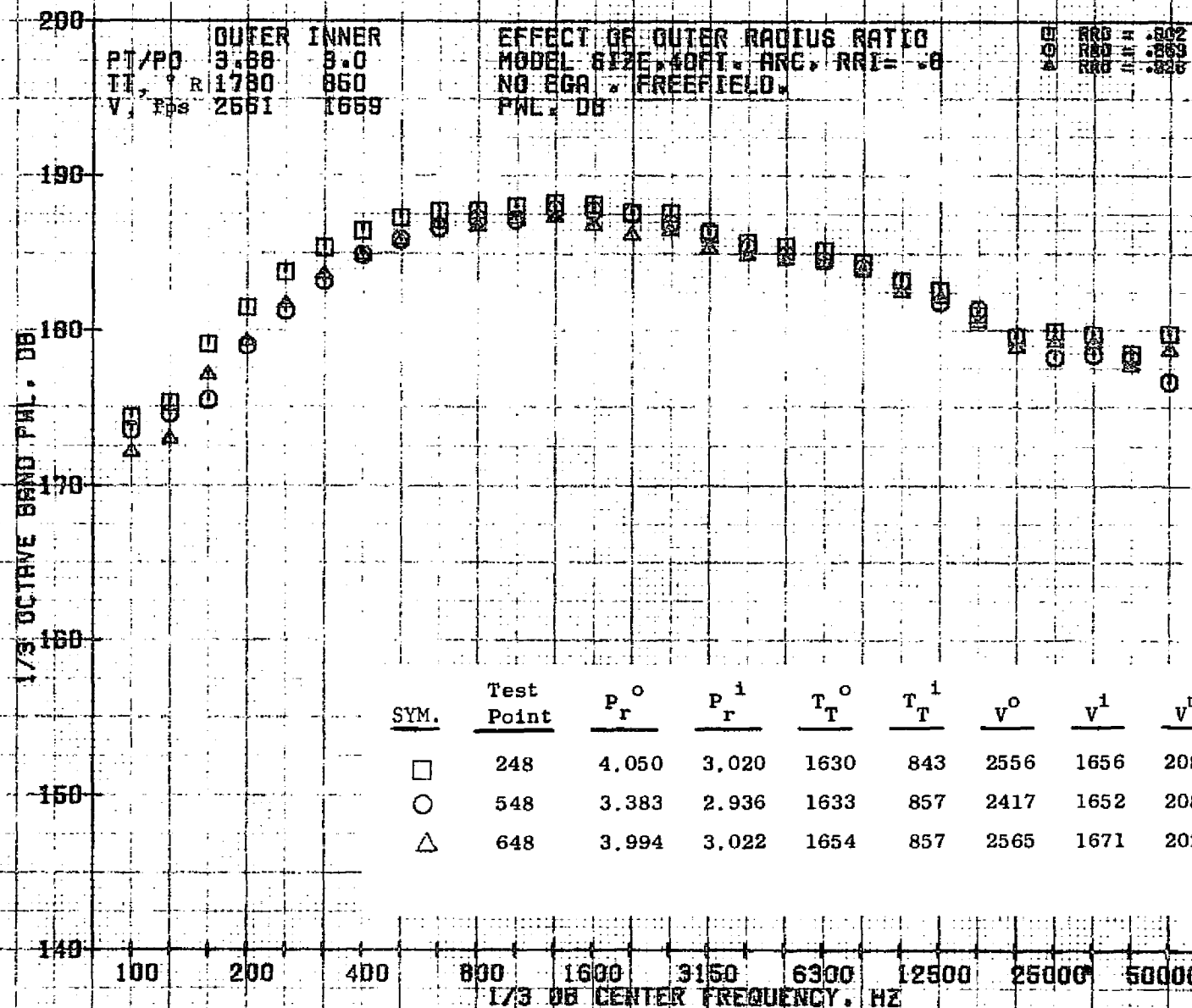
10/29/78
18124-001

79 BURCH A.



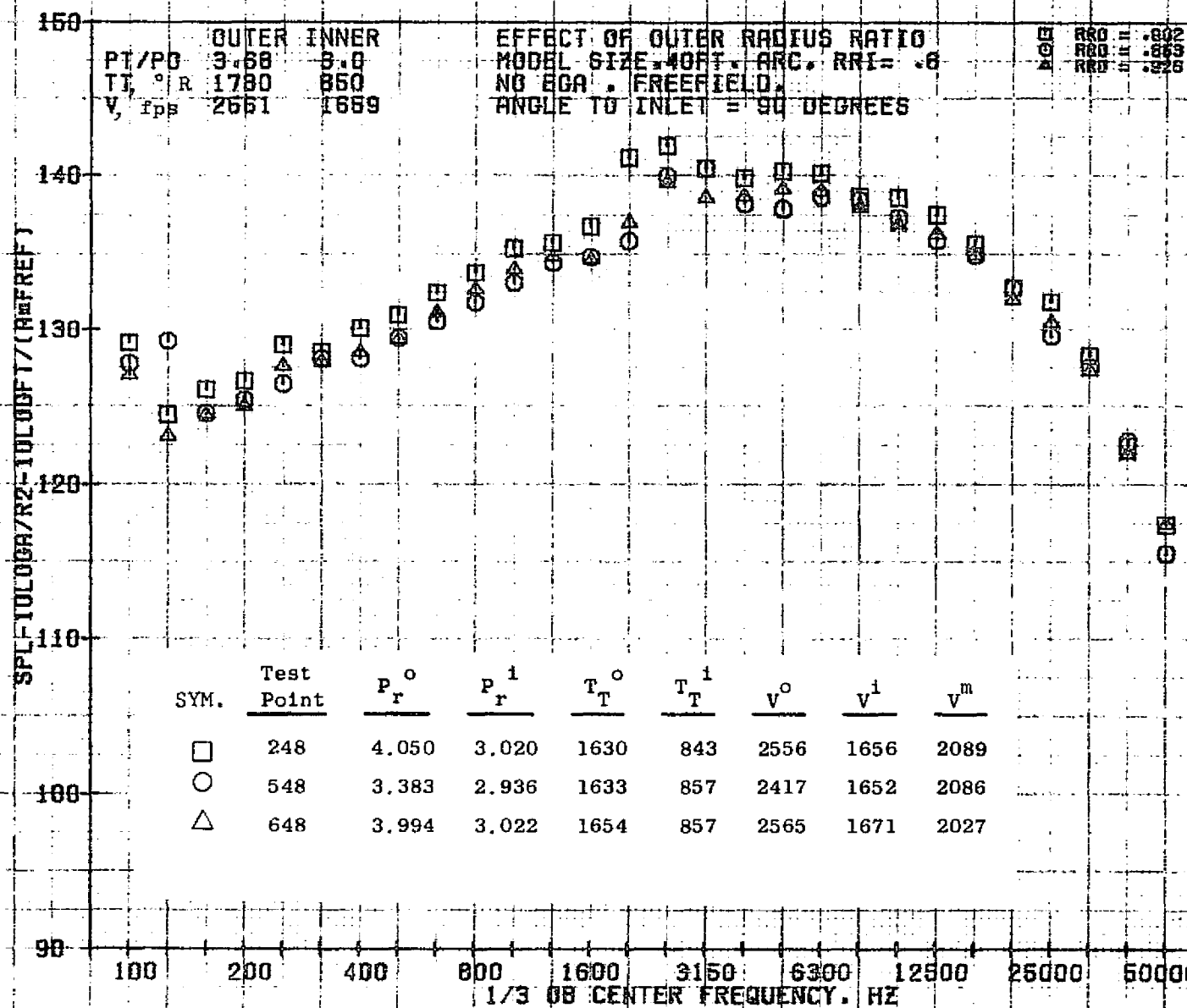
10/27/76
1X824-001

73KOLLSTEDT



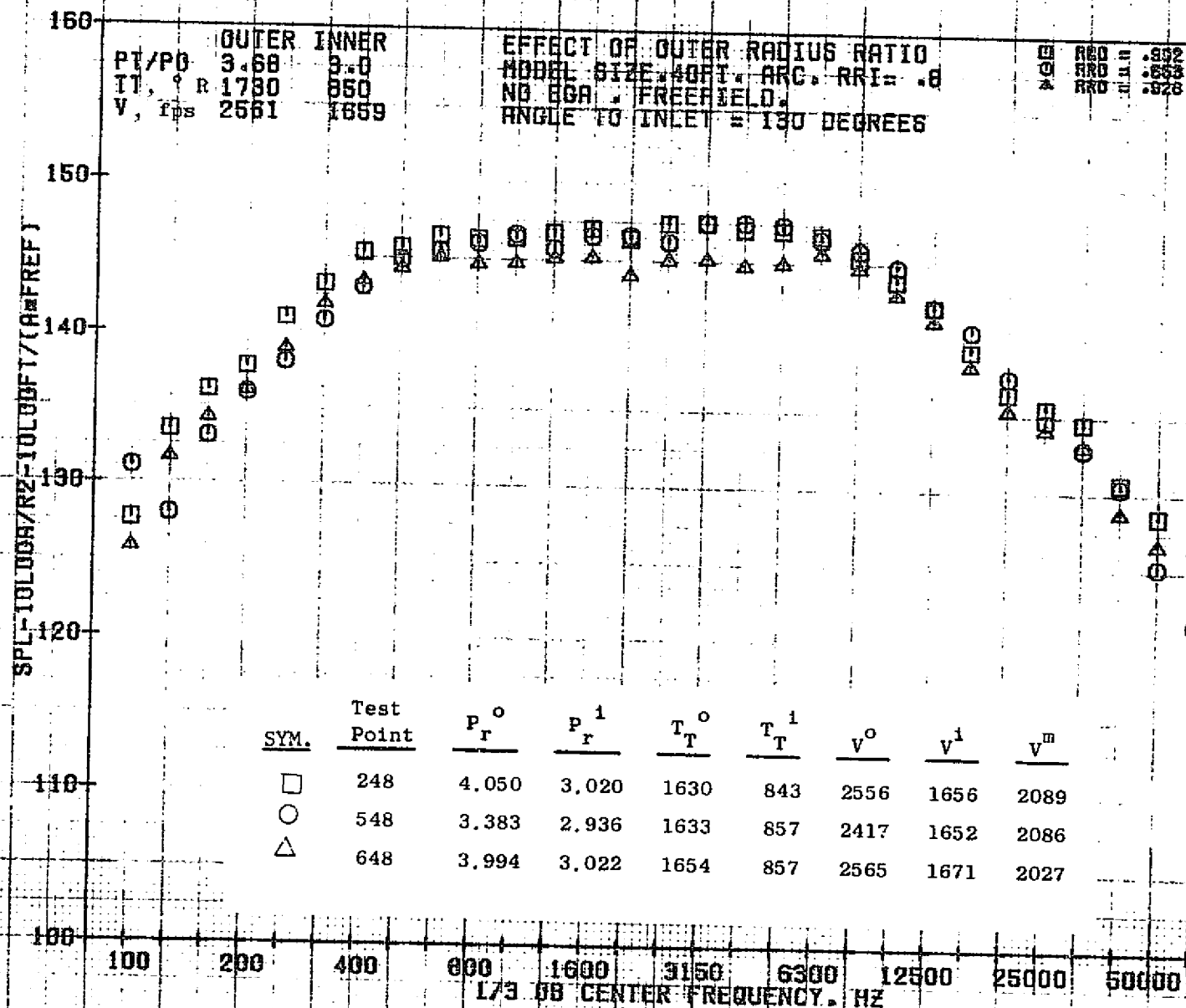
10/27/76
 1X824-001

73KOLLSTEDT



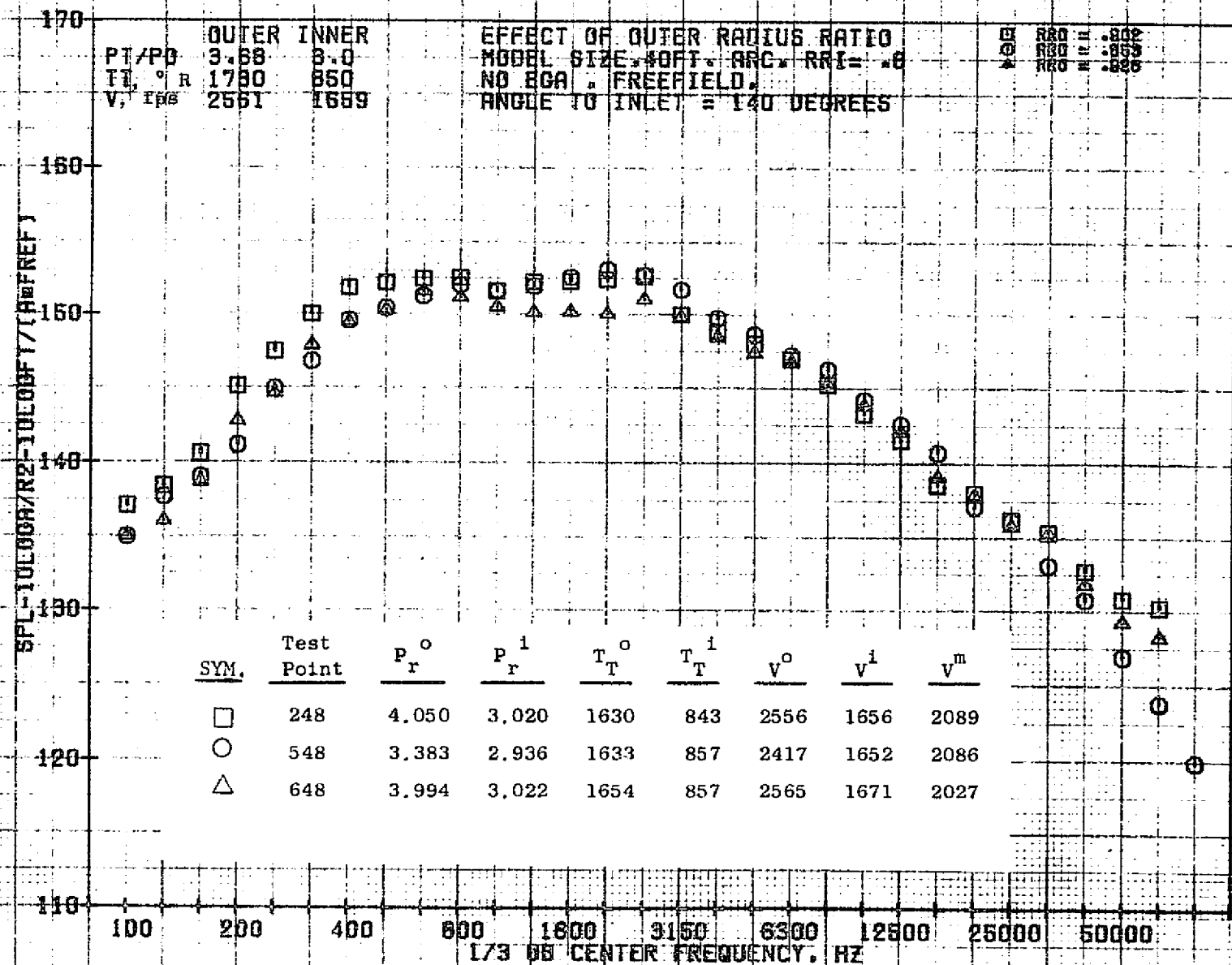
10/27/76
1X824-001

73KOLLSTEDT.



10/27/76
 1X824-001

73KOLLSTEDT

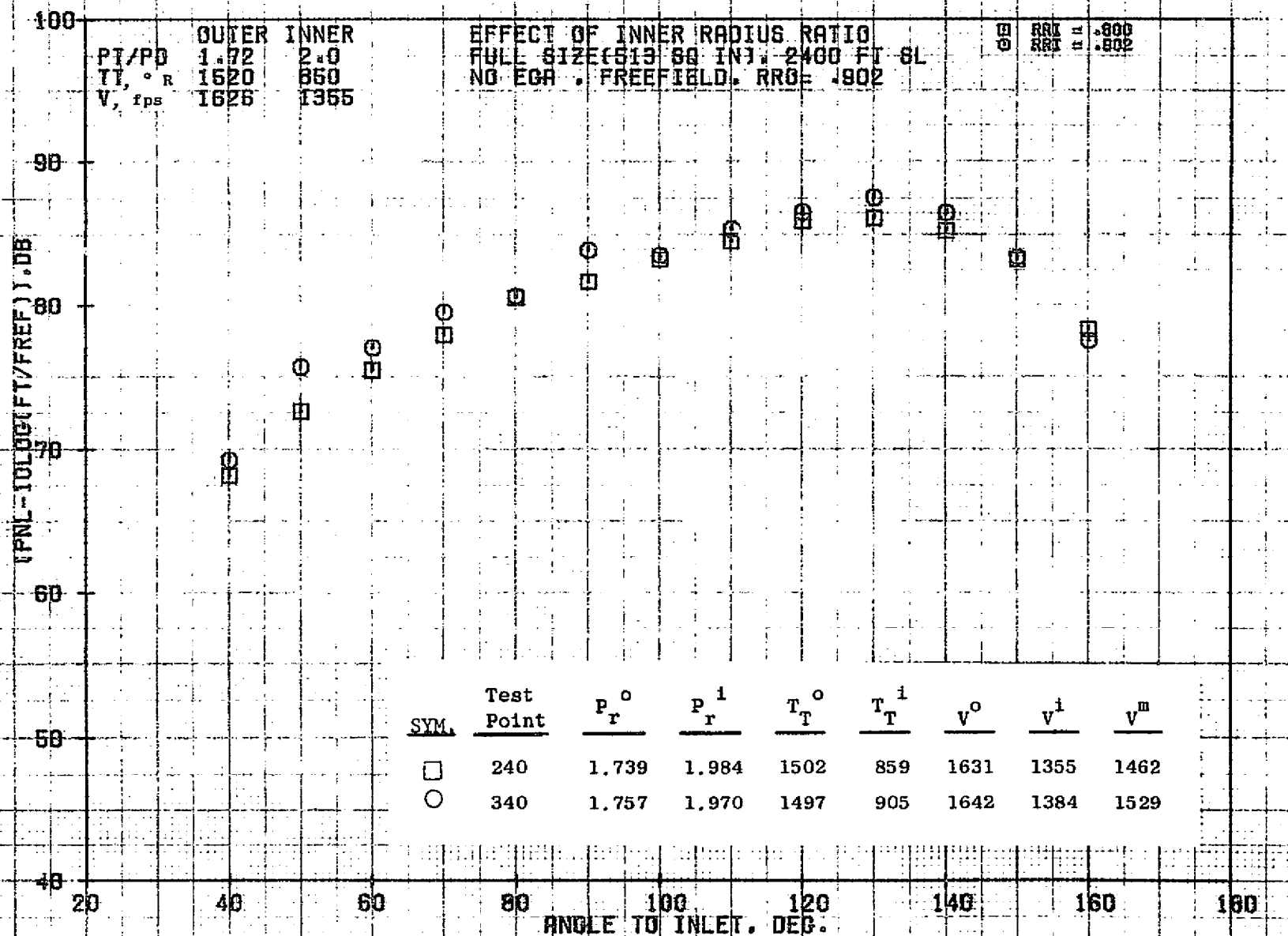


10/27/76
 1X824-001

73KOLLSTEDT

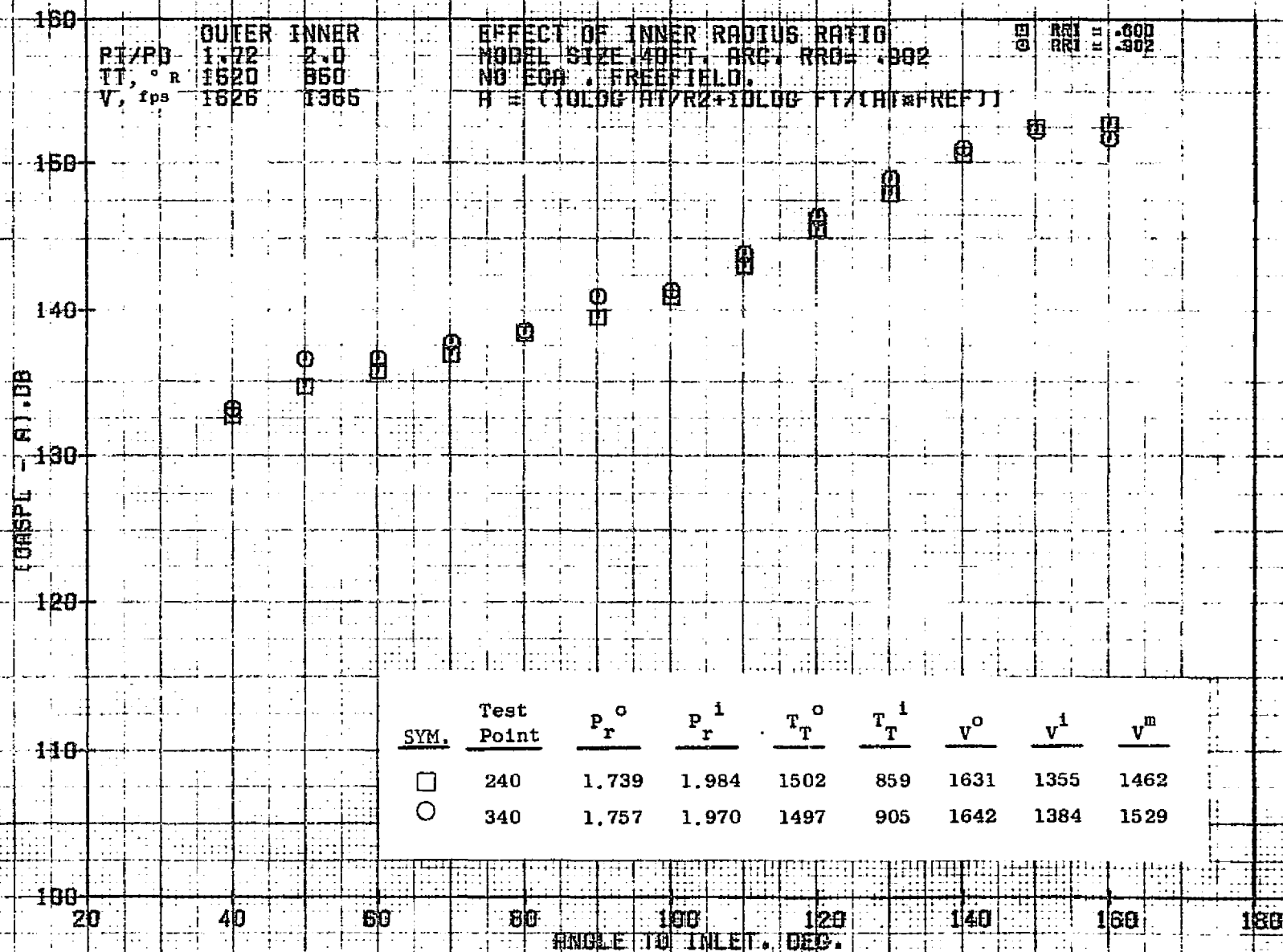
7.4.2 Effect of Inner Radius Ratio

Configurations 2 and 3 have the same outer radius ratio (0.902) but different inner radius ratios, 0.800 and 0.902, respectively. The acoustic results are compared in this section. Configurations 5 and 7 are also compared. These two configurations have a 0.853 outer radius ratio and inner radius ratios of 0.800 and 0.902, respectively.



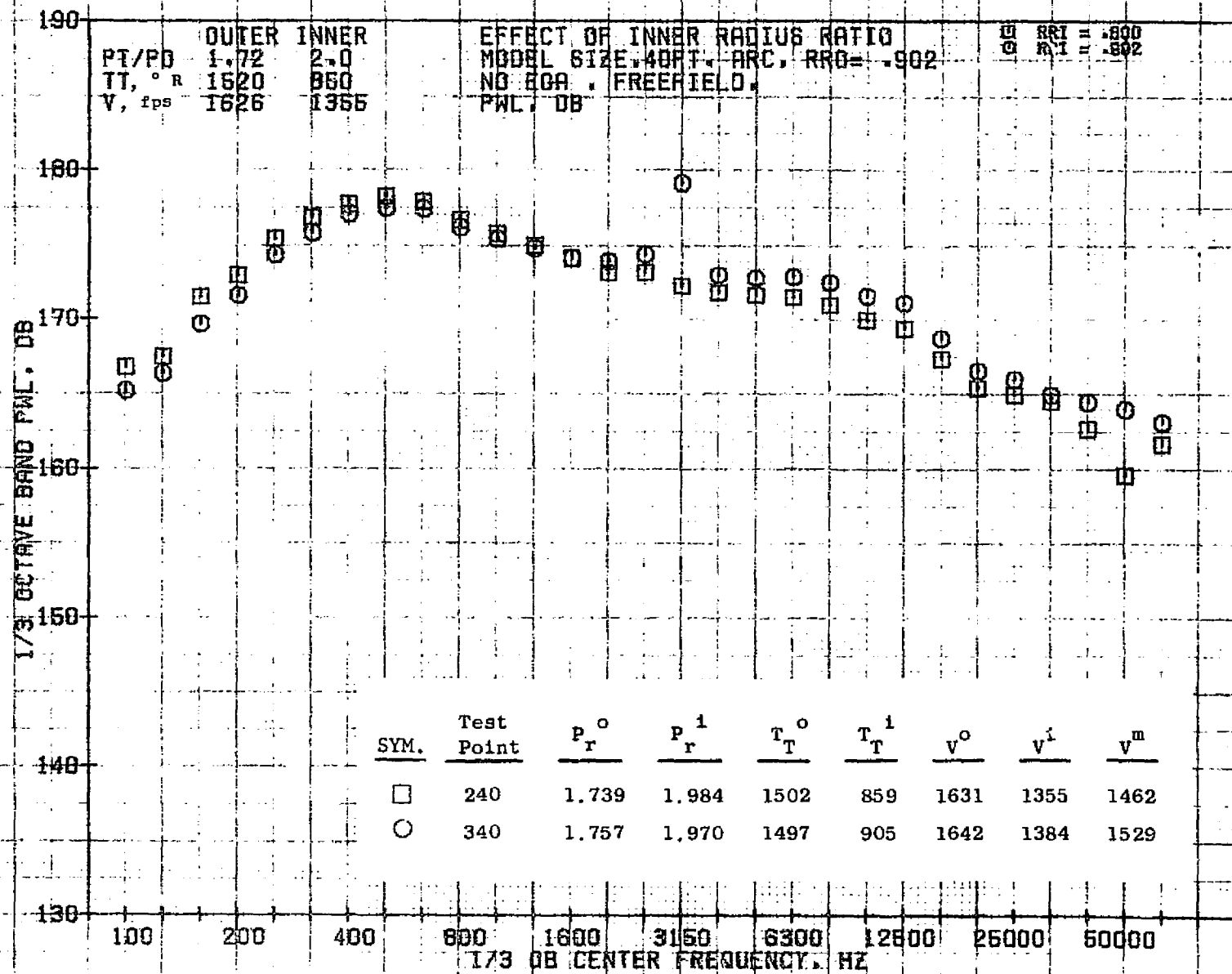
10/29/76
 18124-001

79 BURCH A.



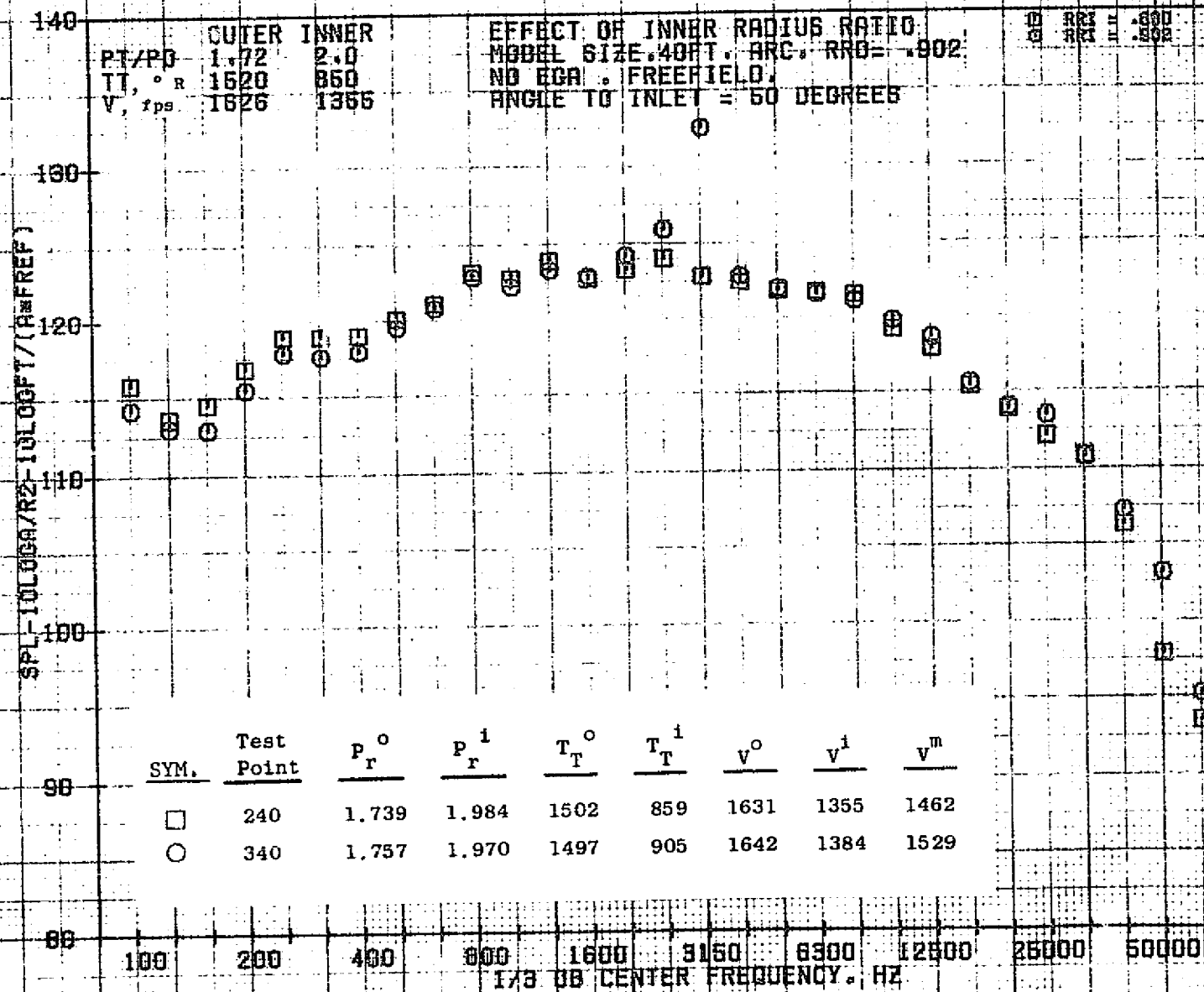
10/29/76
18161-001

79 BURCH A.



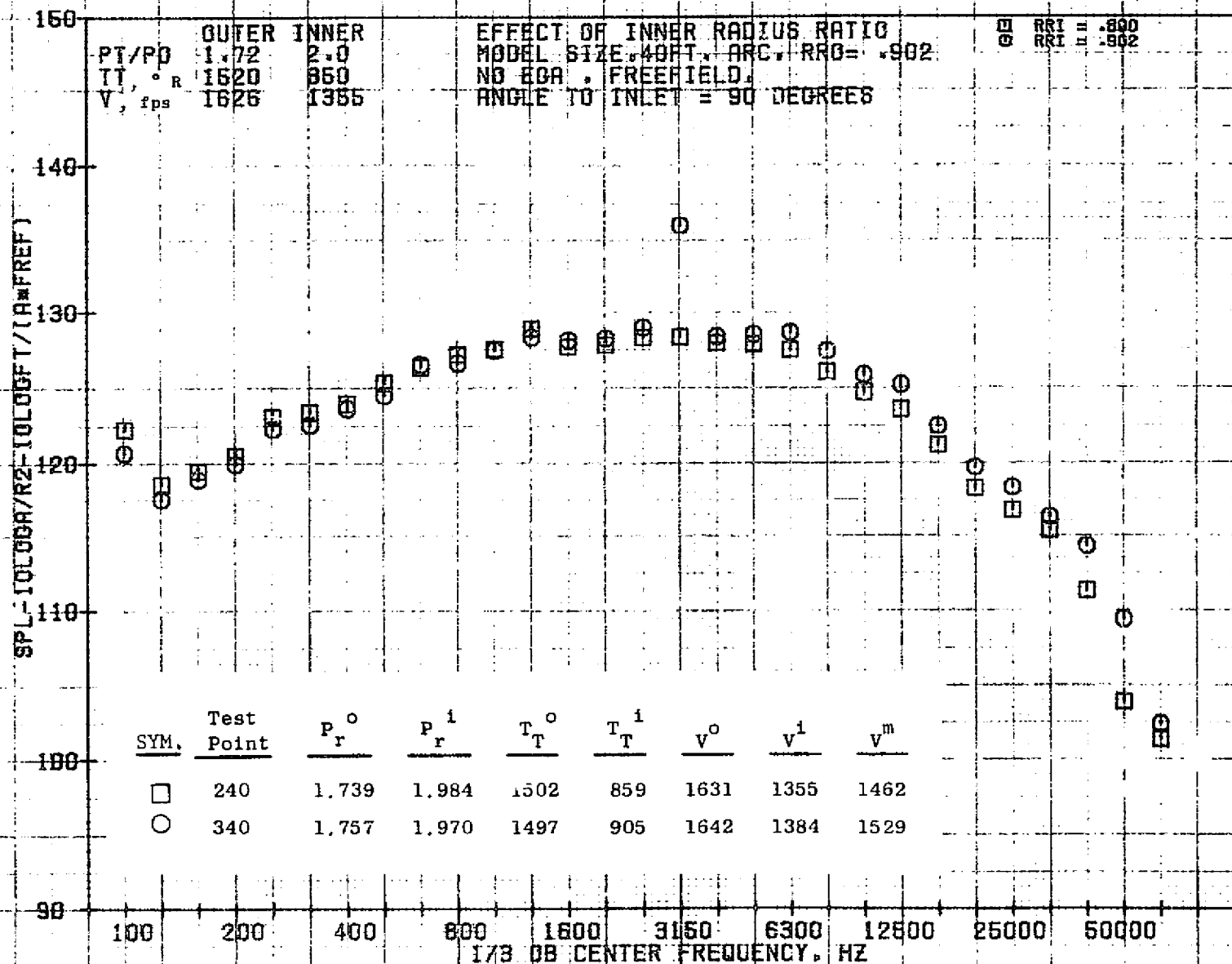
10/29/76
 18161-001

79 BURCH A.



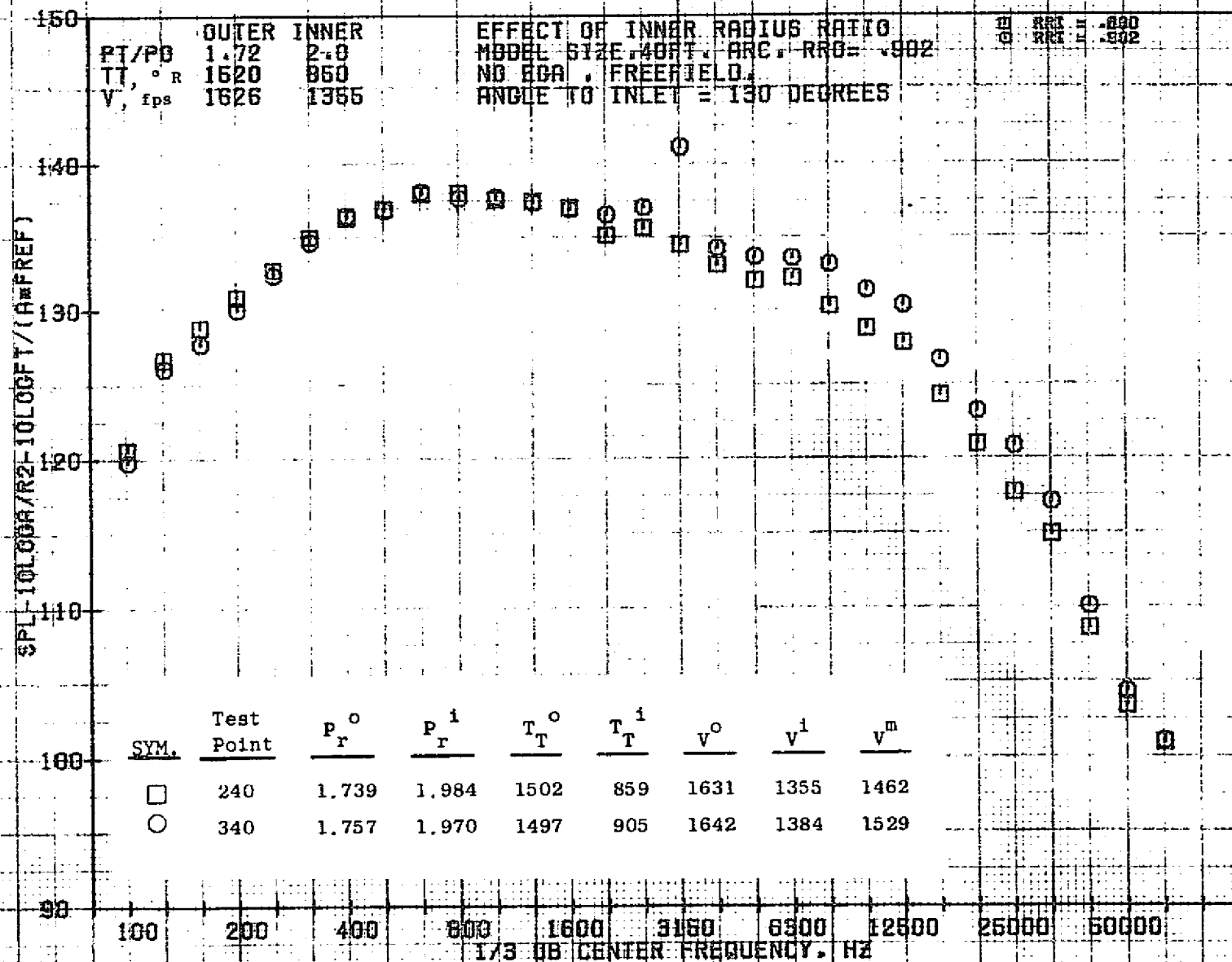
10/29/76
 18161-001

79 BURCH A.



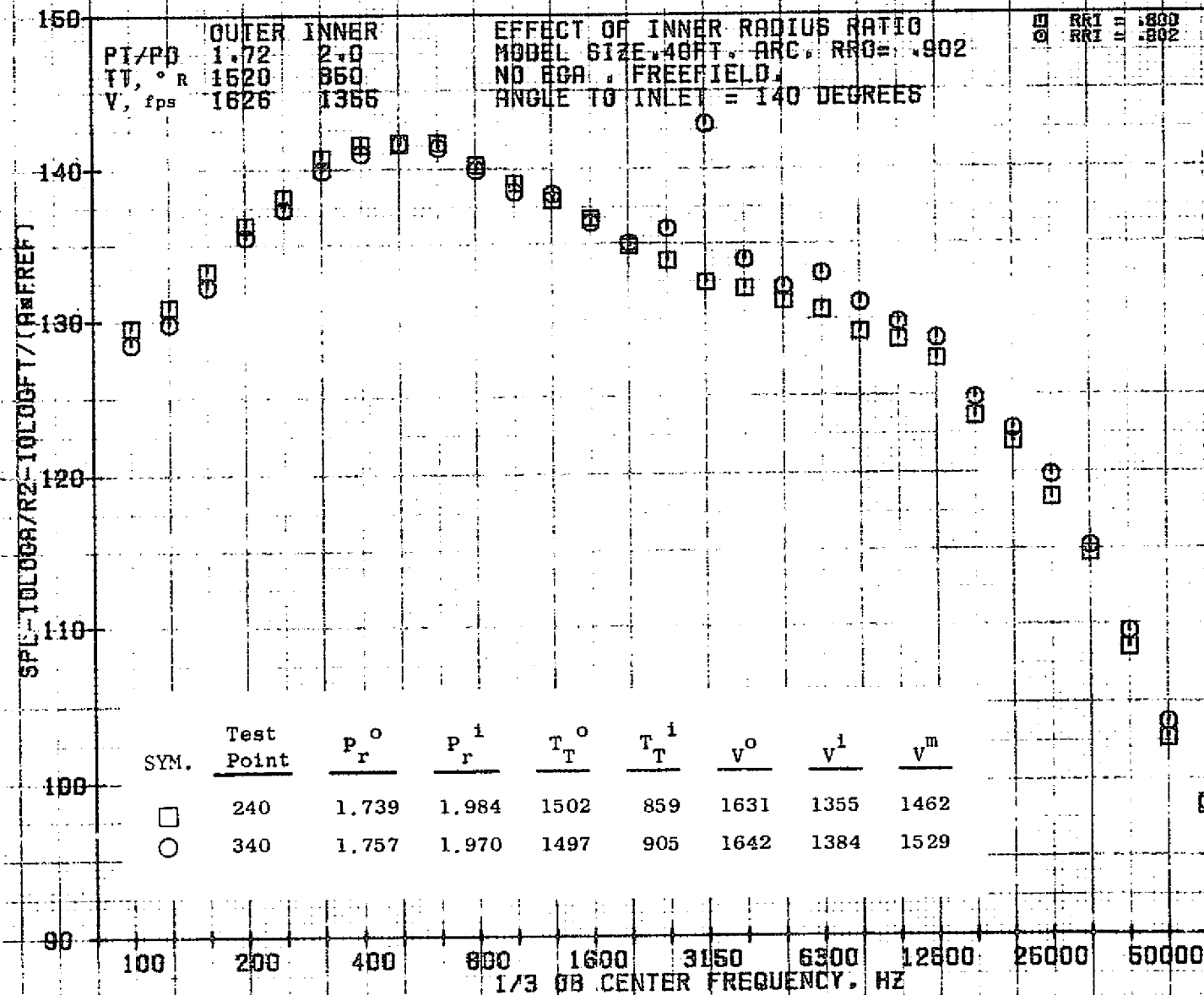
10/29/76
18161-001

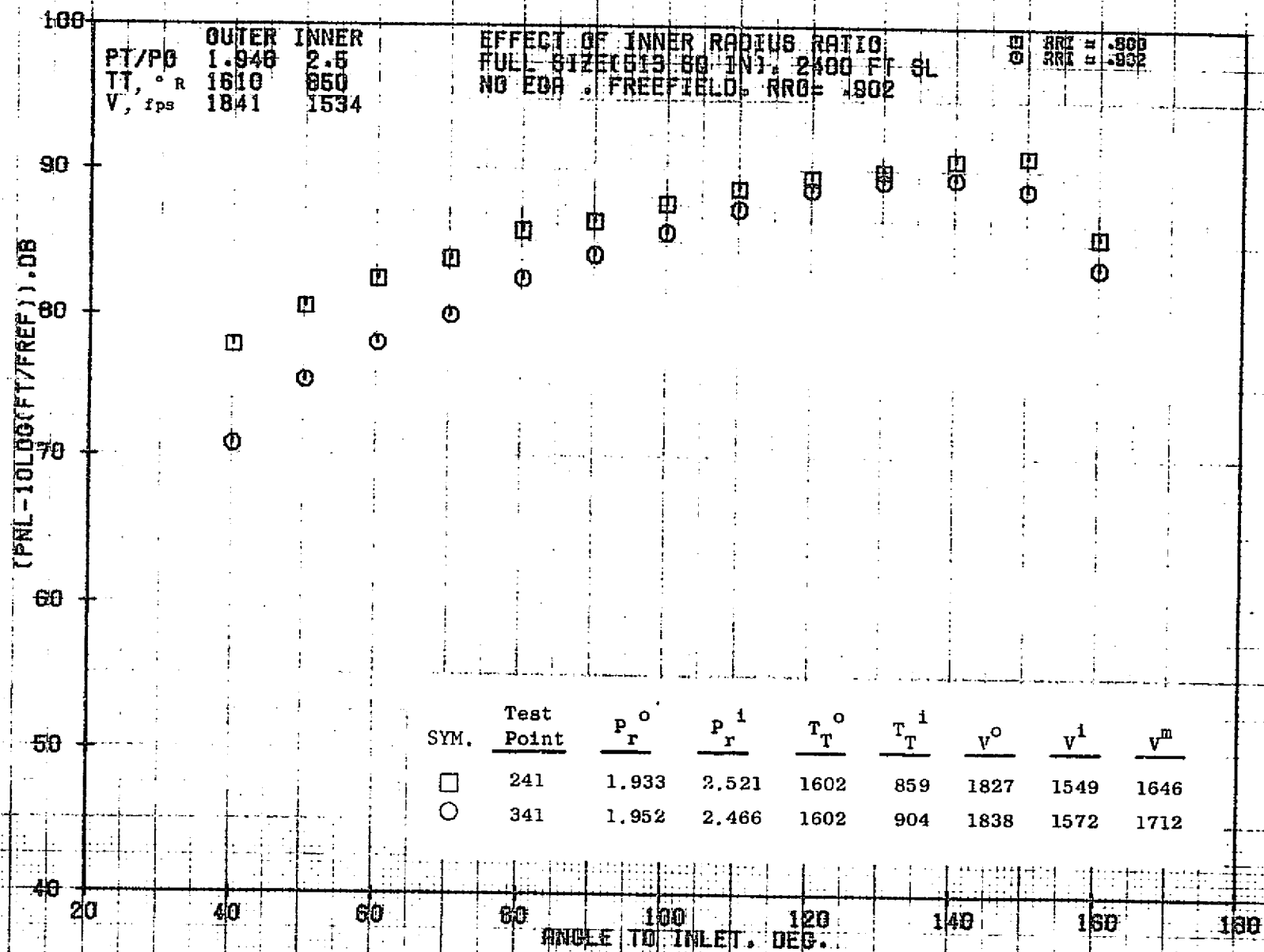
79 BURCH A.



10/29/76
18161-001

79 BURCH A.

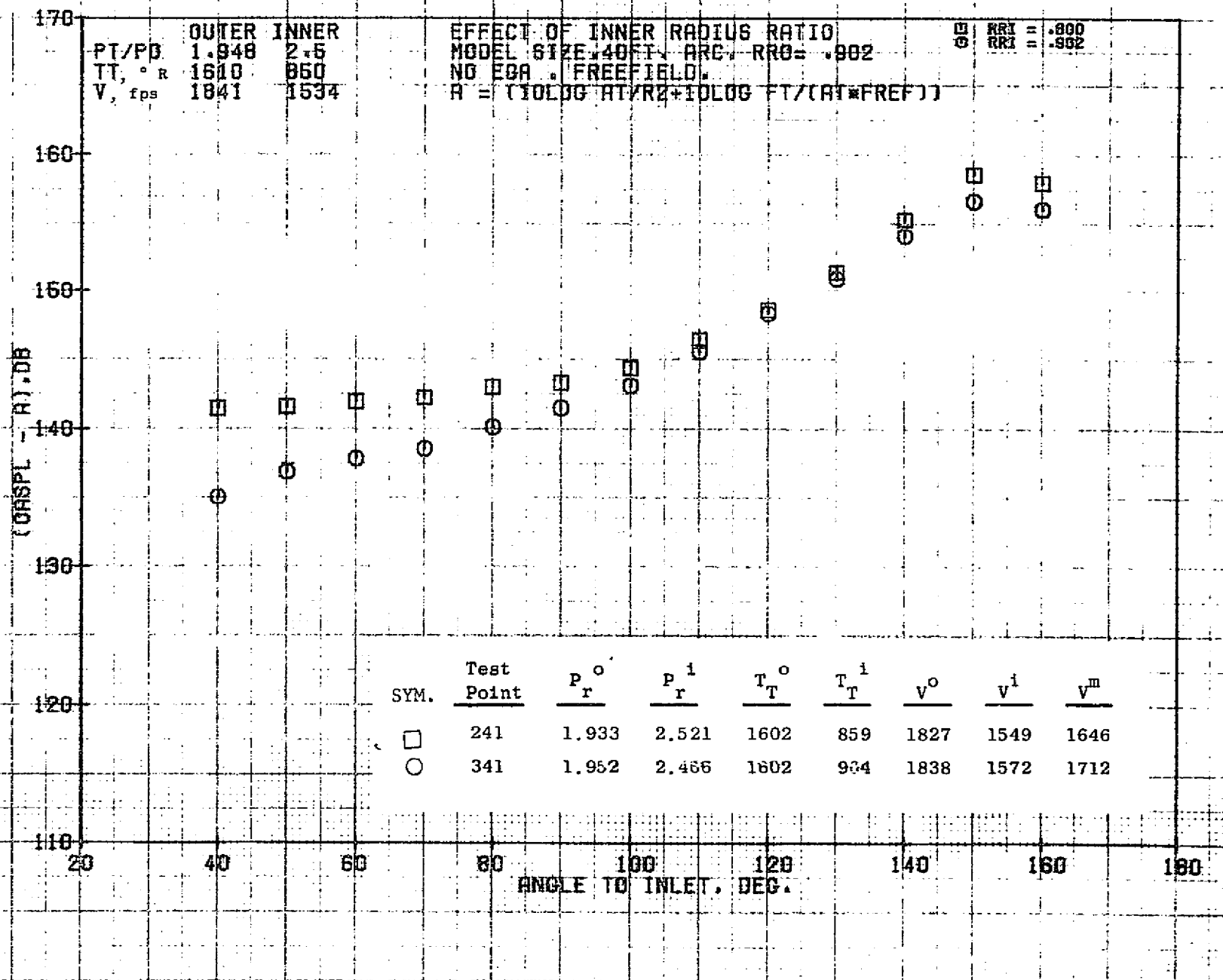




10/29/76
18124-001

79 BURCH A.

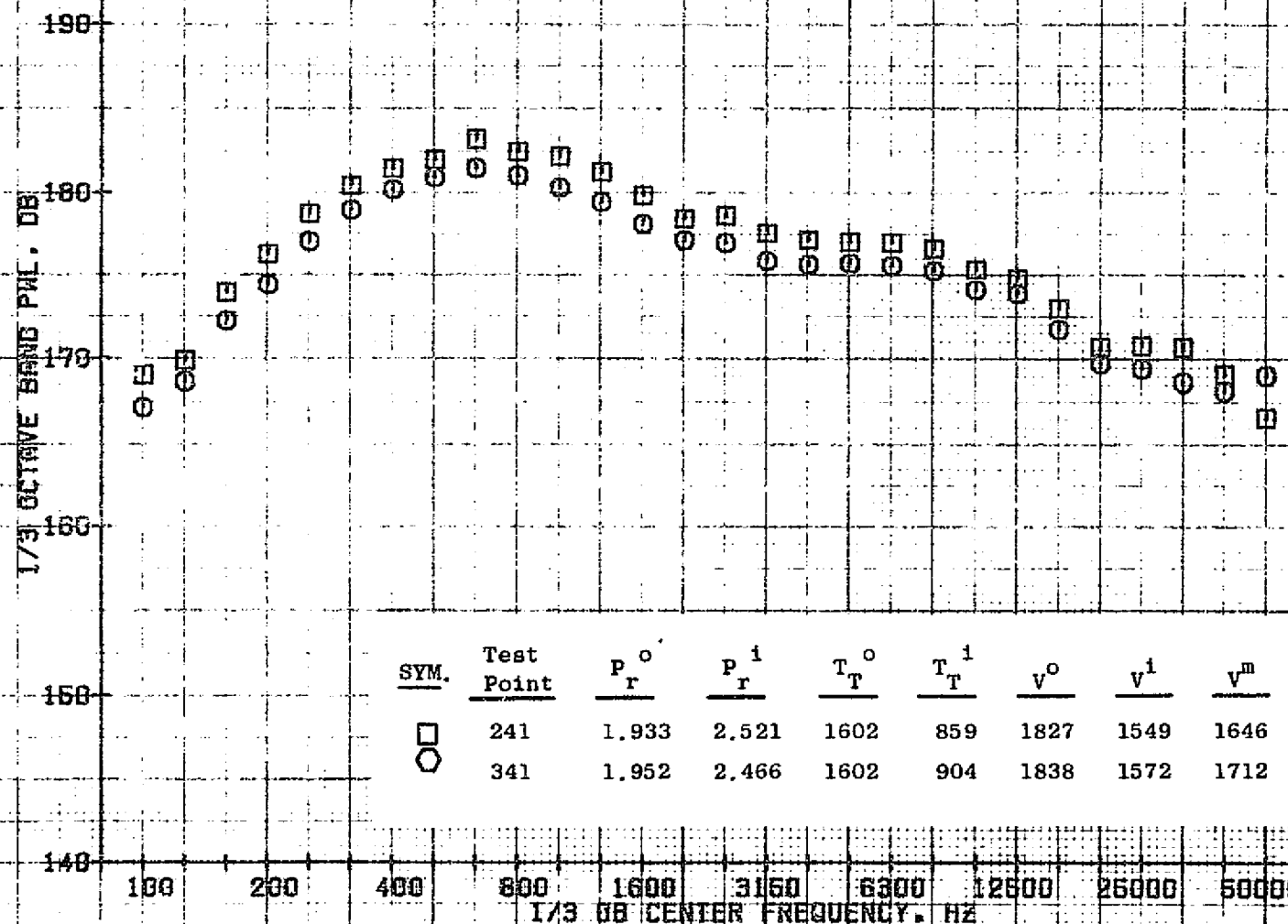
27



10/29/76
1B161-001

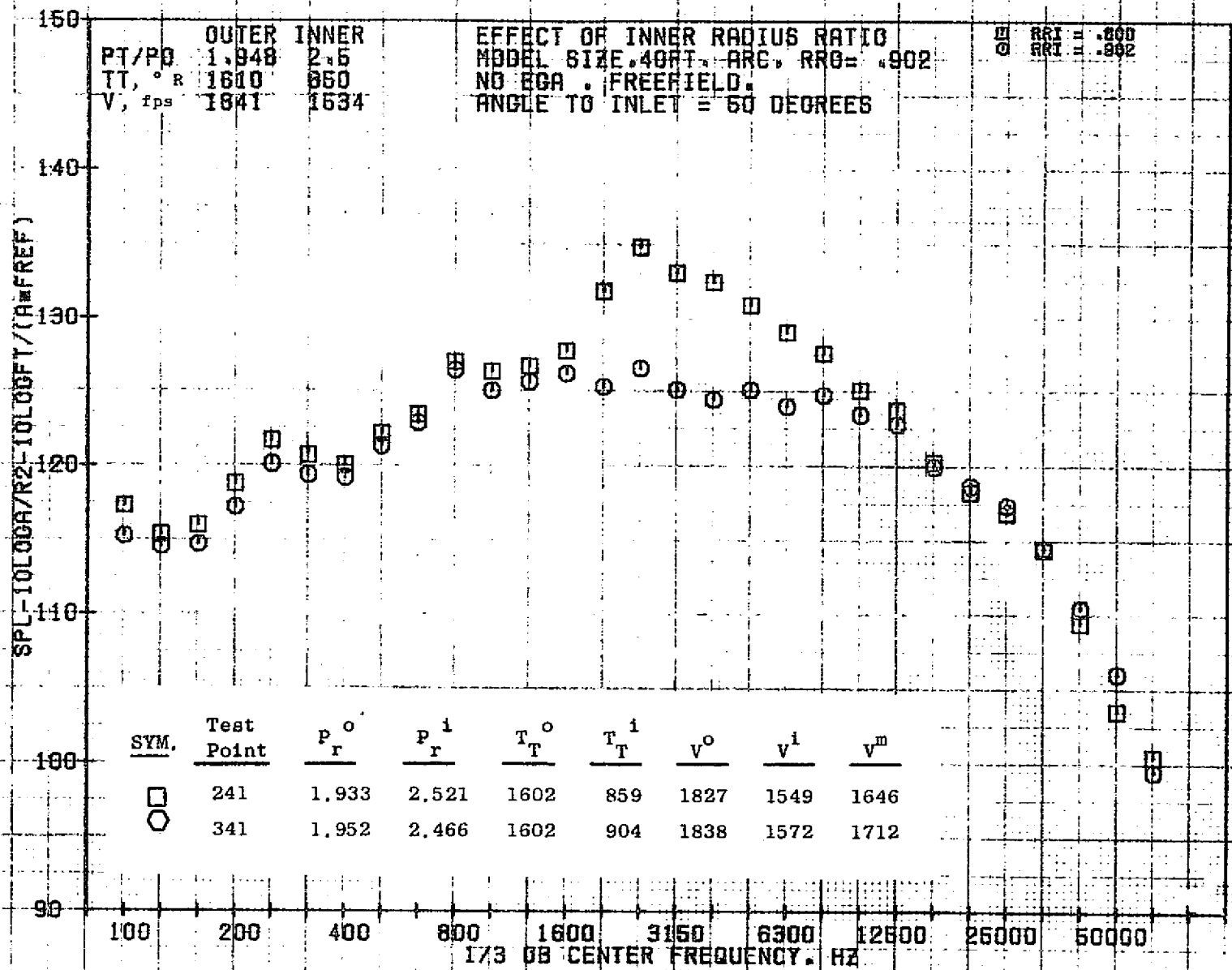
79 BURCH A.

200
 PT/PO
 TT, ° R
 V, fps
 OUTER
 1.948
 1610
 1841
 INNER
 2.5
 850
 1534
 EFFECT OF INNER RADIUS RATIO
 MODEL SIZE 40FT. ARC. RRB= .902
 NO BGR. FREEFIELD?
 PAL, DB
 RET H 800
 RET L 502



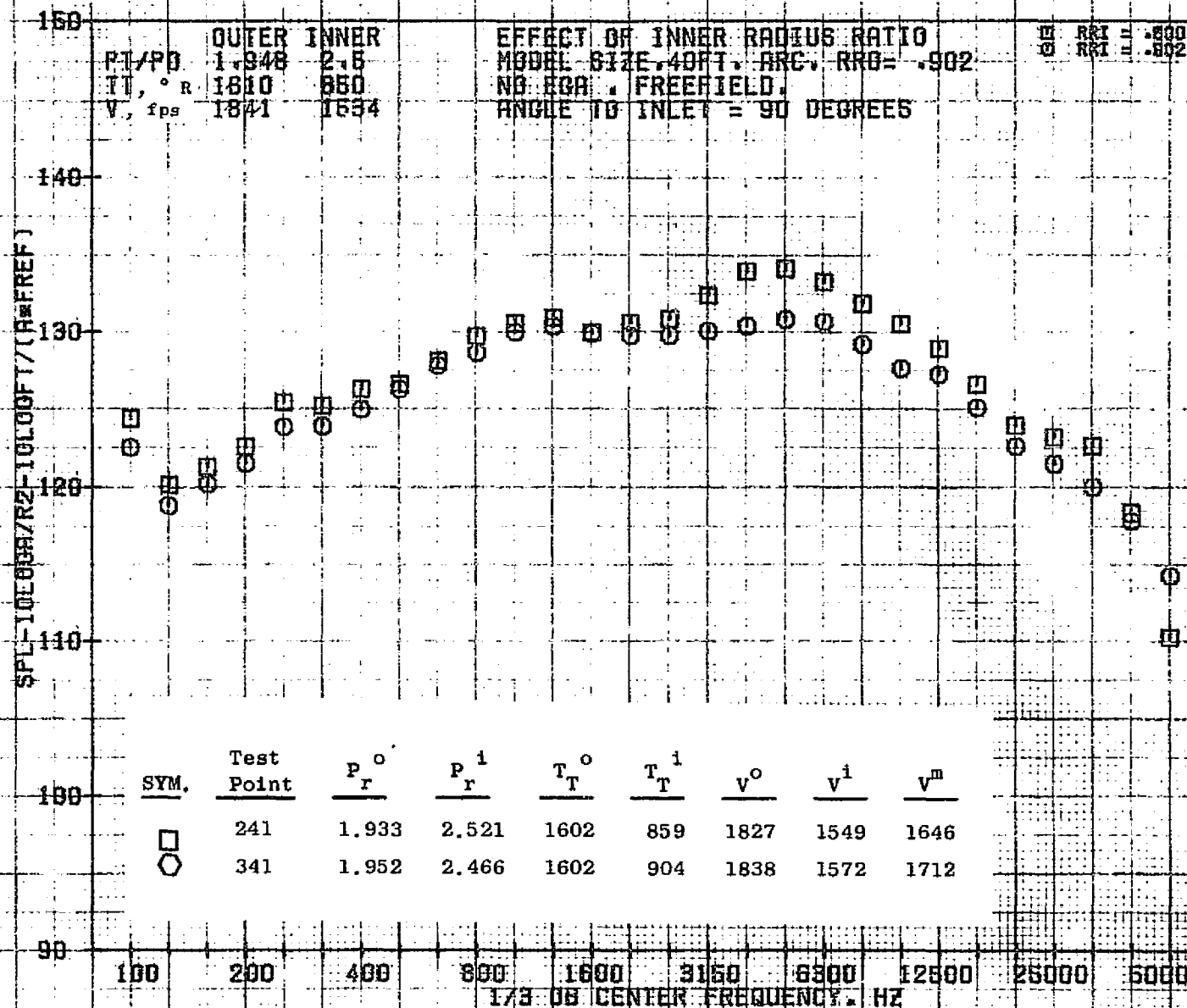
10/29/76
 18161-001

79 BURCH A.



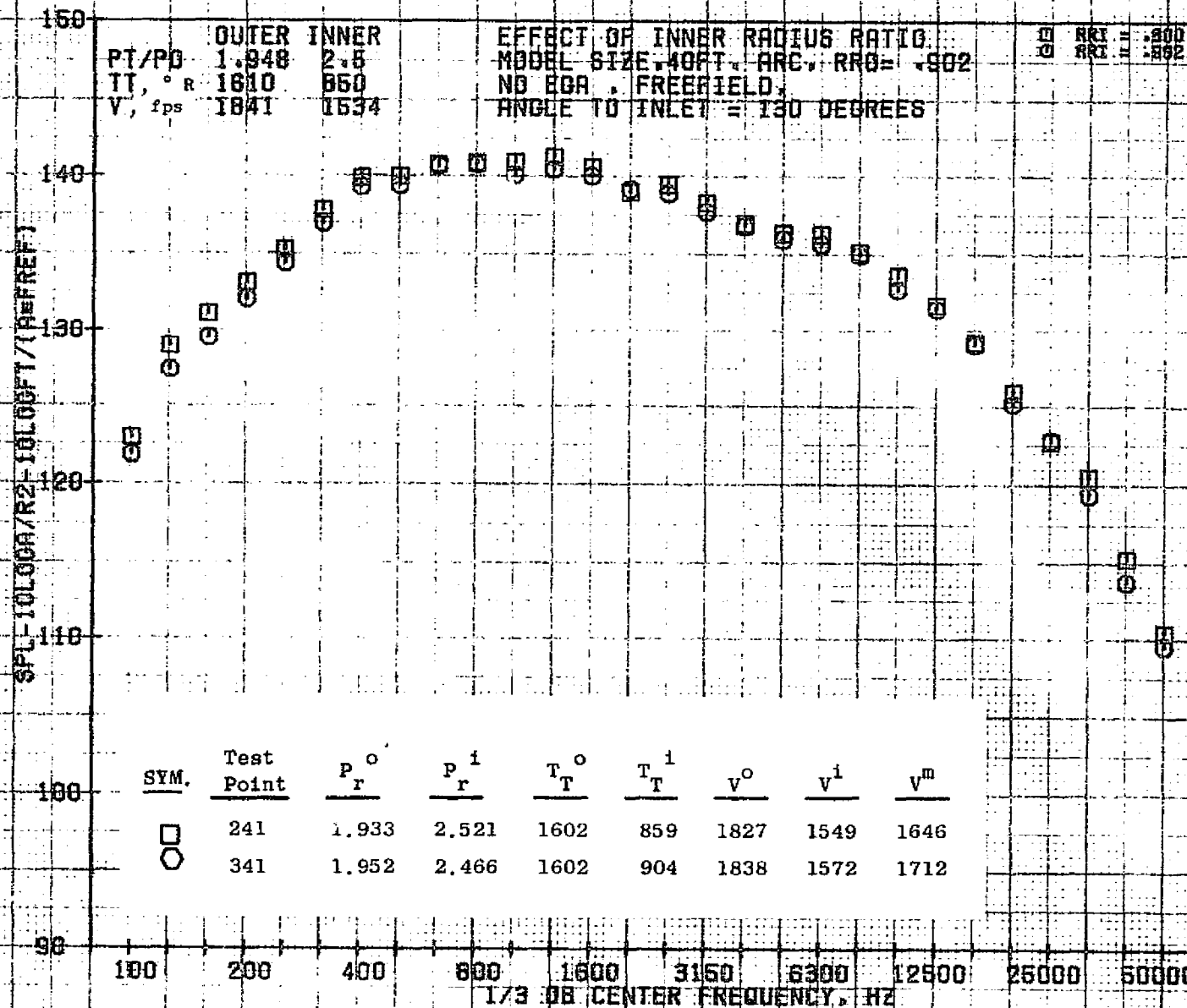
10/29/76
 18161-001

79 BURCH A.



10/29/76
18161-001

79 BURCH A.



10/29/76
18161-001

79 BURCH A.

160
 150
 140
 130
 120
 110
 100

PI/PO
 TV, ° R
 V, fps

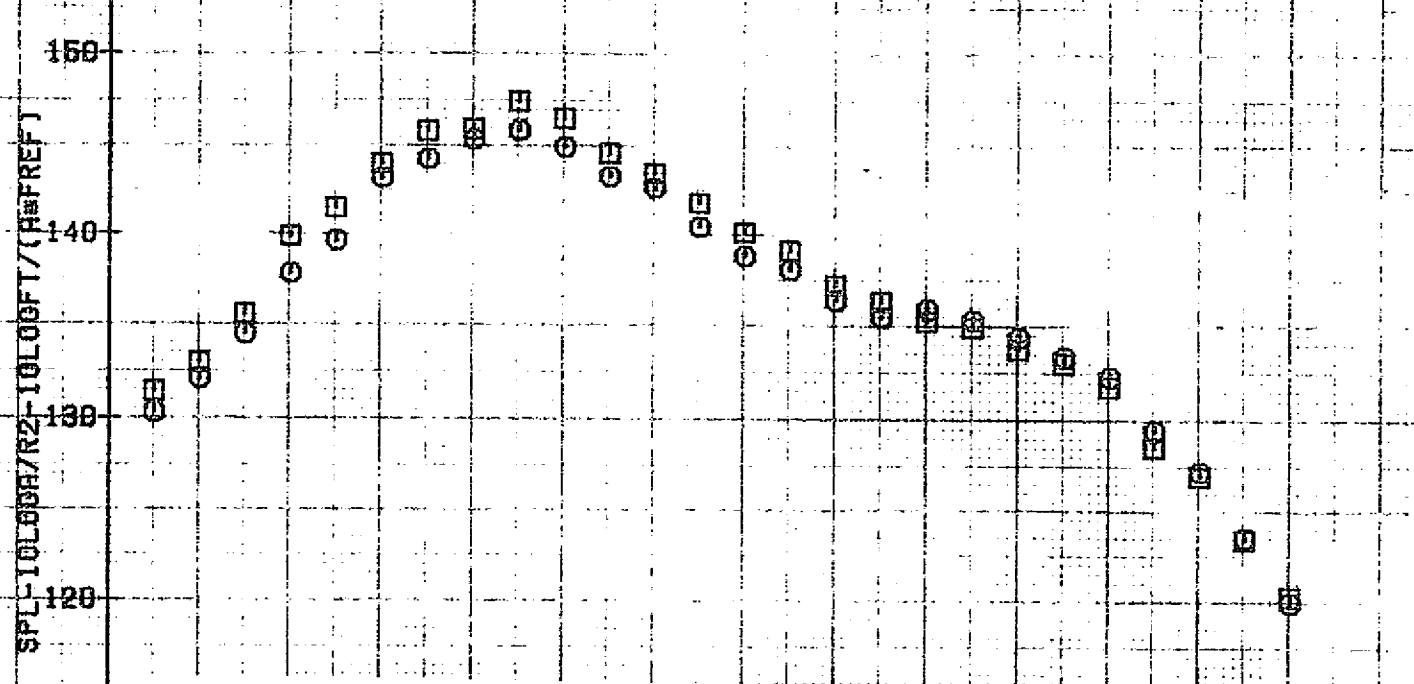
OUTER
 1.948
 1610
 1841

INNER
 2.5
 850
 1534

EFFECT OF INNER RADIUS RATIO
 MODEL SIZE, 40 FT. ARC, RRO = .902
 NO ECA, FREEFIELD
 ANGLE TO INLET = 140 DEGREES

RRT = .800
 RRT = .902

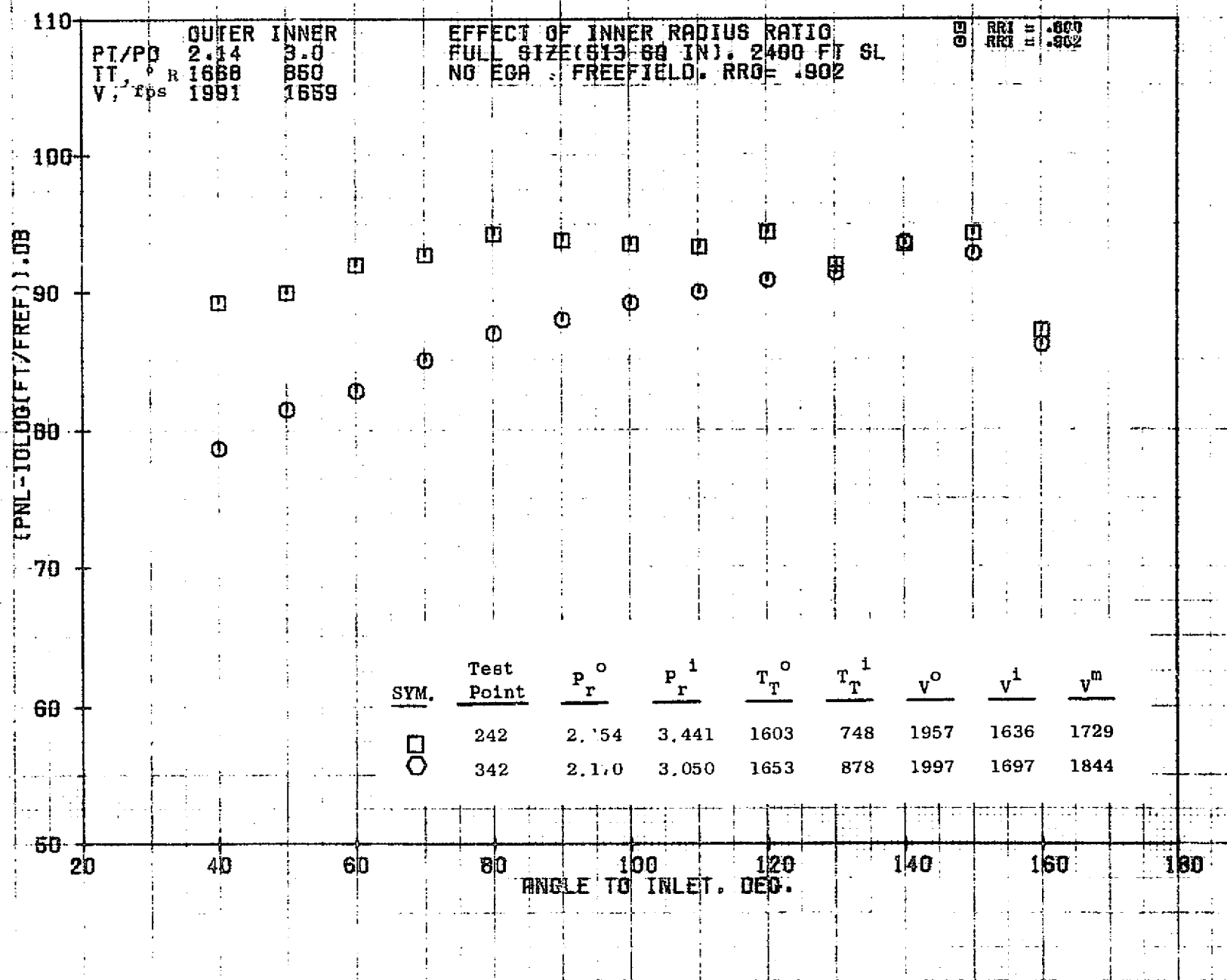
SPL - 10 LOG (PA/R2 - 10 LOG (PT/(Rm FREF))



SYM.	Test Point	P _r ^o	P _r ⁱ	T _T ^o	T _T ⁱ	V ^o	V ⁱ	V ^m
□	241	1.933	2.521	1602	859	1827	1549	1646
○	341	1.952	2.466	1602	904	1838	1572	1712

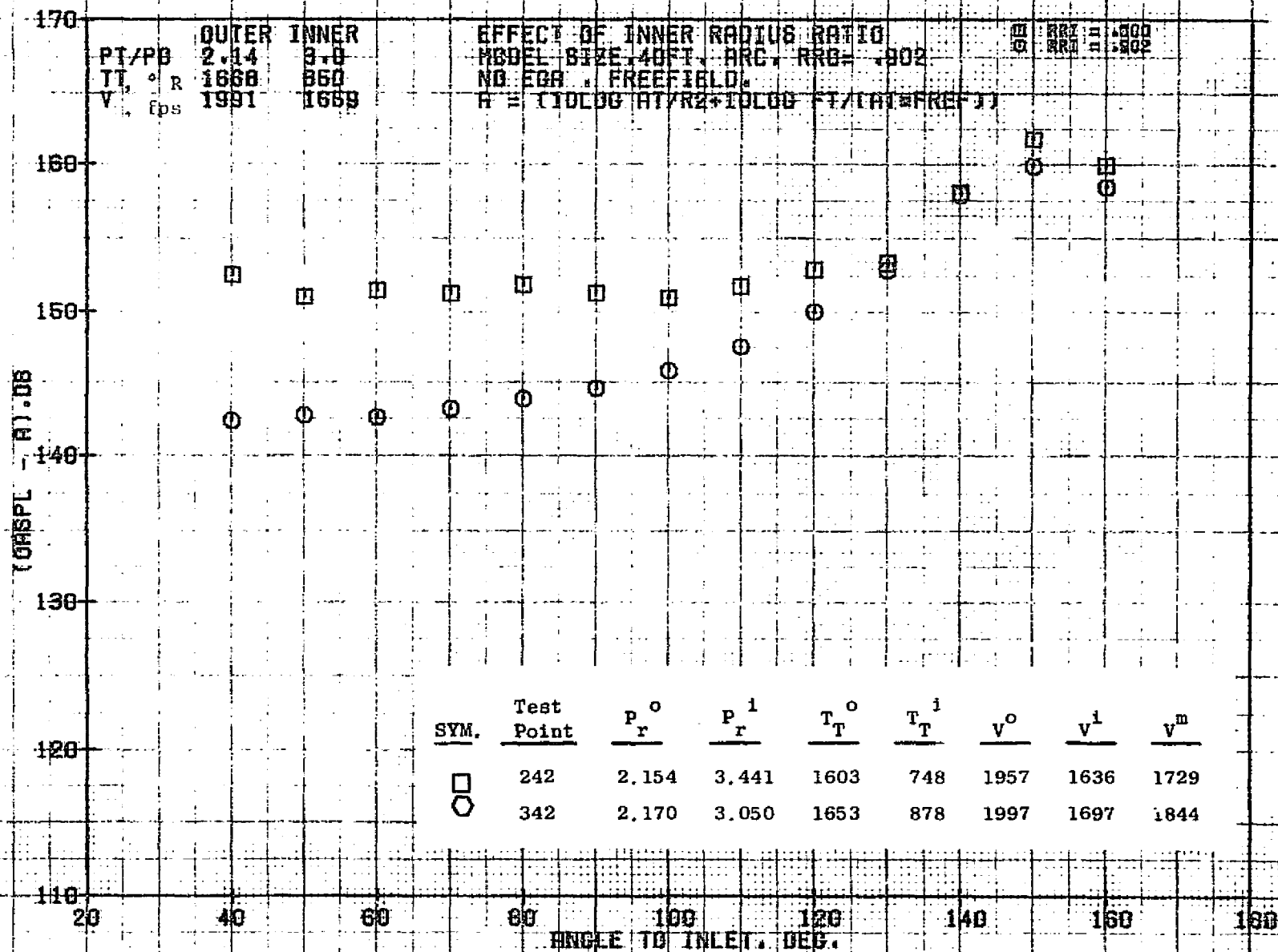
100 200 400 800 1600 3150 6300 12500 25000 50000

1/3 OBT CENTER FREQUENCY, HZ



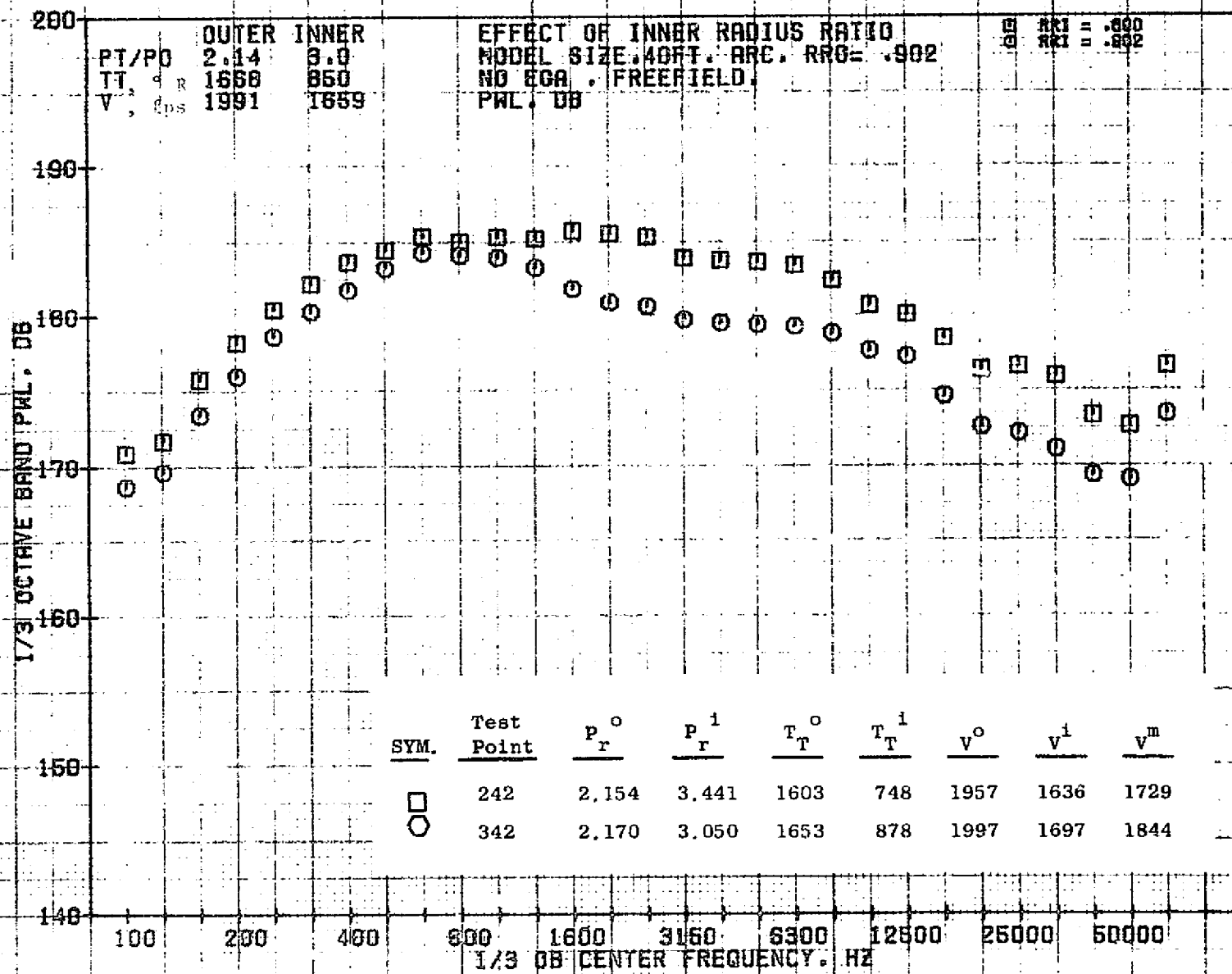
10/29/76
18124-001

79 BURCH A.



10/29/76
18161-001

79 BURCH A.

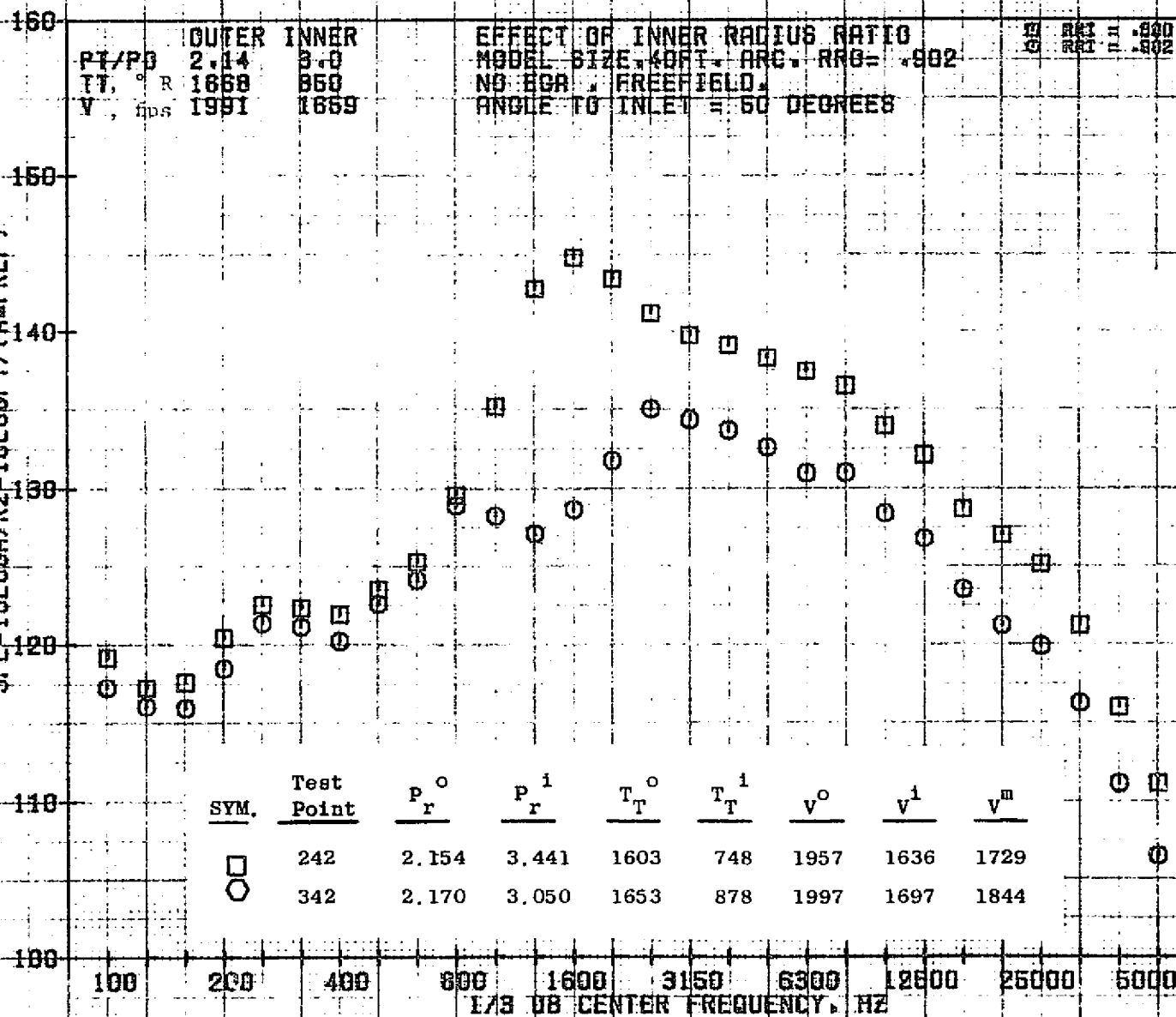


10/29/76
18161-001

79 BURCH R.

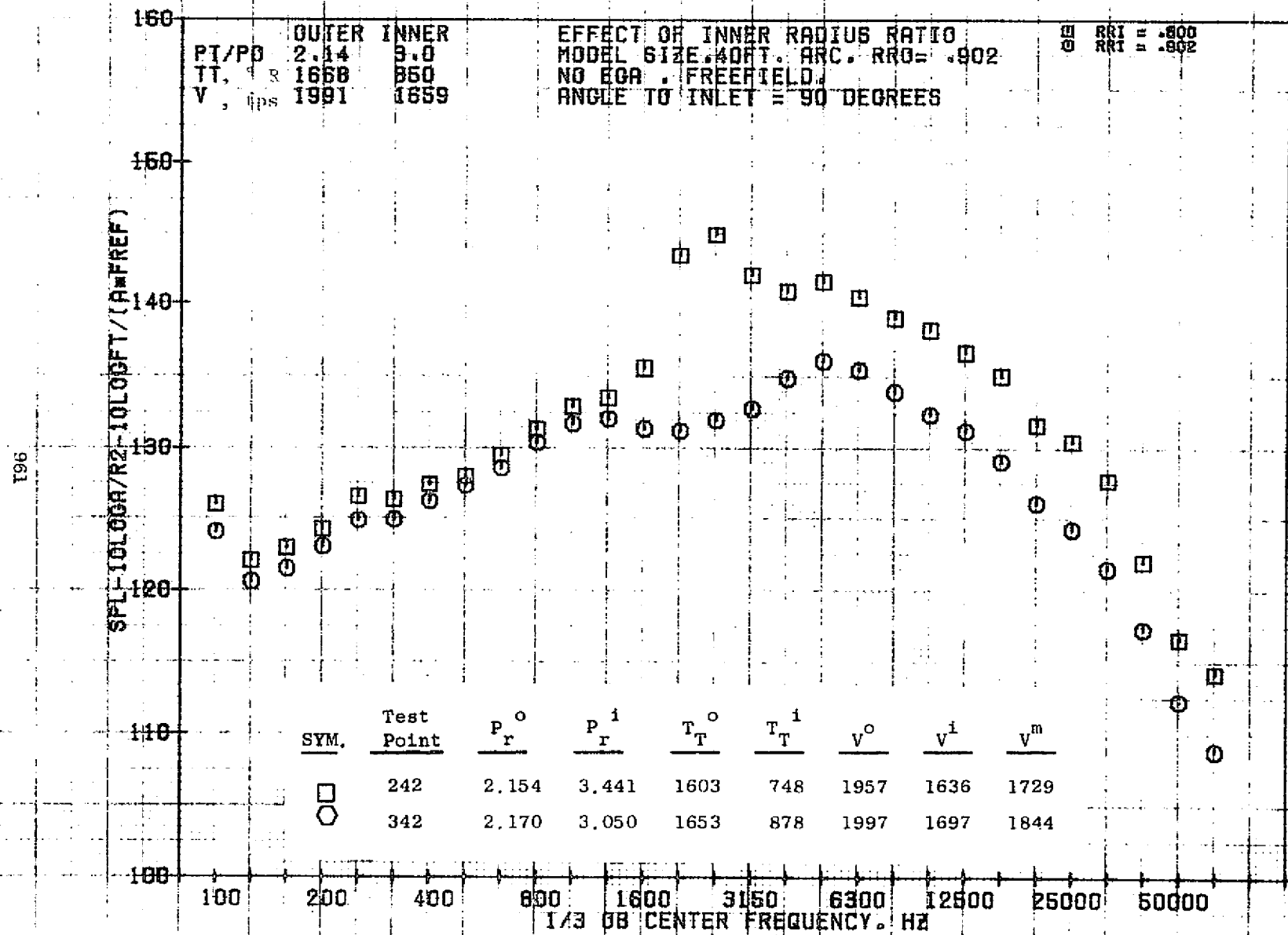
096

SPL-10LOG(R/R2-10LOGFT/(R2-FREF))



10/29/76
1B161-001

79 BURCH A.



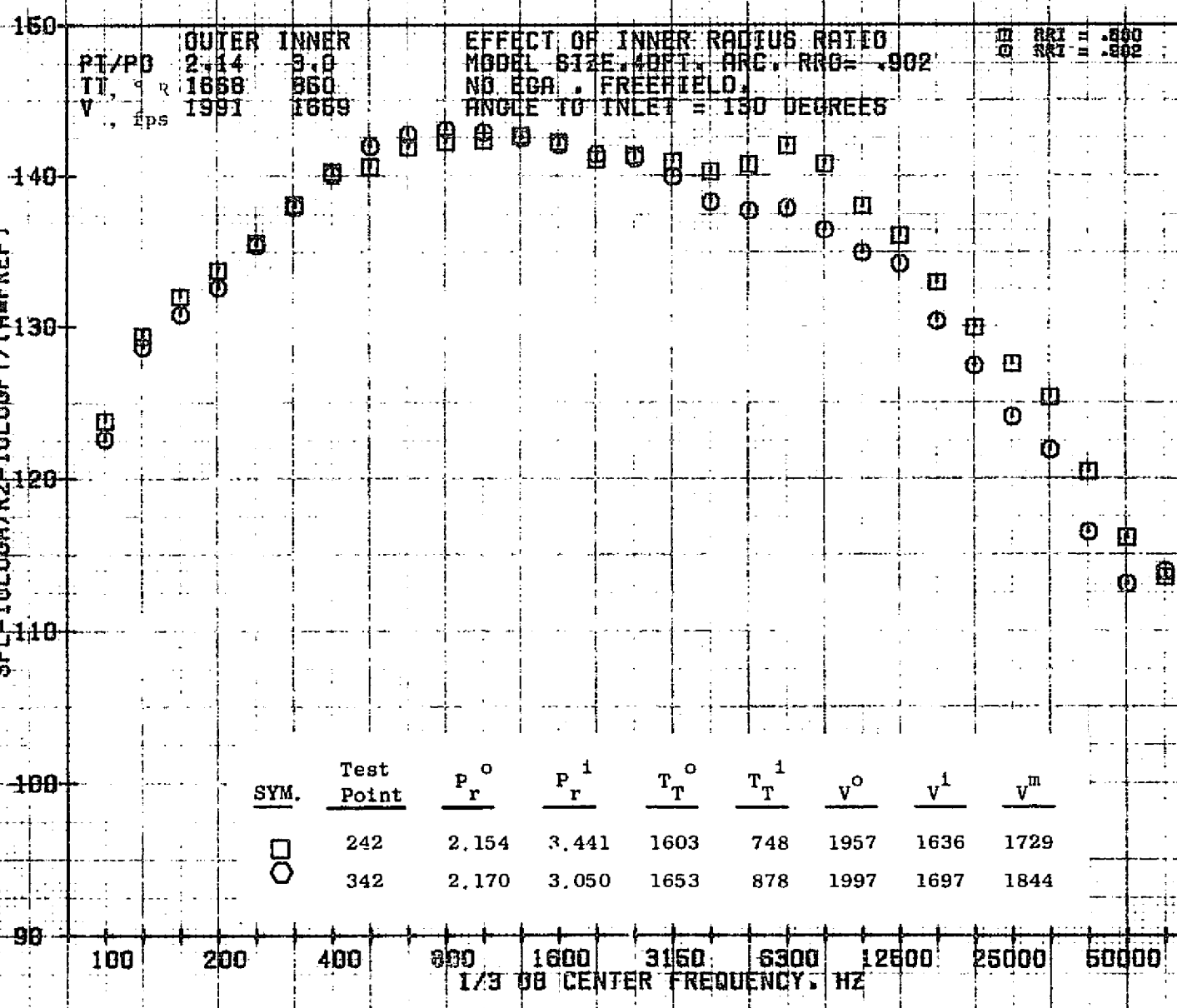
962

SPL 10LOG(R/R2-10LOGFT/(AMFREF))

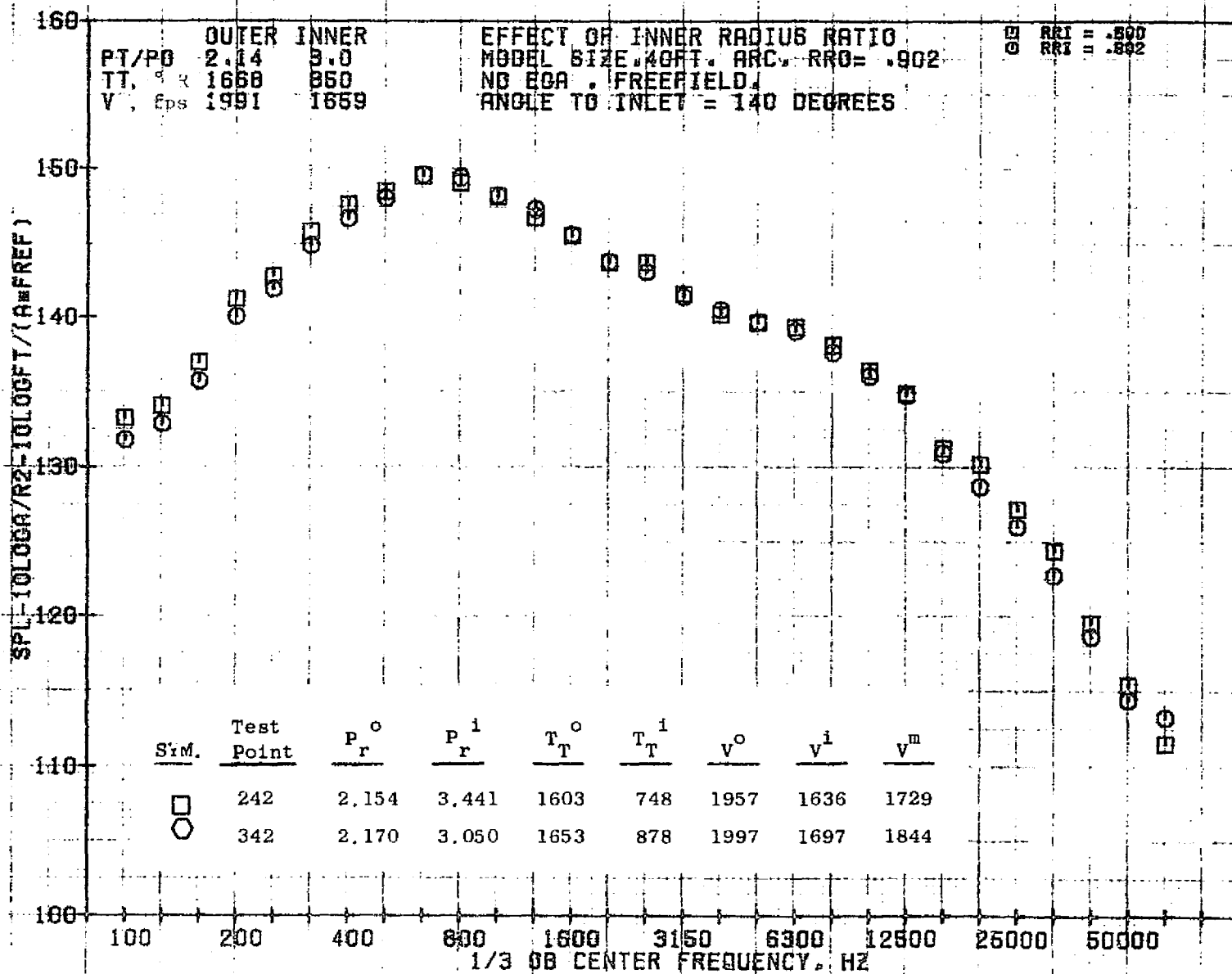
PT/PO 2.14 3.0
 TT, ° R 1658 960
 V, fps 1991 1689

EFFECT OF INNER RADIUS RATIO
 MODEL SIZE, 40FT. ARC. RRG = .902
 NO ECA, FREEFIELD,
 ANGLE TO INLET = 130 DEGREES

□ RRT = .850
 ○ RRT = .902

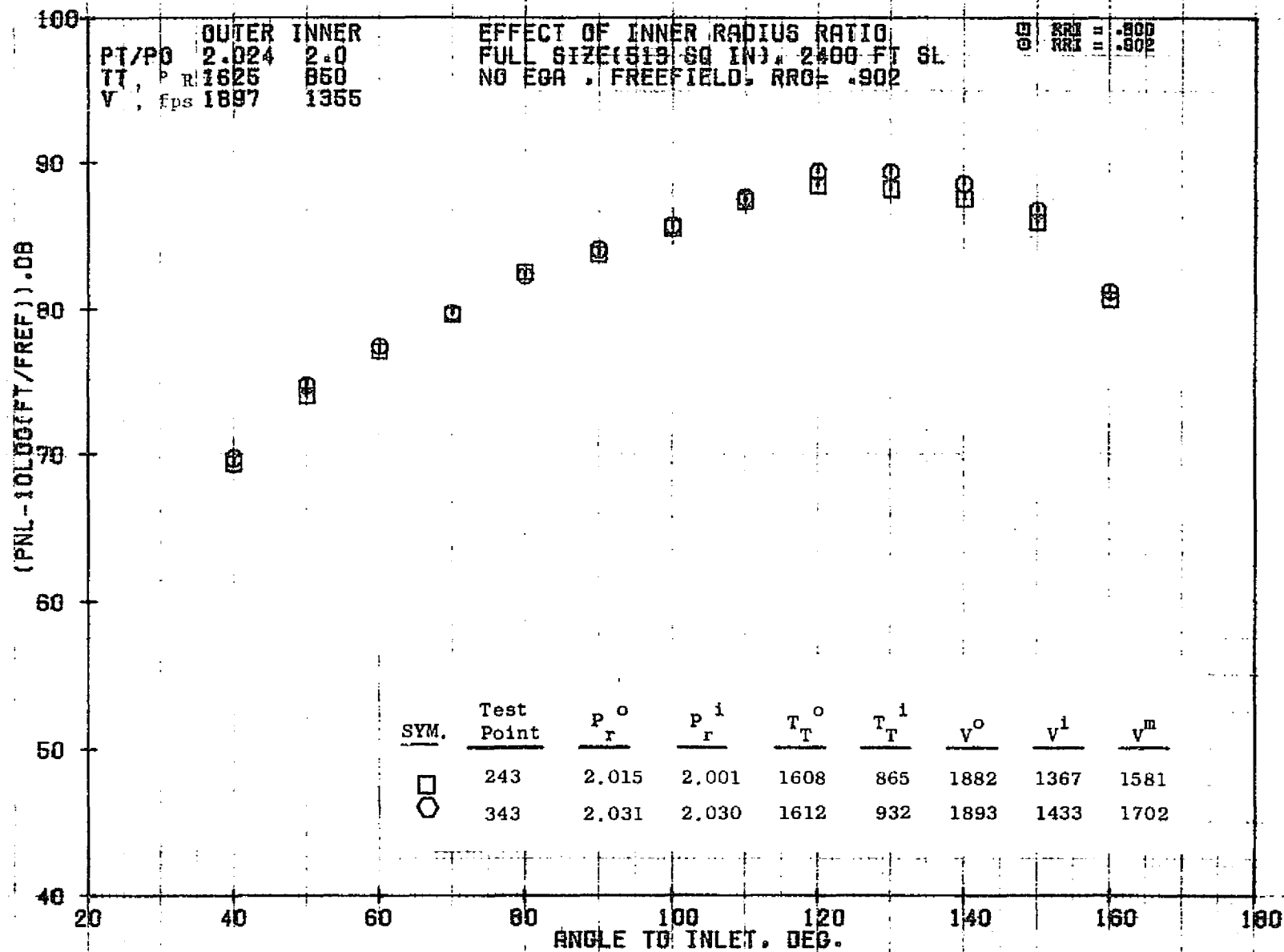


SYM.	Test Point	P_r^o	P_r^1	T_T^o	T_T^1	V^o	V^1	V^m
□	242	2,154	3,441	1603	748	1957	1636	1729
○	342	2,170	3,050	1653	878	1997	1697	1844



10/29/76
18161-001

79 BURCH A.



PT/PO 2.024 2.0
 TT. ° R 1625 850
 V, fps 1897 1366

EFFECT OF INNER RADIUS RATIO
 MODEL SIZE 40 FT. ARC. RRG = .902
 NO EGR. FREEFIELD.
 $R = (10 \log R1/R2 + 10 \log F1/F2) / (2 \log F1/F2)$

RTT 11.800
 RRT 11.802

(OASPL - R) .05

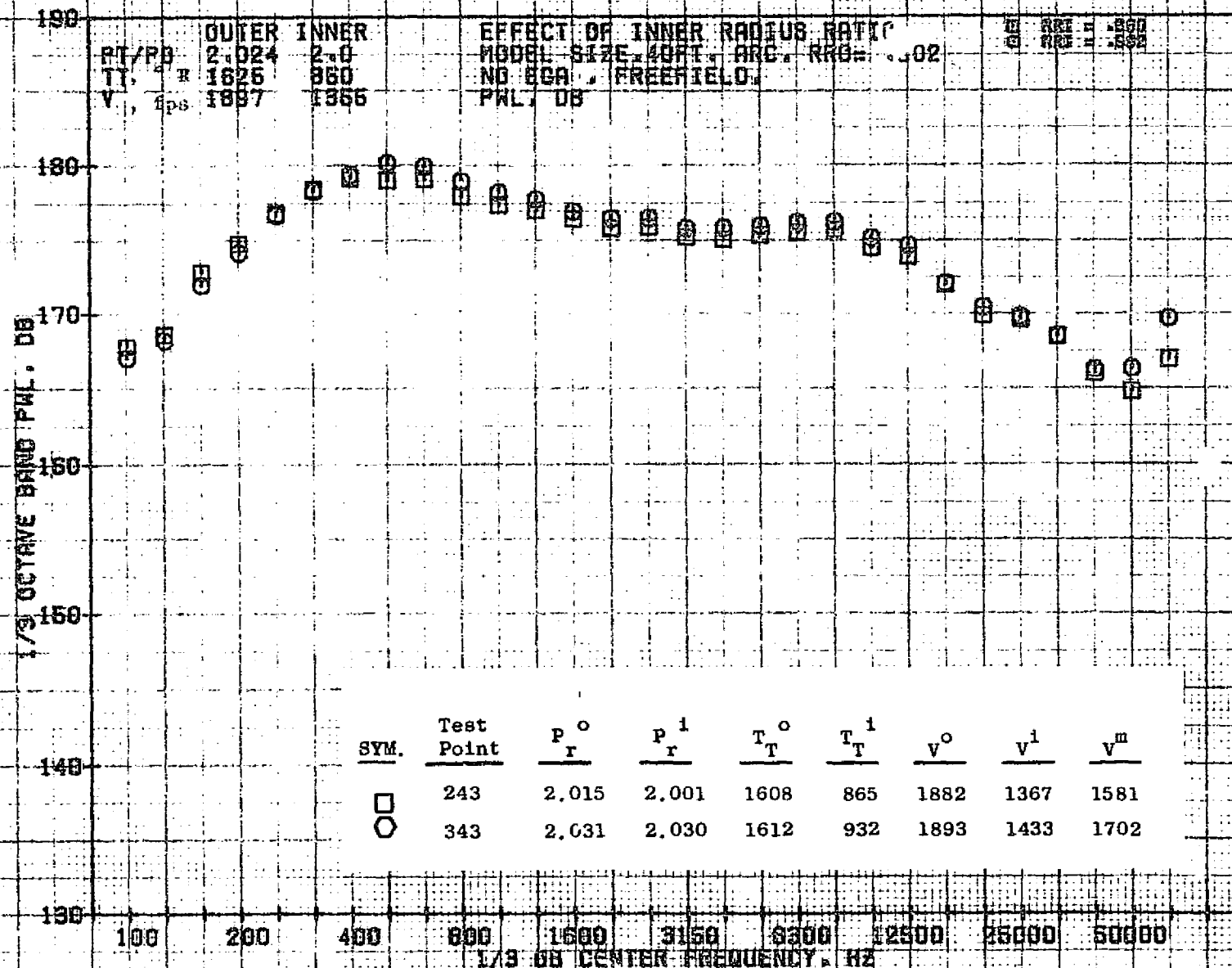
598

SYM.	Test Point	P_r^o	P_r^1	T_T^o	T_T^1	V^o	V^1	V^m
□	243	2.015	2.001	1608	865	1882	1367	1581
○	343	2.031	2.030	1612	932	1893	1433	1702

20 40 60 80 100 120 140 160 180
 ANGLE TO INLET, DEG.

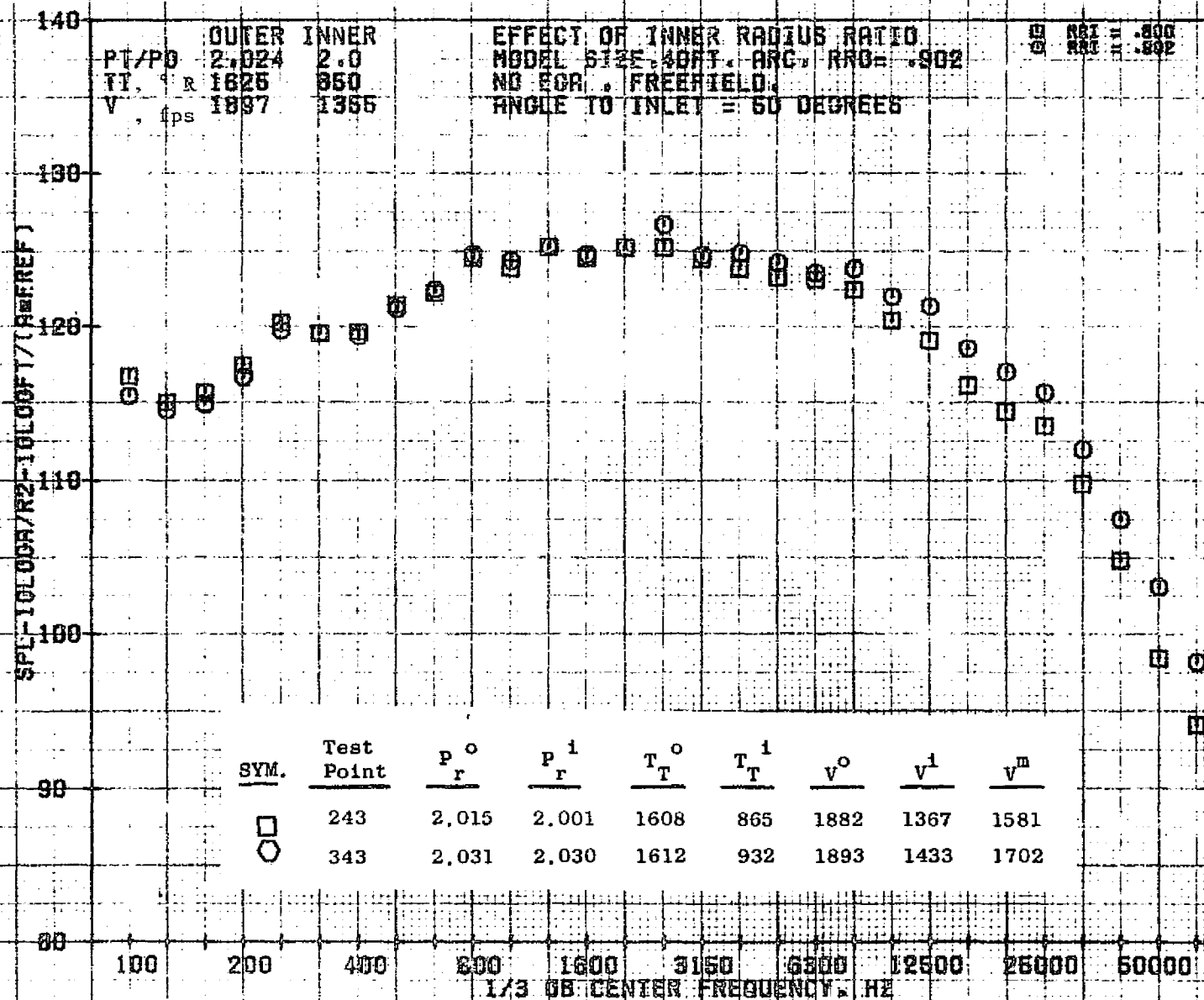
10/29/76
 18161-001

79 BURCH A.



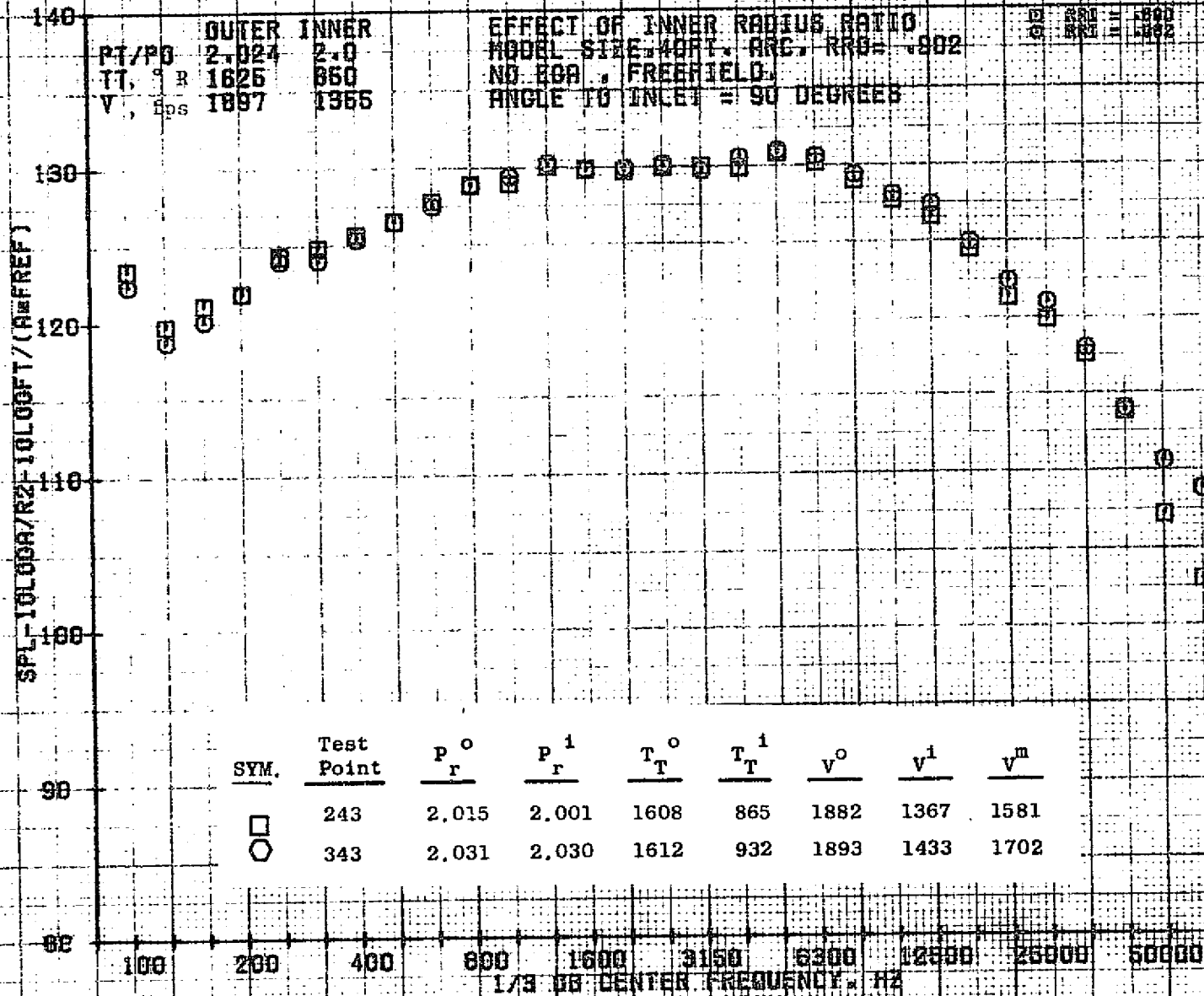
10/29/76
18161-001

79 BURCH A.



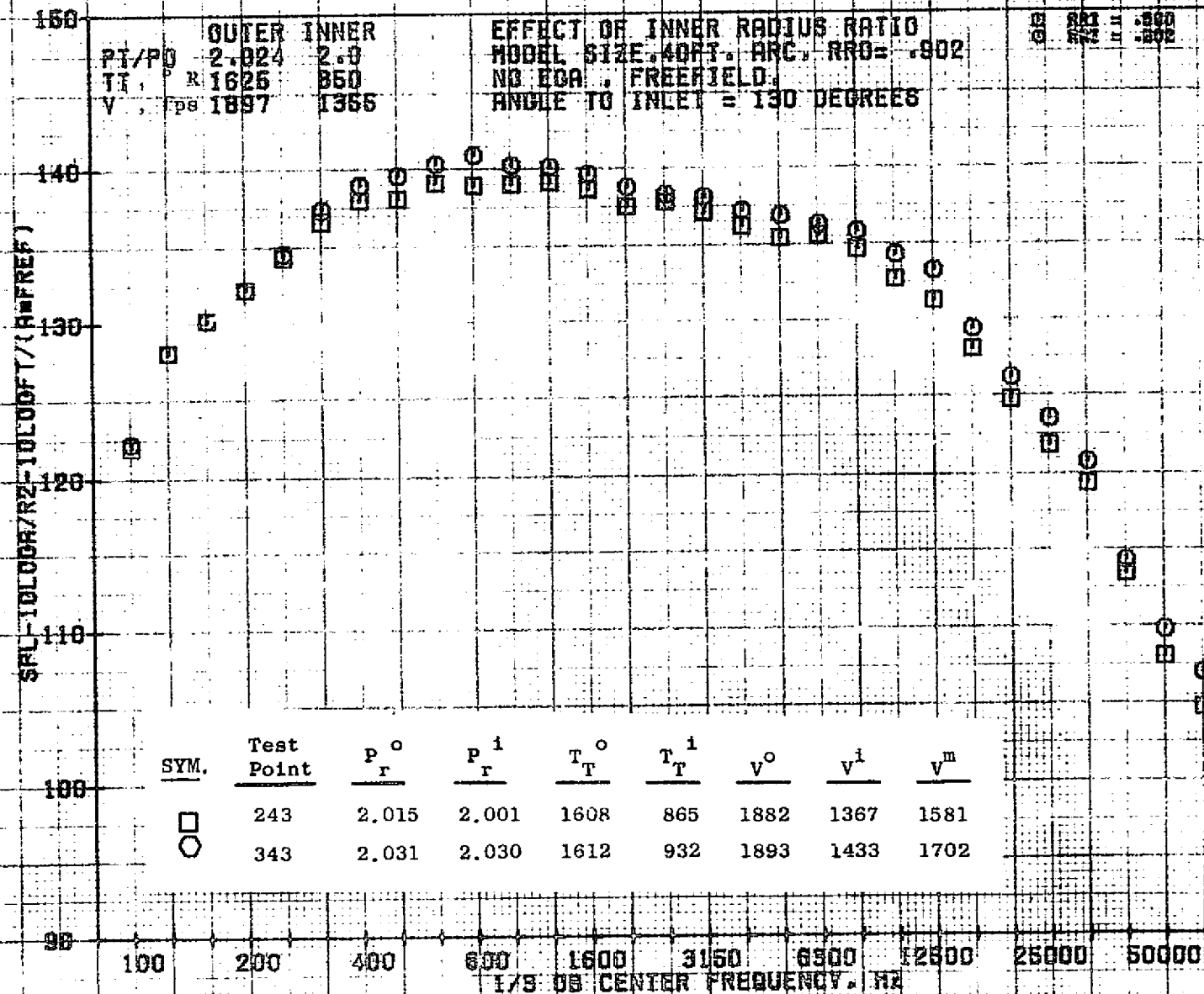
10/29/76
 18161-001

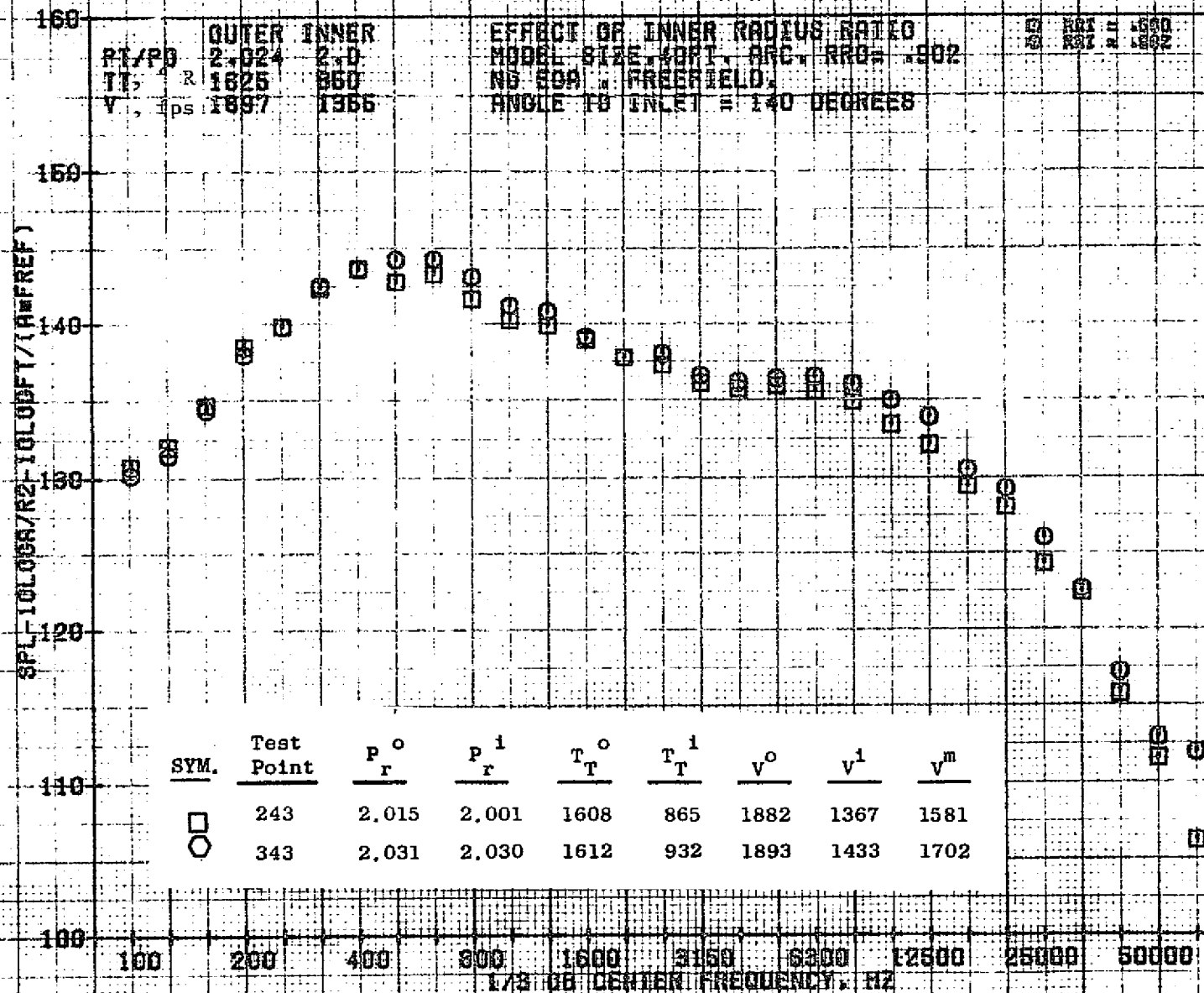
79 BURCH A.



10/29/76
 18161-001

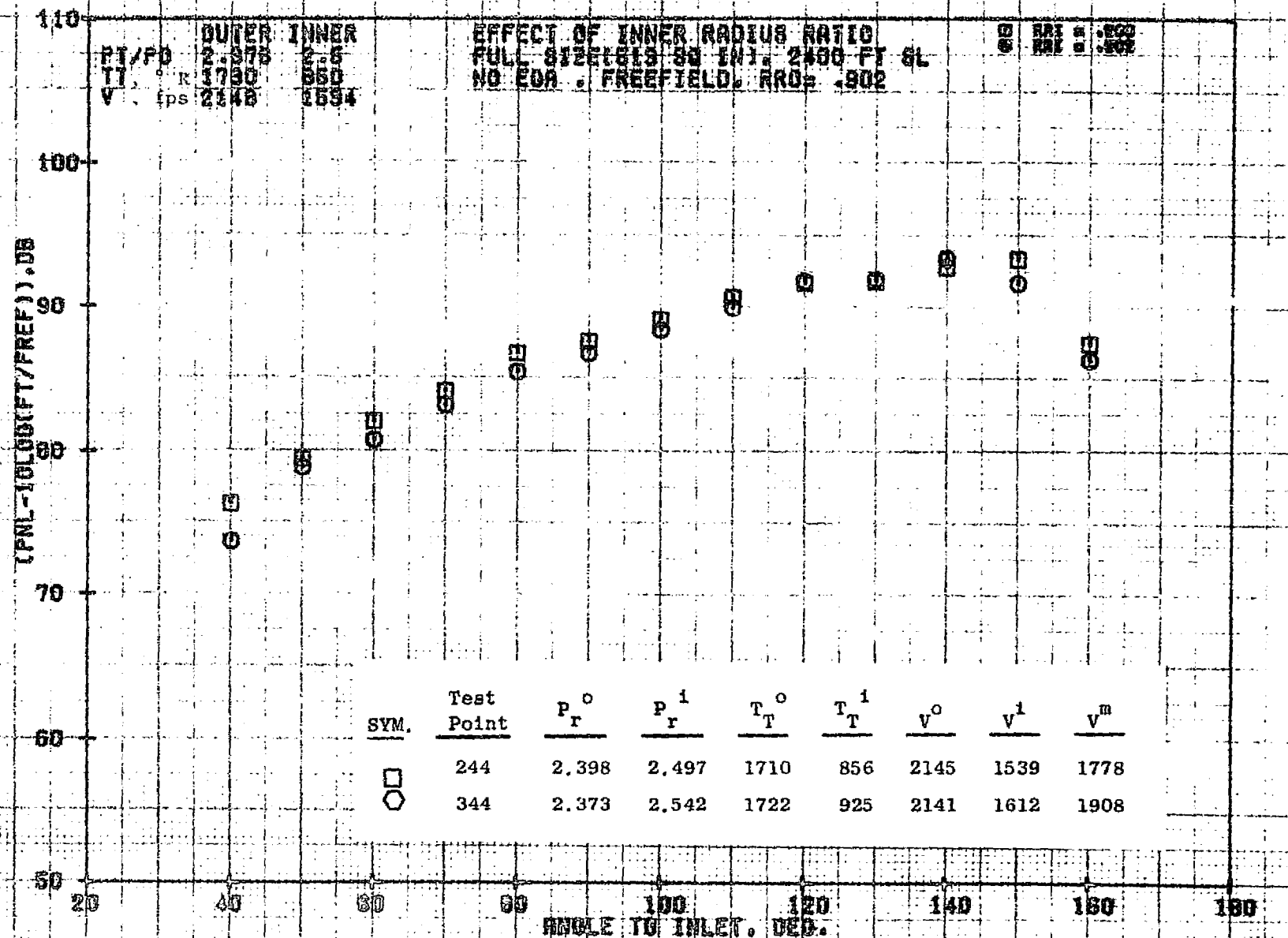
79 BURCH A.





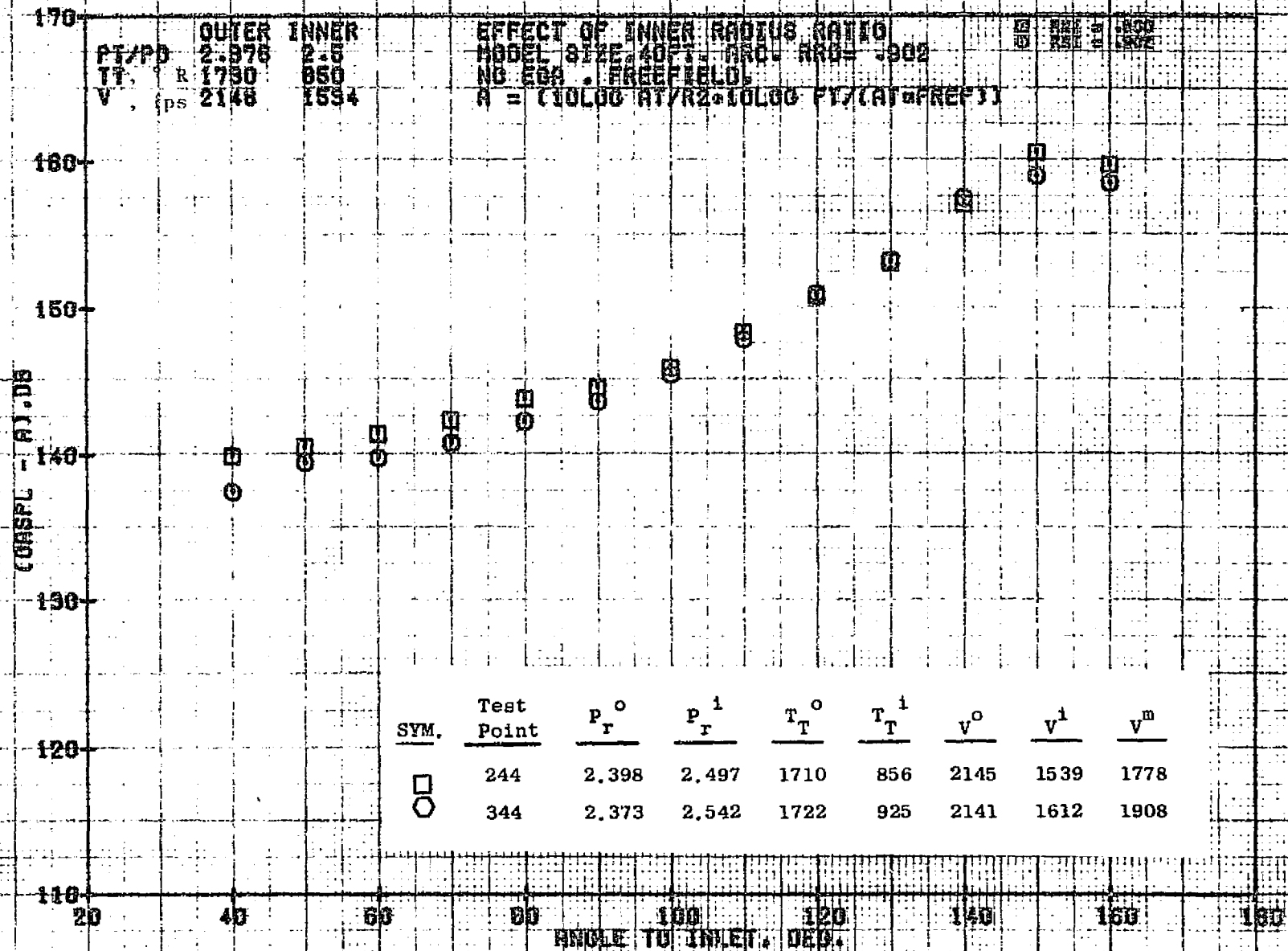
10/29/76
18181-001

79 BURCH A.



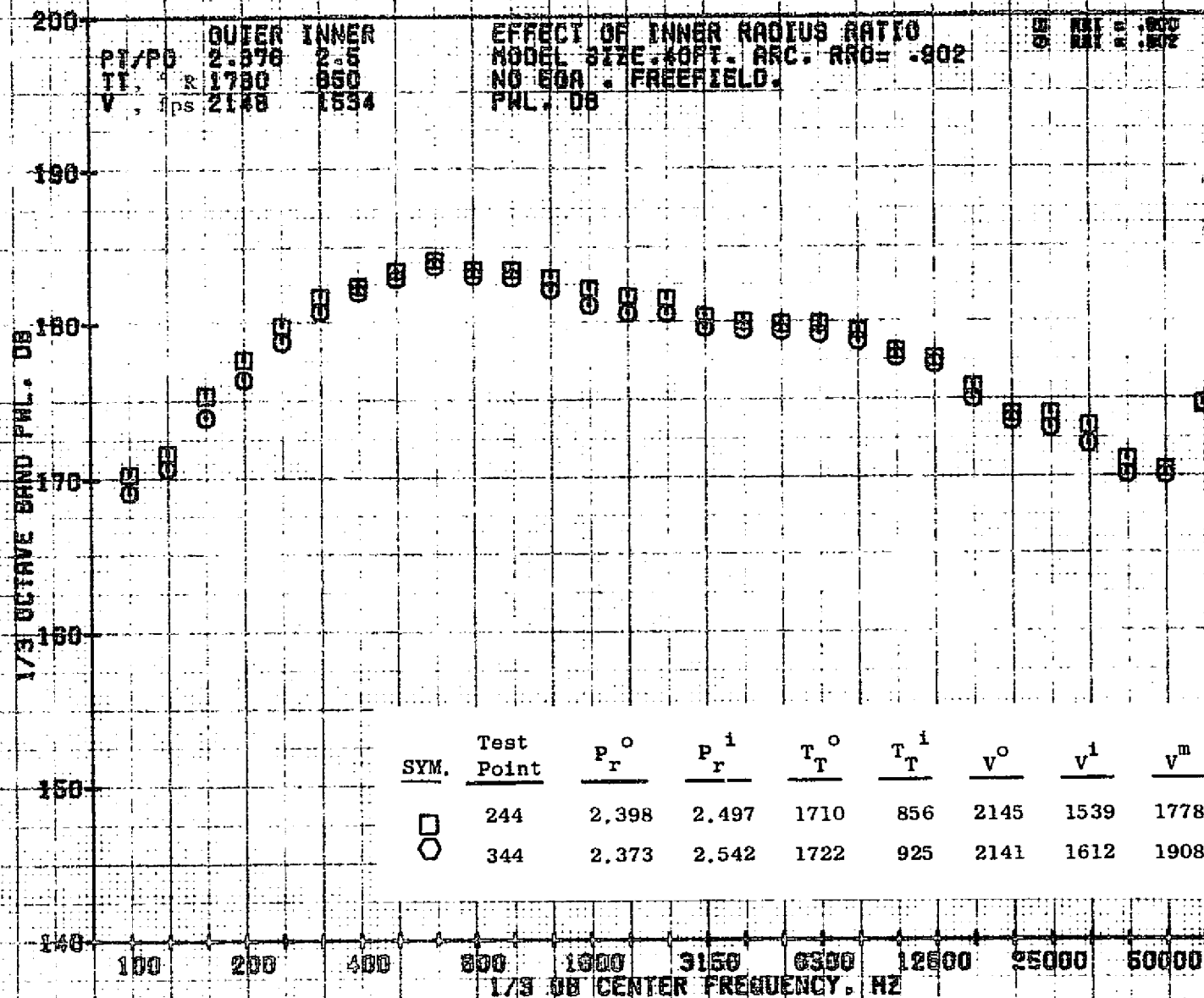
11/04/76
18690-001

79 BURCH A.



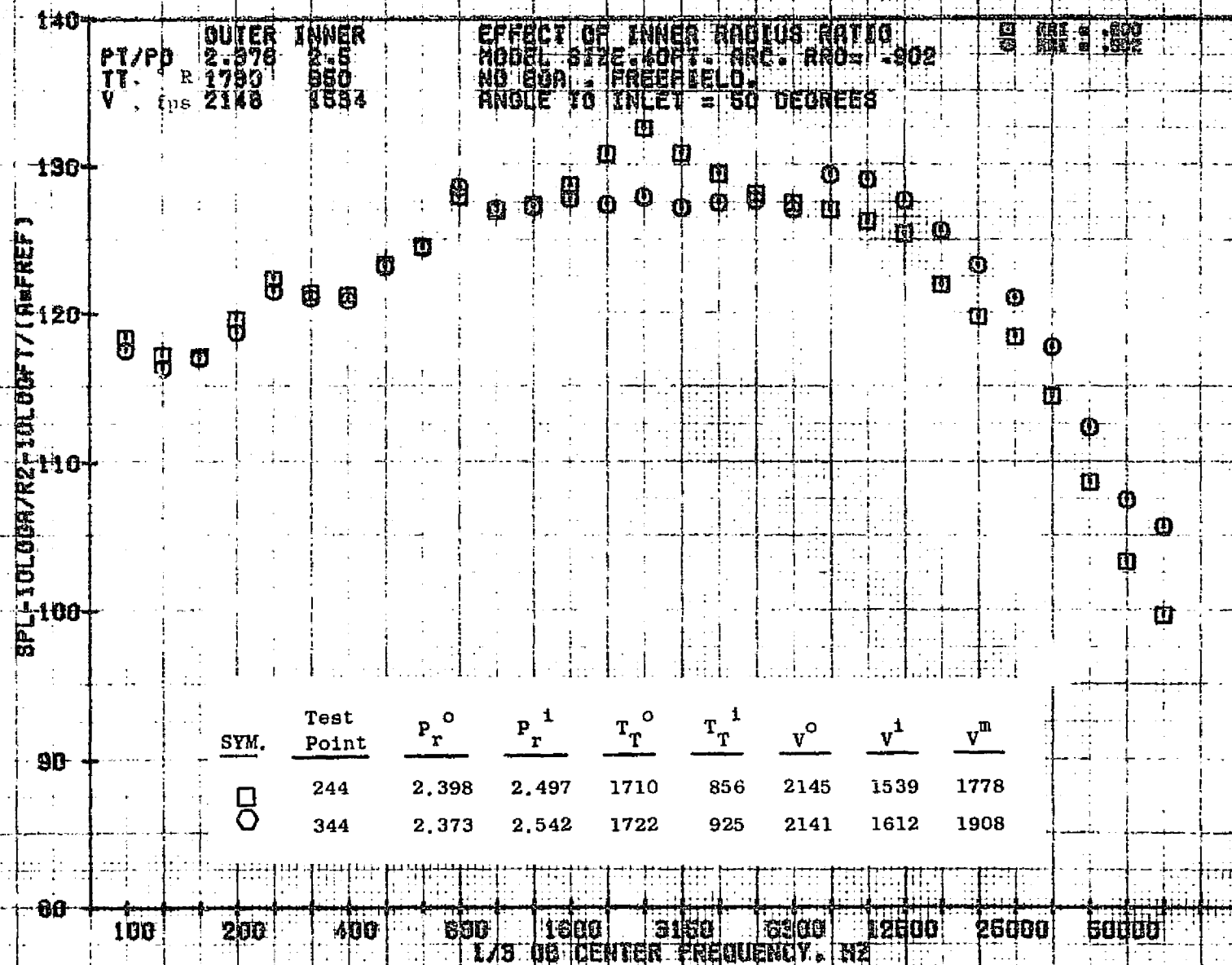
11/04/76
 18727-001

79 BURCH A.



11/04/76
 16727-001

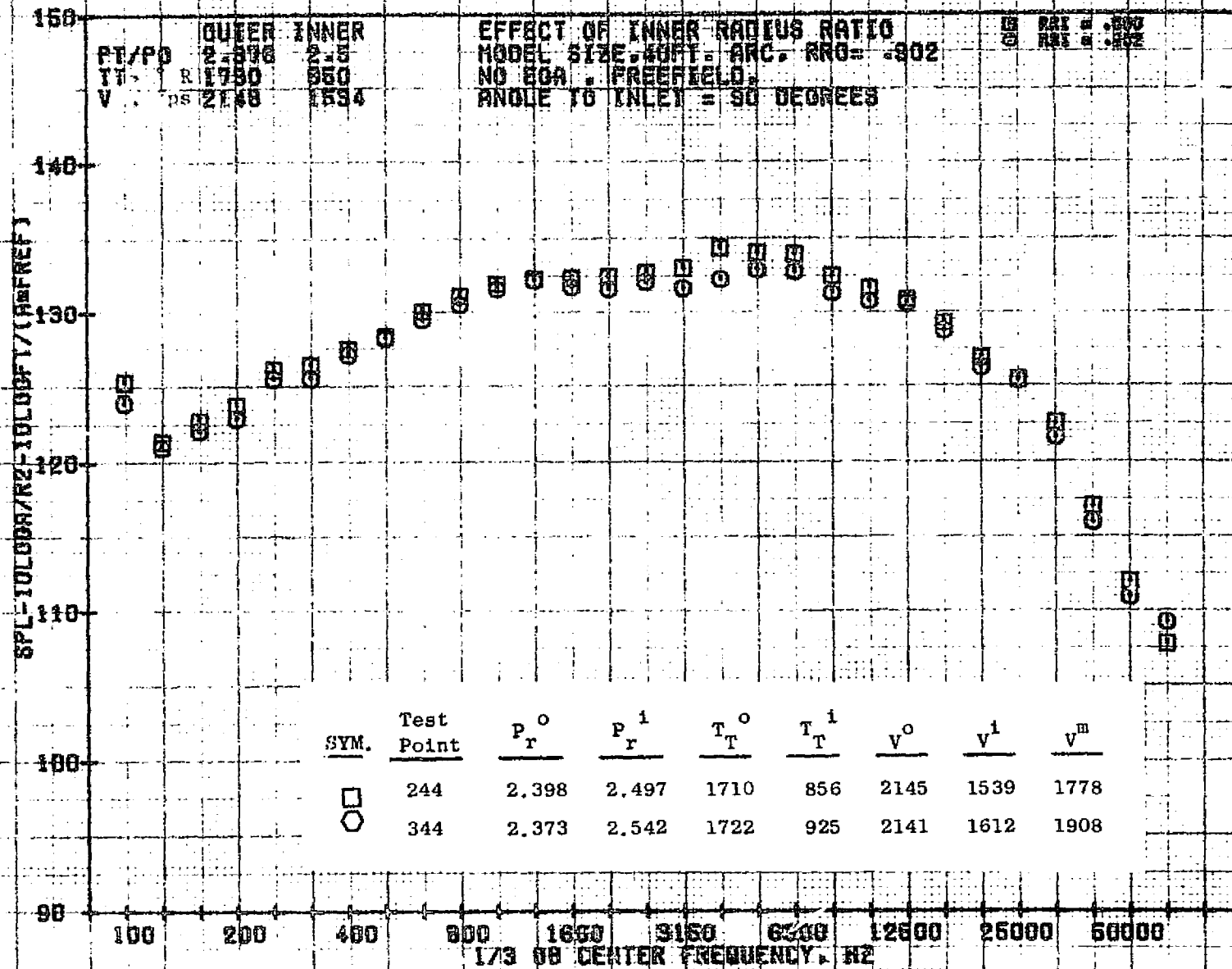
79 BURCH A.



11/04/76
18727-001

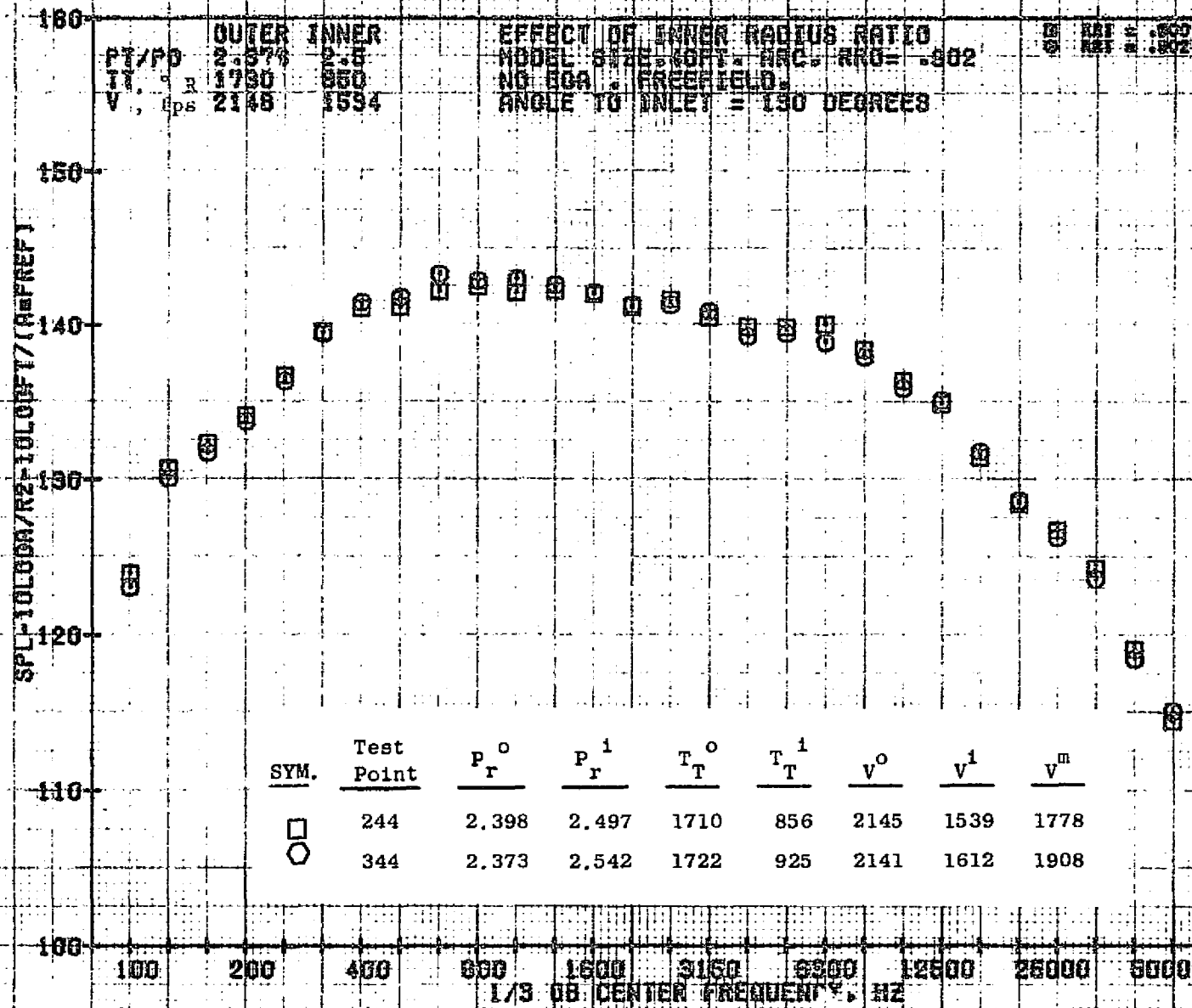
79 BURCH A.

975



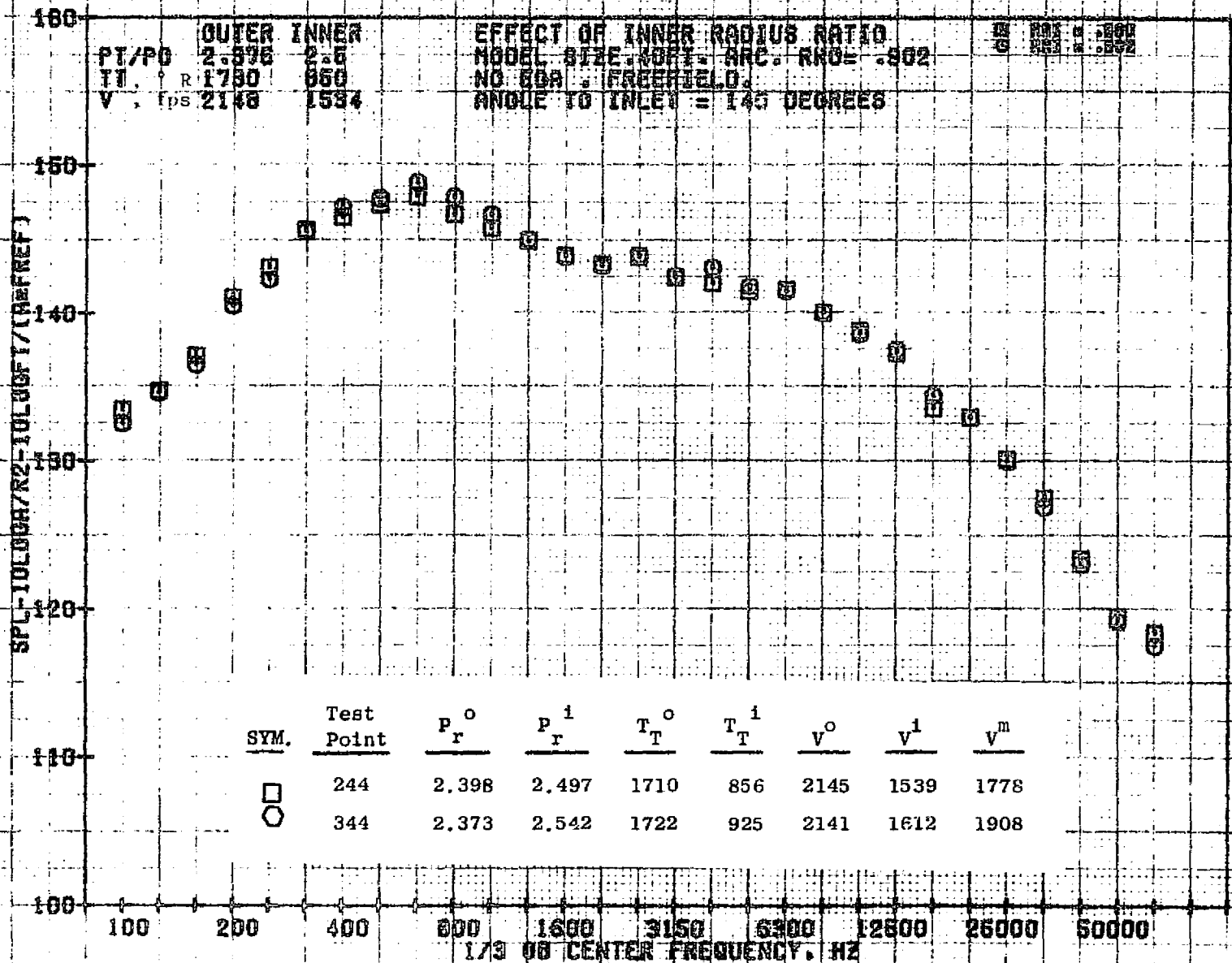
11/04/78
 18727-001

79 BURCH A.



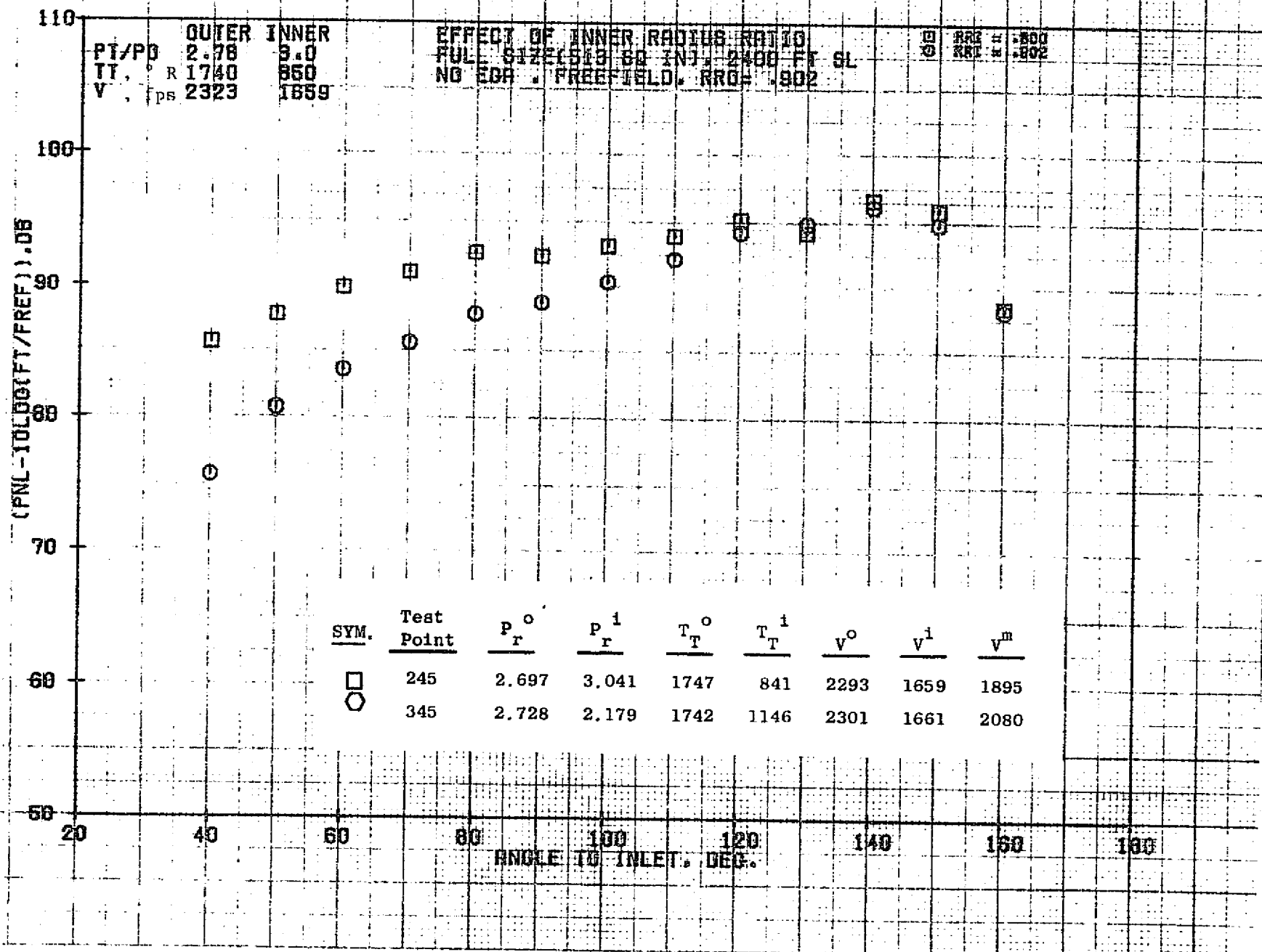
11/04/76
18727-001

79 BURCH A.



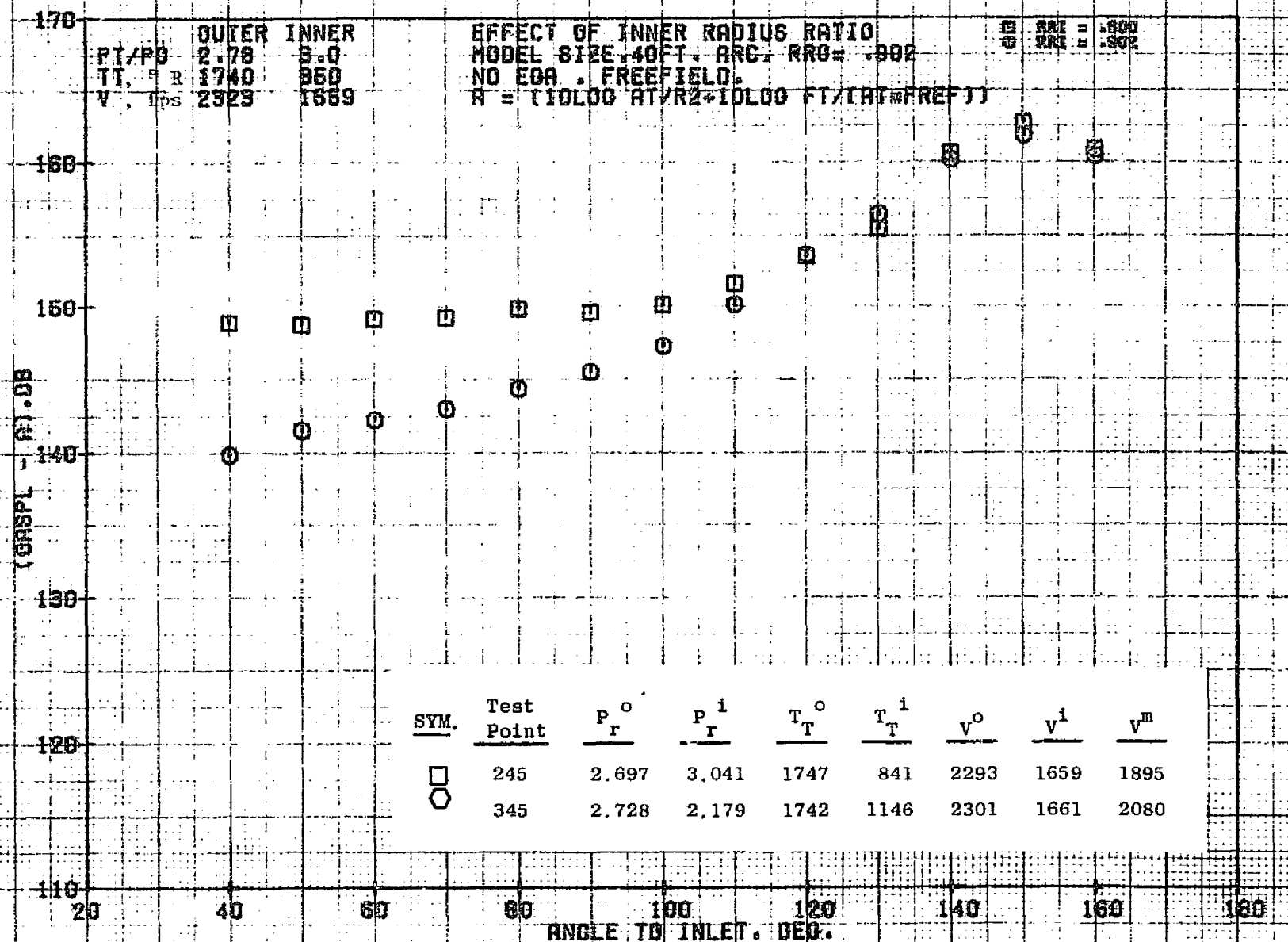
11/04/76
 18727-001

79 BURCH A.



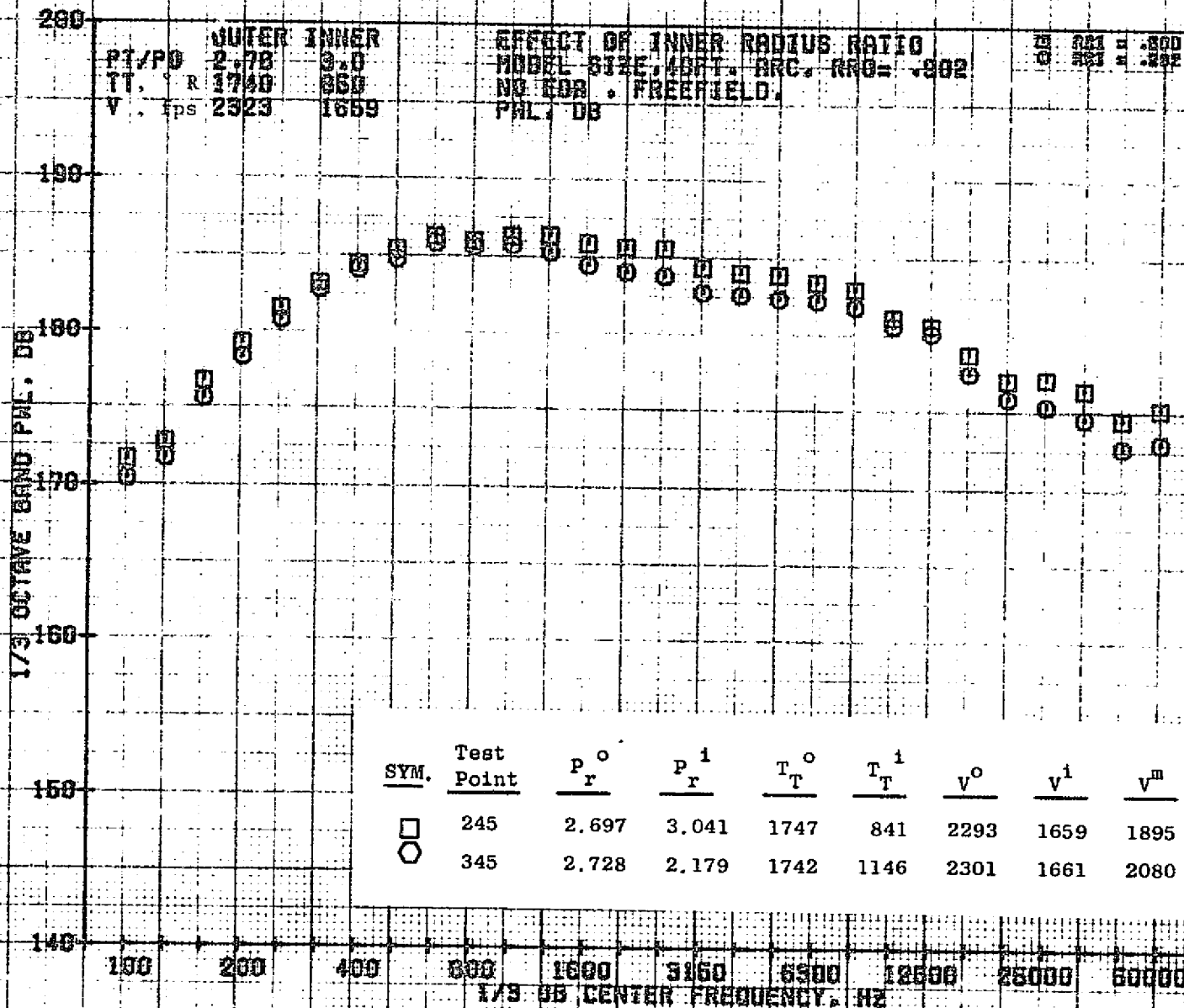
10/29/76
18124-001

79 BURCH A.



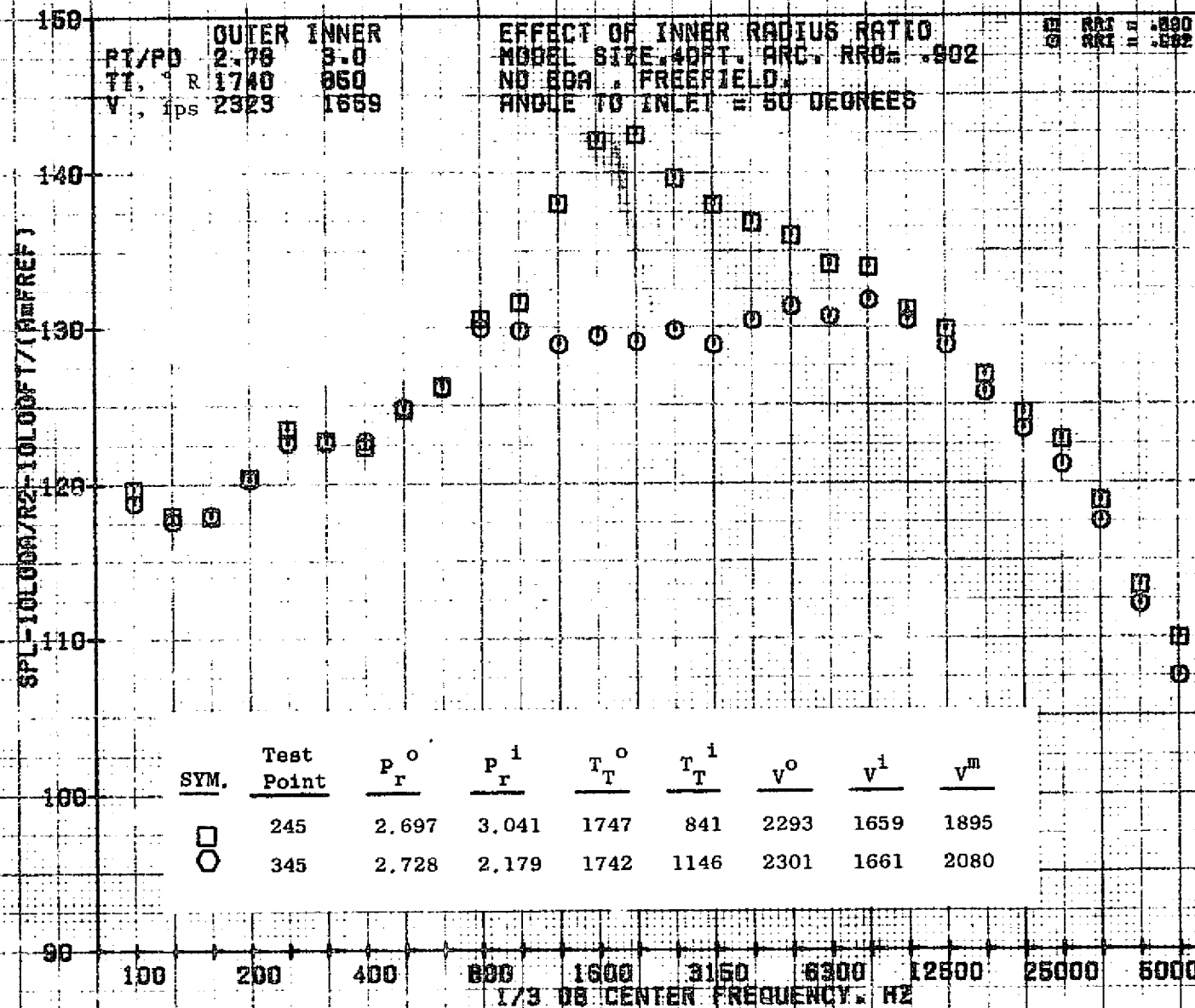
10/29/76
1B161-001

79 BURCH A.



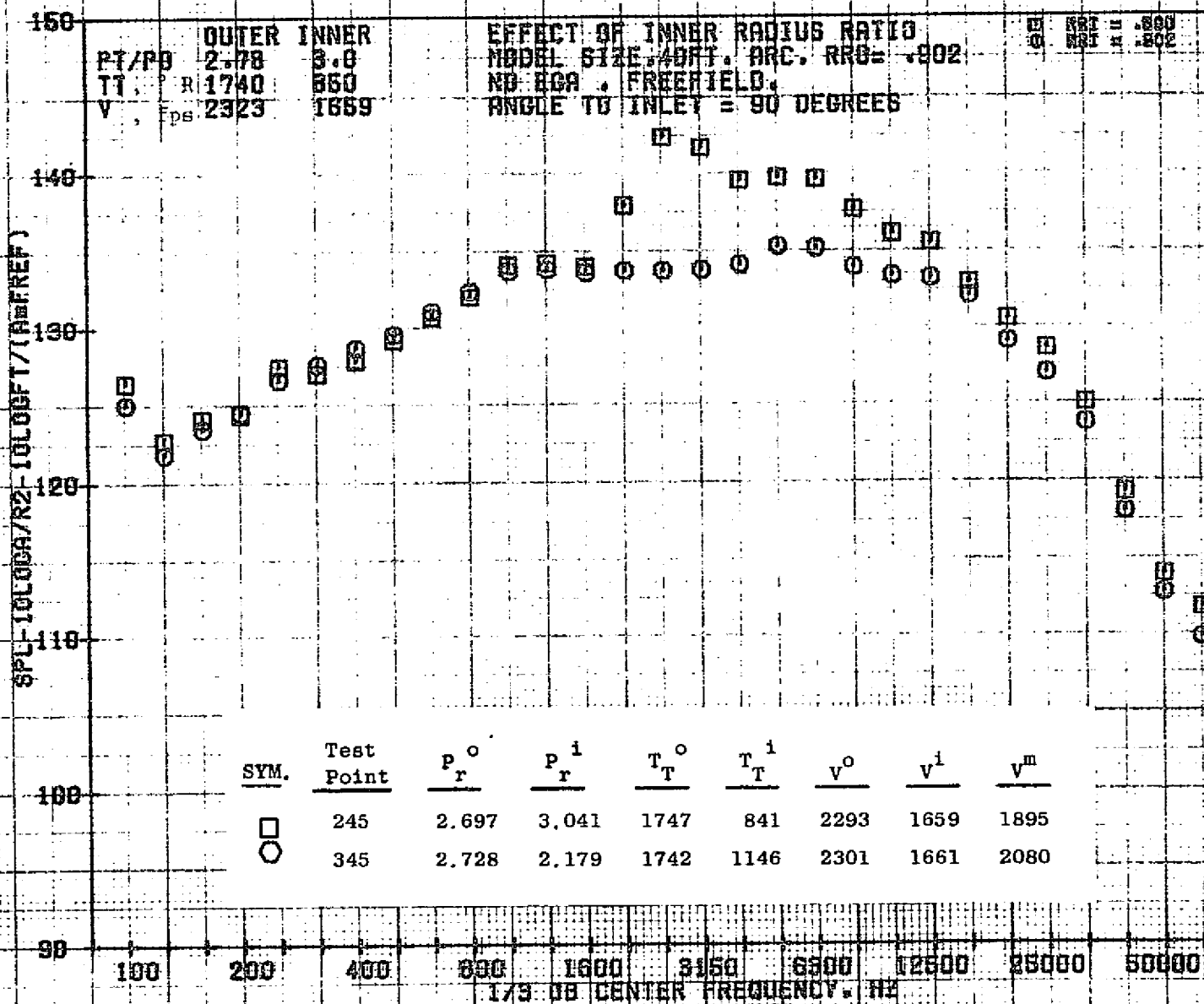
10/29/76
18161-001

79 BURCH A.



10/29/76
 18161-001

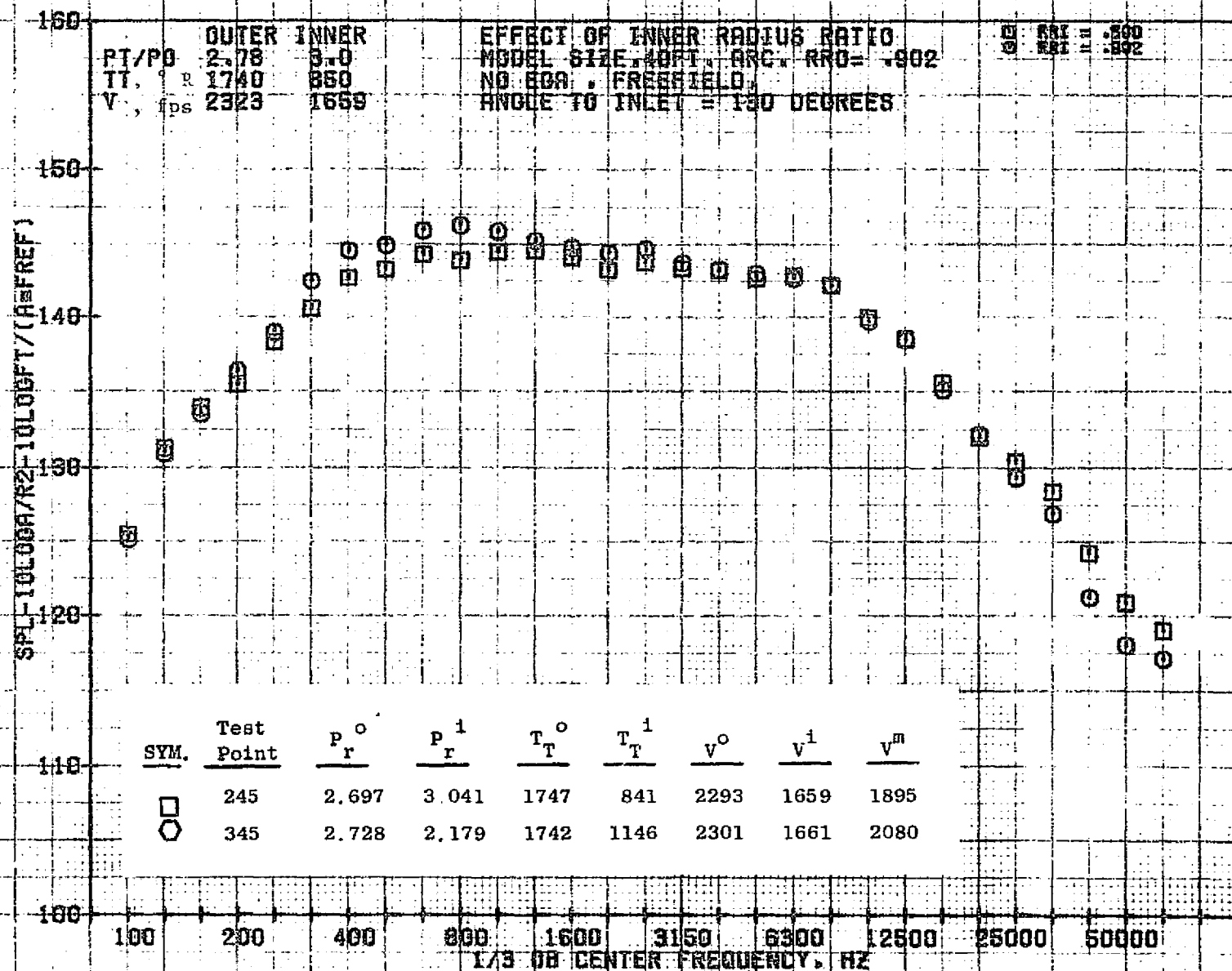
79 BURCH A.



10/29/76
18161-001

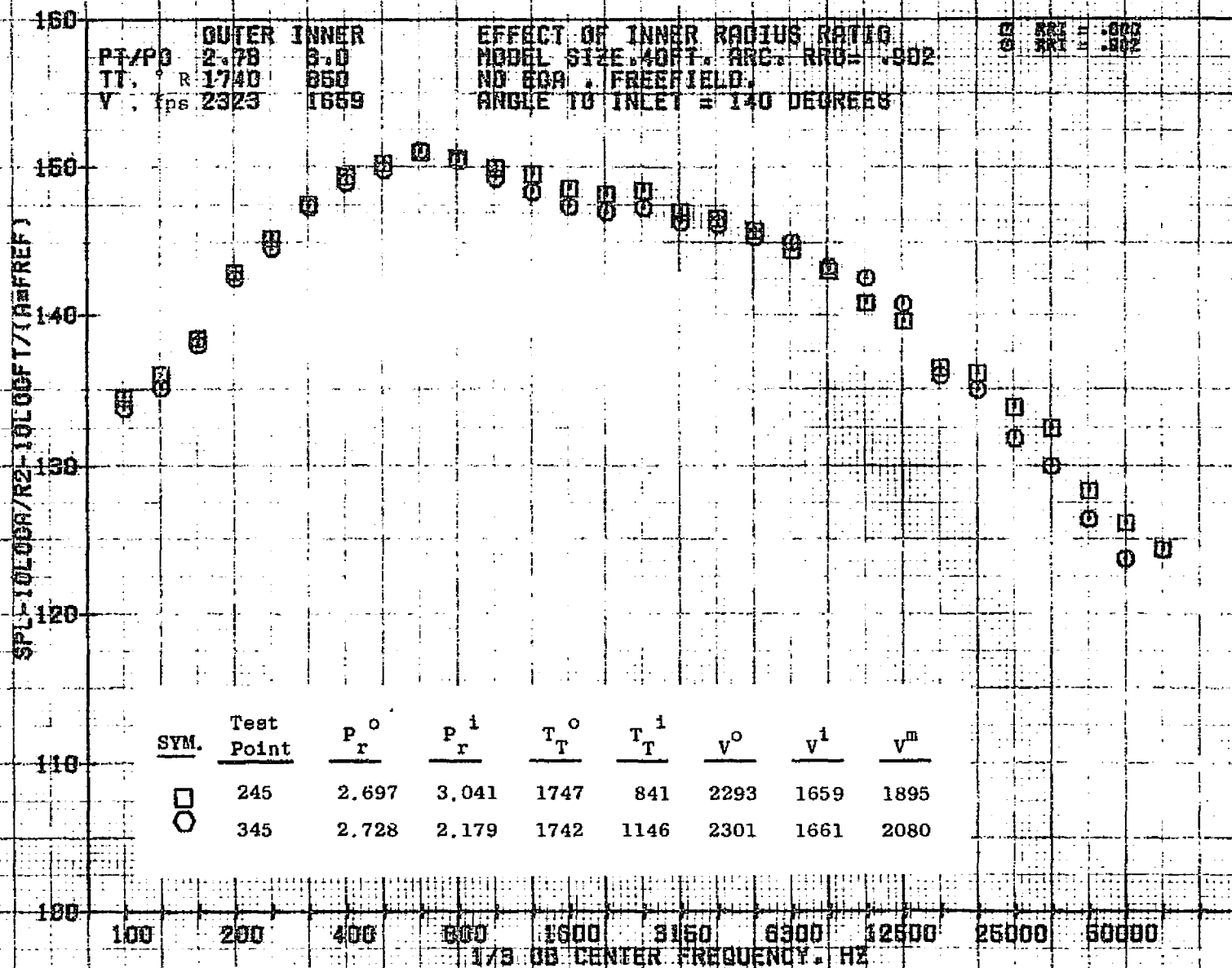
79 BURCH A.

986



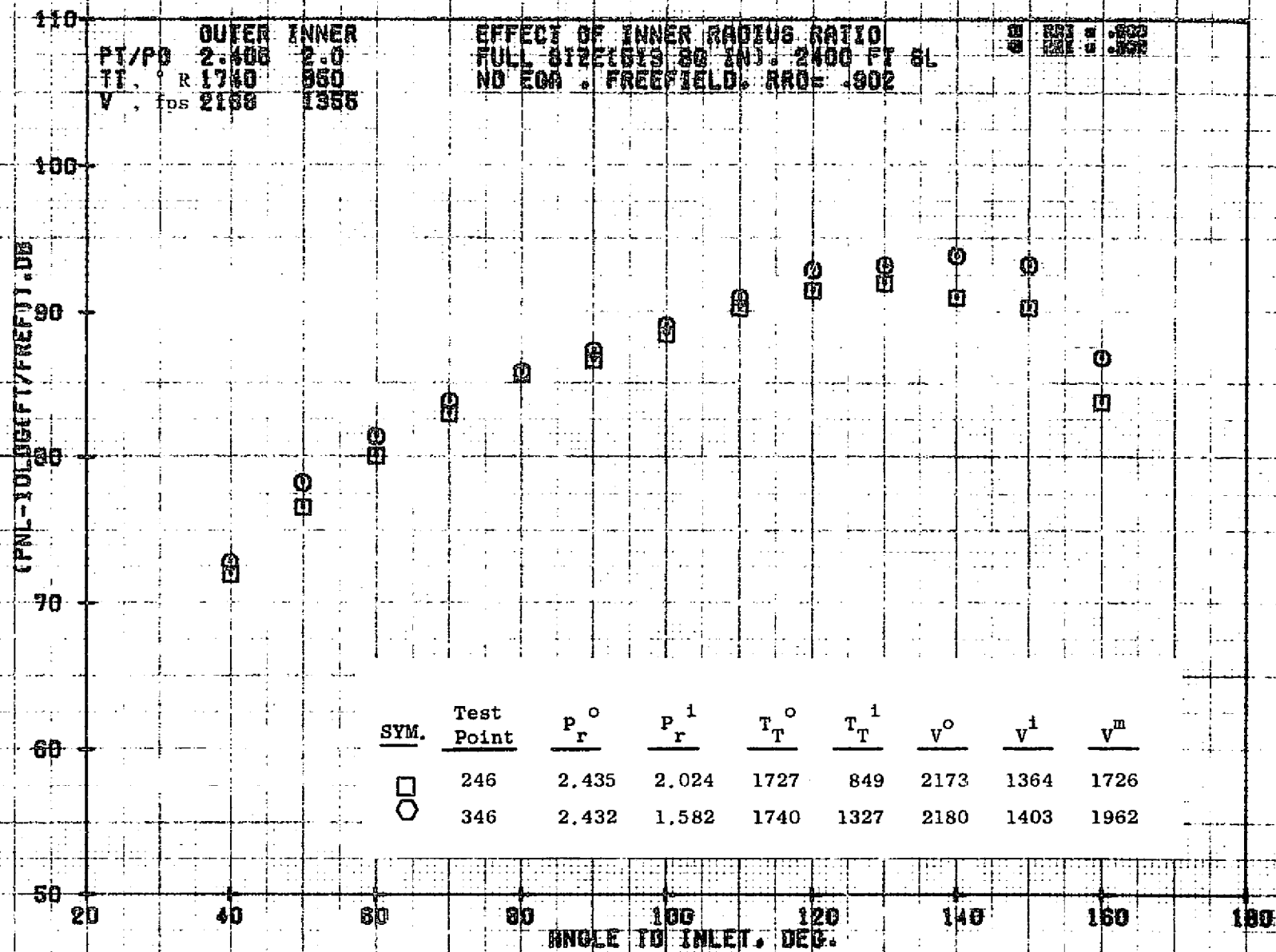
10/29/76
 18161-001

79 BURCH A.



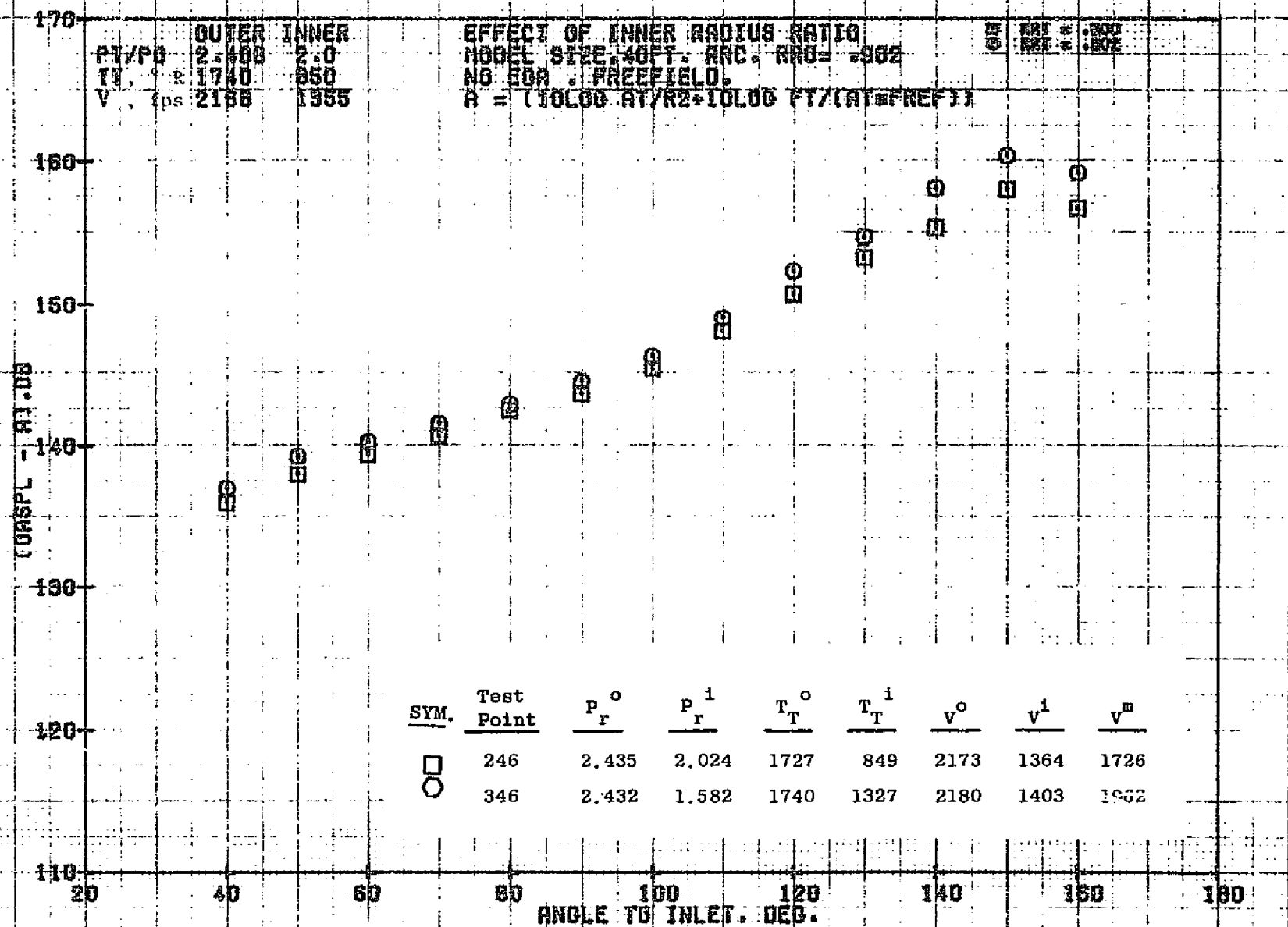
10/29/76
 18161-001

79 BURCH A.



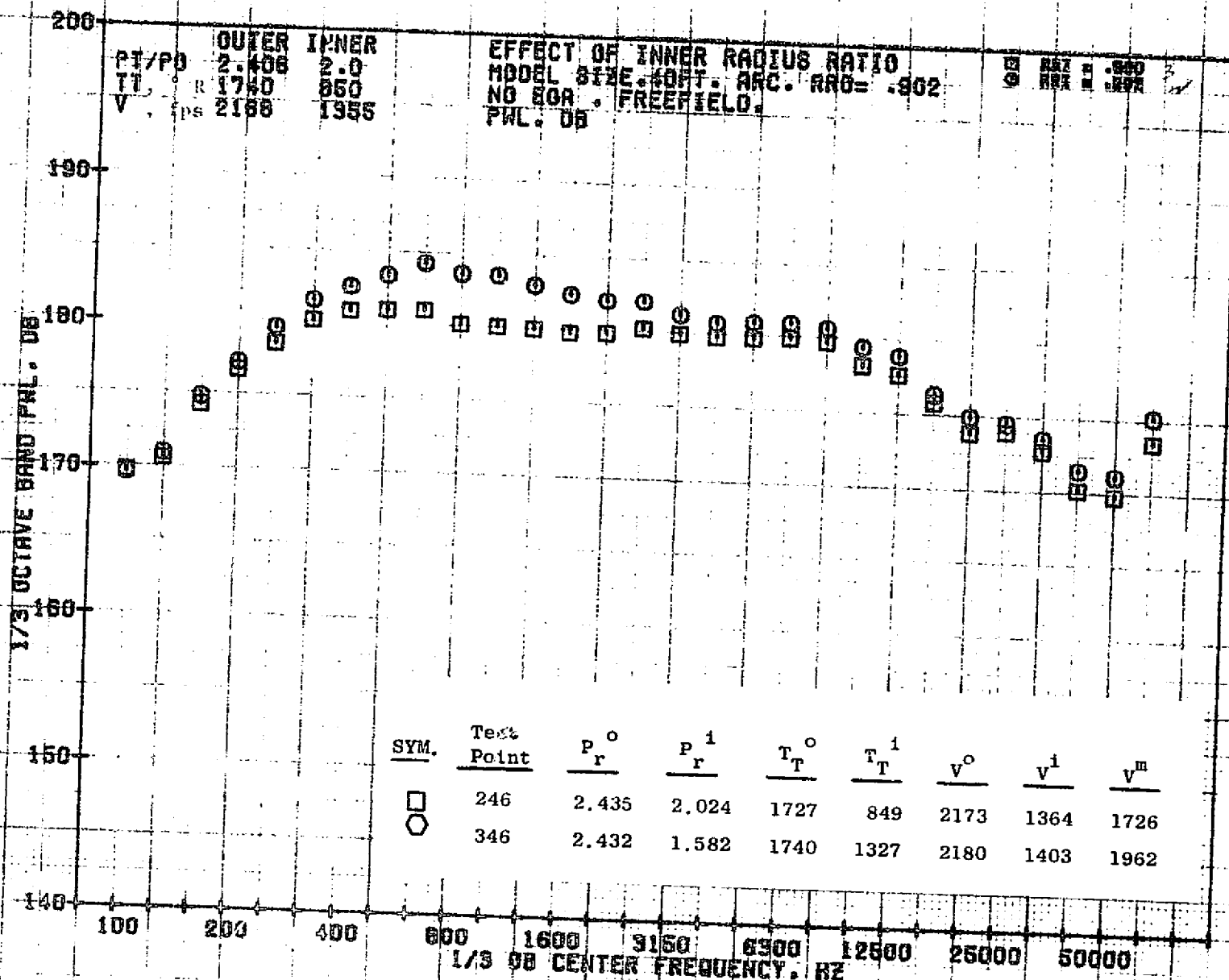
11/04/76
 18880-001

79 BURCH A.



11/04/76
 18727-001

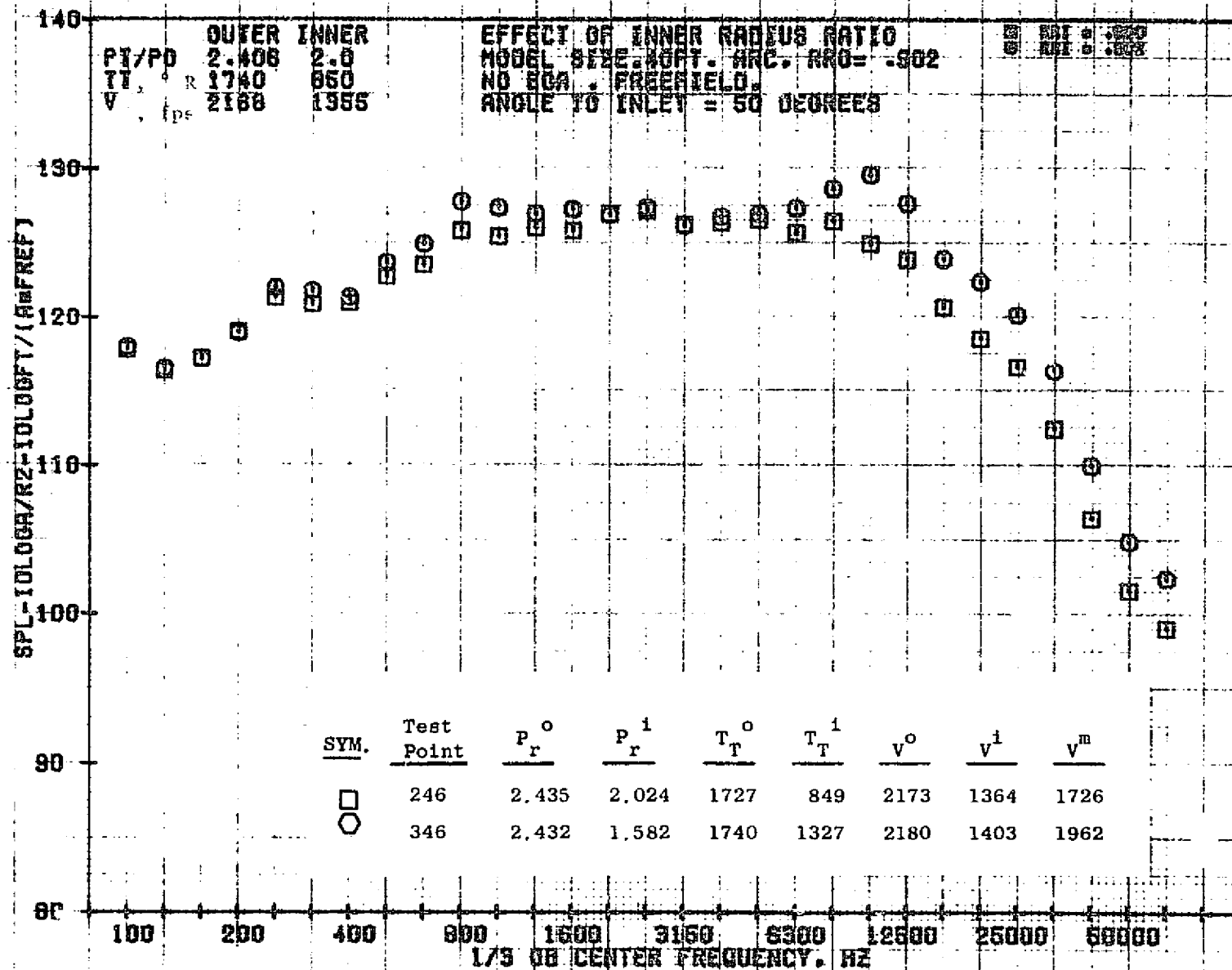
79 BURCH A.



11/04/76
 18727-001

79 BURCH A.

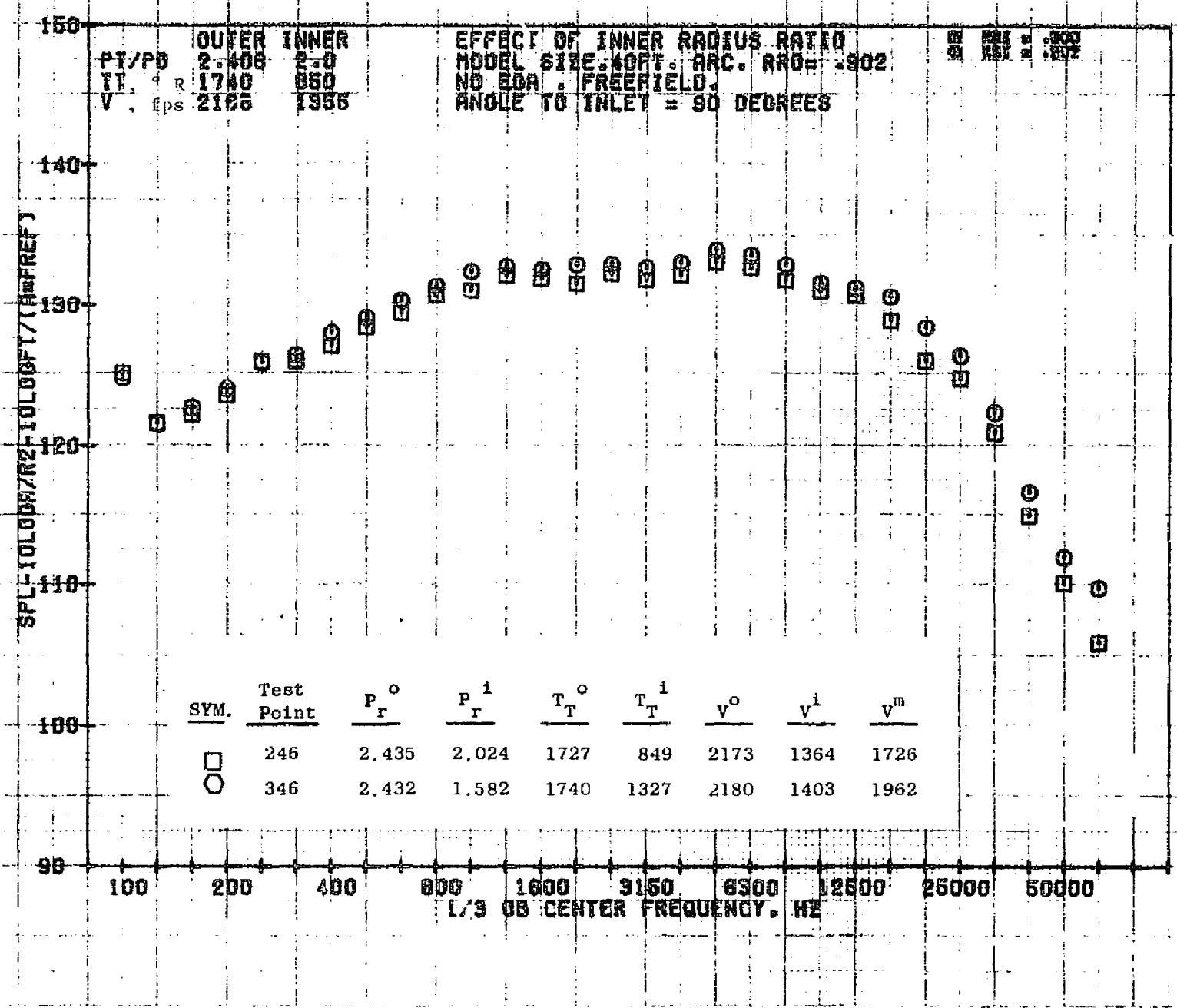
386



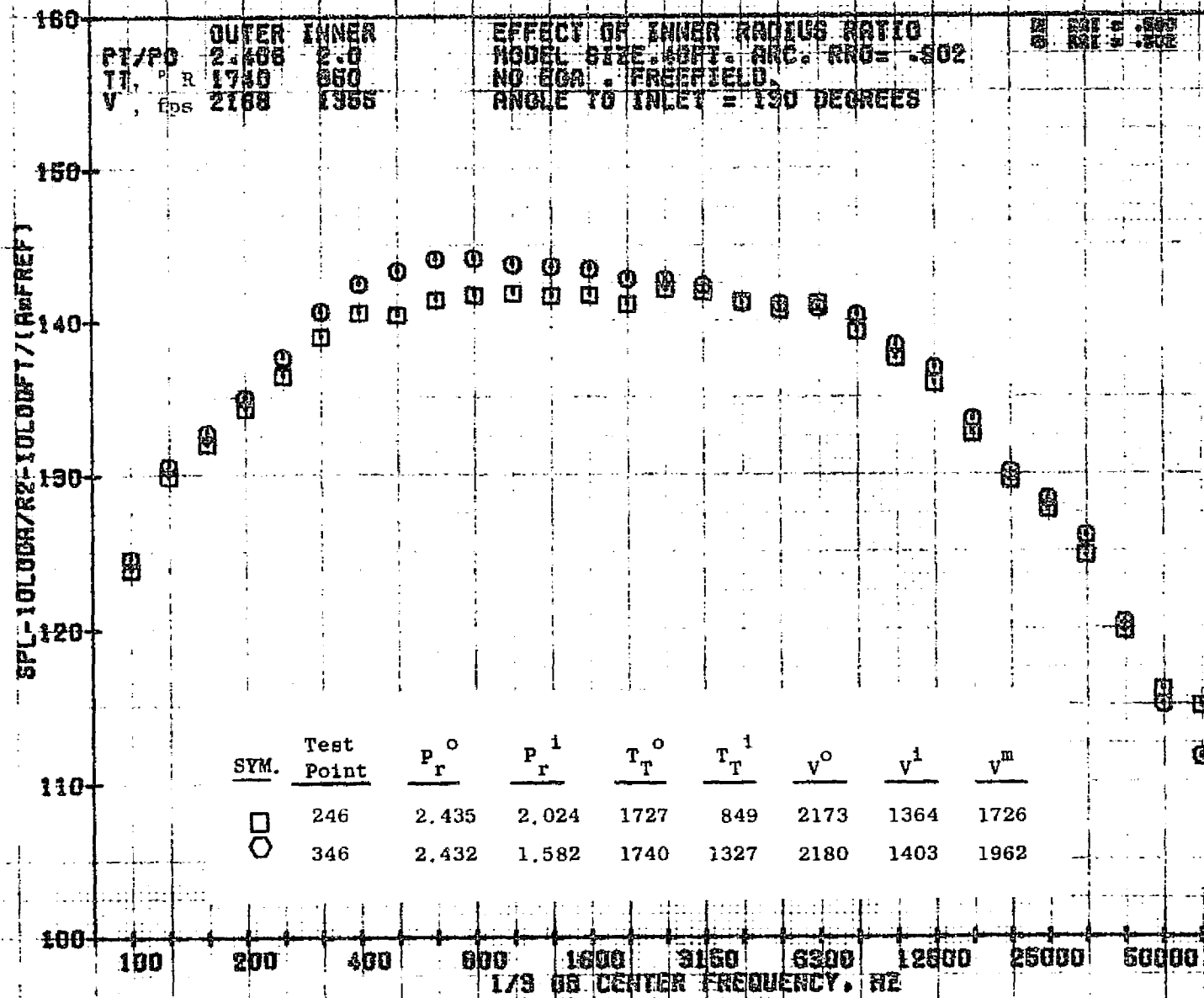
11/04/78
 18727-001

79 BURCH A.

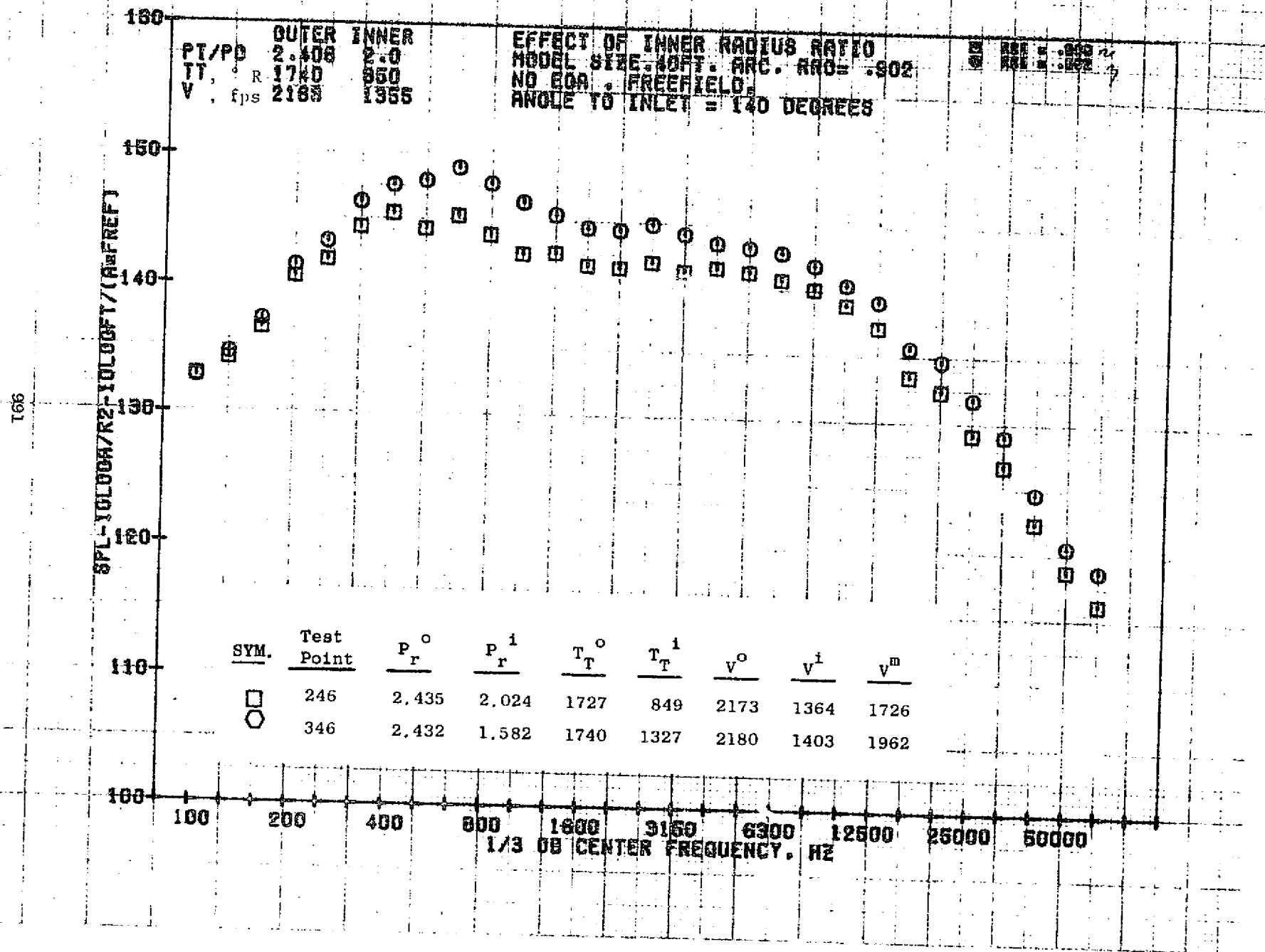
686



066

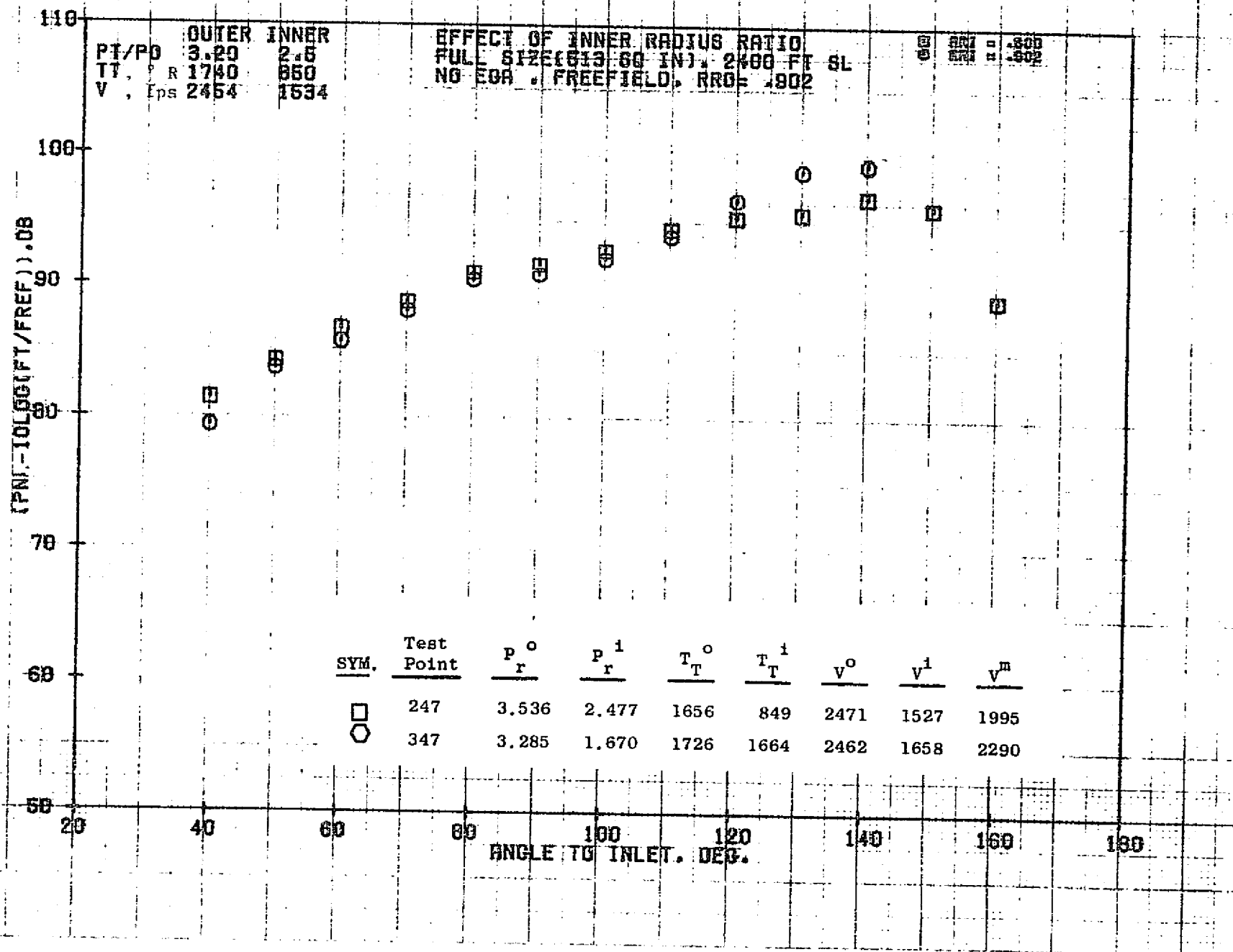

 11/04/76
 18727-001

79 BURCH A.



11/04/76
18727-001

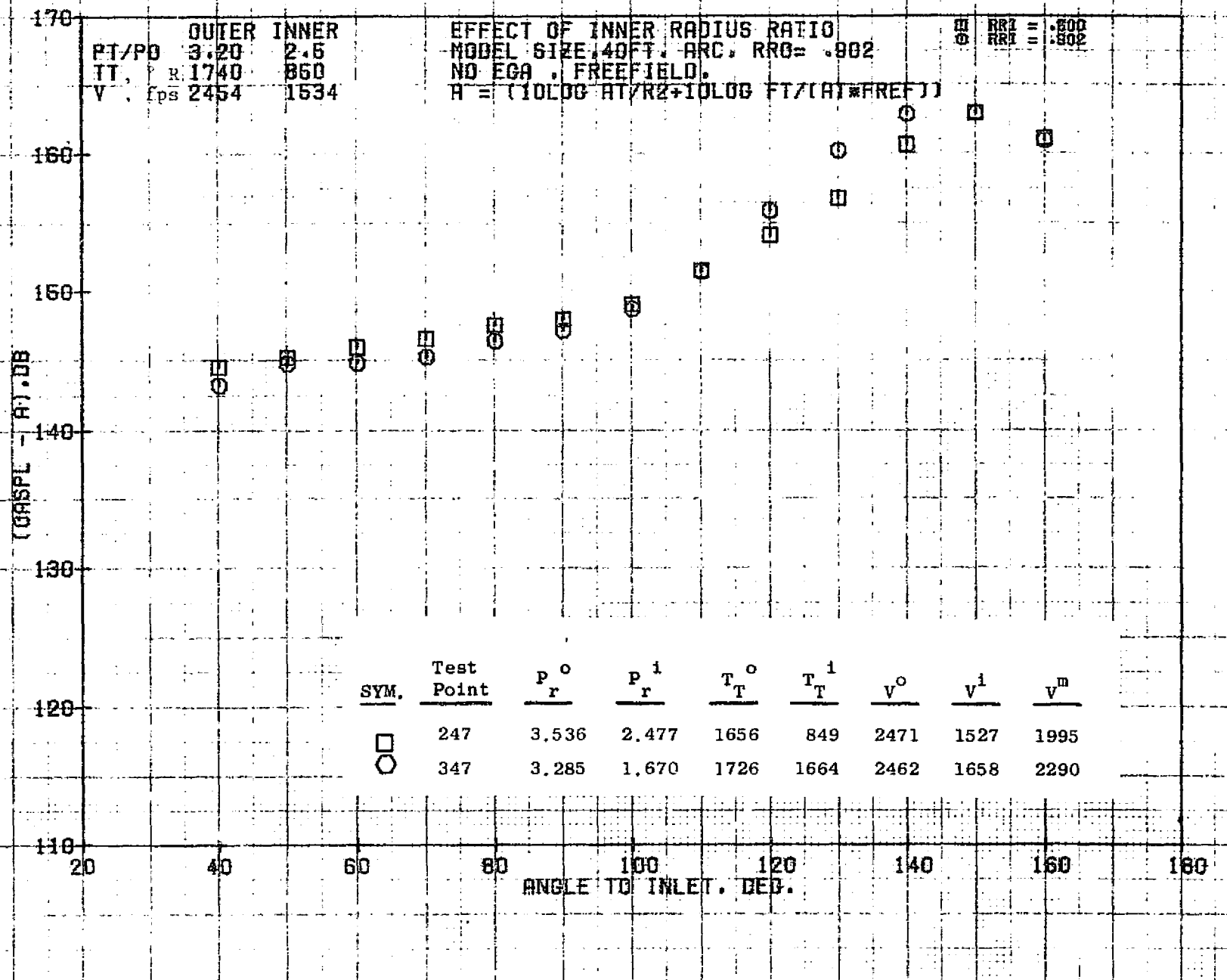
79 BURCH A.

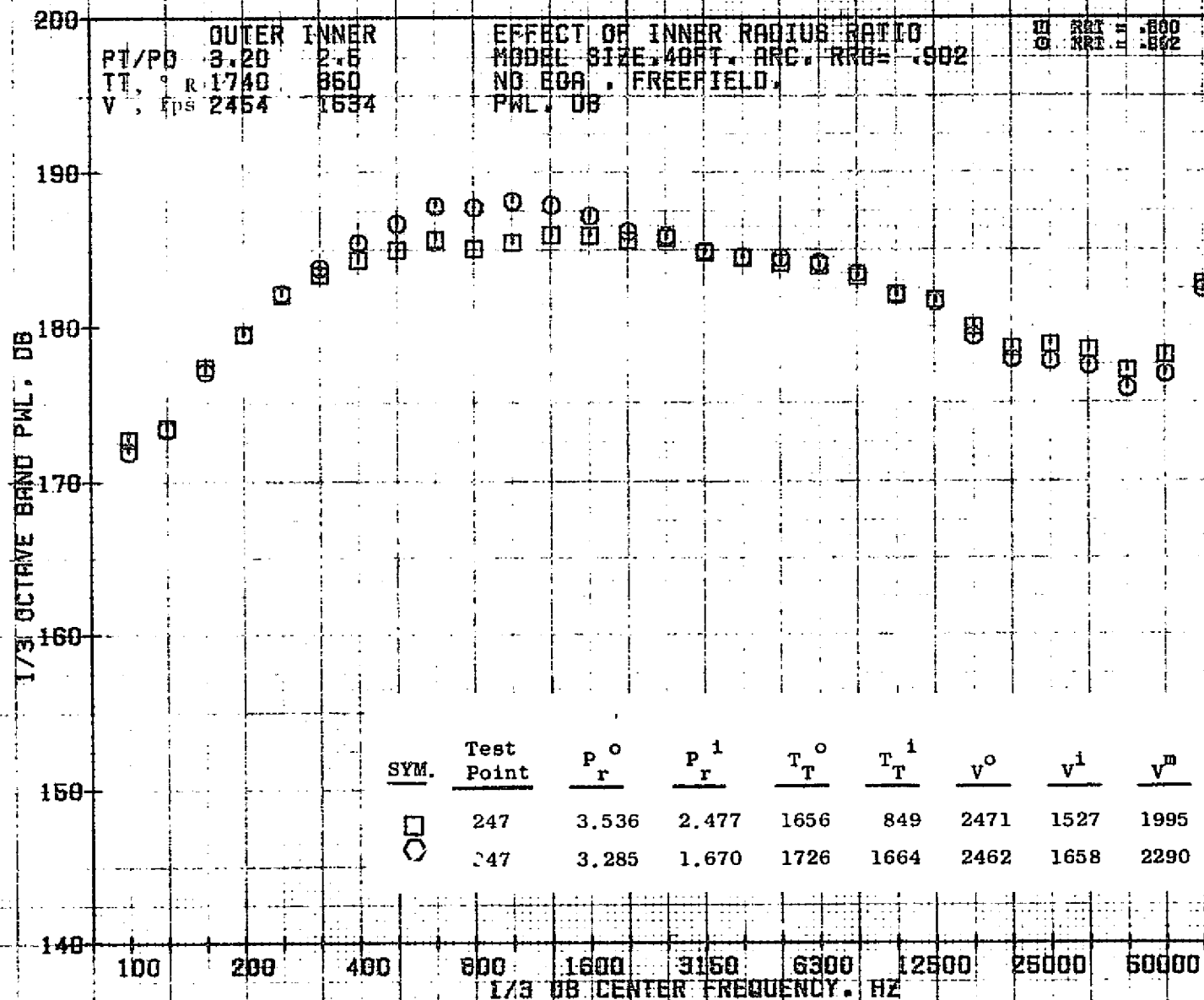


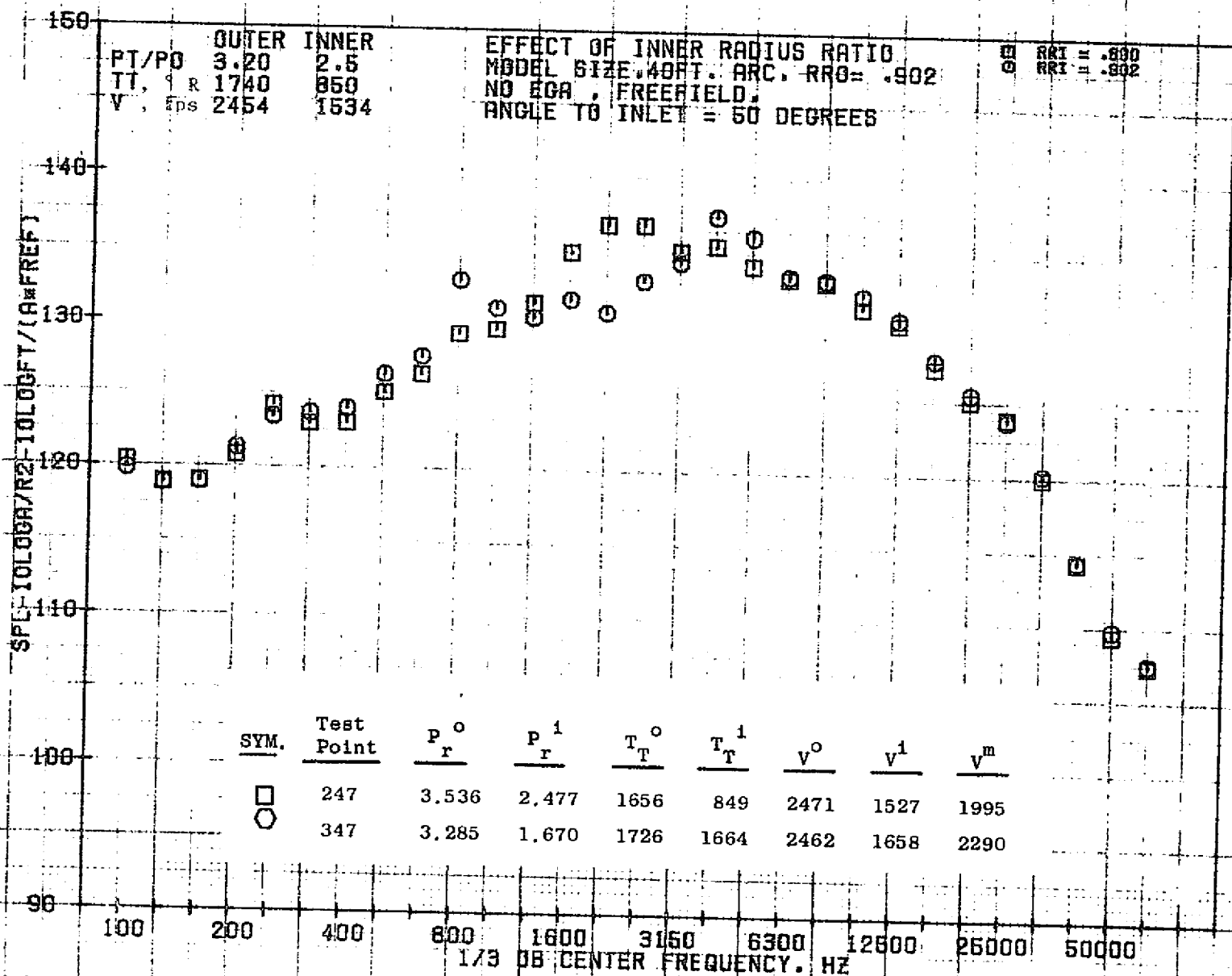
10/29/76
18124-001

79 BURCH A.

963



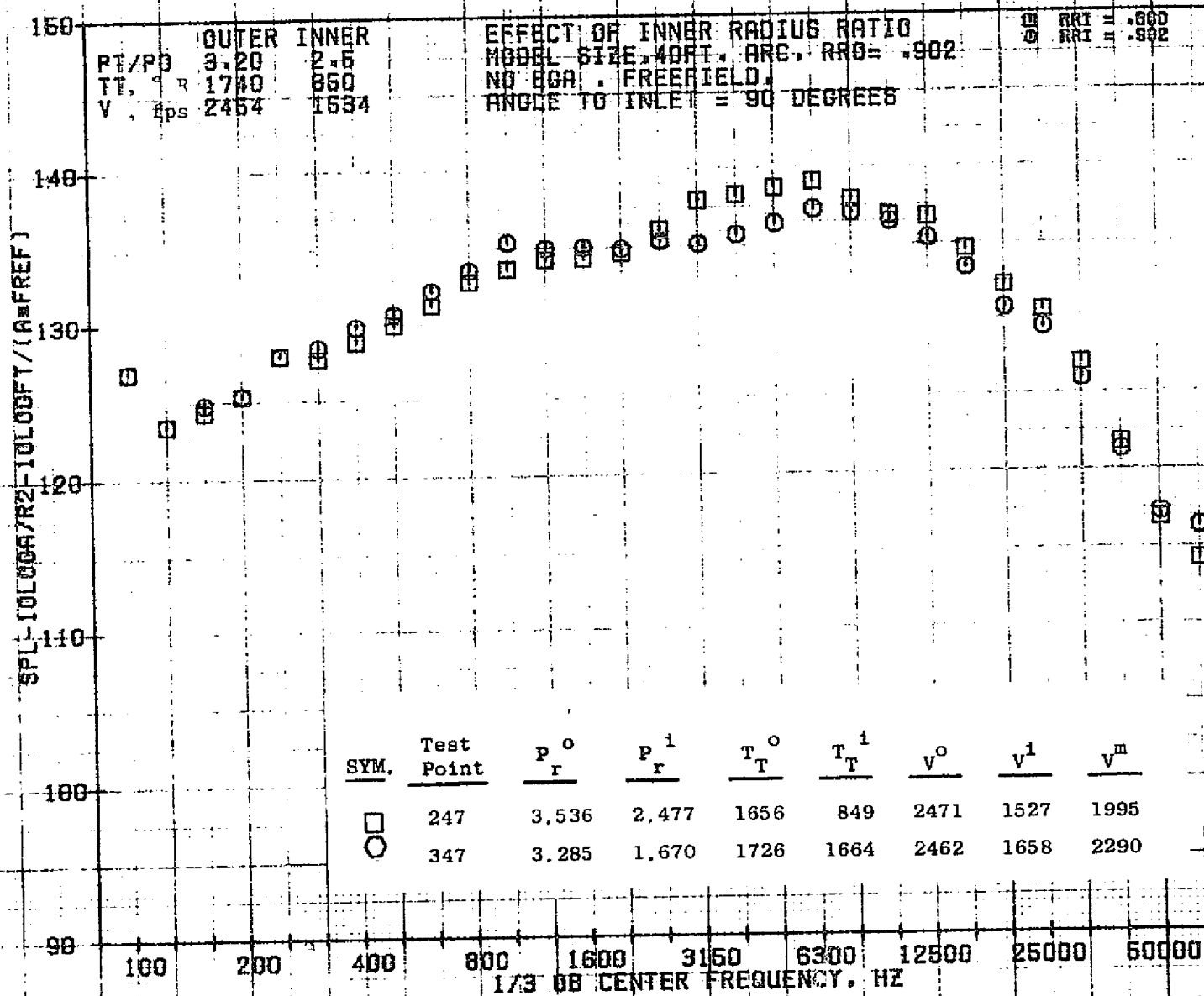




10/29/76
18161-001

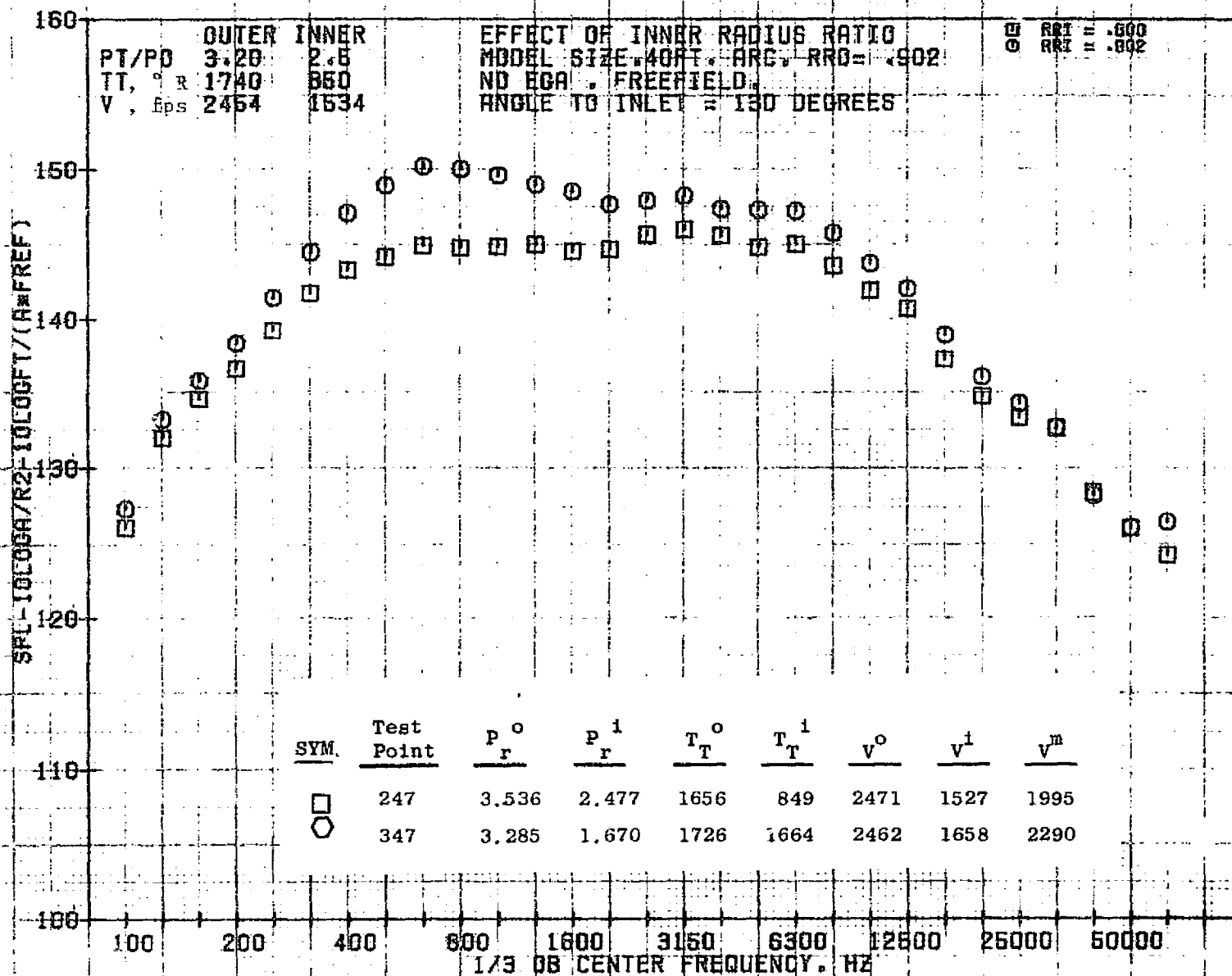
79 BURCH A.

966



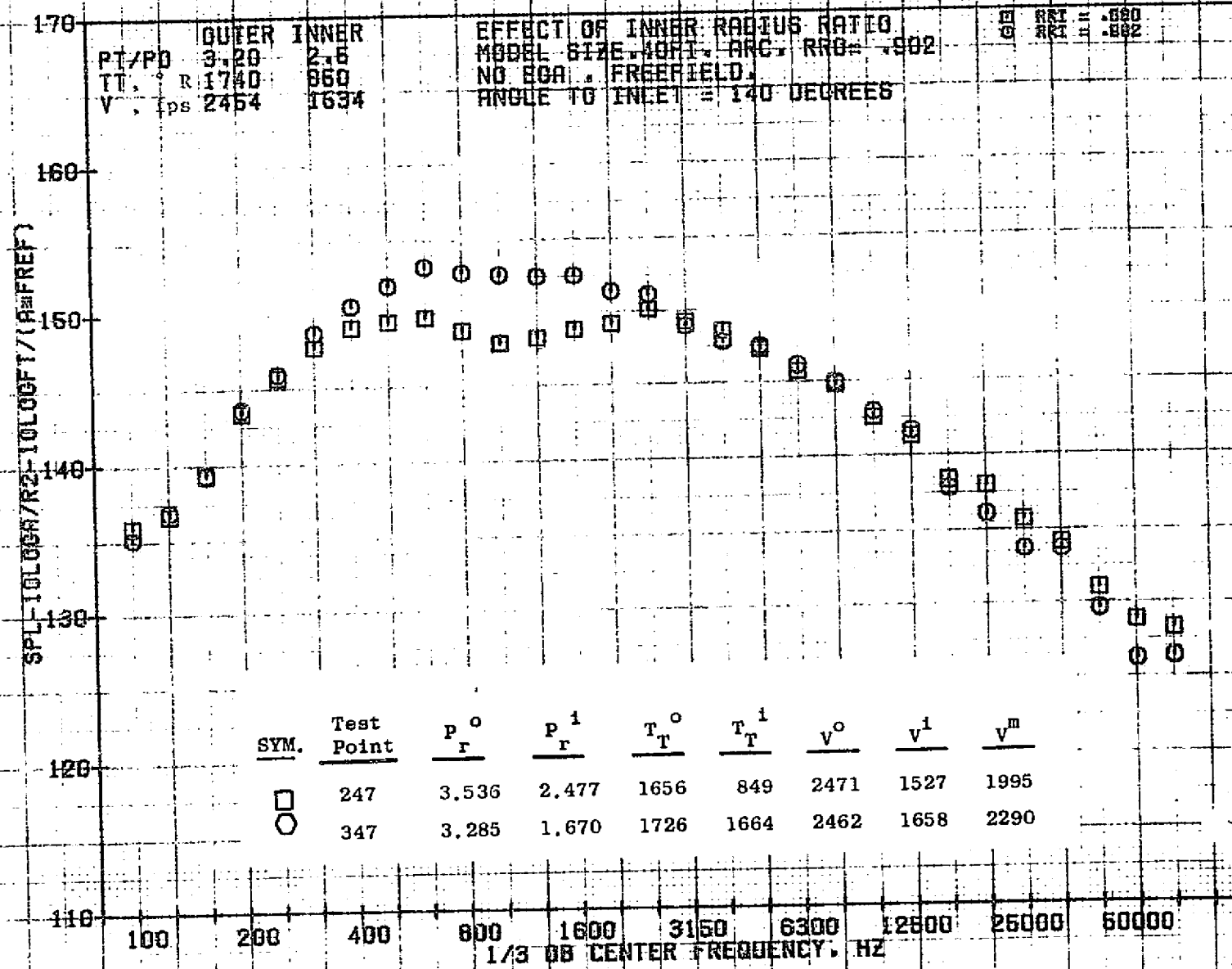
10/29/76
1R161-001

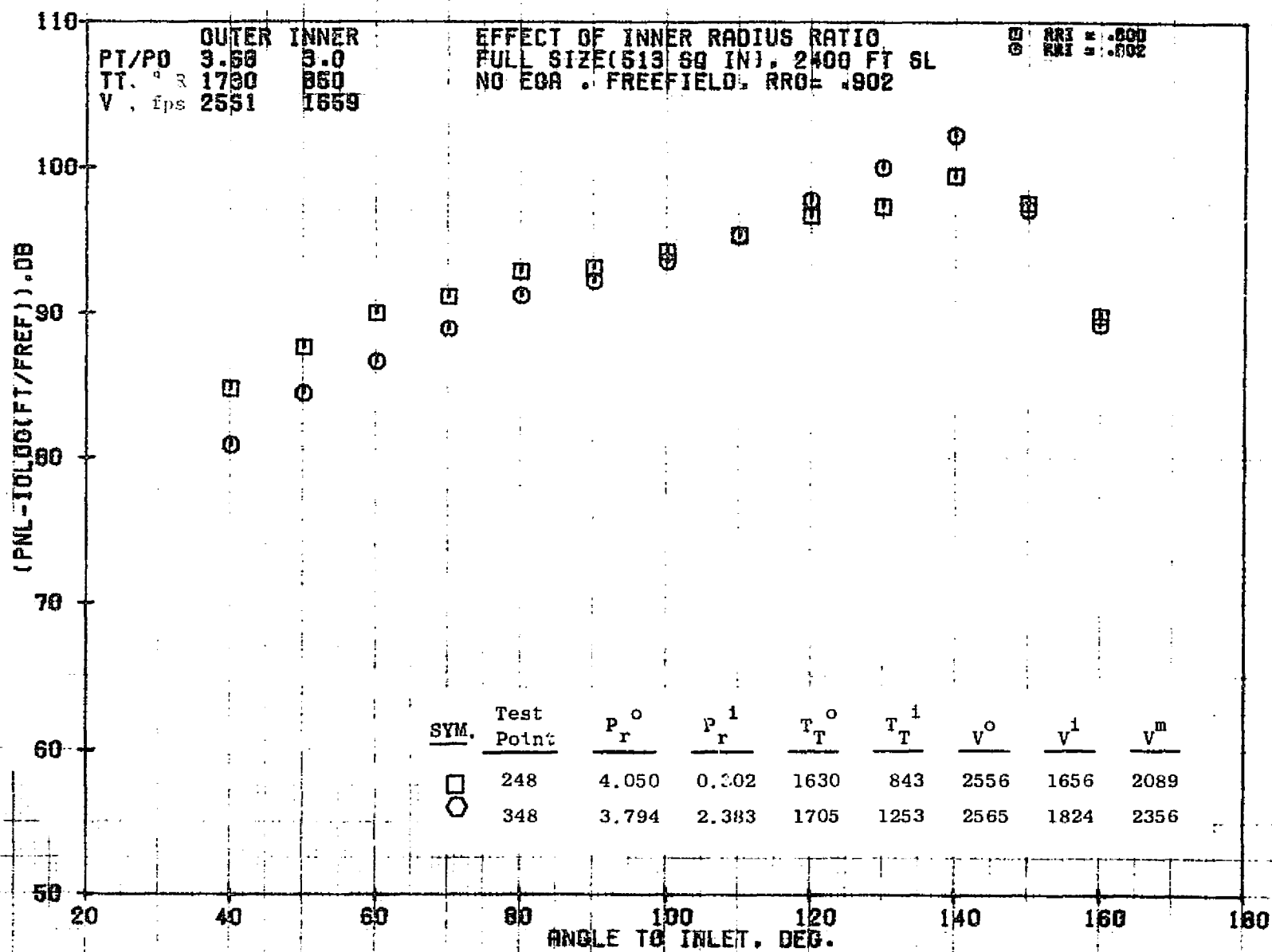
79 BURCH A.



10/29/76
1B161-001

79 BURCH A.

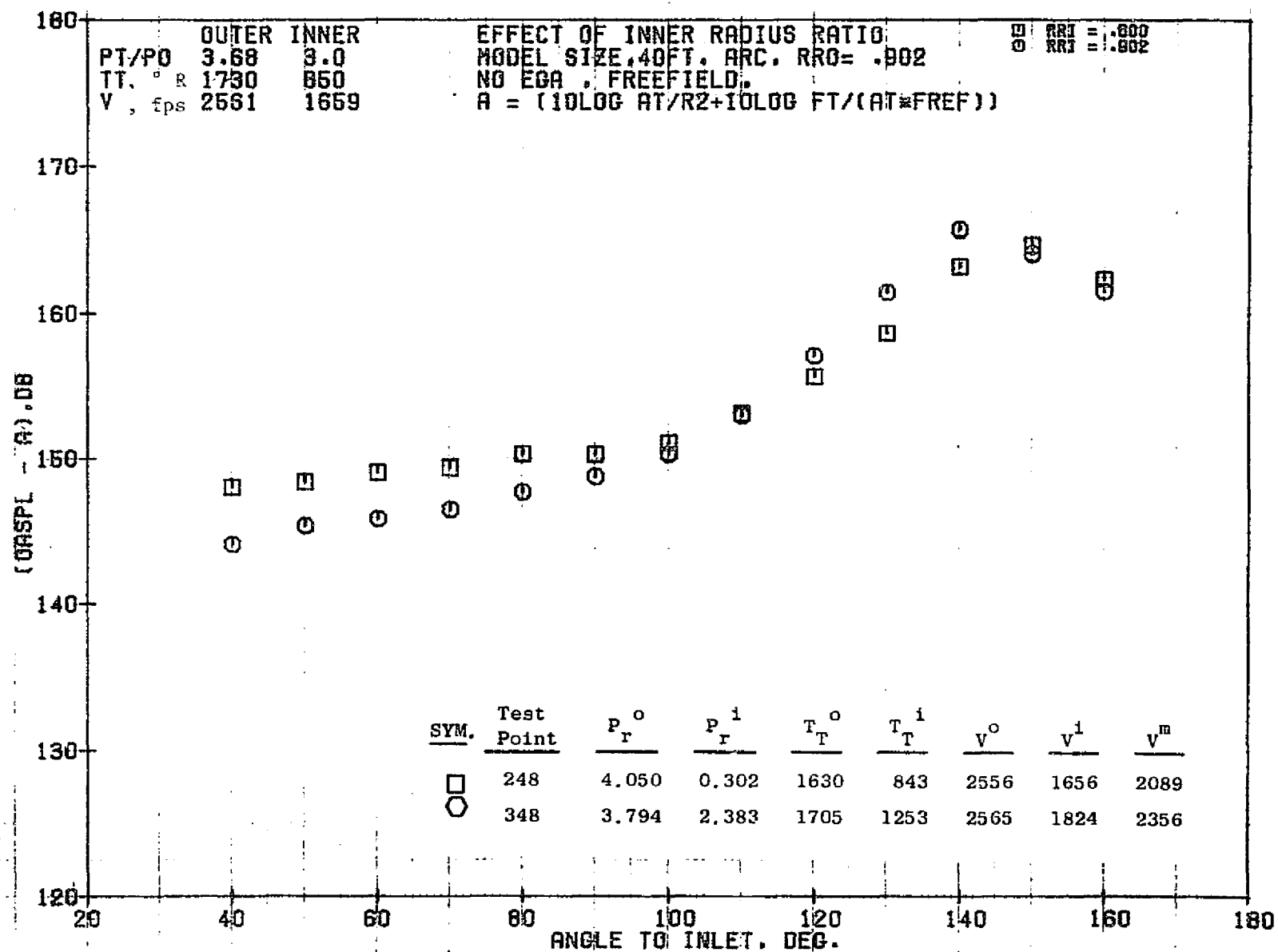




10/29/76
 18124-001

79 BURCH A.

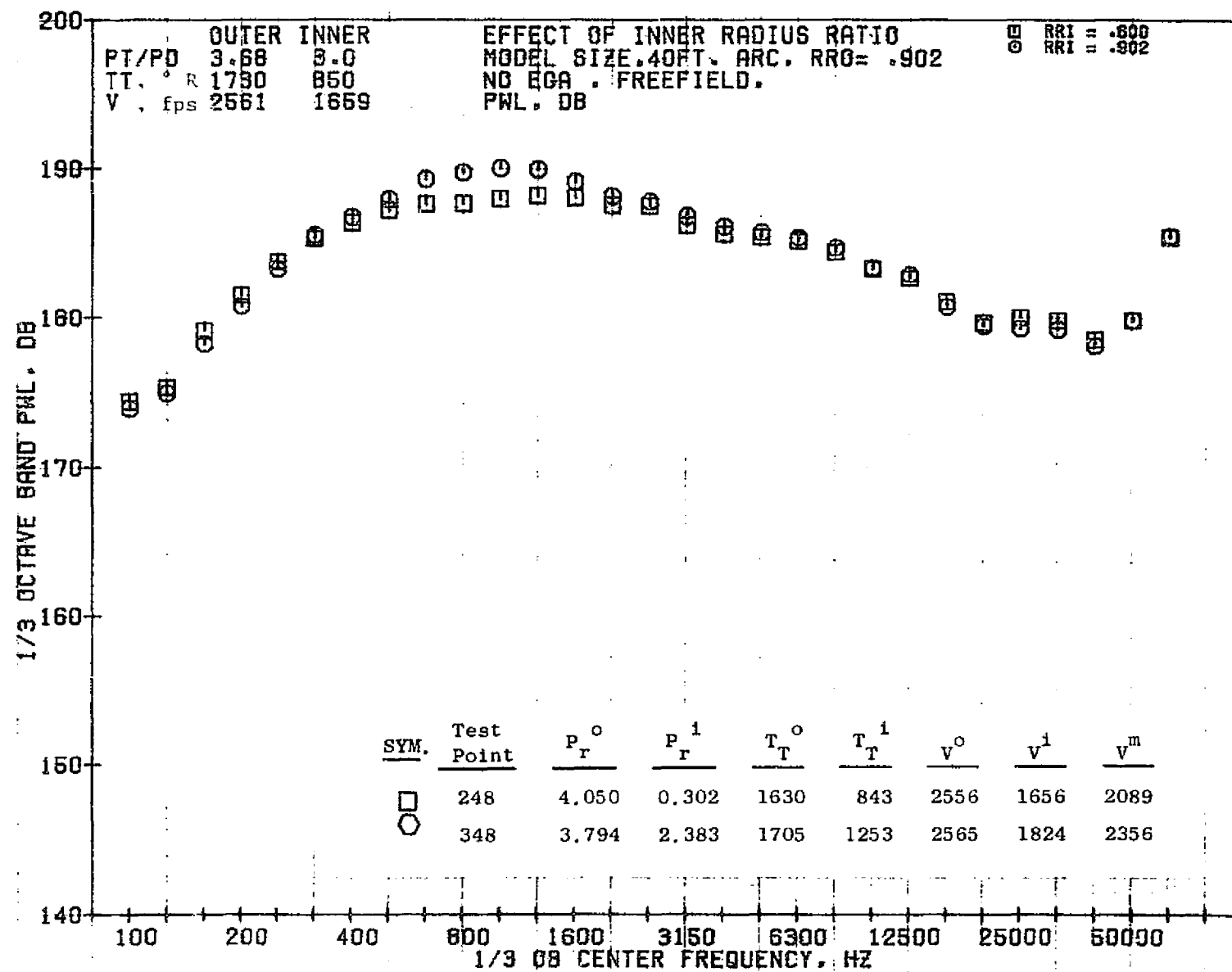
0001



10/29/76
18161-001

79 BURCH A.

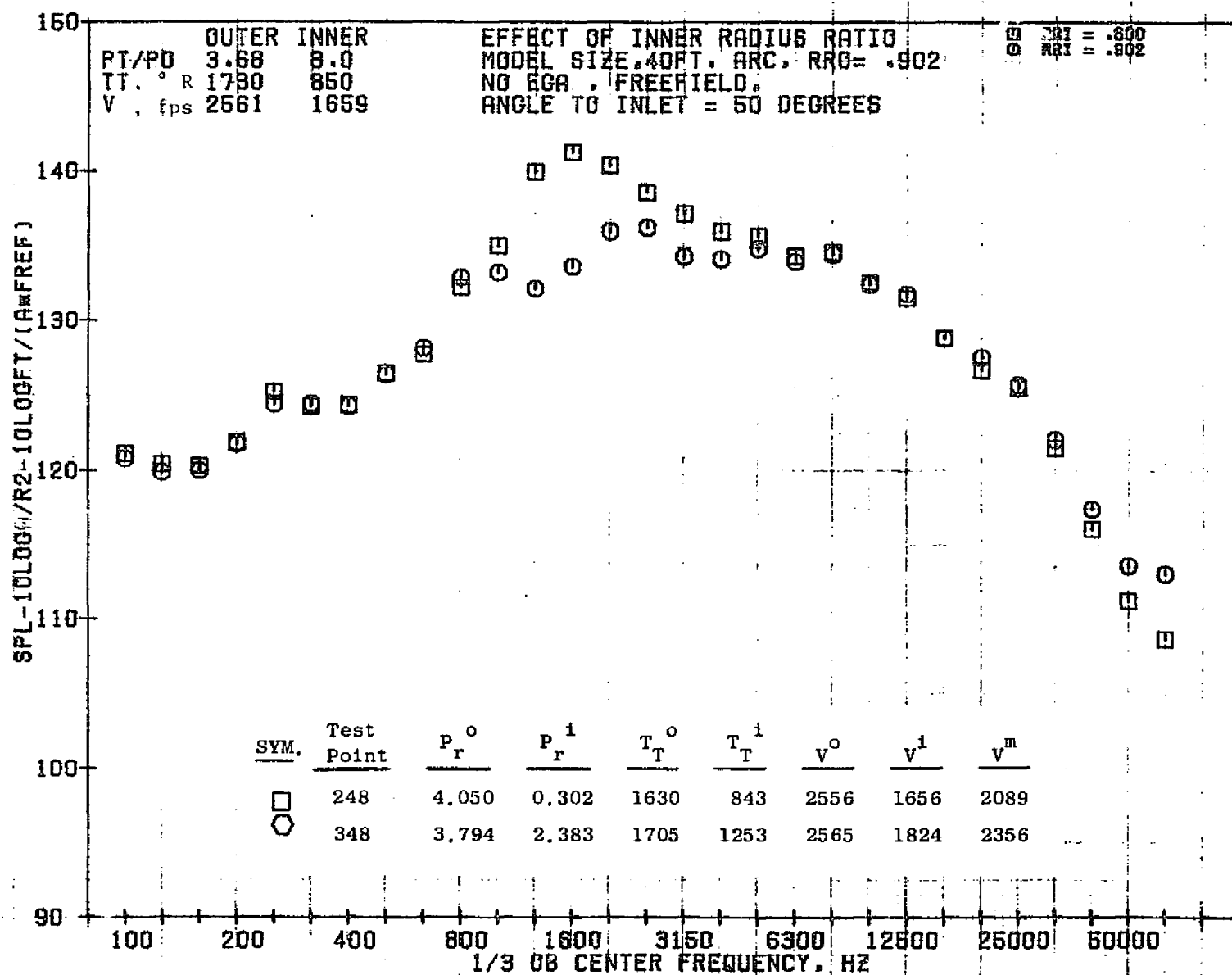
1001



10/29/76
18161-001

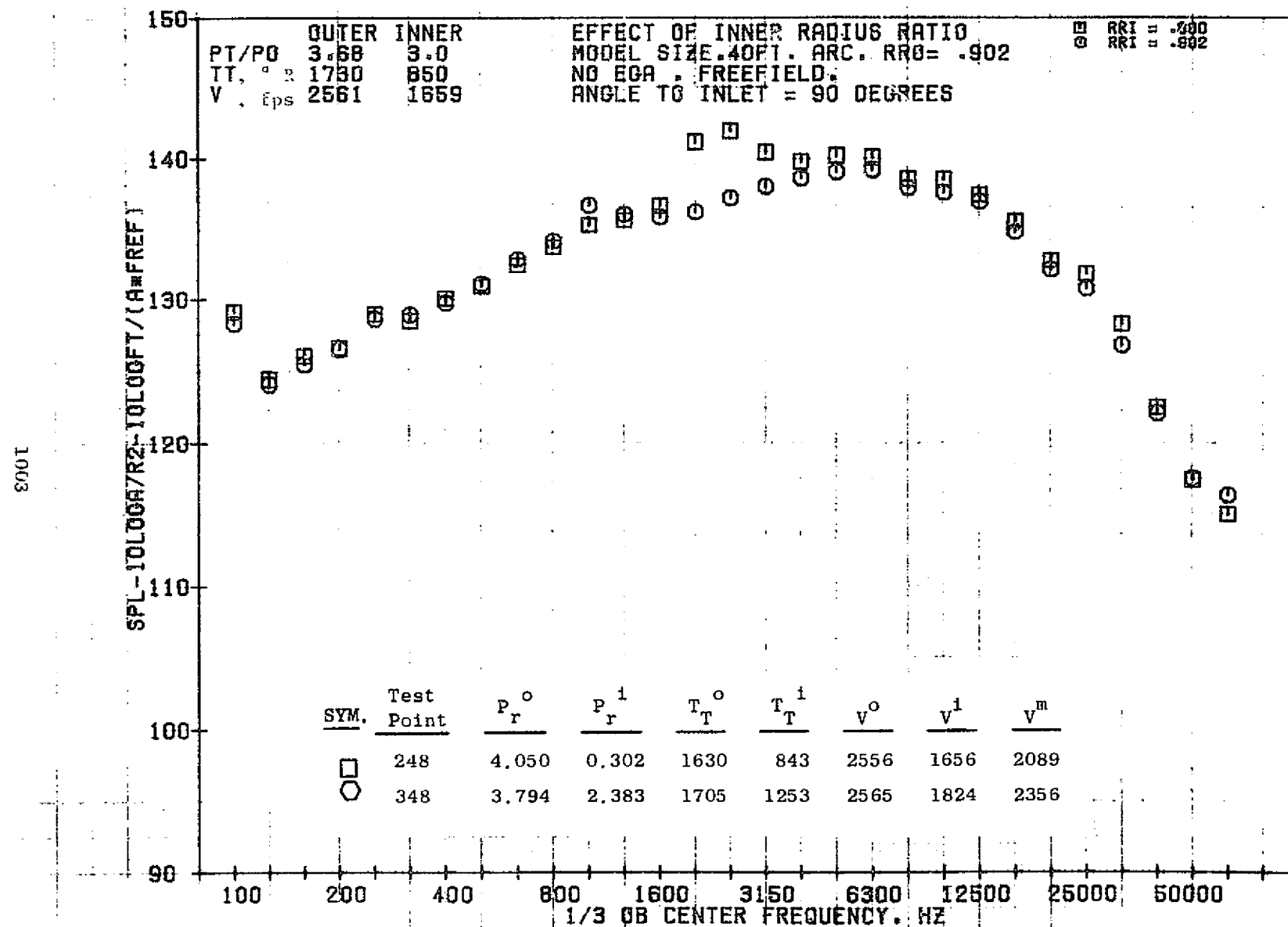
79 BURCH A.

2001



10/29/76
18161-001

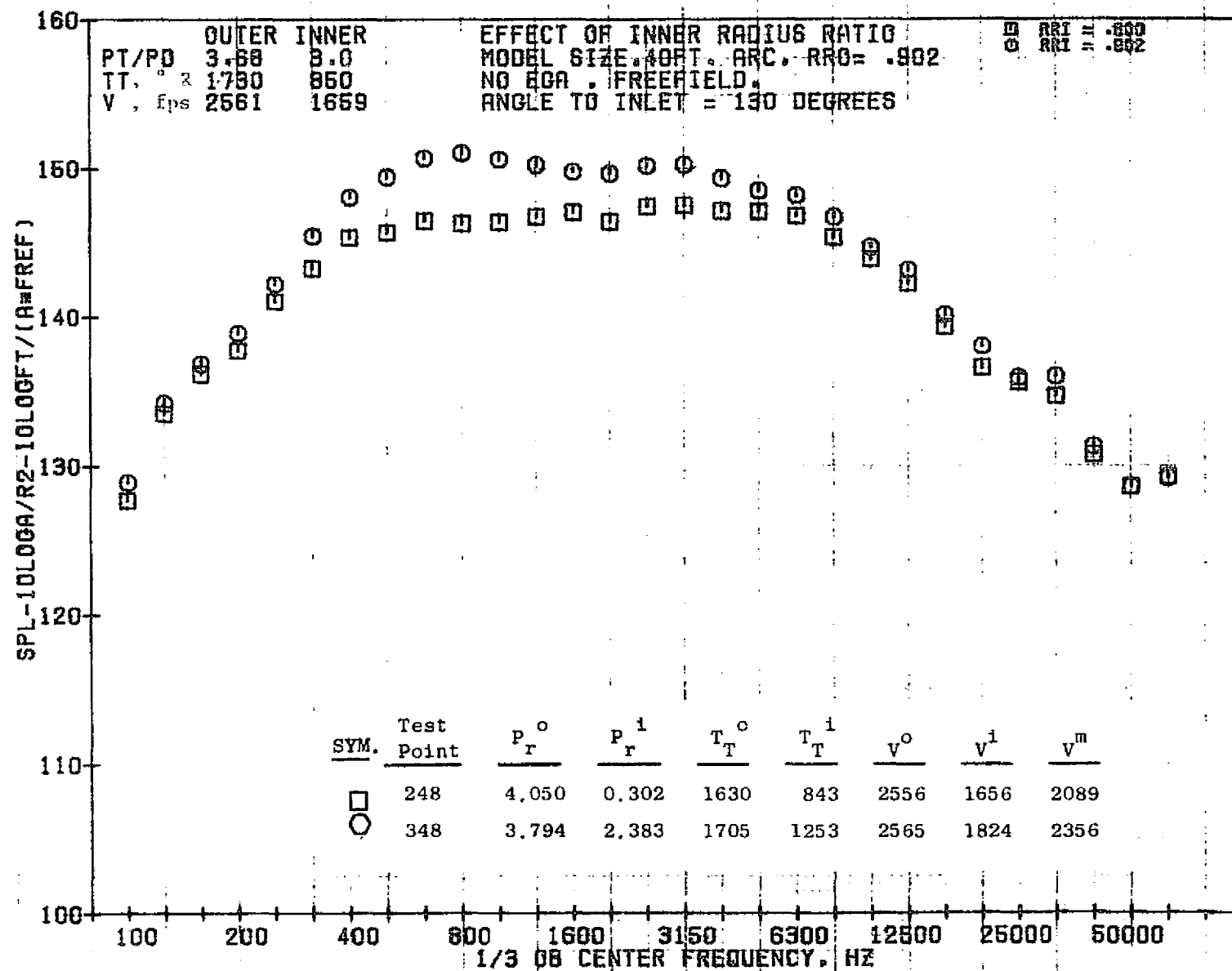
79 BURCH A.



10/29/76
18161-001

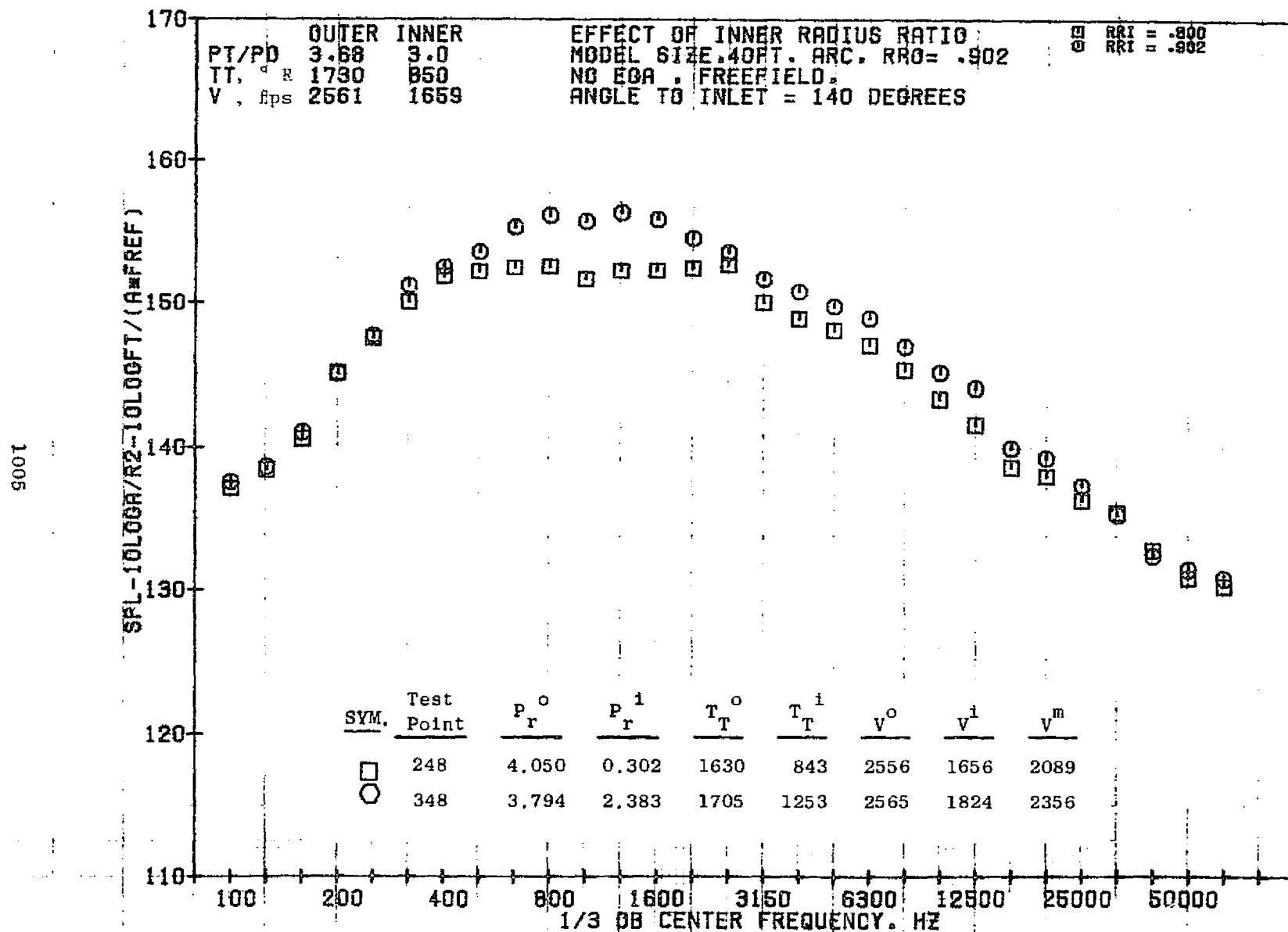
79 BURCH A.

1004



10/29/76
18161-001

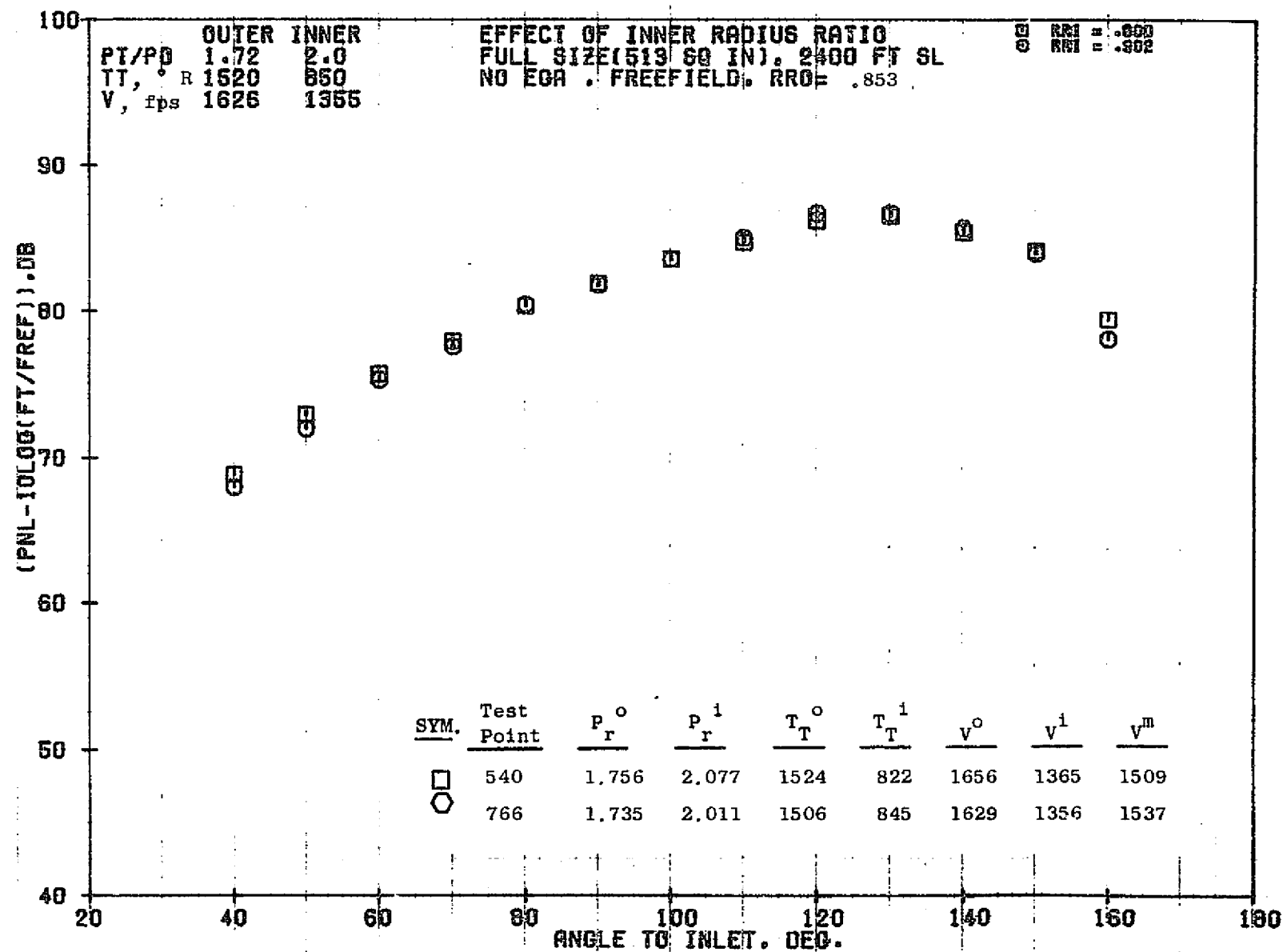
79 BURCH A.



10/29/76
18161-001

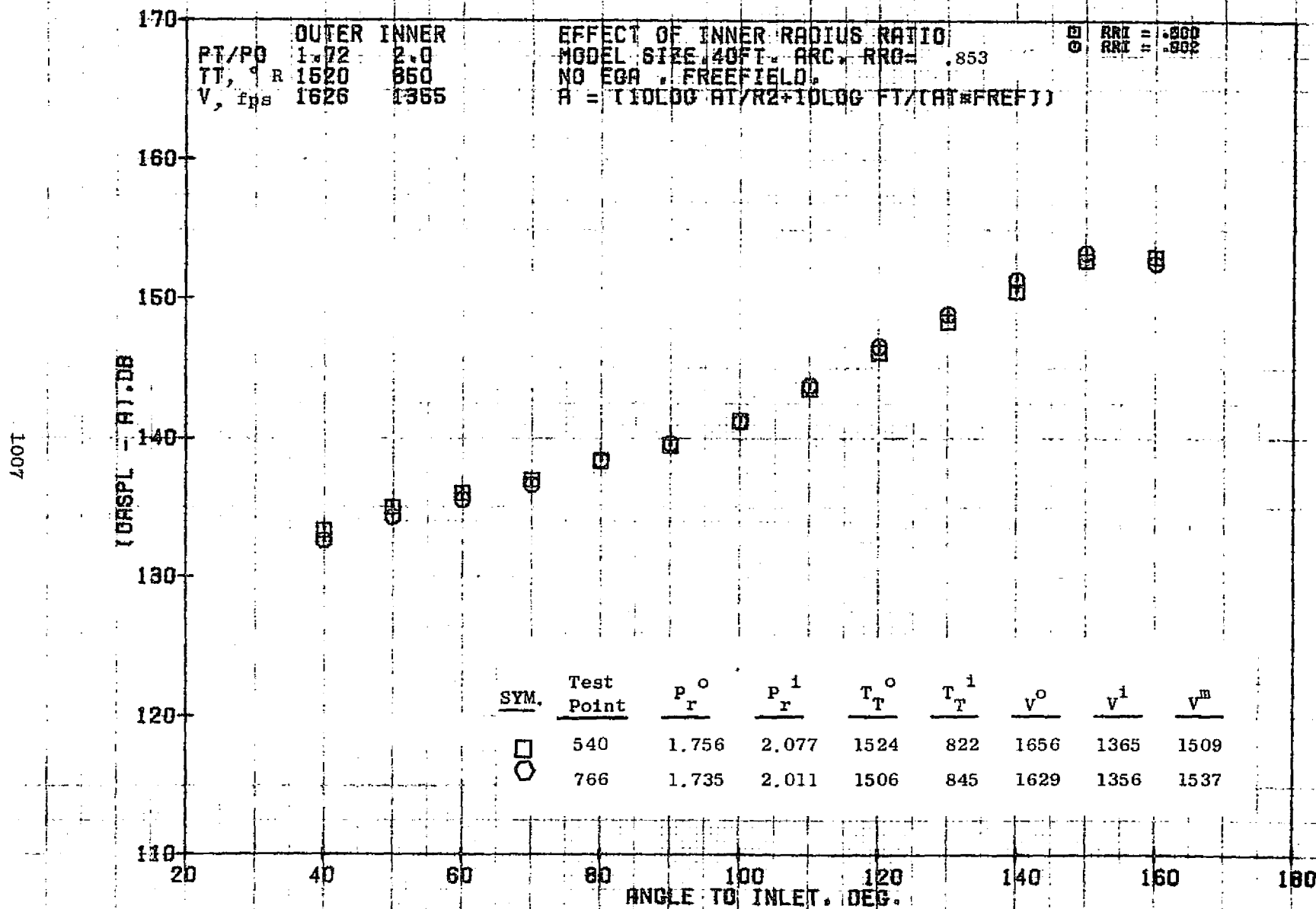
79 BURCH A.

1006



10/29/76
 18124-001

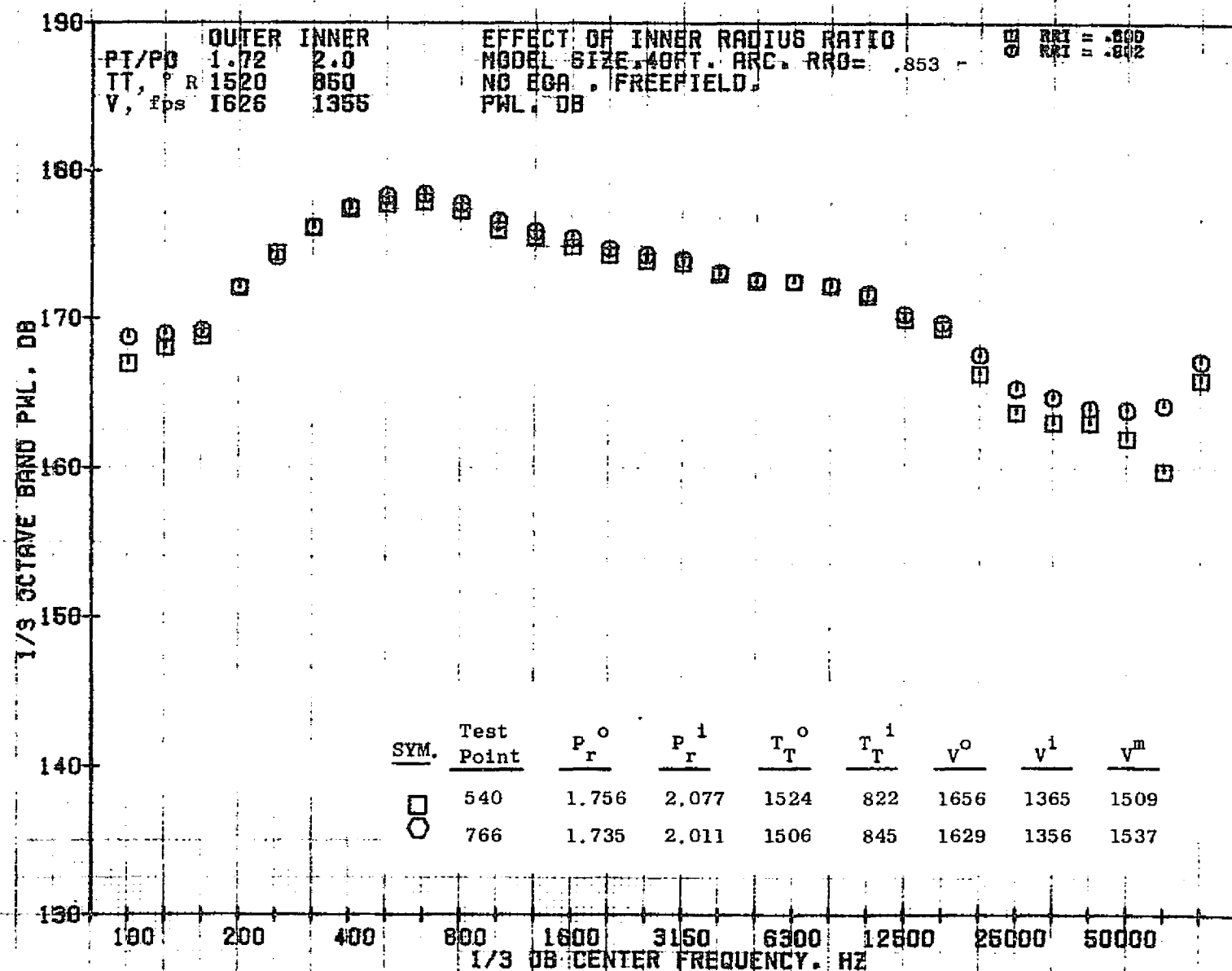
79 BURCH A.



10/29/76
18161-001

79 BURCH A.

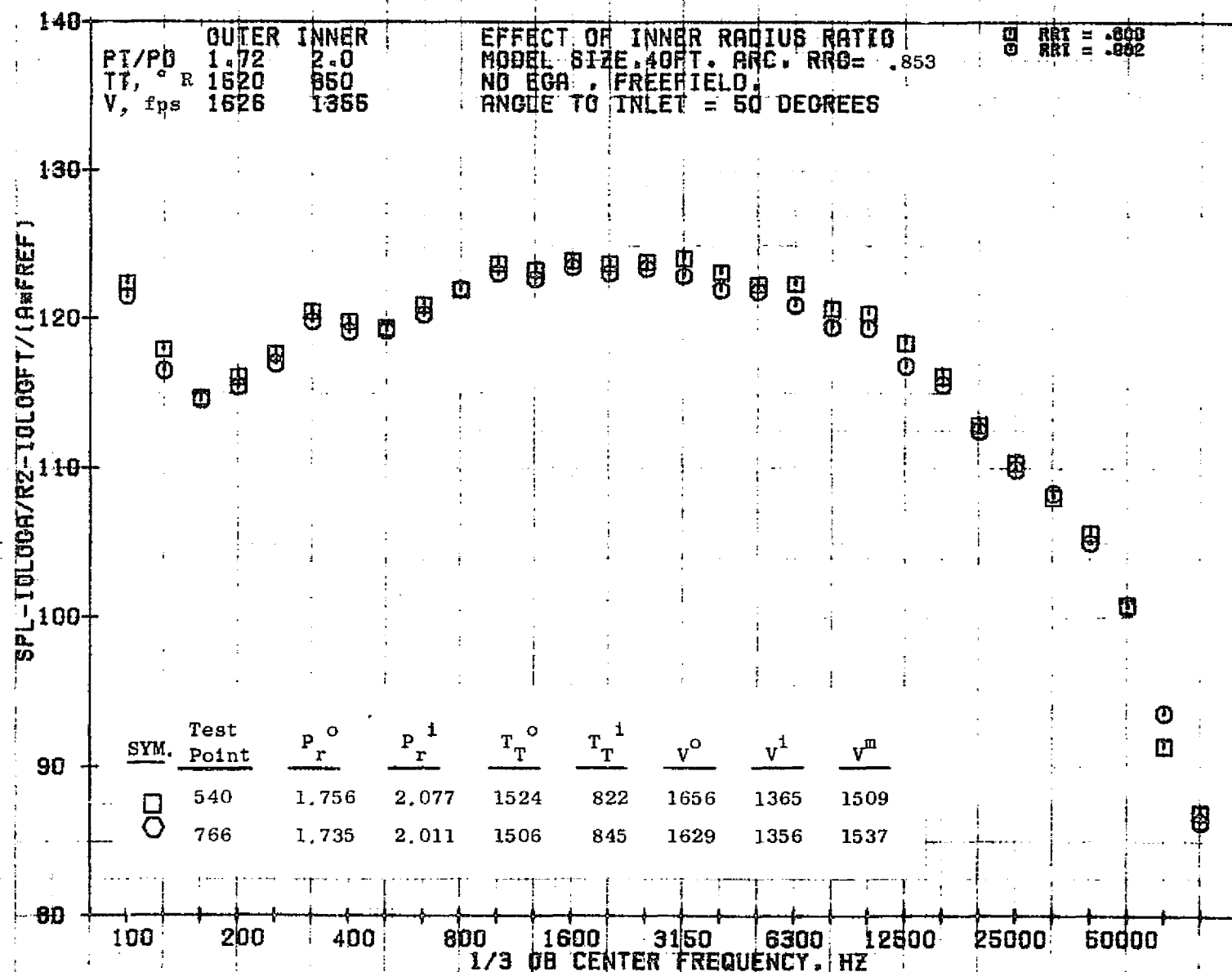
8001



10/29/76
1B161-001

79 BURCH A.

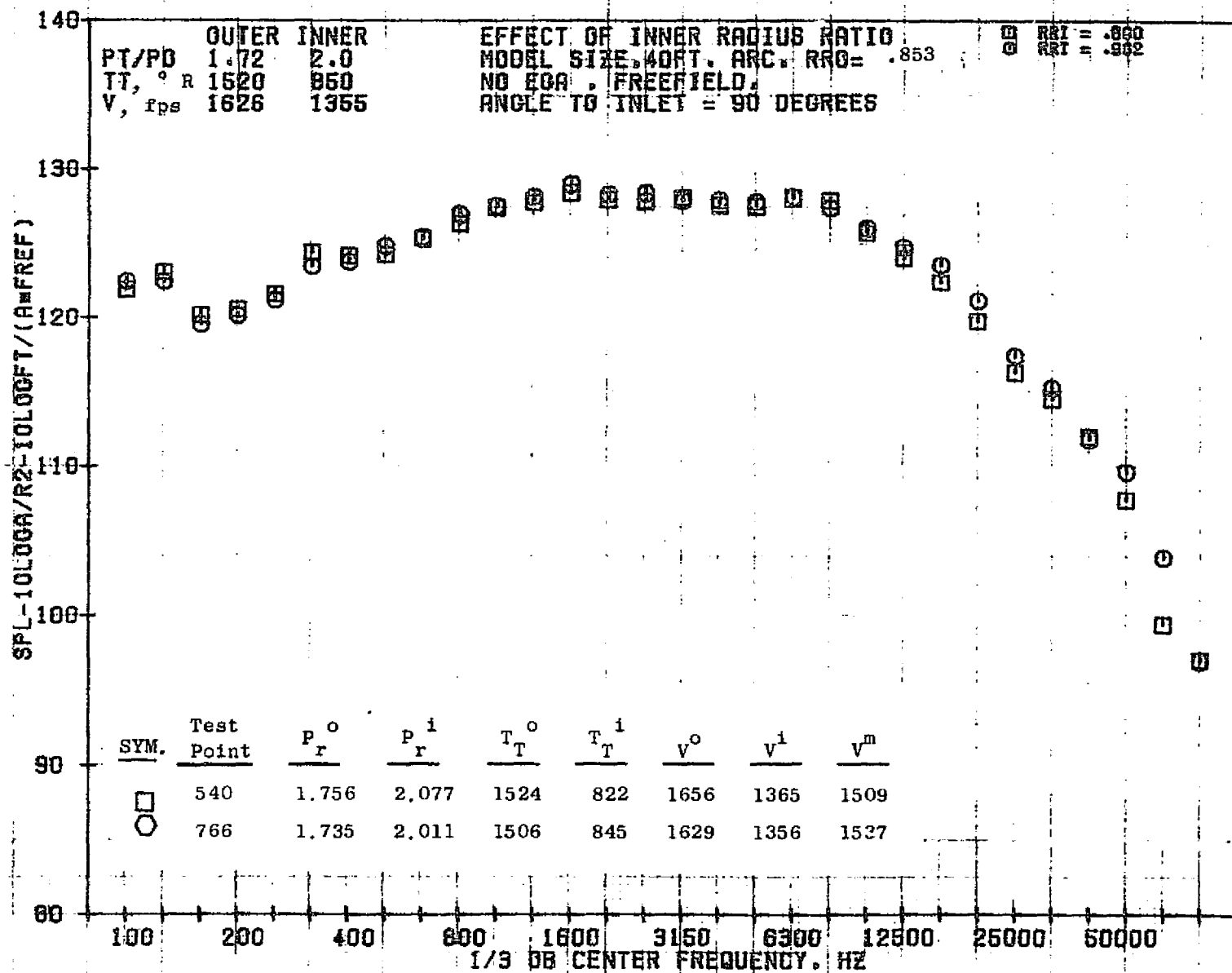
600T



10/29/76
 18161-001

79 BURCH A.

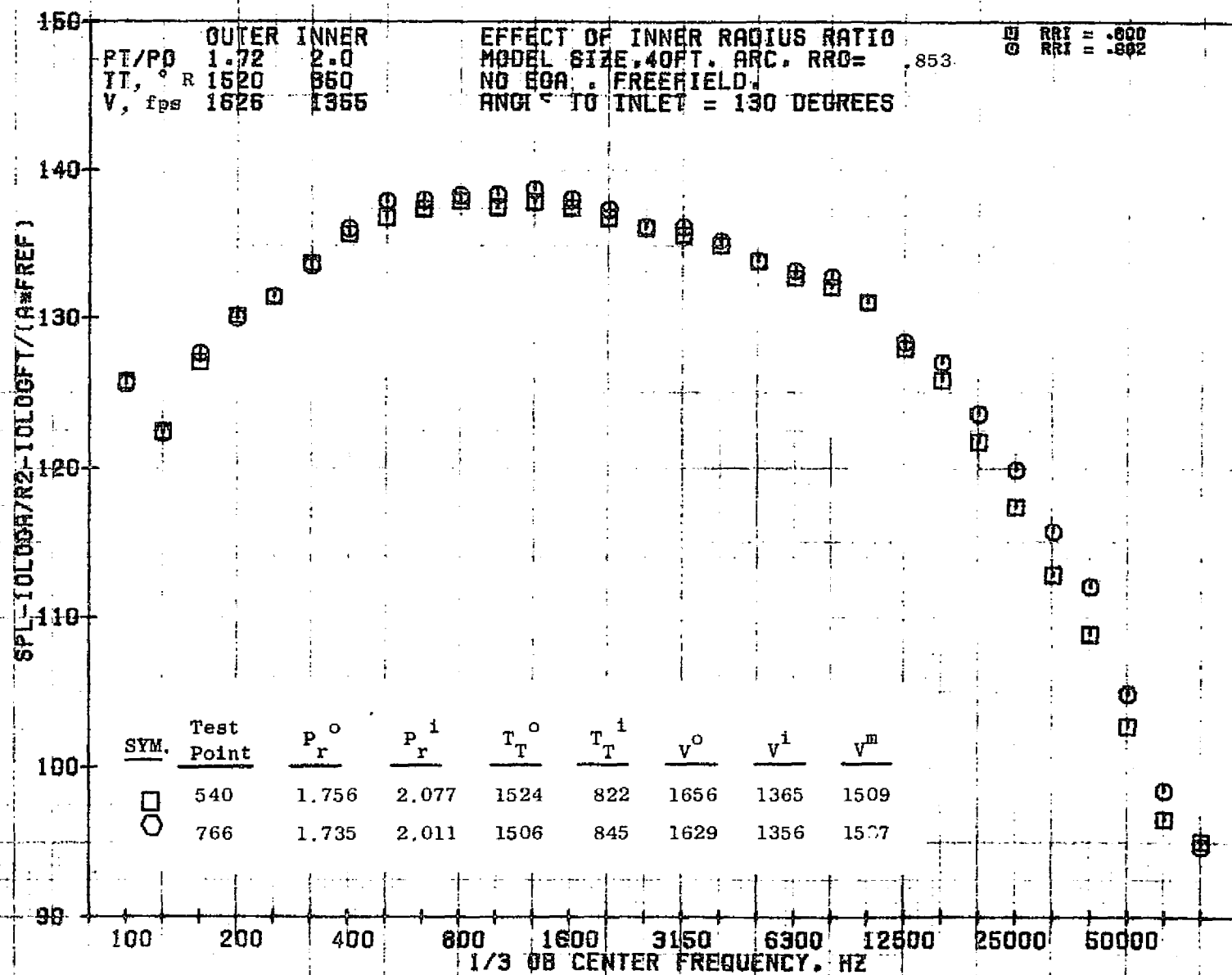
0101



10/29/76
 18161-001

79 BURCH A.

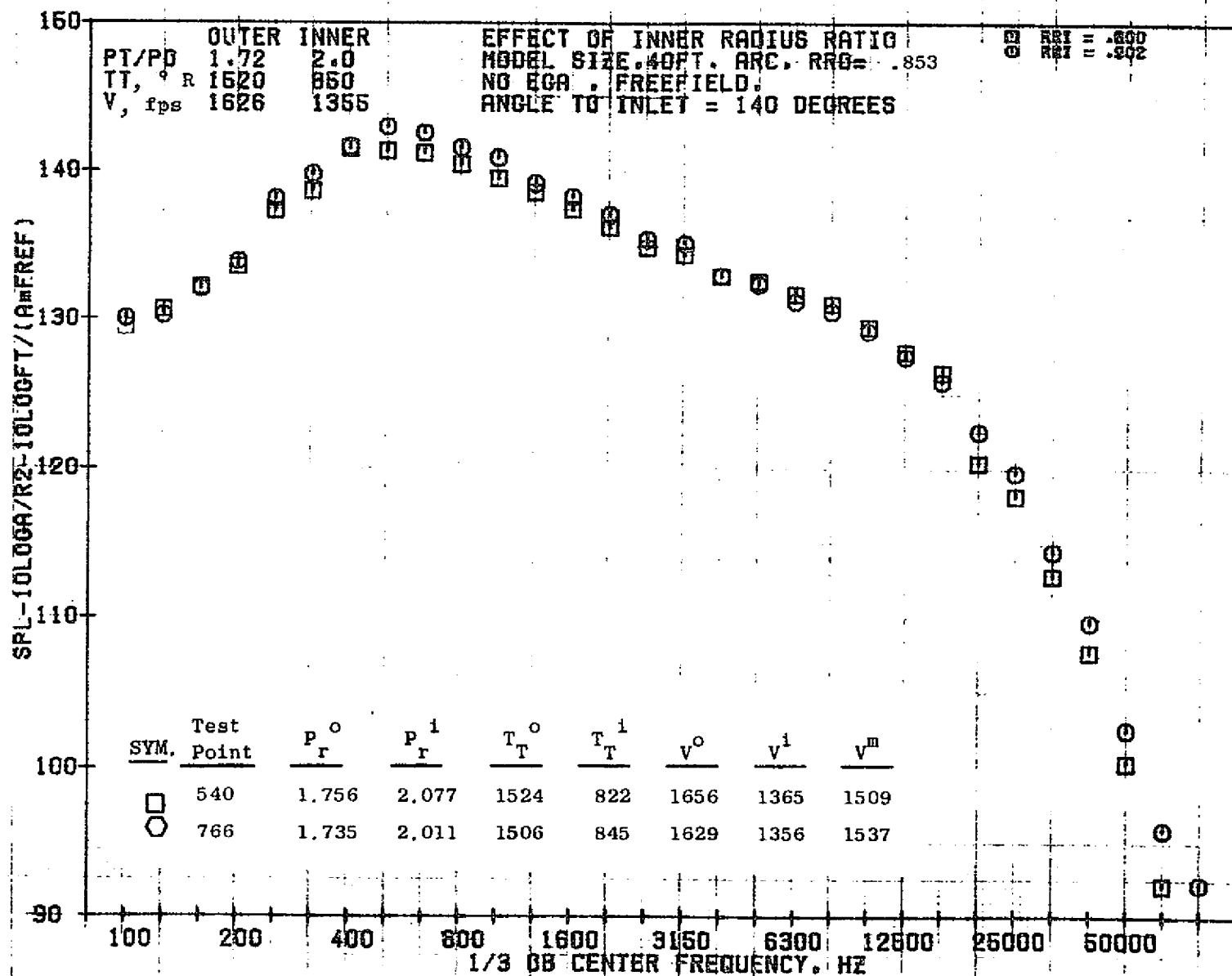
1101



10/29/76
18161-001

79 BURCH A.

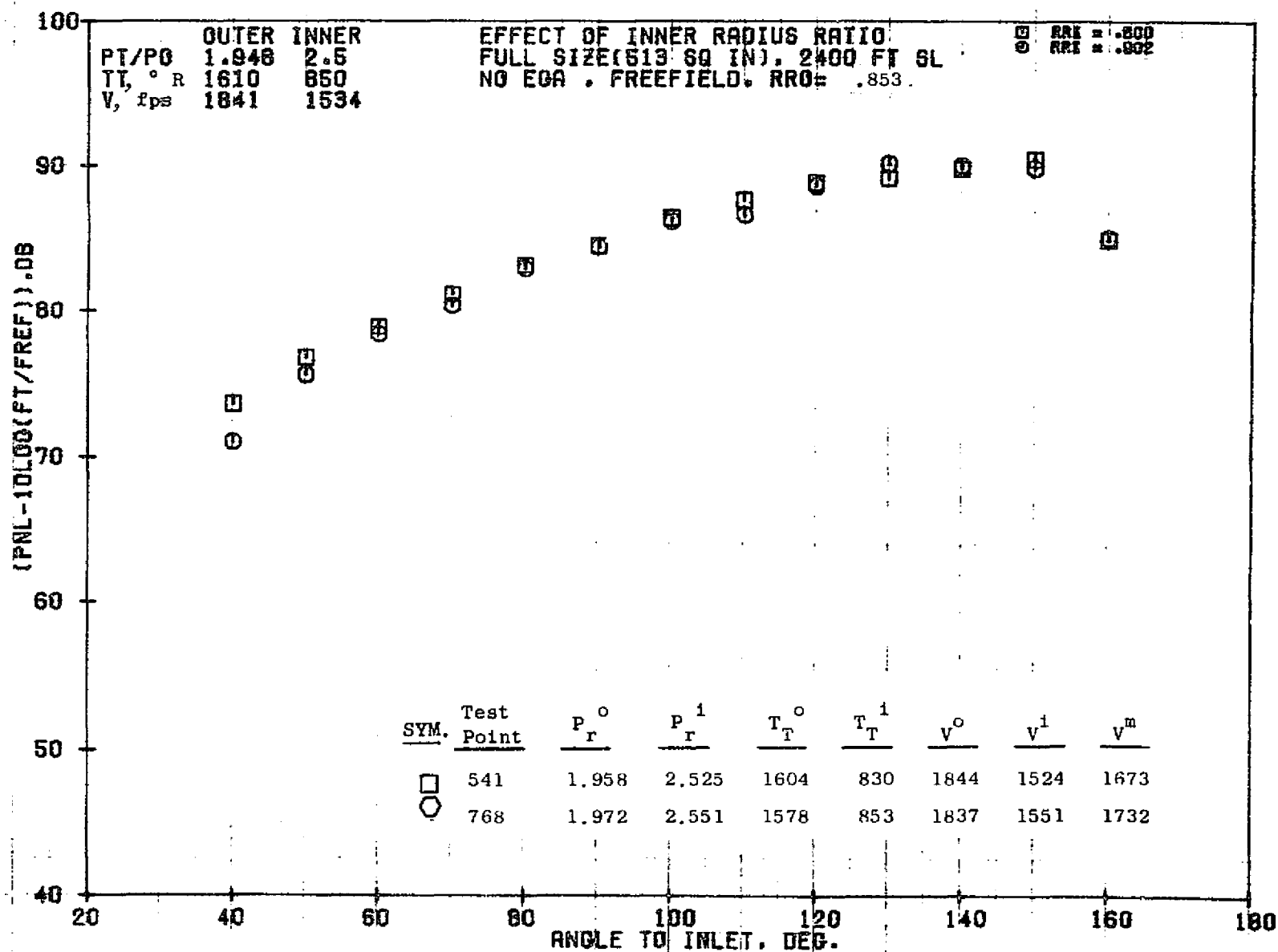
1012



10/29/76
 18161-001

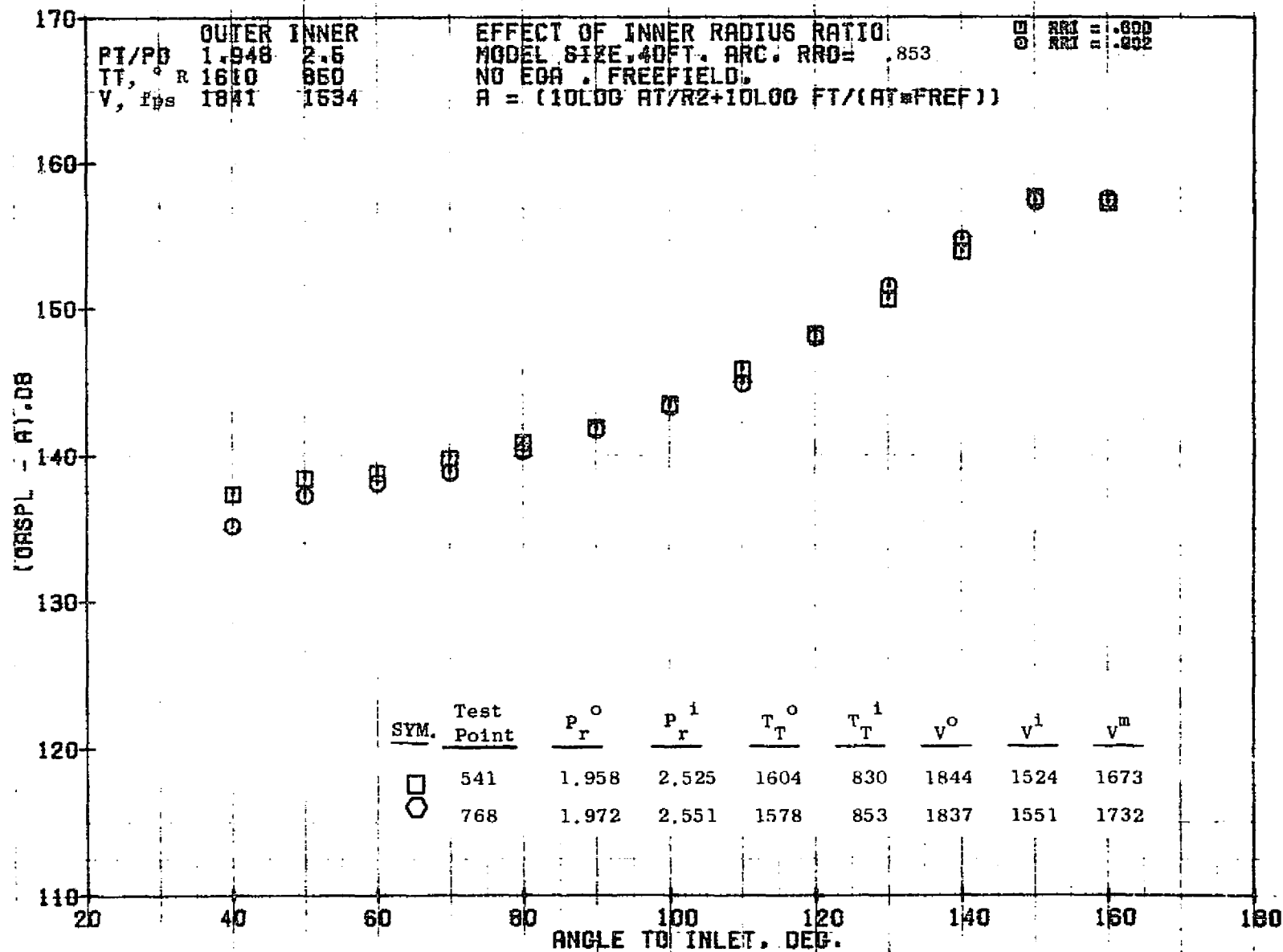
79 BURCH A.

1013



10/29/76
18124-001

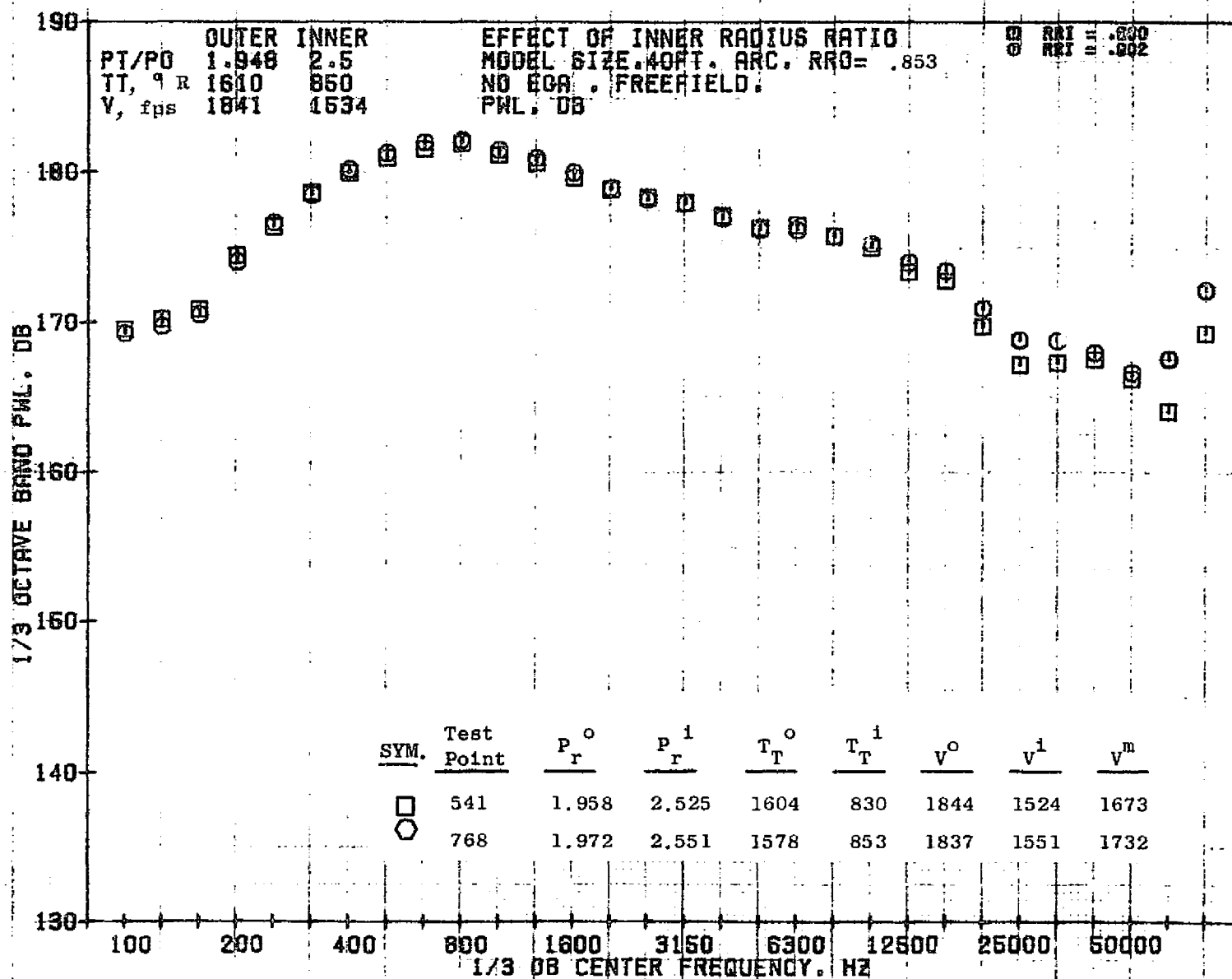
79 BURCH



10/29/76
18161-001

79 BURCH A.

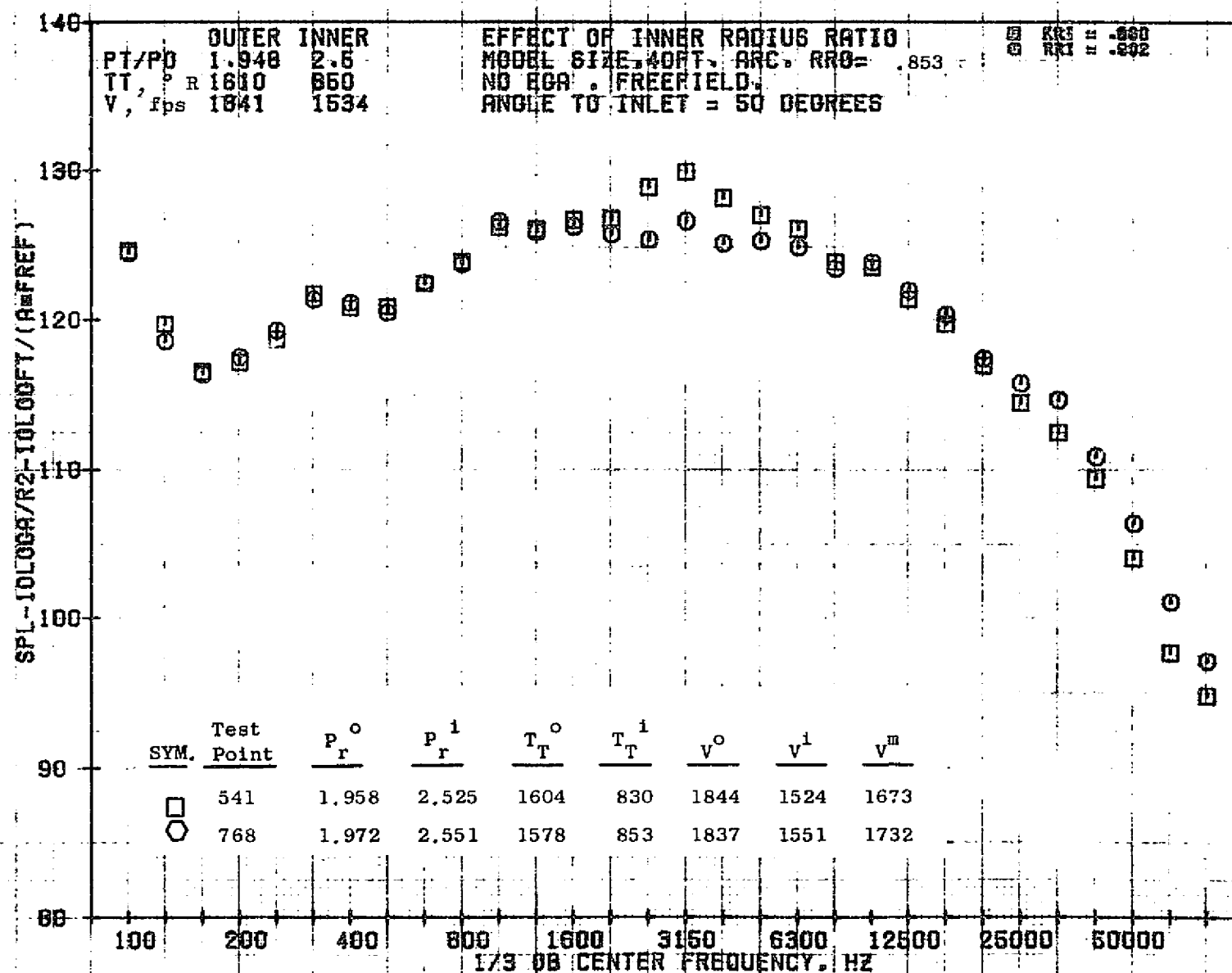
1015



10/29/76
 18161-001

79 BURCH A.

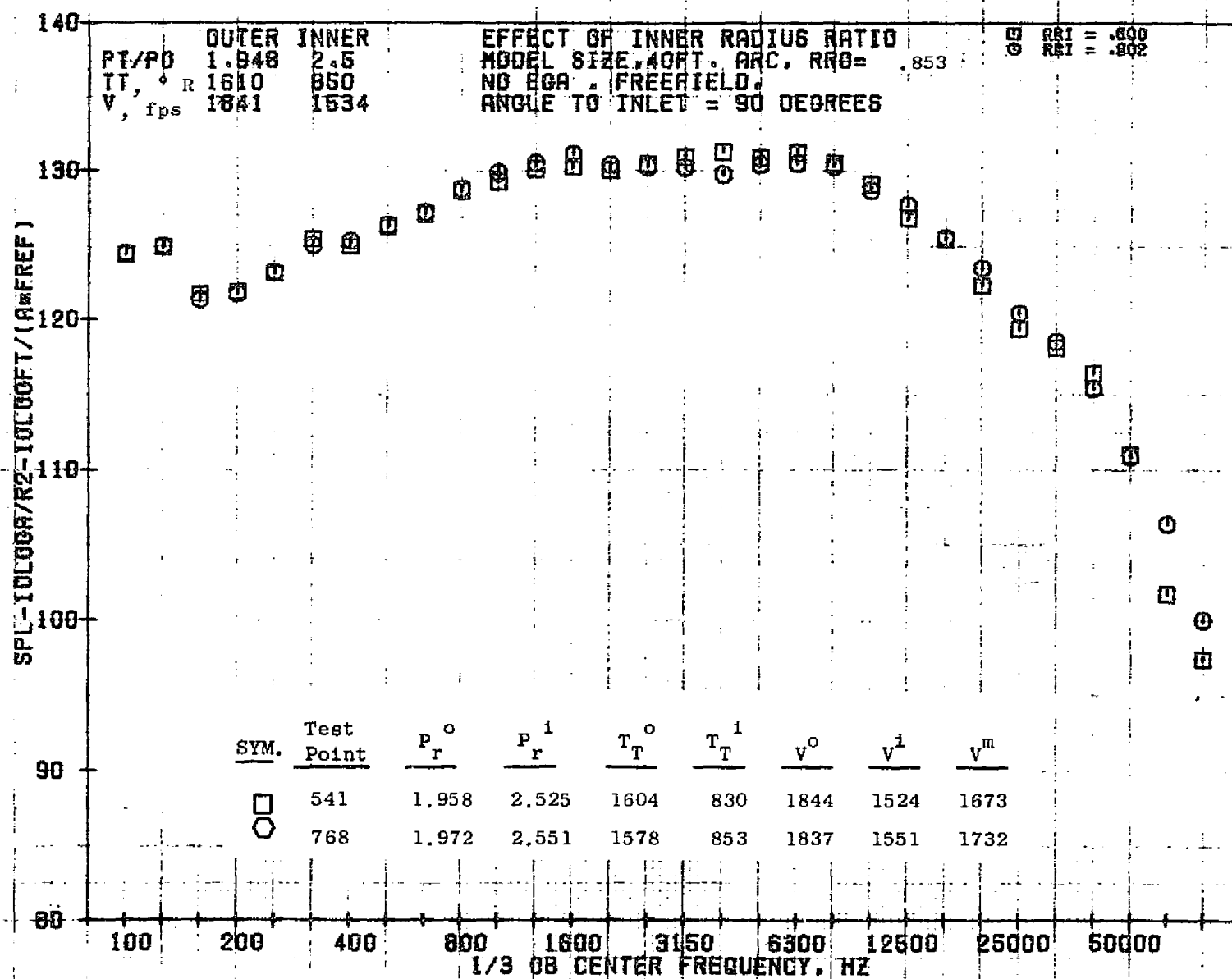
9101



10/29/76
 18161-001

79 BURCH A.

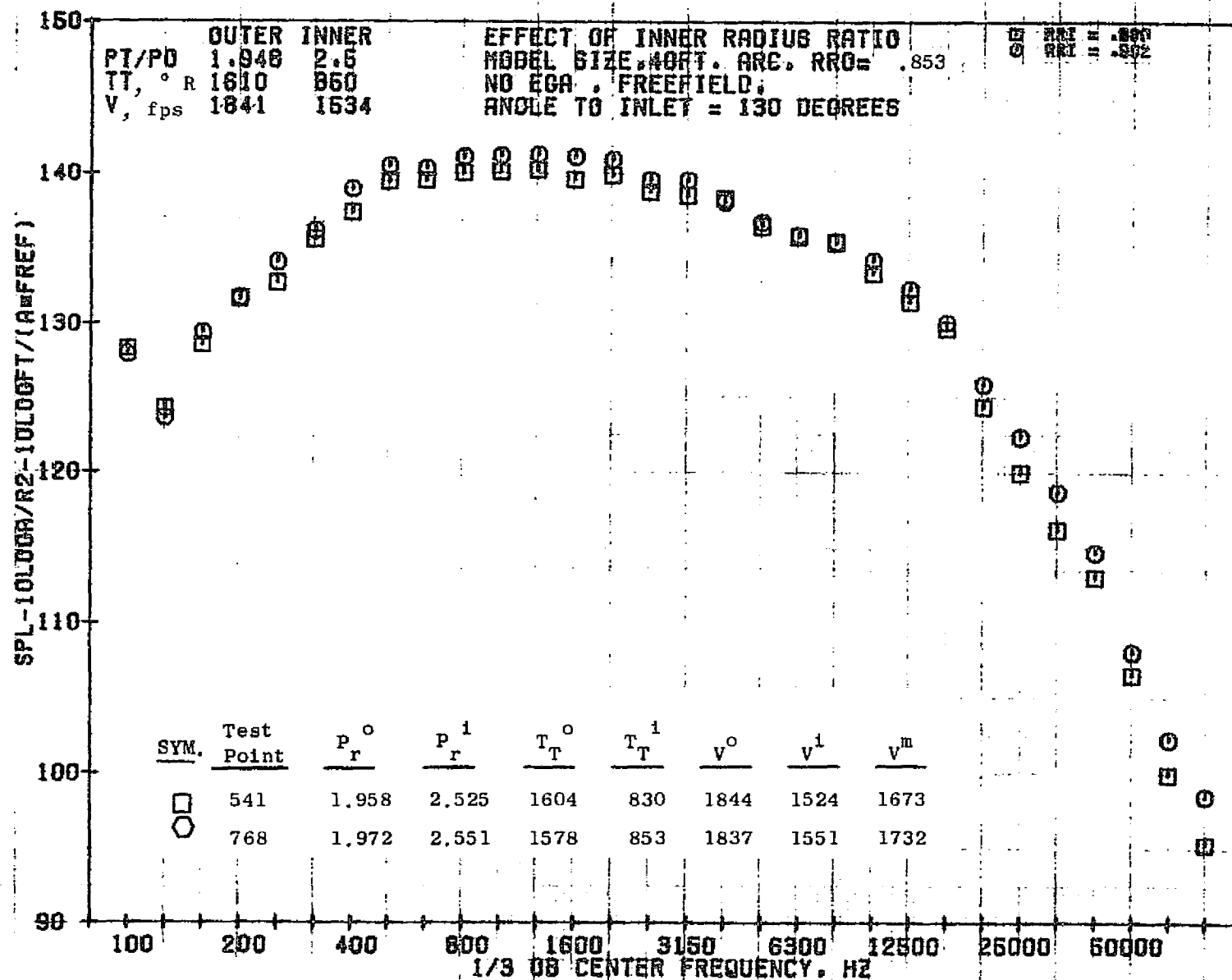
1017



10/29/76
18161-001

79 BURCH A.

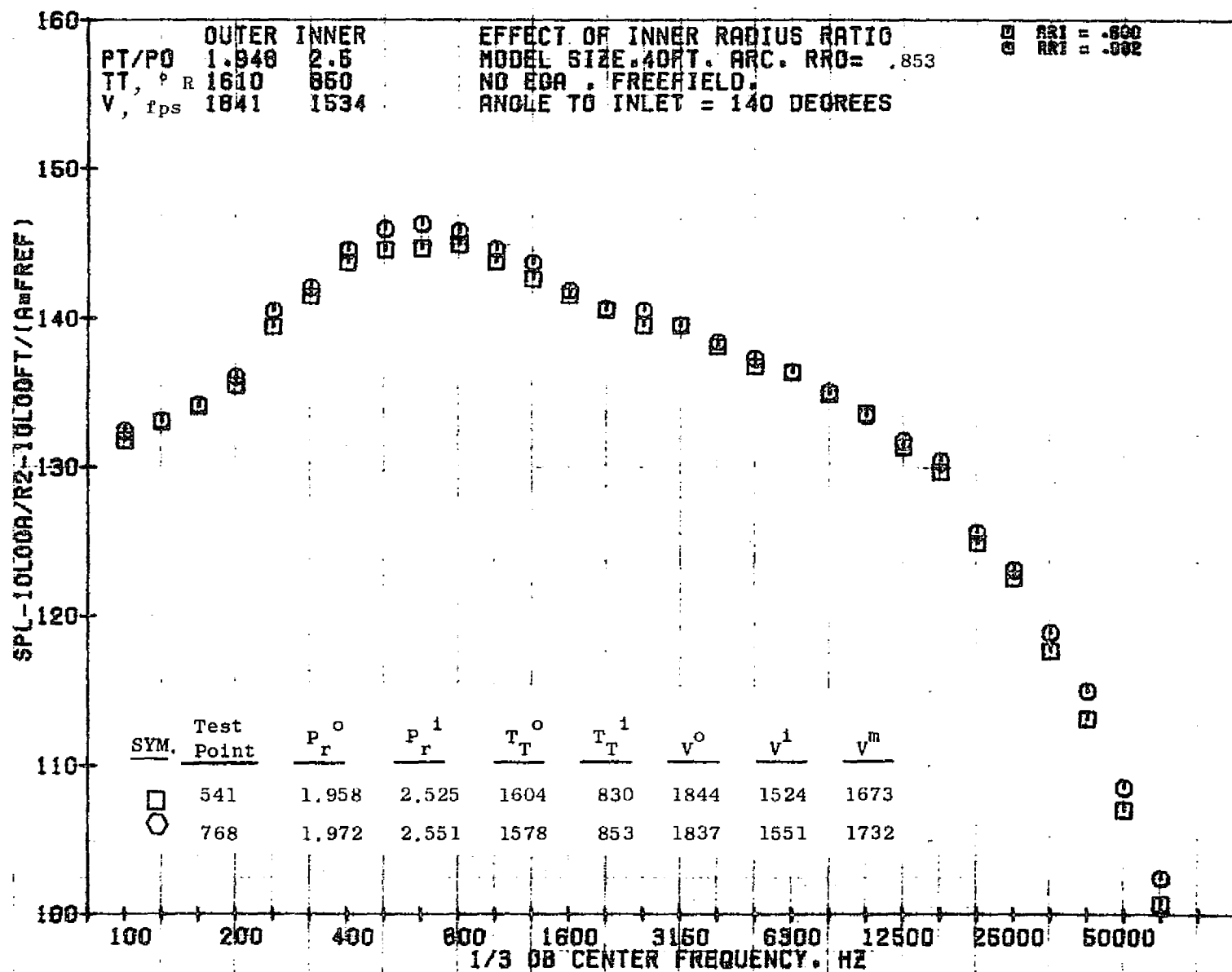
1018



10/29/76
 18161-001

79 BURCH A.

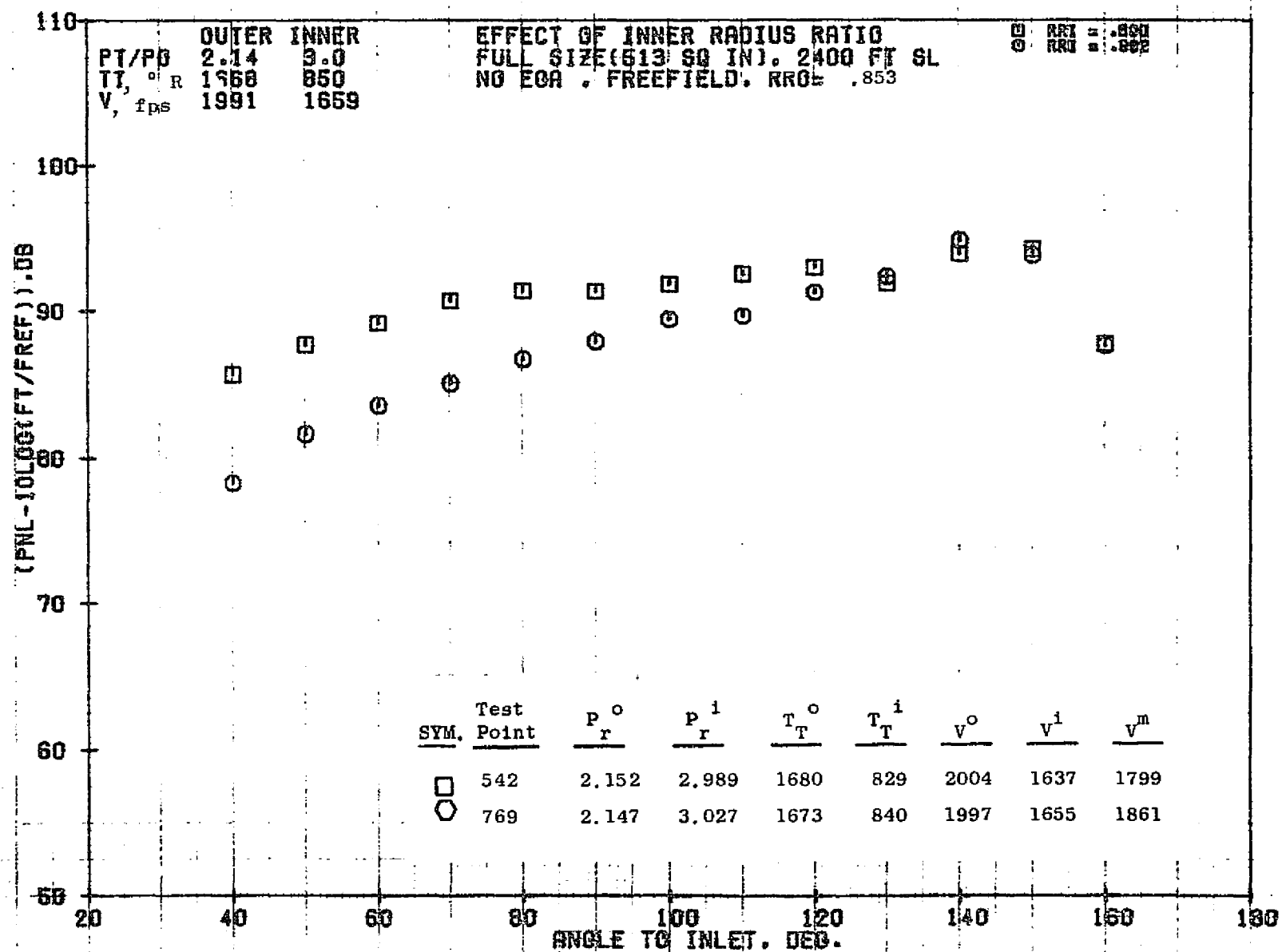
6101



10/29/76
18161-001

79 BURCH A.

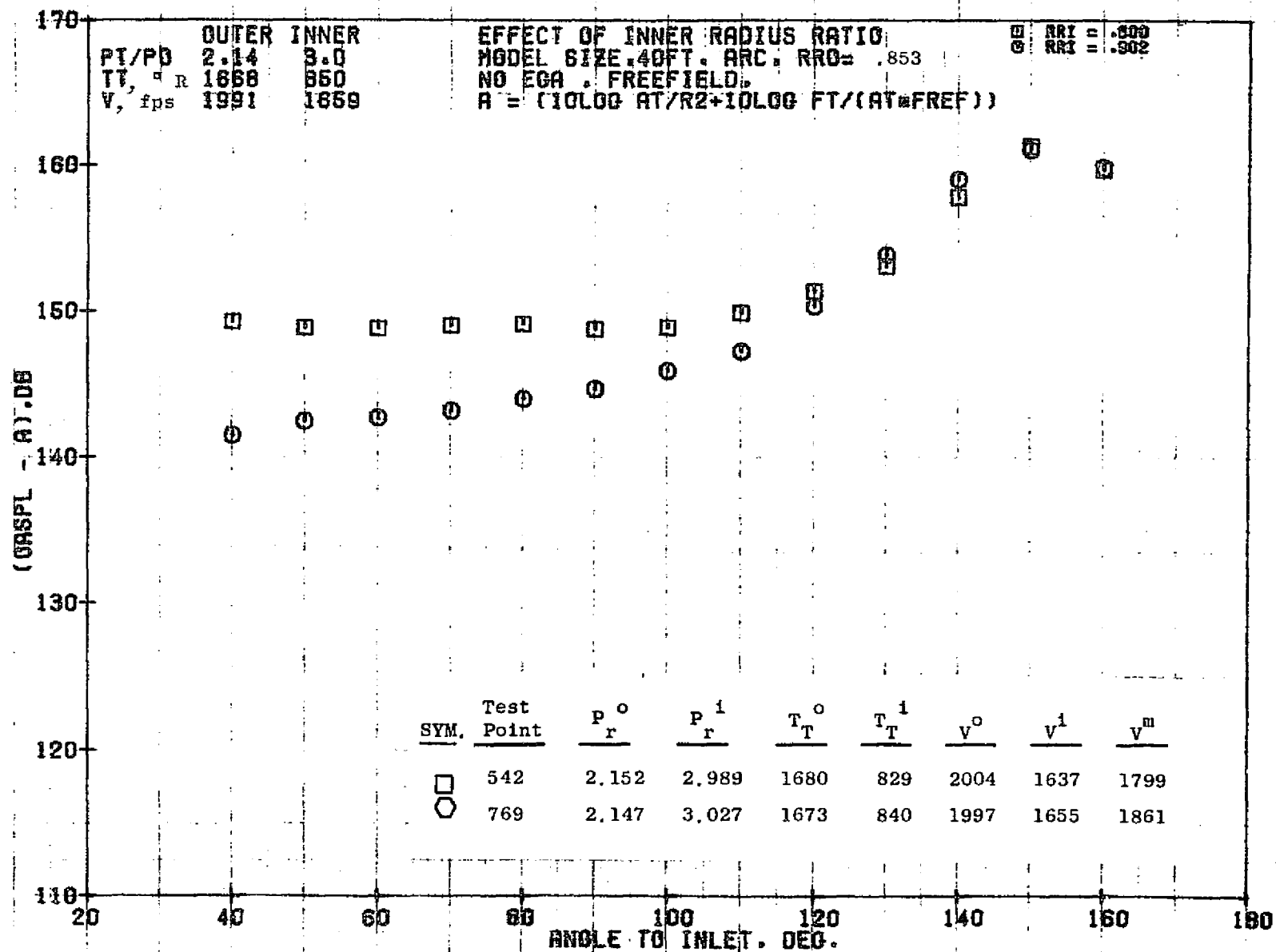
1020



10/29/76
18124-001

79 BURCH A.

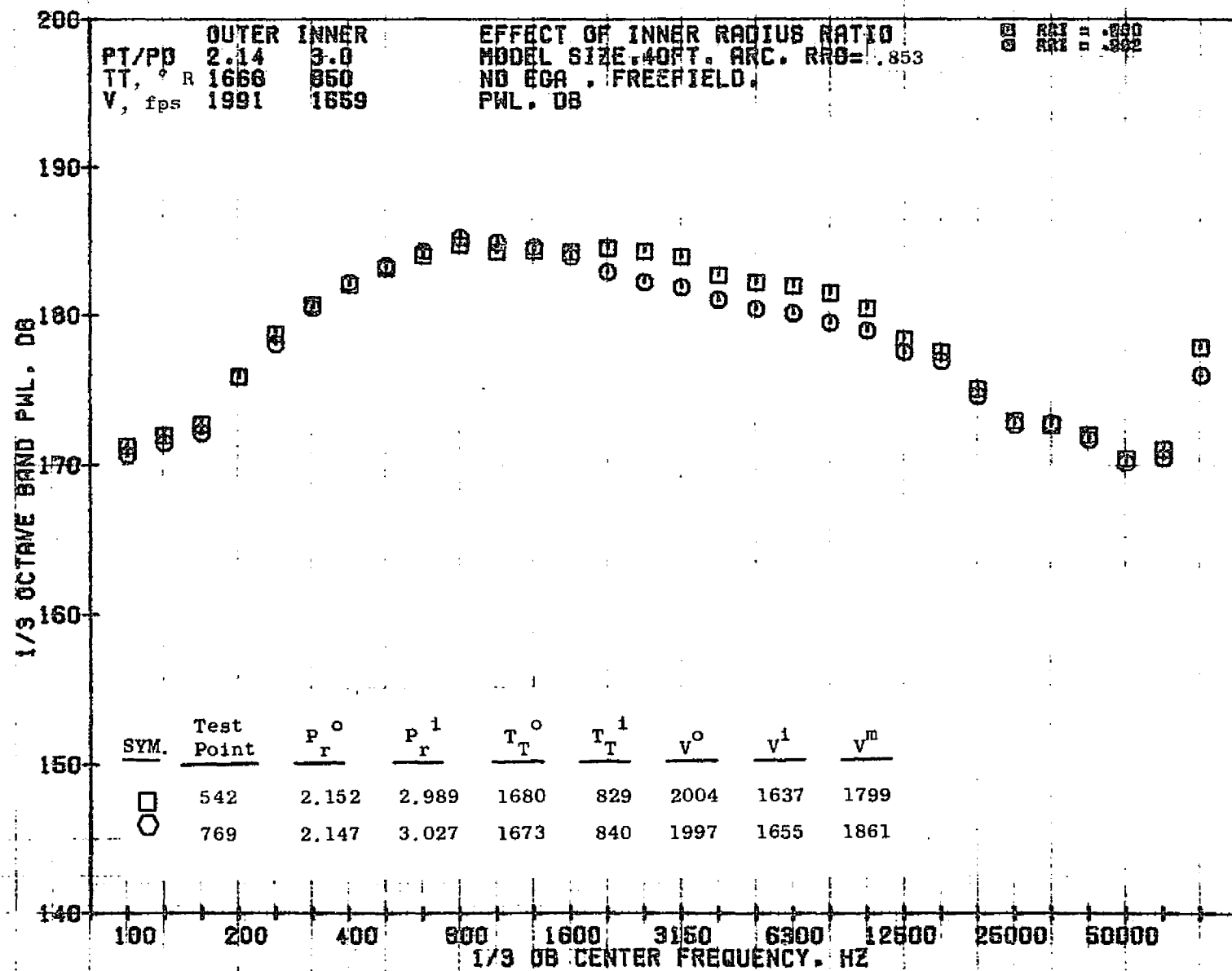
1021



10/29/76
18161-001

79 BURCH A.

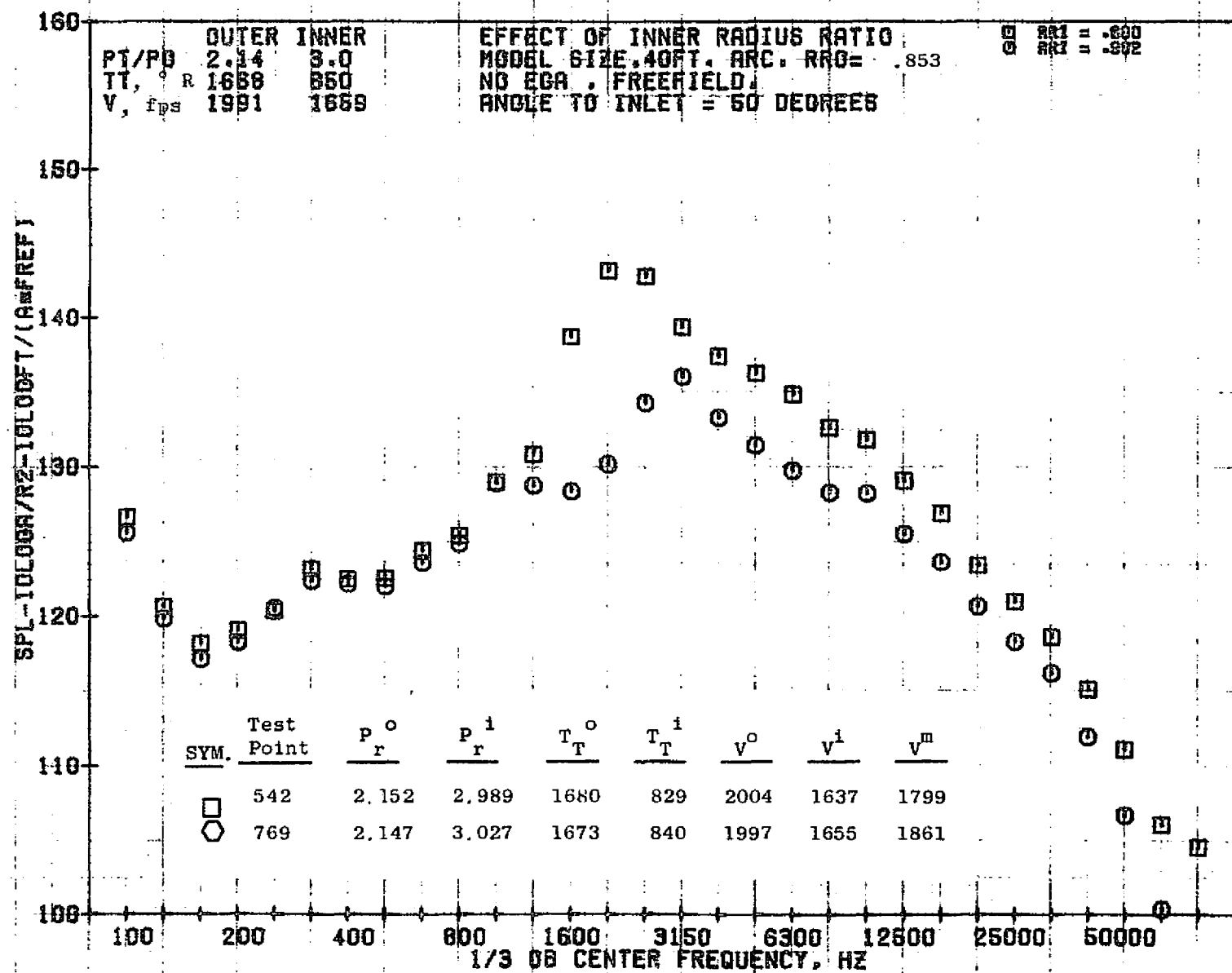
1022



10/29/76
18161-001

79 BURCH A.

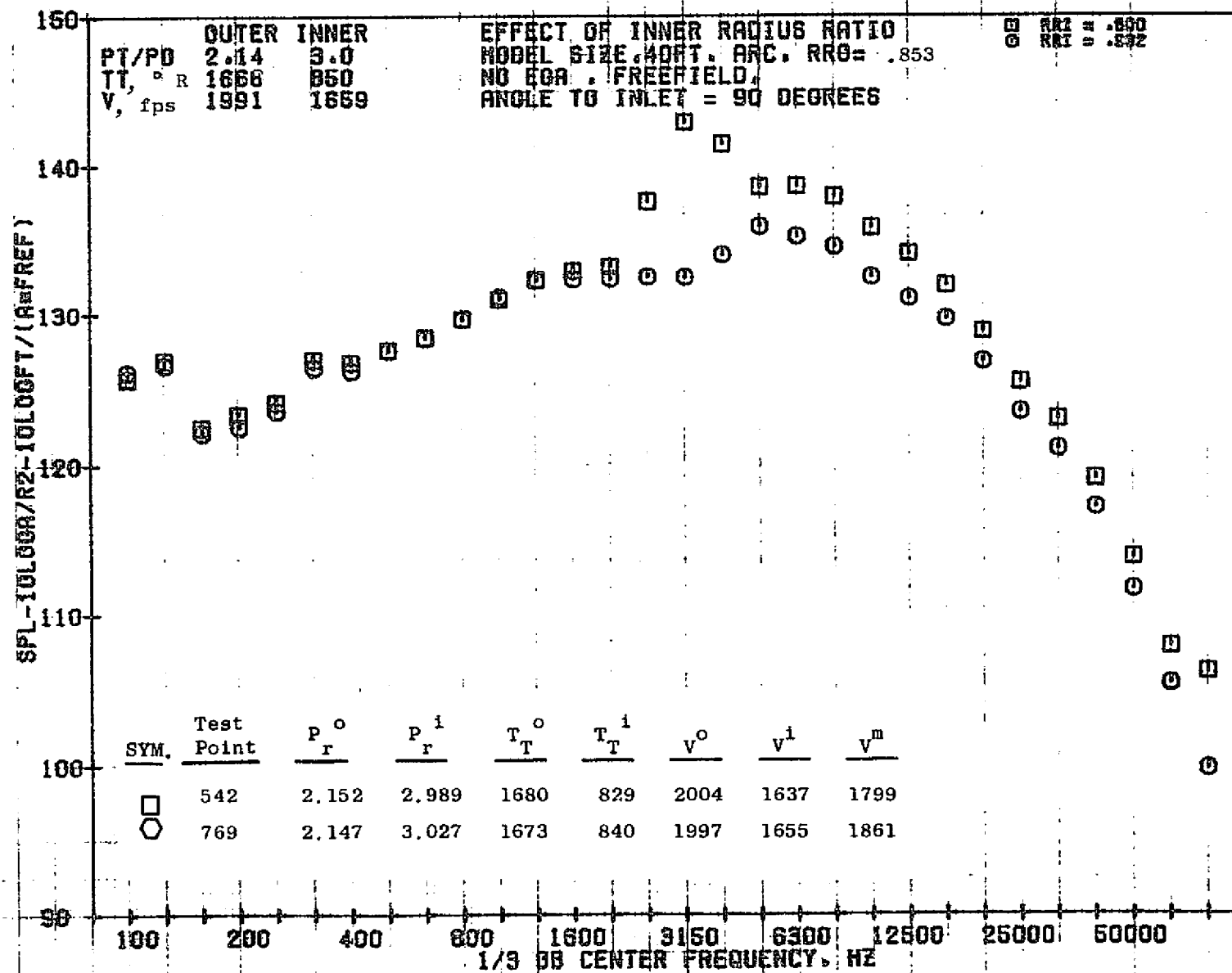
1023



10/29/76
 1B161-001

79 BURCH A.

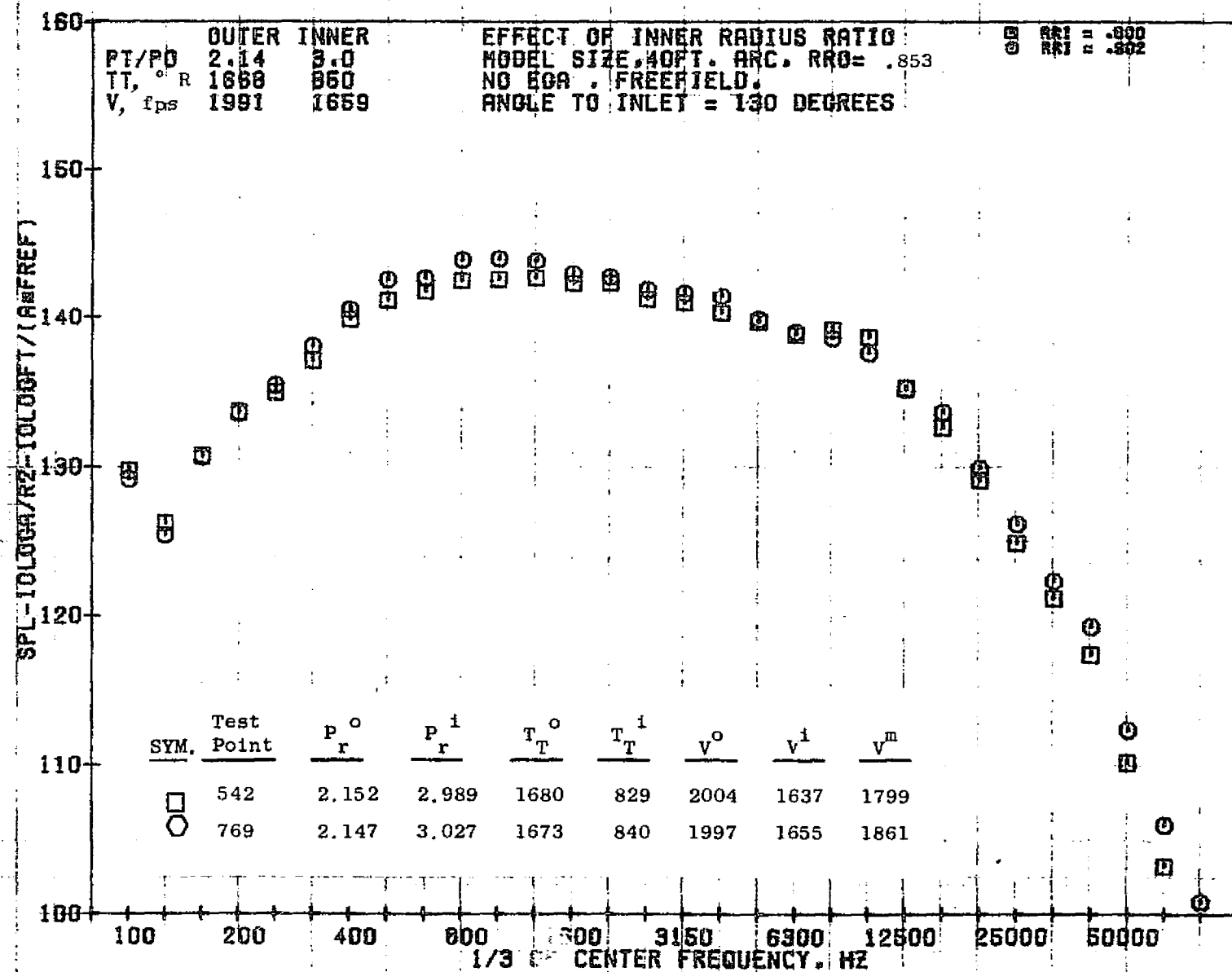
1024



10/29/76
 19161-001

79 BURCH A.

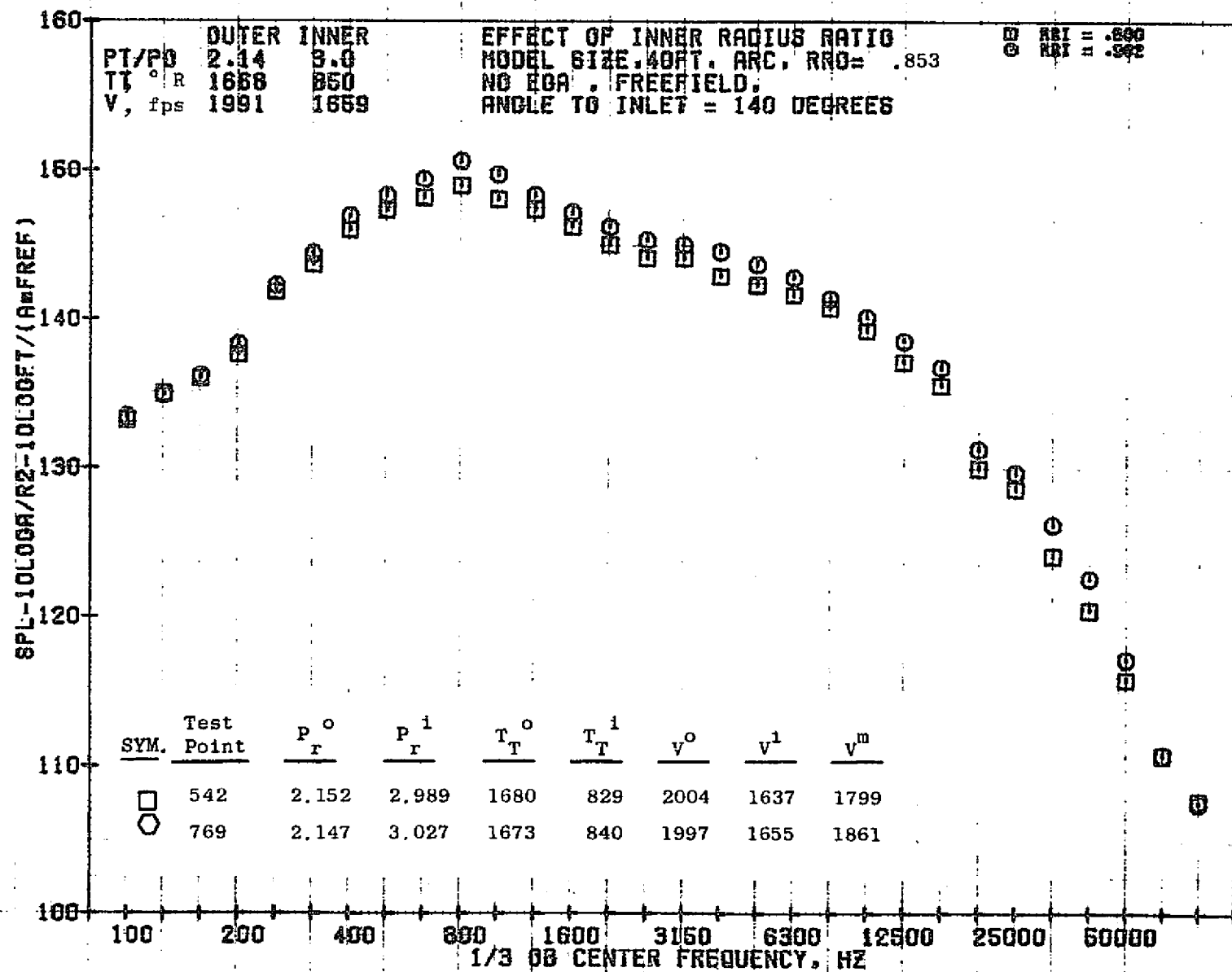
1025



10/29/76
18161-001

79 BURCH A.

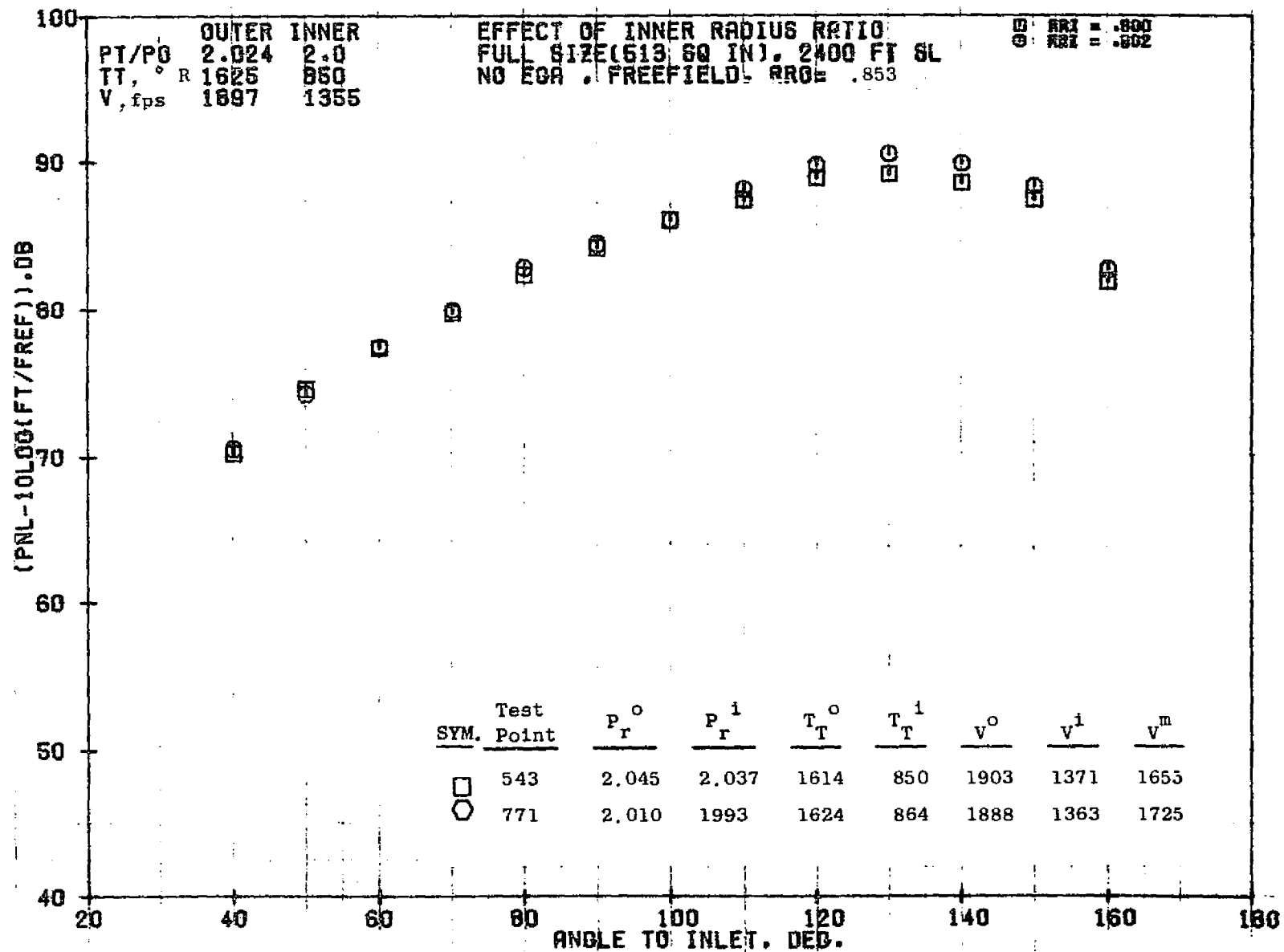
1026



10/29/78
 1B161-001

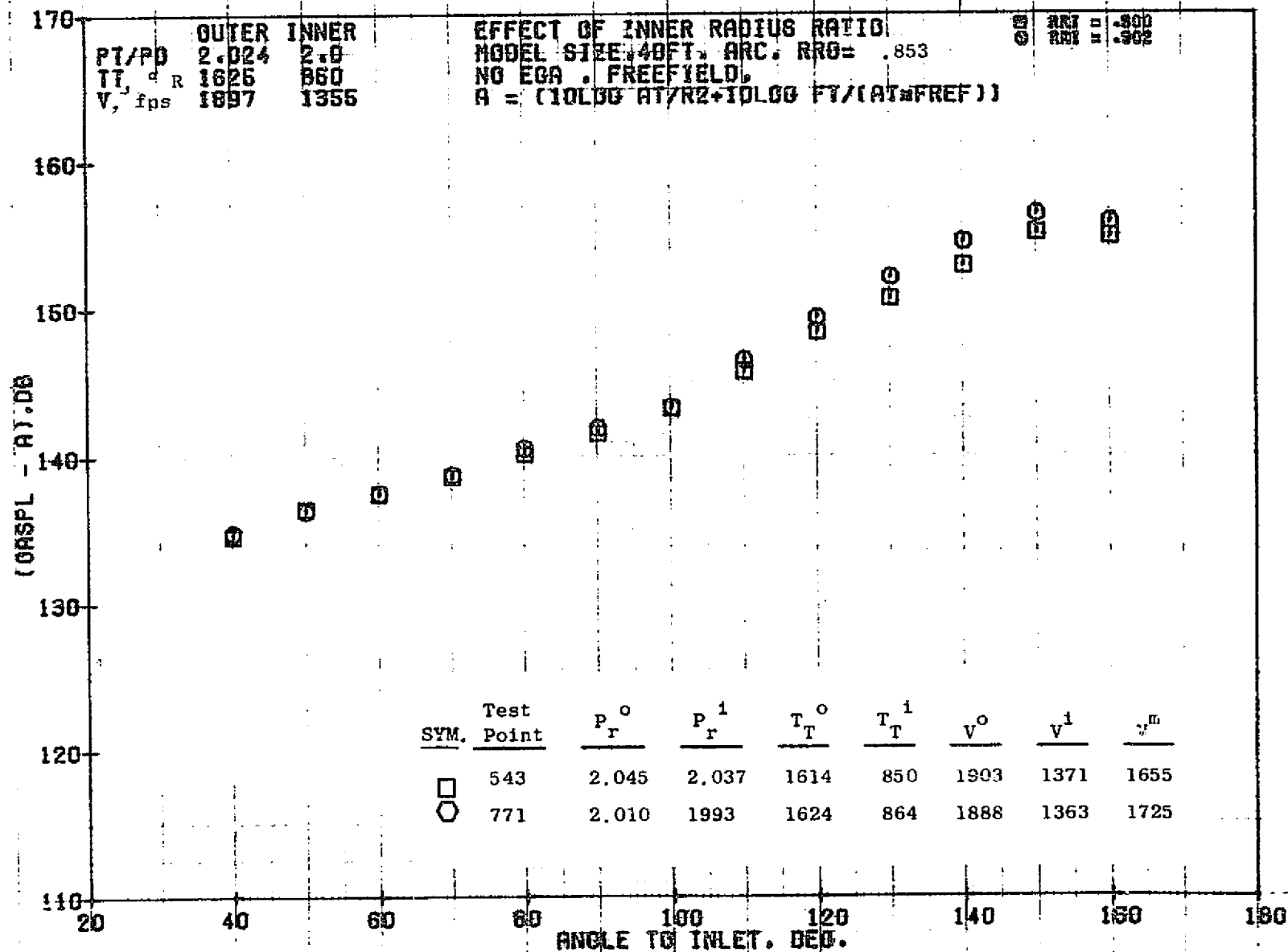
79 BURCH A.

1027



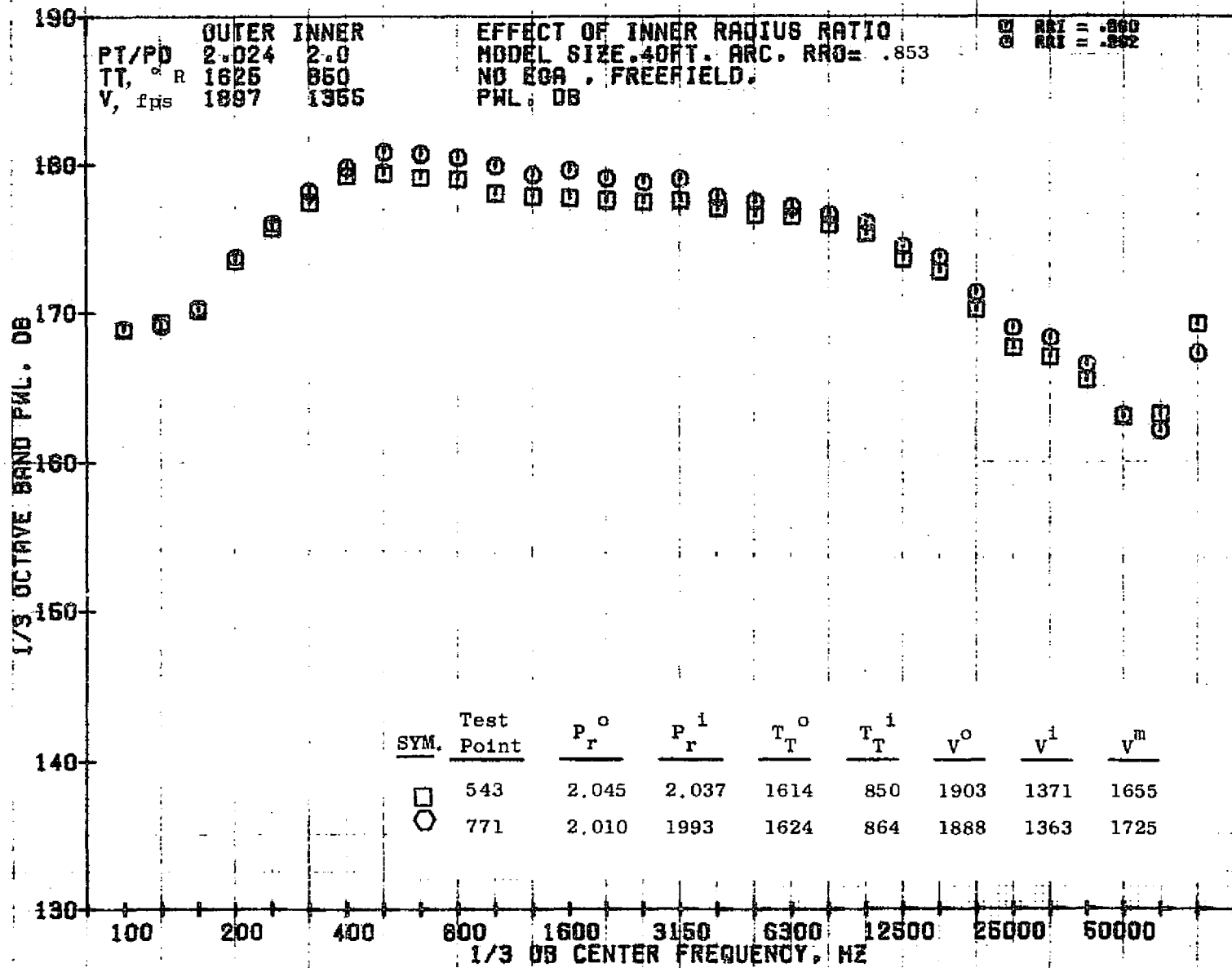
10/29/76
18124-001

79 BURCH A.



10/29/76
 18161-001

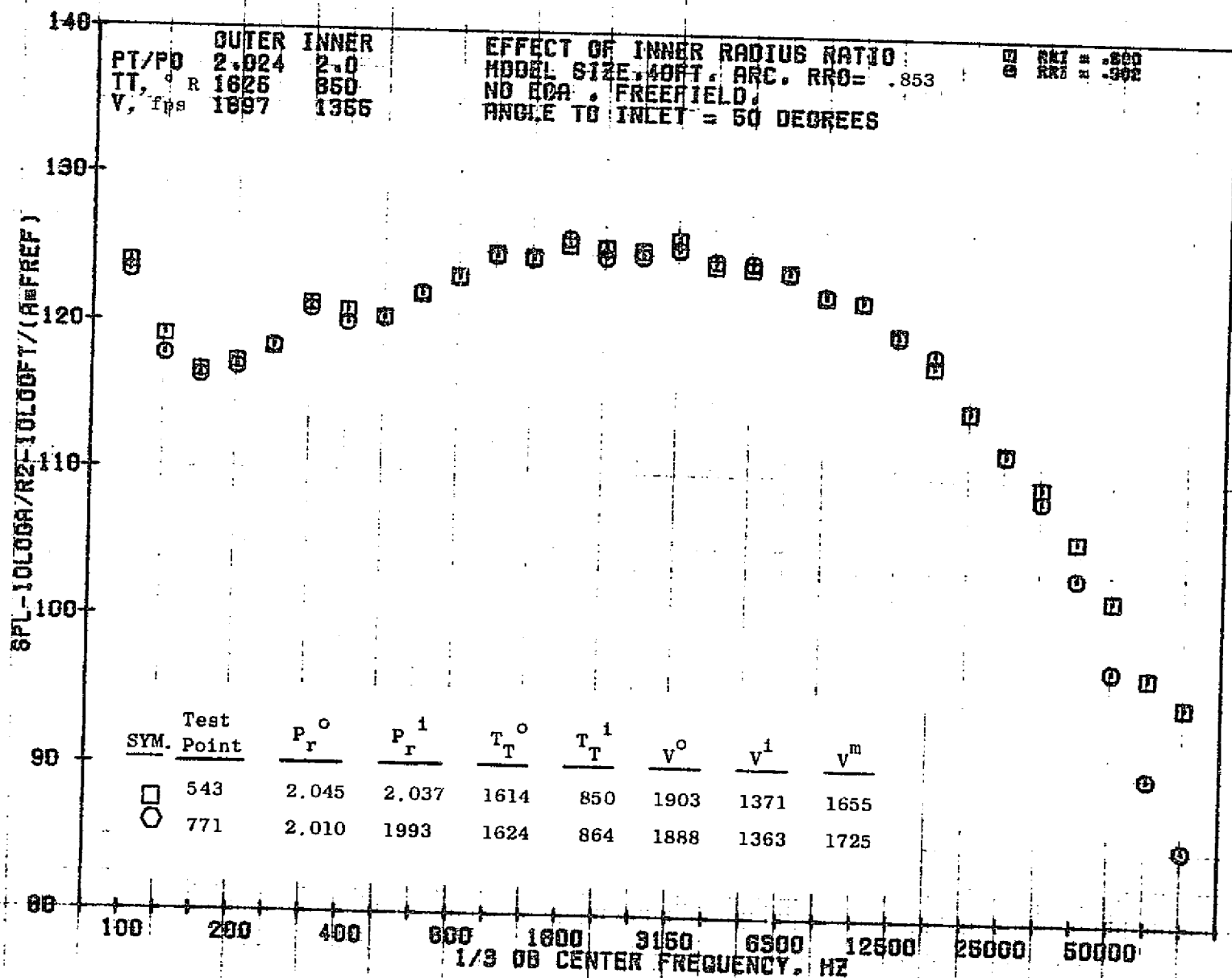
79 BURCH A.



10/29/76
 18161-001

79 BURCH A.

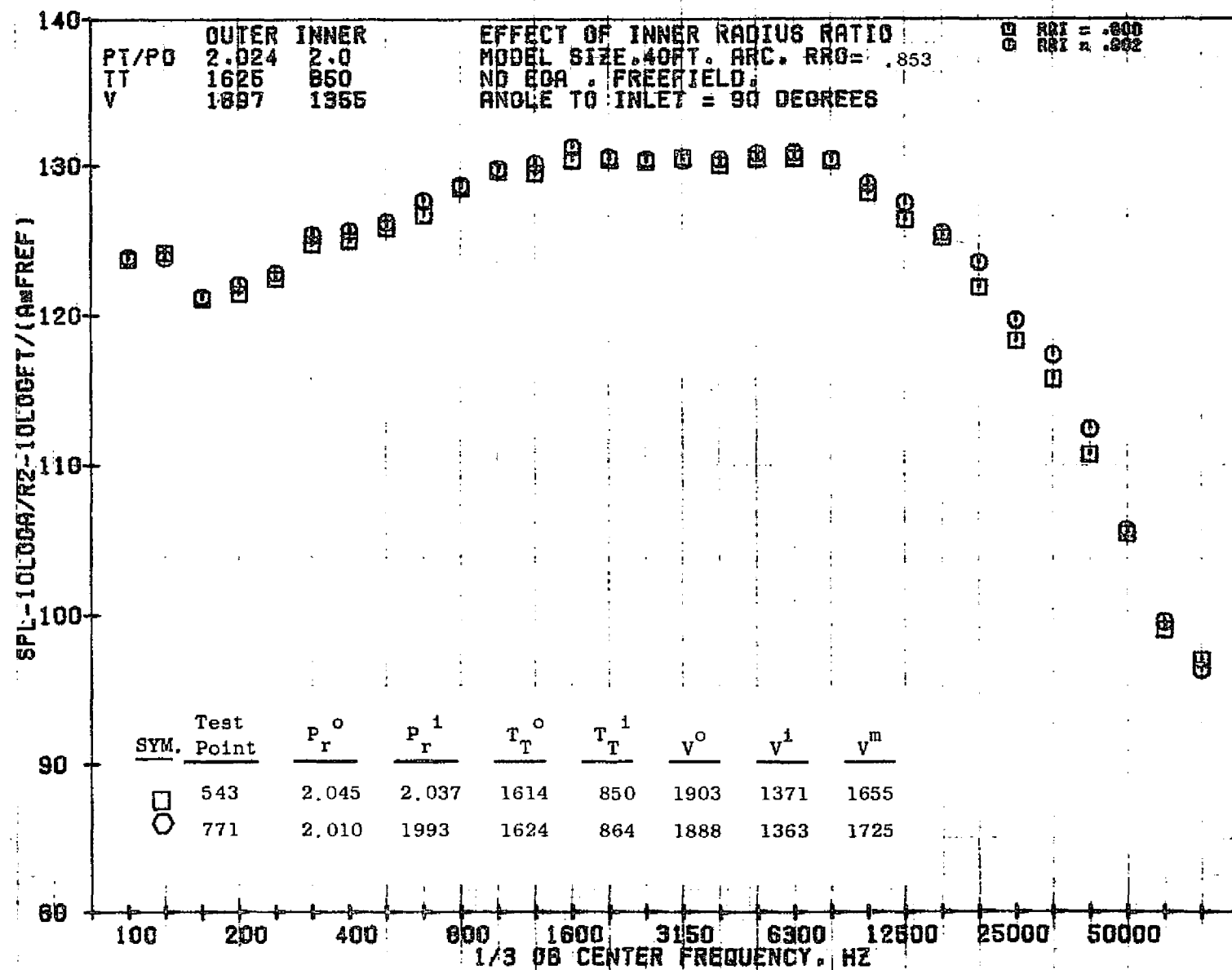
1030



10/29/76
 10161-001

79 BURCH A.

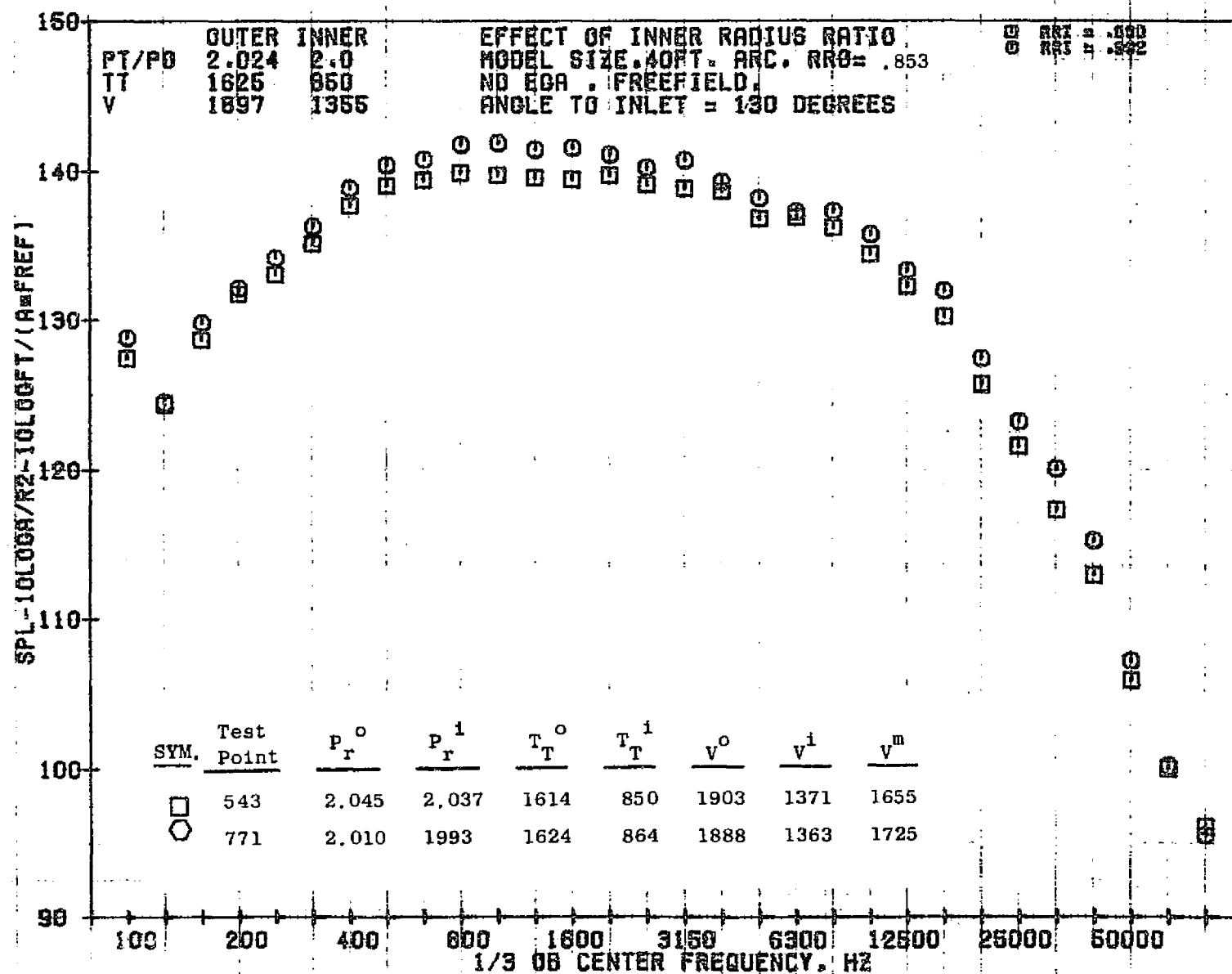
1031



10/29/76
 18161-001

79 BURCH A.

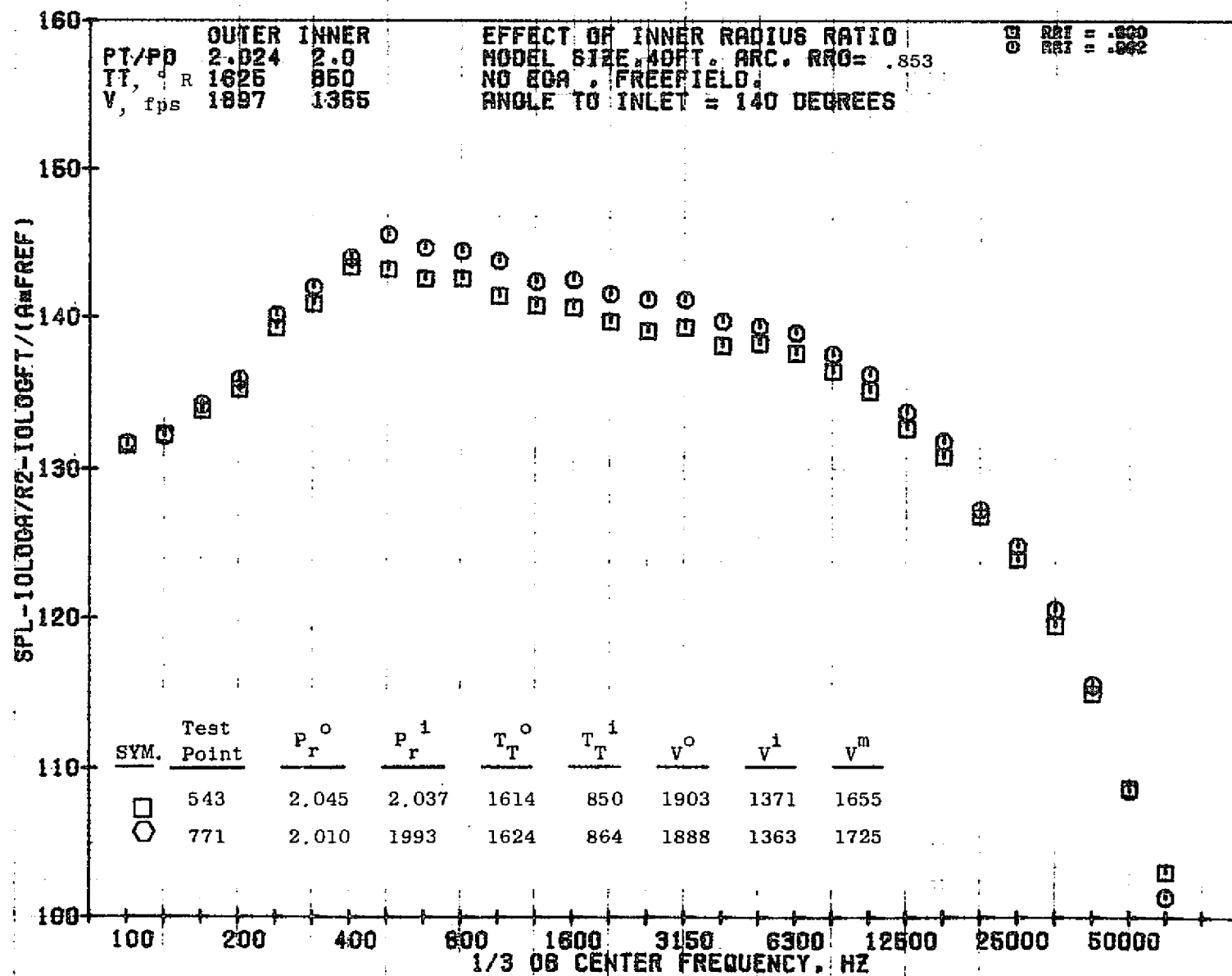
1032



10/29/76
18161-001

79 BURCH A.

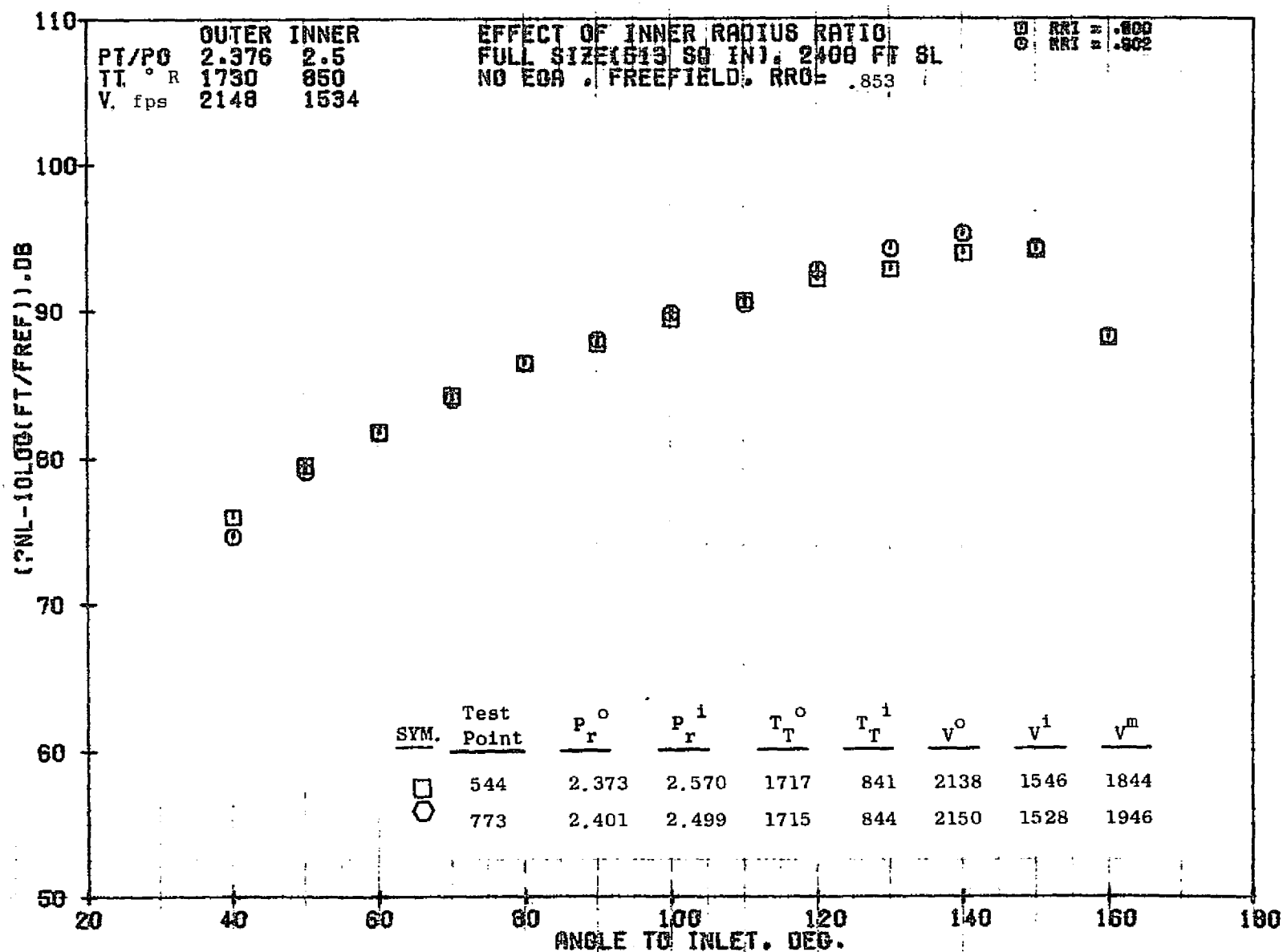
1033



10/29/76
18161-001

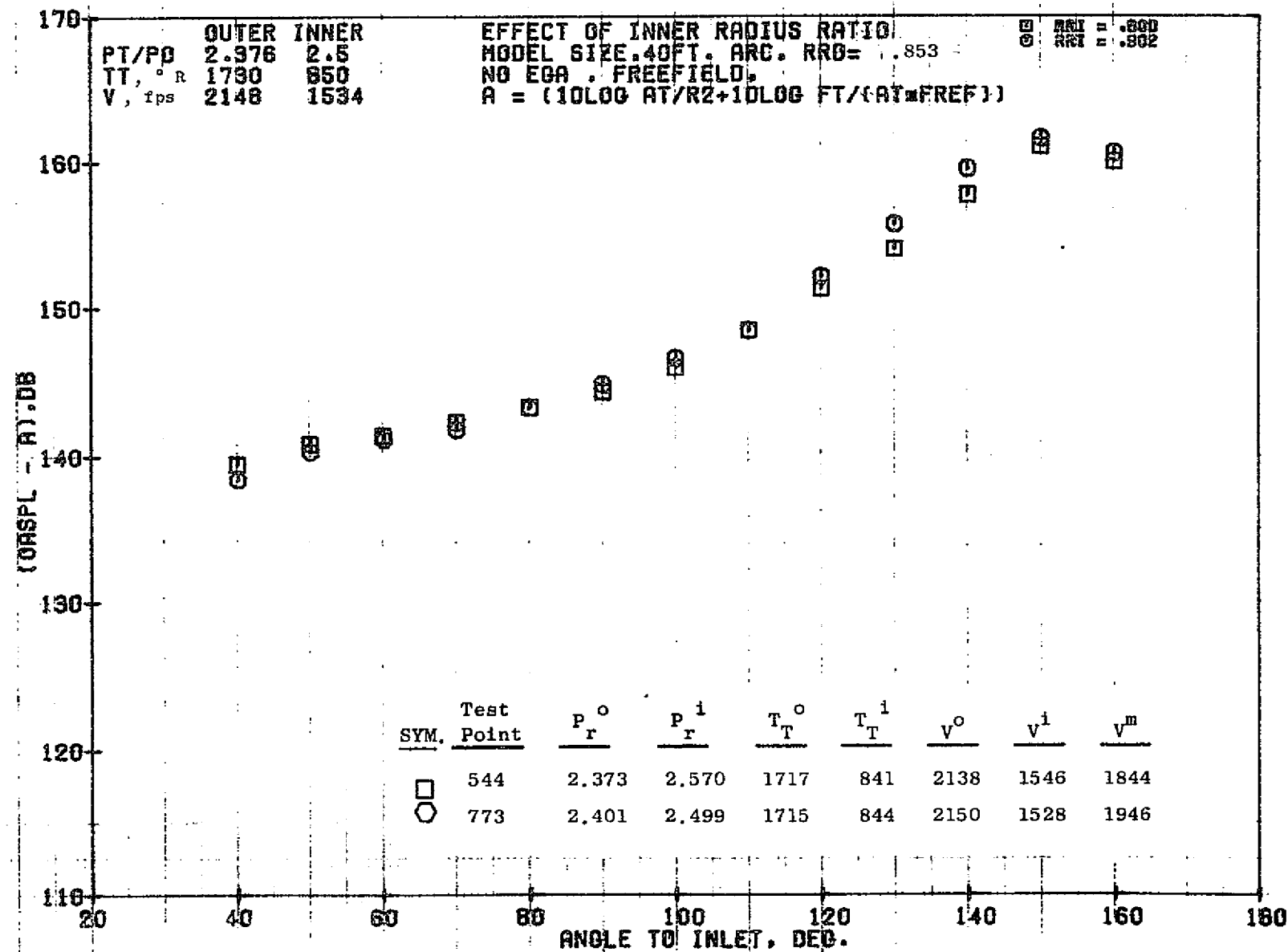
79 BURCH A.

1034



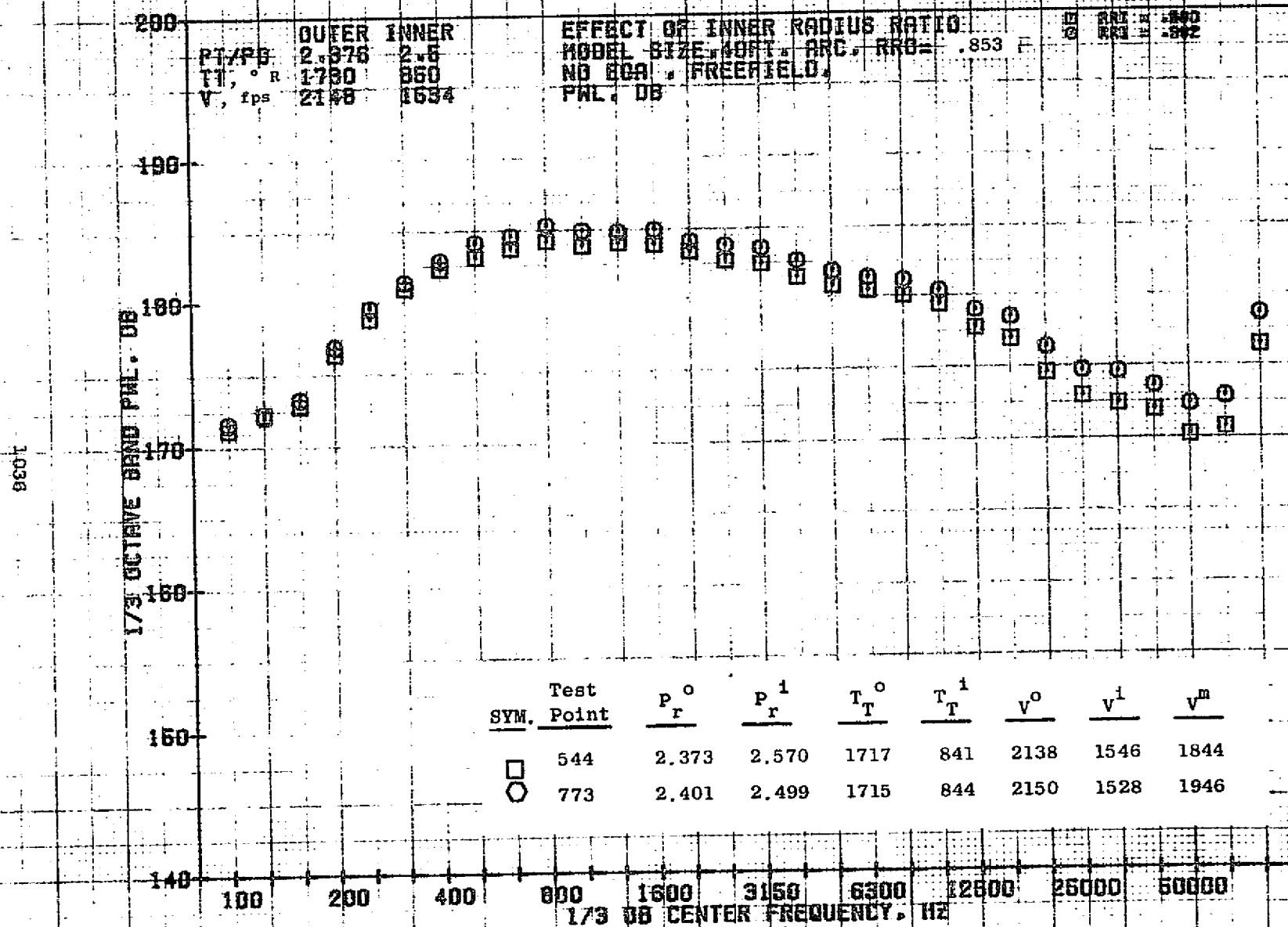
10/29/76
 18124-001

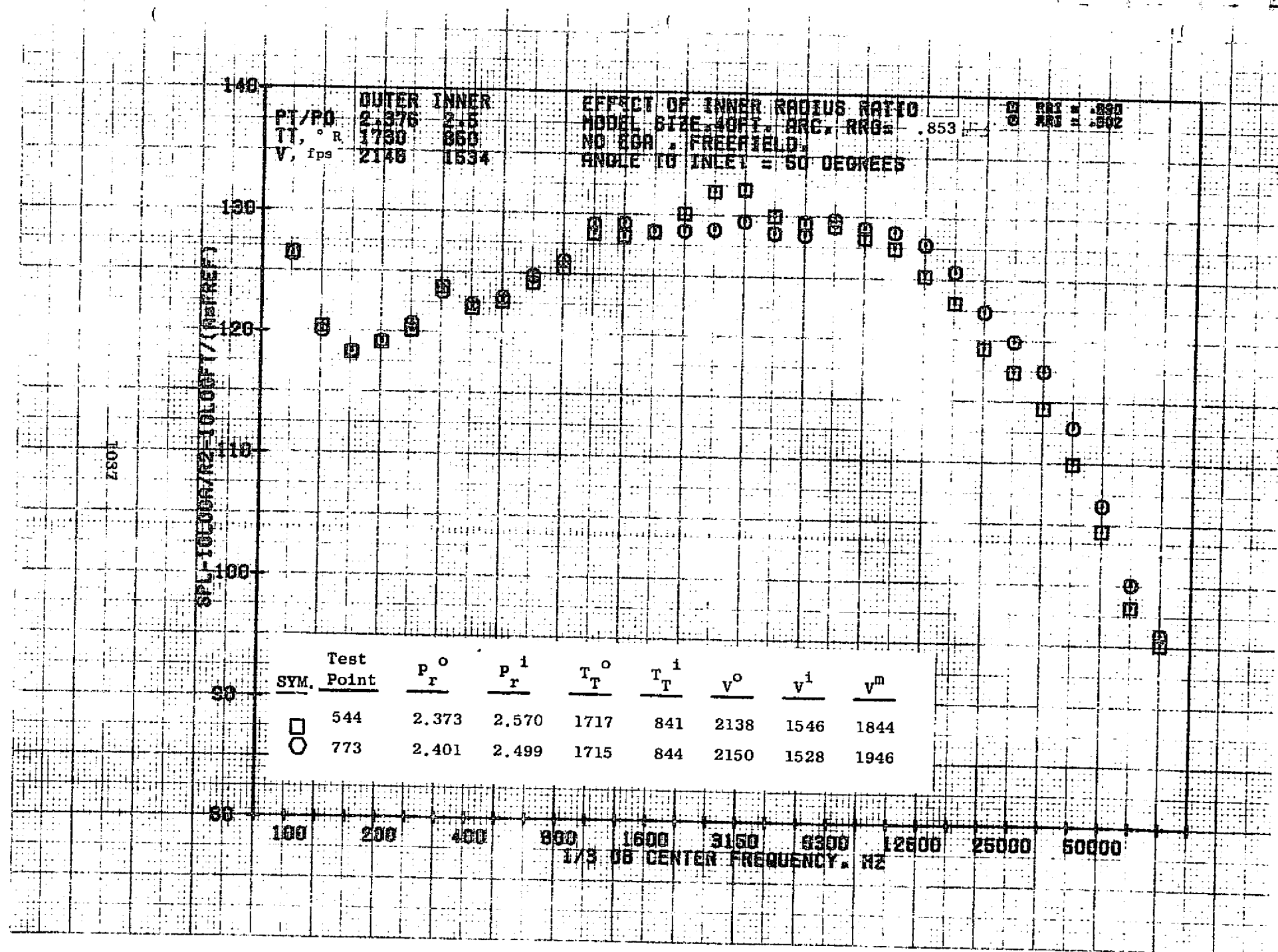
79 BURCH A.



10/29/76
1B161-001

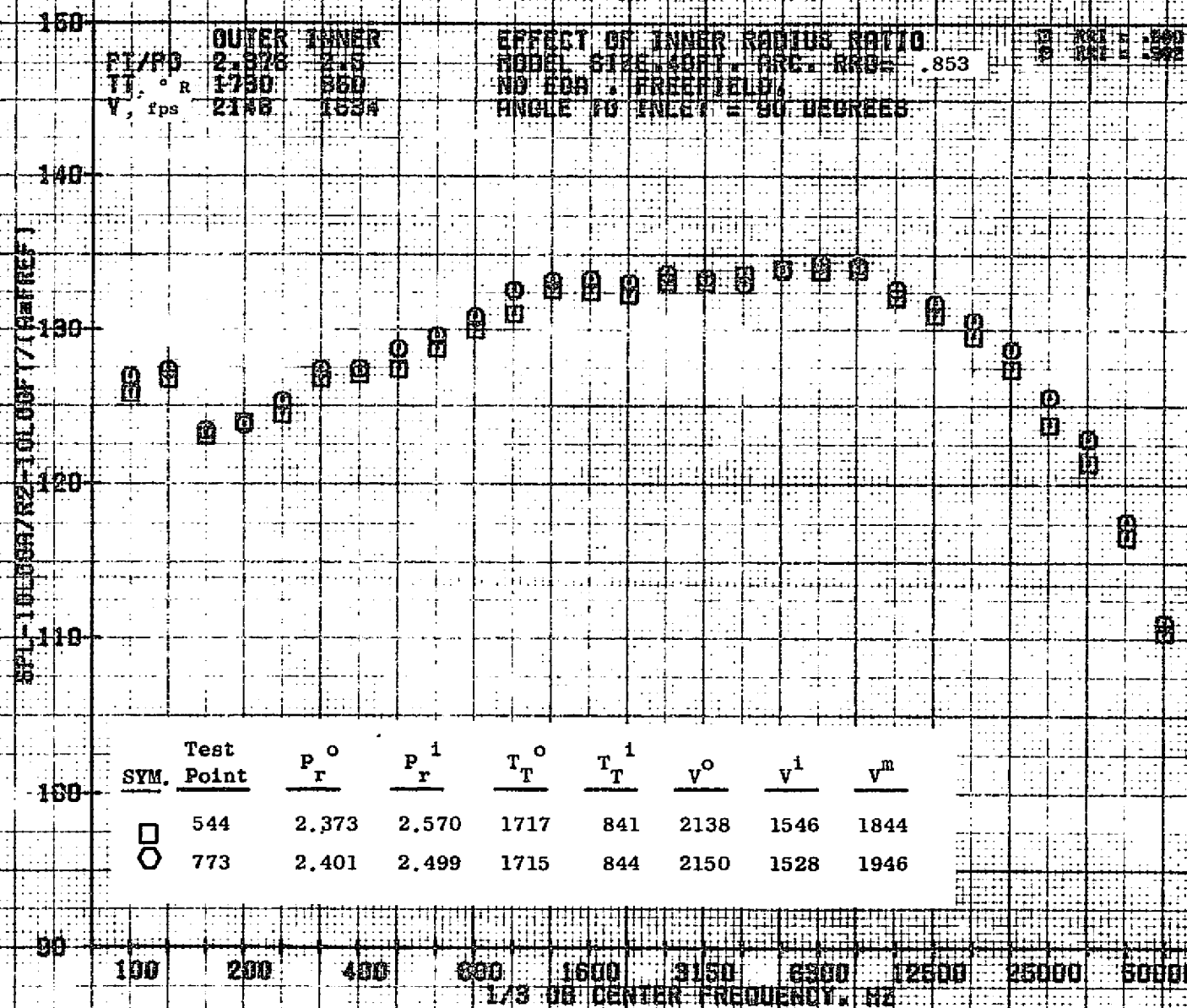
79 BURCH A.





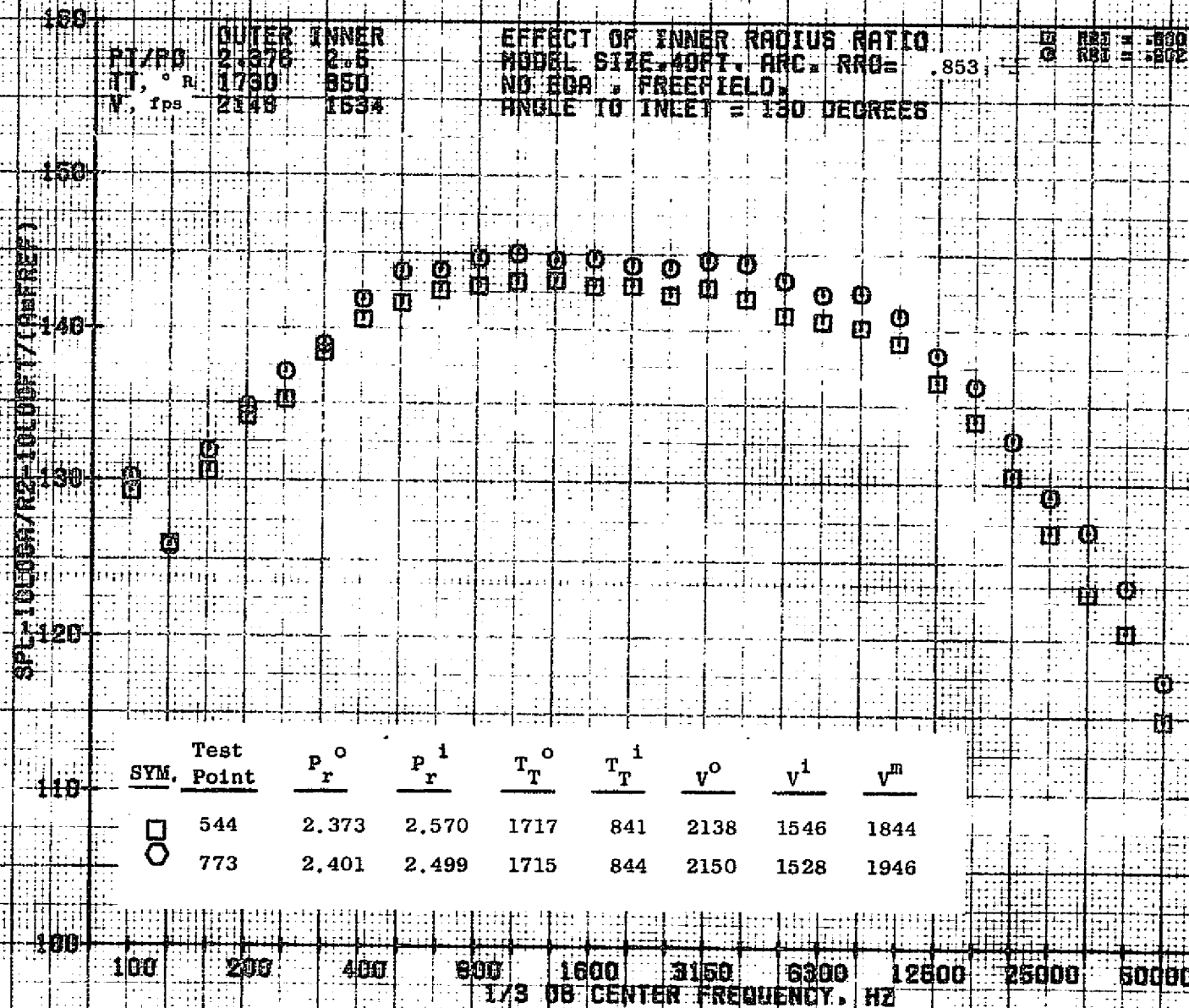
10/29/76
18161-001

79 BURCH A.



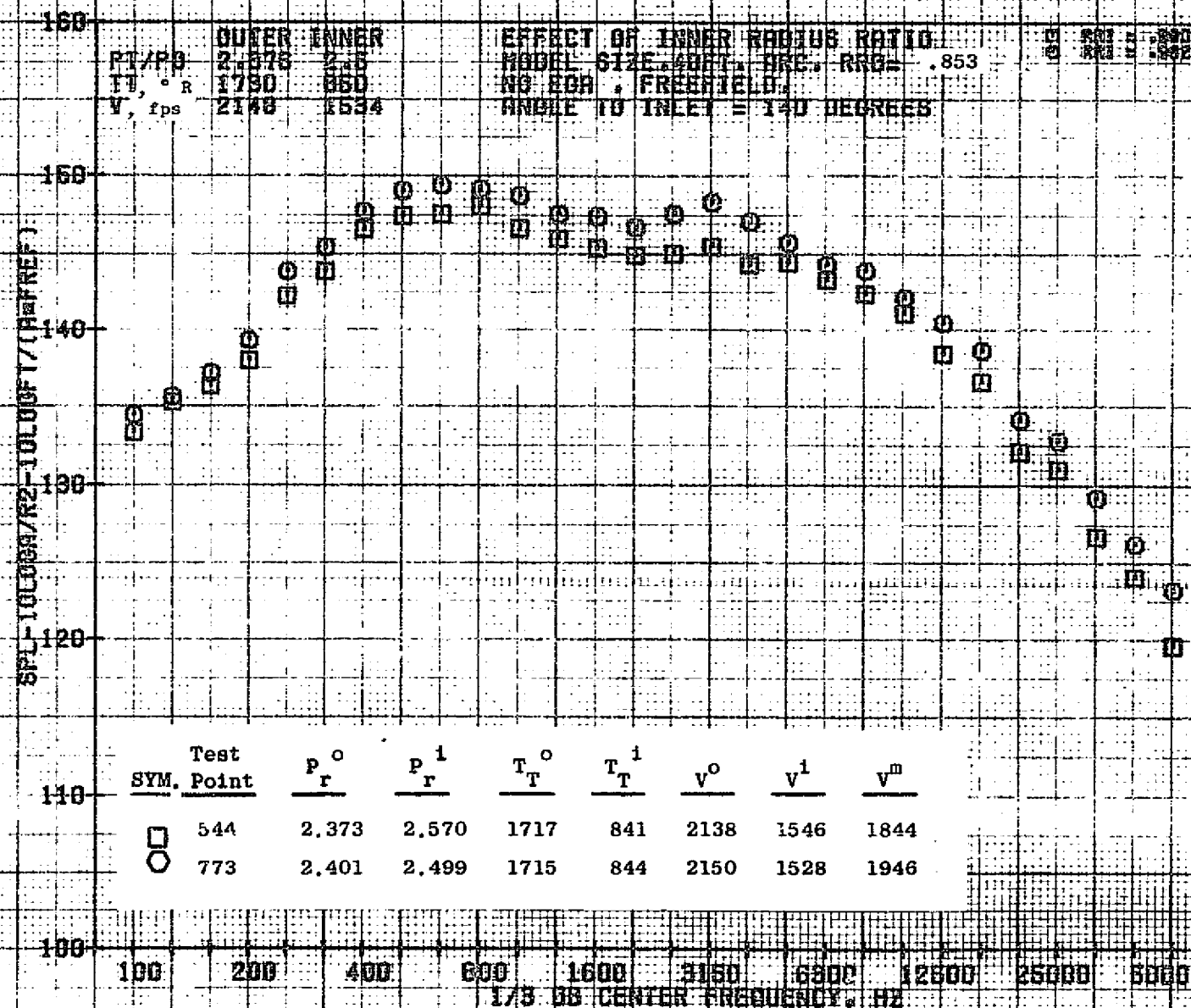
10/29/76
18161-001

78 BURCH A.



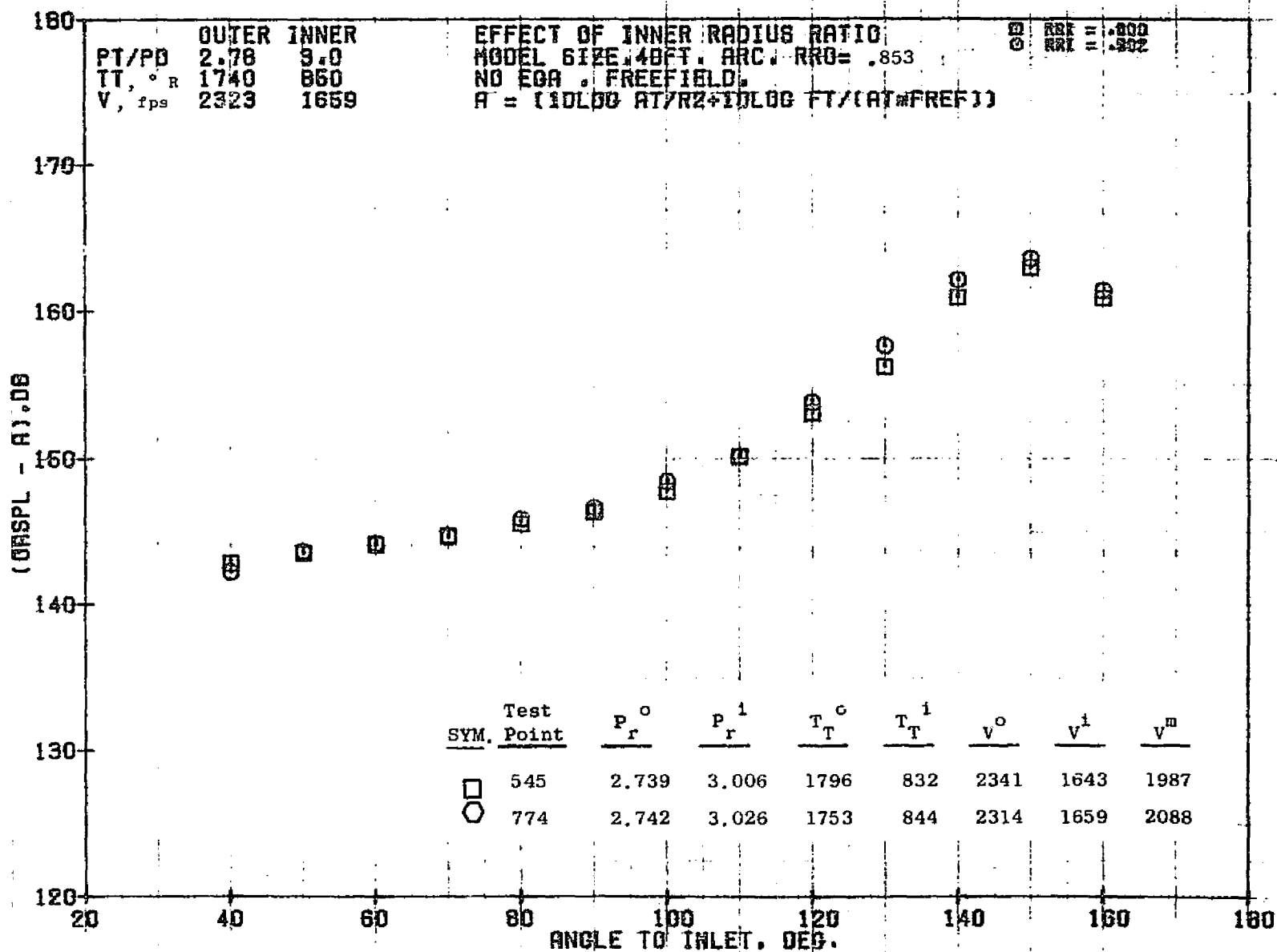
10/29/76
18161-001

79 BURCH A.



10/29/76
 18161-001

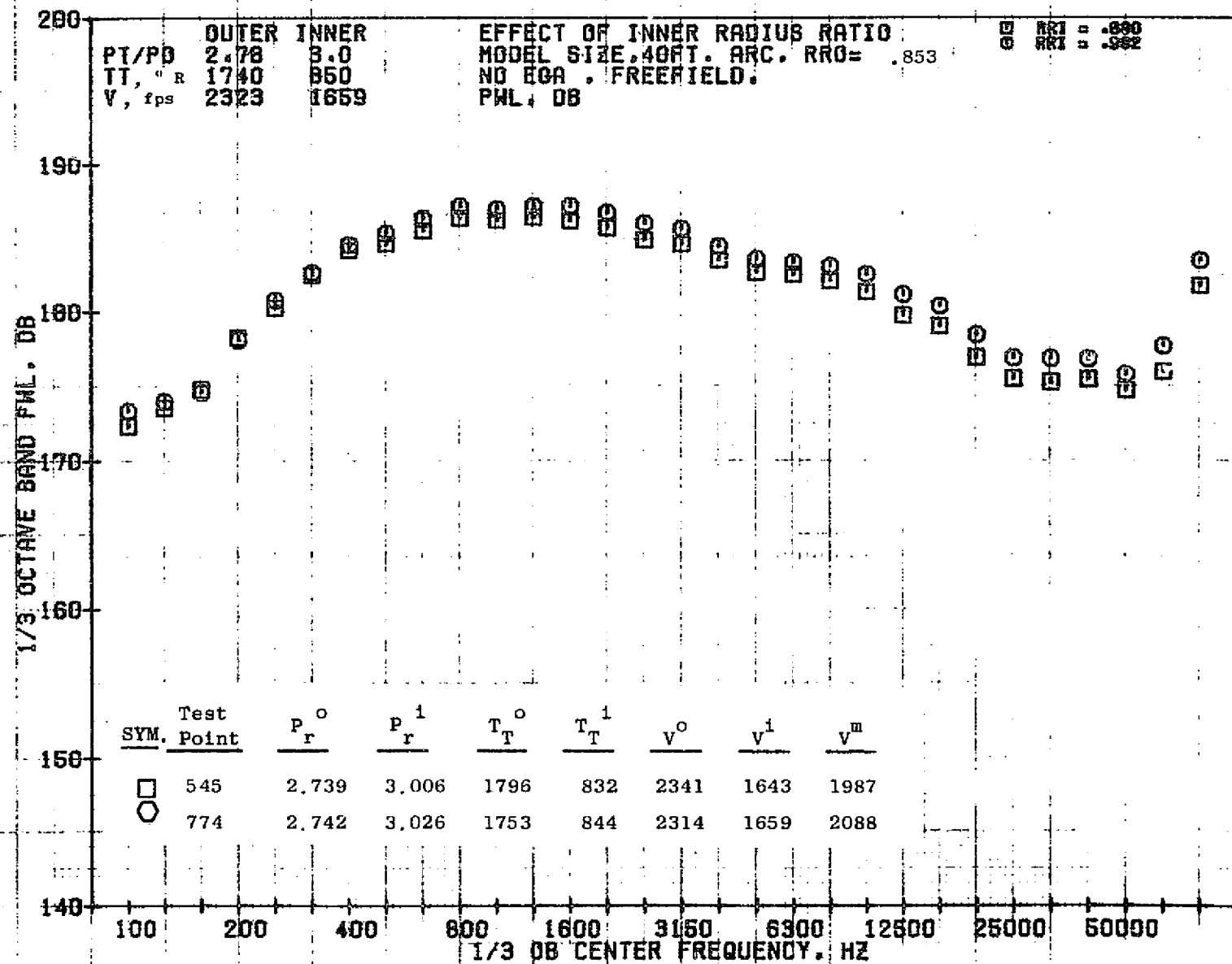
79 BURCH A.



10/29/76
18161-001

79 BURCH A.

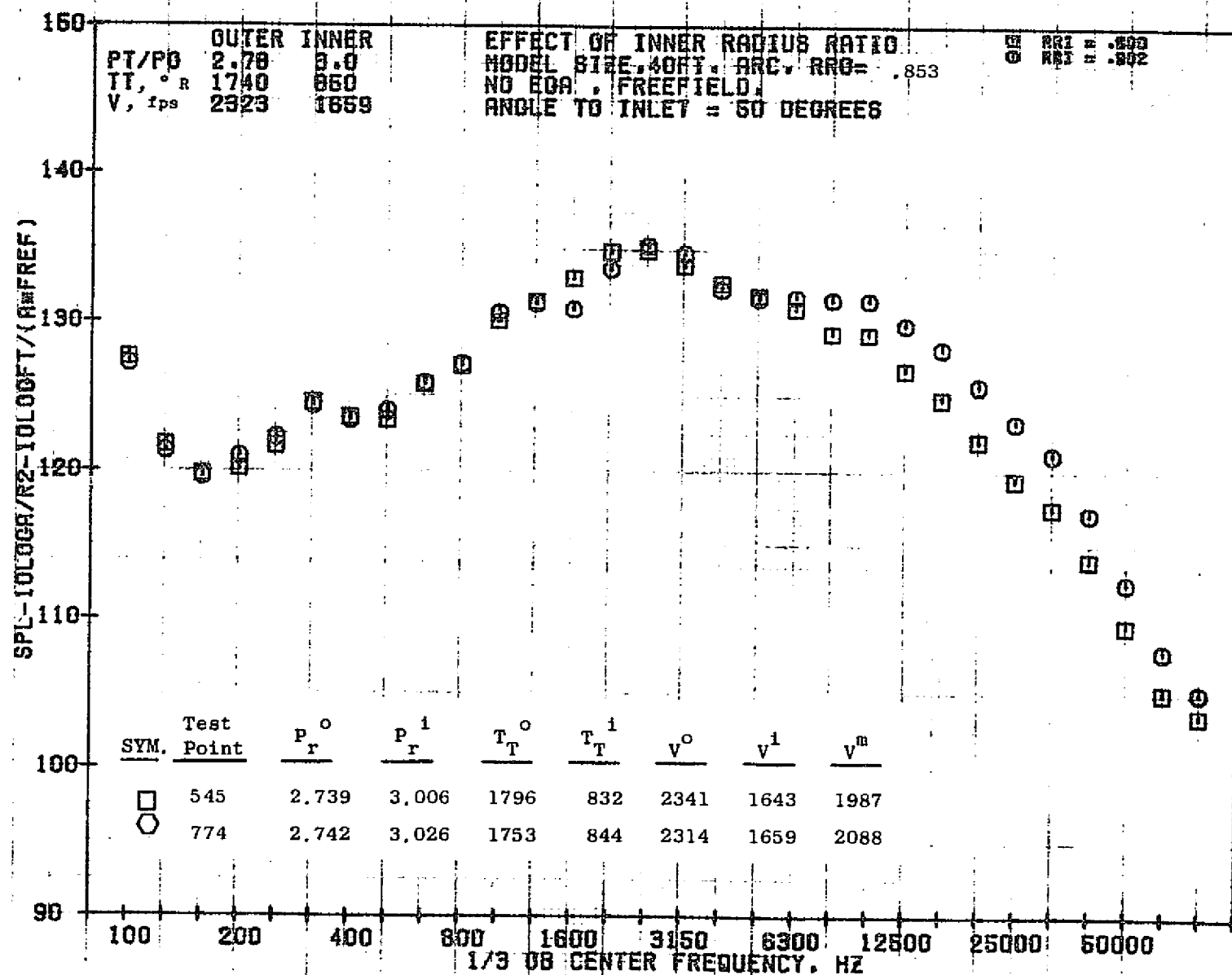
1043



10/29/76
18161-001

79 BURCH A.

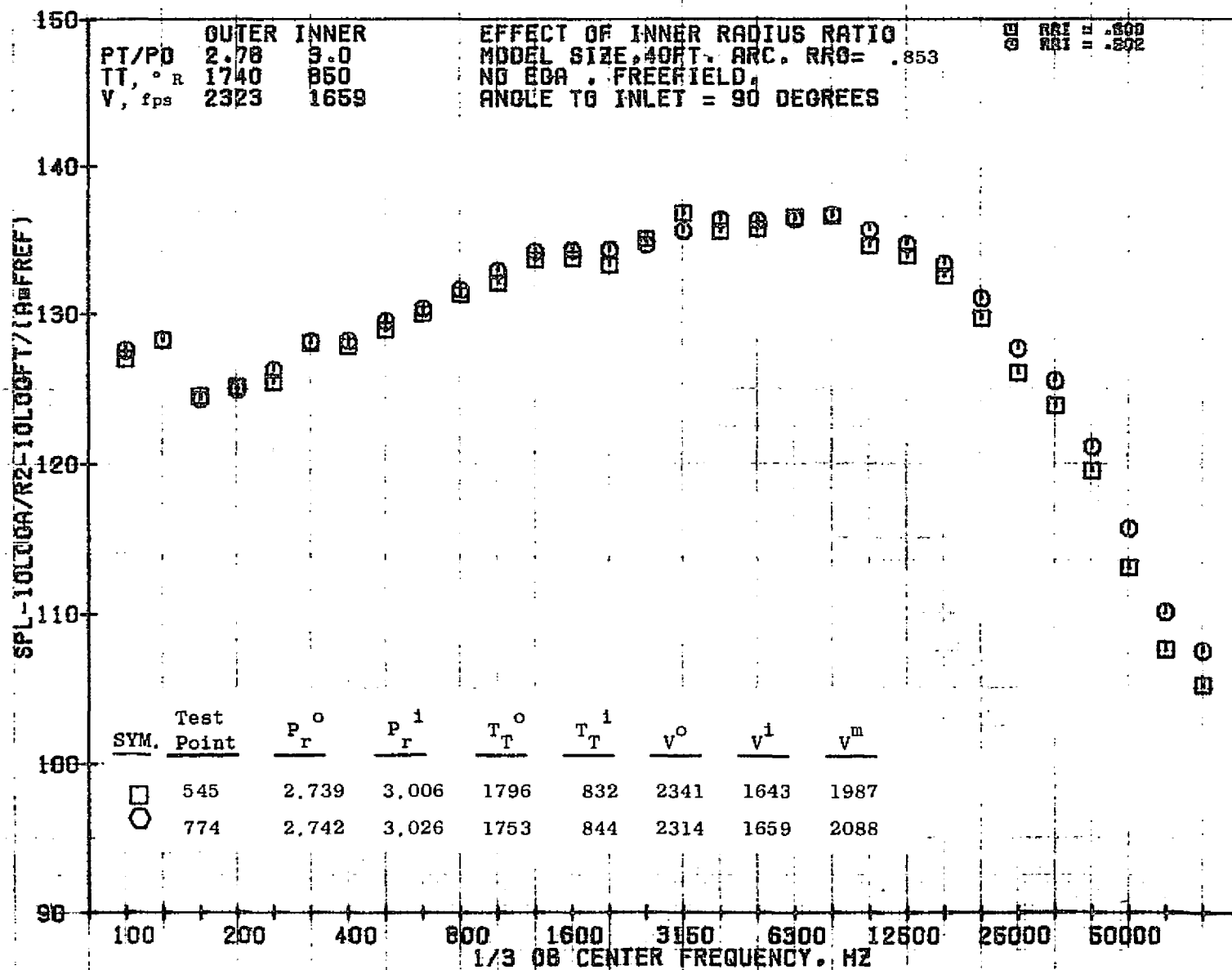
1044



10/29/76
18161-001

79 BURCH A.

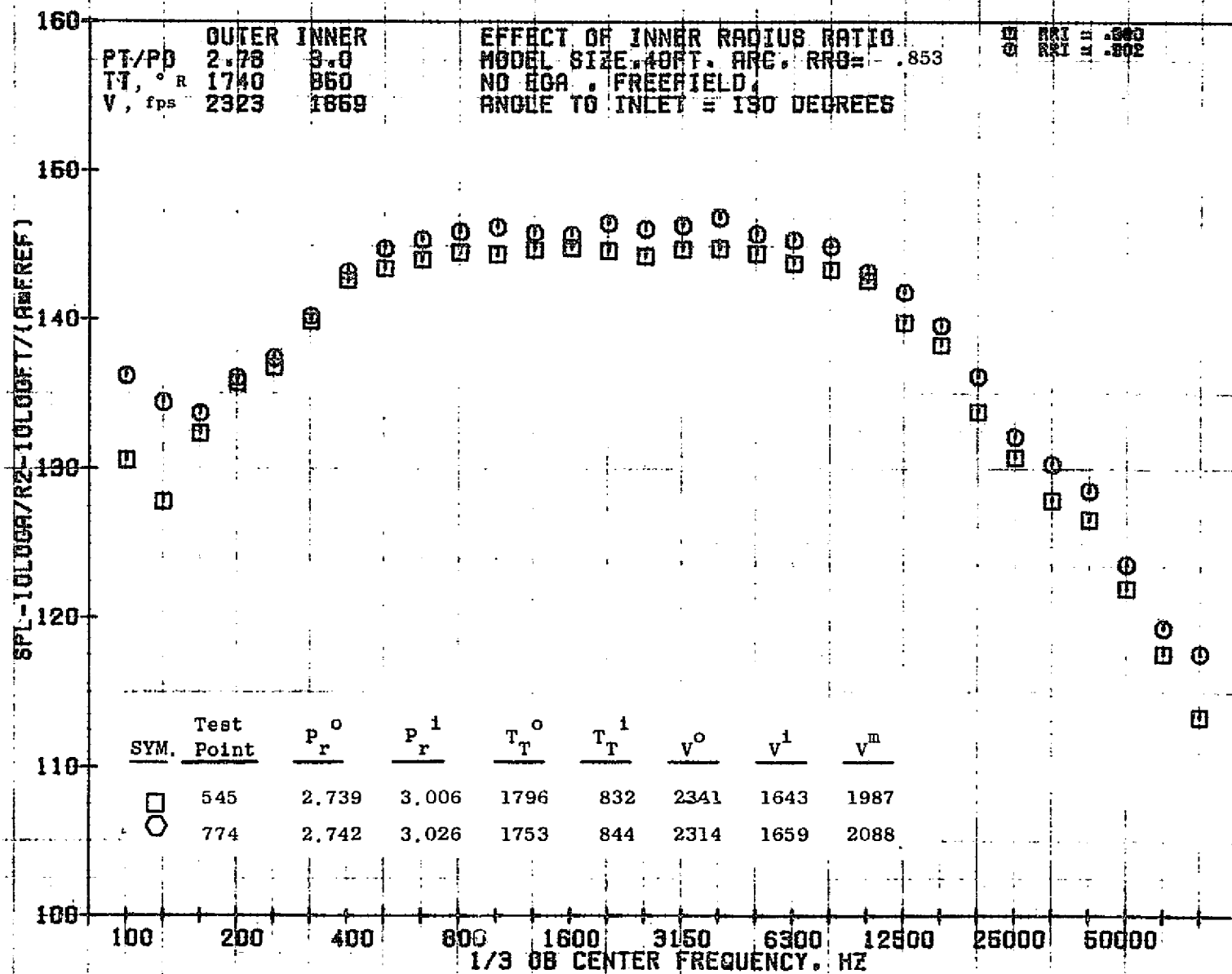
1045



10/29/76
 18161-001

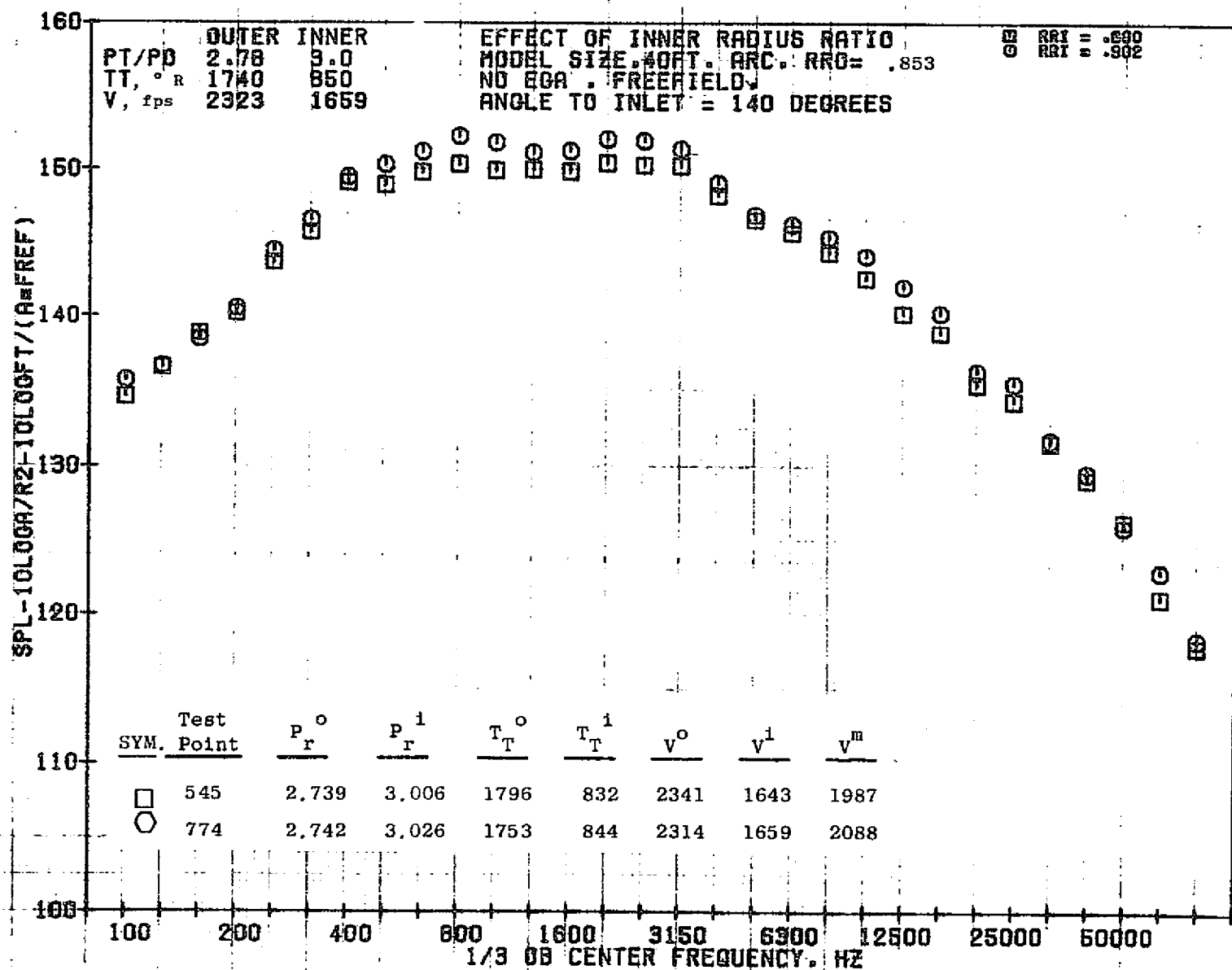
79 BURCH A.

1046

10/29/76
18161-001

79 BURCH A.

1047



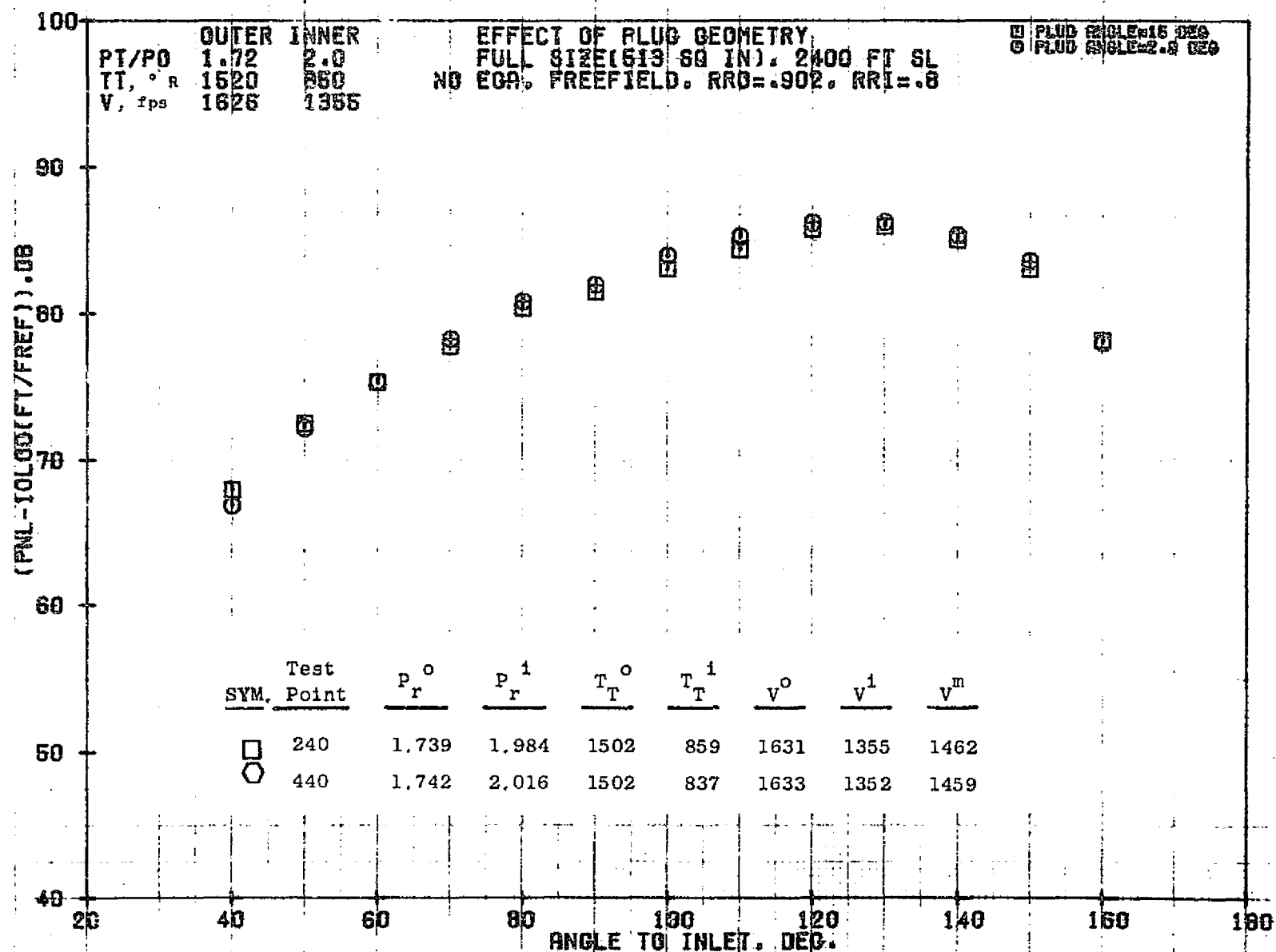
10/29/76
 18161-001

79 BURCH A.

7.4.3 Effect of Plug Geometry

The effect of plug geometry is examined in this section. Configurations 2 and 4 have the same inner and outer radius ratios but different plug geometries. Configuration 2 has a smooth plug contour while Configuration 4 has a somewhat flat plug crown.

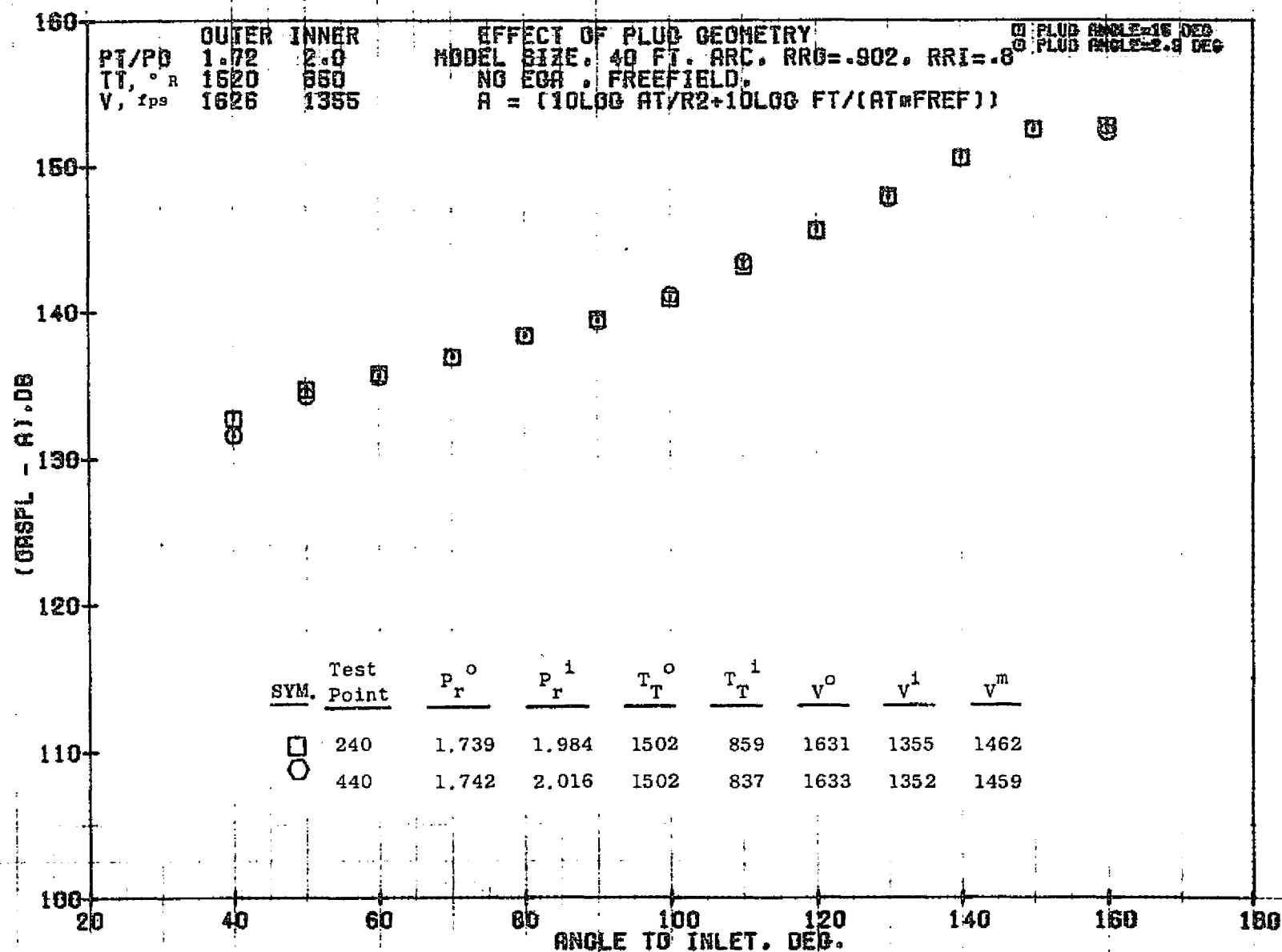
1049



10/29/76
 18130-001

79 BURCH A.

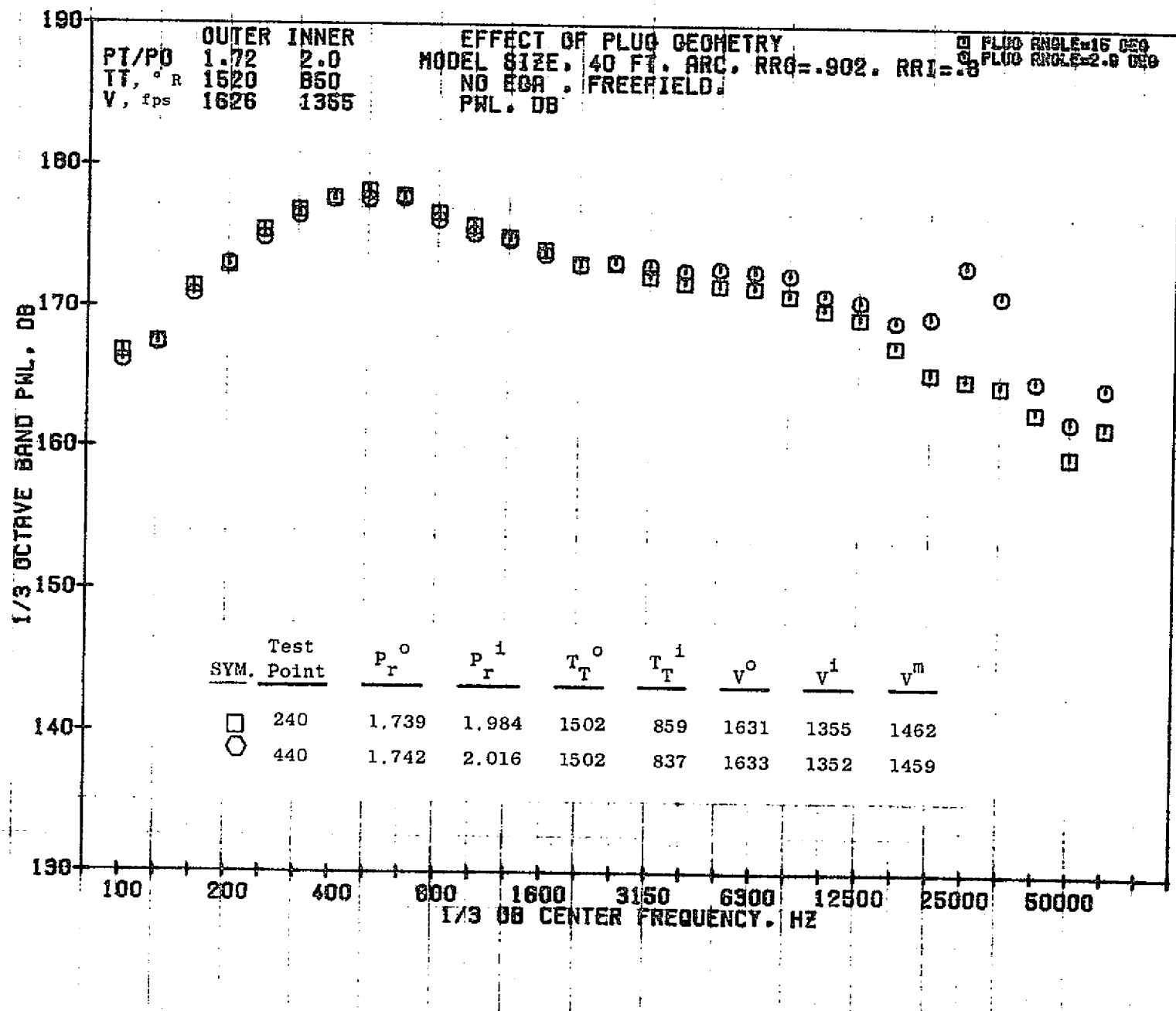
1050



10/29/76
18159-001

79 BURCH A.

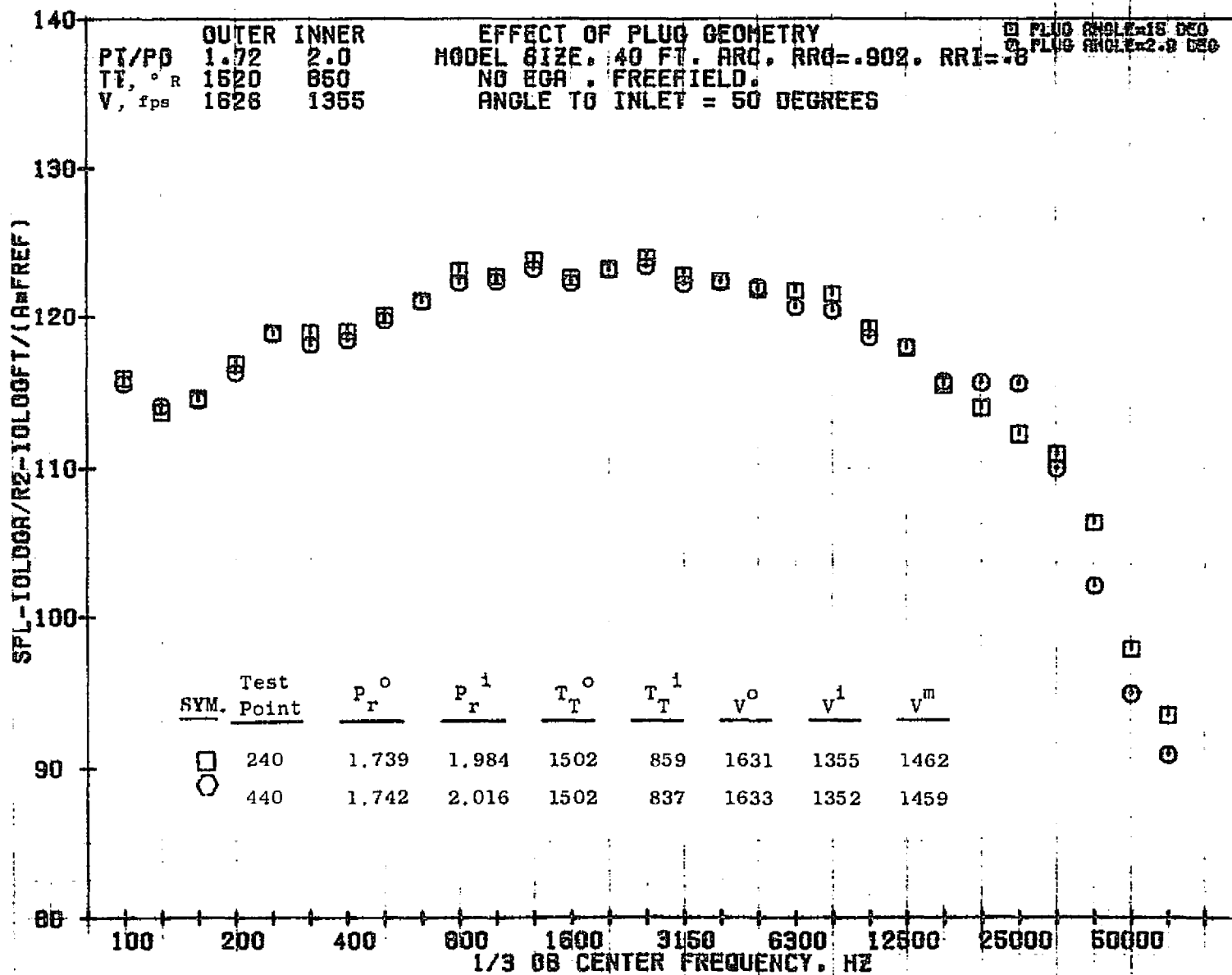
1051



10/29/76
 18159-001

79 BURCH A.

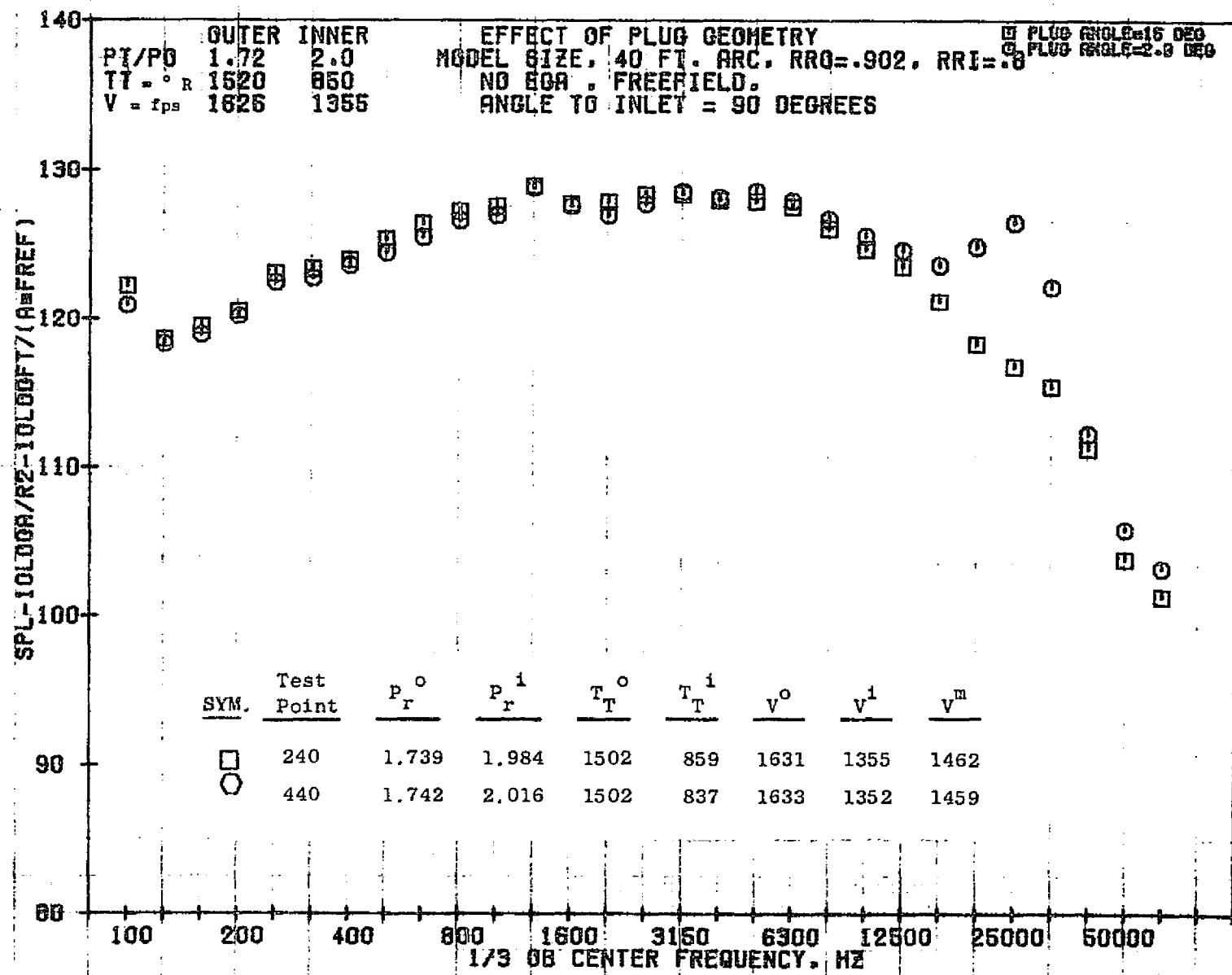
1052



10/29/76
 18159-001

79 BURCH A.

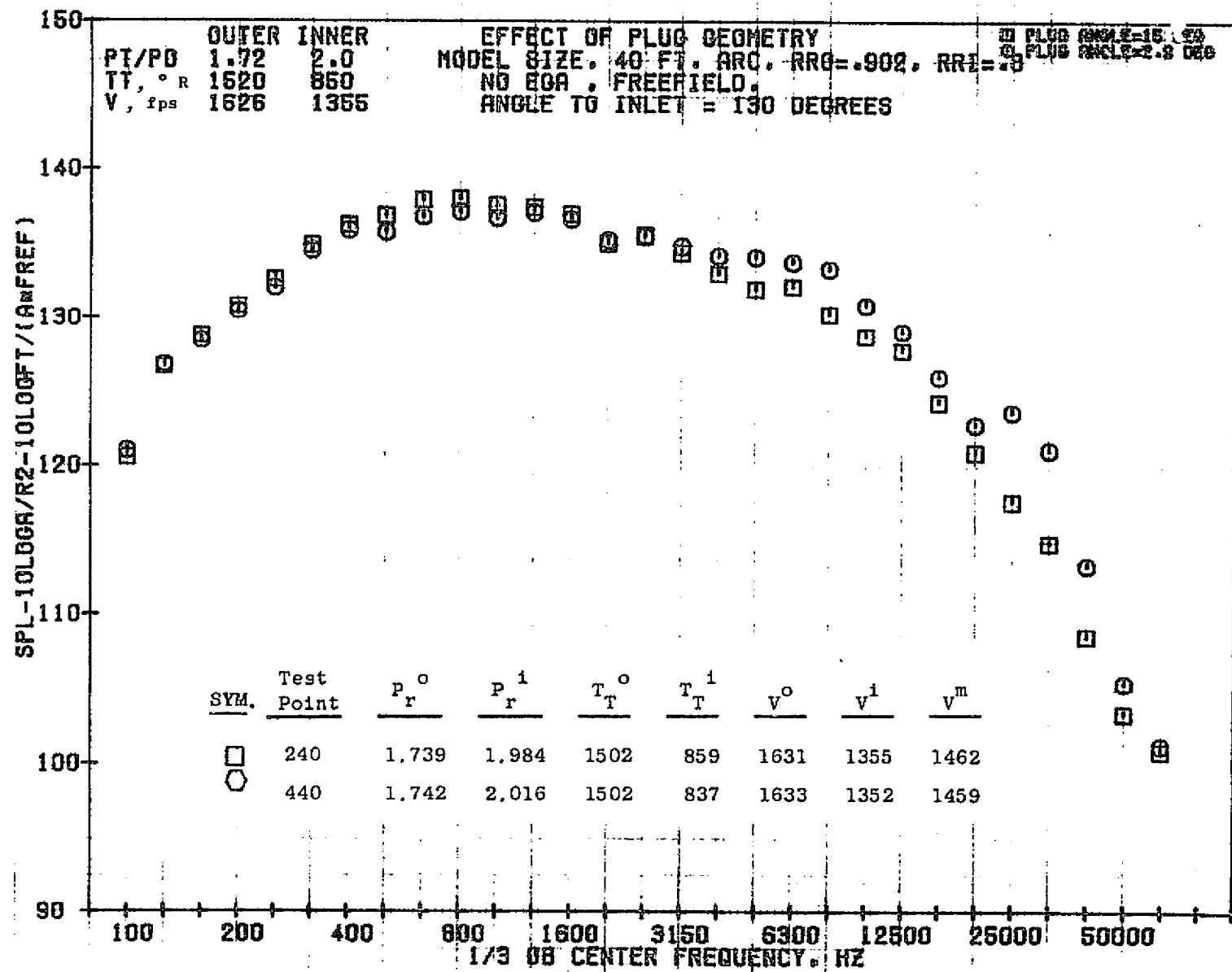
1053



10/29/76
 18159-001

79 BURCH A.

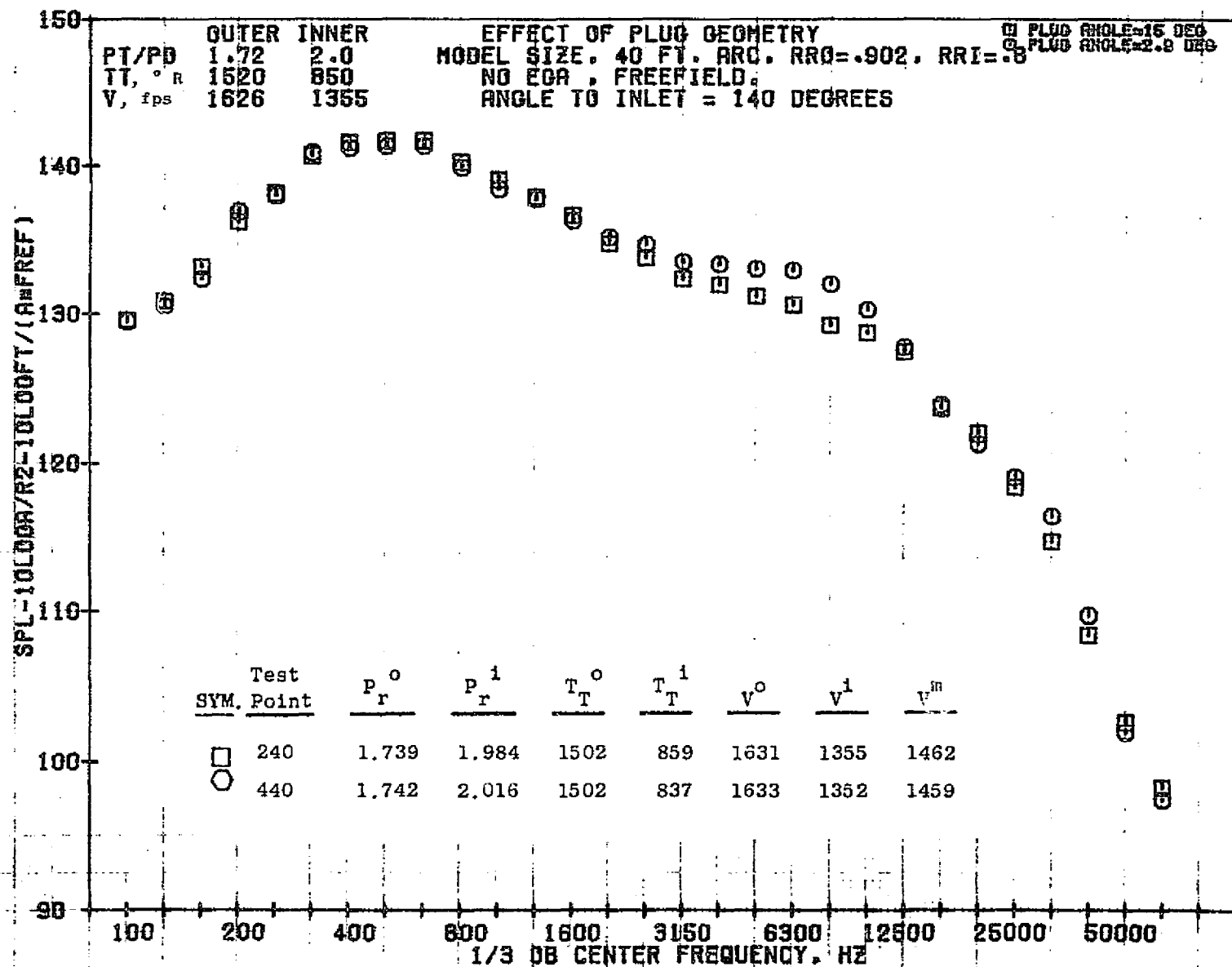
1054



10/29/76
 1B159-001

79 BURCH A.

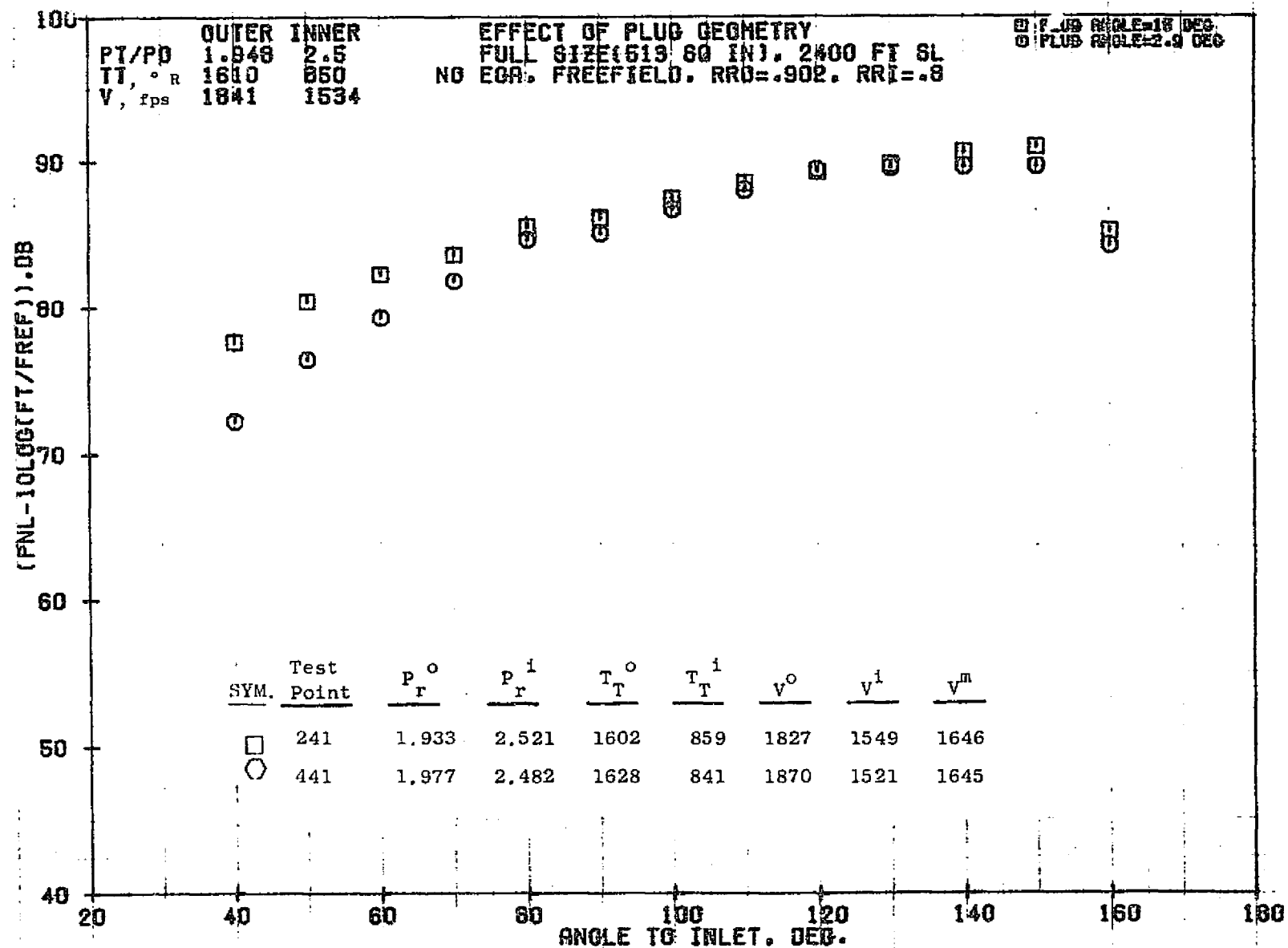
1055



10/29/76
 1B159-001

79 BURCH A.

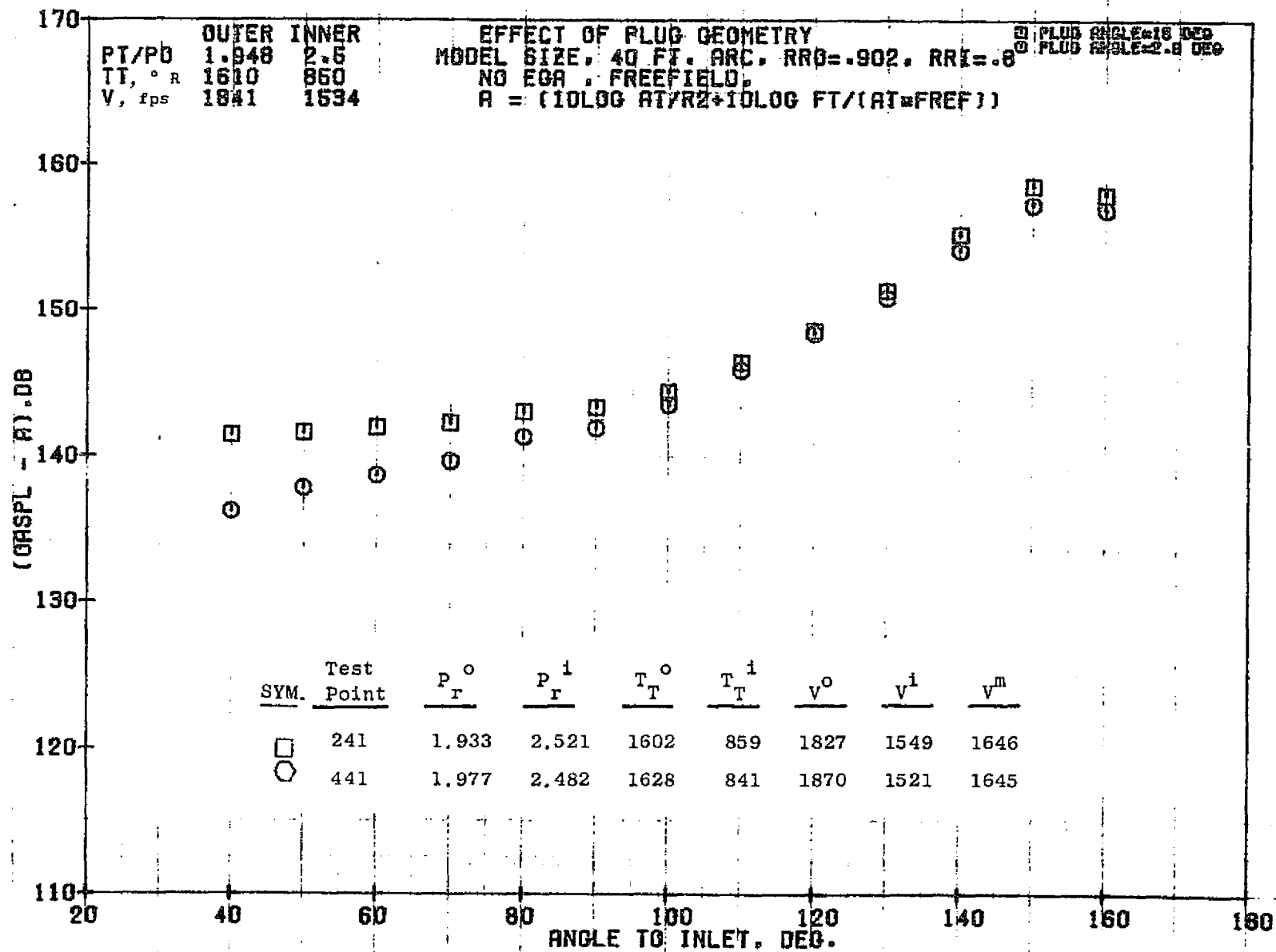
1056



10/29/76
 18130-001

79 BURCH A.

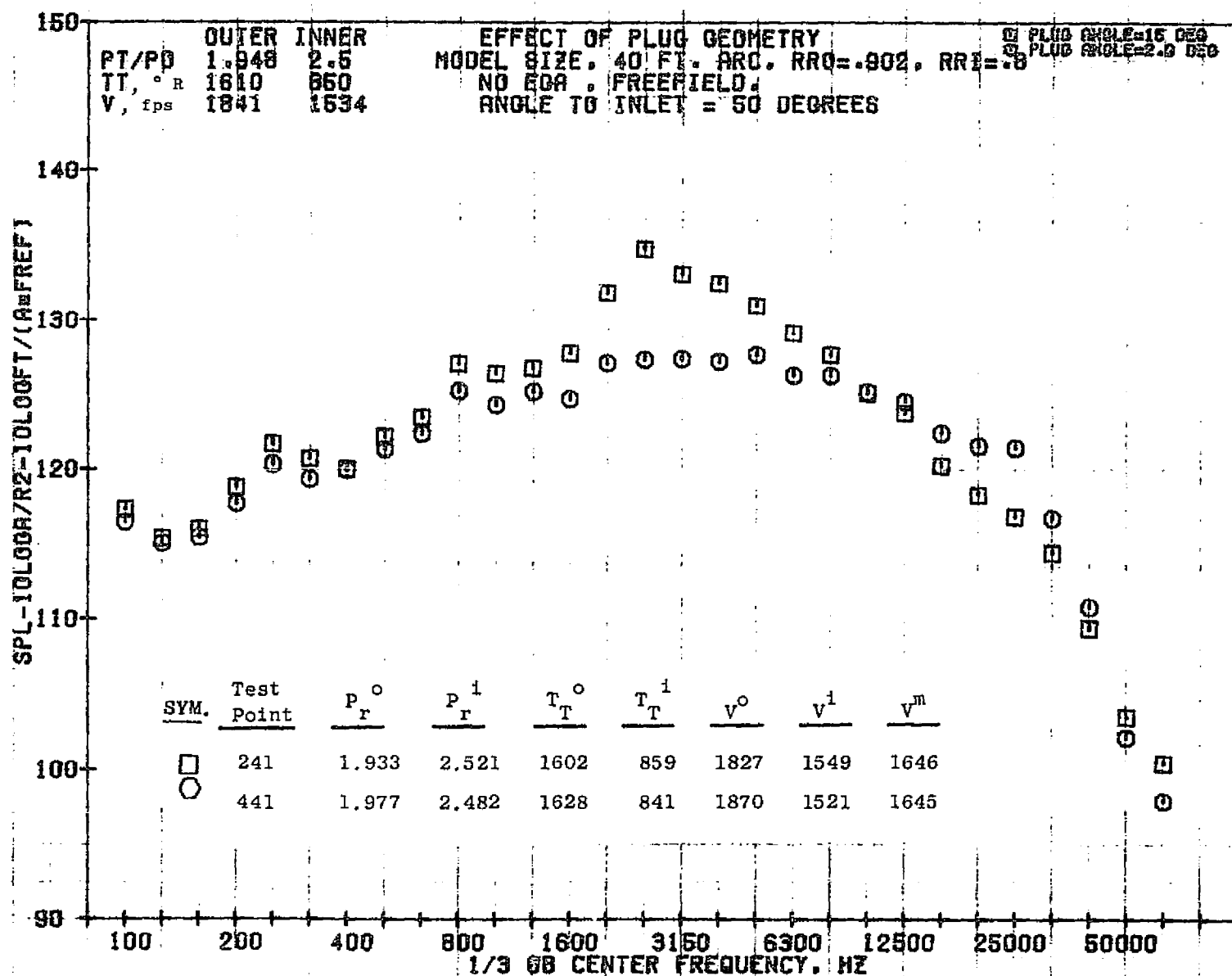
1057



10/29/76
 18159-001

79 BURCH A.

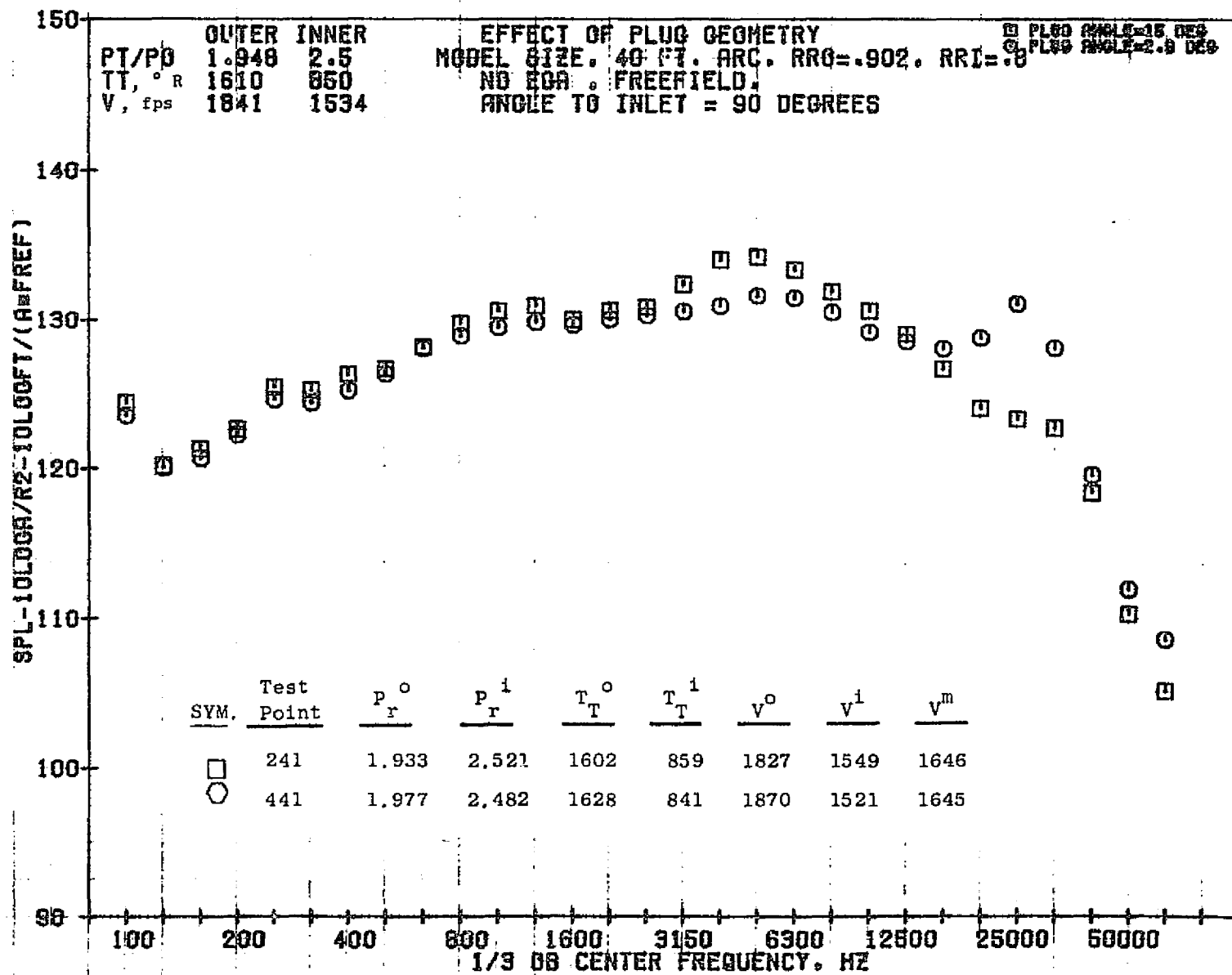
6501



10/29/76
 18159-001

79 BURCH A.

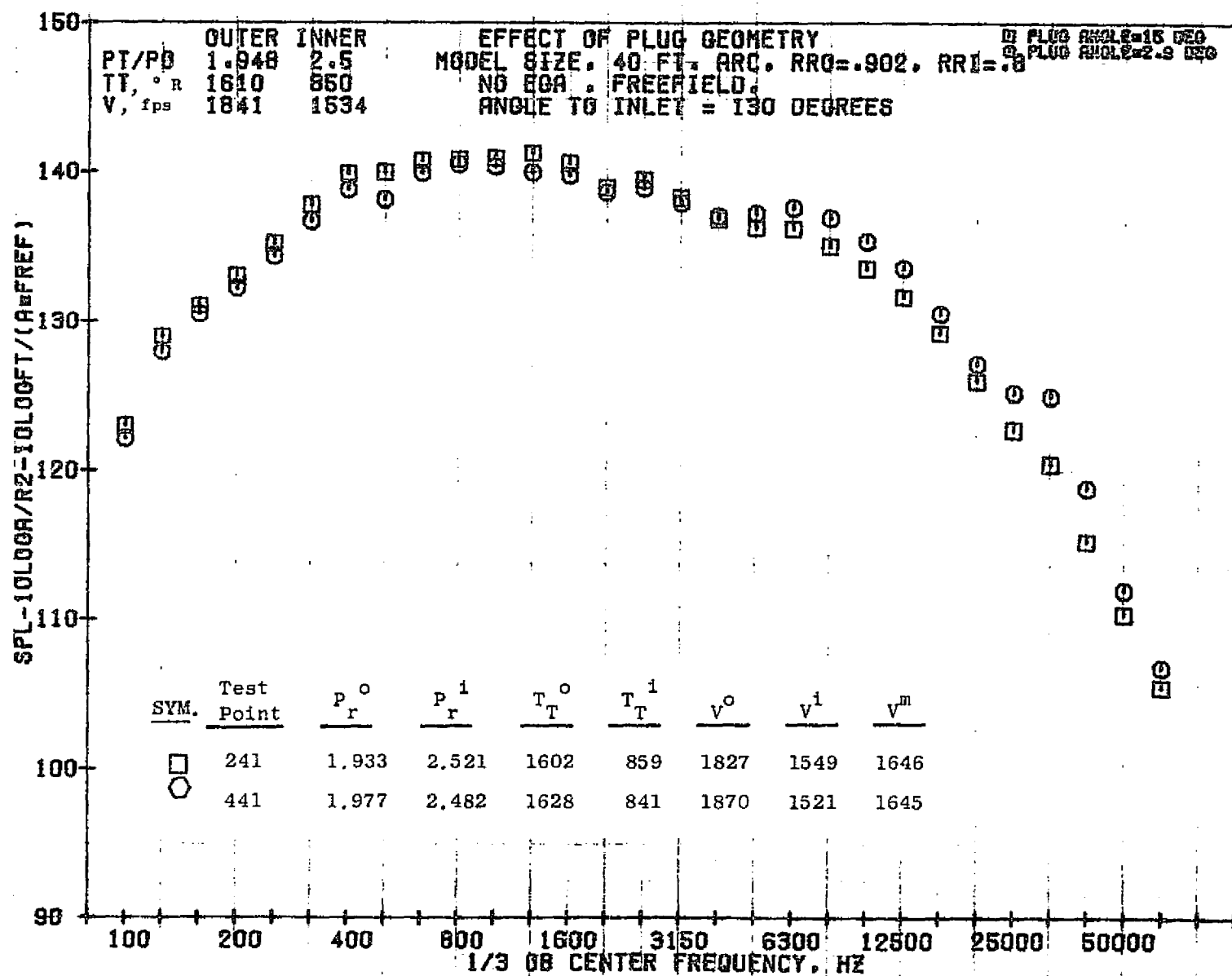
1060



10/29/76
 18159-001

79 BURCH A.

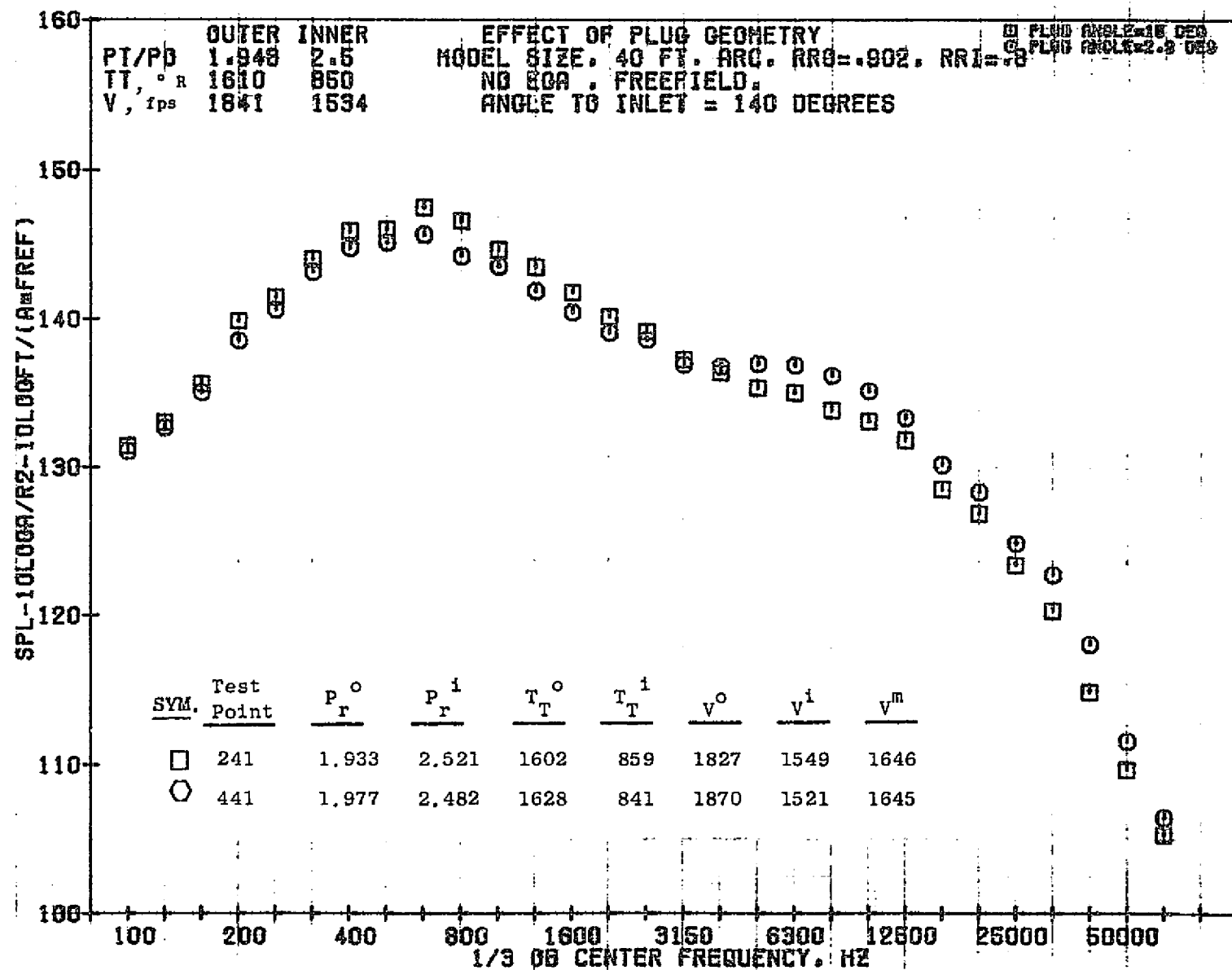
1901



10/29/76
 18159-001

79 BURCH A.

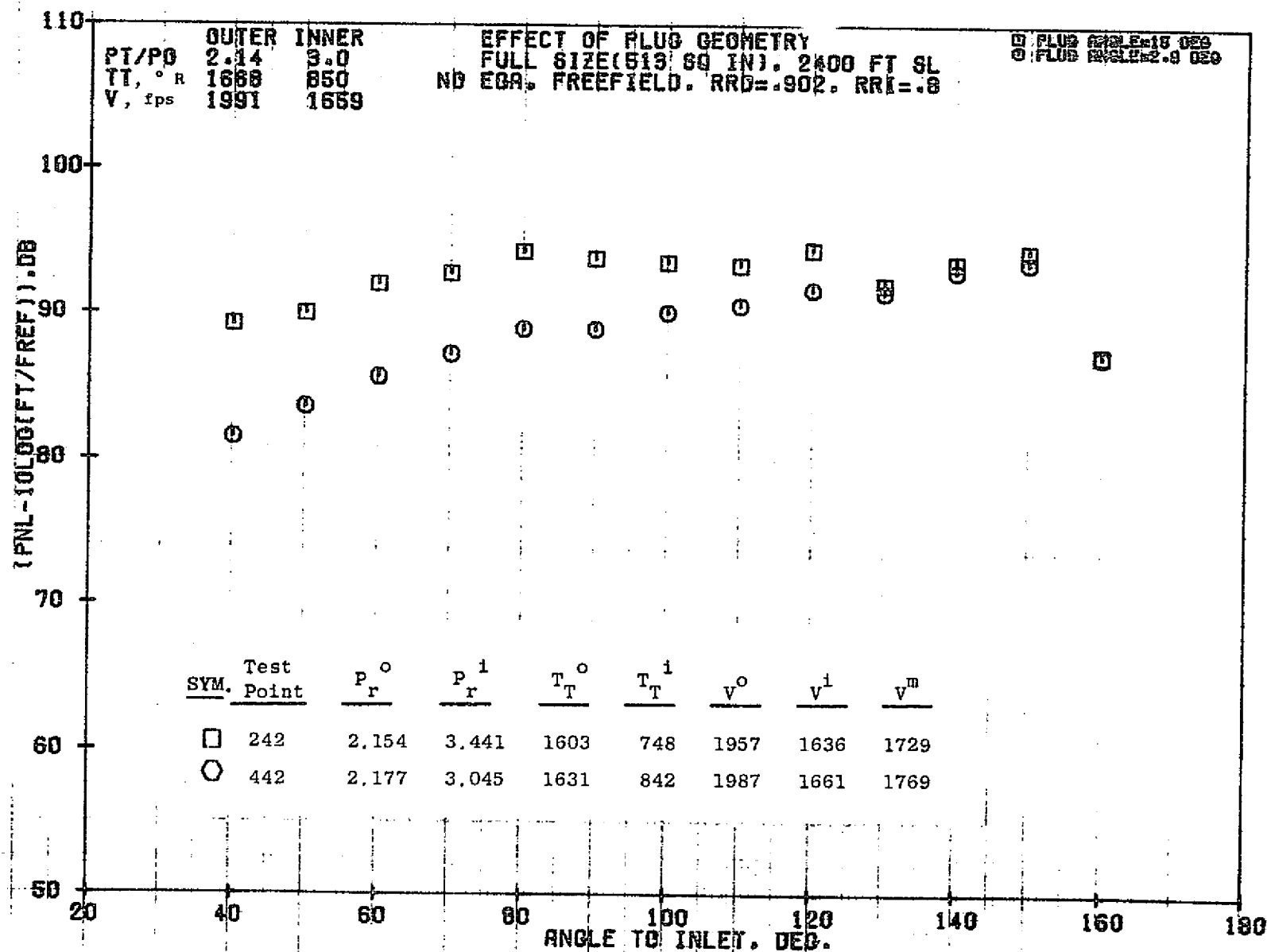
1062



10/29/76
 18159-001

79 BURCH A.

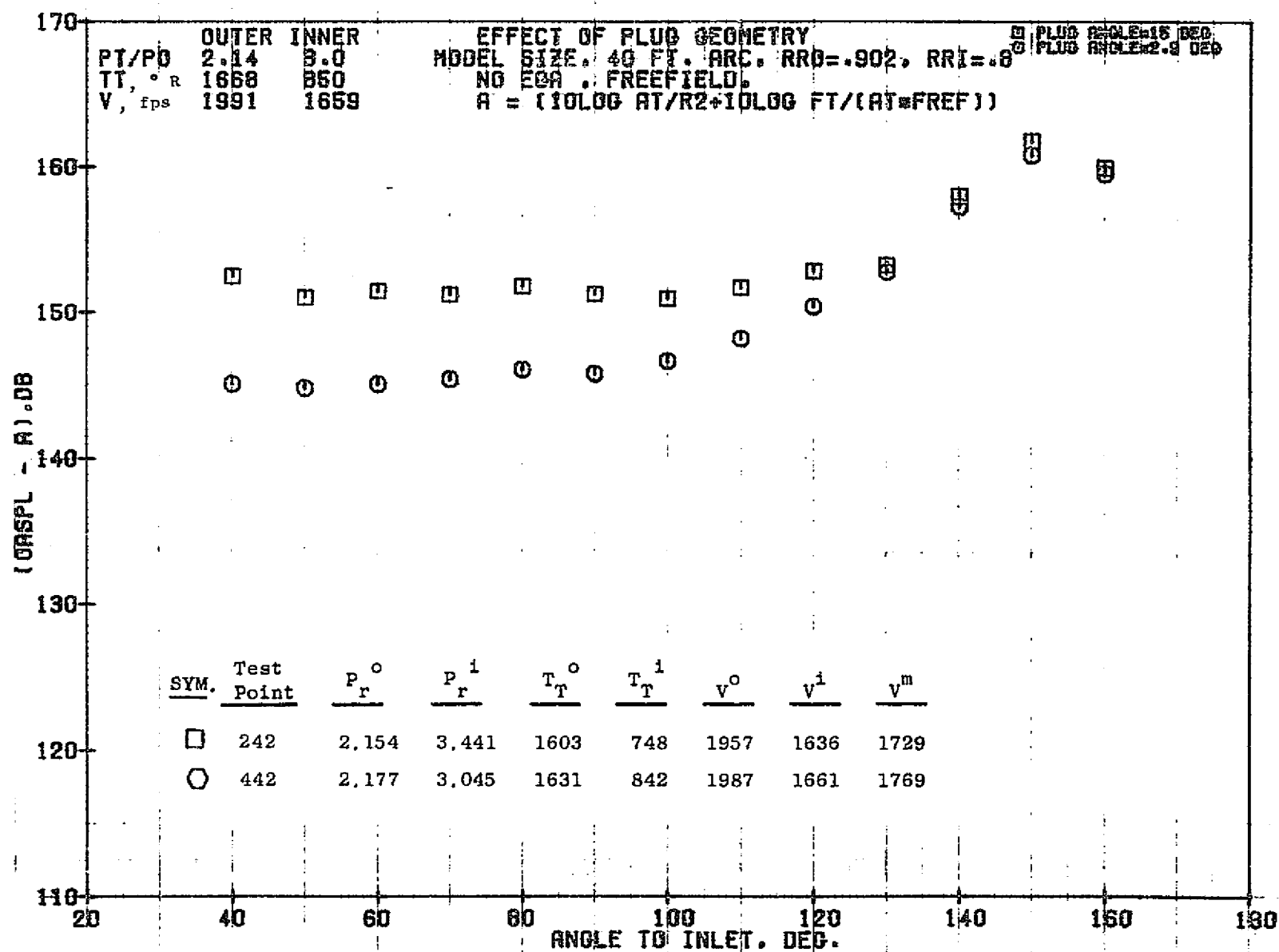
1063



10/29/76
 18130-001

79 BURCH A.

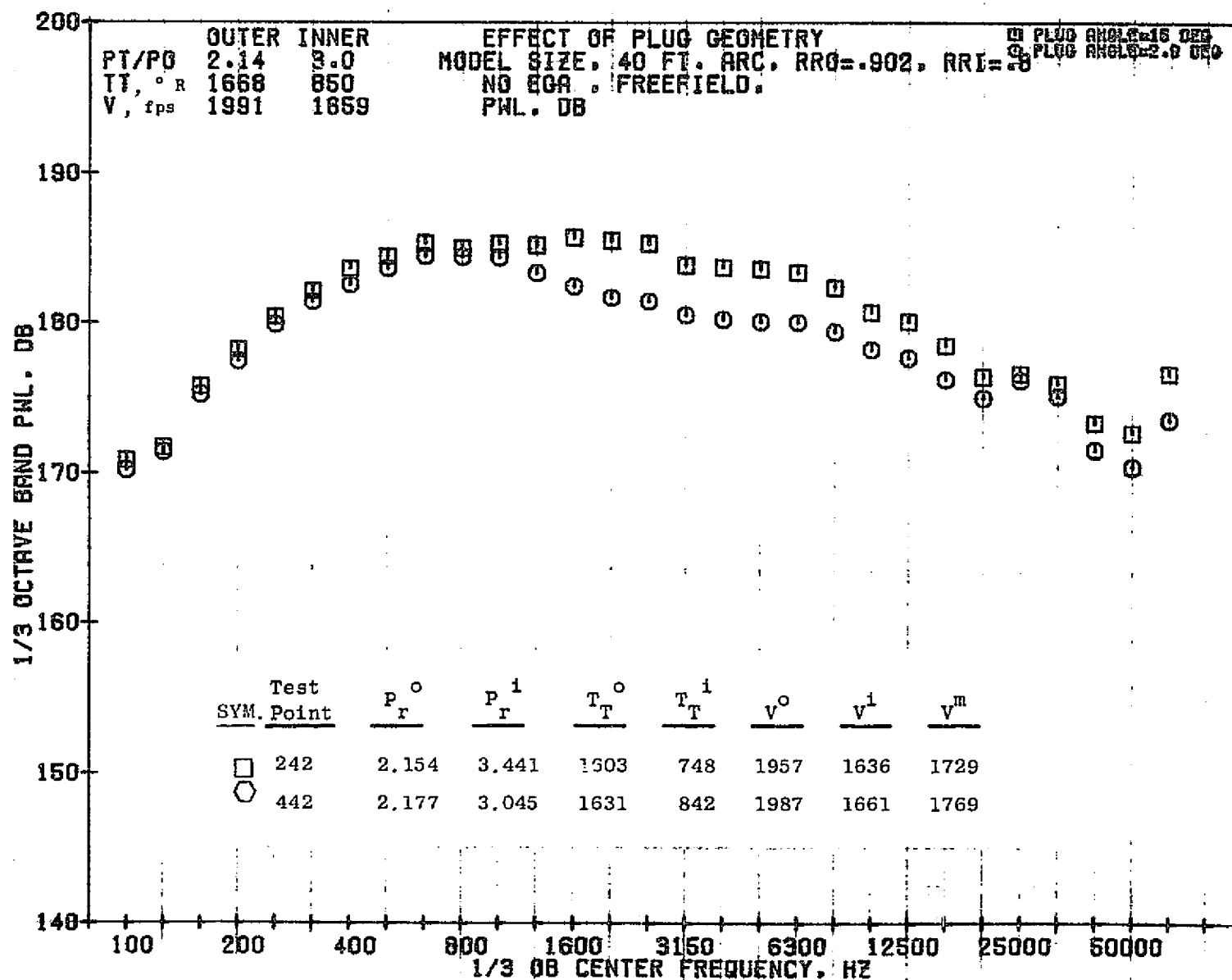
1064



10/29/76
 18159-001

79 BURCH A.

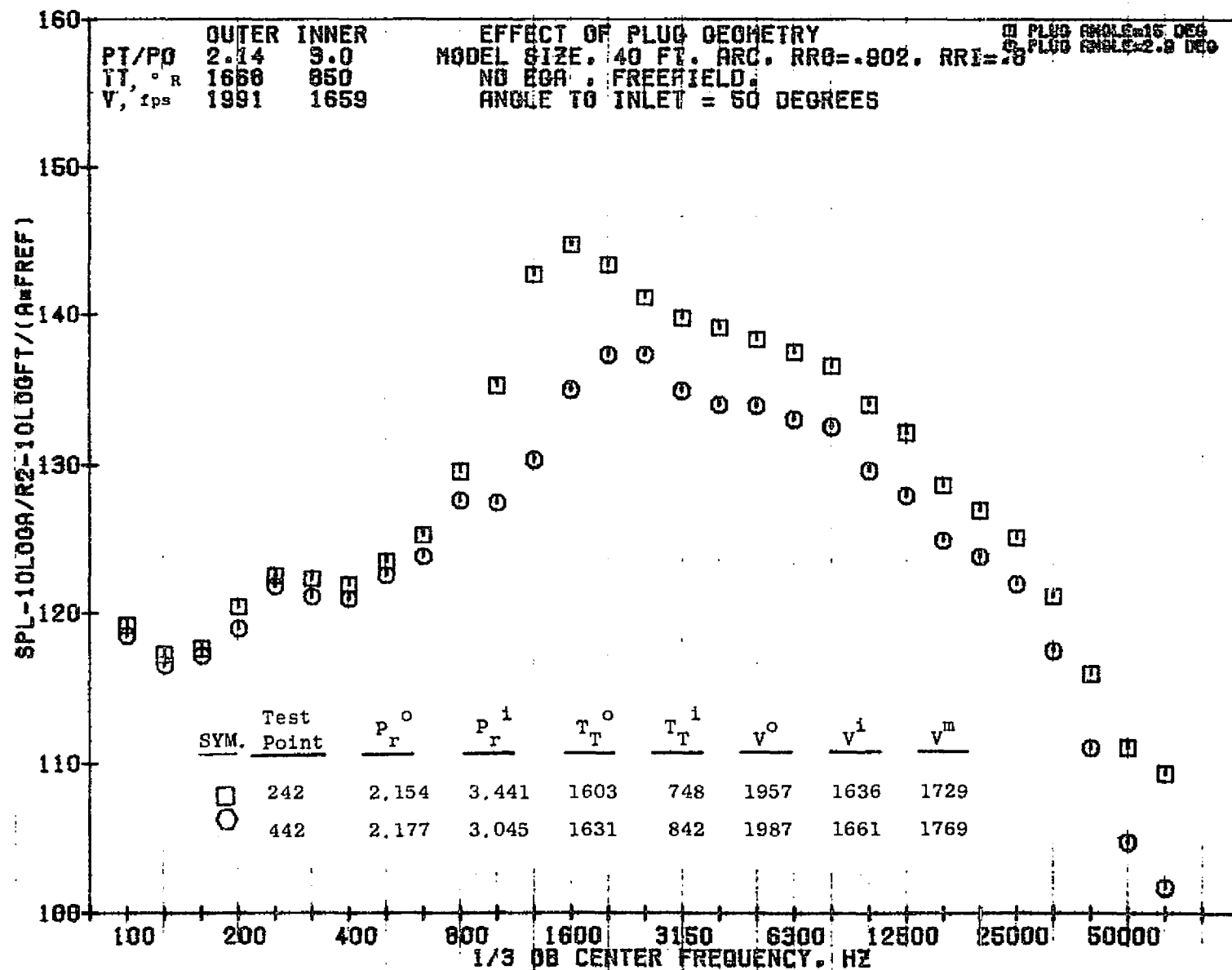
1065



10/29/76
 18159-001

79 BURCH A.

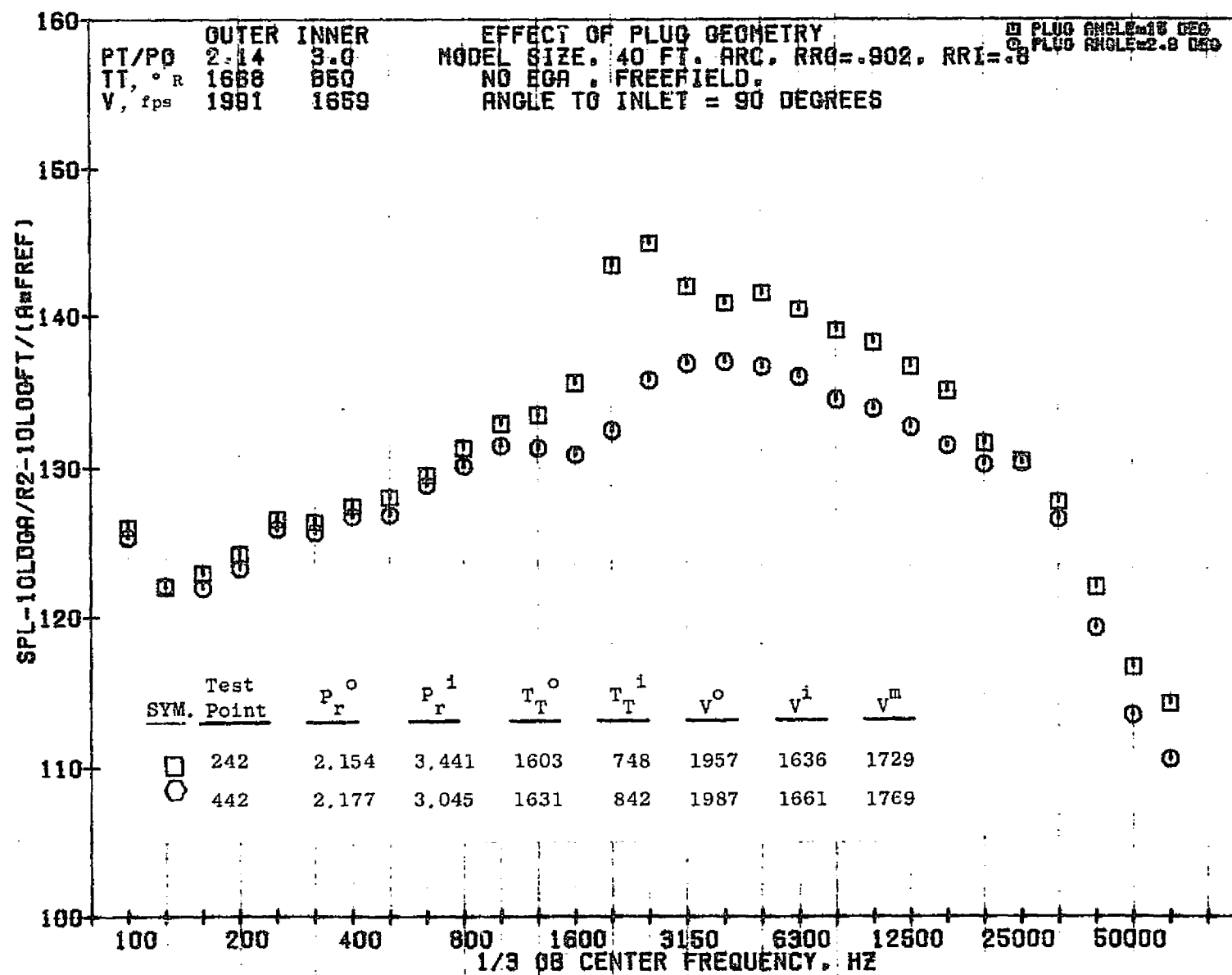
9901



10/29/76
 18159-001

79 BURCH A.

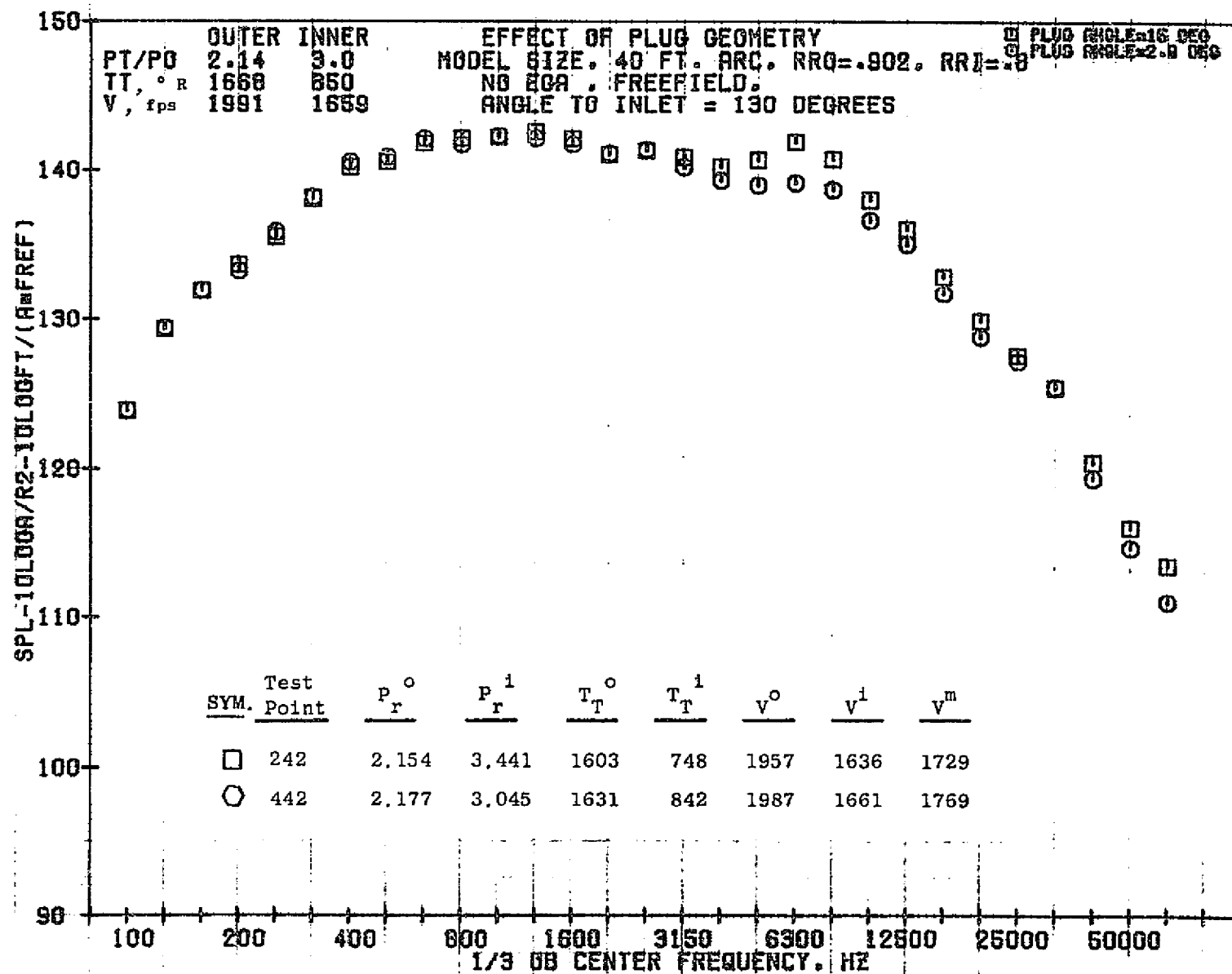
1067



10/29/76
 18159-001

79 BURCH A.

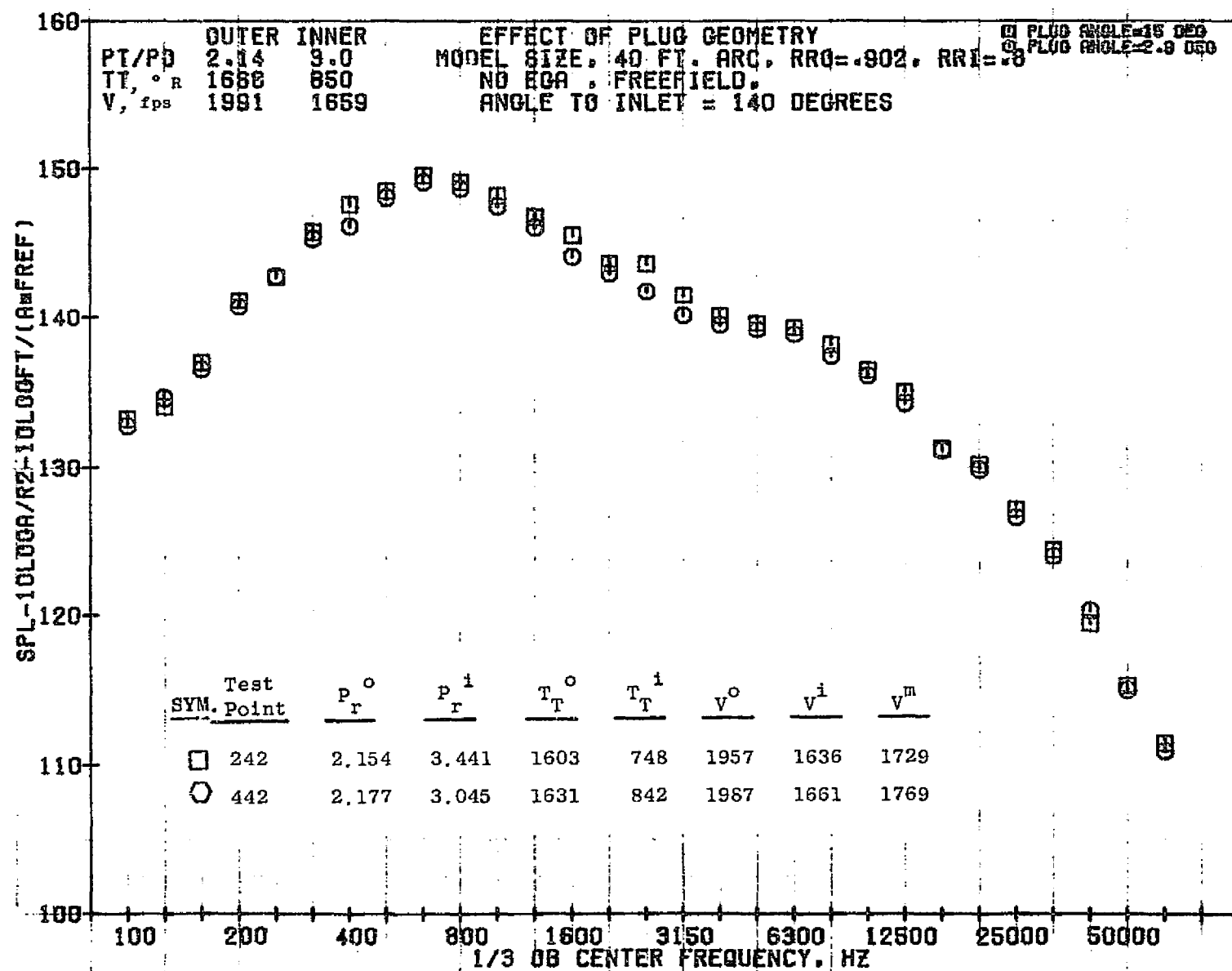
1068



10/29/76
 1B159-001

79 BURCH A.

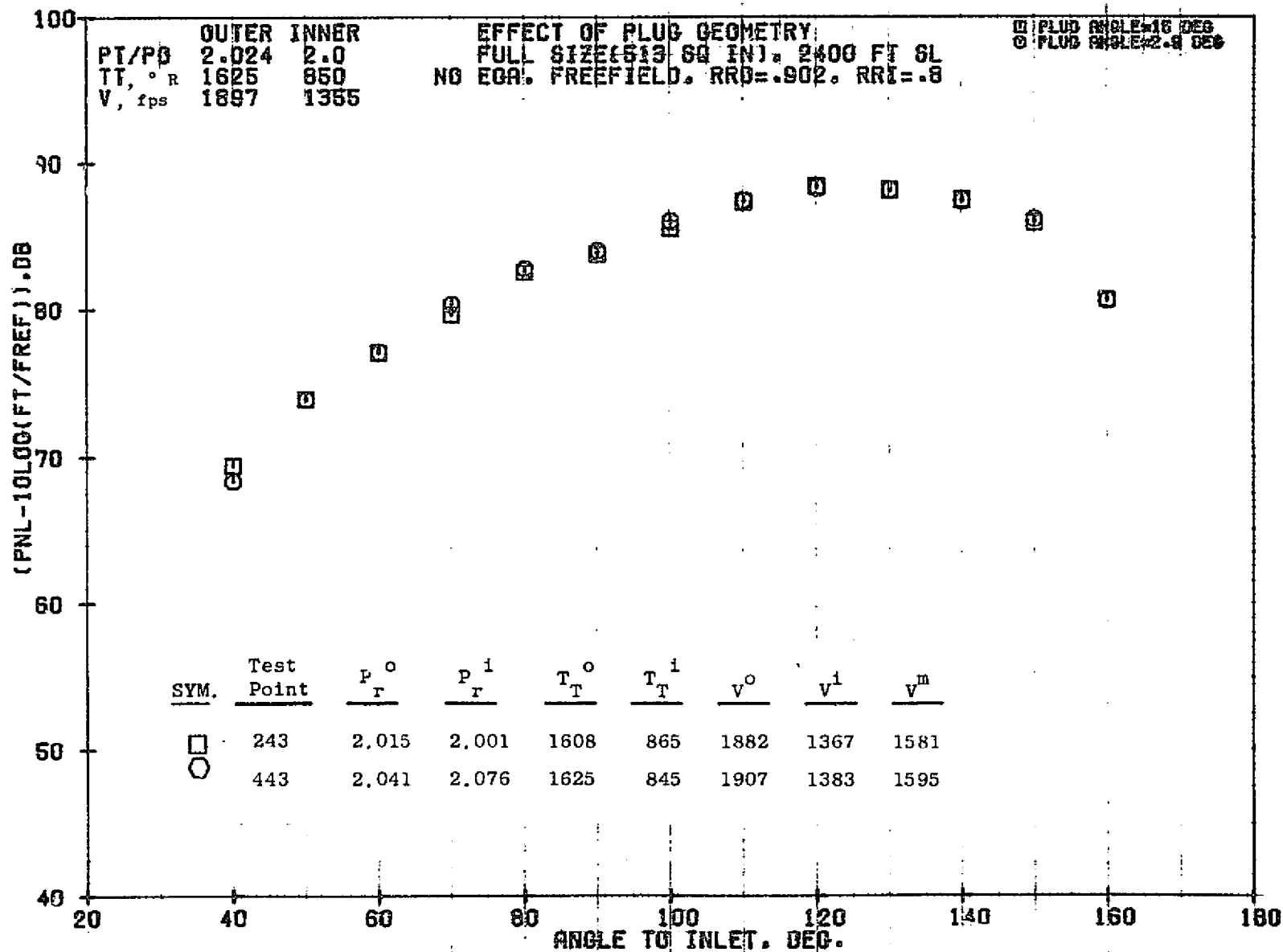
6901



10/29/76
 18159-001

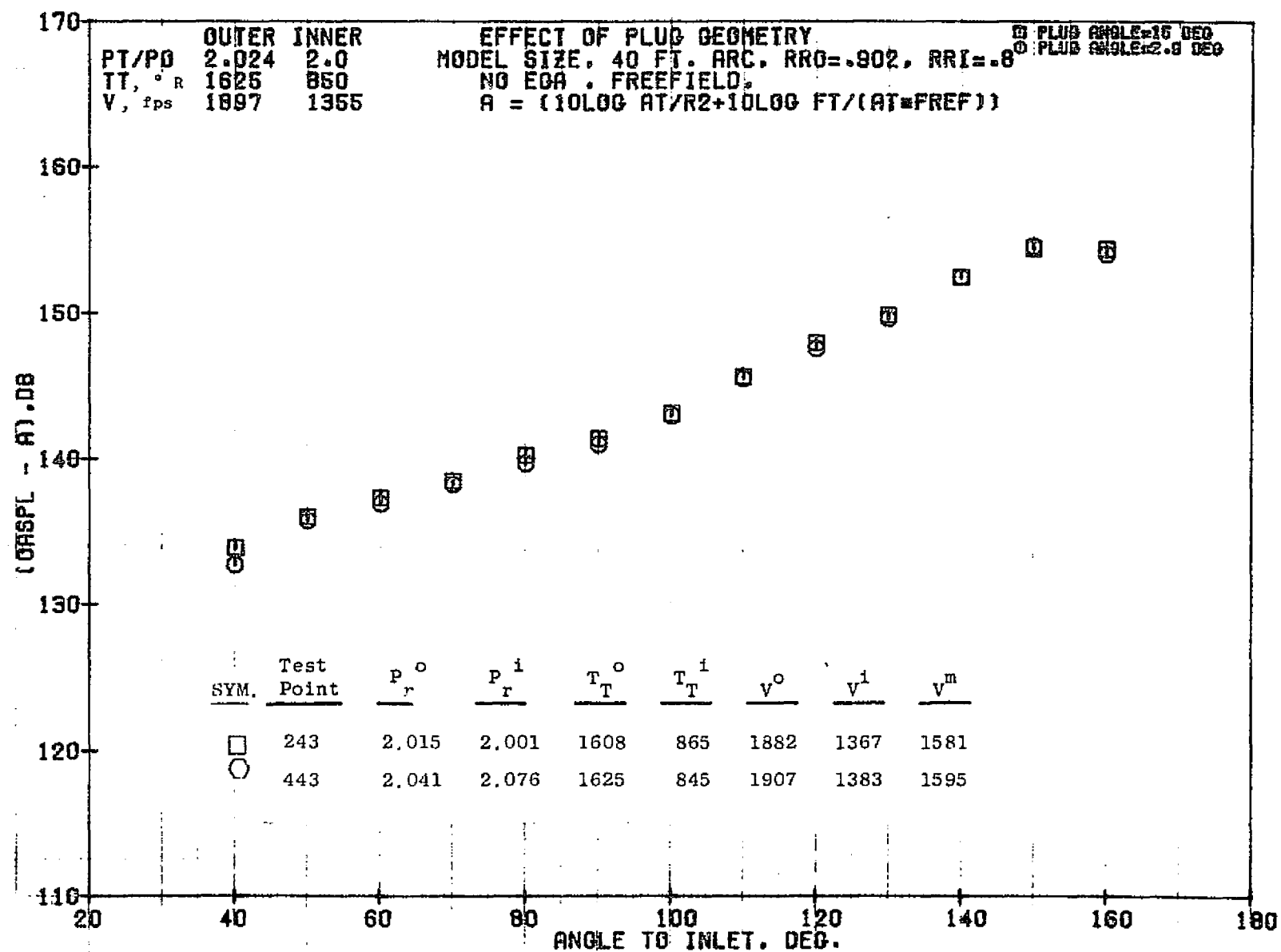
79 BURCH A.

1070



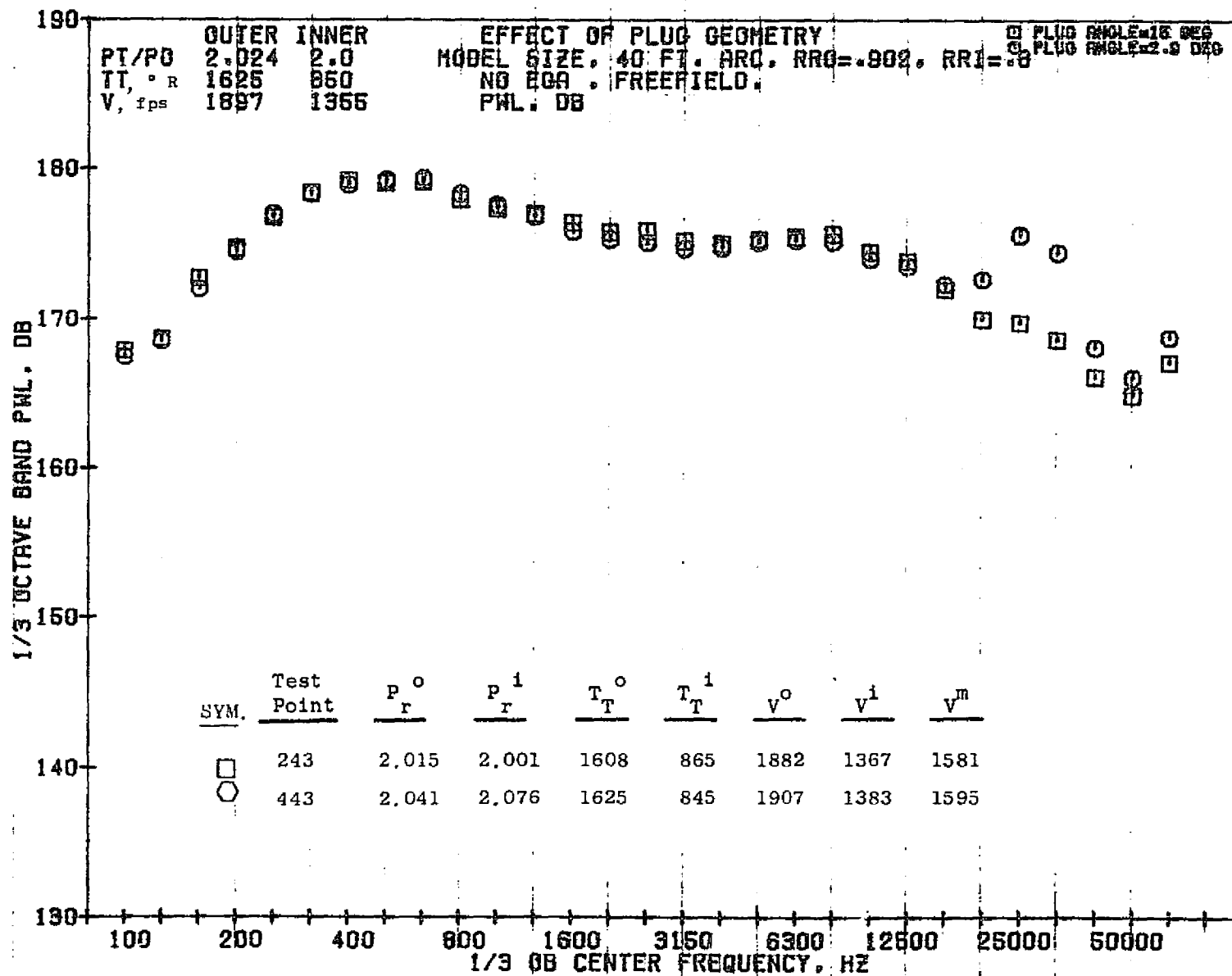
10/29/76
 18130-001

79 BURCH A.



10/29/76
 18159-001

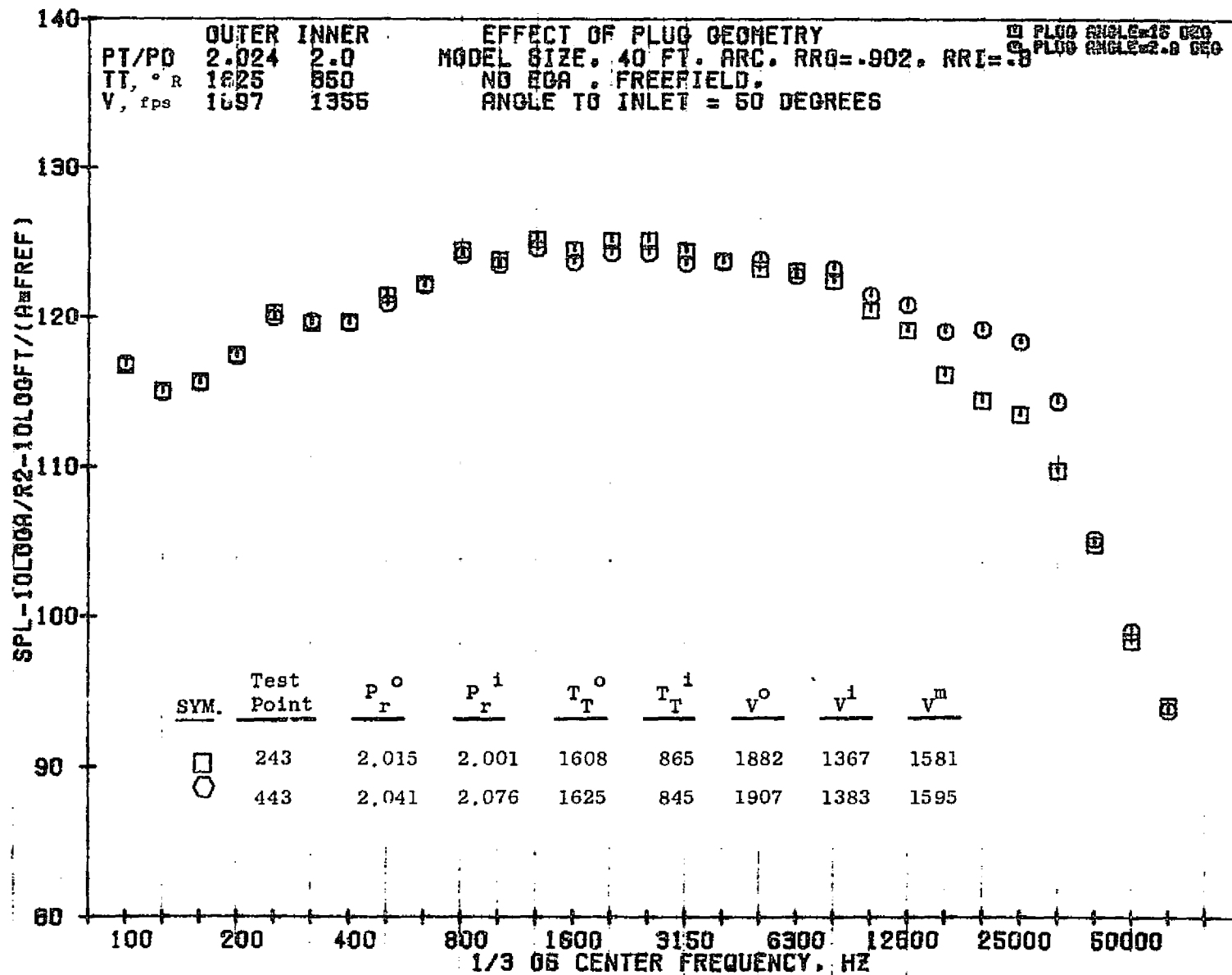
79 BURCH A.



10/29/76
18159-001

79 BURCH A.

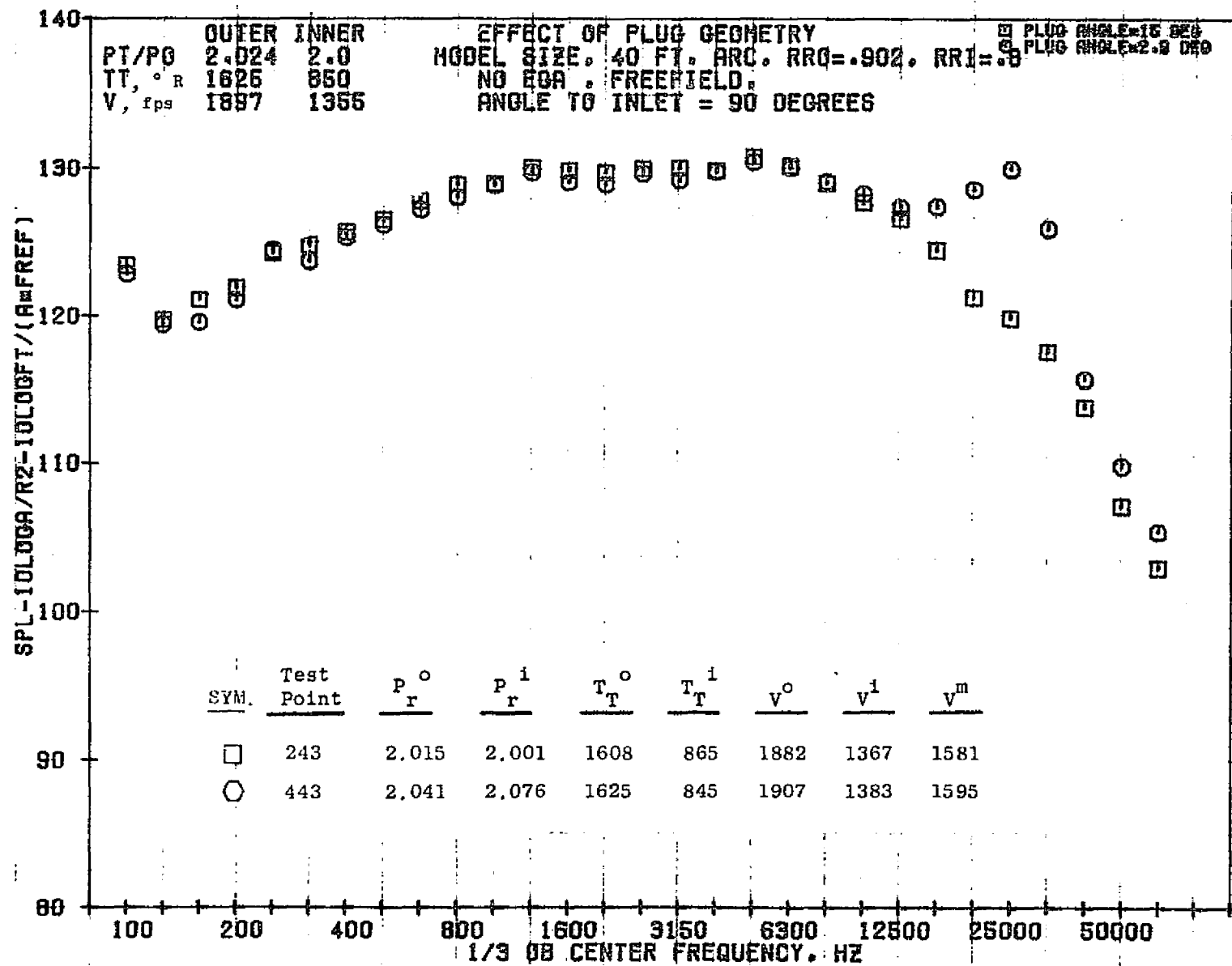
1073



10/29/76
 18159-001

79 BURCH A.

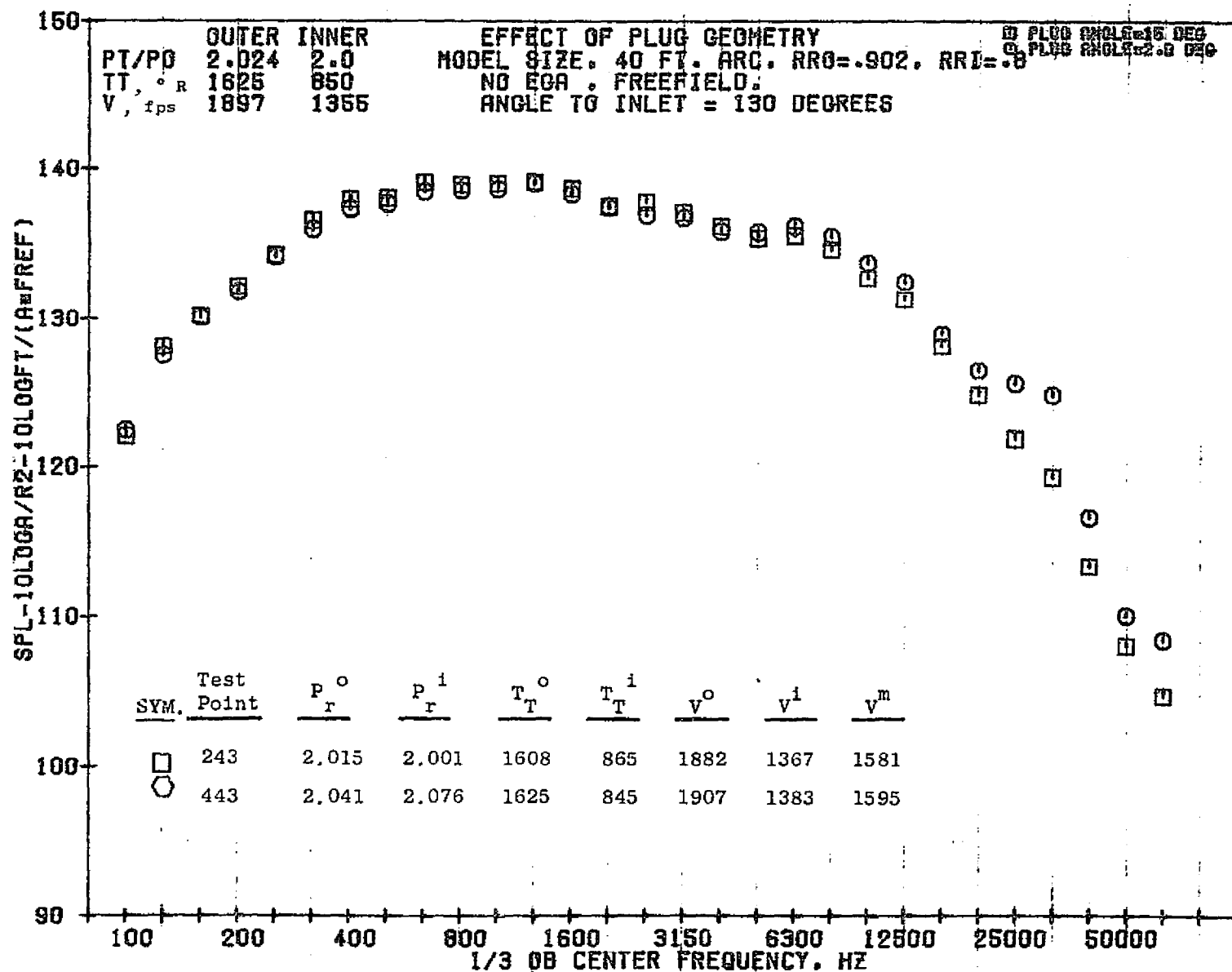
1074



10/29/76
 18159-001

79 BURCH A.

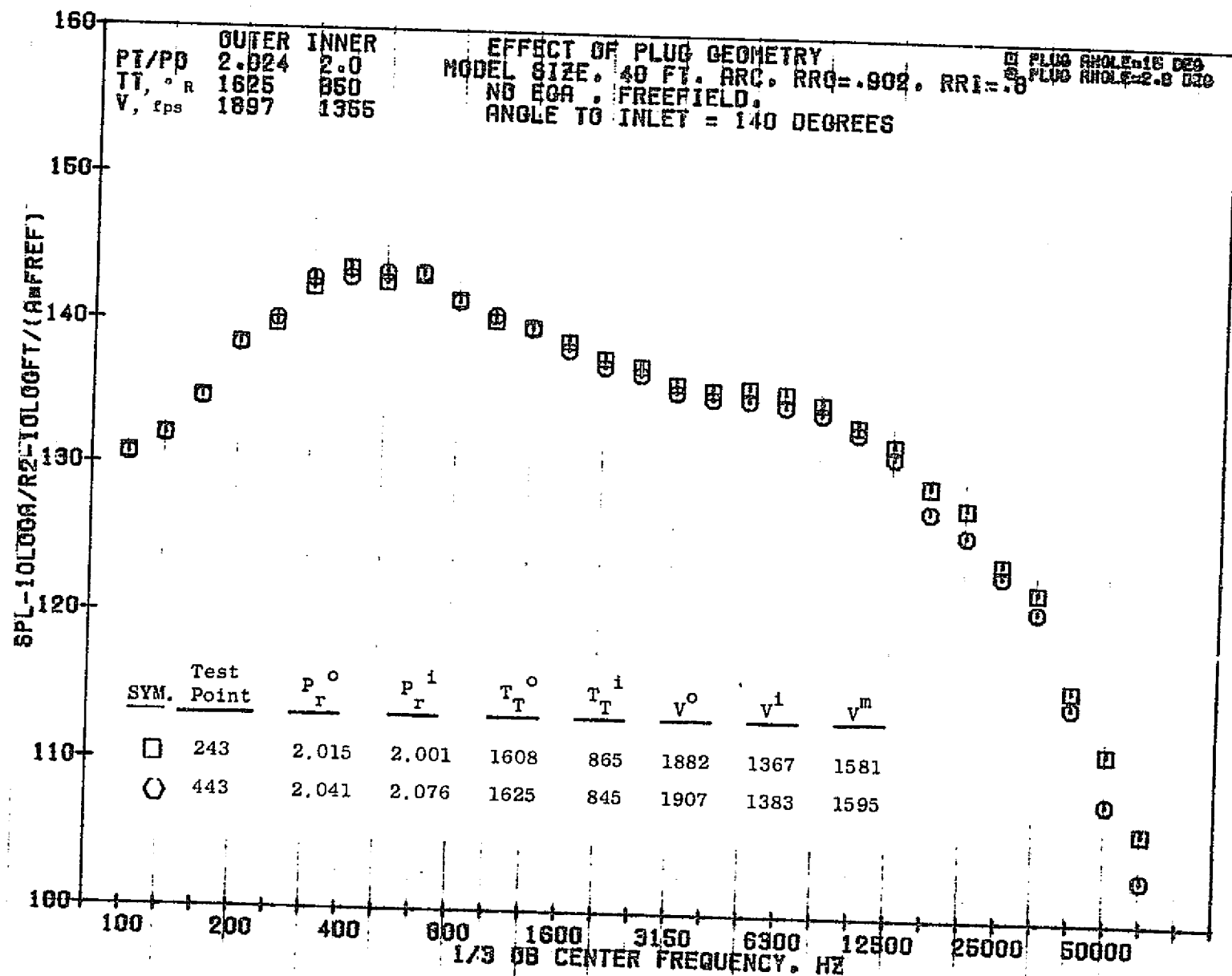
1075



10/29/76
 18159-001

79 BURCH A.

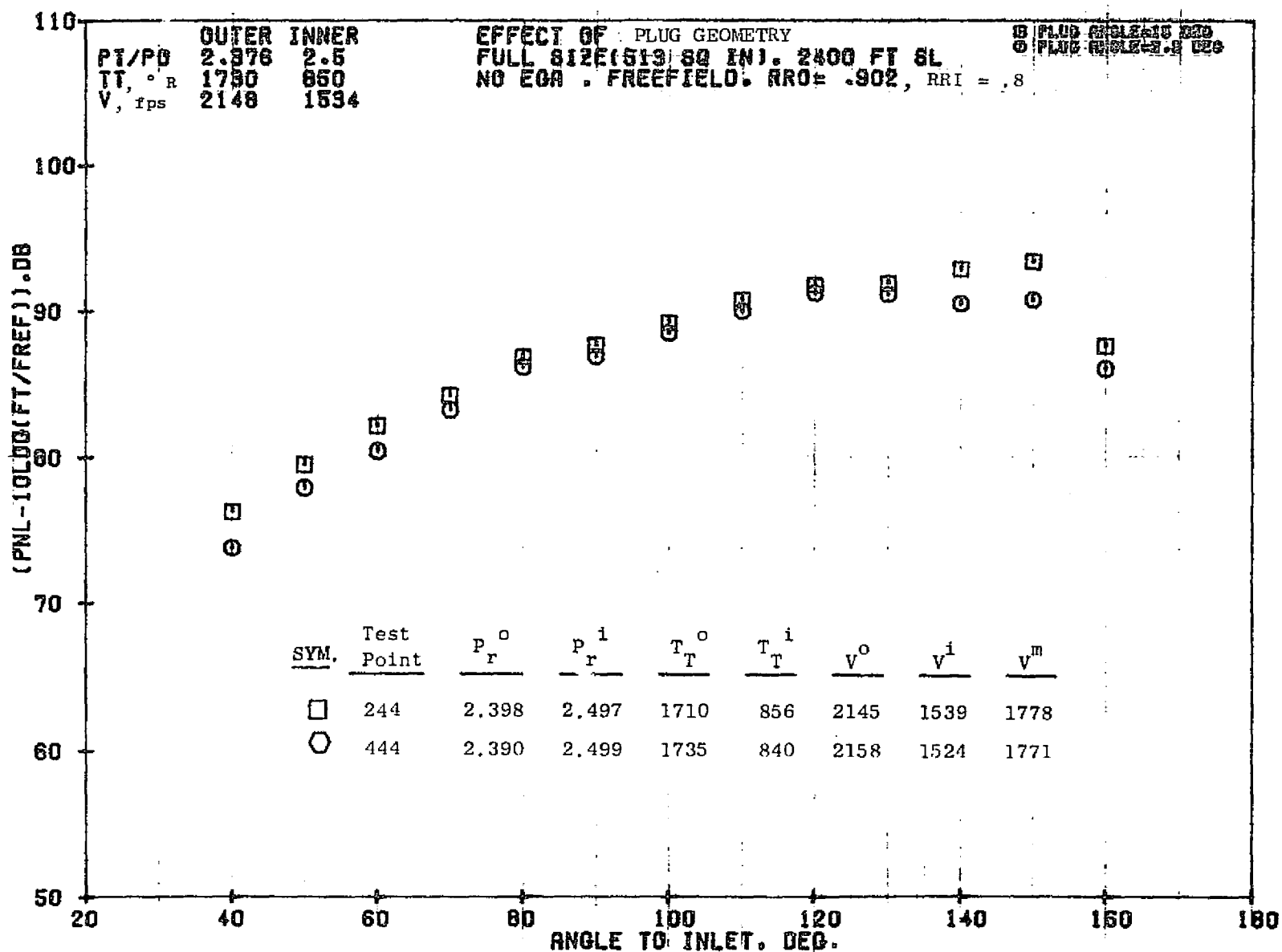
1076



10/29/76
 1B159-001

79 BURCH A.

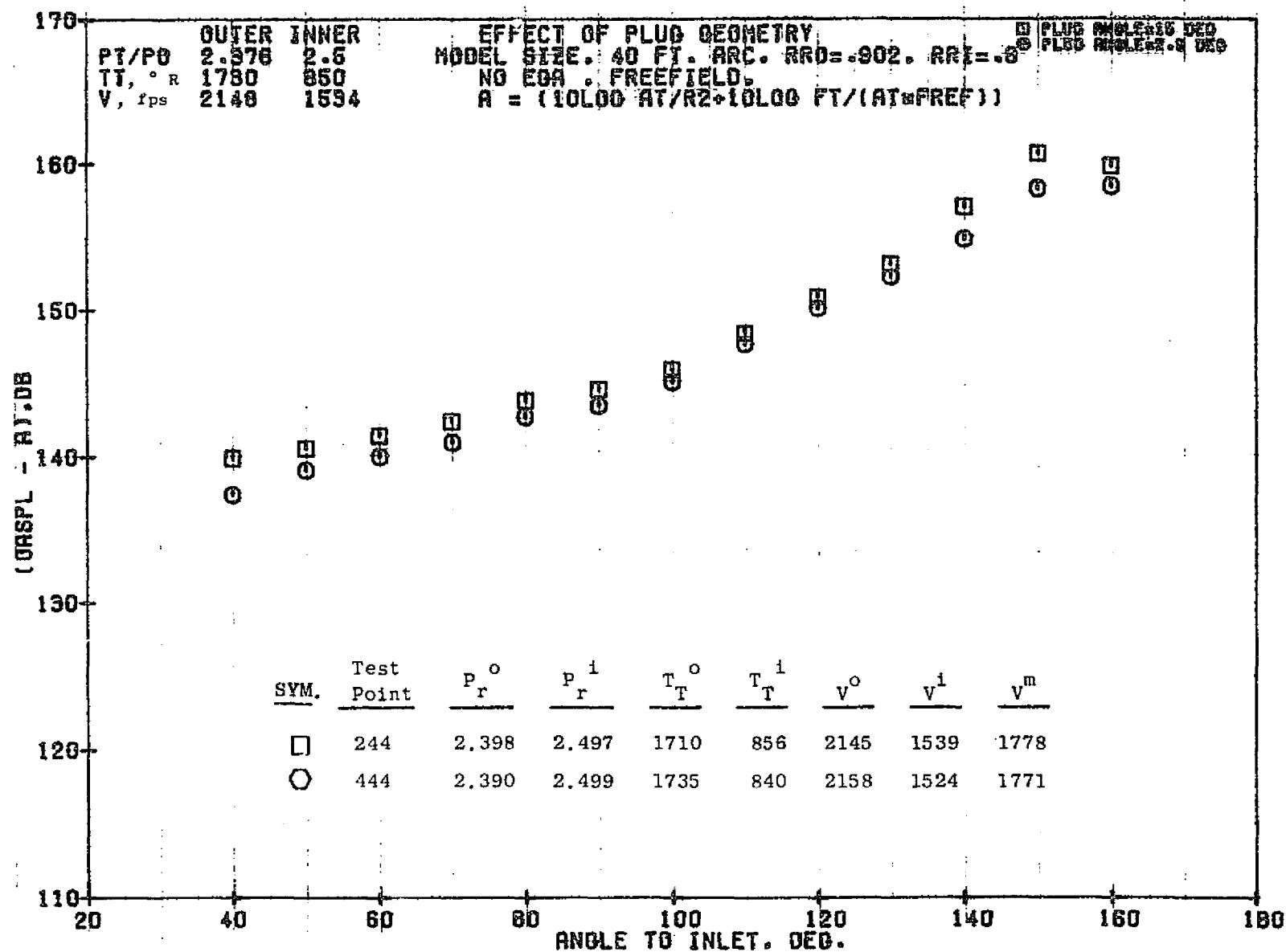
1077



11/04/76
 18680-001

79 BURCH A.

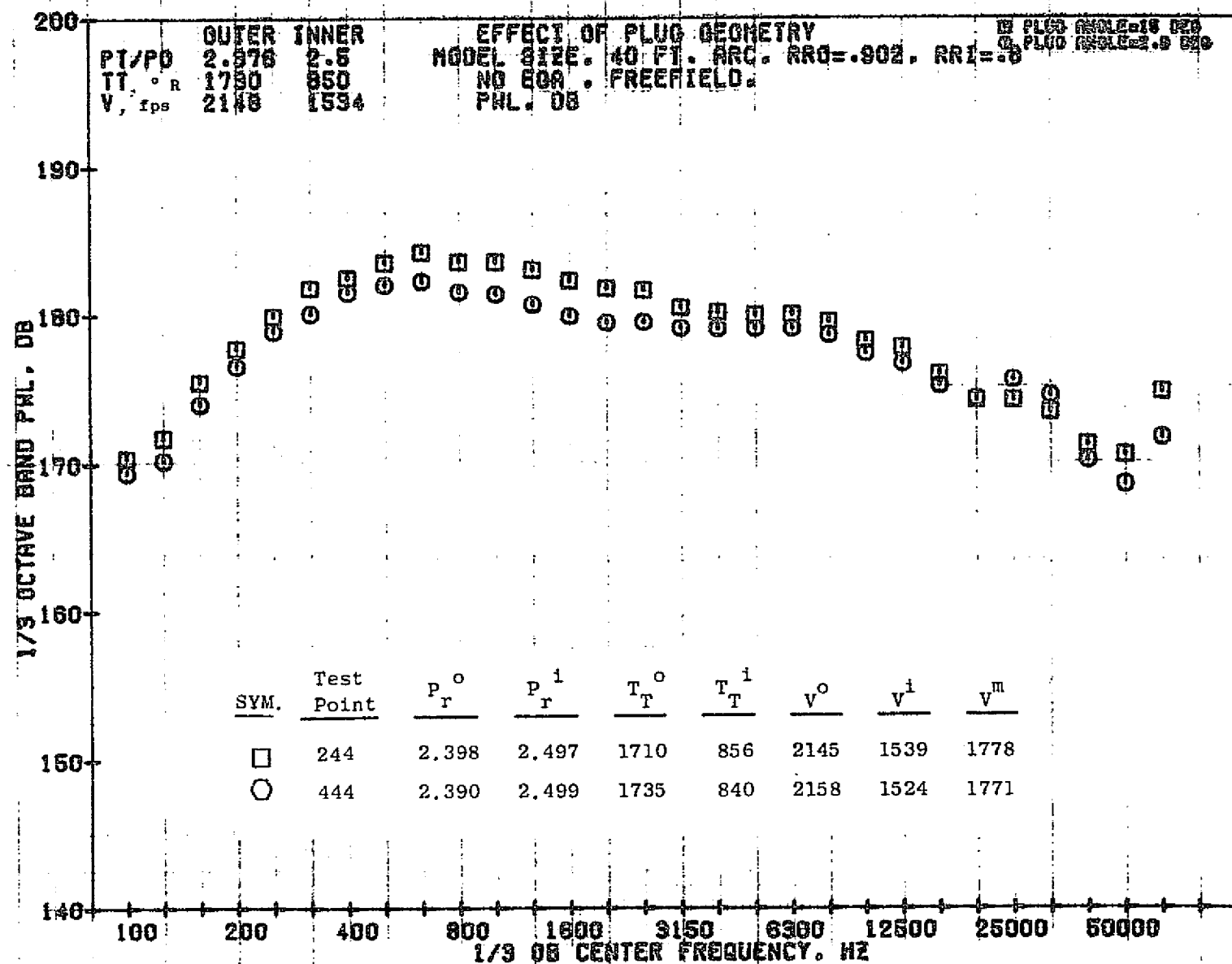
1078



11/04/76
 18727-001

79 BURCH A.

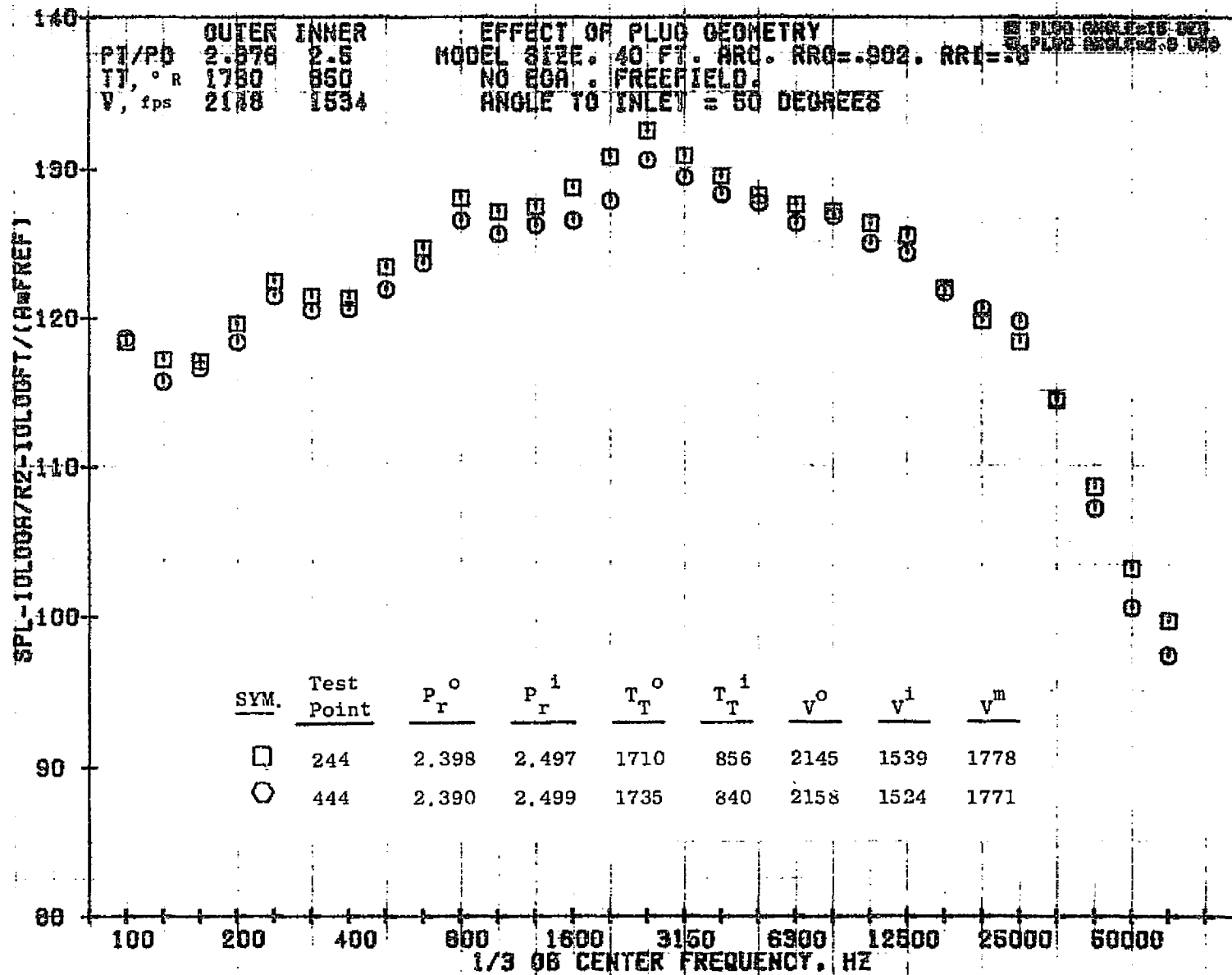
6201



11/04/76
 18727-001

79 BURCH A.

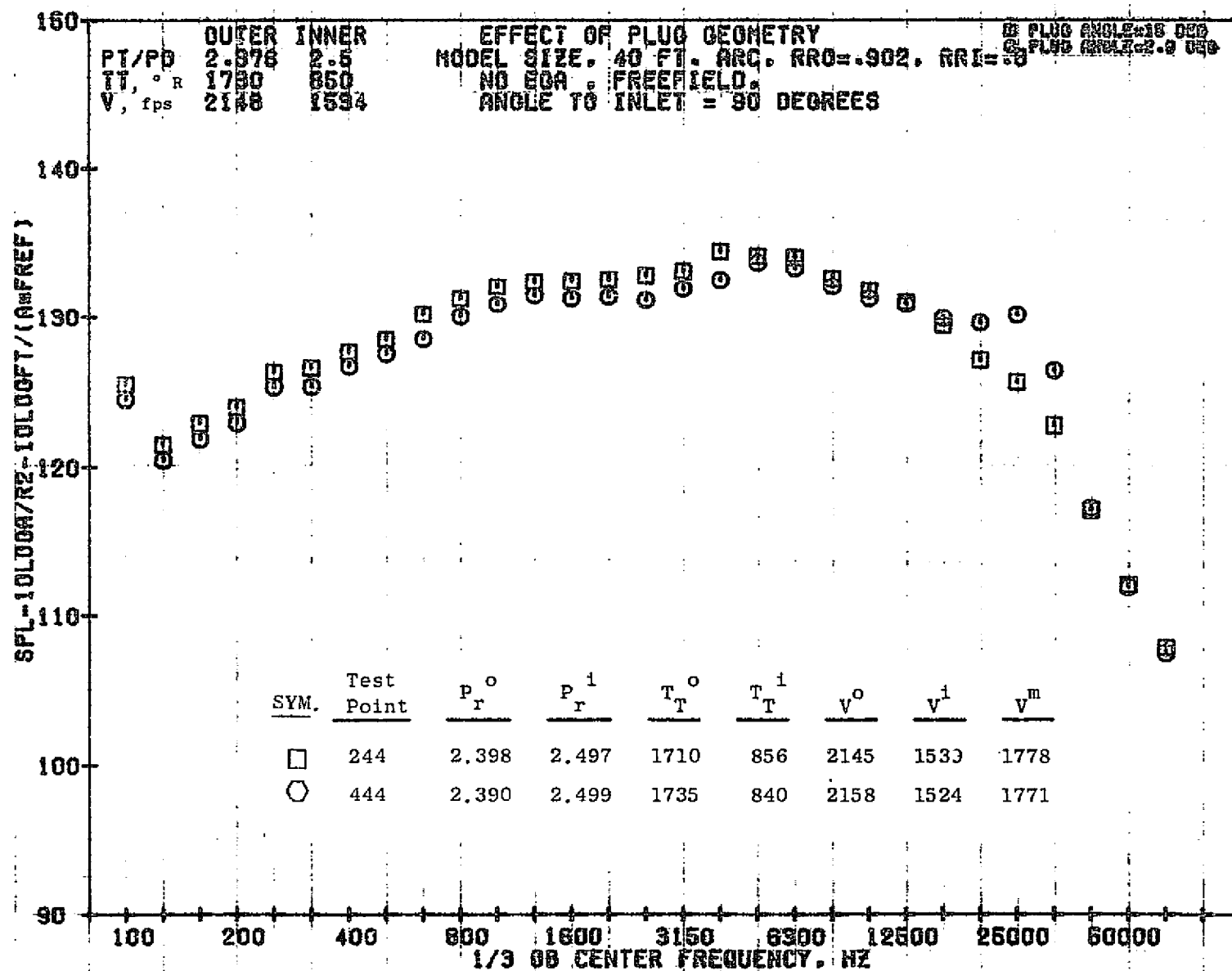
0801



11/04/76
 18727-001

79 BURCH A.

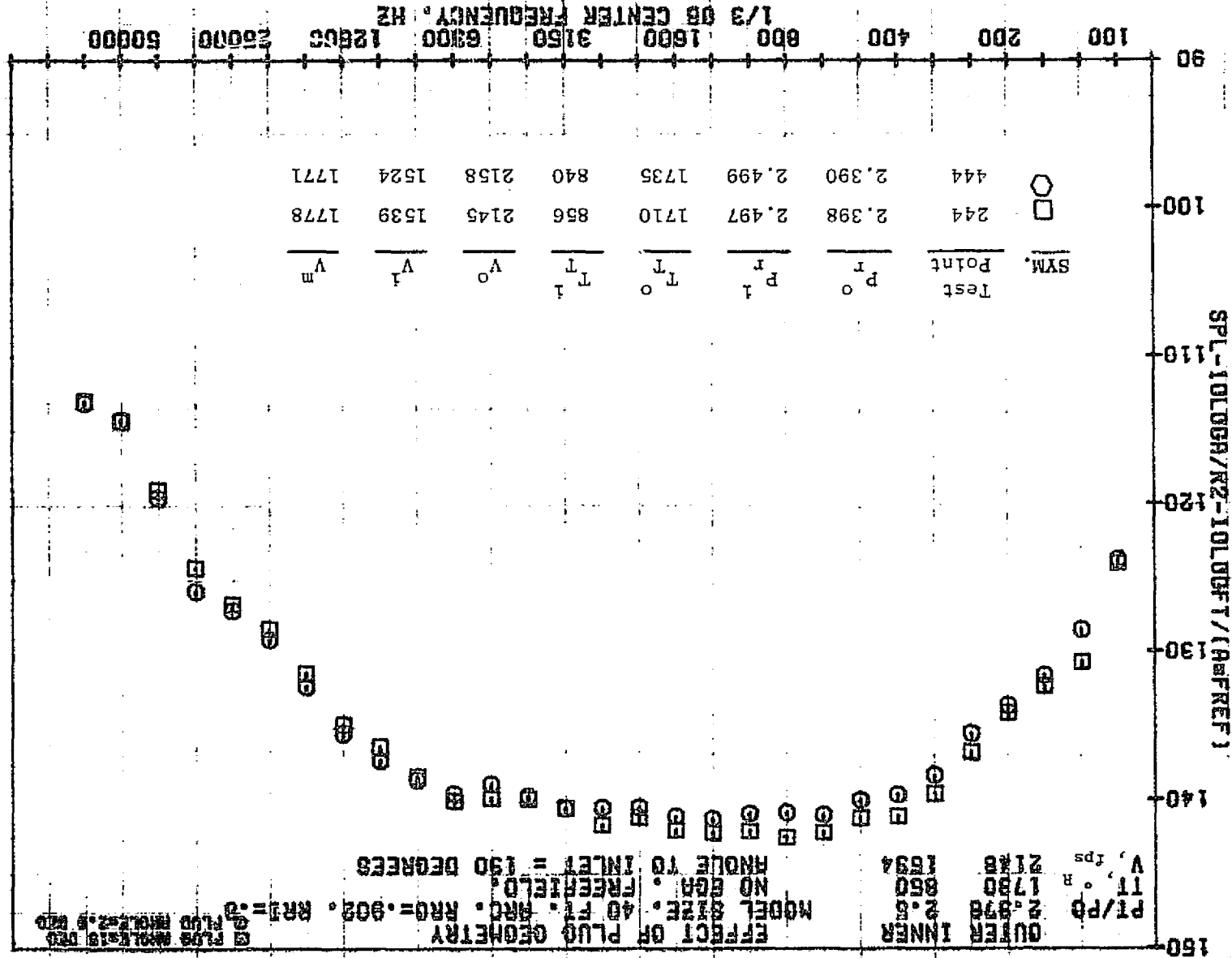
1801



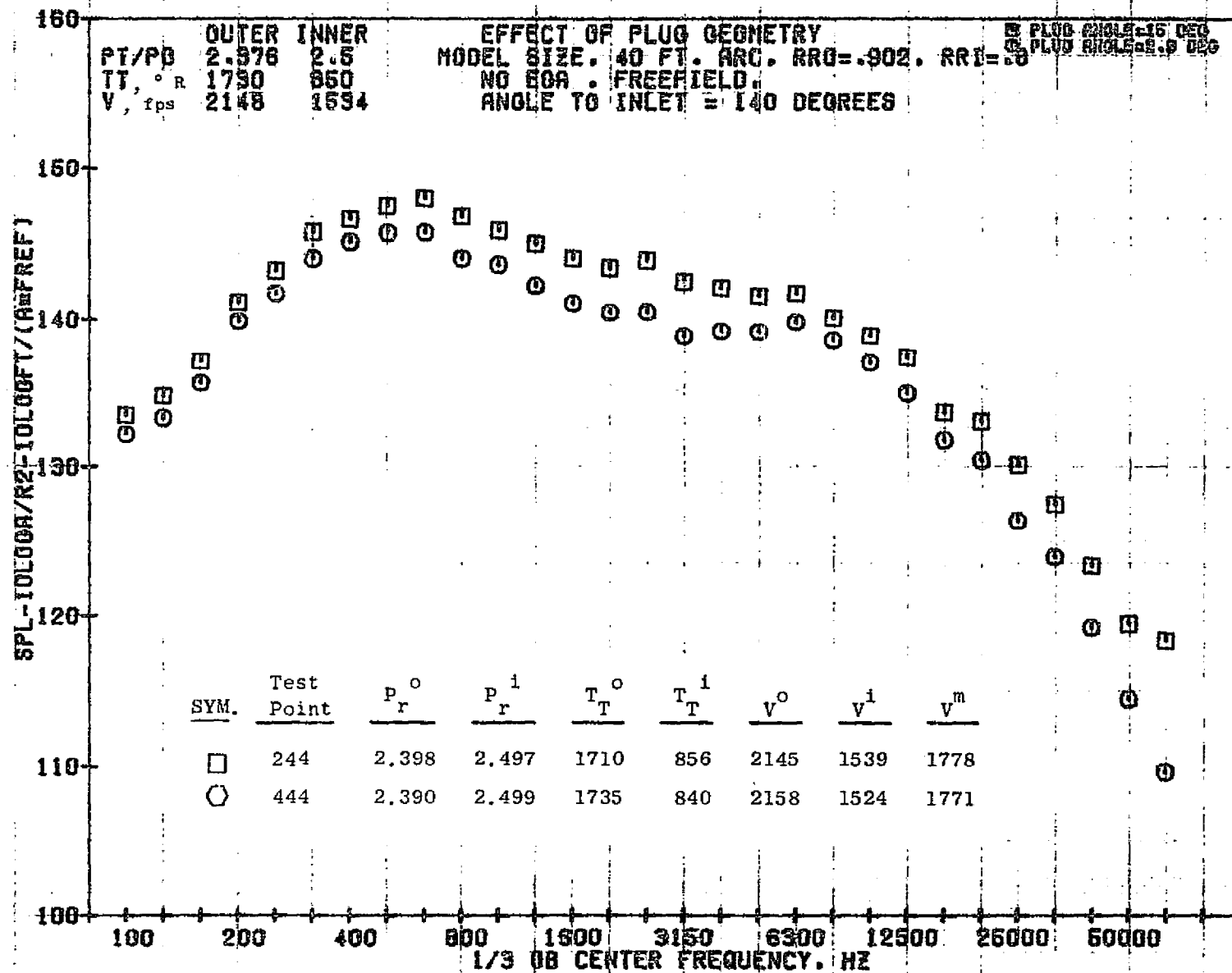
11/04/76
 18727-001

79 BURCH A.

EFFECT OF PLUG GEOMETRY
 MODEL SIZE: 40 FT. HRC. RHO=.902. RRI=.0
 NO EGM. FREEFIELD.
 HOLE TO INLET = 190 DEGREES
 P1/P0 2.876 2.5
 TT, ° 1780 860
 V, f/s 2148 1894
 OUTER INNER
 FLUG MOLE-18 DEG
 FLUG MOLE-2.5 DEG



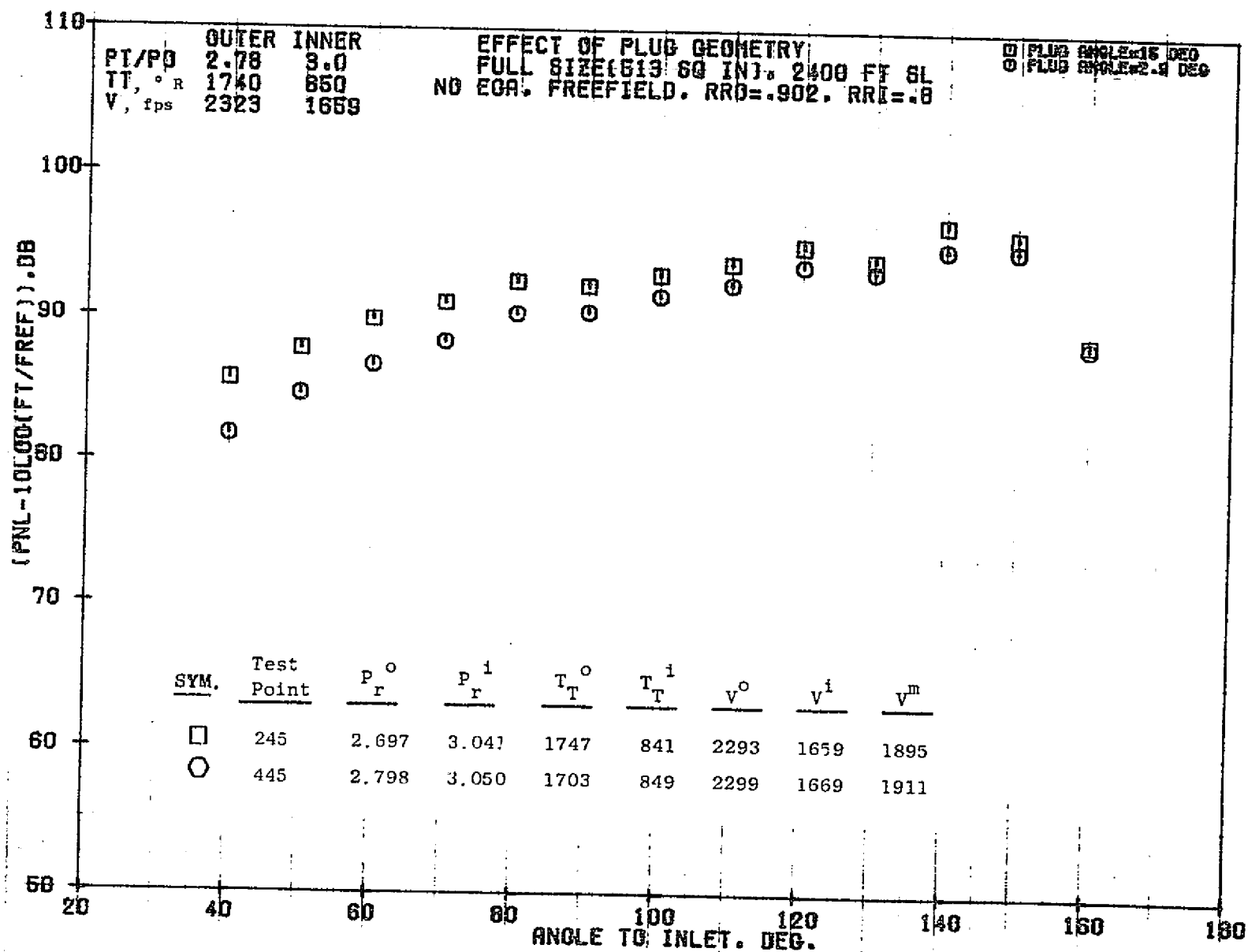
1083



11/04/76
 18727-001

79 BURCH A.

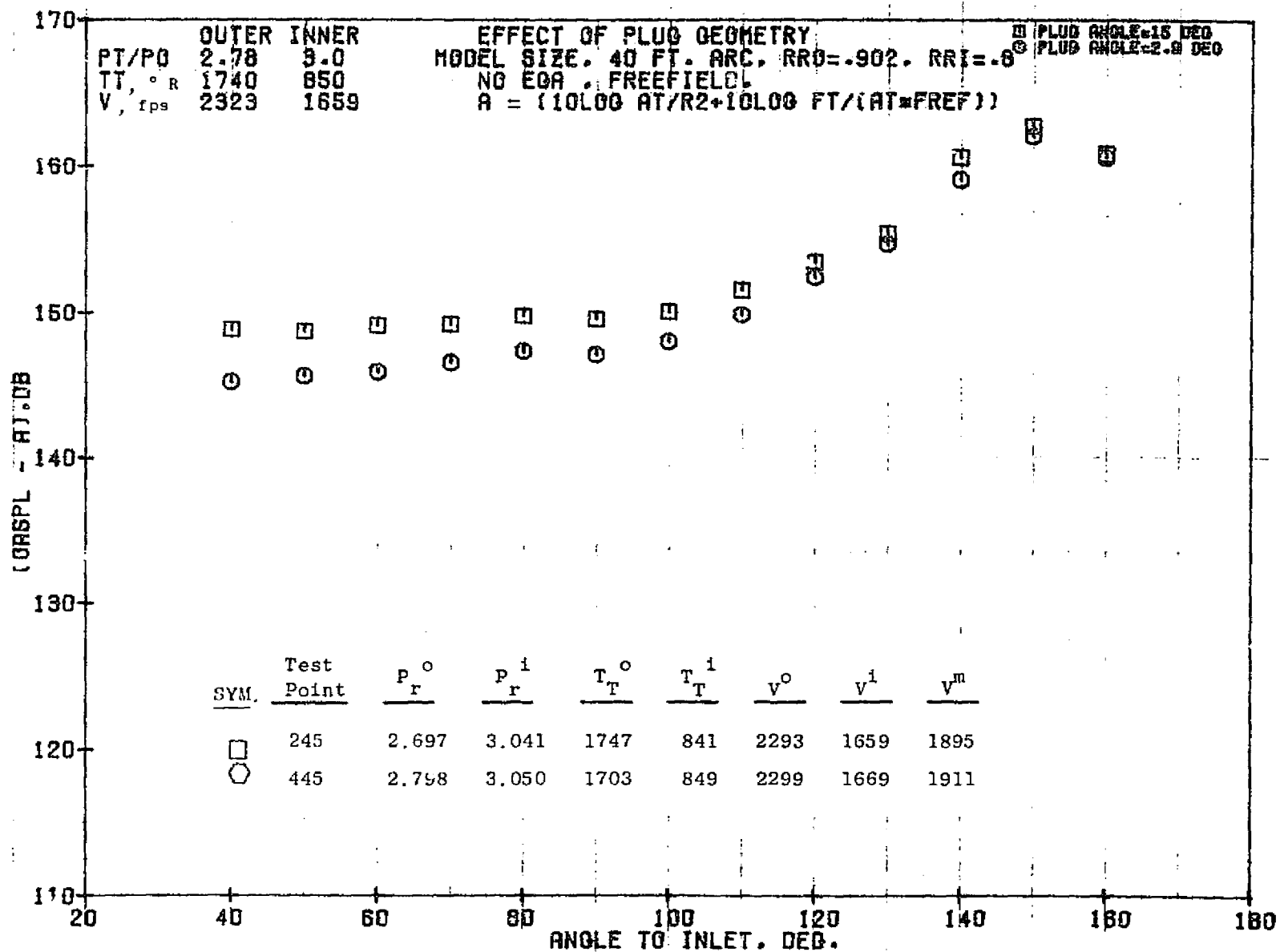
1084



10/29/76
 18130-001

79 BURCH A.

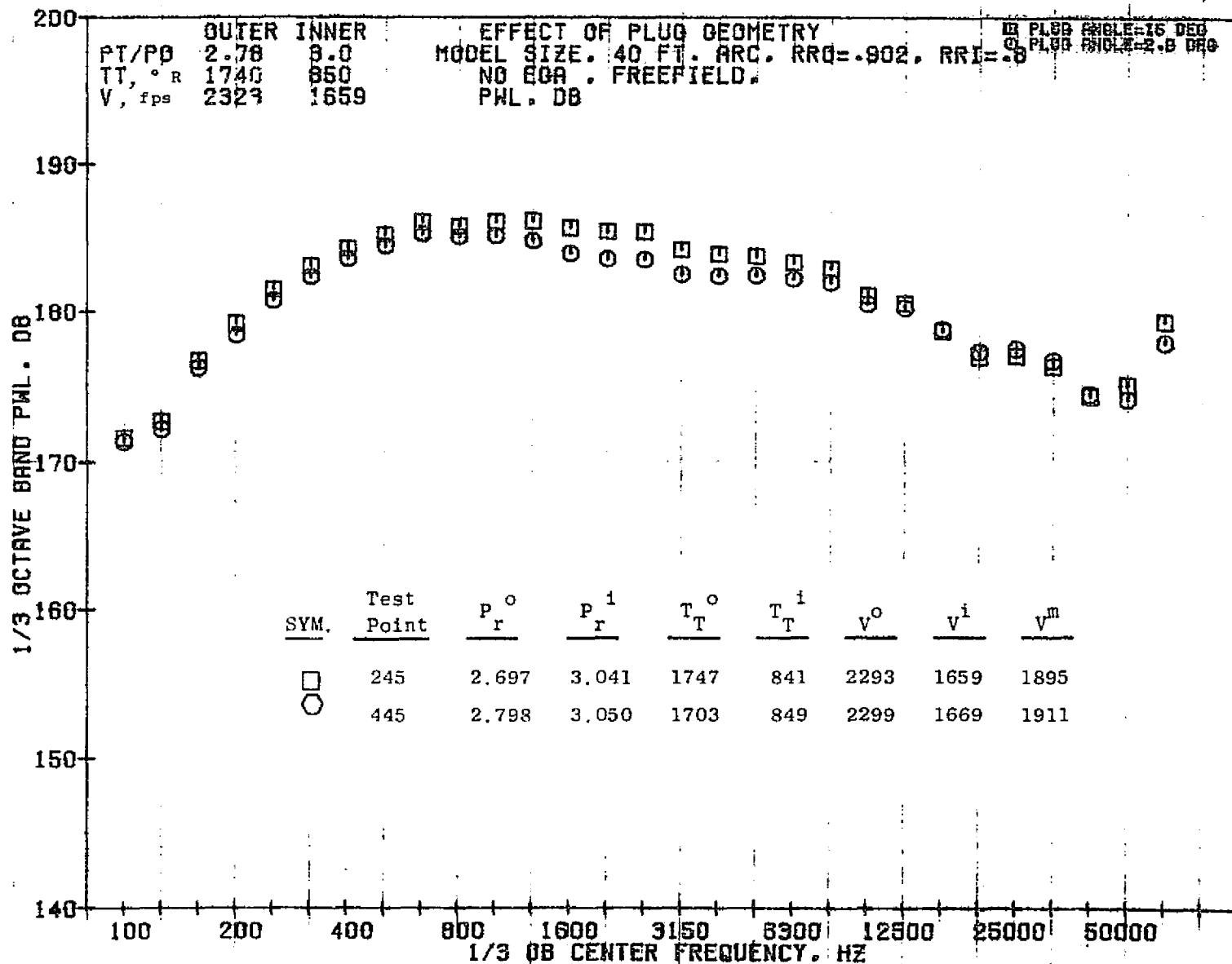
1085



11/03/76
 18360-001

79 BURCH A.

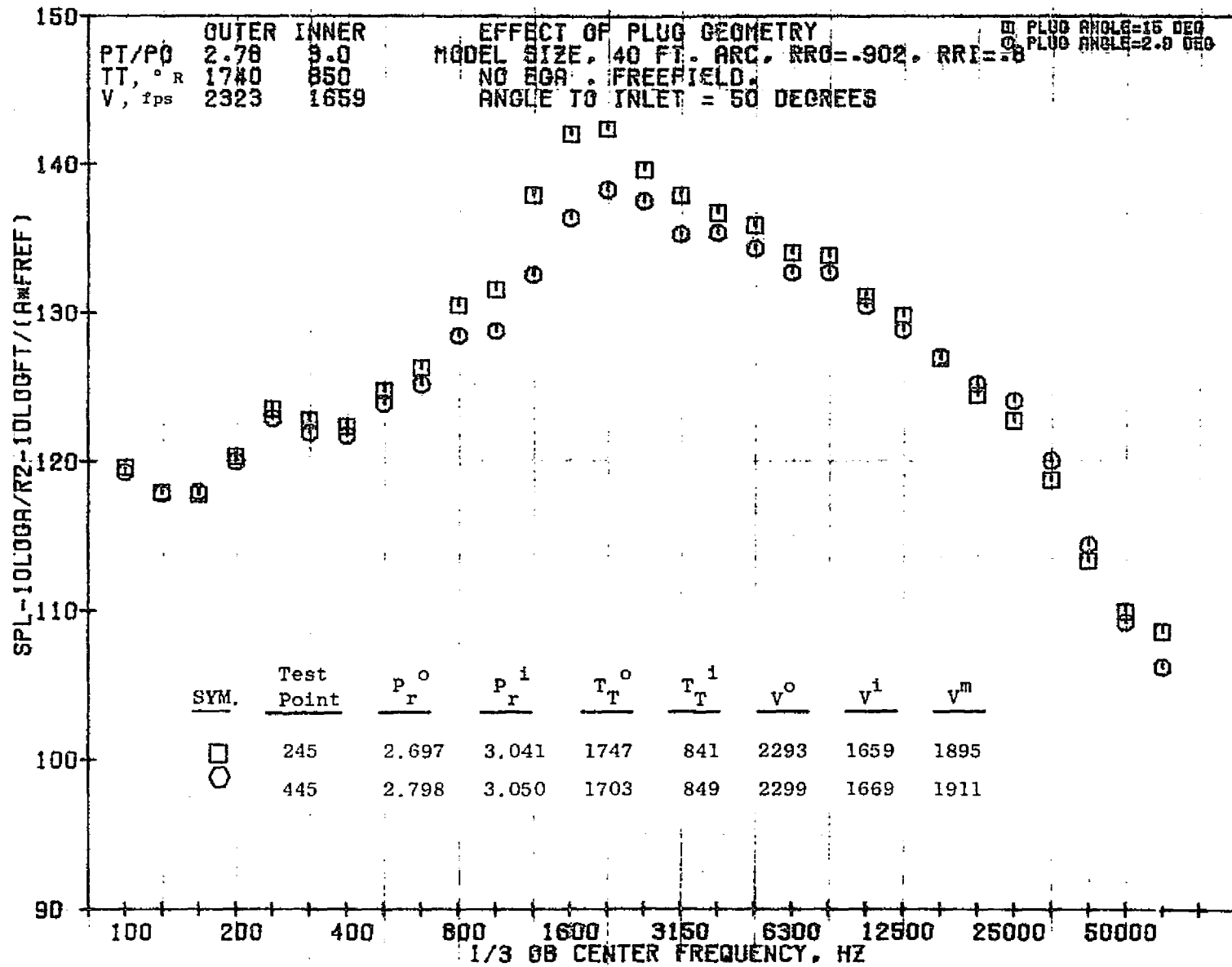
1086



11/03/76
18360-001

79 BURCH A.

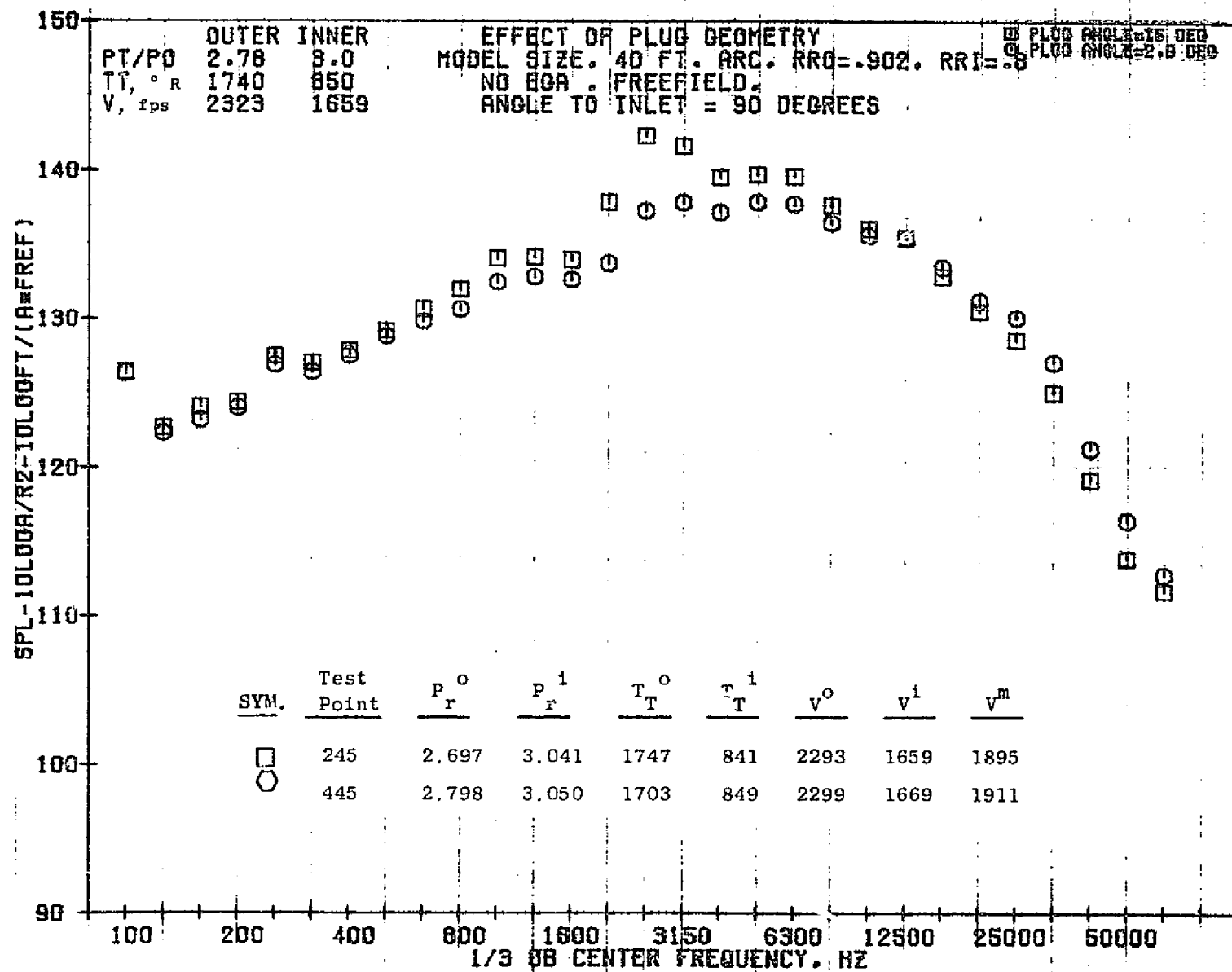
1087



11/03/76
 18360-001

79 BURCH A.

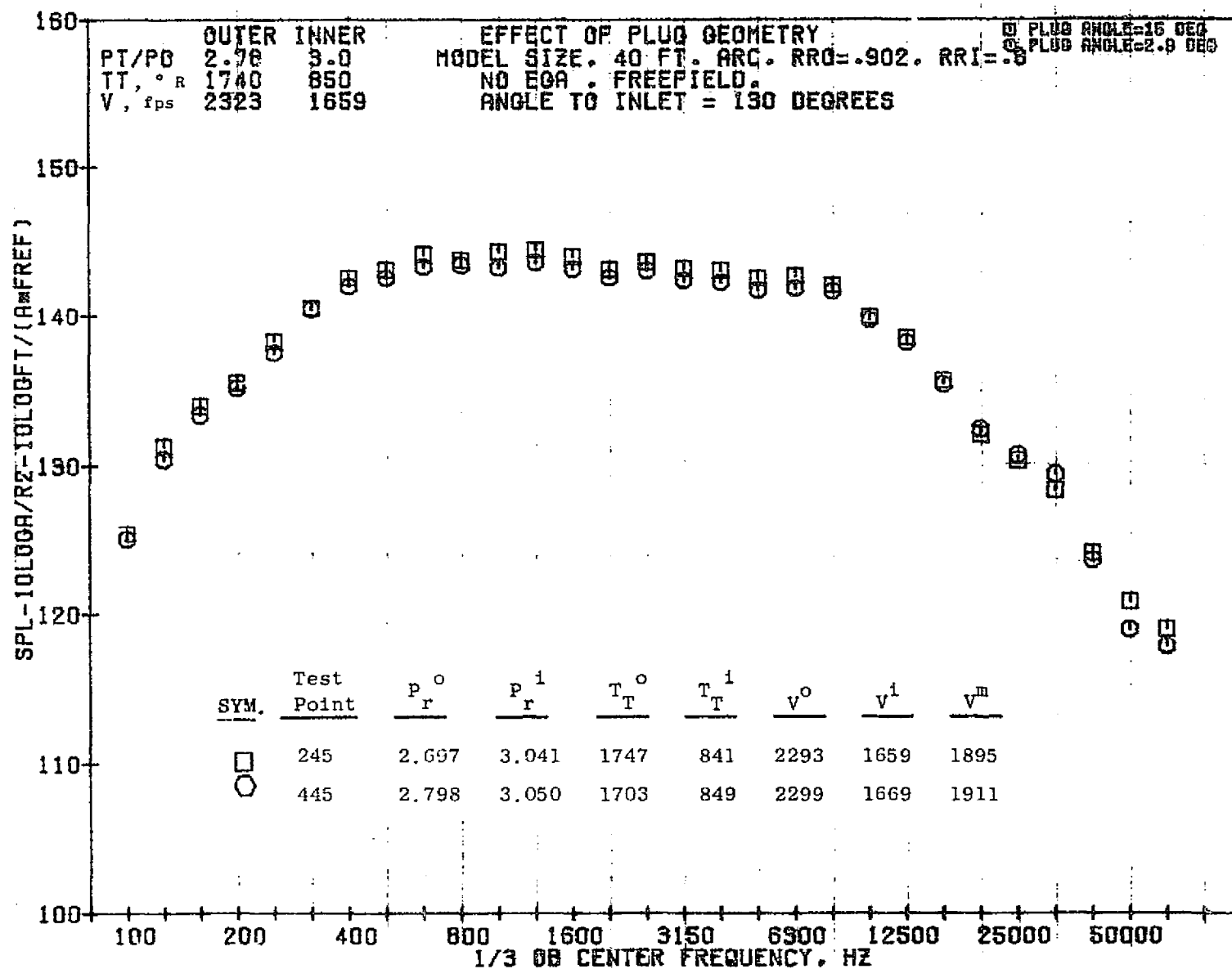
8801



11/03/76
 18360-001

79 BURCH A.

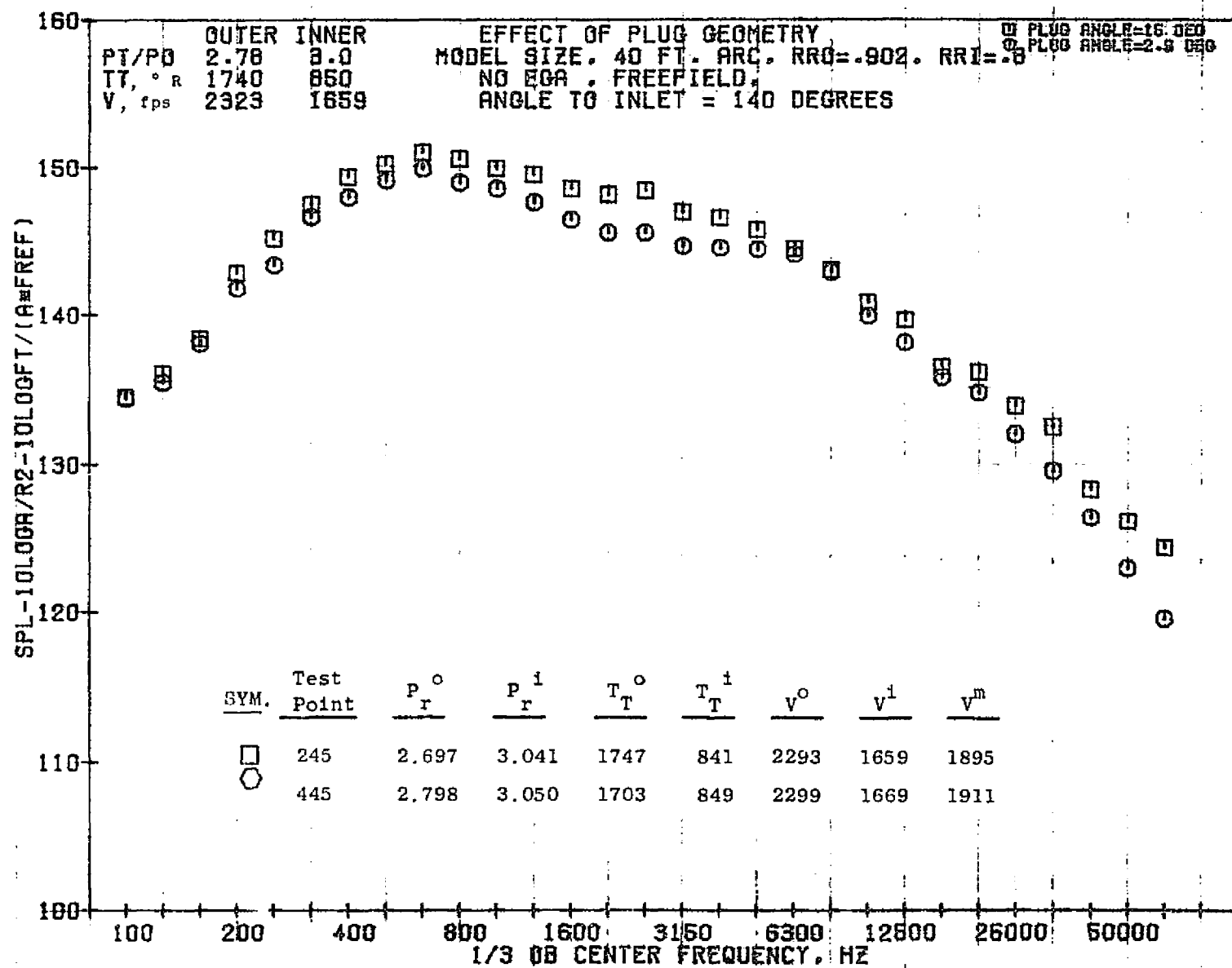
6801



11/03/78
 18360-001

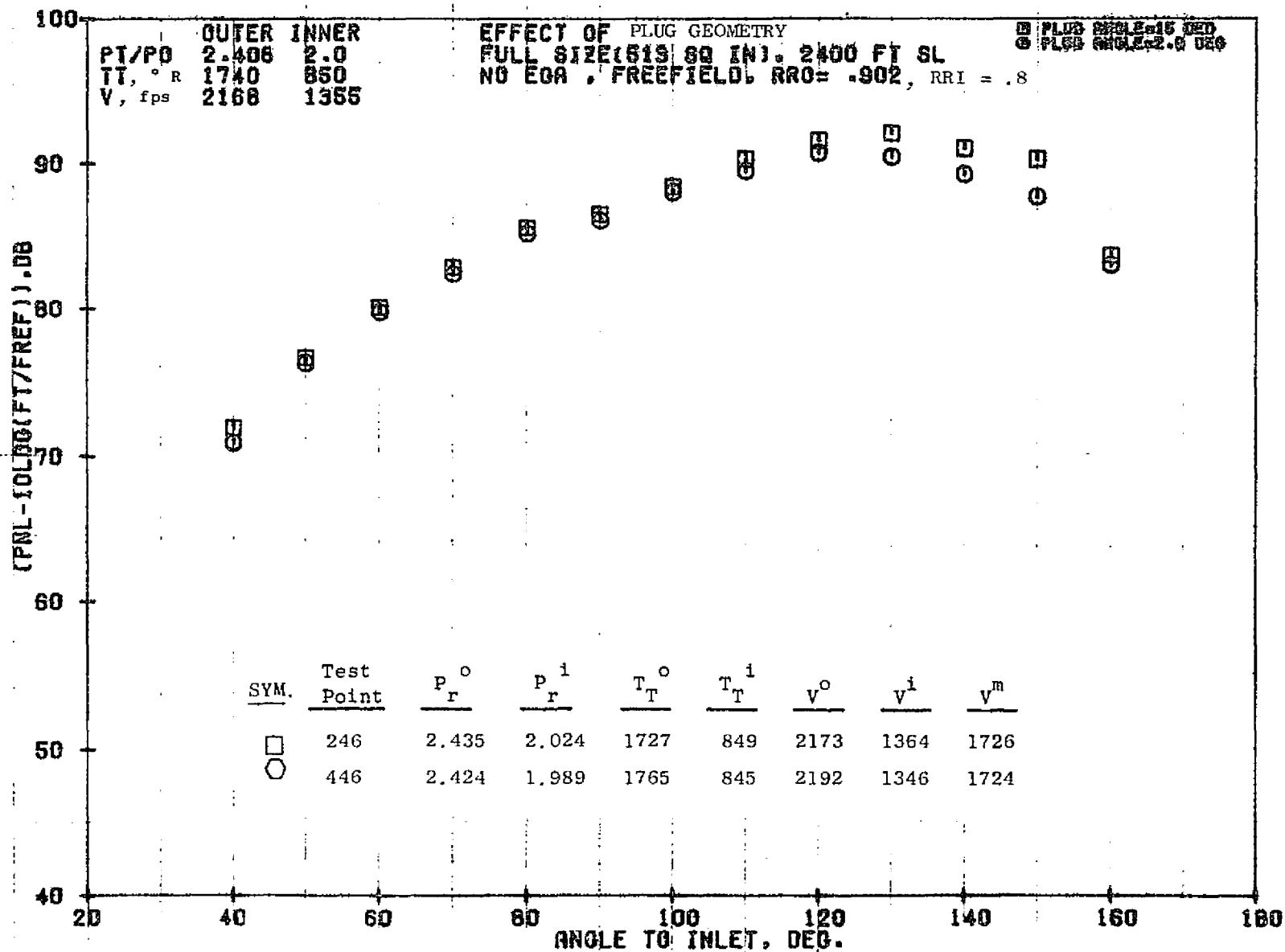
79 BURCH R.

0601


 11/03/76
 18360-001

79 BURCH A.

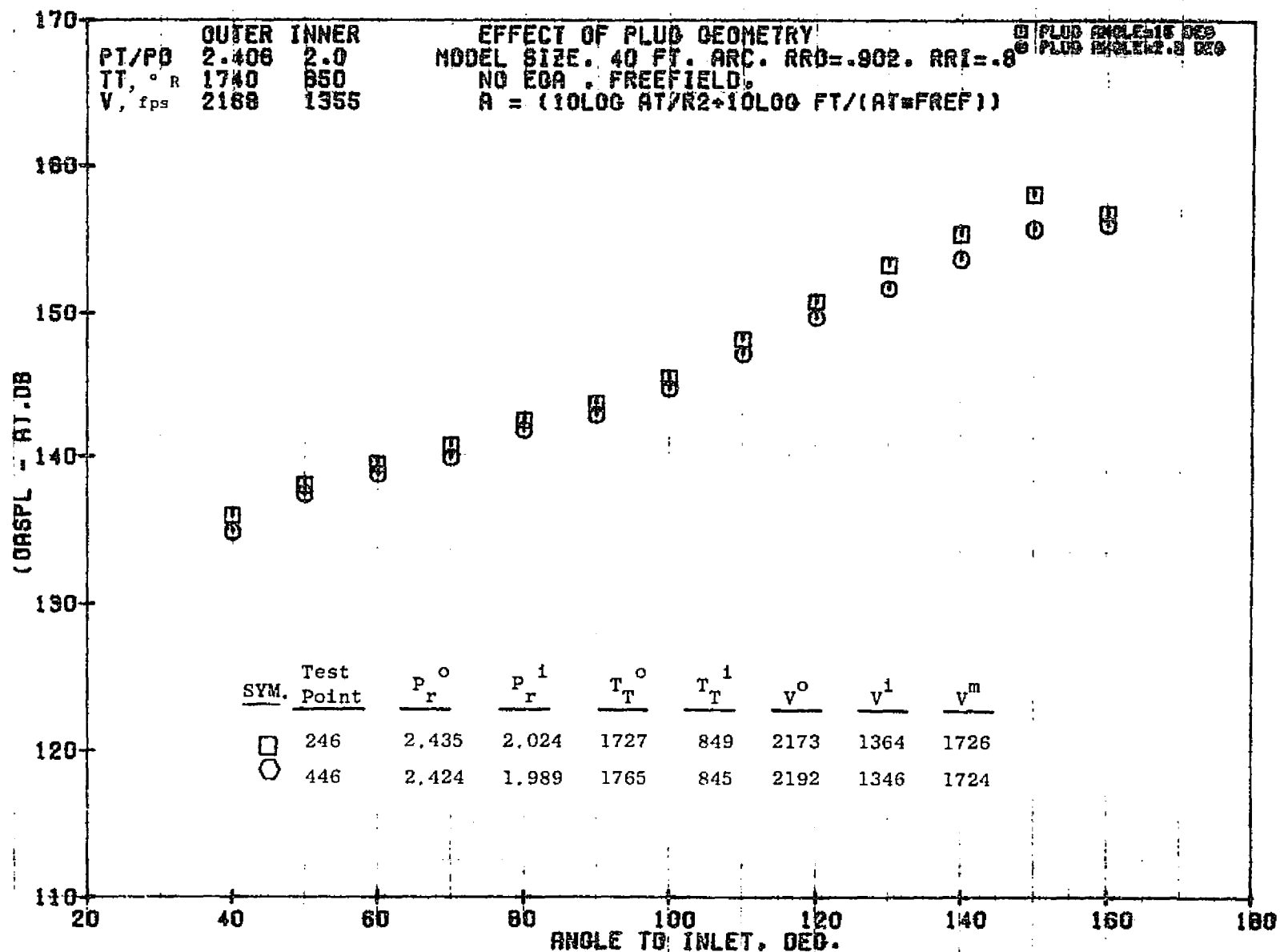
1601



11/04/76
 18680-001

79 BURCH A.

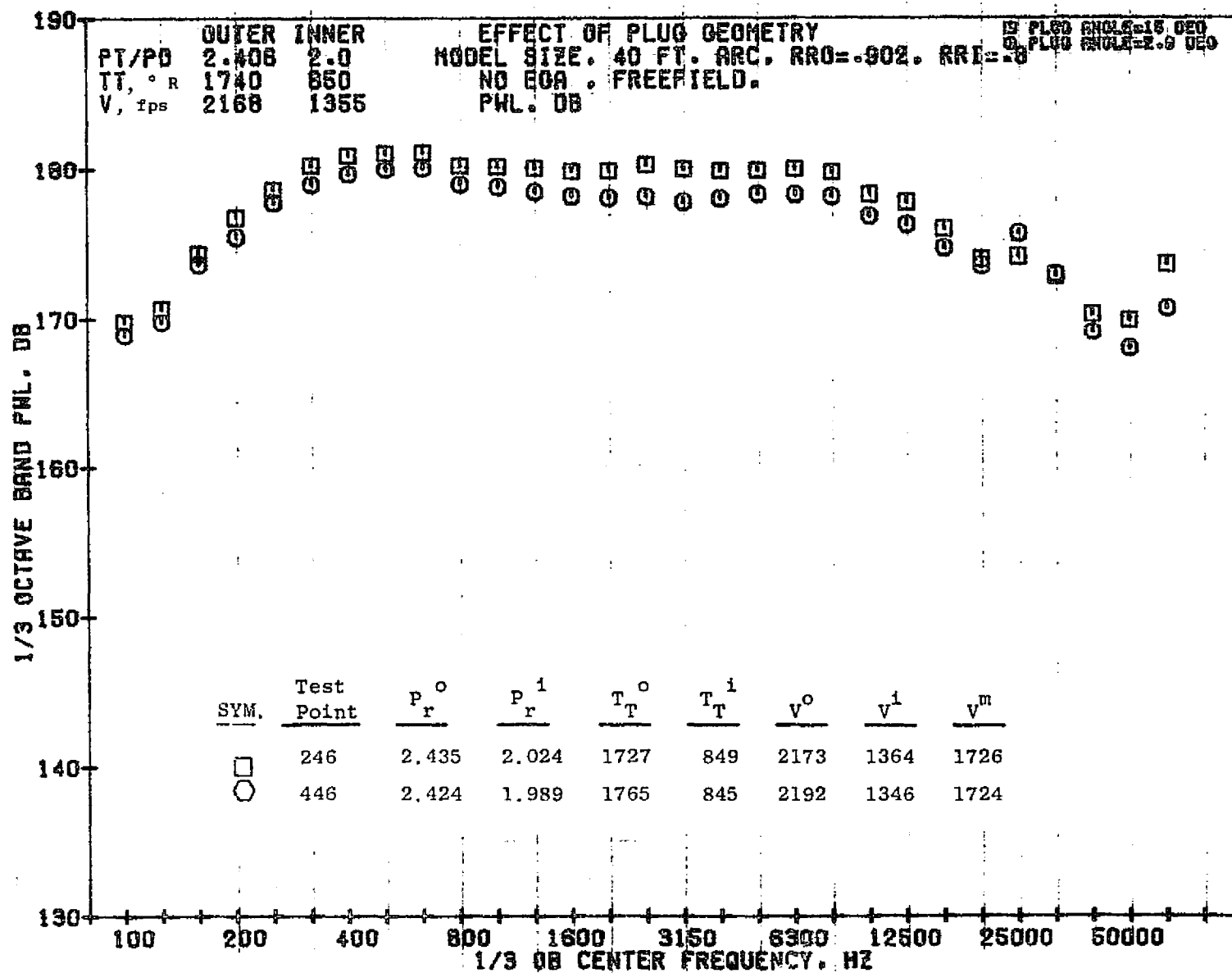
1092



11/04/76
18727-001

79 BURCH A.

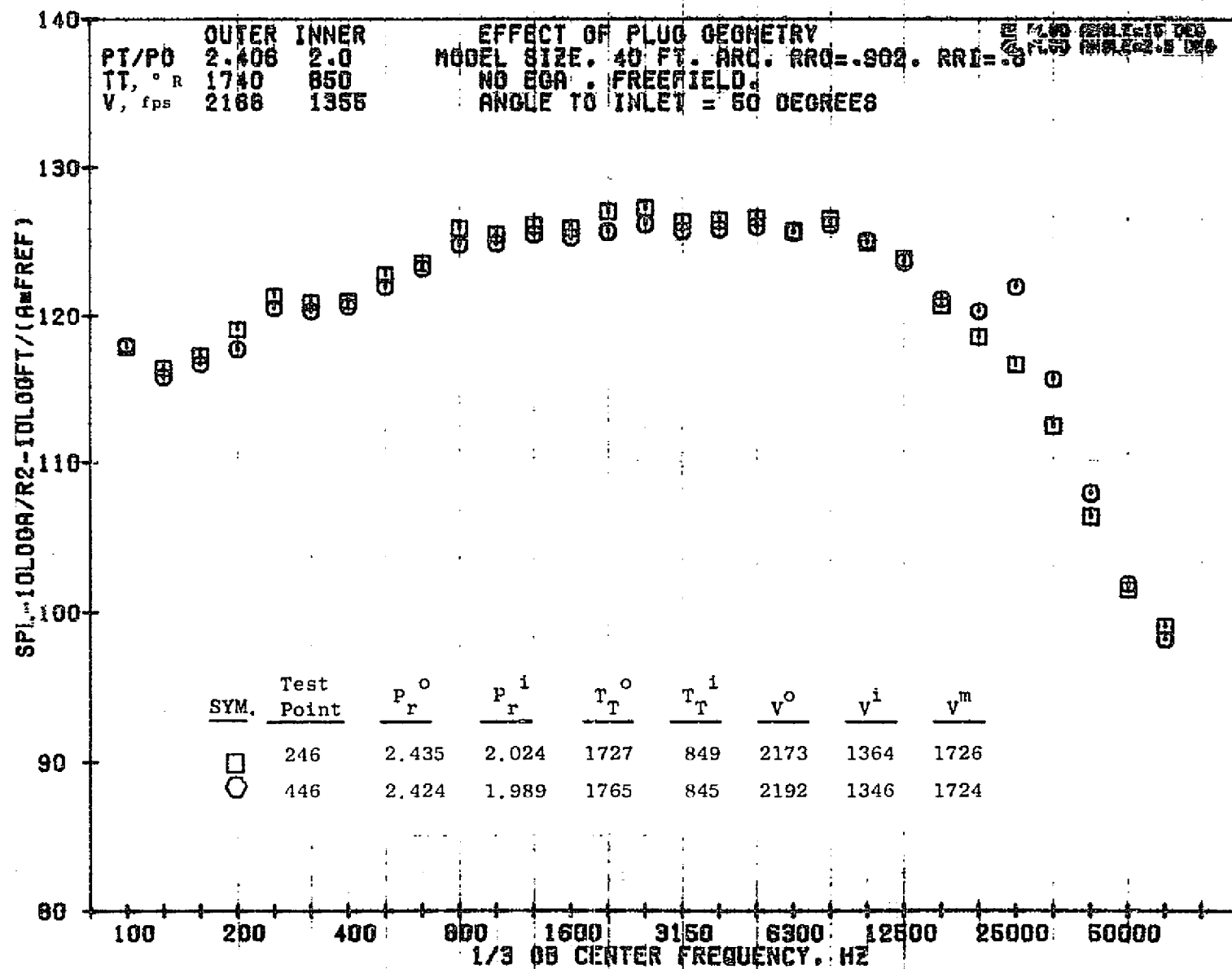
1093



11/04/76
 18727-001

79 BURCH A.

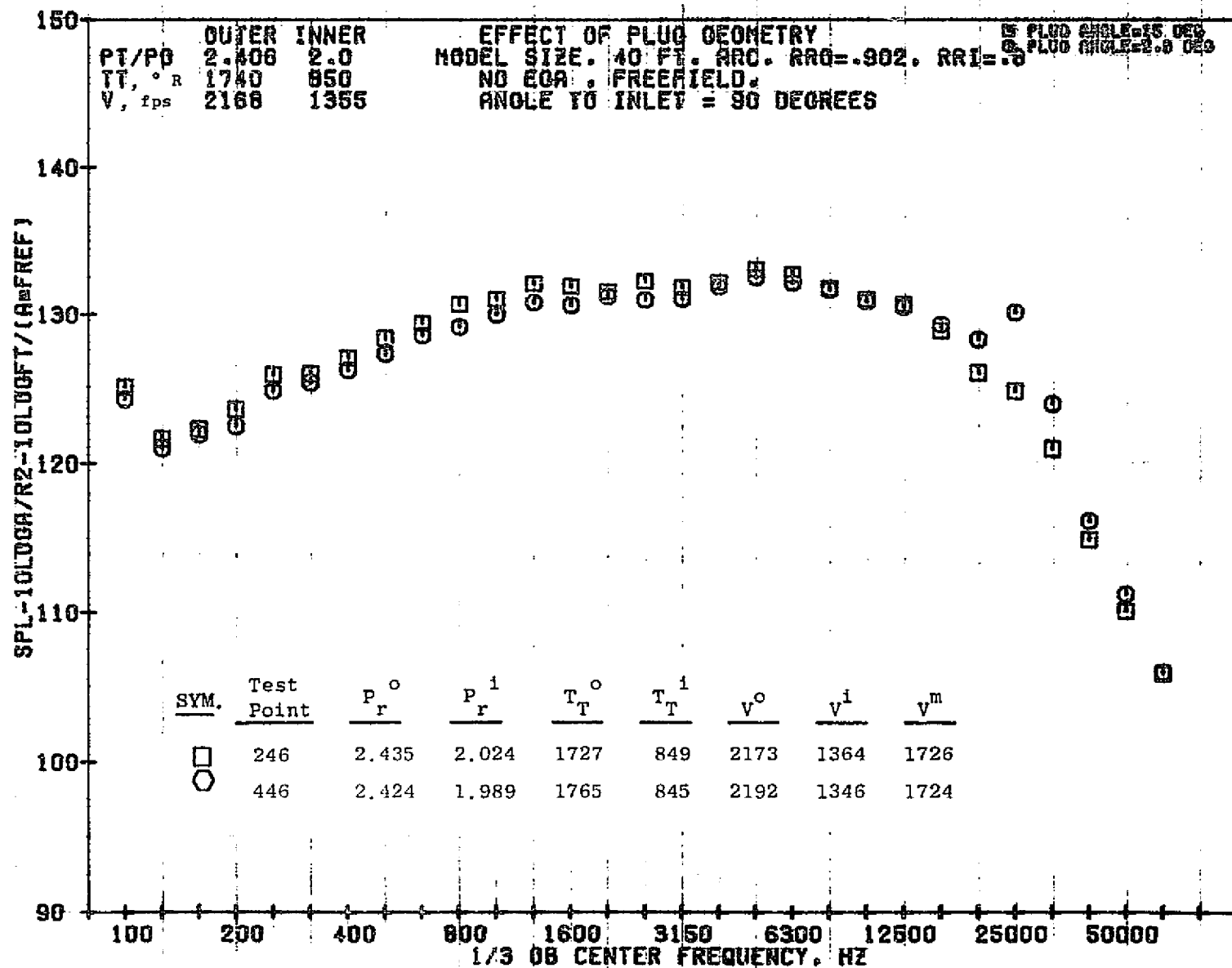
1094



11/04/76
 18727-001

79 BURCH A.

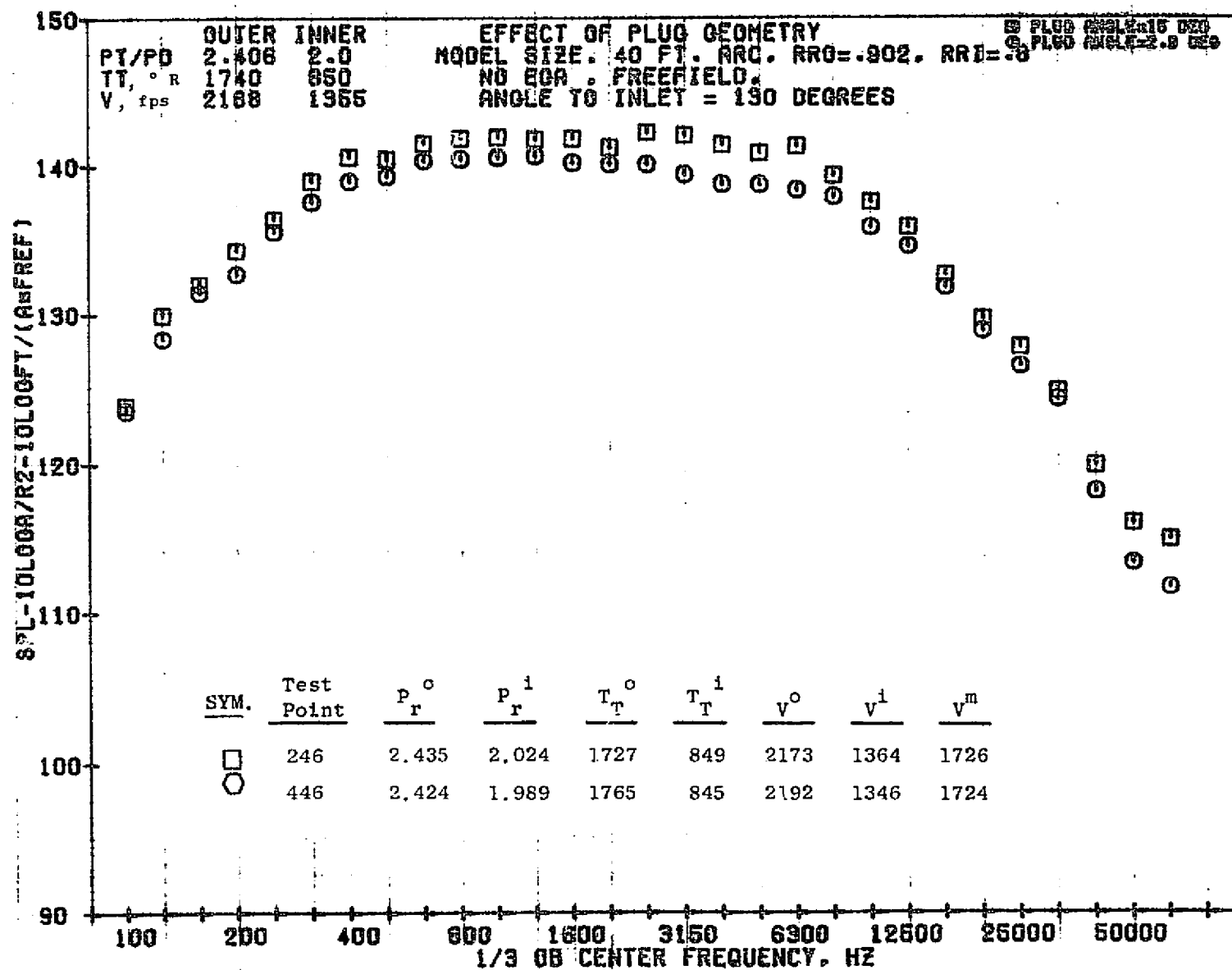
9601



11/04/76
 18727-001

79 BURCH A.

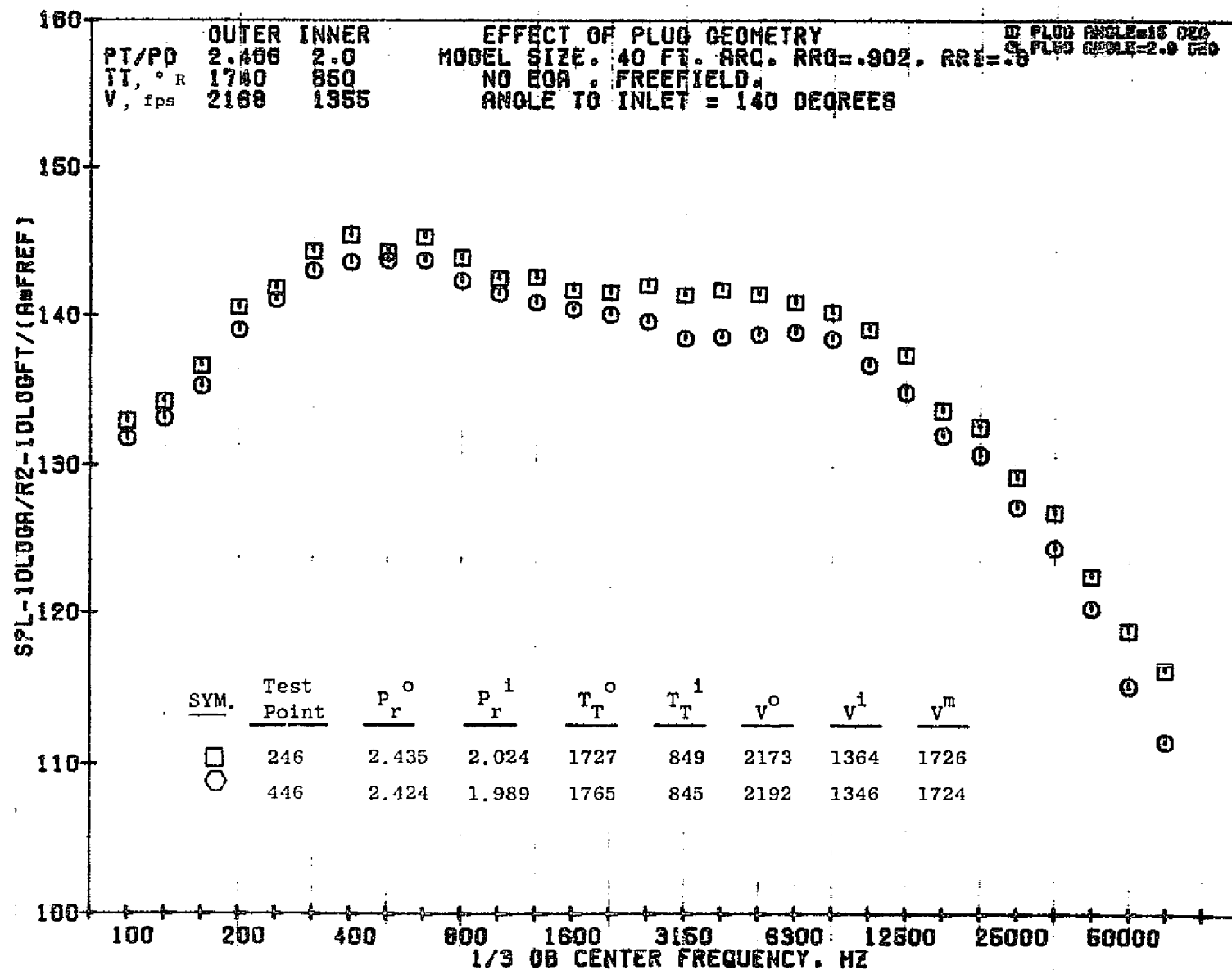
1086



11/04/76
 18727-001

79 BURCH A.

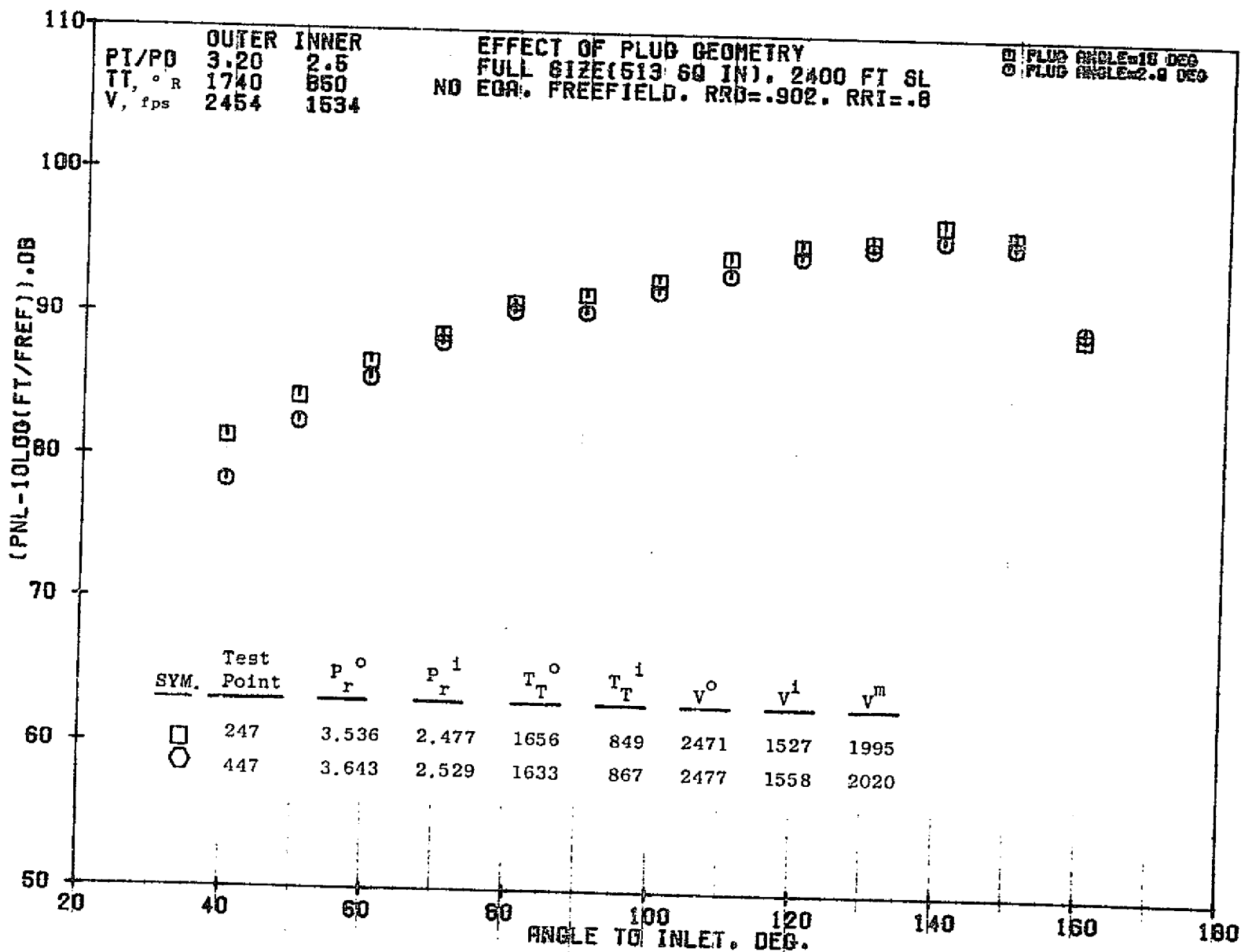
1097



11/04/76
 18727-001

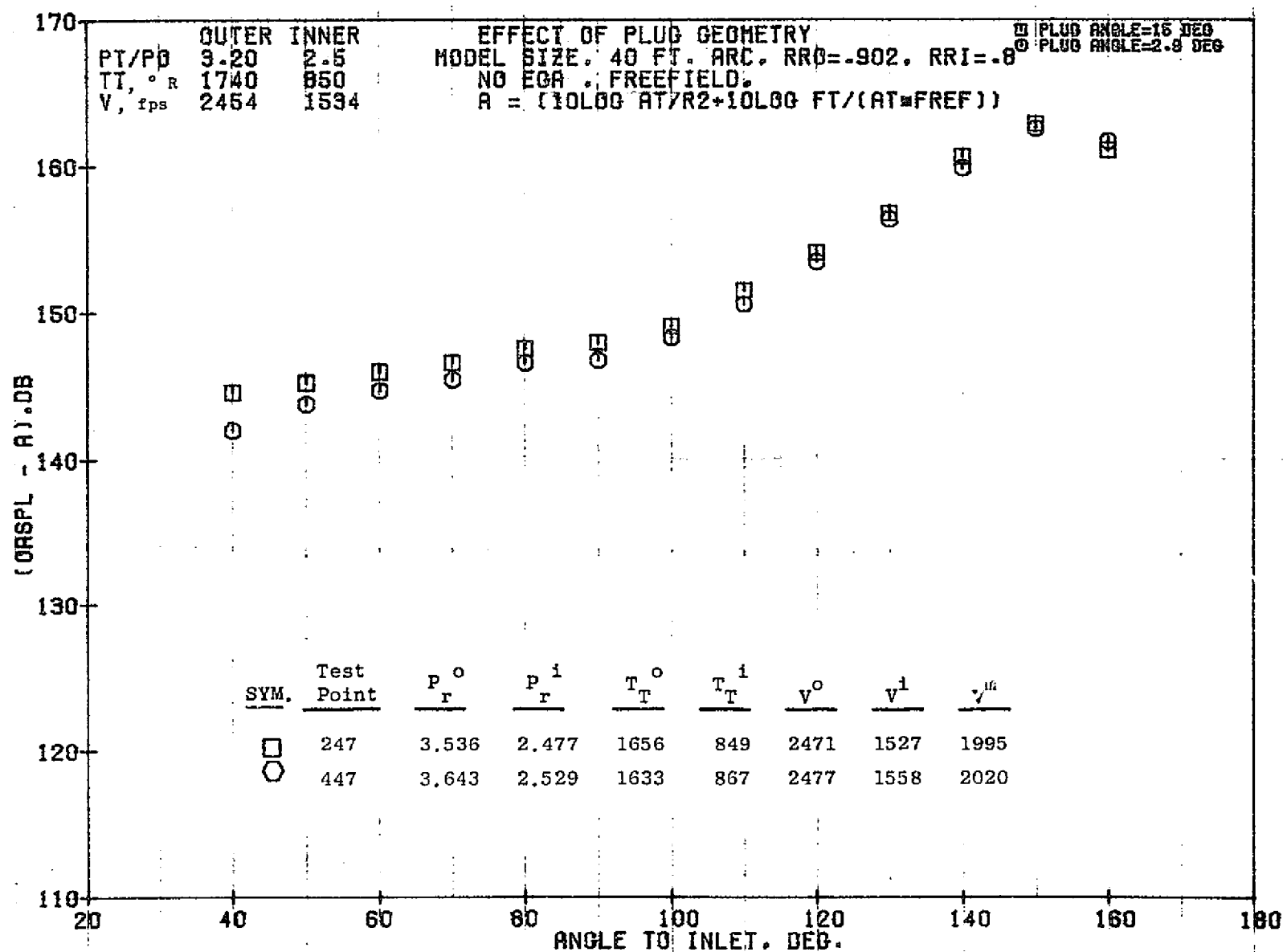
79 BURCH A.

1098



10/29/76
 18130-001

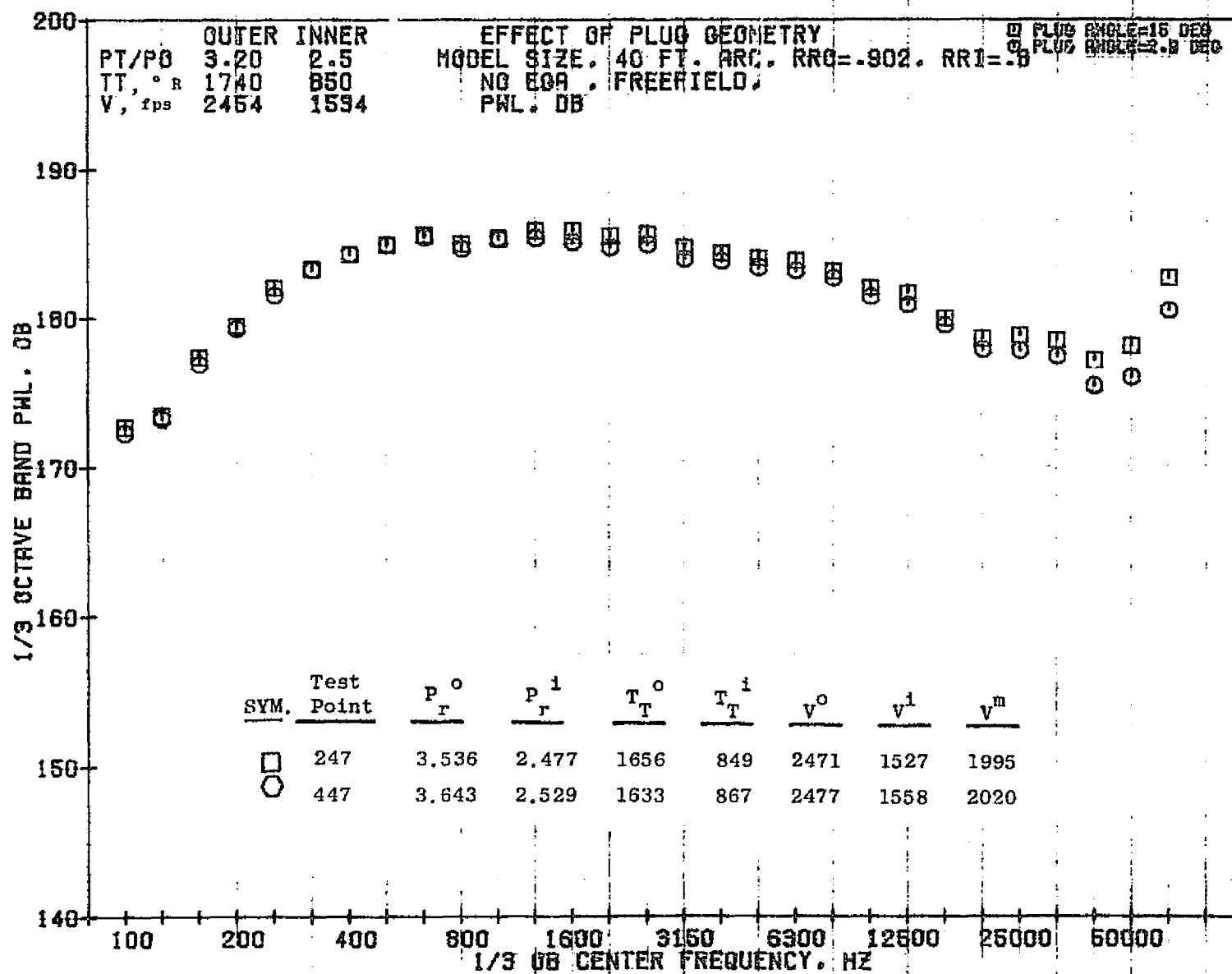
79 BURCH A.



11/03/76
1B360-001

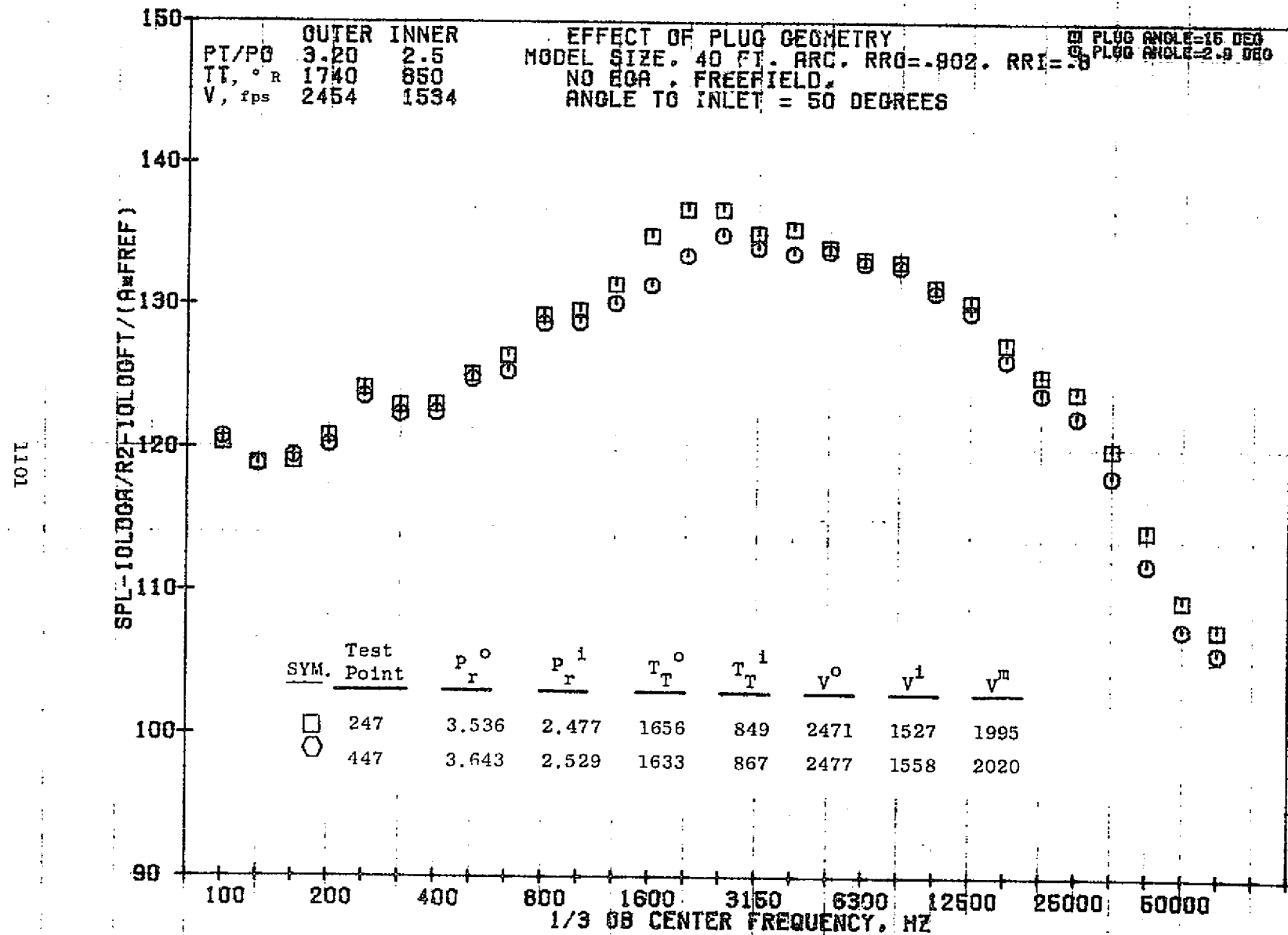
79 BURCH A.

1100



11/03/76
18360-001

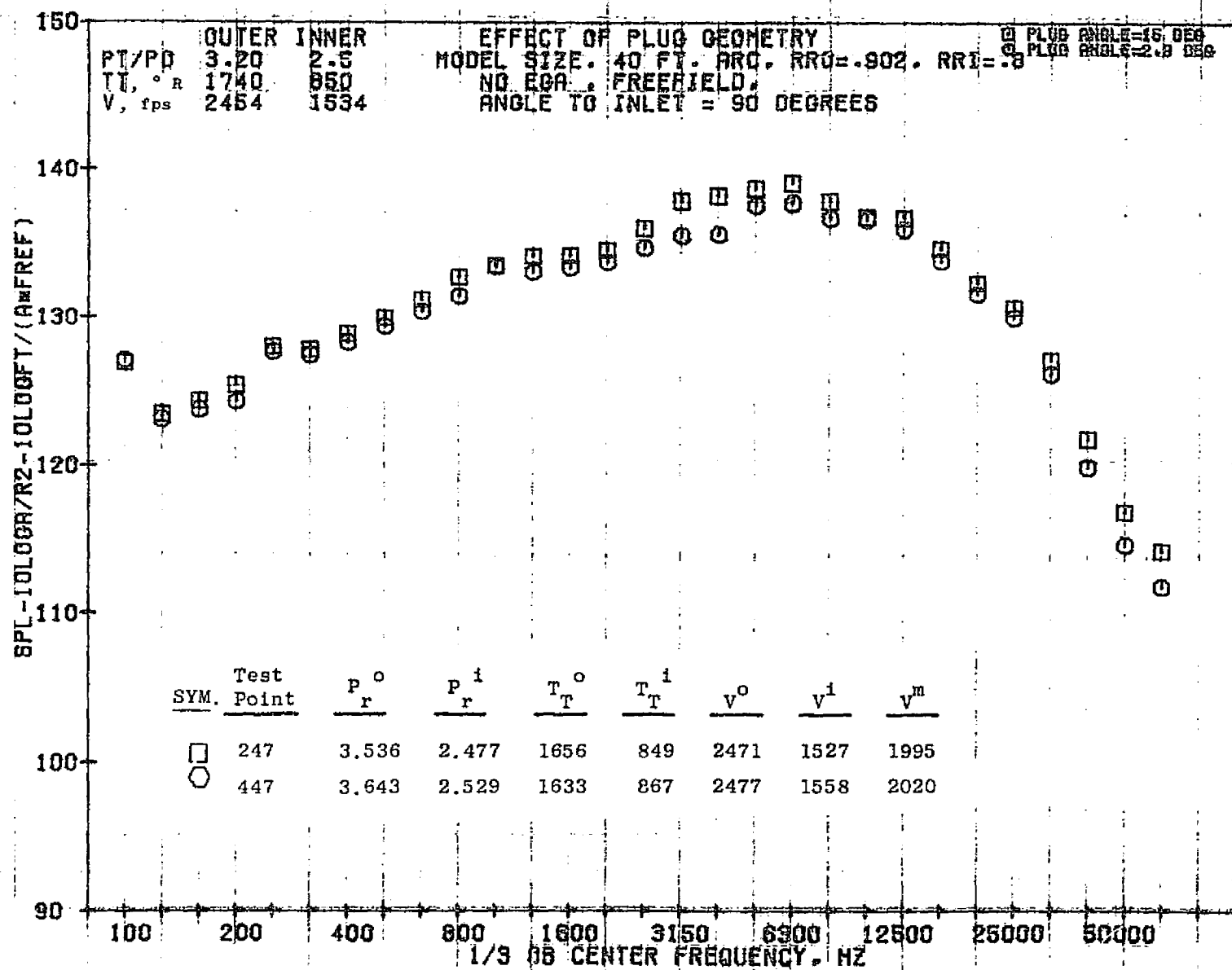
79 BURCH A.



11/03/76
 18360-001

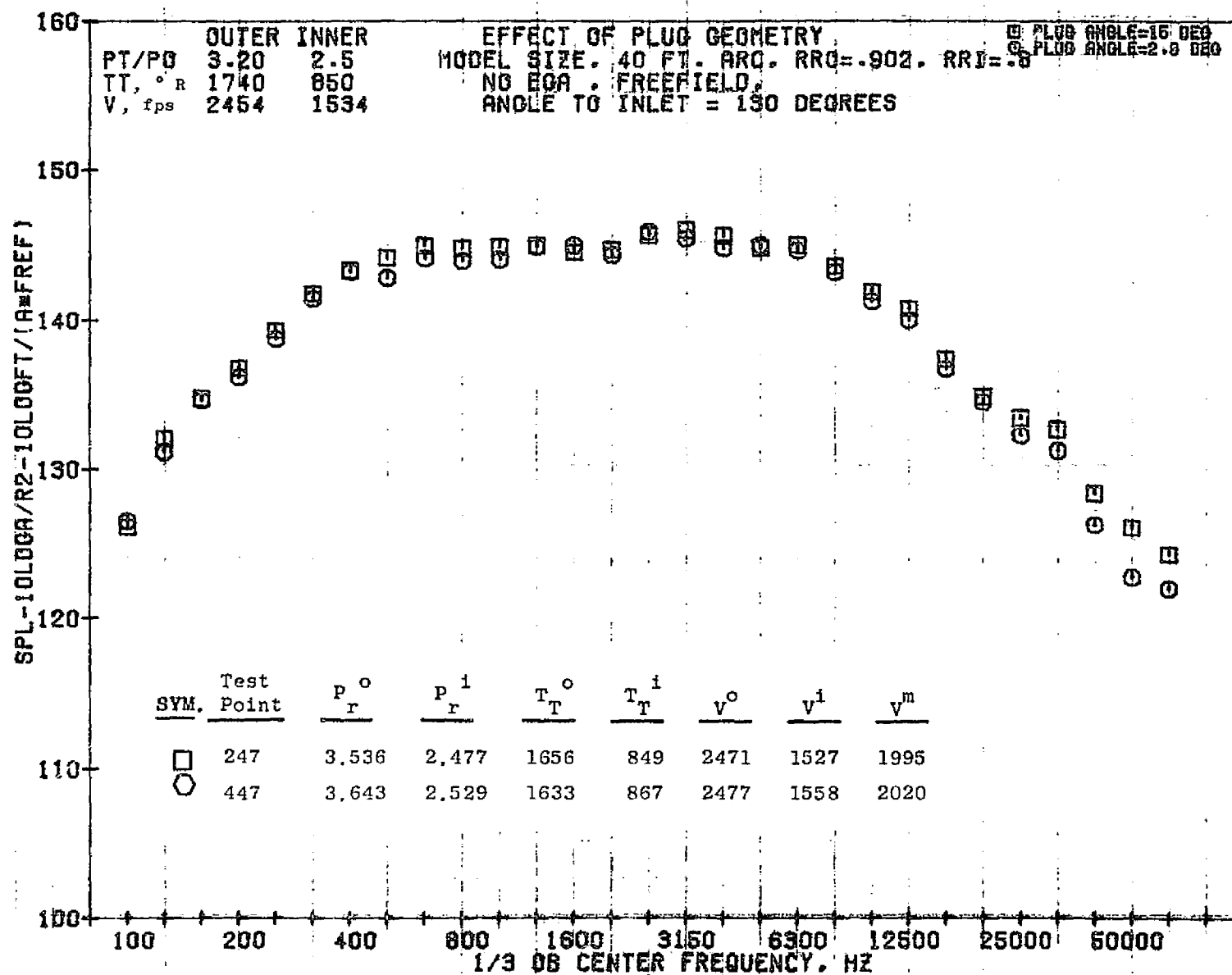
79 BURCH A.

1102



11/03/76
18360-001

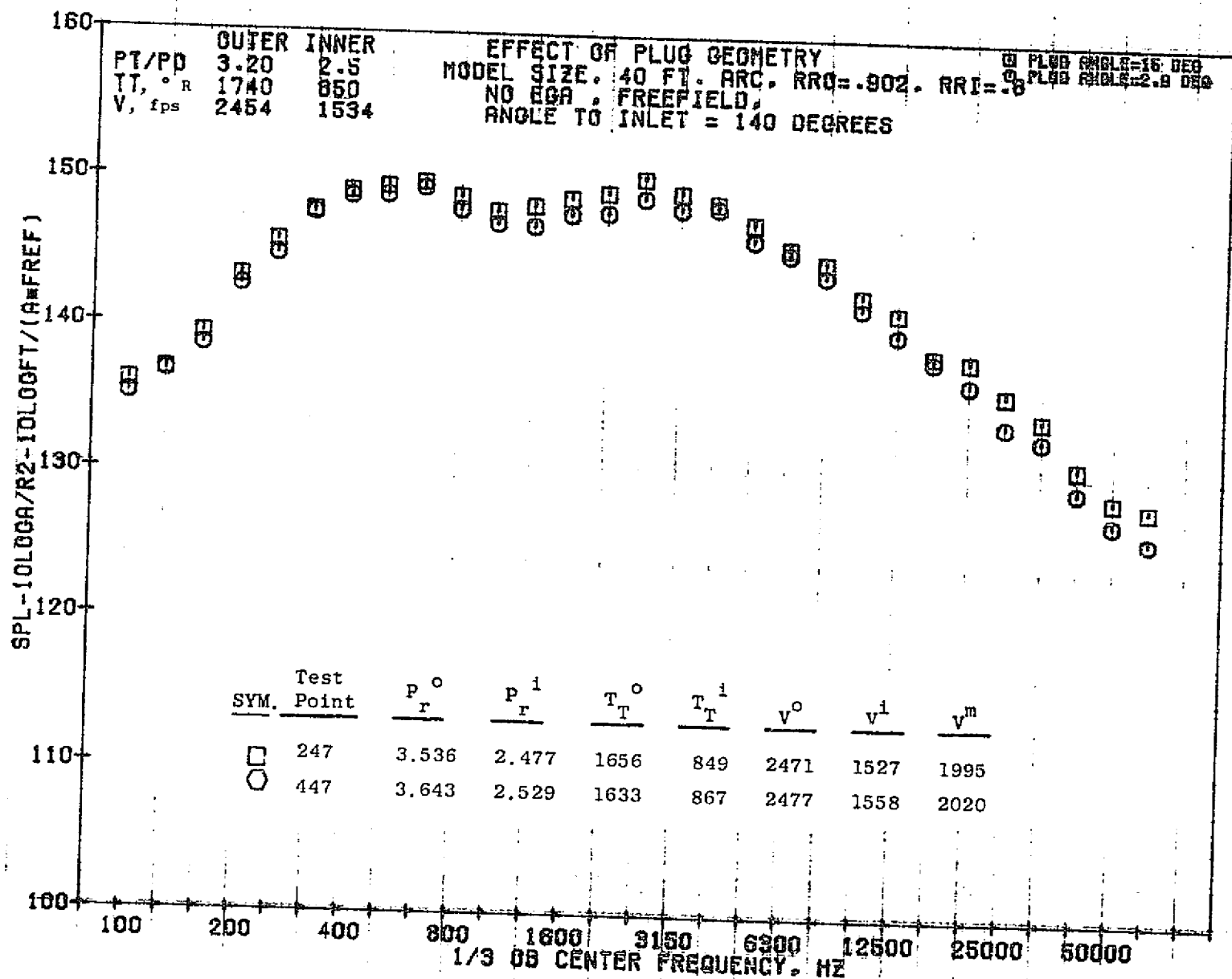
79 AIRCH A.



11/03/76
 18360-001

79 BURCH A.

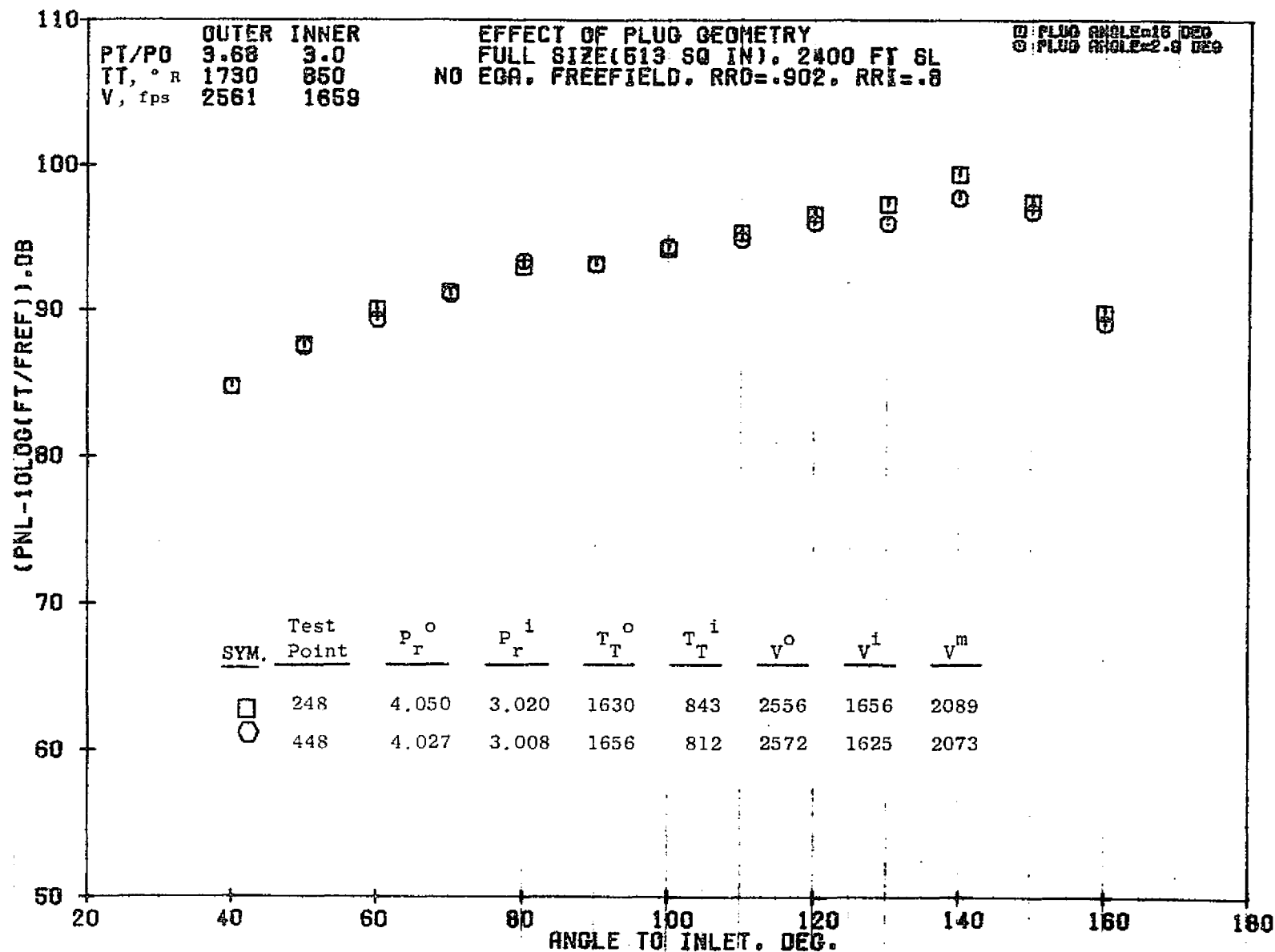
1101



11/03/76
 18360-001

79 BURCH A.

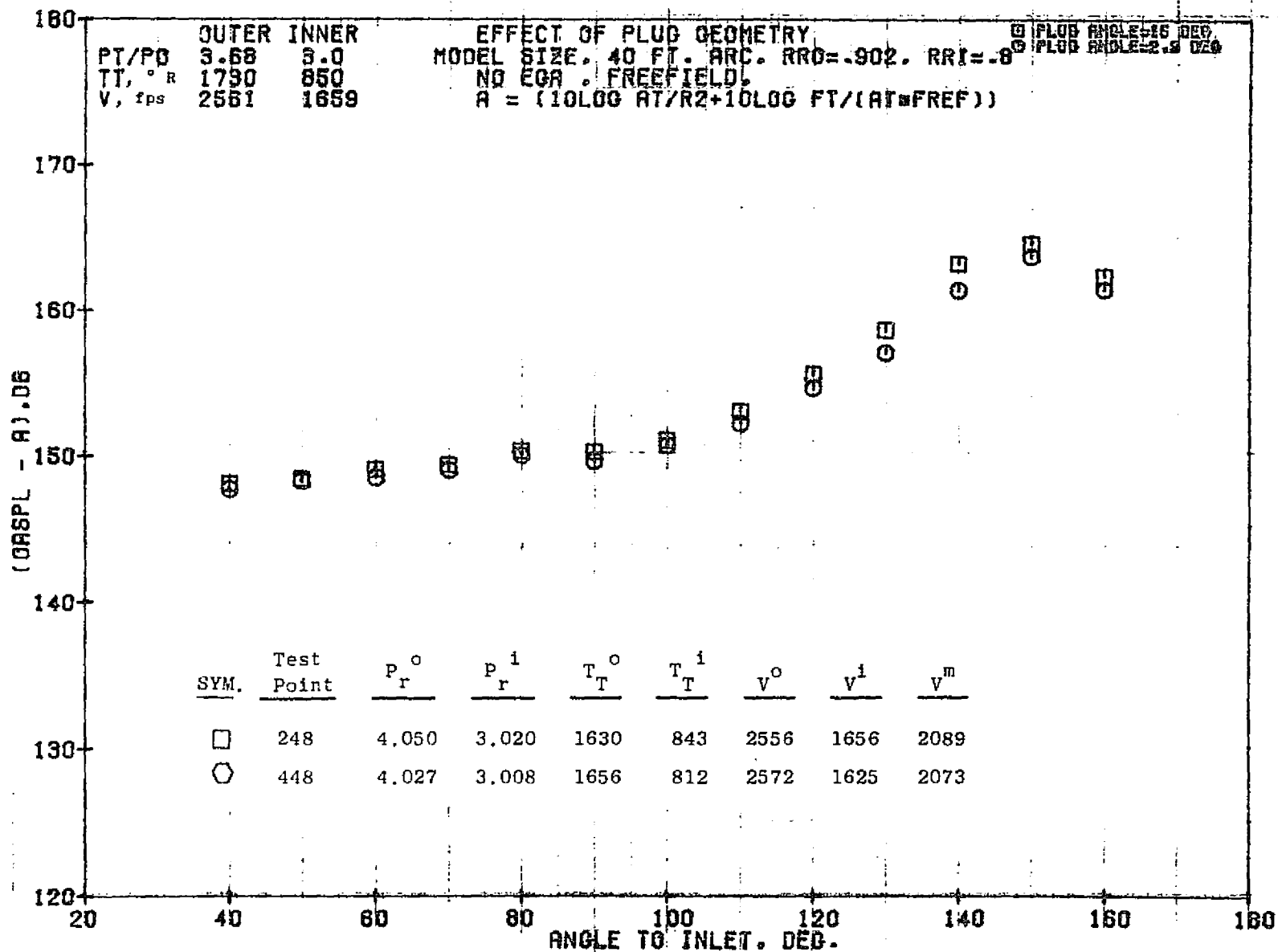
1105



10/29/76
 18130-011

79 BURCH A.

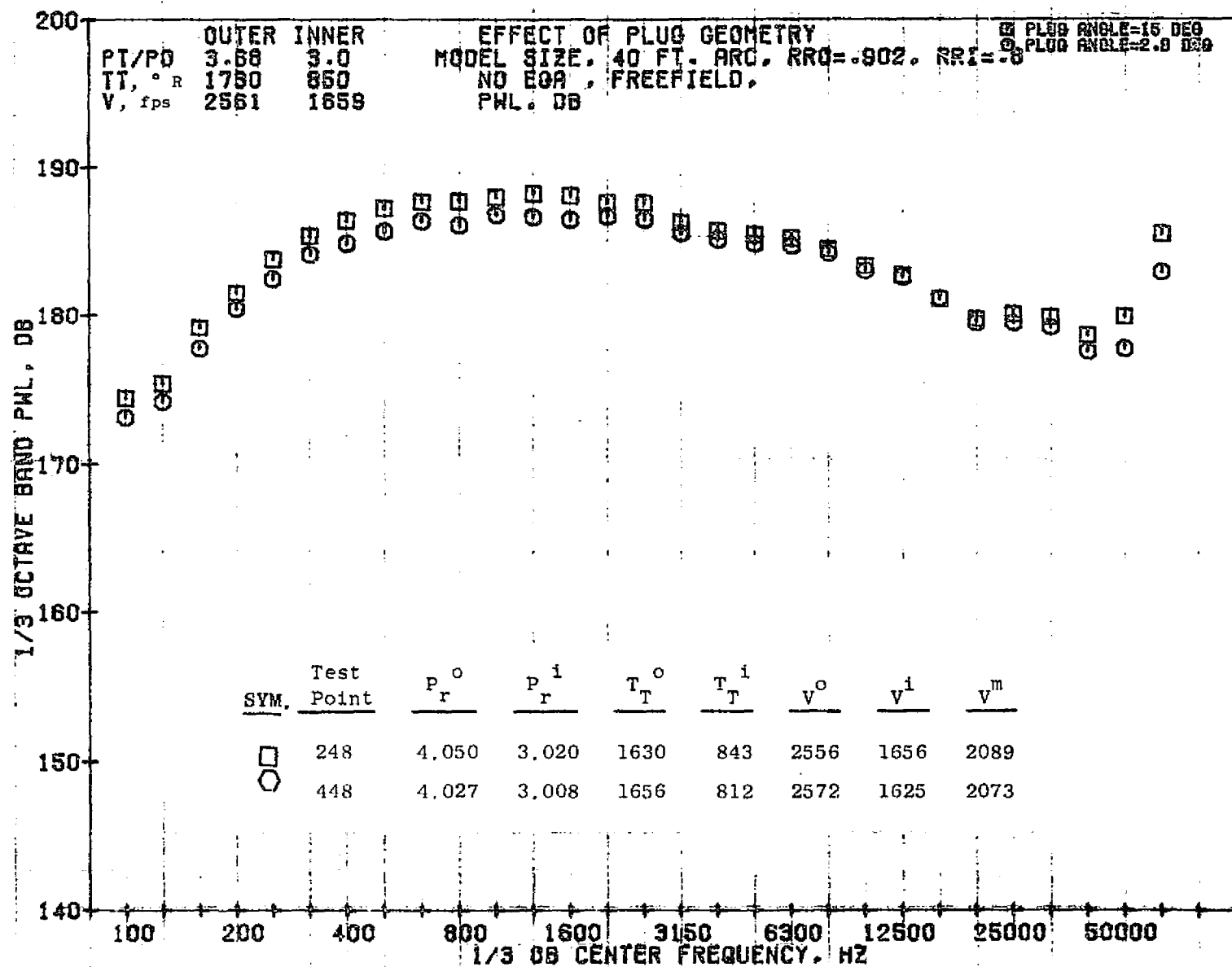
1106



11/03/76
18262-001

79 BURCH A.

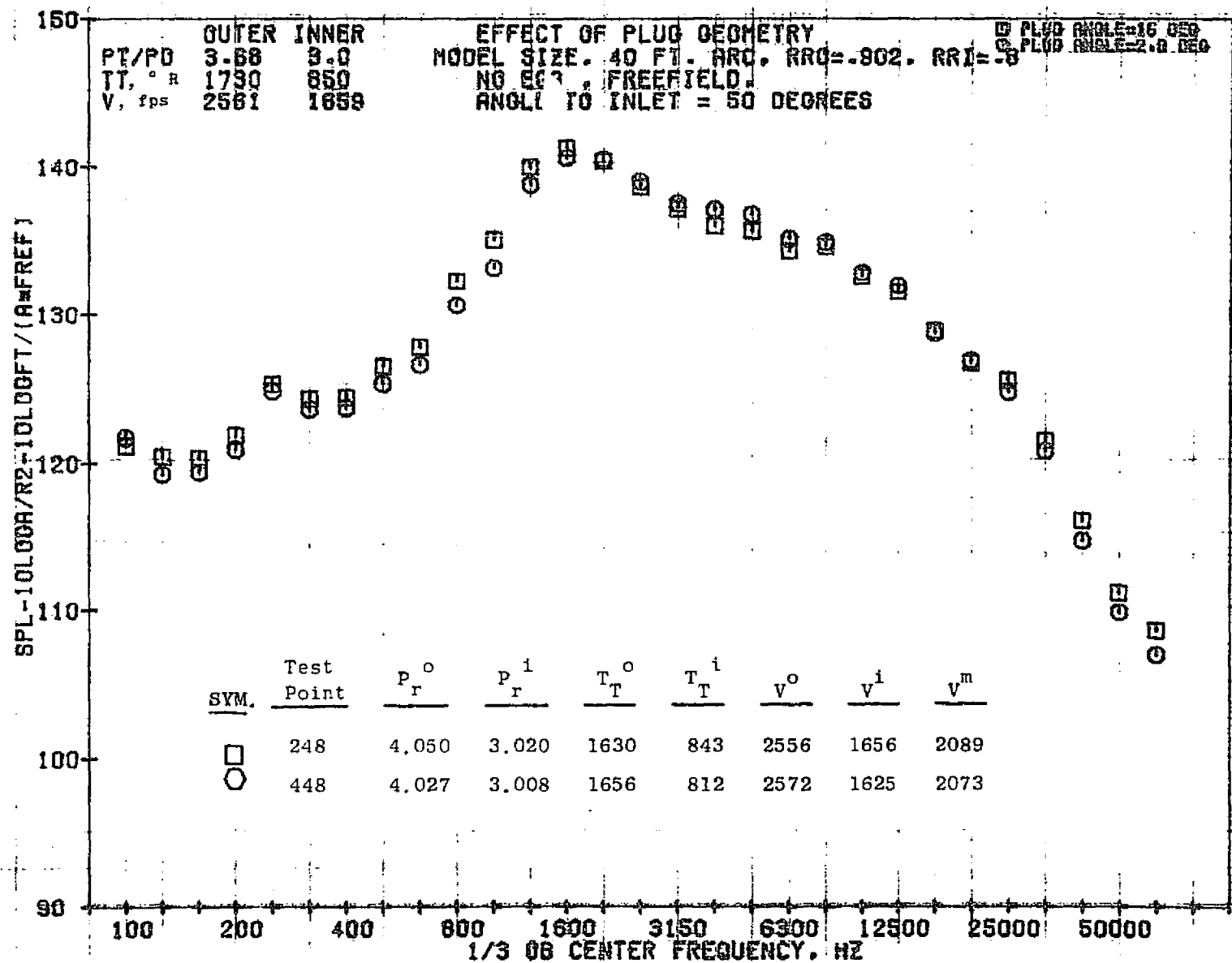
1107



11/03/76
18360-001

79 AIRCRAFT

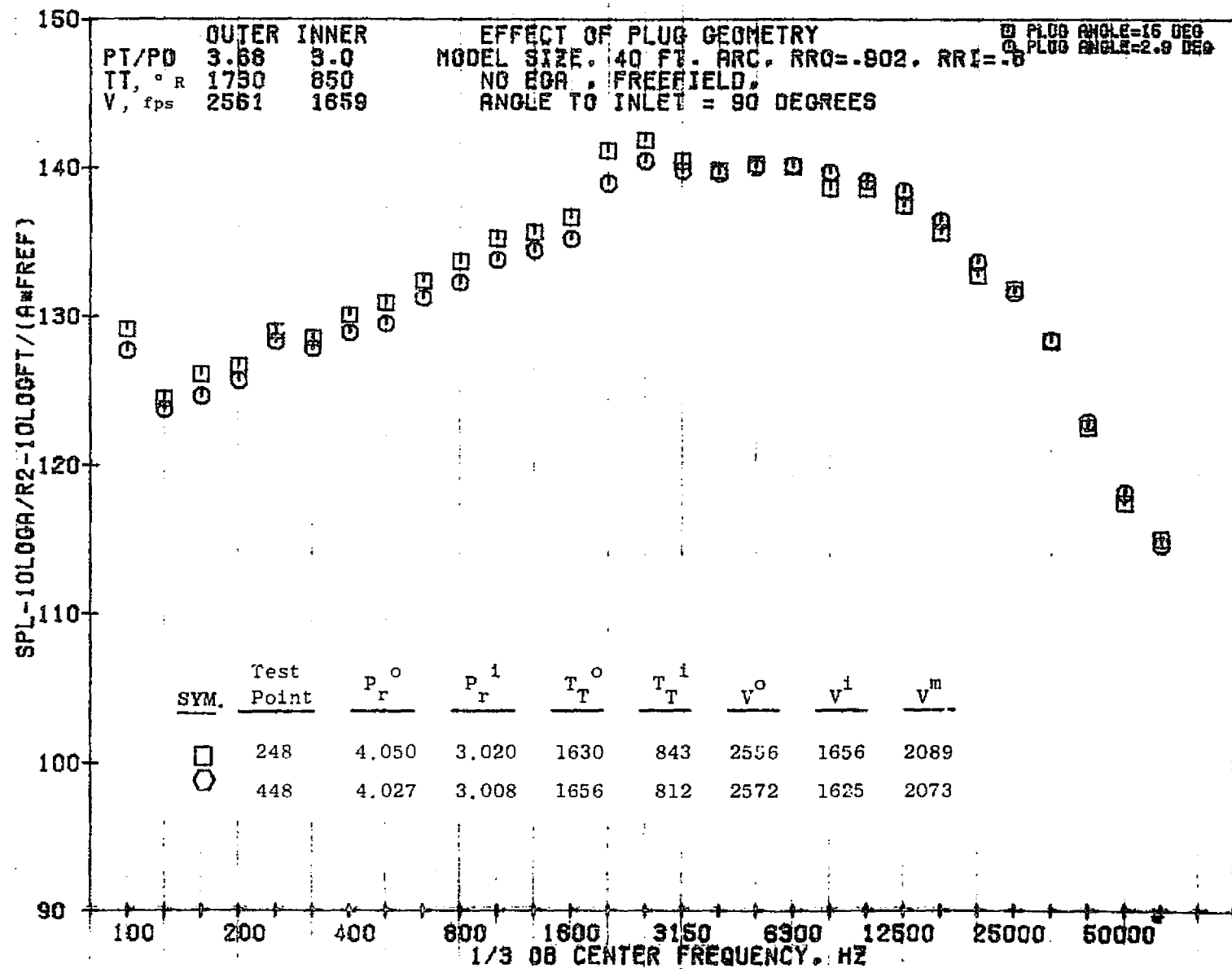
8011



11/03/76
 18280-001

79 BURCH A.

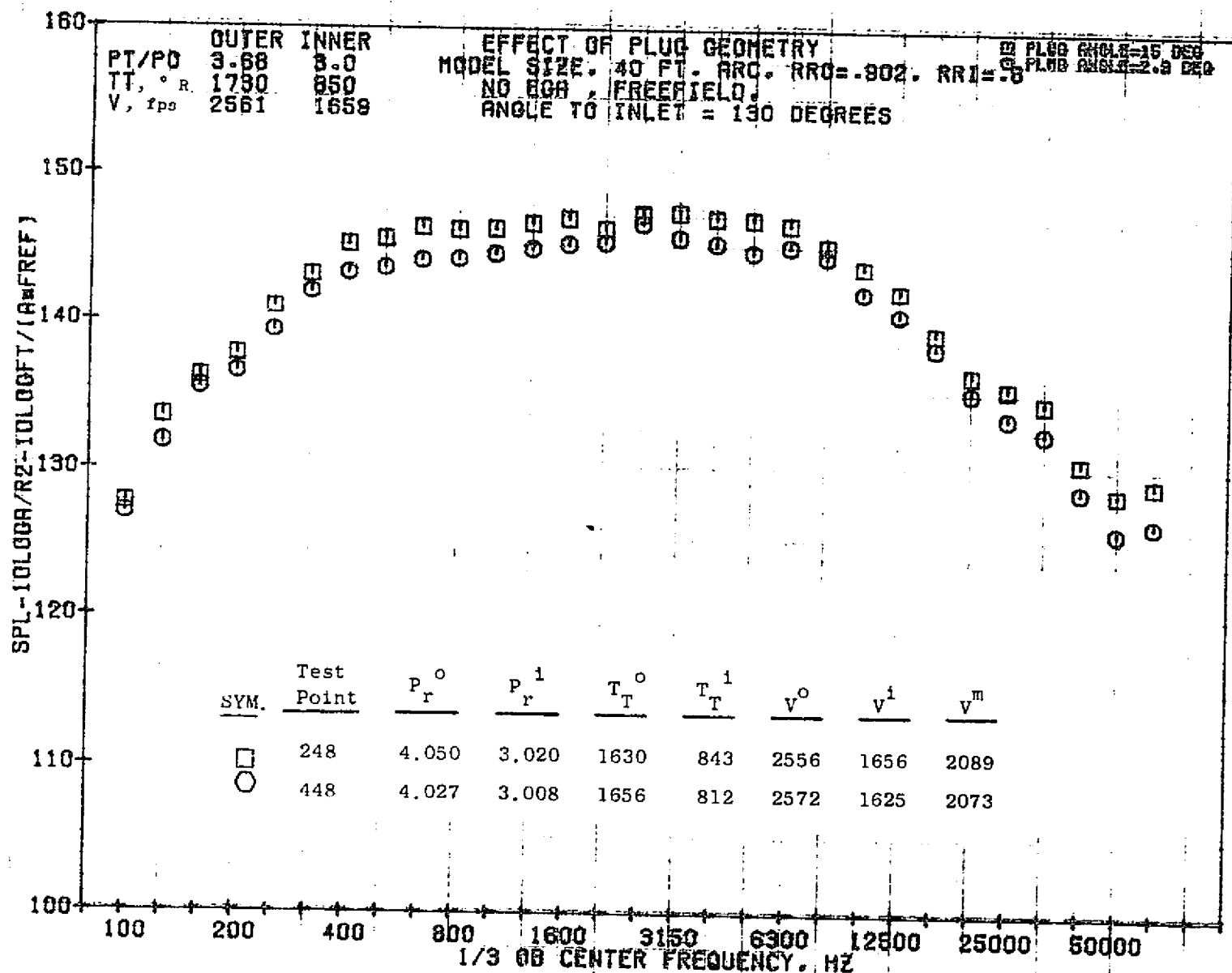
6011



11/03/76
18360-001

79 AIRCH A.

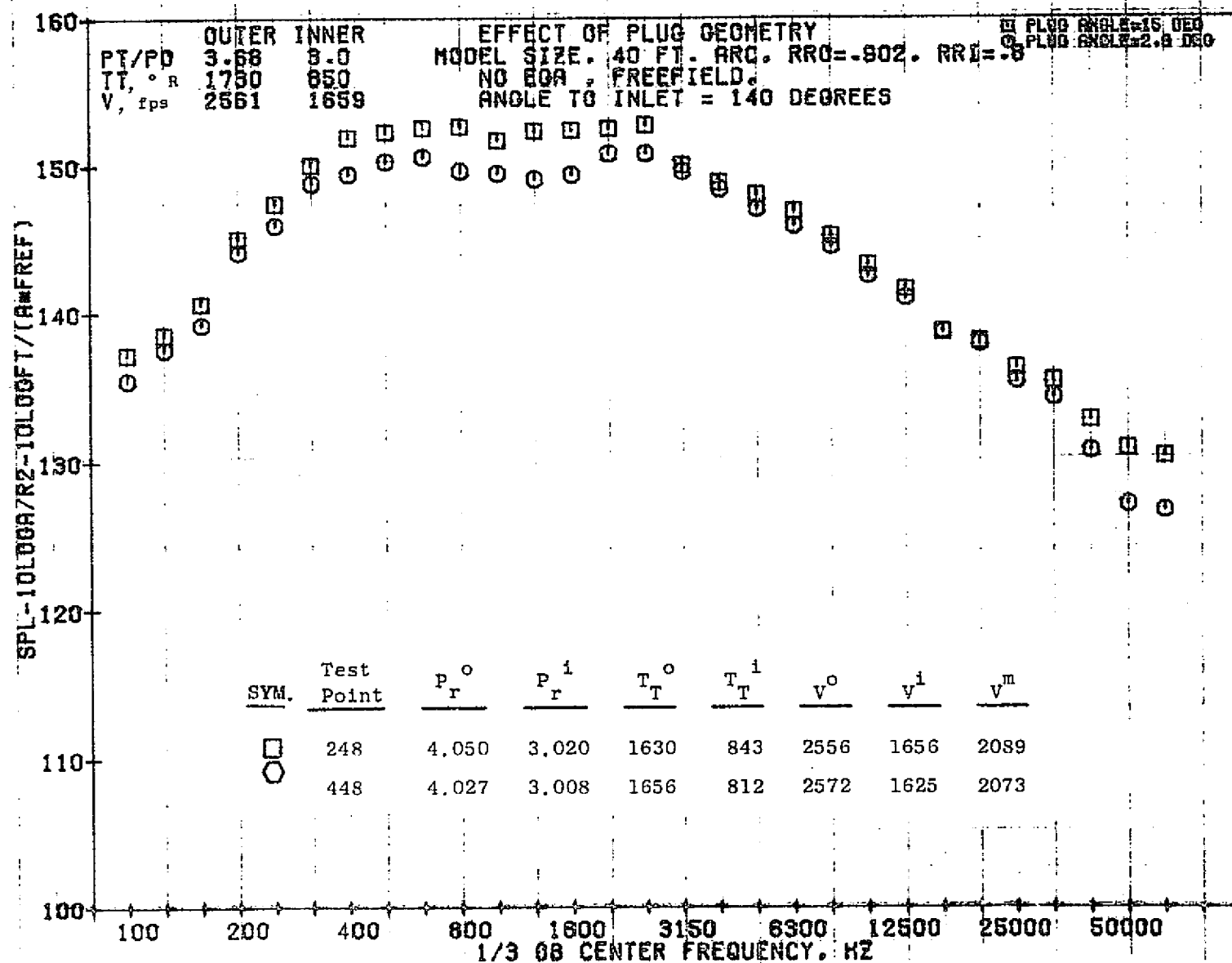
0111



11/03/76
18260-001

79 BURCH A.

TTTT



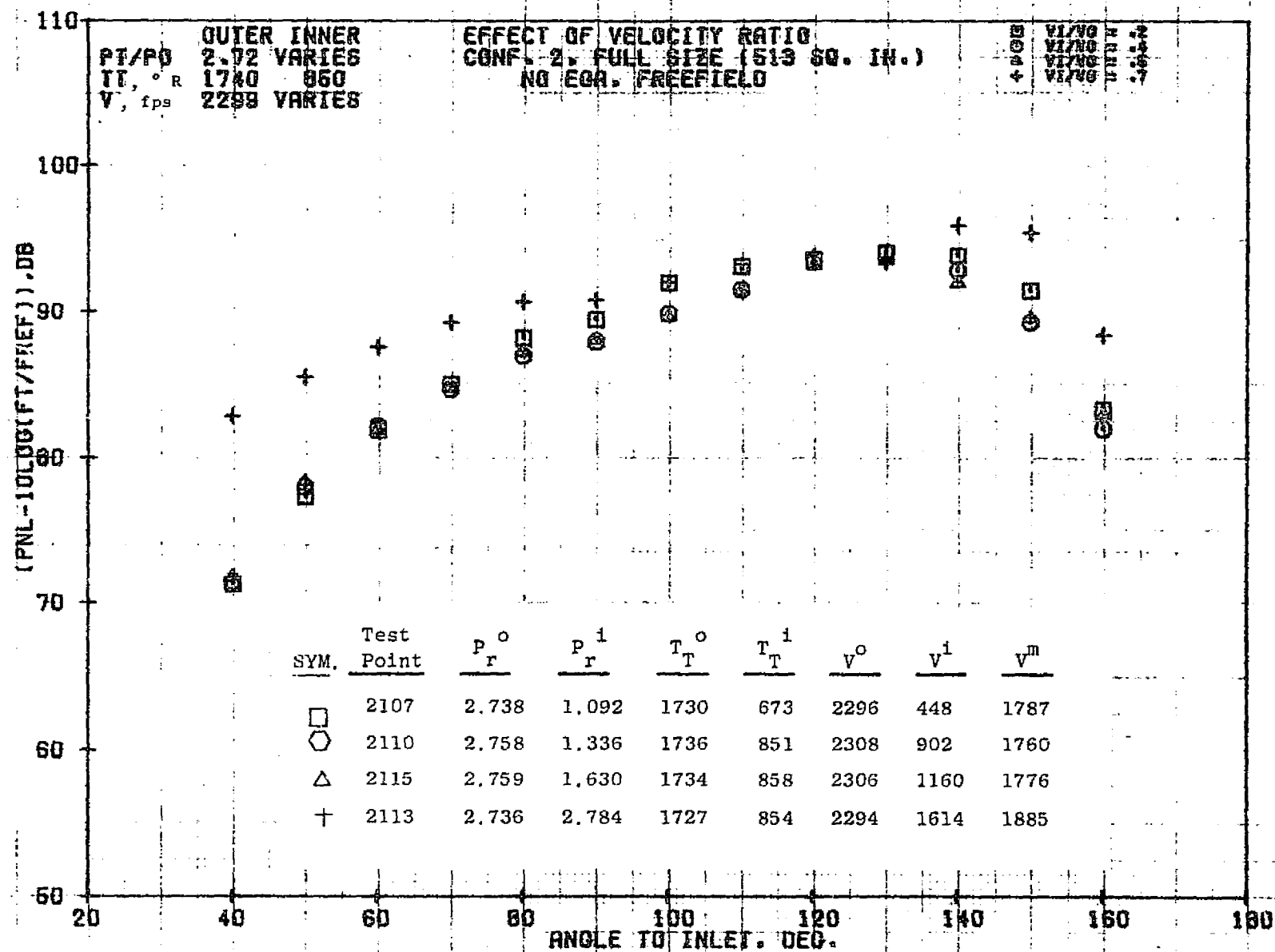
11/03/76
 18360-001

79 BIRCH P.

7.4.4. Effect of Velocity Ratio

For Configurations 2 through 7, test points were run with the outer stream aerodynamic parameters held constant while the inner stream velocity was varied to determine the effect of velocity ratio. The results are shown in this section.

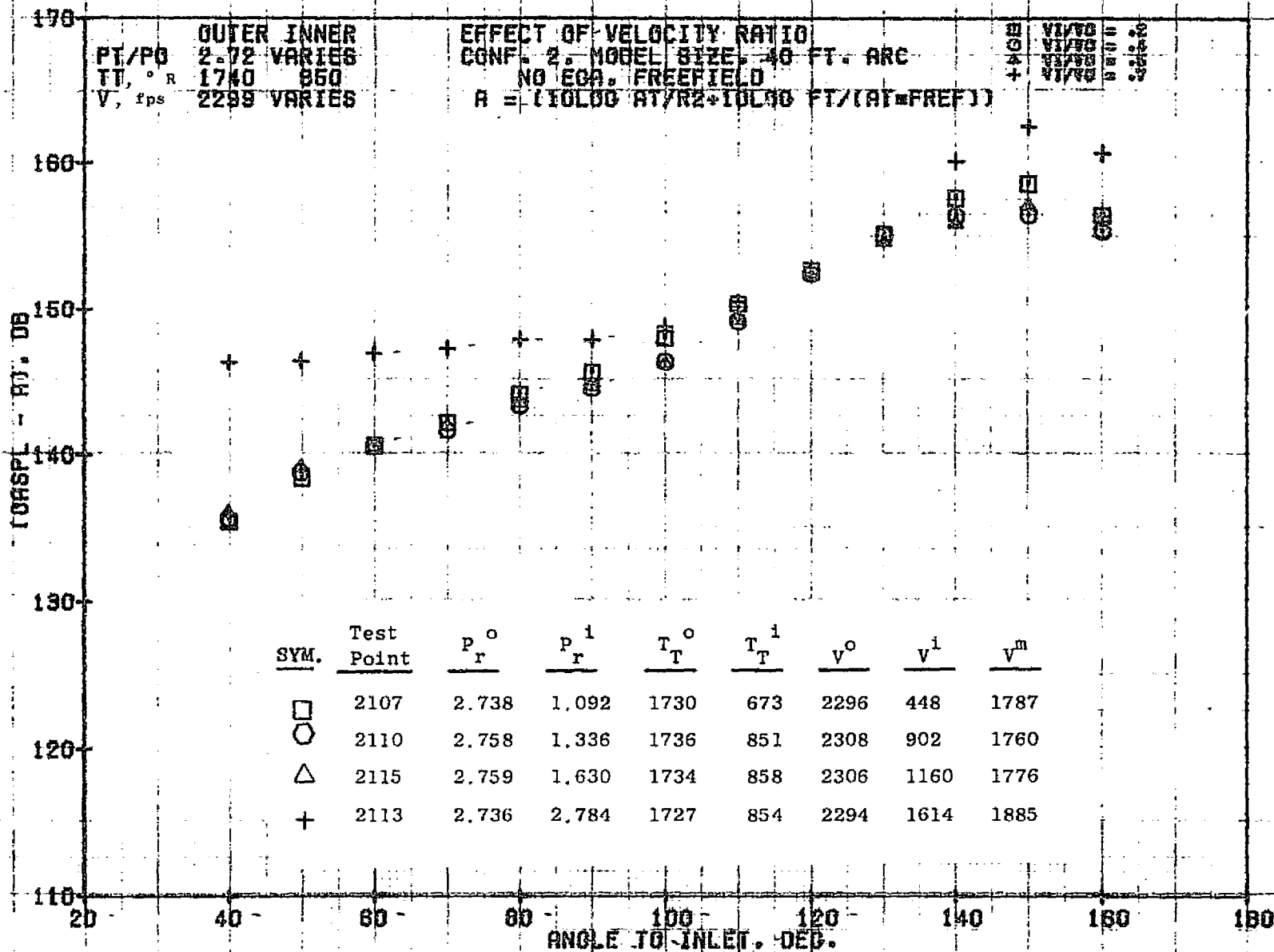
1113



11/01/76
18421-001

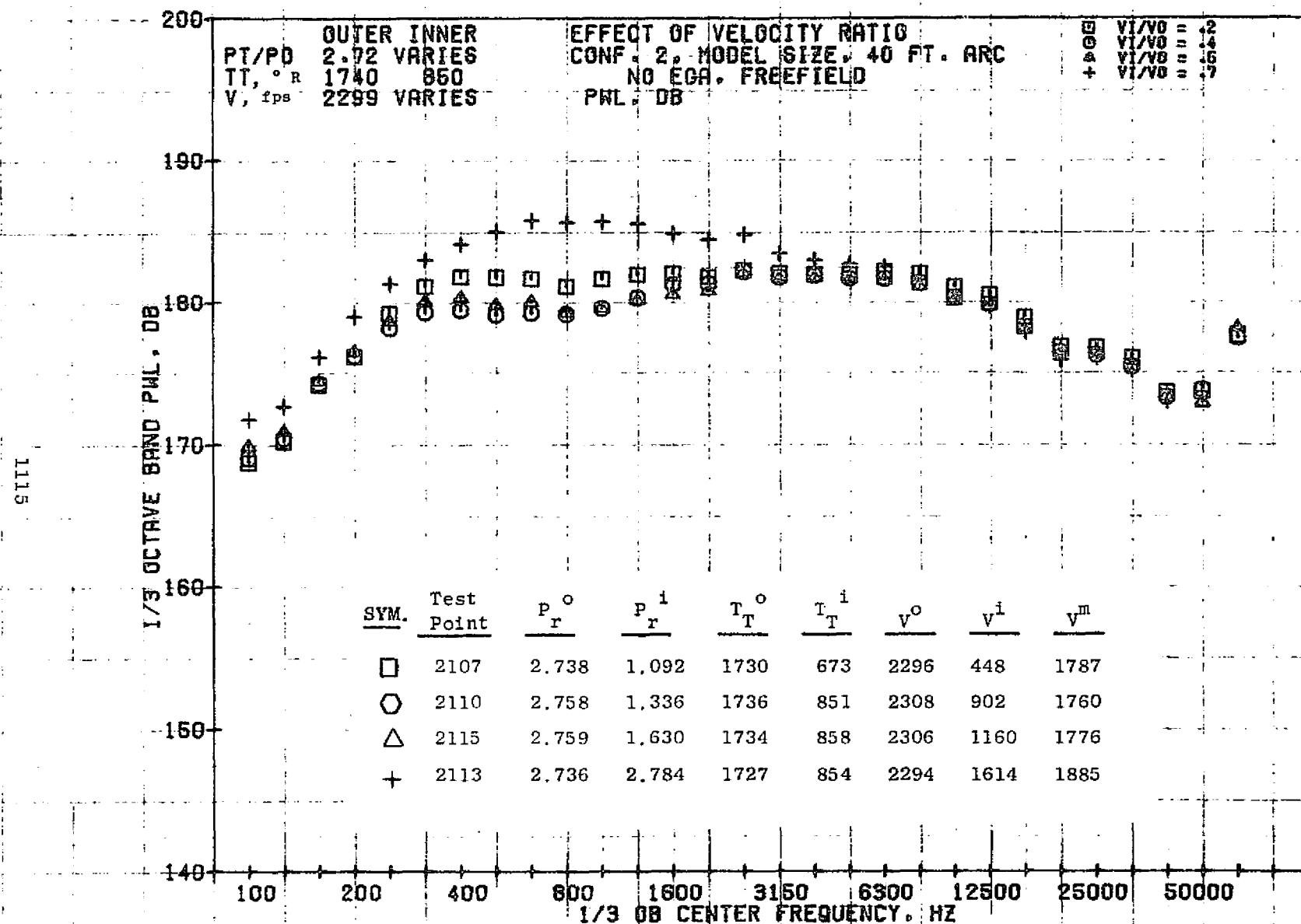
79 BURCH A.

1114



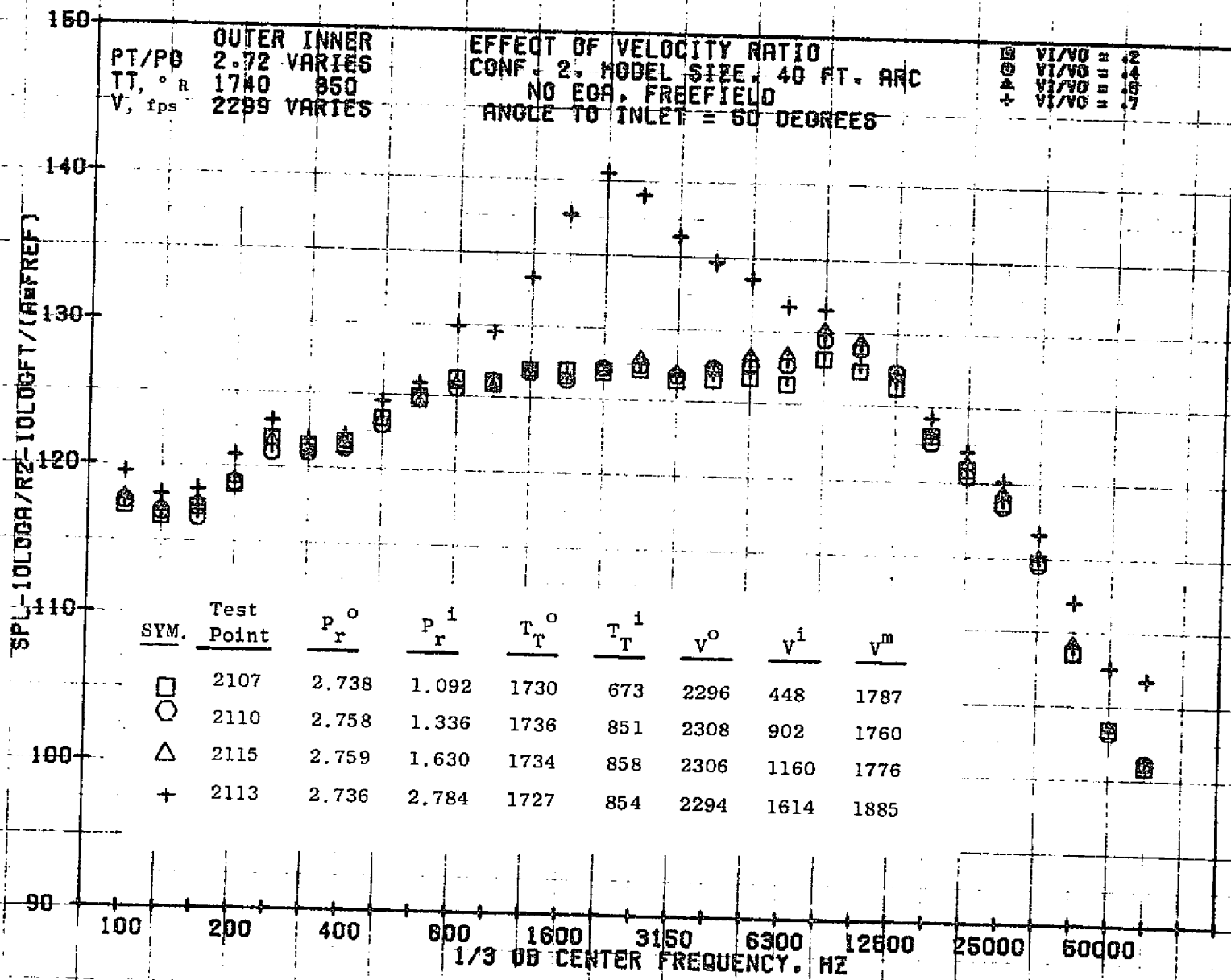
11/09/76
1R343-001

79 BURCH A.



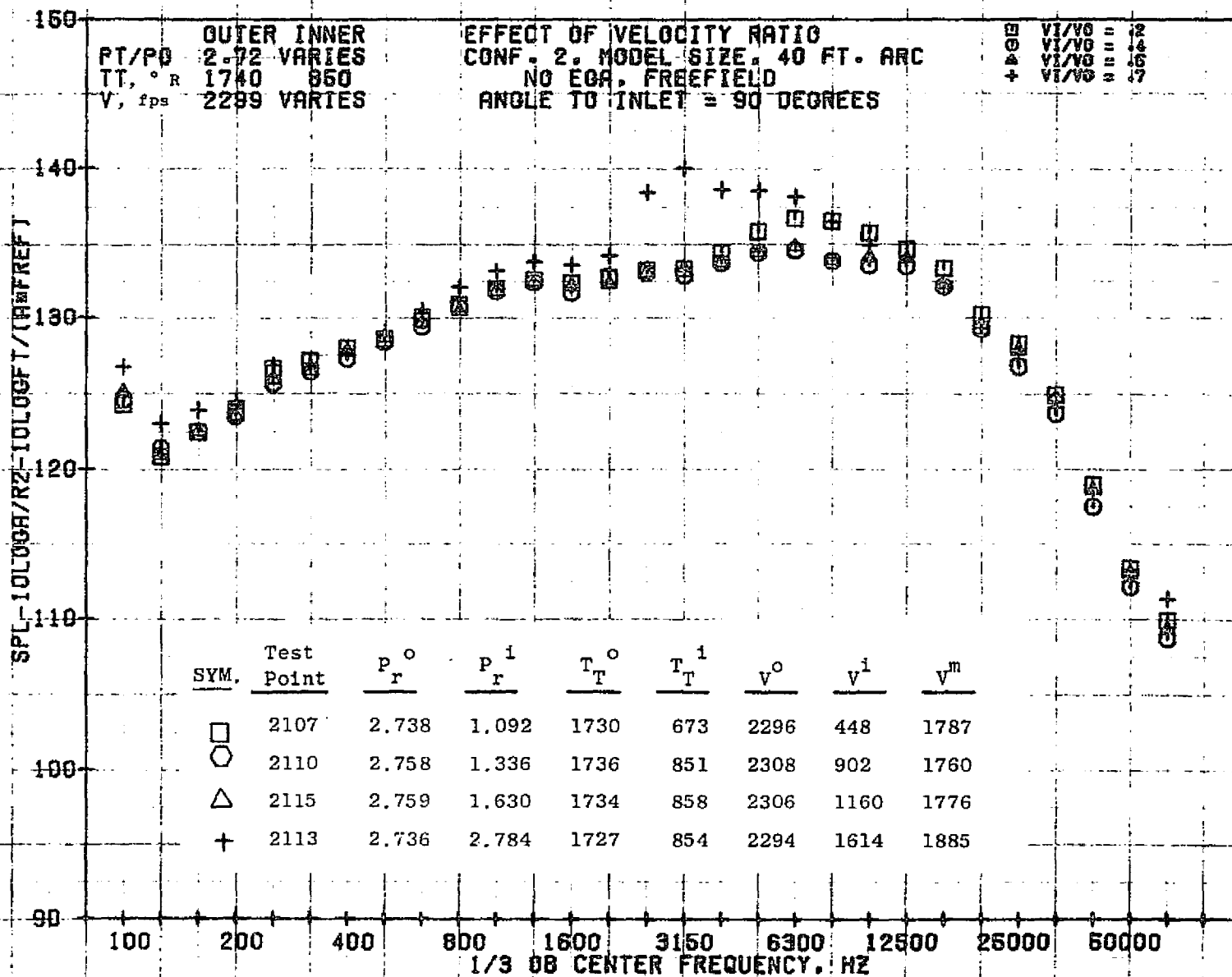
11/01/76
18391-001

79 BURCH A.



11/01/76
18391-001

79 BURCH A.

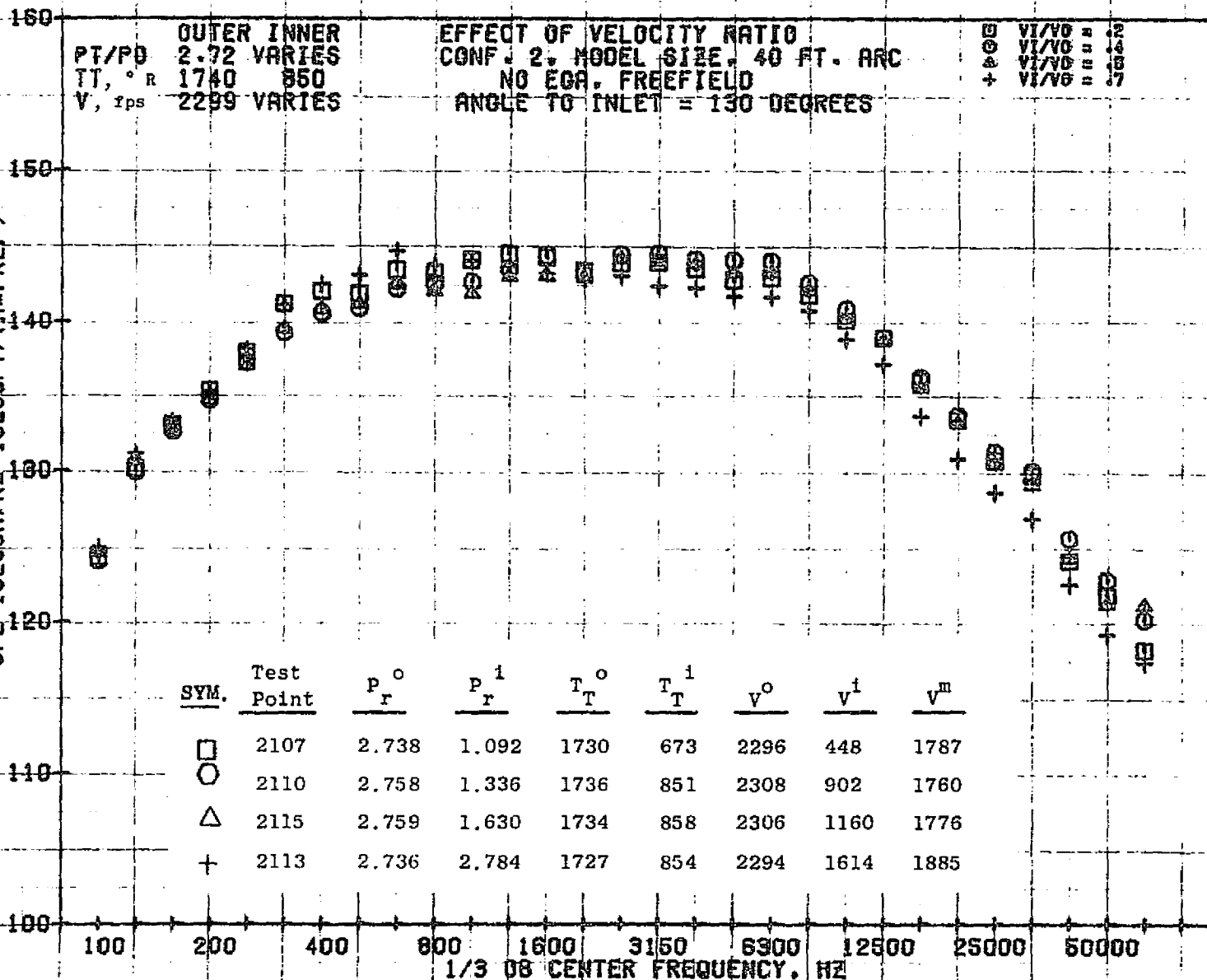


11/01/76
 18391-001

79 BURCH A.

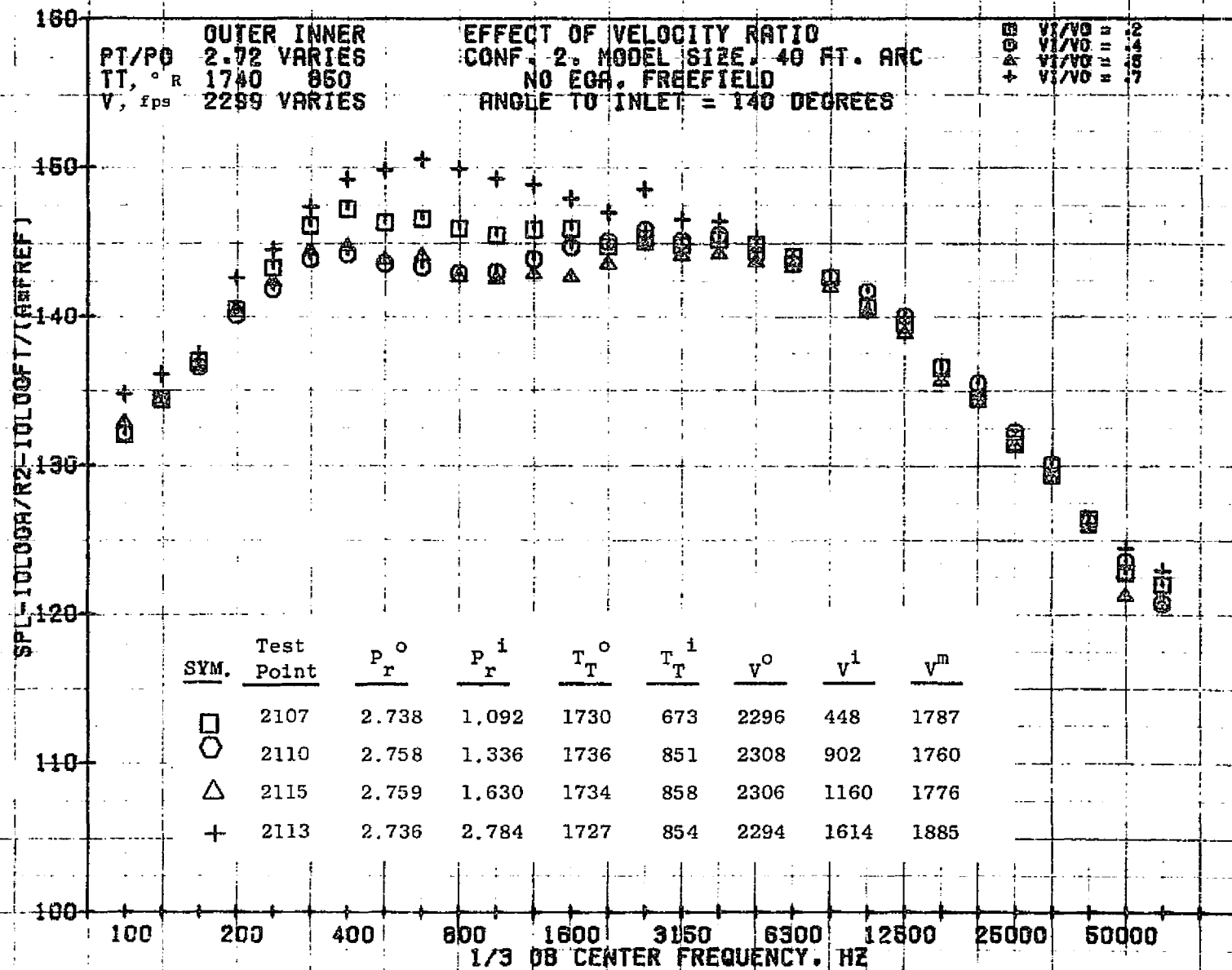
18111

SPL-10LOGA/R2-10LOGFT/(HMFREF)



11/01/76
18391-001

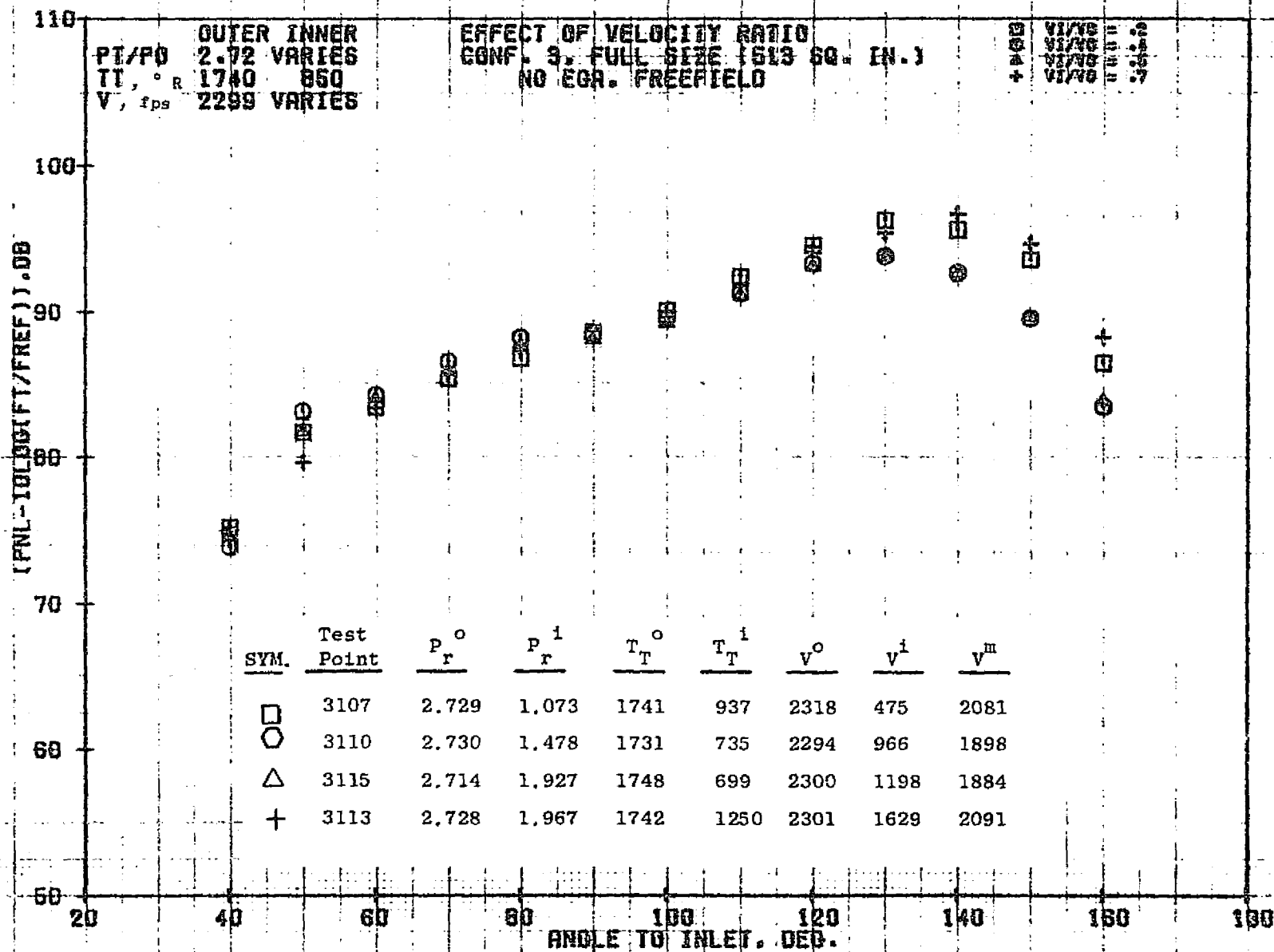
79 BURCH A.



11/01/76
 18391-001

79 BURCH A.

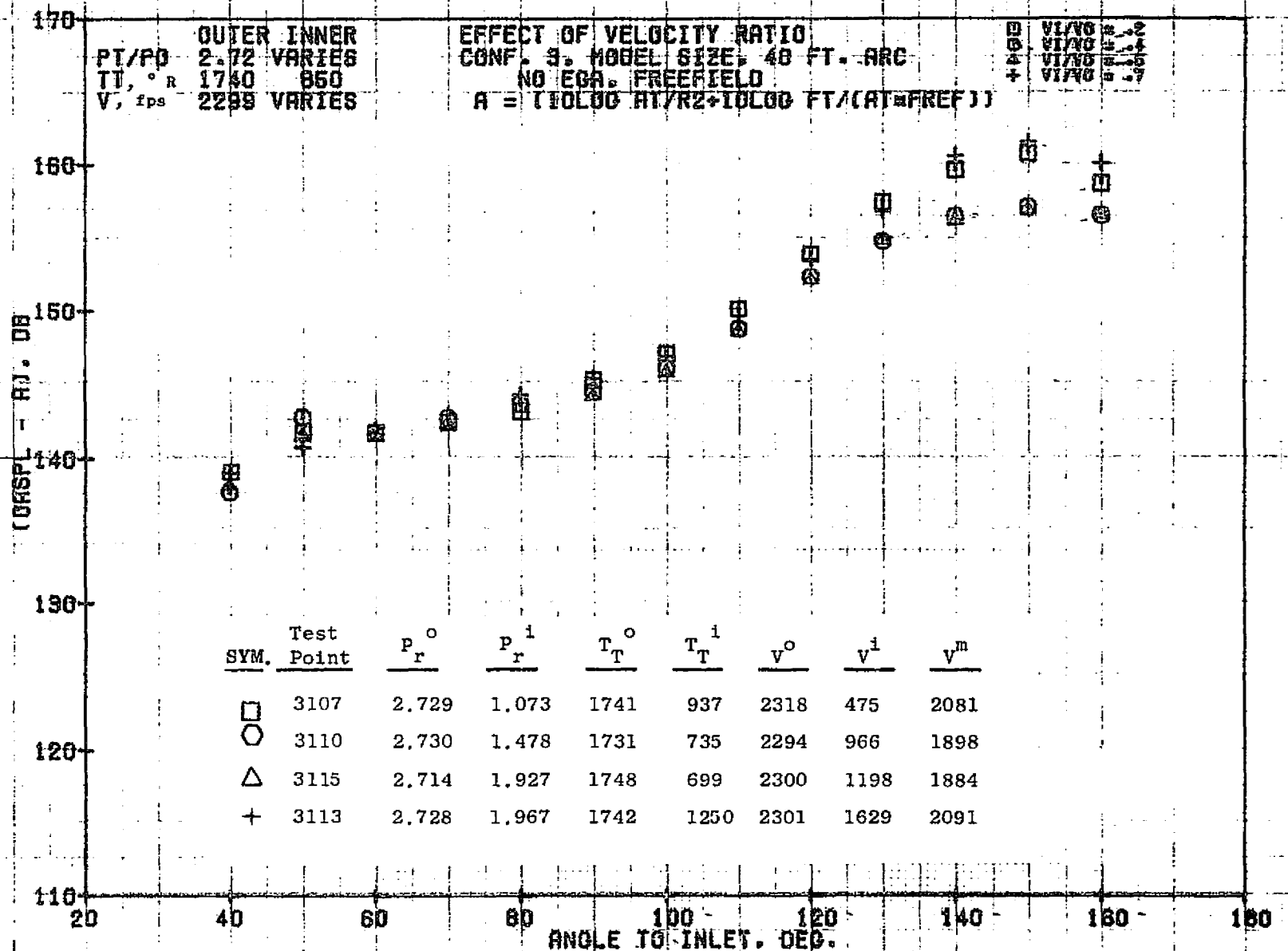
1120



11/01/76
18421-001

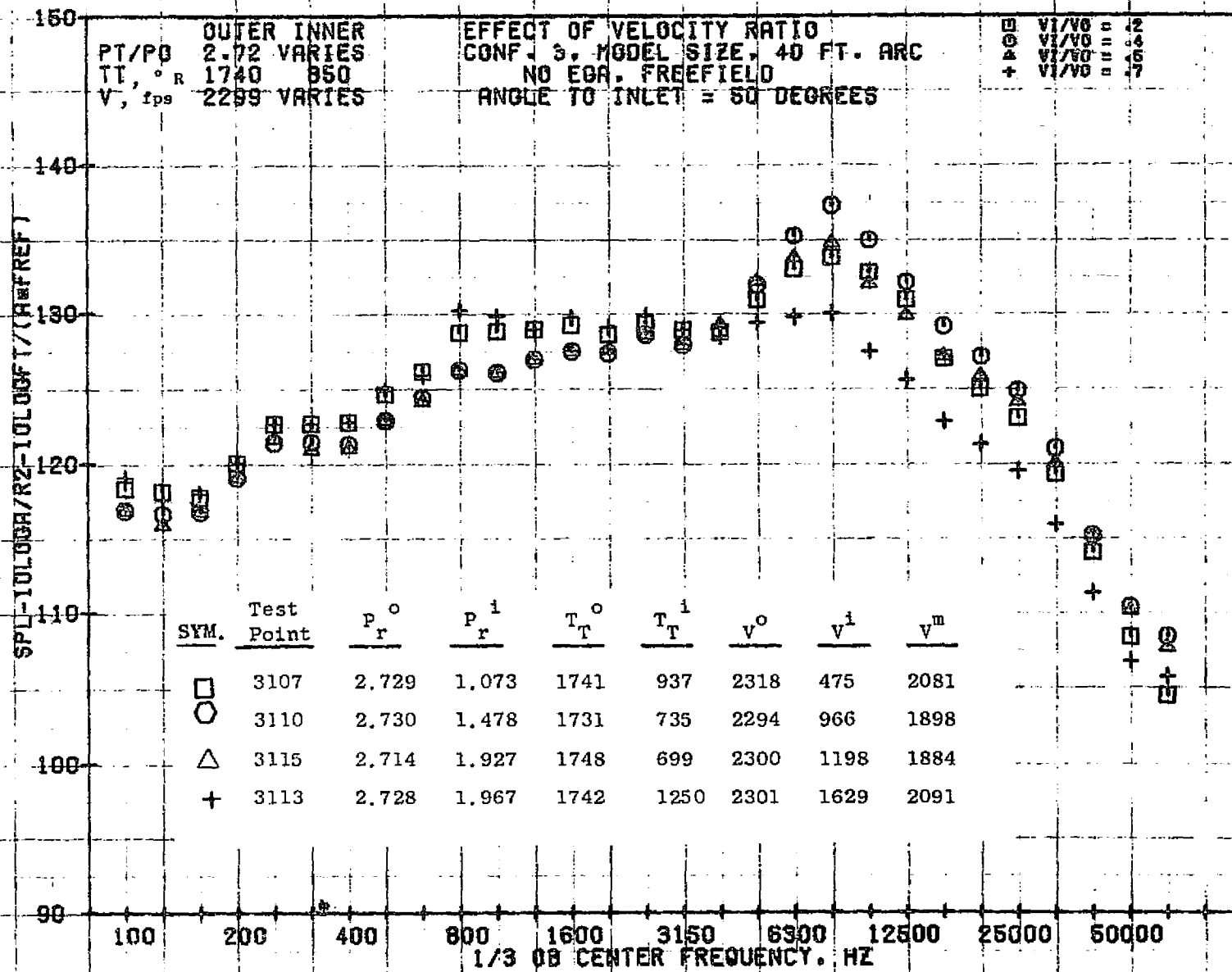
79 BURCH A.

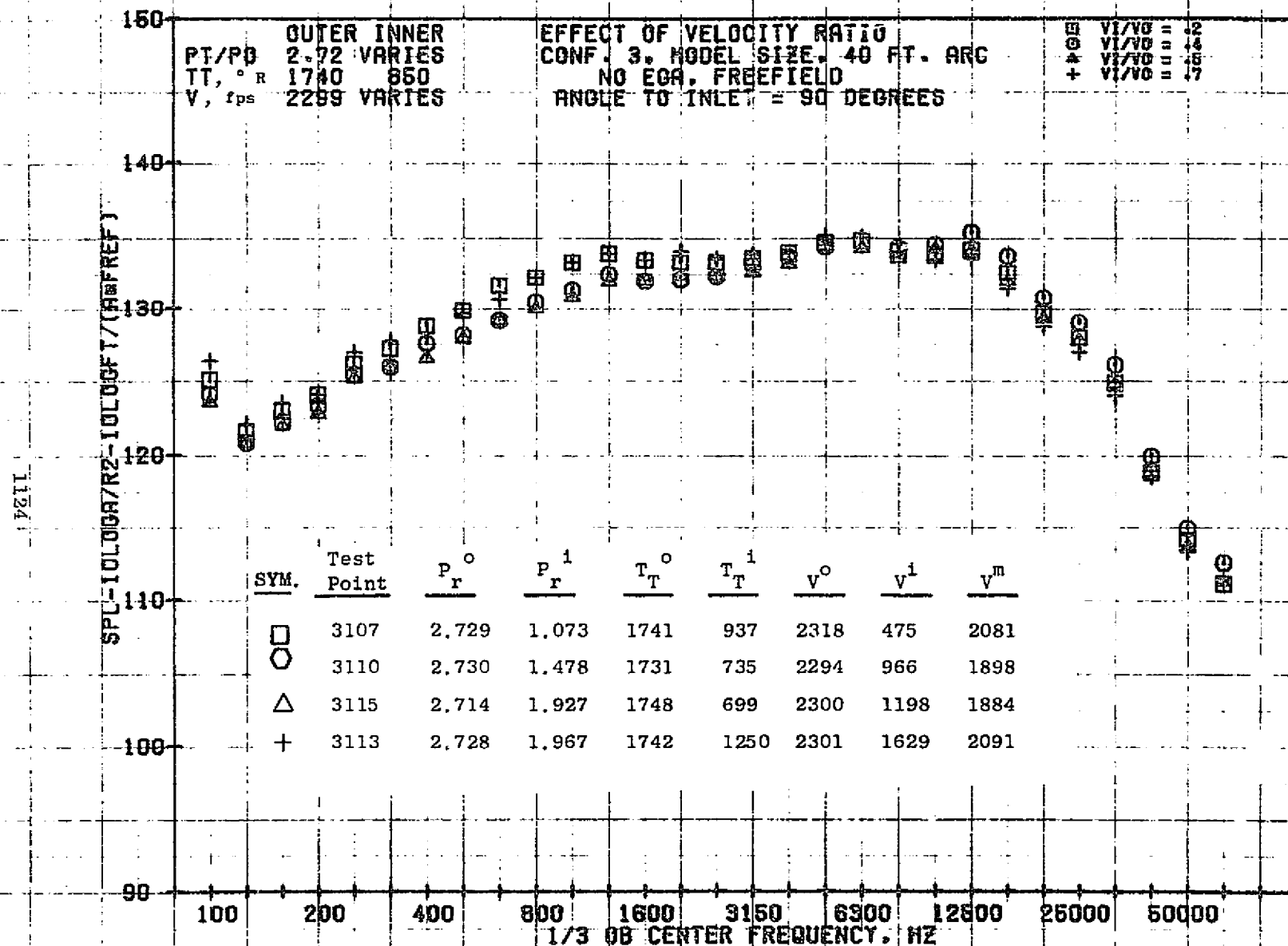
1121



11/09/76 -
 1A343-001

79 AIRCRAFT



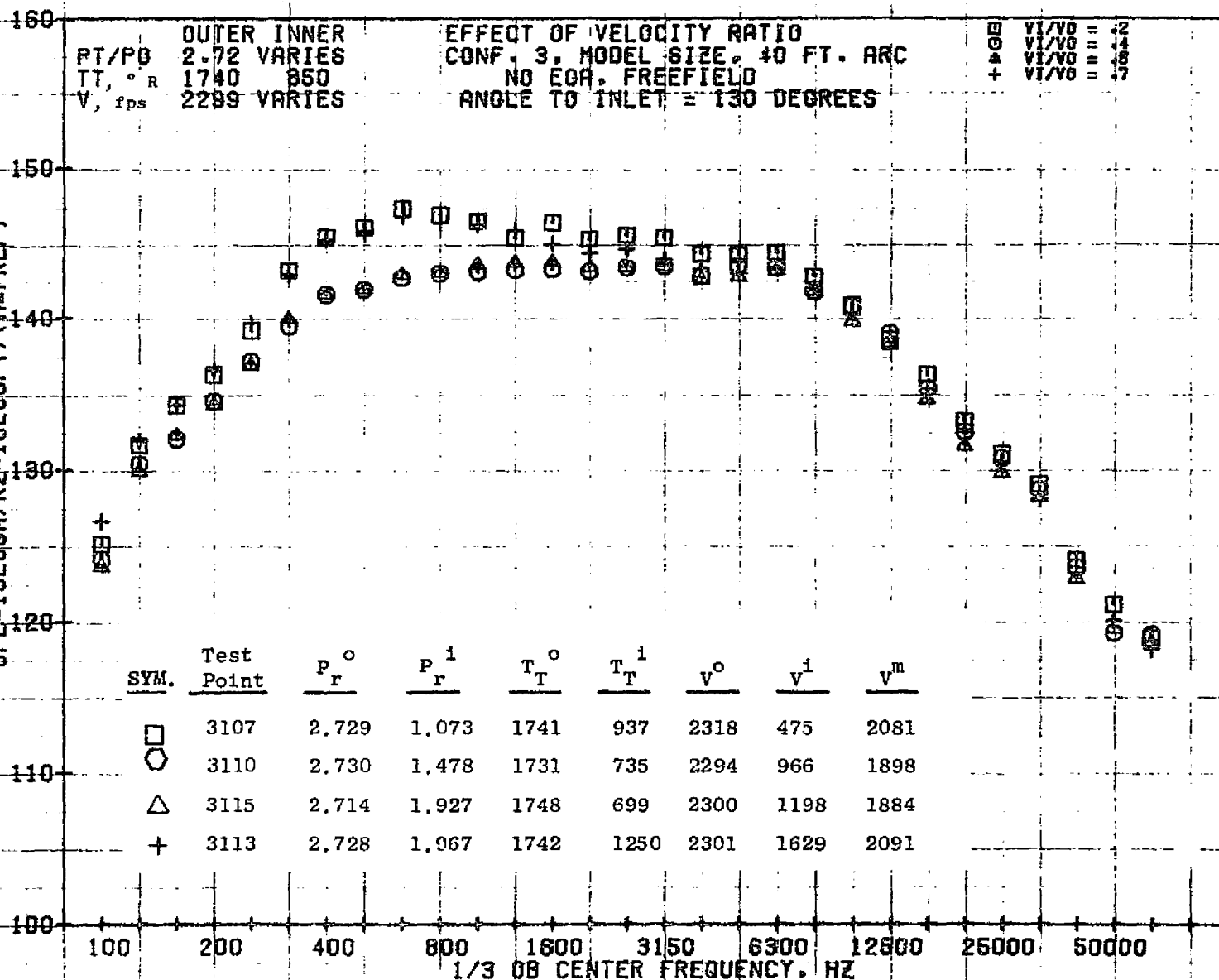


11/01/76
1839-001

79 BURCH A.

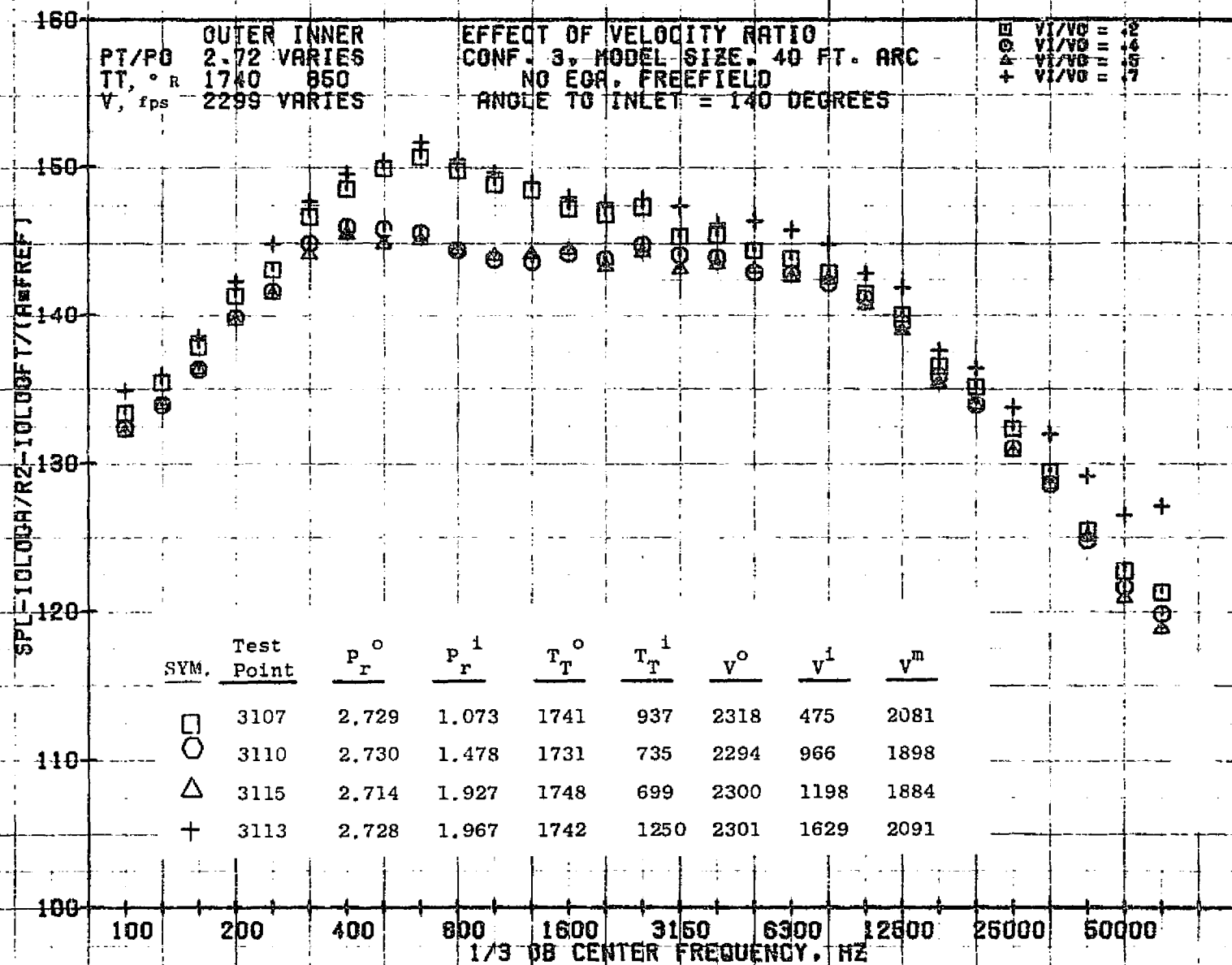
1125

SPL-10LOG(R/R2-10LOGFT/(AMFREF))



11/01/76
1B391-001

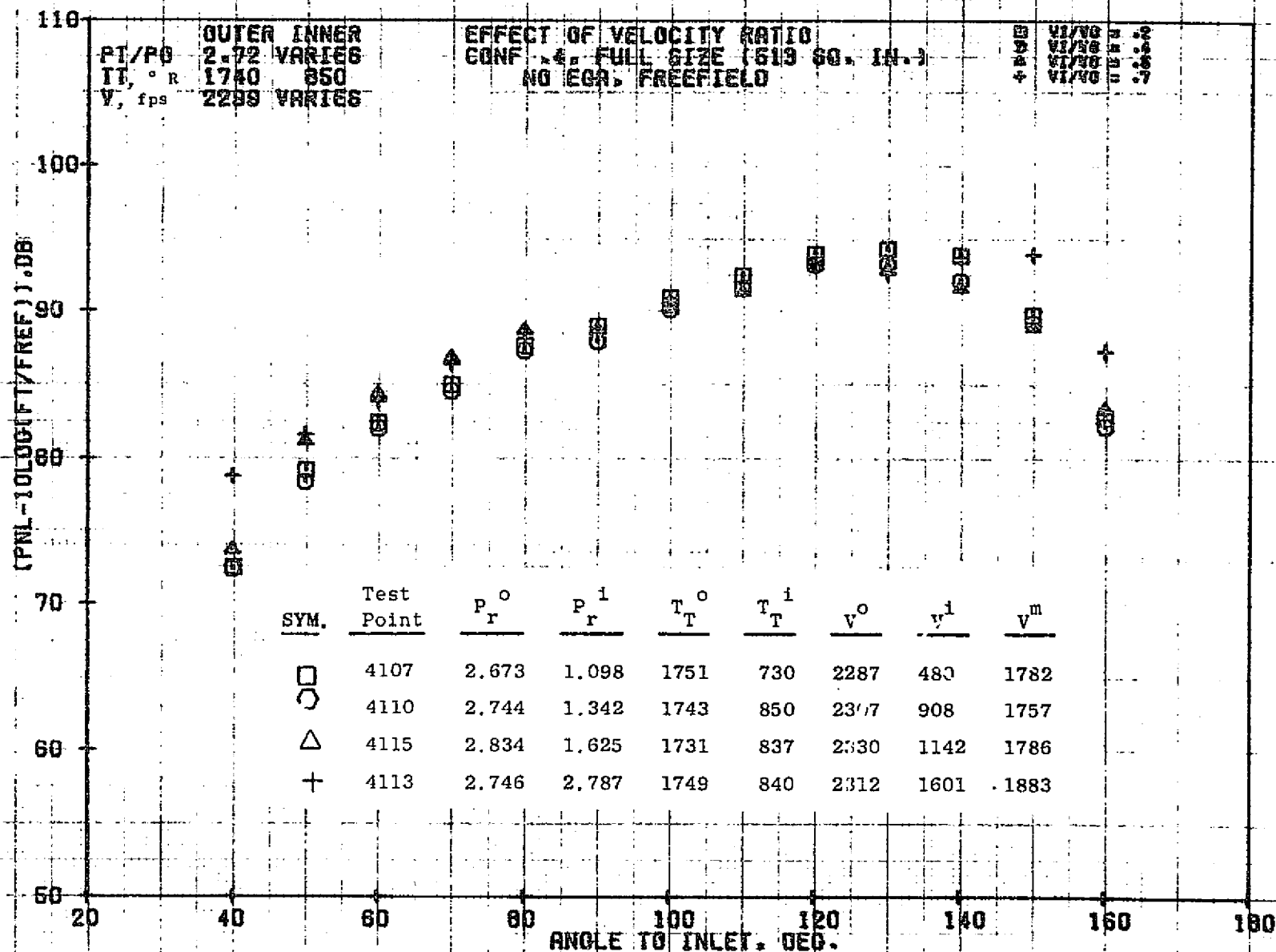
79 BURCH A.



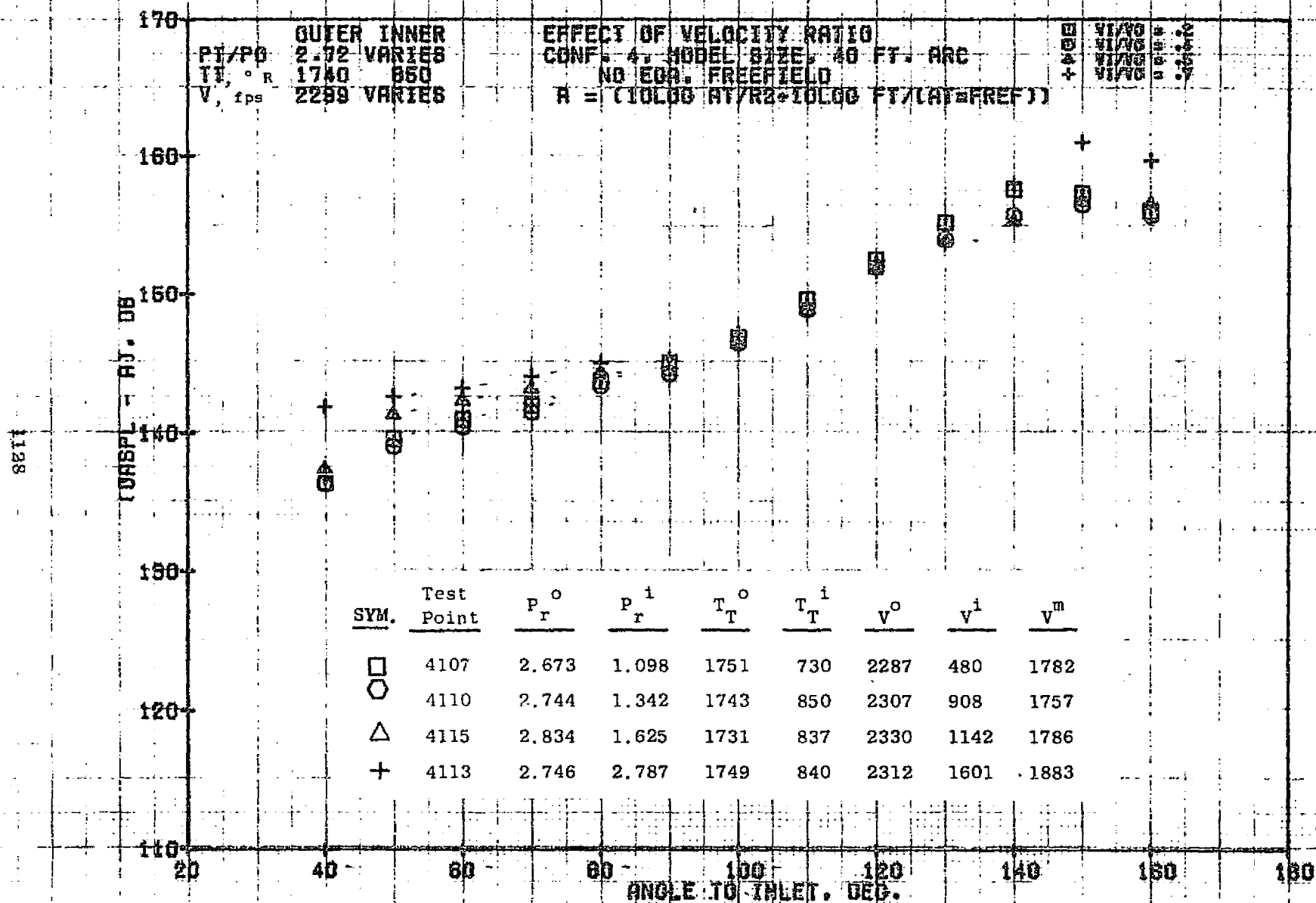
11/01/76
18391-001

79 BURCH A.

1127


 11/01/76
 18421-001

79 BURCH A.

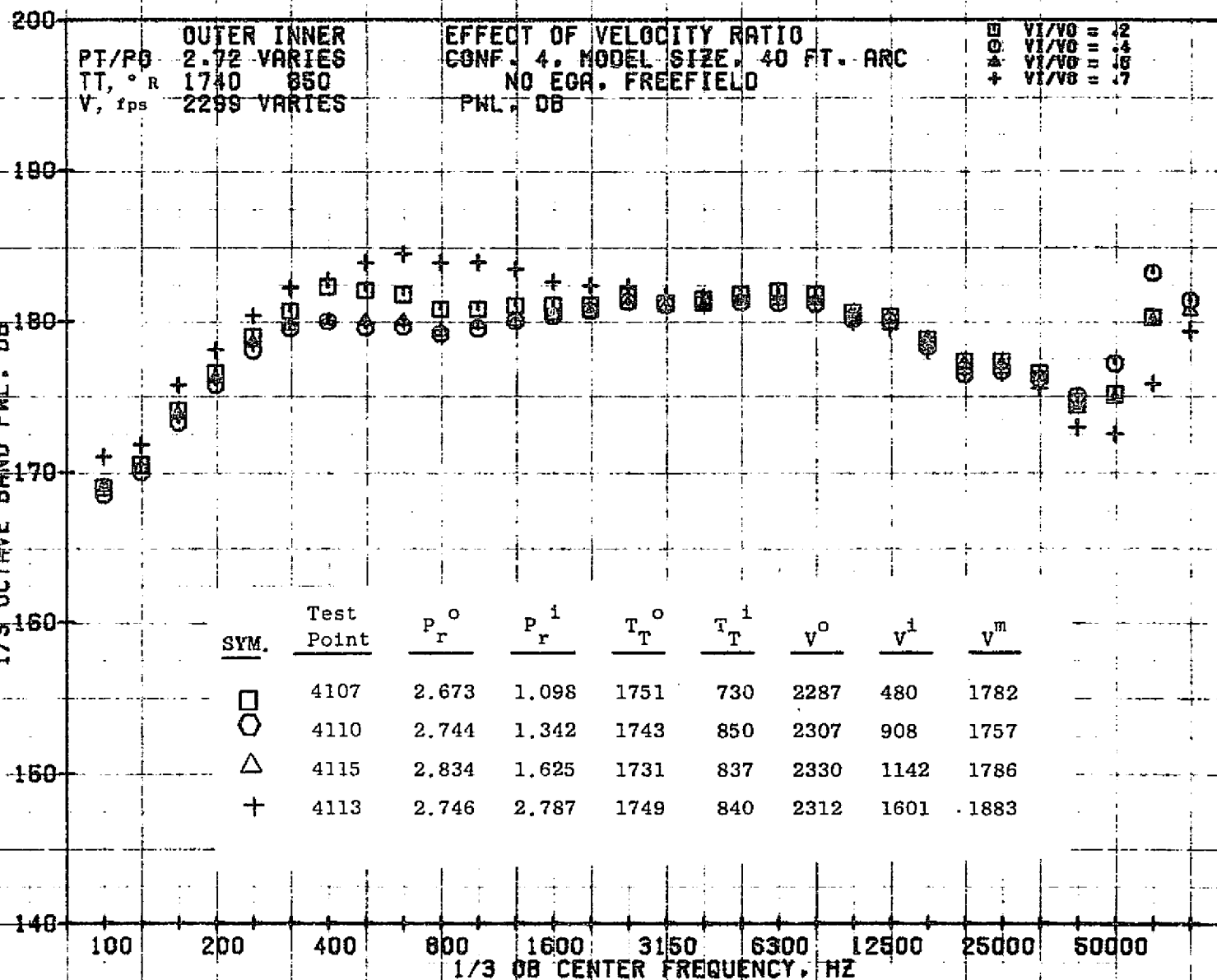


11/09/76
18343-001

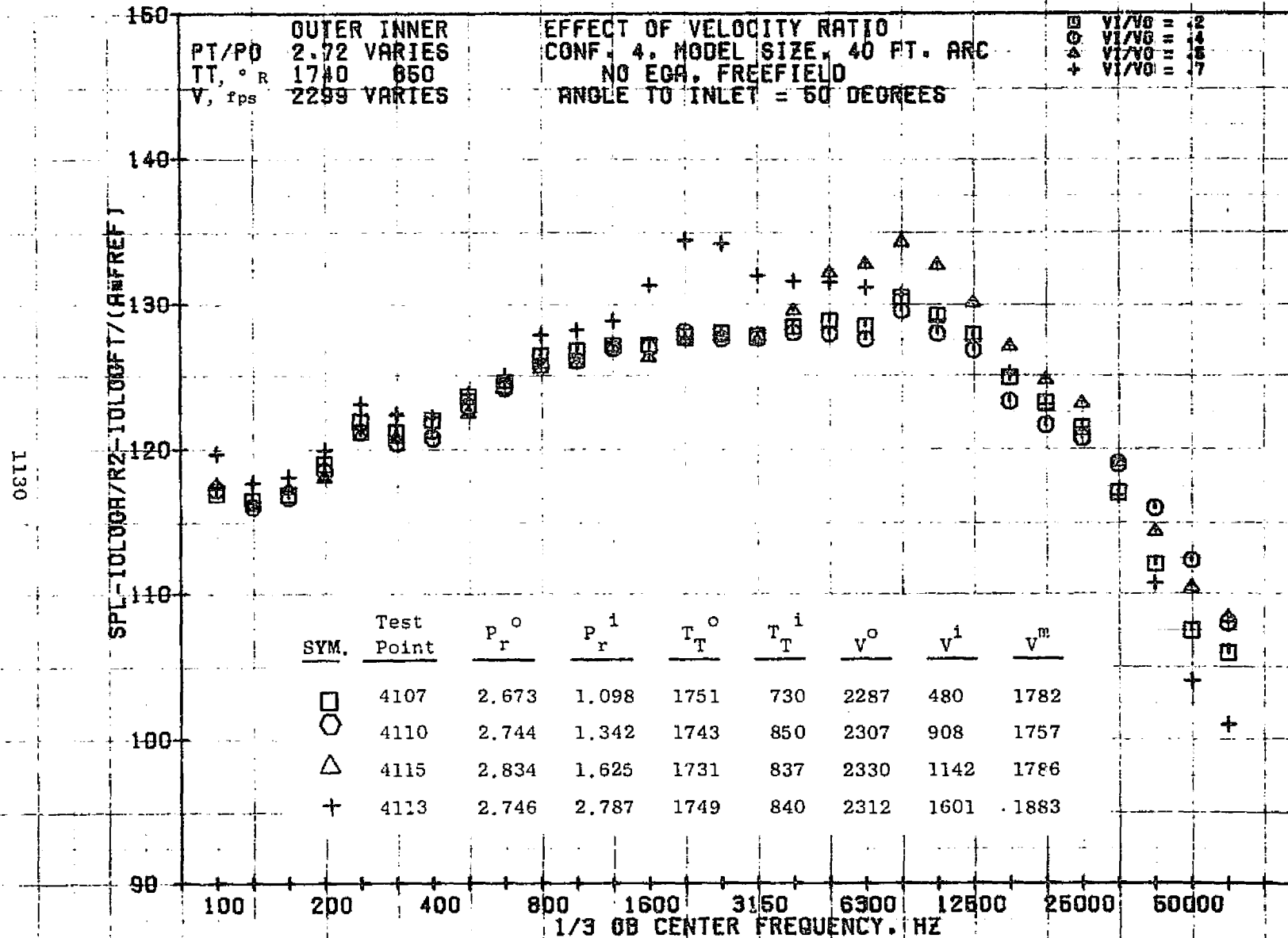
79 BURCH A.

1129

1/3 OCTAVE BAND PWL, DB

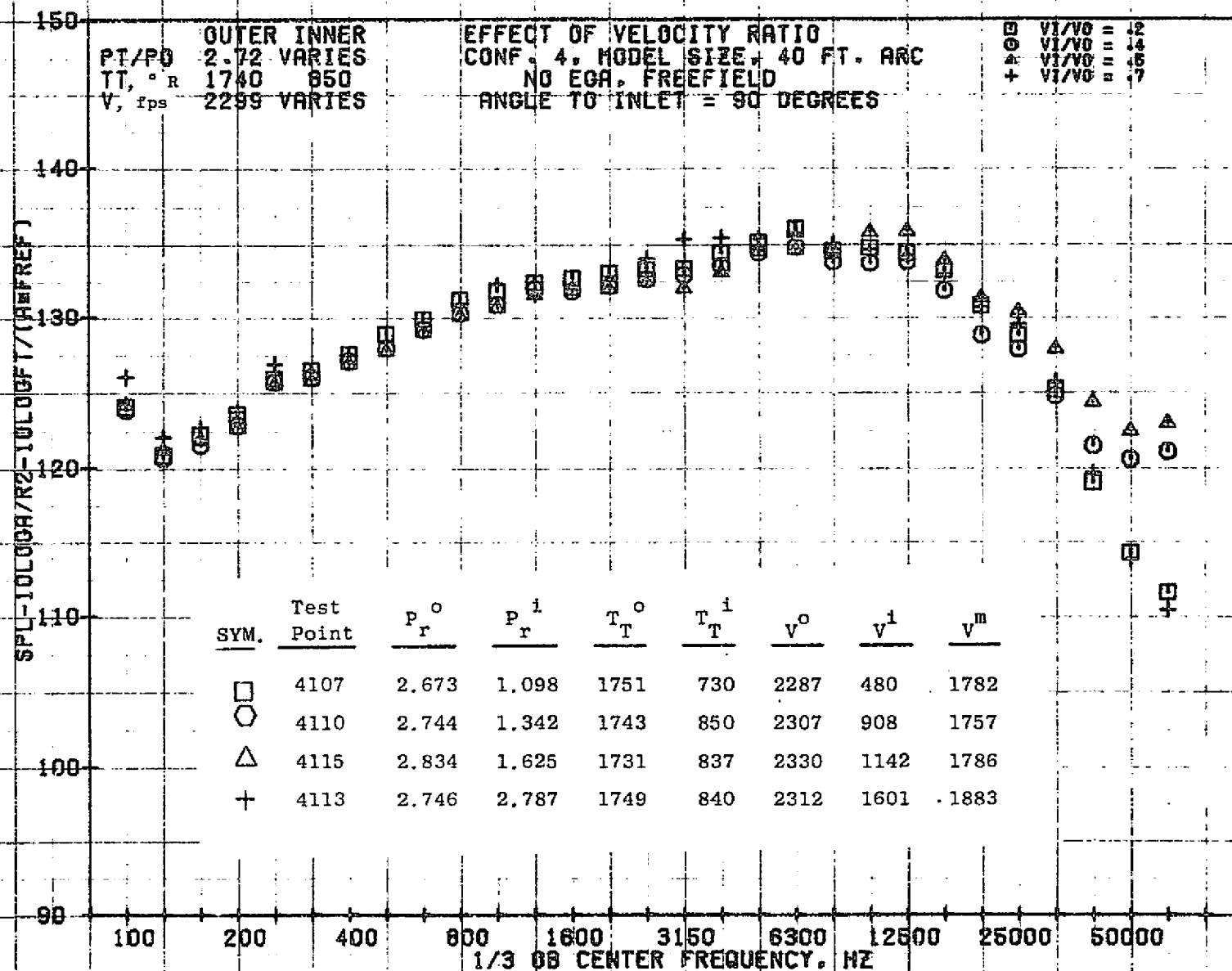

 11/01/76
 18391-001

79 BURCH A.



11/01/76
1B391-001

79 BURCH A.



1132

SPL-10LOGA/R2-10LOGFT/(AMFREF)

160

150

140

130

120

110

100

PT/PO
TT, ° R
V, fps

OUTER INNER
2.72 VARIES
1740 850
2299 VARIES

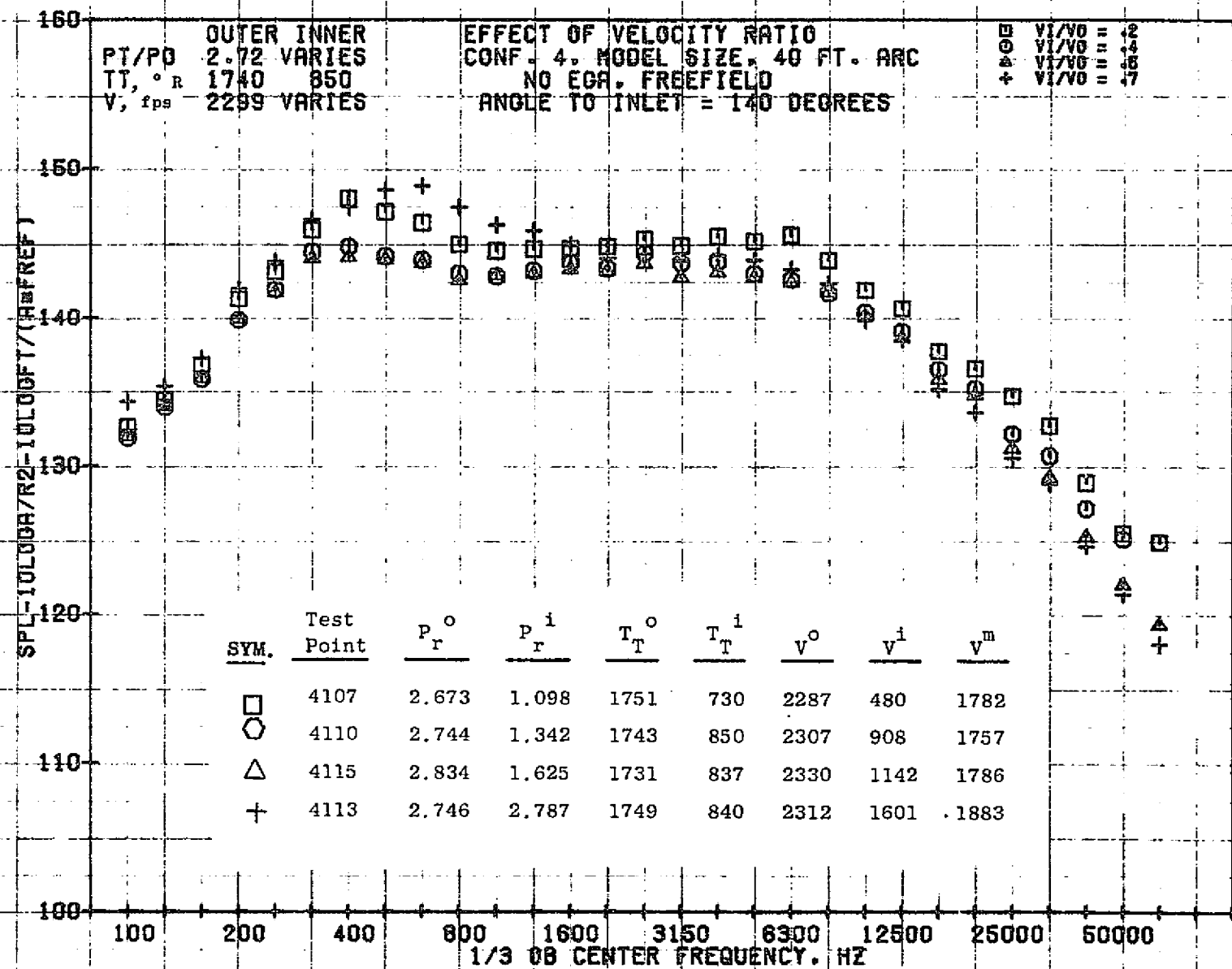
EFFECT OF VELOCITY RATIO
CONF. 4. MODEL SIZE, 40 FT. ARC
NO EGA. FREEFIELD
ANGLE TO INLET = 130 DEGREES

□ V1/V0 = 2
○ V1/V0 = 4
△ V1/V0 = 8
+ V1/V0 = 9

SYM.	Test Point	P_r^o	P_r^i	T_T^o	T_T^i	V^o	V^i	V^m
□	4107	2.673	1.098	1751	730	2287	480	1782
○	4110	2.744	1.342	1743	850	2307	908	1757
△	4115	2.834	1.625	1731	837	2330	1142	1786
+	4113	2.746	2.787	1749	840	2312	1601	1883

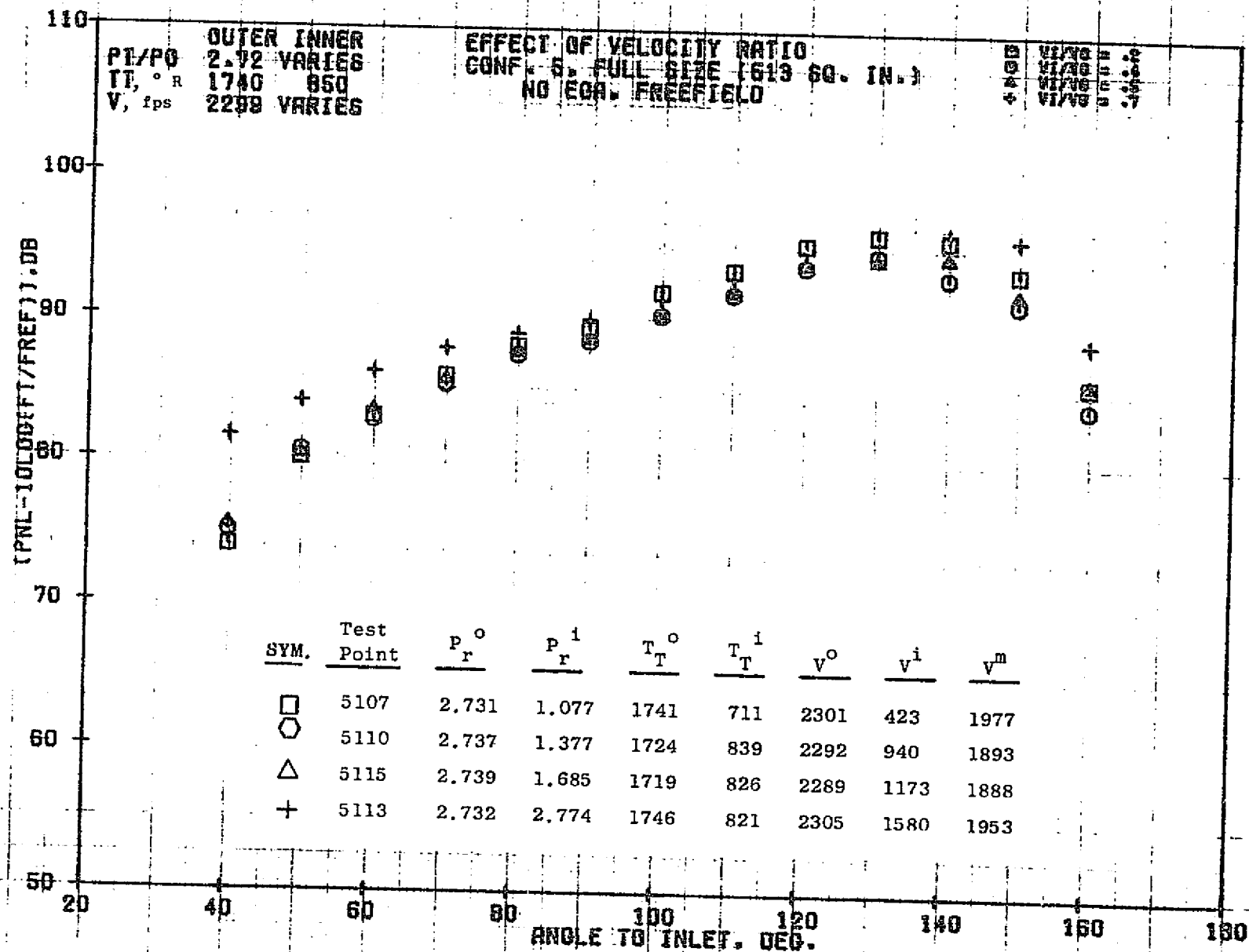
11/01/76
18391-001

79 BURCH A.



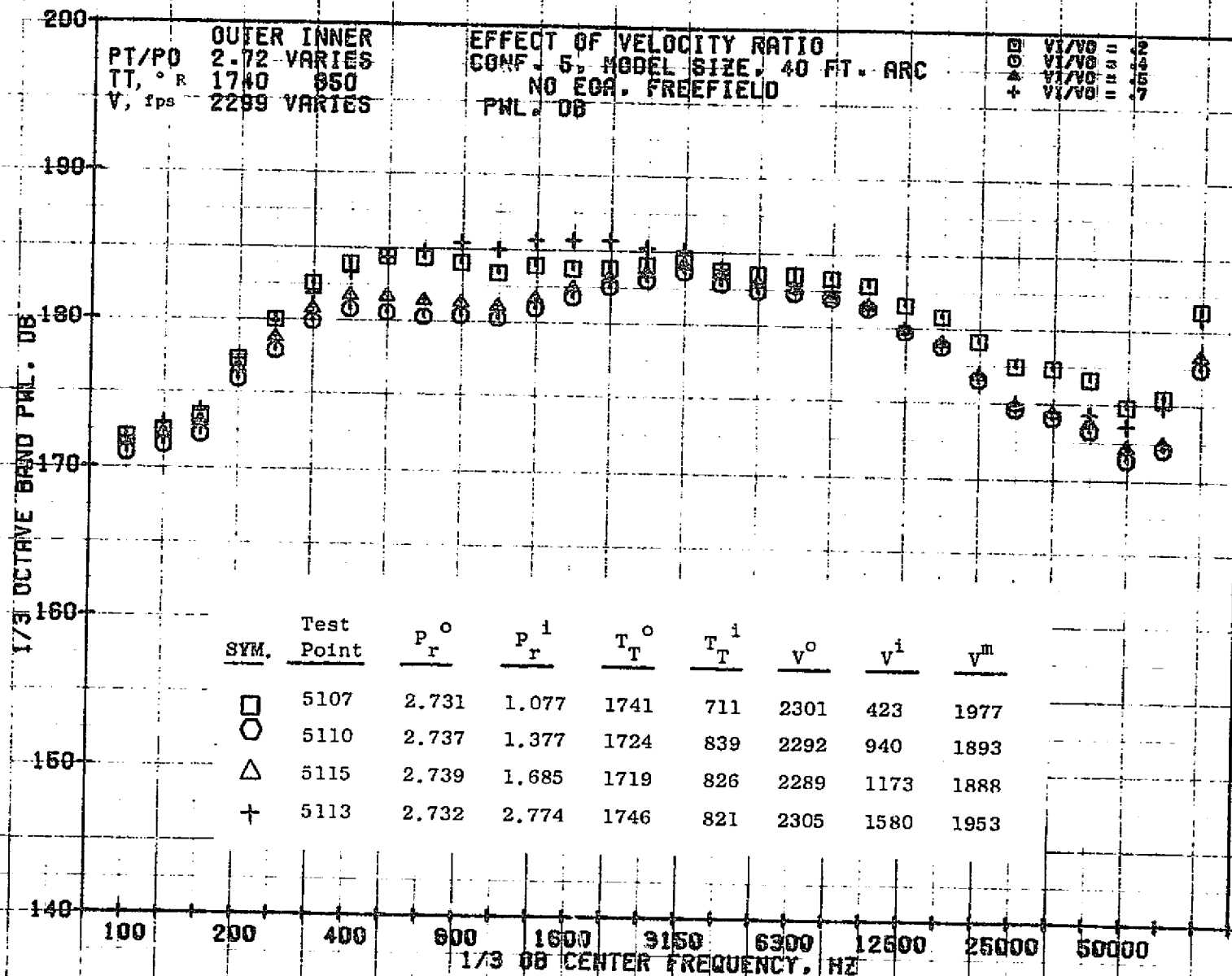
11/01/76
 18391-001

79 BURCH A.



11/01/76
 16421-001

79 BURCH A.

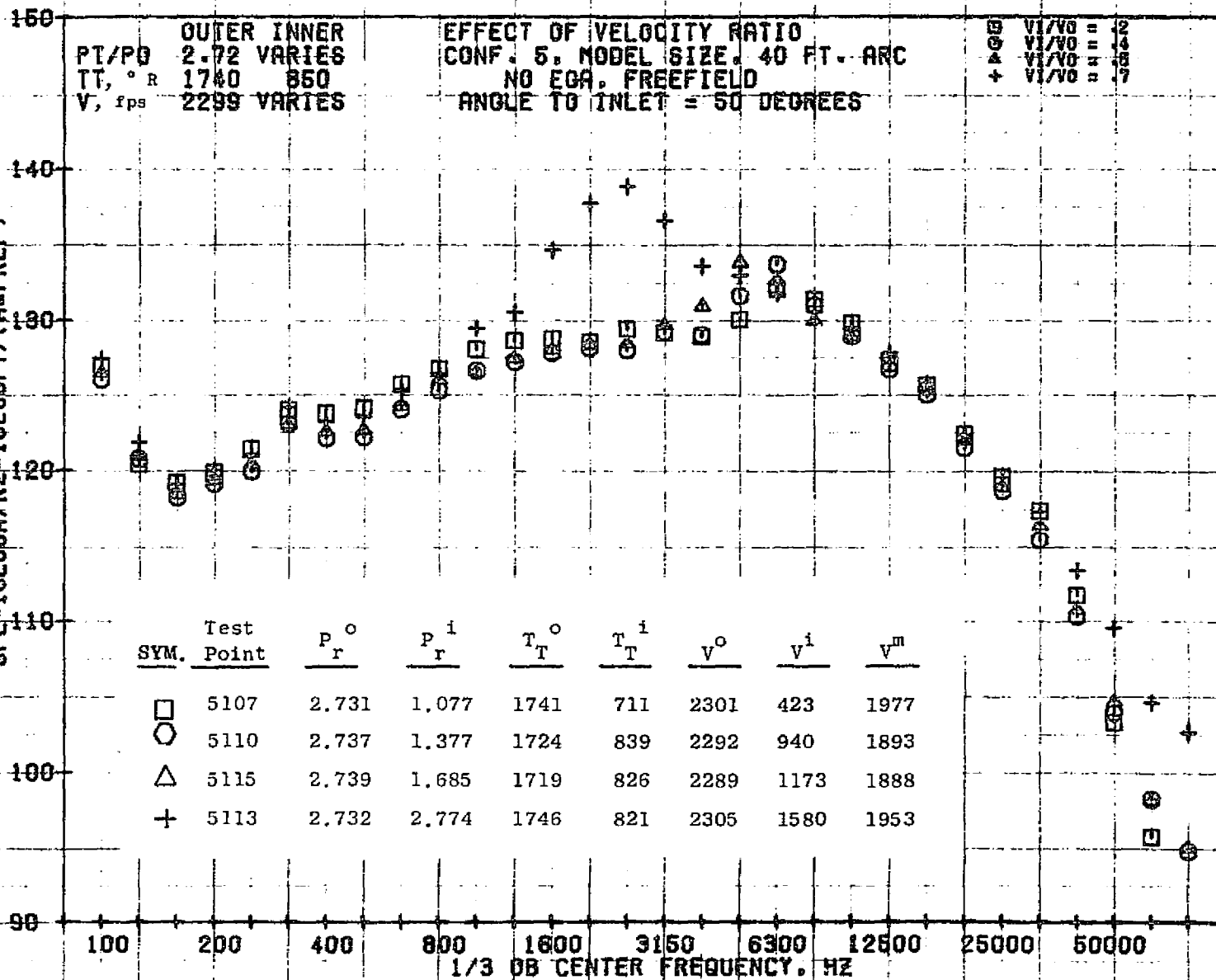


11/01/76
18391-001

79 BURCH A.

1137

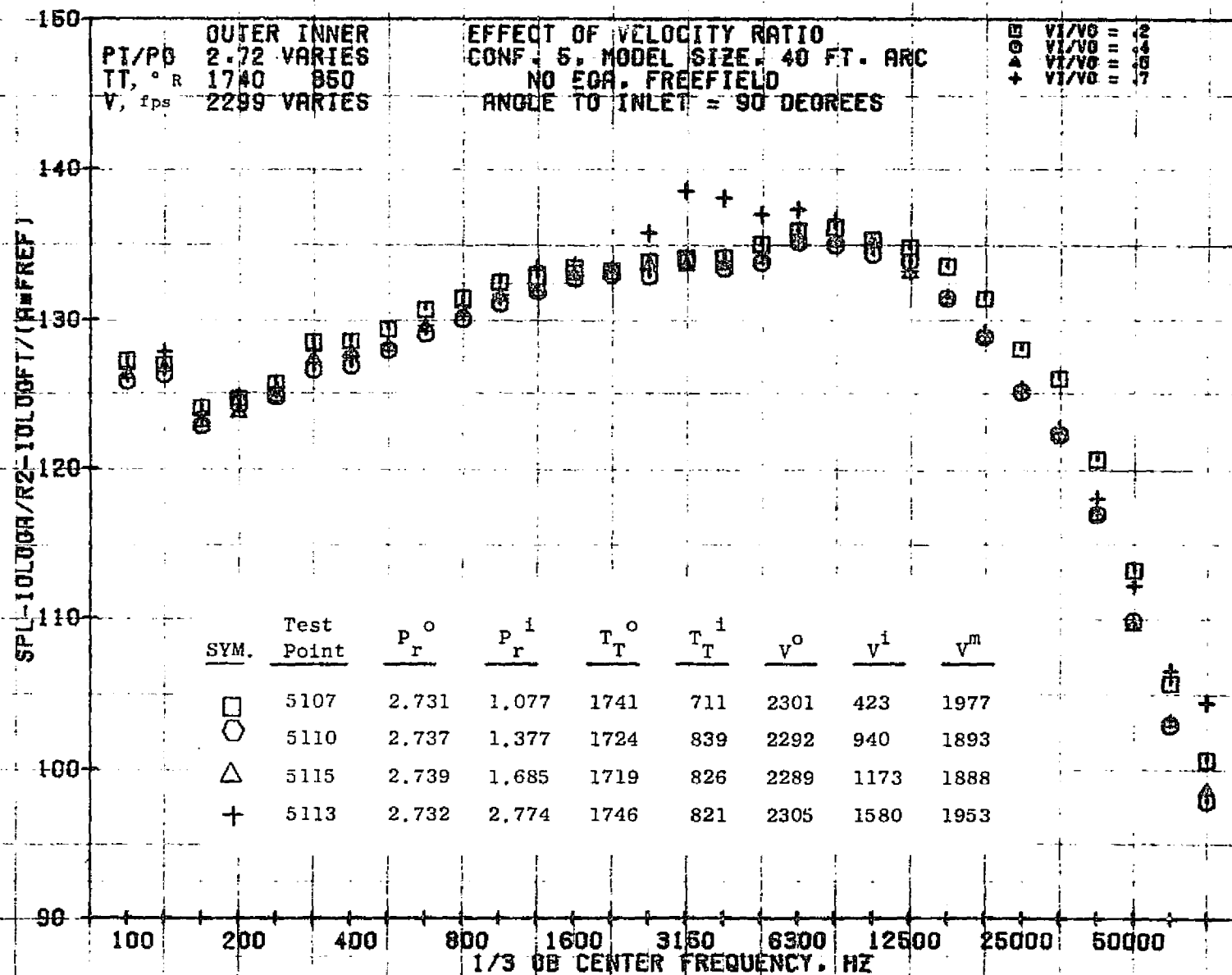
SPL-10LOGA/R2-10LOGF1/(RMFREF)



11/01/76
 18391-001

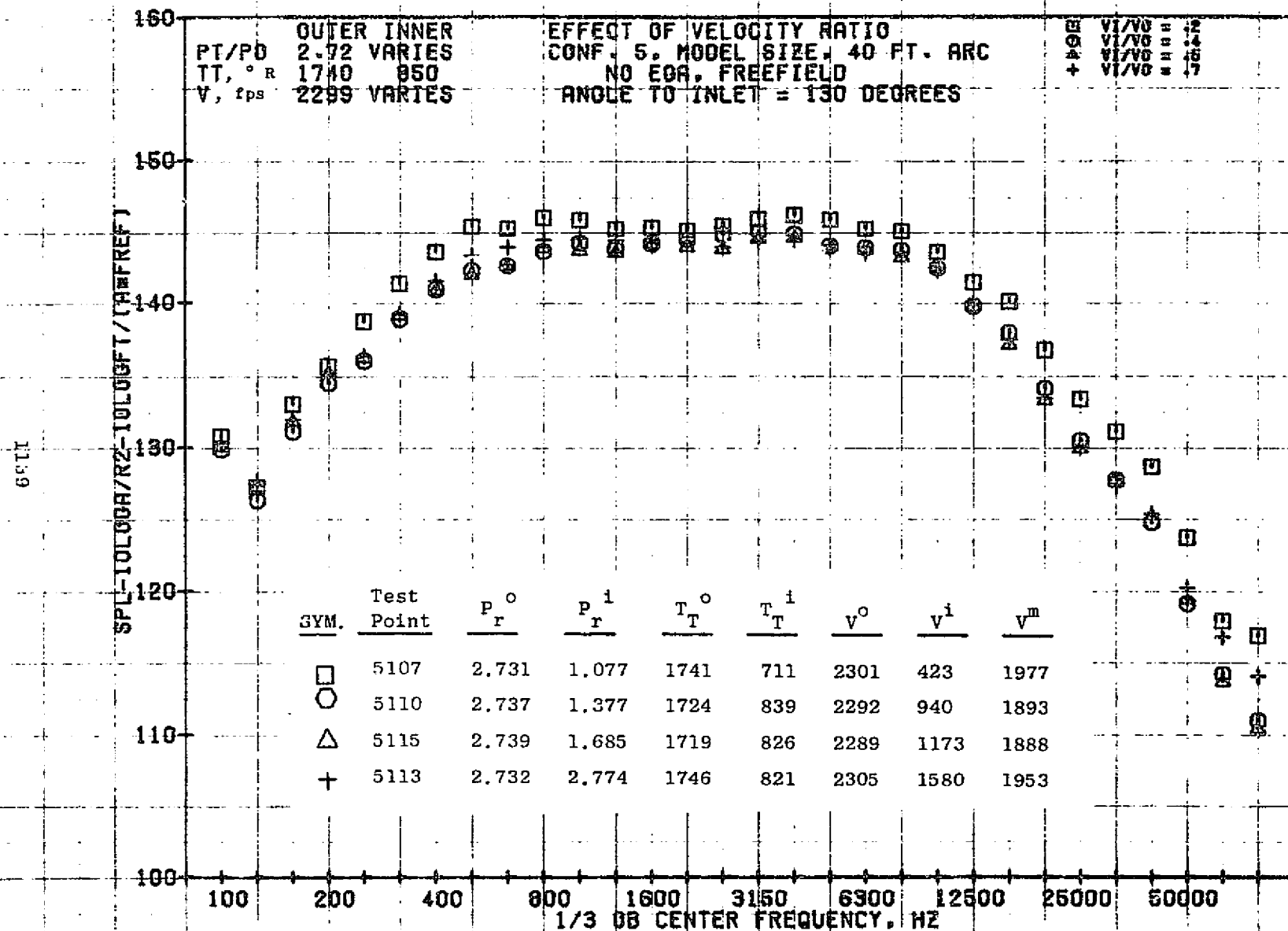
79 BURCH A.

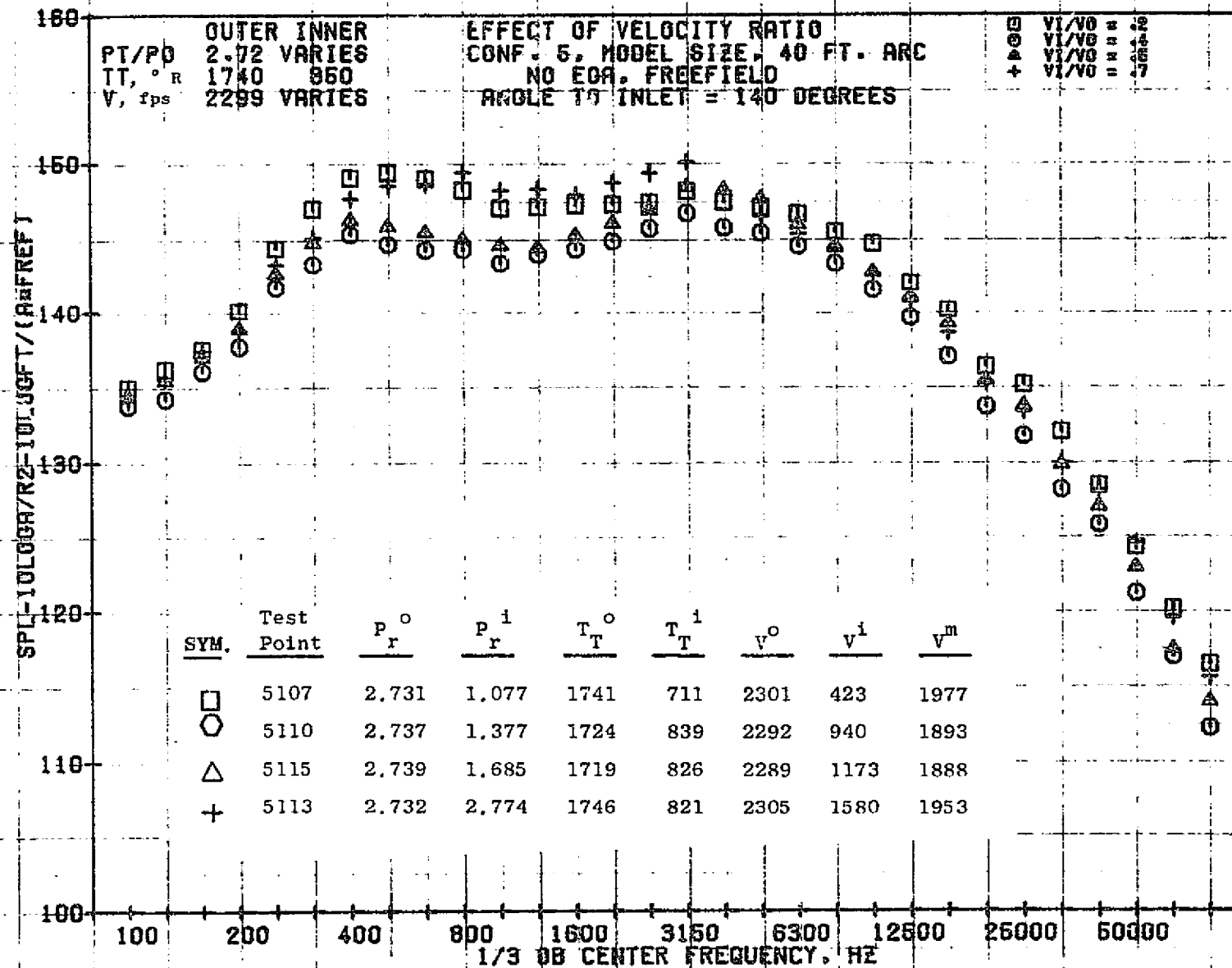
1138

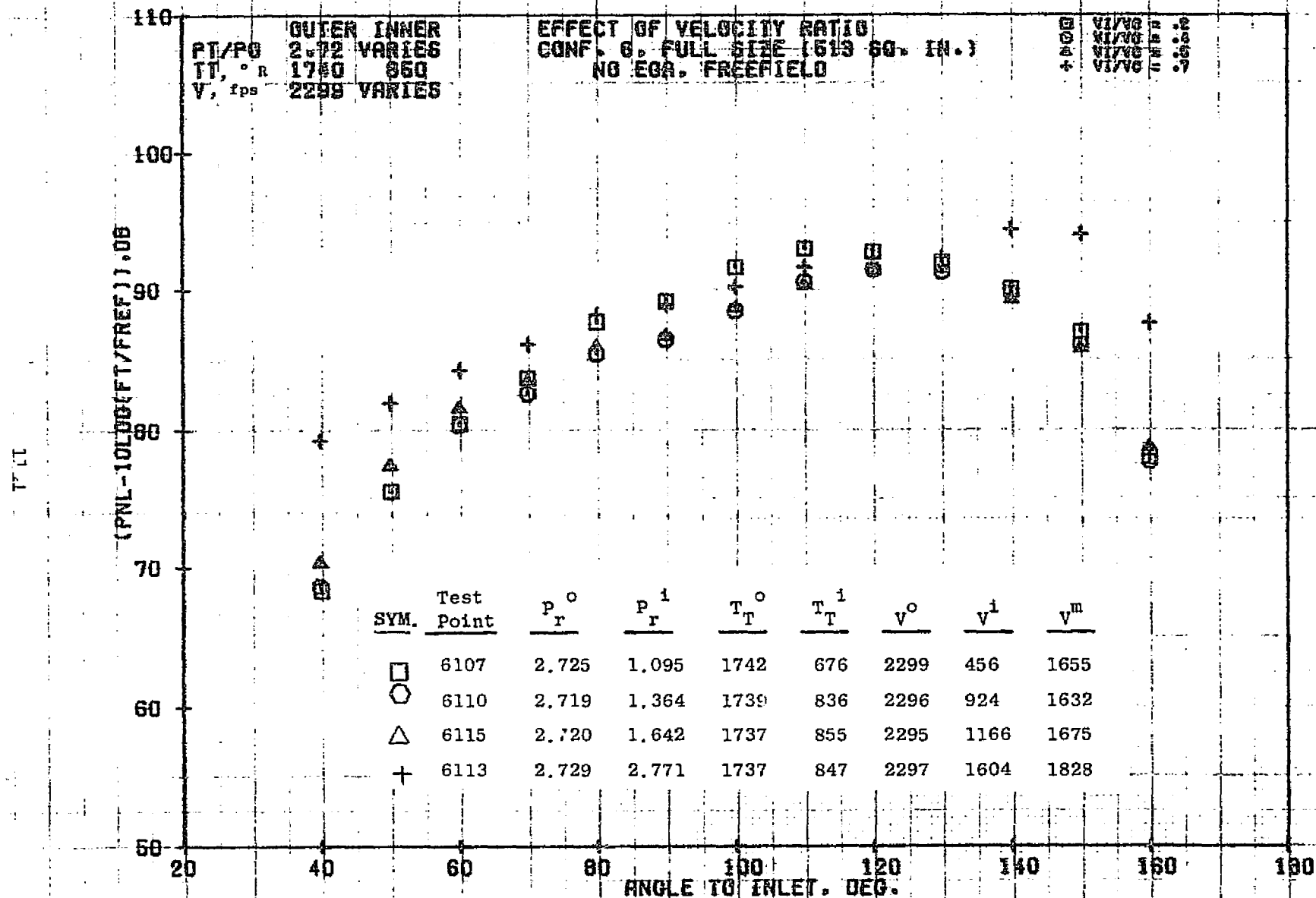


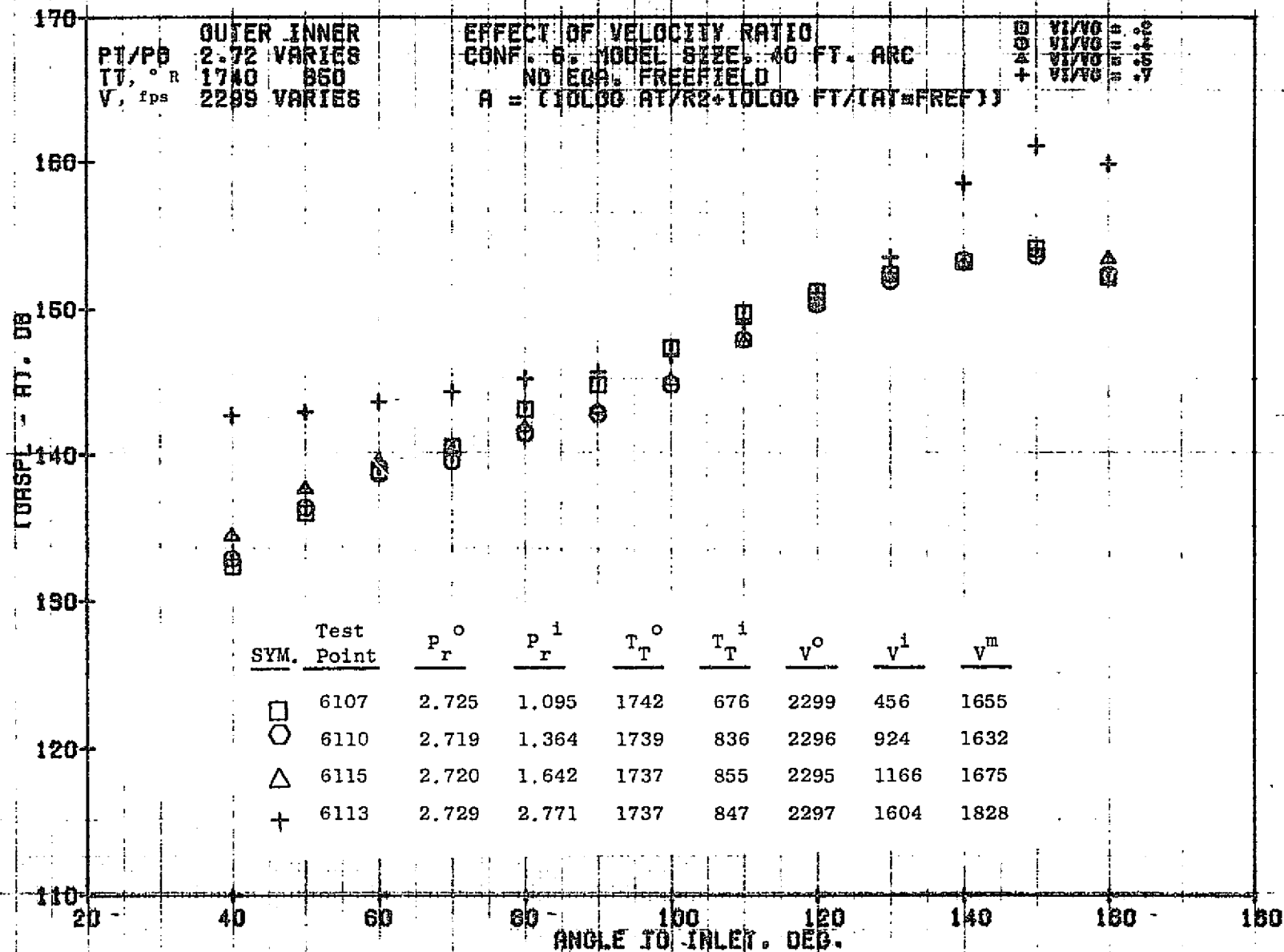
11/01/76
18391-001

79 BURCH A.



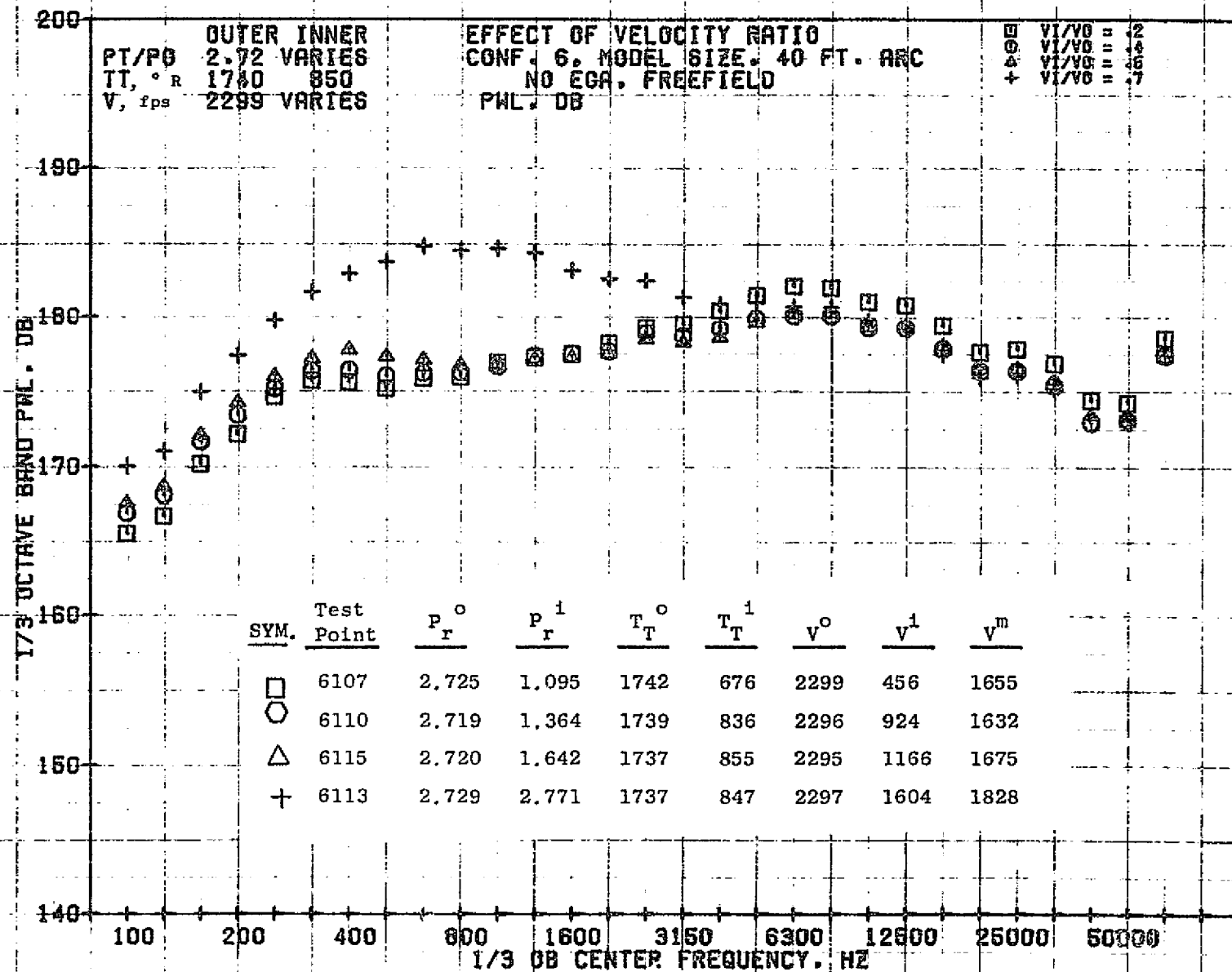






11/09/76
1R443-001

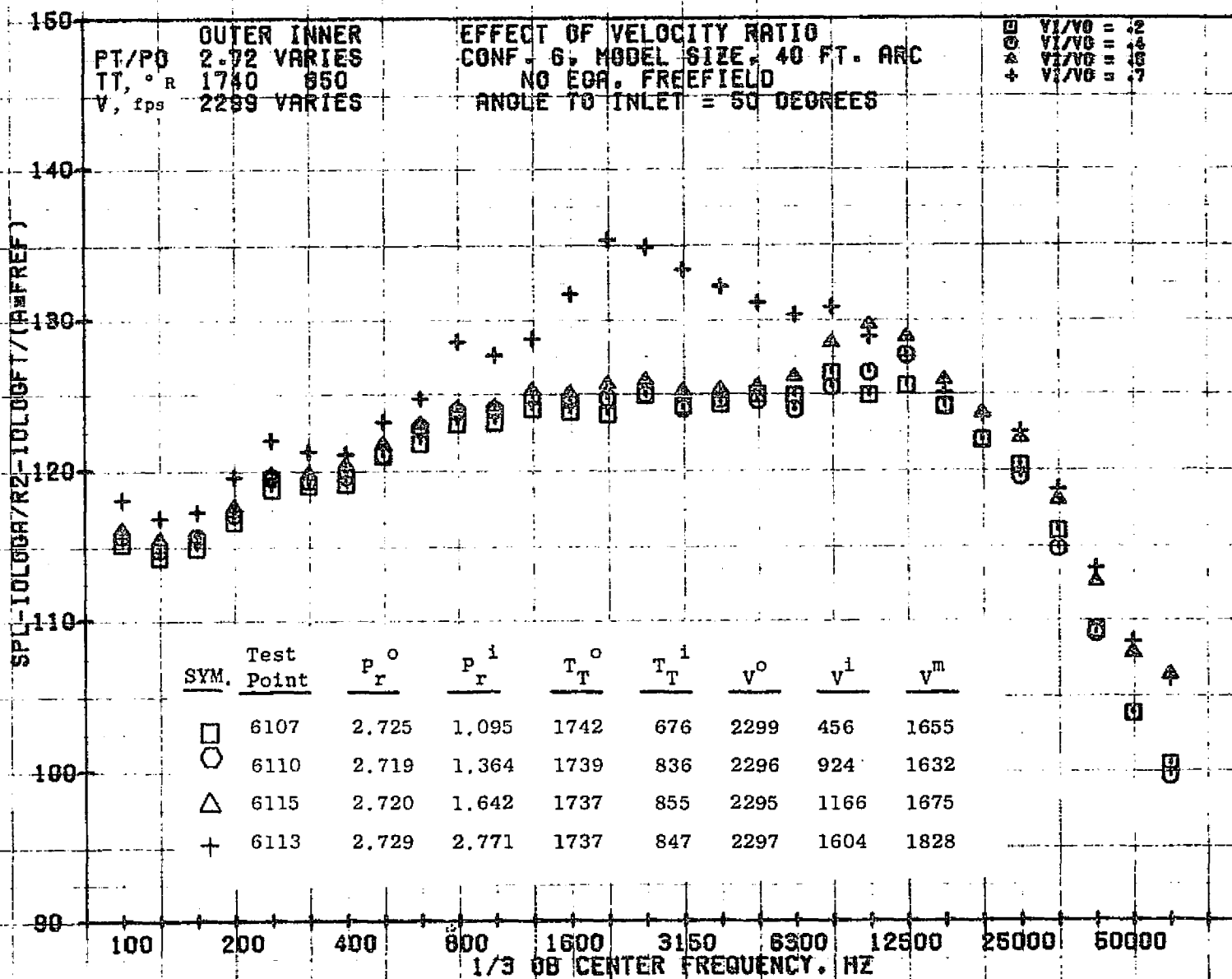
79 AIRCRAFT



11/01/76
18391-001

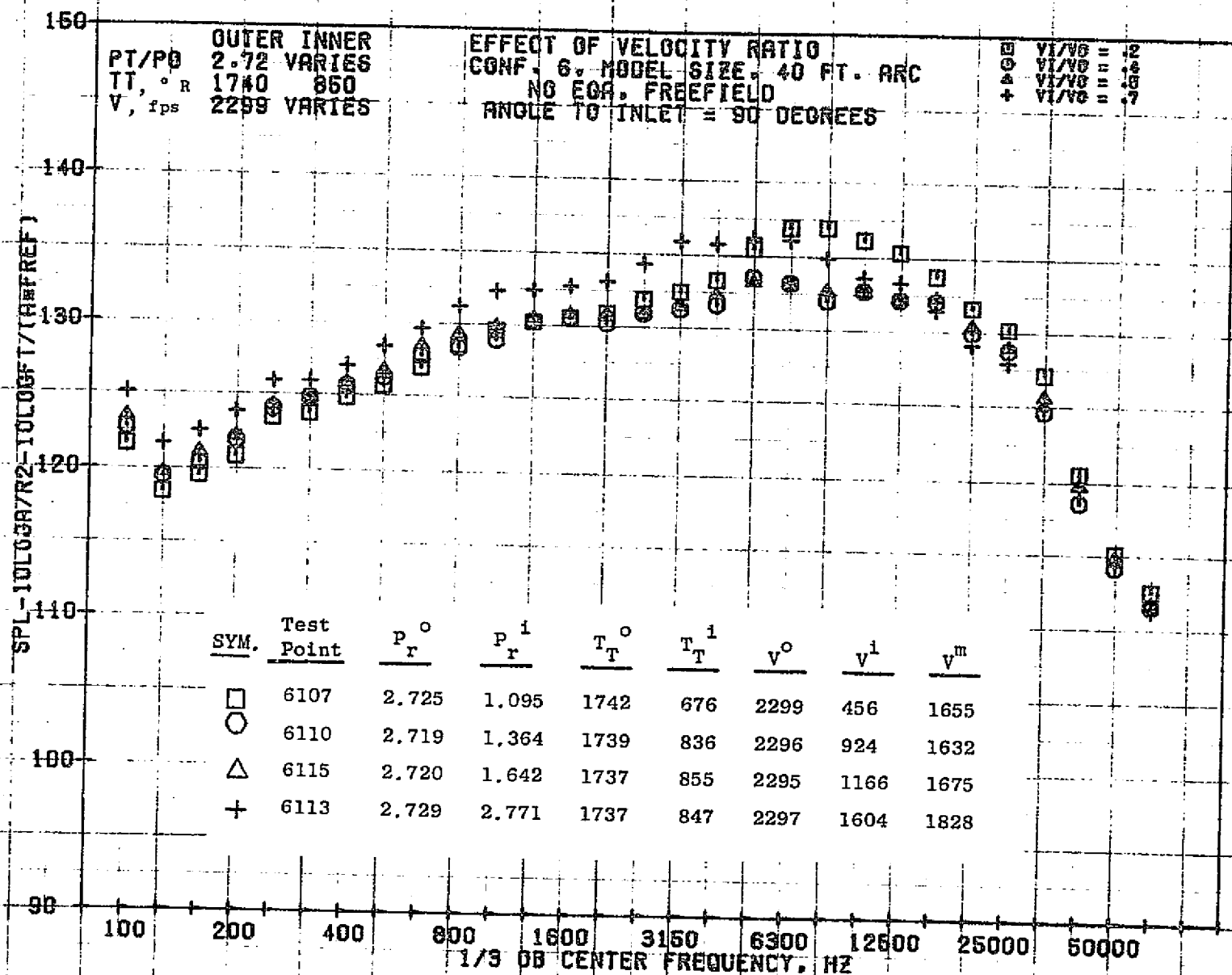
79 BURCH A.

1144



11/01/76
18391-001

79 BURCH A.

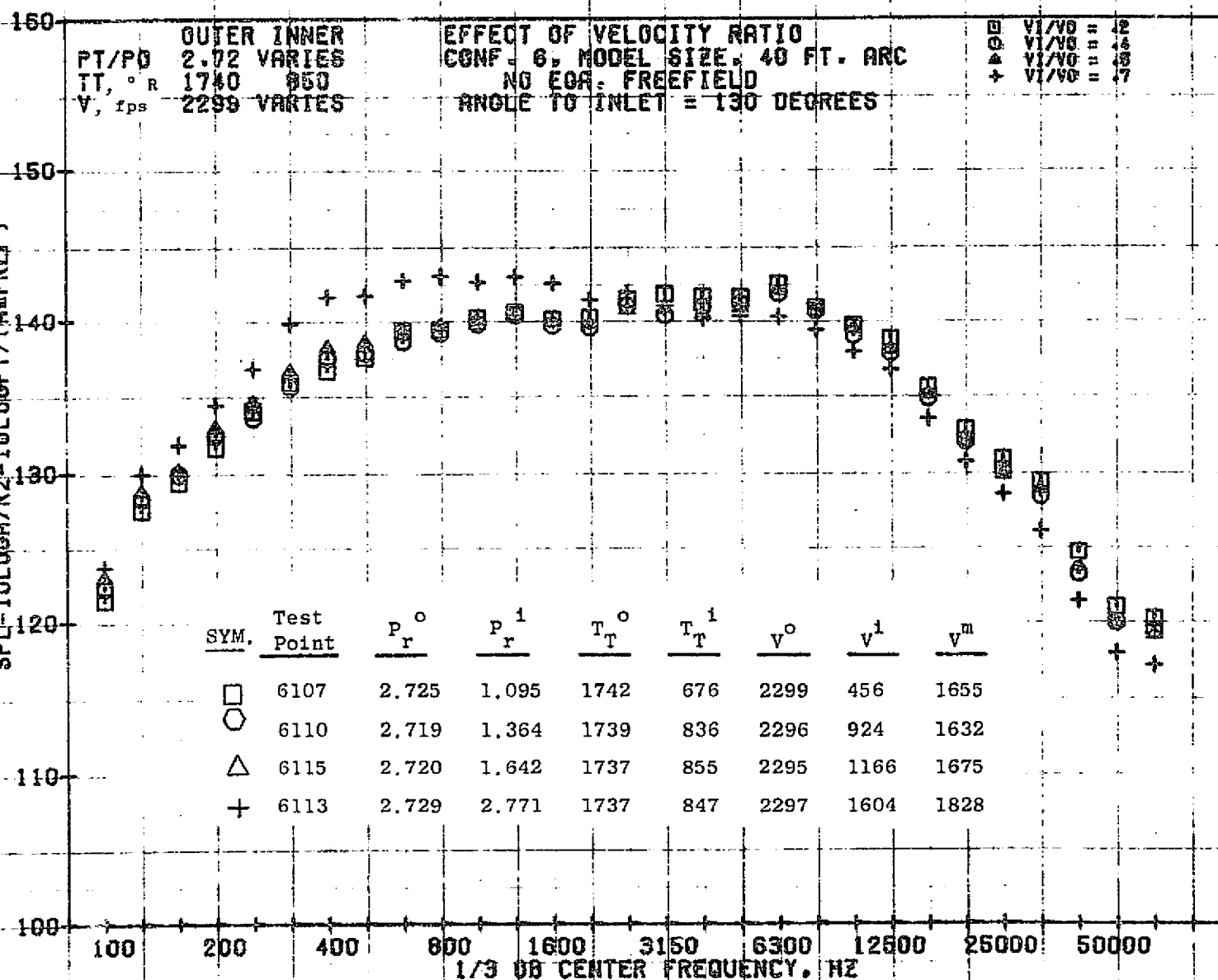


11/01/76
18391-001

79 BURCH A.

1146

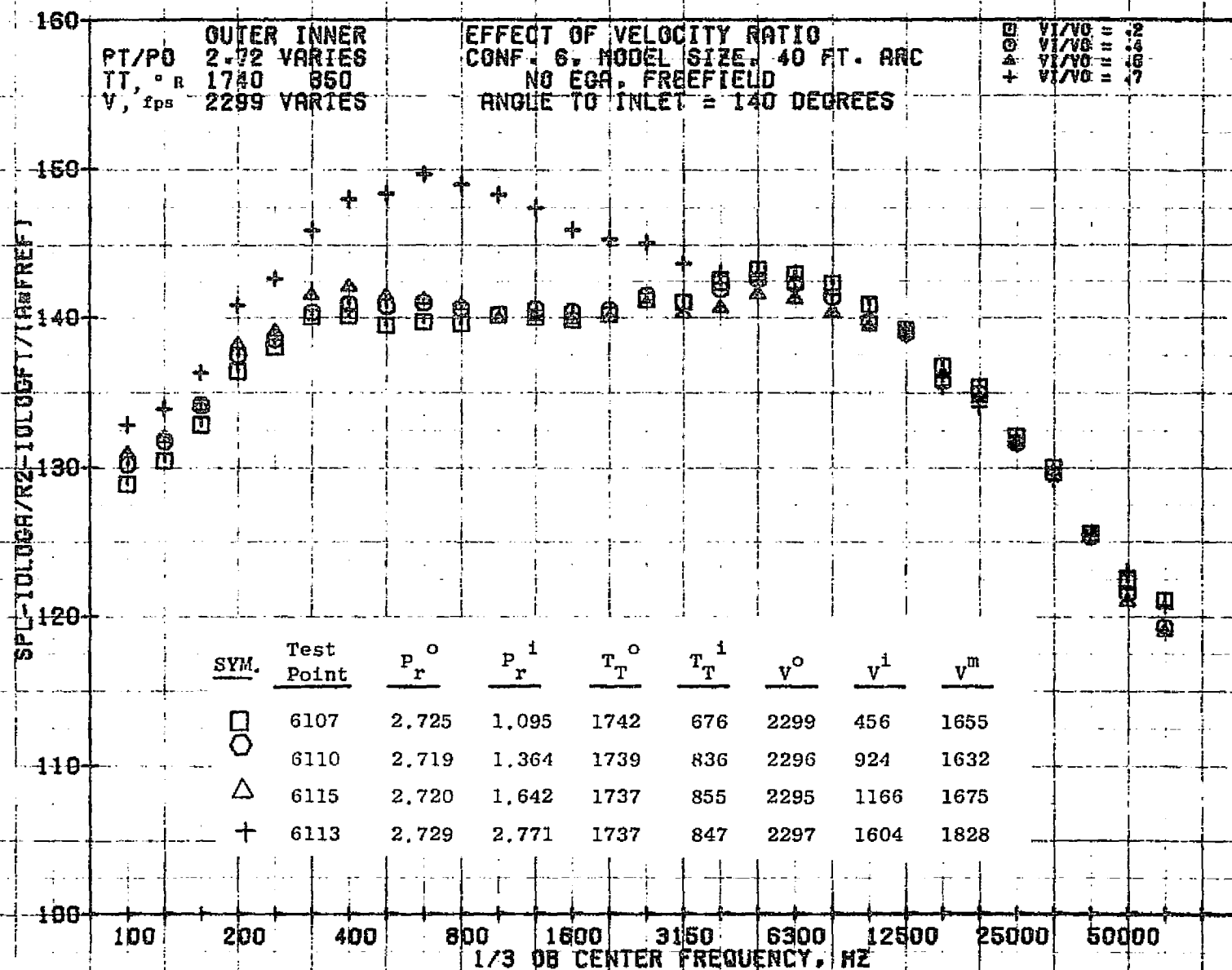
SPL-10LOGR/RZ-10LOGFT/(REF F)



11/01/76
18391-001

79 BURCH A.

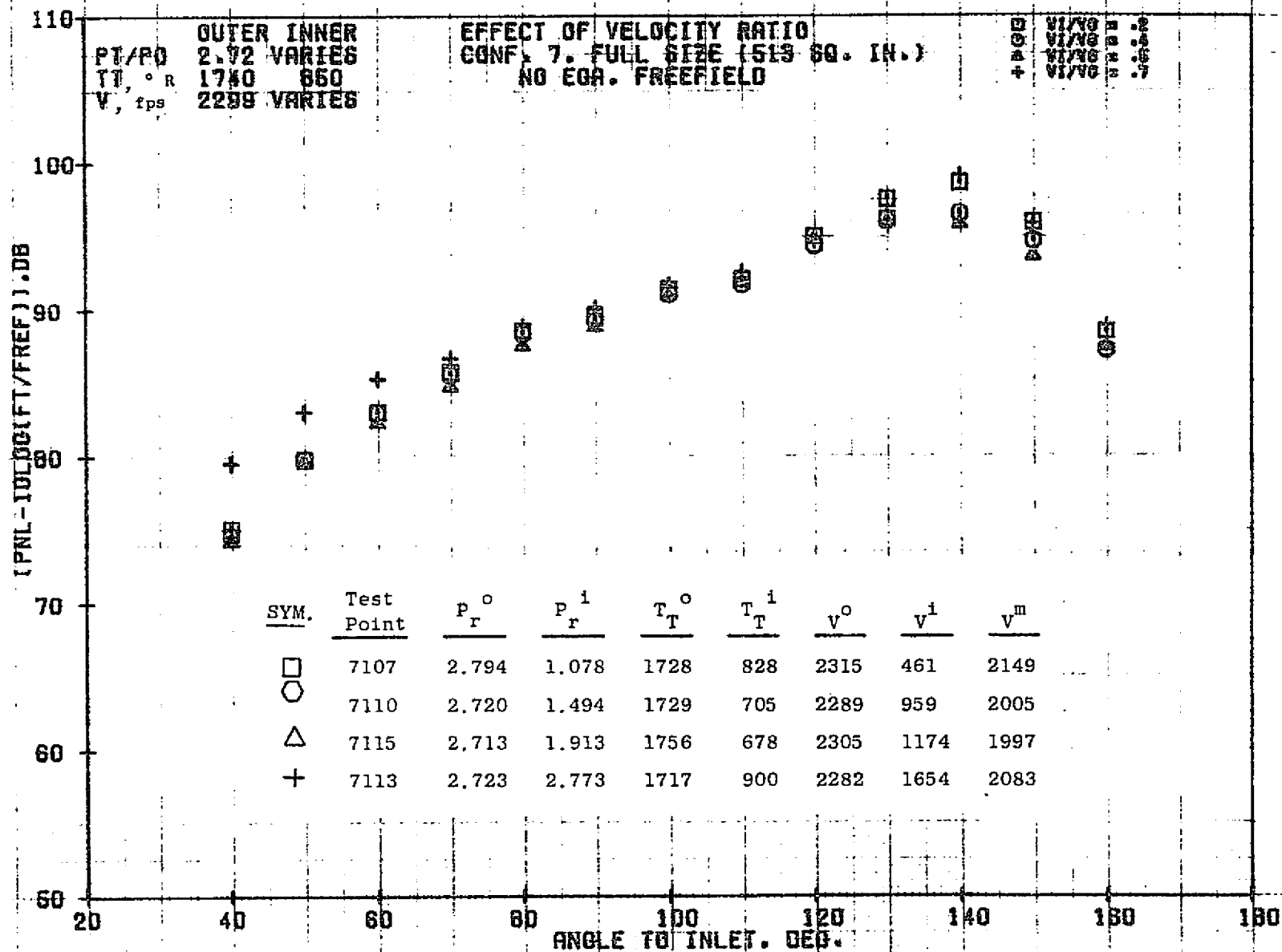
1147



11/01/76
18391-001

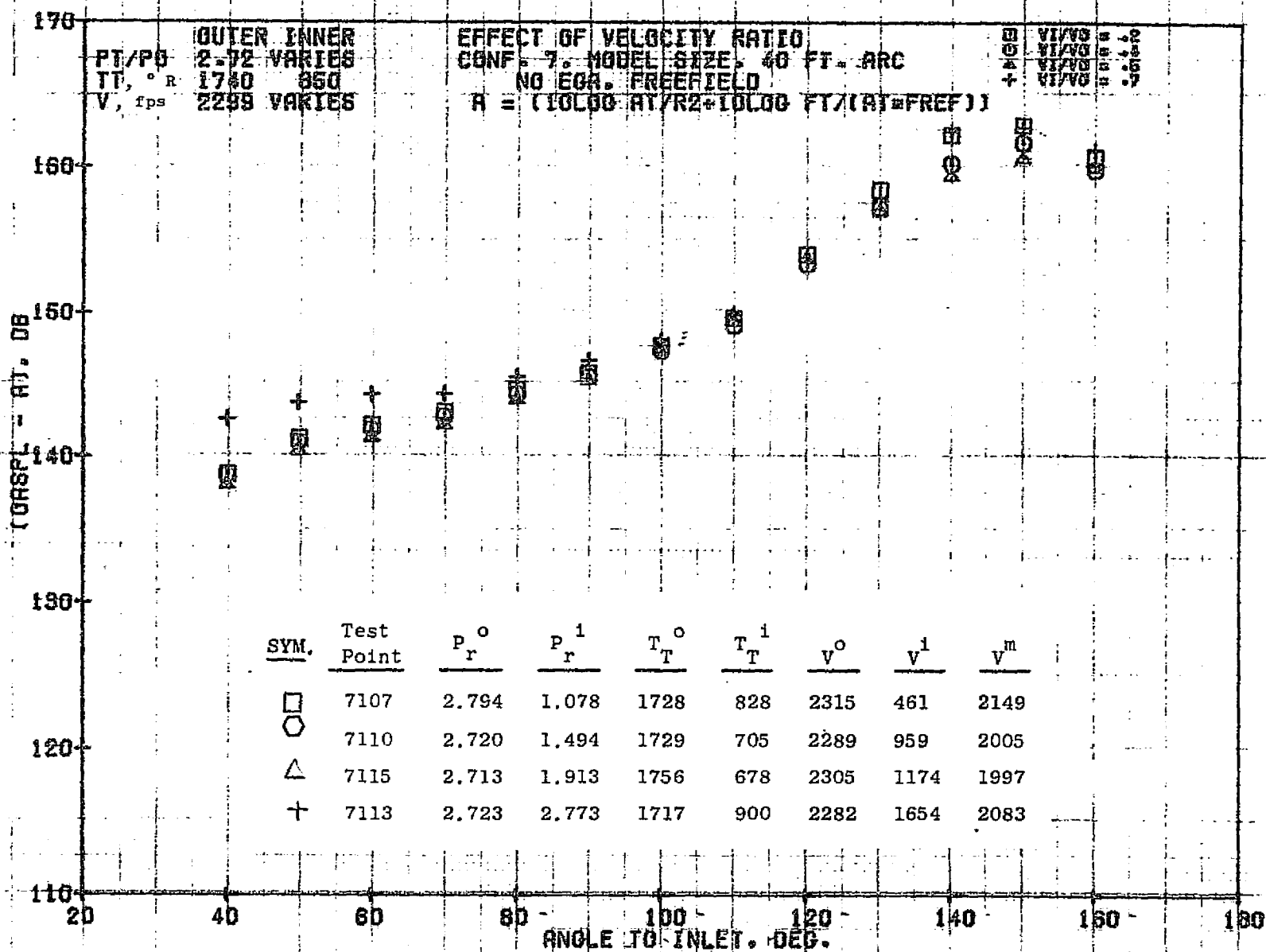
79 BURCH A.

1148



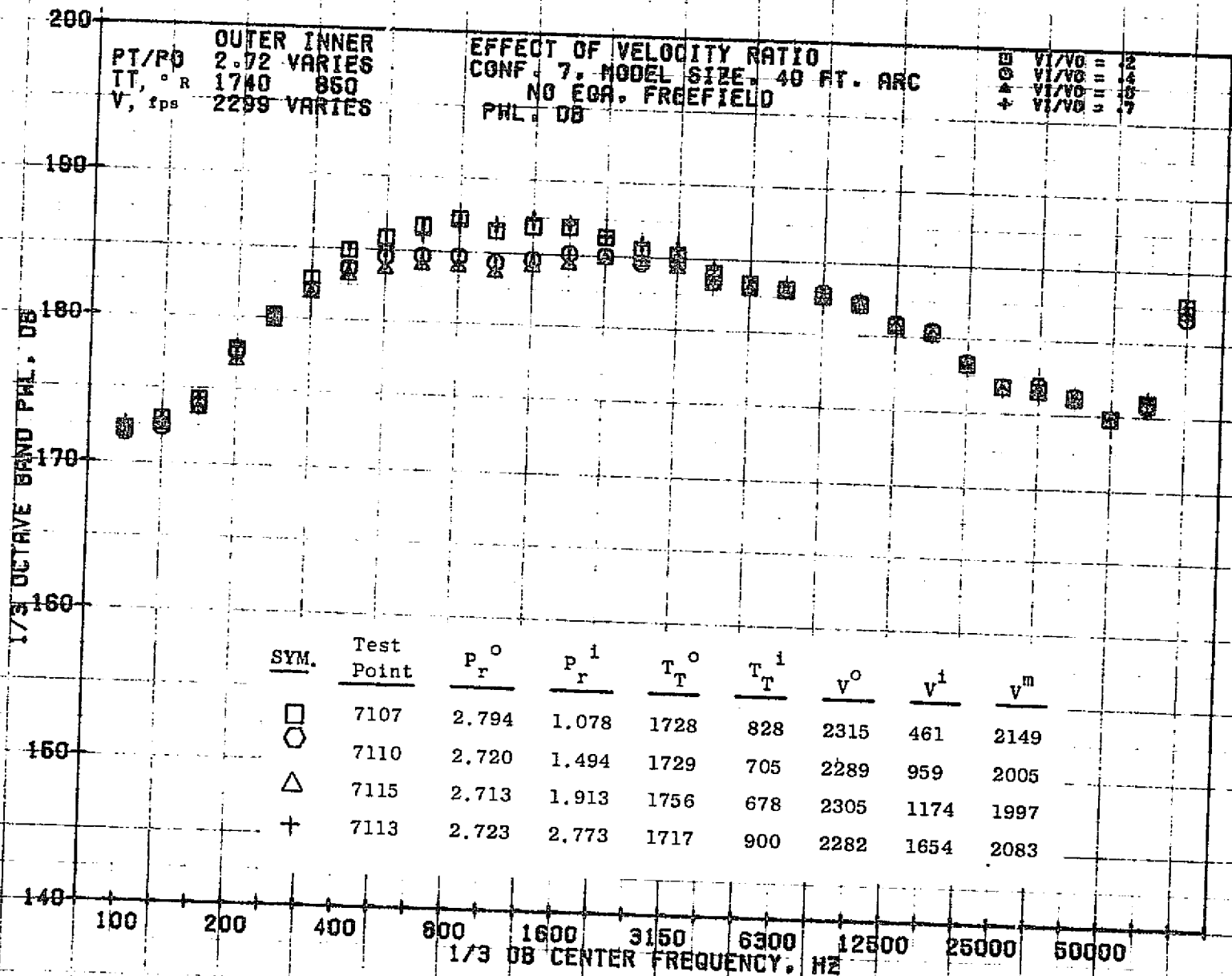
11/01/76
18421-001

79 BURCH A.



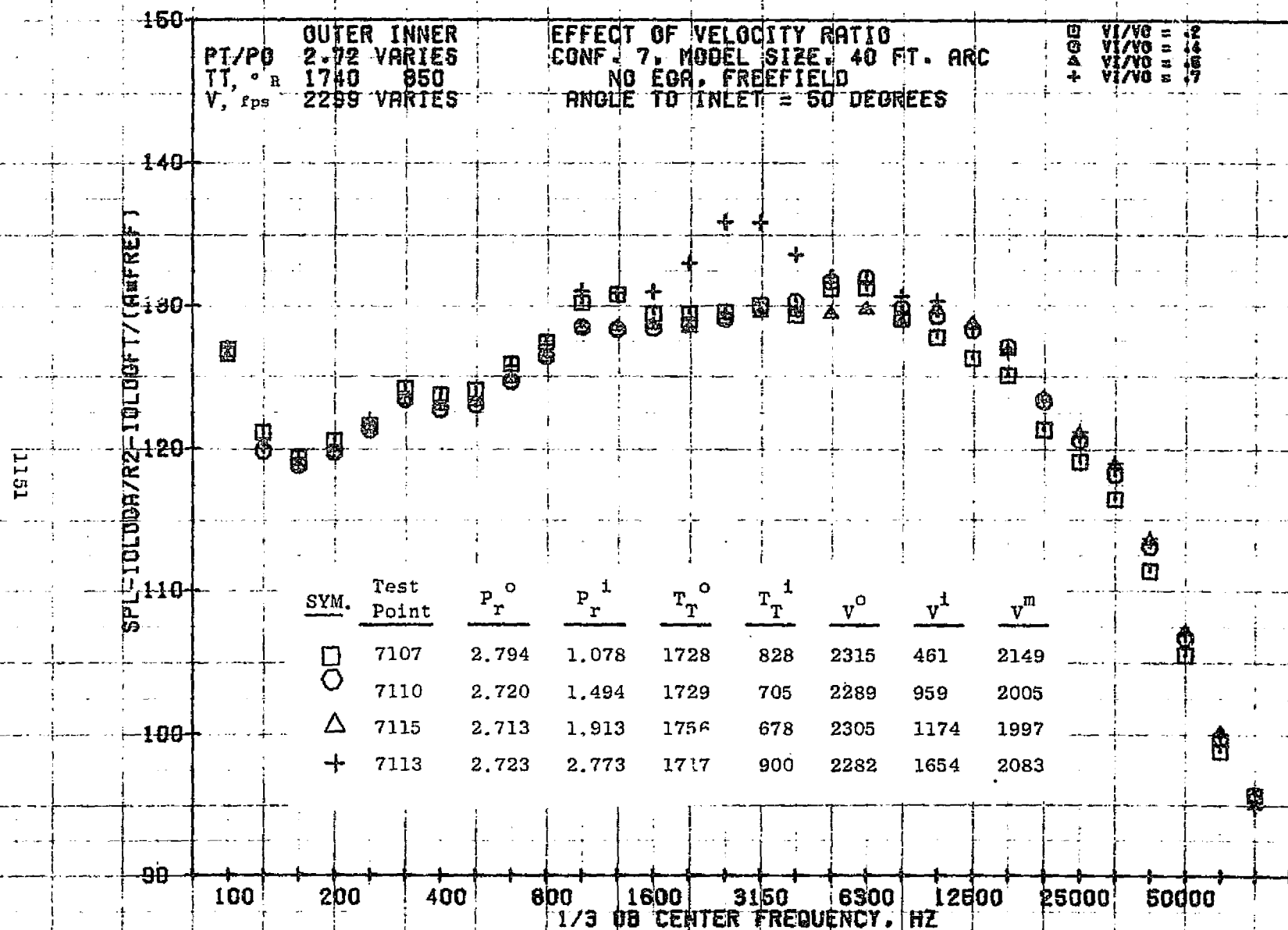
11/09/76
18343-001

79 BURCH D.



11/01/76
18391-001

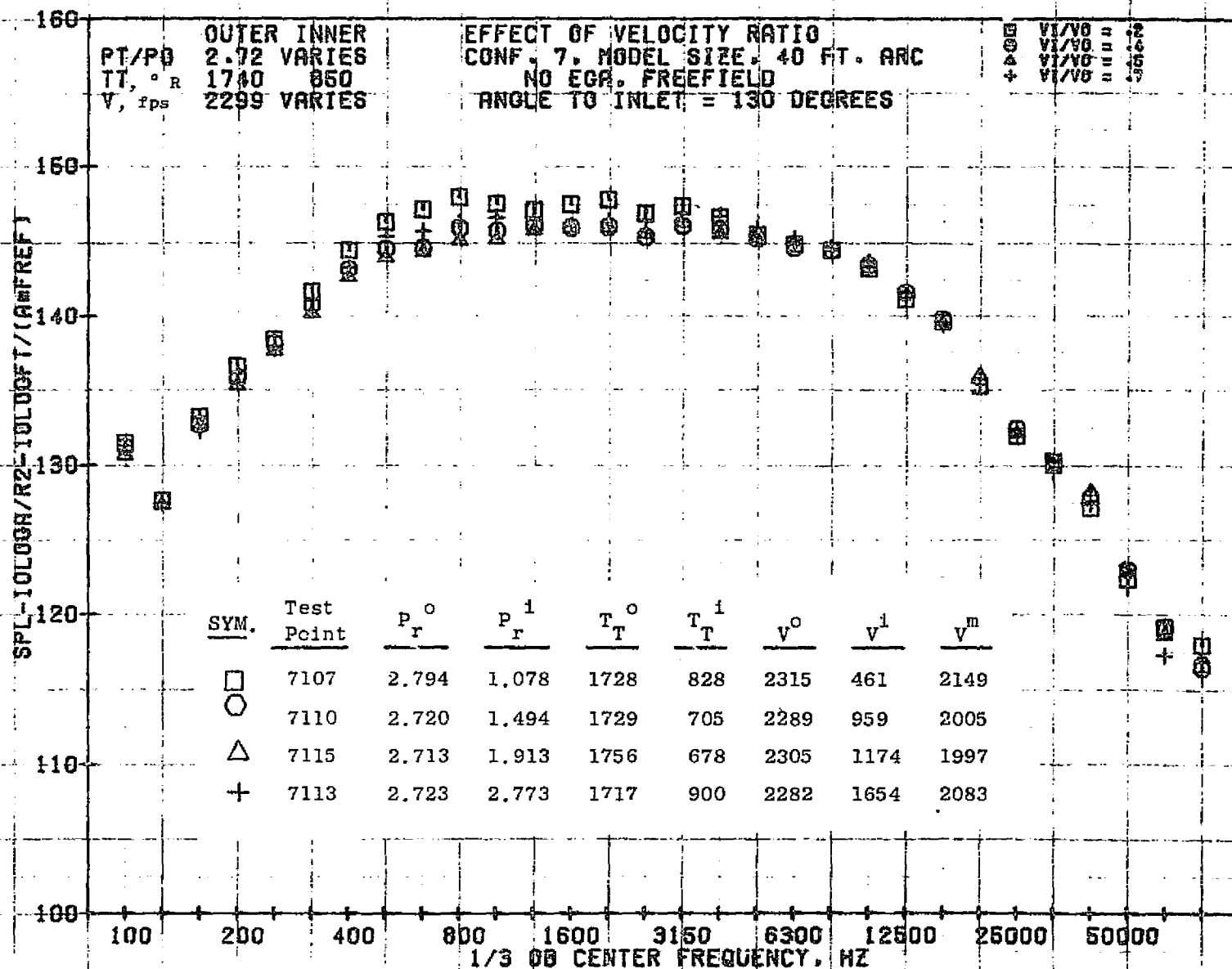
79 BURCH A.



11/01/76
18391-001

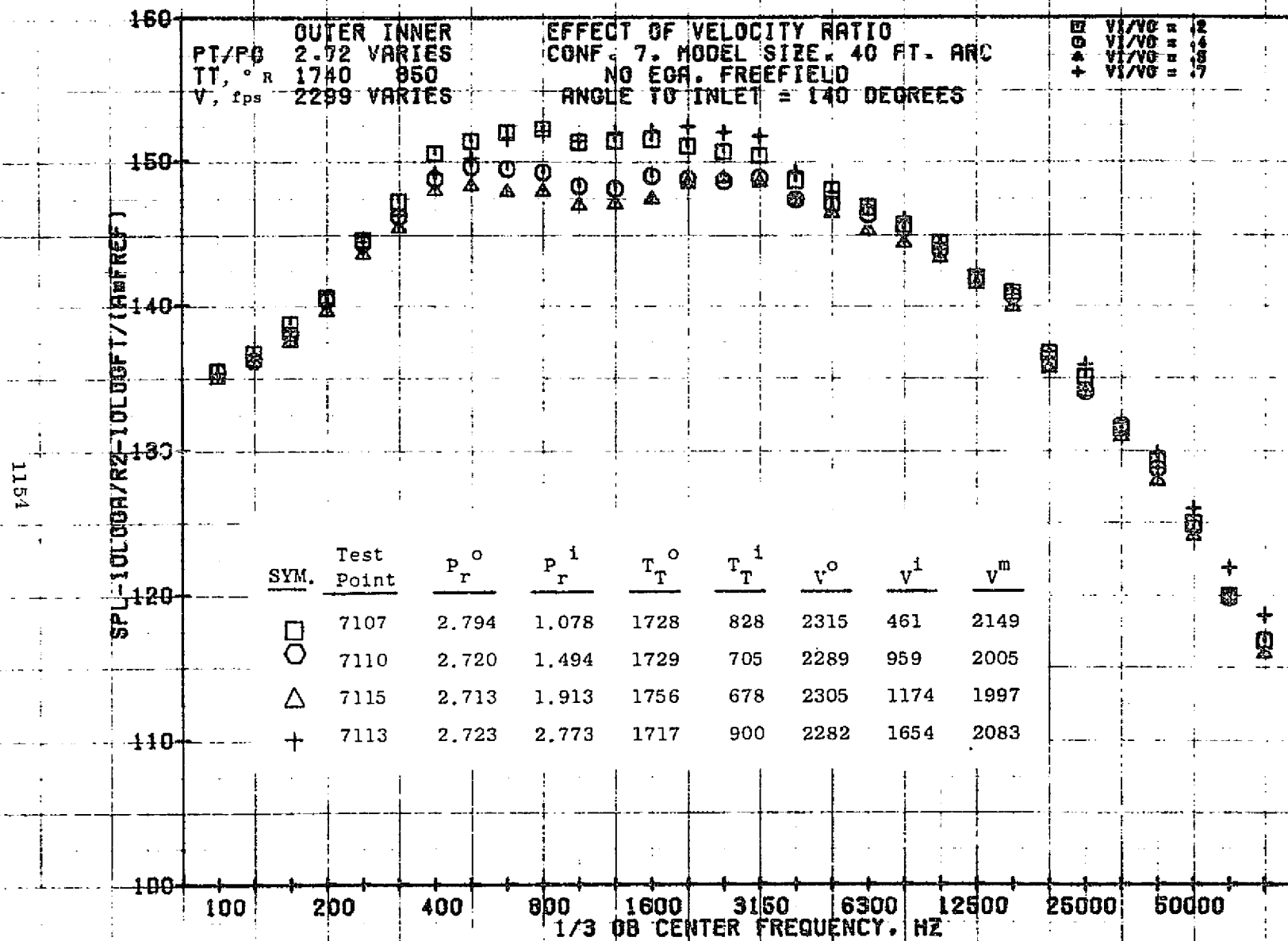
79 BURCH A.

1153



11/01/76
19391-001

79 BURCH A.

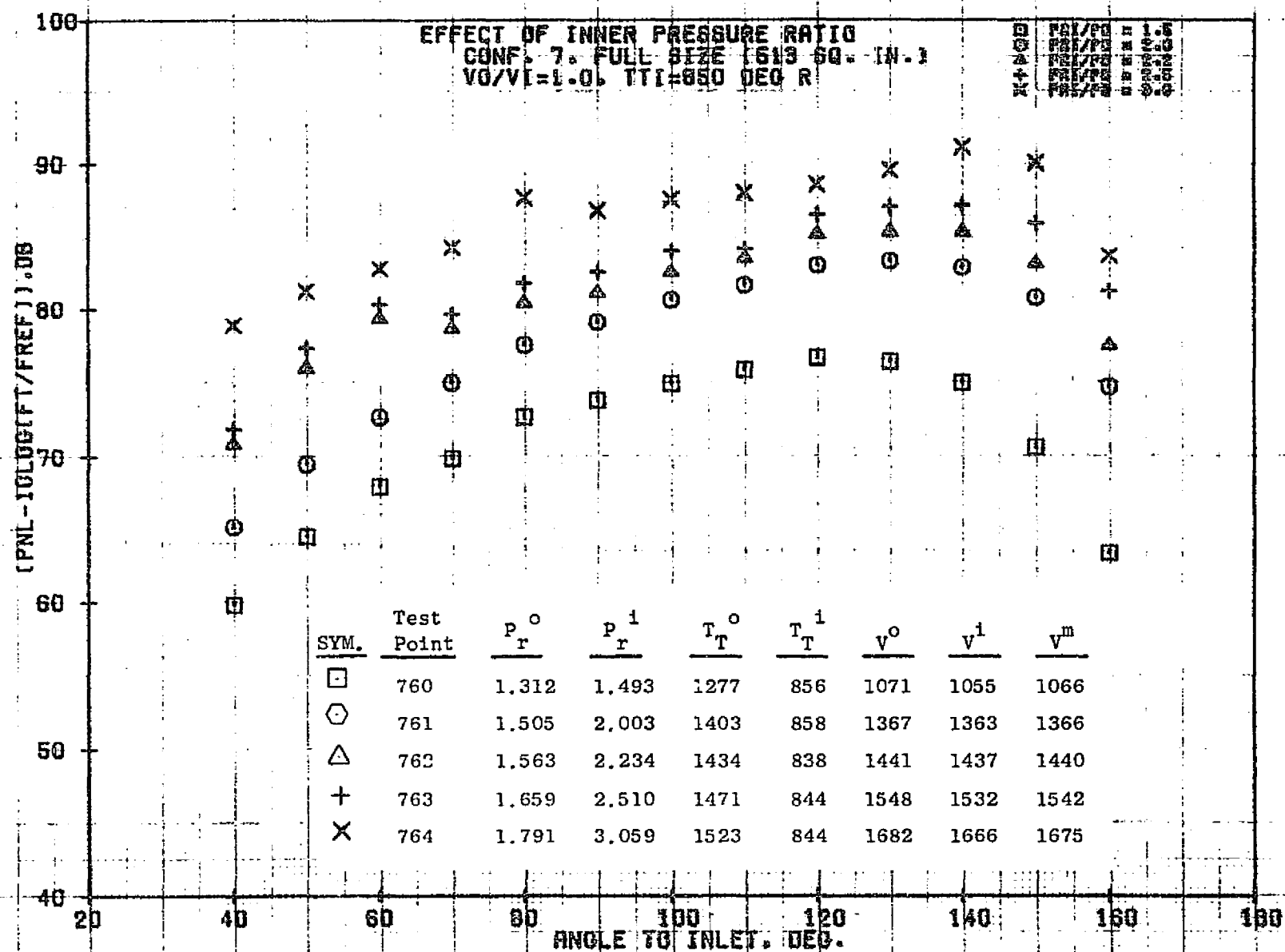


11/01/76
18391-001

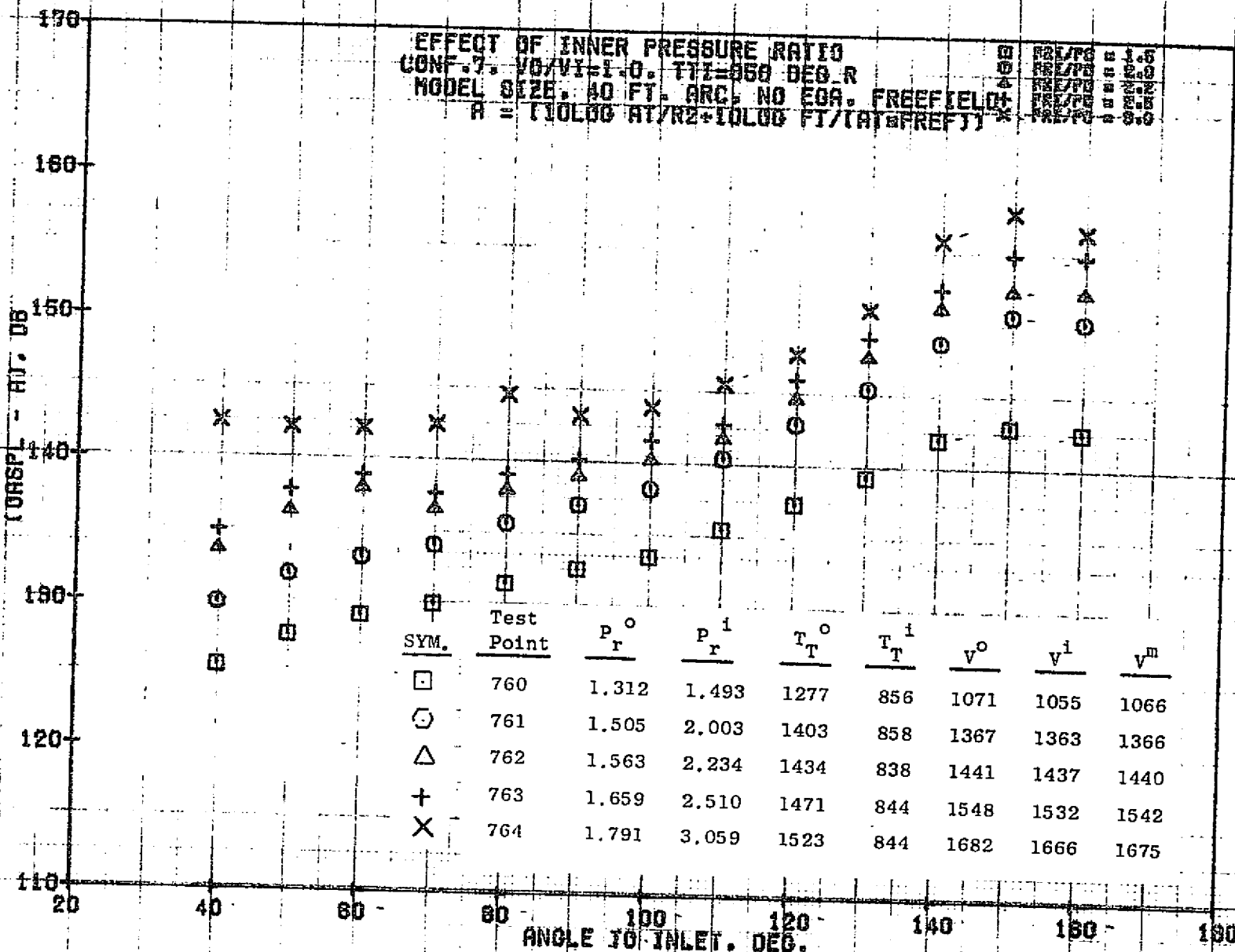
79 BURCH A.

7.4.5 Effect of Inner Pressure Ratio at Constant Velocity Ratio

For Configuration 7, a test series was run in which the velocity ratio was held constant at different levels and the inner pressure ratio was varied. The results are shown in this section.



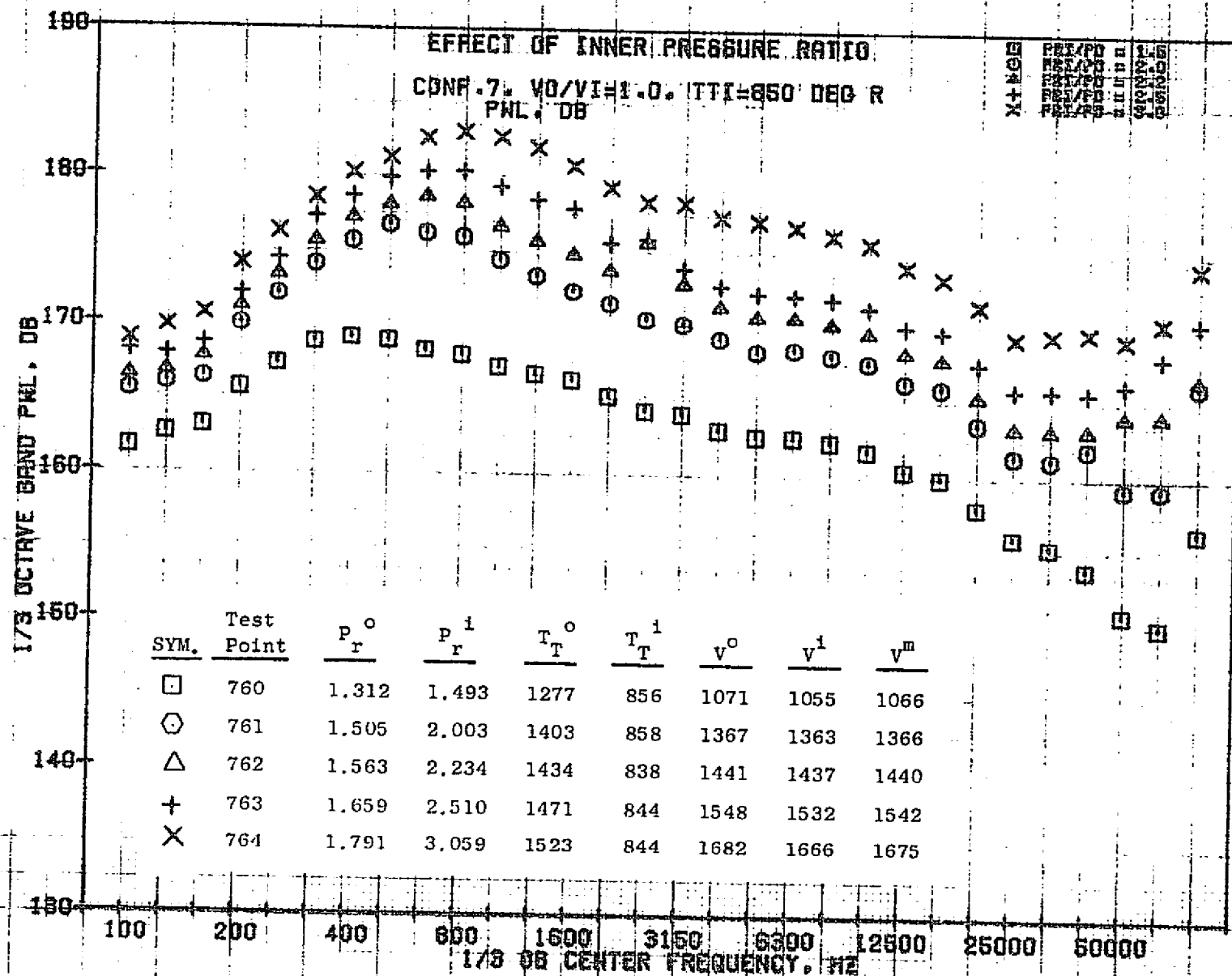
1157



11/09/76
18336-001

79 AIRCRAFT

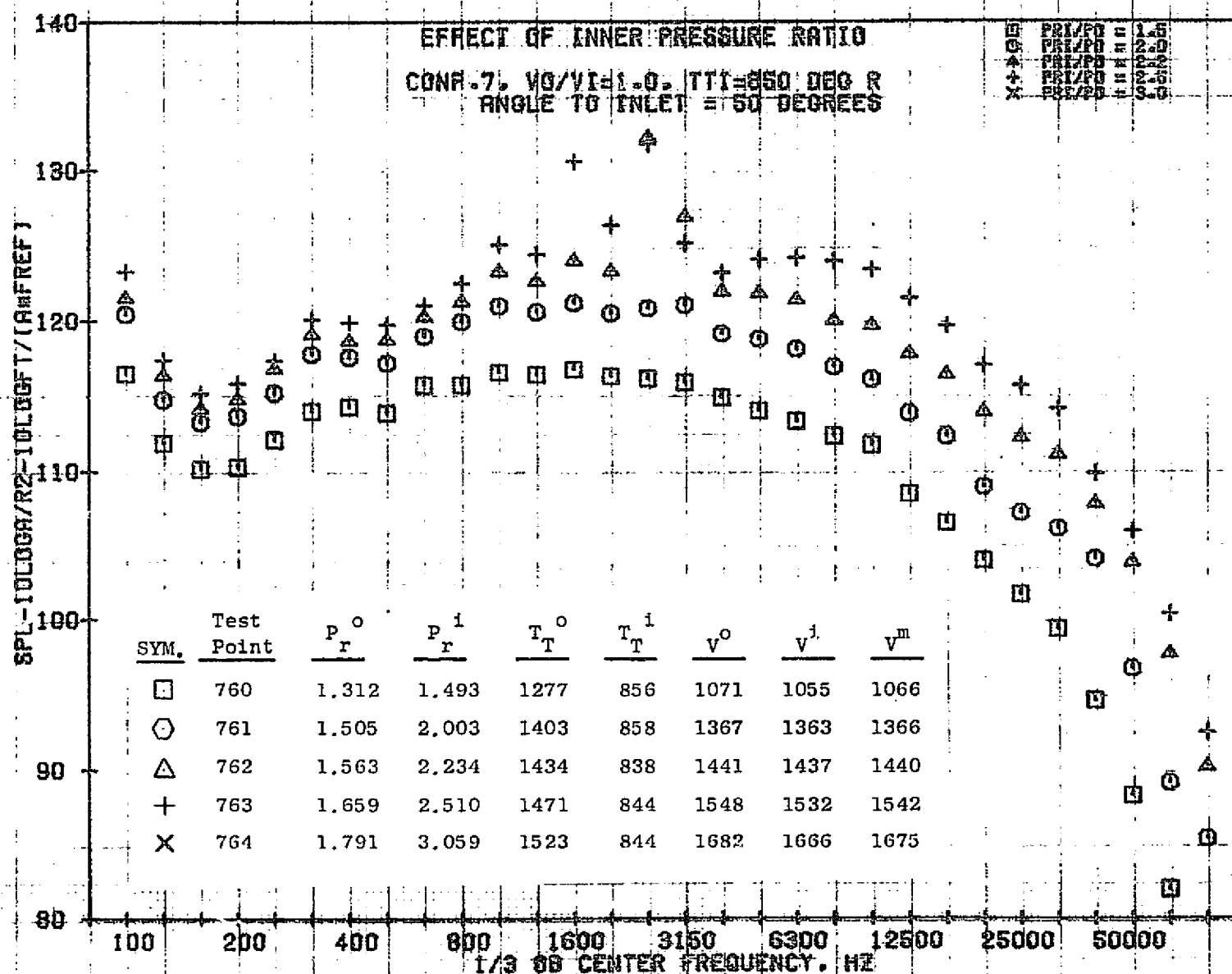
1158



11/03/76
 18575-001

79 BURCH A.

6971

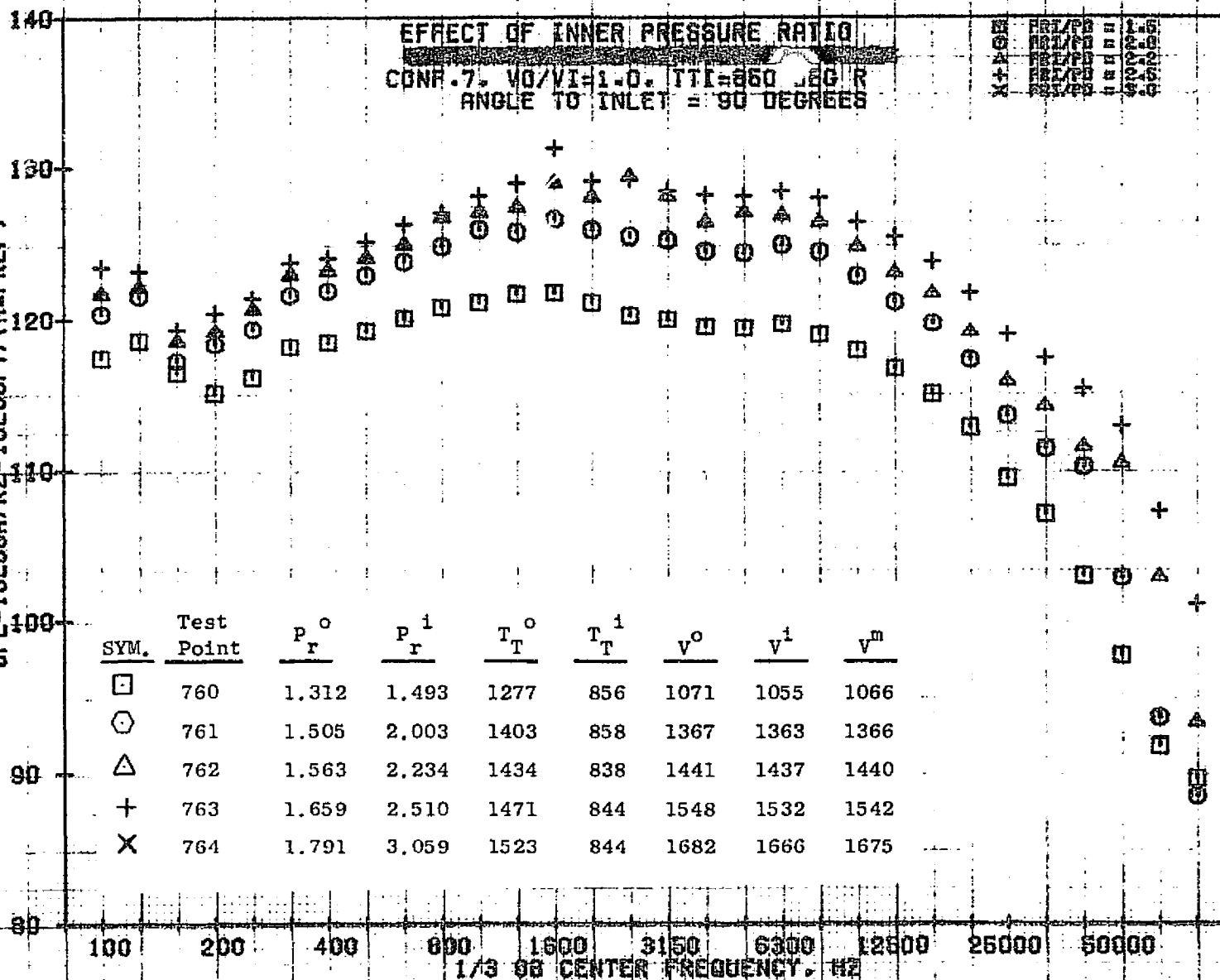


11/03/76
18575-001

79 BURCH A.

09th

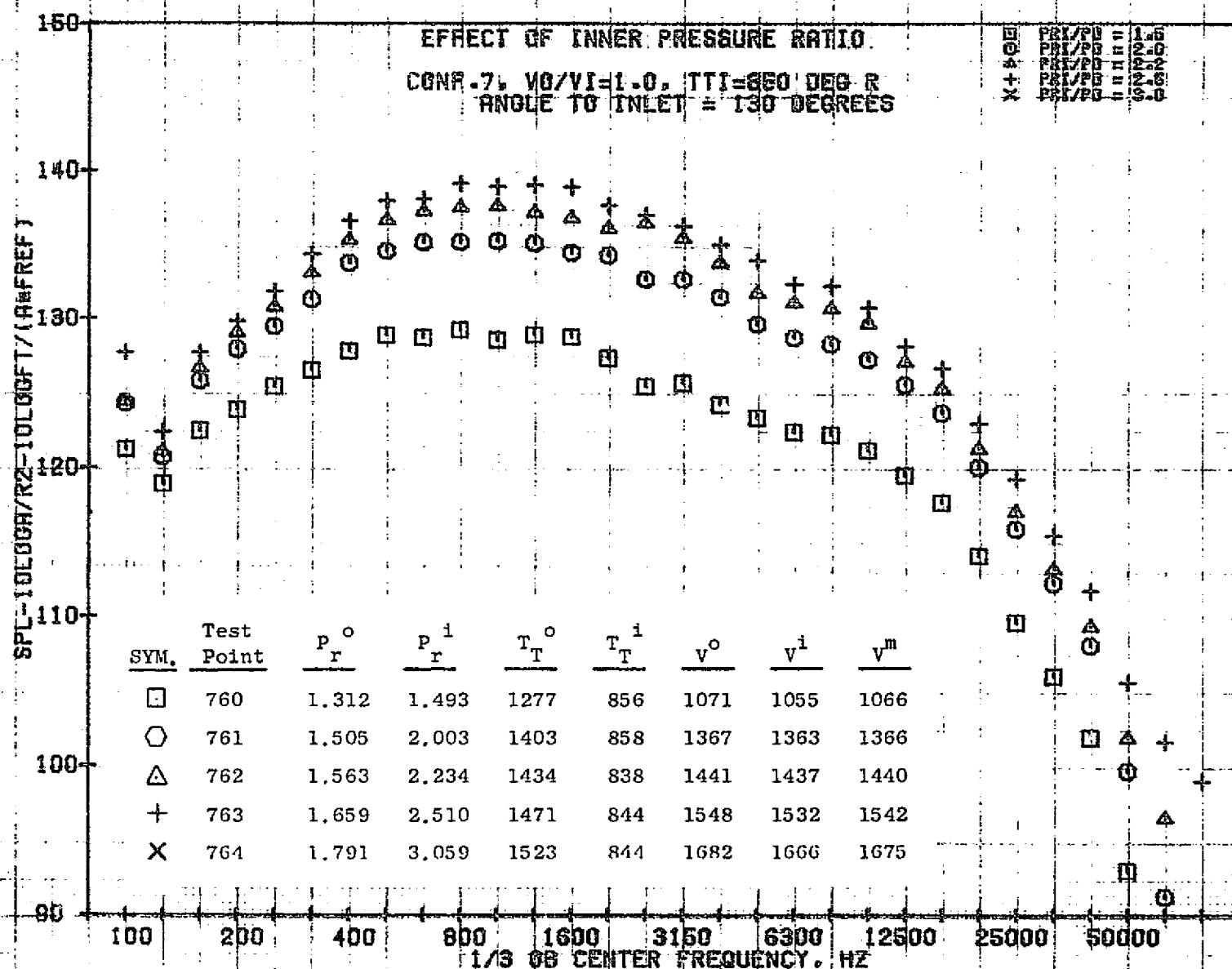
SPL-10L03H/R2-10L03FT/(HREF)



11/03/76
 18675-001

79 BURCH A.

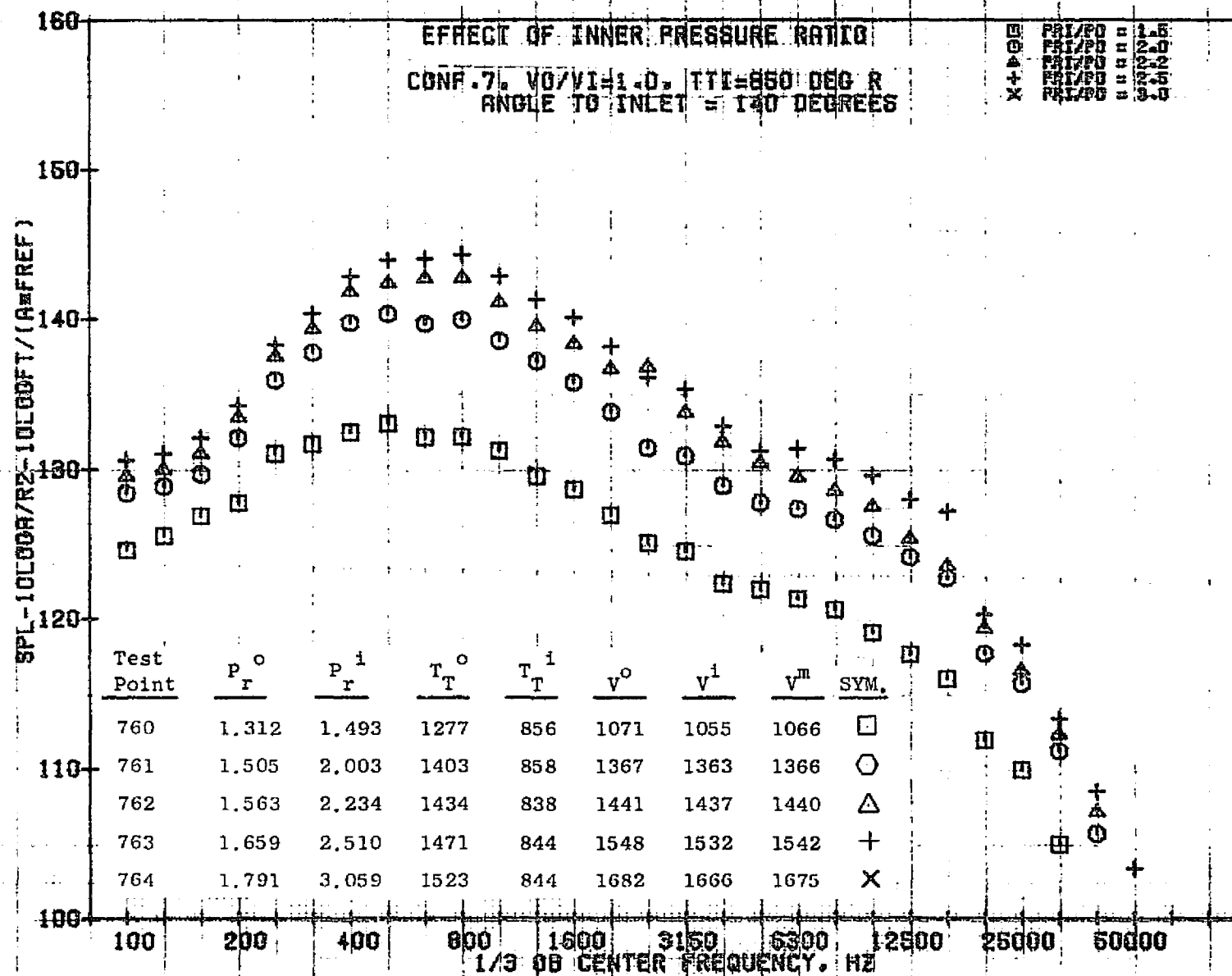
1161



11/03/76
1B575-001

79 BURCH A.

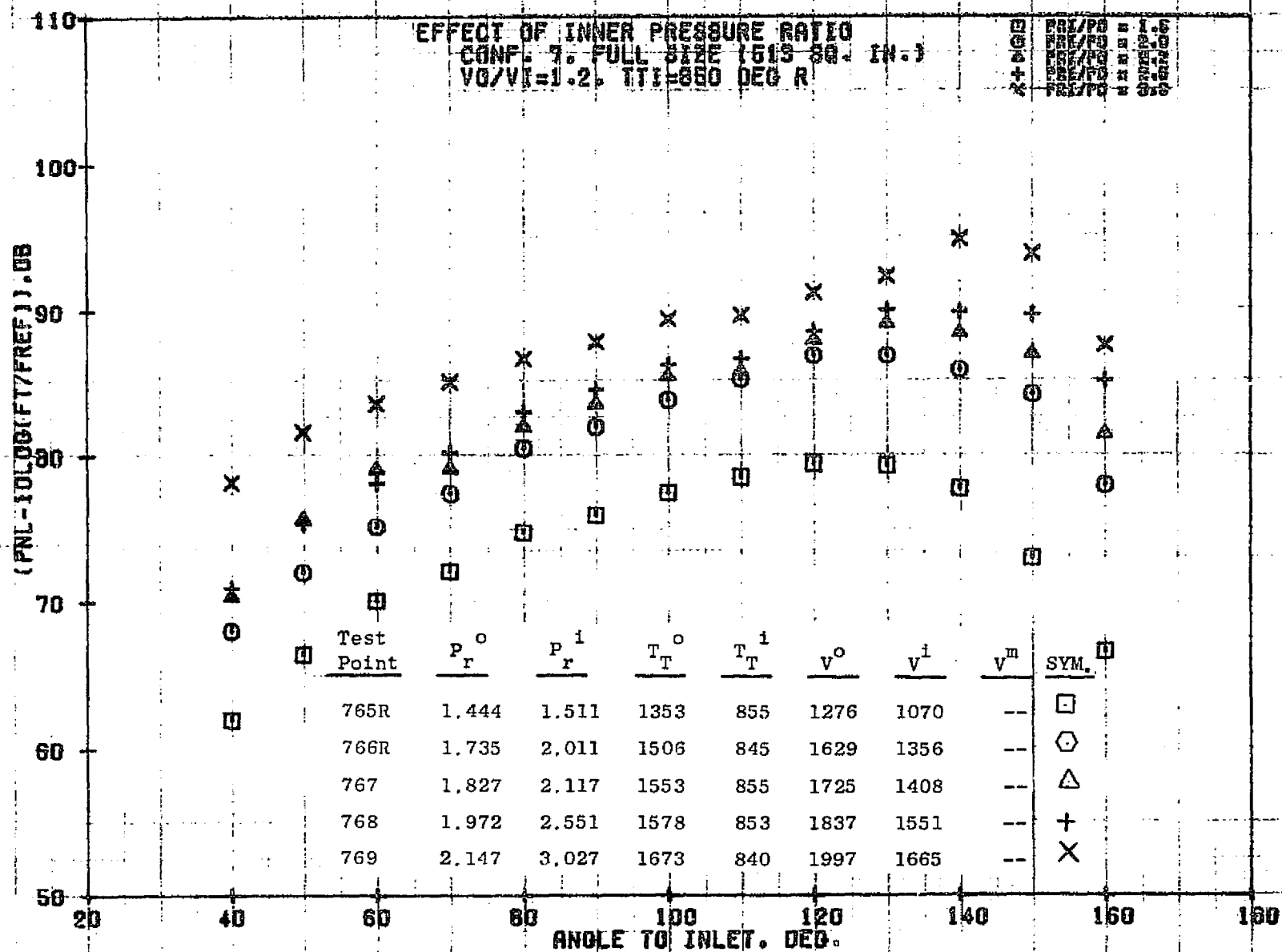
1162



11/03/76
18575-001

79 BURCH A.

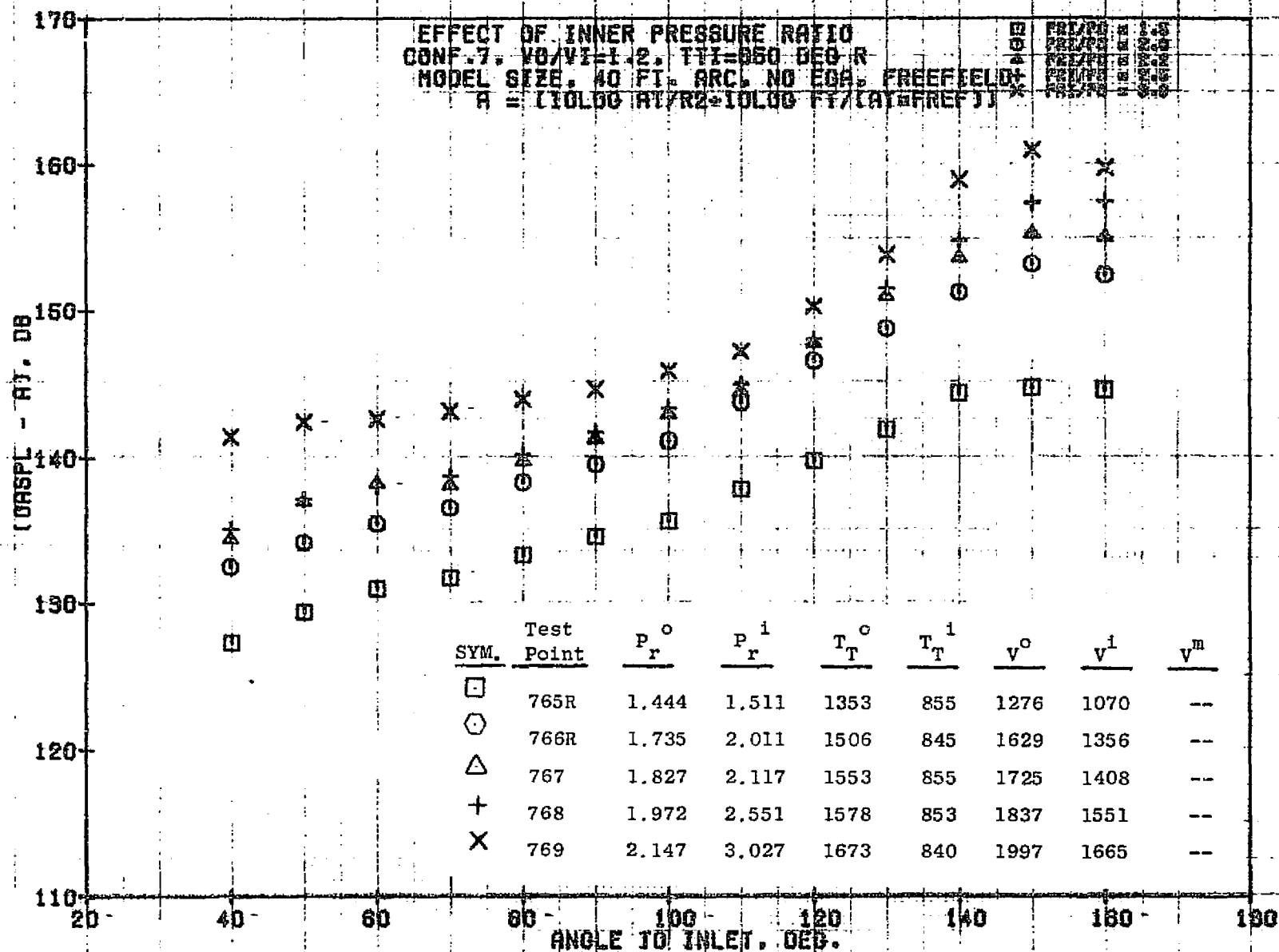
1163



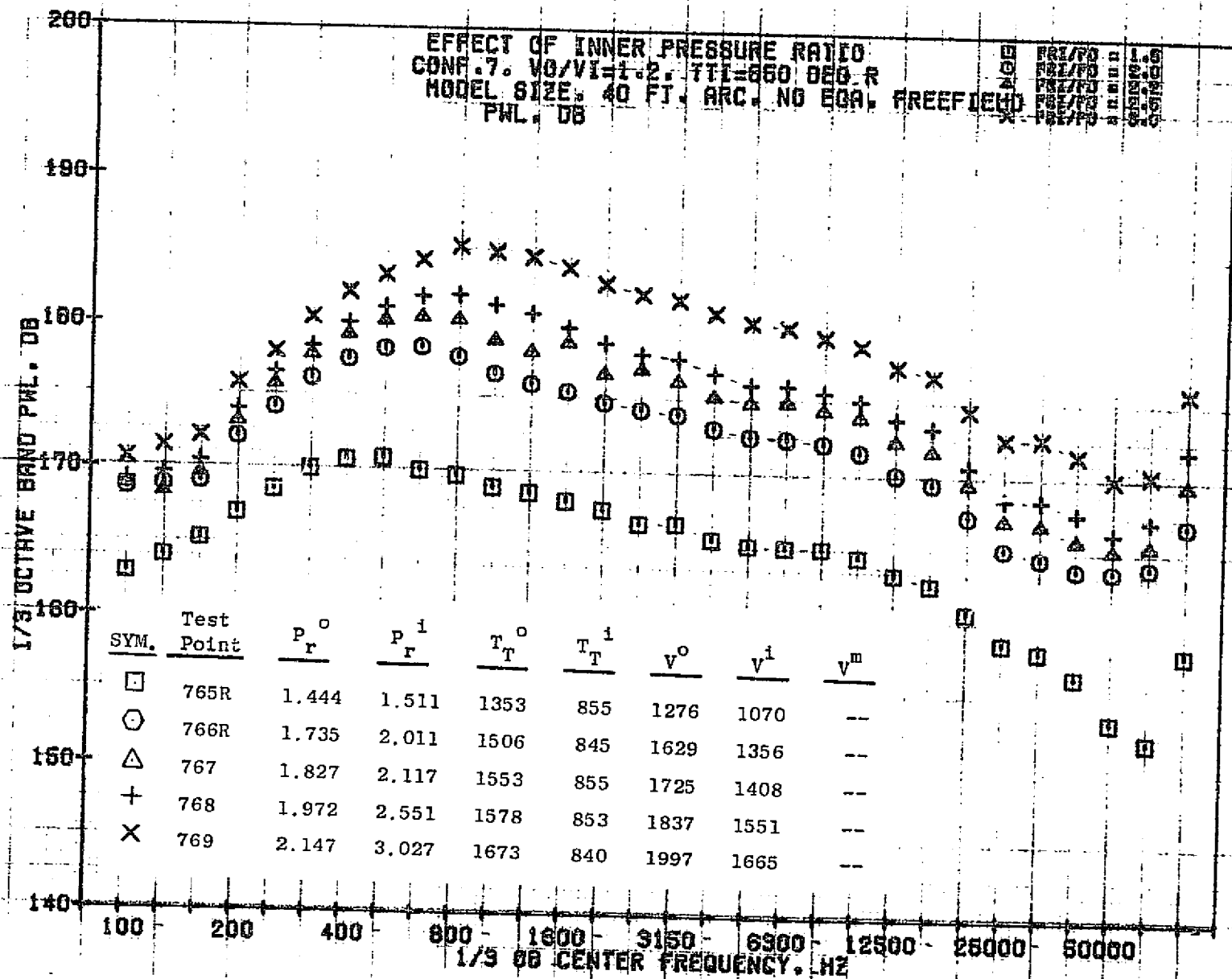
11/04/76
 18680-001

79 BURCH A.

1164

11/09/76
1A336-001

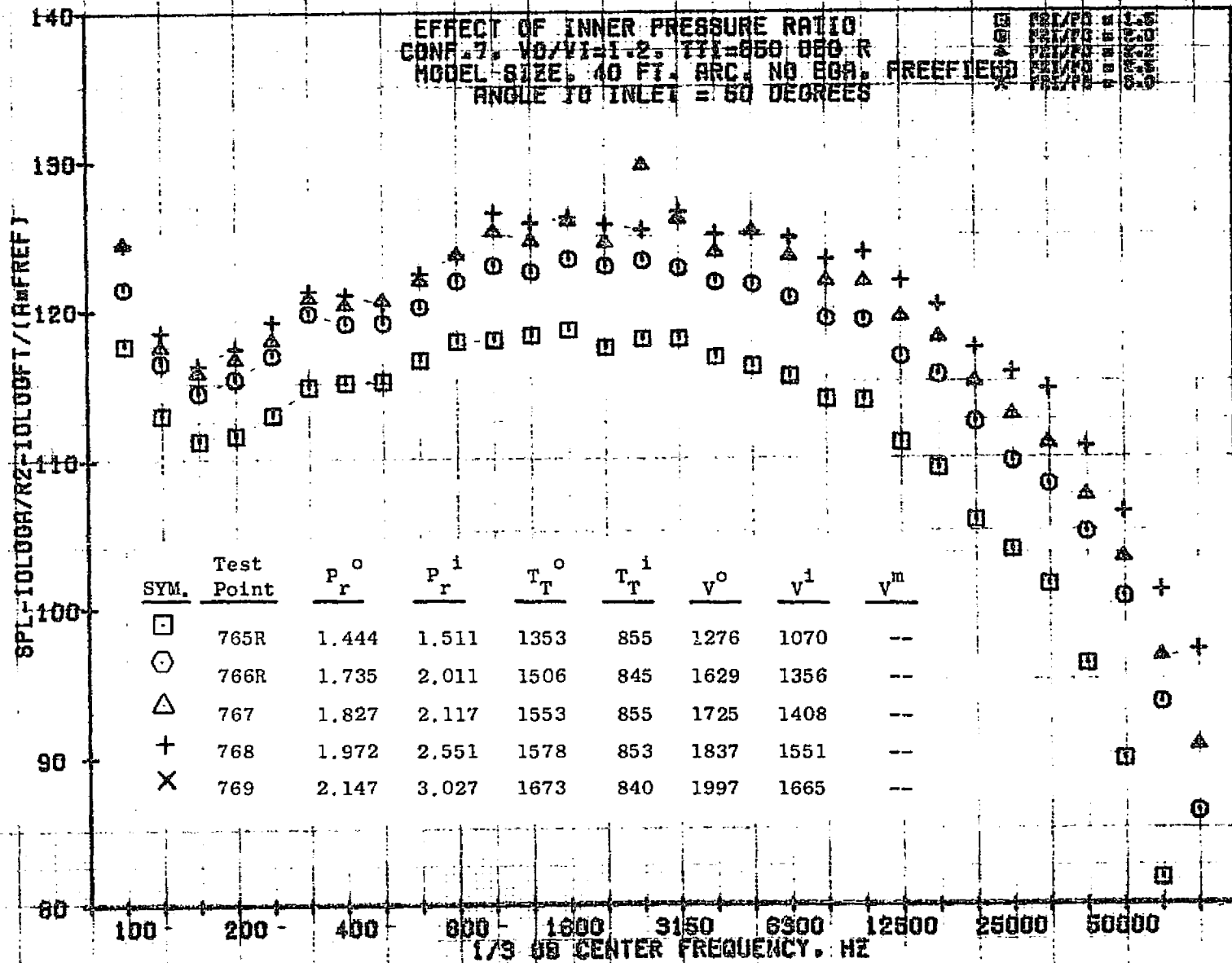
79 AIRCH A.



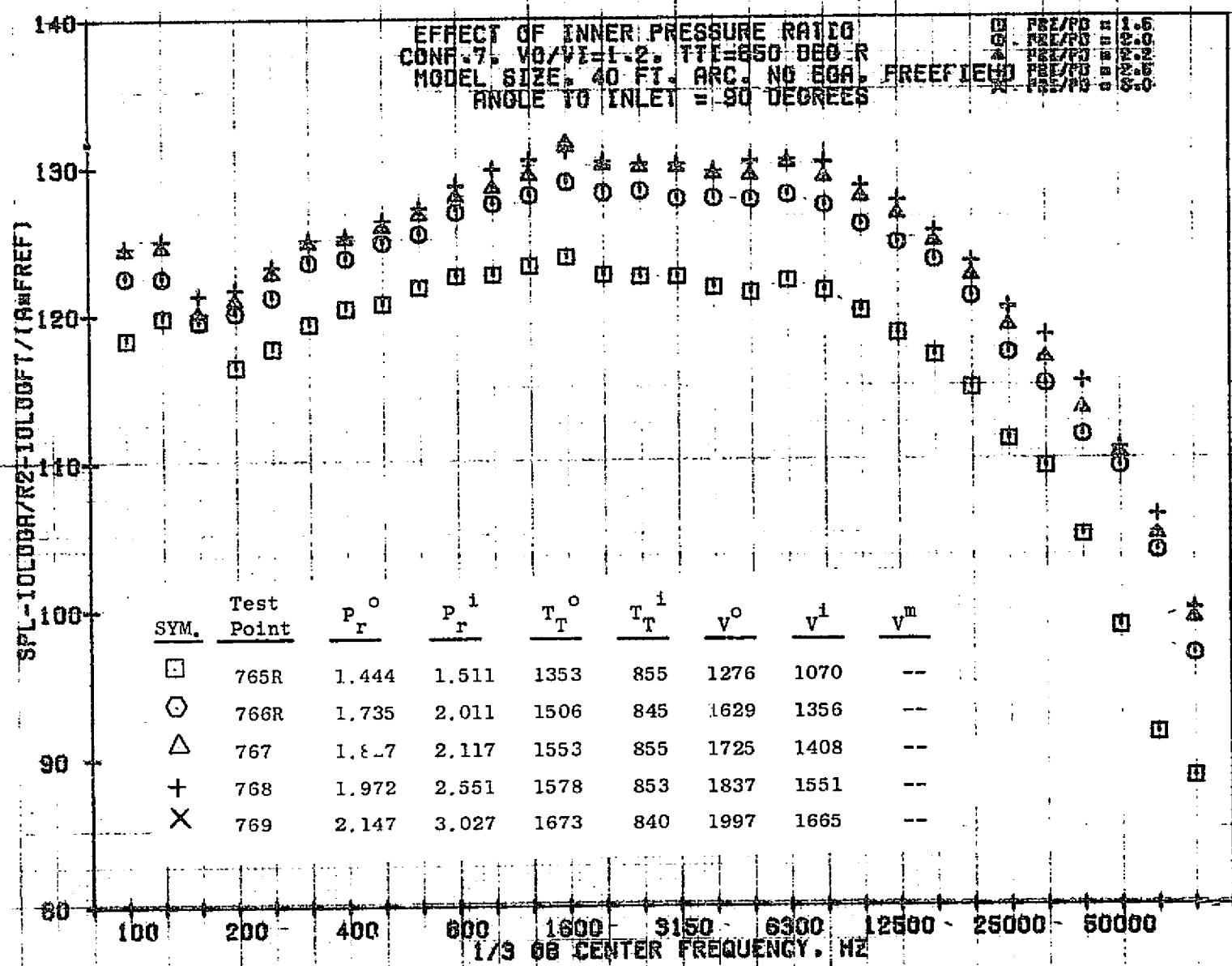
11/09/76
1R33A-001

79 BURCH R.

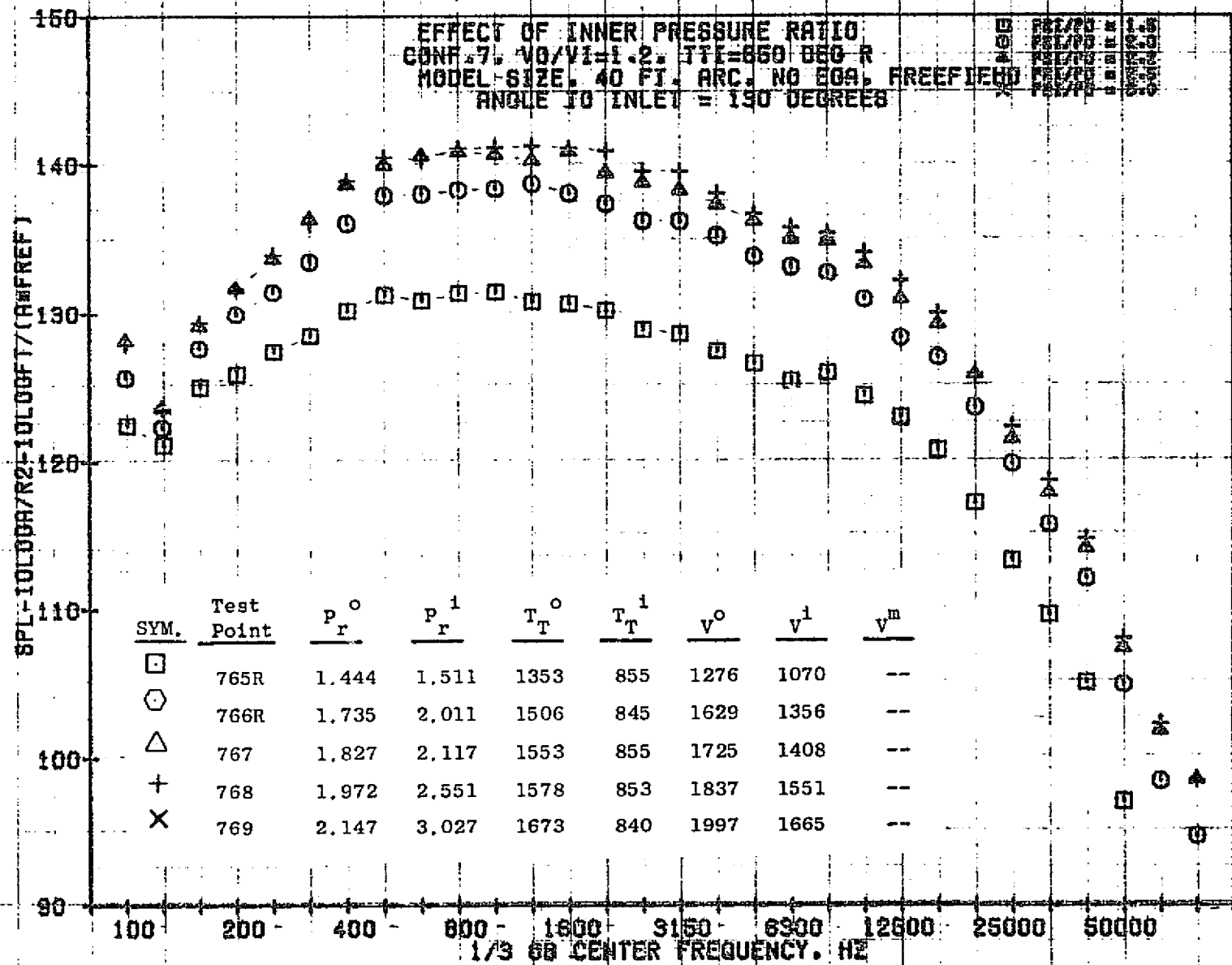
1166



4911

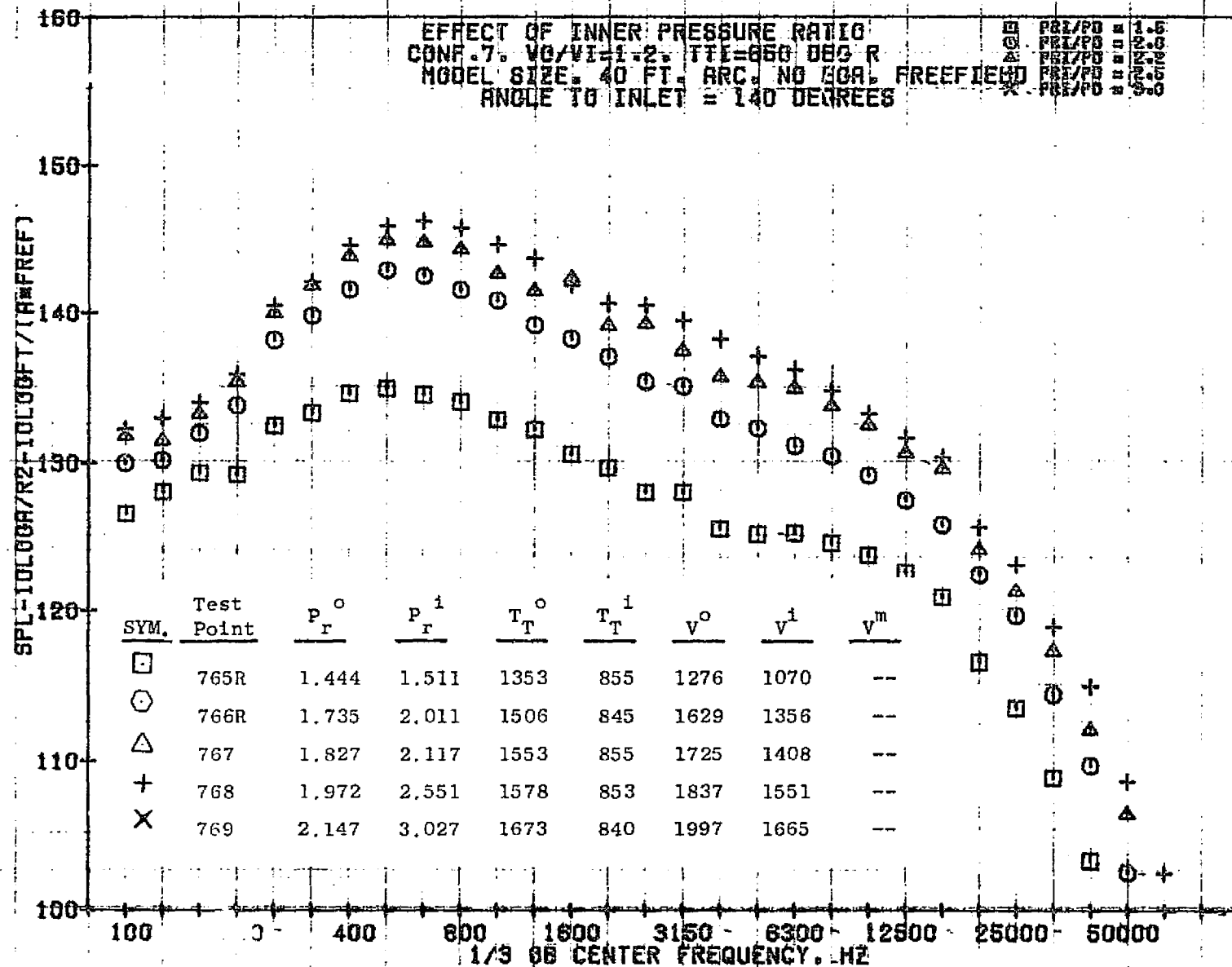


8911



11/09/76
 1R396-001

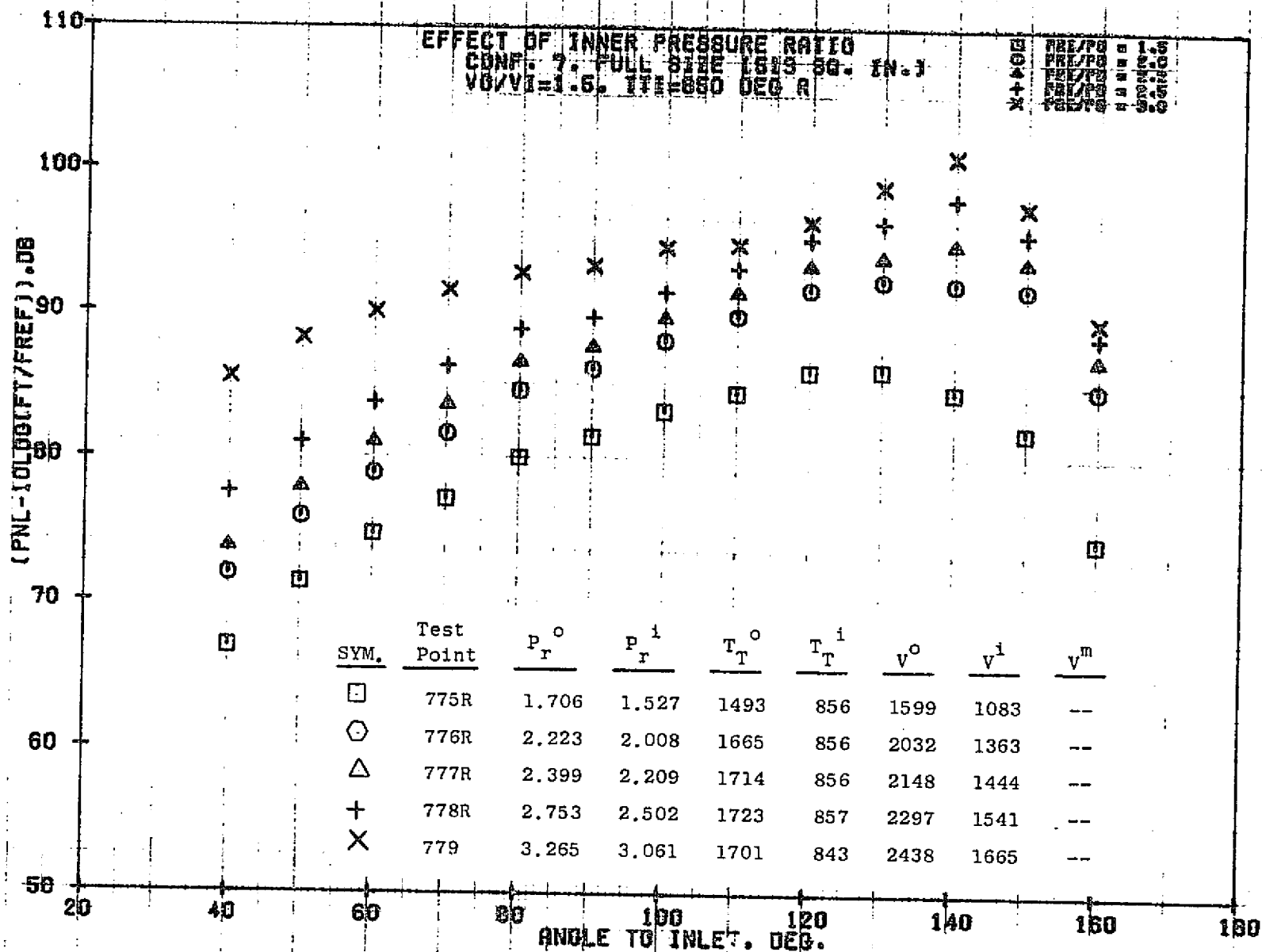
79 AIRCH 2.



11/09/76
 18336-001

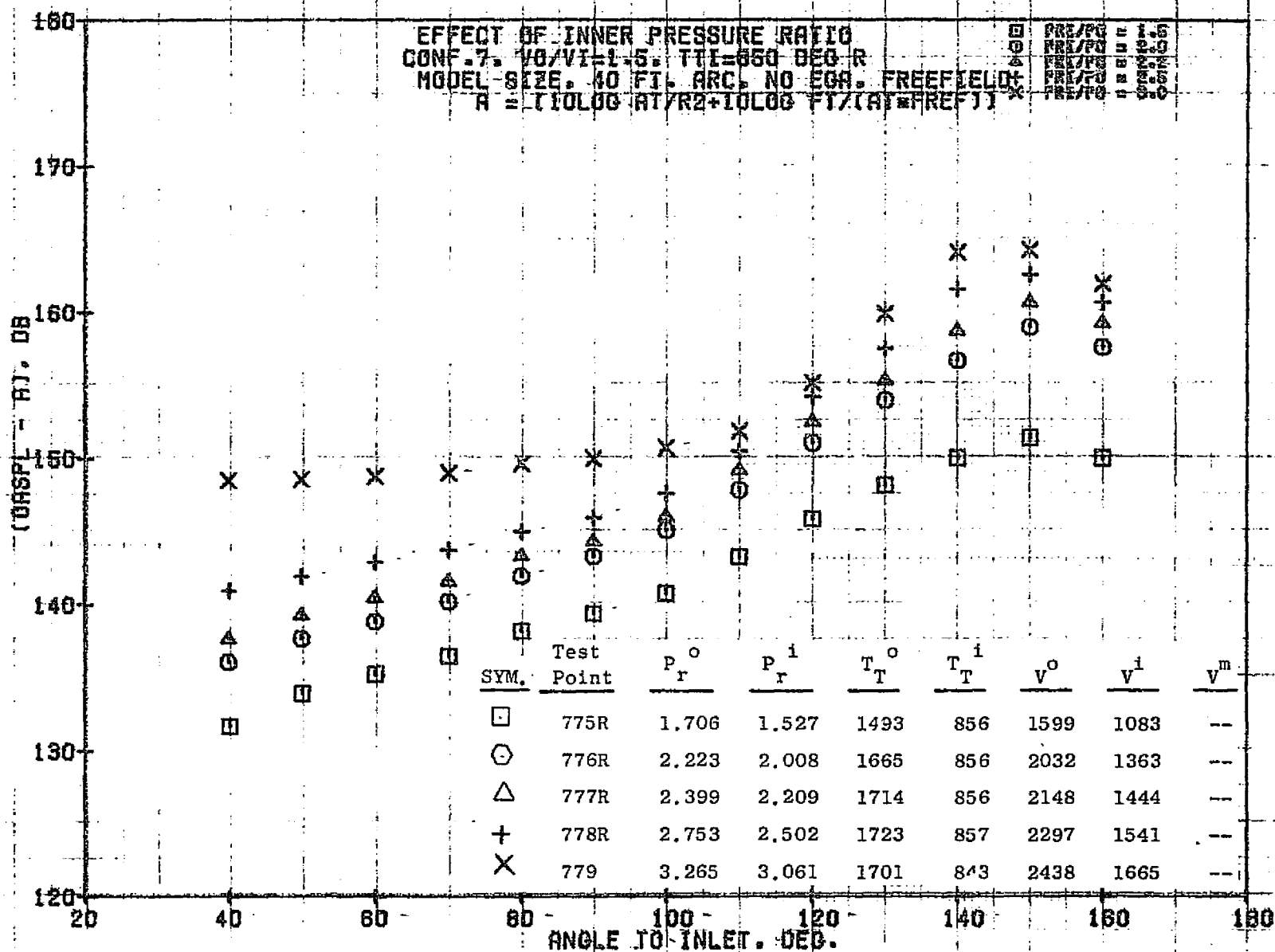
79 AIRCH 2.

0211

11/04/76
18680-001

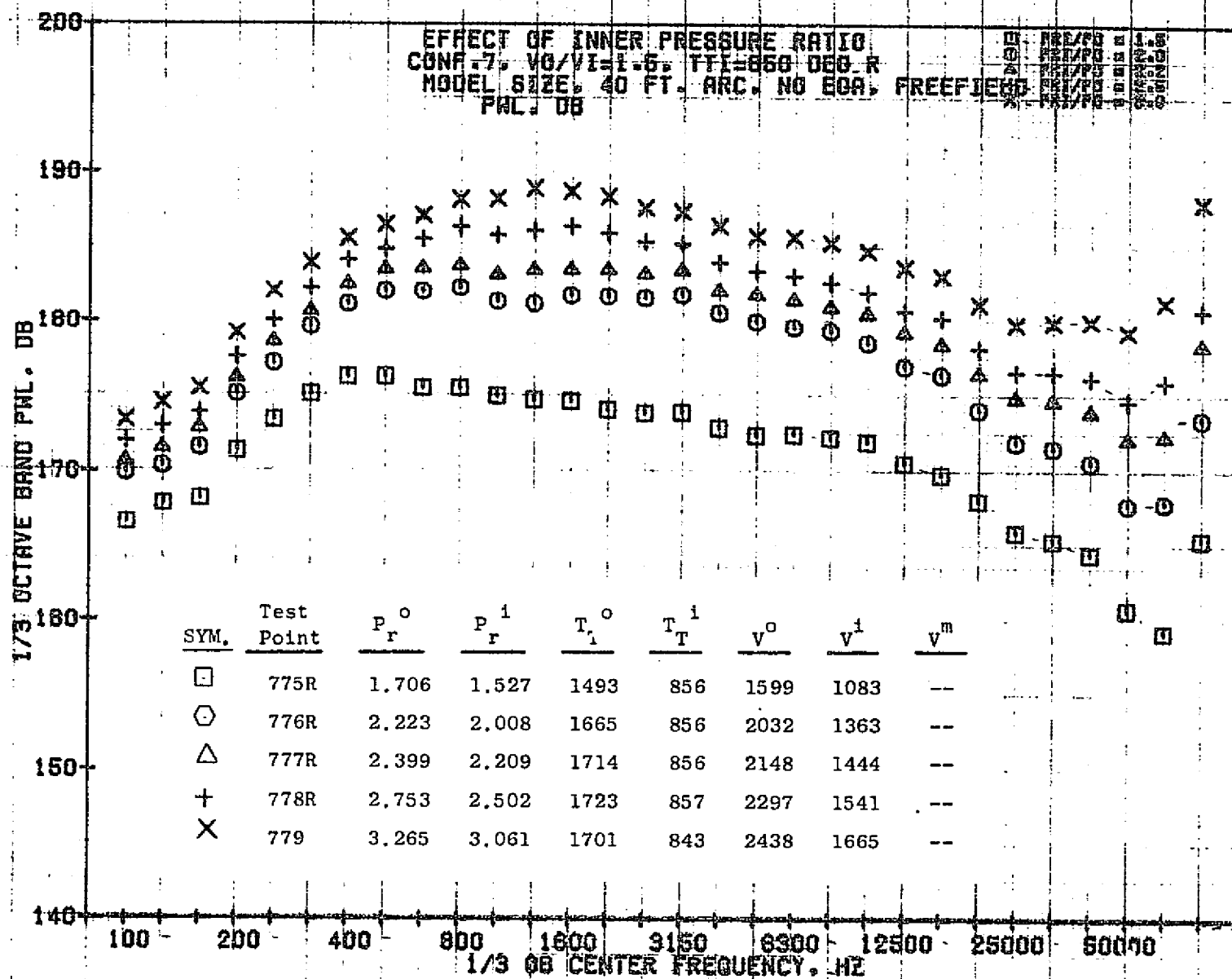
79 BURCH A.

1211


 11/09/76
 1R33R-001

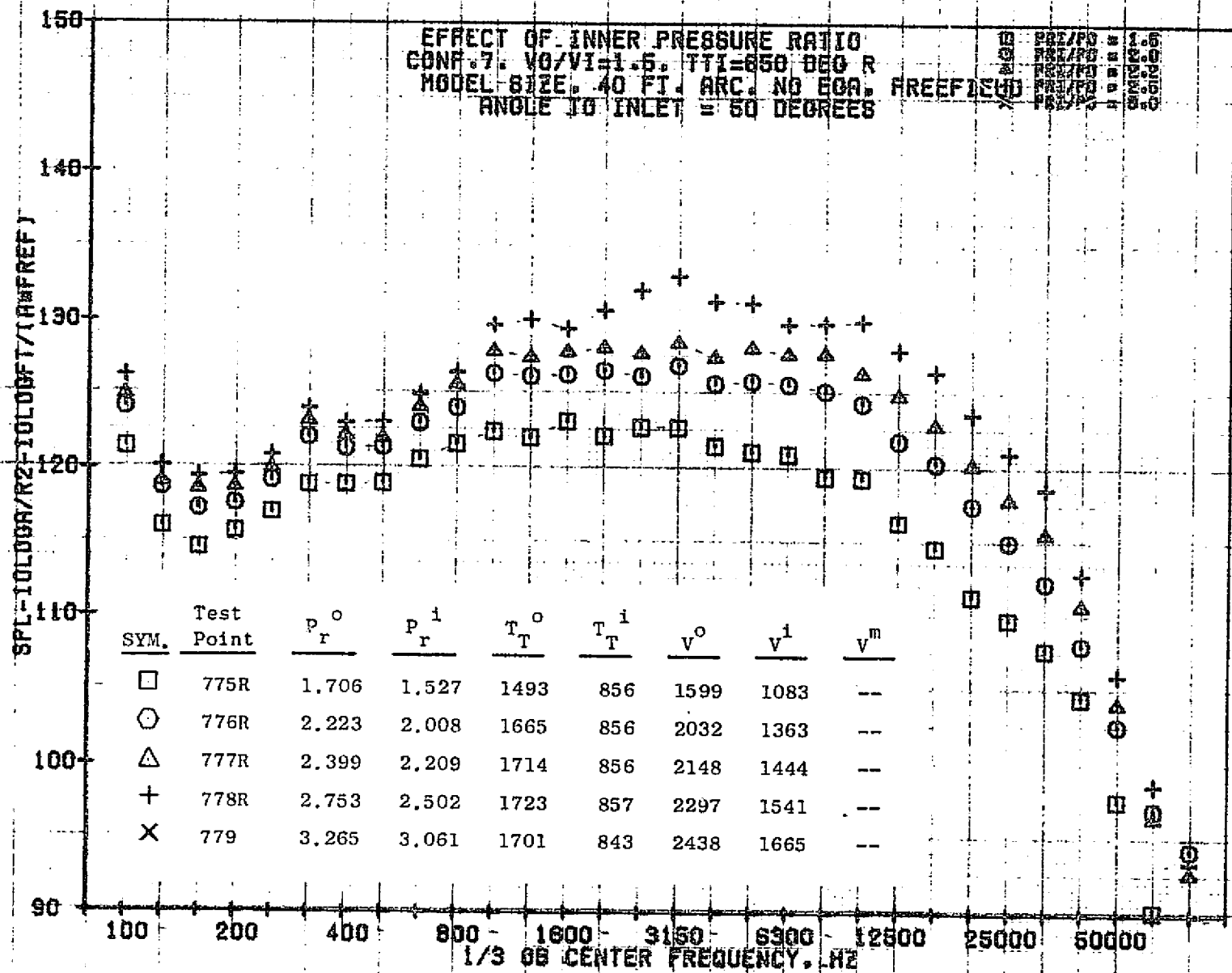
79 BURCH A.

1172

11/09/76 -
1A336-001

79 AIRCH A.

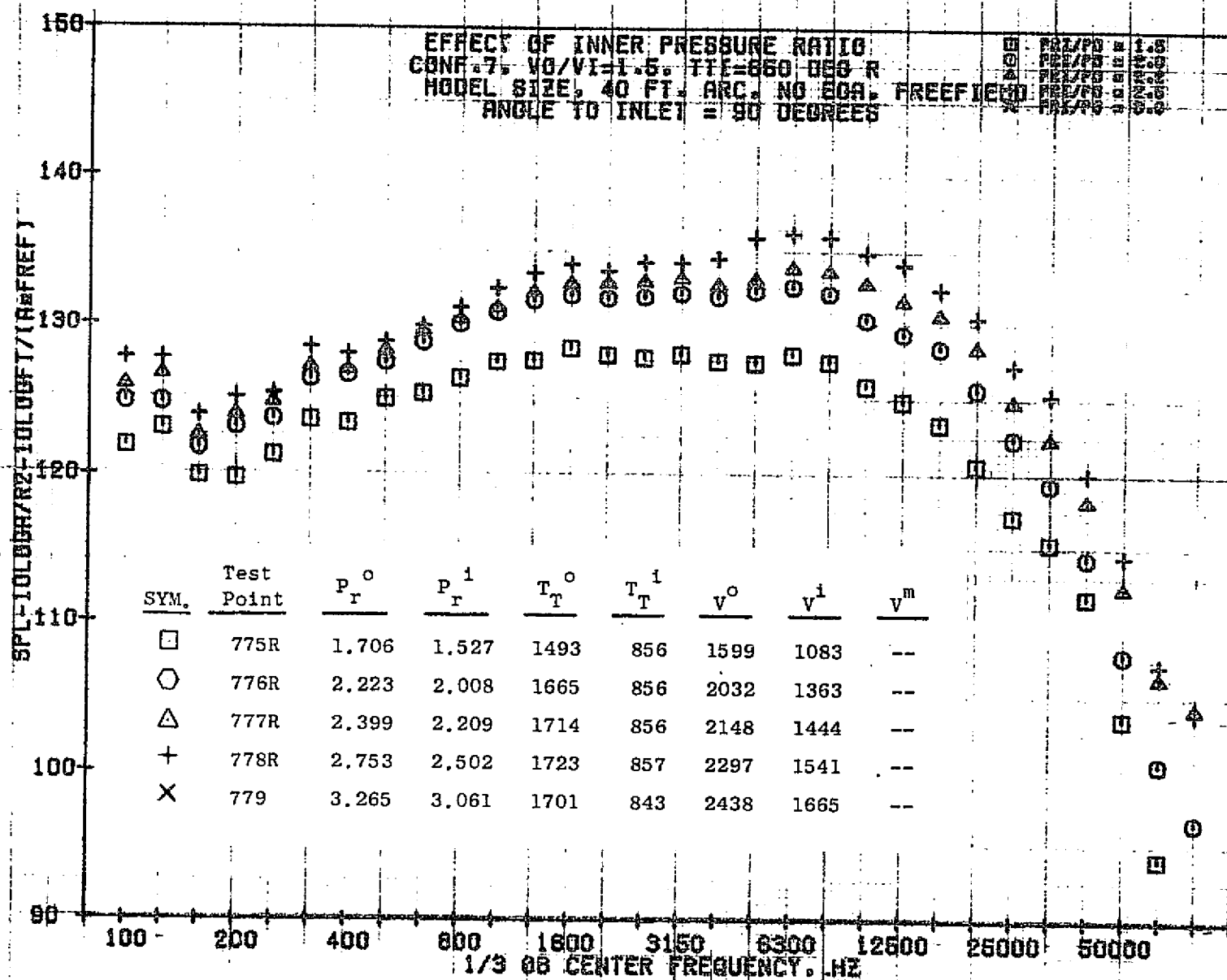
1171



11/09/76
18336-001

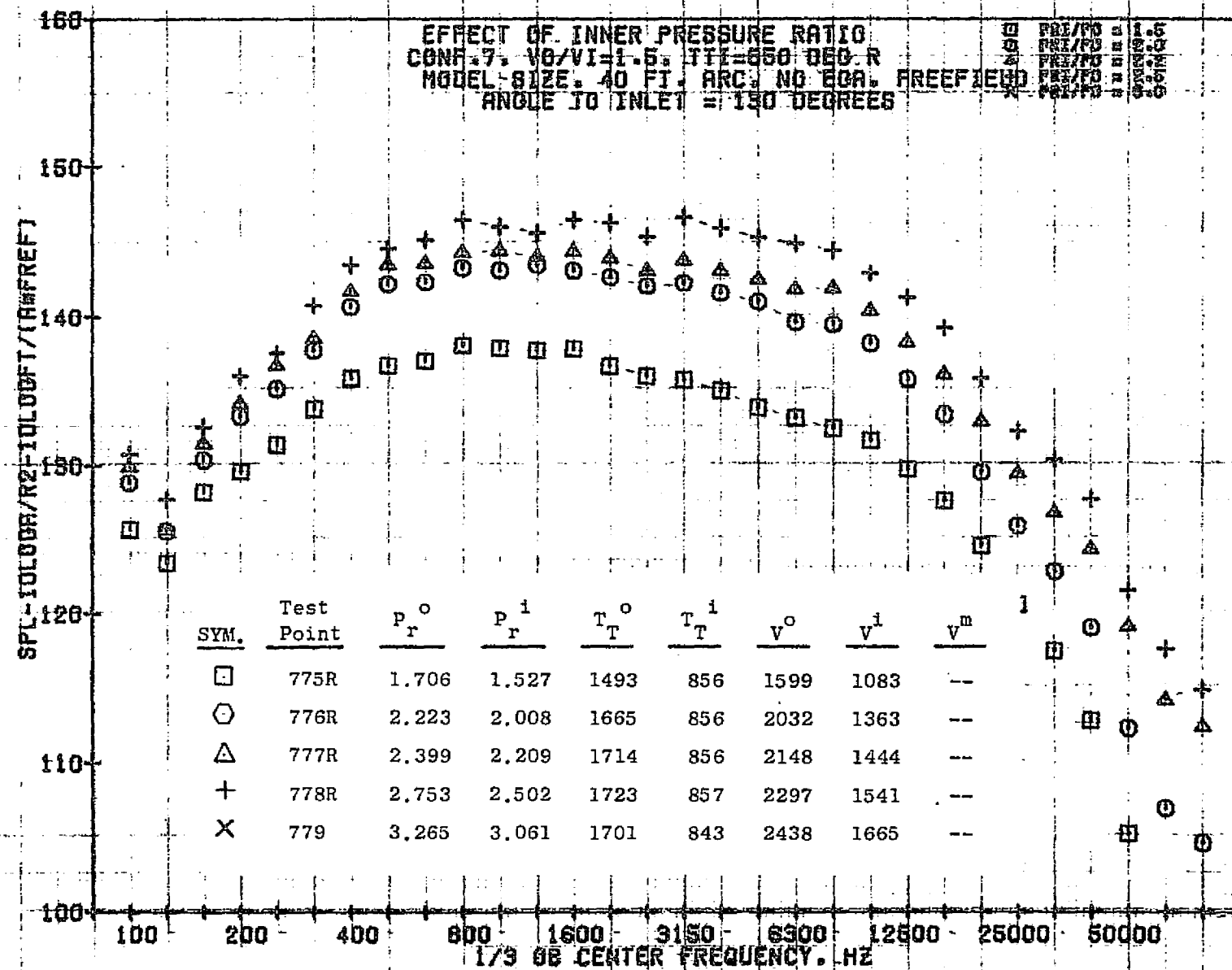
79 BURCH A.

1174

11/09/76
1A33A-001

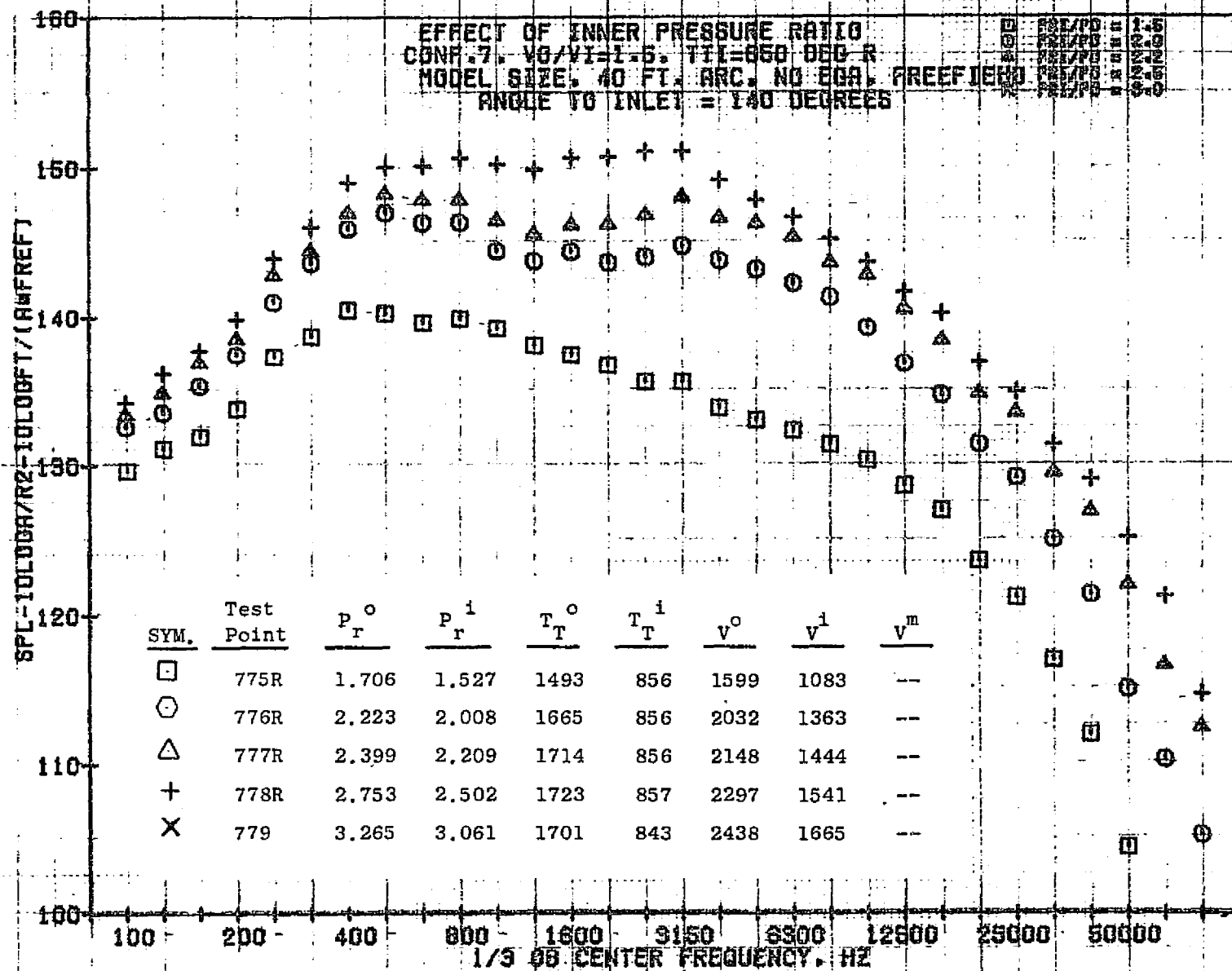
79 AIRCRAFT

1375



11/09/78
 18336-001

79 AIRCRAFT



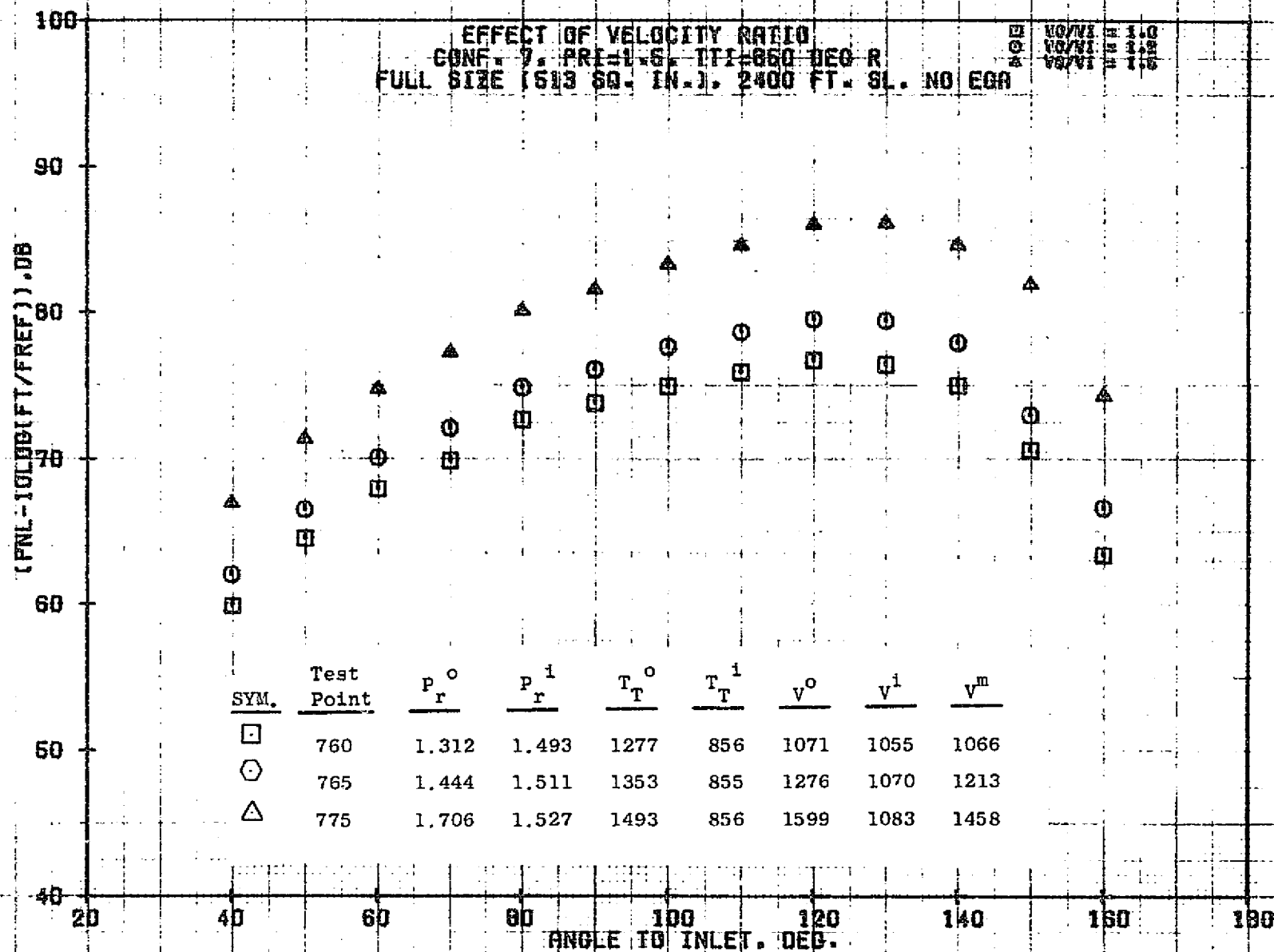
11/09/76 -
 1A99R-001

7A AIRCH A.

7.4.6 Effect of Velocity Ratio at Constant Inner Pressure Ratio

This section presents comparisons showing the influence of velocity ratio for a series of tests for Configuration 7 where the inner pressure ratio was held constant at different levels.

1178



11/01/76
18421-001

79 BURCH A.

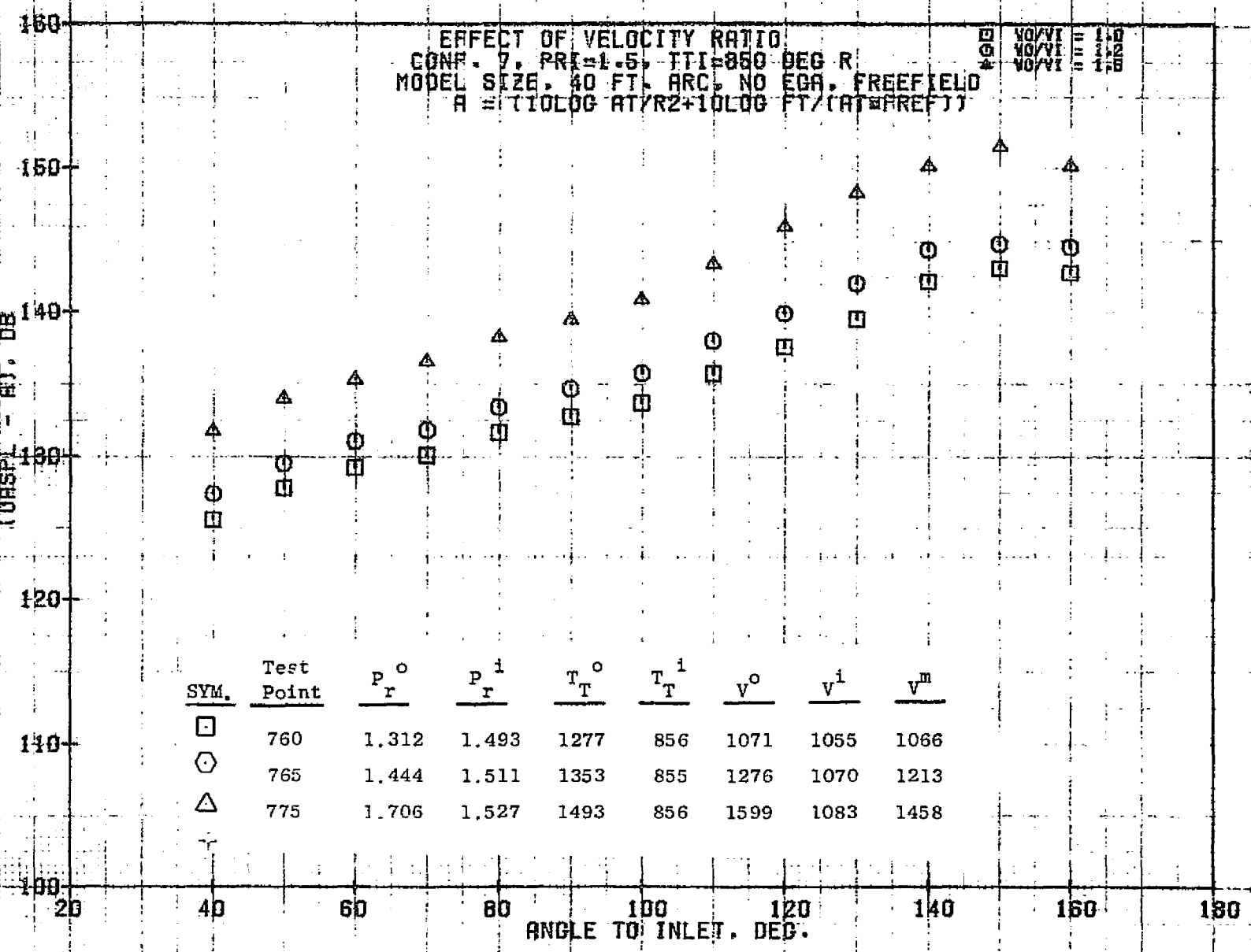
57

621E

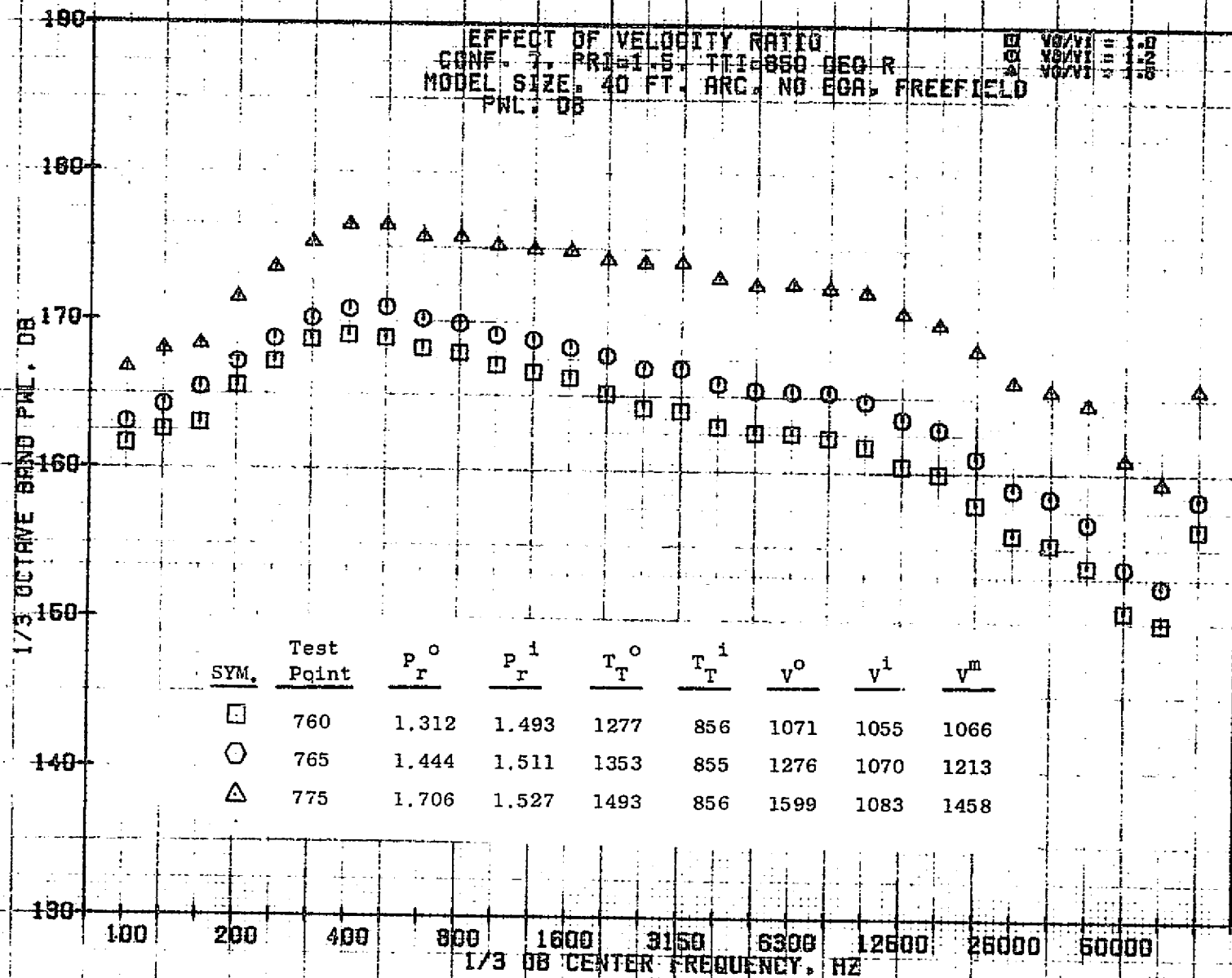
(URSP - H). DB

EFFECT OF VELOCITY RATIO
 CONF. 7, PRE=1.5, TTI=850 DEG R
 MODEL SIZE, 40 FT. ARC, NO EGA, FREEFIELD
 $A = (10 \log AT/R^2 + 10 \log FT/(AT \cdot P_{REF}))$

$V_0/V_1 = 1.0$
 $V_0/V_1 = 1.2$
 $V_0/V_1 = 1.5$

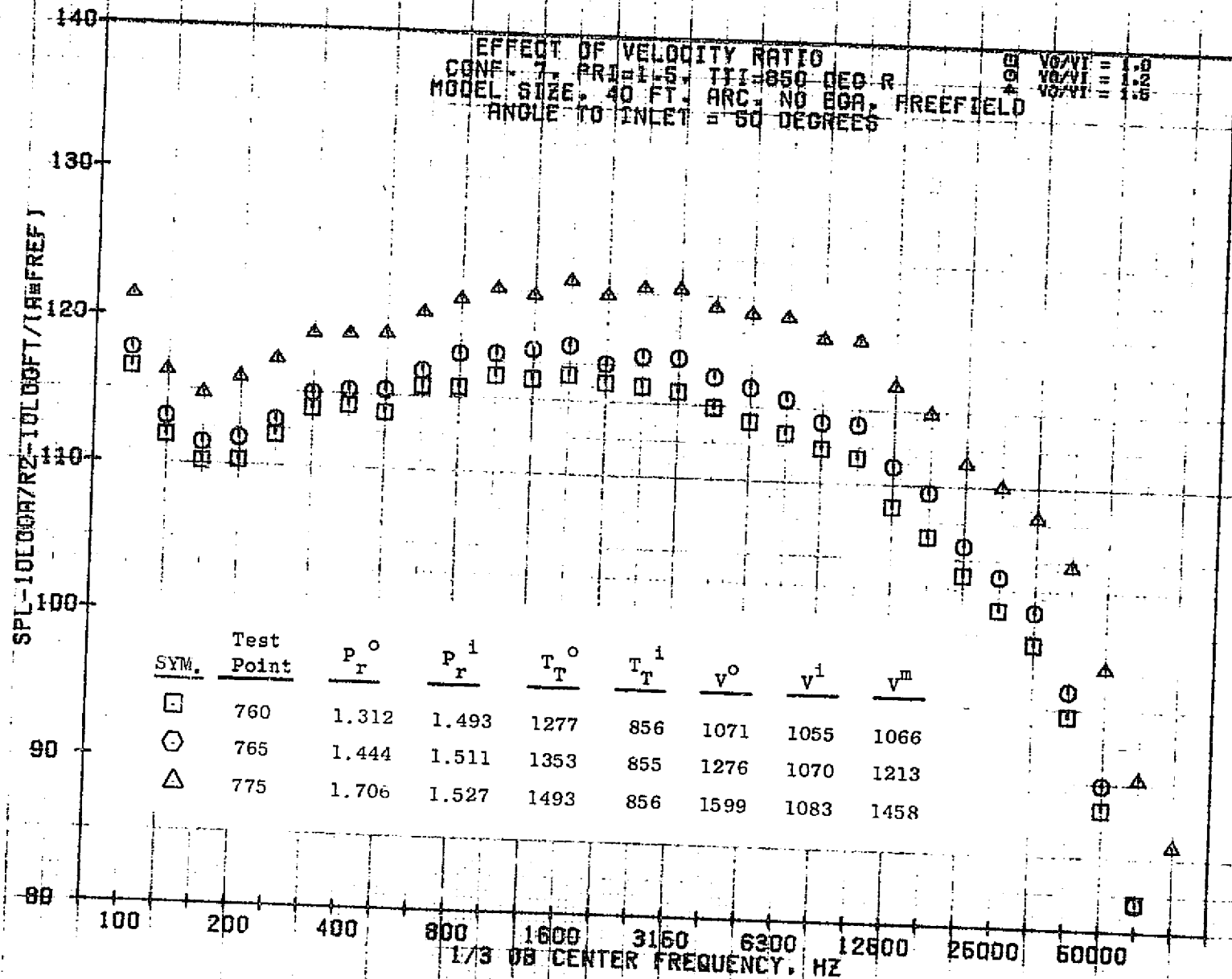


0811



11/10/76
18048-001

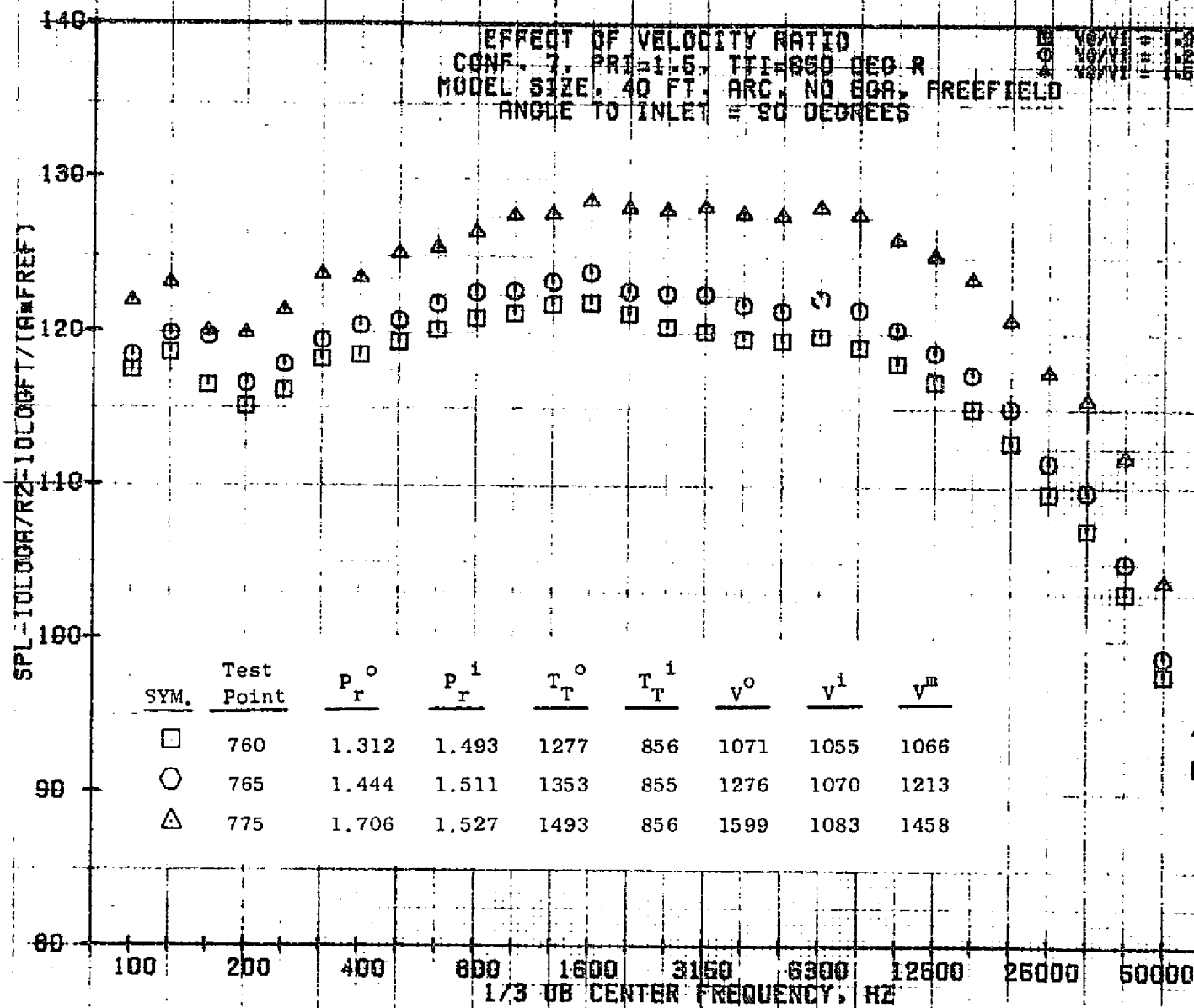
79 BURCH A.



11/10/76
 18048-001

79 BURCH A.

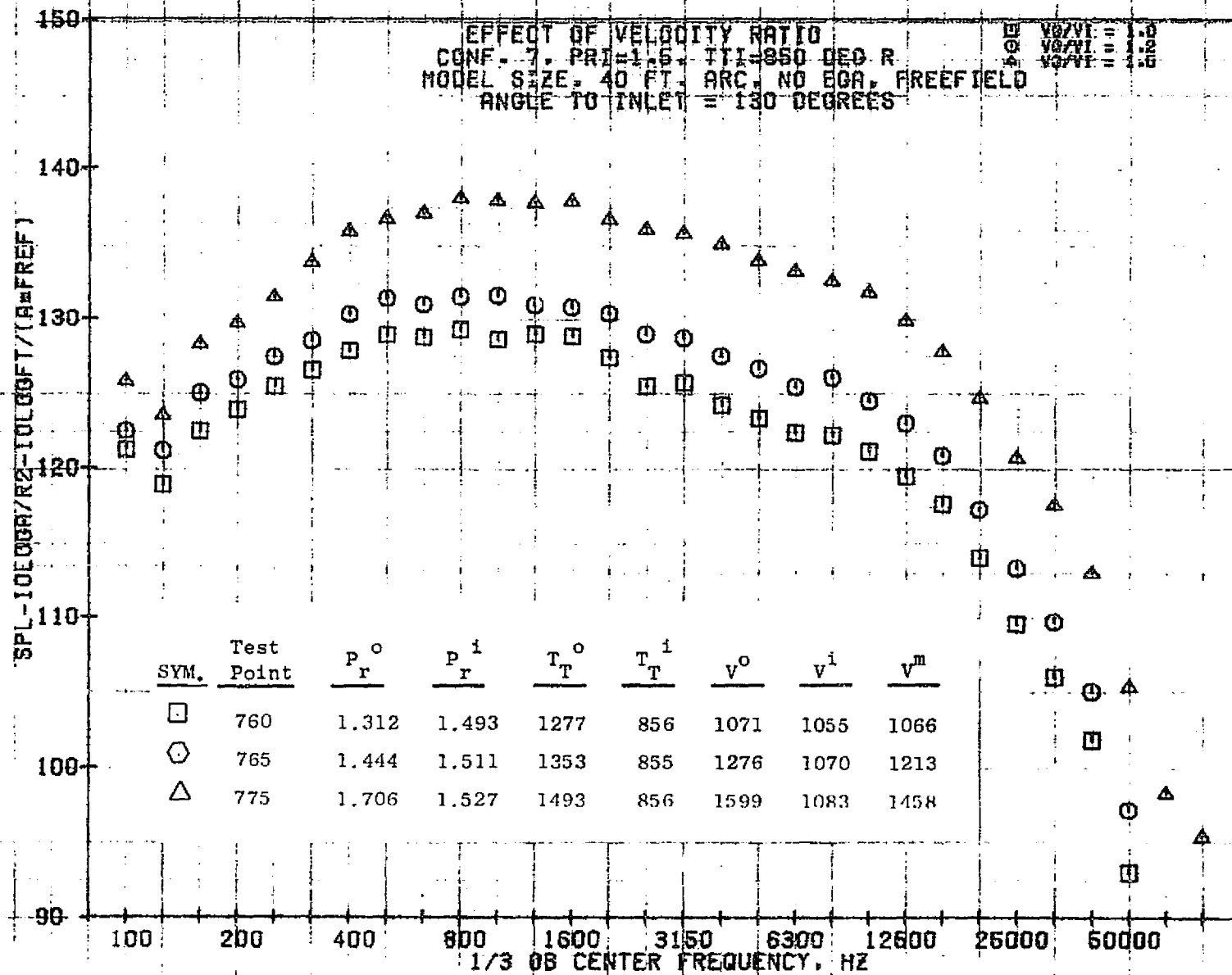
8871



11/10/76
18048-001

79 BURCH A.

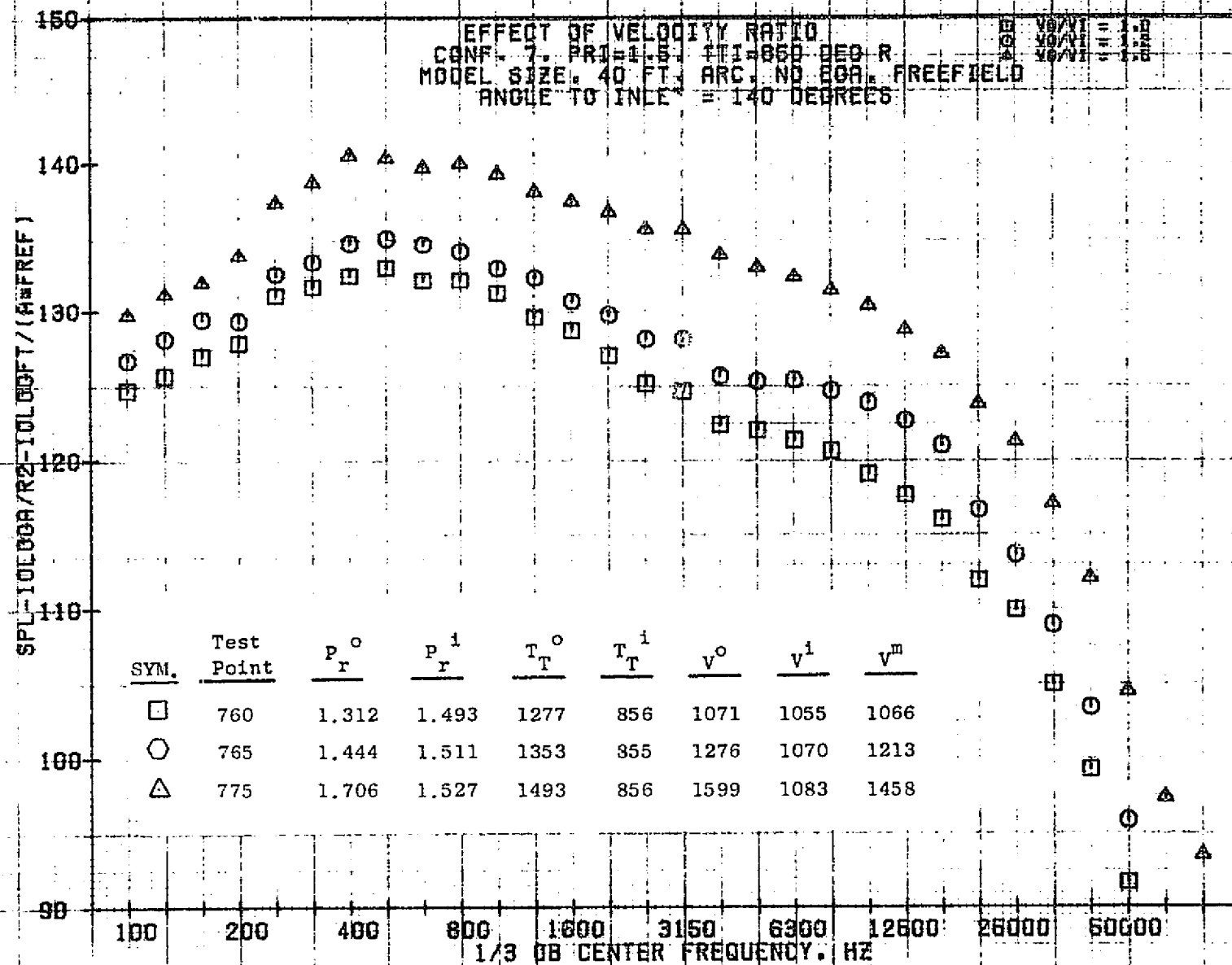
1188



11/10/76
 18048-001

79 BURCH A.

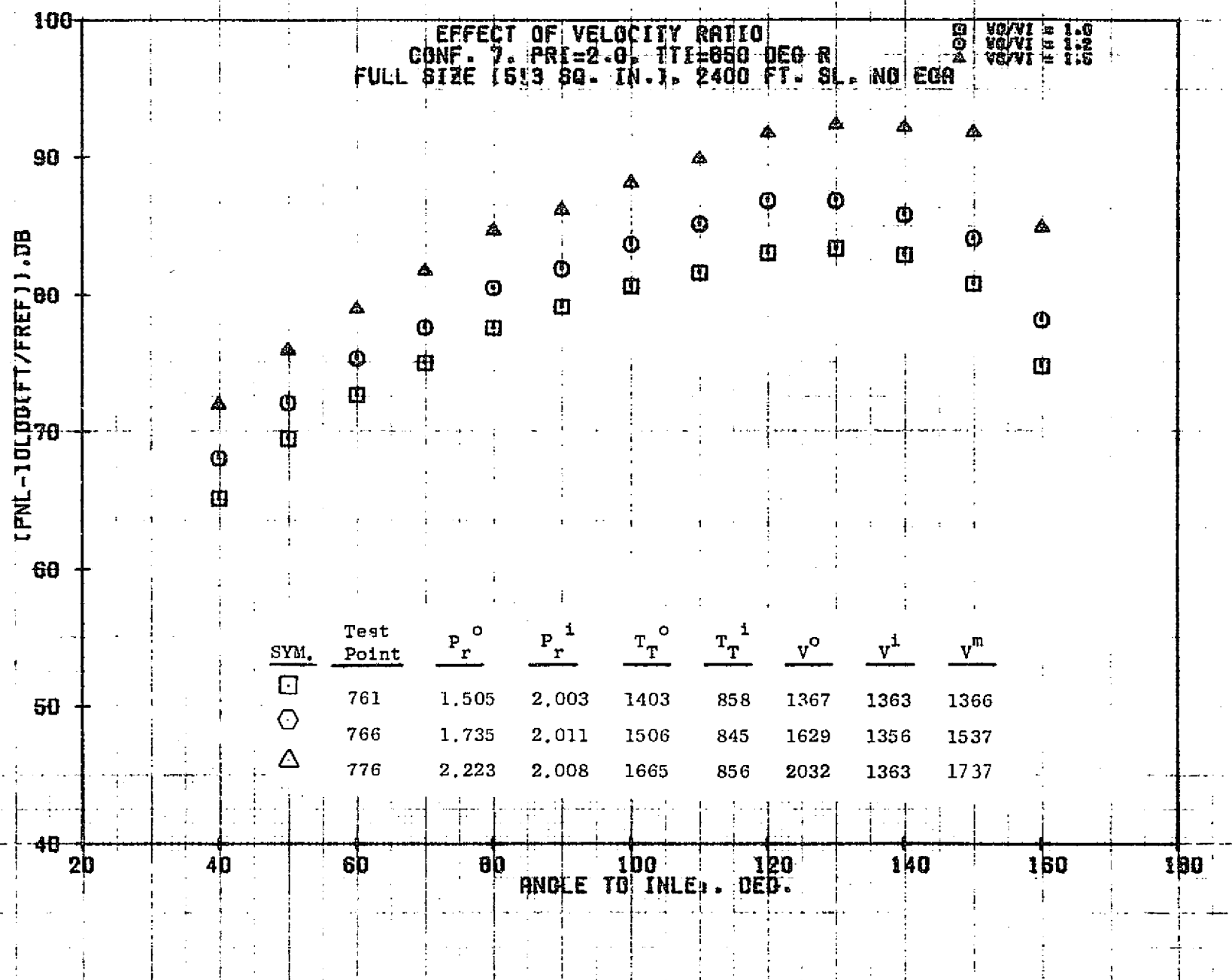
188



11/10/76
 18048-001

79 BURCH A.

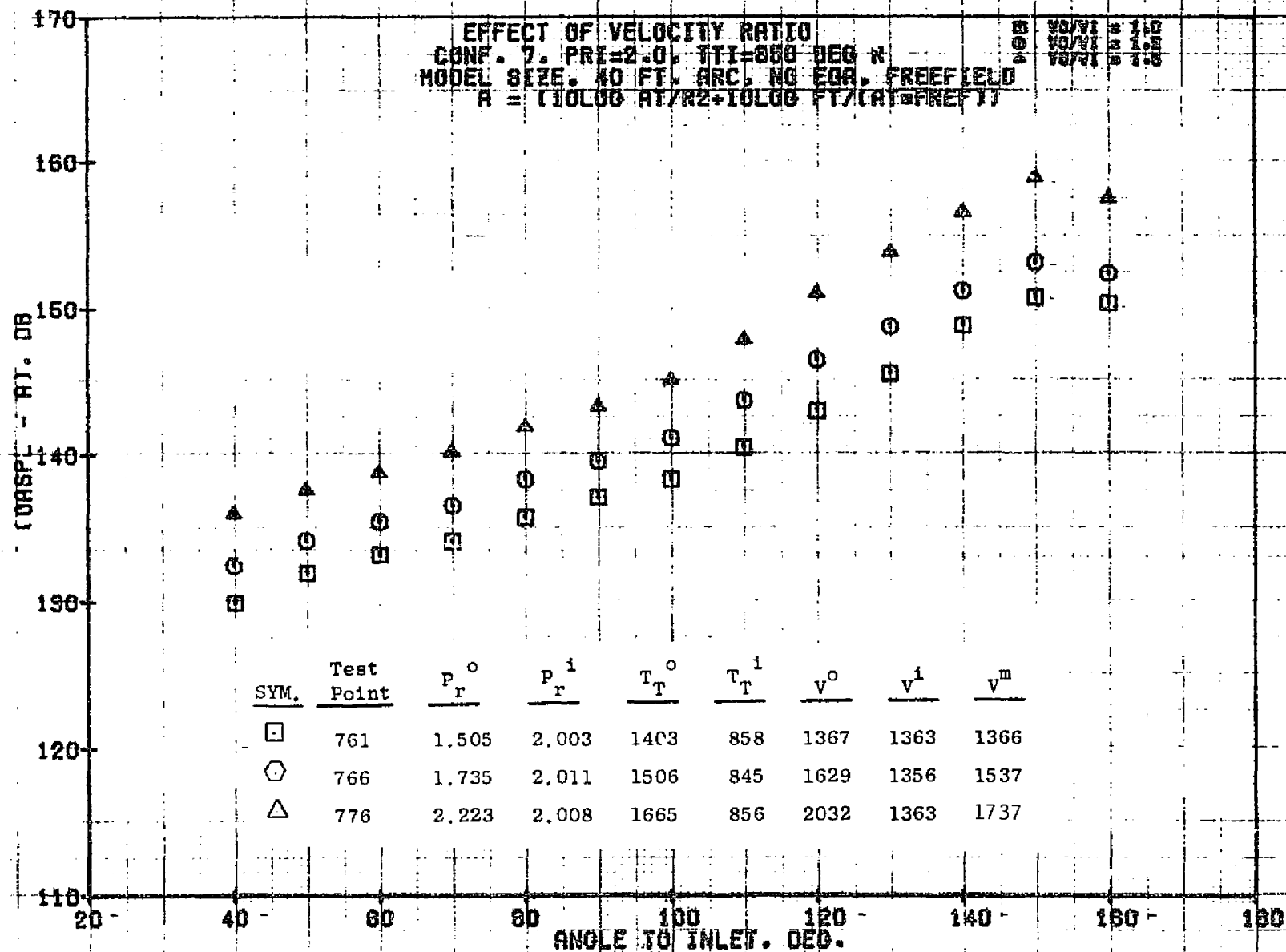
1185



11/01/76
18421-001

79 BURCH A.

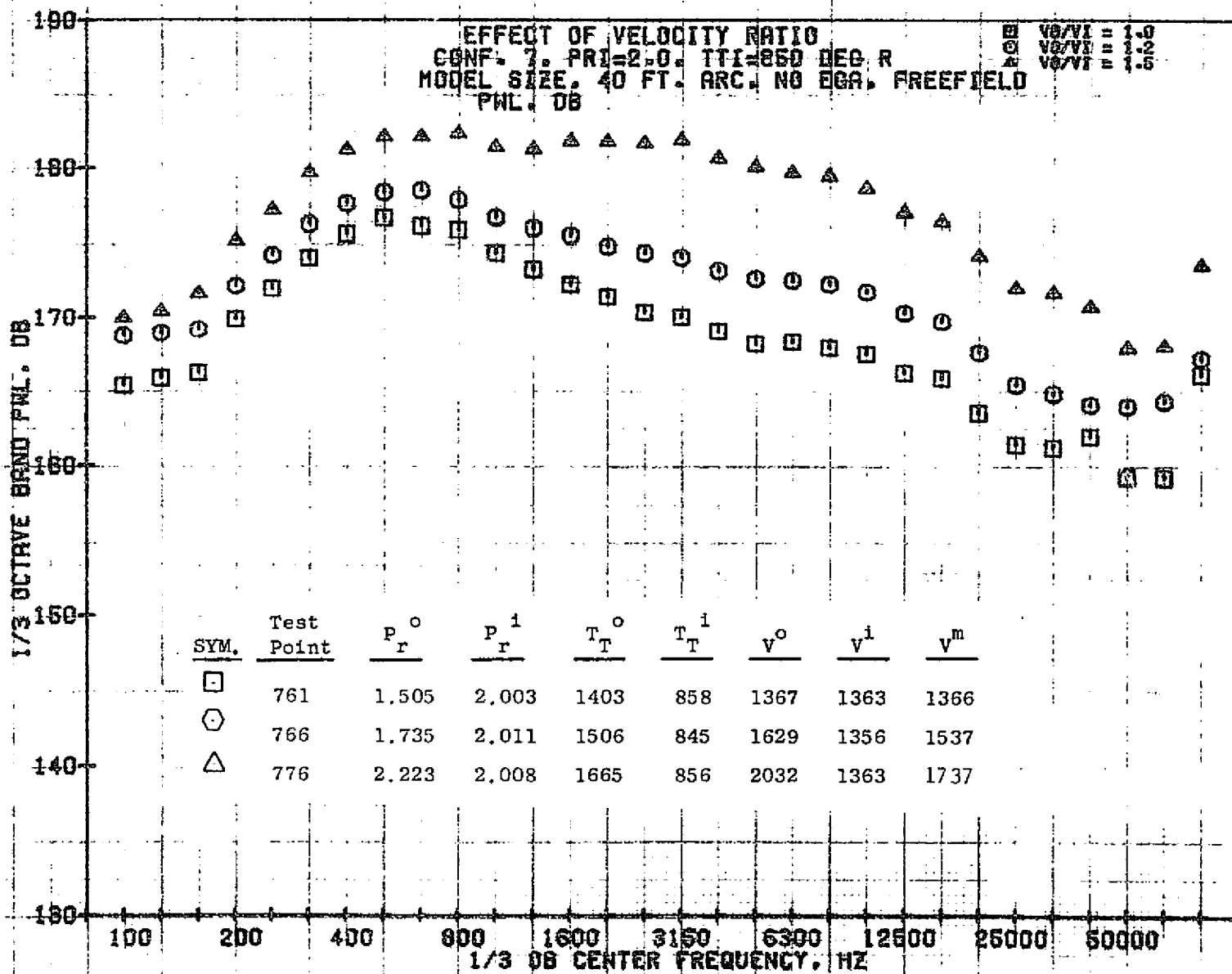
1186



11/09/76 -
 1A996-001

7A AIRCH A.

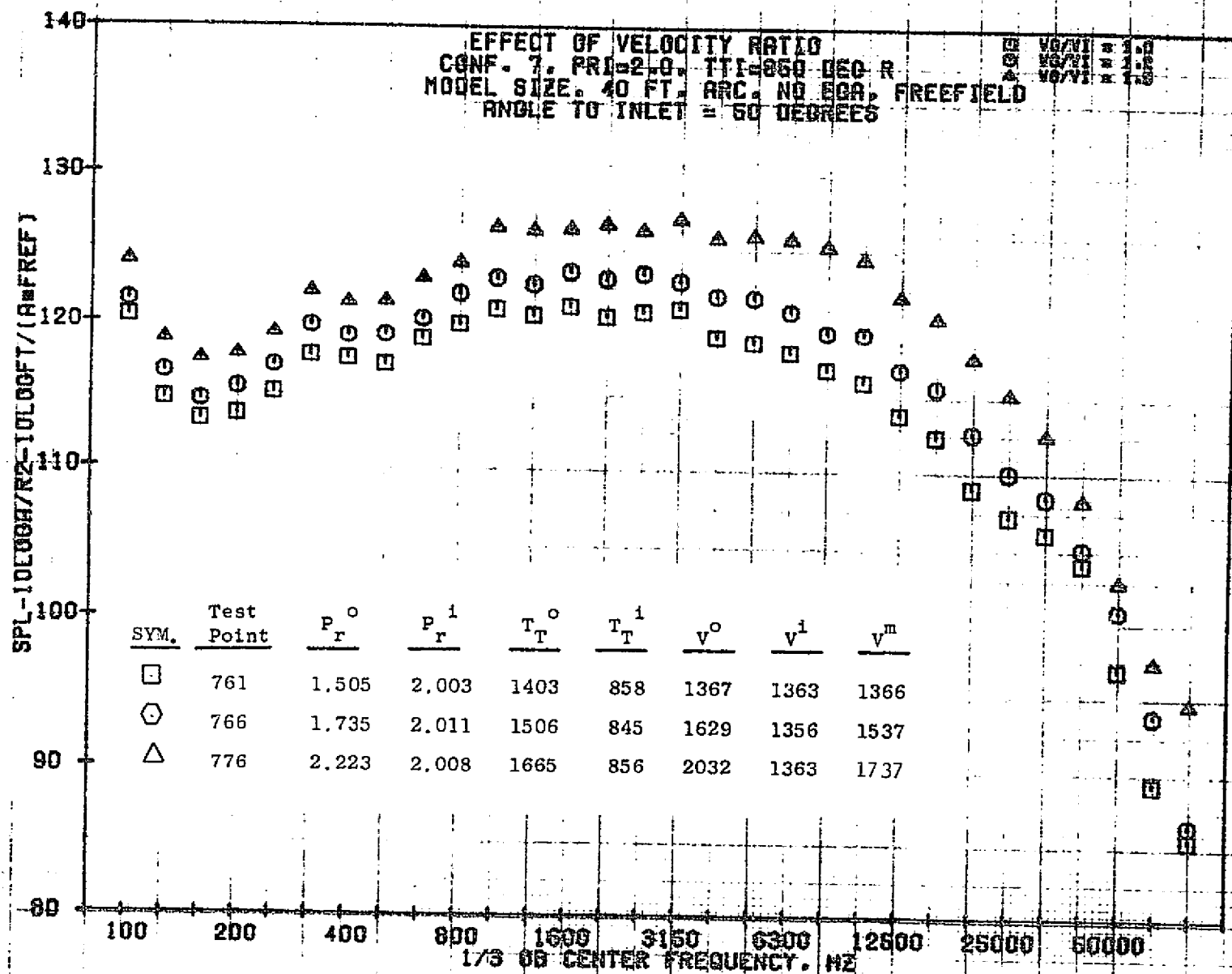
1187



11/03/76
18575-001

79 BURCH A.

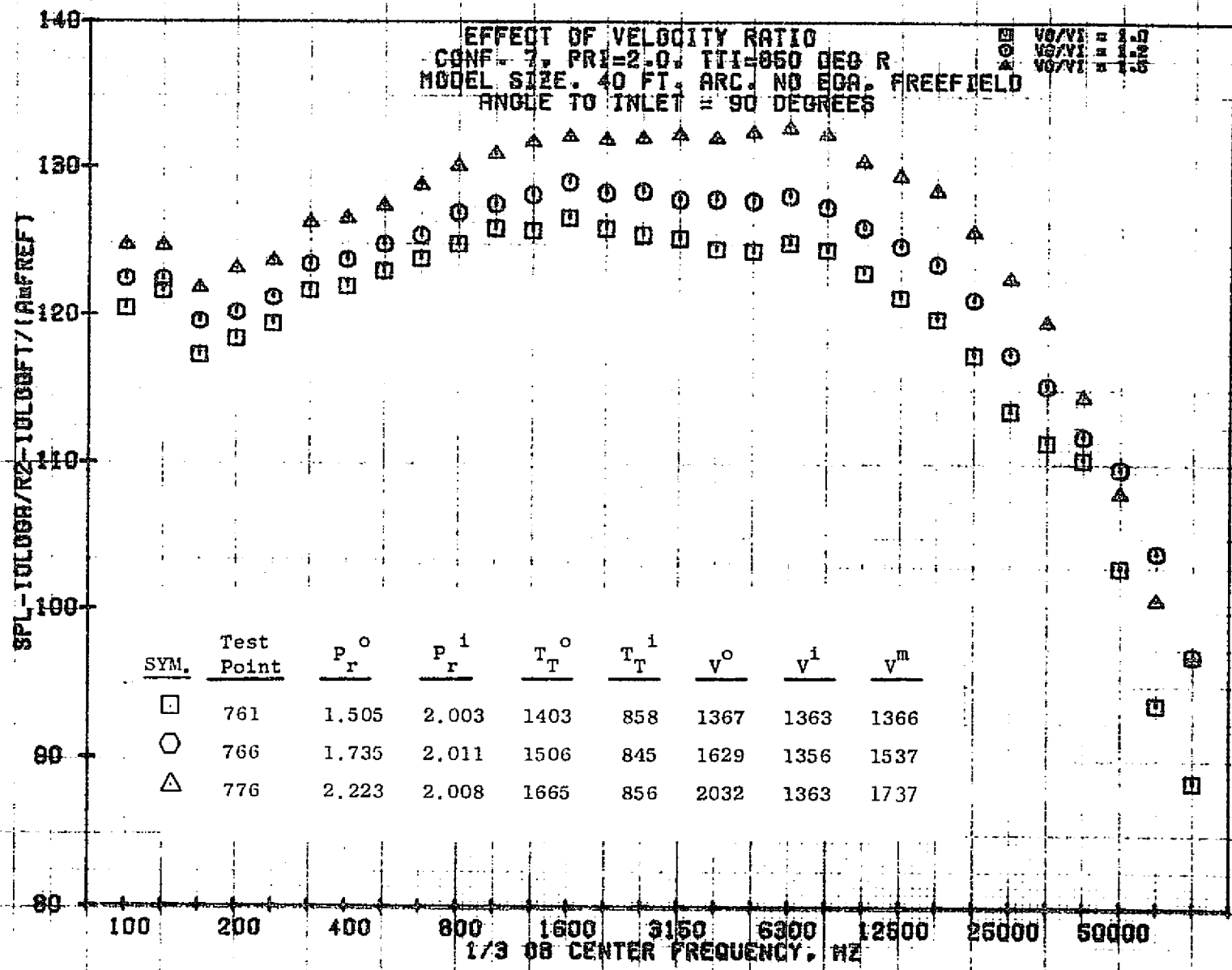
1188



11/03/76
 18575-001

79 BURCH A.

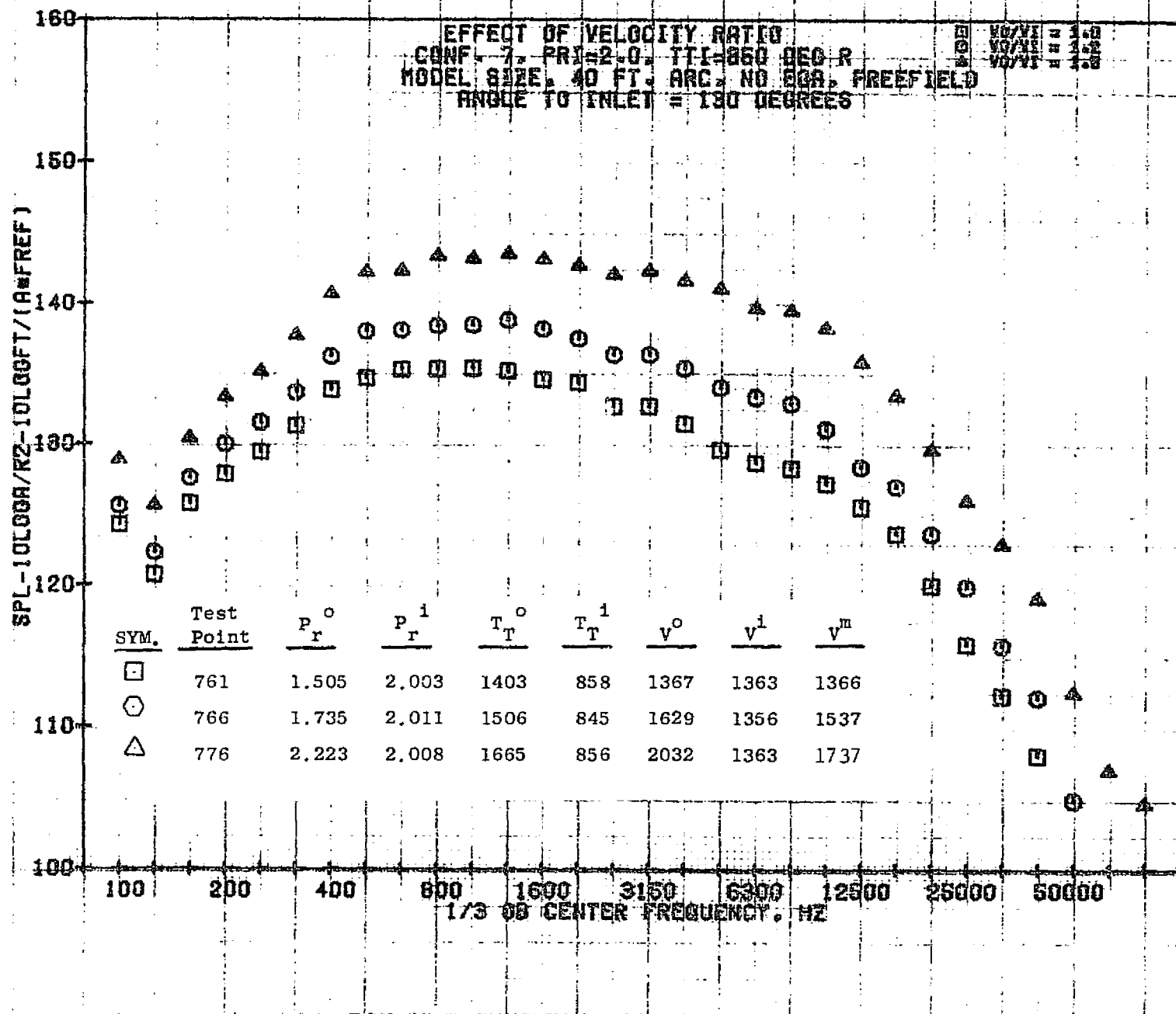
6811



11/03/76
 18575-001

79 BURCH A.

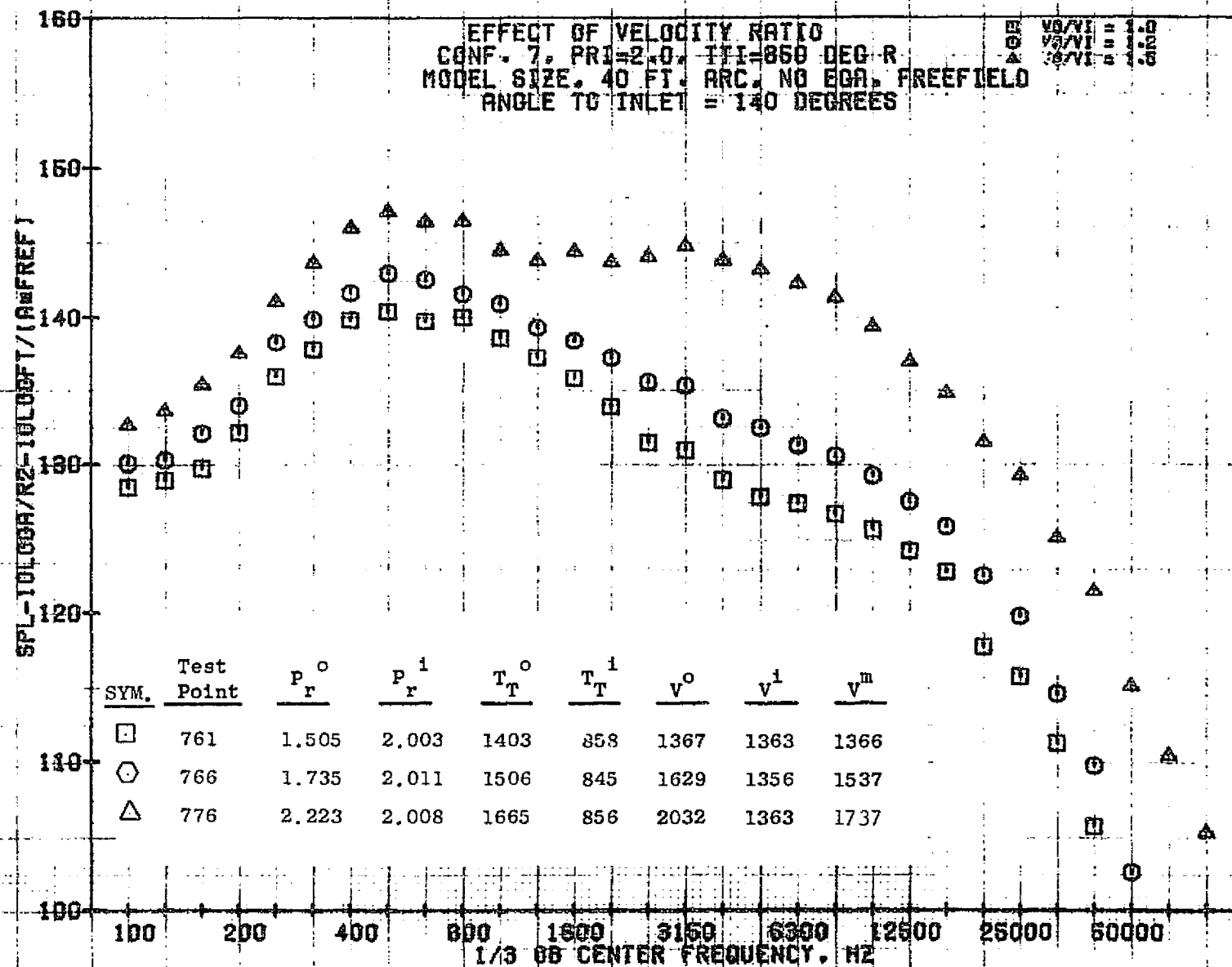
0611



11/03/76
18675-001

79 BURCH A.

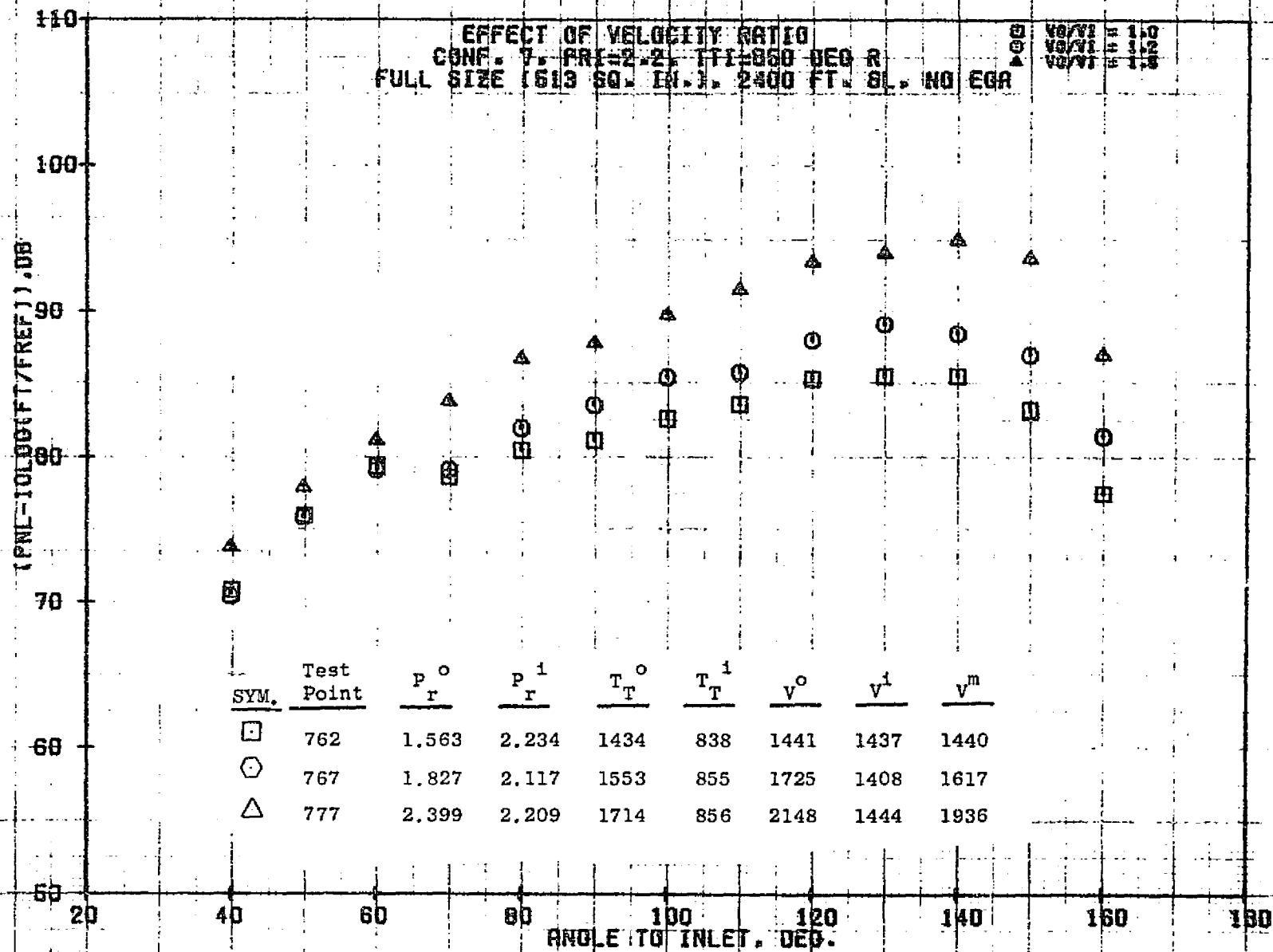
1611



11/03/76
 18575-001

79 BURCH A.

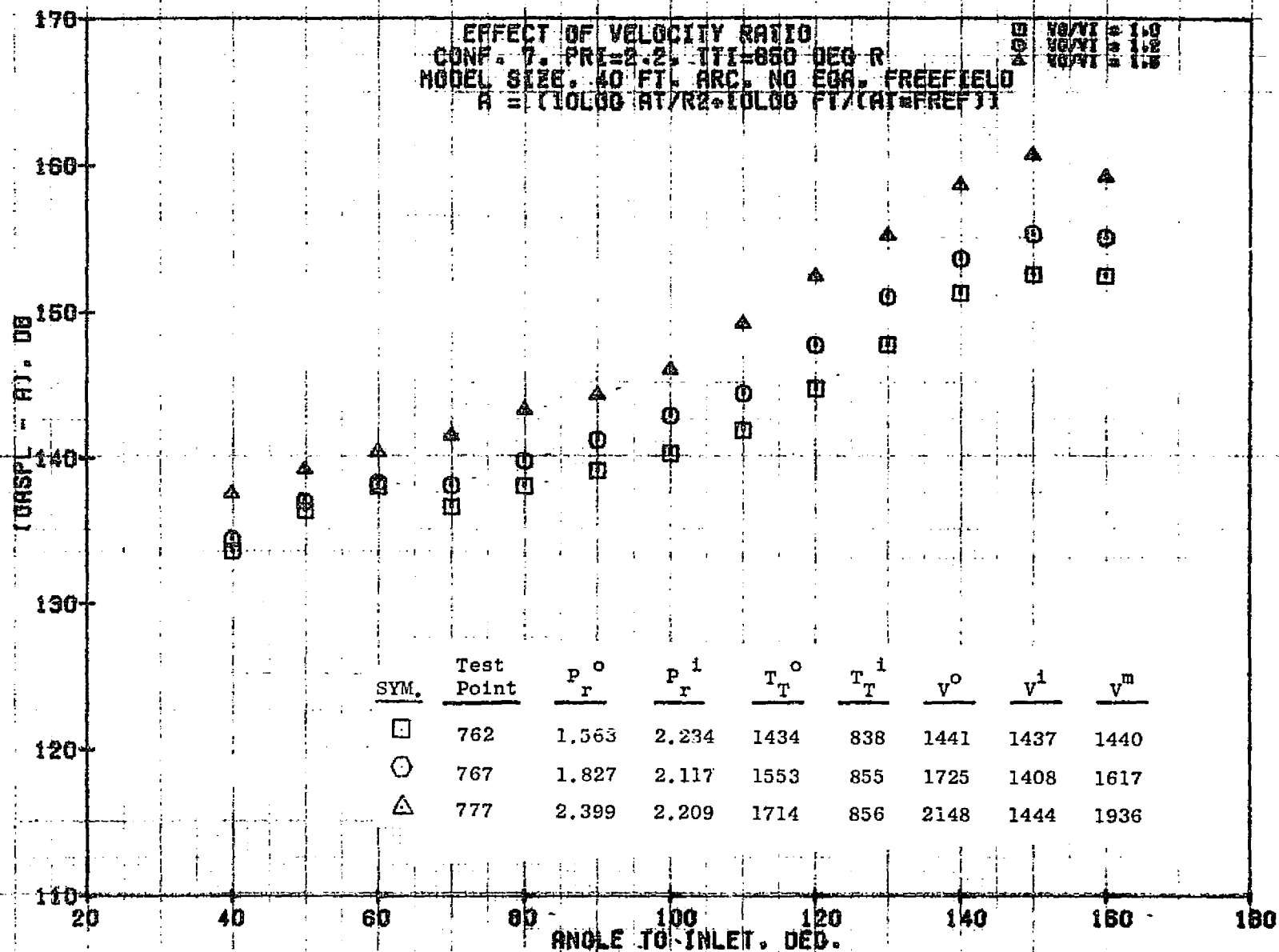
1192



11/01/76
 18421-001

79 BURCH A.

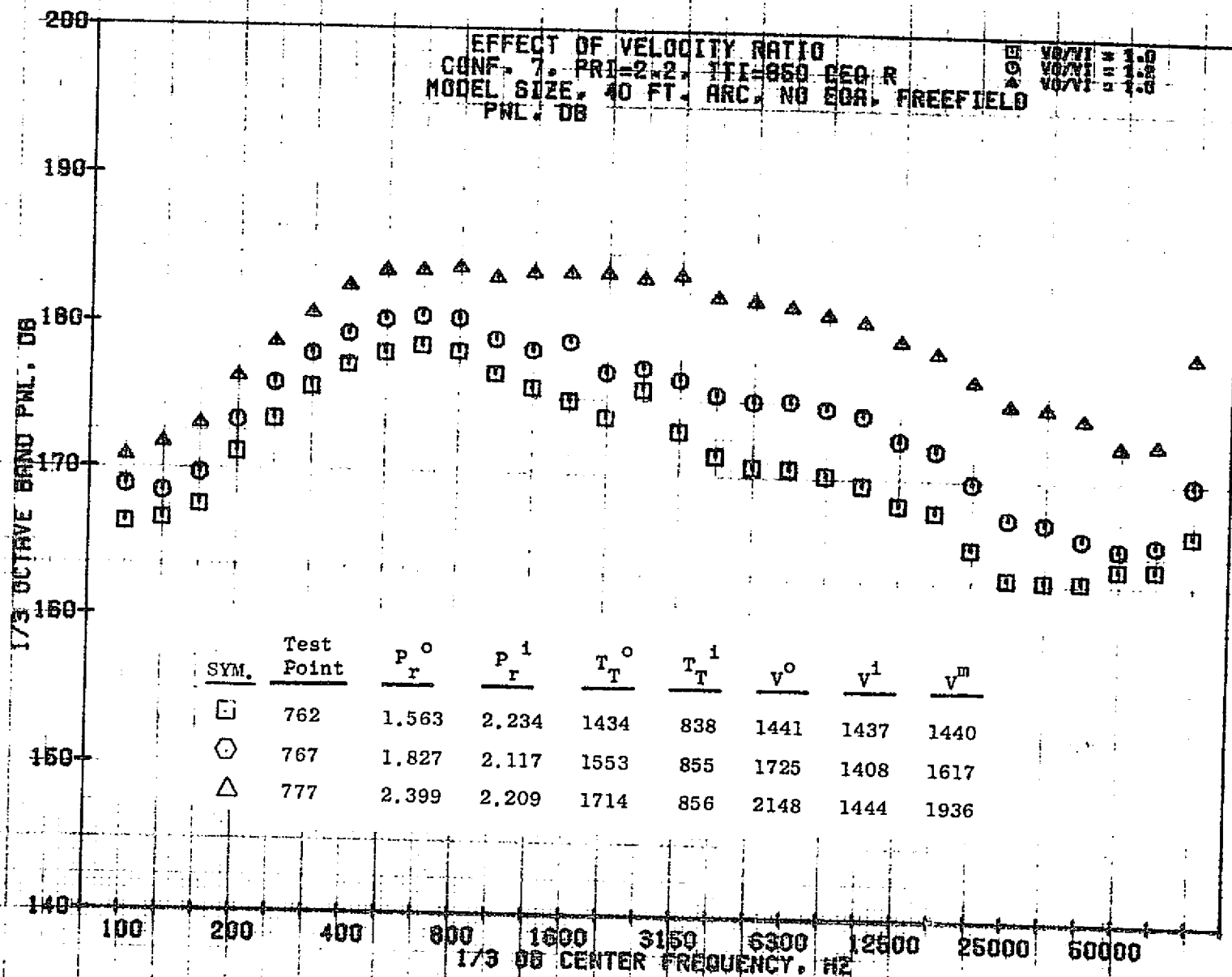
1193



11/09/76
 18938-001

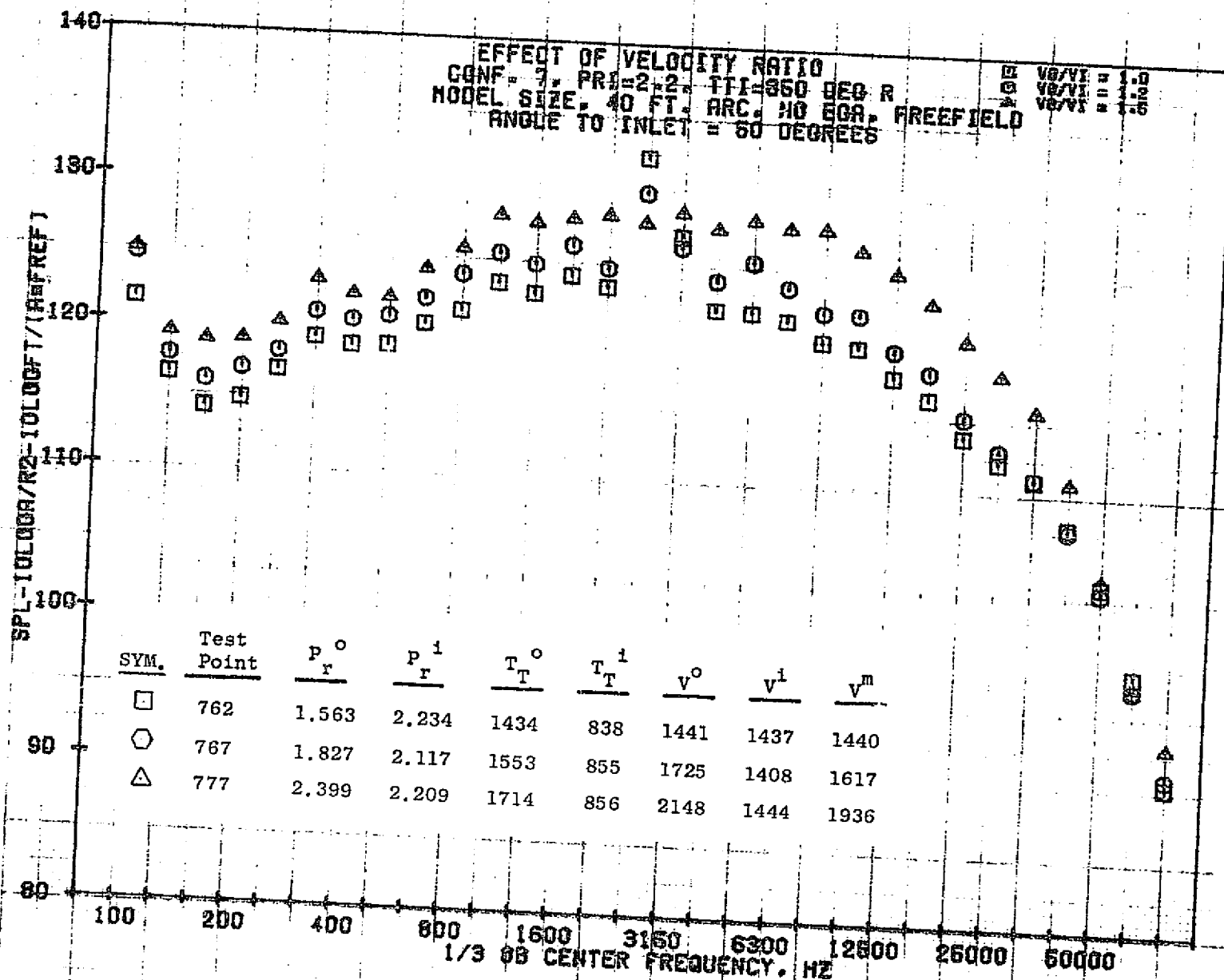
79 AIRCRAFT

1194

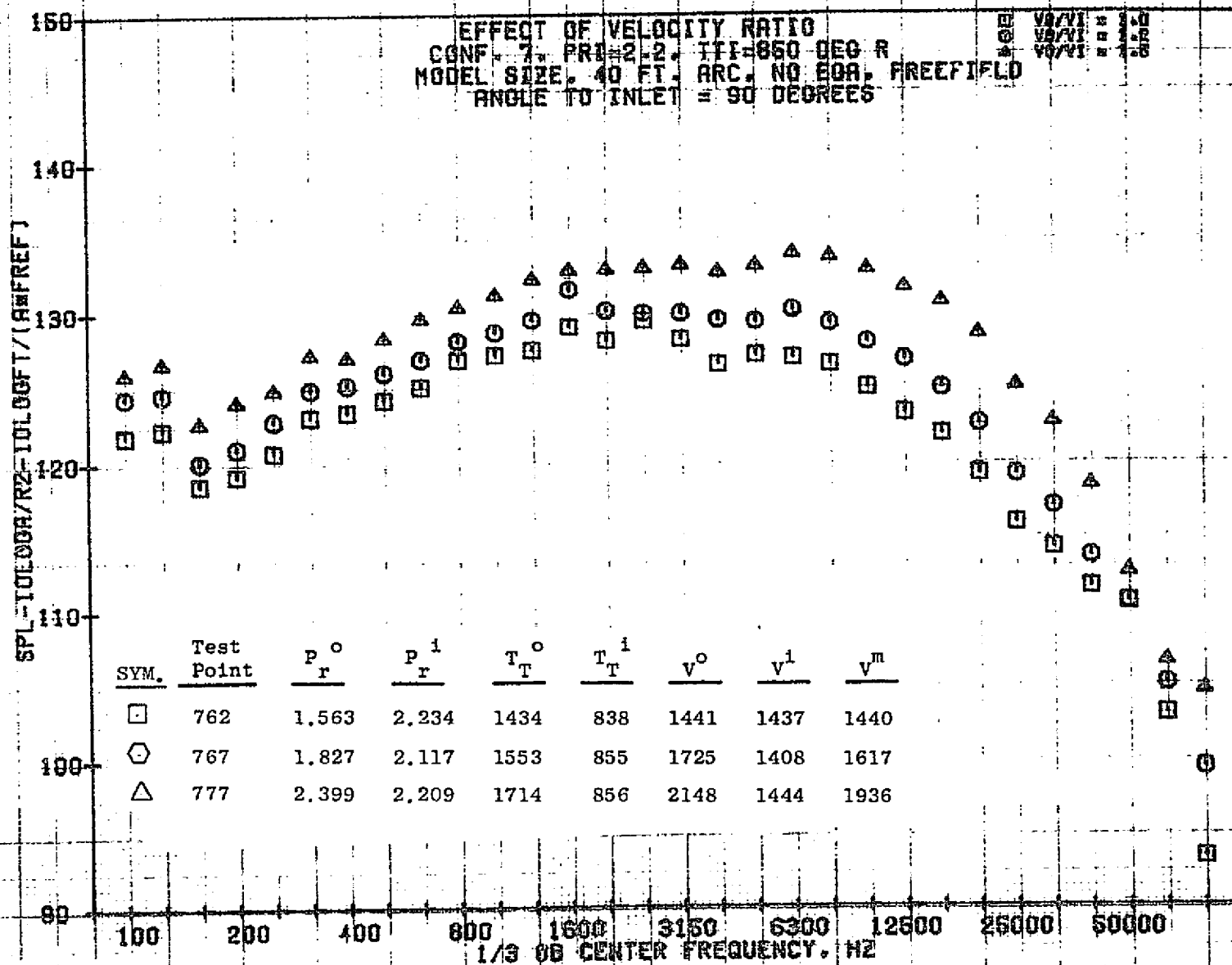


11/03/76
 18575-001

79 BURCH A.



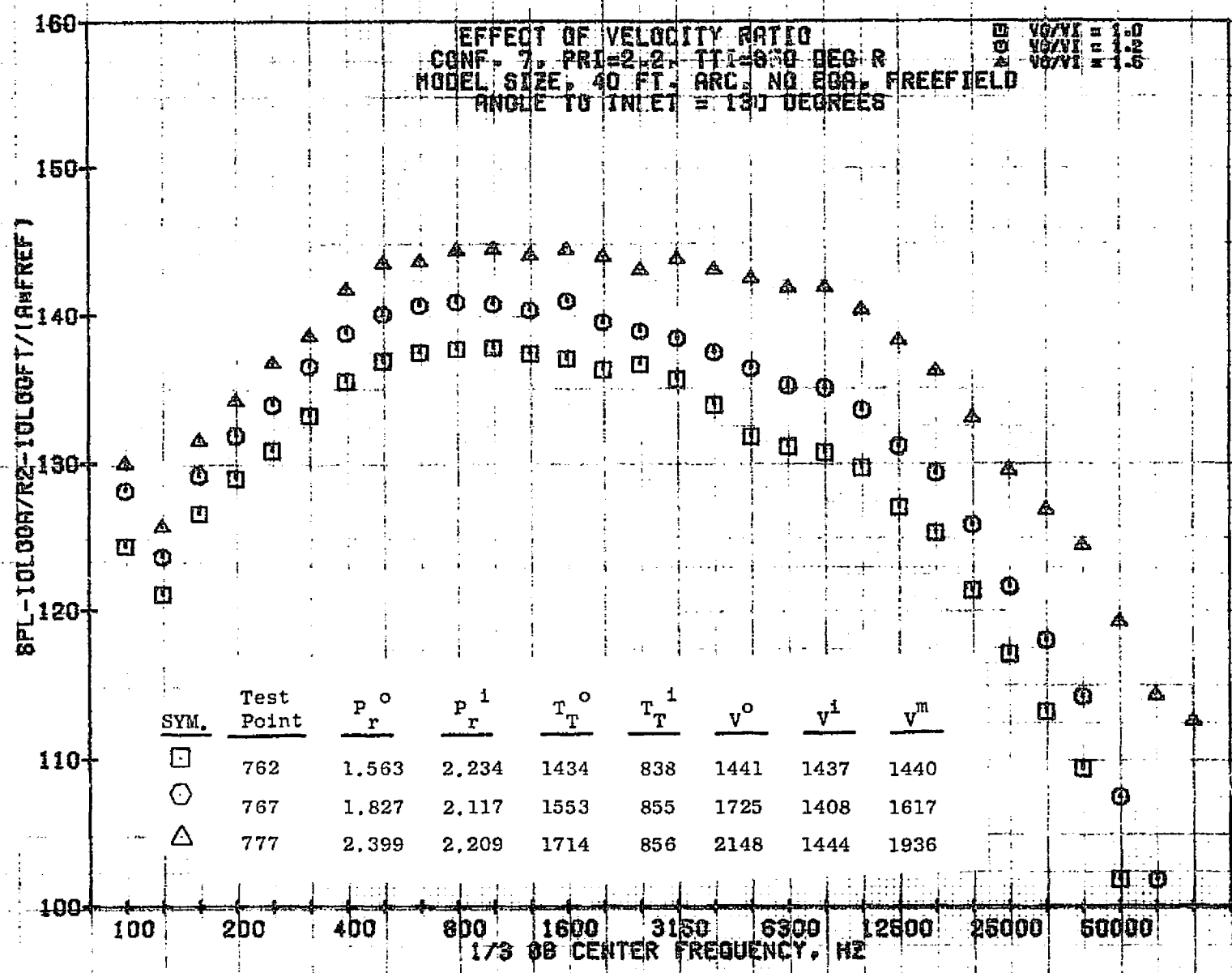
9611



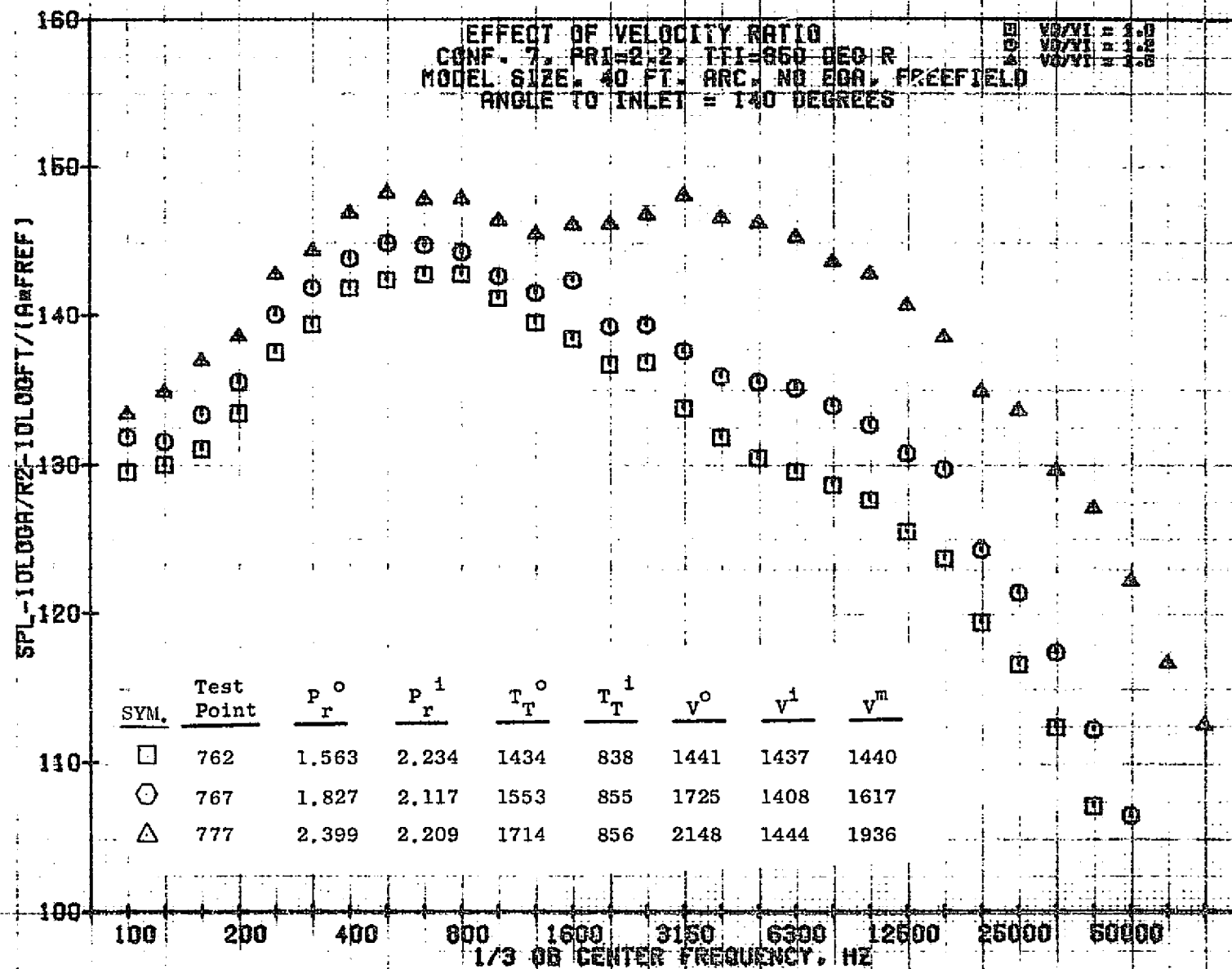
11/03/76
 18575-001

79 BURCH A.

2611

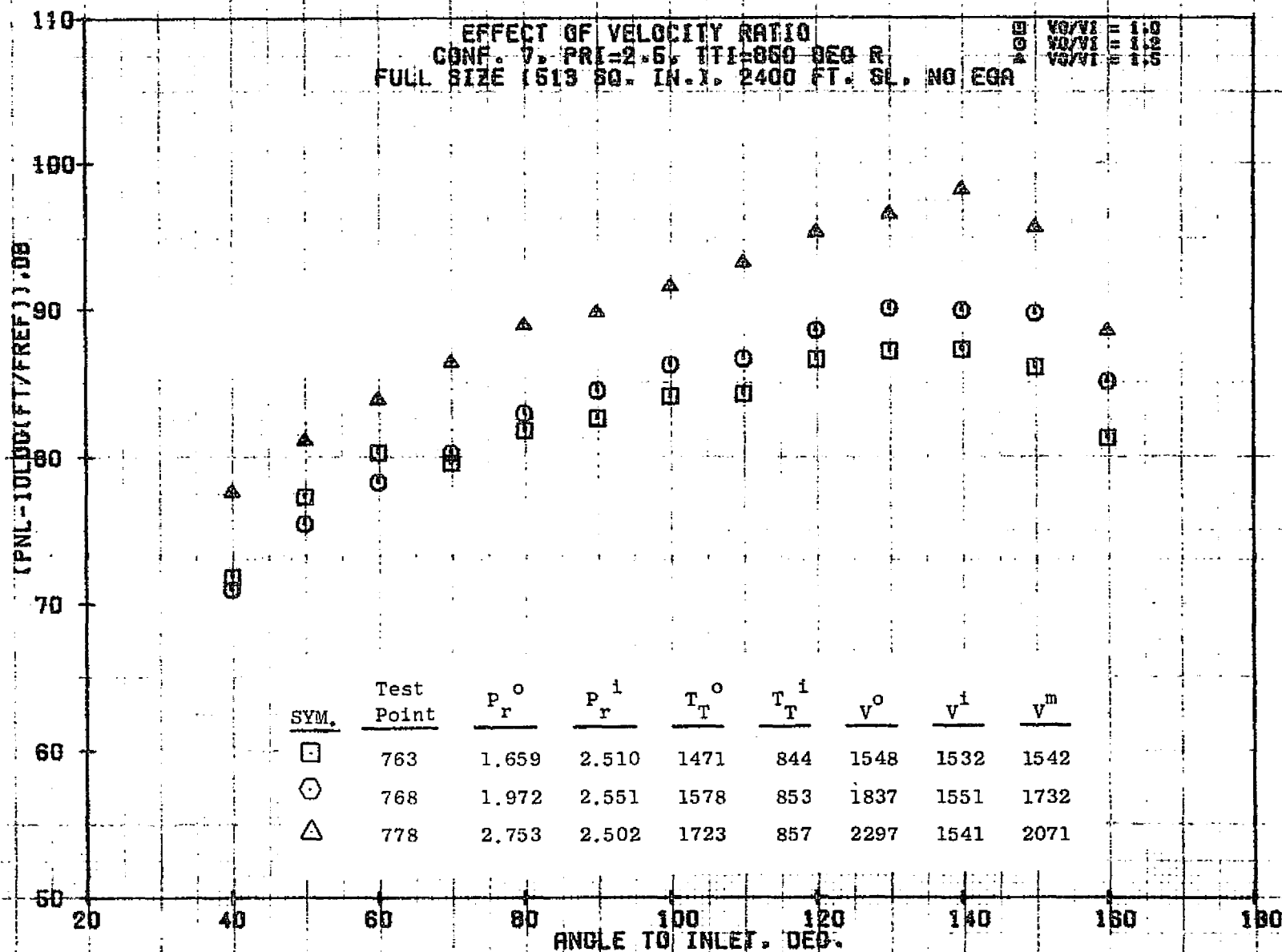


861E



11/03/76
 18575-001

79 BURCH A.

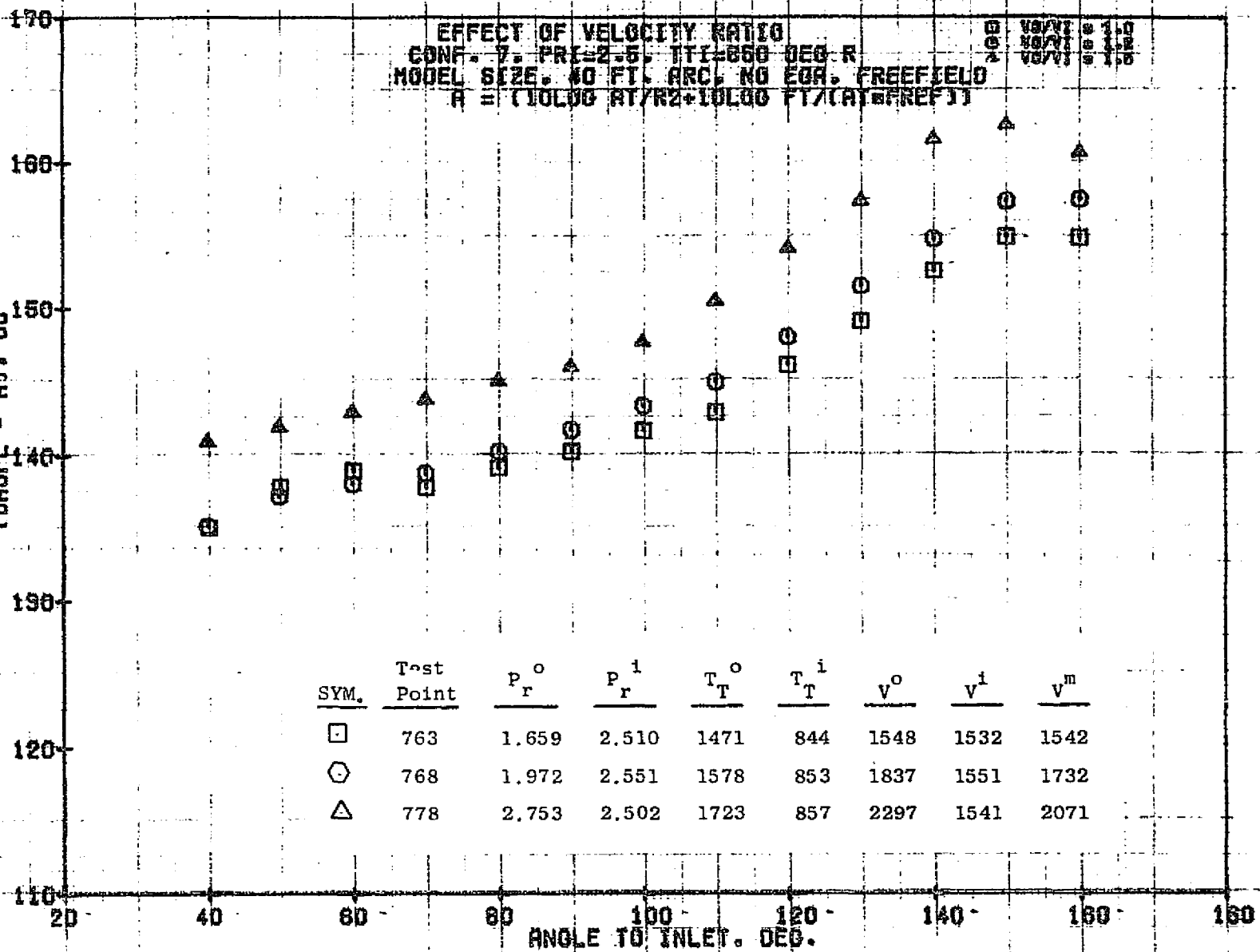


11/01/76
 18421-001

79 BURCH A.

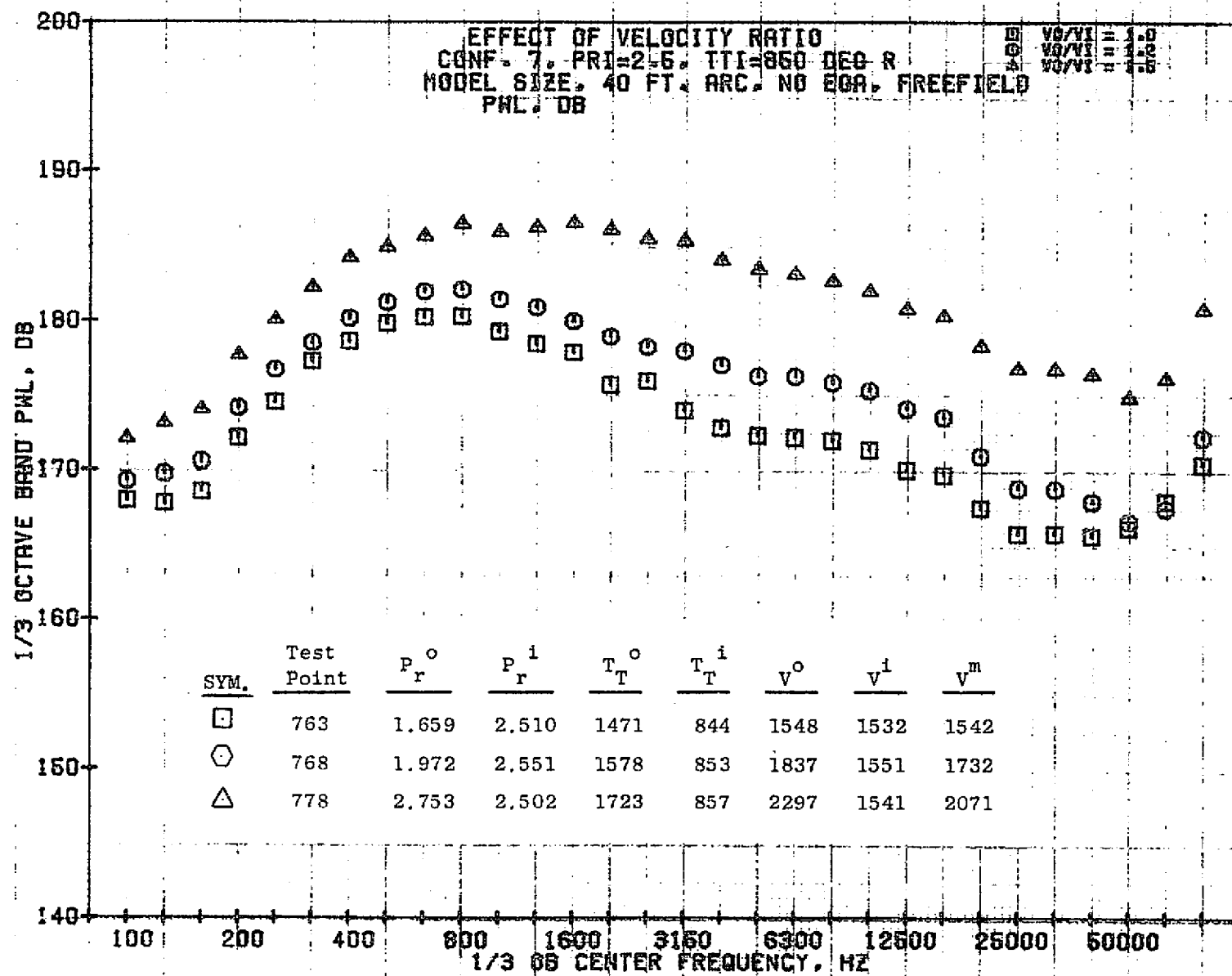
1200

TORSION - RJ. DB

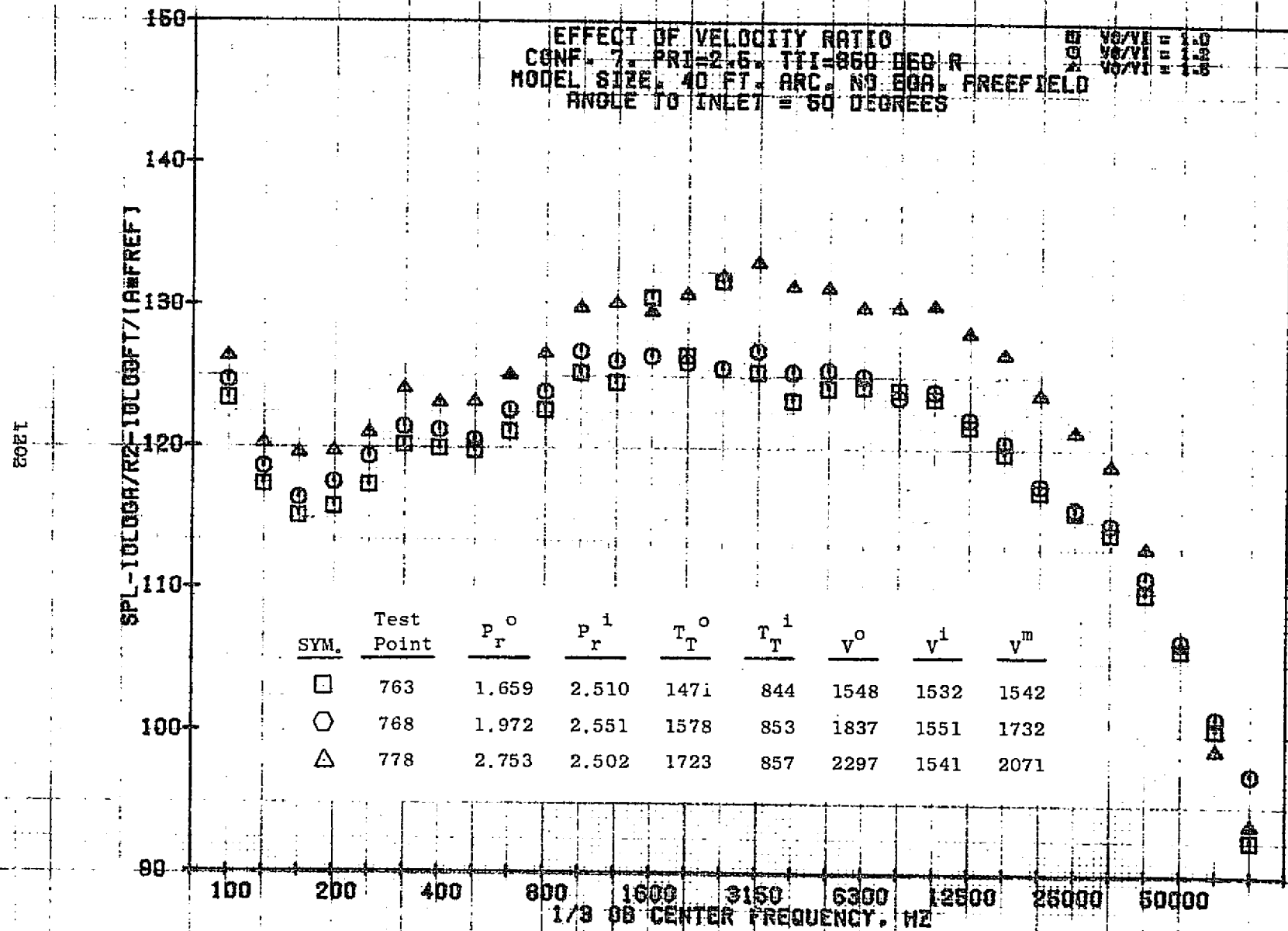
11/09/76
18336-001

79 AIRCH A.

1201


 11/03/76
 18675-001

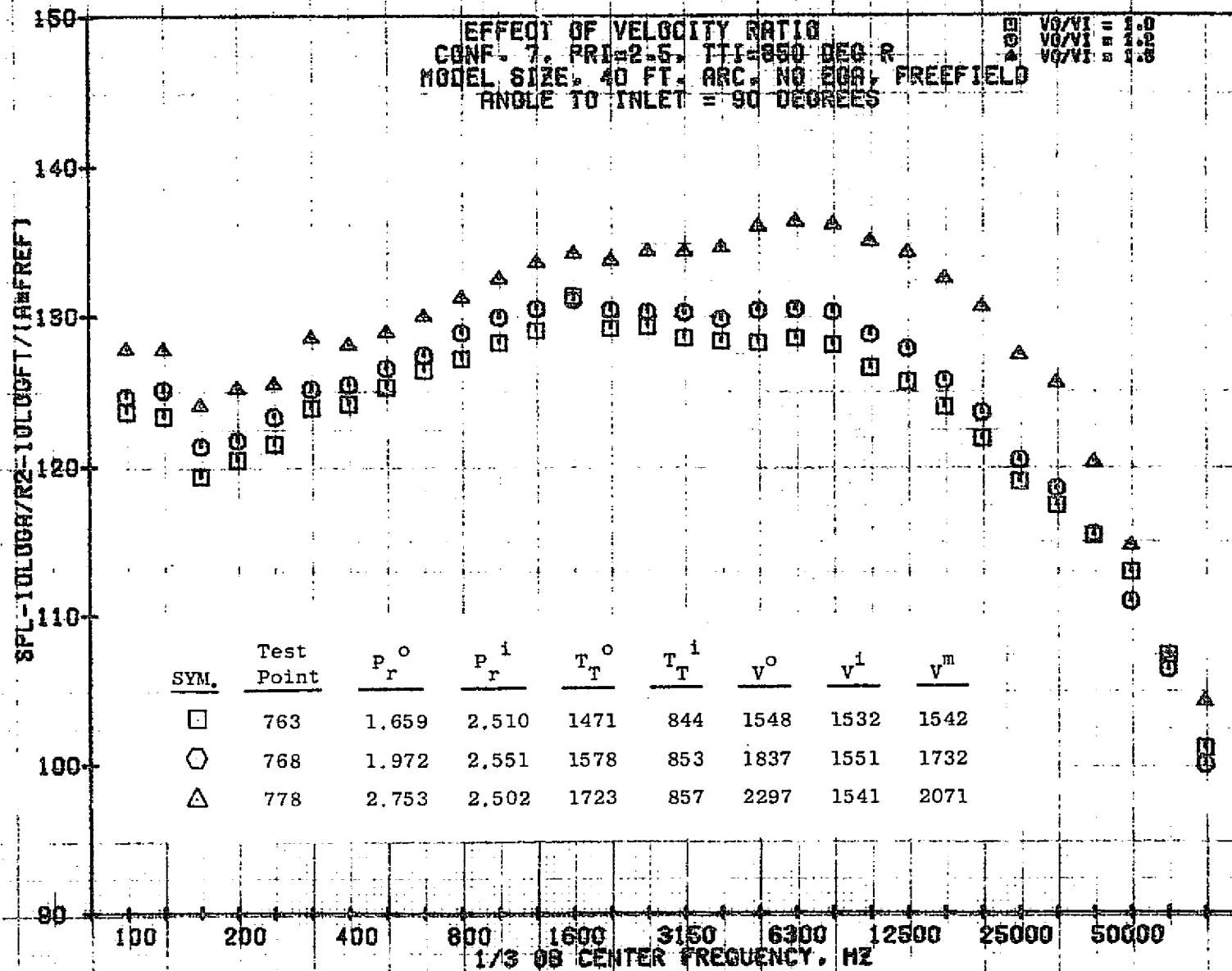
79 BURCH A.



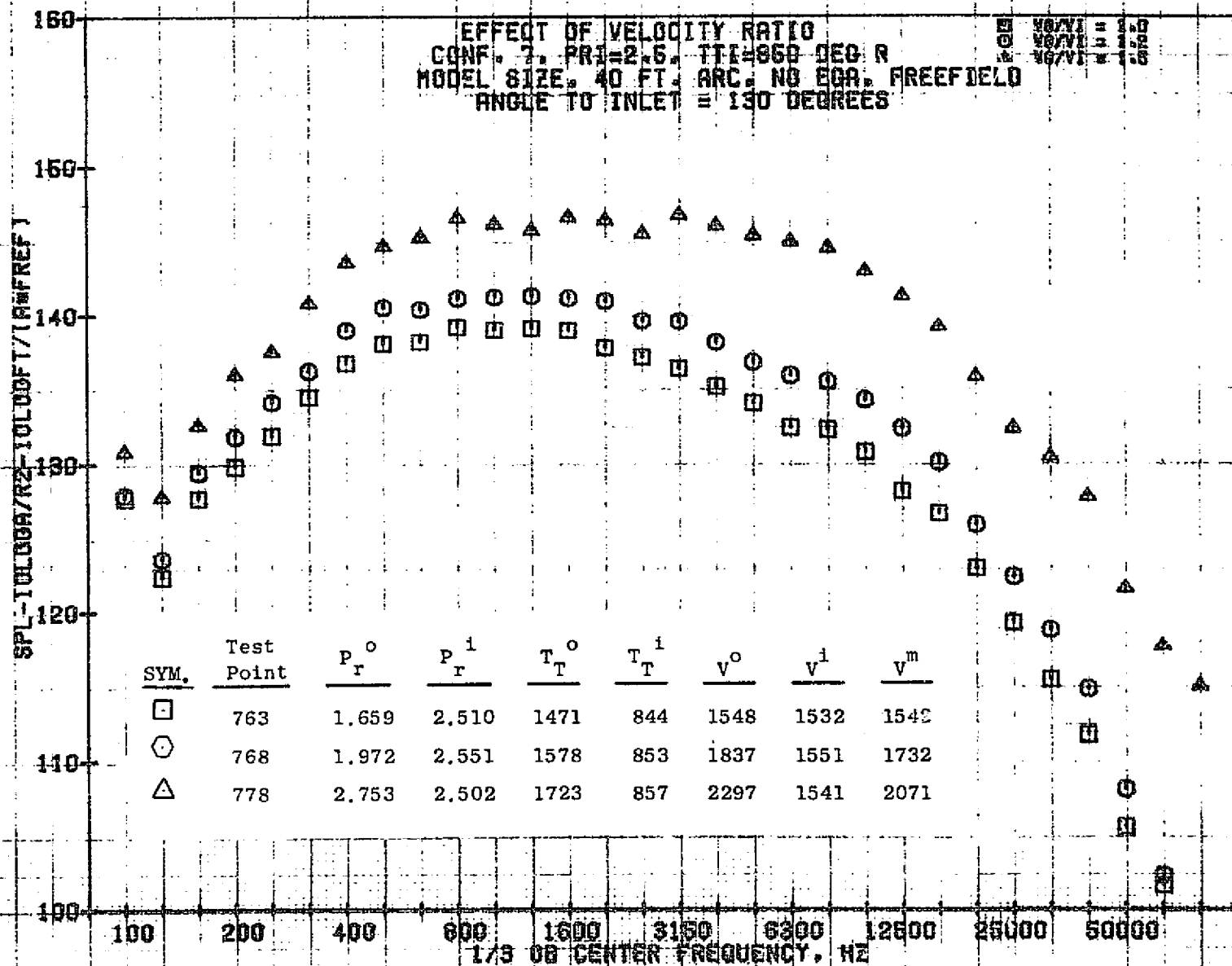
11/03/76
18575-001

79 BURCH A.

1208

11/03/76
18575-001

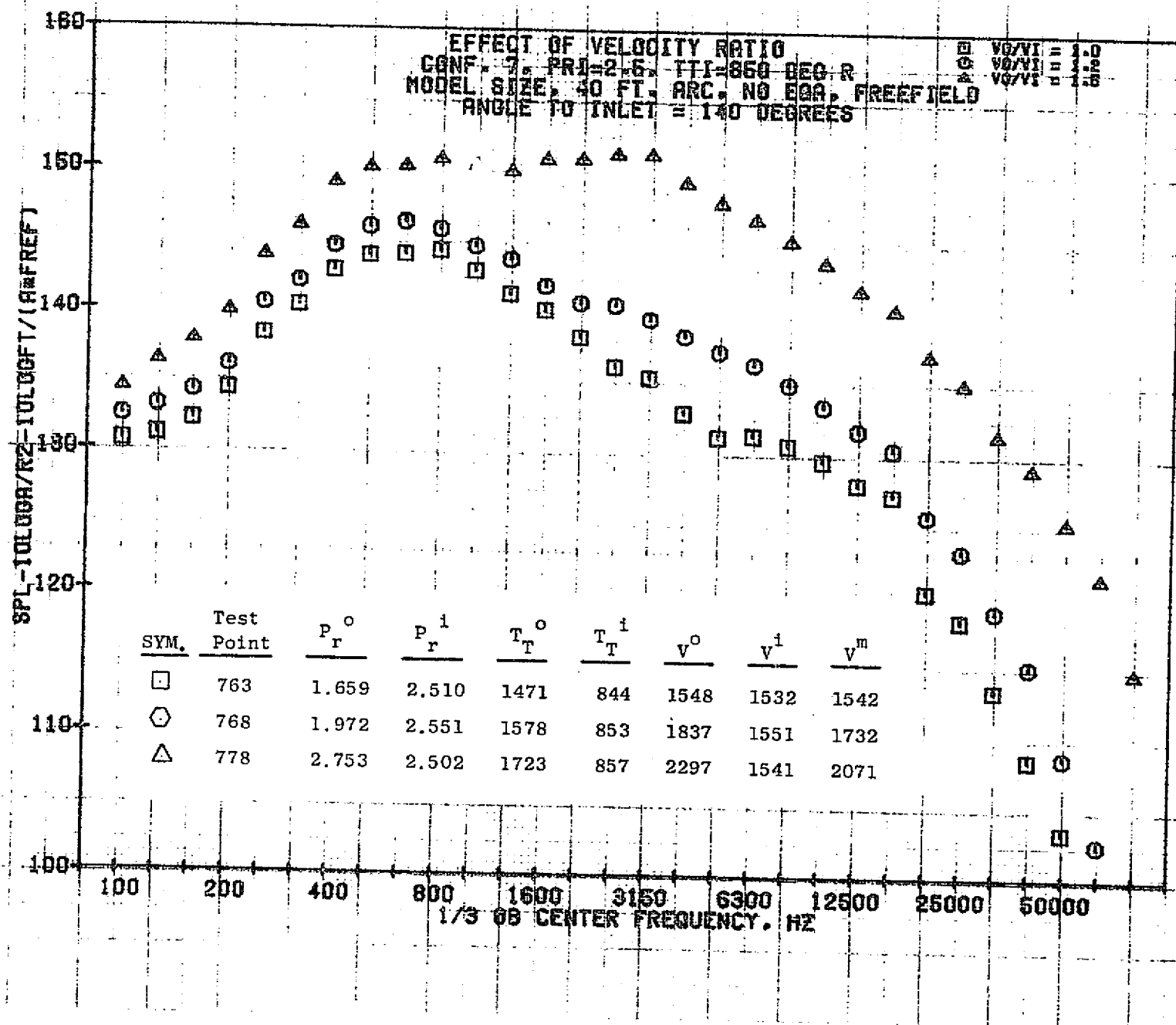
79 BURCH A.



11/03/76
18575-001

79 BURCH A.

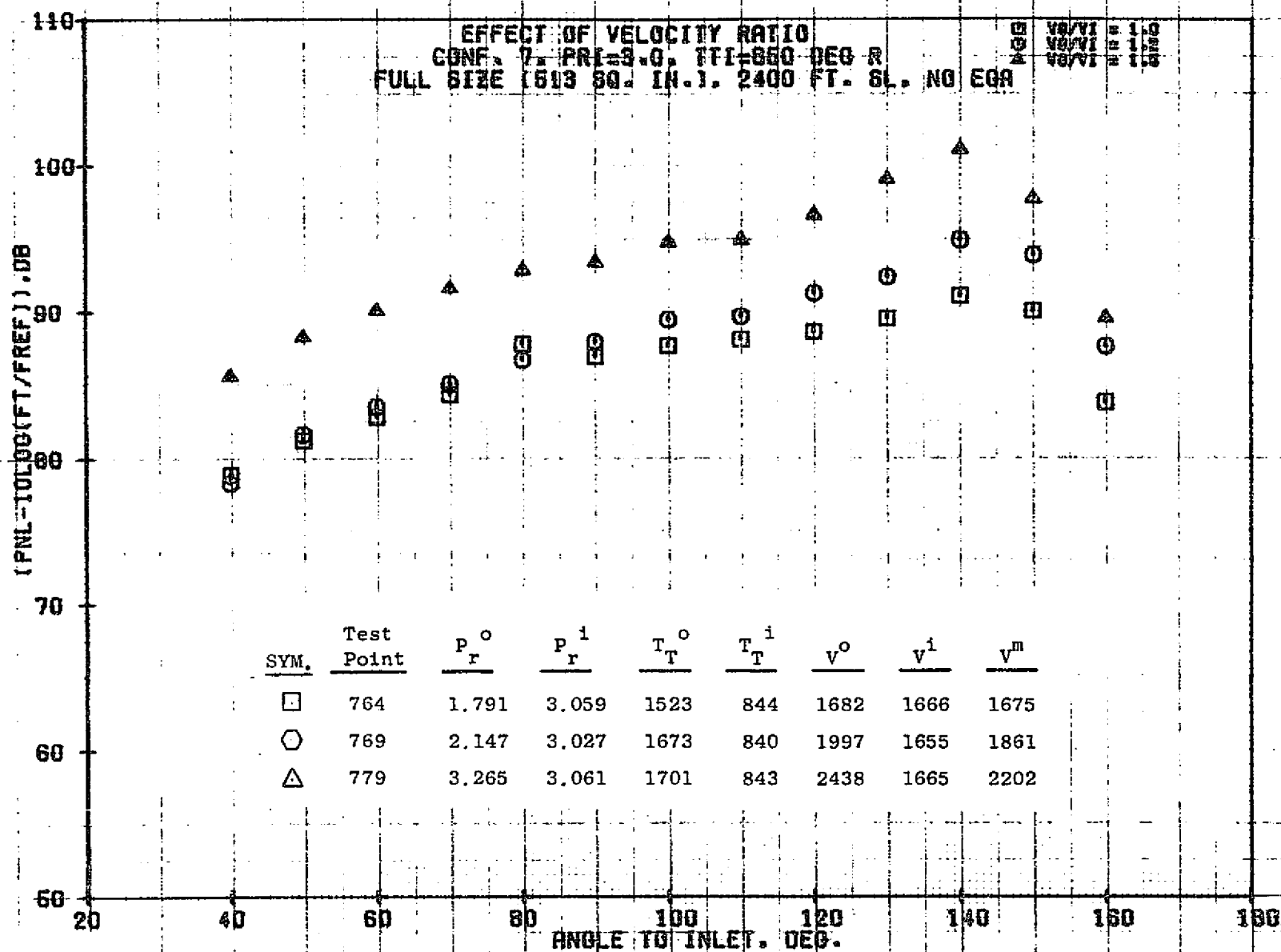
1205



11/03/76
 1B575-001

79 BURCH A.

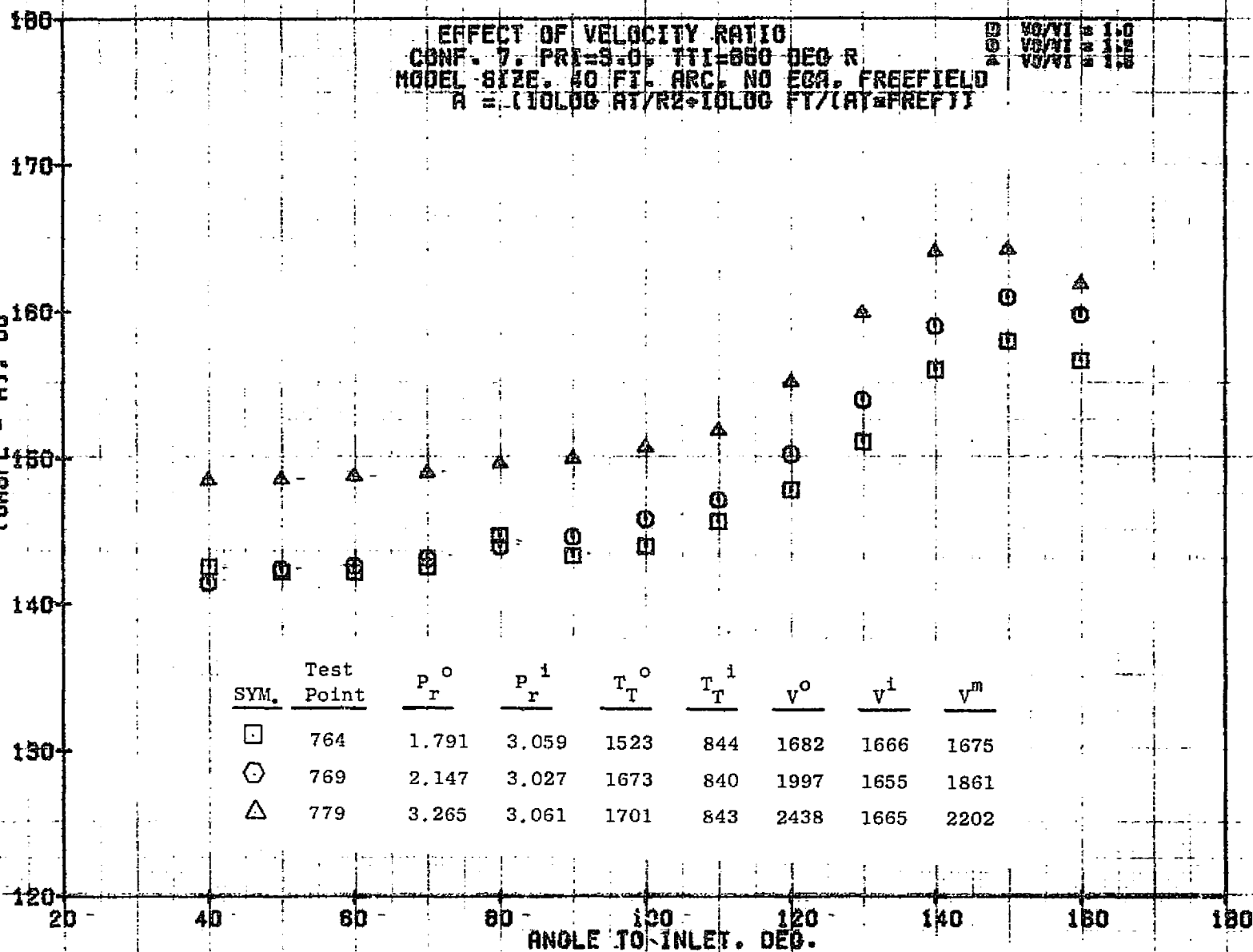
1P08


 11/01/76
 18421-001

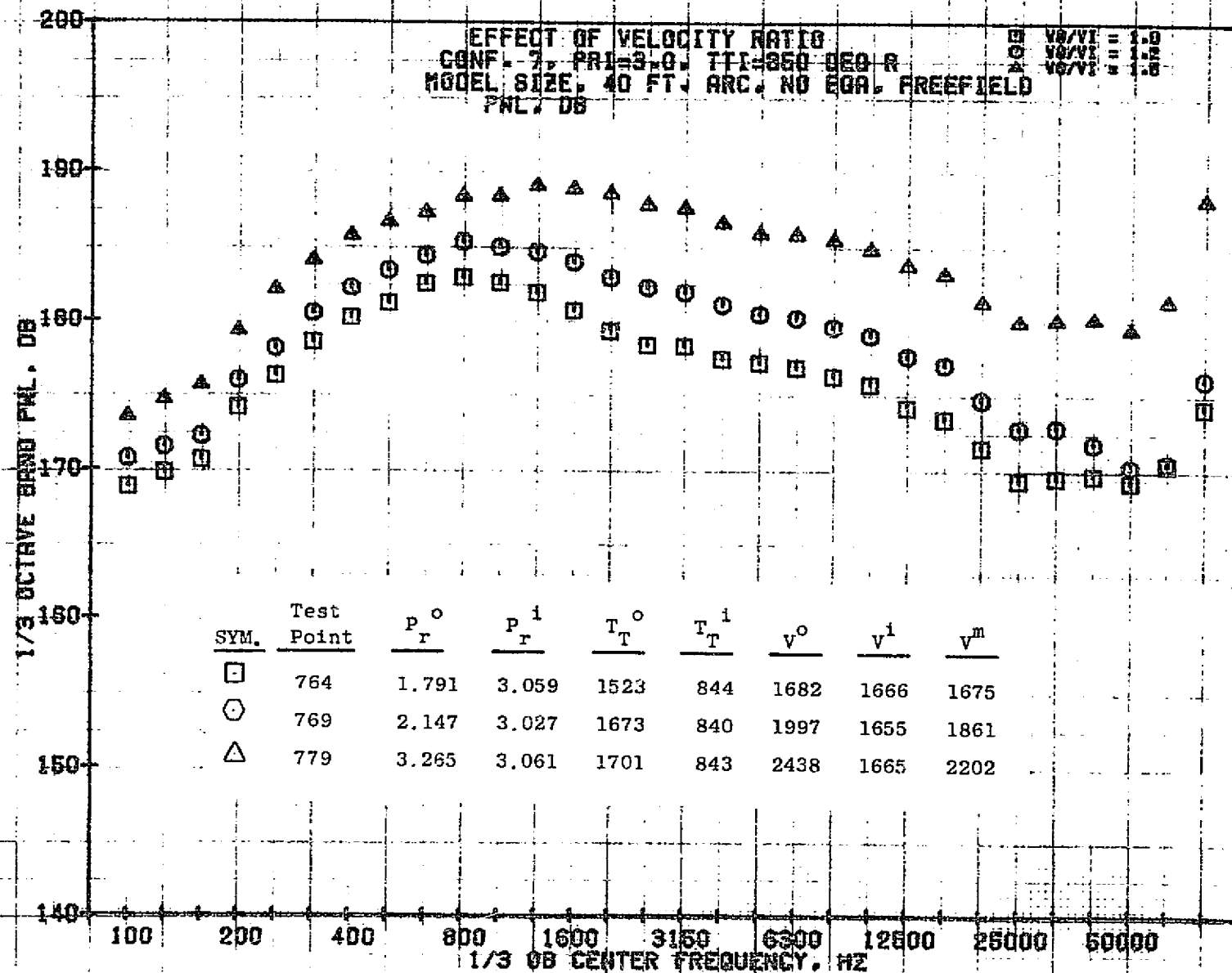
79 BURCH A.

1207

SPL. DB - AJ. DB

11/09/76
18736-001

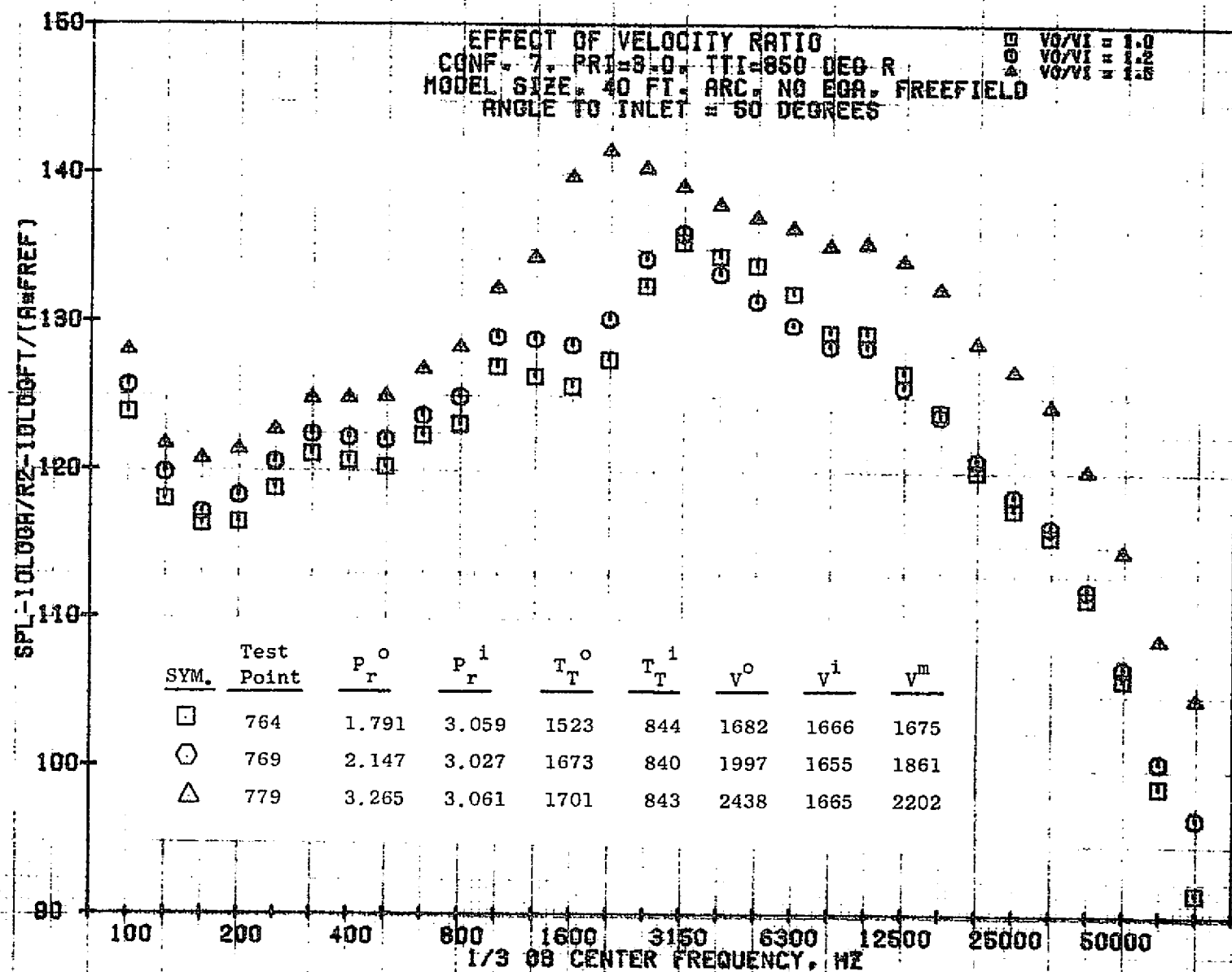
79 AIRCRAFT



11/03/76
18575-001

79 BURCH A.

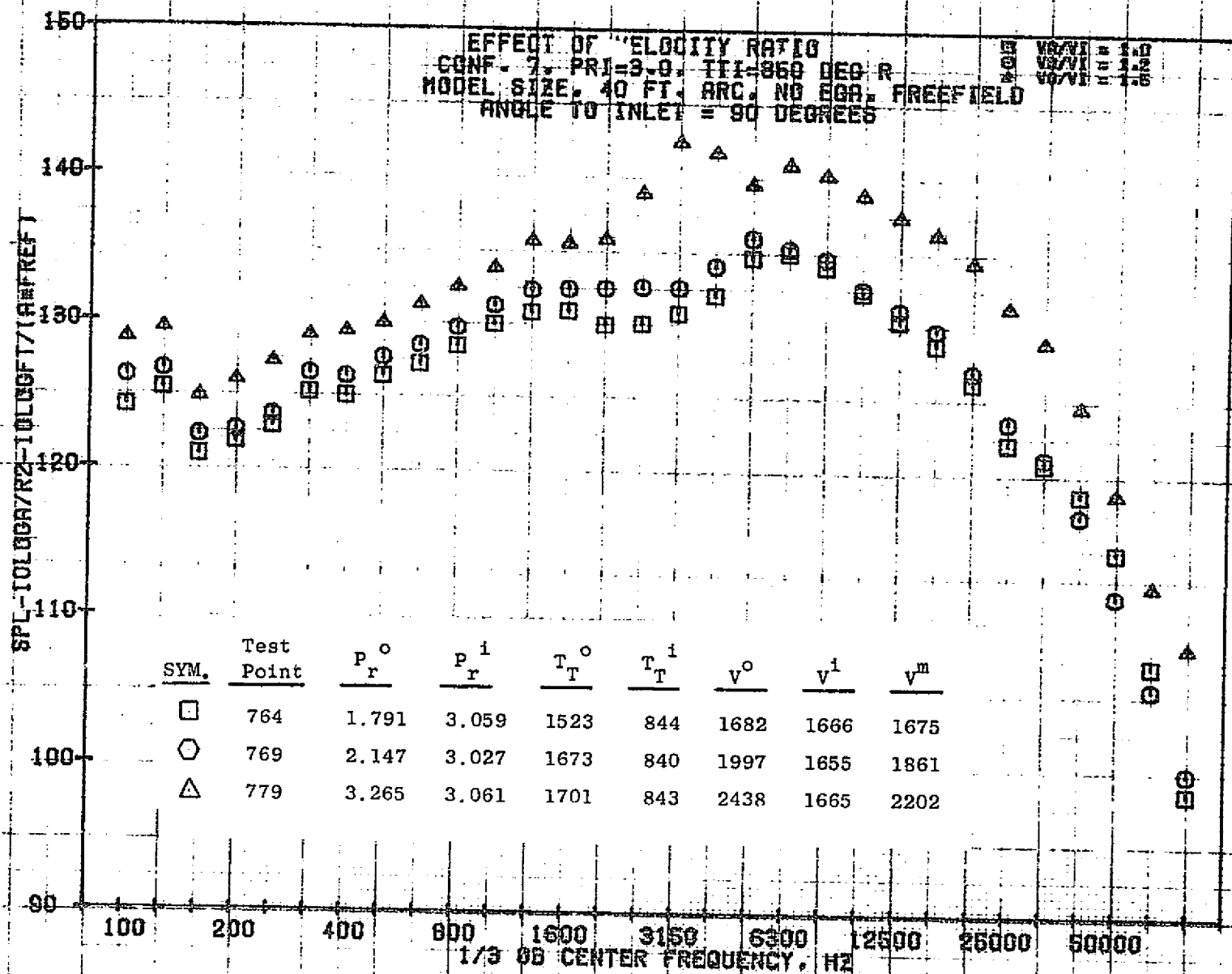
1209



11/03/76
 18575-001

79 BURCH A.

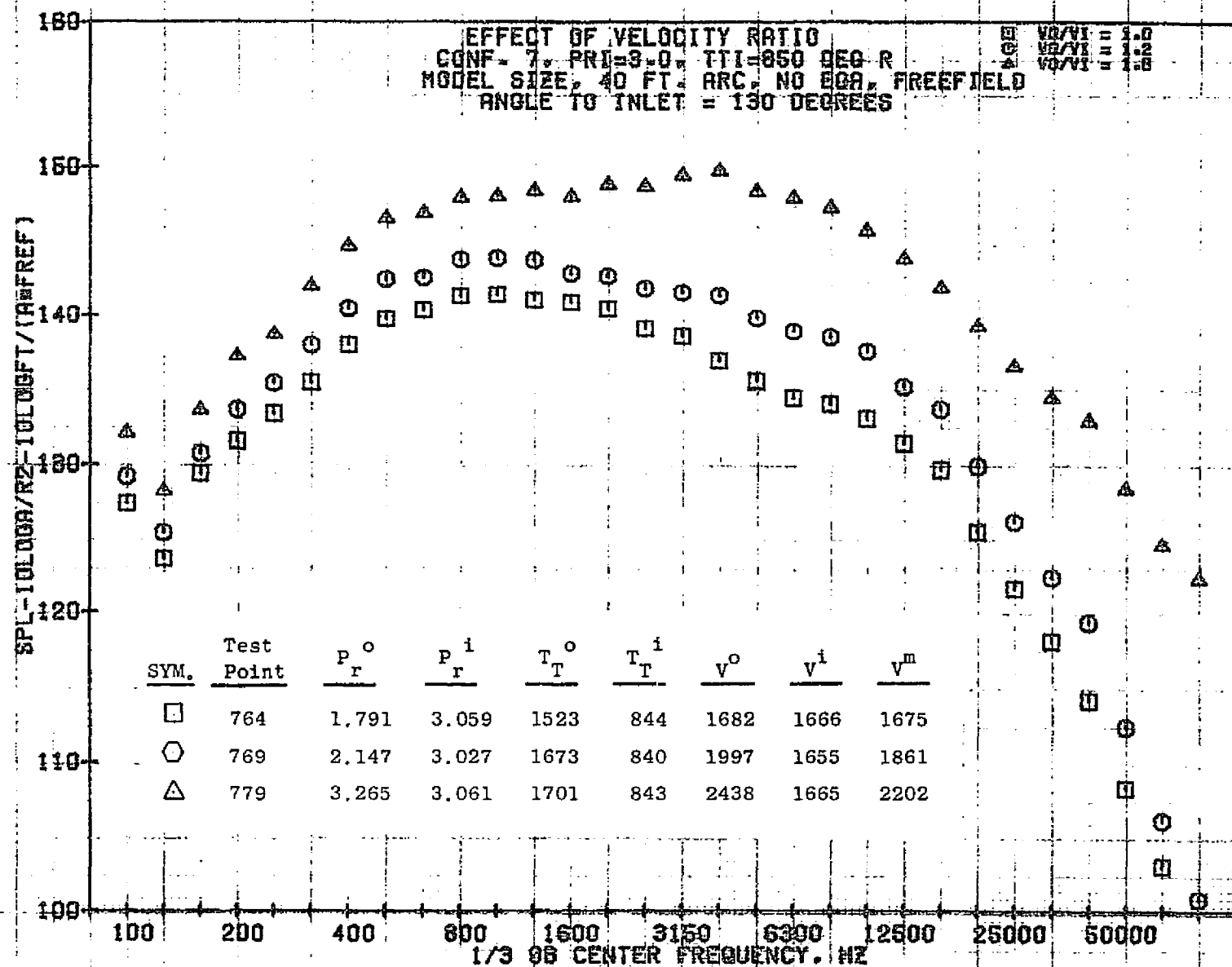
1210



11/03/76
 18575-001

79 BURCH A.

1211



11/03/76
18575-001

79 BURCH A.

1212

SPL-10LOGA/RZ-10LOGT/(A/RREF)

EFFECT OF VELOCITY RATIO
 CONF. 7, PRI=3.0, TTI=360 DEG R
 MODEL SIZE, 40 FT. ARC, NO EBA, FREEFIELD
 ANGLE TO INLET = 140 DEGREES

□ $V_0/V_1 = 1.0$
 ○ $V_0/V_1 = 1.2$
 △ $V_0/V_1 = 1.5$

SYM.	Test Point	P_r^0	P_r^1	T_T^0	T_T^1	V^0	V^1	V^m
□	764	1.791	3.059	1523	844	1682	1666	1675
○	769	2.147	3.027	1673	840	1997	1655	1861
△	779	3.265	3.061	1701	843	2438	1665	2202

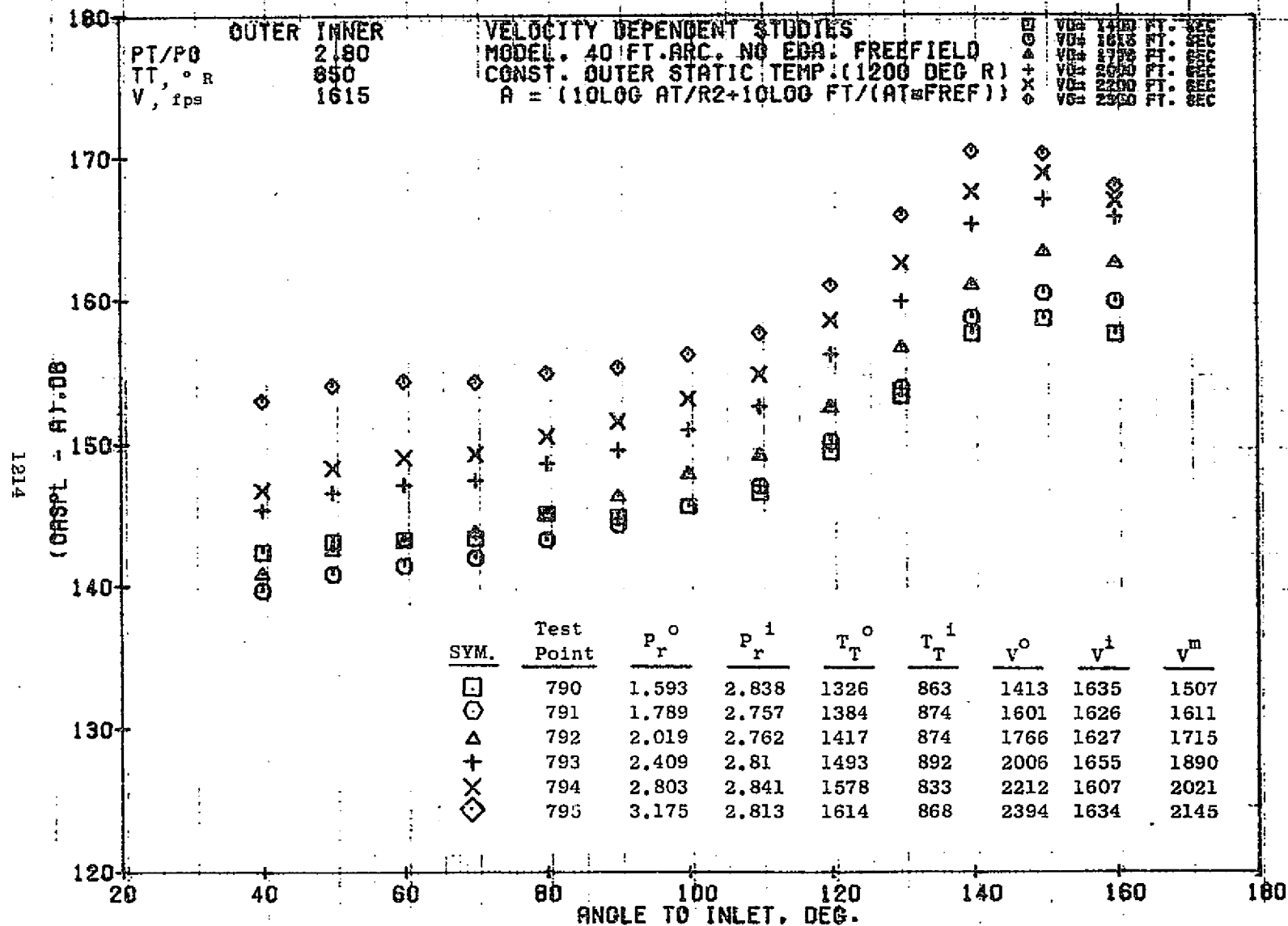
110 100 200 400 800 1600 3160 6300 12600 25000 50000
 1/3 OR CENTER FREQUENCY, HZ

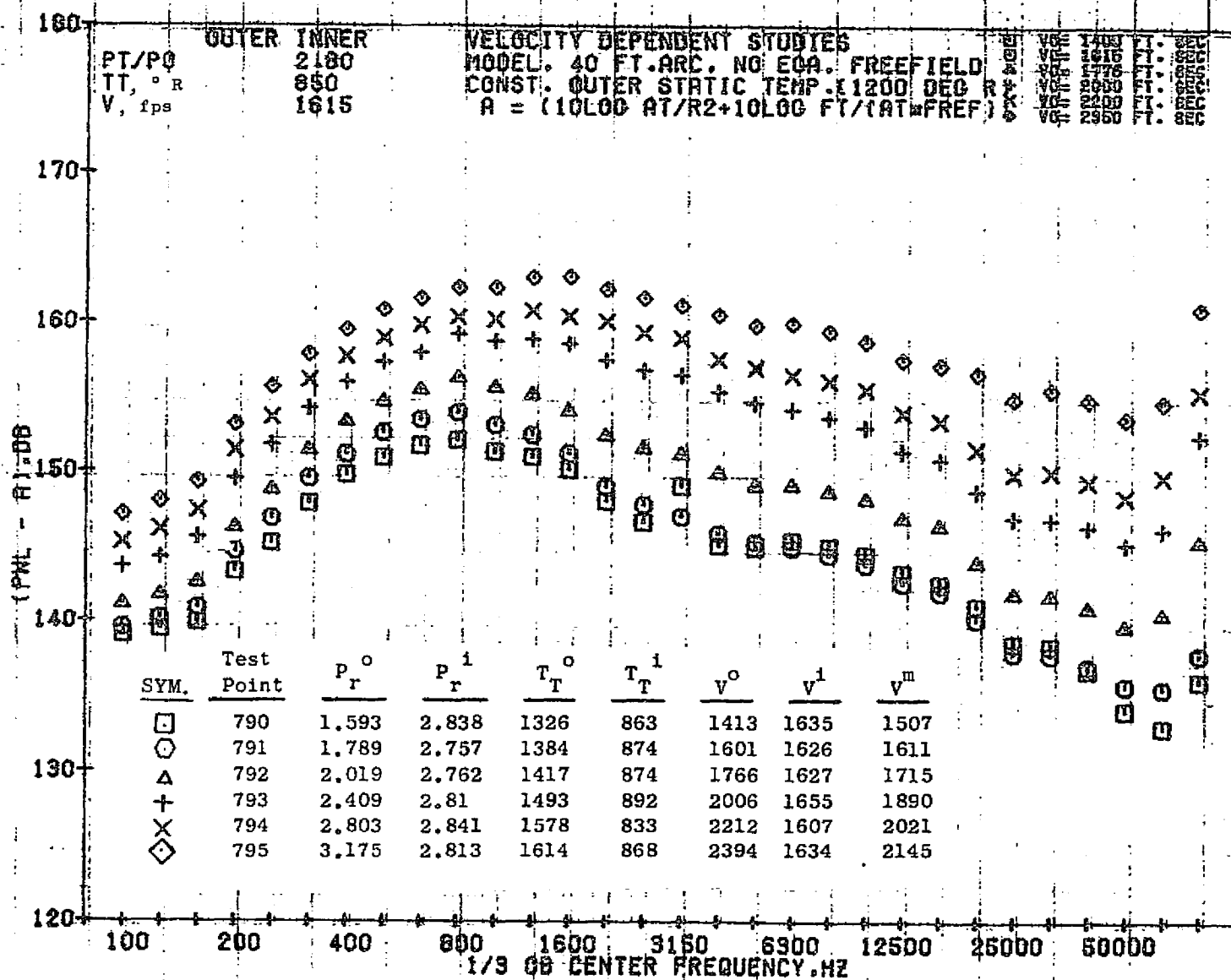
11/03/76
 18575-001

79 BURCH A.

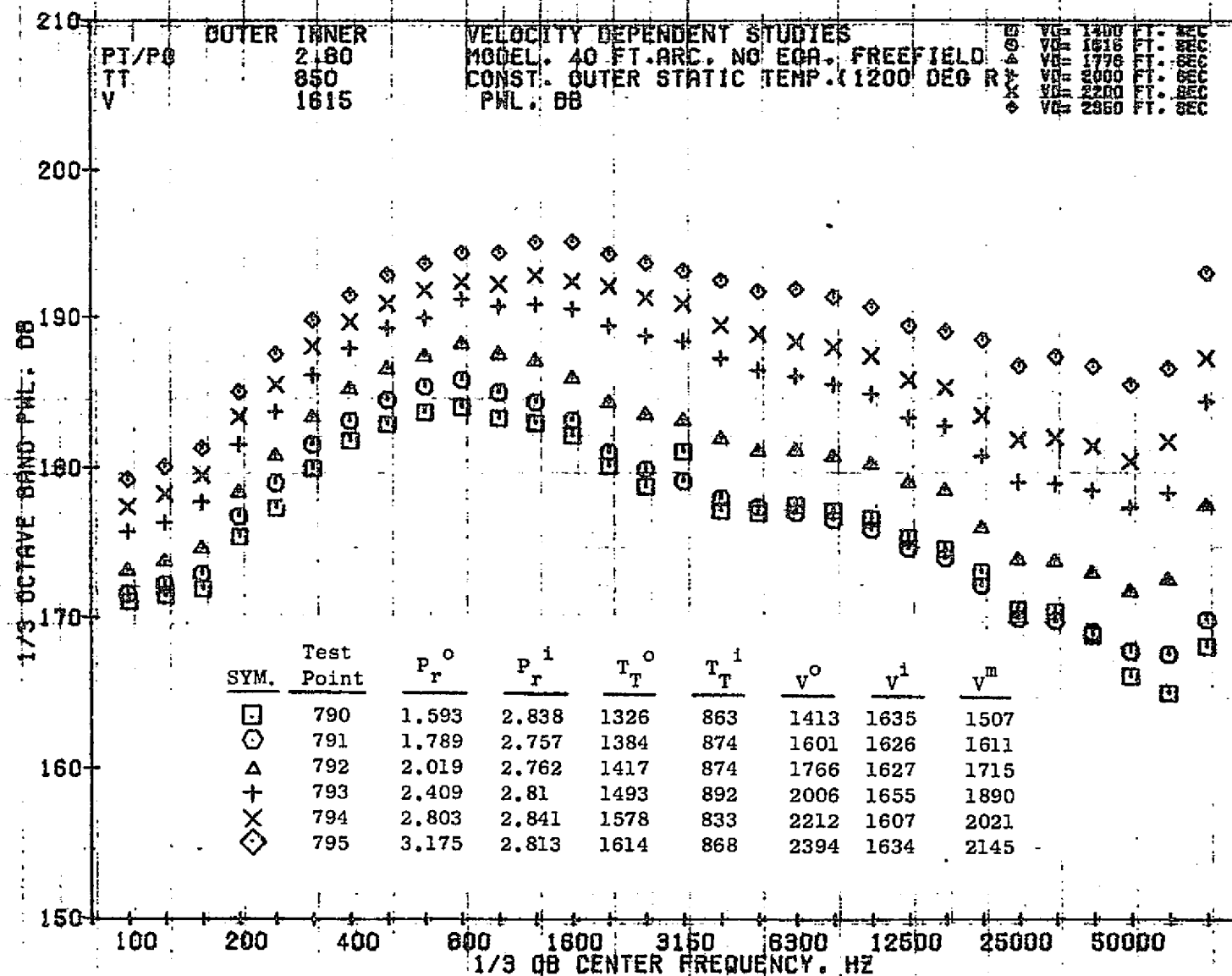
7.4.7 Velocity Dependence Study

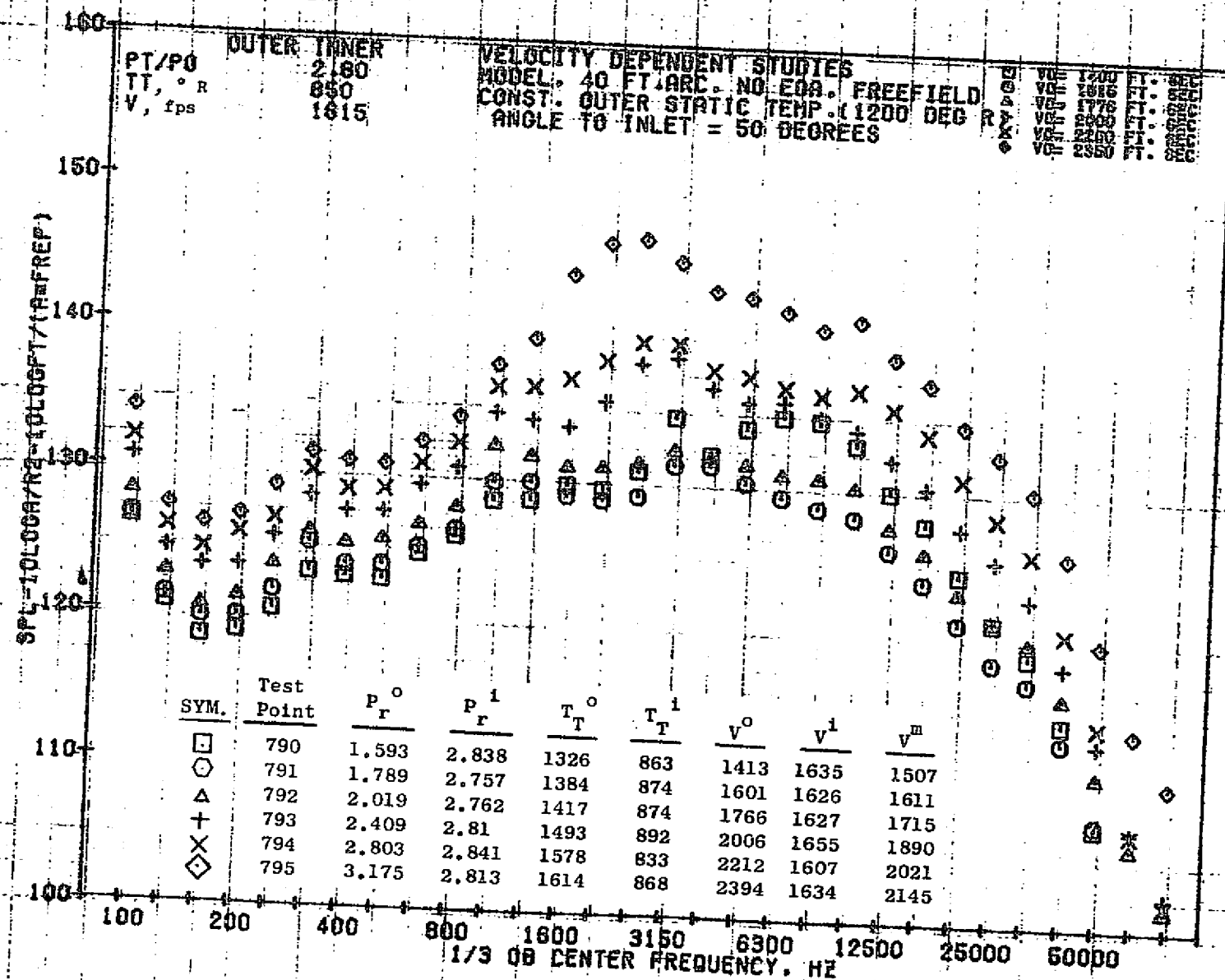
For Configuration 7, a series of tests was run to examine the velocity dependence of a high inner flow annular nozzle. Seven test points were taken at constant inner flow conditions and constant outer stream static temperature. The outer stream velocity was varied from point to point. The results are presented in this section.



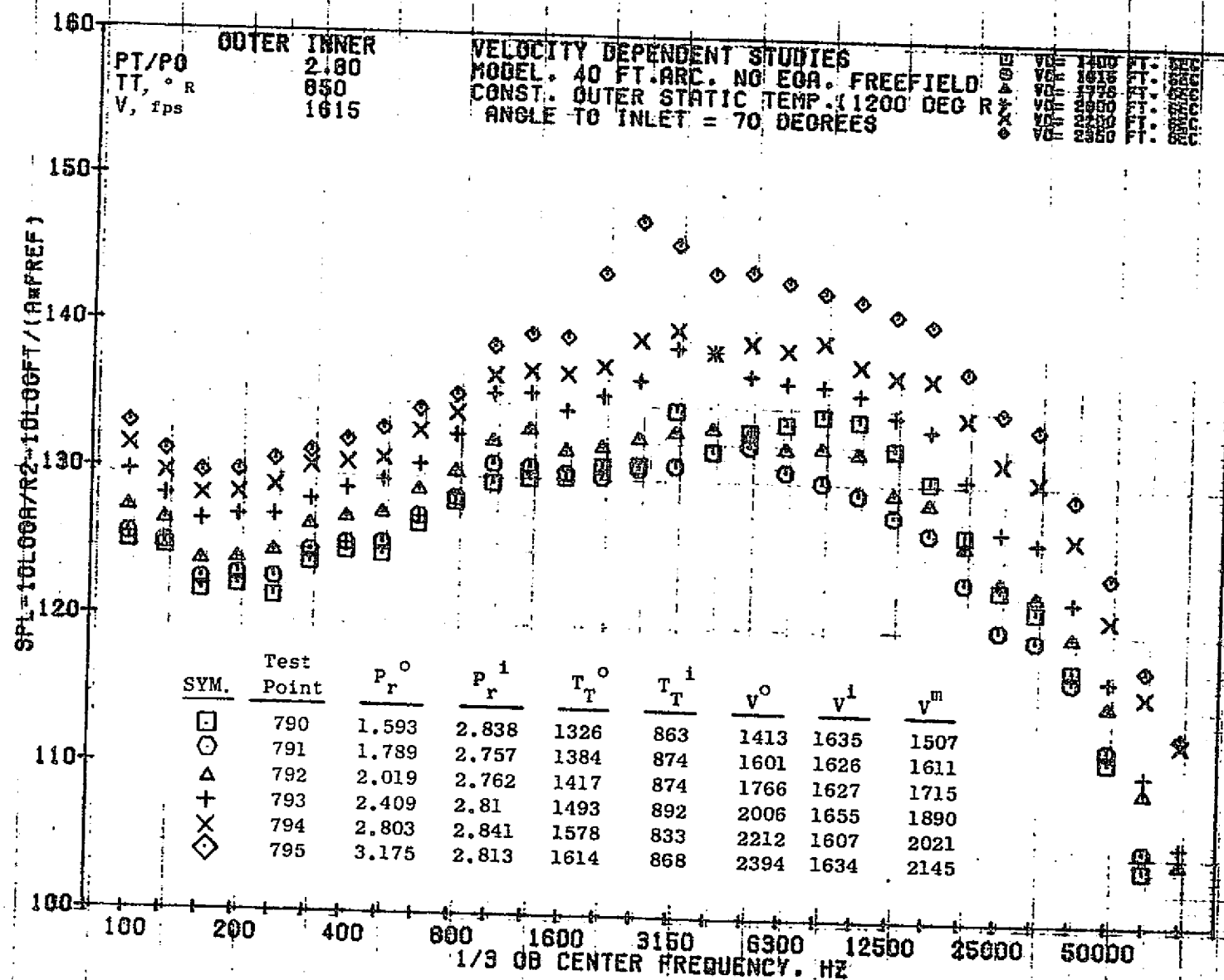


1216

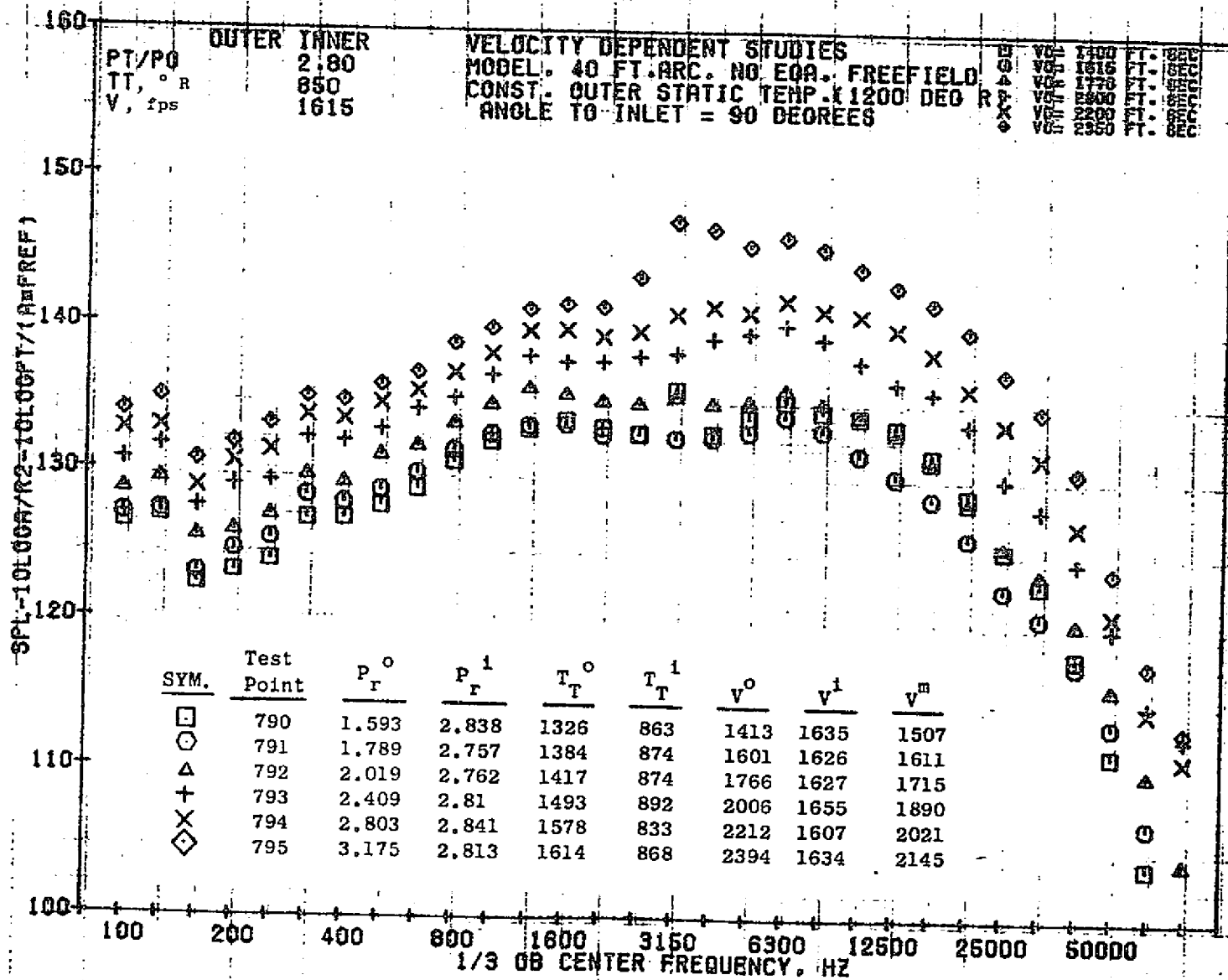




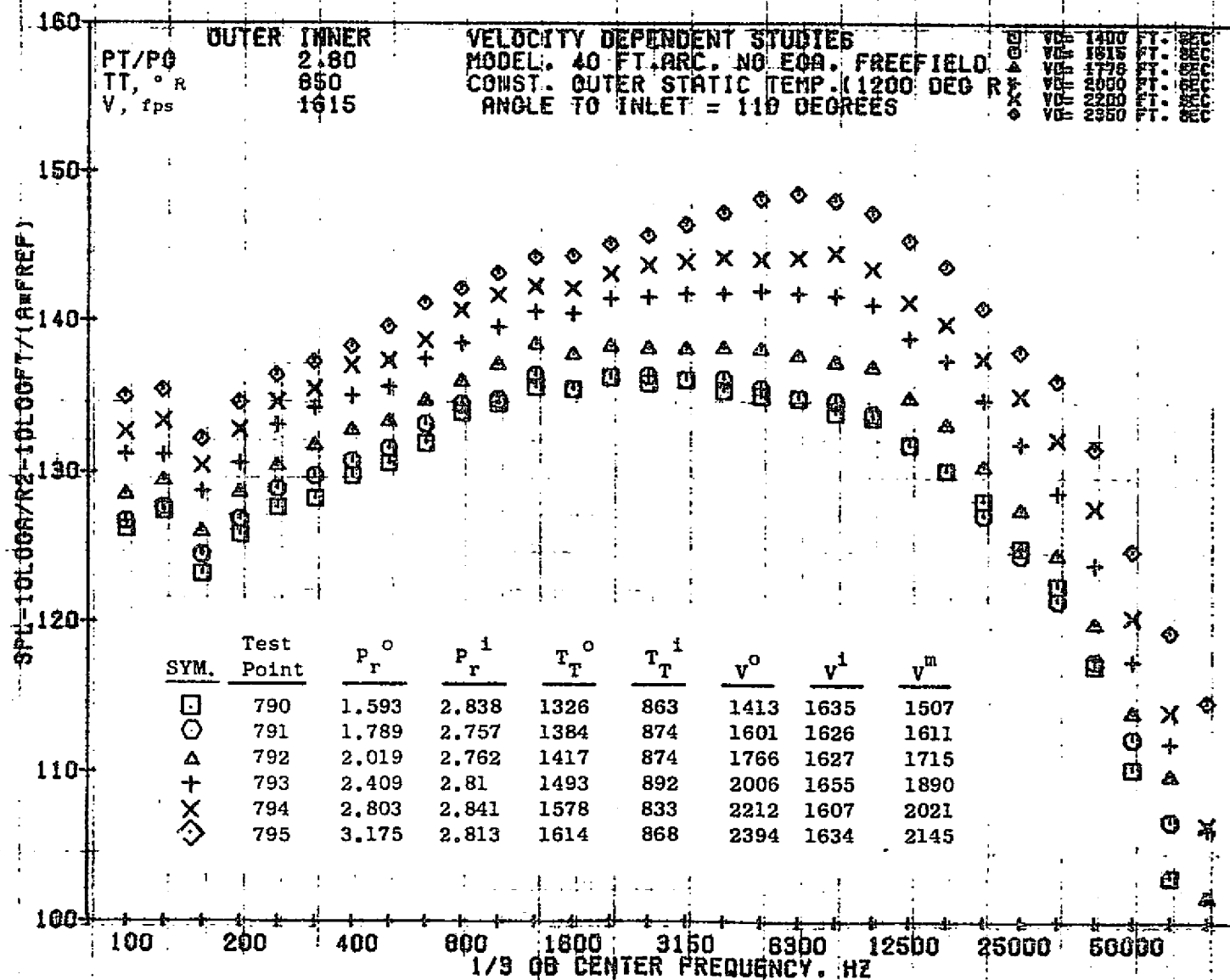
1218

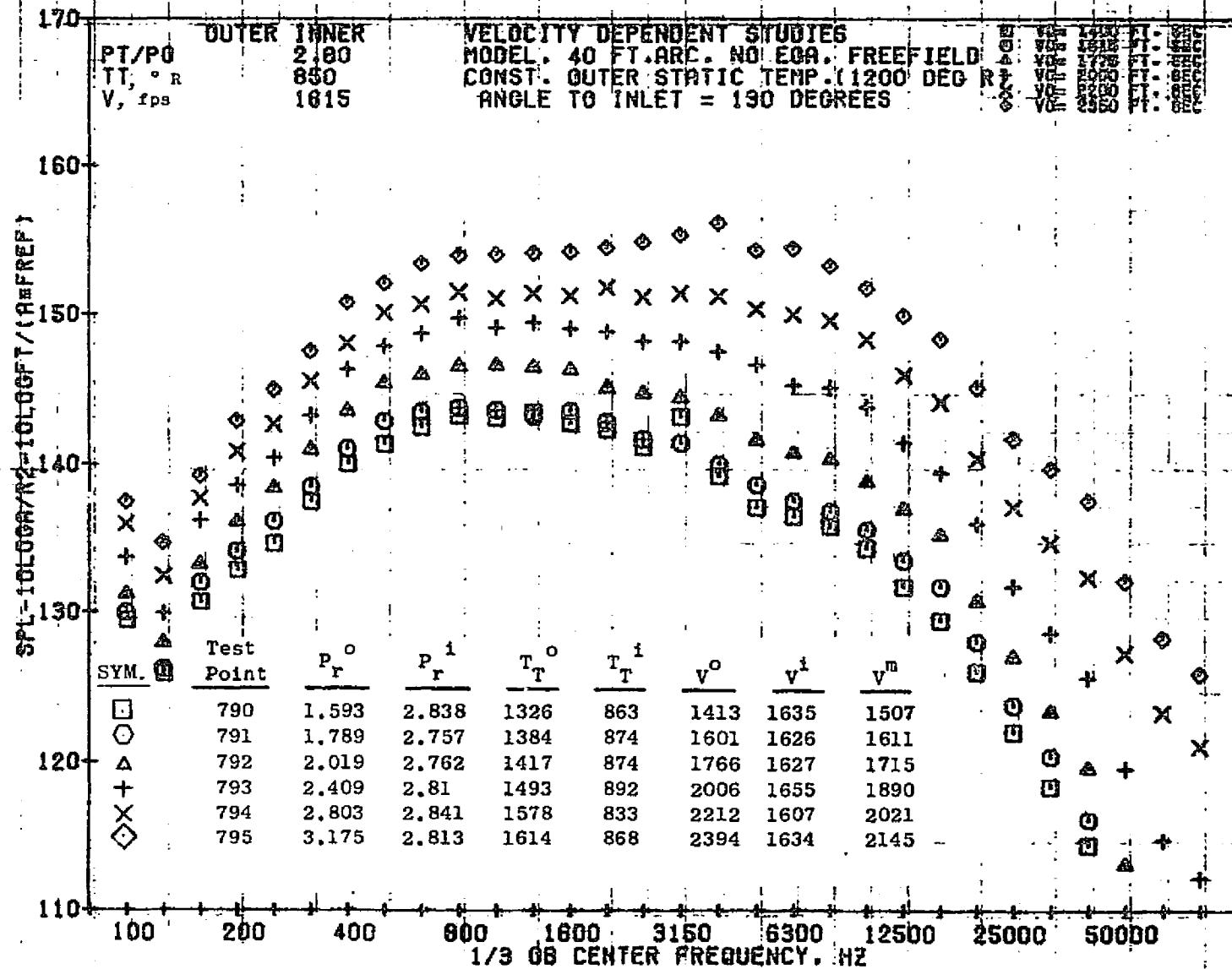


1219



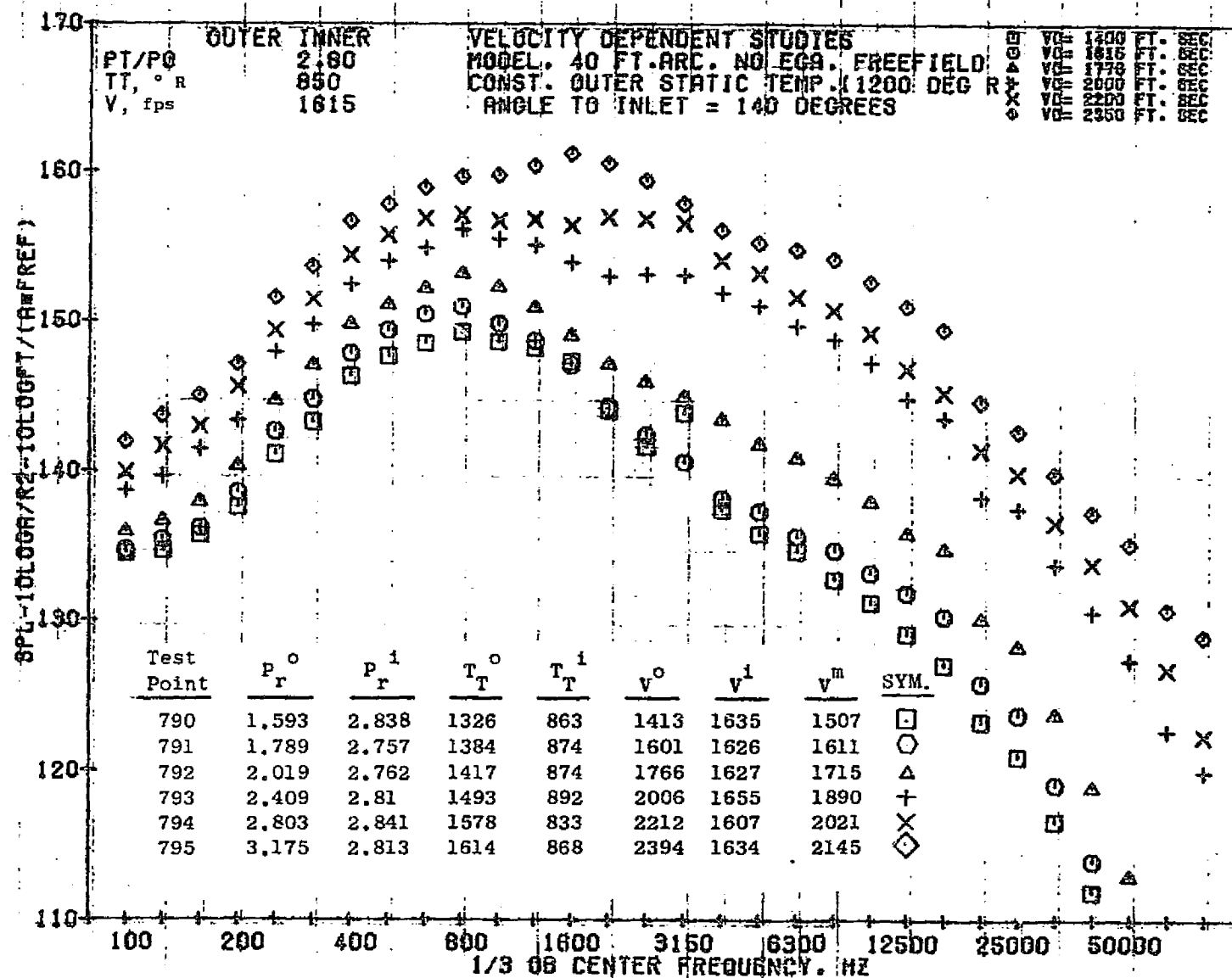
1220





10/13/76
1X930-001

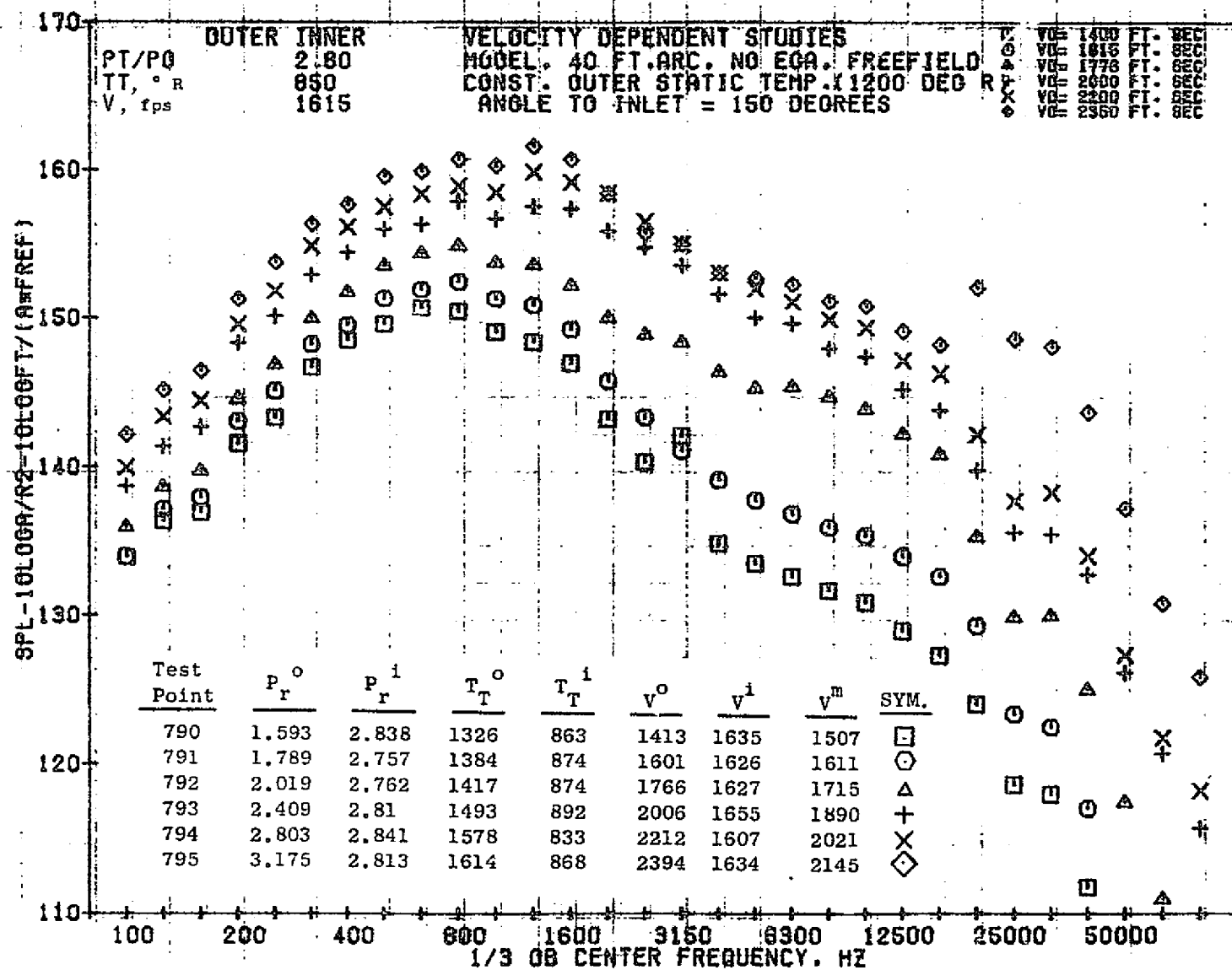
73KOLLSTEDT



10/13/76
1X930-001

73KOLLSTEDT

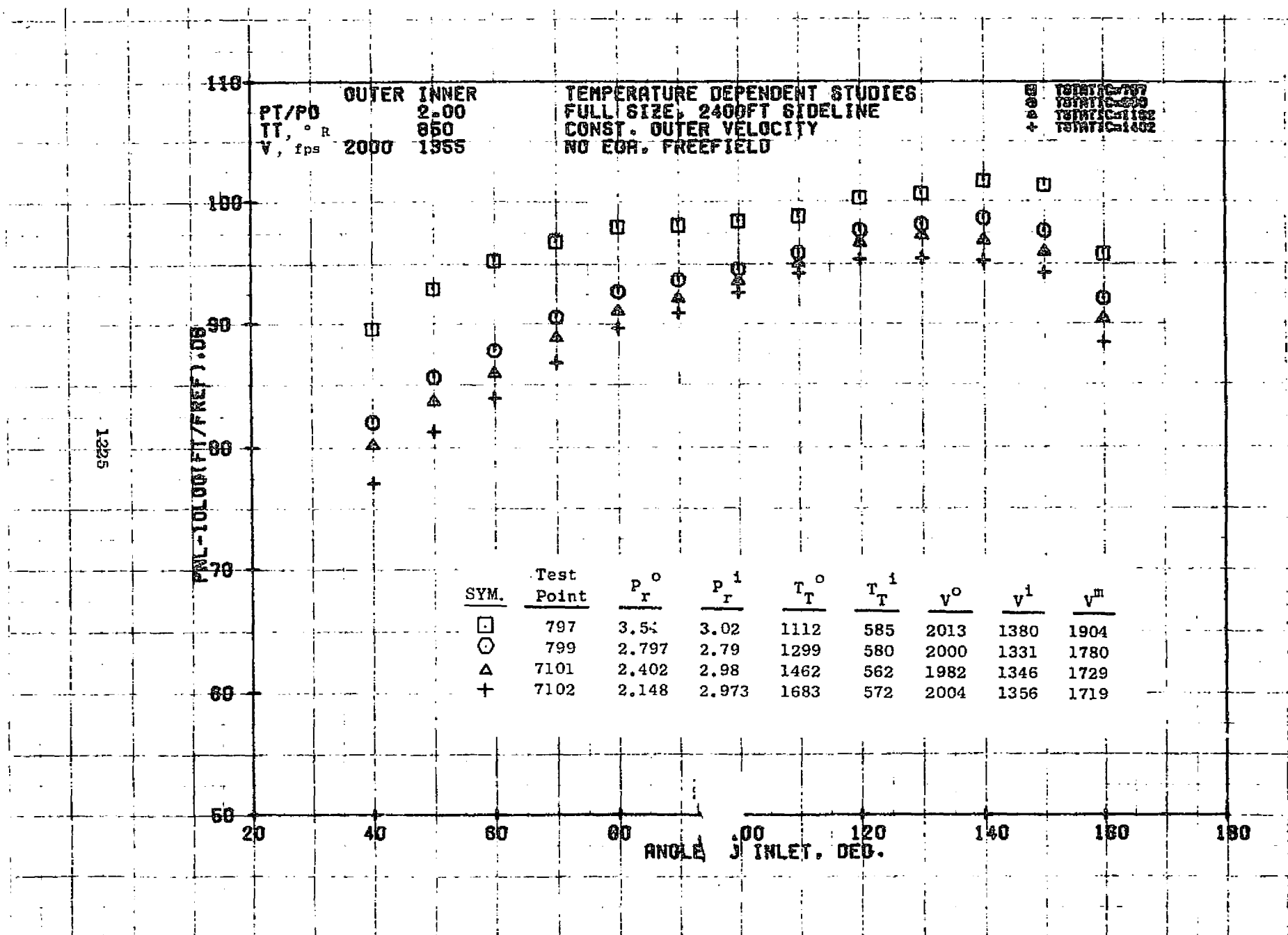
1223

10/13/76
1X930-001

73KOLLSTEDT

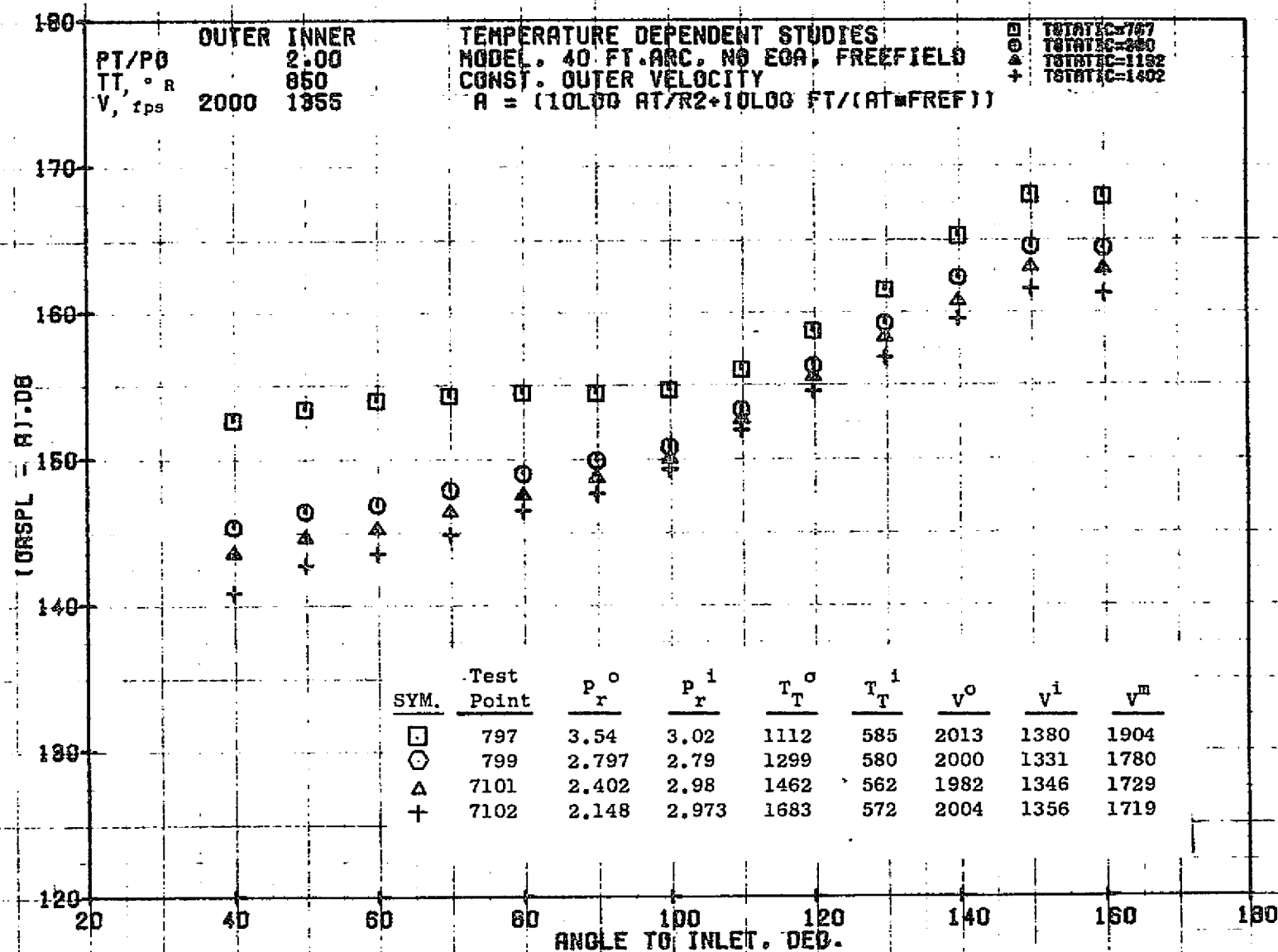
7.4.8 Temperature Dependence Study

For Configuration 7, another series of tests was run to examine the temperature dependence of a high inner flow annular nozzle. For this study, the inner stream conditions were held constant, while the outer stream velocity was held constant and the static temperature of the outer stream was varied. The results are presented in this section.



10/25/78
1X898-001

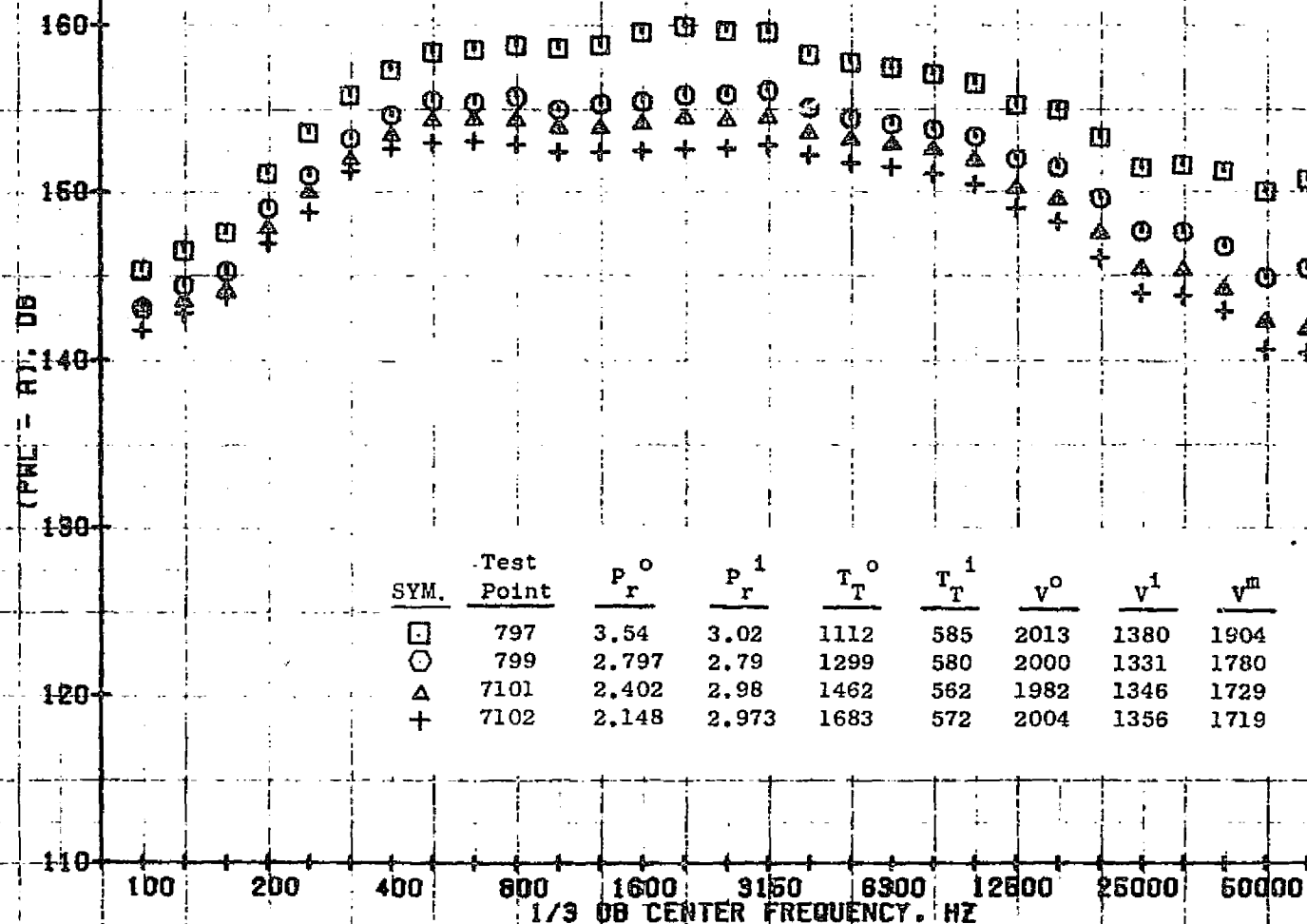
73KOLLETEDT



10/25/76
1X945-001

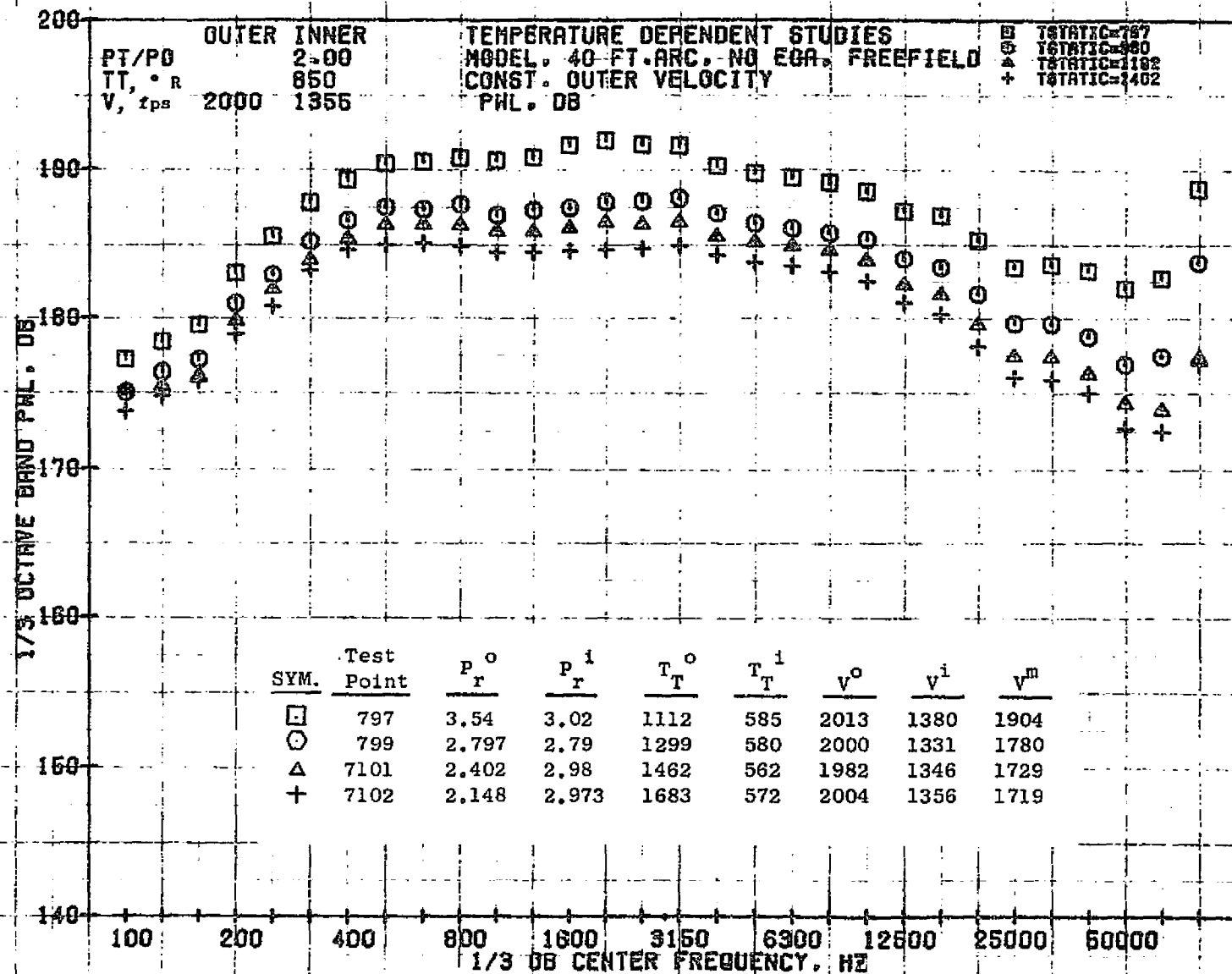
73KOLLSTEDT

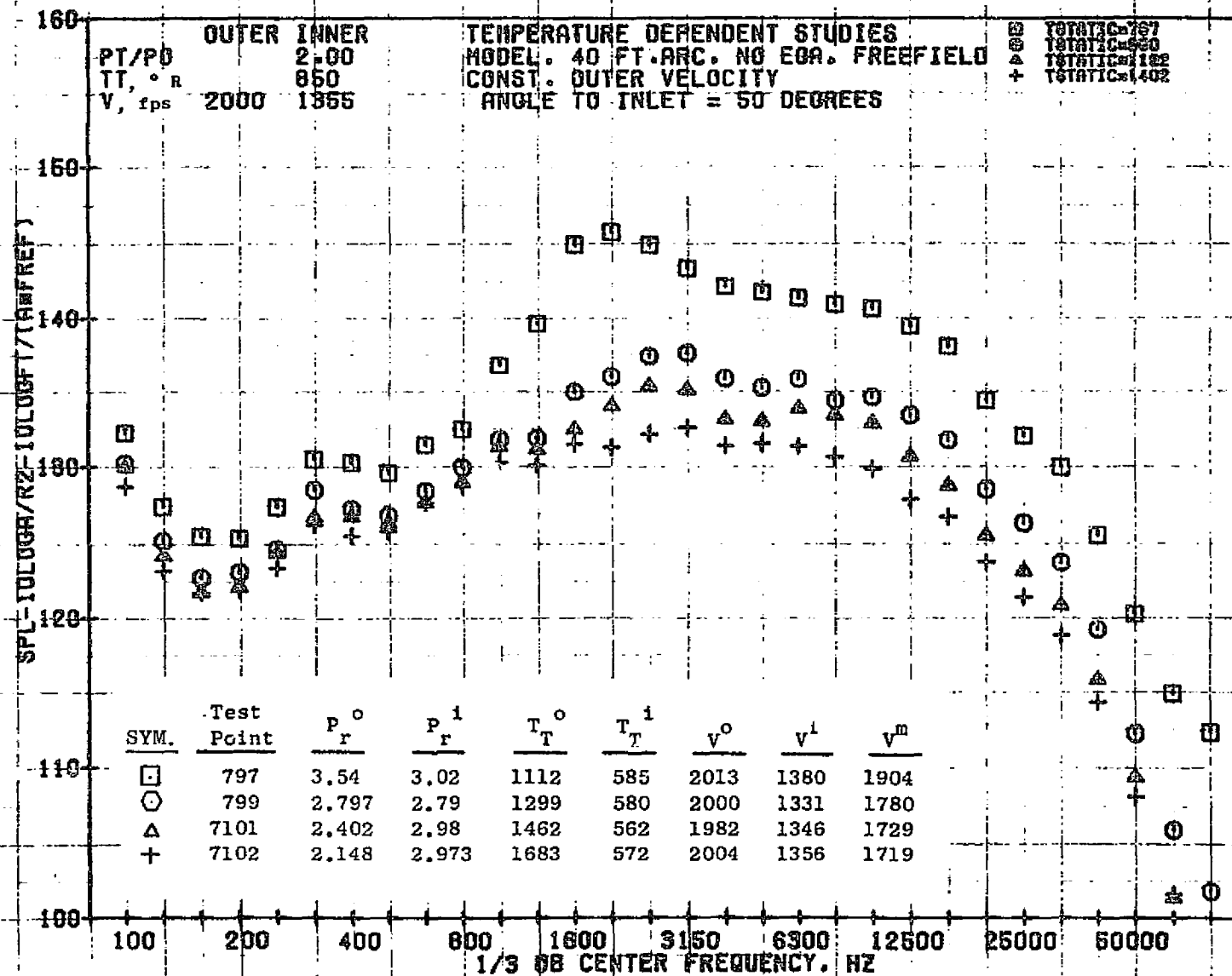
170
 PT/PO OUTER INNER
 TT, °R 2.00
 V, fps 2000 1355
 TEMPERATURE DEPENDENT STUDIES
 MODEL, 40 FT. ARC, NO EOA, FREEFIELD
 CONST. OUTER VELOCITY
 $A = (10 \log A_1/R^2 + 10 \log FT/(AT \cdot FREF))$
 T6TATIC=787
 T6TATIC=880
 T6TATIC=1182
 T6TATIC=1402



10/25/76
 1X946-001

73KOLLSTEDT





10/25/78
1X945-001

73KOLLSTED

160

PT/PO

TT, ° R

V, fps

OUTER INNER

2.00

850

2000 1355

TEMPERATURE DEPENDENT STUDIES

MODEL, 40 FT. ARC, NO EGA, FREEFIELD

CONST. OUTER VELOCITY

ANGLE TO INLET = 70 DEGREES

□

○

△

+

T_{STATIC}=787T_{STATIC}=880T_{STATIC}=1192T_{STATIC}=1402

1230

SPL-10LOGA/R2-10LOGF1/(A-REF)

110

100

SYM.

Test Point

P_r^oP_rⁱT_T^oT_TⁱV^oVⁱV^m

□

797

3.54

3.02

1112

585

2013

1380

1904

○

799

2.797

2.79

1299

580

2000

1331

1780

△

7101

2.402

2.98

1462

562

1982

1346

1729

+

7102

2.148

2.973

1683

572

2004

1356

1719

1/3 DB CENTER FREQUENCY, HZ

10/05/78

PT/PO
TT, °R
V, fps

OUTER
2.00
850
2000

INNER
1355

TEMPERATURE DEPENDENT STUDIES
MODEL, 40 FT-ARC, NO EGA, FREEFIELD
CONST. OUTER VELOCITY
ANGLE TO INLET = 90 DEGREES

□ TSTATIC=787
○ TSTATIC=850
△ TSTATIC=1182
+ TSTATIC=1402

SPL - 10 LOG (P_r² - I₀ I₀ / (R₀ R₀ P_r P_r))

1231

SYM.	Test Point	P _r ^o	P _r ⁱ	T _T ^o	T _T ⁱ	V ^o	V ⁱ	V ^m
□	797	3.54	3.02	1112	585	2013	1380	1904
○	799	2.797	2.79	1299	580	2000	1331	1780
△	7101	2.402	2.98	1462	562	1982	1346	1729
+	7102	2.148	2.973	1683	572	2004	1356	1719

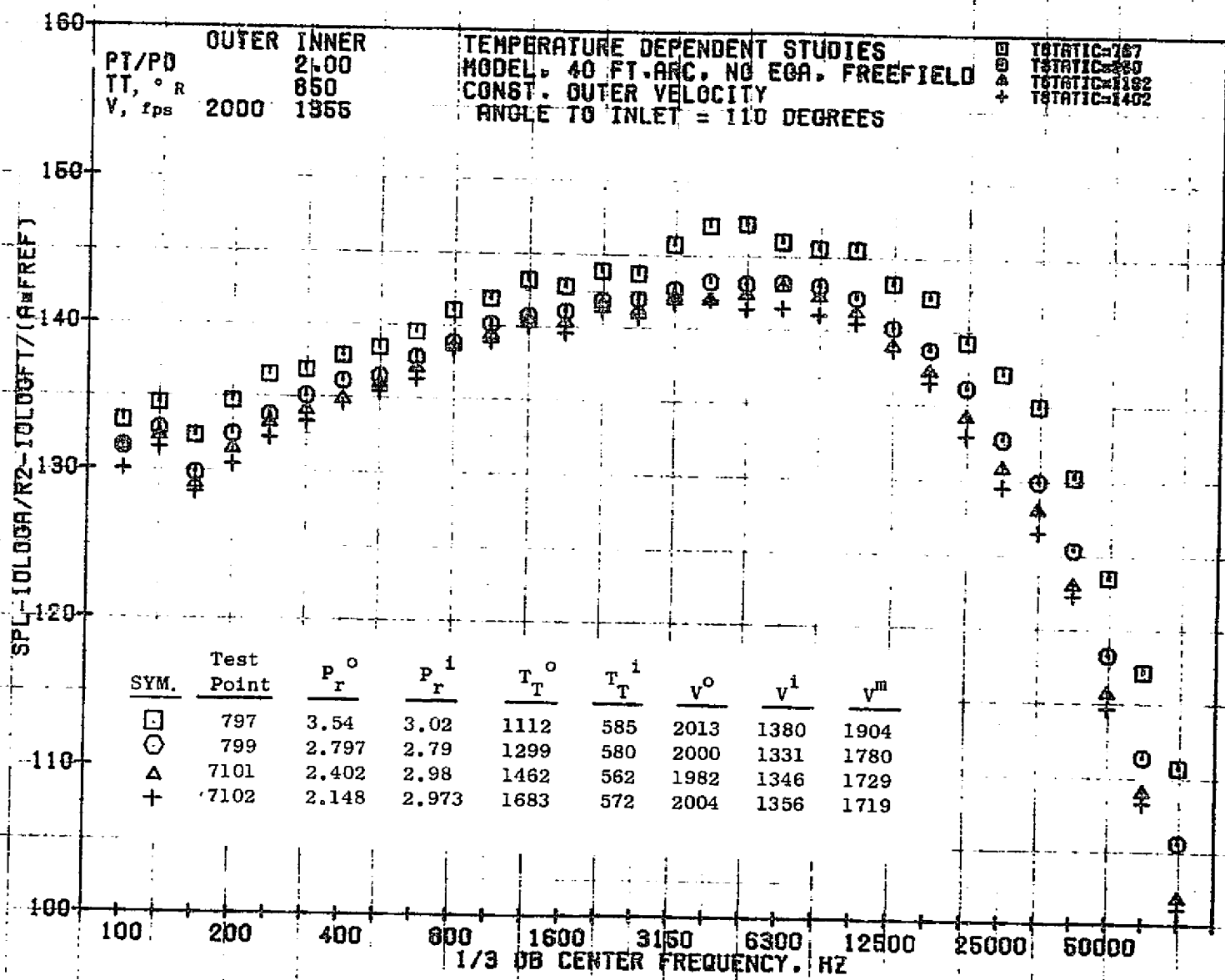
100 200 400 800 1600 3150 6300 12500 25000 50000

1/3 DB CENTER FREQUENCY, HZ

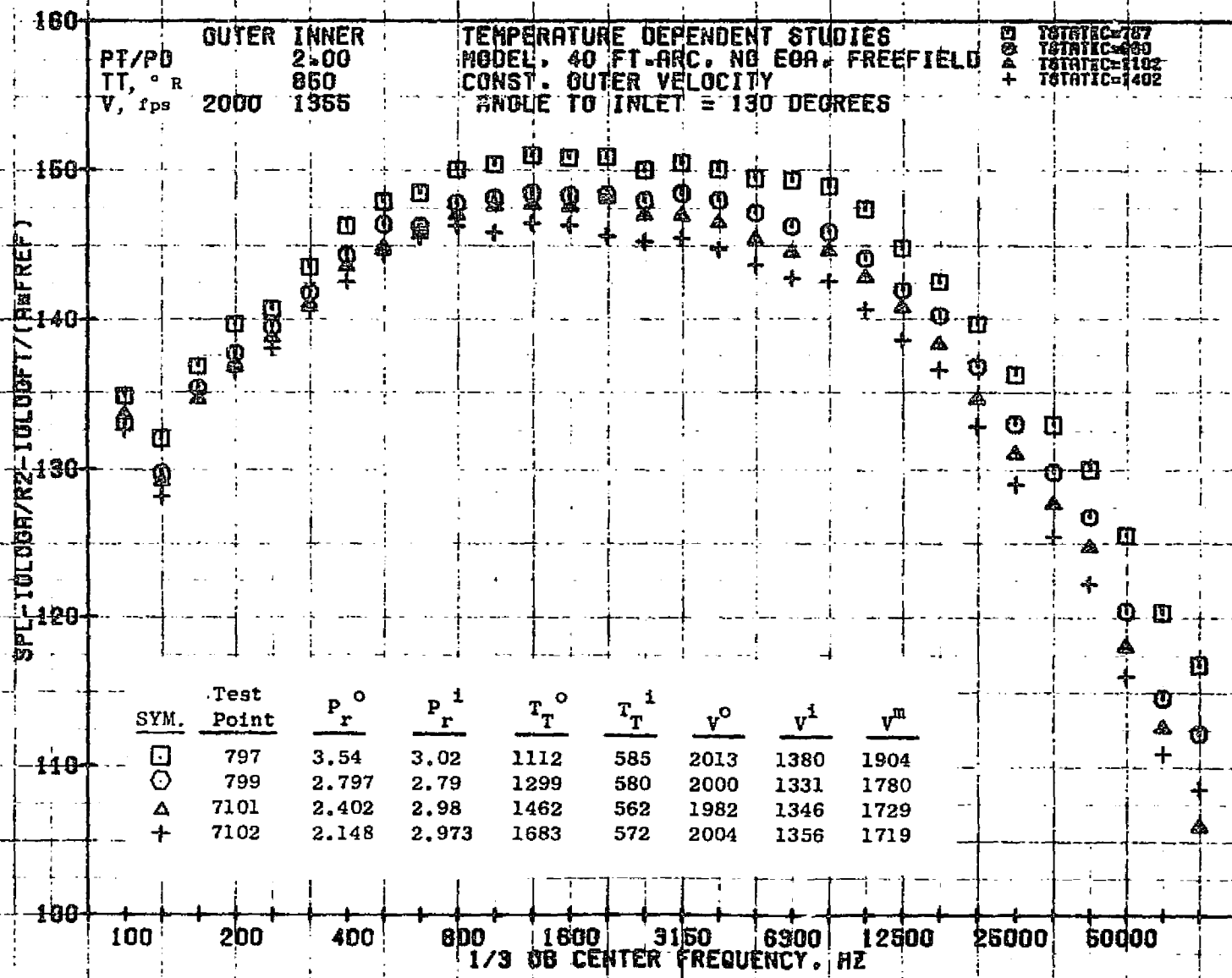
10/25/76
1X945-001

79KOLLSTED

1232



10/25/76

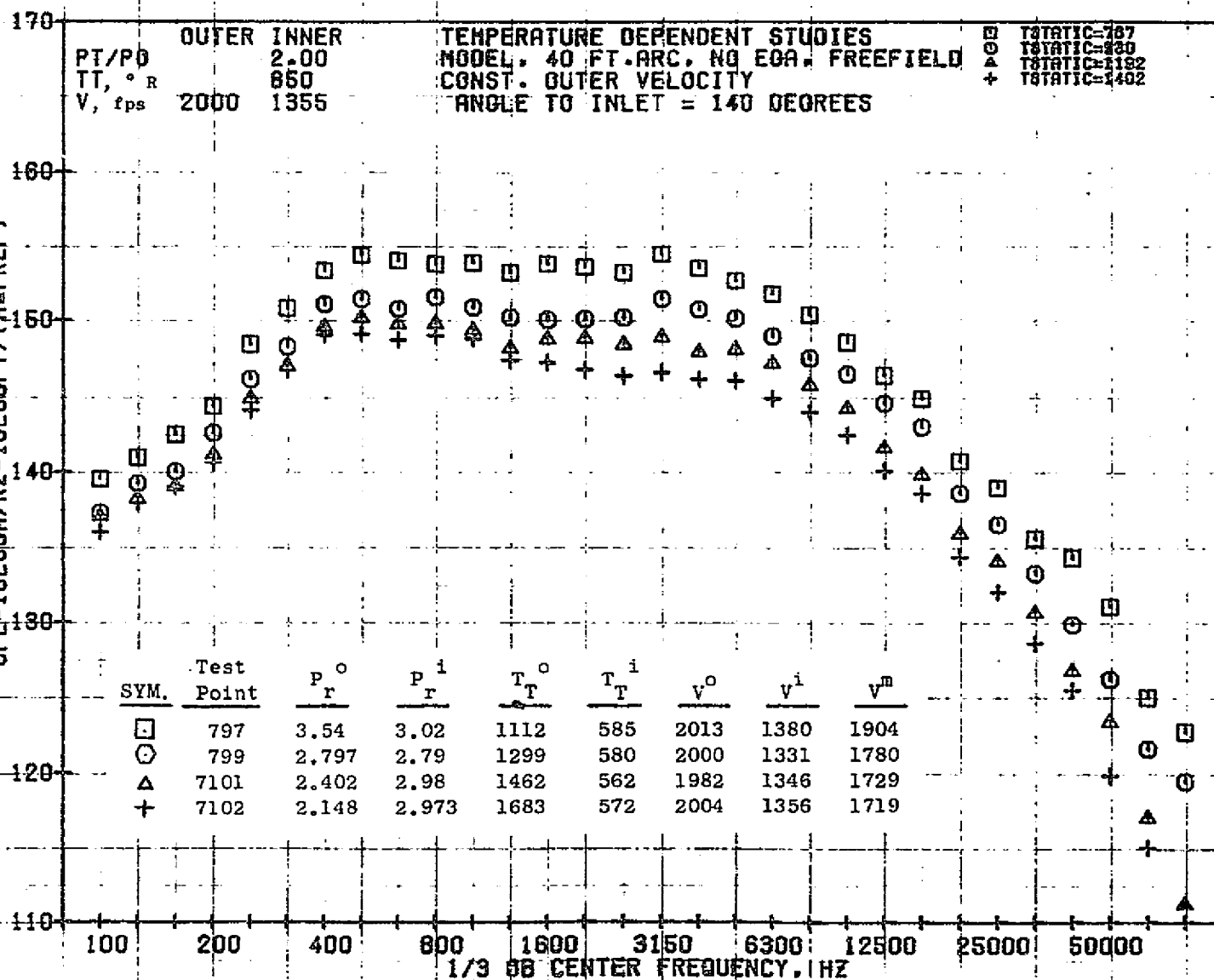


10/25/76
1X945-001

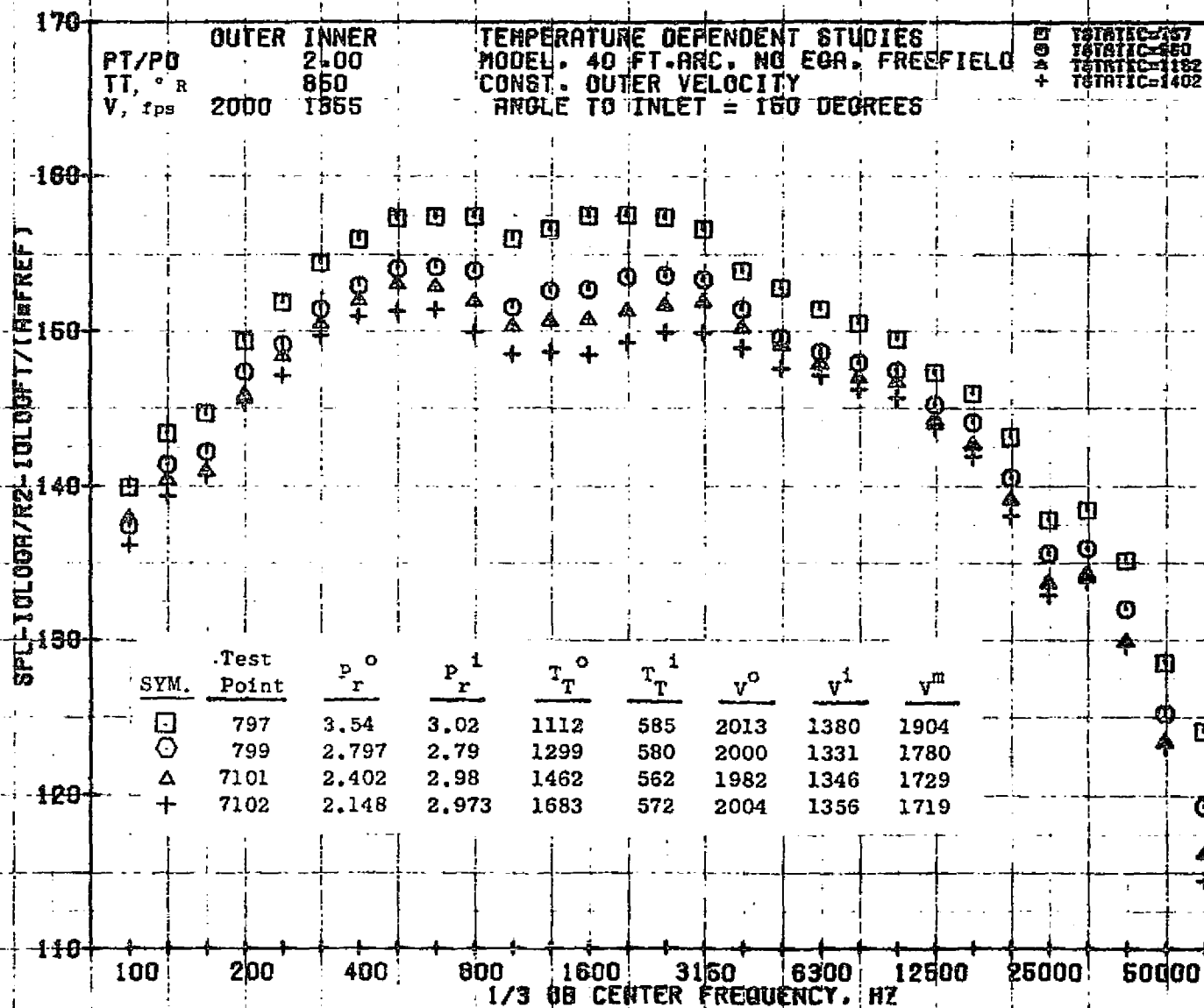
79KOLLSTEDT

1234

SPL-10LOGA/R2-10LOGFT/(A=FREEF)



10/25/76



10/25/78
1X945-001

79KOLI STEDT